Concrete for Extreme Conditions

Proceedings of the International Conference
held at the University of Dundee, Scotland, UK
on 9-11 September 2002

Edited by

Ravindra K. Dhir
Director, Concrete Technology Unit
University of Dundee

Michael J. McCarthy
Lecturer, Concrete Technology Unit
University of Dundee

and

Moray D. Newlands
CPD/Consultancy Manager, Concrete Technology Unit
University of Dundee

Thomas Telford

Published by Thomas Telford Publishing, Thomas Telford Ltd, 1 Heron Quay, London E14 4JD. www.thomastelford.com

Distributors for Thomas Telford books are
USA: ASCE Press, 1801 Alexander Bell Drive, Reston, VA 20191-4400, USA
Japan: Maruzen Co. Ltd, Book Department, 3–10 Nihonbashi 2-chome, Chuo-ku, Tokyo 103
Australia: DA Books and Journals, 648 Whitehorse Road, Mitcham 3132, Victoria

First published 2002

The full list of titles from the 2002 International Congress 'Challenges of Concrete Construction' and available from Thomas Telford is as follows

- Innovations and developments in concrete materials and construction
- Sustainable concrete construction
- Concrete for extreme conditions
- Composite materials in concrete construction
- Concrete floors and slabs
- Repair, rejuvenation and enhancement of concrete

A catalogue record for this book is available from the British Library

ISBN: 0 7277 3178 5

Printed and bound in Great Britain by MPG Books, Bodmin, Cornwall

PREFACE

Concrete is a global material that underwrites commercial well-being and social development. Notwithstanding concrete's uniqueness, it faces challenges from new materials, environmental concerns and economic factors, as well as ever more demanding design requirements. Indeed, the pressure for change and improvement of performance is relentless and necessary.

The Concrete Technology Unit (CTU) of the University of Dundee organised this Congress to address these issues, continuing its established series of events, namely, Creating with Concrete in 1999, Concrete in the Service of Mankind in 1996, Economic and Durable Concrete Construction Through Excellence in 1993 and Protection of Concrete in 1990.

The event was organised in collaboration with three of the world's most recognised institutions: the Institution of Civil Engineers, the American Concrete Institute and the Japan Society of Civil Engineers. Under the theme of Challenges of Concrete Construction, the Congress consisted of three Seminars: (i) Composite Materials in Concrete Construction, (ii) Concrete Floors and Slabs, (iii) Repair, Rejuvenation and Enhancement of Concrete, and three Conferences: (i) Innovations and Developments in Concrete Materials and Construction, (ii) Sustainable Concrete Construction, (iii) Concrete for Extreme Conditions. In all, a total of 350 papers were presented from 58 countries.

The Opening Addresses were given by Mr Jack McConnell MSP, First Minister of the Scottish Executive, Sir Alan Langlands, Principal and Vice-Chancellor of the University of Dundee, Mr John Letford, Lord Provost, City of Dundee, Professor Adrian Long, Senior Vice-President of the Institution of Civil Engineers, Dr Taketo Uomoto, Director of the Japan Society of Civil Engineers and Dr Terence Holland, President of the American Concrete Institute. The Congress had six Opening and six Closing Papers dealing with the main themes of the Seminars and Conferences. Opening Papers were presented by Professor Gerard Van Erp, University of Southern Queensland, Australia Dr Peter Seidler, Astradur Industrieboden, Germany and Professor Kyosti Tuttii, Skanska Teknik AB, Sweden, Professor Surendra Shah, Northwestern University, USA, Dr Philip Nixon, Building Research Establishment, UK and Mr Hans de Vries, Ministry of Transport, the Netherlands. Closing Papers were presented by Dr Gier Horrigmoe, NORUT Technology Ltd, Norway, Professor Andrew Beeby, University of Leeds, UK, Professor Peter Robery, FaberMaunsell, UK, Professor Heiki Kukko, VTT Building and Transport, Finland, Dr Mette Glavind, Danish Technological Institute, Denmark and Professor Yoshihiro Masuda, Utsunomiya University, Japan. The Congress was closed by Professor Peter Hewlett, Chief Executive of the British Board of Agrément, UK.

The support of 23 International Professional Institutions and 32 Sponsoring Organisations was a major contribution to the success of the Congress. An extensive Trade Fair formed an integral part of the event. The work of the Congress was an immense undertaking and all of those involved are gratefully acknowledged, in particular, the members of the Organising Committee for managing the event from start to finish; members of the International Advisory and National Technical Committees for advising on the selection and reviewing of papers; the Authors and the Chairmen of Technical Sessions for their invaluable contributions to the proceedings.

All of the proceedings have been prepared directly from the camera-ready manuscripts submitted by the authors and editing has been restricted to minor changes where it was considered absolutely necessary.

Dundee
September 2002

Ravindra K Dhir
Chairman, Congress Organising Committee

INTRODUCTION

Concrete is a unique material in that it can resist extremes of heat, cold, water and load, yet provide the engineer with an economic solution to the construction of complex buildings and infrastructure. It has very few weak points and where these exist, eg acid chemical attack, its composition can be manipulated to provide satisfactory performance.

As the limits of technology expand, so to do the conditions into which structures and elements must be placed. These include for example, deep water, the conditions to recover hitherto inaccessible oil reserves and roads, which span deserts. Furthermore concrete has an important role to play in containing the conditions associated with climate change, anticipated in the medium to long-term.

Recent events illustrate that concrete must be able to cope with severe blasts and explosive responses. Indeed, the very future of tall structures may depend on the ability of concrete to resist occurrences, which even a few years ago would be unthinkable.

The world is developing rapidly and populations are ever growing. As this occurs, the need for structures for accommodation, business, commerce and education in areas where seismic activity is commonplace, becomes ever more pressing. It is clearly the duty of the developed world technologies to facilitate this.

This century will also see increasing demands for energy, both fossil and nuclear and concrete will play a central role in achieving this. Furthermore, the worlds nuclear generating facilities are ageing and the need for decommissioning and the nettle of the containment of toxic and radioactive materials must be grasped. It can also be anticipated that this century will see concrete become extraterrestrial and thereby enable the further exploration and understanding of the universe.

The Proceedings of this Conference *'Concrete for Extreme Conditions'* deals with all of these subject areas and the issues raised under six clearly defined themes: (i) Chemically and Physically Aggressive environments, (ii) Marine and Underwater Concrete, (iii) Temperature and Humidity Effects on concrete, (iv) Design for Accidental Damage, (v) Extreme Loading Conditions and (vi) Concrete for Specialist Situations. Each theme started with a Keynote Paper presented by the foremost components in their respective fields. There were a total of 79 papers presented during the International Conference which are compiled into these Proceedings.

Dundee
September 2002

Ravindra K Dhir
Michael J McCarthy
Moray D Newlands

ORGANISING COMMITTEE

Concrete Technology Unit

Professor R K Dhir OBE (Chairman)

Dr M D Newlands (Secretary)

Professor P C Hewlett
British Board of Agrément

Professor T A Harrison
Quarry Products Association

Professor V K Rigopoulou
National Technical University of Athens, Greece

Dr S Y N Chan
Hong Kong Polytechnic University

Dr N Y Ho
L & M Structural Systems, Singapore

Dr M R Jones

Dr M J McCarthy

Dr T D Dyer

Dr K A Paine

Dr L J Csetenyi

Dr J E Halliday

Dr L Zheng

Dr S Caliskan

Dr A Iordanidis

Ms P I Hynes (Congress Assistant)

Mr S R Scott (Unit Assistant)

INTERNATIONAL ADVISORY COMMITTEE

Dr C Andrade, *Director of IETCC*
Institute of Construction Sciences Eduardo Torroja, Spain

Professor G Balázs, *Head of Department*
Budapest University of Technology, Hungary

Professor Y Ballim, *Associate Professor*
University of the Witwatersrand, South Africa

Professor A Bentur, *Head Division of Building Materials*
Technion Israel Institute of Technology, Israel

Professor J M J M Bijen, *Professor*
Delft University of Technology, Netherlands

Professor A Brandt, *Head of Department*
Insistute of Fundamental Tech Research, Poland

Professor K-J Byun, *Dean/Professor in Concrete Engineering*
Yonsei University, Korea

Dr J-M Chandelle, *Chief Executive*
CEMBUREAU, Belgium

Professor T-P Chang, *Professor*
National Taiwan University of Science & Technology, Taiwan

Professor M Collepardi, *Professor*
Politecnico Di Milano, Italy

Dr J Duncan, *Manager, Building Industry Research*
BRANZ, New Zealand

Professor R I Gilbert, *Head of School*
University of New South Wales, Australia

Professor S Ikeda, *Professor*
Yokohama National University, Japan

Professor B L Jensen,
Danish Technological Institute, Denmark

Dr H Justnes, *Chief Scientist*
SINTEF Civil & Environmental Engineering, Norway

Professor V Kristek, *Head of Department*
Czech Technical University, Czech Republic

Dr A K H Kwan, *Associate Dean of Engineering*
University of Hong Kong, Hong Kong

Professor F de Larrard, *Director MMCER*
LCPC Centre de Nantes, France

INTERNATIONAL ADVISORY COMMITTEE (CONTINUED)

Professor R W Lindberg, *Professor*
Tampere University of Technology, Finland

Dr H-U Litzner, *Senior Chief Executive*
German Concrete Society (DBV), Germany

Mr J E McDonald, *Research Civil Engineer*
US Army Corp of Engineers, USA

Professor S Mirza, *Professor*
McGill University, Canada

Mr J V Paiva, *Head, Building Department*
LNEC, Portugal

Dr T Philippou, *Manager*
Heracles General Cement Company, Greece

Mr S A Reddi, *Deputy Managing Director*
Gammon India Limited, India

Professor F Saje, *Professor of Concrete Structures*
University of Ljubljana, Slovenia

Professor S P Shah, *Director, ACBM*
Northwestern University, USA

Professor H E R Sommer, *Consultant*
Austria

Dr S Tangtermsirikul, *Head of School of Civil Engineering*
Thammasat University, Thailand

Professor K Tuutti, *Director*
Skånska Teknik AB, Sweden

Professor T Uomoto, *Head of Uomoto Concrete Laboratory*
University of Tokyo, Japan

Dr O H Wallevik, *Head of Concrete Division*
Icelandic Buidling Research Institute, Iceland

Professor T H Wee, *Associate Professor*
National University of Singapore, Singapore

Professor M A Yeginobali, *Director, R&D Institute*
Turkish Cement Manufacturers Association, Turkey

Professor H M Z Al-Abideen, *Deputy Minister*
Ministry of Public Works and Housing, Saudi Arabia

NATIONAL TECHNICAL COMMITTEE

Professor S A Austin
Professor of Structural Engineering, Loughborough University

Professor A W Beeby
Professor of Structural Design, The University of Leeds

Professor T Broyd
Research & Innovations Director, W S Atkins

Professor J H Bungey
Head of Department, The University of Liverpool

Mr N Clarke
Publications Manager, The Concrete Society

Mr G Cooper
Development Director, Fosroc International Ltd

Mr S J Crompton
Divisional Manager, RMC Readymix Ltd

Dr S B Desai OBE
Visiting Professor, University of Surrey

Professor R K Dhir OBE (Chairman)
Director, Concrete Technology Unit, University of Dundee

Dr K Elliott
Senior Lecturer, University of Nottingham

Dr S Garvin
Director (Scotland), Building Research Establishment

Professor F P Glasser
Professor, University of Aberdeen

Mr P G Goring
Technical Director, John Doyle Construction

Professor T A Harrison
BRMCA Consultant, Quarry Products Association

Professor P C Hewlett
Chief Executive, British Board of Agrement

Mr A Johnson
Divisional Director and Manager, Mott MacDonald Special Services

Dr M R Jones
Senior Lecturer, Concrete Technology Unit, University of Dundee

Professor R J Kettle
Head of Department, Aston University

Mr P Livesey
National Technical Services Manager, Castle Cement Limited

NATIONAL TECHNICAL COMMITTEE (CONTINUED)

Professor A E Long
Dean of Faculty of Engineering, Queens University Belfast

Mr N Loudon
Senior Technical Adviser, Highways Agency

Mr A C Mack
Operations Director, Bovis Lend Lease (Scotland) Ltd

Professor P S Mangat
Head, Civil Engineering & Construction, Sheffield Hallam University

Mr G G T Masterton
Director, Babtie Group

Professor G C Mays
Deputy Principal, Cranfield University

Professor W J McCarter
Professor, Heriot-Watt University

Dr J Moore
Director, Standards & Technical, British Cement Association

Dr P J Nixon
Director, Centre for Concrete Construction, Building Research Establishment

Mr M Peden
Partner, W.A. Fairhurst & Partners

Dr W F Price
Senior Research Manager, British Cement Assocation

Professor P C Robery
Divisional Director - Midlands, Maunsell Ltd

Mr J M Ross
Chairman, Blyth & Blyth Consulting Engineers

Dr R H Scott
Reader in Engineering, University of Durham

Dr I Sims
Director (Materials), STATS Limited

Professor G Somerville OBE
Independent Consultant

Mr P Titman
Quality and Environment Manager, Edmund Nuttall Ltd

Dr P R Vassie
Research Fellow, Transport Research Laboratory

Professor S Wild
Head, Building Materials Research Unit, University of Glamorgan

COLLABORATING INSTITUTIONS

Institution of Civil Engineers, UK

American Concrete Institute

Japan Society of Civil Engineers

SPONSORING ORGANISATIONS WITH EXHIBITION

Aggregate Industries plc
Babtie Group
British Board of Agrement
British Cement Association
Building Research Establishment
Caledonian Slag Cement
Castle Cement Limited
CEMBUREAU, Belgium
Danish Technological Institute, Denmark
Degussa Construction Chemicals, Italy
Dundee City Council
Elkem Materials Ltd
FaberMaunsell
Fosroc International Ltd
Heidelberg Cement, Germany
Heracles General Cement Company, Greece
Institution of Civil Engineers
John Doyle Construction
Lafarge Cement UK
Makers UK Ltd
MBT Admixtures
Netzsch Instruments, Germany
North East Slag Cement
Palladian Publications
RMC Readymix Ltd
Rugby Cement
ScotAsh Ltd

SPONSORING ORGANISATIONS WITH EXHIBITION (CONTINUED)

Scottish Enterprise Tayside
Thomas Telford Publishing
UK Quality Ash Association
Waste Recycling Action Programme (WRAP)
Wexham Developments
Zwick Testing Machines Ltd

SUPPORTING INSTITUTIONS

American Society of Civil Engineers
Austrian Concrete Society
Belgische Betongroepering, Belgium
Concrete Institute of Australia
Concrete Society of Southern Africa, South Africa
Concrete Society, UK
Concrete Association of Finland
Czech Concrete Society
Entreprises Generales de France, France
European Concrete Societies Network
Fédération de l'Industrie du Béton, France
German Society for Concrete and Construction
Hong Kong Institution of Engineers
Indian Concrete Institute
Institute of Concrete Technology, UK
Instituto Brasileiro Do Concreto, Brazil
Irish Concrete Society
Japan Concrete Institute
Netherlands Concrete Society
New Zealand Concrete Society
Norwegian Concrete Association
Singapore Concrete Institute
Swedish Concrete Association

CONTENTS

THEME 3 TEMPERATURE AND HUMIDITY EFFECTS ON CONCRETE

DURABILITY OF CONCRETE: A MAJOR CONCERN TO OWNERS OF REINFORCED CONCRETE STRUCTURES

H De Vries
Ministry of Transport
Netherlands

ABSTRACT. As long as we used to build concrete structures some of them suffer from durability problems. Think about reinforcement corrosion, alkali aggregate reaction, ettringite formation, frost damage etc. But is it that bad with our structures? As a representative of an owner of a lot of concrete structures I must say no. First of all, let us be happy about that fact! But it cannot be denied that there are some problems, most of the time due to bad workmanship or unknown behaviour of (new) materials. A major concern of an (future) owner of a concrete structure is how to get a robust and reliable structure in term of costs, maintenance and repair. The next question is how to specify requirements for these points in the contract? Can we rely on the existing codes or should we prescribe more details? Specifications concerning durability in existing codes are on an empirical base. The conventional building codes give in principle only construction rules. If these rules are fulfilled, it is assumed that the structure will have an adequate durability. Specifications for durability in terms of service life or years are not given. Therefore, an update of the design method and durability related codes are desired. A performance and reliability based service life (re)design method has been developed for concrete structures in a recent European Brite/Euram project "DuraCrete". The framework of this method can however be used for other structural and building materials. A further advantage is that it is very similar to the structural design method that is present in most modern structural building codes, like the Eurocode. The method has been put into practice in The Netherlands for the design of several large structures for rail and highway infrastructure. This new approach gives an owner the opportunity the specify his wishes into a contract, while the contractor can 'play' with different solutions in order to get to most optimal or cost-effective result. This paper is based on previous publications [1, 2, 3] on the subject of service life design with the DuraCrete method.

Keywords: Concrete, Durability, Service life design, Reliability, Performance, Quality control

Hans de Vries, Project Engineer and material specialist, Tunnelling Department, Ministry of Transport, Civil Engineering Division, Utrecht, The Netherlands.

INTRODUCTION

The design and construction of several bored tunnels in the Netherlands was a major reason to set additional requirements with respect to durability. The enormous investment of tax money should be acceptable only if the service life of these tunnels was guaranteed for a certain long period. With this aspect in mind it was clear that the requirements in the existing codes were not sufficient. Therefore the use of another method for durability design was necessary. This performance based method has been developed in the European research project DuraCrete and was put into practice in two projects. First in a highway tunnel – the Western Scheldt Tunnel – containing two 6.6 km long bored tubes with two traffic lanes in each tube. Second in a high speed railway tunnel – the Green Heart Tunnel – with one 8.6 km long single tube for two tracks.

Lack of durability can cause serious safety and serviceability problems for structures. Despite this, designers pay considerably more attention to load and resistance based structural design than to durability design. Recent history however has shown that due to a lack of durability, various types of damages and in some cases, even collapses can occur with tremendous overall costs for repair.

HISTORICAL OVERVIEW OF SERVICE LIFE DESIGN

The present design approach, with respect to durability of concrete structures, is based on a reasonable understanding of the main degradation processes for concrete, reinforcement and pre-stressed steel. The design is however not explicitly formulated in terms of service life. It is based on deem-to-satisfy rules like for example minimum cover, maximum water/binder ratio and crack width limitation. If these rules are met, it is assumed that the structure will achieve an acceptably long but unspecified life. In general a service life of at least 50 year is expected when the existing codes are used.

The information about the service life to be achieved is to a large extent empirically: Improving the durability results in increasing building costs without any quantification of the reduction of maintenance costs or failure costs. Current design methods only permit to calculate the whole life cycle costs from assumptions with respect to maintenance and failure rates. There are thus no objective means for demonstrating that future maintenance and repair costs will be acceptably low. This common design approach to durability has other disadvantages. The rules are inadequate in some aggressive environments, while they are too rigorous in other environments. In some cases, this results in a 'belts and braces' approach (many different types of measures on top of each other) which may contain unnecessary and even counteractive measures.

For large infrastructures the requirements with respect to durability are in general, more stringent than the codes. Some examples of storm surge barriers in the Netherlands can demonstrate this:

- For the Haringvlietsluizen (1965) the requirements were based on the experts opinions at that time. The concrete cover was raised to 70 mm, the water/cement ratio was restricted to 0.45 and blast furnace slag cement was used as binder.

- For the Eastern Scheldt Barrier (1985), the durability requirements were for the first time expressed in terms of time. A service life of 200 years was required. For the concrete cover, this was not feasible. A mean service life of about 85 years was therefore accepted. After that period, the concrete cover will be replaced.

- For the Maeslandtkering (1995) a service life of 100 year was specfied. The concrete cover of this barrier was been enlarged with a factor $\sqrt{100/50} = \sqrt{2}$.

In none of these designs a proper approach for predicting the service life was applied.

In the last decades much effort has been put into the development of models and methods for predicting deterioration of concrete structures. A number of methods have matured to a level where these can be used in a formalised approach to assess and design concrete structures with respect to destructive mechanisms.

Recent Developments

Past decades have taught us that the classical procedures for design, construction and use of concrete structures often have failed to provide reliable, long-term performance. Deterioration processes, in particular corrosion of reinforcement, frost action, alkali aggregate reactions and sulphate attack have caused serious damage to concrete structures. To improve this situation a new concept for durability design needs to be established. Similar to the current procedures for structural design, a design for durability should be performance based taking into account the probabilistic nature of the environmental aggressiveness, the degradation processes and the material properties involved.

In order to quantify the durability the concept of a service life design has been introduced. In this respect the performance requirements for a service life design as stated in the CEB-FIP Model Code 1990 [5] has been adopted: *Concrete structures shall be designed, constructed and operated in such a way that, under the expected environmental influences, they maintain their safety, serviceability and acceptable appearance during an explicit or implicit period of time without requiring unforeseen high costs for maintenance and repair.*

Such a rational design for durability, however, requires both an overall methodology and calculation models for the actual degradation processes of concrete structures. Similar to the structural design code for loads, safety requirements and limit states must be defined for the design service life. Controlling the durability of concrete structures will be a fundamental challenge for the engineer in the next years!

The DuraCrete Project

The new durability design methodology should be able to document the efficiency of the materials to resist the aggressiveness of typical environments. The structural designer will, therefore, be able to document the fulfilment of a specific limit state. For the designer deterioration models are valuable tools, showing the degradation over time, or showing the service life as a function of appropriate design parameters. With the aid of this methodology for service life design, the designer can make decisions on the required dimensions and material specifications for structures.

One consequence of the requirements to service life design is that structural engineers and designers need to be educated in the durability aspects of various materials as well as in the structural layout, the effect of workmanship on the in situ qualities, and the interaction between structure and environment. To make this possible the design engineer will need a new design guide to assist him in making a proper service life design, not only for new structures but also for the redesign of existing concrete structures. A first edition of such a guide [6] has been developed in the project 'DuraCrete'.

FRAMEWORK FOR PERFORMANCE BASED SERVICE LIFE DESIGN

The design strategy is to select an optimal material composition, construction method and structural detailing for a reliable performance with respect to safety and resistance against degradation for a specified service life.

Structural Design

In modern codes, like the Eurocode, the basis of the conventional design procedure for the safety and the serviceability of structures is expressed as a limit state function. This limit state defines the border between an adverse state (such as collapse, buckling, deflection, and vibration) and the desired state. The limit state can in principle be formulated as:

$$R - S = R(X_1, X_2, ..., X_n) - S(X_{n+1}, X_{n+2}, ..., X_m) = 0 \quad (1)$$

In which: R - a function that describes the load bearing capacity of the structure
S - a function that describes the influence of the load on the structure
Xi - a basic variable for the functions R or S.

The structural design procedure is worked out in such a way that the failure probability is restricted:

$$P\{\text{failure}\} = P_f = P\{R - S < 0\} < P_{target} = \Phi(-\beta) \quad (2)$$

In which: $P\{\text{failure}\}$ - the probability of failure of the structure
$1 - P_f$ - the reliability of the structure
P_{target} - the accepted maximum value of the failure probability
Φ - standard normal distribution function
β - reliability index (this parameter is normally used in codes)

With the aid of probabilistic techniques this failure probability can be calculated. In practice the design has however been simplified to a semi-probabilistic level with characteristic values and partial factors γ, those are calibrated in such a way that the target reliability will be achieved:

$$R_c / \gamma_R - S_c \cdot \gamma_S = R_d - S_d > 0 \quad (3)$$

In which: Rc - load-bearing capacity of the structure based on characteristic values
γ_R - material factor

Sc - characteristic value of the influence of the loading
γ_S - load factor.
Rd - design value of the load bearing capacity
Sd - design value of the load.

Time Dependent Design

In the structural design both the resistance R and the load S are considered to be time indepenent. However, the load can vary with time or the capacity can change in time due to degradation. Relationship (1) should than be rewritten as a time dependent limit state function [6], that takes such effects into consideration:

$$R(t) - S(t) > 0 \tag{4}$$

Relationship (4) applies for all values of t in the time interval (0,T). T is the intended service period (i.e. reference period). From a mathematical point of view it can be stated that relationship (4) can be used for service life design. The service life concept can be expressed in a design formula, equivalent to relationship (2):

$$P_{f,T} = P\{R - S < 0\}_T < P_{target} = \Phi(-\beta) \tag{5}$$

In which: $P_{f,T}$ - the probability of failure of the structure within T
T - intended service period.

Probably it will be possible to simplify in a later stage relationship (5) to a similar one as for the conventional structural design procedure (3).

The mathematical model for describing the event 'failure', i.e. passing a durability limit state, comprises a load variable S and a resistance variable R, see Figure 1. Failure occurs if the resistance is smaller than the load.

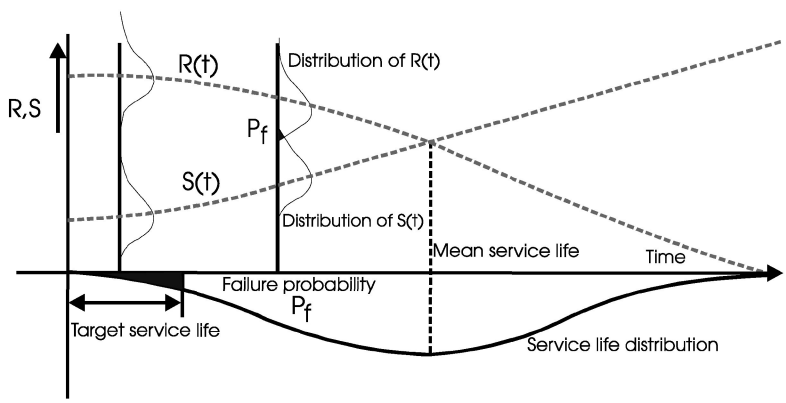

Figure 1 Failure probability and target service life (illustrative presentation)

Design for Service Life

The methodology for service life design will be based upon:

- realistic and sufficiently accurate definitions of loads and environmental actions with respect to the type of degradation.
- material parameters for concrete and reinforcement.
- mathematical models for degradation processes.
- performances expressed as limit states.
- reliability.

The essential items in the methodology have been copied from the structural design [7]:

- performances are related to limit states.
- reference period is similar to the design service life.
- the reliability index is used to reduce the failure probability.

The new items in the approach are the introduction of environmental actions and models describing the degradation of the concrete and the reinforcement.

The limit states that have been defined in the structural codes, are the serviceability limit state (SLS) and the ultimate limit state (ULS). If a SLS is exceeded, the functioning of the structure is restricted. This is the case for example if the deflection of a beam is more than 20 mm. If an ULS is exceeded, it implies that the structure has collapsed, fractured, turned over etc.

The limit states of the structural codes may be extended with other limit states. For example the water tightness of a tunnel can be expressed as a SLS (the amount of leakage water hinders the traffic in the tunnel) or as an ULS (the amount of leakage water is so high that the tunnel floods). Also new types of limit states may be introduced. For example the limit state to reduce the amount of repair. In case of possible corrosion of the reinforcement, the probability that repair is necessary can be reduced by requiring that no corrosion occurs.

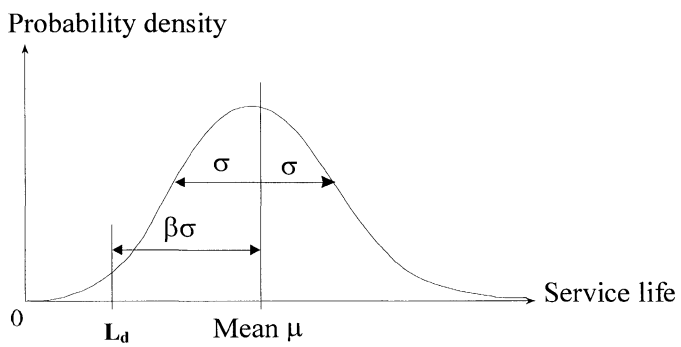

Figure 2 Example of a probability density function for the service life

In Figure 2, an example of a service life distribution is given. The main parameters in such a distribution are the mean value μ (magnitude parameter) and the standard deviation σ (parameter for the scatter). Instead of the standard deviation, we can also use the variation coefficient $V = \sigma/\mu$. By means of the reliability index β, the probability that the service life is lower than the design service life L_d is identified. The margin $\beta\sigma$ can be regarded as a safety margin between the design service life and the mean service life.

For every performance a unique service life distribution function is connected, depending on the geometry of the structure, the material properties, the mechanical loads and the environmental actions. This implies that for every relevant performance the distribution function has to be established, and that the design service life as well as the reliability index must be defined.

In Table 1 some values for the reliability index β and the corresponding approximate failure probabilities are given (European Code EC 1 and Dutch Building Code NEN 6700). These codes refer in the first place to structural aspects. The reliability indexes can however also be used if lack of durability leads to an event that leads to an unacceptably loss of serviceability or to a loss of structural safety.

If failure leads only to economical consequences, serviceability limit states (SLS) are applied, e.g. onset of corrosion. If failure leads to a severe consequence, e.g. total loss of the structure or victims, ultimate limit states (ULS) are applied. The owner or investor may define other reliability indexes in order to reduce repair costs, ensuring the structural appearance, etc.

Table 1 Examples of some reliability indexes in structural codes

TYPE OF PERFORMANCE	RELIABILITY INDEX β FOR 100 YEAR SERVICE LIFE DESIGN		APPROXIMATE FAILURE PROBABILITY	
	EuroCode EC 1	Dutch Building Code NEN 6700	Per Year	Within 100 years
ULS	3.8	3.6	10^{-6}	10^{-4}
SLS	1.5	1.8	10^{-4}	10^{-2}

Before making a probabilistic calculation, it seems illustrative to give an example to show the consequences of these reliability indexes.

In Figure 3, the consequences of the reliability indexes from the Dutch Building Code are given in a service life distribution for the ULS. In this example, it has been assumed that the service life distribution is lognormal with a variation coefficient of 30 % ($\sigma = 0.3\ \mu$). These assumptions are more or less realistic for this kind of durability problems. To illustrate the effect of the value for the design service life, the figures are given for 50 years and 100 years.

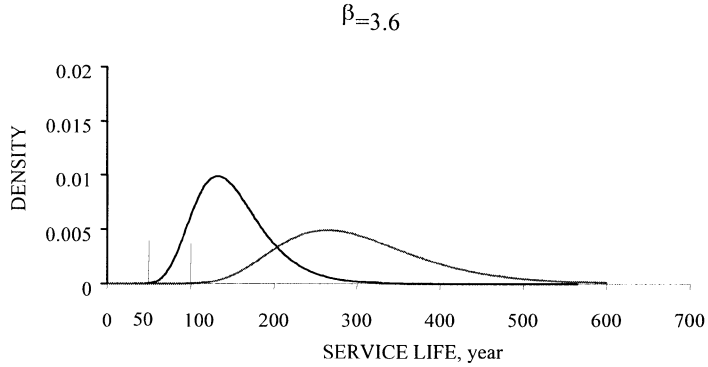

Figure 3 Example of a service life distribution for the ULS ($\beta = 3.6$) for a design period of 50 year and for a design period of 100 year

In Table 2 this has been quantified and extended also to the SLS. The reliability index for the ULS has been taken as 3.6 and for the SLS as 1.8. The margin γ_L depends on the type of distribution and the variation coefficient.

Table 2 Mean service life and margins γ_L for design service of 50 years and 100 years

TYPE OF PERFORMANCE	DESIGN LIFE 50 YEARS		DESIGN LIFE 100 YEARS	
Acc. Dutch Building Decree NEN 6700	Mean service life	Margin γ_L	Mean service life	Margin γ_L
SLS: $\beta = 1.8$	89	1.8	177	1.8
ULS: $\beta = 3.6$	150	3.0	300	3.0

SERVICE LIFE DESIGN

The first step of this design is the definition of the desired/required performance of the structure. The client or the owner of the structure is asked to define his requirements for quality and target service life. Further requirements can be given in building codes. The definition of performance criteria will be related to a limit state criterion. Figure 4 shows an example of the performance (by means of a damage progress function) of a concrete structure with respect to reinforcement corrosion and related limit states. This example is taken from [3] where a description is given of the Western Scheldt Tunnel in The Netherlands, being the first concrete structure designed according to this service life design. In general depassivation and cracking represent serviceability limit states related to durability. Spalling and collapse represent ultimate limit states, where spalling relates to both durability and safety.

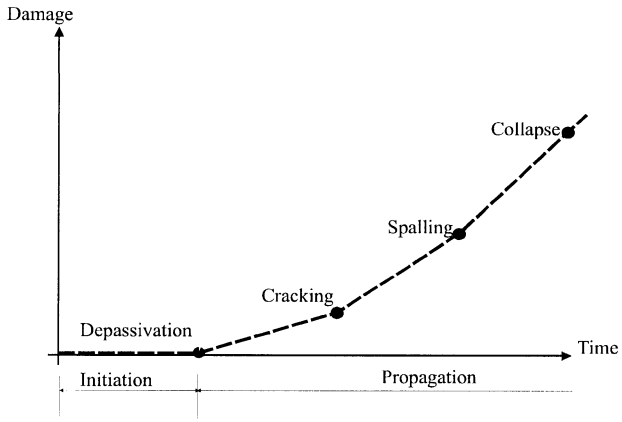

Figure 4 Determination of service life and limit states with respect to reinforcement corrosion

Degradation Models

The second step of the durability design is to analyse the environmental actions and to identify the relevant degradation mechanisms. Mathematical models must describe the time dependent degradation processes and the material resistance against it. The big step forward is that these models enable the designer to evaluate the time-related changes in materials and structures depending on the specific material and environmental conditions.

The different models used for this durability design consist of design parameters such as structural dimensions, environmental parameters and material properties that correspond to the load and resistance variables of the structural design procedure. Models are available for degradation processes due to carbonation and chloride ingress.

DURABILITY OF CONCRETE SEGMENTS FOR A BORED TUNNEL

This example is based on the Western Scheldt Tunnel in the Netherlands. This tunnel consists of two bored tubes with a diameter of 11.30 metre. The length of each tube is 6.6 kilometres. The tunnel has for safety and maintenance cross-links each 250 metres. The construction of the bored section of the tunnel was finalised early this year. The greatest depth of the tunnel is 63 metres below sea level. The required service life is 100 year. The total cost of the project, including connecting roads is about 0.75 billion US dollars.

This example is restricted to the design of a tunnel lining for a bored tunnel. It will be clear that in reality the whole tunnel design must be based on the service life concept. The example deals with the ingress of chlorides into the lining of a bored tunnel on the inside of the tunnel. The chlorides may originate from leakage of salt-laden ground water or from de-icing salts.

Onset of corrosion (depassivation) will be considered as serviceability limit state. When corrosion has started, maintenance is much more complicated to perform and therefore is considered to be much more expensive than for a structure without already started corrosion activity. Consequently there is an economic risk present. From this point of view the onset of corrosion is a serviceability limit state (SLS). According to the requirements of the Dutch Building Code the reliability index should be 1.8 or higher. The ultimate limit state, for instance flooding of collapse of the tunnel, is not taken into account in this example.

Taking the example of onset of chloride induced corrosion the durability inputs are as follows:

- The limit state is given by the requirement that the chloride concentration at the surface of the reinforcement may not reach the critical chloride concentration.

- The resistance R is given by the critical chloride concentration and the quality and thickness of the concrete cover.

- The load S is represented by the actual chloride concentration at the reinforcement level. This depends on material parameters (chloride diffusion coefficient) and environmental effects.

In the case of chloride induced corrosion the following model describing the initiation of corrosion has been identified:

$$x(t) = 2 \cdot k \cdot \sqrt{D_{RCM,0} \cdot k_e \cdot k_c \cdot t \cdot \left(\frac{t_0}{t}\right)^n} \tag{6}$$

In which: $x(t)$ = required concrete cover

$$k = \text{erf}^{-1}\left(1 - \frac{C_{cr}}{C_s}\right) \quad \text{where :} \quad C_{cr} = \text{critical chloride concentration}$$

$$C_s = \text{chloride surface concentration}$$

$$D = D_{RCM,0} k_e k_c \left(\frac{t_0}{t}\right)^n = \text{chloride diffusion coefficient}$$

A full probabilistic calculation is made using relationship (6) for chloride penetration. The input parameters are quantified in table 3. These parameters are typical for the concrete and the environment used in this example. In other cases they could be totally different.

With the arranged data from Table 3, it is now possible to calculate the reliability. The required statistical calculation was carried out with the software package STRUREL. The result of the evaluation is shown in Figure 5. A more detailed description of this calculation is presented in [3].

The environmental factor k_e (accounting for the actual environmental class), the curing factor k_c (accounting for the actual curing period) and the age factor n (accounting for the desired service life t) are neutral factors, i.e. neither load nor resistance factors. These factors are used to determine the actual, effective chloride diffusion coefficient. These factors correct the compliance value $D_{RCM,0}$ that is determined with the Rapid Chloride Migration (RCM) test on concrete specimens under laboratory conditions [8,9].

Table 3 List of stochastic variables influencing the duration of the initiation period

PARAMETER	DIMENSION	μ	σ	DISTRIBUTION
x_c – Concrete cover	[mm]	37	2	Exponential.
$D_{RCM,0}$ – Cl^- migration coeffi.	[$10^{-12}m^2/s$]	4.75	0.71	Normal
CCrit – Critical chloride content	[wt.-%/binder]	0.70	0.10	Normal
n – Age exponent	[-]	0.60	0.07	Normal
k_t – Test factor	[-]	0.85	0.20	Normal
k_e – Environmental factor	[-]	1.00	0.10	Normal
K_c – Execution factor	[-]	1.00	0.10	Normal
C_{SN} – Surface concentration	[wt.-%/binder]	4.00	0.50	Normal Distr.
T_0 – Reference time	[year]	0.0767	-	Deterministic

Figure 5 shows the decrease of the reliability index β over time. The obtained reliability index is $\beta_{SLS} = 1.50$ after 100 year. This value is lower than the minimum required value $\beta_{SLS} = 1.8$. Additional measures had to be taken into account to improve the design. Options could be a higher concrete cover, applying a surface coating, use of stainless steel or cathodic protection. In this case the application of a hydrophobic coating on those parts with a cover less than 50 mm was chosen.

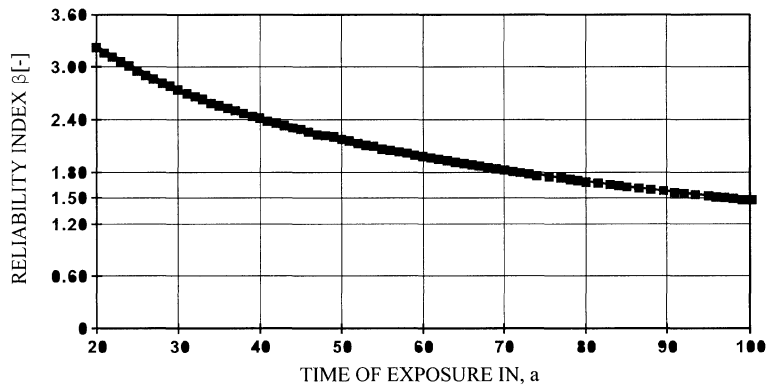

Figure 5 Reliability index versus time of exposure (SLS: Onset of Corrosion)

This example shows that, with the tested material and the chosen concrete cover, one can achieve a durable structure concerning chloride induced steel corrosion with the minimum required safety according to the defined serviceability limit state 'Onset of Corrosion'.

QUALITY CONTROL AND RELIABILITY

The knowledge about the structural and material characteristics of a structure is uncertain due to the variations in structural layout, material properties, execution and environmental input. These variations influence the results of the calculations with the selected degradation models. This uncertainty is taken into account in the probability density functions of the basic variables, including their parameters like the mean value and the standard deviation. This means that during construction and use of the structure, measures must be taken to guarantee that the uncertainties are not exceeded.

Testing and quality control is therefore important at several stages during the life of a structure. The real performance of the structure has to be checked by quality control of the material properties and geometrical and execution variables. The aim is to define and to update the statistical quantities (type of distribution, mean value, standard deviation) of these affected stochastic variables.

Quality control

If a high degree of quality control can be documented and quantified it serves as a basis for documenting service live. In this way the updating of the statistical quantities by reducing the coefficient of variation will result in the possibility to consider lower partial factors. The combined set of problems to be considered can be summarised as follows:

- The actual information on the aggressiveness of the environment, the characteristics of the materials in the structure, and the structure-environment interaction, is uncertain.
- The degree of uncertainty depends on the type and direct relevance of the available data on the above variables.
- The reliability of the available information is different depending on the stage being considered, such as the design stage, the construction stage, the handing over stage, and the period of use.
- From a durability design point of view this means that design input data with different levels of reliability must be used at the different stages.

Compliance Tests

Compliance tests are meant to measure in the laboratory the potential quality of the defined concrete composition (type of binder, binder content, and water-cement ratio) under standardised conditions. By means of this the quality of the concrete can be checked against the design requirements.

Quality control (QC) in the sense of a service life design is mainly to control the variation of the material parameters and the geometrical variables at the different stages of the construction process. For concrete the quality control can be based on cement or concrete properties on basis of compliance tests to measure the relevant quality of the cement or the concrete under standardised conditions.

The test results may serve as input for the designer in the design situation. The concrete producer can classify the potential material resistance against degradation, measuring for example the following quality controlled material parameters:

- Carbonation: carbonation penetration coefficient D_{eff}
- Chloride ingress: chloride diffusion coefficient, $D_{RCM,o}$
- Corrosion resistance: electrical resistivity, ρ_o.

In the DuraCrete project is, for example, a compliance test introduced for the chloride diffusion coefficient. The test is named Rapid Chloride Migration Test (RCM-test). This test has been developed at Chalmers University in Sweden [8, 9]. The test set-up is given in Figure 6.

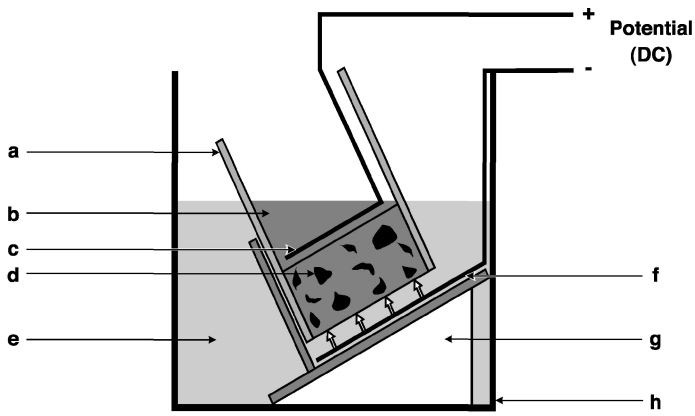

a: rubber sleeve
b: solution of 0,2 M KOH
c: anode (stainless steel)
d: concrete specimen
e: solution of 3-10 % NaCl in 0,2 M KOH
f: cathode (stainless steel)
g: plastic support
h: container

Figure 6 Test set-up for the RCM-test

Beyond the compliance testing, the quality level achieved in the laboratory should be reached on the construction site as well, since the quality of the built-in material determines the service life of the construction. The continuous examination of the material variable $D_{Cl,0}$ cannot be undertaken on the construction site without significant effort, because for the construction site this method is too complicated to perform. Research at the Technical University of Aachen (ibac) has shown [10] a good correlation between the chloride migration coefficient $D_{RCM,0}$ and the electrolytic resistivity of concrete $\rho_{WER,0}$ (see Figure 7) undertaken with the so-called WENNER-probe. How to execute the WENNER method is described in detail in [11]. Considering this aspect, the material resistance towards a chloride penetration can be verified indirectly on the construction site by an examination of electrolytic resistivity of the concrete.

Finally, verification tests are needed to determine the actual quality of the concrete in the structure in service. The actual resistance of the concrete to premature degradation is influenced by execution (compaction, curing) and micro environment.

Another important issue is the measurement of the actual concrete cover (x_c) during construction. Obvious it should be clear that the measured performance of x_c is equal to the required performance of x_c.

Similar to the classification system used in structural design (for example the concrete strength classes) the durability design can be based on durability classes of concrete which corresponds to specified values (characteristic values) with regard to the carbonation rate, the chloride diffusion coefficient and the electric resistivity.

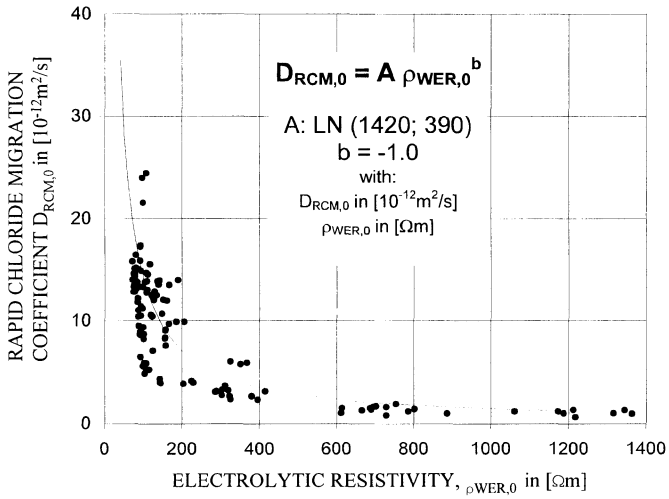

Figure 7 Relationship between $D_{RCM,0}$ and $\rho_{WER,0}$

CONCLUDING REMARKS

The existing codes are not sufficient for specifying service life in terms of performance and reliability. A performance based service life design requires limit states, a reference period and degradation models. These items are not included in the codes nowadays. But developments are ongoing.

The DuraCrete service life design method is based on the same principles and framework as the performance based structural design. It is based on terms as performances, limit states, reliability and reference period or design service life. It may be expected that this approach will be the general basis for service life design of concrete structures in the future.

The service life design method comprises a system of compliance test methods and in situ testing methods that are the bases for the quality control process. To give the service life design method a firmer basis for application in practice it will be necessary that the design method and testing methods is standardised.

Further development of the design method and practical experience are a sound base for improving codes, measurements, testing and standardisation related to durability and maintenance. Defining the limit states, degradations, environmental conditions and gaining experience with relevant testing are things to be done now and in the near future. This work will be the basis of a situation in which the new design approach is well accepted and can be used in common practice.

The design method gives an (future) owner of a structure the opportunity to incorporate specific requirements with respect to durability in the contract. On the other side of the contract, the contractor has tools within range to control durability during design and construction. This combination gives a strong basis for mutual understanding and confidence. At the end a structure has been build that meets the expectations of the owner.

REFERENCES

1. SIEMES, T., DE VRIES H., Service Life Design of a Bored Tunnel Made of Reinforce Concrete, 5th CAMET/ACI International Conference on Durability of Concrete, Barcelona Spain, 2000, pp 663 – 676.

2. SIEMES, T., EDVARDSEN, C., Duracrete Service Life Design for Concrete Structures - A Basis for Durability of Other Building Materials and Components, 8DBMC, 1999.

3. BREITENBÜCHER, R., GEHLEN, C., SCHIEβL, P., HOONAARD, J.V.D., SIEMES, T., Service life design for the Western Scheldt Tunnel, 8th International Conference on Durability of Building Materials and Components, Vancouver Canada, 1999, pp 3 –15.

4. SIEMES, A.J.M., New developments towards a performance based durability design for concrete structures; Symposium Advanced Design of Concrete Structures, Götenborg; Uitg. Chalmers University S, June 1997, pp. 138 –148.

5. CEB/FIP Model Code for Concrete Structures, Recommendation of FIP and CEB, 1990.

6. BE-1347/TG7/.Report R14 "General Guidelines for Durability Design and Redesign", Bruxelles: Brite-Euram, Project No. BE95-1347, 1999.

7. SIEMES A.J.M., ROSTAM, S., Durable safety and serviceability a performance based design format, IABSE report 74: IABSE colloquium 'Basis of design and Actions on Structures Background and Application of Eurocode 1, Delft, 1996, pp. 41-50.

8. TANG, L., NILSSON, L.-O., Rapid determination of chloride diffusivity of concrete by applying an electric field, ACI Materials Journal 49(1), 1992,pp 49-53.

9. NILSSON, L.O., POULSEN, E., SANDBERG, P., SORENSEN, H.E., KINGHOFFER, O., Chloride penetration into concrete, Hetek Raport 53, The Road Directorate, Denmark, 1996.

10. BREIT, W., Untersuchungen zum kritischen korrosionsauslösenden Chloridgehalt für Stahl in Beton. Schriftenreihe Aachener Beiträge zur Bauforschung, Institut für Bauforschung der RWTH Aachen, Nr. 8, Aachen. Technische Hochschule, Dissertation, 1997.

11. GEHLEN, C.; LUDWIG, H.M., Compliance Testing for Probabilistic Design Purposes : Bruxelles: Brite-Euram, Project No. BE95-1347, 1999, report R8, 114 pp.

THEME ONE:

CHEMICALLY AND PHYSICALLY AGGRESSIVE ENVIRONMENTS

Keynote Paper

EXPERIMENTAL AND NUMERICAL MODELLING OF CORROSION IN REINFORCED CONCRETE

M Brem

H Böhni

Swiss Federal Institute of Technology Zurich

Switzerland

ABSTRACT. The rate of localized corrosion of steel in concrete depends on various concrete and environmental parameters. The concrete humidity, the temperature and the ratio of anode to cathode areas are of primary importance. This paper presents the numerical modelling of corrosion in reinforced concrete performed by means of commercial software for boundary element method analysis. With the numerical simulation, it is possible to calculate the potential and the current density in every point of the electrolyte boundary. The results of the simulation can be used to study the influence of different parameters on the corrosion rate by varying the input data or the geometry of the system. It is also possible to predict corrosion rates. The influences of the environment, as well as changes in temperature and humidity can be taken into consideration by selecting the appropriate conductivity values and polarisation curves.

The measurement of polarisation curves in mortar and concrete and the electrolytic resistivity as the basic input data for the numerical simulation is described. The results of the numerical simulation are compared with experimental data measured within a large reinforced concrete element.

Keywords: Steel corrosion, Reinforced concrete, Polarisation curve, Numerical modelling.

Dr M Brem, is a Research Assistant at the Department for Civil, Environmental and Geomatic Engineering, Swiss Federal Institute of Technology (ETH), Zurich, Switzerland. He specialises in corrosion mechanisms of reinforcing steel in concrete, electrochemical techniques for corrosion measurement and numerical modelling of corrosion phenomena.

Professor H Böhni, is full Professor at the Department for Civil, Environmental and Geomatic Engineering, Swiss Federal Institute of Technology (ETH), Zurich, Switzerland. His main research areas are: Corrosion and corrosion protection of metals as well as of steel in concrete, electrochemistry and electrochemical techniques on a micro– and macrometer scale.

INTRODUCTION

The corrosion of reinforcing steel bars in concrete has caused serious damage to a vast number of concrete structures. The reinforcing steel is embedded in the concrete which initially provides an alkaline environment. Under these conditions the steel is protected by surface passivation and metal dissolution takes place at an extremely low rate. However, depassivation of the steel surface can take place due to chloride ingress from deicing salts or sea water. While chloride induced corrosion is of principal interest here, it should be noted that as a result of exposure to atmospheric carbon dioxide, concrete carbonation reactions leading to corrosion are also possible.

Chloride induced corrosion is characterised by a localized depassivation of the reinforcement. The coexistence of small corroding (active) steel areas and large passive steel areas form a short-circuited galvanic element with a high corrosion rate of the active area. This leads to a loss in cross section at the active areas of the reinforcing steel bars. Galvanic corrosion takes place as a result of electrical contact of two pieces of metals with different steady state potentials E_{corr} in an ion conducting corrosive environment. The more noble metal is acting as a cathode where an oxidising species is reduced, the more active metal is acting as the anode of the galvanic couple. The driving force for galvanic corrosion is the difference in potential U_{0c} between the anodic and cathodic sites. The electrochemical interaction between areas of steel with different steady state potentials can be explained graphically by superposing the polarisation curves for the individual anodic and cathodic components of the macro corrosion cell on the same graph [1]. For the simple case of a two component galvanic cell, this situation can be shown in an Evans diagram (Figure 1).

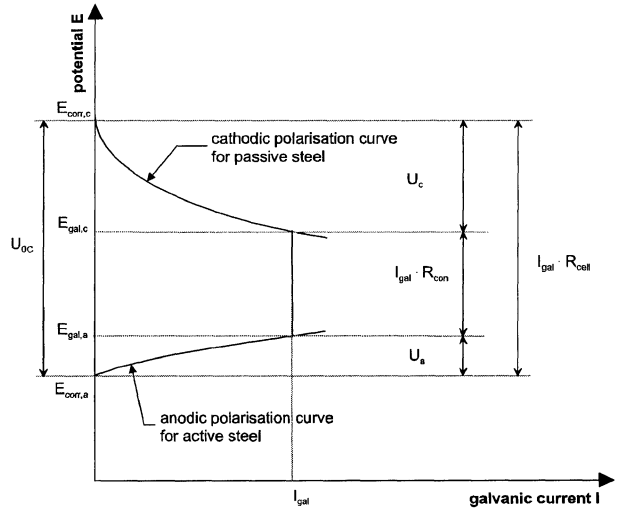

Figure 1 Evans diagram

Nomenclature:

I_{gal}	galvanic current
U_{0C}	driving voltage
$E_{corr,a}$	anodic steady state corrosion potential

$E_{corr,c}$	cathodic steady state corrosion potential
$E_{gal,a}$	potential of the anodic steel area
$E_{gal,c}$	potential of the cathodic steel area
R_{cell}	macrocell resistance
U_a	anodic polarisation
U_c	cathodic polarisation
R_{con}	concrete resistance (electrolyte)

The potential difference U_{0C} can be divided into three parts: the potential drop on the anodic steel surface U_a, the potential drop on the cathodic steel surface U_c, and the potential drop in the electrolyte $I_{gal} * R_{con}$. For galvanic cells in concrete the potential drop in the concrete (electrolyte) may have a large value. In this case the galvanic current is controlled by the electrolyte resistance.

Most macro cells however are more complex as they usually involve a multicomponent macro cell [2]. The resulting galvanic interaction between the reinforcement bars can then be studied only by a numerical analysis which takes into account the electrochemical behaviour of the steel bars and the distribution of concrete resistivity as well as the spatial arrangement of the steel within the structural element.

Numerical modelling of macro cell corrosion has recently received considerable attention for its potential applications in predicting corrosion rates of steel in concrete. Numerical methods can be used to obtain current distributions for geometrically complex corrosion cells. Accurate results from numerical modelling are obtained, if the input data for the mathematical models are representing the electrochemical reactions taking place in real concrete structures. In the past, finite difference, finite element and boundary element methods have been applied to reinforcing steel corrosion and related problems [3-7]. The boundary element method (BEM) is an important technique in the computational solution of a number of scientific or engineering problems. In common with the better-known finite element method and finite difference method, the boundary element method is essentially a method for solving partial differential equations.

The boundary element method has the important advantage that only the boundary, the domain of interest, requires discretisation by elements. Hence the computational advantages of the BEM over other methods can be considerable.

EXPERIMENTAL

Cathodic polarisation curves

The cathodic reaction kinetics of embedded steel in mortar and concrete, were studied with potentiodynamic polarisation measurements. The mortar and concrete samples were cured for 7 days in the formwork at 80% relative humidity and subsequently exposed to different relative humidities. For all the specimens the mixture given in Table 1 was used.

Common reinforcement steel was used for the investigations. The chemical composition is given in Table 2. Before embedding the steel bars were degreased with ethanol.

Table 1 Mortar and concrete mix (w/c 0.5)

	MORTAR	CONCRETE
Water	226	170
Cement CEM I 42.5	453	340
Sand 0-1 mm	793	465
Sand 1-4 mm	793	465
Sand 4-8 mm	-	390.6
Sand 8-16 mm	-	539.4

Table 2 Chemical composition of mild steel

C	Si	Mn	P	S	Cr	Mo	Ni	Al	Cu	Nb
0.15	0.17	0.59	0.012	0.043	0.09	0.02	0.12	.002	0.45	.001

The measurement of the cathodic polarisation curves was performed with cylindrical mortar and concrete samples (Figure 2). The steel sample was mounted in the centre. The counter electrode consisted of a stainless steel grid. A gold plated brass wire was positioned on the steel surface serving as reference electrode. The reference electrode was calibrated against a saturated calomel electrode (SCE).

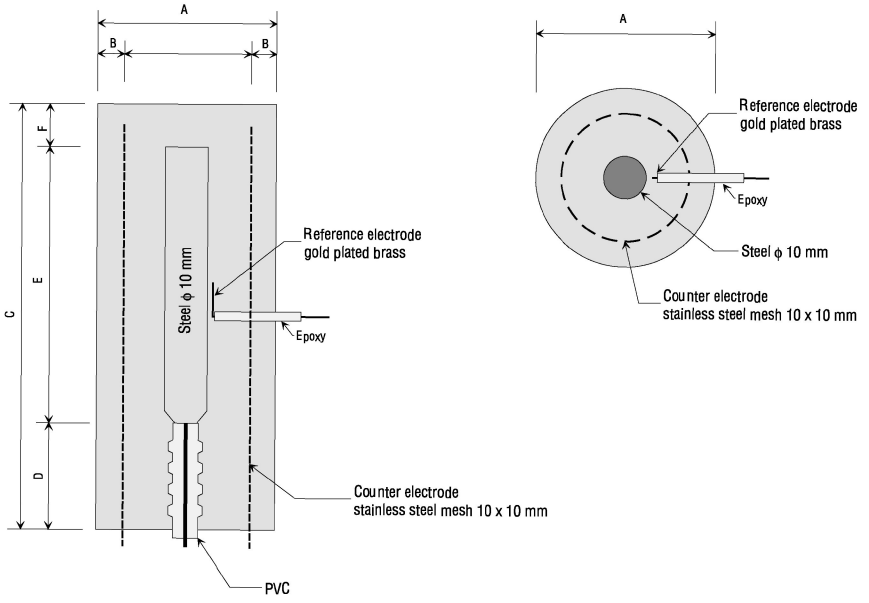

Figure 2 Specimen for cathodic polarisation measurement
The dimensions are specified in Table 2

Table 3 Dimensions of mortar and concrete specimens

	MORTAR	CONCRETE
A	42 mm	170 mm
B	6 mm	35 mm
C	100 mm	125 mm
D	25 mm	25 mm
E	65 mm	65 mm
F	10 mm	35 mm

The mortar and concrete samples were exposed to the relative humidities of 45, 66, 76, and 93 %. All the potentiodynamic measurements started at the open circuit potential with a scan rate of 1 mV/s. The reported potentials are always in respect to a saturated calomel electrode and the ohmic potential drop has been corrected. The measurement was repeated every month in order to study time dependence. The weight of the specimens was also recorded for verifying if equilibrium of humidity had been reached.

Corrosion Current Measurement

A three dimensional macro cell arrangement was prepared. A small steel bar (Ø10mm, length 20mm) was embedded in mortar containing sodium chloride (3% of cement weight). For the adjacent steel bars a stainless steel (DIN 1.4301) was used to prevent activation of these steel sections. The steel bars were heated for 10 minutes up to 700°C. This treatment forms a passive film that has similar electrochemical properties as mild steel [8]. Figure 3 shows the anodic part of the macro cell with the wires for making electrical contact.

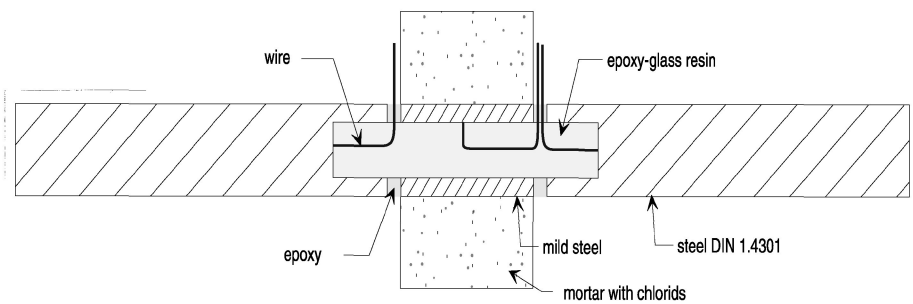

Figure 3 Sketch of activated steel area

A schematic drawing of the whole macro cell is given in Figure 4. The steel bars had a length of 960 mm. Each bar was electrically isolated and had a wire to connect it to the measuring instrument. This made it possible to change the cathodic steel area by disconnecting the steel bars. The galvanic current was measured with a zero resistance ammeter and recorded on a personal computer. Measurements were taken after 1 month exposure to 45% relative humidity. Before and after the current measurements the concrete resistance between the upper two steel layers and the lower two steel layers was measured with a LCR meter at 1 kHz.

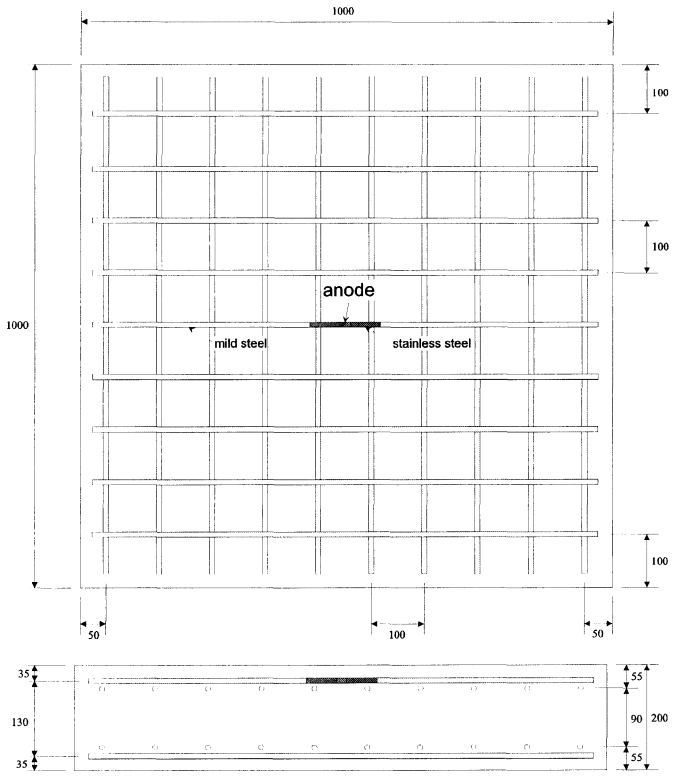

Figure 4 Three-dimensional macro cell for corrosion current measurement [mm]

RESULTS

Cathodic Polarisation Curves

Figure 5 shows the measured cathodic polarisation curves of the mortar specimens that were exposed to different relative humidities for six months. During the measurements the concrete resistance between the counter electrode and the embedded steel was measured. From the measured resistance the specific concrete resistance was calculated with the values obtained from a calibration of the specimen geometry. The curves show a clear dependence of concrete resistance on the cathode kinetics. The sample exposed to 93% relative humidity has a different behaviour for over-potentials up to 500 mV. Even though the concrete resistance is smaller the current density is lower than at the curves measured at 76 and 66%.

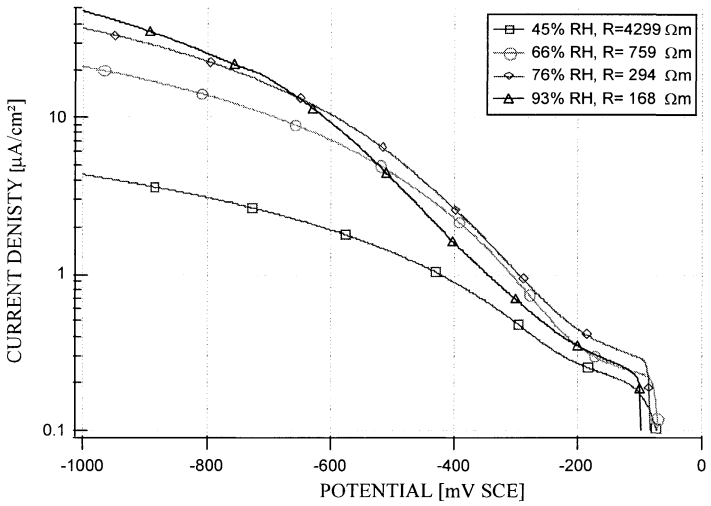

Figure 5 Cathodic polarisation curves of mild steel in mortar after six months storage in different relative humidity

For large over-potentials the increase of oxygen reduction current densities levels out versus a limiting current. Compared to investigations in synthetic pore solution [9] a clearly limiting current was not found. This levelling out at large over-potentials can not be explained solely by oxygen diffusion processes since it was also observed in very dry conditions. Figure 6 shows the cathodic polarisation curves of the specimen exposed to 45 % relative humidity. With increasing curing time the polarisation curve decreases and the concrete resistance rises. After six months, equilibrium of concrete humidity has still not been reached.

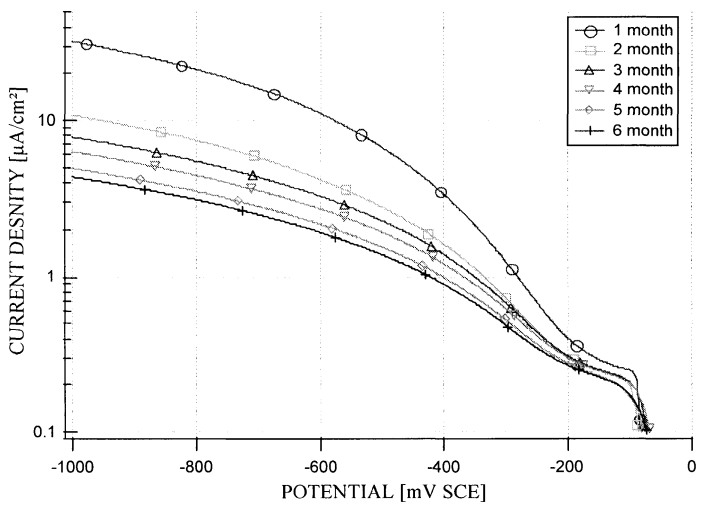

Figure 6 Cathodic polarisation curve of mild steel in mortar exposed To 45 % relative humidity

Figure 7 shows the cathodic polarisation curves of concrete and mortar measured after having been exposed to 45% relative humidity for one month. Because of different cover depths of the embedded steel the curves can only be compared qualitatively. The mortar specimen dries faster than the concrete specimen and the conditions on the steel surface might not be the same. However, the polarisation curves do not show a significant difference and for general considerations cathodic kinetics of steel in concrete and mortar need not to be strictly distinguished.

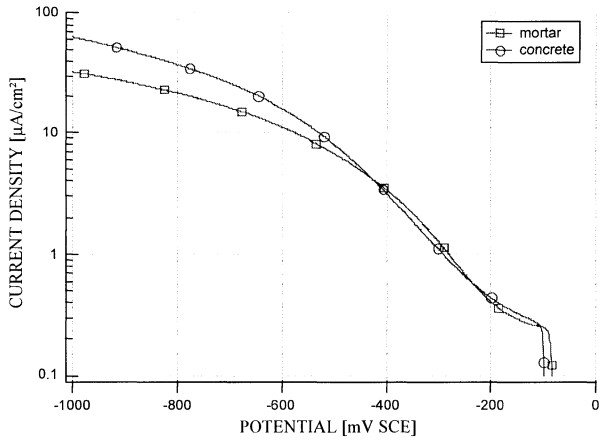

Figure 7 Comparison of cathodic polarisation curves of mild steel measured in mortar and concrete after one month of exposure to 45% relative humidity

Macrocell Current

The galvanic current measured between anode and cathode of the concrete element (Figure 4) is shown in Figure 8. First the total macrocell was measured. In a next step the bars in the layer furthermost of the anode were separated from the anode. Then the next layer was disconnected. Table 4 shows the corresponding cathodes and the ratio of cathode to anode area for the numbers in Figure 8. At the end of the measurement the total macro cell was measured once again.

Table 4 Arrangement of contacted cathodic areas

NUMBER	CATHODE	A_c/A_a
1	4 layers	1823
2	3 layers	1391
3	2 layers	911
4	1 layer all bars	431
5	1 layer 7 bars	335
6	1 layer 5 bars	239
7	1 layer 3 bars	143
8	1 layer 1 bar	47
9	1 layer 1 bar 600 mm length	30

The galvanic current decreases with decreasing cathode area. In addition to this effect a decrease of galvanic current is caused by increase of concrete resistance. The measured concrete resistance before current measurement and thereafter was 70.5 Ωm and 73.6 Ωm respectively.

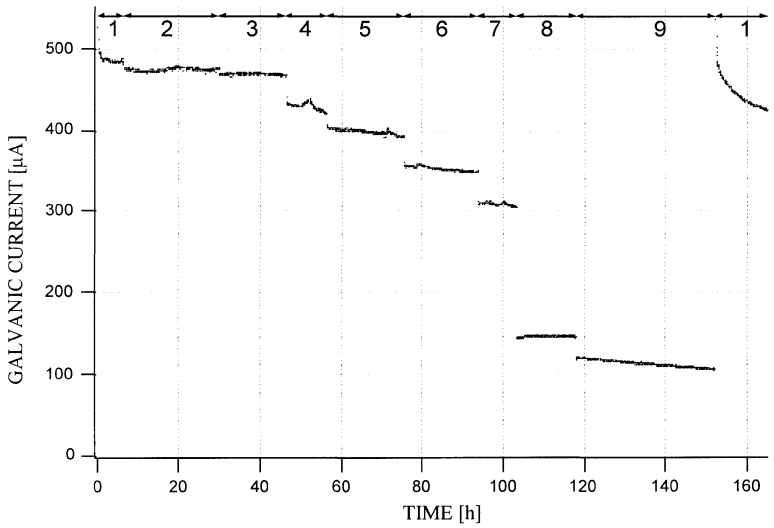

Figure 8 Galvanic current in the concrete element after one month of exposure to 45% r.H

NUMERICAL SIMULATION

Numerical Model and Input Values

The numerical simulation was carried out with the BEASY 8.0 software by Computational Mechanics. This boundary element program uses the anodic and the cathodic polarisation curves and the concrete conductivity as input values. A numerical model of the measured macro cell was generated. Because of the symmetric arrangement of the sample only one quarter of the concrete element had to be modelled. The measured mortar resistivity was converted into the concrete conductivity. For the anodic polarisation curve the values of a dynamic polarisation measurement of steel in 0.1 M HCl was used [10]. For the cathodic polarisation curves the results of the measurements described in the first section of this work were used. The concrete resistivity was assumed to be homogeneous over the entire concrete element.

Results of Numerical Simulation

The change of cathodic area was modelled in the same way as described for the current measurement. For each geometric arrangement (except Number 9 in Table 4) a simulation was performed. For the cathodic polarisation curve the measured curve in concrete after one month was used (Figure 7).

Figure 9 shows the comparison of measured and calculated values.

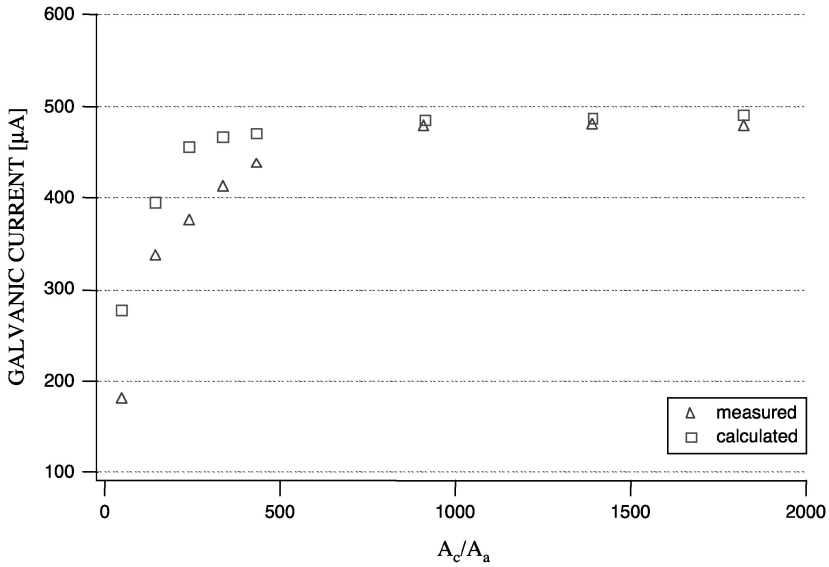

Figure 9 Comparison of calculated and measured galvanic current in the concrete element after one month exposure to 45% r.H

A good agreement between experimental and calculated values was found. The first five values (all in layer 1) show a deviation between experiment and calculation. The reason for this could be a change of concrete resistivity in the outer part of the concrete element. This had not been taken into account for the numerical simulation.

In a second simulation the galvanic current and the current distribution was calculated for the cathodic polarisation curves shown in Figure 5. For one set of simulations the polarisation curves and the resistivity were changed. For the second set of simulations the polarisation curve measured at 93% relative humidity was taken and only the resistance was changed.

Figure 10 shows the dependence of galvanic current on concrete resistance. The deviation of the two sets of calculation is small. This means that for this geometric arrangement the galvanic corrosion current is controlled mainly by the concrete resistance.

For the calculations shown in Figure 10 the current distribution was also calculated. Figure 11 shows the integration of the current flowing through the cathodic steel area in dependence on the horizontal distance from the anode centre.

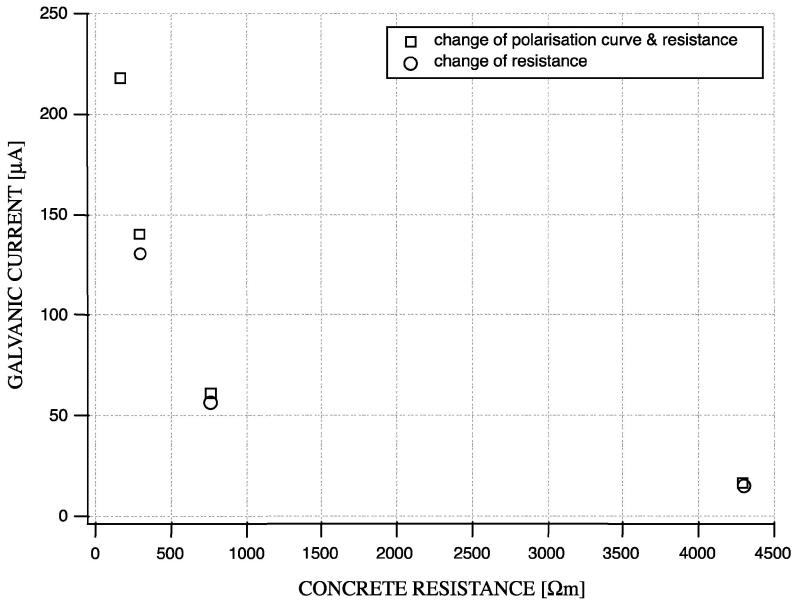

Figure 10 Influence of concrete resistance and cathode kinetics

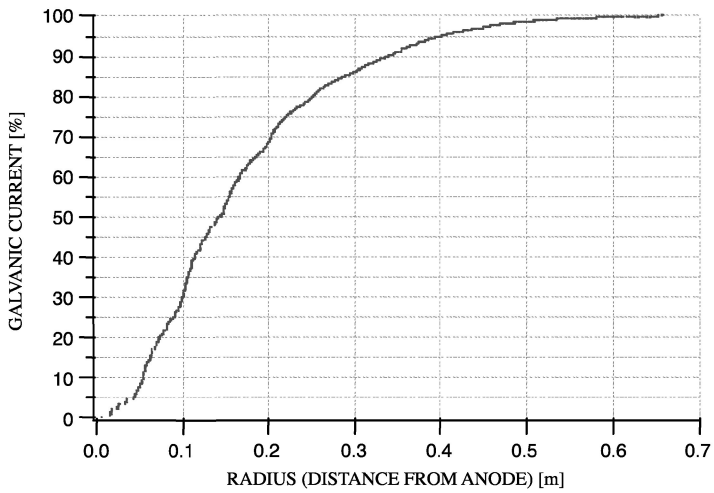

Figure 11 Current distribution (polarisation curve of 93% r.H., 168Ωm)

In Table 5 the values of the radius where 50, 75 and 95% of the total current was reached are given for the calculations shown in Figure 10. In the description in column 1, R,P means that the resistance and the polarisation curve was changed. R means that only the resistance was changed.

Table 5 Propagation of macro cell

SIMULATION	RADIUS 50% [m]	RADIUS 75% [m]	RADIUS 95% [m]
93% rh, R,P	0.145	0.221	0.401
76% rh, R,P	0.151	0.371	0.584
76% rh, R	0.126	0.231	0.527
66% rh, R,P	0.113	0.272	0.497
66% rh, R	0.149	0.396	0.529
45% rh, R,P	0.109	0.307	0.488
45% rh, R	0.327	0.419	0.517

CONCLUSIONS

- From the laboratory study on the cathodic kinetics of steel in mortar it can be concluded that the oxygen reduction on passive steel shows a strong dependency on mortar humidity.

- A good agreement between numerical modelling with the boundary element program and the experimental results was found. The numerical simulation shows that the current distribution in a realistic macro cell has a high complexity.

- For the investigated macro cell arrangement the concrete resistance has a major influence on the galvanic current. A macro cell propagation of about 0.5 meters was found.

- The macro cell propagation is influenced by different parameters. A more detailed study on the interaction of polarisation and concrete resistance could provide more insights. Further investigations are necessary to understand the behaviour of macro cell corrosion in concrete structures.

REFERENCES

1. EVANS, U R, An introduction to metallic corrosion, Edward Arnold LTD, London, 1963, p 294.

2. GULIKERS, J, SCHLANGEN, E, Numerical analysis of galvanic interaction in reinforcement corrosion, Corrosion of Reinforcement in Concrete Construction, The Royal Society of Chemistry, 1996, p 3 - 12.

3. KRANC, S C, SAGÜES, A A, Detailed modelling of corrosion macrocells on steel reinforcing in concrete, Corrosion Science, 2001, Vol 43, No 7, p 1355-1372.

4. JÄGGI, S, BÖHNI, H, ELSENER, B, Macrocell corrosion of steel in concrete - experiments and numerical modelling, Proceedings of Eurocorr 2001, Riva di Garda, Italy, Associzione Italiana Metallurgia (AIM), Milano, 2001.

5. MIYASAKA, M, et al, A boundary element analysis on galvanic corrosion problems - computational accuracy on galvanic fields with screen plates, Corrosion Science, 1990, Vol 30, No 2-3, p 299-311.

6. KORETSKY, M.D, ABOOAMERI, F, WESTALL, J C, Effect of concrete pore saturation on cathodic protection of steel-reinforced concrete bridges, Corrosion, 1999, Vol 55, No 1, p 52-64.

7. BALABANIC, G, BICANIC, N, DUREKOVIC, A, Numerical analysis of corrosion cell in concrete, Engineering Modelling, 1995, Vol 8, p 1-5.

8. BERTOLINI, L, et al, Experiences on stainless steel behaviour in reinforced concrete, Proceedings of Eurocorr 98, Utrecht, Netherland, 1998.

9. JÄGGI, S, ELSENER, B, BÖHNI, H, Oxygen reduction on mild steel and stainless steel in alkaline solutions, Corrosion of Reinforcement in Concrete: Corrosion Mechanisms and Corrosion Protection, Papers from Eurocorr 99, European Federation of Corrosion, London, 2000, Vol 31, p 3-12.

10. JÄGGI, S, Experimentelle und numerische modellierung der lokalen korrosion von Stahl in beton unter besonderer berücksichtigung der temperaturabhängigkeit, Thesis Nr.14058, Eidgenössische Technische Hochschule, Zürich, p. 136.

DETERIORATION OF LONG SERVING CEMENT BASED SANDCRETE STRUCTURES IN NIGERIA

J O Odigure
Federal University of Technology
Nigeria

ABSTRACT. The fall in standard of the Nigerian economy, starting from the mid 1980s, has encouraged massive import of second hand goods, most especially industrial machines, cars, motorcycles, etc. It is a well-known fact that the majority of these are very inefficient and produce lot of pollutants (Cl^-, SO_2, CO_2, CO, N_xO_y, etc) particularly as a result of incomplete fuel combustion. The presence of these pollutants has contributed not only to the depreciation of the peoples' quality of life but also to the degradation of cement based structures' physio-chemical, mechanical and aesthetic qualities. This paper is aimed at developing a deterministic model, based on a mechanism of cement corrosion, to predict the deterioration of cement-based structures in Nigeria. The deterministic model equation developed is only used for a given depth of the sandcrete block. It does not represent the relationship between the concentration of pollutant C_A and depth of penetration in the entire block volume. Variation in the type of pollutant and possible reaction, including leaching must also be considered in order to develop a more generic model.

Keyword: Sandcrete, Deterioration, Pollutants, Modeling.

Dr J O Odigure is a Senior Lecturer and Head of Department of the Chemical Engineering Department, Federal University of Technology, Minna, Nigeria. He specializes in chemical technology of binding materials and refractories non-metallic materials. He is interested in environmental pollution and protection. He has published widely and written two books.

INTRODUCTION

The compressive strength of cement-based structures is expected to increase steadily with age [1]. However, this statement may not be true for many structures especially those serving in aggressive environments. In some areas, most cement-based structures were found to develop micro cracks within few years after construction, despite the fact that acceptable standards were observed. It has been proved by various researchers that long exposure of cement based structures to aggressive medium containing acids, alkalis and salts immensely enhance their physico-chemical and mechanical properties deterioration [1].

Results of various researchers have shown that the weak point in hardened cement microstructure remains the presence in it of soluble and reactive $Ca(OH)_2$ [2]. Much work has been done in investigating the mechanism of various destructive processes responsible for cement based structure deterioration [2-4]. In his work Moskivic formulated the basic points for developing the theory of cement based structure deterioration [2]. It was established that in order to qualitatively assess the kinetics of corrosion process, it is necessary to study the internal diffusion of an aggressive substance, the formation on the cement based structure surface layer of the reaction products, crystallization of corrosive components and products of their interaction with hardened cement minerals in the voids and other processes.

This paper is aimed at developing a deterministic model based on the mechanism of cement corrosion, to predict the deterioration of cement-based sandcrete commonly used as building material in Nigeria.

MATHEMATICAL MODELLING

Diffusion of Pollutants into Sandcrete Structures

The sandcrete block consists of a mixture of cement and coarse sand mixed with water to obtain a normal consistency. The mix is then poured into form and vibrated. Sandcrete structure may have porosity of more than 25% depending on the extent of vibration. The sandcrete block forms the major construction material in Nigeria building industry. Nigeria is a developing country. Pollution problem associated with heavy industrialization is today being experienced globally.

However, all mitigating features to combat the trend of event have all failed in the developing world as a result of these countries being converted to dumping ground for used and inefficient machinery. Today no community is free from gaseous pollutants from automobiles and motorcycles manufactured using outdated technologies. Consequently the major pollutants of our cities include products from incomplete burning of hydrocarbon fuel such as CO_2, SO_2, Cl^-, CO, NO_x, etc. The presence of these pollutants has contributed not only to the depreciation of the peoples' life quality but also to the degradation of cement based structures physico-chemical, mechanical and aesthetic qualities [1].

These pollutants affect the properties of cement-based structures only when they are in direct contact. This is possible through adsorption and diffusion of these pollutants into the structure's matrix. Therefore the rate of the pollutants' diffusion into the matrix will determine to a great extent the longevity of the cement-based structure. This is the focus of this research with particular reference to long serving sandcrete structures in Nigeria.

Basic Assumptions

The following assumptions were made to facilitate the derivation of the deterministic model equation.

1. The cement block is well compacted and therefore available inter pore space is spherical.
2. The Fick's law holds for the diffusion mechanism.
3. The product of the chemical reaction is retained on the surface of the particles in a monomolecular layer.
4. Diffusion is predominantly in one direction of gas flow, except for particles at the edges.
5. The pollutant gases obey the general gas law
6. Surface flux is based on the total area of the solid particles perpendicular to the direction of diffusion.

By analogy to Fick's law, the molar rate per unit of pore surface N_s is [6-8]

$$N_s = -D_s \frac{dC_s}{dr} \quad \text{.....1}$$

where C_s = surface concentration, mole gas/m^3 [8].

For diffusion in a porous solid the surface flux $(N_s)_e$ should be based on the total area perpendicular to the direction of diffusion on the co-ordinate r:

$$(N_s)_e = -\rho_b D_e \frac{dC_A}{dr} \quad \text{.....2}$$

where D_e = effective diffusivity, per unit of the total cross sectional area, C moles adsorbed per gram solid, mole/g, ρ_b – density of the block.

The equilibrium concentration of the net rate of adsorption of gases on the solid, according to Langmuir's law can be represented as

$$C_A = K\overline{C}_m C_g \quad \text{.....3}$$

where C_A = adsorbed concentration on the solid surface, mole/g, $\overline{C}_m$ - concentration corresponding to complete monomolecular layer on the solid, C_g – concentration of adsorbable component in the gas phase; it is proportional to P, K – linear form of equilibrium constant, m^3/g.

Due to the long exposure of the sandcrete blocks under investigation, equilibrium is assumed to exist between the gas and the surface concentration. Equation 3 can be represented as

$$C_A = K_A \overline{C}_m C_g = K_A \frac{py_A}{R_g T} \quad \text{.....4}$$

Substituting Equation 4 into 2

$$(N_s)_e = -\frac{p}{R_g T} K_A D_e \rho_b \frac{dy_A}{dr} \quad \text{..... 5}$$

The total surface flux is

$$(N_s)_t = N_s + (N_s)_e \quad \text{.....6}$$

Therefore

$$(N_s)_t = -\frac{p}{R_g T}(D + \rho_b K_A D_s)\frac{dy_A}{dr} \quad \text{..... 7}$$

or

$$(N_s)_t = -(D + \rho_b K_A D_s)\frac{dC_A}{dr} \quad \text{..... 8}$$

Therefore

$$(D_e)_t = D + \rho_b K_A D_s \quad \text{..... 9}$$

The overall rate of reaction W_A of component A on the structure is

$$W_A = (N_A)_t V \quad \text{..... 10}$$

where V – volume of the structure = length x width x height (LBr).

Therefore Equation 8 becomes

$$W_A \frac{dr}{r} = -LB\,(D + \rho_b K_A D_s)dC_A \quad \text{..... 11}$$

$$W_A \int_{r=0}^{r=r} \frac{dr}{r} = LB\,(D + \rho_b K_A D_s) \int_{c=c_A}^{c=0} dC_A \quad \text{..... 12}$$

$$W_A Inr = LB\,(D + \rho_b K_A D_s)C_A \quad \text{..... 13}$$

Let LB is a constant and it was assumed that no diffusion took place except on the perpendicular surface to the direction of gas flow. In the linear form y = mx eq. 13 can be presented as

$$C_A = \frac{W_A}{D_c} Inr \quad \text{.....14}$$

taking

$$D_c = LB(D + \rho_b K_A D_s)$$

Equation 14 is the modeling equation for the research.

EXPERIMENTAL DETAILS

The samples A (20 years old) and B (15 years old) were collected from exposed long serving sandcrete blocks used for fencing at highly industrialized layouts A and B in Lagos, Nigeria. The choice of samples was based on the age of the fence and centrality of the structure in the two industrial layouts. Most industries in Nigeria use natural gas and black oil for energy generation. Consequently, the bulk components of emission from these areas are oxides of carbon. All samples were collected by drilling using a hand drilling machine, equal distance into the blocks wall used for the fence at the top, middle and ground levels. The control sample (1 day old) was collected from a block industry in Minna; about 500km north of Lagos. All samples were produced by mixing sand and cement with potable water. The mixture with moisture content of 30 – 40% is then poured into mould and compressed either manually or vibrated mechanically. Minna is a city with practically no functional large-scale industry, consequently except from automobile and the homes not many pollutants are generated. Each of the collected samples were ground in a ceramic lined mill to a fineness of about 6 – 8% residue on a 80μm size mesh. All the chemical analyses were conducted according to [9].

RESULTS AND DISCUSSION

Results of the experiments are presented in Figures 1 and 2 and Table 1. From Equation 14 C_A is directly proportional to the natural logarithm of depth of pollutant penetration, lnr. The gradient of the line so obtained will be equal to W_A/D_C. W_A for a given pollutant is calculated from the quantity of reaction product deposited in the sandcrete over the experimental period. The results of analysis of the rate of reaction for the various pollutants are presented in Tables 2 and 3.

Table 1 Average concentration of $Ca(OH)_2$ at different depths

DEPTH r, mm	SAMPLE CONCENTRATION g/l x10^{-2}		
	Control	A	B
0.9	9.3	8.0	7.7
10.0	10.4	8.3	7.8
20.0	10.7	8.5	7.9

The CO_2, SO_2 and Cl^- were the pollutants investigated in this paper. Analysis, based on the quantity of deposition of the rate of penetration showed that the CO_2 and Cl^- were more likely to be introduced to sandcrete blocks than SO_2 (Figures 1 and 2 and Table 2). The concentration of CO_3^{2-} and Cl^- in the block increased by 3 – 10.5 and 1 –2 times respectively over a 15 – 20 years period. The significant disparity in the CO_3^{2-} concentration maybe connected to the conversion of the insoluble $CaCO_3$ to soluble $Ca(HCO_3)$ and its subsequent leaching [2-4). The concentration of SO_3 increased by 1.6 – 6.5 times for sample A and 2.3 – 6.0 times for B in comparison to the control sample. The $Ca(OH)_2$ concentration during this 15 – 20 years decreased only by about 1.4 times for B and 1.3 for A.

The mechanism of cement mineral hydration showed that the extent of hydration tends to 1 after many years [10]; with only about 60% extent of hydration attained after 180 days even for fast hydrating cement [11]. The free $Ca(OH)_2$ is continuously utilized through various reactions such as in presence of SO_3, or CO_2 or Cl^- and water to produce gypsum, $CaCO_3$, $Ca(HCO_3)_2$ and $CaCl_2$ respectively. In presence of active SiO_2, $Ca(OH)_2$ will react to produce various solid solution of C-S-H [11]. The porous nature of sandcrete block ensures that the increased volume experienced as increased stress during the formation of ettringite in the course of the reaction involving $CaSO_4.2H_2O$ and calcium aluminate/ferrite hydrates is completely adsorbed. Unlike SO_2 pollutant and sometimes CO_2, Cl^- will always lead to increased porosity of the structure as the resultant soluble $CaCl_2$ or unstable monochloroaluminates can be easily removed via leaching.

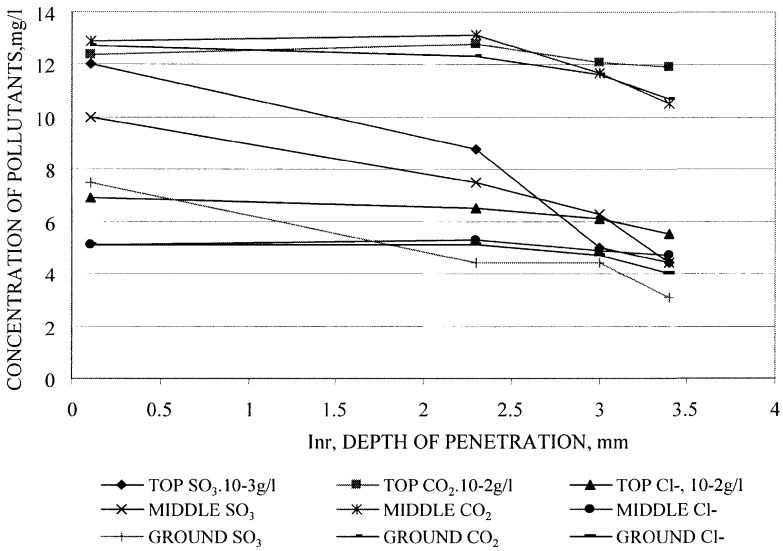

Figure 1 Concentration of pollutants versus depth of penetration in Site A

Analysis of Table 2 showed that the rate of all the pollutants investigated is higher at the outer surface. There is no linear relationship between the rate of reaction and the depth of the pollutants' penetration. The rate of deposition of CO_2 in the sandcrete block was the highest irrespective of the depth or age of the samples. The CO_3^{2-} was fairly well distributed in all the depth investigated; with 4 – 25% variation between the outer and the inner layers. It is followed by SO_3, however the extent of variation was relatively high; 37 to 57%. The extent of variation for Cl^- was the least. The difference in the various rates of reactions involving SO_2, Cl_2 and CO_2 for samples A and B, showed that the observed $Ca(OH)_2$ content (Table 1) could not have been the products of the primary reactions of cement minerals hydration [10, 11]. Their continuous presence is the resultant of various secondary reactions involving the cement minerals' hydrates and pollutants introduced into the sandcrete block.

Analysis of the diffusivities coefficients, D, mm/hr (Table 3) showed that SO_2 has the least value. The (-) sign indicates that the resultant product is being accumulated on the particular

depth. Except for CO_3^{2-}, no other resultant product of the pollutants' reactions with $Ca(OH)_2$ was accumulated on the outer surface of the sandcrete block. The outer layer diffusivity coefficients for all the pollutants investigated were for most cases, higher than those of the interior. However, the observed disparities of D values between layers' depth might be connected with the non-uniform rates of leaching of the reaction products and the resultant exposure of the cement minerals hydrates surfaces.

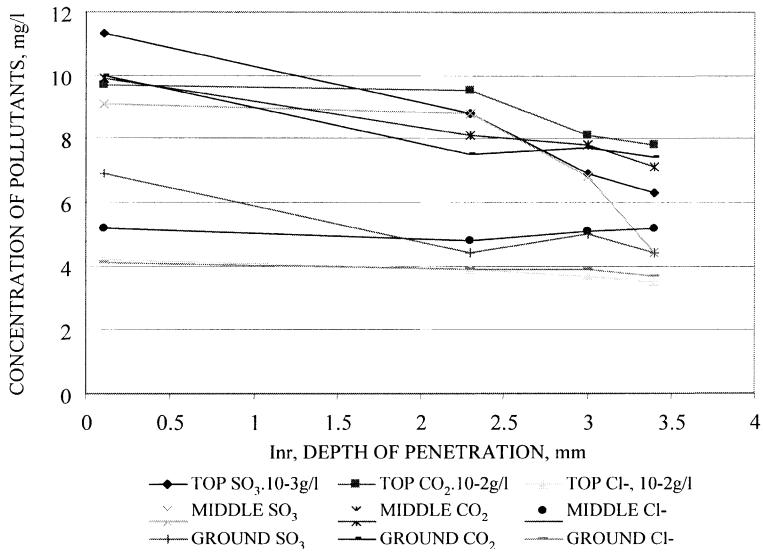

Figure 2 Concentration of pollutants versus depth of penetration in Site B

Among the pollutants investigated SO_2 has the least D values, however the high porosity of the sandcrete block structure coupled with the small percentage concentration in the mix, made its degrading effect very minimal. The degrading effect of CO_2 was enhanced by its relative abundance in the atmosphere.

The deposition of $CaCO_3$ on the outer surface of sandcrete block reduces the penetration of CO_2 into the structure. The non uniformity in the D values with increasing depth could be attributed to inconsistency in the diffusion of pollutant and the transformation of the resultant reaction product $CaCO_3$ to $Ca(HCO_3)_2$ and the possible leaching from the structure.

Chloride (Cl^-) showed serious inconsistencies in the D values. This could be attributed to the relative ease with which the product of C-S-H and Cl^- reaction is leached from the structure. In general it is difficult to establish the overall pollutants' D values in sandcrete structure, based on the evaluated data (Table 3).

The type of pollutant and its product of reaction with cement minerals, the rate of leaching of these products, influence the overall D value.

Table 2 Rate of various pollutants' deposition in sandcrete block

DEPTH, r, mm	RATE OF SO_3 DEPOSITION, . g/l/hr x 10^{-9} at depths, for samples from sites A and B					
	Top		Middle		Ground	
0.9	69	87	59	72	44	53
10.0	50	67	43	67	25	33
20.0	28	53	36	48	25	38
30.0	25	48	25	33	17	33
	RATE OF CO_2 DEPOSITION, g/l/hr x 10^{-8} at depths, for samples from sites A and B					
0.9	72	75	75	76	73	77
10.0	74	73	76	63	71	73
20.0	70	63	68	60	67	59
30.0	69	60	61	55	62	57
	RATE OF Cl^- DEPOSITION, g/l/hr x 10^{-8} at depths for samples from sites A and B					
0.9	40	49	3.0	40	30	32
10.0	38	46	3.1	37	30	30
20.0	35	46	2.8	39	27	30
30.0	32	45	2.7	40	23	29

Table 3 Diffusivities coefficients of pollutants in samples at different depths

DEPTH, mm	DIFFUSIVITY OF SO_3, 10^{-6} mm/hr at depths, for samples from Sites A and B					
	Top		Middle		Ground	
	A	B	A	B	A	B
0.9 –10	14.3	19.2	10.0	24.0	19.2	25.0
10 – 20	4.05	5.16	4.09	6.64	*	*
20 – 30	0.17	3.3	2.31	2.5	2.46	3.3
	CO_2					
0.9 –10	*	25	*	17.3	11.8	3.84
10 – 20	4.0	5.0	4.0	7.0	4.0	4.83
20 – 30	0.5	4.0	2.3	2.86	2.22	2.66
	Cl^-					
0.9 –10	12.0	25.0	*	10.0	*	25.0
10 – 20	5.88	*	5.26	*	5.26	*
20 – 30	2.0	2.0	3.3	*	2.28	2.0

* Shows an increase in the relative rate of pollutants' deposition in the sandcrete block. It is assumed that diffusivity of these pollutants is retarded.

Deterioration mechanism of a serving structure is dependent on:

- In-built or self-destructive mechanism, which in this case include the quality of the cement, sand and water and the block production technique.
- External or prevailing environmental conditions and
- The extent of interaction of a and b to be defined by time.

These factors are adequately represented in the model Equation 14. For any structure; even when serving in the same locality, the above-mentioned factors cannot be the same due to variation in especially the internal factors. This could account for observed variations in data presented in Table 2 and 3. The developed model and the methodology of application can be used to determine the rate of deterioration of serving sandcrete in any environment and it will serve as a base for comparative analysis of the extent of depreciation of the structure.

CONCLUSIONS

The developed deterministic model equation can only be used for a given depth of the sandcrete block. It does not represent the relationship between C_A and Inr in the entire block volume. Variation in the type of pollutant and possible reaction, including leaching need to be considered in order to developed an acceptable model.

ACKNOWLEDGEMENTS

I wish to acknowledge the contribution of the Federal University of Technology Board of Research and the Third World Academy of Sciences, Italy for their sponsors of this research.

REFERENCES

1. AKPAN U. G., ODIGURE J. O. The effect of pollution on building structure and its control. Proc. National Eng. Conf. Vol. 4, N^{o} 1, Nee publ. Pp. 116 – 121, 1997.

2. MOSKIVIN V. Concrete and reinforced concrete deterioration and protection. Mir publ. Pp. 111-169, 1983.

3. HARAID JUSTICES. Why concrete is not always durable. Proc. 10th Internat. Congr. On the chemistry of cement. Vol. 1. Amarkai AB and Gote'borg AB publ. Pp.31, 1997.

4. LUDWIG U. Durability of cement mortar and concrete. ASTM.STP 691, pp. 269 – 281, 1980.

5. GHOSH S. N., MATHOR V. K. Testing and quality control in cement industry. Vol. 3. Akademia book Internat. New Delhi, pp. 424 – 448, 1997.

6. ODIGURE J. O. General chemical engineering technology. Jodigs and associates publ. Minna, Nigeria. Pp. 30 – 31, 1995.

7. LYBEN W. L. Process modeling, simulation and control foe chemical engineering. McGraw Hill Internat. Publ. NY, 1995.

8. SMITH J. M. Chemical engineering kinetics. 3rd ed. McGraw Hill publ. Ny, pp. 450 – 482, 1981.

9. BAEV A. K. Handbook of chemical analyses of silicate minerals. Belorussian Tech. Institute, Minsk, Belorus, p. 38, 1983.

10. ODIGURE J. O. Hydration of cement paste and concrete from raw containing metallic particles. Cem. and Concr. Res. Vol. 24, N° 8, pp. 1549 – 1557, 1994.

11. VOLJINSKII A. V. Mineral binding substances. 4th ed. Stroiizdat, Moscow, p. 239, 1986.

LOW HEAT SULFATE RESISTANT CEMENT – ITS STRENGTH AND DURABILITY IN CHEMICALLY AGGRESSIVE ENVIRONMENT

M Singh

M Garg

Central Building Research Institute

India

ABSTRACT. The paper deals with the development of low heat sulfate resistant (LHSR) cement produced by activation of granulated slag obtained from blast furnace, copper and phosphate industries with calcium sulfate hemihydrate. A rapid setting cement of high strength was obtained. The setting time of cement was prolonged with a small addition of set retarder without adverse affect on strength. Better strength results with low heat of hydration than the anhydrite activated cement were achieved. Data confirmed that granulated blast furnace slag can be replaced with copper or phosphatic slag upto 10 percent by mass without appreciable fall in strength. The LHSR cement on hydration produce ettringite, C-S-H and C_4AH_{13} as the major hydraulic products. The durability of LHSR cement vis-a-vis ordinary Portland cement (OPC) was examined for its use in sulfate solutions such as $Na_2SO_4.10\ H_2O$, $(NH_4)_2SO_4$, $MgSO_4$ and in a mixture of NaCl and $Na_2SO_4.10\ H_2O$. Data upto 180 days of curing in sulfate solution is reported. A fall in compressive strength of LHSR cement as well as OPC was recorded. However, fall of strength was lower in LHSR cement than the OPC. The gain in higher strength in LHSR cement in sulfate solutions may be assigned to the formation of enhanced quantity of C-S-H and decrease in $Ca(OH)_2$ and ettringite. The LHSR cement may be used in construction work prone to sulfate attack.

Keywords: Cement, Slag, Hemihydrate, Compressive strength, Durability, Low heat, Sulfate resistance.

Dr M Singh, is a senior scientist at Central Building Research Institute, Roorkee,India. His field of specialization is cement and gypsum products. He has published several research papers in reputed National and International journals and worked as building material expert in various countries under CSIR-UNCHS-USSR Mission and bagged several awards.

Dr M Garg, is a scientist at Central Building Research Institute, Roorkee, India. Her field of specialization is gypsum products. She has published many research papers in reputed National and International journals and received awards.

INTRODUCTION

About 10 million tonnes of slag are produced annually as a by-product from blast furnace and metallurgical industries in India. Granulated slag can be activated by various agencies like alkali, lime and sulfate to form cementing materials [1-2]. These slags are used in the manufacture of cement and cementing materials in concrete, as rail ballast and as a filler [3-4]. The copper and phosphatic slags are mostly used as an aggregate and pozzolanic materials but their use in the manufacture of blended cements has yet to be explored.

Super-sulfated cement is a well known blended cement, which is produced by activation of granulated blast furnace slag with 10 to 15 percent gypsum anhydrite in the presence of 2 to 5 percent cement or lime. Super-sulfated cement is low heat sulfate resistant cement as it gives low heat of hydration and adequate sulfate resistance than the ordinary Portland cement [5] hence, the name low heat sulfate resistant (LHSR) cement. The Indian slags are characterized by low lime and high alumina content and are less reactive than the foreign slags. By increasing anhydrite content to 20-25 percent, the strength of cement can be increased considerably.

However, for the production of anhydrite, high temperature (800^0-850^0C) is required. Investigations were therefore, undertaken to produce LHSR cement with and without copper / phosphatic slag by activation with calcium sulfate hemihydrate ($CaSO_4$. ½ H_2O) made at much lower temperature (150-160 ^{0}C). Experimental cements were produced by blending ground granulated slag with hemihydrate plaster and Portland cement clinker in suitable proportions and their characteristics were compared with the cement made using anhydrite as well as Portland cement. The heat of hydration and sulfate resistance of the cement were determined. The hydraulic products as determined by DTA and X-ray diffraction are reported.

Durability of concrete due to sulfate attack is an important matter. The use of cement mortar and concrete in sulfate bearing soils, ground water or marine atmosphere deteriorate concrete due to formation of ettringite, gypsum or thaumosite [6-8]. To combate sulfate attack on cement mortar and concrete, blended cements are preferred over OPC [9].

LHSR cement is a blended cement and its use in aggressive atmosphere could be an asset for cement mortar and concrete. Hence, performance of LHSR cement mortar in sulfate solutions such as Na_2SO_4.10 H_2O, $(NH_4)_2SO_4$, $MgSO_4$ and in a mixture of NaCl and Na_2SO_4.10 H_2O upto a period of 180 days was studied in term of measurement of compressive strength of mortar cubes. The strength development in mortar cubes during immersion in sulfate solutions was examined by DTA and XRD. The results are reported and discussed in the paper.

EXPERIMENTAL DETAILS

Materials

The raw materials such as granulated blast furnace slag, phosphogypsum and Portland cement clinker of chemical composition (Table 1) were employed to formulate LHSR cement. Granulated slag contains 90 % glass.

Table 1 Chemical composition of raw materials

CONSTITUENTS	GBFS	PHOSPHOGYPSUM	CEMENT CLINKER
P_2O_5	--	0.47	--
F	--	0.86	--
Organic matter	--	0.59	--
SiO_2 + insoluble in	33.83	0.29	22.50
HCl	--	--	--
Al_2O_3 +Fe_2O_3	22.93	0.54	9.80
CaO	34.93	31.09	61.70
MgO	7.46	1.31	2.80
SO_3	0.84	43.21	0.06
Na_2O	--	0.29	Tr.
LOI	0.20	18.38	2.1
Mn_2O_3	0.10	--	--

GBFS : Granulated blast furnace slag

Preparation of Low Heat Sulfate Resistant Cement

The LHSR cements were produced by uniformally blending the ground granulated blast furnace slag (410 m^2/kg, Blaine) with the calcium sulfate hemihydrate (320 m^2/kg, Blaine) and cement clinker (330 m^2/kg, Blaine) in different proportions. The hemihydrate plaster was produced at 150^{0}C in the Gypsum Calcinator fitted with mechanical churner whereas anhydrite was made at 850^{0}C in the electrical furnace. The composition of LHSR cements is listed in Table 2. The LHSR cements were evaluated for properties such as setting time, compressive strength and Lechatelier expansion (cold expansion) as per methods given in IS:4031-1996 [10]. The initial and final setting times of the neat cement was tested using Vicat apparatus at normal consistency and the compressive strength was determined using 1:3 cement-standard sand (triple graded) cubes (7.06x7.06x7.06cm) produced by 2 minutes vibration method. While the cold expansion was determined by measuring the expansion of neat cement cast in ring moulds submerged under water. The progress in hydration of LHSR cement was examined with DTA (Stanton Red Croft, U.K.) and X-ray diffraction (Philips, Netherlands). The sulfate resistance of LHSR cements was studied as per method described in IS:12330 - 1988 [11]. According to test, a mixture of LHSR cement and natural gypsum was prepared in such a way that the total SO_3 content was 7.0 percent by mass. The granulometry of natural gypsum was maintained as 100 percent passing 150 micron IS sieve, at least 95 percent passing 75 micron sieve and at least 75 percent passing 45 micron IS sieve respectively. Bars of size 250mm x 25mm x 25mm were cast using cement (containing gypsum) and sand in the proportion 1:2.75 at W/C 0.485. The bars were demoulded after 24 hours of their casting and then immersed in the water horizontly. The average expansion of 3 bars was recorded at 14 days.

Table 2 Composition of LHSR cements

CEMENT DESGN.	MIX COMPOSITION (% by mass)					
	GBFS	Phosphatic Slag	Copper Slag	$CaSO_4.½ H_2O$	Cement Clinker	Retarder
A	75	--	--	15	10	--
B	75	--	--	15	10	0.2 Borax
C	75	--	--	15	10	0.1 T.acid
D	65	10	--	15	10	0.1 T.acid
E	65	--	10	15	10	0.1 T.acid
F	75	--	--	15 (Anhydrite)	10	--
G	--	--	--	--	96	4.0 (Gypsum)

T.acid : Tartaric acid.

Performance of LHSR Cement in Sulfate Solutions

The mortar cubes (5 cm x 5 cm x 5 cm) comprising 1 : 3 cement - sand (F.M. 1.2) were cast at 105 % flow and cured for 28 days in water at 27 $\pm$ 2^{0}C. The hardened cubes were immersed in acetone and then dried to constant weight at 100^{0}C,cooled to ambient temperature and then submerged in $Na_2SO_4.10\ H_2O$ (5%), $(NH_4)_2SO_4$ (4%), $MgSO_4$ (4%) and NaCl (2%) + $MgSO_4$ (2%) solutions. The cubes were tested for their compressive strength after certain periods vis-a-vis OPC mortars. The hydration studies of of LHSR cement and OPC mortars during immersion was checked with the help of DTA and XRD.

RESULTS AND DISCUSSION

Properties of Low Heat Sulfate Resistant Cement

The physical properties of LHSR cements are listed in Table 3. The results show fast setting of cements due to higher concentration of sulfate ions in cement matrix. To regulate setting time, chemical retarders such as borax, tartaric acid, sugar, citrate, phosphates etc. were added to cement to enhance their setting times. Borax and tartaric acid (< 0.2%) have been found effective to prolong setting times of the cement. Strength wise these cements compared well with conventional super sulfated cement based on slag, anhydrite and portland cement (cement 'D') and the ordinary Portland cement designated as cement 'G'. These cements are sound as they show cold expansion much within the maximum specified value of 5.0 mm as given in IS: 6909[12].

The results, furthermore, show that on replacing GBFS with 10 % (by mass) of phosphatic and copper slags (cements 'D' and 'E') conform to the requirement of IS: 6909.

It is therefore, established that LHSR cement can be manufactured by activating the slag with hemihydrate ($CaSO_4.1/2H_2O$) plaster in place of anhydrite ($CaSO_4$). These cements possess low heat of hydration and are sulfate resistant as they showed sulfate expansion within maximum specified value of 0.045 % covered in IS : 12330.

Table 3 Properties of LHSR cements

CEMENT DESIGN	PROPERTIES					
	Setting time (Minutes)		Compressive strength (MPa)			Soundness(Cold Expn.) (mm)
	Initial	Final	3d	7d	28d	
A	10	65	16.1	23.7	35.4	1.0
B	60	120	15.9	22.3	43.1	1.1
C	55	106	16.9	38.4	56.1	1.2
D	70	142	15.7	23.0	44.7	0.8
E	66	150	17.5	28.8	35.0	1.1
F	62	170	15.8	35.2	55.3	0.9
G	110	205	17.5	28.0	46.0	1.0
IS: 6909 Limits	Min.30	Max.600	Min.15	Min.22	Min.30	Max.5.0

The LHSR cement on hydration produce ettringite ($C_3A.\ 3\ CaSO_4.\ 32\ H_2O$), tobermorite (C-S-H) and C_4AH_{13} as predominant hydraulic products [13]. The microstructure of hardened LHSR cement showed enhanced intensity of ettringite and tobermorite peaks with increase in curing period. However, the gypsum and $Ca(OH)_2$ peaks grossly reduced and almost disappeared at 28 days and on subsequent hydration.

Performance of LHSR Cements in Sulfate Solutions

The compressive strength of 1 : 3 cement - sand mortar cubes tested after 3, 7, 28 and 180 days of immersion in sulfate solutions is listed in Table 4. A fall in strength of LHSR cements activated with hemihydrate plaster as well as anhydrite was noted. However, the fall in strength was less pronounced in LHSR cement mortars than the ordinary portland cement mortar. It can be seen that even in 90 days cured portland cement mortar, the strength could not be measured due to development of cracks and breakage in the cubes during their curing in sulfate solutions.

The strength development in cement mortar cubes cured in sulfate solutions up to 90 days was monitored by DTA and XRD. Figure 1 shows DTA of the LHSR cements 'C' and 'F' and that of cement 'G' (OPC) cured in 5 % $Na_2SO_4.10\ H_2O$ solution. The endotherms formed at 100^0C, 130^0C, 150^0C, 220^0 - 230^0C, 490^0C, 640^0 - 660^0C, 780^0 - 830^0C may be assigned to

the decomposition of C-S-H gel, ettringite, gypsum, C_4AH_{13}, $Ca(OH)_2$, tobermorite and $CaCO_3$ respectively. The appearance of exotherms at 920^0 - 930^0C in cements 'C' and 'F' is due to devitrification of slag. It can be seen that with increase in curing period, the intensity f C-S-H gel, C_4AH_{13} and tobermorite peaks increased whereas intensity of $Ca(OH)_2$ and ettringite reduced

Table 4 Performance of LHSR Cement in Sulfate Solutions

CEMENT DESIGN	CURING PERIOD (DAYS)	COMPRESSIVE STRENGTH IN SULFATE SOLUTIONS, (MPa)				
		$MgSO_4$ (4%)	$(NH_4)_2SO_4$ (4%)	$Na_2SO_4.10\ H_2O$ (4%)	NaCl + $MgSO_4$ (2%)	(2%)
C	3	18.7	16.7	22.1	12.6	
	7	22.1	19.7	23.0	23.9	
	28	24.2	32.2	24.0	26.6	
	90	32.0	26.4	27.2	22.9	
	120	33.2	25.4	26.4	23.2	
	180	35.2	24.8	25.5	24.8	
F	3	21.1	26.7	14.7	14.0	
	7	24.3	27.1	20.8	16.2	
	28	36.0	24.0	22.8	29.7	
	90	24.2	19.7	29.0	20.0	
	120	23.8	19.6	28.4	21.9	
	180	19.9	18.6	26.7	23.2	
G	3	29.3	29.4	15.9	10.3	
	7	35.3	22.2	21.6	10.2	
	28	15.3	12.0	28.5	11.9	
	90	All cubes broken	7.5 (Craking started)	All cubes broken	10.1	

However, no $Ca(OH)_2$ was found at 90 days and on subsequent hydration. In contrary to LHSR cements 'C' and 'F', the intensity of C-S-H gel, tobermorite and $Ca(OH)_2$ are grossly reduced in cement 'G'. Moreover, disappearance of gypsum endotherm (150^0C) was observed at 90 days as wellas at 180 days.

Hence, increase in tobermorite and C_4AH_{13} may be correlated with residual higher strength in LHSR cements than OPC based mortars and thereby confirming better durability of former than latter in sulfate solutions. The XRD plots of LHSR cements 'C','F'and 'G' cured in 5.0% $Na_2SO_4.10\ H_2O$ solution are shown in Figure 2.

It can be seen that reflections of ettringite, tobermorite C_4AH_{13} and $Ca(OH)_2$ are formed. The intensity of tobermorite and C_4AH_{13} reflections increased with the increase in curing period whereas reflections of ettringite and $Ca(OH)_2$ reduced. However, in cement 'G', intensity of C-S-H and ettringite were further mitigated leading to cracking and disruption of mortar cubes. In essence, the cement mortars based on LHSR cement 'C' showed better sulfate resistance than the LHSR cement 'F' in $MgSO_4$, $(NH_4)_2SO_4$ and NaCl + $MgSO_4$ solutions. The sulfate resistance of LHSR cement C' and cement 'F' was similar in $Na_2SO_4.10H_2O$ solution due to close strength characteristics. However, the sulfate resistance of LHSR cements was better than the Portland cement 'G'. The XRD results corroborate the findings of DTA. Similar pattern of XRD and DTA results were obtained by curing cement mortars in $MgSO_4$, $(NH_4)_2SO_4$, and NaCl + $MgSO_4$ solutions.

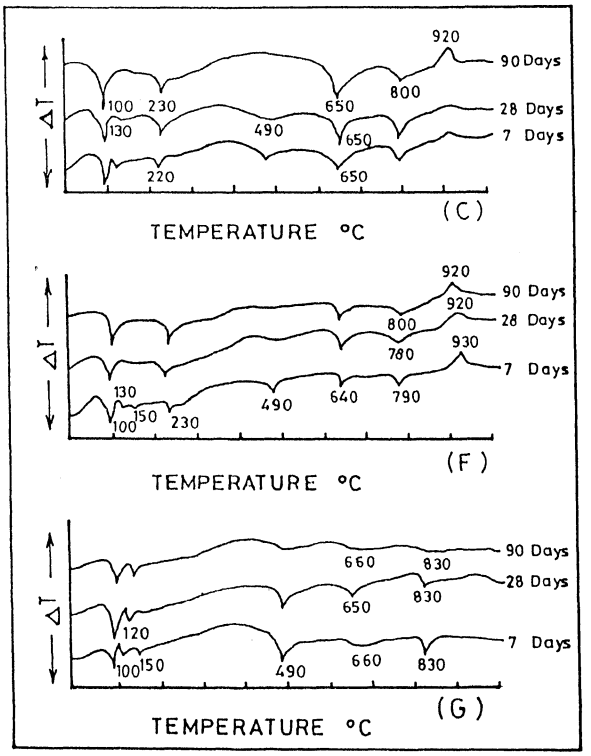

Figure 1 DTA of LHSR cements 'C' and 'F' and Portland cement 'G' cured for different periods in 5% Na_2SO_4 $10H_2O$ solution

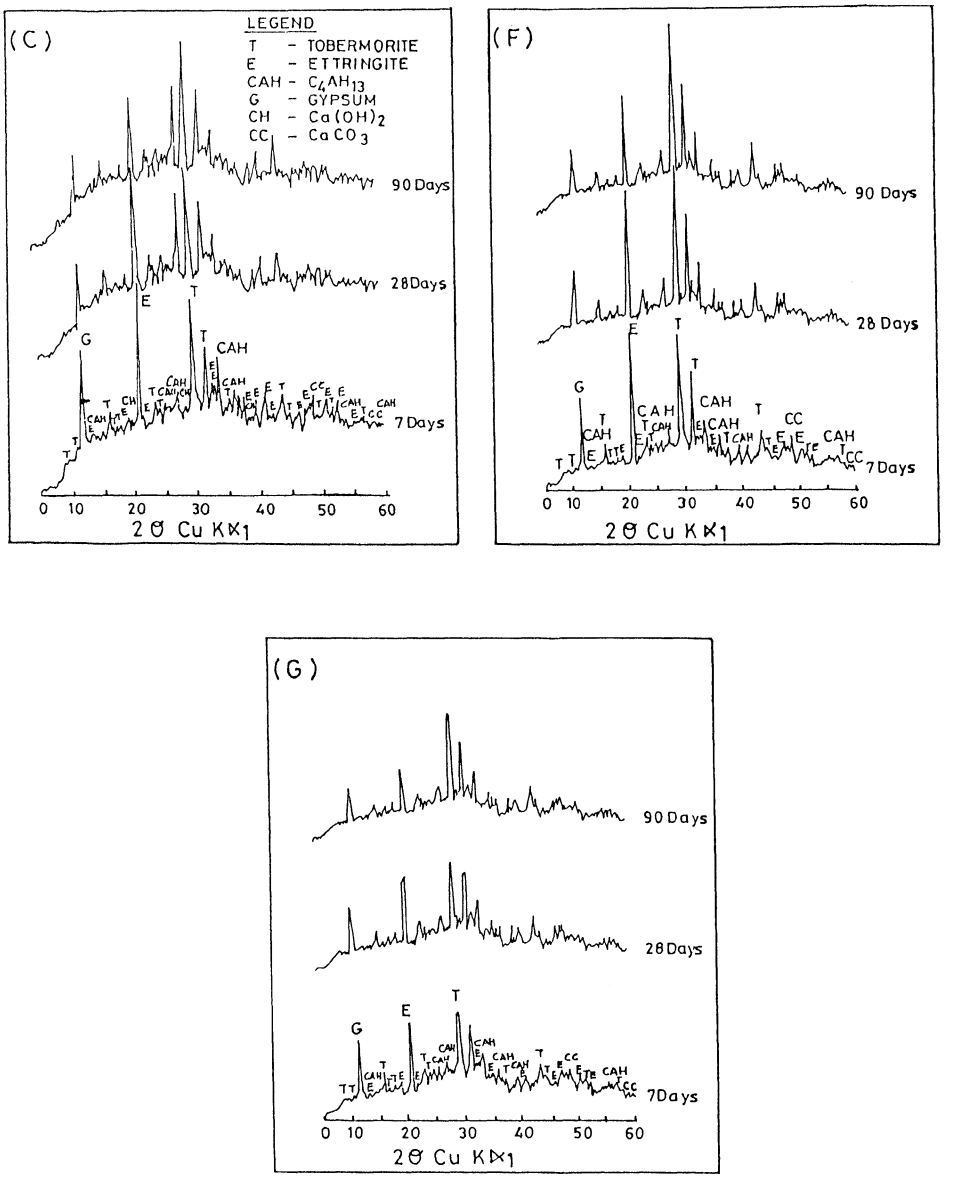

Figure 2 X-Ray diffractograms of LHSR cement 'C' and 'F' and Portland cememt 'G' cured in 5% $Na_2S0_4H_20$ solution

CONCLUSIONS

The low heat sulfate resistant cement can be manufactured by activating granulated blast furnace slag with hemihydrate plaster produced at 150^{0}C instead of using anhydrite formed at 850^{0}C. In this way saving in thermal energy may be achieved. It is also concluded that phosphatic and copper slags may be replaced with the granulated blast furnace slag up to 10 % by mass in making LHSR cement without any appreciable effect on the compressive strength. The performance of cement mortars in different sulfate solutions showed decrease in strength of LHSR cement to lesser extent than OPC mortars. The formation of tobermorite and C_4AH_{13} phases of higher intensity confirm attainement of higher strength in LHSR cement. The curing of LHSR cement mortars in sulfate solutions beyond 180 days is in progress.

ACKNOWLEDGEMENTS

The authors are grateful to Shri V.K.Mathur, Director, Central Building Research Institute, Roorkee for permitting presentation of the paper.

REFERENCES

1. ROY, D.M., IDRON, G.M., Hydration structure and properties of blast furnace slag cements, mortars and concrete, ACI Journal,Vol.79, 1982, pp 444-451.

2. SINGH, M., Portland slag cement as building material, Proceedings of National Seminar on Portland Slag Cement-Its Superior Characteristics and Suitability for All Civil Constructions and Mass Concrete Works, Bhubaneswar,1992, pp. 31-51.

3. DOUGLAS, E., MAINWARING, P.R., Hydration and pozzolanic activity of nonferrous slags, Ameriacn Society Bulletin, Vol.64, 1985, pp. 700-706.

4. TIXIER, R., et.al., Effect of copper slag on the hydration and mechanical properties of cementitious mixtures, Journal of Cement & Concrete Research, Vol.27, 1997, pp. 1569-1580.

5. CHOPRA, S.K., LAL KISHAN., Manufacture of supersulfated cement from the Indian slags, experimental work at C.B.R.I., Indian Concrete Journal, Vol.35, No.4, 1961, pp. 114-116.

6. KURDOWSKII, W., Durability of blended cements in aggressive media, Progress in Cement and Concrete, Mineral Admixtures in Cement and Concrete, by Shondeep L. Sarkar and S.N. Ghosh :First ed. New Delhi, Akademia Books International, 1993, p. 448.

7. REGOURD, R., Physico - chemical studies of cement pastes, mortars and concretes exposed to sea water. ACI Special Publication, SP-65, Det roit, 1980, p. 63.

8. NIKITINA L.V., KRASSILINIKOV K.G., APCHINA A.I., La Nature physico - chemiqua des autocontraintes des ciments expansifs, Proceedings of Seventh Intl. Cong. Chem. Cem., Paris, 30 June-4 July 1980.

9. MEHTA, P.K. et.al., Performance and durability of concrete systems, Proccedindgs of Nineth Intl.Cong. Chem.Cem., New Delhi, 23-28 November 1992.

10. BUREAU OF INDIAN STANDARDS. IS : 4031, Methods of physical tests for hydraulic cement, 1996.

11. BUREAU OF INDIAN STANDARDS. IS : 12330, Specification for sulfate resistant Portland cement, 1988.

12. BUREAU OF INDIAN STANDARDS. IS : 6909, Specification for super-sulfated cement, cement, 1990.

13. SINGH, M., GARG, M., Investigations into activation of slag by calcium sulfate hemihydrate, Proceedings of 5th Intl. Conf. On Concrete Technology for Developing Countries, New Delhi, Vol.1, 1999, pp. 1-45-1-53.

AMMONIUM SULFATE ATTACK ON CEMENT MORTAR

F Rendell

University of East London

United Kingdom

R Jauberthie

INSA

France

ABSTRACT. Chemicals storage in concrete silos often presents durability problems due to their chemical attack, the situation being severe due to the high concentration. The paper aims to examine the effects of ammonium salts, - ammonium sulphate and nitrate, noted for their aggressive behaviour. Two laboratory programmes are reported which study the influence of ammonium solutions on PC mortar samples. Modification to mortar properties are reported. Ammonium sulphate undergoes a strong swelling that is correlated with the reduction in strength. These mortars also undergo rapid cracking after removal from solution and exposure to air. Ammonium nitrate undergoes a rapid decalcification which is accompanied by a strength loss.

Key words: OPC, Sulfate attack, Ammonium nitrate, Ammonium sulphate, Durability.

F Rendell, Senior Lecturer. University of East London, Longbridge Road, Barking, London, UK. His research work is directed at material durability in water and wastewater systems.

R Jauberthie GRGC Maître de Conférences. Matériaux, INSA, 20 Av. des Buttes de Coësmes 35043 Rennes, France. His main research interests include the properties of different phases in hydrated cements, the durability and the protection of concrete.

INTRODUCTION

Deterioration of concrete in the presence of ammonium salts has been observed since the 1930's, many of these cases being associated with the industrial processes used in the production of coal gas. The reaction between certain ammonium salts and concrete has long been recognised as potentially aggressive, ammonium chloride, phosphate, sulphate, sulphide, sulphite and bicarbonate being considered the most harmful whereas ammonium carbonate, oxalate and fluoride being harmless [1]. Most codes, e.g. EN 206 would consider concentration of in excess of 60 mg NH_4^+ /l as an extreme exposure condition. Ammonium compounds are found to occur in sewage, typically 30 mg NH_4^+ /l, certain industrial wastewater and sludge treatment processes will have concentrations of ammonium compounds in a significant concentration, e.g. supernatant liquor from sludge can have concentration of up to 500 mg NH_4^+ /l. The most severe conditions that are likely to exist are found in the storage silo where an ammonium compound is stored in bulk [2]. The principle process involved in the deterioration of concrete in the presence of ammonium compounds involves the reaction between the portlandite (lime) and the ammonium salt.

$$Ca(OH)_2 + 2NH_4Y \rightarrow CaY_2 + 2H_2O + 2NH_3$$

Where Y is the anion associated with NH_4^+

Ammonium sulphate and ammonium nitrate are usually considered as the most aggressive of the ammonium salts.

Ammonium Nitrate

Ammonium nitrate provokes a solubilisation and leaching of the lime in the cement paste, this is accompanied be a reduction in the pH of the concrete and thus creating a danger of depassivation of the steel in reinforced concrete. The leaching of the lime would also lead to a weakening of the matrix of the material. It is often observed that the surface of a mortar will undergo visible signs of cracking, this has been attributed to the formation of calcium nitro-aluminate [3]. It is proposed that the nitrate reacts with the hydrated aluminates in the cement paste thus forming the expansive calcium nitro-aluminate. Lea [4] has shown that it has a low solubility in a lime rich solution i.e. high pH, however the nitro-aluminate decomposes as the lime is leached from the cement matrix, i.e. decreasing pH. This would imply that in a saturated state the leaching of lime is a dominant factor and the conditions do not favour the formation of the nitro-aluminate. The converse is true in the case of mortar subjected to wetting and drying cycles. Cadre [5] has confirmed the presence of nitro-aluminate by X Ray diffraction analysis of mortar samples conserved in dry conditions and then immersed in ammonium nitrate solution.

Ammonium Sulphate

Lea [6] expresses the opinion that ammonium sulphate is the most destructive of the sulphate salts, a 5% solution capable of causing 3.8% linear expansion in a cement mortar after 12 weeks. He proposes that the expansion may be due to the formation of an expansive double salt $CaSO_4.(NH_4)_2SO_4.H_2O$. Considering the general reaction between an ammonium salt and lime it can be seen that one would expect the formation of Ca $SO_4.2H_2O$ gypsum and a liberation of ammonium; this gas liberation being common to most ammonium salts. It has been observed that during the period of immersion of a PC CEM I mortar in ammonium sulphate solution there is the formation of needle like crystals over the surface of the concrete, these have been identified as gypsum [7, 8].

EXPERIMENTAL PROGRAMME

An experimental programme was conducted with the aim of observing the deterioration of a PC CEM I mortars immersed in ammonium sulphate solution and ammonium nitrate solution. Both programmes quantify the modification to the material by measuring swelling strength and depth of pH reduction in normal mortar specimens immersed in ammonium compound with control samples stored in water. The mortar used in the test is a normal mortar conforming to EN196. The aggregate type being a standard sand conforming to ISO 679, with an aggregate/cement ratio of 3.0. The cement type used is an Ordinary Portland Cement, CPA CEM 1 (52.5N) CP2, manufactured in SAINT-PIERRE-LA-COUR (France). An analysis of the cement type is summarised in Table 1.

Table 1 Oxide analysis of the cement used in the tests

BULK OXIDE, % (WEIGHT BY MASS)										
Ins	SiO_2t	Al_2O_3	Fe_2O_3	CaO	MgO	K_2Ot	Na_2Ot	SO_3	P.F.	CaO_{free}
0.26	20.15	5.18	2.76	65.13	0.69	0.99	0.17	2.85	1.51	1.31

A summary of the two experimental protocols is set out in Table 2. In both programmes a set of control samples were conserved in water at 20°C. The samples were cured for 1 day at 100% RH and then stored at 20°C 50% RH for 10 days prior to immersion.

Table 2 Experimental protocols

	PROGRAMME A	PROGRAMME B
W/C ratio	0.5	0.8
Cure at 100%RH	1 d	1 d
Duration of immersion	90 d	180 d
Solution and concentration ($g\ NH_4^+/l$)	Ammonium sulphate (5.4)	Ammonium sulphate (36) Ammonium nitrate (36)

EXPERIMENTAL RESULTS

Observations

In programme A and B it was noted that there was a strong liberation of ammonia gas for all samples immersed in an ammonium solution. This was apparent from the second day of immersion and persisted until the end of the exposure time. After approximately a week it was noted that needle like crystals form and the surface of the samples immersed in ammonium sulphate solution. The samples immersed in the ammonium nitrate solution developed a thin white coating on their surface and the formation of a scum on the surface of the solution.

At the end of the exposure period the samples were removed from the solution and washed in tap water prior to testing, it was noted that the samples immersed in ammonium sulphate developed cracks along the edges and end faces. This cracking occurred within minutes of washing, Figure 1, left hand side, shows a sample from Programme B where most of this severe cracking occurred during and after washing. The surface zone of samples immersed in ammonium sulphate were examined by scanning electron microscope, observed formations were identified using microanalysis (EDS). Figure 1, right hand side (lower), shows the formation of the acicular gypsum crystals on the surface, and the internal gypsum formations (right hand upper) were found to a depth of approximately 200 mm.

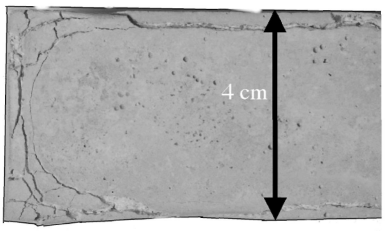

Detail of crack damage

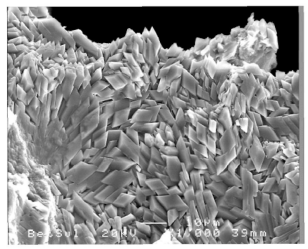

Interior gypsum formation (x1000)

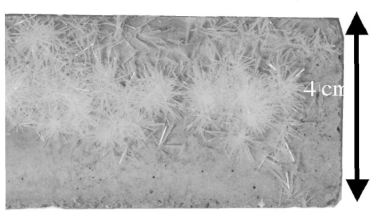

Surface crystallisation

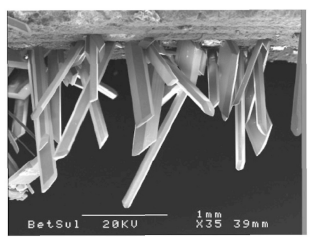

Surface gypsum formation (x35)

Figure 1 Damage to a mortar sample after 90 d immersion in ammonium sulphate solution.

In the case of samples immersed in ammonium nitrite there was a slight deterioration after washing however this was very minor in comparison with the sulphate solution.

Mechanical Properties

The results of the final tests on the samples are set out in Table 3. The strength tests were carried out when the samples were saturated to avoid the effects of chemical modification to the sample during the drying process. A 3 point bending configuration was used to determine the flexural strength.

An assessment of the depth to which the cement paste was chemically modified was determined by the use of phenolphthalein alcohol solution, the presumption being that loss of the lime will cause a drop in pH below the indicators change point, approximately 9-10.

Table 3 Mechanical properties of mortar samples after exposure.

PROPERTY	PROGRAMME A		PROGRAMME B		
	Control water	Ammonium sulphate	Control water	Ammonium sulphate	Ammonium Nitrate
Flexural strength (MPa)	8.3	7.7	5.6	1.7	2.5
Compressive strength (MPa)	53.7	41.0	32.6	20.3	10.7
Swelling (mm/m)	0.20	0.50	0.47	2.94	0.53
Depth of pH loss (mm)	2	2	1	2.5	7.0

DISCUSSION

It is evident from the results that the porosity of the sample has had a great effect on the kinetics of the reactions. Programme B, high concentration and high water cement ratio, presents the most rapid deterioration. Previous work carried out in Programme A [9] showed that a mortar with w/c ratio of 0.5, immersed in 0.016 mol/l ammonium sulphate (0.29 g NH_4^+/l) for 6 months did not exhibit any significant change in properties.

In programme A an attempt was made to correlate the reduction in the flexural strength (β) to the depth of pH loss and the swelling. The results of this exercise showed that for the case of mortar immersed in ammonium sulphate solution there is no correlation between depth of pH reduction, this being in agreement with the results shown in Table 3 i.e. the same depth being found for two radically different materials and exposures. However there is a strong correlation, see Figure 2, between swelling and strength loss. This result is again in broad agreement with Table 2 where the greatest strength loss is associated with the highest degree of swelling. Extrapolating the linear regression of the data set used in Figure 2 one can observe that a relative strength loss of 0.3 corresponds to a sample swelling of 3mm, which is in reasonable agreement with the results seen in Programme 2.

The mechanism of strength loss associated with immersion in ammonium sulphate appears to be closely related to swelling and therefore related to formation of internal cracking within the matrix of the material. The rapid cracking observed after removal from the solution and washing would infer a rapid internal stress build up on exposure to air; this could be due to a rapid liberation of gaseous ammonia as the pore pressure is reduced. In the case of samples immersed in ammonium nitrate the results confirm the observation that there is a large zone in which the pH of the mortar is reduces, most probably due to leaching of the portlandite. The very minor cracking observed before and after washing could possibly be due to the expansive action of calcium nitro-aluminates.

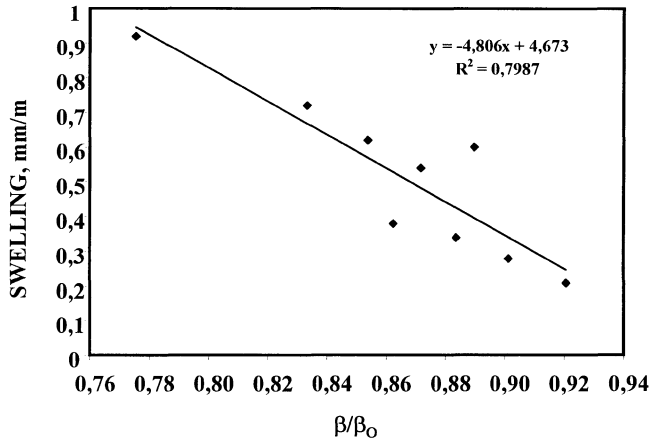

β flexural strength after exposure βo flexural strength of control

Figure 2: Correlation between sample swelling and the reduction in flexural strength

CONCLUSIONS

The study has confirmed that the action of ammonium compounds can be extremely detrimental to the durability of concrete. A knowledge of the mechanism involved in this type of deterioration is of particular importance for the design and repair of fertiliser storage silos. It is shown that the concentration of the solution and the porosity of the mortar have an effect on the kinetics of the reaction. Ammonium nitrate solution appears to provoke a deterioration in material performance by the leaching of the portlandite from the cement paste, this could lead to depassivation of reinforcement. The formation of expansive calcium nitro-aluminates may cause surface deterioration however the formation of this compound is inhibited by the reduction of pH due to leaching. Wetting and drying cycles are the exposure pattern favouring this expansive action.

In the tests carried out on mortars immersed in ammonium sulphate it is evident that the sample swelling is severe, however for a dense mortar the effects are insignificant below a concentration of 0.016 mol/l. The exact mechanism of deterioration has not been identified however it is apparent that the loss of strength is related to swelling and therefore internal crack damage. The rapid cracking effect seen after washing and exposure to air has a serious consequence for the durability of a material, if concrete is in contact with ammonium sulphate solution and exposed to wetting and drying cycles it is concluded that severe damage may occur.

REFERENCES

1. BICZOK, J., Concrete corrosion and concrete protection, Akademiai Jiadl, 8th edition, Budapesta, 1972.

2. New Civil Engineer - 5th July 2001.

3. UKRAINCIK, V. BJEGOVIC, D. DJUREKOVIC., A. Concrete corrosion in a nitrogen fertilizer plant Durability of Building Materials and Components, Proceedings ofthe First International Conference, Ottawa, Canada, 1978 pp 30-41.

4. LEA, F.M., The action of ammonium salts on concrete, Magazine of concrete research, Vol 17 n° 52 pp115-116.

5. CARDE, C., Caractérisation et modélisation de l'altération des propriétés mécanique due à lixivation des matériaux cimentaires, Thèse No D'ordre 375 INSA Toulouse , March 1996.

6. LEA, F.M., The chemistry of cement and concrete, Edward Arnold, 3rd Edition, London, 1970.

7. RENDELL, F., JAUBERTHIE, R, The deterioration of mortar in sulphate environments, Construction and Building Materials, 1999, 13, pp 321 – 327.

8. RENDELL, F, JAUBERTHIE, R, CAMPS, J P,. The effect of surface gypsum deposits on the durability of cementitious mortars under sulphate attack, Concrete Science and Engineering, RILEM, April 2000, Vol 2, pp231-244.

9. RENDELL, F,. Le comportement des bétons dans les systèmes d'assainissement. Thèse No D'ordre D00-01 INSA Rennes, January 2000.

EFFECTIVENESS OF SUPPLEMENTARY CEMENTING MATERIALS FOR REDUCING THE SULFATE ATTACK IN BLENDED CEMENTS

R E Rodriguez-Camacho

R Uribe-Afif

J J Flores-Martinez

Cementos Mexicanos CEMEX

Mexico

ABSTRACT. The use of supplementary cementing materials for reducing the sulfate attack has increased; due to they form cementing compounds that increase this resistance. This study shows an evaluation of different Mexican natural pozzolans and mineral admixture finely divided. It was determined their chemical composition and pozzolanic activity according to ASTM C 311 and 1240 Methods. Mortar bars with blended cements were making according to ASTM C 1012 test method using 5% sodium sulfate solution. It was determined the length change in the mortar bars exposed to a sulfate solution. Expansion measurement was conducted for one year to allow an adequate penetration of sulfate ions to the interior of mortar. Besides, microscopic observations were made to verify the formation of cracks on the mortar bars that showed an increase in the expansion and their state after one year in sulfate solution. The results of expansion development are showed. Satisfactory evidences about performance of the blended cements and the supplementary cementing material type used were gotten.

Keywords: Natural pozzolans, Sulfate attack, Silica fume, Fly ash, Expansion. Petrographic observations, Sulfate attack resistance.

Ms R E Rodríguez-Camacho, is currently undertaking research into the development of performance concrete durability focused mainly on sulfate attack and alkali aggregate reaction.

Mr R Uribe-Afif, is currently undertaking research in to the development of performance specifications for durability. His research focuses mainly on concrete durability, pathology and aggregates.

Dr J J Flores-Martinez, is currently undertaking research into the development of performance concrete durability. Besides, his research focuses mainly pathology and aggregates.

INTRODUCTION

Sulfate attack of cement mortar and concrete has been studied for several decades. It is commonly believed that sulfate attack of portland cement pastes is caused by chemical reactions between cement ingredients and sulfate ions from various sources [1], that result in the formation of ettringite and gypsum, can lead to excessive expansion, cracking, and strength loss. Typically, these constituents are the monosulfate hydrate (C_4ASH_{12}), calcium aluminate hydrates (C-A-H), and calcium hydroxide (CH). The sulfate attack can be controlled when the presence de (C_4ASH_{12}), calcium aluminate hydrates (C-A-H) is reduced or even eliminated by either restricting the C_3A content of the Portland cement, or by substituting a portion of the Portland cement with suitable blending material. The later method can be effectively employed to reduce also the CH content of the hydrated cement paste, such as in the case of pozzolanic additions. [2].

In respect to world requirements of quality assurance in the production of concrete have encouraged the use of the supplementary cementing materials, which combined with Portland cement, allows us improve the durability of concrete. In Mexico there is a great amount of deposits of natural pozzolans and the use the pozzolanic Portland cement is usually using to make concrete: others materials as fly ash and silica fume have been used too.

Possible technological benefits from the use of supplementary cementing materials in concrete include enhanced impermeability and chemical durability, improved resistance to thermal cracking, and increase in ultimate strength [3].

In Mexico has been found regions where the sulfate concentrations vary since moderate to severe, according to ACI 201 (Guide to Durable Concrete), as shown in Table 1. It has determined sulfate (SO_4^{2-}) concentrations in soils since 0,11 % to 0,70 % being sodium sulfate-rich soils; in ground waters and wastewaters have been the sulfate (SO_4^{2-}) concentrations since 288 to 10 000 ppm. At Pacific Coast the sulfate content vary from 3500 to 6700 ppm and in the Gulf of Mexico from 2500 to 5700 ppm. The contact of concrete with these soils and waters may cause expansion, chemical deterioration and disruption, so is very important to consider the using supplementary cementing materials in the concrete that is subject to sulfate attack to improve their resistance and reduce this type of attack.

One way to improve the sulfate resistance is to use the supplementary cementing materials mainly in concrete exposed to marine environmental or soils with high sulfate content. This investigation was conducted to show the advantages of using different supplementary cementing materials, as natural pozzolans, fly ash and silica fume, to improve the sulfate resistance.

SCOPE OF INVESTIGATION

The objective of this study is to present the results of a experimental program that consisted in determining the sulfate attack of different Portland cement, pozzolanic cements and, blends with fly ash-Portland cement and silica fume-Portland cement according to ASTM 1012 "Standard Test Method for Length Change of Hydraulic Cement Mortar Exposed to a Sulfate Solution". The proportioning of the mortar remained constant as 1 part of cement and 2.75 parts of standard sand and the bars were stored in 5% sodium sulfate solution.

A series of four mixes combinations constituting Portland cement-fly ash and three combinations of silica fume replacement levels were tested.

Table 1 Sulfate content in different regions of Mexico

PLACE IN MEXICO	WATER SOLUBLE SULFATE (SO_4^{2-}) IN SOILS, PERCENT	SULFATE IN WATER (SO_4^{2-}), ppm	ACI 201.2R-92
Texcoco. Mex.	0,11 - 0,18		0,10 –0,20 % (Exposure moderate)
Altamira, Tamps.	0,70		0,20 – 2,00 % (Exposure severe)
Coatzacoalcos, Ver.	0,20 - 0,28		150- 1500 ppm (Exposure moderate)
Wastewater, Toluca, Mex.		760	500- 10,000 ppm (Exposure severe)
Groundwater, Progreso, Yuc.		1995	
Seawater, Pacific Coast		3500 - 6700	
Seawater, Gulf of Mexico Coast		2500 - 5700	

The pozzolanic activity and chemical analysis of supplementary cementing materials was made. These include composition, reactivity and amount of pozzolan used with the Portland cement. The classification of every natural pozzolan includes its mineralogical-petrological characteristics, chemical composition, and pozzolanic activity index with lime and Portland cement. The pozzolanic activity with Portland cement and chemical composition were made for fly ash and silica fume.

EXPERIMENTAL METHODS

Materials

Natural pozzolans, fly ash and silica fume

In this study, representative samples from 6 natural pozzolanic deposits located in different states of the Mexican Republic were used. These materials were dried at a temperature of 100 °C, they were ground and the fineness was determined (amount of material retained in No. 325 sieve -45 μm-) according to ASTM C 430 [4]. The fly ash from North of Mexico is Class F (low- calcium) and silica fume were used.

Cements

The cements used included the follow: Three Portland cements (Type I, II and V) and seven portland-pozzolan cements. The characteristics of pozzolans used are shown in Table 5. The physical and chemical analysis of the cements is given in Table 2. The portland-pozzolan cements have different pozzolan content depending from source. At the Table 2 is shown the content of each pozzolan in each cement, the range varies from 11 to 30 percent. The pozzolan was intergrinding in the cement mill. The fly ash was combined with Portland

cement at 20, 30, 40 and 60 percent by mass replacement of Portland cement. The silica fume was used replacement 10, 15 and 20 percent by mass replacement of portland cement. The identification is as following: FA20-PC, FA30-PC, FA40-PC, FA60-PC, SF10-PC, SF15-PC, SF20-PC.

Table 2 Physical properties and chemical analysis of portland and pozzolanic cements

	ASTM TYPE I CEMENT	ASTM TYPE II CEMENT	ASTM TYPE V CEMENT	CPZ -A	CPZ -B	CPZ -H	CPZ -I	CPZ -J	CPZ -J-1	CPZ -ATC
Fineness										
- passing 45 μm, %	80.0	87.1	77.8	93.6	90.2	95.5	97.1	88.6	-	-
- Blaine, m^2/kg	319	372	272	488	444	434.5	387.5	380	-	-
Compressive Strength of 51-mm cubes, MPa									-	-
- 3 days	20.0	23.9	13.0	17.2	11.9	24.2	24.8	17.5	-	-
- 7 days	25.8	33.3	19.5	22.2	16.4	28.2	27.6	24.2	-	-
- 28 days	30.7	44.4	27.5	31.9	24.7	37.6	36.2	34.6	-	-
Chemical Analysis, %										
SiO_2	20.8	20.6	20.7	39.7	38.2	31.2	29.8	37.6	29.9	26.2
Al_2O_3	5.8	5.1	4.9	4.1	4.9	3.3	2.9	4.5	6.5	6.2
Fe_2O_3	3.1	3.4	4.8	2.1	2.4	3.1	3.7	1.8	2.7	2.9
CaO	61.5	62.7	62.9	45.2	48.0	54.0	54.4	48.4	52	56.6
MgO	2.4	2.2	1.6	0.8	1.8	1.3	1.4	1.4	1.3	1.1
SO_3	2.4	2.6	2.4	3.3	3.8	2.3	1.9	2.5	3.1	2.9
Na_2O	0.41	0.09	0.22	0.61	0.49	0.15	0.45	0.29	0.85	0.85
K_2O	0.56	0.50	0.40	0.82	0.66	0.60	0.70	066	1.40	1.11
Loss on ignition	1.5	1.5	1.8	2.7	3.4	3.6	3.2	2.3	1.8	1.58
Amount of Pozzolan	-	-	-	30	22	19	14	24	16.2	10.94
Bogue Potential Compounds Composition, %										
C_3S	42.0	52.2	50.8	-	-	-	-	-	-	-
C_2S	28.0	19.7	21.1	-	-	-	-	-	-	-
C_3A	10.1	7.8	4.9	-	-	-	-	-	-	-
C_4AF	9.4	10.3	14.6	-	-	-	-	-	-	-

TEST METHODS

Petrographic Examination

In order to make the petrographic identification, thin layers of each sample of natural pozzolans were prepared and observed under the petrographic microscope.

X-Ray Diffraction

The identification of the clay fraction in pozzolans was done on Siemens X-ray diffractometer; the powder method and radiation KαCu were used. Their mineralogical and physical characteristics and identification by XRD are shown in Table 3 and 4.

Chemical Analysis

The chemical composition of pozzolans, supplementary cementing materials and cements were determined by wet chemical methods according to ASTM C 114 [5]. The results are shown in Table 5.

Pozzolanic Activity with Lime and Portland Cement

It was determined according to ASTM C 311 [6]. Physical and chemical properties as pozzolanic activity with lime and Portland cement of each material are shown in the Table 5.

Tests Performed According to ASTM C 1012 Method

ASTM 1012 standard test method [7] cover the determination of the length change of mortar bars stored in 5 % sodium sulfate solution. Mortar mixtures proportioned as 1 part of cement, 2.75 parts of sand and W/C of 0.485, were used cast prismatic specimens 25 by 25 by 285 mm in size. The water content was adjusted to keep flow of the mortar within ± 5% of the obtained with W/C of 0.485. Specimens were cured at 35 °C for 24 h , after are cured at 23 °C until the mortar cube strength reached a value of 20 MPa. Typically, the strength was reached of 24 h to four days. Only for combinations with 30, 40 and 60 of fly ash content this strength was obtained in more time since 17 days until 6 months (cured at 23 °C as it is indicated an ASTM C 511) depending the fly ash content. The results as expansions of mortar bars for 52 weeks are shown in Figure 2

Petrographic Observations

The mortar bars were observed under the stereoscopic microscope to identify mainly cracking and spalling of the mortar surface.

RESULTS AND DISCUSSION

Natural Pozzolans. Petrographic characteristics

Natural pozzolans in Mexico are materials of pyroclastic origin as a result of explosive volcanic eruptions, where eruptive fragments are transported by air to be finally deposit of ground of water, once deposited as incoherent materials they can be submitted to diagenetic processes transforming them into compacted rocks called tuffs.

In the case of Mexican pozzolans, they are indistinctly exploited as incoherent materials as compact rocks. In the incoherent pozzolans, these correspond to similar deposits with very little lithological variations causing small changes in the chemical composition. The products show an evident acid composition. In relation with this aspect the pozzolan PZ-B that is in another region, it shows a low content of SiO_2, which classifies as a basic material but not acting in detriment of the pozzolanic activity index. It is very common that these materials

are found partially cemented with a vitreous paste with several degrees of alteration. The mineralogycal-petrologycal characteristics and the diagenetic processes affecting reach deposit, in particular can be consulted in Table 3.

Mexican tuffs (compacted materials) used as pozzolans have a first characteristic in their components (pyroclastic and matrix) in which outstanding process is zeolitization, which shows the great capacity, that volcanic materials have to produce this diagenetic transformation [8]. A zeolitic mineral identified (X-ray) in pozzolans, PZ-H and PZ-I is clinoptilolite. It is clear that there exists an important association between the alteration of the vitreous matrix of these tuffs with the presence of a pair of mineralogical species of diagenetic origin of zeolite type, evidence that has been proved in laboratory tests by Sersale [9]. As in the case of incoherent materials, its characteristics are shown in Table 3.

X-Ray Diffraction

By means of the X-ray diffraction patterns, the following constituents were identified at natural pozzolans: feldspars, quartz, cristobalite, clay minerals as chorite-montmorillonite and zeolitic compounds as clinoptilolite. Results are given in Table 4.

Table 3 Mineralogical and Petrological Characteristics of Natural Pozzolans

POZZOLAN/ CLASSIFICATION	MINERALOGICAL COMPONENTS (ESSENTIAL)	SPECIAL CHARACTERISTICS
PZ-A Tuff Vitreous Acid (*)	G and pumice lithics	• Pyroclastic texture • Voids and fluid structure
PZ-B Tuff crystal-vitreous Dacitic (*)	AN, Q, G, Andesite and Dacite Lithics	• Pyroclastic texture • Devitrification 20% • Andesite and dacite lithics altered by sericite 10%
PZ-C Tuff vitreous-lithic Rhyolitic (*)	G, Q,OL and pumice	• Pyroclastic texture • Voids structure • Lithics sericitized and oxided less than 10%
PZ-H Tuff vitreous Rhyo-dacitic ®	OL, Q, G and Andesite, dacite and pumice lithics	• Pyroclastic texture • Voids structure • Devitrification less than 30% • Lithics altered of dacite and andesite
PZ-I Tuff crystal-vitreous-lithics Andesitic ®	OL, AN, G and volcanics lithics	• Pyroclastic texture • Voids and cracked structure • Devitrification 100% • Some crystal dissolution • Matrix quartz-feldespatic • Mafics altered to clay
PZ-J Tuff vitreous Rhyolitic (*)	G, Q, S and OL	• Pyroclastic texture • Voids and fluid structure • Devitrification 10%
Notes: OL: Oligoclase AN: Andesine G: Glass	Q: Quartz S: Sanidine R: Rock	* : Incoherent material

Natural pozzolans

In the pozzolans it is possible to find characteristics easily measurable and correlate with their activity. Among these characteristics, the chemical composition plays an important part. In the Table 5. It can be seen that the chemical composition of Mexican natural pozzolans have a strong acid character, having a high (SiO_2 + Al_2O_3) content ranging around 75 to 84% of the total. Between the two oxides, silica prevails in all cases; it reaches percentages greater than 55%.

The importance of the content (SiO_2 + Al_2O_3) is clearly emphasized by the fact that the active vitreous phases of pozzolans generally are richer in silica and alumina content. Chemical composition of Mexican natural pozzolans either incoherent and tuffs are rich in silica. It is important to emphasize that the total alkalis content in Mexican pozzolans, is lower than 6,9%, whereas the loss on ignition is between 3,3-13,3% and the content of other elements like lime is less than 7%.

Chemical Analysis

The natural pozzolans to use as a mineral admixture in portland cement must meet certain chemical and physical requirements. For instance, ASTM C 618 Class N admixtures must have a minimum content of 70% in SIO_2 + Al_2O_3 + Fe_2O_3, whereas Mexican natural pozzolans have between 76,5 to 86,2%. This chemical requirement is arbitrary for the purpose, and does not have direct relationship with properties of material. Although, the importance of the content (SIO_2 + Al_2O_3) is emphasized by the fact that the active vitreous phases generally are richer in silica and alumina content. The Mexican natural pozzolans show a strong acid character, having a (SIO_2 + Al_2O_3) content ranging around 75 to 84% of the total.

Table 4 Mineralogical Identification by X-Ray Diffraction of Natural Pozzolans

POZZOLAN	MINERALS IDENTIFIED	IDENTIFICATION
PZ-A	F, Q and Crt	Cl: Chlorite
PZ-B	F and Crt	M: Montmorillonite
PZ-C	F	Crt: Cristobalite
PZ-H	Cl-M, Q, Clp and F	Q: Quartz
PZ-I	Q, Crt, F and Clp	F: Feldspar
PZ-J	Crt and F	Clp: Clipnoptilolite

Fly ash (FA) and silica fume (SF)

The silica content in FA is 57,7% and 73 % in SF; it is important to say that FA has a strong acid character due to it has a high (SiO_2 + Al_2O_3) content (85%); this is the main indication of its pozzolanic activity. The silica fume has a high silica content (73%); however do not meet with specified with ASTM C 1240 (13) the minimum content is 85%.

Pozzolanic Activity with Lime

The evaluation of pozzolanic activity is essential to consider and utilize a material as pozzolan. Lea [10] has proposed different methods to evaluate it. Mechanical strength tests nowadays are a basic complement to the petrographic and chemical methods. Besides, the two fundamental pozzolan characteristics are: a) ability to react with lime and b) ability to form products with binding properties [8]. According to results shown in Table 5, compressive strength of Mexican natural pozzolans ranged between 4,78 to 6,58 MPa, one case was less than 5,39 MPa specified by the ASTM Standard C 618.

It is well known that one of the fundamental conditions for a rapid zeolitization is the structure of finely subdivided volcanic glass [11]. In fact most easily zeolitizable pozzolans are those which have a more marked hydraulic activity as those presented mainly in PZ-H and PZ-I deposits. This reaction produces neohydrated phases (hydrated calcium silicates and aluminates in excess of lime) which are important to form binding compounds, which is very advantageous when the material contains silica and alumina easy mobilized, this is typic of amorphous structures and particularly of acid glasses [11].

In this study the materials containing zeolites were detected and they presented more reactivity than those containing vitreous constituents, this confirms work cited by R. Sersale [11]. This is due to probably to the more open porous structure of the zeolites, therefore more likely to be attacked. Indeed these pores allow chemical agents to penetrate, attacking their crystalline structure destroying and liberating silica, alumina and alkalis, the first of which combine with lime.

Pozzolanic Activity with Portland Cement

Although the principal pozzolanic reaction is the chemical reaction involving lime and silica, cementitious products are also formed as a result of the chemical reactions between lime, alumina or iron oxide. The essential difference between the pozzolanic reactions and the reactions involving the hydratation of portland cement alone is not in the composition of the hydration products [12].

The behavior of the Mexican natural pozzolans shows different compressive strength of the mortars pozzolan-portland cement mixture regard to Portland cement alone. Mechanical strength tests are still today the indispensable complement to chemical and physical methods. According to Table 5 strength activity index with Portland cement ranging of 91-103,1% at 28 days old, which over 75% specified by ASTM standard C 618 [13]. The pozzolans which contain zeolitic minerals as clinoptilolite they have a marked increase hydraulic activity as PZ-H (103,1% and 6,58 MPa) and PZ-I (97,3 and 5,98 MPa).

Fly ash (FA) and Sílica Fume (SF)

In regard to fly ash exhibit a pozzolanic activity of 72%, but is lightly less to 75% according to specified by the ASTM C 618. Sílica fume has a pozzolanic activity with Portland cement of 130%, however it has 73% of silica.

Table 5 Physical Properties and Chemical Analysis of some Natural Pozzolans, Fly Ash and Silica Fume

	PZ-A	PZ-B	PZ-C	PZ-H	PZ-I	PZ-J	FA	SF
Physical Tests								
Fineness , - passing 45 μm, %	93.9	93.6	93.6	93.8	94.5	94.6	32	63.0
Chemical Analysis, %								
SiO_2 (S)	69.2	55.1	70.1	62.1	64.8	69.1	57.7	73.1
Al_2O_3 (A)	13.6	19.9	13.9	11.6	14.1	14.7	27.2	8.3
Fe_2O_3 (F)	2.8	6.4	2.2	2.8	1.5	2.1	5.5	-
S + A + F	85.6	81.4	86.2	76.5	80.4	85.9		
CaO	1.8	6.4	1.0	5.8	3.1	1.7	4.4	1.5
MgO	1.0	3.9	0.5	1.7	0.6	0.8	0.8	13.3
SO_3	0.1	0.1	0.1	0.1	0.2	0.1	0.5	0.4
Na_2O	2.92	2.56	2.96	1.04	1.28	2.88	-	-
K_2O	3.20	2.44	5.98	1.94	1.76	5.20	-	-
Equivalent alkalis (as Na_2O)	5.02	4.17	6.89	2.32	2.44	6.30	-	-
Loss on ignition	5.0	4.2	3.3	13.3	10.7	3.6	2.6	3.0
Pozzolanic Activity with Portland Cement								
Activity index at 28 days	90.9	90.9	98.5	103.1	97.3	94.6	72	130 *
Pozzolanic Activity with Lime								
Compressive Strength at 7 days, MPa	6.58	4.78	5.75	5.93	5.98	5.64	-	-

* At 7 days

Results of Tests Performed According to ASTM C 1012 Method

Due to the expansion value is normally used to indicate the extent of sulfate attack. With the standard ASTM 1012 Test Method for Length Change of Hydraulic-Cement Mortars Exposed to a Sulfate Solution is possible to evaluate the performance of mortars made with Portland cements, blended cements, and blends of Portland cement with some supplementary cementing materials producing a sulfate-resisting cement mortar. The primary cause of the sulfate attack in mortars or concrete is the reaction between the C_3A present in the Portland cement and the sulfate ions (SO_4^{2-}) from the environment, resulting in the formation of expansive ettringite. The formation of gypsum, another expansive product, also takes place due to the reaction with $Ca(OH)_2$, a by-product of cement hydration and the sulfates. Although recent publications in the last 10 years dealing with physical sulfate attach, chemical sulfate attack, both internal and external (DEF), and holistic approach about sulfate attack. This paper deals to find which are the better supplementary cementing materials that can be used in Mexico to avoid that concrete structures suffer sulfate attack when are in service in a aggressive environmental of sulfate.

An experimental program was performed on the sulfate resistance of portland-pozzolan cements and blends with fly ash or silica fume with Portland cement replacement different levels of these materials, and reference mortars made with ASTM Type I, II and V cements. The results of performance tests on mortar bars exposed sulfate attack in 5% solution over a period of 52 weeks for the pozzolanic cements and FA-PC and SF-PC are shown in Table 6. The portland-pozzolan cement (CPZ-H, CPZ-I, CPZ-A and CPZ-J) mortars showed the lowest sulfate expansion at 52 weeks, so are considered of very high resistance sulfate attack. Figure 2 followed by, and the reference Type V cement mortar (Figure 1), in that order

(Figure 2). These cements contain pozzolans with very good pozzolanic activity forming products with binding properties improving the resistance sulfate. Instead, the reference Type II cement considered moderate sulfate attack resistance has a greater expansion than the pozzolanic cements at 52 weeks, besides mortar bars showed little cracks. The change length of the reference Type I and II are also illustrated in Figure 1. ASTM Type I has expansion very high at ages early (after 8 weeks) and the mortar bars are curved and with big cracks. ASTM Type II showed great change length after 26 weeks. Obviously, ASTM Type I is not resistance sulfate attack.

The performance of blends with fly ash-Portland cement show a moderate resistance sulfate attach with replacement level of 20% because it presents an expansion less than 0,1% at six months (26 weeks). With 30% of replacement resulted of high resistance and with 40 and 60% replacement levels showed an expansion less than 0,05% at 52 weeks being considered of very high resistance sulfate attack. The relative order of improvement is shown in Figure 2 Although the fly ash has a pozzolanic activity less than specification requirements of ASTM C 618 [15] and it is not very fine it is able to improve the sulfate resistance maybe by the dilution effect alone or part fly ash composition has constituents vitreous able to produce cementing compounds that improve the sulfate resistance. When is used silica fume replacement, the mortar bars show a good performance, all of the replacement levels improve sulfate resistance. The relative order of improvement found in this investigation is shown in Figure 2.

Petrographic Examination of Mortar Bars

In the Figure 3 are shown the mortar bars features seen under field sterioscopic microscopic. The microphotograph 3a) shows a great amount of cracks on all of surface of the bar mortar of ASTM Type I Portland cement exposed for 4 months in sulfate solution. The cracks showed salt precipitation and have irregular shapes and ramifications. Mortar presents a bad quality.

Table 6 Performance of sulfate attack at pozzolanic cements and blends with Silica Fume and Fly Ash and Portland Cements

Type	PC-I	PC-II	PC-V	CPZ-A	CPZ-B	CPZ-H	CPZ-I	CPZ-J	CPZ-J1	CPZ-ATC	SPECIF. ASTM C 1157 MS	SPECIF. ASTM C 1157 HS
26 weeks > 1		0,1	0,042	0,027	0,055	0,016	0,017	0,024	0.036	0.039	0.1	0.05
52 weeks		0,35	0,082	0,031	0,084	0,033	0,030	0,042	0.057	0.062		0.1
		FA20-PC	FA30-PC	FA40-PC	FA60-PC	SF10-PC	SF15-PC	SF20-PC				
26 weeks		0.057	0.04	0.019	0.016	0.027	0.027	0.016			0.1	0.05
52 weeks		0.113	0.08	0.034	0.020	0.042	0.042	0.034				0.1

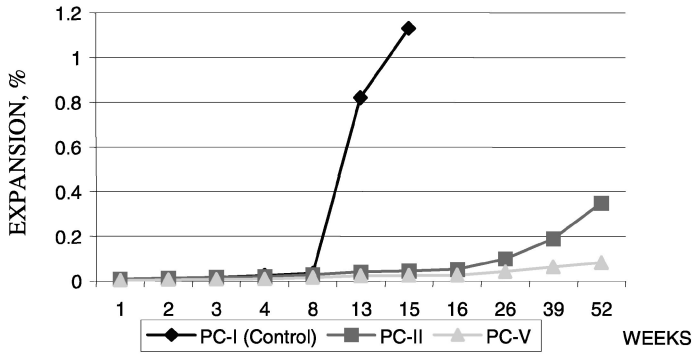

Figure 1 Performance of Portland cements exposed sulfate attack in 5% of Na_2SO_4 solution

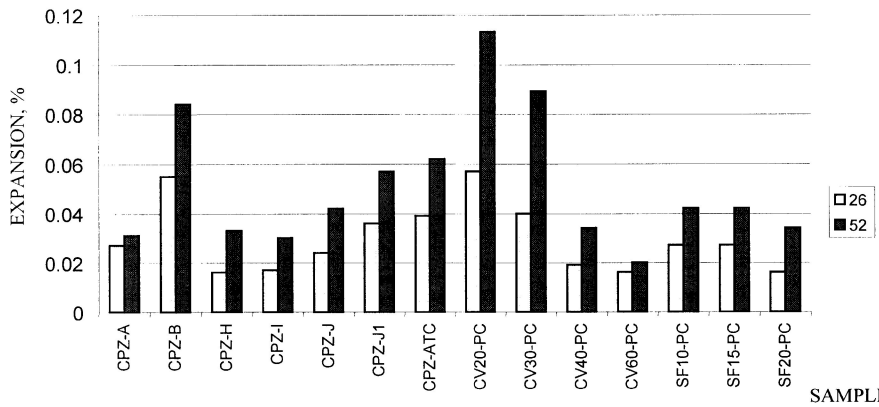

Figure 2 Expansion of mortar bars with different type of supplementary cementing material at 26 weeks and 52 weeks in 5% of Na_2SO_4 solution

The combination Portland cement-fly-ash with 20% replacement -FA20-PC-(Figure 3b) at one year exposed in sulfate solution shows some cracks mainly in edge of bars. They do not show ramifications. These cracks are partially filled with salt precipitation. Regarding the combination Portland cement-fly-ash with 60% replacement, Figure 3c at one year exposed in sulfate solution shows a homogeneous texture out cracks practically does not have damage. Mortar is qualified of good quality.

The combination SF10-PC (Microphotograph 3c) at one year exposed in sulfate solution shows a mortar of good features. Only it was observed some little cracks, neither there is damage evidence, and it is qualified of good quality.

In the case of pozzolanic-portland cements mortar bars at one year exposed in sulfate solution have a good performance, it was observed some little cracks. There is not damage evidence, and mortars are qualified of good quality.

It is important to consider of different types of attack sulfate, because nowadays there controversies about this subject. Frequently, physical attack by salt crystallization is being confused with classical attack which involves chemical interaction between sulfate ions from an external source and the constituents of cement paste or about internal –a chemical attack in which the source of sulfate ions reside in the concrete aggregates or cement [18].

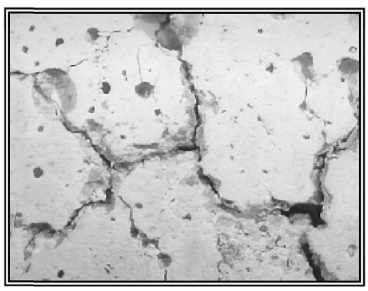

a) ASTM Type 1 Portland Cement-I. 4 months age

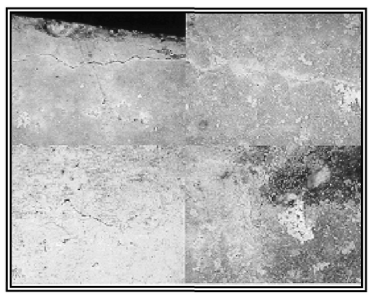

b) Combination FA20-PC. A year age

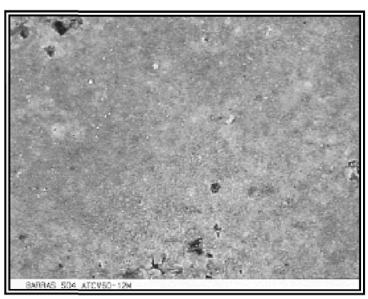

c) Combination FA60-PC. A year age

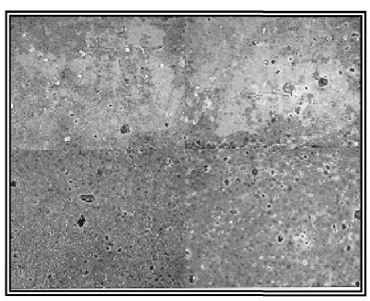

d) Combination SF10-PC. A year age

Figure 3 Microphotographs of different mortar bars observed under field stereoscopic microscopic

CONCLUSIONS

The Mexican natural pozzolans are characterized to be of pyroclastic origin, with diagenetic processes in a different scale; these processes were identified by means of the used test methods as: devitrification, sericitization, chloritization, oxidation and zeolitization.

Representative minerals of this lithological groups are: glass, oligoclase, andesine, quartz, pumice and volcanic lithics mainly of acid composition.

The principal finding from this study is that substantial sulfate resistance can be achieved equal to, or greater than Type II and V by using portland-pozzolan cements. This is particularly significant because the pozzolans used that show high pozzolanic activity increase sulfate resistance when are added as a mineral admixture. Mainly when the pozzolan contains zeolitic minerals as pozzolan PZ-H and PZ-I even containing less than 20 % in the cement, showing expansion less than 0,05%, how present very low expansion they can be considered of very high sulfate resistance, so CPZ-A and CPZ-J. The CPZ-B, CPZ-J1 and CPZ-ATC cements show expansion less than 0,1% a year and they can consider of high sulfate resistance.

The low expansion levels of mortars (less than 0,05%) at one year containing supplementary cementing materials are indicative of a total protection sulfate attack.

From this work was concluded that all of fly ash and silica fume replacement improve sulfate attack in a different grade, considering that by using fly ash replacement 40 and 60% and silica fume 10, 15 and 20% have a very high sulfate resistance.

REFERENCES

1. OUYANG, C H, A Damage Model for Sulfate Attack of Cement Mortars., Cement, Concrete and Aggregates, 1989, Vol11, No 2, p 92-99.

2. MEHTA, P K, Effect of Fly Ash Composition on Sulfate Resistance of Cement, ACI Journal Proceeding, 1986, Vol 83, No 6, November-December, p 994-1000.

3. RAMACHANDRAN, V S, Concrete Admixture Handbook, Properties, Science and Technology. Noyes Publications, p 304.

4. ASTM C 430, Test Method for Fineness of Hydraulic Cement by the 45 μm, (No 325), sieve.

5. ASTM C 114, Test Methods for Chemical Analysis of Hydraulic Cement, p 99-128.

6. ASTM Standard C 311-98, Tests Methods for Sampling and Testing Fly Ash or Natural Pozzolans for use as a Mineral Admixture in Portland-Cement Concrete, pp 185-192.

7. ASTM Standard C 1012-97, Test Method for Length Change of Hydraulic- Cement Mortars Exposed to a Sulfate Solution.

8. MASSAZZA, F, Chemistry of Pozzolanic Additions and Mixed Cements., The VI International Congress on the Chemistry of Cement, 1974, Volume I, Moscow, September, p 65.

9. SERSALE, R, The Constitution, genesis and Chemical behavior of Volcanic Tuffs, Rend. Soc. Min. Ital., 1961, No 17, p 499-536.

10. LEA, F M, The Chemistry of Cement and Concrete, Chemical Publishing Company Inc., New York, 1971, p 727.

11. SERSALE, R, Structure and Characterisation of Pozzolans and Fly Ashes, 7th International Congress of the Chemistry of Cement, Paris, 1980, Vol I.

12. MALHOTRA, V M, (Editor), Supplementary Cementing materials, CANMET Special Publication SP 86-8E, Energy, Mines & Resources Canada, Ottawa, Canada, 1987, p 25.

13. ASTM Standard C 1240-97b, Silica Fume for Use as a Mineral Admixture in Hydraulic-Cement concrete, Mortar and Grout, p 635-639.

14. METHA, P K, Sulfate Attack on Concrete: Critical Review, Concrete Durability, 1993, p 106-132.

15. ASTM Standard C 618-98, Specification for Fly Ash and Raw or Calcined Natural Pozzolan for Use as a Mineral Admixture in Portland Cement Concrete, p 298-300.

16. ASTM C 1157M-95, Standard Performance Specification for Blended Hydraulic Cement, 1996, p 481-484.

17. ACI 201.2R-92, Guide for Durability Concrete.

18. MEHTA, P K, Sulfate Attack on Concrete-Separating Myths from Reality,Suplementary Papers Fifth CANMET/ACI International Conference on Durability Concrete, Barcelona, Spain, 2000, p 1-112.

RESISTANCE OF PLAIN AND BLENDED CEMENTS UNDER DIFFERENT SULFATE ENVIRONMENTS

K K Sideris

A E Savva

University of Thrace

Greece

ABSTRACT Sulfate resistance of plain and blended cements under different sulfate environments is experimentally investigated in this paper. A total of eight different cements were used for the production of mortar specimens. All specimens were immersed in two different solutions: a 5% Na_2SO_4 solution and a 2.5%Na_2SO_4 + 2.5% $MgSO_4$ solution. Length change measurements were taken for a time period of two years. At the age of 2 years, compressive strength as well as flexural strength measurements were taken for all mixtures. Results indicate that fly ash blended cements have a very good performance in both curing environments.

Keywords: Blended cements, Fly ash, Length change, Natural pozzolan, Sulfate resistance.

Dr Kosmas K Sideris is lecturer at the Civil Engineering Department, Democritus Univercity of Thrace, Greece. He received his Ph.D. from Democritus University of Thrace, Greece, in 1996. His research interests include hydration of portland and blended cements, concrete technology and durability of cement and concrete.

Dr Athina E Savva is lecturer at the Civil Engineering Department, Democritus Univercity of Thrace, Greece, from which she received her B.Sc (Eng) and Ph.D. Her teaching and research interests are in cement and concrete technology, and she has authored or co-authored many papers on various aspects of concrete technology and durability.

INTRODUCTION

Sulfate attack is one of the mechanisms minimizing the effective life of concrete structures. Sulfates usually exist in significant concentrations in underground water and attack mainly underground concrete structures. The attack mechanism mainly depends on the cation of the salt [1]. In the case of Na_2SO_4, cementitious matrix of the material is corroded through the formation of crystalline compounds of ettringite ($C_6A\bar{S}_3H_{32}$) and gypsum ($C\bar{S}H_2$).

$$CaOH + Na_2SO_4 + 2\,H_2O \rightarrow CaSO_4.2H_2O + NaOH \quad (1)$$

$$C_4AH_{13} + 3\,CaSO_4.2H_2O + 14\,H_2O \rightarrow 6CaOH.Al_2O_3.3H_2SO_4.32H_2O + CaOH \quad (2)$$

$$4CaOH.Al_2O_3.H_2SO_4.12H_2O + 2CaOH.H_2SO_4.2H_2O + 16H_2O \rightarrow 6CaOH.Al_2O_3.3H_2SO_4.32H_2O \quad (3)$$

$$C_3A + 3CaSO_4.2H_2O + 26H2O \rightarrow 6CaOH.Al_2O_3.3H_2SO_4.32H_2O \quad (4)$$

Since ettringite is expansive in nature (it has a density of 1.73 g/cm^2 compared with an averaged density of 2.50 g/cm^2 for the other products of hydration), expansion and cracking of concrete are the results of sulfate attack caused by Na_2SO_4 [2]. The principal methods available to limit sulfate attack caused by Na_2SO_4 is the use of cements with lesser amounts of C_3A such as ASTM Type II or Type V Portland cements instead of Type I Portland cement. An alternative method is the use of additives – such as natural pozzolanas, fly ashes or silica fume. These materials decrease the total amount of C_3A available in the mixture, when they replace a portion of the cement. On the other hand they help by reducing the total $Ca(OH)_2$ content available in the mixture, as following:

$$\underset{(from\ pozzolan)}{Silica} + \underset{(from\ \text{cement})}{Portlandite} \xrightarrow[Normal\ \text{Temperature}]{H_2O} Secondary\ \text{C-S-H} \quad (5)$$

The attack mechanism is different in the presence of $MgSO_4$:

$$CaOH + MgSO_4 + 2H2O \rightarrow CaOH.H_2SO_4.2H_2O + MgOH \quad (6)$$

$$CxSyHz + xMgSO_4 + (3x-0.5y-z)H_2O \rightarrow x\,CaOH.H_2SO_4.2H_2O + xMgOH + 0.5y2SiO_2.H_2O \quad (7)$$

$$4MgOH + SHn \rightarrow M_4SH_{8.5} + (n-4.5)H_2O \quad (8)$$

Magnesium Hydroxide formed in Equation (6) is insoluble and its saturated solution has a pH value equal to 10.5 instead of 12.4 and 13.5 which is the pH value of saturated solutions of $Ca(OH)_2$ and NaOH respectively. The consequences of this low pH value can be summarized as follows [3-5]: i) Secondary ettringite will not form (not stable in low pH values); ii) $MgSO_4$ reacts with CSH to produce gypsum, brucite (MgOH) and silica gel (S_2H) (Equation 7); iii) CSH tends to liberate lime to raise the decreased pH. Liberated lime reacts further with $MgSO_4$ producing more MgOH (Equation 6); iv) concentration of gypsum and brucite will increase while CSH is destabilizing and becomes less cementitious; v) magnesium silicate hydrate formed by the reaction of brucite with hydrosilicates (Equation 8) is non-cementitious.

The main cause of deterioration due to $MgSO_4$ is therefore the conversion of CSH in a fibrous, amorphous material with no binding properties [3]. Protection solutions against Na_2SO_4 mentioned above are less effective in the case of $MgSO_4$ environments simply because there are different mechanisms to be faced: C_3A, C_4AF and their hydrates are not involved in equations 6 to 8 whereas $Ca(OH)_2$, which is the primary reactant constituent in Na_2SO_4 environments (Equation 1) constitutes in $MgSO_4$ environments the first line of defense by protecting CSH. It is well documented [5] that mixtures having sufficient resistance against Na_2SO_4 attack (such as blended cements and especially silica fume blended cements) suffer extended deterioration in $MgSO_4$ environments. In the latter those mixtures performed worst even from portland cement mixtures mainly because of their low content of portlandite [3, 5-6, 8].

Although there is a sufficient and clear view for the behavior of different mixtures under magnesium or sodium sulfate attack, there is little information concerning the influence of additives on the behavior of mixtures under mixed sulfate solutions [1, 7]. In this work the influence of additives in the performance of mixtures under mixed sulfate solution is experimentally investigated and compared with the corresponding one under sodium sulfate solution.

MATERIALS AND METHODS USED

The cements used were one normal portland cement and six blended cements, all of them produced in the laboratory by grinding together clinker, the appropriate pozzolanic material and gypsum ($CaSO_4.H_2O$). The gypsum content was different for each mixture, in order to keep the total SO_3 content of the binder (clinker + pozzolan) equal to 3.5%. A commerciall available cement, type II/A-M 32.5N according to EN 197-1 was also used, for comparison reasons. The pozzolanic materials used were a greek natural pozzolan of volcanic origin, Milos' Earth (ME) and two lignite fly ashes, Megalopoli fly ash (MFA) and Ptolemaida treated fly ash (PFA) Chemical composition of those materials, as well as the one of portland clinker are presented in Table 1.

Table 1 Chemical composition of the materials used

OXIDE CONTENT (% wt)	CLINKER	II32.5N CEMENT	MILO'S EARTH (ME)	MEGALOPOLI'S FLY ASH (MFA)	PTOLEMAIDA'S FLY ASH (PFA)
SiO_2	22	28	65.9	47.08	45.15
Free SiO_2	--	--	23.21	15.69	22.58
Al_2O_3	5.2	9	15.7	18.62	17.50
Fe_2O_3	1.9	5.5	3.95	6.72	8.18
CaO	65.4	48.0	4.0	17.50	14.87
Free CaO	1,53	--	--	2.96	1.64
MgO	2.0	2.2	1.4	3.81	3.44
SO_3	1.3	3.2	-	3.28	4.72
Na_2O	0.5	0.5	5.65	0.68	-
K_2O	1.0	1.5		1.52	-
Fineness (retainer %R45)	52.9	64	62.9	65.5	26

The cements produced are presented in Table 2.

Table 2 Cements used for mortar production

MIX NO	MIXTURE	CEMENT TYPE	SO_3 CONTENT OF THE MIXTURE CLINKER+GYPSUM
1	I42.5N	93,58% clinker+6,42% gypsum	3.5%
2	II32.5	CEM II32.5N	3.2%
3	10%ME	10%ME+84.24% clinker+5.76% gypsum	3.5%
4	30%ME	30%ME +65.52% clinker+4.48% gypsum	3.5%
5	10%MFA	10%MFA+84.78% clinker+5.22%gypsum	3.5%
6	30%MFA	30%MFA+67.57% clinker+2.43%gypsum	3.5%
7	30%PtFA	30%PtFA+66.18 clinker+3.92%gypsum	3.5%
8	40%PtFA	40%PtFA+58,61clinker+1,38%gypsum	3.5%
9	50%PtFA	50%PtFA+49,36%clinker+0,64%gypsum	3.5%

All mixtures were produced according to German Standard DIN 1164 using EN-196-1 standard sand. Mixtures immersed in Na_2SO_4 solution were prepared first. The water/binder ratio was different in order to achieve the same flow for all mixtures. Mixtures of second sere (immersed in mixed solution) prepared with a water/binder material ratio equal to 0.45. In this case different dosages of superplasticizer (Daracem 205) were added in order to keep the flow constant. The water/cementitous material ratio and the dosage of superplasticizer are presented in Table 3.

Table 3 Water/binder materials ratio of produced mortars

MIXTURES IMMERSED IN Na_2SO_4 SOLUTION			MIXTURES IMMERSED IN MIXED SOLUTION		
Mixture	w/binder ratio (%wt)	Flow meter (%)	Mixture	w/binder ratio (%wt)	Superplasticizer (%wt cem. mat.)
I 42.5N	0.456	114.75	I42.5N	0.45	1%
II 32.5N	0.53	114.5	II32.5N	0.45	1%
10% M.E.	0.48	111.5	10%ME	0.45	1%
30% M.E	0.52	113.5	30%ME	0.45	1%
10%MFA	0.48	105	10%MFA	0.45	1%
30% MFA	0.567	110	30%MFA	0.45	1%
30% PtFA	0.50	79.75	30%PtFA	0.45	2%
40% PtFA	0.55	94.25	40%PtFA	0.45	2%
50% PtFA	0.58	100	50%PtFA	0.45	3%

RESULTS AND DISCUSSION

Sulfate resistance was measured according to ASTM C-1012 [9]. Length change as well as bending flexural strength was measured at mortar prisms (40x40x160 mm) whereas cube specimens (50x50x50 mm) were used for compressive strength measurements. All specimens cured in warm curing room with relative humidity 95-98% and temperature of 35 °C until their compressive strength, measured on 50 mm cubes became equal or greater than 20 MPa. This happened for most mixtures after 24 hours. Only the 32.5N, 30% ME and 50% PFA specimens had to remain for 48 hours in the above room in order to achieve the 20 MPa strength. After that point they were immersed in the above aggressive solutions in a temperature of 20 °C.

Additional specimens were produced for both series and cured in a curing room with relative humidity 95-98% and temperature of 20 °C after their initial curing in the as above mentioned chamber. Length change measurements were taken up to the age of 2 years or the final deterioration of specimens, whichever happened first. Compressive and flexural strength measurements were also performed at the final test age. Length change measurements are presented in figures 1-2 whereas strength measurements are presented on Tables 4 and 5.

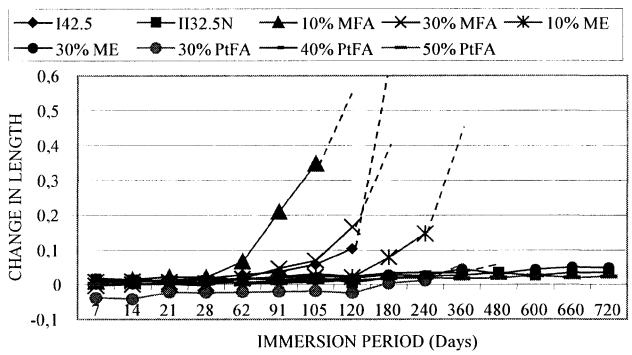

Figure 1 Length change measurements of specimens immersed in 5% Na_2SO_4 solution

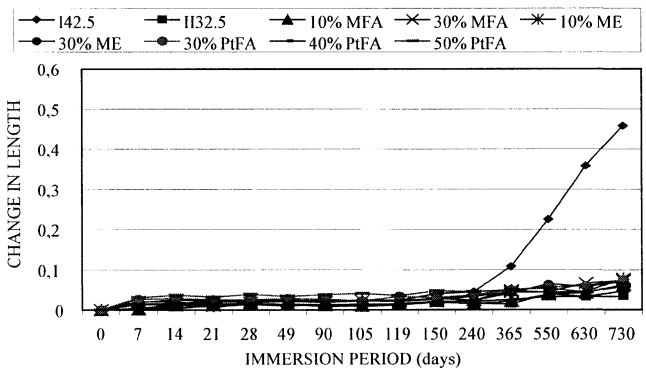

Figure 2 Length change measurements of specimens immersed in 2.5%Na_2SO_4 + 2.5%$MgSO_4$ solution

Table 4 Compressive and flexural strength reduction (%), final expansion (%), deterioration age and first crack observed age (months) for all mixtures immersed in Na_2SO_4 solutions

MIXTURE	COMPRESSIVE STRENGTH REDUCTION (%)	FLEXURAL STRENGTH REDUCTION (%)	EXPANSION (%)	DETERIORATION AGE (months)	FIRST CRACK (months)
I 42.5N	30	67.5	1.1	6-8	6
II 32.5N	15.4	-3.5 *	0.0354	Not deteriorated	16
10% ME	26.3	79.7	0.79	16-20	8
30% ME	0.4	44.3	0.0484	Not deteriorated	20
10% MFA	-	-	0.5443	4-6	No cracks
30% MFA	30	-	0.4081	4-6	No cracks
30% PtFA	19	17	0.049	12-16	No cracks
40% PtFA	15.3	14.7	0.0552	16-20	16
50% PtFA	-0.8 *	-153 *	0.0224	Not deteriorated	No cracks

Compr. Strength reduction = reduction to the compr. strength measured at the deterioration age due to sulfate attack
Flexural Strength reduction = reduction to the flexural strength measured at the deterioration age due to sulfate attack
(-) : Totally deteriorated, not measured
(*) : Strength increased

Table 5 Compressive and flexural strength reduction (%), final expansion (%), deterioration age and first crack observed age (months) for all mixtures immersed in mixed solutions

MIXTURE	COMPRESSIVE STRENGTH REDUCTION (%)	FLEXURAL STRENGTH REDUCTION (%)	EXPANSION (%)	DETERIORATION AGE (months)	FIRST CRACK (months)
I 42.5N	61.09	69.18	0.4583	Not deteriorated	No cracks
II 32.5N	44.8	11	0.0344	Not deteriorated	No cracks
10% ME	59.73	24.74	0.0781	Not deteriorated	No cracks
30% ME	69.01	24.73	0.07	Not deteriorated	No cracks
10% MFA	69.61	38.02	0.0625	Not deteriorated	No cracks
30% MFA	65.3	19.41	0.074	Not deteriorated	No cracks
30% PtFA	66.05	36.5	0.075	Not deteriorated	No cracks
40% PtFA	66.96	23.08	0.0469	Not deteriorated	No cracks
50% PtFA	61.6	14.04	0.0583	Not deteriorated	No cracks

Compr. Strength reduction = reduction to the compr. strength measured at the deterioration age due to sulfate attack
Flexural Strength reduction = reduction to the flexural strength measured at the deterioration age due to sulfate attack

Length change expansion

i) under Na_2SO_4 solution.

Different results are obtained when the sulfate resistance of the mixtures is examined. The 10% MFA mixture is the one with the greatest expansion from the age of 2 months, whereas all MFA mixtures started to deteriorate after exposure of 16 to 24 weeks (4 to 6 months) (Figure 1). Deterioration was very sudden. The control mixture performed cracks at the age of 6 months and from that point onwards deteriorated very fast, between 6 and 8 months. Mixture produced with commercial cement (CEM II32.5N) had a very good performance during the period of the test. In that case cracks

appeared after 16 months of exposure. No deterioration was observed until the age of 2 years.

Mixtures produced with natural pozzolans had a better sulfate resistance performance. The 10% ME mixture started to expand from the age of 4 months, cracks appeared at 8 months and it deteriorated between 12 and 16 months. The 30% ME mixture did not deteriorated during the period of the test. This mixture also suffered small expansion whereas it showed its first crack at the age of 20 months.

a) Na_2SO_4 attack b) $Na_2SO_4 + MgSO_4$ attack

Figure 3 Mode failure due to sulfate attack

Sulfate resistance of PtFA mixtures was satisfactory. Those mixtures underwent small expansions through the first year of immersion whereas the 30% showed signs of shrinkage during the first months. Deterioration occurred first on the 30% PtFA mixture, between 12 and 16 months. No cracks were observed at earlier ages. The 40% PtFA specimens deteriorated next, between 16 and 20 months. Specimens produced with 50% PtFA mixtures did not deteriorate until the end of the test.

Most of the mixtures produced with blended cements performed better sulfate resistance than the control mixture, although they had higher w/binder ratios. It also seems that as the replacement of clinker by a pozzolanic material increases, the sulfate resistance of the mixture also increases. This conclusion, which is in accordance with other research results [10-12], indicates that the decrease of C_3A content of the mixture is more critical than the

total porosity (which increases as the w/binder ratio also increases) when sulfate resistance is of primary interest. OPC mixture, as well as mixtures prepared with low pozzolan content cement, had the smallest sulfate resistance. Those mixtures also had the lowest w/binder ratio and the lowest total porosity [13].

ii) under Na_2SO_4+$MgSO_4$ solution.

Length change of all mixtures immersed in the mixed solution was different. No deterioration occurred during the 2 years time immersion period. The control mixture was the one who first started to expand from the age of 8 months (240 days). This mixture also had the greatest expansion at the age of 2 years, almost six times the expansion of 10% ME mixture (Table 5). The mixture produced with II32.5N cement had a very satisfactory sulfate resistance during the 2 years immersion period.

Mixtures produced with natural pozzolan had the worst total performance among all blended mixtures immersed in mixed solution The 10% ME mixture performed the second greater expansion after the one of the control specimen. On the other hand, the 30% ME mixture performed the smallest expansion among all blended cements with a 30% additive, irrespective of the material added.

Fly ash mixtures performed well at general, especially those produced with PtFA. MFA did not deteriorate and did not performed any cracks during the period of the test. Those mixtures had the worst performance when immersed in Na_2SO_4 solution. PtFA mixtures performed the smallest expansion among all blended mixtures tested, especially when the material replaced cement at percentages of 40% and 50%.

Strength reduction

Regarding strength reduction of mixtures due to Na_2SO_4 sulfate attack, it appears that the use of blended cements is generally effective (Table 4). Residual compressive strength of all blended cement mixtures is less affected or even equal (in the case of 30% MFA) to the strength of the control mixture. The same conclusion is drown for the flexural strength (except the flexural strength of 10% ME). All MFA specimens were totally deteriorated (Figure 3). This happened very suddenly, so the residual strength could not be measured.

Compressive as well as flexural strength increases in the 50% PtFA mixture. Those specimens also demonstrated the smallest expansion (Table 7) whereas they did not deteriorate and developed no cracks during the whole immersion period. According to other researchers [14], compressive strength of specimens immersed in Na_2SO_4 solutions initially increases beyond that of the control due to the pore filling by the reaction products of sulfate attack. Subsequently, the disruption of the cement matrix by those reaction products resulted in a strength decline. This means that in these cases the deterioration due to sulfate attack is very much prolonged, since the phenomenon is still in the first stage. It is also noticeable that those specimens were produced with the higher w/binder ratio (Table 3).

Compressive strength of mixtures immersed in mixed solution was significantly reduced (Table 6). This reduction is the result of the $MgSO_4$ deterioration mechanism [1]. Although it it well documented ([1, 3, 6-8] that compressive strength of blended mixtures is more affected than the one of portland cement mixture under $MgSO_4$ attack, this is not valid for the specimens immersed here in the mixed solution. All mixtures performed almost the same

reduction in compressive strength, but not in flexural strength as well. In this case specimens of the control mixture suffered the greater reduction whereas blended mixtures with great content of pozzolanic material (30% ME, 30% MFA and 50% PtFA) did not.

The failure mode under different sulfate environments is presented in Figure 3. In the case of Na_2SO_4 solutions deterioration is associated with the development of cracks (Figure 3a). Those cracks initially appeared at the edges of the specimen and gradually moved to its interior. Formation of crystalline compounds of ettringite as described in Equations (1) to (4) was mainly responsible for this phenomenon.

On the contrary, there were not any cracks in the case of mixed solutions (Figure 3b) although significant expansions were also observed. A thin layer of brucite formed on the major part of specimens' surface whereas deterioration also started from the edges of both prisms and cubes. Hydrated cement paste in these areas changed to a cohesionless granular mass which dissolute in the solution and left the aggregates exposed. This is mentioned elsewhere [6] as acidic type of sulfate attack.

CONCLUSIONS

Blended cement mixtures performed the best against Na_2SO_4 attack. It was also observed that the resistance of the mixture increased as the pozzolan content also increased. It is also noticeable that those mixtures were prepared with the higher water to binder ratio.

Those mixtures also had a very good performance against attack caused by the mixed solution. Blended cement mixtures suffered a compressive and flexural strength reduction almost equal to the one of the control mixture, but they performed significantly smaller expansion.

The attack mechanism under mixed sulfate solution could be explained as the simultaneous presence of two different mechanisms: the one of Na_2SO_4 attack (causes the expansion), and the one of $MgSO_4$ attack (causes the compressive and flexural strength reduction). It is proposed therefore to measure both length change and strength reduction of mixtures immersed in mixed solutions in order to investigate their resistance under this kind of sulfate attack.

Regarding the influence of the materials used in this research, it seems that addition of natural pozzolan, although it has a beneficial effect on Na_2SO_4 resistance of the mixture, results in less resistant mixtures under mixed solution attack. Among the lignite fly ashes used, PtFA has a beneficial effect, especially when it replaces cement at high contents, whereas MFA has a catastrophic effect in Na_2SO_4 solutions and a negative one in mixed solutions.

Results reported here are limited for the mixtures and solutions used in this research, since specimens immersed in Na_2SO_4 had greater porosity and were more permeable. Although it seems this was not reflected in their sulfate resistance (on the contrary, mixtures with the highest w/binder ratio performed the best sulfate resistance), further research has to be done in order to obtain a more representative icon regarding the attack mechanism as well as the influence of additives under different sulfate solutions.

REFERENCES

1. AL-AMOUDI, O.S.B.: "Mechanisms of sulfate attack in plain and blended cements: A review." Proceedings of the conference Extending Performance of Concrete Structures, pp. 247-260, International Congress "Creating with Concrete", Dundee, 6-10 September 1999.

2. LEA F.M.: The chemistry of Cement and Concrete, 3rd edition, Edward Arnold, London, 1970.

3. RASHEEDUZZAFAR, AL-AMOUDI, O.S.B., Abduljauwad, S. N. and Maslehuddin, M.: Magnesium-sodium sulfate attack in plain and blended cements. ASCE Journal of Materials in Civil Engineering, 1994, Vol. 6, No 2, May, pp201-222.

4. AL-AMOUDI, O.S.B., MASLEHUDDIN, M. AND SAADI, M. M.: Effect of Magnesium Sulfate and sodium sulfate on the durability performance of plain and blended cements. ACI Materials Journal, 1995, Vol. 92, No 1, pp. 15-24.

5. COHEN, M.D. AND BENTUR, A.: Durability of portland cement – silica fume pastes in magnesium sulfate and sodium sulfate solutions. ACI materials Journal, 1988, Vol. 85, No 3, May-June, pp.148-157.

6. AL-AMOUDI, O.S.B.: Sulfate attack and reinforcement corrosion in plain and blended cements exposed to sulfate environments. Building and Environment, 1998, Vol. 33, No 1, pp.53-61.

7. AL-AMOUDI, O.S.B.: Performance of fifteen reinforced concretes in magnesium-sodium sulfate environments. Construction and Building Materials, 1995, Vol. 9, No 1, pp. 25-33.

8. AMERICAN SOCIETY FOR TESTING AND MATERIALS: ASTM C-1012, "Length change of Hydraulic-cement Mortars Exposed to a Sulfate Solution», Annual Book of ASTM Standards, 1995, V.04.01, Philadelphia.

9. SERCALE R., GIOFFI R., DE VITO B., FRIGIONE G., ZENONE F.: "Sulphate Attack on Carbonated and Uncarbonatted Portlant and Blended Cement Mortars", Proceedings of the 10th International Congress on the Chemistry of Cements, Gotemburg, Sweeden, 1997, paper 4iv017.

10. MANGAT P.S., EL-KHATIB J.M.: "Influence of Initial Curing on Sulfate Resistance of Blended Cement Mortars", Cement and Concrete Research, Vol. 22, 1992, No 6, pp. 1089-1100.

11. IRASSAR E.F.: "Sulphate Resistance of Blended Cements: Prediction and Relation with Flexural Strength", Cement and Concrete Research, Vol. 20, 1990, No 1, pp. 209-218.

12. SIDERIS K. K.: "Influence of Natural Pozzolans on the Compressive Strength and Porosity of Cement Paste and Concrete", Ph.D. Dissertation, Democritus University of Thrace, Xanthi, Greece, 1996 (in Greek).

13. BROWN P. W.: "An Evaluation of the Sulfate Resistance of Cements in a Controlled Environment", Cement and Concrete Research, Vol. 11, pp. 719-727, 1981.

DURABILITY OF CONCRETE MADE WITH PORTLAND COMPOSITE CEMENTS CONTAINING LARGE QUANTITIES OF MINERAL CONSTITUENTS

A Garbacik

S Chladzynski

IMMB

Poland

ABSTRACT. In the paper performance characteristics of concrete made with Portland composite cements CEM II/B have been described. For investigation Portland-limestone cement, Portland-fly ash cement and Portland-slag cement containing respectively up to 35 % of limestone, fly ash or granulated blast-furnace slag were used. The investigation program of the concrete mixes covered standardised properties and some additional performance characteristics creating concrete durability. Frost resistance, sulphate resistance, permeability and porosity of concrete specimens were tested. It was stated that some non-clinker constituents of cement positively create performance properties of concrete with respect to durability. A high resistance against sulphate attack of Portland-fly ash cement have been proved. On the base tightness and permeability measurements of concrete specimens a very favourable influence of fly ash and slag Portland cement on cement matrix structure have been confirmed.

Keywords: Cement, Additions, Slag, Fly ash, Limestone, Durability, Heat of hydration, Porosity, Freeze-thaw, Sulfates.

Dr Eng Albin Garbacik, is Manager of Cement and Building Chemistry Department at IMMB. Specialist in technology of cement and concrete. Author of tens of publications connecting with cement and concrete and their applications into the building materials industry. Author of many applications of new technologies in Polish cement plants.

Dr Eng Slawomir Chladzynski, is Assistant Professor in Cement and Building Chemistry Department at IMMB. Specialist in technology of cement and concrete. His research interests include the durability of concrete. Author of several publications.

INTRODUCTION

Using of non-Portland clinker constituents in the cement technology is conditioned by some factors, which improve efficiency of cement production process. It is connected with replacement of energy-consuming clinker in cement by cheap secondary composites often waste materials. Ecological aspects to reduce CO_2 emission are also very important. On the other hand, non-clinker composites of cement play a significant role in shaping the processes of hydration and hardening of cement. Composite Portland cements containing Pozzolanic and hydraulic non-clinker constituents are characterised by many performance properties, which advantageously create durability parameters of concrete. This is a very important factor, which is responsible for large scale of production of cements containing mineral additives and universality of their application in concrete technology. The new cement standards that are elaborated according to the European Commission directives for CE marked products covers many kinds of cements containing large quantities of very different non-clinker constituents [1]. At the national levels, implementation of the European Standard makes the users afraid of durability of concrete made of some cements. So, the necessity of more detailed assessment of new kind of cements on account of durability features of concrete is especially important to choose proper cement for concrete constructions.

MATERIALS AND TESTING METHODS

The following commercial cements have been investigated:

- Portland-fly ash cement CEM II/B-V 32.5,
- Portland-slag cement CEM II/B-S 32.5 R,
- Portland-limestone cement CEM II/B-L 32.5.

As reference cement, Portland cement CEM I 32.5 R has been used. The normative properties of the cements have been specified in Table 1. The investigation program of the cements covered the following measurements: heat of hydration, concrete properties and resistance against sulphate corrosion. The heat of hydration of the cements was determined by usage of semi-adiabatic method, in accordance with the standard EN 196-9 [2]. The investigation of concrete was carried out on concrete mixtures and testing procedures as defined by the concrete standard EN 206 [3]. Resistance of cements to sulphate corrosion was investigated in accordance with the pr ENV 196-10 [4].

Table 1 Physical and mechanical properties of cements
(All tests were made according to the EN 196 Standard)

CEMENT	NON-CLINKER CONSTITUENT	WATER DEMAND, %	SETTING TIME, MIN		COMPRESSIVE STRENGTH AFTER DAYS, Mpa			
			Initial	Final	2	7	28	90
CEM I 32.5 R	none	25.0	145	205	20.9	34.2	46.2	54.3
CEM II/B-V 32.5 R	28 % of fly ash V	27.5	255	330	11.8	24.6	37.2	57.8
CEM II/B-S 32.5 R	32 % of slag S	24.5	155	225	17.1	34.7	51.2	62.2
CEM II/B-L 32.5	31 % of limestone L	26.5	210	295	8.8	23.3	35.7	42.2

RESULTS

Heat of Hydration of the Cements

Heat of hydration is of crucial importance as far as selection of proper cement for making concrete constructions is concerned. It is the feature of cement which is connected with destruction of concrete being a result of thermal cracks originating from usage - for certain kinds of massive constructions - cements of excessive heat of hydration [5]. Cements with some mineral additives show lower heat of hydration when compared with the Portland cement CEM I without non-clinker constituents. The heat of hydration of the cements CEM II/B under investigation has been presented in Table 2 and on Figure 1. It can be stated that slow-hardening cements 32.5 are characterised by very low heat of hydration. Cements CEM II/B-V and CEM II/B-L meet requirements for low heat cements. It makes them very useful for massive structures, where the process of self-heating of concrete becomes a serious hazard for its durability on account of possible destruction of concrete as result of thermal cracks.

Table 2 Heat of hydration of cements

CEMENT	HEAT OF HYDRATION, J/g			
	After 1 day	After 41 hours	After 3 days	After 7 days
CEM I 32.5 R	244	281	322	369
CEM II/B-V 32.5	122	212	225	271
CEM II/B-S 32.5R	209	252	290	331
CEM II/B-L 32.5	161	191	218	254

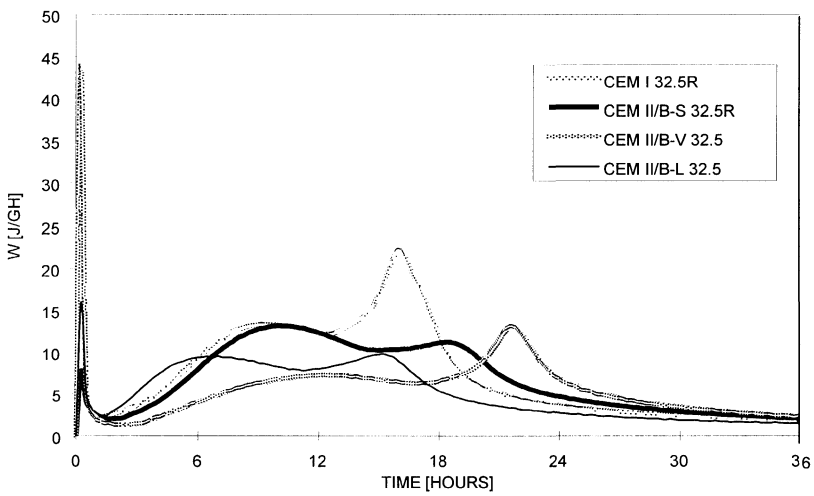

Figure 1 Kinetic curves of the heat of hydration of cements

Concrete Properties

The compositions of the concrete mixtures made of the cements listed in Table 1 have been presented in Table 3. The design assumption of the mixtures was done keeping the same parameters of aggregate selection and the concrete mixture consistency for all the cements under investigation. The scope of investigation of concrete properties covered: compressive strength, freeze resistance, water-permeability, water-absorbability and porosity. The measurements of compressive strength were made on cube samples 15×15×15 cm, after 7, 28 and 90 days of water curing. The results of the determination have been presented in Table 4 and Figure 2. The testing of resistance of concrete against freezing was conducted after 50 and 150 cycles of freezing and thawing. The results have been presented in Table 5. The tightness of concrete structures has been determined on the base of the measurement of water-permeability, water-absorbability and porosity. The results have been presented in Table 6. The porosity testing were made by using mercury porosimetry determining the fraction of pores in the range from 3.7 to 53600 nm in samples 8×8×30 mm cut out of the standard concrete cubes 15×15×15 cm.

Table 3 Concrete mixes composition

COMPONENT/ PARAMETER	UNIT	CEM I 32.5 R	CEM II/B-V 32.5	CEM II/B-S 32.5R	CEM II/B-L 32.5
Sand 0/2	kg/m^3	566	566	566	547
Gravel 2/8	kg/m^3	625	625	625	604
Gravel 8/16	kg/m^3	761	761	761	736
Cement	kg/m^3	320	320	320	350
w/c	-	0.54	0.55	0.53	0.47
Consistency	s	10	10	10	10
Air content	%	1.90	1.92	1.88	1.88

Table 4 Compressive strength of concrete

Cement	COMPRESSIVE STRENGTH AFTER DAYS, MPa		
	R_7	R_{28}	R_{90}
CEM I 32.5 R	39.1	45.3	48.8
CEM II/B-V 32.5	30.2	38.8	47.6
CEM II/B-S 32.5 R	28.9	39.5	45.3
CEM II/B-L 32.5	24.3	30.9	40.4

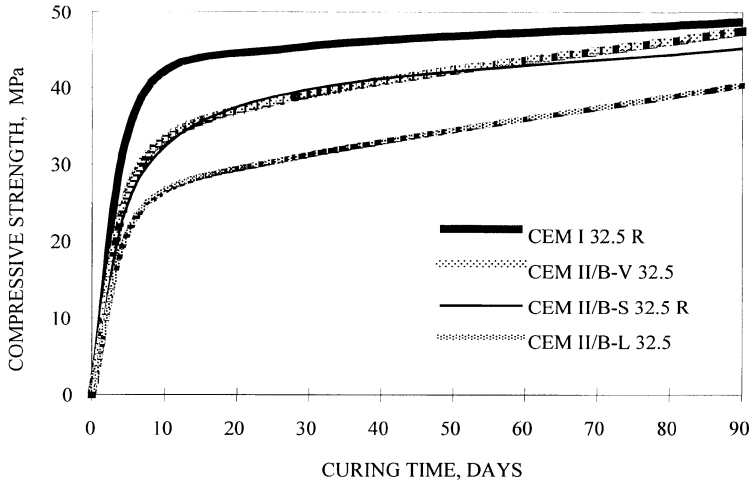

Figure 2 Compressive strength of concrete specimens

Table 5 Freeze / thaw resistance of concrete

CEMENT	50 CYCLES		150 CYCLES	
	Loss of mass, %	Loss of strength, %	Loss of mass, %	Loss of strength, %
CEM I 32.5 R	0.11	3.6	0.10	3.6
CEM II/B-V 32.5	0.06	2.8	0.05	10.1
CEM II/B-S 32.5 R	0.11	7.5	0.08	7.0
CEM II/B-L 32.5	0.29	0.9	0.19	3.4

Table 6 Permeation properties of concrete

PARAMETER	CEM I 32.5 R	CEM II/B-V 32.5	CEM II/B-S 32.5 R	CEM II/B-L 32.5
Water-permeability, cm (water penetration at 1.2 MPa)	7.6	9.4	3.9	7.6
Water-absorbability, %	5.09	3.99	5.43	5.86
Porosity, cm^3/g				
- after 2 days	0.051	0.073	0.057	0.067
- after 7 days	0.038	0.046	0.055	0.046
- after 28 days	0.028	0.042	0.038	0.036
- after 90 days	0.024	0.017	0.032	0.034

The results of investigation of the compressive strength of the concrete samples (Table 4) reflect the features of hydraulic activity of the applied cements (Table 1). The initial compressive strength of concrete samples made of Portland cement CEM I 32.5 R is significantly higher than the compressive strength of concrete made of Portland-composite cements CEM II/B. It gives evidence of higher dynamics of hardening of cement CEM I 32.5 R at the initial stage of hardening. Nevertheless, what is worth noticing is the very high dynamics of compressive strength development at later stages of hardening of concrete made of fly ash and slag Portland cements: CEM II/B-V 32.5 and CEM II/B-S 32.5 R. The compressive strength of concrete made of these cements after 90 days of curing is close to the compressive strength of concrete made of Portland cement CEM I.

The data given in Table 5 show very good freeze resistance of concrete made of Portland-composite cements CEM II/B. It should be underlined that these results have been obtained in case of not air entrainment concrete of nearly the same air content of about 1.9 % for all the cements (Table 3). The listed in Table 6 results of investigation of tightness of concrete structure also evidently indicate positive features of concrete made of Portland-composite cements CEM II/B. Both the water-permeability and porosity of concrete made of cements CEM II/B-V 32.5, CEM II/B-S 32.5 R and CEM II/B-L 32.5 R are comparable to the parameters of concrete made of cement CEM I 32.5 R.

The results of investigation of porosity and water-absorbability graphically presented in Figures 3 and 4 also confirm how big influence the mineral composites of Portland-composite cement can exert on shaping the tightness of the cement matrix. This effect is especially visible in case of Portland-fly ash cement CEM II/B-V: the porosity of concrete made of this kind of cement reaches, after a long time of concrete curing, the lowest values of all the investigated cements. Low porosity of concrete made of cement II/B-V 32.5 (Figure 3) influences on very low water-absorbability and water-permeability of concrete (Table 6).

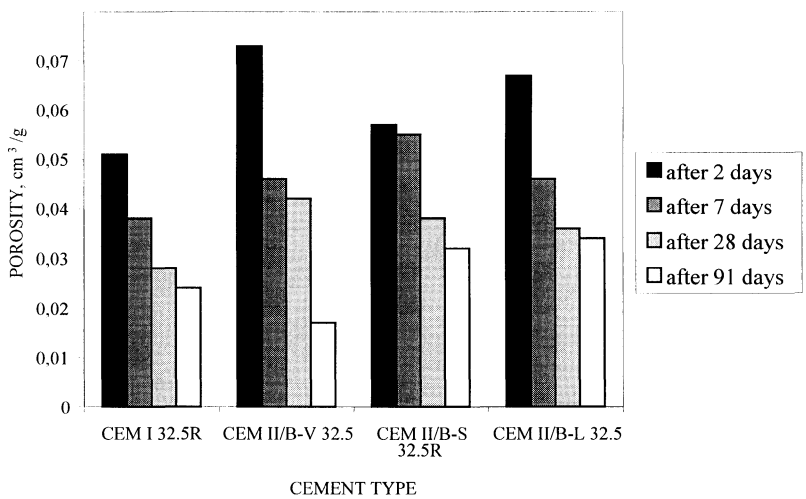

Figure 3 Porosity of the concrete specimens

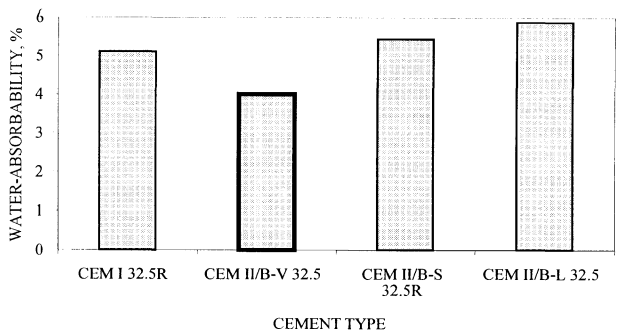

Figure 4 Water-absorbability of the concrete specimens

Sulfate Resistance

Mineral composites of cement decide in great measure of concrete resistance against aggressive influence of the environment. The results of determination of interaction between sulphate ions and the cements under investigation: fly ash, slag and limestone Portland cement have been listed in Figure. 5. According to the procedure involved in the investigations, the cement resistance against SO_4^{-2} attack is expressed by the value of expansion of cement mortar curing in sulphate solution. The results (Figure 5) confirm positive influence of mineral constituents on sulphate resistance of cement. Extraordinary favourable features in this respect shows Portland-fly ash cement CEM II/B-V 32.5. The resistance against sulphate aggression of the cement CEM II/B-V is comparable with the resistance of blast-furnace cement CEM III/B that is considered as very high sulphate resistance cement HSR. In practice it means that Portland-fly ash cement CEM II/B-V 32.5 can be the object of selection when concrete structures exposed to the corrosive action of sulphate environment are under consideration.

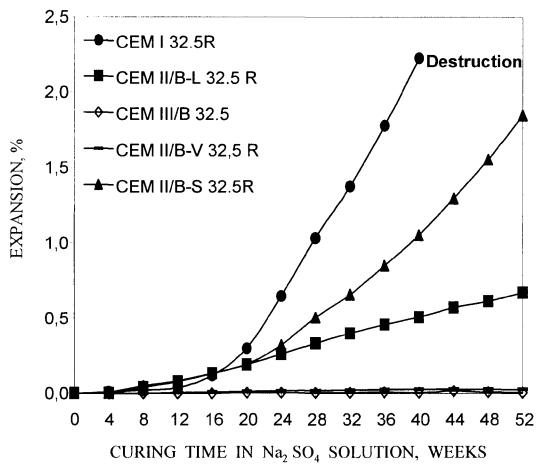

Figure 5 Expansion of cements in Na_2SO_4 solution

CONCLUSIONS

The national cement standards amendment according to the European standardisation system cover many kinds of new cements containing large quantity of different non-clinker constituent. Especially large group of this cements are Portland-composite cements CEM II. The CEM II/B cements can contain up to 35 % of fly ash, slag, limestone and Pozzolanic constituents. Mentioned non-clinker mineral constituents of cement can positively create performance properties of concrete. In the paper performance characteristics of concrete made of commercial cements: Portland-fly ash CEM II/B-V 32.5, Portland-slag CEM II/B-S 32.5 R and Portland-limestone CEM II/B-L 32.5 have been described. The presented investigations confirmed high quality of these cements and their good usability in concrete technology. The properties of Portland-composite cements CEM II/B allow to design and performance concrete of similar or even better - when compared with net Portland cement - usable features: strength development, water-permeability and water-absorbability, freeze resistance, resistance to aggressive influence of the environment. The Portland-slag cement CEM II/B-S 32.5 R which contains up to 35 % of the granulated blast-furnace slag is to be considered as especially favourable product which, on account of improved: water-tightness, shrinkage, water-absorbability, lowered heat of hydration, as well as extended workability time, can replace Portland cement CEM I 32.5 R. Characteristic features of Portland-fly ash cement CEM II/B-V 32.5 such as low heat of hydration, very high resistance to sulphate aggression, high water-permeability and low water-absorbability determine its special usability for massive concrete structures of high durability in aggressive sulphate environment.

REFERENCES

1. EN 197-1:2000, Cement - composition, specifications and conformity criteria. Part 1: Common cements.

2. EN 196-9:1998, Methods of testing cement- Part 9: Heat of hydration - Semi-adiabatic method.

3. EN 206:2000, Concrete - Performance, production, placing and compliance criteria.

4. prENV 196-10:1995, Methods of testing cement- Part 10: Determination of the resistance of cements to attack by sulphate solution or by sea water.

5. BENSTED, J., Low heat Portland cements. World Cement. Vol. 11, 42 (1993).

COMPUTATIONAL MODELLING OF CHLORIDE ION TRANSPORT IN REINFORCED CONCRETE

S J H Meijers **J M Bijen**
R de Borst **A L A Fraaij**
Delft University of Technology
Netherlands

ABSTRACT. Exposure to a saline environment is a major threat with respect to the durability of reinforced concrete structures. The chloride ions, which are present in seawater and de-icing salts, are able to penetrate the concrete to the depth of the reinforcement, where they eventually trigger a pitting corrosion process. The assessment of a corrosion-free service life of concrete structures is of paramount economic interest. However, the modelling of the ingress of chloride ions is complicated due to various influencing factors and transport mechanisms. Here a computational model for chloride ion transport through a porous material is presented. Chloride ion transport in reinforced concrete is modelled by focusing on centimetre-level and setting up three coupled equations for heat, moisture and chloride ion transport respectively. The model is handled computationally by discretising in space according to the finite element method and discretising in time according to the finite difference method. Stationary and transient, linear and non-linear, homogeneous or heterogeneous calculations can be performed. Moisture migration according to Bazant and Roelfstra has been implemented and Saetta's concept of chloride transport is followed. This is illustrated with a numerical example, which focuses on the coupling between chloride ion and moisture flow.

Keywords: Chloride penetration, Reinforced concrete, Corrosion, Coupled transport, Porous media, Durability, Finite element method

Sander Meijers got his MSc degree in civil engineering from Delft University of Technology in 1998. Currently he is PhD student at that university.

Jan Bijen has been director of INTRON for 20 years, the institute for quality assessment in the building industry in The Netherlands. Nowadays he is involved as a consultant. He is also a part-time professor in civil engineering materials at Delft University of Technology and director of FEMMASSE BV.

René de Borst has studied civil engineering at Delft University of Technology, where he graduated cum laude in 1982 and received his PhD in 1986, also cum laude. Since 1988 he is professor of computational mechanics at Delft University of Technology. He has received the Composite Structures Award (1995), the Max-Planck Research Award (1996), the IACM Computational Mechanics Award (1998) and the NWO/Spinoza Prize (1999).

Alex Fraaij is associated professor at the faculty of civil engineering of Delft University of Technology. His field of interest is additions in concrete, materials and environment.

INTRODUCTION

The design of concrete structures involves mainly the evaluation of strength, stability and durability. A major threat to concrete durability is chloride. As chlorides are present in salty water and de-icing salts, special care has to be taken in the design of off-shore structures, bridges and parking garages. Also buildings in coastal areas are subjected to chloride ion ingress. The deterioration mechanism is the following: chloride ions penetrate the concrete to the level of the reinforcement, when they are in a sufficient quantity they depassivate the rebars, pitting corrosion starts if also oxygen is available, the effective cross section of the rebars decreases and cracks appear due to the expansion of rust products. The cracks and the decrease of the effective cross section of the reinforcing steel bars imply a strength loss, while the cracks also enhance the deterioration process.

Chloride ion ingress in reinforced concrete has been subject of research for many decades and traditionally this process has been modelled by Fick's second law. The only material parameter in this model is the effective chloride diffusion coefficient. The adjective "effective" already suggests that many effects are hidden in this coefficient. Very few attempts have been made to substantially refine the modelling, e.g. by Saetta [1]. With the aid of current computing techniques, complex problems can be solved which could not be handled in the time the effective diffusion approach was proposed. Here a refined approach is presented based on the interaction of three simultaneous processes: chloride ion transport, moisture migration and heat flow.

THREE COUPLED BALANCES

Chloride ion transport is closely related to moisture migration, and both of them have relations with heat flow. Among the various processes that occur in reinforced concrete after it has been cast, these three are selected for the model, thereby excluding cement hydration, oxygen flow and the corrosion process. Since only the corrosion initiation phase is considered and the latter two processes are relevant just for the corrosion propagation phase, they are not taken into account. Cement may still be hydrating, even years after casting. However, if calculations are to be performed for the service life of concrete structures, periods of 50 to 100 years are of interest. Then the effect of cement hydration may as well be summed up in the initial conditions for such a calculation and the actual process can be disregarded.

While focusing on cm-level, the three coupled balances for heat, moisture and chloride ion transport are represented mathematically by:

$$\begin{bmatrix} c_{11} & c_{12} & c_{13} \\ c_{21} & c_{22} & c_{23} \\ c_{31} & c_{32} & c_{33} \end{bmatrix} \begin{Bmatrix} \dfrac{\partial T}{\partial t} \\ \dfrac{\partial H}{\partial t} \\ \dfrac{\partial C}{\partial t} \end{Bmatrix} = \nabla \cdot \left(\begin{bmatrix} k_{11} & k_{12} & k_{13} \\ k_{21} & k_{22} & k_{23} \\ k_{31} & k_{32} & k_{33} \end{bmatrix} \begin{Bmatrix} \nabla T \\ \nabla H \\ \nabla C \end{Bmatrix} \right) + \begin{Bmatrix} f_1 \\ f_2 \\ f_3 \end{Bmatrix} \tag{1}$$

in which the derivates of the quantities (E, W and C) with respect to the potentials (T, H and C) have been replaced by c_{ij}. Thermodynamical backgrounds of equation 1 are described in [2,3].

The capacities (c_{ij}), conductivities (k_{ij}) and sources (f_i) are in principle functions of the potentials. This makes the set of equations a set of coupled non-linear second order partial differential equations, or coupled non-linear diffusion equations.

SUBSTITUTED MODELS

Currently, this computational model is equipped with moisture migration according to Bazant [4] and Roelfstra [5], and follows the concept of chloride ion transport according to Saetta [1]. At some points Saetta's chloride model has been modified, as will be clarified in this section. The entire model has been implemented in the finite element code FEAP [6]; the computer routine is able to deal with stationary and transient (using Euler backward time stepping), linear and non-linear (using the Newton-Raphson method), homogeneous and heterogeneous, and coupled and uncoupled problems.

Moisture Migration

Basically, moisture migration is described with the following differential equation:

$$\frac{\partial W}{\partial t} = \frac{\partial W}{\partial T}\frac{\partial T}{\partial t} + \frac{\partial W}{\partial H}\frac{\partial H}{\partial t} = \nabla\left(\lambda_w \nabla H\right) \tag{2}$$

with W the moisture content (in kg/m^3), H the macroscopic pore humidity (dimensionless) and λ_w the moisture conductivity (in kg/ms). Division by the derivative of the moisture content with respect to the macroscopic pore humidity yields:

$$\frac{\dfrac{\partial W}{\partial T}}{\dfrac{\partial W}{\partial H}}\frac{\partial T}{\partial t} + \frac{\partial H}{\partial t} = \frac{1}{\dfrac{\partial W}{\partial H}}\nabla\left(\lambda_w \nabla H\right) \tag{3}$$

According to Bazant the righthand-side of the last equation can be replaced by:

$$\frac{1}{\dfrac{\partial W}{\partial H}}\nabla\left(\lambda_w \nabla H\right) = \nabla\left(k_{22}\nabla H\right) \tag{4}$$

with:

$$k_{22} = a_1\left(a_2 + \frac{1-a_2}{1+\left(\dfrac{1-H}{1-a_3}\right)^{a_4}}\right) \tag{5}$$

(in m^2/s), in which a_1 to a_4 are coefficients.

The moisture content W is described by the desorption isotherms given by Roelfstra:

$$W(T,H) = a_5 + a_6T + a_7H + a_8TH + a_9H^2 + a_{10}TH^2 \tag{6}$$

in which the coefficients a_5 to a_{10} are functions of the (initial) water-cement ratio and the degree of hydration. In this computational model, however, the water-cement ratio and the degree of hydration are constants. In [5] the moisture content is given in g per g cement; multiplication by the cement content of concrete yields kg per m^3 concrete. Then it follows that:

$$c_{21} = \frac{\frac{\partial W}{\partial T}}{\frac{\partial W}{\partial H}} = \frac{a_6 + a_8H + a_{10}H^2}{a_7 + a_8T + 2a_9H + 2a_{10}TH} \tag{7}$$

(in 1/K). It is clear that c_{22}=1. For the moment c_{23}, k_{21} and k_{23} all equal zero.

Chloride Ion Transport

Saetta sets up a balance for total chlorides C_{total} (in kg per m^3 concrete), i.e. the sum of free C_{free} (in kg per m^3 water) and bound C_{bound} (in kg per m^3 solid matrix) chlorides:

$$C_{total} = W^*C_{free} + \left(1 - W^*_{\max}\right)C_{bound} \tag{8}$$

with W* the volumetric moisture content (in m^3 water per m^3 concrete) and W^*_{max} the maximum volumetric moisture content (constant). Consequently, the factor 1-W^*_{max} equals the volumetric solid matrix content (in m^3 solid matrix per m^3 concrete), onto which chlorides can be adsorbed. The relation between the two definitions of moisture content is:

$$W = \rho_w W^* \tag{9}$$

with ρ_w the density of water (998 kg/m^3). Then equation 8 can be written as:

$$C_{total} = \frac{1}{\rho_w} WC_{free} + \frac{1}{\rho_w}\left(\rho_w - W_{\max}\right)C_{bound} \tag{10}$$

According to Saetta the ratio between bound and free chlorides can be considered to be fixed:

$$C_{bound} = \gamma C_{free} \tag{11}$$

in which γ is the constant of proportionality (dimensionless). Next, the last equation is substituted in the last but one equation:

$$C_{total} = \frac{1}{\rho_w}\left[W + \left(\rho_w - W_{\max}\right)\gamma\right]C_{free} = \varphi(T,H)C_{free} \tag{12}$$

in which φ replaces the factors preceding C_{free} in the last equation. As φ depends on W and W is a function of temperature and humidity, φ is a function of temperature and humidity as well.

Diffusive and Convective Chloride Ion Fluxes

The diffusive chloride flux $q_{c,diff}$ (in kg/m^{2}s) is given by:

$$q_{c,diff} = -\lambda_c \nabla C_{free} \tag{13}$$

in which λ_c is the macroscopic chloride conductivity (in m^2/s). This macroscopic chloride conductivity increases when more water paths are available in the porous medium or, alternatively, lack of water paths restrains the chloride diffusivity in a porous medium [1]. Hence λ_c is scaled (linearly) with the moisture content. Furthermore, λ_c is temperature dependent via the Arrhenius function. Then the macroscopic chloride conductivity becomes:

$$\lambda_c(T,H) = \left[(\lambda_{cw} - \lambda_{cd}) \frac{W(T,H) - W_d(T)}{W_w(T) - W_d(T)} + \lambda_{cd} \right] e^{\frac{U}{R}\left(\frac{1}{T_{ref}} - \frac{1}{T}\right)} \tag{14}$$

with λ_{cw} the chloride conductivity at H=100 % (constant), λ_{cd} the chloride conductivity at H=35 % (also constant), W_w the water content at H=100 % (temperature dependent) and W_d the water content at H=35 % (also temperature dependent). The Arrhenius function includes the following constants: U as the activation energy of the diffusion process (in J/mol), R the gas constant (8.3143 J/molK) and T_{ref} the reference temperature.

The convective chloride flux $q_{c,conv}$ (in kg/m^{2}s) is expressed by:

$$q_{c,conv} = -\frac{C_{free}}{\rho_w} \lambda_w \nabla H \tag{15}$$

In order to find an expression for λ_w, equation 4 is elaborated:

$$\nabla \left[\frac{\partial W}{\partial H} k_{22} \nabla H \right] - k_{22} \frac{\partial^2 W}{\partial T \partial H} (\nabla T)^T \nabla H - k_{22} \frac{\partial^2 W}{\partial H^2} (\nabla H)^T \nabla H = \nabla (\lambda_w \nabla H) \tag{16}$$

in which T in superscript denotes transposition. Assuming that the second order derivatives in the second and third term on the lefthand-side of the last equation can be neglected, the following substitution is valid:

$$\lambda_w = \frac{\partial W}{\partial H} k_{22} \tag{17}$$

Total Chloride Ion Content Balance

The balance for total chlorides can now be set up. The change of the total choride content within a reference volume is equal to the net diffusive and convective influx of free chlorides:

$$\frac{\partial C_{total}}{\partial t} = \nabla\left[\lambda_c(T,H)\nabla C_{free} + \frac{C_{free}}{\rho_w}\frac{\partial W}{\partial H}(T,H)k_{22}(H)\nabla H\right] \tag{18}$$

Substitution of equation 12 yields:

$$\frac{\partial C_{total}}{\partial t} = \nabla\left[\lambda_c(T,H)\nabla\left(\frac{C_{total}}{\varphi(T,H)}\right) + \frac{C_{total}}{\rho_w\varphi(T,H)}\frac{\partial W}{\partial H}(T,H)k_{22}(H)\nabla H\right] \tag{19}$$

This balance for total chlorides makes it possible for the free chloride content to increase when the water content decreases due to evaporation and vice versa. The balance can be further elaborated, which results in:

$$\frac{\partial C_{total}}{\partial t} = \nabla\left(k_{31}\nabla T + k_{32}\nabla H + k_{33}\nabla C_{total}\right) \tag{20}$$

with:

$$\begin{aligned} k_{31}(T,H,C_{total}) &= -\frac{\lambda_c(T,H)C_{total}}{\rho_w\varphi^2(T,H)}\frac{\partial W}{\partial T}(H) \\ k_{32}(T,H,C_{total}) &= \left[k_{22}(H) - \frac{\lambda_c(T,H)}{\varphi(T,H)}\right]\frac{C_{total}}{\rho_w\varphi(T,H)}\frac{\partial W}{\partial H}(T,H) \\ k_{33}(T,H) &= \frac{\lambda_c(T,H)}{\varphi(T,H)} \end{aligned} \tag{21}$$

Clearly, this balance for total chlorides is directly coupled to the temperature and moisture balance, and the corresponding differential equation is very non-linear. Obviously, it holds that c_{33}=1, and that c_{31} and c_{32} both equal zero. As compared to [1] the following modifications have thus been introduced:

- the free chloride content is not assumed to be constant within a small region of material
- the moisture balance does not appear in two different forms
- desorption isotherms are included for temperatures ranging from 293 to 343 K
- φ is a function of temperature and humidity and differentiated accordingly
- the degree of hydration is constant
- λ_c varies linearly with the moisture content

NUMERICAL EXAMPLE

This example shows a 10·10 mm^2 piece of concrete which is exposed to a chloride solution on the left side; the other sides are impermeable for chlorides. Simultaneously, drying takes place in vertical direction. This direction has been chosen perpendicular to the direction of chloride ingress to visualise the effect of coupling between the two flows. The moisture

potential on the top side is prescribed to be 36 % and on the bottom side 100 %; the moisture cannot escape through the other sides. The temperature has been kept constant in this example. The model parameters can be found in Tables 1 and 2.

Table 1 Material functions input parameters. If the material function is a function of other parameters (see Table 2), these parameters are enclosed in parentheses

MATERIAL FUNCTIONS					
capacities		conductivities		sources or sinks	
c_{11}	$2.40 \cdot 10^6$ J/m^{3}K	k_{11}	2.40 J/Kms	f_1	0 J/m^{3}s
c_{12}	0 J/m^3	k_{12}	0 J/ms	f_2	0 kg/m^{3}s
c_{13}	0 J/kg	k_{13}	0 Jm^2/kgs	f_3	0 kg/m^{3}s
c_{21}	(a_6 ... a_{10}) 1/K	k_{21}	0 m^2/Ks		
c_{22}	1	k_{22}	(a_1 ... a_4) m^2/s		
c_{23}	0 m^3/kg	k_{23}	0 m^5/kgs		
c_{31}	0 kg/m^{3}K	k_{31}	(λ_{cw},λ_{cd},a_5 ... a_{10},U,T_{ref},γ,W_{max}) kg/Kms		
c_{32}	0 kg/m^3	k_{32}	(λ_{cw},λ_{cd},a_1 ... a_{10},U,T_{ref},γ,W_{max}) kg/ms		
c_{33}	1	k_{33}	(λ_{cw},λ_{cd},a_5 ... a_{10},U,T_{ref},γ,W_{max}) m^2/s		

If the piece of concrete is exposed to a chloride solution of 50 g NaCl per 1 water (corresponding to a 3.0 % solution), then the boundary condition for the total chloride ion content is obtained by assuming that at this boundary:

- all pores are water-filled, so $W=W_{max}$
- the concentration of free chloride ions in these pores is the same as in the salty water to which the concrete is exposed, so $C_{free}=(35.5/(23.0+35.5))50=30.3$ kg/m^3 (kg Cl^- per m^3 of water)

For a certain concrete mixture the total pore volume can be calculated according to [7]. Then the boundary condition follows from equation 12. In case of ordinary Portland cement, a water-cement ratio of 0.59, a cement content of 320 kg/m^3, a degree of hydration of 95 %, γ equal to 0.7 [1] and the chloride concentration mentioned earlier, this boundary condition becomes 22.5 kg/m^3 (kg Cl^- per m^3 of concrete).

The problem type in this example is transient, partly non-linear, homogeneous and partly coupled. The computed total chloride ion distribution is shown in Figure 1. The total chloride ion contents range from 0.3 to 25.9 kg/m^3, which is equivalent to 0.1 to 8.1 %. When comparing Figure 2 (the total chloride ion distribution in the absence of a moisture potential field) and Figure 1 the building up of chlorides in the upper left corner becomes apparent. Clearly the upward moisture flow drags the chloride ions in the same direction and together

with the continuous supply of chloride ions from the left, this leads to an excess of chlorides in the upper left corner (note that the chloride content in that area is higher than the boundary condition).

Table 2 Parameters of the moisture and chloride model

MOISTURE MODEL					
basic moisture content parameters			derived moisture content parameters		
degree of hydration	0.95			0.35<H<0.85	0.85≤H≤1.00
water-cement ratio	0.59	a_5		38.1 kg/m^3	4.48·10^3 kg/m^3
cement content	320 kg/m^3	a_6		0 kg/m^{3}K	-12.2 kg/m^{3}K
conductance parameters		a_7		1.59·10^3 kg/m^3	-8.90·10^3 kg/m^3
a_1	1.00·10^{-10} m^2/s	a_8		-5.25 kg/m^{3}K	23.6 kg/m^{3}K
a_2	0.05	a_9		-1.38·10^3 kg/m^3	4.83·10^3 kg/m^3
a_3	0.70	a_{10}		4.77 kg/m^{3}K	-12.3 kg/m^{3}K
a_4	4				

CHLORIDE MODEL					
Arrhenius parameters		conductance parameters		adsorption parameters	
U	32.0·10^3 J/mol	λ_{cw}	1.00·10^{-12} m^2/s	W_{max}	138 kg/m^3
T_{ref}	296 K	λ_{cd}	1.00·10^{-12} m^2/s	γ	0.7

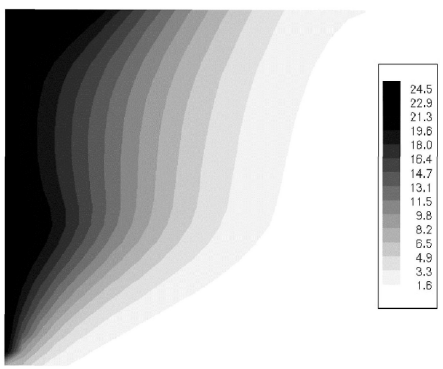

Figure 1 Computed total chloride ion content (in kg/m^3) after 40 days of exposure. Clearly the bottom-up moisture flow influences the chloride-ion flow from left to right. Consequently, the chloride accumulates in the upper left corner

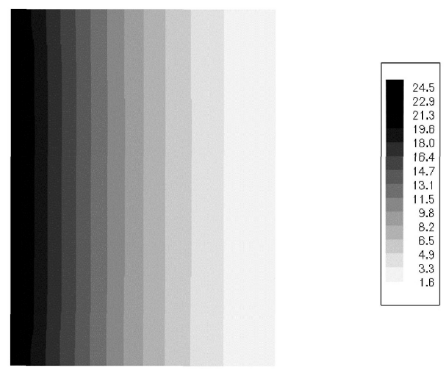

Figure 2 Reference total chloride ion distribution (in kg/m^3) after 40 days of exposure in the absence of a moisture potential field (H=90 %)

CONCLUSIONS

Since chloride ingress in concrete is closely related to moisture migration, while both of them are temperature-dependent, it is essential to involve all three processes in calculations. Currently, the implemented finite element routine is able to deal with stationary and transient, linear and non-linear, homogeneous and heterogeneous, and coupled and uncoupled problems. The combination of moisture migration according to Bazant and Roelfstra, and Saetta's concept of chloride transport has been studied. An example illustrated the behaviour of the computational model. In the future more models and sets of parameters will be tested and verified to reach the goal of reliable service life prediction.

ACKNOWLEDGEMENTS

The computational mechanics group of the faculty of civil engineering and geosciences is greatly acknowledged for providing outstanding computational facilities and for kindly helping with the implementation.

REFERENCES

1. SAETTA, A.V., SCOTTA, R.V., VITALIANI, R.V., Analysis of chloride diffusion into partially saturated concrete, ACI Materials Journal, September 1993, Vol.90, No.5, pp 441-451.

2. GROENEVELT, P.H., BOLT, G.H., Non-equilibrium thermodynamics of the soil-water system, Journal of Hydrology, 1969, No.7, pp 358-388.

3. GRUNEWALD, J., Diffusiver und konvektiver Stoff- und Energietransport in kapillarporösen Baustoffen, Dissertation, Technischen Universität Dresden, Dresden 1997, Germany.

4. BAZANT, Z.P., NAJJAR, L.J., Nonlinear water diffusion in nonsaturated concrete, Matériaux et Constructions, 1972, Vol.5, No.25, pp 3-20.

5. ROELFSTRA, P.E., A numerical approach to investigate the properties of concrete, Numerical concrete, Dissertation, Ecole Polytechnique Fédérale de Lausanne, Lausanne 1989, Switserland, 199 pp.

6. ZIENKIEWICZ, O.C., TAYLOR, R.L., The finite element method, Ed.4, McGraw-Hill, Berkshire 1997, England, United Kingdom.

7. REINHARDT, H.W., Beton als constructiemateriaal, Eigenschappen en duurzaamheid, Delft University Press, Delft 1985, The Netherlands.

SILICA PHOSPHATE IN ENGINEERING MATERIALS

N Abdel-Rahman

N M Naghoj

Al-Balqa' Applied University

Jordan

ABSTRACT. This research presents the results of an experimental investigation carried out to study the technological basics of a new material characterised by its high compressive strength and its resistance to acids. One hundred and thirteen cylindrical 45 x 30 mm samples with height to diameter ratio of 1.5 were prepared by mixing suitable ratios of quartz sand and phosphoric acid, burned in a furnace to temperatures between 800-1400° C for 2 hours. On the basis of test results gathered from this study, a new silica-phosphate material is suggested.

Keywords: Silica, Phosphoric acid, Mixing ratio, Burning temperature, Properties.

Dr N Abdel-Rahman, is an Assistant Professor of Civil Engineering in Amman College for Engineering Technology at Al-Balqa' Applied University, Jordan. Dr Abdel-Rahman has been involved in research in building materials and soil stabilization.

Dr N M Naghoj, is a Lecturer in the Department of Civil Engineering, Amman College for Engineering Technology at Al-Balqa' Applied University, Jordan. Dr Naghoj received his B.Sc. from Alexandria University, Egypt, and his Ph.D. from University of Edinburgh, U.K.

INTRODUCTION

A number of investigations looked at the bonding effect of Silica-phosphate. Iler in 1962, and Yates in 1972, found that the reaction of P_2O_5 with silica at a relatively low temperature develops high bond strength in refractory compositions. Both of them come to the fact that silica sol may be mixed with ammonium phosphate or other P_2O_5 precursors at relatively low pH and used in minimal quantities as a binder in refractories [1].

In 1961 Nobel, Bradstreet and Rechter found that improved bond strength in ceramic bodies is attained with mixtures of mono aluminum phosphate and colloidal silica when used with finely divided refractory powders of ziricon, ziriconnia, or alumina [1].

Researchers have not come to an agreement about the nature of the bond of silica-phosphate. Some published literature [2] related the nature of bond to two compounds SiO_2 .P_2O_5 and $2SiO_2$, others related the bond nature to $3SiO_2.P_2O_5$ compound. According to a study conducted by Tien and Hummel [2] in 1962, the compound $SiO_2.P_2O_5$ melt congruently at 1290° C, and exists in two polymorphic modifications, with a transition temperature of 1030° C. The compound $2SiO_2.P_2O_4$ melts incongruently with decomposition into $SiO_2.P_2O_5$ and silica-rich liquid at 1120° C. In 1968 Liebau and Bissert [3] have obtained different modifications of $P_2O_5.SiO_2$ by using various forms of SiO_2 and P_2O_5. These modifications are cubical, tetragonal, two monoclinic, orthorhombic, hexagonal and pseudo-hexagonal modifications. They also obtained a hexagonal phase of variable composition, which includes the compounds, $P_2O_5.3SiO_2$ and $2P_2O_5.3SiO_2$.

Nurse, Welch and Gutt [4] have investigated high-temperature phase equilibria in the system $2CaO,SiO_2$-$3CaO,P_2O_5$ by high-temperature microscopy and *X*-ray analysis. The system was presented a continuous series of solid solutions with a melting-point maximum at 2240° C. A new high-temperature form of $3CaO,P_2O_5$ was discovered but it was not survived quenching to room temperature. At lower temperature two compounds were formed by solid-state reactions, the known silicocarnotite stable below 1450° C and a new phase denoted as "A," stable below 1125° C, having the approximate composition $7CaO,P_2O_5,2SiO_2$. The properties of building materials governing their suitability for service under various conditions depend first on chemical and mineralogical composition of the material. The present work is directed to develop a new acid resistance building material taking into consideration the effect of acid rain on some parts of the world. Two important factors should be considered when developing it, the availability of cheap raw materials and the material suitability to withstand different conditions.

This investigation aims to find cheap engineering building materials from local raw materials to produce ceramics, thermal bricks and blocks characterised by solid physical, dynamical and chemical properties.

EXPERIMENTAL WORK

A total of one hundred and thirteen samples of silica-phosphate cylinders, that are 45 mm in height and 30 mm in diameter, were tested to study their physic-chemical features and their resistance to acid mediums. The mineralogical and chemical analysis of the tested quartz sand samples was achieved by using the x-ray fluorescence method.

The method used to produce silica-phosphate material consists of four stages:

In the first stage, the raw sand material, mostly of silica, was ground to very fine grains with the sand surface weight kept between 3000 to 4000 cm^2/gm. In the second stage, the silica sand was mixed with phosphoric acid with a ratio varying between 5 to 15% of the total silica sand weight. In the third stage, the silica-phosphoric acid mixture was cast in steel moulded cylinders. The samples then were removed from moulds, ready for their furnace heat treatment. In the fourth and final stage, the cast samples were placed inside a muffle furnace, in which a maximum temperature of 1400° C can be achieved. Four burning temperatures were adopted, these temperatures were 800° C, 1000° C, 1200° C and 1400° C. The sample maintained at these temperatures for 2 hours. Then the samples were removed to cool at laboratory temperature.

The specimens were tested under axial compression using screw type machine. The load was applied and increased continuously at a nominal rate within the range 0.2 $N/(mm^2.s)$ to 0.4 $N/(mm^2.s)$ conforming to BS 1881: Part 116: 1983 [5]. The specific gravity and the water absorption of the specimens were obtained by a standard method generally used for the determination of specific gravity and absorption of coarse aggregate [6]. The specimens were first immersed in water for approximately 24 hours, to essentially fill the pores. It is then removed from the water, the water dried from the surface of the particles, and specimens then were weighed. Subsequently they were weighed while they were submerged in water. Finally they were dried in an oven at 110 ± 5° C for 24 hours and massed. Using the mass and weight measurements obtained and formulas in the standard method, the specific gravity and absorption were obtained. In order to obtain the specimens porosity, the specimens absolute specific gravity were determined. The specimen whiteness was obtained using colour charts. The percentages of specimen resistance to acids were obtained after weighing the specimens before and after acid soaking for 72 hours.

RESULTS AND DISCUSSION

The percentage ratios of the raw sand components to their weight are given in Table1.

Table 1 Mineralogical and chemical analyses of used materials

COMPOSITION (%)	SiO_2	Al_2O_3	Fe_2O_3	CaO	MgO	SO_3	LOI
Quartz Sand	98.3	0.5	0.2	0.3	-----	0.1	0.4

Table 2 summarises the results of the compressive strength for all samples, and specifies the specific gravity and percentages of porosity, water absorption and whiteness of each group of samples burned at each specified burning temperature.

Figure 1 shows the relationship between the samples percentage of water absorption and the burning temperature for quartz samples mixed with 10% phosphoric acid. The Figure shows a decrease of the water absorption percentage when the burning temperature was 1200° C. Figure 2 shows the compressive strength-temperature curves for samples mixed with 5%, 8%, 10% and 15% phosphoric acid. Compared to samples mixed with 5% phosphoric acid, the curves show a 47.8%, 88.7% and 68.5% increase in the compressive strength when burning temperatures was 800° C for samples mixed with 8%, 10% and 15% phosphoric acid respectively.

Table 2 Physic-chemical features of silica-phosphate material

BURNING TEMP (°C)	MIXING (%)		NUMBER WHITENESS OF SAMPLES	COMPRESSIVE STRENGTH (N/mm²)	POROSITY (%)	SPECIFIC GRAVITY (%)	WATER ABSORPTION (%)	(%)
	SiO_2	H_3PO_4						
800	95	5	5	3.18	18.8	2.08	7.8	95.2
	92	8	5	4.7				
	90	10	5	6.0				
	85	15	5	5.36				
1000	95	5	5	13.75	7.8	2.22	3.2	95.8
	92	8	5	17.27				
	90	10	5	21.94				
	85	15	5	27.88				
1200	95	5	5	32.05	1.27	2.29	0.5	97.4
	92	8	5	40.47				
	90	10	5	51.09				
	85	15	5	43.65				
1400	90	10	5	39.83	6.8	2.25	1.4	96.5

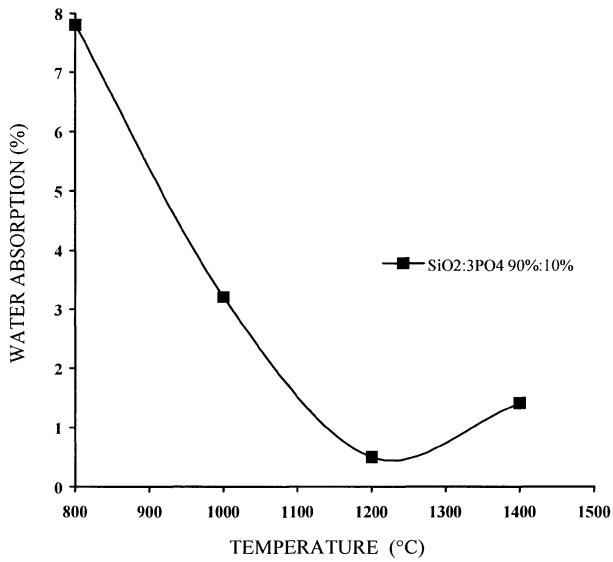

Figure 1 Effect of burning temperature on water absorption

The Figure shows that the compressive strength was increased by 25.6%, 59.7% and 102.8% when burning temperatures was 1000° C for samples mixed with 8%, 10% and 15% phosphoric acid respectively. The increase was 26.3%, 59.4% and 36.2% when burning temperatures was 1200° C for sample mixed with 8%, 10% and 15% respectively. For sample with 10% of phosphoric acid the Figure shows a decrease of 22% in compressive strength when the burning temperature was increased from1200° C to 1400°C.

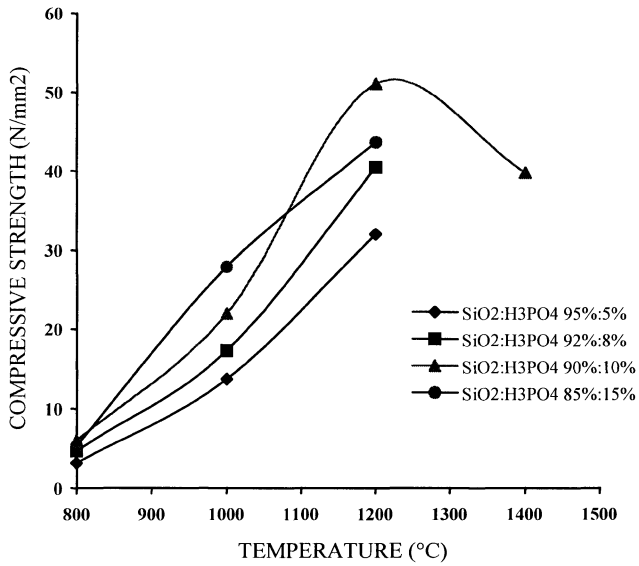

Figure 2 Effects of burning temperatures on compressive strength

Table 3 summaries the results of the resistance of the silica phosphate sample to acid mediums. The acids used were hydrochloric acid, sulfuric acid, nitric acid and phosphoric acid.

Table 3 The resistance of silica phosphate material to acid medium

MIXING		BURNING TEMPERATURE	NUMBER OF	RESISTANCE TO ACIDS (%)			
SiO_2	H_3PO_4	(°C)	SAMPLES	H_3PO_4	H_2SO_4	HNO_3	H_3PO_4
90	10	800	12	92.9	91.4	92.1	90.3
90	10	1000	12	97.3	95.6	96.4	94.7
90	10	1200	12	99.7	99.5	99.8	99.4
90	10	1400	12	98.2	97.4	96.6	98.3

Figure 3 shows the percentage of the resistance of silica-phosphate material to acid medium-temperature curves, each curve presents the percentage of the resistant of the silica-phosphate material sample to one individual acid at burning temperature of 800° C, 1000° C, 1200° C and 1400° C. The results obtained from the Figure shows that the silica-phosphate resistance to the acid medium was improved. The maximum resistance occurred when the burning temperature was 1200° C.

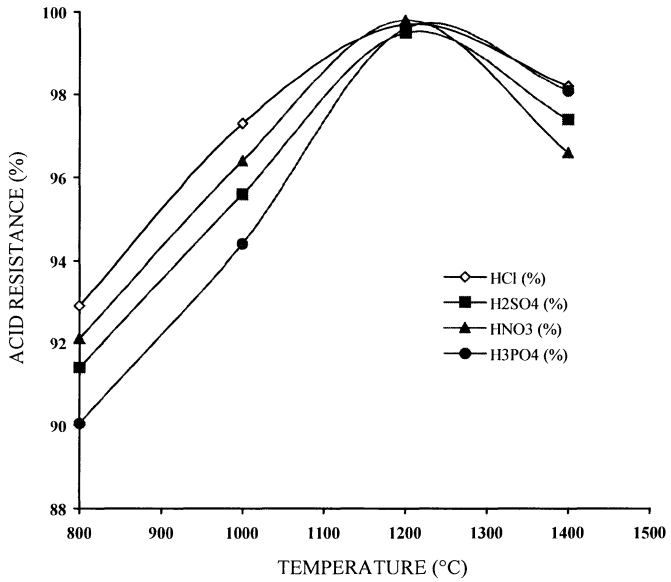

Figure 3 The resistance of the silica phosphate materials to acid mediums

SCOPE OF USING

Silicate technology has been going through a tangible development. Steam moistening of quartz sand for molding parts has become widespread at brickyards. This set up the opportunity of more quantity, in the same time raised the quality, that ends with better structural, architectural, decorative, every day use, refractory and acid resistant materials. Silica phosphate can be used to construct buildings, roads, and drainage systems for the acid rain regions. It can be also used due to its characteristics as wall materials, hollow bricks, tiles, roofing material and as covering layer of bricks and stones.

CONCLUSIONS

1) A new, cheap building material characterised by high compressive strength, low porosity, and low water absorption, notable for its lightweight, whiteness and its resistance to acid mediums, can be made when burning silica with phosphoric acid with a suitable mix at about 1200° C.

2) The high compressive strength of the new material is attributed to the stabilization of the silica and phosphate in many aspects of its structural formation, the reformation of free silica oxide and also for the decrease of the voids caused by high temperatures and consequent chemical reactions.

REFERENCES

1. ILER, R. K., The chemistry of silica, Willey, New York, 1979, p 866.

2. TOROPOV, N. A., BARZAKOVSKIV, V. P., LAPPIN, V. V., KURTSEVA, N. N., Handbook of phase diagrams of silicate systems, Toropov, N A (Ed), 2nd Edition, Izdatal, stvo "Navka", Leningradskoe otdelenie, Leningrad, 1969. [Engl. Transl., Keter press, 1972, p 723].

3. NURSE, R. W., WELCH, J. H., GUTT, W., High-temperature phase equilibria in the system dicalcium silicate-traicalcium phosphate, Journal of the Chemical Society, London, 1959, Part I, p 1077-1083.

4. LIEBAU, F., BISSERT, G., Synthesis and crystallographic data of some phases in the system SiO_2-P_2O_5, Bull. de la Soc. Chim. de France, 1968, p 1742- 1743.

5. BRITISH STANDARDS INSTITUTION, Testing concrete: Methods for determination of compressive strength of concrete cubes, BS 1881, Part 116, 1983.

6. AMERICAN SOCEITY FOR TESTING AND MATERIALS, Specific gravity and absorption of coarse aggregate, ASTM C127-84, 1986.

A NEW SPECIAL CLINKER COMPOSITION WITH LOW CLINKERABILITY TEMPERATURE THAT PRODUCES A CEMENT HAVING HIGH RESISTANCE TO STRONGLY AGGRESSIVE SULFATE ATTACK

F G Gomà

M D Vicente

Polytechnic University of Barcelona

Spain

ABSTRACT. Certain naturally occurring cements, having constant raw composition, have been found to possess raw properties with low clinkerability temperature. These provide cement that possesses a much higher resistance to the attack of strongly aggressive sulfate solutions. The resistance to sulfate attack was determined by means of series of 20 x 20 x 20 micro-cubes, and series of prisms 40 x 40 x 160 mm, in accordance with the 196-1 EN standard, of pure paste with a water/cement ratio of 0.4, which were similarly cured in water at 20ºC. The physical and chemical parameters were determined for the prepared mortars compressive strength, the results of which are provided. A study of the modification of the internal porosity of the samples in function of the sulfate ions was carried out. The results and conclusions appear to provide a new aspect to the influence of structure density of the C-S-H phases in expansion due to ettringite formation, when the silicate content is low and there is also sufficient space for occupation by the ettringite. The need to locate clinkers having a low degree of clinkerability temperature for sustainable energetic and ecological reasons and to obtain information that leads to better understanding of the effects of expansion due to sulfates justify the interest in this work. A new parameter is suggested both for the control of concrete sensitivity to sulphate attack as well as in the verification of actual behaviour in field studies.

Keywords: Calcium sulfoaluminate, Low energy cements, Sulfate attack.

Professor F G Gomà, is Director of the Research Chemistry Laboratory and Professor in Department of Architectural Construction at the Polytechnic University of Barcelona. He specialises in Analytical Chemistry and Durability of Concrete and Materials, and has been associated with the research of the manufacturing of Portland cement (Asland associated with Blue Circle).

Dr M D Vicente, is an Associated Chemist in the Research Chemistry Laboratory, Department of Architectural Construction at the Polytechnic University of Barcelona.

INTRODUCTION

Natural cements with constant raw chemical composition have been found in certain cretaceous geological strata associated to cretaceous coals as in "torre de Foix", Vallcebre in Berga, Catalonia, Spain, which possess chemical compositions which are very similar to ordinary raw Portland cements. When these materials are calcined at low temperatures, between 1.000 and 1.200ºC, they display technically significant characteristics and properties, unknown up to now and which are examined in this paper. The work reported in this paper is part of an extensive study to investigate whether the Ettringite formation as a major component of the C-A-H phases in the products of a hydrated cement could be an alternative binder.

In the sulfate resistance tests performed using the micro-cube technique by the described aggressive solution attack [1] and prism 40X40X160 mm., in accordance with the 196-1 EN standard, it was found that they possess very high sulfate attack resistance.

The mortar samples, after curing in the usual manner, and maintained in highly aggressive 5% sulfate solutions, underwent a progressive increase in compression strength. In this case, reaching values of up to 45 Mpa from between six months and one year, and which have since been under observation for more than two years to the present date. This means that, in this case, the aggressive solution unexpectedly behaves as a curing solution which contributes extrinsic sulfate to the formation of secondary Ettringite as the cause of an increase in strength instead of its destruction. Finally, an interpretation of the secondary Ettringite formation mechanism for these cements which do not reveal themselves as being expansive, could lead to new orientations of current knowledge on the resistance of concrete to sulfate attack.

EXPERIMENTAL DETAILS

Determination of Chemical and Mineral Composition of Clinker of this Natural Cement

A representative sampling was taken of the industrial clinker in which the variation in the major components did not exceed 3%. The chemical composition of the obtained mean sample of clinker was analysed in accordance with current standard EN 196-2 procedures, with the exception of the silica determination which was carried out using a version of the classic gravimetric procedure modified by the author [2]. The results include a representative sample of Ordinary Portland Cement clinker for comparative reference.

The natural cement clinker under study was calcined at a temperature of 1,200ºC and its composition had a lime Kstll "British Lime Saturation Factor" of 61.1%, whereas that of the Portland cement clinker used as a reference was 96.1%.

The SO_3 content in the natural cement clinker was 3.0%, while that of the Portland clinker was 0.66%. The natural cement clinker silica ratio (SR) was 1.85. This is lower than the 2.23 of the Portland clinker. The analysis results are shown in Table 1.

The clinkerability temperature of the raw mix of this ordinary Portland clinker, taken as a reference, was evaluated using the author's procedure [3] and was determined to be 1.625ºC, whereas the natural cement clinker, which was calcined in a vertical kiln at1.200ºC produced a free lime value of less than 2%. The energy consumption is therefore, considerably less, as is the produced level of pollution.

Table 1 Chemical analysis and physical properties of binders

	NATURAL CEMENT WHOLE SAMPLE	SOLUBLE[2] FRACTION AS WHOLE SAMPLE	INSOLUBLE RESIDUE AS WHOLE SAMPLE	ORDINARY PORTLAND CLINKER AS REFERENCE
TiO_2	0.24	0.09	1.16	0.15
SiO_2	22.0	13.9	60.6	20.8
Al_2O_3	8.9	6.6	16.7	6.1
Fe_2O_3	3.0	1.6	10.8	3.2
CaO	45.3	43.8	3.3	64.9
MgO	0.82	2.2	0.80	1.8
Na_2O	0.30	0.16	1.1	0.19
K_2O	1.7	1.2	3.9	0.54
SO_3	3.0	3.2	0.2	0.66
L.O.I.950°	12.2	12.2	0.2	1.1
Insoluble Residue[1]	14.6	-	-	0.50
$\overline{A}/\overline{S}$ Molar ratio	23.32	-	-	7.25
CaO Free	1.6	-	-	0.8
KstII %	61.1	-	-	96.1
Bogue Potential Compounds (%)				
C_3S	-	-	-	60
C_2S	-	-	-	16
C_3A				11
C_4AF	-	-	-	10
Fineness				
% passing 88 μm 32	-	-	-	99
% passing 63 μm 18	-	-	-	95
Compression Strength N/mm^2				
R_2	8.5	-	-	34.3
R_{28}	11.3	-	-	63.1

[1] Soluble in 10% HCl when cold
[2] Soluble Fraction Gomà method [18]

Clinker Finishing and Mechanical Strengths

The examined representative clinker sample was ground up in accordance with the special conditions for technical use as a building cement and no additives was added. The Portland cement clinker sample was ground with added gypsum in order to obtain 3.0% SO_3 in the resulting cement, together with a fineness equivalent to a cumulative value of 95%, which would pass through a 63-micron sieve. Three series of micro-cubes 20X20X20 mm., and three series of prisms 40 x 40 x 160 mm, in accordance with the 196-1 EN standard, with a water/cement ratio of 0.5 and an S/C ratio of 1:3, with standardised sand, were prepared and cured by immersion in water at 20°C.

One of these series of each type of mould was employed in obtaining the compression strength results and the other two for post curing attacks in aggressive solutions of 5% sodium sulfate and 5% magnesium sulfate respectively. The cement obtained from the natural cement clinker was ground, without any added additives, to a fineness equivalent to an accumulative value of 82%, which passed through a 63-micron sieve, and had a maximum particles size of 600 microns. This was used to prepare another three series of 20 x 20 x 20 micro-cubes, and three series of prisms 40 x 40 x 160 mm, in accordance with the 196-1 EN standard, of pure paste with a water/cement ratio of 0.4, which were similarly cured in water at 20°C. For natural cement mixtures were prepared with de-ionised water and 0.4 %, over the cement, of the citric acid was employed to delay setting and hardening by 30 to 40 minutes in order to mould under suitable conditions. After 28 days of water curing, they were all checked for compression strength.

After 28 days of water curing, one series of each type of mortar and cement were immersed in aggressive solutions of 5% sodium sulfate and 5% magnesium sulfate respectably both saturated with $Ca(OH)_2$. In all these samples, the compression strength was periodically determined during a period of two years. These results are shown in Figure 1.

Hydration Specifications and Aggressive Attacks Conditions

All the pure paste specimens and micro-cubes were hydrated at 20°C in water, chamber-cured for 24 hours, removed from the moulds and immersed in de-ionised water at 20°C in order to carry out prior water curing up to 28 days. They were then placed in aggressive solutions of Na_2SO_4 at 5 % and $MgSO_4$ at 5 %, respectably saturated with $Ca(OH)_2$ on a long-term basis for up to two, after which the XRD patterns for the samples were determined and the results are given in Figure 2, in values KαCu. In order to establish any variations occurring to the physical parameters of the material in the pure paste specimens with natural cement due to the aggressive treatment, the physical parameters were determined in accordance with the standard ASTM C-642 method using cement paste micro-cubes which had been cured for 28 days in water and, at the end of this period, placed into the aggressive solution treatment period. The results are given in Table 2.

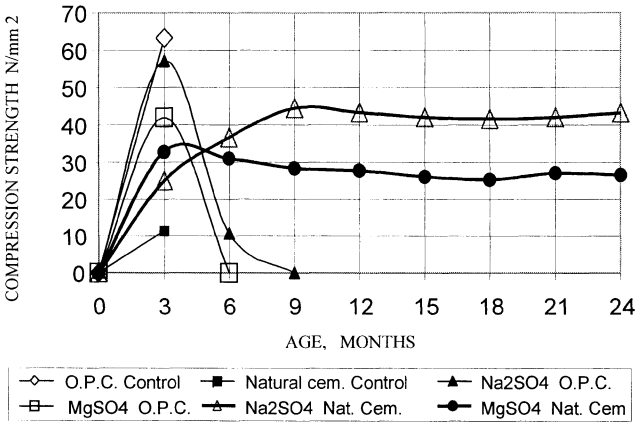

Figure 1 Compression strengths development

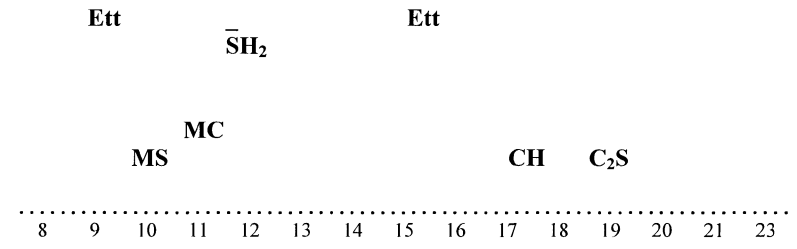

Ett = Ettringite
MC = monocarboaluminate
SH_2 = Gypsum
MS = calcium monosulfoaluminate
CH = calcium hydroxide
C_2S = β calcium disilicate

Figure 2 X-ray patterns of natural cement pure paste attacked 1 year with Na_2SO_4

Table 2 Physical properties of natural cement pastes A/C 0.4

	AFTER WATER 28 d CURED	AFTER 1 YEAR Na_2SO_4 ATTACKED	AFTER 1 YEAR $MgSO_4$ ATTACKED
Absorption after immersion %	32.7	20.4	22.9
Bulk specific gravity cm3/g	1.45	1.67	1.55
Apparent density cm3/g	2.78	2.53	2.45
Volume of permeable voids %	47.7	34.0	35.5

DISCUSSION OF RESULTS

The experimental facts which we established in our work are described as follows: after water curing, the natural cement having the described composition and specifications, has a strength of between 12 to 15 N/mm^2 when tested as a pure paste under the described granulometric conditions and with a water/cement ratio of 0.4 When the specimens were previously cured in water for 28 days and then exposed to highly aggressive water containing 5% sodium sulfate and/or 5% magnesium sulfate both saturated with calcium hydroxide ($Ca(OH)_2$) at 20°C, they undergo a progressive increase in compression strength during between six and twelve months, which can reach 40 to 45 N/mm^2. No expansion or degradation phenomena were observed in any of the cases and the levels of strength attained remained constant during observation of up to two years at the time of writing. This progressive increase in strength occurred at the same time as the physical parameters were modified, with a reduction in porosity of some 13 to 15% in the sodium sulfate solutions and noticeably less, 11 to 13%, in the magnesium sulfate solutions.X-ray diffraction confirmed that the amount of ettringite formed is very significant and is present in the dominant phase.

Background to this Fact Found in the Literature

The differences found between the natural cement clinker under study and the OPC clinker taken as a reference is summarised in the following Table:

Table 3 The differences found between the natural cement clinker and OPC clinker

	$\bar{A}/S$ MOLAR	SO_3 %	LIME SATURATION FACTOR % KstII	MS	CLINKERABILITY T °C
Natural cement clinker	2.32	3.0	61.1	1.85	1.200
Portland cement clinker	7.25	0.6	96.1	2.23	1.625

We have therefore compared it with the clinkers and cements of the $CaO\text{-}SiO_2\text{-}Al_2O_3\text{-}SO_3$ system.

There are background studies into these types of clinkers/cements by Nakamura and Sodoh [4]; Mehta and Klein [5]; Deng-Jun [6]; and Sodoh [7]. These show that obtained compression strength values are comparable to those of OPC (Ordinary Portland Cement) and that the Ettringite is either controlled or is not produced.

The common factor in these cements is the fact that the dominant phase is the secondary Ettringite as a hydrolysis product.

Among which, those of Sodoh [7] produced cements from clinkers with A/′ molar ratios close to 1.3, in which the compression strength tests carried out in accordance with the JIS R 5201 standard, produced a value of 59 MPa at 28 days. The authors used scanning electron techniques to determine that this Ettringite has a crystallisation of 1 to 2 μm within hardened mass having a large specific surface area that has undergone a total porosity loss in volume in function of time up to 28 days with mercury porosimeter monitoring.

Our work has enabled us to confirm this reduction is porosity due to the formation of secondary Ettringite in the natural cement studied by the determination of the usual physical parameters in accordance with the ASTM C-642 standard, with the results demonstrating a marked reduction as shown in Table 3.

The obtaining of high resistance on a level of those provided by Portland cement was also observed by other authors, such as Zang and Glasser [8], who obtained an increase in compression strength, based on sulfo-aluminates, together with the formation of Ettringite.

These reached the same levels as Portland cements after some four months with an asymptotic growth up to six years later, together with stable concrete during twelve to sixteen years in constant immersion.

Expansive Behaviour of the Ettringite Formed in this Class of Cements

The cited background studies, carried out using these types of clinkers/cements were focused on obtaining cements with controlled expansion for specific applications.

The expansion conditions in clinkers for expansive cements have been examined by Nakamura, with the conclusion that low free limestone and low chalk content are required. The common factor in these cements is the fact that the dominant phase is the secondary Ettringite as a hydrolysis product. The papers by Sodoh [7] demonstrated that when the formation of Ettringite is micro-crystalline of 1 to 2 microns and the free limestone content is low, then expansion is not produced.

The tested cement from Catalonia has an A/′ molar ratio is 2.32, and the SO_3 contribution for the formation of secondary Ettringite comes from the sulfate attack solution and is therefore extrinsic, whereas the Sodoh cement, and the cements of other authors cited have anhydrite incorporated clinker or in cement grinding as intrinsic SO_3 contribution. It must be emphasised that this is an important difference and that the extrinsic sulfate action under the conditions of the tested natural cement clinker did not reveal any expansion during the secondary ettringite formation and this has been revealed by x-ray diffraction. This leads to the conclusion that the ettringite formation produces high strength without any degradation or expansive effects.

New Aspects of Sulphate Attack

In the 40s, independently of the laboratory work, the U.S. Road Administration commenced a field study, based on the work of Jackson [9] "The durability of concrete in service", into the state of real structures affected by sulfate attack and those which were not. The discrepancies which were found between the actual results and those predicted by the laboratory placed even more emphasis on the need to review the causes.

As from the 50s, a large number of researchers have contributed to the establishment of various causes associated with the ettringite formation which explains the destruction of concrete due to sulphate attack and which may be resumed as follows: a C3A content is excess of 5% as a general criterion from the beginning; the expansive forces produced by osmosis as described by Torwaldson [10]; the topo-chemical formation of ettringite Lafuma [11]; the influence of pH on expansion as proposed by Chatterji [12]; the absorption of water by the poorly crystallised ettringite , and the loss of strength of the CSH phases when the pH is reduced and the disappearance of the CH phase Mehta [13]; the need and/or concomitant micro-cracking of the concrete in presence of water as defended by Collepardi in his holistic view [14]; The introduction of the osmosis process as being the most significant generalized cause of expansion as has been accepted. Osmotic pressure, which has been extensively studied in the alkali-aggregate reaction implies the formation and existence of a semi-permeable membrane, which is caused by the existence of alkaline silicates coming from the Newkirk [15] phases and which exists in all Portland cements to a greater or lesser degree, and the eventual presence of small amounts of clay material in the concrete aggregates aids this membrane formation.

Recently, in traditional concretes or mortars by comparing these Ettringite formations with those produced in Portland mortar and concrete, Diamond [16], and Famy and Scrievener [17], were able to obtain information through "SEM observations of micro-structures" in the C-S-H phases. Two different manifestations in the hydrated C-S-H phase masses, a light grey internal one, called the inner C-S-H product that surrounds the non-hydrated clinker grains, together with another darker mass or outer product, or non-differentiated product housing the formation of secondary expansive Ettringite which is produced over time with mortar or concrete having the original sulfate ions, both intrinsic and extrinsic. These authors reached the conclusion that Ettringite crystallisation takes place inside the outer exterior C-S-H phase micro pores and that this is associated with the expansion phenomenon.

In summing up, there is a large number of controversial contributions for the interpretation of the behaviour of conventional concrete without active additions in which there does not appear to be any single generalised prevalent conclusion, in spite of being ever-closer to a more thorough understanding.

A conclusive interpretation from Professor Mehta [16] could be schematically resumed as follows: from the use of cements with higher strength at early ages as a general proposal for cement users according to major of the authors and cement manufacturers, the cements having a high C_3S and C_2S content produce a general tendency for the concrete to crack more easily under lower levels of creep and higher drying shrinkage and thermal shrinkage. As this micro-cracking increases, the concrete penetrability and the durability decrease.

New Contributions to Critical Aspects

There are still certain critical aspects and suggestions from the author to this updated summary.

The conditions for Ettringite formation in both cement types are really quite different. The most active phases in Portand clinker during hydrolysis are the C-A-H, so that it is well-known that the C_3S and C_2S silicates do not commence to hydrolyse until after the first two days, forming a binder network once the primary Ettringite has been produced.

The C-S-H gel develops much more resistance than that produced by the Ettringite for two reasons, first, because it is present in greater amounts 75% *of* (C_2S + C_3S) against 20% of aluminates, and secondly because the C-S-H gel is a colloid with a smaller range of particle size, together with great cohesive power due to its large specific surface area of between 21.000 and 25.000 cm^2/g, which it strengthened by the polymerisation action of the silica. In accordance with our own criteria, it seems understandable that the primary Ettringite is not expansive in any type of Portland because it forms within the first 48 hours, in other words, before the C-S-H gel is formed. There is always space available to hold the primary Ettringite. When the hydrated cement is 80% hydrated at 28 days of curing, the C-S-H gel formation is almost complete.

The Ettringite which then forms due to intrinsic or extrinsic attack or because of Delayed Ettringite Formation (DEF) is the secondary Ettringite which crystallises within the indeterminate outer C-S-H phase, with a higher level of cohesion, which is rigid, together with the possibility of having formed semi-permeable membranes capable of creating osmotic pressure etc, and which is therefore expansive.

In natural or ASC sulfo-aluminate-based cements, and certain ones from the $CaO-SiO_2$ – Al_2O_3-SO_3 system, expansion is not produced because the C_2S content is very low and C_3S is non-existent. The resistance of these cements to sulfate attack therefore seems understandable and this, together with the growing formation of secondary Ettringite, increases these levels of resistance to those of Portland cements as we pointed out in our research. In Table 2, we can see how the total porosity of the samples attacked by sulfate dissolutions has been decreased.

From our point of view, the main problem of expansion would appear to be one of a lack of compatibility in the binding systems in the C-A-H and C-S-H phases so that the sulfate pathology generates the rigidity in the C-S-H formation. The natural cement under study therefore, is not only resistant to sulfate attack, but, because of its contribution, attains O.P.C. compression strength in the medium and/or long terms.

It also includes how the pozzolanic additions fragment because of interposition within the C-S-H gel mass with micro-porous material that opens spaces in which the Ettringite is able to crystallise and prevents the excessive formation of semi-permeable membranes. Meta-kaolin or silicates which have been calcined above 800°C, in which amorphous masses of SiO_2 and Al_2O_3 are formed, have been demonstrated as being especially useful as pozzolana.

The cement which we have investigated was calcined at low temperature and contained an average value of 15% silica material, which also means that it is pozzolanic.

The conclusions reached concerning the applications of this type of cement appear to lead towards the opening of a new road forward in the research into new cements which are immune to sulfate attack, possess high compression strength, involve much lower energy costs and a very significant reduction in pollution. In this way, it is possible to understand how the use of active additions appears as a generalised solution, providing good, practical, coherent results.

We therefore believe that this is good method of following the influence of sulfate attack on the concrete, in which the ratio

$$\frac{\text{Porous space of pozzolanic material}}{\text{Space of CSH phases}}$$

is suggested as a new parameter that to should will be have into account to control of concrete on it's sensibility to sulfate attack and the evaluation on field study of its durability behaviour.

CONCLUSIONS

A raw cement with a composition very close to that of a raw Portland cement, with a 3% SO_3 content and calcined at a low temperature of 1.150 to 1.200 °C produced a type of natural ground cement which is resistance to attack by 5% sodium sulfate solution.

Its medium and long-term compression strength is increased to that of Portland cement through the formation of secondary Ettringite with the sulfate.

The Ettringite formation does not manifest itself as expansive when the amount of the C_2S is very low and there is no C_3S. Its most significant application is use in situations of heavy aggression due to high sulfate concentrations.

The increase in compression strength may allow a new type of alternative use cement to be created with a notable reduction in energy costs, together with very significant reduction in levels of pollution.

The commencement of an extensive study, both in the laboratory, in order to determine all its physical-chemical parameters, and through work in the field on structures with real volumes, is justified, and will enable a specific standard for its use to be established by the standards committees.

REFERENCES

1. GOMÀ, F, VICENTE, M, Determination and classification of the causes of the loosening of aglomerate materials from building façades, Fifth Canmet/ACI International Conference on Durability of Concrete, Barcelona, Spain, 2000, Supplementary Papers, p 553 – 568.

2. GOMÀ, F G, Sobre la determinació gravimètrica de la sílice, Tesi Doctoral, Departament de QuímicAnalítica, Universitat de Barcelona, 1975.

3. GOMÀ, F G, Generalized clinkerability function, 7th International Congress on Chemistry of Cement, Paris, 1980, Vol II, p 67/73.

4. NAKAMURA, et al, Mineralogical composition of expansive cement clinker reach in SiO_2 and its expansivity, Proceedings of Fifth International Symposium of the Chemistry of Cement, Tokyo, 1968, Supplementary Papers IV –74, p 351 – 365.

5. KLEIN, A, Mehta, P K, Nature of hydratation products in the system $4CaO.3Al_2O_3.SO_3.CaO.H_2O$, Proceedings of Fifth International Symposium of the Chemistry of Cement, Tokyo, 1968, Supplementary Papers IV –66, p 336 – 350.

6. DENG JUN – AN, et al, Sulfoaluminate Cement Series, 7th International Congress on the Chemistry of Cement, Paris, 1980, Supplementary Papers IV – Theme V, p 381 – 386.

7. SODOH, G, OTHA, T, HARADA, H, High strength cement in the $CaO-Al_2O_3-SiO_2-SO_3$ system and its applications, 7th International Congress on the Chemistry of Cement, Paris, 1980, Vol III, Comunications, p 152-157.

8. ZHANG, L, GLASSER, F P, New concretes based on calciumsulfoaluminate cement, International Conference Creating with Concrete, (Ed. R K Dhir) University of Dundee, UK, September 1999, Vol Modern Concrete Materials, p 261.

9. JACKSON, F H, The durability of concrete in service, ACI Journal, Vol 18, No 2, October 1946, p 165-180.

10. THORVALDSON, T, Chemical aspects of the durability of cement products, Third International Symposium on the Chemistry of Cement, London 1952, p. 436-484.

11. LAFUMA, H, Theory of expansion of cements, Ren. Mat. Constr. Trav. Publ., Vol 243, 1929, p 441-444.

12. CHATTERJI, S, Mechanism of sulfate expansion: A reappraisal of literature, 7th International Congress on the Chemistry of Cement, Paris, 1980, Vol IV, Tema 5, p 586-591.

13. MEHTA, P K, Sulfate attack on concrete, Critical Review, Material Science of Concrete, Ed. J Skalny, 1992, p 105-129.

14. COLLEPARDI, M, Concrete sulfate attack in a sulfate-free environment, 2nd CANMET/ACI International Conference on High Performance Concrete, Gramado RS, Brazil, 1999, SP-186-1, p 1-19.

15. NEWKIRK, T F, The alkali phases in Portland cement clinker, Third International Symposium on the Chemistry of Cement, London, 1952, p 151-171.

16. DIAMOND, S, Microscopic features of ground water-induced sulfate attack in highly permeable concretes, International Conference on Durability of Concrete, CANMET/ACI, Vol I SP-192-25, p 403-416.

17. FAMY, C, SCRIVENER, K L, Characterization calcium-silicate-hydrate products in expansive and non-expansive heat-cured mortars – electron microscopy study, International Conference on Durability of Concrete, CANMET/ACI, Barcelona, Catalonia, Spain, 2000, Vol I SP-192-24, p 385-401.

18. GOMÀ, F G, VICENTE, M D, Chemical analysis of hardened concretes and morters with active additions: A new procedure for its identification, Proceedings of the International Conference Creating with Concrete, Dundee, U,K September 1999, Utilizing ready-mixed concrete and mortar (Ed. R.K. Dhir and M C Limbachiya).

REINFORCEMENT STRESS LIMITS TO PREVENT STEEL CORROSION IN HPC MEMBERS DUE TO CHLORIDE PENETRATION

N Gattesco

University of Trieste

D Bernardi

University of Udine

Italy

ABSTRACT. A model to predict the chloride ingress into high performance concrete able to consider the time-dependency of both the diffusion coefficient and the surface chloride concentration as well as the effect of the tensile stress in the reinforcement is herein presented. A parametric study allowed evidencing the role of some of the main parameters that govern the phenomenon. For this concern different values for the water-cement ratio, the silica fume content, the concrete cover, the tensile stress in the reinforcement were considered and structures were supposed to be exposed to three marine environments: coastal zone, splash zone, permanently submerged. The results evidence a significant increment of the chloride penetration in the concrete for greater values of the tensile stress in the reinforcement due to the increase in permeability provoked by the microcraking forming in the concrete between two major cracks. Moreover, the results show a considerably different durability among the structures exposed to the splash zone and those exposed to coastal or submerged zone; Eurocode No. 2 durability provisions are in general not conservative in the former case while in the latter some tensile stress limitations in the reinforcement are needed.

Keywords: Concrete durability, Corrosion, Chloride diffusion, High performance concrete, Serviceability limit states, Marine environment, Mix proportions.

Professor N Gattesco, is Associate Professor of Structural Design, Faculty of Architecture, University of Trieste (Italy). His main research interests concern composite beams under cyclic loads, nonlinear analysis of concrete structures with particular attention to high performance concrete, connections in wood elements.

Mr D Bernardi, is a professional Engineer in Gorizia (Italy) and currently undertaking research on the durability of concrete structures with particular concern to the effect of chloride ingress into concrete in the Department of Civil Engineering at the University of Udine (Italy).

INTRODUCTION

The structural design of concrete structures, which is mainly aimed to provide to the structure adequate safety against the collapse and to satisfy some serviceability requirements (e.g. cracking, deformation), cannot neglect to consider the effects of environmental agents that may reduce considerably the durability of the structure.

Among the causes of damage in concrete structures due to these agents, the main chemical-physical phenomena, which significantly affect the durability of structures through the corrosion of steel reinforcement, are the carbonation of concrete and the chloride penetration. In particular the latter phenomenon assumes primary importance for structures exposed to marine environment. Moreover the corrosion due to chlorides is very dangerous because reduces locally the reinforcement section (pitting) very quickly without showing appreciable cracks in the reinforcement concrete cover.

Many existing concrete structures, as bridges, thin precast elements, offshore structures, etc., experienced significant damage due to the corrosion of steel reinforcement (e.g. [1]) so very costly repairing interventions were needed in order to provide again to the structure adequate safety and serviceability features. Moreover, in some cases, the damage was so serious to cause the collapse of the structure. Nevertheless, in most of the codes of practice (e.g. [2]), for durability, only some general rules per each environment exposure are given concerning mix design, water-cement ratio, curing, reinforcement cover, etc.

In the last two decades many researchers (e.g. [3-8]) devoted their studies to the problem of chloride ingress into the concrete with the main scope to provide refined models to be used to predict the durability of structures. The chloride diffusion in concrete is a phenomenon rather complex because it is governed by many parameters, like concrete composition, curing, time, temperature, environment, concrete stress, etc. Only limited experimental investigations were carried out up to now to evidence the interaction between these parameters.

Most of the models [3-7] consider a homogeneous uncracked concrete with unidirectional diffusion of chlorides; they allow evaluating the chloride content at any time in the concrete surrounding the reinforcement; when the critical chloride content, close to the reinforcement, is reached the corrosion propagation phase may start. The papers [7-8] concern a study aimed to point out the influence of the tensile stress in the reinforcement on the chloride diffusion in normal NSC and high-performance concrete HPC. The experimental results evidence an appreciable increase in the chloride diffusion growing up the tensile stress.

The aim of the present research work is to define a model, that considers most of the parameters listed above including the tensile stress in the reinforcement, and to determine some limitations to the reinforcement tensile stress in service, which assures that the fast propagation of the corrosion do not occur for an assigned period of time (e.g. service lifetime of the structure).

For the study three marine environments (coastal area, splash zone, submerged in seawater), corresponding to exposure zone 4a in EC2 [2], were considered; also the role of HPC mix design (water-cement ratio, silica fume content) was evident.

CHLORIDE-INDUCED CORROSION

Reinforcing steel embedded in the concrete develops a protective passivity layer on its surface. This layer is self-generated after the hydration of cement has started and as long as such a protection is present the steel remains intact. The presence of chlorides in the concrete surrounding the reinforcement, due to the exposure of the structure to marine environment, may destroy locally the protective film and in the presence of water and oxygen corrosion occurs.

The corrosion mechanism for uncracked concrete presented in the literature concerns two phases: the incubation phase and the propagation phase (Figure 1a). The incubation period ($t<t_O$) is the time needed to aggressive agents to penetrate to the concrete and to reach, at the surface of the reinforcement, the concentration that provokes the steel depassivation. The second phase may be very fast especially in the case of chloride-induced corrosion (pitting), therefore the sole time interval (0-t_O) is normally assumed as safe life for the structure. As a matter of fact concrete structures are generally cracked in service, so that it is necessary to evaluate how the corrosion develops in this case. The chlorides penetrate faster in the crack reaching the critical concentration at the reinforcement level very soon, which follows the commencement of the corrosion (t'). However the corrosion products tend to re-passivate the steel and consequently to arrest the corrosion process (t'') as long as the critical chloride content in the concrete between two cracks at the level of the reinforcement is reached (t^* in Figure 1b) [7]. For cracked concrete, then, the corrosion mechanism concerns four phases: incubation, commencement, dormancy and propagation (Figure 1b). The crack width influences the incubation and commencement phases, which are however very brief; the tensile stresses in the concrete between two consecutive cracks, due to bond, cause microcrackings and consequently a faster chloride ingress in the concrete. In this case, in fact, the propagation of the corrosion occurs earlier than for uncracked concrete ($t^*<t_O$). The interval (0-t^*) is assumed as service lifetime of structure.

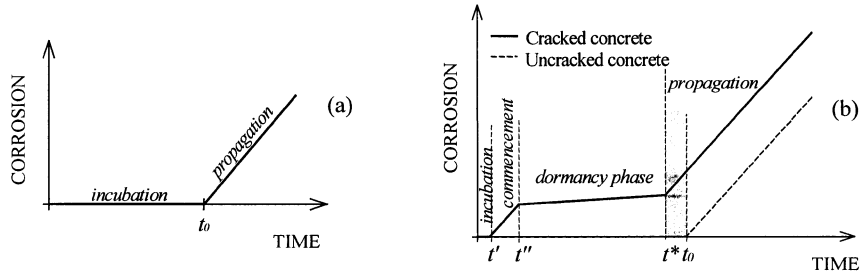

Figure 1 Corrosion procedure for (a) uncracked and (b) cracked reinforced concrete.

CHLORIDE INGRESS MODEL

The first model to describe the chloride ingress into concrete by diffusion was proposed by Collepardi et al. [3]. The chloride content as a function of the distance from the surface (depth) and of the time $C(x,t)$ can be obtained by solving the Fick's second law of diffusion. Several researchers obtained the expression of $C(x,t)$ assuming that the chloride diffusion coefficient D_a and the surface chloride content C_{sa} of the exposed concrete are time-independent. But, this

assumption is acceptable only when applied to old marine concrete structures, while for younger structures and especially for newly cast structures would lead to gross deviation from what is found in practice. In fact, extensive inspection of marine concrete structures evidenced that the chloride diffusion coefficient and the surface chloride content of the exposed concrete, besides their dependence to the concrete composition, the workmanship (casting, compaction, curing) and the environment, are time-dependent [9].

Mejlbro and Poulsen [6] proposed an analytical solution of Fick's second law of diffusion considering the time-dependency of the above parameters. In particular it was assumed that the surface chloride content in the concrete C_{sa} is described by the function

$$C_{sa} = C_i + S_p \cdot \left\{ \left(\frac{t}{t_{ex}} - 1 \right) \cdot \frac{D_a}{D_{aex}} \right\}^p , \tag{1}$$

where C_i is the initial chloride content of the concrete, S_p and p are factors depending on the concrete and environment (Table 1), t and t_{ex} are the concrete age and the time of the first chloride exposure, respectively. The diffusion coefficient D_a varies with time as [9]

$$D_a = D_{aex} \cdot \left(\frac{t_{ex}}{t} \right)^{\alpha} , \tag{2}$$

where D_{aex} is the value of the diffusion coefficient at time $t=t_{ex}$ and α is an exponent which varies between 0 and 1 (Table 1). From Equations (1), (2) the solution of Fick's second law gives [6]

$$C(x,t) = C_i + S_p \cdot \tau^p \cdot \Psi(z), \tag{3}$$

where $C(x,t)$ is the total chloride content in the concrete at distance x from the exposed concrete surface at time t and $\Psi(z)$ are generalized error functions [6] defined as

$$\Psi(z) = \sum_{n=0}^{\infty} \frac{\prod_{i=0}^{n-1} (p-i) \cdot (2 \cdot z)^{2n}}{(2n)!} - \frac{\Gamma(p+1)}{\Gamma(p+0.5)} \cdot \sum_{n=0}^{\infty} \frac{\prod_{i=0}^{n-1} (p-0.5-i) \cdot (2 \cdot z)^{2n+1}}{(2n+1)!} . \tag{4}$$

for $n=0$ the product function Π gives 1, $\Gamma(y)$ is the gamma function. The factors τ and z represents the functions

$$\tau = \left(\frac{t}{t_{ex}} \right)^{1-\alpha} - \left(\frac{t_{ex}}{t} \right)^{\alpha} \tag{5}$$

$$z = \frac{0.5 \cdot x}{\sqrt{\tau \cdot t_{ex} \cdot D_{aex}}} . \tag{6}$$

The four parameters S_p, p, α, D_{aex}, needed in Equations (1) and (2), are evaluated through the Frederiksen derived parameters C_1, C_{100}, D_1, D_{100} (Table 1) [9] which account for the concrete composition and the environment. For concrete the equivalent water-cement ratio is introduced

$$eqv(w/c) = \frac{w}{c + \delta \cdot s} , \tag{7}$$

where w, c, s are the masses of water, cement and silica fume, respectively, per unit volume of concrete; δ is the efficiency factor for silica fume. The relationships for the parameters are summarized in Table 1 [6].

The coefficients k_b, k_t, k_D and k_α represents the types of environment (Coastal area, splash zone, submerged in seawater) and their values are given in Table 2 [6]. Coefficients k_t and k_α are non-dimensional, k_b is in [% of mass binder] and k_D is in [mm^2/yr.]. The efficiency factors δ to be used in Equation (7) are presented in Table 3 [3].

Table 1 Relationships for parameters S_p, p, α, D_{aex} through Frederiksen C_1, C_{100}, D_1, D_{100}

$$\alpha = 0.5 \cdot log_{10}\left(\frac{D_1}{D_{100}}\right) \qquad p = \frac{log_{10}\left(\frac{C_{100}}{C_1}\right)}{log_{10}\left(\frac{100 - t_{ex}}{1 - t_{ex}} \cdot \frac{D_{100}}{D_1}\right)} \qquad S_p = C_1 \cdot \left\{\left(\frac{D_1}{D_{100}}\right)^{\vartheta} \cdot \frac{t_{ex}}{1 - t_{ex}}\right\}^{p}$$

$$D_{aex} = D_1 \cdot \left(\frac{D_1}{D_{100}}\right)^{\vartheta} \qquad \vartheta = 0.5 \cdot log_{10}\left(\frac{1}{t_{ex}}\right)$$

$$C_1 = k_b \cdot eqv(w/c)_b \qquad D_1 = k_D \cdot exp\left(-\sqrt{\frac{10}{eqv(w/c)_D}}\right) \qquad D_{100} = \frac{D_1}{exp\left[k_\alpha \cdot \left(1 - 1.5 \cdot eqv(w/c)_D\right)\right]}$$

$$C_{100} = k_t \cdot C_1$$

Table 2 Values of the coefficients k_b, k_t, k_D and k_α

ENVIRONMENT	k_b *[% MASS BINDER]*	k_t	k_D *[mm^2/years]*	k_α	k_{cr} *[% MASS BINDER]*
Coastal area	2.20	7.0	10000	4.60	0.50
Splash zone	3.70	4.5	15000	0.45	0.75
Submerged	5.15	1.5	25000	2.75	2.00

Table 3 Factors δ

	δ
$eqv(w/c)_b$	-1.50
$eqv(w/c)_D$	7.00
$eqv(w/c)_{cr}$	-3.50

The threshold content of chlorides in concrete suggested in [6] is herein considered. The value represents the total acid soluble chloride content expressed as percentage of the mass binder. The relationship in function of concrete composition and environment features is

$$C_{cr} = 2.6 \cdot k_{cr} \cdot exp\left(-2.4 \cdot eqv(w/c)_{cr}\right), \tag{8}$$

the values of k_{cr} and δ, for $eqv(w/c)_{cr}$, are reported in Table 2 and Table 3, respectively.

However the model proposed by Mejlbro and Poulsen [6] does not consider the influence of cracking on the chloride ingress process. As stated in the preceding section, the starting of the corrosion propagation (t^* in Figure 1) is influenced by the tensile stress in the reinforcement, which causes a significant microcracking in the concrete between major cracks leading to an increase in the chloride penetration with respect to unstressed concrete.

Konin et al. [8] proposed a relationship that considers the variation of the diffusion coefficient with the stress level in the reinforcement. Their relationship is derived from experimental tests carried out on NSC and HPC, measuring the diffusion coefficient after 9 months of exposure.

$$D_a(\sigma_s) = D_a \cdot \left(1 + 5.98 \cdot 10^{-8} \cdot \sigma_s^3\right), \tag{9}$$

where σ_s is the tensile stress applied in the reinforcement and D_a is the diffusion coefficient evaluated for uncracked concrete (σ_s = 0). Substituting Equation (9) in Equation (3) a relationship for the evaluation of the chloride content into concrete that considers concrete composition, environment and reinforcement stress is obtained.

RESULTS

The model described in the preceding section was applied to evaluate the corrosion propagation time (t^* in Figure 1) in function of the main parameters that govern the chloride ingress into concrete (C_i is assumed nil). Such a value can be determined imposing that the chloride content at the reinforcement level be equal to the threshold content of chlorides (Equation 8).

Three different marine environments were considered: A – coastal area, characterized by very fine droplets of sea water raised up by turbulence and carried by wind; B – splash zone, which is wetted by sea water only when the sea is high or the wind is strong; C – submerged in sea water, which means permanently under water level (in Eurocode No. 2 the three environments are all included in the exposure class 4a). The intervals of variation of the other parameters were as follow: water-cement ratio w/c=0.3÷0.5, ratio between silica fume and cement s/c=0÷0.15, concrete cover x=20÷40 mm and tensile stress in the reinforcement σ_s=0÷300 MPa.

The effect of the value of the tensile stress in the reinforcement is evidenced with the chloride concentration profiles plotted in Figure 2. The curves are related to a concrete made with w/c=0.40 and s/c=0.05. In particular in Figure 2a the chloride content in the concrete versus depth after 50 years of exposure in a costal environment (*env.* A) is plotted; each curve corresponds to a different stress value. Analogously in Figure 2b with an exposure of 10 years in a marine splash zone (*env.* B).

The diagrams show that an appreciable increase in chloride concentration occurs at the increase of the tensile stress of the reinforcement. The threshold content of chlorides C_{cr}, evaluated with Equation (8), is also reported in the plots. The intersection between the curves and the threshold of chlorides corresponds to the depth at which the chloride content is equal to its critical value. For higher reinforcement tensile stress values the critical concentration of chlorides reaches larger depths.

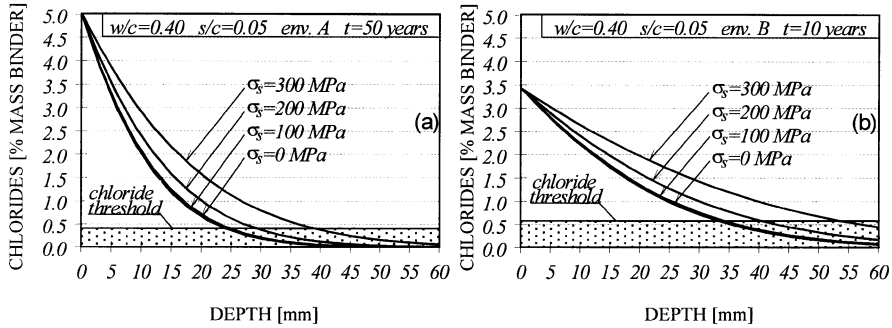

Figure 2 Total chloride content against the depth at various reinforcement tensile stress values: (a) coastal zone – t = 50 years, (b) splash zone - t = 10 years

The corrosion propagation time t^* against the tensile stress σ_s is plotted in Figure 3 for cases with a concrete made with w/c=0.4 and s/c=0.05. Each curve of Figure 3a corresponds to different environment conditions and x=40 mm. For a structure exposed to a marine splash zone (*env. B*) even very small tensile stresses in the reinforcement do not avoid an early appearance of corrosion (10÷15 years) while, for the other two environments considered, corrosion may occur before than 100 years only when the reinforcement stresses are greater than 160 or 230 MPa. The curves of Figure 3b correspond to different values of the concrete cover and refer to a coastal environment (*env. A*). As can be noted a significant reduction in the service lifetime t^* occurs for smaller values of the concrete cover.

In Figure 4 similar diagrams as those of Figure 3 are illustrated; the effect of the silica fume content is evidenced for two different environment conditions. In Figure 4a a w/c=0.5 and x=40 mm in a coastal environment (*env. A*) are considered. The increase in the silica fume content allows for a significant increment in the lifetime for an assigned value of the tensile stress (e.g. for s/c=0.15, t^*>100 years for σ_s<300 MPa. In Figure 4b a w/c=0.4 and x=40 mm in a marine splash zone (*env. B*) are considered. In this case lifetime grows moderately at the increase of the silica fume content: corrosion occurs in a limited number of years. Diagrams similar to those illustrated in Figures 3 and 4, drawn for all possible combinations of the values of the parameters that govern the chloride ingress into concrete, provide the reinforcement stress limits needed to give an assigned durability to concrete structures.

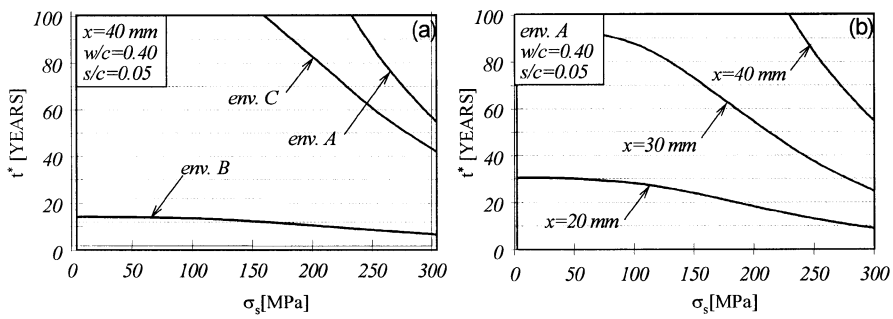

Figure 3 Service lifetime against the tensile stress: (a) influence of the environment, (b) influence of the concrete cover

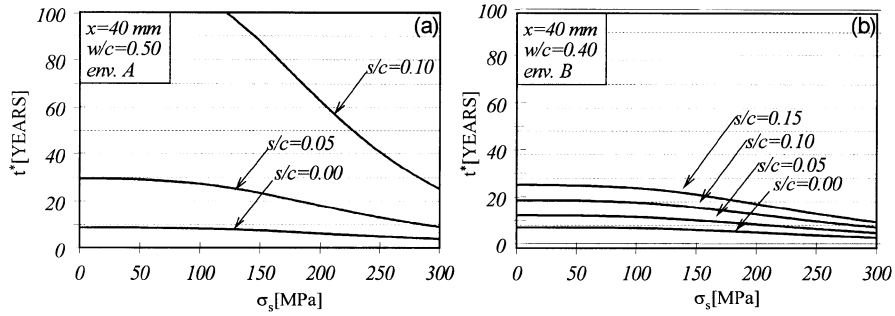

Figure 4 Service lifetime against the tensile stress; influence of the silica fume content (a) x=40 mm, w/c=0.50, coastal area, (b) x=40 mm, w/c=0.40, splash zone

CONCLUSIONS

The Mejlbro-Poulsen [6] model of chloride ingress into concrete was improved introducing also the dependency of the diffusion coefficient to the stress in the reinforcement according to the Konin et al. [8] study allowing to extend the use also for cracked concrete. The results obtained with this model evidenced an appreciable increase in the chloride penetration rate for greater values of the tensile stress in the reinforcement. From the study, the influence of some of the main governing parameters (w/c, s/c, environment, concrete cover) was underlined.

The main results, aimed to determine serviceability requirements in terms of maximum service reinforcement stresses, showed that the provisions of Eurocode No. 2 are in some cases non conservative in exposure class 4a (marine environment); for splash zone, in fact, the service lifetime is in general rather brief, but also for the other two environments considered the service lifetime reduces appreciably for high values of the reinforcement tensile stresses.

The analytical model can be used to draw tables to be easily used in structural design, where the values of the design parameters, as concrete mix proportions, reiforcement cover, steel stresses, etc., are related to needed sevice lifetime for any kind of environment. Moreover, the model can be easily implemented in numerical procedures to design concrete structures so as to check that the required structural durability can be fulfilled.

ACKNOWLEDGEMENTS

The financial support of the Italian Ministry of University and Scientific and Technological Research (MURST) is gratefully acknowledged.

REFERENCES

1. KURTIS, K. E., MEHTA, P. K., A Critical Review of Deterioration of Concrete due to Corrosion of the Reinforcing Steel, L'Industria Italiana del Cemento, 1998, 1, p 78-95.

2. ENV 1992-1-1, Eurocode No. 2, Design of Concrete Structures, Part 1, General Rules and Rules for Buildings.

3. COLLEPARDI, M., MARCIALLIS, A., TURRIZIANI, R., Cinetica di Penetrazione degli Ioni Cloruro nel Calcestruzzo, L'Industria Italiana del Cemento, 1970, 4, pp 157-164.

4. MANGAT, P. S., MOLLOY, B. T., Prediction of Long Term Chloride Concentration in Concrete, Materials and Structures, 1994, Vol 27, p 338-346.

5. DHIR, R. K., JONES, M. R., AHMED, H. E. H., Concrete Durability: Estimation of Chloride Concentration During Design Life, Magazine Conc. Res., 1991, Vol 43, 154, pp 37-44.

6. POULSEN, E., Chloride Ingress into and Lifetime of Marine Reinforced Concrete Structures, L'Industria Italiana del Cemento, 1999, No 5, p 420-433.

7. FRANÇOIS, R., ARLIGUIE, G., MASO, J. C., Durabilité du Bèton Armé Soumis à l'Action des Chlorures, Annales de l'ITBTP, 1994, No 529, p 3-47.

8. KONIN, A., FRANÇOIS, R., ARLIGUIE, G., Penetration of Chlorides in Relation to the Microcracking State into Reinforced Ordinary and High-Strength Concrete, Materials and Structures, 1998, Vol 31, p 310-316.

9. TAKEWAKA, K., MATSUMOTO, S., Quality and Cover Thickness of Concrete Based on the Estimation of Chloride Penetration in Marine Environments, ACI, SP-109, Detroit, 1988, p 381-400.

CONCRETE BEAMS EXPOSED TO AGGRESSIVE INDUSTRIAL ENVIRONMENTS

A Ioani

D Mircea

M Filip

M Mihailescu

Technical University of Cluj-Napoca

Romania

ABSTRACT. In 1973, a comprehensive experimental research programme began in order to evaluate the corrosion effects and the long-term behaviour of different types of concrete elements (reinforced and prestressed, normal and lightweight) maintained in urban and chemically aggressive environments (industrial chlorine, industrial nitrogen) for 10, 15, 20 and 25 years. The other parameters, which were taken into account in the design of the programme, are: cement type and cement content, thickness of concrete cover, beam surface protection type. Protected and unprotected beams maintained in chemically aggressive environments were analysed, then tested up to failure and the results were compared to those resulting from witness elements. In the paper, the principal aspects and conclusions regarding the durability of the concrete beams, after 20 years of exposure, are reported.

Keywords: Reinforced concrete beams, Prestressed concrete beams, Chemical environments, Durability, Corrosion, Monitoring, Ultimate capacity, Time effect.

Professor A M Ioani, is a Professor of Civil Engineering in the Technical University of Cluj-Napoca, Romania. He is an ACI member. His research interests include structural performance of earthquake – resistant structures, fibre-reinforced concrete and concrete durability.

Ms D Mircea, is a Senior Researcher at the National Building Research Institute – Department of Cluj, Romania. She holds engineering degrees from the Technical University of Cluj. Her research interests include: structural behaviour of reinforced elements and concrete durability.

Mr M Filip, is a Senior Researcher at the National Building Research Institute – Department of Cluj. He is a graduate of the Technical University of Cluj-Napoca, (1974). His research interests concern the durability, repair and retrofitting of concrete structures.

Dr M Mihailescu, received his Ph.D. from the Technical University of Cluj-Napoca, Romania. He is Director of Izowest Ltd. Co., specialized in repair, retrofitting and waterproofing systems for concrete structures, including bridges.

INTRODUCTION

The performance of any important concrete structures cannot be correctly appraised without taking into consideration the durability criterion, especially in the present conditions of post-industrial society, characterized by intense chemical pollution. Research programmes in this field are difficult, costly and require suitable long-term tests. The Cluj Department of National Building Research Institute (INCERC) began such a comprehensive experimental programme: 274 full-scale elements (142 R/C and 132 prestressed beams) were cast in three stages (1973, 1977 and 1979) and loaded until they reached a predicted maximum crack width [1]. Long-term loaded, the cracked beams were maintained in different chemically aggressive environments for 10, 15, 20 years and then, after a detailed inspection, were tested up to failure. These results were compared to those of unloaded witness elements, maintained "indoor" in the institute's testing hall.

In the paper, the principal aspects of the programme are discussed and conclusions after 20 years of monitoring and tests on 80 beams maintained in industrial chlorine environment and 36 beams maintained in nitrogen compounds atmosphere are presented.

RESEARCH PROGRAMME

The programme was performed on two types of elements: R/C beams and prestressed concrete beams. The following parameters were taken into account when the research programme was developed: 1) concrete type: normal and lightweight; 2) cement type: high-early strength (RIM), sulphate-resistant (SRA) and ordinary Portland cement (BSS); 3) cement content: 300, 400, 500, 550 and 650 kg/m^3; 4) reinforcement: plain round mild-steel bars and deformed high-yield bars for R/C beams and wire and compacted strands for prestressed beams; 5) concrete cover thickness: 1, 2, 3 and 3.5cm; 6) exposure environment: urban, industrial chlorine atmosphere, industrial atmosphere with nitrogen compounds and laboratory conditions; 7) protections of elements: unprotected and protected by different coatings [2]. Dimensions of elements and reinforcement details for the R/C programme are given in Figure 1.

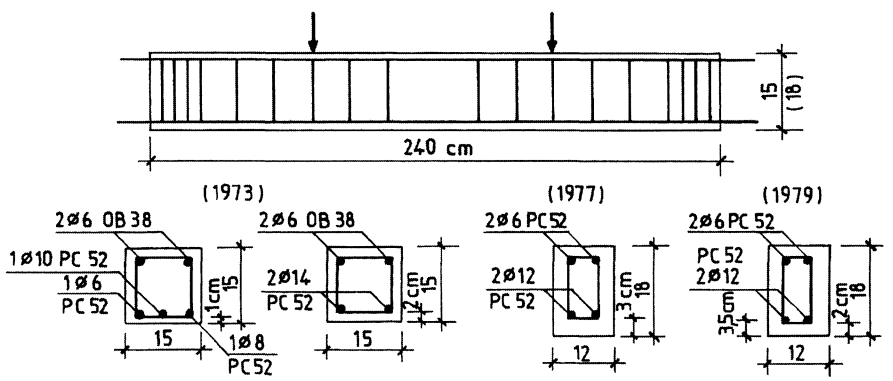

Figure 1 Dimensions and reinforcement details for R/C beams

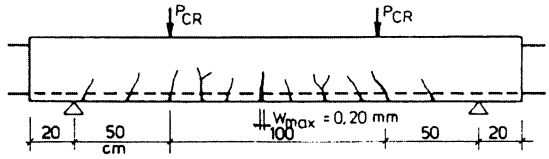

Figure 2 Loading system and the cracking pattern

Each element was loaded in a 3000 KN testing machine and, the force P_{cr} corresponding to a maximum crack width w_{max} = 0.15 – 1.20 mm was recorded, Figure 2. Using the devices shown in Figure 3, pairs of beams were loaded at force levels corresponding to a crack reopening controlled value w_{max} = 0.15 – 0.20 mm. Long-term loaded, these pairs of beams were exposed to different conditions:

- 31 pairs of beams, "outdoor" in the urban environment of our city, Cluj-Napoca;
- 40 pairs of beams in chlorine polluted industrial environment, near the Chemical Products Factory of Turda (Cl_2 concentration of 0.1 to 3.6 mg/m^3 of air and HCl concentration of 0.01 to 3.05 mg/m^3 of air);
- 18 pairs of beams, in industrial atmosphere containing nitrogen compounds, in the yard of the Chemical Factory Azomures, Targu-Mures (NH_4 concentration of 0.16 to 0,38 mg/m^3 of air and NO_2 concentration of 0.015 to 0.5 mg/m^3 of air);
- 36 unloaded, uncracked witness elements (beams) were preserved "indoor", in the laboratory of INCERC – Department of Cluj.

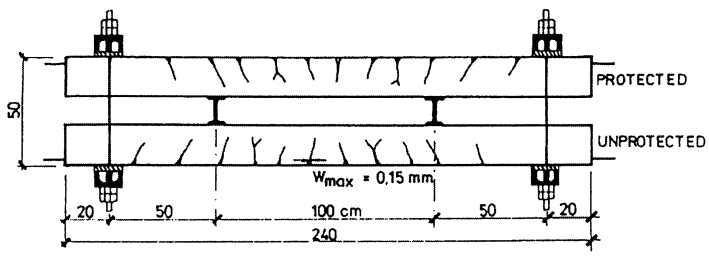

Figure 3 Cracked beams under long-term loads

RESULTS AND DISCUSSION

After 20 years of exposure to different conditions, 94 reinforced and 82 prestressed concrete beams were tested up to failure at different ages: at 28 days – 10 beams, at 5 years – 22 beams, at 11 years – 52 beams, at 16 years – 60 beams and at 20 years – 32 beams.

Durability was appreciated according to the following parameters: concrete characteristics, exterior aspect of exposed elements, carbonation depth of concrete, reinforcement corrosion degree and ultimate strength capacity of beams.

Concrete Characteristics

The results on unit weight w_c, modulus of elasticity E_c and compressive strength of concrete are given in Table 1. The principal findings are as follows:

1. A slight decrease of the unit weight in the range of 2% to 3.1% after 10 years and 20 years respectively, is recorded.

2. The concrete has a significant increase of its E_c: 20% for normal concrete and up to 12% for lightweight concrete. It must be noted that the code ACI 209 R-92 [3] introduces the time effect on E_c using the magnitude of the compressive strength at a given age t of concrete $\left(f_c'\right)_t$:

$$\left(f_c'\right)_t = \frac{t}{a+\beta t}\left(f_c'\right)_{28} = \alpha_t \left(f_c'\right)_{28} \tag{1}$$

$$E_{ct} = 0.043\left[w_c^3 \alpha_t \left(f_c'\right)_{28}\right]^{\frac{1}{2}} = \sqrt{\alpha_t}\left(E_c\right)_{28}. \tag{2}$$

Using estimated values for time-ratio α_t given in Table 2, for normal concrete it results:

$$\left(E_{ct}\right)_{t=1\,year} = 1.077\left(E_c\right)_{28} \; ; \; \left(E_{ct}\right)_{t=10\,years} = 1.081\left(E_c\right)_{28}$$

$$\left(E_{ct}\right)_{t=ultimate} = 1.086\left(E_c\right)_{28}.$$

These estimated increases of E_c in time, in the range of only 7.7% to 8.6%, differ significantly from our recorded data which show an increase of 20% in 10 years for normal concrete specimens and of 12% for lightweight specimens.

Table 1 Concrete characteristics variation

CONCRETE CHARACTERISTICS		AT 28 DAYS	VARIATION (Δ%) AFTER		
			10 Years	15 Years	20 Years
w_c, [kg/m^3]	normal	2210÷2430	-2.0	-2.4	-2.9
	lightweight	1760÷1960	-2.2	-2.7	-3.1
E_c, [Mpa]	normal	26300÷31100	+20.0	-	-
	lightweight	17600÷21100	+12.0	-	-
$f_c^{(1)}$, [MPa]	normal	30	+23.0	+30.0	+34.0
		42	+16.0	+19.5	+22.0
		50	+9.4	+11.0	+12.5
	lightweight	30	+28.0	+35.0	+37.0
		39	+17.0	+20.0	+21.0
		45	+7.0	+8.4	+10.0

(1) Mean values of cube compressive strength of concrete (65 measurements)

Table 2 Time effect on concrete strength
Theoretical and experimental values

TIME	1 YEAR	5 YEARS	10 YEARS	ULTIMATE	15 YEARS	20 YEARS
$\alpha_t^{(1)} = \frac{(f_c')_t}{(f_c)_{28}}$	1.16	–	1.17	1.18	–	–
Experimental values[2]	-	1.112	1.16	-	1.195	1.22

[1] Theoretical values for moist cured concrete, cement type I, ACI 209R-92, [3].
[2] Experimental values for concrete class C25/30 and C30/37, [5].

3. Relative to compressive strength versus time, the experimental values presented in Table 1 show a similar rate of strength development for normal and lightweight concrete. This remark is also reported in different studies [4] and codes [3].

   The rate of strength development seems to be dependent on the concrete grade; it is higher for a concrete grade of between 20-25 MPa and it is slower for concrete having a higher compressive strength. A medium rate of strength development (16%, 19.5% and 22% after 10, 15 and 20 years respectively) which is in good agreement with the theoretical values given by design codes [3] – see Table 2 – corresponds to concrete having a strength class of C30/37 according to Eurocode 2 [5], widely used in Europe.

   We have to underline that all the concretes have continued to increase in strength even after 10 years. This increase is significant between 10 and 20 years – see Table 1 and Table 2.

Exterior Aspect of Exposed Elements

In terms of visual observation:

1. In natural urban environment there are no new cracks, no stains but the exterior reinforcement ends are corroded.

2. In industrial environment with chlorine/nitrogen there appear: new transversal and longitudinal cracks; a medium to severe scaling process of the concrete surface according to the provisions of ACI 201R-92 [6]; highly corroded exterior reinforcement ends. The outward manifestation of steel rusting includes staining, cracking and local spalling of the concrete.

Rate of Concrete Carbonation

The knowledge and the control of the long-term carbonation resistance of any type of concrete is a difficult task due to this large variety of constituents-binders, aggregates and admixtures-on the one hand, and on the other hand owing to the multitude of parameters which influence this process, including the aggressiveness of the environment, too.

Being a relatively slow process (a significant carbonation depth is reached after 10 or 20 years [7]), researchers have tried to develop both simulated natural carbonation methods and accelerated carbonation tests.

The lack of funds and technical means from the 1970-80 made the research team from National Building Research Institute (INCERC) – Department of Cluj select the natural carbonation of concrete elements exposed to different environments (urban area, industrial chlorine and industrial nitrogen areas) as their testing philosophy.

Usually, the cracks represent the "weak" area of any structural concrete element. As a consequence, in the cracked beams the carbonation depth in the crack was up to 16 to 18 mm, but at the same time, the carbonation depth (C.D.) did not exceed 3 to 5 mm between cracks. For this reason we tried to assess the carbonation process in the cracks and not between cracks. Previous results [1] have shown that the carbonation depths of the cracked region depend on several factors:

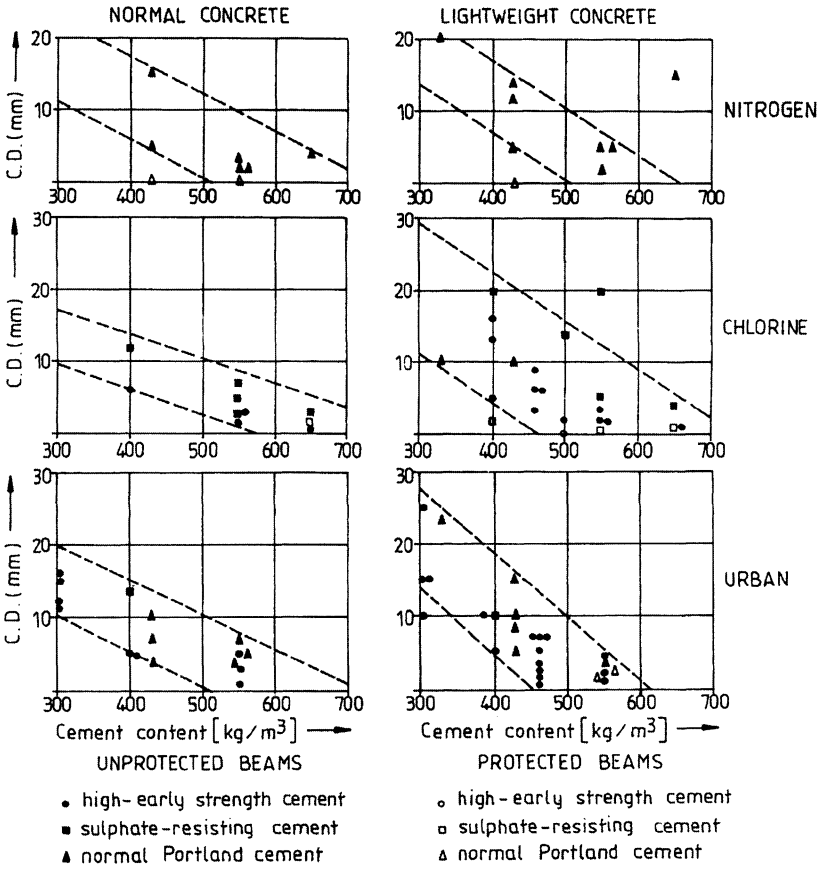

Figure 4 Carbonation depths (C.D.) of concrete elements after 20 years of exposure to different aggressive environments [mm]

1. **Cement content**, where carbonation depths greatly decrease as cement content is increased; a cement content over 430kg/m^3 generally maintains the depths of carbonation under 10 mm, Figure 4.

2. **Concrete strength**, where the carbonation depths are smaller for the reinforced and prestressed concrete beams having a higher concrete grade; for instance, elements made of concrete with compressive strength of 52.7 and 57.7 MPa showed the best behaviour even in the most aggressive environment (chlorine industrial): after 20 years of exposure, the depths of carbonation are only between 2-7 mm, Figure 4.

3. **Cement type**, where for equal cement content and similar conditions of exposure, the use of high-early strength cement leads to the smallest carbonation depths.

4. **Environment type**, but the carbonation process is slightly influenced by the exposure of the specimens in an atmosphere containing chemically products as chlorine (Cl_2) or ammonium (NH_4) as it is more dependent on the relative humidity of the environment, temperature, permeability of the concrete and concentration of CO_2 [6]. For this reason in Figure 4 there are not significant differences regarding the carbonation depths versus environment type.

5. **Concrete type**, where the lightweight concrete is most sensitive to carbonation when cement content below 400kg/m^3 is used; for such situation, the lightweight elements had 10 to 30% deeper carbonation depths versus the normal concrete ones, Figure 4.

Reinforcement Corrosion Degree

In all beam types corrosion was revealed by the presence of rust stains at the lower side of the reinforcement, in the cracked area. Between cracks, the medium length of rust stains (l_r) depends on the thickness of concrete cover, on carbonation depth and on the chemical aggressivity of the environment. After 20 years of exposure the following were observed:

1. All the stirrups that are in the vicinity of the cracks are corroded.

2. At the elements with a concrete cover of 1 cm and 2 cm, rust stains have extended over the whole circumference of the bar and along its whole length.

3. In chemically aggressive environments (chlorine, nitrogen), at the elements with a concrete cover of 2 cm, longitudinal cracks have been produced, followed by the spalling of the concrete on certain zones.

4. In general, the length of the rust stains decreases by half, if the thickness of the concrete cover increases from 2 cm to 3.5 cm. The last three observations show that for reinforced concrete elements, only the use of a 3.5 cm concrete cover provides satisfactory protection. In fact Eurocode 2 [5] has also similar requirements for reinforced elements related to the environmental exposure class 5 (aggressive chemical environment) where, the minimum concrete covers are 2.5, 3.0 and 4.0 cm for 5.a, 5.b and 5.c, respectively.

5. For reinforced concrete elements with cement content of 300kg/m^3, a very significant increase (70-100%) of rust stain length is recorded between 10 and 20 years of exposure.

6. In general, at lightweight concrete elements the rust stains on the reinforcement are more extended in comparison with the elements of the same type of normal concrete.

7. At the elements protected by different coatings the presence of the rust has been noticed only in 2-3 isolated cases, in which the coating were degraded.

8. In industrial chlorine atmosphere were recorded the most significant damages: highly corroded reinforcement ends, corroded hoops, spalling of the concrete between the end of the beam and the first hoop; in the specimen OS 400 BA-P (reinforced concrete beam, normal concrete, sulphate–resistant cement, cement content of 400 kg/m^3, protected) even a reduction of 50% of the bar cross-section was noticed.

9. In similar conditions of exposure, the concrete specimen (OS 500 BA-P) made with an increased cement content of 500 kg/m^3 had absolutely no rust stains, underlining the importance of an adequate cement content for concrete exposed to chemically aggressive environments.

Ultimate Strength of Beams

In terms of beam strength the following may by asserted:

1. There are no significant differences between elements of the same type, maintained in different aggressive environments. Tested up to failure after 20 years of exposure, a similar ultimate capacity for elements exposed to urban and industrial nitrogen is recorded. However, a 10% reduction of the ultimate bending moment M_u for the beams maintained in industrial chlorine environment versus those maintained in urban conditions clearly appears from Figure 5, where data for beams of OS 500 type are given.

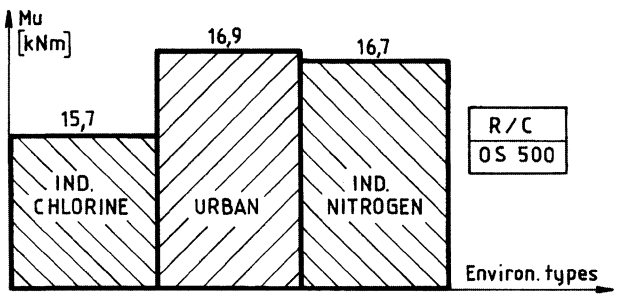

Figure 5 Ultimate beam capacity for different conditions of exposure (20 years): reinforced concrete beam of OS 500 type

2. There is a similar behaviour during the experimental tests for protected and unprotected beams. This aspect is shown in Figure 6 for reinforced concrete elements, made of normal concrete, using sulphate – resistant cement and a cement content of 500 kg/m^3.

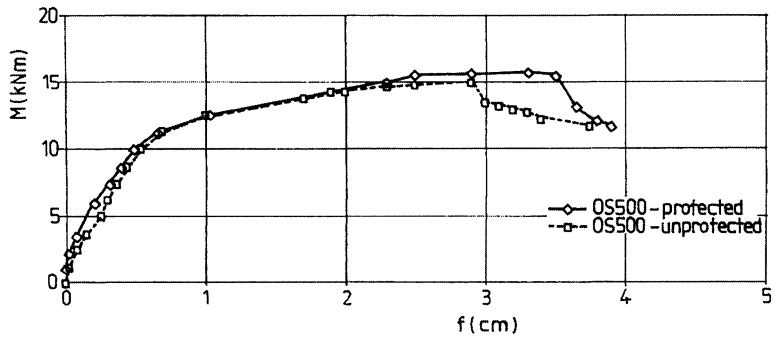

Figure 6 Moment deflection diagrams for protected and unprotected R/C elements (20 years of exposure to industrial chlorine environment)

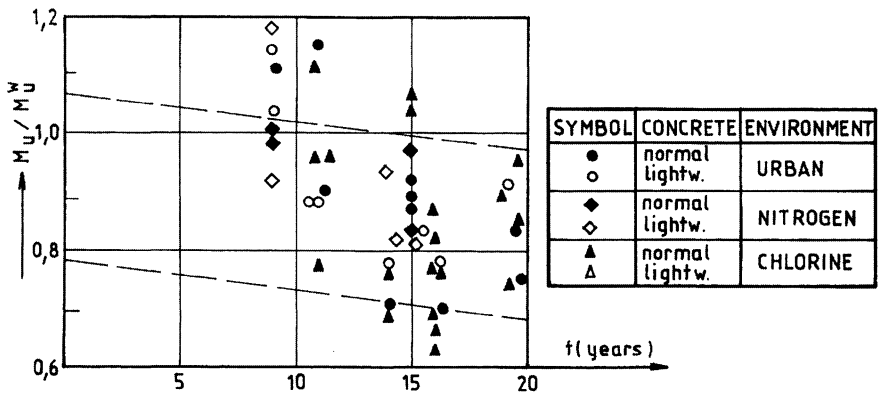

Figure 7 Effect of time on the ultimate capacity of the beams

3. The ultimate capacity (M_u) of the beams decreases in time. Figure 7 shows that the ratio M_u / M_u^w, where M_u^w is the ultimate capacity of the witness beam, is generally substandard: 0.91 after 9 years, 0.78 after 16 years and 0.75 after 20 years. From the analysis of more then 60 tested beams, the following could be reported:

   - Lightweight concrete elements showed a greater reduction of their ultimate capacity (aprox. 10%) than the normal concrete elements.

   - For the beams made of concrete with high-compressive strength $(f_c)_{28}$ = 53-58 MPa (strength class of concrete C35/45 and C40/50 [5]), the reduction of the ultimate bending capacity with time is smaller, only 0.82÷0.92, after 20 years.

CONCLUSIONS

The main results and conclusions are summarised as follows:

1. The rate of strength development is dependent on the concrete grade; the concrete strengths have continued to increase even after 10 years and, between 10 and 20 years this increase is significant.

2. After 20 years of exposure, the aggressive industrial environments have produced a medium to severe scaling process of the concrete surface, staining, cracking and local spalling of the concrete.

3. The rate of carbonation depends on several factors, such as: the cement content, cement type or concrete type, but it is slightly influenced by the environment type.

4. Regarding the protection against the reinforcement corrosion, the importance of an adequate cement content (e.g. 500 kg/m^3) and a minimum of 3.5 cm concrete cover for the R/C beams exposed to industrial chlorine atmosphere is to be kept in mind.

5. The ultimate capacity of the beams decreases in time; reductions of 10 to 25% after 20 years, being recorded.

REFERENCES

1. MIRCEA, D., Long-term durability of reinforced and prestressed elements in aggressive environments, ACI Materials Journal, Vol 91, March 1994, p135-140.

2. IOANI, A., MIRCEA, D., 20 years durability study: reinforced elements in aggressive environments, Proceedings of the International Symposium "High Performance concrete" Hong Kong & Shenzhen, China, December 2000, Vol 1, p 231-236.

3. ACI Committee 209, Prediction of creep, shrinkage and temperature effect in concrete structures (ACI 209R-92 Reapproved 1997), ACI MCP 2000, Part 1.

4. BRANSON, D. E., CHRISTIANSON, M. L., Time-dependent concrete properties related to design-strength and elastic proprieties, creep and shrinkage, Symposium on Creep, Shrinkage and Temperature Effects, SP-27-13, ACI, 1971, pp 257-277.

5. EUROPEAN COMMITTEE FOR STANDARDISATION, Eurocode 2: Design of Concrete Structures, ENV 1992.

6. ACI Committee 201, Guide to durable concrete (ACI 201.2R-92 Reapproved 1997), ACI Manual of Concrete Practice 2000, Part 1.

7. PARROT, L. J., A review of carbonation in reinforced concrete. C&CA/BRE Report C/1-0987, British Cement Association, July 1987, p 45.

THE CONDITIONS OF THAUMASITE FORMATION AND ITS ROLE IN CONCRETE

J Małolepszy

R Mróz

University of Mining and Metallurgy

Poland

ABSTRACT. The following report will mainly be focused on the conditions of thaumasite formation in concrete and mortar. Until now in literature there has been a predominant opinion that the destruction of concrete by sulphate ions is connected first of all with expansive ettringite and gypsum formation. The C_3A content in cement is the main parameter limiting the resistance of concrete to chemical corrosion. However, recent research indicate that CSH also undergoes sulphate corrosion, especially in the presence of CO_2 and in lower temperatures. In this case the thaumasite, which crystals are similar to those of ettringite, is produced. The formation of thaumasite also results in expansion causing the microcracks in concretes and mortars. Preliminary results of the experiments dealing with the influence of C/S ratio in CSH on the thaumasite formation will be presented. In order to identify this phase the XRD and SEM – EDS methods will be used.

Keywords: Sulfate attack, Thaumasite, Concrete

J Małolepszy is Professor at the Faculty of Material Science and Ceramics of University of Mining and Metallurgy in Cracow, Poland. His research activities are focussed on concrete technology and developing of modern buildings materials technologies basing on wastes and secondary raw materials.

R Mróz is post graduated student at the Faculty of Material Science and Ceramics of University of Mining and Metallurgy in Cracow, Poland. In his PhD researches he studying chemical corrosion of concrete. Recently his researches are focused on Thaumasite form of sulphate attack.

INTRODUCTION

Concrete durability can be defined as a complex of assumed properties, which must be attributed to the construction within the longest possible time of utilization [1,18]. There is a number of factors influencing concrete durability, and among them are: section of components, technology, curing and maturing conditions, mechanical load constant and variable, influence of corrosion environment and maintenance / conservation. In many cases the factors mentioned above influence concrete together. The chemical corrosion belongs to the factors which change concrete durability in a significant way [1].

Concrete corrosions in environment sulphate is the most dangerous. As a result the expansion with gypsum and ettringite formation takes place [1]. The amount of gypsum and ettringite depends mainly on the content of calcium hydroxide and hydrated calcium aluminate [2]. The influence of ammonium sulphate and magnesium sulphate can be considered among even more destructive for concrete [3,4]. In case of magnesium sulphate also the most durable CSH phase undergoes decomposition [2].

Another example of CSH destruction in concrete occurs when thaumasite is produced [5]. Thaumasite forms as a result of alkali sulphates and CO_2 attack on concrete in lower temperatures and conditions of high humidity [5,6,7].

C/S ratio in the CSH phase to a large extend depends on the sort of cement. It is known that created CSH phase as a result of cements hydration consisting big amounts of granulated blastfurnace slag or pozzolana is characterized by much lower C/S ratio than in case of traditional portland cements. Moreover, portland cement contains in its mineral composition different amounts of C_3S which will also have influence on the C/S ratio in created CSH phase.

Recently, it has been very popular to add silica fume to concrete mixtures which bind $Ca(OH)_2$ and simultaneously create CSH phase of lower C/S ratio than in traditional cement. Thus, research results indicate practical meaning of choosing mineral composition of clinker and mineral additives to cement, which will be used to create concrete used in the constructions exposed to thaumasite form of sulfate attack.

The investigations of many authors indicate that many concrete constructions may be deteriorated by thaumasite formation as a result of sulphate attack. Typical elements that may suffer from thaumasite sulphate attack are: fundations, colums and pier bases, ground slabs and buried pad fundation, roads pavements, trench fill and concrete drainage pipes, ground cincrete anchors and tunel linings [5]. As a result of thaumasite sulphate attack on the elements mentioned above, the potentially significant structural effects have been identified as: loss of concrete cross-sectional area, loss of cover concrete to the reinforcing bars and, possibly, beyond the bars, loss of bond between reinforcement and concrete in affected zones, settlement, inducing structural damage and loss of durability as a result of loss of protection against reinforcement corrosion [5].

Examples of the thaumasite sulphate attack effects above mentioned are widely described in literature. The British authors, among others point out the numerous cases of thaumasite sulphate attack phenomenon occurring mainly in concrete foundations of industrial buildings, flats and flyovers and bridges in Great Britain [5,6,7]. Such cases have also been noticed in concrete surface and car and train tunnels in the Italian Alps [8]. Also very dangerous - and

described in the literature - are symptoms of thaumasite sulphate attack in concrete constructions in dams located in Italy [9]. There are also cases of similar sulphate attack in historical buildings in Greece and Turkey [10].

In the following report the preliminary research results on the influence of C/S ratio in CSH on the thaumasite formation will be presented.

EXPERIMENTAL PART

Concrete is produced from different cements. The differences may concern mineral composition and mineral additives used. As a reasult of cement hydratation CSH phase is formed with variable C/S ratio of 0,8 to 2,5. In order to follow the C/S effect the CSH has been synthesized with C/S ratio of 0,8, 1,5, 2,0, 2,5.

CSH synthesis

The mechanism of calcium silicate hydrate synthesis has been studied by many authors [11,12,13,14]. This process includes the following stages:

- surface protonation with OH^- formation
- seperation of $Si(OH)_3^-$ into the solution
- reaction between Ca^{2+} from the solution and silicate ions with formation of a product rich in CaO (so-called CSH II of C/S ratio about 1,5 - 2,0)
- reaction of an initial product with SiO_2 dissolution product with CSH phase poorer in CaO synthesis(so-called CSH I of C/S ratio about 0,8 – 1,0)
- depending on the conditions of the synthesis and proportions between SiO_2 and CaO the ordering of structure with formation of tobermorite and xonotlite or other phases takes place.

A relatively slow rate of quartz dissolution is the factor controlling the rate of CSH synthesis. The process can be considered as a hydration reaction "by solution" in which we can identify, in the most general case, the phase of dissolving substrates and precipitation of products. The process of setting and hardening of the products containing calcium silicate can take place in normal temperature under the atmospheric pressure or by using hydrothermal conditions, that is the temperature above 100^0C and saturated water vapour. As a result of the reaction in the reacting mixture we get the products formed in the form of calcium silicate hydrates, characterized by different degree of order.

In the following research a synthesis of CSH phase was carried out in hydrothermal conditions. The materials were put together in the proportions expressed by C/S mole ratio, which were given by the following values 0,8, 1,5, 2,0, 2,5. In the hydrothermal process of CSH phase synthesis the silica flour and burnt lime were used, mixed in proper C/S proportions. Then the mixture was homogenized with added in amount to guarantee putting of lime and hydration of the ingredients (w/s equal 1,0). The mixture was then put into a container where it underwent slaking process in 50^0C within 2 hours. After that it underwent a homogenization process again. The variable parameters of treatment was time of synthesis (8 and 24 h), and C/S ratio. The samples prepared in such a way where subjected to thermal processing at 180^0C under the equilibrium pressure of water vapour.

Preparation of pastes

CSH obtained as mentioned above was used to prepare pastes with composition given in a table 1 and 2. As a mineral additions were used: $CaCO_3$, $Ca(OH)_2$ and $Na_2SO_4 \cdot 10H_2O$ in variable quantities in relation to CSH phase. From the mixtures the pastilles were made with dimensions d x h = 12 x 8 mm. The pastilles were pressed with deaeration of the mass. Pressing took place under pressure of 1kN. The samples prepared in such way were subjected to testing for sulphate attack resistance of CSH phase.

Table 1 Composition of pastes produced from CSH phases of variable C/S ratio, cured in hydrothermal conditions within 8 hours of the autoclaved process

NO	SAMPLE CODE	COMPOSITION OF SAMPLES						
		C/S ratio in CSH phase				$CaCO_3$ p. p. a	$Ca(OH)_2$ p. p. a	$Na_2SO_4 \cdot 10H_2O$
		0,8	1,5	2,0	2,5			
		weight [%]						
1	P/8/1D	75	-	-	-	10	5	10
2	P/8/2D	-	75	-	-	10	5	10
3	P/8/3D	-	-	75	-	10	5	10
4	P/8/4D	-	-	-	75	10	5	10
5	P/8/1	100	-	-	-	-	-	-
6	P/8/2	-	100	-	-	-	-	-
7	P/8/3	-	-	100	-	-	-	-
8	P/8/4	-	-	-	100	-	-	-

Table 2 Composition of pastes produced from CSH phases of variable C/S ratio, cured in hydrothermal conditions within 24 hours of the autoclaved process

NO	SAMPLE CODE	COMPOSITION OF SAMPLES						
		C/S ratio in CSH phase				$CaCO_3$ p. p. a.	$Ca(OH)_2$ p. p. a.	$Na_2SO_4 \cdot 10H_2O$
		0,8	1,5	2,0	2,5			
		weight [%]						
1	P/24/1D	75	-	-	-	10	5	10
2	P/24/2D	-	75	-	-	10	5	10
3	P/24/3D	-	-	75	-	10	5	10
4	P/24/4D	-	-	-	75	10	5	10
5	P/24/1	100	-	-	-	-	-	-
6	P/24/2	-	100	-	-	-	-	-
7	P/24/3	-	-	100	-	-	-	-
8	P/24/4	-	-	-	100	-	-	-

Conditions of maturing

The pastes produced in accordance with the assumptions given in preparation of pastes in the form of pastilles, divided into two testing series, stored in two different temperature ranges [15,16,17]:

- I: 5 ± 1^0C range
- II: 20 ± 2^0C range.

Both series were placed above the distilled water in plastic containers closed tightly. The samples matured in a horizontal position 5mm from the surface of water. Water was not exchanged during entire testing process and its level was maintained only by adding fresh distilled water. The testing took place after: 28, 90, 180, 270 and 360 days.

RESULTS

The influence of $CaCO_3$, $Ca(OH)_2$ and Na_2SO_4 additions used for preparation of CSH phases with variable C/S ratio from 0,8 to 2,5 and conditions of storing samples on possibilities of occurrence of thaumasite were estimated according to results obtained by SEM – EDS and XRD. The results presented here are showing results of investigations of binders after 90 and 180 days of curing.

Analyzing results obtained from observations of samples after 90 days of curing, proved by scanning microscopy, it could come to conclusion that the beginning of crystallization of fibre – like form [Fig.1a] are observed in samples doped with $CaCO_3$, $Ca(OH)_2$ and Na_2SO_4 with C/S ratio 2,5 and stored in temperature 5^0C, apart from method of obtaining CSH phase (time of autoclaved process). The observed beginnings of crystallization take their places in region of cracks, gaps and voids in samples [Fig.2a]. Additionally on the basis of results of analysis of chemical composition of these forms, acquired by EDS method, it could be concluded, that we have to deal with existence of thaumasite forms [Fig.1b,2b].

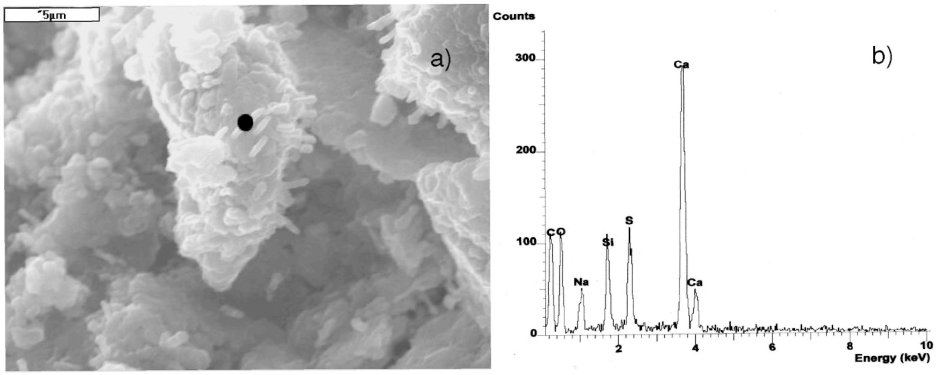

Figure 1 Results of SEM observation sample (P/8/4D) of C/S ratio 2,5 admixtured $CaCO_3$, $CaOH_2$ and Na_2SO_4 stored in 5^0C, after 3 months. a) The beginning of crystallization of fibre – like form, b) EDS analysis of these form

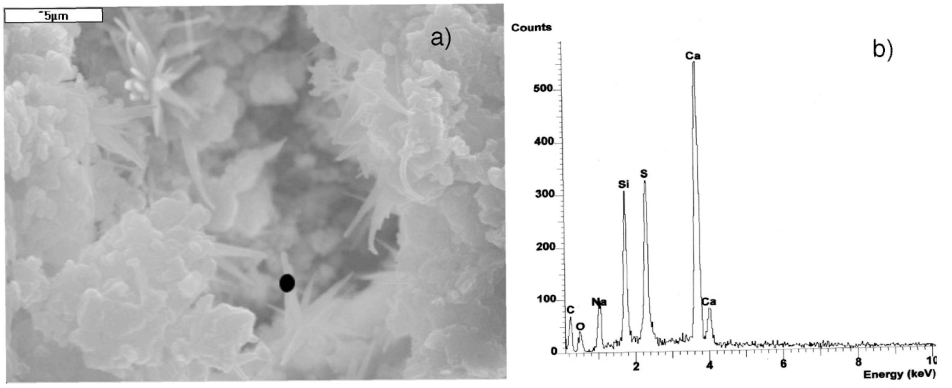

Figure 2 Results of SEM observation sample (P/24/4D) of C/S ratio 2,5 admixtured $CaCO_3$, $CaOH_2$ and Na_2SO_4 stored in 5^0C, after 3 months. a) The beginnings of crystallization in region of cracks and gaps in sample, b) EDS analysis

Analysis of obtained results of samples after 90 days of curing by XRD method let us to claim that in each case, samples of these binders consist of CSH phase with variable C/S ratio and additions of $CaCO_3$, $Ca(OH)_2$ and Na_2SO_4, and also indicates on formation of gypsum.

Results of investigation of samples after 180 days of curing were obtained with same methods, namely SEM – EDS and XRD. Analyzing results obtained from observations of samples after 90 days of curing, proveided by scanning microscopy, let us to conclude, that crystallization of fibre – like forms existing in earlier stage of observation (90 days) in samples with addition $CaCO_3$, $Ca(OH)_2$ and Na_2SO_4 with C/S ratio 2,5 and stored in temperature 5^0C shows changes in microstructure in leading to formation of better crystallized products [Fig 3a]. The EDS chemical analysis proves thaumasite's character of these forms [Fig. 3b].

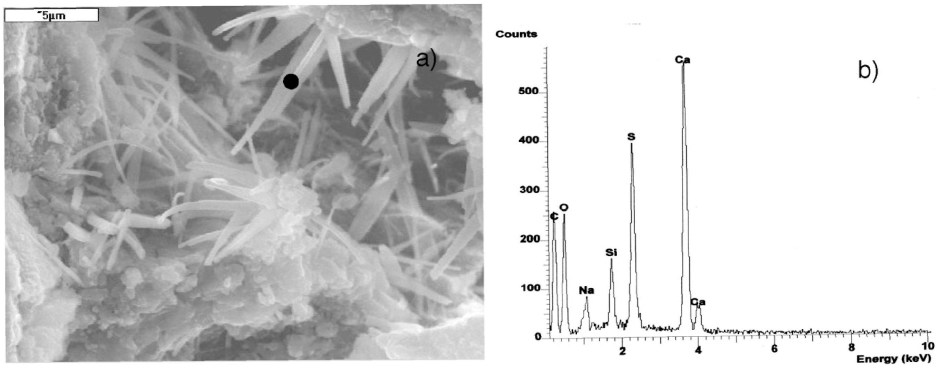

Figure 3 Results of SEM observation sample (P/24/4D) of C/S ratio 2,5 admixtured $CaCO_3$, $CaOH_2$ and Na_2SO_4 stored in 5^0C, after 6 months. a) Formation of better crystallized products, b) EDS analysis of these form

Similar crystallization were observed in CSH samples with C/S ratio 1,5 and 2,0 doped with $CaCO_3$, $Ca(OH)_2$ and Na_2SO_4 stored in 5^0C [Fig. 4a,5a]. Also in this case EDS chemical analysis proved thaumasite's character of these forms [Fig. 4b,5b].

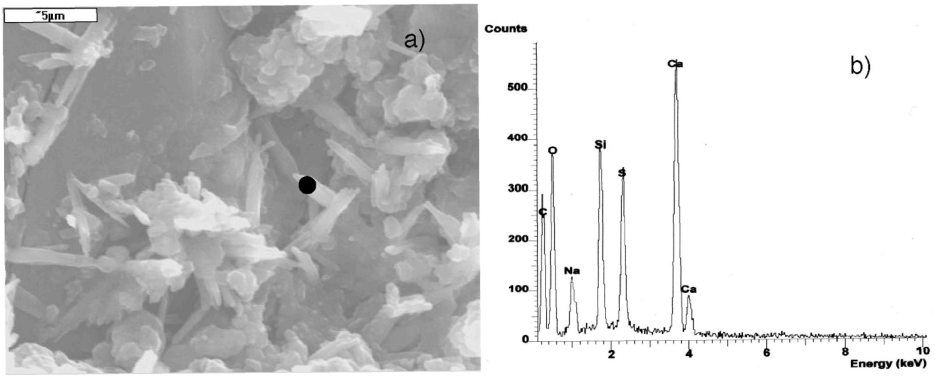

Figure 4 Results of SEM observation sample (P/24/2D) of C/S ratio 1,5 admixtured $CaCO_3$, $CaOH_2$ and Na_2SO_4 stored in 5^0C, after 6 months. a) Crystallization of fibre-like forms, b) EDS analysis of these form

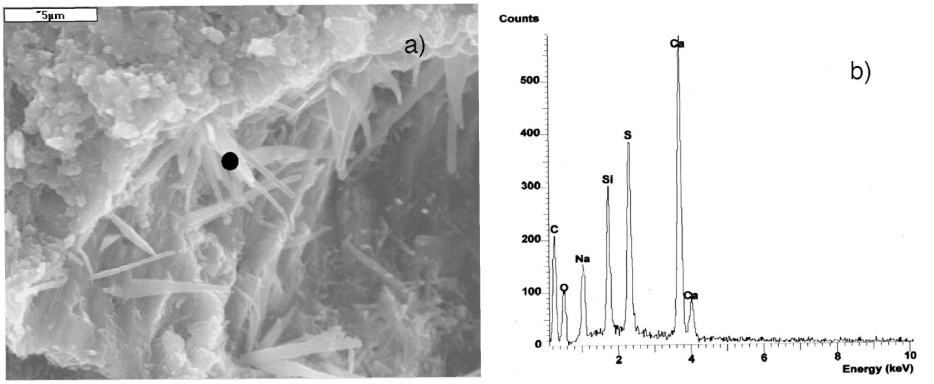

Figure 5 Results of SEM observation sample (P/24/3D) of C/S ratio 2,0 admixtured $CaCO_3$, $CaOH_2$ and Na_2SO_4 stored in 5^0C, after 6 months. a) Crystallization of fibre-like forms, b) EDS analysis of these form

The crystallization of thaumasite's form took place both in cracks and gaps as in region of voids in discussed samples. Whereas SEM observations of samples CSH with C/S ratio 0,8 with additions of $CaCO_3$, $Ca(OH)_2$ and Na_2SO_4 stored in temperature 5^0C, in which fibre – like forms were not observed in cracks, gaps and voids, shows crystallization of portlandite [Fig. 6a], which identification was proved by EDS chemical analysis [Fig. 6b].

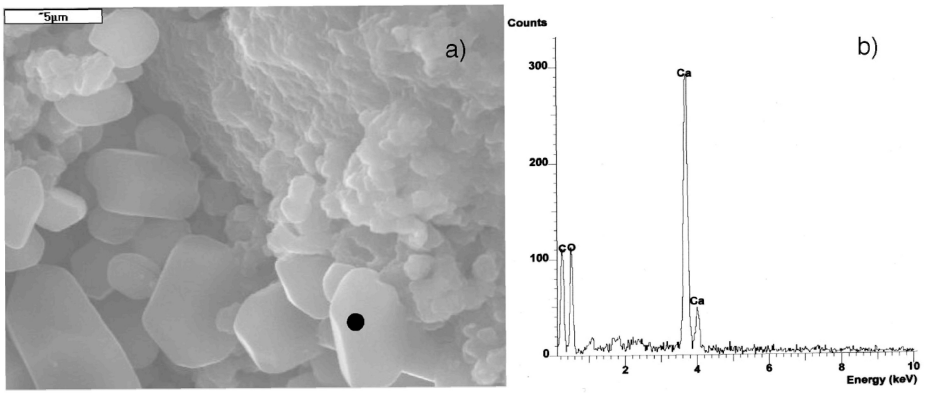

Figure 6 Results of SEM observation sample (P/24/1D) of C/S ratio 0,8 admixtured $CaCO_3$, $CaOH_2$ and Na_2SO_4 stored in 5^0C, after 6 months. a) Crystallization of portlandite, b) EDS analysis of these form

Analysis of the XRD results of samples curing for 180 days, was made on basis of changes in intensity of main reflexes assigned to the mineral phase, it allows to conclude that while time of curing is longer there's less amount of $CaCO_3$ and $CaSO_4 \cdot 2H_2O$ in samples doped with $CaCO_3$, $Ca(OH)_2$ and Na_2SO_4, stored in temperature 5^0C.

DISCUSSION

Synthesised CSH phase, which was used as a alite hydration product was characterised by variable C/S ratio from 0,8 to 2,5. Obtained pastes are characterised by assumed C/S ratio. It should also be mentioned that apart from CSH phase of assumed ratio there is also CSH of different C/S ratio. However the CSH of assumed ratio dominates as it results from SEM-EDS data.

A circumstance which decided about carrying out research of assumed range was variety of cement used currently to concrete production which are characterized by a changeable C/S ratio in CSH phase created during hydration process.

The observation of samples containing apart from CSH, $CaCO_3$, $Ca(OH)_2$ and Na_2SO_4 do prove some volume changes in the form of cracks and scratches. The cracks and scratches appear in samples stored in 5^0C.

The obtained results indicate that a pace and an amount of appearing crystallization of fibre – like form are determined by the C/S ratio in CSH as it results from SEM – EDS data. SEM observation confirm the presence of fibre – like form in binders containing CSH of C/S ratio = 1,5; 2,0 and 2,5 doped with $CaCO_3$, $Ca(OH)_2$ and Na_2SO_4 and stored in 5^0C, which EDS analysis proves thaumasite's character of these form.

The results of XRD analysis allow to say that in the initial period of time (90 days) in the samples containing CSH as well as $CaCO_3$, $Ca(OH)_2$ and Na_2SO_4 stored in 5^0C gypsum is formed. Whereas after 180 days an intensity of reflexes assigned to the gypsum and calcium carbonate decreases visibly.

To confirm the SEM – EDS results more research is carried out, which also includes IR and NMR. Additionally, thaumasite synthesis has been done which will make easier to identify it by using IR and NMR methods.

The range of research aims to find an answer if the presence of ettringite is necessary for the formation of cristalized thaumasite.

ACKNOWLEDGEMENTS

The financial support from Faculty of Minerals Science and Ceramics, University of Mining and Metallurgy (grant No 10.10.160.674) is fully acknowledged.

REFERENCES

1. NEVILLE A. M., „Properties of Concrete", London 1997.
2. TAYLOR H. F. W., „Cement chemistry", Academic Press, London 1990.
3. OBERHOLSTER R. E., VAN AARDT I. H., BRANDT M., „Structure and Performance of Cements", Appl. Science Publ., s. 363, London 1983.
4. ROY D. M., 8^{th} ICCC Rio de Janeiro, t I, s. 362, 1986.
5. THAUMASITE EXPERT GROUP „The thaumasite from of sulfate attack: Risks, diagnosis, remedial works and guidance on new construction. Raport of the Thaumasite Expert Group", DETR, Londyn, 1999.
6. THAUMASITE EXPERT GROUP „Thaumasite form of sulfate attack", Concrete Nr 2, s. 37 - 40, 1999.
7. HOBBS D. W., TAYLOR M. G., „Nature of the thaumasite sulfate attack mechanism in field concrete", Cement Concrete Research 30, s. 529 - 533, 2000.
8. HARTSHORN S., SIMS I., „Thaumasite - a brief guide for engineers", Concrete Nr 10, s. 24 - 27, 1998.
9. BERRA M., BARONIO G., „Thaumasite in Deteriorated Concretes in Presence of Sulfates", Concrete Durability sp 100 - 106, s. 2073 – 2089.
10. PAPAYIANNI I., „Durability lessons from the study of old mortars and concretes", P. K. Mehta Symposium on Durability of Concrete, Nice 1994.
11. TAYLOR H. F. W., „The chemistry of Cements", Academic Press, London 1964.

12. UCHIKAWA H., Proc 9th ICCC, Vol. 1, 797, New Delhi, 1992.

13. KALOUSEK G. L., J. Am. Ceram. Soc., 40, 74 1957.

14. RADEMAKER P.D., REIMAN V., Zement-Kalk-Gips, 47, 636 1994.

15. BENSTED J., „Scientific background to thaumasite formation in concrete", World Cement Research 11, 1998.

16. BENSTED J., VARMA S. P., „Studies of Thaumasite", Sil. Ind. T 2, 1973.

17. BENSTED J., VARMA S. P., „Studies of thaumasite, part II", Sil. Ind. T 39, 1974.

18. KRIVENKO P., "Mineralogical aspects of durability of concretes", Kurdowski Symposium: Science of Cement and Concrete, Kraków, June 20-21, 2001.

ACCELERATED SCREENING TESTS FOR ALKALI AGGREGATE REACTIONS IN HONG KONG

K K Liu W H Tam

T H Kwan W C Lau

Government of the Hong Kong SAR

China

ABSTRACT. Some 50% of the aggregates used for construction in Hong Kong are imported, mostly from nearby quarries in Mainland China. While local aggregates produced from granite are generally regarded as non-reactive with respect to alkali aggregate reaction (AAR), less can be said about imported aggregates. Structures suffering from the effects of AAR have been reported, investigated and confirmed by the Public Works Central Laboratory (PWCL). Accelerated mortar bar test (AMBT) methods were used at the PWCL for testing the alkaline aggregate reactivity of aggregates, including imported aggregates and recycled aggregates. The results of these tests using four different AMBT methods, originated from Hong Kong, the US, Canada and Europe, are presented and discussed in this paper. This paper also describes a study which compares the results of AMBT using high alkaline cement in forming the mortar bars with those using low alkaline cement but with sodium hydroxide or sodium chloride added. The International Union of Testing and Research Laboratories for Materials and Structures (RILEM) method was used for the AMBT. The differences in the results are highlighted and discussed. The study also investigated the role of alkaline in the cement, and of the sodium ions and hydroxide ions added to the mortar mix during the AMBT in the development of AAR.

Keywords: Reactive aggregates, Recycled aggregates, Alkaline, Alkali-aggregate reactions, Accelerated mortar bar tests.

K K Liu, is a Chartered Civil Engineer and Senior Engineer in the Geotechnical Engineering Office in the Civil Engineering Department, Government of the Hong Kong SAR.

W H Tam, is a Chartered Civil Engineer in the Geotechnical Engineering Office in the Civil Engineering Department, Government of the Hong Kong SAR.

T H Kwan, is a Chartered Civil Engineer and Engineer in the Geotechnical Engineering Office in the Civil Engineering Department, Government of the Hong Kong SAR.

W C Lau, is a Chemist in the Geotechnical Engineering Office in the Civil Engineering Department, Government of the Hong Kong SAR.

INTRODUCTION

Concrete is a construction material made by mixing cement with coarse aggregates, fine aggregates, water and possibly admixtures. Good quality concrete should not only have the required minimum strength, but should also be durable. Both the required strength and durability of concrete are achieved by a judicious choice of component materials in the right proportions, proper placing and adequate curing. The alkali in the cement, which is important to the strength development of concrete, may however be the source of severe durability problems. It can react with some forms of silica in the aggregates, and cause expansion and cracking of the concrete. This process is known as alkali-aggregate reaction.

As the characteristics of two of the major components in concrete, aggregates and cement, vary depending on the geographic location, thus affecting the strength and durability of concrete, a local testing method of AAR was developed to suit the local use of aggregates having unique reactivities and cement with low alkaline contents. The Public Works Central Laboratory (PWCL) started to develop its own AAR testing method in 1993 based on the method by Oberholster and Davies [1] of the National Building Research Institute (NBRI). In this method, the mortar bars are stored in one molarity solution of sodium hydroxide (1M NaOH) at a temperature of 80°C for 14 days. The classification of alkali reactivity of aggregates is based on the expansion of the mortar bars after 14 days. This method is aimed to quickly screen aggregates for the potential alkali aggregate reaction in concrete. This local AMBT method, named as the PWCL CON 5.5, has been adopted for use by the PWCL as one of the routine tests for evaluating the alkaline reactivity potential of aggregates.

OCCURRENCE OF AAR IN HONG KONG

Background

Although AAR has been known to be a problem in many parts of the world, it was not discovered in Hong Kong until 1991. The Standing Committee on Concrete Technology (SCCT), formed in 1982 with the principal aim of monitoring and setting the standard of concrete construction in Hong Kong, became aware of the occurrence of AAR which can cause detrimental expansion of concrete. A number of concrete structures in Hong Kong were identified with 'map cracking' – a crack pattern characteristic of AAR. Consequently, an AAR sub-committee of SCCT chaired by the Chief Geotechnical Engineer/Materials of the Geotechnical Engineering Office (GEO) was set up to coordinate all investigative and research work related to AAR in concrete in 1991. The sub-committee comprises representatives from various Government departments. This sub-committee issued a Technical Circular (Works Branch Technical Circular No. 5/94in 1994 [2]) recommending a limit of 3 kg of reactive alkali content per cubic metre of concrete to safeguard concrete against AAR. The most common type of AAR, identified in Hong Kong, is alkali-silica reaction (ASR). ASR is related to the chemical instability of various forms of silica minerals (e.g. opal, cristobalite, micro- to cryptocrystalline quartz) under high pH conditions. These silica minerals were found to present in aggregates from Wu Shek Koo Quarry (located in Shenzhen Special Economic Zone just across the border of Hong Kong). Since the control of alkali content (3 kg/m^3) in concrete had not been imposed prior to 1994, the alkali content of concrete structures constructed using these aggregates could be high, and the occurrence of ASR in these concrete structures could be expected.

Projects investigated

The Materials Division of GEO was requested by SCCT to investigate a number of suspected cases of AAR in Hong Kong. Consequently, an AAR investigation programme was set up in the PWCL of the Materials Division. The investigation included site monitoring, expansion test, and petrographic examination and chemical analysis of concrete specimens obtained from in situ structures. The investigative work was reported subsequently [3, 4 & 5]. Study of aggregates from a number of quarries in Hong Kong and in southern parts of Mainland China close to Hong Kong was also carried out for identifying potential AAR problems by means of AMBT. The case of Shek Wu Hui Sewage Treatment Plant was thoroughly investigated and the techniques used are highlighted below.

Site monitoring

Ten hexagonal rosettes of Demec gauges were installed on the concrete structure to measure strains in three directions. Measurements were taken four times in each of the three rosette directions in each site visit. The strains measured at the ten Demec gauges in the horizontal, the left slanting and the right slanting directions were plotted against time. Details of the results were reported by Tse & Gilbert [6].

Expansion test

The procedure for the expansion tests is based on ASTM C 227-90. Seventeen bars of 25 mm x 25 mm x 70 mm long were prepared from nine 100 mm diameter cores taken from selected locations on the walls of the sedimentation and aeration tanks. They were individually wrapped in wet towel and immersed in water inside a sealed plastic container. The container was then stored in an environmental chamber with the temperature maintained at 38°C and relative humidity above 95%. The expansion of the bars were measured at regular intervals. The results of the tests for the Shek Wu Hui Treatment Plant investigation indicated that all specimens expanded rapidly by about 200 to 300 microstrains (i.e. 0.02 to 0.03%) after fourteen days of testing [6].

Petrographic examination

Petrographic examination of concrete specimens was carried out generally in accordance with the requirements of ASTM C 856-86. Thin sections of 65 mm x 45 mm x 30 μm thick were cut and vacuum impregnated with fluorsecent or colour dyed resin prior to the microscopic examination. The examination provided information on the cement/aggregate relationship, mineral phase in the cement and aggregates, aggregate composition and nature of microcracks. It also allowed the identification and assessment of ASR reaction centres and gel products. An example of observation from a petrographic examination is shown in Figure 1.

Chemical analysis

The white solids obtained from the expansion tests were examined by means of infrared (IR) spectroscopy and scanning electronic microscope and energy dispersive x-ray (SEM-EDX) spectroscopy to identify their chemical composition. The carbonate group (CO_3^{2-}) was identified in the IR spectroscopy with C-O bond stretch absorption peak.

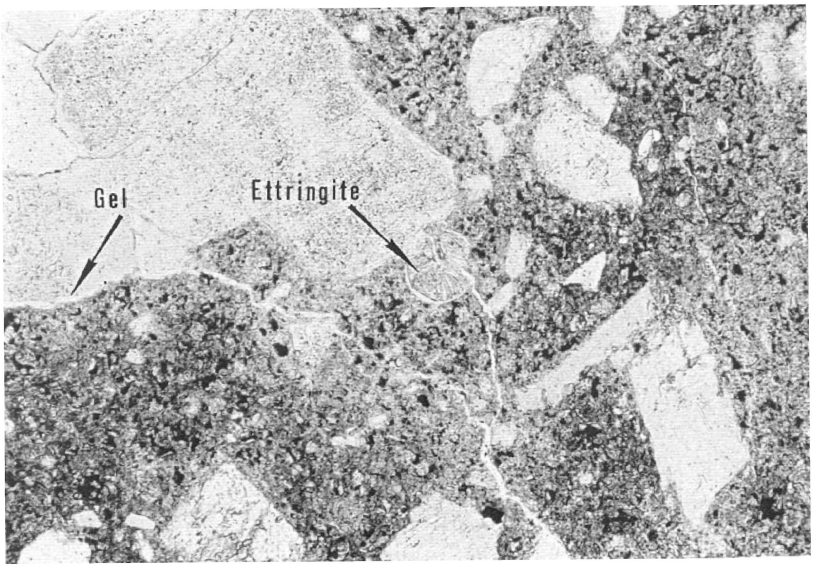

Figure 1 Petrographic examination of a concrete core specimen from a footbridge in Fanling, Hong Kong

The SEM analysis of the white solids revealed that the matrix material was generally poorly crystalline to amorphous with individual crystals of size between 2 μm and 5 μm. From the EDX analysis, calcium was found to be the dominant element in the white solids. These white solids were then concluded as $CaCO_3$. The total alkali content of concrete specimens obtained from sites were tested since high alkalinity conditions can initiate AAR in concrete. The results of alkaline contents were found to be as high as 15 kg/m^3 of concrete in some cases, which far exceeded the limit of 3 kg/m^3 [7] that was not yet introduced at the time the concrete was cast. With such high alkaline contents, it is not surprised that AAR has taken place in the concrete.

ASSESSMENT OF AGGREGATES BY ACCELERATED MORTAR BAR TEST

A number of AMBT methods were continued to be developed, but they often involved the use of a high temperature up to 80°C which can distort the normal behaviour of the constituents of concrete. Several national standard methods (e.g. ASTM C 1260-94, CSA A23.2-25A-94, RILEM AAR-2: 2000 and DD 249: 1999) are available for AMBT. These methods involve the mixing of cement of high alkali content with aggregates of size 5 mm – 125 μm and storage of the mortar bars in sodium hydroxide solution (1M NaOH) at 80°C for 14 days after demoulding. A length-measuring device, accurate to 0.002 mm, is used to measure the changes in length of the bars at regular intervals. A detailed comparison of the various AMBT methods is given in Table 1. In order to assess the susceptibility of various types of aggregates to AAR , the PWCL has carried out a series of AMBT including PWCL CON 5.5 on local and imported aggregates from various sources using different AMBT methods, and the results were shown in Table 2.

Table 1 Comparison of various accelerated mortar bar test methods

	PWCL CON 5.5	ASTM C 1260 (94)	CSA A23.2-25A (94)	RILEM AAR-2 (2000)	DD 249 : 1999[1]
Size of specimen	25 x 25 x 285 mm	25 x 25 x 285 mm	25 x 25 x 285 mm	25 x 25 x 285 mm	25 x 25 x 250 mm
Laboratory conditions	20 ± 2°C; RH ≥ 65%	20°C to 27.5°C; RH ≥ 50%	20°C to 26°C; RH ≥50%	20 ± 2°C; RH: ≥50%	20 ± 5°C; RH: ≥50%
Temp. of water used	20 ± 2°C	23 ± 1.7°C	23 ± 2°C	20 ± 2°C	20 ± 5°C
Specification of cement	Locally available cement, preferably with alkali content >0.55%	Complies with specification C150. Autocave expansion <0.2%	Pass through 710 μm sieve to remove lumps	Specific surface >450 m^2/kg; autocave expansion <0.2 or MgO soundness = 0 mm	Same as RILEM
Alkali content of cement	0.85 ± 0.05%	Negligible or of minor effect on expansion	0.9 ± 0.1%	Min. 1.0%	1 ± 0.1%
Storage cabinet for mould and duration of storage	20 ± 2°C; RH ≥ 95% for 24 ± 2 hrs	23 ± 1.7 °C, RH ≥ 95% for 24 ± 2 hrs	23 ± 2°C, RH >95% for 24 ± 2 hrs	20 ± 1°C; RH ≥ 90% for 24 ± 2 hrs	20 ± 5°C for 24 ± 2 hrs
Volume ratio of NaOH solution to specimen	Min. 4 times vol. of mortar bars	4 ± 0.5 times vol. of mortar bars	4 ± 0.5 times vol. of mortar bars	4 ± 0.5 times vol. of mortar bars	4.8 times vol. of mortar bars
Storage Conditions	1N NaOH at 80°±2°C	1N NaOH at 80°±1°C	1N NaOH at 80±2°C	1N NaOH at 80°±2°C	1N NaOH at 80°±2°C
Measuring time	Within 20 sec	15 ± 5 sec	15 ± 5 sec	Within 15 sec	Within 15 ± 5 sec
Compliance criteria	Not specified	Innocuous if expansion <0.1%	Innocuous if expansion <0.15%	Innocuous if expansion <0.1%	Innocuous if expansion <0.1%
Follow up action	Not specified	Petrographic examination	Petrographic examination	Petrographic examination	Not specified

(1) The DD249 is a Draft for Development and should not be taken as a British Standard

Comparison of accelerated mortar bar tests

The mean percentage expansions of mortar bars prepared using aggregates obtained from local and imported sources and measured using the PWCL CON 5.5, ASTM C 1260, CSA A23.2-25A and RILEM AAR-2 methods were compared in Table 2. As can be seen, these methods are able to clearly identify the reference aggregates of ash tuff and granodiorite, for which a 14-day mortar bar expansion was found to be greater than 0.1%, as reactive aggregates. Aggregates of granite and diorite were found to have 14-day expansion of less than 0.1%. They were therefore considered as innocuous with respect to AAR. This 0.1% expansion is considered by the methods studied as the lowest limit below which aggregates could be considered as innocuous. The above mentioned four AMBT methods produced similar expansion results.

Table 2 Comparison of mean percentage expansion of mortar bars measured using different test methods

AGGREGATE	MEAN EXPANSION OF MORTAR BARS AT 14 DAYS OF TESTING (%)[1]					
	PWCL CON 5.5	ASTM C 1260 (94)	CSA A23.2-25A (94)	RILEM AAR-2 (2000)[2]	RILEM AAR-2 (2000)[3]	RILEM AAR-2 (2000)[4]
San Jian Shan (Granite)	0.017	0.016	0.016	0.054	0.038	0.029
Oi Ling Ding (Granite)	0.019	0.019	0.019	0.043	0.034	0.039
Little Montana Island (Granite)	0.020	0.025	0.024	0.046	0.038	0.039
Chung Hsin Chau (Granite)	0.023	0.024	0.021	0.050	0.036	0.027
Er Chau (Granite)	0.026	0.033	0.025	0.065	0.041	0.041
Chik Wan (Granite)	0.029	0.030	0.026	0.063	0.040	0.052
Nitutou Island (Granite)	0.044	0.050	0.047	0.106	0.092	0.073
Hung Wan (Diorite)	0.059	0.064	0.055	0.083	0.093	0.072
Little Spider Island (Granodiorite)	0.184	0.137	0.135	0.191	0.193	0.186
Wu Shek Koo (Ash tuff)	0.298	0.285	0.224	0.311	0.291	0.217
Spratt (Reference)	0.458	0.421	0.423	0.467	0.504	0.464
Shek O (Granite)	0.026	0.016	0.036	0.049	0.043	0.052
Lam Tei (Granite)	0.068	0.084	0.078	0.102	0.056	0.061
Lamma Island (Granite)	0.074	0.090	0.076	0.158	0.142	0.108
Anderson Road (Ash tuff)	0.350	0.334	0.359	0.448	0.408	0.309
Kai Tak Airport (Recycled)	--	--	0.040	--	--	0.030
Tseung Kwan O (Recycled)	--	--	0.150	--	--	0.160

(1) The results shown in the above table are the mean of at least two sets of results.

(2) The "Asano" band OPC, the specific surface area of which is less than 450 m^2/kg, was used for the test with sodium hydroxide solution added to arrive at an alkali content of 1.25%.

(3) The "Feng Jiang" brand OPC, the specific surface area of which is greater than 450 m^2/kg, was used for the test with sodium chloride solution added to arrive at an alkali content of 1.25%.

(4) The "Norcem" brand OPC, which is specified by the RILEM Standard Method, was used for the test without addition of any chemicals.

Accelerated mortar bar test on recycled aggregates

Recently , Hong Kong has started to consider the inclusion of recycled aggregates in new concrete structures . This will avoid dumping the aggregates unnecessarily as waste to landfill sites thus reducing their useful life. Presently there are two large sites of recycled aggregates. One is at the Kai Tak Airport where the recycled aggregates were produced from the concrete of the runway. The other one is at a landfill site at Tseung Kwan O. The compaction strength, flakiness index and chloride and sulphate contents of these recycled aggregates were tested in a series of laboratory trials. The results of these tests were found to comply with the respective standard for aggregates and were similar to those of normal aggregates [8]. The PWCL CON 5.5 was once again used to evaluate the reactivity of recycled aggregates to screen out those recycled aggregates that may cause AAR in concrete.

RESULTS AND DISCUSSION

Reactivity of local, imported and recycled aggregates

As can be seen from Table 2, all aggregates of granite from the Lam Tei, Lamma Island and Shek O Quarries in Hong Kong, except those of ash tuff from the Anderson Road Quarry [5], are considered as innocuous. In general, aggregates from Mainland China, other than some exceptional ones, can also be considered as innocuous. For recycled aggregates, the AMBT is also found to be an effective method for identifying those which are potentially deleterious, as can be seen from the results of tests on aggregates from Tseung Kwan O (see Table 2). Subject to other tests like the petrographic examination of recycled aggregates to confirm the validity of AMBT, AMBT can be considered as one of the screening test methods for recycled aggregates as well.

Adoption of RILEM in Hong Kong

Based on the research and development work conducted in PWCL, the RILEM AAR-2 has been found to give the maximum mortar bar expansion for the aggregates tested in the accelerated mode. As confirmed by the results of the petrographic examination, the AMBT using the RILEM method and 0.1% expansion as the limit has been found to be able to identify those aggregates which are deleterious. The SCCT is of the view that the RILEM's AMBT method, RILEM AAR-2: 2000, should be adopted as the routine testing method for assessing the alkaline aggregate reactivity in Hong Kong.

The role of alkaline in cement in accelerated mortar bar test

The alkaline ions in cement are crucial in the development of AAR in concrete since the alkaline (Na_2O_{equ}) in cement can react directly with the activated silica of the aggregates in concrete in the presence of water, to produce AAR. In the case where low alkaline cement, 0.4% (of Na_2O_{equ}) by weight is used in the AMBT for preparing the mortar bars, an appreciable volume of sodium hydroxide solution will have to be added to bring the alkaline content up to 1.2% by weight of Na_2O_{equ} in the mortar mix as specified in the AMBT of RILEM. The alkaline in the form of sodium hydroxide can generate calcium hydroxide $Ca(OH)_2$ by the exchange of the sodium and calcium ions in concrete mix. The amount of $Ca(OH)_2$ generated will in turn cause the mortar mix to form lumps quickly. The normal products of cement hydration (tricalcium silicate, dicalcium silicate, tricalcium aluminate

and tetracalcium aluminoferrite) will be disturbed by the extra amount of calcium hydroxide formed in concrete. Some of the calcium ions in the mortar mix will be consumed as calcium hydroxide and the hydrated products of cement will form quickly leading to the formation of lumps. On the other hand, the addition of sodium chloride powder to the mortar mix, as in the PWCL's study, will not lead to the formation of lumps. The sodium chloride still can provide the required amount of sodium ions in the mortar mix and the formation of calcium chloride. The addition of sodium chloride can satisfy the need for the alkaline content in cement but will avoid the fast formation of lumps.

CONCLUSIONS AND RECOMMENDATIONS

Based on the testing and research work conducted in PWCL, the following conclusions and recommendations can be drawn:

1. Petrographic examination can confirm the presence of AAR in the concrete specimens examined. However, petrographic examination on its own is not able to provide information on the extent and rate of deterioration of the concrete resulting from AAR. This should be carried out in conjunction with long term field monitoring.

2. Aggregates of volcanic tuff from the Anderson Road Quarry in Hong Kong contain abundant amount of microcrystalline quartz in the rock matrix and strained quartz in the coarse crystal components. They are therefore widely recognised as potentially reactive with respect to AAR. Qranitic aggregates originated from Hong Kong do not normally give rise to serious AAR problems.

ACKNOWLEDGEMENT

The authors acknowledge the dedicated technical support, making this research work possible, provided by the staff of Public Works Central Laboratory of Civil Engineering Department, and the permission to publish this paper by the Head of the Geotechnical Engineering Office and Director of Civil Engineering, Government of the Hong Kong Special Administrative Region, China.

REFERENCES

1 OBERHOLSTER R.E., DAVIES G. An Accelerated Method for Testing the Potential Alkali Reactivity of Siliceous Aggregates, Cement and Concrete Research, 1986, Vol. 16, pp 181-189.

2 The Government of Hong Kong. Specification Clauses to Guard Against the Occurrence of Alkali-aggregate Reaction in Concrete Structures, Works Branch Technical Circular No. 5/94, June 1994.

3 WONG P.C., KOIRALA N.P. Interim Report: Investigation of Cracks at Shek Wu Hui Treatment Plant, Special Project Report, Geotechnical Engineering Office, Civil Engineering Department, Hong Kong, 1992, 54 pp.

4 GILBERT S.T. Petrographic Examination of Concrete Cores from Shek Wu Hui Treatment Plant, Special Project Report 4/95, Geotechnical Engineering Office, Civil Engineering Department, Hong Kong, 1994, 42 pp.

5 LEUNG W.C., TSE W.L., MOK C.S., GILBERT S.T. AAR Potential of Volcanic Rocks from Anderson Road Quarries, GEO Report No. 49, Geotechnical Engineering Office, Civil Engineering Department, Hong Kong, 1995, 78 pp.

6 TSE W.L., GILBERT S.T. Final Report on Investigation of Cracks at Shek Wu Hui Treatment Plant, Special Project Report 9/94, Geotechnical Engineering Office, Civil Engineering Department, Hong Kong, 1994, 35 pp.

7 LIU K.K., CHAN C.Y. The Investigation of Cracking of the Concrete on Two Footbridges near Fanling KCR Station, Special Project Report 3/2000, Geotechnical Engineering Office, Civil Engineering Department, Hong Kong, 2000, 37 pp.

8 LIU K.K., TAM W.H. A Report on the Use of Recycled Aggregates in Low Grade Concrete Geotechnical Engineering Office, Civil Engineering Department, Hong Kong, in print.

MOZAL I AND II PROJECT – ACHIEVING DURABILITY UNDER DIFFERENT CIRCUMSTANCES

R Amtsbüchler

H van Heerden

Lafarge

South Africa

ABSTRACT. This paper describes the concrete investigations carried out for the production of durable concrete utilizing locally available resources as much as possible for a sensitive industrial structure in Mozambique. A portion of this structure is directly exposed to the harsh marine environment conditions of the Indian Ocean. The only aggregate source available was not only slightly expansive (ASR) but also showed a very high water absorption in excess of 4%. All these problems were overcome through an innovative approach to concrete mix design. Phase I of this project which included two pot lines for an Aluminium smelter, storage silos in Maputo harbour and a new concrete jetty was successfully completed during 2000. Phase II of the project commenced during July 2001 and involves the construction of another pot line and additional storage facilities in Maputo harbour.

Keywords: Durability, Alkali silica reaction, Water absorption and concrete mix design.

Dr R Amtsbüchler, is a Professional Civil Engineer and Manager of the Product Assistance Department, Lafarge South Africa. His experience in all aspects of concrete was gained in Austria, the Middle East and South Africa. He has been involved with various long-term durability investigations using South African cements, fly ash and aggregates.

H van Heerden, is Laboratory Manager – Cement and Concrete at the Lafarge South Africa Product Assistance Department, an internationally accredited Civil Engineering testing facility. He has been involved with all aspects of concrete for more than 25 years, including tunneling and mining applications.

INTRODUCTION

The Mozal Aluminium smelter project in Mozambique's Maputo province turned out to be a major challenge to concrete technologists.

Phase I of this project, a partnership between Billiton, the Mozambique Government, the Industrial Development Corporation of SA and Mitsubisi, included 250 000m³ of mainly high grade 40 MPa concrete for a primary aluminium smelter, three storage silos and a new jetty in Maputo harbour. Site establishment started in September 1998 and construction was completed in March 2002.

Phase II, involving the supply of 48 000t cementitious material for the construction of another pot-line and additional storage facilities at the harbour site commenced in July 2001. Engineering, Procurement and Construction Management for both phases was awarded to SLE, a joint venture between SN-Lavalin of Canada and Engineering Management Services of South Africa. All concrete for Phase I and II with the exception of the new jetty was and is batched on site by a joint venture between Group Five Civils from South Africa and CMC, an Italian Company which also supplies all the aggregates.

Lafarge Cement – South Africa (LSA) is the main cement supplier, whilst classified fly ash is supplied through associate company Ash Resources and admixtures by Lafarge Group Company Chryso. At the feasibility stage (LSA) had carried out extensive studies on the suitability of Mozambican aggregates. Recommendations by LSA influenced the decision on the basic concrete mix design by SLE. Eventually, the aggregates from the only viable quarry owned by CMC were approved[1], despite being slowly expansive and showing a water absorption at over 4%, four times the usual acceptance level used in South Africa.

An innovative approach to concrete mix design made it possible to use these marginal aggregates for the design of durable concrete.

AGGREGATE AND CONCRETE INVESTIGATIONS

During 1997 Lafarge Cement – South Africa (LSA) sent it's Head Office geologist into Mozambique to investigate possible aggregate sources in the Maputo region.

A confidential Company report identified two possible aggregate sources, about 35 km from the proposed construction site at the Beluluane Industria Park outside Maputo.

- CMC Ravenna Quarry: Rhyolite Rock
- Prosul Quarry: Greywacke Rock

Both aggregates are siliceous, a prerequisite to be used as concrete aggregate for an aluminium smelter (resistivity reasons).

Rhyolite and Greywacke

Rhyolite is by origin an Igneous rock (volcanic equivalent of Granite group), whilst Greywacke is a Sedimentary rock (part of the Sandstone group). The bulk chemistry of Rhyolite contains Alumino Silicates (this is rather mineralogical than bulk chemistry), and Greywacke is classified as an Alumino Silicate bearing Sandstone.

Both aggregates are known to have a high potential reactivity in terms of ASR [2] and water absorption in excess of 4.0%. Another common problem is the possible weathering to expansive clay.

Rhyolite is known to generate very little dust during crushing due to grain size and mineralogy, whilst Greywacke can generate major amounts (~30%) of dust during crushing. Based on the information above Greywacke was in principle eliminated as potential aggregate source.

Further evaluations of Rhyolite and River Sand samples gave the following typical results:

- Low dust content of 1.2% during crushing, low flakiness index and a good Aggregate Crushing Value at Rhyolite aggregate.
- High water absorption of 4.1% with both Rhyolite Crusher Sand and Stone.
- Potential ASR, predicted from petrographic investigations on thin sections, confirmed by a linear expansion of 0.12% (= slowly expansive) when tested according SABS method 1245 [3].
- Suitability of local River Sand to be blended with the rather harsh Crusher Sand. This River Sand showed very low organic impurities and a low clay content of 0.35% as measured by Methylene blue adsorption [4].

Concrete evaluations, conducted at the accredited Civil Engineering Testing facility of LSA

Numerous trial batches were undertaken and some of the final mixes are shown below:

Table 1 40 MPa trial mix with Rhyolite (75/25 OPC/FA)

MIX PROPORTIONS (dry in kg/m³)		COMPRESSIVE STRENGTH (MPa)	
w/binder *	0.43	24 hour	7.0
CEM I 42.5 N	330	2d	14.0
Fly Ash	110	3d	19.0
Blended Sand	550	7d	27.0
7/10 Stone	230	14d	34.5
10/19 Stone	115	28d	45.0
14/22 Stone	805	56d	51.5
Adm. (m ℓ)	656	7/28 ratio	0.60
Water (ℓ)	190		
Absorption Water (ℓ)	56		
Slump (mm)	80		

* Water-excluding Absorption Water, Binder = Cement + Fly Ash

Table 2 Precast trial mix with Rhyolite (80/20 OPC/FA)

MIX PROPORTIONS (dry in kg/m³)		COMPRESSIVE STRENGTH (MPa)	
w/binder *	0.41	24 hour	9.0
CEM I 42.5 N	350	2d	19.0
Fly Ash	85	3d	26.0
Blended Sand	580	7d	37.0
7/10 Stone	225	14d	45.0
10/19 Stone	115	28d	52.0
14/22 Stone	790	56d	62.5
Adm. (m ℓ)	700	7/28 ratio	0.71
Water (ℓ)	180		
Absorption Water (ℓ)	56		
Slump (mm)	40		

Table 3 40 MPa trial mix with Greywacke (75/25 OPC/FA)

MIX PROPORTIONS (dry in kg/m³)		COMPRESSIVE STRENGTH (MPa)	
w/binder *	0.42	24 hour	4.5
CEM I 42.5 N	340+23	2d	10.0
Fly Ash	110+8	3d	12.5
Crusher Sand	525	7d	17.0
19 mm Stone	1150	14d	21.0
Adm. (m ℓ)	660	28d	25.5
Water (ℓ)	190+13	56d	32.5
Absorption Water (ℓ)	73	7/28 ratio	0.67
Slump (mm)	zero		

These trial mixes confirmed the non-suitability of the Greywacke aggregate. The high dust content of 25.9% together with a very flaky aggregate rendered a sticky, unworkable mix with high water demand and low strength.

The Rhyolite aggregate on the other hand performed well despite a high water absorption, provided absorption water was added to the mix (in excess to 50 ℓ/m³). On site, pre-wetting of aggregates has obviously to be undertaken.

The Rhyolite mixes also confirmed the positive effect of a high quality Fly Ash in terms of water reduction, good compactibiltiy and excellent early as well as late compressive strength.

Original concrete specification based on the Hillside smelter (Alusaf) project in South Africa (main points):

- Siliceous aggregate with a maximum water absorption of 0.25% (!)
- Electrical resistivity of concrete ≥ 1000 Ohm meter
- Cementitious material: OPC/CSF (Condensed Silica Fume)
- Max water / binder ratio 0.50

Proposed changes by LSA for the Mozal specification

- Maximum water absorption of 4.5%

  The decision to propose the use of absorptive aggregates was based on experience gained at the Construction of the Corumana dam in Mozambique, where 250 000m³ concrete were placed using Rhyolite as aggregate [5]. Further experience had been gained during the construction of Katse dam in Lesotho [6], where Basalt aggregates with >2% water absorption was used successfully. Pre-wetting of aggregates as used on both projects was strongly recommended.

- Cementitious make-up for the project: CEM I 42.5N and Fly Ash.

  The use of quality Fly Ash was proposed for the following reasons:

  1. To prevent ASR – a minimum of 20% FA is specified by the South African Code of Practice, SABS 0100-2 [7].
  2. To reduce concrete water demand, which will enhance durability and resistivity.
  3. To achieve long term durability through dense, impermeable concrete required in the harsh coastal environment of the Indian Ocean, in particular to prevent chloride induced corrosion.

  Additional benefits of Fly Ash are: increased concrete resistivity [8] and greater abrasion resistance [9] as required for the material silos.

The following materials were finally proposed to the SLE Consultants:

- CEM I 42.5N (Lichtenburg): a cement with a low Sodium Equivalent of ~0.30, complying with all the requirements of SABS EN 197-1 [10].
- Fly Ash: an air classified Fly Ash complying with SABS 1491, Part II [11].
- Concrete admixtures: products from Chryso.
- Aggregates: "Pink" Rhyolite coarse aggregate and a blend of Rhyolite Crusher Sand with River Sand.

An independent evaluation (undertaken for SLE) by the Cement & Concrete Institute of South Africa confirmed the correctness of the proposals by LSA. Subsequently the following amended specification was drawn up by SLE (main points):

- Rhyolite aggregate approved as Concrete aggregate.
- Maximum water absorption of 4.5%
- Cementitious material: CEM I 42.5N and Fly Ash
- Maximum water / binder ratio of 0.445 (for added durability)

CONCRETE CONSTRUCTION

Mozal Phase I

The Group Five / CMC joint venture set up three 50 m³/h power drive batch plants on site, supplying a fleet of 34 truck mixers (6 m³). All concrete mixes except for the concrete jetty were designed by the Group Five Concrete Technologist, using as a rule a combination of 70% CEM I 42.5N (OPC) from Lafarge and 30% Fly Ash from Ash Resources.

Only for the sliding operation of the two coke silos, where a 3 m lift was achieved per 12-hour shift was the Fly Ash reduced to 25%. During the intensive pouring period of the contract for Phase I (mainly pile concrete) 1 200 m³/day where achieved on average, with a highest pour rate of 1 800 m³/day, consuming more than 450 tons of cement a day.

To keep up with this high production rate, 15 to 17 road tankers of cement a day had to be cleared through the Mozambican border. Cement had to be railed for about 600 km from the Lichtenburg factory West of Johannesburg to the Nelspruit depot, unloaded, stored and re-loaded into road tankers for another 250 km journey. This logistical operation required extensive preplanning. Fly Ash was delivered directly from Matla Power Station with road tankers, a round trip of 1 100 km.

Concrete Silos – Matola harbour site

The 45 000 tons capacity raw materials silo for alumina powder in Maputo harbour, one of the largest silos in Africa, required 3 000 m³ concrete for the base and 2 000 m³ for the slide walls.

The continuous supply of cement and Fly Ash was critical for this structure, as well as for the continuous thirteen days and nights of sliding the two coke silos with 30 000 tons capacity each.

Concrete Jetty – Matola harbour site

Design and construction of the new jetty was awarded to Basil Read (Pty) Ltd of South Africa. The total jetty structure took a total of 14 800 m³ concrete, using a 70/30 OPC/FA mix and the same aggregate as the Group Five / CMC joint venture [12].

All concrete was batched directly on site, 3 400 m for piling, 4 600 m³ for pre-cast work and the balance for in-situ pours for the deck and the "cope" (service tunnel).

High durability (marine exposure) was required for this structure which received the first shipment of alumina raw material from Western Australia during April 2000.

Mozal Phase II

Further work for a third pot-line and additional storage facilities in Maputo harbour has commenced during July 2001.

All concrete is again batched by the Group Five / CMC joint venture, using the same input materials which had proven themselves during Phase I.

CONCLUSIONS

Phase I of this prestigious project was successfully completed ahead of time, with no concrete related failures.

Durability was not neglected despite the use of potentially marginal aggregates. This was achieved through the correct choice of cementitious material, an innovative mix design taking a rather high amount of absorption water into account and good concrete practice.

Phase II of this project is well underway.

REFERENCES

1. Team Work solves problems. CONCRETE Trends, Volume 3, April 2000, pp. 14-17.

2. ADDIS, B., OWENS, G., Fulton's concrete technology, 8th edition, Cement & Concrete Institute, South Africa, 2001, pp. 163-189.

3. SABS Method 1245: 1994, Potential reactivity of aggregates with alkalis (accelerated mortar prism Method).

4. SABS Method 1243: 1994, Deleterious clay content of the fines in aggregates (Methylene blue adsorption indicator test).

5. DIGA DI CORUMANA (Corumana Dam). Edito da CO.BO.CO Corumana Consortium, Roma, 1989.

6. AMTSBÜCHLER, R., Fly Ash in large Water Supply project: A South African Case History, Supplementary papers, Fith CANMET / ACI Int. Conference on Fly Ash, Silica Fume, Slag and Natural Pozzolans in concrete, 1995, pp. 531-575.

7. SABS 0100-2: 1992, Code of practice, The structural use of concrete Part 2: Materials and execution of work.

8. CABRERA, J. G., GHODDOUSSI, P., The influence of Fly Ash on the resistivity and rate of corrosion on reinforced concrete. Durability of concrete. Third Int. Conference, Nice, France 1994.

9. DHIR, R. K., PFA CONCRETE: ABRASION RESISTANCE, Contract Report : RKD / BCC / 8, Dundee University, 1991.

10. SABS EN 197-1: 2000, Cement, Part 1 : Composition, specifications and conformity criteria for common cements.

11. SABS 1491: Part II – 1989, Standard Specification for Portland Cement extenders, Part II : Fly Ash.

12. Fly Ash for Matola jetty and silos. The Civil Engineering & Building Contractor, June 2000, pp. 36-39.

BIOGENIC SULPHURIC ACID CORROSION: A MICROSCOPIC INVESTIGATION

A Beeldens **J Monteny** **E Vincke** **N De Belie**
D Van Gemert **W Verstraete**
Katholieke Universiteit Leuven Ghent University

Belgium

ABSTRACT. Biogenic sulphuric acid corrosion is one of the most severe corrosion mechanisms in sewer pipes. Simulation of the tests in laboratory conditions is a demanding task due to the presence of bacteria. In this paper, the influence on the microstructure is investigated of two chemical immersion tests and a biochemical test. To ameliorate the resistance of concrete sewer pipes against biogenic sulphuric acid corrosion, polymer emulsion is added to the fresh mixture with a polymer-cement ratio of 7.5%. Analysing the eroded surface of mortar and concrete samples revealed a similar deterioration process for the different test methods. Gypsum crystals were formed preferably at places with larger porosity. However, due to the presence of bacteria, a different type of gypsum crystals was formed. A more twisted type of crystal with unsharp edges appears on the biochemical attacked specimens. The presence of polymer film results in a better retention of the attacked layer on the surface and a reduced size of the corrosion products.

Keywords: Biogenic sulphuric acid attack, Microstructure, Polymer modification, Biochemical corrosion test, TAD-test, Chemical immersion test, gypsum crystals

A Beeldens is PhD Candidate at the Department of Civil Engineering of Katholieke Universiteit Leuven, Belgium.

J Monteny is PhD Candidate at the Magnel Laboratory of Concrete Research, Department of Structural Engineering of Ghent University, Belgium.

E Vincke is PhD Candidate at the Laboratory of Microbial Ecology and Technology of Ghent University, Belgium.

N De Belie is Professor at the Magnel Laboratory of Concrete Research, Department of Structural Engineering of Ghent University, Belgium.

D Van Gemert is Professor at the Department of Civil Engineering of Katholieke Universiteit Leuven, Belgium.

W Verstraete is Professor at the Laboratory of Microbial Ecology and Technology of Ghent University, Belgium.

INTRODUCTION

Biogenic sulphuric acid attack (BSA) is one of the most severe corrosion processes occurring in sewer pipes. It is a well known type of erosion in countries with warmer climates, but also in regions with a milder climate, this type of damage could increase due to a different policy towards wastewater transportation and treatment. The tendency towards more separate sewer systems may result in an increase in temperature, an increase in BOD-content and therefore an increased risk on damage due to BSA.

Laboratory simulation of BSA is a demanding task. Different studies have shown a discrepancy between pure chemical tests where specimens are submerged in a H_2SO_4 - solution and biochemical tests, which incorporate the cultivation of the bacteria. An overview of the test methods is presented by Monteny et al. [1].

The influence of chemical as well as biochemical simulation tests on the microstructure of mortar and concrete is investigated. Different types of polymer emulsions were added to the fresh mixture in order to increase the resistance against BSA. The main point of interest of this paper is the influence of the test method and of the material composition on the microstructure of mortar and concrete subjected to sulphuric acid attack. Therefore, emphasis is put on the SEM study of corroded and non corroded specimens. Only a brief description of the test methods is given to point at the differences between the tests used. Part of the results were presented in literature [2,3,4].

BIOGENIC SULPHURIC ACID CORROSION

Considering the durability of sewer pipes, biogenic sulphuric acid corrosion is mentioned in literature as one of the most important corrosion mechanisms [5]. The process of biogenic sulphuric acid attack is studied since 1945. It was Parker who first associated the presence of bacteria with the formation of sulphuric acid and the concrete attack [6]. Bacterial activity in sewers helps to develop a portion of the sulfur cycle, leading to the formation of sulphuric acid. The sulphur cycle can be divided into four consequent phases. The first phase is the reduction of sulphate compounds in the wastewater at anaerobic conditions by sulphate-reducing bacteria, e.g., *Desulfovibrio*. The second phase is the transition of the hydrogen sulphide in the wastewater to the sewer atmosphere. The third phase is the re-oxidation of the hydrogen sulphide to sulphuric acid H_2SO_4 on the exposed surface of the sewer pipe by aerobic sulfur oxidizing bacteria *Thiobacillus Thiooxidans*, also called *Thiobacillus Concretivorus*. The final phase is the erosion of the material of the sewer pipe. A more detailed description of the BSA mechanism is presented in literature [7,8].

This attack takes place at very low pH values. The bacteria can survive at pH values as low as 0.2 [7]. The type of bacteria present on the surface depends on the pH of the condense layer. The lower the pH of the condense water, the more aggressive the bacteria are. If cement bounded material is used for the sewer pipe, the main type of attack is the reaction of $Ca(OH)_2$ present in the cement stone with the sulphate to form gypsum (calcium sulphate). The cement bounded material converts to a pasty white mass consisting of the calcium sulphate and the residual sand and gravel used in making the pipe. The influence of type of cement and polymer modification on the resistance towards biogenic sulphuric acid is investigated by different authors [9].

TEST METHODS

Three different test methods were used: a chemical immersion test, an accelerated chemical test and a biochemical test.

Immersion Test

The immersion test was carried out on concrete as well as on mortar with similar p/c-ratio. The test consisted of 10 immersion cycles. Each cycle contained an immersion period over 6 days in a 0.5% H_2SO_4 solution, followed by a 1-day immersion in water. After the day of water immersion, the samples were rinsed with tap water and brushed with a soft nylon brush. The weight was measured before and after brushing. After each cycle, the H_2SO_4 solution was renewed. Reference samples were stored in water during the whole test. No drying period was included in the cycle.

TAD-accelerated Corrosion Test

A standardized and automated chemical exposure to sulphuric acid was performed using a Testing apparatus for Accelerated Degradation tests (TAD) as described by De Belie et al. [10]. Three concrete cylinders, ⌀ 270 x 70 mm in height, of the different concrete mixtures were mounted on rotating axles, fixed on a frame. During the cycles, the cylinders turned through containers with a solution of 0.5% sulphuric acid at a speed of 1.04 revolutions per hour, in such a way that the outer 50 mm was submersed. In this way, submersion and drying were altered. The solution had a pH of around 1.0. One exposure cycle lasted 6 days. The solution was renewed after every cycle. After each exposure cycle, the concrete cylinders were brushed with rotary brushes to remove the weakly adhering concrete particles.

Concrete degradation was measured with automated laser sensors. For each concrete cylinder, six profiles, equally distributed along the cylinder width, were scanned after each exposure cycle. The change of the concrete surface (either swelling or shrinkage of the specimen) of each cylinder was calculated by comparing the profiles after exposure with the initial profiles at the same place. According to the British Standard BS 1134, the Ra-value, a measure of the surface roughness, was calculated for each cylinder. Similar concrete mixtures were used for the TAD test as for the immersion test.

Microbiological Test Method

The microbiological test was carried out on small concrete prisms, glued on glass plates. The prisms were treated with a sulfur suspension. This suspension contained all necessary elements (mixture of Thiobacilli bacteria, elemental sulfur particles and nutrients) to produce sulfuric acid in a microbiological way. The test method consisted is given more detailed in [4]. One cycle consisted of four subsequent steps as is indicated in table 1.

During step 1 the test specimens were placed in a H_2S atmosphere for 2 days. The initial gas concentration of the atmosphere was around 250 ppm H_2S and decreased, due to the absorption of the H_2S-gas by the concrete. Next, the test specimens were subjected during 10 days to the sulfur suspension. They were completely immersed in 600 ml of the suspension and constantly stirred. Therefore the recipients were placed on a shaker. During this step (step 2) the bacteria, present in the suspension, converted elemental sulfur to sulfuric acid which caused deterioration of the concrete. In step 3 the test specimens were stirred during one day

in separate glass recipients containing milli-Q water, to remove corrosion products and possible adhering bacteria. During step 4 the test specimens were dried during 4 days and afterwards slightly brushed to remove weakly adhering concrete particles. 3 to 4 cycles were applied to the specimens, every cycle lasted 17 days. During step 2, the pH and the sulfate concentration of the sulfur suspension were measured. At the end of the experiment, the loss of mass of the different prisms was determined as well as the change in height of the specimen

Table 1 Cyclic procedure of the biological test, total duration of 1 cycle: 17 days

CYCLIC PROCEDURE BIOLOGICAL TEST
- 2-day incubation in H_2S atmosphere
- 10-day exposition to bio-S (bacterial culture)
- 1-day rinsing with water
- 4-day drying at laboratory conditions

Mixture Composition

Two types of specimens were prepared: mortar specimens and concrete specimens. Three different cement types were investigated: a normal Portland cement, CEM I/42.5/LA/R; a blast furnace slag cement, CEM III/A/42.5/LA, and a sulphate resistant cement, CEM I/42.5/HSR/LA. Different types of polymer emulsions were tested, two are discussed in this paper: SAE and SBR1. The minimum film forming temperature of SAE is equal to 32°C and of SBR1 to 5°C. Both types of polymer emulsions were chosen to see the influence of the MFT on the properties of the material, with the MFT of SAE slightly higher than the curing temperature and the MFT of SBR1 lower than the curing temperature. The influence of the MFT on the properties of polymer modified material is discussed in[9]. A polymer cement ratio equal to 7.5% (weight of solids of emulsion/weight of cement) was used for the mortar samples as well as for the concrete samples. The water-cement ratio varied between 0.5 and 0.35. The mortar mixture composition was varied to obtain an equal flow for the different mixtures. Detailed results can be found in previous publications [2,3,4].

MICROSTRUCTURE OF CORRODED MATERIAL

The microstructure of the samples submitted to chemical and biochemical corrosion tests was studied by means of SEM technique. A SEM type JSM-6400 Jeol was used. The samples were coated with a thin gold layer under vacuum. Eroded surfaces as well as broken and sawn surfaces were looked at.

Mechanism of Corrosion

Three types of corrosion tests were used: chemical immersion test, TAD-test and biochemical test with Bio-S. The corrosion mechanism varied especially between the chemical and biochemical test. However, some general points could be detected, such as a large porosity and crystal growth at the transition zone between the aggregates, release of smaller aggregates, large crystal growth in the pores and erosion of the binder matrix.

Unmodified samples

The study of the surface subjected to chemical or biochemical produced H_2SO_4 pointed out that the reaction between $Ca(OH)_2$, C-S-H hydrates and the sulphuric acid , the gypsum formation and the erosion were the most severe at places with larger porosity, it is in the pores or at the transition zones between the aggregate and the binder matrix. This resulted in typical views of the microstructure, namely pores filled with larger crystals, uncovered aggregates, enlarged porosity at the interface between the aggregate and the binder matrix, and spots where the aggregate was released from the surface.

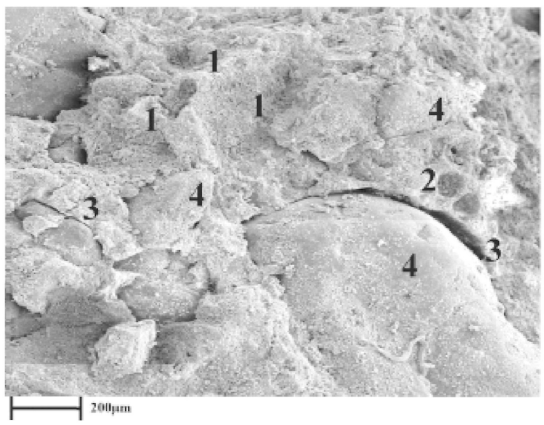

Figure 1 Mortar, subjected to immersion test, 50x
1: spots where aggregates are released
2: pores filled with crystals
3: larger porosity at the transition zone aggregate-mortar
4: uncovered aggregates

The size of the gypsum crystals present in the transition zone lets presume that primarily the aggregates are released from the surface due to the reduced adherence between the aggregates and the binder matrix as a consequence of the reaction between the cement hydrates and the sulfates. Only secondarily the crystals may grow and develop extra pressure on the aggregate. Once the aggregate is gone, the crystals may grow freely. The larger porosity at the interface between the aggregate and the binder matrix also facilitates the migration of the sulfates towards the transition zone to react with the free $Ca(OH)_2$ and the C-S-H hydrates.

The occurrence of crystals in the pores of the matrix also points at the reaction between the sulfates and the cement product but does not cause immediate damage since enough space is available for the crystals to develop. As is pointed out by Ambroise [11], the main attack due to sulfuric acid is an intensive dissolution of the cement hydrates rather than a spalling due to volume expansion of the crystal formation.

Figure 1 gives an overview of the attacked surface of a mortar specimen, CEM III/A/42.5/LA subjected to the chemical immersion test. The different phenomena are indicated on the figure. No distinction could be made on the base of the corrosion products between the different cement types. However, the impression arose that in the case of ordinary Portland cement, a smaller amount of gypsum crystals were present throughout the sample. This could

point at ettringite formation. Ettringite is less stable at lower pH so dissolving more easily during the immersion period. The weight loss after 10 cycles of immersion was the highest for the specimen with Portland cement. The depth of the damaged layer on the surface however was the smallest. This is due to the fact that the Portland cement matrix is less capable of retaining the aggregates onto the surface. For the modified samples, the depth of the damaged layer was even higher. The aggregates and the gypsum crystals were held by the polymer film on the surface. If mechanical interaction is omitted, the damaged layer in that case may become very wide.

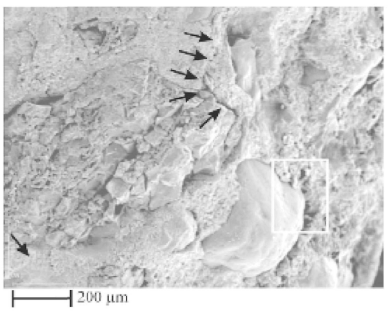

Figure 2 Concrete, subjected to immersion test, CEM III/B/42.5, 50 x

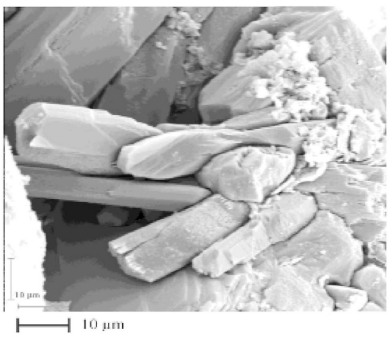

Figure 3 Enlargement of figure 2, 1000 x

Figures 2 to 6 give an overview of the corroded surfaces of unmodified concrete submitted to the chemical immersion test and the biological test. In figure 2, the inner surface of the sample is looked at. The damaged layer is visible at the right sight of the figure. A transition zone is visible between the unattacked and the attacked surface marked by the arrows. The broken parts visible at the left side of the picture are caused by the sawing of the specimen. Again uncovered aggregates are visible as well as large gypsum crystals at the transition zone between the aggregate and the cement matrix as is shown in figure 3. Figures 4 and 5 give an overview of binder matrix, made with CEM III/32.5/R and submitted to the biochemical test. Large crystals are present in the pores and at the transition zones aggregate-matrix. The crystals however have a much more irregular form as if the sides are weaker and more easily broken down, as can be seen in figure 6.

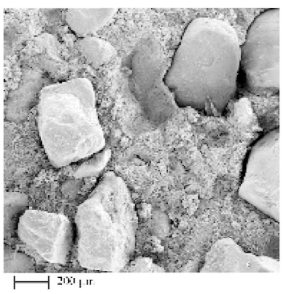

Figure 4 Concrete, submitted to biological test, CEM III/32.5/R, 50 x

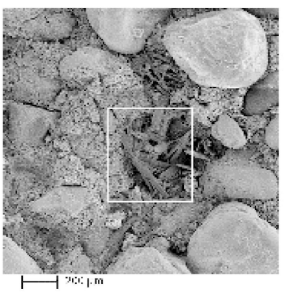

Figure 5 Different zone on surface of shown in Figure 4, 50 x

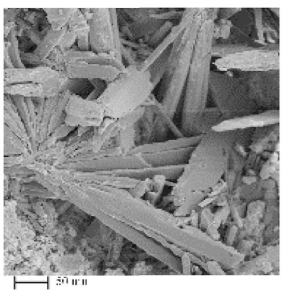

Figure 6 Enlargement of Figure 5, 200 x

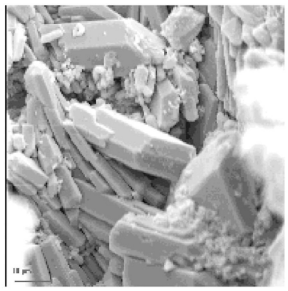

Figure 7 Concrete, submitted to immersion test, CEM I/42.5/R, 1000 x

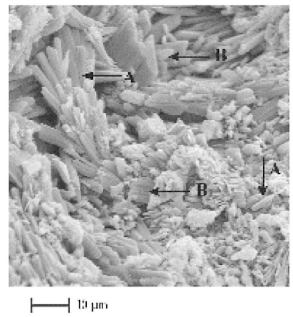

Figure 8 Mortar, submitted to immersion test, CEM III/A/42.5, 1000 x

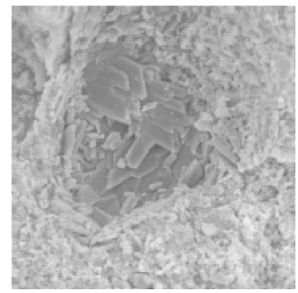

Figure 9 Mortar, submitted to immersion test, CEM III/A/42.5, 500 x

Comparing figures 7 to 9 with figure 6, the difference in shape is clearly visible between the gypsum crystals formed during chemical immersion and the gypsum crystals formed in the presence of biological produced sulphuric acid. In the former case, the crystals have well specified and straight edges. In the latter case, the crystals are more twisted as if they have followed the movement of the bacteria. The edges of the crystals are more serrated. The idea arises that the bacteria are partly encapsulated by the crystals and influence the morphology of the crystals, similar to $CaCO_3$ "Bacteries Baptiseuses". However, due to the use of the high-vacuum in the SEM and the preliminary drying and coating of the sample, it is not possible to reveal the bacteria in this case. ESEM could give better results.

Modified samples

The general appearance of the eroded surfaces is similar for the modified specimens as for the unmodified specimens. Again an increased porosity at the transition zone aggregate-cement polymer co-matrix, released aggregates due to decohesion and internal pressure and large crystals in the pores were noticed. Figure 10 shows the transition between the damaged zone and the intact concrete, indicated by arrows. The surface is sawn perpendicular to the specimen surface. As can be seen, the surface transforms from a flat, even and dense, undamaged surface at the top left to a rough surface in which aggregates are clearly visible (4) or pushed off (1). An enlarged porosity at the transition zone aggregate- co-matrix (3) and large crystals in the pores (2) are visible.

The difference between the eroded microstructure of modified and unmodified samples lays in the size of the crystals formed. In the case of modified samples, the gypsum crystals formed in the bulk co-matrix are much smaller as if their growth is obstructed by the presence of the polymer. Of course, in the case enough space is available as in air pores, the crystals grow in a similar way as for the unmodified specimens. [Figure 1.(2)].

Figures 11 and 12 are an enlargement of the transition zone between the aggregate and the binder matrix indicated by the rectangle in Figure 10. Comparing the size of the gypsum crystals with those on Figure 8; a much reduced size is noticed for the polymer modified material. This is observed for the crystals formed at the transition zone as well as in the bulk matrix.

On places where a continuous polymer film is present, crystal growth is strongly limited, as can be seen in figure 13. If no restriction is present, the gypsum crystals can grow as was noticed for the unmodified samples.

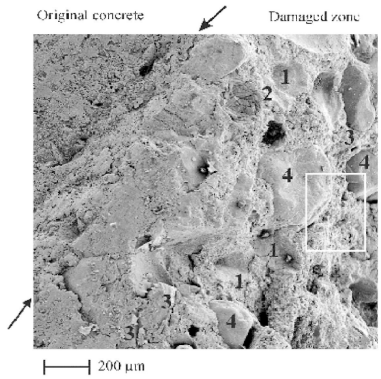

Figure 10 Concrete, modified with SBR1, subjected to TAD (numbers identical to Figure 1)

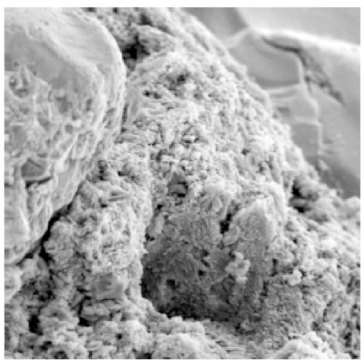

Figure 11 Concrete, modified with SBR1, subjected to TAD, 500 x

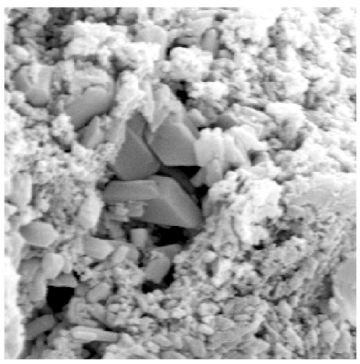

Figure 12 Concrete, modified with SBR1, subjected to TAD, 3000 x

The presence of a continuous polymer film is not always visible, as can be seen in Figure 12. This could point at the fact that modification the polymer-cement ratio of 7.5% was too low to assure a continuous film throughout the sample. Although the effect of the polymer modification is visible in the results by a retarded erosion and in the microstructure, an increase in polymer-cement ratio could lead to an improved resistance against sulphuric acid.

Figure 14 shows the eroded surface of concrete specimens modified with 7.5% SAE subjected to the biochemical test. In this case, the polymer film is present. This is remarkable since the MFT of the polymer emulsion is higher than the curing temperature. The surface is comparable to the surface obtained after etching the sample with HCl. The $Ca(OH)_2$ and C-S-H hydrates have reacted with the sulfates to form gypsum. The polymer film does not react, and remain as small bridges between the aggregates and the crystals.

In the presence of the polymer, crystal growth is limited. If no restriction is present, the gypsum crystals can grow as was noticed with the unmodified samples. A clear example of this is shown in figure 13, taken in a pore of the specimen modified with7.5 % SAE and submitted to an immersion test. On places where no polymer film is present, the crystals grow freely in the pore. At the right-hand side of the pore, a more continuous film is present. In this case, only small crystals are visible through the gaps in the film.

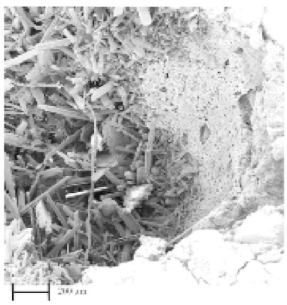

Figure 13 Concrete, modified with 7.5% SAE, submitted to immersion test, 50 x and 150 x enlargement. Polymer film in combination with gypsum crystals

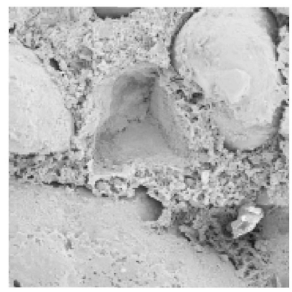

Figure 14 Concrete, subjected to bio-S, modified with SAE, 100 x

CONCLUSIONS

The influence of different test methods on the microstructure of modified and unmodified mortar and concrete is investigated. Two chemical and one biochemical tests were used. In general, identical corrosion products were formed. Large gypsum crystals in the pores and at the transition zone between aggregate and binder matrix, released aggregates due to a weakened adhesion between the aggregates and the binder matrix and erosion of the binder matrix itself resulting in an uncovering of the aggregates.

A difference between the chemical test methods and the biochemical method occurred in the shape of the gypsum crystals. When the specimens are submitted to a chemical test, the crystals have a hexagonal form with well defined edges. In the case of the biochemical test, when bacteria are present, the gypsum crystals are more twisted as if they intermingle with the bacteria. The edges of the crystals are more serrated.

Polymer modification influences the microstructure by the size of the crystals formed. Due to the presence of the film, the growth of the crystals is restricted. The polymer film itself is not attacked by the sulphuric acid and assures to a certain extend the connection between the different aggregates. However, if mechanical action is applied, the depth of the damaged layer which is present on the surface largely decreases.

ACKNOWLEDGMENTS

The authors grateful acknowledge the financial support from the Fund for Scientific Research - Flanders (FWO) through research grant nr. G.0274.98. J. Monteny also acknowledges the support of the IWT (Flemisch Institute for the Improvement of Scientific Technological Research in the Industry).

REFERENCES

1. MONTENY JOKE, VINCKE E., BEELDENS A., DE BELIE N., TAERWE L., VAN GEMERT D., AND VERSTRAETE W., Chemical, Microbiological, and in Situ Test Methods for Biogenic Sulfuric Acid Corrosion of Concrete, Cement and Concrete Research, volume 30, nr. 4, 2000, Elsevier Science, pp. 623-634.

2. BEELDENS ANNE, et al., Accelerated Biogenic Sulphur Attack on PCC, 10th International Conference on Polymers in Concrete, 2001, May, Hawaii, pp. 14 (CD-rom)

3. MONTENY JOKE, VINCKE E., DE BELIE N., TAERWE L., AND VERSTRAETE W., Chemical and Microbiological Corrosion Tests on Concrete Made With and Without Addition of Polymer, Proceedings of the International Conference on infrastructure regeneration and rehabilitation, Sheffield, pp. 715-724.

4. MONTENY JOKE, ET AL., Chemical and Microbiological Corrosion Tests on Polymer Modified Concrete, 10th International Conference on Polymers in Concrete, 2001, May, Hawaii, pp. 15 (CD-rom)

5. POLDER ROBERT, Duurzaamheid Rioolleidingen - Een Literatuurstudie Naar Aantastingsmechanismen, 1987, editor: Commissie voor Hydrologisch onderzoek TNO, 's-Gravenhage, pp. 53.

6. PARKER C. D., The Function of Thiobacillus Concretivorus (Nov.Spec.) in the Corrosion of Concrete Exposed to Atmospheres Containing Hydrogen Sulphide, Australian Journal Exp.Biol.and Med.Science, volume 23, 1945, pp. 91-98.

7. VINCKE ELKE, MONTENY J., BEELDENS A., DE BELIE N., TAERWE L., VAN GEMERT D., AND VERSTRAETE W., Recent Developments in Research on Biogenic Sulfuric Acid Attack of Concrete, Environmental Technologies to Treat Sulfur Pollution, Principles and Engineering, Chapter 22, editor: Lens, Piet and Hulshoff, Pol Look, IWA Publishing, London, pp. 515-542.

8. BIELECKI R. AND SCHREMMER H., Biogene Schwefelsäure-Korrosion in Teilgefüllten Abwasserkanälen, Sonderdruck aus Heft 94/1987 der Mitteilungen des Leichtweiss-Instituts für Wasserbau der Technischen Universität Braunschweig, 1987, pp. 275.

9. BEELDENS ANNE, MONTENY J., VINCKE E., DE BELIE N., VAN GEMERT D., TAERWE L., AND VERSTRAETE W., Resistance to Biogenic Sulphuric Acid Corrosion of Polymer-Modified Mortars, Cement and Concrete Composites, volume 23/1, 2001, pp. 47-56.

10. DE BELIE NELE, VERSCHOORE R., AND VAN NIEUWENBURG D., Resistance of Concrete With Limestone Sand or Polymer Additions to Feed Acids, Transactions of the ASAE, volume 41(1), 1998, pp. 227-232.

11. AMBROISE JEAN, CHABANNET M., ROLS S., AND PERA J., Resistance of Different Cements to Ammonium Sulfate, Proceedings of the Twenty-first International Conference on Cement Microscopy, Las Vegas, Nevada, April 25-29,1999, pp. 47-57.

VARIATION OF CONCRETE BASE'S CLEANING GRADE AND ESTIMATION OF PROTECTIVE COATINGS

J Jasiczak

M Szczeszek

Poznan University of Technology

Poland

ABSTRACT. The investors try to execute durable concrete and avoid an expensive protective coating in new build waste-water-treatment plants. The similar establishment at the currently building waste-water-treatment plants in Stuttgart, Gubin and Poznan is applied. This approach is based on principle of the material and structural protection of construction in a new build waste-water-treatment plants erected by execute suitable durable concrete and formed in system formwork which are equipped in special active mat. The most important role of active mat (for example Zemdrain or described in this paper Agepan RS) is to noble the on surface layer of concrete by local reduce w/c ratio. The concrete surface formed in special active mat characterised by following properties: higher homogenous, smaller absorption, flexibility for carbonisation and chloric ion diffusion, higher freeze resistance and strength. [1] This paper presents the effects of research of the adherence of firm's mat combinations (for example Polyment, Sika, and Schomburg) on concrete bases, formed in system formwork. The authors analysed a few cases of adhesion one- and multilayer coating covered on an ordinary concrete bases formed in an active curing mat. Dissolving using the flow - abrasive method, cleaned the surfaces. At the end of etching process the layer of the thickness of 1mm was grinded. The results of tests were the base to execute a project for concrete protection in bioreactor wall in waste-water-treatment plants built in Poznan.

Keywords: Corrosion, Durability, Adhesion, Protective coating, Concrete surfaces.

Professor Dr J Jasiczak, is Vice-Dean of the Faculty of Civil Engineering Poznan University of Technology, Poland. He specialises in the use of statistical methods for quality control ready mix production and the durability and protection of concrete structures working in the aggressive environment. He is a member of Building Materials Association Polish Academy of Science. Professor Jasiczak has published on many International Conferences Proceedings. In the last time he wrote the book: Technology of Concrete Modified by Admixtures and Additives, Domestic and foreign tendencies.

Mr M Szczeszek, is a Lecturer in Institute of Structural Engineering Poznan University of Technology, Poland. Her main research interest includes the permeability properties of concrete, the prediction and modelling of concrete degradation processes. She published in Concrete Engineering International in October'99 and in Polish conferences about Waste concrete as a source of aggregate.

INTRODUCTION

The biological reactors responsible for removing of nitrogen and phosphorus from sewage's have been designed and realised in Europe for some time and in Poland for a shorter period of time. Many institutions are currently doing the research over biological cleaning of sewage's and the concrete protection methods. The problems of biological cleaning of sewage have been described in the paper [2]. The problems of concrete protection in bioreactors was researched and studied by many authors, for example [3] and [4].

THE PROGRAM OF LABORATORY RESEARCH

Three versions of surface preparations were adopted:

1. Smooth surface – concreting of walls in PERI formwork.
2. Relief surface - PERI system formwork covered with protective mat – Agepan, affecting concrete for different period of time.
3. Surface formed by Agepan, wet cleaned by means of flow - abrasive method.

Wooden panel Agepan RS is a lining put on the formwork system before concreting of the construction. The panel is made of 5-leyer of wood. It is impregnated by preparat which presents adhesion to concrete and is the hot water and alkali effects resistant (concrete pH=12,5). The part of the panel is shown in Figure 1.

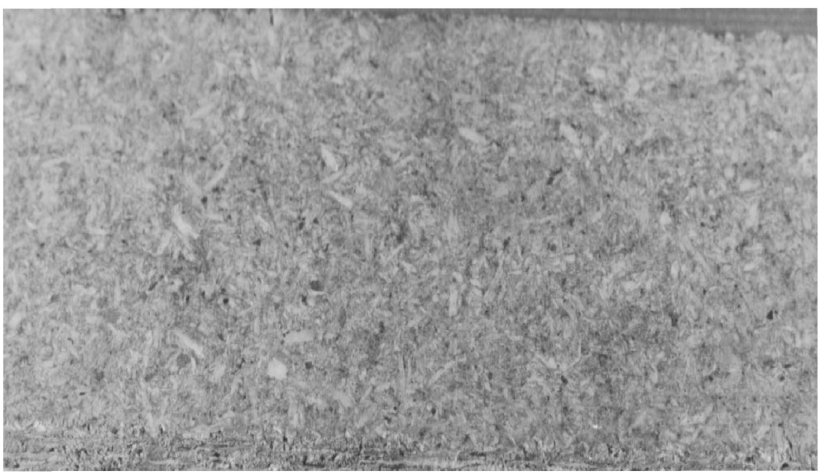

Figure 1 The Agepan RS panel

Due to use of Agepan panels a mat, slightly relief surface of concrete is obtained with coarse structure, irregular arrangement of greyness. Thanks to absorbing structure the concrete surface is mostly free from porous. To cause of that Agepan it is numbered as an active mat. The properties of concrete made in Agepan presents the paper [1]. According to this publication [1] an active mat is also called CPF (Controlled Permeability Formwork).

The wall formed in Agepan RS it is shown in Figure 2. The basis technical information about panel is shown in Table 1.

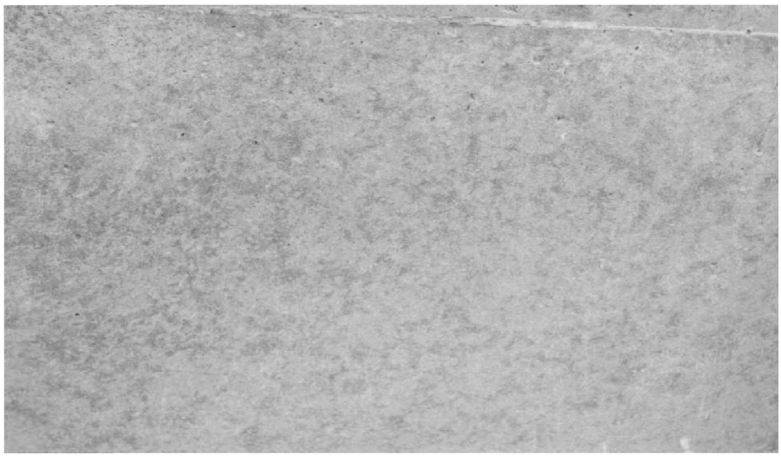

Figure 2 The fragment of concrete wall formed in mat (coat) Agepan

Table 1 The technical parameters of Agepan panels

SPECIFICATION OF THE PROPERTIES	TECHNICAL PARAMETER
Structure of panel	Wood material, high quality, 5-layer
Betterment surface	Impregnation by antyadhesion preparat
Glue	Hot water and alkali effects resistant (DIN 68791)
Dampness	9-12%
Thickness of panel	11-21 mm
Mass of panel	13,9 kg/m^2
Flexural strength	20 N/mm^2
Young's model	3000 N/mm^2

On that prepared surface one- or multilayer following characterisations materials put on:

LM6 – two-component epoxide resins without dissolving for varnishing mineral basis. That material is a protective coating for settlink tank wall in water – waste – treatment plants. LM6 is delivered as two-component; component A – resins, component B – hardener.

P1400 – colourless, without dissolving, without filler, two-component epoxide resins, and slightly viscosity, with big penetration ability and high glue ability, which causes the mineral, base strengthened. It is using as grounding liquid under epoxide resins coat.

FS – a dry repair surfacer PCC, one-component modified by resins of cement to levelling, evening and lute the concrete surface. That product should be diluted only by water. The mortar should be cleaned good bounded and not freeze. It's necessary to several damped the base before put on a coat.

The described materials were put on variantitly prepared concrete base as one- two- or three-layer coat.

THE COAT ADHERENCE TO CONCRETE BASE SETTLED IN THE LABORATORY RESEARCH

The control sample 0,15m*0,15m*0,15m was done from the same concrete as used in bioreactor (concrete grade B30, waterproof W8, absorption 4,5%, freeze resistance F150). The adherence coating to concrete base was measured. The part of samples formed in an ordinary steel form, the rest formed in form with Agepan. The samples at first were hold in a steel form. After extraction from a steel form was successive outformed from Agepan after 3, 6, 9 and 28 days. Through 28 days of hardening samples were water curing, then Agepan was adhered to concrete surface the water influence directly on Agepan and indirectly on the concrete. After tear off Agepan mat the whole samples was dipped in water.

It was prepare two types of samples (in steel form and steel form with Agepan). The part of them was appropriate to immediately put on a coat and the rest was additionally cleaned by flow – abrasive method. After cleaning a protective coating covered the concrete. In that way obtained the four groups of surface i.e.: steel form and with Agepan and as above but cleaned by the flow – abrasive method. The prepared surface covered by protective coating comply the following rules:

- The top of sample (series 1) and lateral surface (flank) (series 2) – without coating.
- An ordinary surface and formed on an active mat with coat P1400 (series 3) and with coats P1400+LM6 (series 4).
- Surface as above but cleaned by the flow – abrasive method with coat P1400 (series 6), with surfacer FS and with coat P1400 (series 7), with surfacer FS and with coats P1400+LM6 (series 8).

The mechanical properties of the base and value of adhesive forces the coat to these base was measured by tester "pull-off" DYNA 15 – by Proceq, according to standard procedure. Figure 3 presents the value of tear off forces the on surface concrete layer and one- and two-layer protective coat. Figure 4 presents results of experiments of the adhesive forces to the cleaned base by flow – abrasive method.

According to product regulation a surface cleaned flow should be additional levelled by surfacer (lute) FS. The obtained results are presented in conclusions in the end of this paper.

FIELD TESTING MECHANICAL PROPERTIES OF THE SURFACE CONCRETE LAYER

The Massive Walls of Biological Reactor

Using the Agepan RS panel as active mat fixed to PERI system formwork in biological reactor and secondary settlink tank was formed in water – waste – treatment plant. The experiments of mechanical properties and on surface were realised under supervision of the authors of this paper. There is only a main type of research from many marked mechanical properties formed concrete walls (partitions). At first it was marked a value of an axial tear off on surface concrete layer. Applying the "pull-off" DYNA15 value of tear off forces was measured for the case the concrete surfacer was formed in a system formwork and with Agepan RS. The control pulley (roller) was glued to both surfacer is shown in Figure 5.

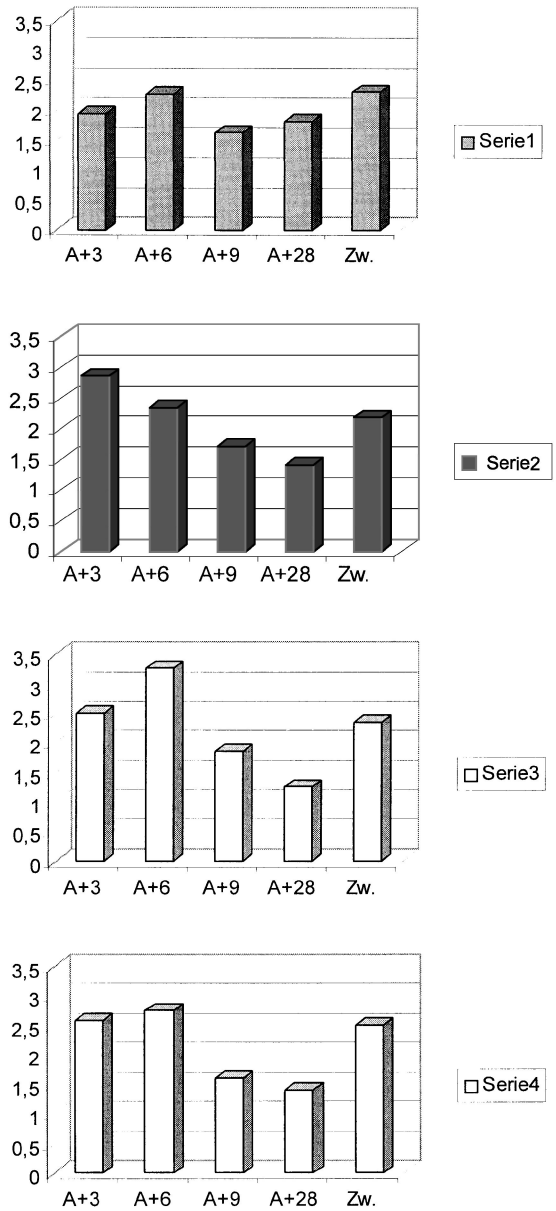

Figure 3 The value of tear off forces [N/mm2] for series: 1 – the top of sample, 2 - lateral surface (flank) of sample, 3 – coat with P1400, 4 – coat with P1400+LM6

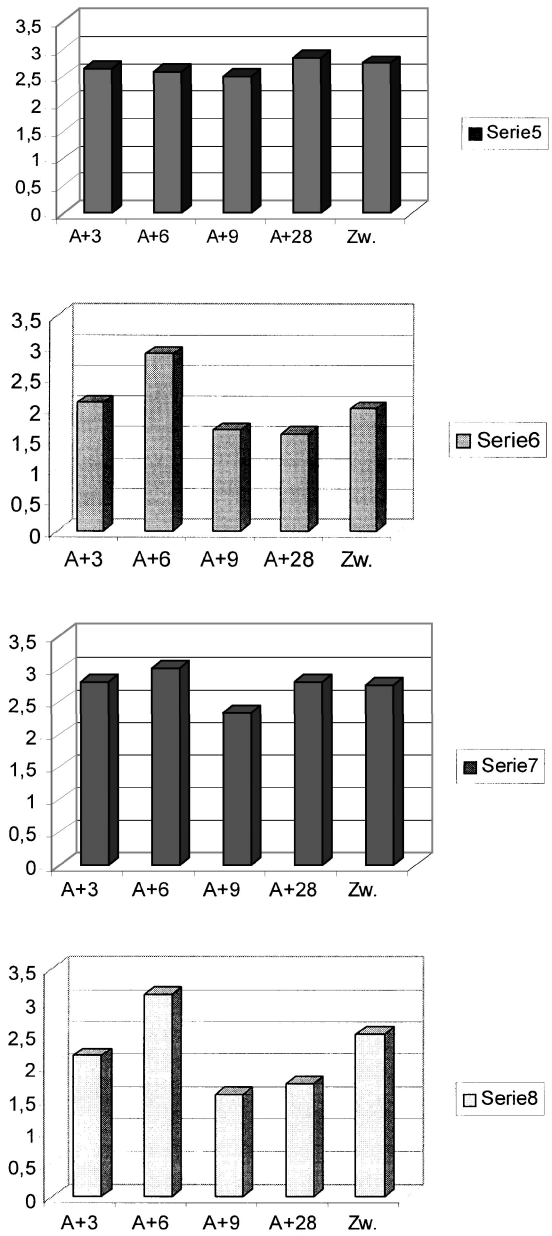

Figure 4 The value of tear off forces [N/mm2] for series: 5 – sand-blast cleaning coat + P1400, 6 - sand-blast cleaning coat + FS + P1400, 7 - sand-blast cleaning coat + P1400 + LM6, 8 - sand-blast cleaning coat + FS + P1400 + LM6

A view on tear off part of concrete for two types (an ordinary and with Agepan) is shown in Figure 6.

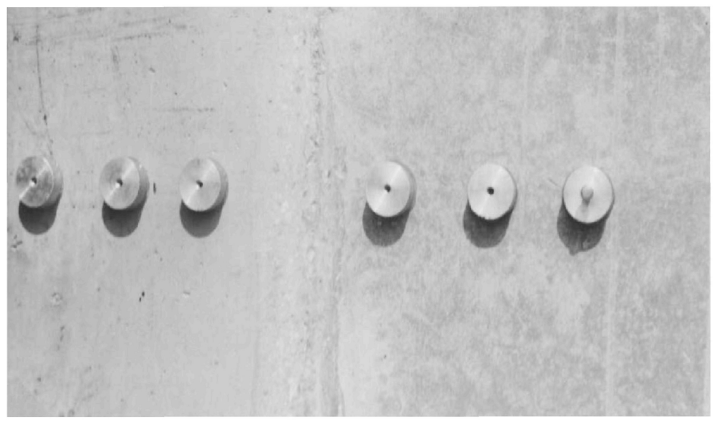

Figure 5 The view of pulley control (roller) glued to the two types of the concrete surface, by the left an ordinary formwork, by the right with Agepan

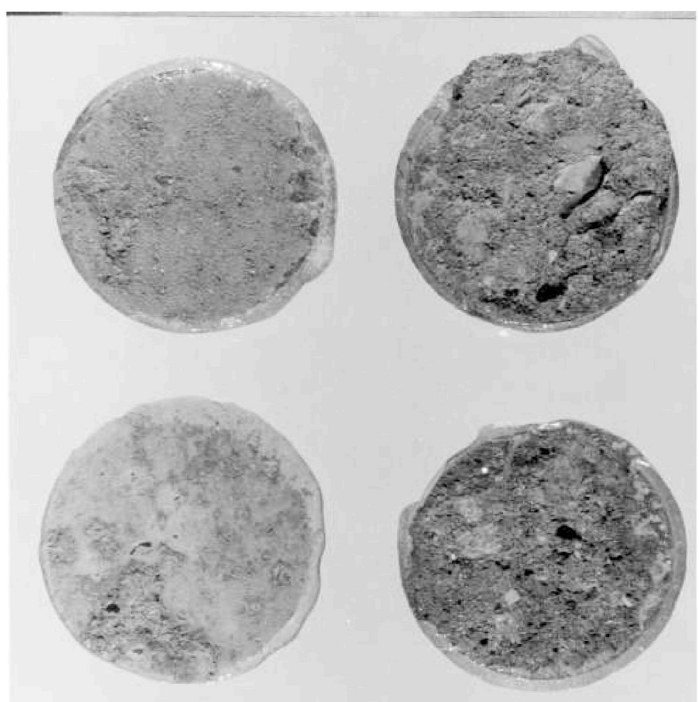

Figure 6 The effect of tear out the pulley control (roller) from ordinary concrete (by the left) and concrete formed in Agepan (by the right)

The mean value of tear off forces was appropriate a suitable 5,4 N/mm^2 and 6,5 N/mm^2 (at the quarantine the good adherence coat f $\geq$ 1,5 N/mm^2). It should be marked that walls were executed by following parameters: concrete grade B30, waterproof W8-W10 and freeze resistance F>150. The protective coating was put on only on strand oscillating of the sewage's level. Due to necessary of the reduce the cost of protection a biological reactor it was accepted that only a facture wall formed by Agepan was enough coarse and it is not required an additional cleaning the wall by flow – abrasive method. To proof that procedure was executed a pull off sample (i.e. pull off coat) from wall surface in the following:

1 – wall without any cleaning.
2 – wall clean by dissolving.
3 – grinding the wall on the surface.

Those prepared walls were covered by two-layer coat with resin K24 with parameters like described about LM6. The acceptance 3 types of prepare base with covered coating, which was treat as:

A – coat without machining
B – coat grinding used an abrasive paper "100" before glue a control pulley (roller).

The results of tear off forces are shown in Table 2.

Table 2 The tear off forces (N/mm^2) registered at pull off coat the K24

NOT CLEANING CONCRETE		CONCRETE CLEANED BY DISSOLVING		GRINDING CONCRETE	
A	B	A	B	A	B
5,5	6,5	6,0	6,9	6,5	7,3

From results shown in Table 2 appear that accepted type of prepare surface of wall formed in coat Agepan RS has not an influence on value of adhesion forces coat to base. In all analysed cases obtained adhesion > 1,5 N/mm^2, consider as minimum good adhesion parameter.

The Thin Walled Element of Secondary Settlink Tank

The research of mechanical properties of on surface concrete layer in bioreactor and the adhesion to protective coating type K24 previously presented, proved that it is not necessary (besides of dust removal water under pressure) an additional prepare surface like sand – blast -cleaning, grinding or lute etc. The good results of Agepan effects influence on formation the concrete layer surface could be achieve on the other constructions formed in Agepan too, for example the thin walled element of secondary settlink tank. The research made with pull-off tester on drain walls about thickness 0,10m didn't confirm that theory. The macroscopic research of drain proves that the concrete surface has not a homogenous relief facture, it is results of fibre scheme of Agepan. The reason of different in use Agepan was the relatively small thickness of drain walls (0,10m) which was bilaterally strengthened by reinforcing

fabrics. The concreting in those conditions made difficult at consolidation work and in press to the fibre scheme of Agepan. The consequence of these was the put tear off strength too low and obtained the information as:

- When mechanical properties of concrete was lower the adherence specified by "pull-off" tester was 2,5-4,0 N/mm^2 and f>1,5N/mm^2.
- When the load of drain was partially aggressive then should be used a typical multilayer protective coat.

Table 3 The mechanical properties of concrete in drain (sewer)
(the results for 6 measurement places)

THE COMPRESSIVE STRENGTH MPa	THE TEAR OFF STRENGTH N/mm^2	COMMENT
27,3	3,70	the surface tear off
24,0	2,50	
27,7	2,80	partly pull off concrete
28,0	3,40	the surface tear off
29,1	4,10	
25,1	2,80	partly pull off weak concrete
26,9	3,38	-

CONCLUSIONS

The experimental laboratory testes gave many dates about qualitative and numerical character at realised bioreactor walls. It is possible to contain the conclusions in 3 groups:

- Tear off strength the concrete surface layer realised in on ordinary formwork and with Agepan is diverse (series 2). The different in the strength after 3 days of curing in Agepan and then in water with relation to curing only in water is cross 40%. The curing in Agepan in the long time gave worse effects. The reasons of that are not explaining now, but may be helpful for the contractor of concrete work.
- The analyse 3 and 4 series of experiments confirm the conclusion that longer than 6 days curing in an active mat it is not profitable to get higher adhesion forces than for an ordinary concrete
- Cleaning surface formed in an ordinary way and in Agepan, by flow – abrasive method could be commented variantitly. Cleaning surface by flow – abrasive method and cover only resins coat (with good penetration parameters) causes to very good adherence the coat to base (series 5 and 7) regardless of character and curing range. Using a mineral lute (surfacer) obtained a differentiation value of adherence (series 6 and 8) similar obtained in series 2.

The realised in technical approach an effectively used Agepan RS are satisfactory. Thanks of Agepan can increase the axial tensile strength of on surface concrete layer. The research of adherence protective coating (type LM6 or K24) has given a clear higher adherence. The concrete formed in Agepan have better adherence than the concrete surface formed in

traditional formwork (above 10% to 47%). To avoid the expensive cleaning by flow – abrasive method it is necessary to form the concrete in an active mat used formwork in a suitable period of time. In order to use construction about higher corrosion load it should be used an active mat to forming concrete construction.

ACKNOWLEDGMENTS

The authors would like to acknowledge the support provided for the tests by the Polish Committee of Science. The test is included in research programme number 11-181/02 DS and Individual Grant KBN 8T11A – 01017: Climbing robot for on line inspection internal walls in prefabricated buildings.

REFERENCES

1. WILSON, D, Durability problems: is formwork the cause?, Concrete Engineering, Vol 5, No 2, 2001, p 35-38.

2. HARTMANN, L, Biologische Abwasserreiningnug Springer – Verlag, Berlin Heidelberg 1992, p 271 (printed in Poland).

3. JASICZAK, J, Influence the roughness grade and curing conditions of concrete on the adhesion of protective coatings in waste and water treatment plants, Scientific Papers of the Institute of Building Engineering of the Wrocław University of Technology, Poland, No 74, 1999, p 197-202.

4. OWAKI, E, OKAMOTO, R, NAGASHIO, D, Determination of concrete in an advanced water treatment plant, Proceedings of the Second International Conference on Concrete under Severe Conditions CONSEC'98, Tromsφ, Norway, 1998, pp 438-447.

THEME TWO:

MARINE AND UNDERWATER ENVIRONMENTS

Keynote Paper

MARINE AND UNDERWATER CONCRETE – BUILDABILITY AND DURABILITY

D Slater
Halcrow Group Limited
United Kingdom

ABSTRACT. In addition to the primary requirements of structural strength and function, the critical issues when designing concrete structures for the marine and underwater environment are buildability and durability. Buildability is essential for safety and economy during construction and can have a major influence on the long-term performance of the structure. Durability is influenced by design and by construction methods in addition to the environmental conditions. Understanding concrete technology, the process of construction in the marine and underwater environments and the mechanisms for the degradation of concrete in these hostile environments is necessary if durable structures are to be built. These aspects are discussed, a methodology is outlined and examples are given with reference to the latest British Standards for concrete specification, performance, production and conformity.

Keywords: Marine concrete, Underwater concrete, Design, Construction, Curing, Durability, Safety.

Mr David Slater, is Technical Director, Materials Technology, Halcrow Group Limited, with wide experience of the design, construction and performance of maritime structures in aggressive conditions. He is a member of the DETR Expert Group on Thaumasite, the Concrete Society Design Group and was active in the BSI Working Group B/517/1/1 considering the selection of concrete for chloride environments for BS 8500-1:2002 Concrete – Complementary British Standard to BS EN 206-1 published earlier this year. He has written numerous publications including chapters on design and specification in Concrete in Coastal Structures edited by R.T.L. Allen and published by Thomas Telford in 1998.

INTRODUCTION

What may appear to be the most straightforward construction project can become very difficult when part or all of the structure is underwater. The logistics of working between tides, the extra precautions needed to support the temporary works against current and wave action and prevent damage to the environment and/or the concrete itself due to washout or premature exposure to seawater and the difficulties of working underwater, all make the constructor's job difficult. The constructor, therefore, needs every possible assistance from the designer and the designer needs to understand concrete technology if they are to succeed as a team. This paper will outline the problems and the decision process needed to solve them, with examples using the latest British Standards for the Specification, performance, production and conformity of concrete. The design process, as always, involves trade-off between considerations of practicality, durability and economy and is iterative. The paper examines the main issues of safety, the marine environment, the form of construction, selection of an appropriate concrete mix and nominal minimum depth of cover, placement and curing to achieve a durable structure that is relatively straightforward to build with minimum risk.

BUILDABILITY

Safety

Since March 1995, designers of all types of structure that are to be built, altered, renovated or demolished in the United Kingdom, including temporary works, are required under the Construction (Design and Management) Regulations 1994 to consider, during the design process, the safety of those who are to construct, maintain or repair the structure. The CDM Regulations are aimed at improving the overall management and co-ordination of health, safety and welfare throughout all stages of a construction project to reduce the large numbers of serious and fatal accidents and cases of ill health which occur every year in the construction industry.

Two of the designer's key tasks under the CDM Regulations, therefore, are to identify significant health and safety hazards and risks of the design and to give adequate regard to the heirarchy of risk control. This is a series of steps which need to be taken to control the risks, with the first consideration being prevention of a hazard by altering the design to avoid the risk if at all possible. If this cannot be achieved, the risk should be combated at source by means of design details if reasonably practicable. Failing this, priority should be given to measures to control the risk that will protect all workers, occupiers and the public at large. Only as a last resort should measures be taken to control the risk by means of personal protection.

Safety is therefore paramount in the consideration of the designer. Safety risk assessments must be carried out to identify the hazards, the likelihood of occurrence, the severity of harm that would arise from the hazard and, by multiplying the likelihood by the severity, the risk level associated with the hazard. Actions for avoidance or, if not reasonably practicable, mitigation and the residual risk must then be evaluated and recorded. A duty of the designer under the CDM Regulations is to provide adequate information about the health and safety risk of the design to those who need it. This will involve including a risk assessment with the design to alert others to the risks which they cannot reasonably be expected to know.

This is essential for the parties who have to use the design information such as the planning supervisor, the principal contractor and other contractors who use the design information and the actual individuals carrying out the work.

If the basic design assumptions affect health or safety, or health and safety risks are not obvious from the standard design document, designers must provide additional information on drawings, in written specifications or outline method statements on the assumptions taken during the design about the precautions needed for dealing with the risks. The level of detail recorded is determined by the nature of the hazards involved and the associated level of risk.

Further details of the CDM Regulations and how they are to be applied by designers are set out in publications by HMSO [1], Health & Safety Executive [2-4] and CIRIA [5, 6].

One of the best methods of controlling the safety risks in marine and underwater works is to choose the season for carrying out the work carefully to minimise the risk of high waves and storm surges in maritime works or high water flows in rivers. The key to achieving this for coastal works is in persuading clients that carrying out construction works during the holiday season, which is usually the time when the risk of high winds and storm surge is least, can be accomplished without adversely affecting the tourist trade. For each construction stage of caisson structures, for example, the designer has to specify the waves which can be tolerated, in height, period and direction, ie the limiting sea conditions for the construction windows during float-out and sinking [7, 8].

Another method of controlling the safety risk during construction is to minimise the time spent on underwater or inter-tidal activities by utilising precast concrete components as much as possible. This also has the advantage of allowing the concrete to be cast and cured under controlled conditions, thus avoiding poor workmanship due to difficult working conditions or early exposure to seawater, which may compromise long-term durability due to rapid chloride ingress whilst the concrete is immature. Precast concrete components that are not cast and cured under properly controlled conditions, however, could be less durable than in-situ concrete if the emphasis is solely on the speed of production and cost saving.

It is worth noting that the requirement of the CDM Regulations for designers to consider safety during the service life and through to demolition of the structure and to avoid hazards by design where possible, means that the durability and maintenance of the structure must be considered at the outset. The hazards associated with in-service repairs to reinforced concrete marine structures can be avoided if the structure is designed to be durable from the outset. Buildability and durability, therefore, must be considered in detail by the designer from the outset to deliver safety.

The Marine Environment

The environmental conditions for maritime structures vary significantly from the lowest level of construction, usually beneath the seabed, to the highest level of construction, often well above the level of extreme waves. They alter the physical loading on the structure in terms of water pressure, waves and currents and also the environmental loading in terms of abrasion, temperature, rainfall, frequency of wetting by seawater and exposure to drying conditions.

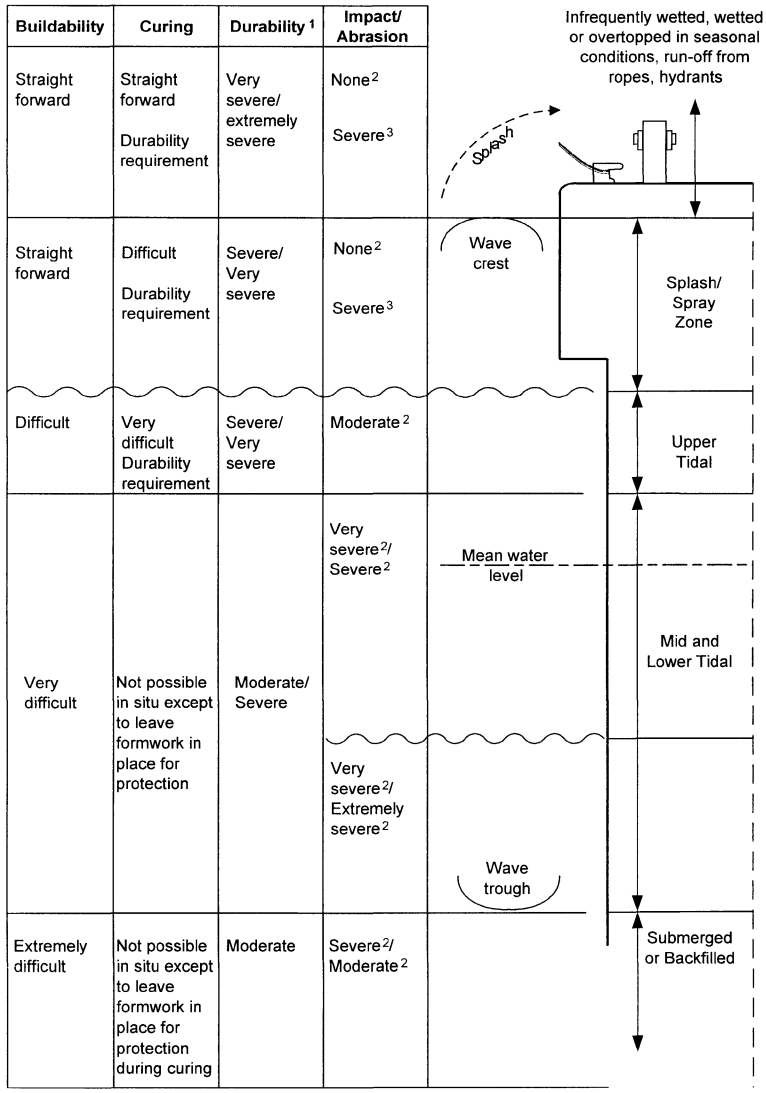

1. For chloride-induced corrosion of embedded steel, reinforced concrete structures only. The degree of severity will depend upon the climate zone - see Ref 7, or 9 Chapter 6, or 10

2. Applies to ice free locations with shingle (pebbles) beach deposits exposed to wave action only. Degree of abrasion in each zone depends upon wave climate and level of seabed/beach relative to structure, mean sea and tide levels.

3. Applies to impact and abrasion from steel ropes on cope, cargo handling on quay and mooring forces on face of cope.

Figure 1 Suggested severity and difficulty ratings for buildability, curing, durability and abrasion relative to tide levels in the marine environment

The physical loading will dictate the size of members and the robustness of temporary works needed during construction but the environmental loading will determine the long term durability of the structure within each exposure zone. Because the environmental loading determines the degree of risk of corrosion of embedded steel reinforcement and the risk of abrasion, it will also influence the importance of curing the concrete before its exposure to the degrading conditions. Selecting the correct type of construction as well as the most appropriate concrete mix is essential for each of the exposure zones if the effort to achieve the required durability is not to be wasted because of inadequate curing or premature exposure to chlorides.

Figure 1 shows the author's suggestions for the severity and difficulty ratings for buildability, curing, durability against corrosion of steel in reinforced concrete and impact/abrasion for concrete structures in the marine environment relative to tide levels. The durability exposure zones are determined by the exposure to drying conditions, with the worst case conditions for corrosion of reinforcement in areas of long term drying with occasional wetting by seawater. The higher the temperature and the longer the drying period between wetting events, the more severe the conditions become.

Form of Construction

Guidance on the selection of structural form for concrete structures in the marine environment is given in BS 6349: Part 1[10] and BS 6349: Part 2 [11]. For general guidance on the strategy to adopt in the design of maritime structures, BS 6349:Part 2 offers the following good advice: 'Greater economies are generally made by aiming at simplicity of construction and robustness of design than by trying to reduce the quantities of materials in the structure by complicated details. If in situ concrete is used within the tidal zone, members should be detailed so that the concrete can be easily placed and effectively compacted. For reinforced or prestressed concrete work in the tidal zone, it is generally better to use precast units with the minimum of in situ concrete connections.'

In the submerged zone, the practicalities of construction favour piled construction, precast caissons and precast blockwork. By understanding the environmental exposure zones relative to the tidal levels for each specific structure location, the form of construction can be selected to optimise the design for each zone. The change in exposure conditions for durability design tend to coincide with the levels at which changes in working practices are needed to allow for tidal and underwater working. For example, because the durability risk in relation to corrosion is relatively low for parts of the structure which are below mean tide level because they are permanently saturated, the use of reinforced or prestressed concrete for this zone can often provide the most economic solution without the precautions to limit chloride ingress that are necessary at higher elevations (as described later).

The form of construction, or at least the design of the depth of cover and concrete mix, can then be changed for those parts of the structure above the mid-tide level and exposed to the greater risk of corrosion of reinforcement. For example, under extreme hot dry conditions as found in the Middle East, a plain precast concrete cope unit can be fixed to the main reinforced concrete structure beneath by means of stainless steel dowels for durability and the flexibility of future replacement following abrasion and impact damage.

Working over water favours precast construction with in situ concrete connections between concrete members and grouted connections between concrete members and tubular steel supporting piles. The precast concrete can be in the form of permanent formers above and around the tops of the supporting piles in which concrete is placed to give composite structural action, which can lead to large section sizes, or fully precast. For decking, the most economic solution is usually to cast an in situ topping above precast concrete planks with steel shear connections in the form of links between the two through which the top reinforcement is added before the topping is poured. The concept and application of a composite precast, prestressed concrete system for wharfs has been described by Peeples et al [12]. Cost comparisons between a cast-in-place deck and a composite deck above water has shown 23% cost savings from the precast composite deck system [13].

DURABILITY

Marine Concrete Specification

Recently there has been significant progress in the recognition of exposure conditions and deterioration mechanisms for concrete in the marine environment culminating in the publication of revised British Standards BS 6349-1:2000 [10], BS 8500-1:2002 [14] and BS 8500-2:2002 [15]. Durability modelling, however, is in its infancy and there are a wide variety of opinions on how different concrete mixes will perform in the different microclimate zones within the marine environment. The committee chairpersons tasked with arriving at a consensus view for each of the British Standards had difficult jobs and each committee comprised different people, so it is not surprising that there are some slight discrepancies between the recommendations given in BS 6349-1:2000 on concrete mixes for maritime structures and those given in Table A.13 of BS 8500-1:2002 for concrete exposed to seawater. The exposure classes for the latter had been defined as part of the pan-European development of Eurocode EN206-1:2000 [16], so the committee for BS 8500-1:2002 did not have the latitude to sub-divide the exposure class for XS2 to distinguish between the permanently submerged and the frequently wetted zones in the lower tidal zone that was exercised by the committee for BS 6349-1:2000 when they developed Class XS2/XS3. The designer needs to be aware that the slight differences between these Standards reflect only part of the range of opinion on durability design because the subject is complex. The selection of a particular combination of concrete mix and depth of cover for a given environmental exposure will have an associated probability of failure which, at present, we are unable to quantify with precision as we lack detailed studies of a large number of actual structures. The selection of higher grades of concrete with increased percentages of cementitious additions, lower water/cement ratios and larger depths of cover will, however, reduce the risk of failure if these concretes can be placed and cured properly before exposure to seawater. The designer can therefore select different relative risk levels for different structural components depending upon their criticality to the performance of the structure and/or their difficulty to repair.

It is also worth noting that these British Standards generally relate to environmental conditions in the United Kingdom and could be applied to similar temperate climates with similar sea water salinity. BS 6349-1:2000, however, also gives comparative ratings for chloride-induced corrosion of reinforced concrete in three different climate zones, namely cool/temperate, tropical hot wet and desert hot dry conditions as defined by Fookes [17, 18]. In addition, BS 6349-1:2000 gives suggestions for concrete mixes and depths of cover to reinforcement under these different marine climates [7, 9, 11].

Table 1 Suggested alternative concrete mixes for external concrete in coastal areas not directly in contact with seawater for 50 years service life in temperate, UK conditions

CONSTRUCTION	REINFORCED CONCRETE	REINFORCED CONCRETE
Casting & curing	Cured 4 days	Cured 7 days
Exposure	Airborne salt	Airborne salt
	XS1	XS1
Grade	C45	C40
Cement Type	100% Pc	50% ggbs or 25% pfa
Cement content[1] (kg/m^3)	360 minimum 425 maximum	340 minimum 400 maximum
Max free water-cement ratio	0.45	0.50
Admixtures	BS5075 Pts 1 & 3	BS5075 Pts 1 & 3
Cover (mm)		
Minimum	55	40
Nominal[2]	70	55

Note 1 Maximum aggregate size 20 mm
Note 2 Tolerance of 15 mm added to minimum for workmanship

Tables 1 to 3 give the author's suggestions for some alternative concrete mixes in the marine environment in the UK which are mainly in agreement with the recommendations of either BS 6349-1:2000 or BS 8500-1:2002 or lie between the two. The exception is in the use of 100% ordinary Portland cement in reinforced concrete that will be exposed to airborne salt in coastal areas, where the author considers that the minimum depth of cover should be increased to 55 mm from 40 mm recommended by the British Standards to allow for wind-borne salt water spray and the relatively poor performance of this mix in resisting chloride ingress. Again, it is a matter of selecting the degree of risk of corrosion damage considered appropriate.

These tables show only a few of the many alternatives available for each exposure class. It was the intention of the technical subcommittee B/517/1 who drafted BS 8500 to encourage designers to consider "trade-off" between depth of cover and concrete quality to optimise designs for particular circumstances. Therefore, Tables A.10 to A.13 of BS 8500-1:2002 recommend different limiting values of the concrete properties for different depths of cover.

Table 2 Suggested alternative concrete mixes for reinforced concrete in the upper tidal and splash zone for 50 years service life in temporate, UK conditions

CONSTRUCTION	REINFORCED CONCRETE	REINFORCED CONCRETE	REINFORCED CONCRETE	REINFORCED CONCRETE
Casting & curing	Cured 4 days	Cured 7 days (or precast)	Controlled Permeability formwork[2] Cured 7 days	Cured 14 days (or precast)
Exposure	Upper Tidal and Splash	Upper Tidal and Splash	Upper Tidal and Splash	Upper Tidal and Splash
	XS3	XS3	XS3	XS3
Grade	C50	C45	C40	C35
Cement Type	100% Pc	50% ggbs or 25% pfa	50% ggbs or 25% pfa	70% ggbs or 30% pfa
Cement content[1] (kg/m^3)	400 minimum 450 maximum	370 minimum 425 maximum	360 minimum 410 maximum	340 minimum 400 maximum
Max free water-cement ratio	0.40	0.45	0.50	0.50
Admixtures	BS5075 Pts 1 & 3	BS5075 Pts 1 & 3	BS5075 Pts 1 & 3	BS5075 Pts 1 & 3
Cover (mm)				
Minimum	60	50	40	50
Nominal	75	65	55	65

Note 1 Maximum aggregate size 20 mm
Note 2 Controlled permeability formwork reduces chloride diffusion coefficient in surface zone by reducing effective water/cement ratio, allowing reduced cover.

What Tables 1 to 3 demonstrate is that designers have to consider each mix selection carefully to cover the lifecycle of the concrete from placement and curing through to the end of the design service life. Because the curing requirements for the mixes vary with cement type and the exposure conditions, the choice of cement type affects both buildability and durability.

It is worth noting that, whilst the maximum free water/cement ratios given in Tables 1 to 3 generally follow the recommendations of the British Standards, reducing the water/cement ratio will be beneficial for all the mixes in terms of improved strength and durability and reduced sensitivity to poor curing conditions. As a rule-of-thumb, it is considered that a reduction in water/cement ratio of 0.05 is equivalent to an increase in cover depth of 5 mm as research shows that it is the water/cement ratio which controls the resistance to chlorides and not cement content per se.

The higher allowable maximum water/cement ratios in combination with reduced depths of cover for mixes containing ggbs or pfa are in recognition of their superior chloride barrier properties.

Table 3 Suggested alternative concrete mixes for reinforced and plain concrete in the lower tidal zone for 50 years service life in temperate, UK conditions

CONSTRUCTION	REINFORCED CONCRETE	PLAIN CONCRETE
Casting & curing	In situ curing not possible except to leave formwork in place for extended period for protection	In situ curing not possible except to leave formwork in place for extended period for protection
Exposure	Lower tidal XS2/XS3 to BS 6349-1:2000; XS2 to BS8500-1:2002	Lower tidal
Grade	C40	C35
Cement Type	100% Pc, 50% ggbs or 25% pfa	100% Pc, 50% ggbs or 25% pfa
Cement content[1] (kg/m^3)	360 minimum 410 maximum	320 minimum 375 maximum
Max free water-cement ratio	0.50	0.55
Admixtures	BS5075 Pts 1 & 3	BS5075 Pt 1
Cover (mm) Minimum Nominal	 50 65	 Not applicable Not applicable

Note 1 Maximum aggregate size 20 mm

Design Details

To achieve durability, the structure must be designed to eliminate the risk areas as far as possible. Plain concrete should be chosen wherever practicable, but where reinforced concrete is necessary for structural reasons or for early thermal crack control to permit monolithic forms of construction, durable mixes with ground granulated blastfurnace slag or pulverised fuel ash additions should be the first choice for precast concrete or in situ work

that can be protected by the formwork until it is cured. These blended cement mixes will require an allowance for the slower early strength gain in thin sections and the need for extended formwork striking times. Sharp corners should be avoided, particularly in abrasive conditions (where the mixes listed in Tables 1 to 3 are likely to be inadequate and further precautions such as increased strength and the addition of steel fibres should be considered), and if unavoidable, large chamfers or rounded corners detailed instead. Any details which increase the surface area relative to the volume of concrete, such as T or I-section beams, should be avoided to minimise the surface available for ingress of chlorides. Flat slabs with smooth soffits and no support beams should be adopted wherever possible. Abrupt changes in section should also be avoided to eliminate the risk of cracking. The upper surfaces in the splash zone should be detailed to drain without maintenance cleaning of channels and, in hot dry climates, any drainage channels should be lined with waterproof material as a further safeguard against chloride ingress. In situ reinforced concrete connections and/or box outs should be avoided in the tidal or splash zones and horizontal construction joints in reinforced concrete located above the tidal zone where possible. Circular piles should be chosen instead of square to maintain uniform cover and eliminate corners. Precast concrete should be utilised as far as possible. The design and spacing of movement joints should allow for settlements on rockfill embankments or breakwaters and early thermal contraction of thick sections to avoid excessive cracking. For reinforced concrete that must be concreted below water level, the section size and reinforcement spacing should be designed for ease of access of the tremie or pump discharge pipe to the centre of the section and flow of concrete around the bars.

Placement and Curing

To avoid damage to concrete placed in situ under water, the fresh concrete must be protected from washout during placing by careful placing technique or by mix design, using underwater admixtures for increased cohesion. Underwater concrete placement to form foundations, prevent scour or strengthen and repair existing structures will usually require formwork. For foundation slabs, steel frames with integral levelling jacks lifted by crane and positioned by divers is a tried and tested method of construction [19]. The design of concrete mixes for underwater placement has historically involved the use of higher cement contents than normal, partly to allow higher workability to achieve self-levelling properties and partly to allow for the perceived washout of cement from the surface. According to Cooke[19], the use of greatly increased cement contents is not necessary as cement loss is minimal with carefully placed concrete, and the extra cement can create a significant layer of laitence. Unless the water velocity is in excess of 0.5 metres/second, only the outer film of cement is likely to be lost from the mobile advancing face and top surface. Excessive cement contents can also lead to thermal cracking during cooling from the peak temperatures generated during hydration, which may be of concern in some applications. Modern guidance, such as BS 6349 Part 1, also confirms that high cement contents are not necessary.

In situations where the water velocity is higher than 0.5 metres/second, or where there is an environmental requirement to prevent washout of fines, or where high structural integrity is needed, then the use of cellulose or gum underwater anti-washout admixtures in conjunction with superplasticisers is the solution for underwater concreting. McDonald [20] has very usefully described the research carried out by the US Army Corps of Engineers in evaluating methods for repair of concrete underwater and the concrete mixes and methods used. He advises that concrete mixes proportioned for underwater placement, with self-compaction and

moderate resistance to water erosion, generally require a minimum cementitious content of 356 kg/m^3 and a maximum water/cement + pozzolan ratio of 0.45, whilst mixes proportioned for maximum flowability and cohesiveness have cementitious contents approaching 415 kg/m^3 and a water/ cement + pozzolan ratio of 0.40 or less. Slumps of 150 to 230 mm are generally required.

Cullen [21] has described the successful use of a Grade C40 self-compacting concrete with anti-washout admixture for the placement of a mass concrete foundation block for the Low Level Refuelling Facility at Devonport Royal Dockyard.in Plymouth, UK. The mix was developed to be placed within a cofferdam measuring 46 m by 27 m and under approximately 10m of water without reinforcement and yet providing a low risk of cracking. Mix development trials found the optimum solution contained 75% ggbs, 450 kg/m^3 total cement content, a maximum water/cement ratio of 0.45, and flowed with a surface gradient of approximately 1 in 10. This allowed the tremie spacing to be increased to approximately 7 m in each direction. The reduced heat of hydration of this mix, which contained limestone aggregates which increased its tolerance to early thermal temperature gradients, allowed the thickness of each layer to be increased up to 4 m if sufficient, uninterrupted concrete supplies had been available.

For placing plain concrete under water in relatively large areas, skips have traditionally been used. They have the advantages of ready availability and the precise load, jib radius and angle for each position allows the pours to be planned. They can be used over a wide tidal range and depth of water. Their disadvantages are that the skip placing has to be controlled by diver, often in poor or nil visibility, which determines the quality that can be achieved and the speed of delivery. Each insertion of the skip into the fresh concrete creates laitence, which is likely to be trapped within the pour, so it is not suitable for structural grade concrete. It is also a potentially dangerous operation as the divers are at risk from falling objects and the skip swings in strong tidal conditions, so this would rule it out under such conditions on grounds of safety to satisfy the current CDM regulations.

Placement within formwork and below water level is most easily and safely achieved by pumping directly into place or through a tremie pipe. In both cases the delivery pipe is positioned at the bottom of the pour and gradually lifted out as the level of concrete rises. If flexible hose is used for the tremie pipe which will allow water pressure to close the pipe between charges of concrete and reduce the risk of segregation, then allowance needs to be made for the elastic stretching of the hose with the load of concrete inside when calculating the length required to leave sufficient gap at the bottom of the pour. Interruptions to the placement sequence are to be avoided and the end of the discharge pipe must be kept embedded in the fresh concrete and behind the flowing face to avoid the inclusion of seawater.

For pours within formwork that are longer than a few metres, a series of pump or tremie positions will be required, with the flow of concrete and delivery sequence planned to avoid the inclusion of seawater between placement positions. Lateral movement of tremie pipes within a pour is normally undesirable as the seal may be lost or some wash out may occur. A detailed description of the procedure of placing concrete by tremie has been produced by The Concrete Society [22]. Consideration of the concrete's cohesion and flow properties is an essential part of planning such pours to optimise the overall cost of the operation. It is normal practice to select a self-compacting concrete with high flow properties. Anti-washout properties may not be needed for concrete placed directly within formwork if the concrete is

protected from waves and currents, but the increased cohesion of the concrete achieved with a stabilising admixture will improve the quality of the concrete in place and reduce the risk of defective workmanship.

Other methods of concrete placement underwater have been used, including re-usable, bottom-opening canvas bags, hessian bags half-filled with a very plastic concrete mix [22], bottom-dumping buckets, tilting pallets and grouted, pre-placed aggregates [20]. The hessian bags are only useful for small permanent works and repairs or for temporary works where high structural standards are not required.

Table 4 Examples of underwater concrete mixes

Construction	Plain concrete Foundation 900 mm thick [19]	Plain concrete,large pour,minimum thermal cracking,self-levelling withanti-washout admixture [21]	Typical self-levelling, underwater concrete with anti-washout admixture [23]
Casting & curing	Skip placed by crane Curing not possible	Tremie placement in layers 1.4 m – 2.75 m deep Curing not possible	Pump or tremie Curing not possible
Exposure	Submerged	Submerged	Submerged
Grade	C25	C40	C35
Cement Type	100% Pc	75% ggbs	30% pfa
Cement content[1] (kg/m^3)	400 minimum 450 maximum	400 minimum 475 maximum	400
Max free water-cement ratio	0.50	0.45	0.42
Admixtures	BS5075 Parts 1 and 3	BS5075 Part 3 + Underwater /stabiliser admixture	BS5075 Part 3 + Underwater/ stabiliser admixture
Workability Flow	Not quoted	600 + or – 50 mm	600 mm

Note 1 Maximum aggregate size 20 mm

In the author's experience, their main drawback is in the lack of good bond between the bags or between bags and the structure being repaired. Unless a positive mechanical bond is achieved, individual bags can be easily disturbed by wave action.

In the splash zone, it is a worthwhile precaution to wash reinforcement that has been exposed to seawater splashes with fresh water immediately prior to placing concrete to limit built-in chloride levels. This is particularly important in hot dry conditions, where the contamination of chlorides can build up on the steel from wind-blown sources and the risk of corrosion is high. Below high-tide level, where the reinforcement is exposed during low tide there is no need as the risk of corrosion is low due to the regular wetting of the concrete stifling the flow of oxygen to the steel.

In the tidal zone, it is necessary to protect the young concrete through the hydration phase until discontinuous capillaries are achieved before exposing it to seawater otherwise there could be an early build-up of chlorides within the cover zone. The most practical method is simply to leave the formwork in position for longer than usual to keep the seawater away from the immature concrete.

Above the tidal zone, in the splash zone and higher, then normal fresh water curing is recommended for a duration depending upon ambient conditions and cement type. The curing periods given in Tables 1 to 3 are for UK conditions in temperatures above 5°C.

For scour prevention and for encasement repairs of existing concrete piles, high strength woven textiles can be used to construct fabric forms as mattresses or jackets [24]. These have been developed from the concrete-filled sandbag technique traditionally used to block holes underwater or provide scour protection. The mixes employed for filling textile formwork has often been a micro-concrete with sand up to 1.5 mm size as the coarsest aggregate or a pump mix with a maximum aggregate size of 10 mm and a cement content between 450 and 600 kg/m^3 to facilitate flow and placement in relatively thin sections.

CONCLUSIONS

The marine and underwater environments pose a tremendous challenge to the ingenuity of the engineer in designing structures that can be built safely, with control of the risks during construction, and that provide durability over the service life required.

Developments in legislation in UK place more onus on the designer to consider during the design process the safety of those who are to construct, maintain or repair the structure. By using ingenuity and having due regard to buildability and durability, the designer can ensure he meets this requirement and minimises the need for maintenance and repairs which introduce further hazards.

Advances in the specification of concrete mixes for the marine environment in British Standards has given the design engineer the guidance needed to produce durable concrete and improve sustainability by reducing maintenance repairs.

The emergence of self compacting concrete technology for underwater applications has recently been demonstrated successfully on a major project, which has shown the way forward for concrete technology in many applications.

This is an exciting time for the development of concrete technology in the marine and underwater environments. The requirements of buildability and durability are converging with the application of improved understanding of concrete durability in the marine environment and the use of admixtures and cement replacement materials which deliver the concrete properties needed for safety, economy and sustainability.

REFERENCES

1. PARLIAMENT, Construction (Design and Management) Regulations 1994, SI 1994 No 3140, HMSO, 1995, 10 pages.

2. HEALTH & SAFETY COMMISSION, Managing health and safety in Construction, HSE Books, London, 2001, 100 pages.

3. HEALTH & SAFETY COMMISSION, A guide to managing health and safety in construction, Health & Safety Commission, HSE Books, Sudbury, Suffolk, 1995, 76 pages.

4. HEALTH & SAFETY COMMISSION, Health and Safety in Construction, HSE Books, Sudbury, Suffolk, 1996, 116 pages.

5. COOKS, J., BRIFFA, G., DEW, K., WATSON, D., STOKES, M., ET AL, CDM Regulations - case study guidance for designers: An interim report, Report 145, CIRIA, London, 1995, 176 pages.

6. OVE ARUP & PARTNERS, CDM Regulations – work sector guidance for designers, Report 166, CIRIA, London, 1997, 170 pages.

7. INTERNATIONAL NAVIGATION ASSOCIATION (PIANC), Mar-Com 28 (previously PTC II Working Group 28), Recommendations for the Construction of Breakwaters with Vertical and Inclined Concrete Walls, Report of Sub-Group C, Investigations into the implication of construction aspects in design, performance of concrete and identification of "hot spots" in design and construction, International Navigation Association, Brussels, July 1997, 58 pages.

8. INTERNATIONAL NAVIGATION ASSOCIATION (PIANC), Working Group 28 Mar-Com, Breakwaters with Vertical/Inclined Concrete Walls, Main (Summary) Report, International Navigation Association, Brussels, publication due 2002-2003.

9. ALLEN, R.T.L., (EDITOR), Concrete in Coastal Structures, Thomas Telford Ltd, London, 1998, 301 pages.

10. BRITISH STANDARDS INSTITUTION, Maritime structures – Part 1: Code of practice for general criteria, BS 6349-1:2000, BSI, London, 2000, 202 pages.

11. BRITISH STANDARDS INSTITUTION, Code of practice for Maritime structures – Part 2: Design of quay walls, jetties and dolphins, BS 6349-2:1988, BSI, London, 1998, 118 pages.

12. PEEPLES, F. K., CHEN, T. L., P. LEONARD VAN DYKE P.E., COBURN, M., MANCILL, E., A Composite Prestressed Concrete System for Marine Wharfs, PCI Journal, Precast/Prestressed Concrete Institute, Chicago, November-December 1996, pp110-115.

13. TANNER, J.A., Composite Deck Systems for Marine Structures, Concrete International, American Concrete Institute, Farmington Hills, Michigan, December 1999, pp 57-61.

14. BRITISH STANDARDS INSTITUTION, Concrete – Complementary British Standard to BS EN 206-1 Part 1: Method of specifying and guidance for the specifier, BS 8500-1:2002, BSI, London, 2000, 43 pages.

15. BRITISH STANDARDS INSTITUTION, Concrete – Complementary British Standard to BS EN 206-1 Part 2: Specification for constituent materials and concrete, BS 8500-2:2002, BSI, London, 2000, 32 pages.

16. EUROPEAN COMMITTEE FOR STANDARDISATION, Concrete – Part 1: Specification, performance, production and conformity, EN 206-1:2000, CEN, Brussels, 2000, 69 pages.

17. FOOKES, P. G., SIMM, J. D., BARR, J. M., Marine concrete performance in different climatic environments, Marine Concrete, Proc. International Conference on Concrete in the Marine Environment, The Concrete Society, London, 1986, pp 115-130.

18. FOOKES, P. G., A Simple Guide to risk assessment for concrete in hot dry salty environments, 4th Int. Conference, Deterioration & Repair of Reinforced Concrete in the Arabian Gulf, The Bahrain Society of Engineers and The Concrete Society, Bahrain, 1993, pp 161-212.

19. COOKE, A.R., SIMPSON, J., Underwater concrete construction of Phuket port quay wall foundation, The Dock & Harbour Authority, September 1991, pp 127-140.

20. MCDONALD, J. E., NEELY, B., Underwater Concrete Placement: Materials, Methods and Case Studies, Keynote Paper, Specialist Techniques and Materials for Concrete Construction, Theme Four: Underwater Concrete, Proc.of International Conference held at the University of Dundee, Scotland on 8-10 September 1999, pp 239-255.

21. CULLEN, D., WILLIAMS, R., KNIGHTS, J., Constructing Beneath the Waves, Concrete Engineering, Summer 2001, pp 13-17.

22. CONCRETE SOCIETY, Underwater Concreting, Technical Report No.35, The Concrete Society, Crowthorne, Berkshire, UK, 1990, 40 pages.

23. MCLENNAN, L., Underwater Concrete construction, Specialist Techniques and Materials for Concrete Construction, Theme Four: Underwater Concrete, Proc.of International Conference held at the University of Dundee, Scotland on 8-10 September 1999,
pp 281-288.

24. CANNON, E. W., BOYES, R. G. H., Permeable woven fabric formwork, Civil Engineering, March 1987, pp 9-33.

THE REINSTATEMENT OF A POST-TENSIONED MARINE STRUCTURE – AN UNUSUAL CHALLENGE

A R Evans
Scott Wilson
United Kingdom

ABSTRACT. A routine inspection of a prestressed concrete dock dividing wall revealed significant cracking. At the time of the inspection, the wall retained up to 13m of sea water. Concerns for safety led to flooding of the dock in order to reduce pressures on the wall. Against the background of known problems with post-tensioned structures and the concern of possible loss of prestress, a number of options for repair were considered. These included the construction of major remedial works. In the event a novel and challenging approach was adopted. This involved the monitoring of the behaviour of the structure under varying load conditions. This work, together with an intrusive investigation led to a restoration of confidence in the wall and the possibility of more modest repairs.

Keywords: Prestress, Marine, Repair, Concrete, Monitor, Analysis, Underwater.

André Evans, is a Regional Director with Scott Wilson, based in their Plymouth office. He graduated from City University, London in 1972 and completed a Masters Degree in structures at Manchester University in 1974.

After working in Local Government and for an Iranian Consultant he joined Scott Wilson in 1978. Since that time he has worked for the firm in the UK, in the Middle East and in Hong Kong. He has been involved in all manner of civil engineering projects and has a special interest in the deterioration and reinstatement of concrete structures.

He has been Chairman of the Concrete Society (Devon and Cornwall branch). He is a reviewer for the ICE Chartered Professional Review and an Associate of the University of Plymouth.

INTRODUCTION

The operator of a major dry dock decided some years ago to divide it into two parts in order to create two smaller facilities. This was achieved by constructing a prestressed concrete wall at the mid-point of the dock.

The design and construction of the wall in the medium of prestressed concrete followed naturally from the popularity if this material at the time (1970). Reinforced concrete had become a universally used material which was considered by many to have an almost limitless lifespan. Prestressed concrete was a natural progression which allowed greater spans and more slender construction. The problems which have afflicted the concrete industry had not yet emerged to any great degree at that time. The wall served its purpose for some years retaining up to 13m of seawater without incident. However when a routine inspection in 1993 by a Scott Wilson Engineer revealed significant cracking, a potentially serious problem was recognised.

Between 1970 and that time, concrete construction had been plagued by problems. In particular, prestressed construction in bridges of the precise kind used in the wall had been subject to chloride attack. Similar construction in a dock in Greece was the subject of failure (1). The presence of sea water in the vicinity of the cracks in the wall raised the spectre of loss of prestress and hence the greater part of the strength of the wall.

In order to reduce the risk of structural failure of the wall, the operator decided to flood the dock on one side of the wall thus reducing the differential head of water. Whilst taking away the immediate urgency of the situation, the use of the dock facility was lost.

The investigation of the problem and design of the remedial works is the subject of this paper.

THE DESIGN OF THE WALL

Two major reinforced concrete beams were designed which spanned horizontally at the top and bottom of the dock, the prestressed wall spanning about 13m vertically between them.

Figure 1 overleaf shows an elevation and section through the wall.

The upper horizontal beam incorporated a man-entry size subway for water, power and various other services.

The original dock, which was constructed around the turn of the last century comprises stone-clad mass concrete resting on a shale substrate. More recent reinforced concrete extensions have been added to the walls of the dock.

The wall, which was designed by T F Burns & Partners, was constructed in situ in five equal lifts and incorporated the BBRV prestressing system. Forty-five pairs of tendons were used, each comprising 55 No. 7 mm diameter wires. Each tendon was stressed to 230 tonnes against a working load of 220 tonnes. After stressing, the enclosing sheaths were grouted from a point close to the base of the wall.

Aside from the main reinforcement for the horizontally spanning beams, the wall was generally lightly reinforced against shrinkage/thermal cracking.

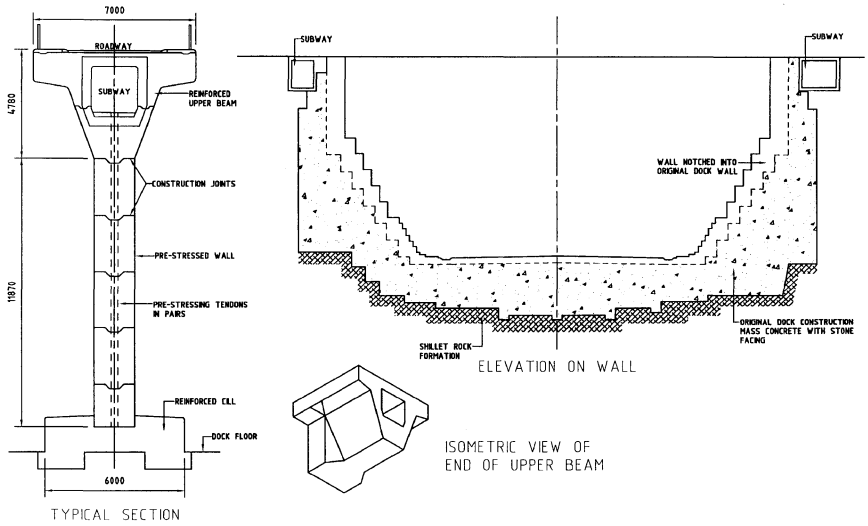

Figure 1 Typical section and elevation on wall

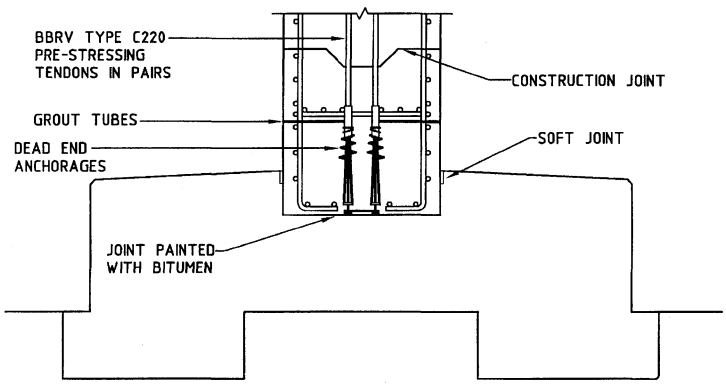

Figure 2 Wall base detail

Articulation of the wall at its base was catered for by means of bitumen coating and a 20 mm slot with flexible infill.

A check calculation was carried out based upon unyielding supports in accordance with BS8110 pt 1. This revealed satisfactory factors of safety against bending, but there was doubt concerning the shear capacity at the base. If prestress had been lost in part due to corrosion of the tendons, then collapse of the wall with severe consequences was possible.

CRACKS IN THE WALL

The cracks which were discovered were sharp indicating relatively recent origin. They were up to a few millimetres wide and extended around 10m in length close to the base and on both sides of the wall.

After discovery of the cracks, a limited monitoring exercise was carried out over several months which showed a small but progressive increase in crack width. A Scott Wilson report of 1994 suggested that the cracking could be caused by shrinkage or thermal strains, loss of prestress or movements in the foundations or original stepped dock wall.

At around this time the decision was made to flood the dock. It was not possible after this to continue monitoring the crack widths in the manner which had been instigated as the gauges were under water.

A diving survey carried out in 1997 indicated that the cracking had not increased to a significant degree although it was difficult to be precise.

Figure 3 Cracking to wall elevation

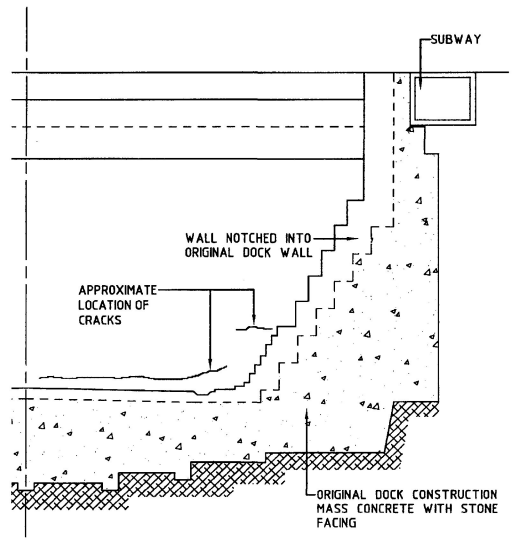

Figure 4 Position of cracks on elevation

REPAIR OPTIONS

In 1997 the Dock Operator requested that Scott Wilson put forward ideas for strengthening the wall on the assumption that prestress had been lost and that work should be carried out with the docks flooded. Ideas which emerged from a brainstorming exercise included using mass concrete cast under water with permanent shuttering, reinforced concrete, mass concrete with reusable shuttering and the addition of further prestress. A rapid estimating exercise revealed repair costs to be in the region of £0.75-£1.25 million.

MONITORING PROPOSAL

While the repair options were under consideration, the dock operator received a proposal from Structural Statics Ltd which offered the possibility of restoring confidence in the wall with reduced expenditure.

The essence of the proposal involved monitoring the behaviour of the wall under varying loads and comparing this with the behaviour predicted using analytical techniques. A sophisticated system was proposed which had been developed for steel caissons and had succeeded in prolonging their life. The equipment which had previously been used on the steel caissons was available for re-use.

This exercise would be able to demonstrate whether prestress had been lost.

It was proposed by Scott Wilson that the monitoring be backed by an intrusive investigation in order to physically inspect the tendons and the concrete.

In the event, the dock operator accepted the proposals and requested that Scott Wilson lead the team.

INTRUSIVE INVESTIGATION

The intrusive investigation involved the extraction and testing of cores and the inspection of tendons, grout and prestressing anchorages. Whilst working under water, further inspections of the cracks were also undertaken.

A total of 8 cores were drilled and extracted from the wall. In order not to cause damage, the final stage in exposing the tendons was carried out with an ultra high pressure water jet. Underwater CCTV was used to inspect and record the condition of the exposed tendons. A single core was taken at the location of the crack.

Anchorages were carefully exposed within the subway at the top of the tendons.

The conclusions of the investigation are summarised below:

1. Exposed tendons showed no significant loss of section or penetrative corrosion (see figure 5).

2. Grouting appeared to have been reasonably well accomplished.

3. Anchorage heads were in good condition.

4. Concrete quality was good. Chloride levels, cement contents and sulphates were all satisfactory. Strengths and moduli of elasticity were at reasonable levels (see Table 1).

5. The core taken through the crack appeared to demonstrate that the crack did not penetrate right through the wall but terminated at the compression zone (see Figure 6).

Figure 5 Still image showing tendons and grout

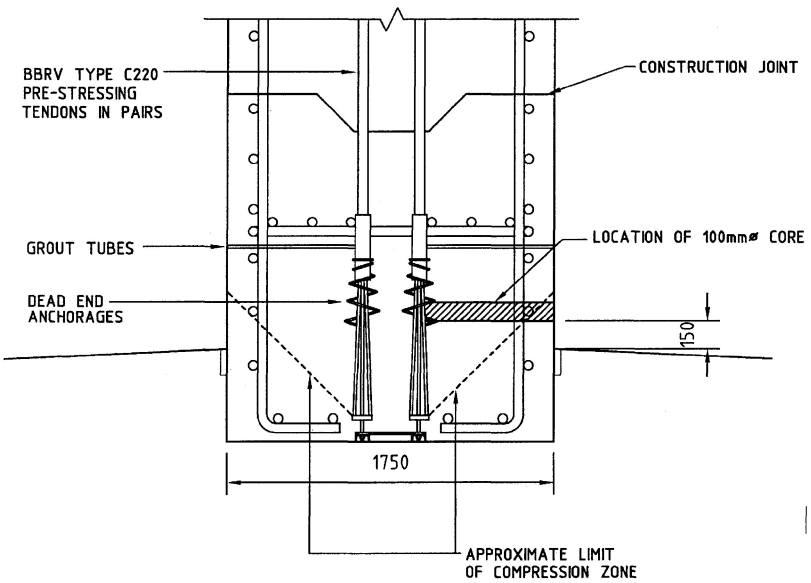

Figure 6 Compression zone in wall base

THE MONITORING EXERCISE

Detailed monitoring was carried out of the behaviour of the wall between 1998 and 2000. During this period, problems were encountered with the system due to accidental damage, long delivery of specialised parts, IT problems and even the interference by fish. It should be recognised that highly sensitive equipment was installed under water with minimal visibility and hence such problems might be expected.

Table 1 Physical Tests

CORE REFERENCE No.	3	6	7
Condition of sample at receipt	Dry	Dry	Dry
Curing/Storage conditions	Tank	Tank	Tank
Sample type	Core	Core	Core
Mean length (mm)	146	146	146
Mean diameter (mm)	68	68	68
Saturated density (kg/m^3)	2380	2370	2380
Gauge Type	Vibrating wire	Vibrating wire	Vibrating wire
Gauge length (mm)	90	90	90
No. of gauges per sample	2	2	2
Compressive strength of companion specimen (N/mm^2)	48.5	48.5	48.5
Compressive strength of test sample (N/mm^2)	49.5	46.5	39.5
Compressive strength of test sample within 20% of estimated strength	Yes	Yes	Yes
Static modulus of elasticity (N/mm^2)	34000	26500	21500
Failure mode	Normal	Normal	Normal

Equipment which measured minute variations in angle and linear strain was installed at various locations on the wall. In addition, water levels and temperature gauges were installed on both sides of the wall.

During the course of the work, water levels were adjusted within safe limits, by pumping water in or out of the dock. This, in conjunction with the tidal variations which acted on the one side of the wall, gave a range of loading patterns.

The results of the exercise, which were not entirely as expected, are discussed in following sections of this paper.

FINITE ELEMENT ANALYSIS

In parallel with the monitoring exercise, a finite element analysis was carried out by Scott Wilson in order to compare the measured behaviour with that predicted.

The wall was analysed using the LUSAS package incorporating 366 solid elements. Different scenarios were modelled assuming full prestress and no prestress and pinned and encastré boundary conditions.

Results of deflections and stresses showed a predictable 'skewed dish' format typically as shown on figure 7 below.

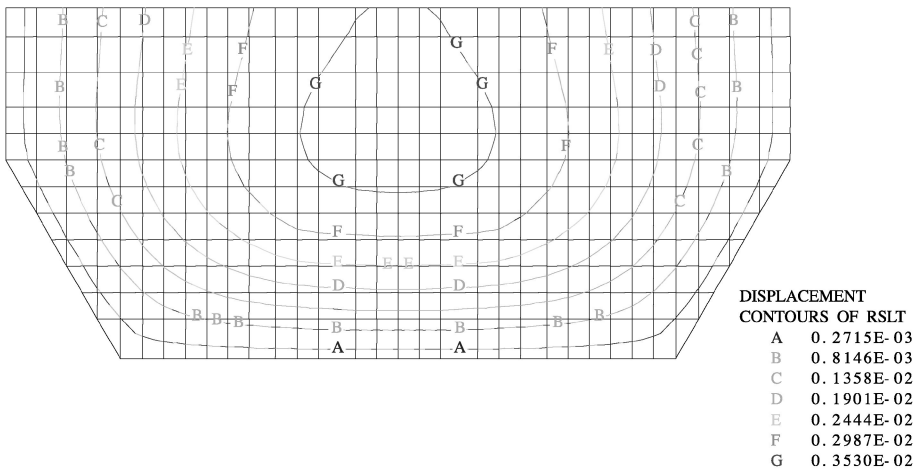

Figure 7 Typical displacement contours

RESULTS AND CONCLUSIONS OF MONITORING EXERCISE

The enormous volume of data emanating from the monitoring regime was carefully scrutinised so that a thorough understanding of the behaviour of the wall and the reasons for the cracking was gained. A brief summary of the results is given below:

- Flexing of the wall under lateral loading corresponded to a fully prestressed configuration.

- A complex thermal regime exists to which the wall responds. Water temperatures vary significantly with depth. Insolation occurs which is pronounced due to the East-West orientation of the wall.

- Rather than being rigid as the designers will have assumed, the substrate appears to move depending on the level of water present and the temperature.

- The base of the wall moves in its slot longitudinally and transversely with the cracks allowing articulation of segments of concrete independently.

The behaviour of the wall is the result of a complex interaction between the wall, which in its own plane, is massively stiff and the adjacent dock structures that are in some regards not as rigid as the designers assumed.

As temperatures vary on a daily and seasonal cycle, the wall seeks to expand and contract and this results in relative movement between itself and the adjacent structures. Where such

movement cannot occur, very large stresses will result that are easily capable of 'tearing' inadequately prestressed concrete (such as that outside the anchorage 'cone'). The measures incorporated by the designers to accommodate such articulation probably sufficed for some years but ultimately failed.

RECOMMENDATIONS

There is a requirement to enhance the shear capacity of the base of the wall while still allowing articulation. An indicative scheme comprising steel gallows brackets is shown in Figure 8 below:

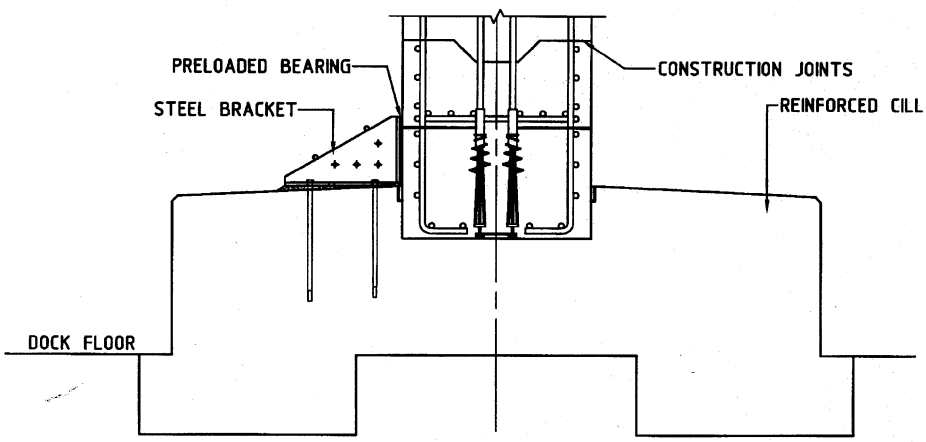

Figure 8 Shear Capacity Enhancement

In addition to these works, a monitoring system which is alarmed to detect any unexpected change of behaviour, together with an inspection regime is recommended.

This proposal can be installed quickly at modest cost. It will represent significant savings to the client over more conventional solutions.

At the time of preparation of this paper, a value engineering exercise is planned to ensure that all possible solutions have been explored prior to implementation of the repair scheme.

REFERENCES

1. MARTIN G. P., ARNOLD A. C., Failure of dry dock floor in Scaramanga, Greece, resulting from stress corrosion damage to anchor pile tendons. Proceedings of the Institution Civil Engineers, Water Maritime and Energy 1992, pages 211-225.

FREEZE-THAW RESISTANCE OF BLASTFURNACE CEMENTS: LABORATORY TEST AND LONG TERM EXPERIENCE

E Lang

Forschungsgemeinschaft Eisenhuttenschlacken

Germany

ABSTRACT. Most of the marine structures in the German part of the North Sea are constructed with blastfurnace cement. Furthermore, so are all of the sluices in the Rivers Mosel and Saar. The history of these constructions is well documented and allows one to judge the performance precisely. Performance tests, for instance the CDF-test for freeze-thaw resistance with sodium chloride solution, are becoming increasingly important. However, problems arise with laboratory tests, especially in the case of freeze-thaw resistance, in the correlation between the laboratory conditions and the environmental conditions that occur in practice. This paper describes the results of a research programme in which some marine constructions of between 25 and 70 years old were investigated. Drill cores from the constructions and laboratory concretes made with the same mix design, but stored in accordance with CDF test regulations, were tested for comparison. The results show that the laboratory tests are not always capable of reflecting performance in practice. This mainly occurs with the measurement of the internal damage of the concrete during the CDF/CIF test.

Keywords: Blastfurnace cement, Marine structures, Durability, Carbonation, Freeze-thaw resistance

Dr Eberhard Lang, is the Head of the Research Department for Building Materials of Forschungsgemeinschaft Eisenhüttenschlacken, Duisburg-Rheinhausen, Germany. His main research interests include blastfurnace cement, high-performance concrete, durability of concrete with particular reference to freeze-thaw resistance, multiaggressive attack on concrete made with blastfurnace cement, and alkali-silica-reaction.

INTRODUCTION

Most of the marine structures in the German part of the North Sea are constructed with blastfurnace cement. Furthermore, so are all of the sluices in the Rivers Mosel and Saar. The history of these constructions is well documented and allows one to judge the performance precisely. Performance tests, for instance the CDF/CIF test for freeze-thaw resistance with sodium chloride solution or with water, are becoming increasingly important. However, problems arise with laboratory tests, especially in the case of freeze-thaw resistance, in the correlation between laboratory conditions and the environmental conditions that occur in practice.

This paper describes the results of a research programme in which some marine constructions of between 25 and 70 years old were investigated. Drill cores from the constructions and laboratory concretes made with the same mix design, but stored in accordance with the CDF test regulations, were tested for comparison. The tests were completed with examinations of concretes with a mix design (limit values) in accordance with exposure classes XF3 and XF4 of the European Concrete Standard EN 206.

The results show that laboratory tests are not always capable of reflecting the performance in practice. This mainly occurs with the measurement of the internal damage of the concrete during the CDF/CIF test.

SEA LOCKS AND FLOOD BARRIER

In 1998 a group of concrete experts visited some different marine structures, mainly flood barriers, which were often combined with a sluice, on the Baltic and North Seas. Table 1 gives some information about a few of these buildings and the concrete which was used.

Table 1 Marine structures and the used concrete

BUILDING	YEAR OF CONSTRUCTION	STRENGTH CLASS	TYPE OF CEMENT	CEMENT COMMENT	W/C-RATIO	ADDITION
				kg/m³		kg/m³ / type
Harbour Kiel, quay	1978	C25	CEM III/B-32,5 NW/HS/NA*	330	0,47	-
Harbour Kiel, quay	1978	C25	CEM I 42,5-N	330	0,47	-
Sluice, Everschop	1970	C30	CEM III/B 32,5	300	0,54	25 / fly ash
Sluice Schlüttsiel	1959	C30	CEM III/B 32,5	300	0,45	35 / Trass**
Sluice Schlüttsiel	1959	C45	CEM II/B-S 32,5	300	0,45	-
Sluice Holmer	1984	C35	CEM III/B 32,5-NW/HS/NA	300	0,50	70 / fly ash
Sluice Wilhelmshaven	1938/42	C15	CEM III/B 32,5 NW/HS/NA	300	?	60 / Trass
Sluice Wilhelmshaven	1958/63	C25	CEM III/B 32,5 NW/HS/NA	295	0,55. 0,60	30 / Trass 30 / pulv. stone

* NW = low heat of hydration, HS = high sulphate resistance, NA = low alkali content
** Trass = natural pozzolanic material

The monitoring of these marine constructions has shown that, also sometimes appearing damaged, they are in good condition, and that high slag blastfurnace cements are an excellent binder for these applications. Some damage is not the result of the type of cement used. For example the quay of the harbour in Kiel looks like washed concrete, because of insufficient curing. The damaged surface was already visible after the first winter. In the last 20 years this state has not changed any more. Some parts of the Everschop sluice how damage as a result of insufficient concrete cover and the use of aggregates without a high freeze-thaw-resistance.

RIVER SLUICES

In accordance with the completing of the European waterways the River Saar in Germany between the border with France and the River Mosel has six sluices. The first one was finished in 1976 and the last in 1998. Five sluices were built with concrete using CEM III/B 32,5-NW/HS and one using CEM III/A 32,5. In all cases natural sand and gravel from the Rivers Mosel, Saar or Rhine of 32 mm diameter and air-entraining admixtures were used.

In 1999 a group of experts visited the sluices of the River Saar. The results were published [2]. With reference to the concrete the expert group sums up: we found that it is possible to build sluices having extremely high durability with used concrete. The use of blastfurnace cement is successful. Some deficiencies are not the result of the building material but the result of the manufacturing and curing. It depends on the seasons and the weather at the time of curing is very important.

A similar judgement was made in respect of the sluices of the River Mosel [3]. The finishing and completion of the River Mosel to a navigable waterway was finished in 1964. The sluices were built up with concrete using blastfurnace cements with slag content between 60 and 80 percent by weight. The cement content ranged from 240 to 300 kg/m³, and in some cases Trass (40 to 75 kg/m³) was used. Unlike the sluices of the River Saar air-entraining agents were not used.

PROBLEMS

The ultimate test of the durability of structures is to measure their performance in practice. Regardless of how good laboratory tests are, and the dedication of the scientists conducting them, it is impossible to replicate real-life conditions in a laboratory. This is especially true with freeze-thaw and de-icing salt-resistance, because the stress levels that occur in practice and under laboratory conditions are too different.

The results in practice show a very high performance when concrete is made with blastfurnace cement basis that all requirements of the German Concrete Standard DIN 1045 [6] are fulfilled, especially the water-cement-ratio and the curing conditions. The European Concrete Standard EN 206-1 increases the requirements. In comparison with the German regulations the water-cement ratio is lower for freeze-thaw durable concrete. This means that under the old regulations there is already a concrete with a high resistance to seawater, freeze-thaw or de-icing salt attack, and under the new regulations there will be a higher safety level.

On the other hand performance was developed [5]. The problem is to calibrate the results from the performance test with the behaviour of the concrete in practice. In the past there has sometimes been an insufficient correlation between test results and the behaviour in practice. In particular the testing conditions of the CDF-test and the proposed acceptance criterion of 1500 g/m² after 28 freeze-thaw cycles are not suitable to describe the freeze-thaw resistance for all concretes. The behaviour in practice must be the fix point to find test conditions and acceptance criteria.

EXPERIMENTAL DETAILS

Materials

One Portland cement and four blastfurnace cements with different slag contents and two different strength classes were used. The blastfurnace cements were based on the same clinker as the blastfurnace cements. Table 2 shows some important physical properties. The coarse and the fine aggregates consisted of natural gravel and sand from the Rhine area. These aggregates are comparable with the most of the aggregates used in the sluices.

Table 2 Properties of cement

		CEM I 32,5	CEM III/A 32,5	CEM III/A 42,5	CEM III/B 32,5-NW/HS/NA*	CEM III/B 42,5-NW/HS/NA*
Spec. Surface	cm²/g	3100	3910	4040	4040	4630
Slag content	%	-	63	44	74	67
Compressive strength						
2 d	MPa	26,9	10,8	18,5	7,8	13,6
28 d		50,8	55,8	57,4	52,6	62,5
91 d		58,9	64,5	66,8	61,9	71,3
Heat of Hydration	J/g	280	220	260	160	240

*NW = low heat of hydratation, HS = high sulphate resistance, NA = low effective alkali content

Test Methods

The fresh and hardened concrete properties were tested in accordance with the German Standard DIN 1048 or European standards if available. On the basis of the existing standards and recommendations the Task Group 4 "Freeze-Thaw Resistance of Concrete" of CEN TC 51 has prepared a draft for a European standard: "Test Methods for the Freeze-Thaw Resistance of Concrete – Tests with Water or with Sodium Chloride Solution, Part 1: Scaling" [5]. This draft contains as a reference method the Slab test and, as an alternative method the Cube- and CDF-/CIF-test. For the investigations described in this paper the CDF-test with salt was used.

TEST PROGRAMME

The test programme comprises four steps: 1) Making and testing of concrete in laboratory scale, 2) on taking of fresh concrete during the construction of a marine structure and the testing of this concrete after different curing conditions, 3) sampling drill cores from waterway structures, which have shown a high performance in the past, and 4) making and testing concretes with the same composition of old marine structures.

RESULTS AND DISCUSSION

In laboratory tests at a constant temperature of 20°C and a relative humidity of 65 per cent the carbonation rate of blastfurnace cement concrete is higher than Portland cement concrete having the same strength class. The laboratory climate favoured the carbonation. Cements with a lower degree of hydration in the first weeks of hydration are more sensitive under such conditions.

The compressive strength and the carbonation rate of the laboratory concretes with a w/c-ratio of 0,50 as shown Table 3.

Table 3 The compressive strength and carbonation depth of the laboratory concretes

STRENGTH		CEM I 32,5 R		CEM III/A 42,5		CEM III/A 32,5		CEM III/B 42,5-NW/HS/NA		CEM III/B 32,5-NW/HS/NA	
2 d	MPa	24,7		16,9		9,5		10,3		7,8	
7 d		33,1		31,5		32,0		30,5		21,9	
28 d		47,3		48,8		39,4		51,6		35,4	
CARBONATION		LC*	OD*	LC	OD	LC	OD	LC	OD	LC	OD
28 d	mm	0.8	0	-	-	2.0	0.5	0.8	< 0.5	2.0	1.0
90 d		1.5	0.3	1.8	0.3	3.1	0.8	1.2	0.2	2.4	1.2
180 d		2.2	0.5	2.0	0.5	4.1	2.0	1.6	0.2	4.9	1.8
360 d		3.5	1.7	3.8	2.4	7.4	2.8	2.0	0.9	6.8	2.9

* LC = laboratory climate, OD = outdoor storage (unprotected)

The higher the slag content the higher the carbonation depth, except the concrete with CEM III/B 42,5. The fineness of this cement is much higher and therefore the capillary porosity of the concrete made with this cement is, in its early life, much lower, and it has a higher compressive strength. After 28 days the carbonation depth in laboratory climate is already much higher as by outdoor storage.

It is well known that the capillary porosity in the carbonated layer of blastfurnace cements concrete is higher than in the uncarbonated concretes [7]. Marine structures are unprotected and their carbonation depth is very low. The concrete of the harbour access at Wilhelmshaven, constructed between 1938 and 1942 using a blastfurnace cement with 75% granulated blastfurnace slag, shows a maximum carbonation depth of 2 mm in the tidal zone and of 2 to 6 mm in the splash zone [8]. The sea lock at Wilhelmshaven is now about 60 years old. In laboratory climate the concrete with a blastfurnace slag content of 67% shows after only 28 days a carbonation depth of 2 mm.

The scaling of the laboratory concretes in the CDF-test is high, see Figure 1. After 28 cycles the scaling is near the proposed acceptance criterion of 1500 g/m².

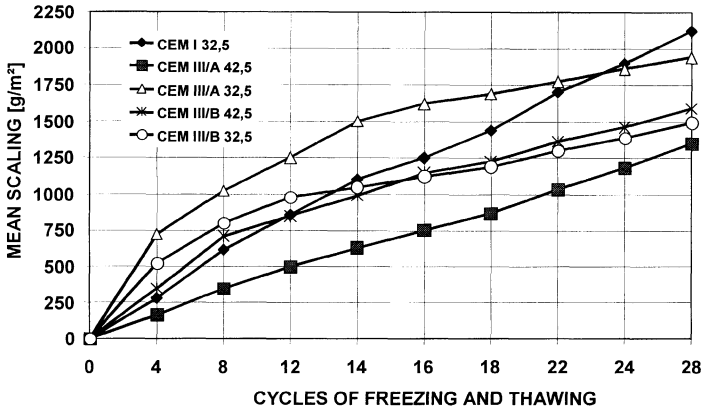

Figure 1 Scaling of laboratory concretes

During the construction of a marine structure samples were taken and were tested according to the CDF-test after 28 days. Samples of the same concrete were stored in laboratory climate and outdoors unprotected and protected under roof. The concrete contains 340 kg/m³ CEM III/B 32,5-NW/HS/NA, 60 kg/m³ fly ash, 1750 kg/m³ natural sand and gravel and 175 kg water. The carbonation depth of the concrete is shown in Table 4.

Table 4 Carbonation depth depends uponboth the kind of storage and the time [mm]

TIME OF STORAGE	LABORATORY CLIMATE	PROTECTED OUTDOORS	UNPROTECTED OUTDOORS
28 d	1.3	0.1	< 0.1
90 d	2.0	0.1	< 0.1
180 d	4.7	1.7	0.6
360 d	6.1	2.9	1.4

In laboratory climate the carbonation depth of this concrete is after 28 days nearly the same as after one year outdoors storage. Therefore, the scaling (Figure 2) of both samples is nearly the same too. The carbonation depth of the samples stored protected outdoors for a year is 2.9 mm. This value is about double the size of the concrete stored unprotected outdoors and the scaling is double the size too. The relative values for carbonation depth, scaling and the increase of weight during the capillary suction in the CDF-test, are about equal, as shown in Table 5.

Table 5 Relative carbonation depth, scaling and increase of weight (samples stored unprotected outdoors = 1)

	LABORATORY CLIMATE	PROTECTED OUTDOORS	UNPROTECTED OUTDOORS
Carbonation depth	4,4	2,1	1
Increase of weight	4,8	2,3	1
Scaling	5,8	2,1	1

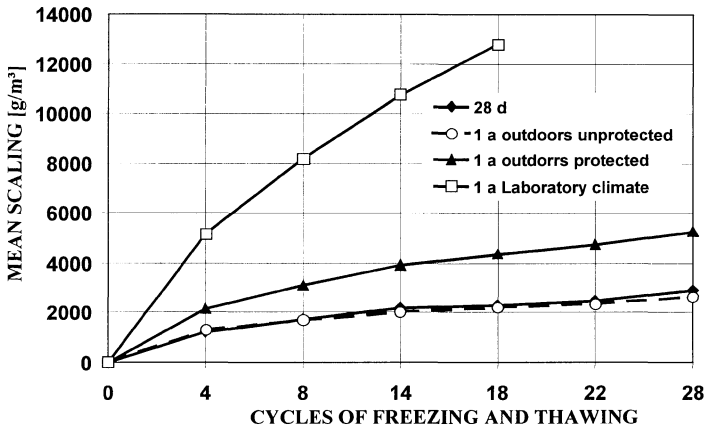

Figure 2 Scaling depends on the kind of storage

The scaling of the concrete is higher than the proposed acceptance criterion of 1500 g/m². The marine structure was built with this concrete three years ago. There is not yet any visible evidence of alterations.

Drill cores were tested from different marine structures. The next results are from concrete produced in 1974 with blastfurnace cement similar to CEM III/B 32,5 according to EN 197-1. This concrete has a cement content of 300 kg/m³, 725 kg/m³ Sand 0/3 mm, 1215 kg/m³ Gravel 7/30 mm, 20 kg/m³ fly ash and a w/c-ratio of 0.46.

After 27 years' use of this marine structure there is no sign of any damages and no repairs have been necessary; nor will they be in near future. Contrary to the behaviour in practice, in the CDF-test the concrete shows a very high scaling, see Figure 3. According to the CDF-test only 28 cycles are necessary.

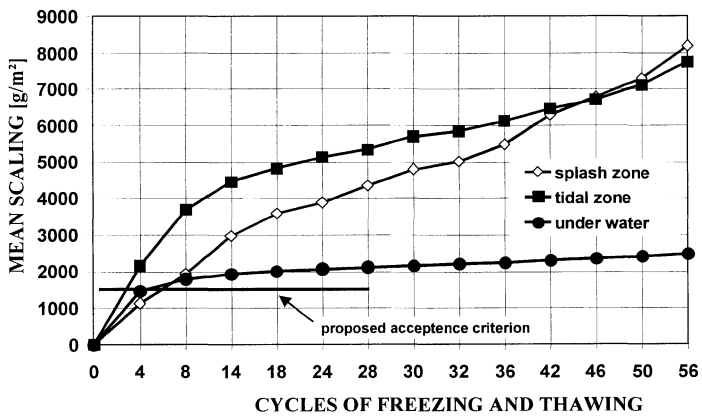

Figure 3 Scaling of drill corse from a 27-year-old marine structure

In laboratory scale the concretes of this old marine structure and from some other marine structures were produced and tested exactly according to the regulations of the CDF-test. The scaling after 28 cycles was about 2000 g/m². This value is higher then the proposed acceptance criterion. What is the meaning of the result? On one hand, the structure was built up according to the rules of the German Concrete Standard (description method) and the concrete quality is, after a use of 27 years, very good. On the other hand with respect to the performance test (CDF) and the proposed acceptance criterion of 1500 g/m², a concrete of this quality would be not allowed.

CONCLUSIONS

Long-term practical experiences show concretes with blastfurnace cement have a high durability in marine structures. If there are any problems the reason is not the cement, the reason is an offence against the rules (for instance higher w/c-ratio, insufficient curing).

The main reason for the scaling of concrete made with blastfurnace cement is the higher capillary porosity in the carbonated surface layer. In laboratory climate the carbonation of a blastfurnace cement is much higher than in natural atmosphere.

It is not possible to describe the performance of concretes made with blastfurnace cement or other slowly hardened cements with the CDF-test. All results show that performance in practice is better then the laboratory test.

It is necessary to change the storage conditions in the CDF-test or to find different acceptance criteria for different kinds of cement in correlation to their behaviour in practice.

REFERENCES

1. Bereisung von Wasser- und Meerwasserbauwerken an der Ost- und Nordsee, Final report of the montanzement Marketing GmbH, 1998.
2. BAYER, E, KUNZ, C, Die Saarschleusen nach 12-jährigem Betrieb, Beton , 3, 2000, pp 122-127.
3. HALLAUER, O, Beurteilung der Betonbauwerke des Moselausbaus nach 25jährigem Betrieb, Beton-Informationen, 31, 1, 1991, pp 3-9.
4. DIN 1048, Prüfverfahren für Beton, Part 1-5, Issue June 1991.
5. CEN TC 51, Document CEN TC 51/WG12/TG4: 04/99, Test Methods for the Freeze-Thaw Resistance of Concrete – Tests with Water or with Sodium Chloride Solution, Part 1: Scaling.
6. DIN 1045, Beton und Stahlbeton – Bemessung und Ausführung, Issue July 1988.
7. LANG, E, Die Carbonatisierung der Betonrandzone – Porenstruktur und Frost-Tausalzwiderstand. Report der Fachtagung Quecksilberdruckporosimetrie an Baustoffen. Bundesanstalt für Materialprüfung und –forschung, Berlin 30, März 2000.
8. GEISELER, J, LANG, E, Long-term durability of non-air-entrained concrete structures exposed to marine environments and freezing and thawing cycles, Third CANMET/ACI International Conference on Durability of Concrete, Nice, France 1994, Supplementary Papers, pp 715-737.

ACCELERATED CHLORIDE PENETRATION TEST RESULTS FOR DIFFERENT CONCRETE COMPOSITIONS

A S Poupeleer

D Van Gemert

Katholieke Universiteit Leuven

Belgium

ABSTRACT. Chloride contamination in real structures is a long-term process. It takes a long time to initiate the degradation process in most cases. However, once the propagation is started the degradation can go really fast. To make the investigation of the subject possible in the laboratory, an accelerated test method is used to analyse the corrosion problems. An accelerated chloride penetration test based on an electrochemical principle is executed on cylindrical samples. Voltages of 3 or 5 Volt are applied over the specimens and the electrolyte. Besides, the different voltages, used to accelerate the movement of the chlorides, and the effect of chlorides mixed into the concrete is examined. Next to all these parameters different concrete mixes are employed. In particular the influence of the test conditions is evaluated. The property to make statements about all the circumstances and the used samples is the CPT (chloride penetration time). Also the evolution of the current, measured continuously during the tests, is discussed.

Keywords: Accelerated Chloride Penetration Time test (CPT), hydrophobic agent, diffusion, Polymer Cement Concrete (PCC).

A-S Poupeleer is research assistant at the Department of Civil Engineering of Katholieke Universiteit Leuven

D Van Gemert is Professor at the Department of Civil Engineering of Katholieke Universiteit Leuven

INTRODUCTION

Chloride ions that penetrate through the concrete cover towards the reinforcement can initiate corrosion by breaking down the passivating patina layer. However, because this process takes quiet some time it is difficult to investigate the problem in laboratory or on site. Therefor, several accelerated tests are proposed in literature [1, 2, 3]. Most of them simulate an accelerated diffusion process only. Although calibration of accelerated tests to real time remains problematic, such tests are frequently used for comparison of concrete protection systems. This paper deals with a forced chloride ion penetration test [4]. Not only the transport process of the chlorides will be studied, but also the corrosion initiation on a steel bar in the concrete. The usefulness of this accelerated test concerning the evaluation of different concrete mixes will be discussed. Within the framework of this particular investigation several test programmes have been carried out. The first investigation part (Series A) deals with the effect of hydrophobic agent [5] on the diffusion of chlorides and the influence of the curing circumstances on it. Series B deals with additional tests on hydrophobic treated samples and the influence of chlorides mixed into the concrete. Also the effect of gluing the reinforcement bar afterwards in the centre of the concrete test cylinder by using some cement pasta has been investigated. This procedure is always used for testing concrete taken from the site.

MATERIALS AND METHODS

Materials

Table 1 Concrete mixes for test series

COMPONENTS	SERIES A		SERIES B		
	1	2	3	4	5
Portland cement P40 [kg/m^3]	350	350	400	400	400
Water/cement-ratio [-]	0.5	0.7	0.5	0.5	0.5
Gravel 4/14 [kg/m^3]	1189	1156	/	/	/
Aggregates 2/7 and 7/10 [kg/m^3]	/	/	1175	1175	1175
Sand 0/2 [kg/m^3]	650	631	587	587	587
NaCl [kg] (Cl^- % per weight of cement pasta)				2.64 (0.4)	5.28 (0.8)

This table shows that in each series there are some deviations on the basic composition. This makes it possible to control the effect of different parameters on the diffusion process and the corrosion initiation. In series A different w/c-ratios are used to investigate a structure with higher water content. The composition used in the second series deviates from the others through a different cement content and a different type of aggregates. The concrete mixes used are numbers 3, 4 and 5. In mix number 3 no chlorides are added to the concrete. In the other two respectively 0.4 and 0.8 % Cl^- per weight of cement are added to the mix.

Test Sample

The specimens (type 1) used for the forced diffusion test are cylinders of 50 mm diameter and 150 mm length. They contain a smooth reinforcement bar of 8 mm diameter in the centre. In the second part of the investigation there are also some samples (type 2) where the reinforcement bar is placed afterwards in a drilled hole in the concrete. This procedure is always used for testing concrete taken from the site.

Test Set-up

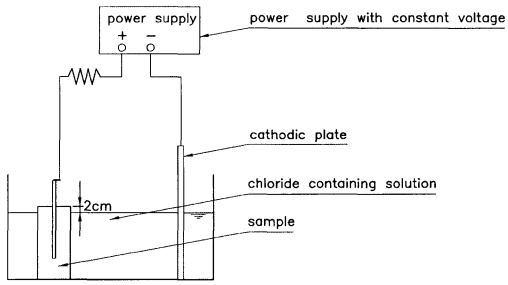

Figure 1 Scheme of the test set-up

The effectiveness of the protection against chloride penetration is measured electrochemically. Before testing the samples are saturated with tap water. Subsequently, they are immersed in a chloride containing solution (3% NaCl), in such a way that there are at least two centimetres between the surface of the solution and the top of the specimen. Further an electric circuit is imposed on these samples. A constant voltage drop of 3 or 5 V is put over the cylinders and the electrolyte solution. The electric current in the circuit is measured. An overview of the test set-up is shown in figure 1. All the tests are executed in the climatised room with constant ambient temperature of 20°C and a relative humidity of 65%.

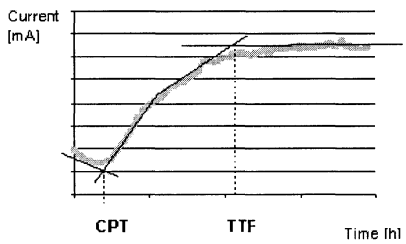

Figure 2 Graphical determination of the CPT

The registered current normally has a typical form (Fig. 2). Because the electrical current is mainly carried by the chlorides, the measured electrical current will be very small as long as the chlorides are not penetrated up to the reinforcement bars. During the first period the current is very small and decreasing. This decline can be explained by the polarisation of the

anode. At a certain moment a strong current increase is noticeable. This is assumed to be the time on which the chloride ions reach the patina and destroy it. This moment is also called the chloride penetration time or CPT. From that moment on there is a strong current increase due to the attack of the steel bar by the chlorides. The reason is a diminishing of the resistance of the electrolyte through the concrete for ion transport. Consequently, more chloride ions get access to the steel. The first cracks become visible. Finally, the reinforcement will corrode and this leads to a rise of the diffusion resistance. A maximum height for the current will be reached. At that moment the 'time to failure' or TTF is achieved. In most cases a vertical crack appears in the surface of the concrete. The corrosion products are pressed out of this fissure and it starts to silt up. So, the current starts to decline again.

RESULTS

Although the current versus time graphics contain a lot information, only the CPT will be used to compare the results (table 2, 3), for the time being. In the future it can be interesting to look also at the current level and the slopes of the current to make valuable conclusions.

Series A [5, 6]

The first series deals with the efficiency of the hydrophobic agents. These hydrophobic agents are applied on dry samples after they reached a constant weight by drying at 105°C. The CPTs for different treatments like drying, immersing and saturating are mentioned in table 2.

Series B [7]

Two different hydrophobic agents are compared in this section. Dynasylan BHN (Huls; H) and Tegosivin HL 100 (Goldschmidt; G). Dynasylan contains silanes. It is an isobutyl-tri-ethoxy-silane. Tegosivin is an oligomer alkylalkoxysiloxane. The difference between the two agents is the difference in penetration depth. The penetration depth of Dynasylan is much higher than that of Tegosiven. The reason is the size of the building stones of the molecules. The first is built out of monomer (small molecules), the second one is slightly polymerizated and forms bigger chains.

Besides hydrophobic addition, each sample is made in two ways. Or the reinforcement is already present in the concrete while casting (first placed; FP) or the bars are added afterwards in a suitable hole drilled in the concrete slabs (placed afterwards; PA). The influence of both conditions is examined.

DISCUSSION

Series A

Dried samples (applied voltage of 3V)

Two different graphs can be distinguished during the forced diffusion test. The non-hydrophobic dried samples show a high current peak a few hours after the test is started. Afterwards the current decreases exponentially. The peak corresponds to the rapid chloride ingress, mainly caused by capillary suction. Visual observation confirms the fact that after 48 hours the samples are completely deteriorated.

Table 2 Chloride ion penetration time (CPT) for the different tested samples of series A

CODE	VOLTAGE	W/C-factor	CPT [hours]	MEAN CPT [hours]	σ [hours]
ref; dry;	3V	0,5	12, 12, 12, 15	12.75	1.5
ref; im;	5V	0,5	60, 80	70	14.1
ref; sat;	3V	0,5	230, 230, 245	235	8.6
hyd; dry;	3V	0,5	> 800	/	/
hyd; im;	5V	0,5	> 140	/	/
hyd; sat;	3V	0,5	105, 110, 135, 160	127.5	25.3
ref; dry;	3V	0,7	6, 6, 6, 8	6.5	1
ref; im;	5V	0,7	35, 35	35	0
ref; sat;	3V	0,7	100, 130, 130, 115	118.75	14.4
hyd; dry;	3V	0,7	> 800	/	/
hyd; im;	5V	0,7	> 140, 65	/	/
hyd; sat;	3V	0,7	80, 115, 140, 155	122.5	32.8

ref: non treated concrete; dry: dried at 105°C; sat: saturated under vacuum conditions; hyd: concrete treated with hydrophobic agent; im: immersed in water for 7 days

Table 3a CPT for the different tested samples of series B with no chloride in the concrete

CODE		VOLTAGE	W/C	SALT SOLUTION	CPT [hours]	MEAN CPT [hours]	σ [hours]
ref; dry	FP	3V	0.5	3% NaCl	couple of hours	/	/
ref; dry	*PA*	*3V*	*0.5*	*3% NaCl*	*couple of hours*	/	/
ref; im	FP	3V	0.5	3% NaCl	234,200,183,146, 252	203	42
ref; im	*PA*	*3V*	*0.5*	*3% NaCl*	*215,143,162,184*	*176*	*31*
ref; sat	FP	3V	0.5	3% NaCl	110,120,194,215, 109	150	51
ref; sat	*PA*	*3V*	*0.5*	*3% NaCl*	*130,98,151,110, 142*	*126*	*22*
H; dry	FP	3V	0.5	3% NaCl	>2600,>2600,> 2600,>2600	>2600	/
H; sat	*PF*	*3V*	*0.5*	*3% NaCl*	*161,194,214,180, 203*	*190*	*21*
G; dry	FP	3V	0.5	3% NaCl	1089,1133,998, 1068	1072	61
G; dry	*PA*	*3V*	*0.5*	*3% NaCl*	*1417,1417,1417*	*1417*	*0*
G; sat	FP	3V	0.5	3% NaCl	117,110,108,144	120	16
G;sat	*PA*	*3V*	*0.5*	*3% NaCl*	*148,90,107*	*115*	*30*

Table 3b CPT for the different tested samples of series B with chloride mixed in the concrete

CODE		VOLTAGE	W/ C	SALT SOLUTION	CPT [hours]	MEAN CPT [hours]	σ [hours]
ref; dry	FP	3V	0.5	0.4 % Cl^-	16,12,13	14	2
ref; dry	FP	3V	0.5	0.8 % Cl^-	10,11,7	9	2
ref; im	FP	3V	0.5	0.4 % Cl^-	<1,<1,<1	<1	/
ref; im	FP	3V	0.5	0.8 % Cl^-	<1,<1,<1	<1	/
ref; sat	FP	3V	0.5	0.4 % Cl^-	15,10,13	13	3
ref; sat	FP	3V	0.5	0.8 % Cl^-	<1,<1,<1	<1	/
H; dry	FP	3V	0.5	0.4 % Cl^-	>688,>688,>688	>688	/
H; dry	FP	3V	0.5	0.8 % Cl^-	>688,>688,>688	>688	/
H; im	FP	3V	0.5	0.4 % Cl^-	>688,>688,>688	>688	/
H; im	FP	3V	0.5	0.8 % Cl^-	>688,>688,>688	>688	/
H; sat	FP	3V	0.5	0.4 % Cl^-	<1,37,11	16	19
H; sat	FP	3V	0.5	0.8 % Cl^-	<1,<1,<1	<1	/

The curves of the dry treated samples also differ from the typical current versus time graphic (Fig. 2). Only after a considerable period of time the current is visible and increases very slowly. In this case the test specimens do not seem to deteriorate. The hydrophobic product seems to offer a good resistant to the penetration of chloride ions, even under external potential difference.

Saturated samples (applied voltage of 3V)

The good working of the hydrophobic product on the dried samples seems to be destroyed by the saturation. The product does not longer seal the pores and diffusion is still possible in the pore solution. In the current versus time curves of these samples the typical shape (Fig. 2) can be recognised.

Immersed samples (applied voltage of 5V)

From the samples, which are immersed in tap water during 7 days, those who were not treated with hydrophobic agent show a similar behaviour as the samples cured in saturated conditions. The only difference is the higher current in the case of immersing, which is caused by the higher applied voltage of 5 V. Besides, it can also be remarked that the CPT in this particular case is higher in the concrete with a w/c of 0.5 than in the concrete with w/c of 0.7. Using the hydrophobic agent before immersing results in a clearly different behaviour. The current only starts after some hours and is rather low. After 140 hours exposure none of the samples with w/c of 0.5 showed sudden current increase or damage. Also with a w/c of 0.7 one of the samples stayed intact for more than 140 hours. The other one showed an increase of the current, but later than the CPT of the same concrete not treated with hydrophobic agent.

Series B

External chloride ingress

The CPT of the dried reference samples of mix number 3 are obviously smaller than those of the immersed and saturated ones. Instead of ion diffusion, which takes a certain time, the chloride ions penetrate almost immediately by means of capillary suction into the dried samples. Although the ion diffusion in the other cases is accelerated by the electrical field, it still is a lot slower than the capillary suction. Further, the CPT of the saturated specimens is a lot lower than that of the immersed ones. Like it is known the immersed ones contain still a lot of air in the pores. This forms an extra barrier against chloride diffusion. On the other hand the vacuum saturated cylinders have an air content of approximation zero. This is also the reason why the saturated samples have a higher start current: the electrical resistance is lower. Due to this the electrical resistance of the saturated samples is lower and consequently the start current is higher.

When a hydrophobic agent is used, the relationship between the dried and the other samples is right the opposite. The dried samples can profit from the water-repellent characteristic of the hydrophobic agent. It acts as a buffer between the water and the air in the pores.

In the case of vacuum saturation, all the air is removed out of the pores. Consequently, the waterproof capacity of the hydrophobic agent disappears and the pores can be filled with water. The remaining hydrophobic working is probably not strong enough for the difference in pressure. However, the reinforcement in the dried specimens finally does corrode due to the fact that the hydrophobic agents do not prevent water vapour diffusion. So, capillary condensation can not be stopped. In this way the chloride ions will reach the reinforcement after all, even in the dried samples, although it can take a while. The currents versus time graphics show that the current stays zero as long as there is no continue channel of water between the surface and the reinforcement. As long as this is the case, there is air on the way and this forms an isolator on the electrical path.

The CPT of the immersed samples is longer than that of the saturated ones because of the extra resistance formed by the included air. Moreover, the same phenomena arise as in the case of the dried samples. The current only occurs when there is a water channel between the surface and the reinforcement.

The hydrophobic agent does not seem to work after saturation. It has only an effect if the samples are dried or immersed. Besides, the quality of the protection depends on the type of hydrophobic agent. The reason is probably the difference in penetration depth. After a while the pores in the untreated zone will be filled by capillary condensation. The hydrophobic zone will act as an inflatable cushion surrounded by two fluids. Consequently, it is understandable that the protection increases with the thickness of the cushion. The hydrophobic treatment makes that the moisture transport changes from capillary suction into water vapour diffusion.

Generally, the CPT of the saturated samples, where the bars are placed afterwards (PA = placed afterwards), are a bit shorter than the CPT of the samples, where the reinforcement is placed before the concrete is cast (FP = first placed). The transport mechanism in this case is ion diffusion, which is stimulated by a greater permeability. First of all there is the presence of the transition zone between the concrete and the cement pasta and

secondly the water/cement-ratio of the cement pasta is higher. Nevertheless, the standard deviations are so big, that no significant distinguish can be made between the two types of samples. No conclusions can be made. Still, it can be claimed that the presence of the cement pasta accelerates the suction and the chloride diffusion in saturated samples.

For the other samples (dry, immersed) it is more difficult to say. The results are not so unambiguous. Theoretically the mortar forms an extra barrier. There are two different zones where the chlorides have to pass trough. In a first phase the water vapour will condense in the concrete area. In a second phase the chlorides start to penetrate through the concrete and a secondary diffusion process starts towards the reinforcement. From the moment that the chlorides find a continuous water line to the reinforcement the diffusion will propagate.

Internal chloride presence

Difference has to be made between the dried and the saturated or immersed reference samples. For the dried samples the CPT will be determined by the capillary suction of water. In the other two cases the water is already present and time is only needed to augment the concentration of chlorides on the spot of the reinforcement until the critical concentration is reached.

As far as the hydrophobic samples are concerned the same observations can be made as for the first stadium with external chlorides.

The current of the tests with the samples prepared with 0.8 % (chlorides per weight of cement pasta) are always higher than those with 0.4 % and the CPT are smaller. The explanation is ambient. The higher chloride concentration causes an higher conduction and the maximum current can never be higher by using a lower salt concentration, because the total amount of free chlorides will be lower and consequently the reserve will be exhausted earlier.

CONCLUSIONS

The treatment with a hydrophobic agent is very effective, as long as the concrete is not water saturated. For example, constructions above the seawater level, along the shore and also in the tidal zone are suitable places to treat with hydrophobic products.

It is demonstrated that the difference in penetration depth of the hydrophobic agent results in a different behaviour towards chloride penetration. Further, it can be mentioned that the way of fixing the reinforcement in the concrete affects the transport mechanisms of the ions. A cement mortar in the centre can accelerate the transport by saturated conditions and it can slow down the transport in not saturated conditions.
The logically expected differences by mixing 0.4 or 0.8 % Cl^- in the concrete are also confirmed. A higher concentration leads to a higher current and a faster deterioration.

Advantages of the Forced Diffusion Test

It is obvious that the forced chloride test offers a good instrument to analyse the chloride diffusion in different materials. Some of the advantages are mentioned below:

1. The CPT test offers a criterion to determine the effectiveness of different concrete mixes.

2. The test gives reproducible values for the CPT in contrast with some of the free diffusion tests [8], where a salt solution is put on top of the samples and gravity diffusion is measured.

   The CPT test is also very sensitive to the circumstances of the test, which makes it very interesting to investigate the effect of the different exposition situations of the concrete.

3. The continuous measurement of the current makes it also possible to follow the changes during the chloride penetration process. This is a big advantage for such a long during tests.

4. The time for the performance of the test is not too long.

5. The necessary number of samples is limited.

Disadvantages of the Forced Diffusion Test

1. Further investigations are needed to establish the relationship between the free diffusion test and the forced diffusion test.

2. The forced diffusion test is purely a laboratory situation. It would be extremely interesting to have a reliable relation between the testing time and the real time situation

3. More tests should be done by using different voltages to know more on the reliability of these electric forces. Also a relation between different voltages would be useful.

4. A more accurate analysis of the different aspects of the transport mechanisms along the distinct stages of the curve is necessary.

5. Because of the immersed test conditions only the transport of ions and the corrosion initiation is measured. The CPT test is not intended to follow up real corrosion processes.

REFERENCES

1. J.-Z. ZHANG, N. BUENFELD, "Development of the Accelerated Chlorine Migration Test as a Measure of Chloride Diffusivity in Concrete", Corrosion and corrosion protection of steel in concrete, Vol. 1, 1994, pp. 395-403.

2. M. BASHEER, A.A. SHA'AT, A.E. LONG, F.R. MONTGOMERY, "Reliability of the Accelerated Chloride Migration Test as a Measure of Chloride Diffusivity in Concrete", Corrosion and corrosion protection of steel in concrete, Vol. 1, 1994, pp. 446-460.

3. C. ANDRADE, C. ALONSO, M. ACHA, "Chloride Diffusion Coefficient of Fly Ash Containing Concrete Calculated from Migration Tests", Corrosion and corrosion protection of steel in concrete, Vol. 2, 1994, pp. 783-793.

4. P.C. LIU, Y.-Y. SHEN, R. SRI RAVINDRARAJAH, "Influence of Binder Materials Type on Corrosion Protection for Steel Reinforcement", Corrosion and corrosion protection of steel in concrete, Vol. 2, 1994, pp. 817-824.

5. REPORT HÜLS AG, "Chloride ion diffusion tests on concrete samples treated with Dynasylan BHN", 1992.

6. D. VAN GEMERT, "Betonbescherming tegen chlorideindringing", Bouwkroniek Beton, November 1992.

7. FREDERIC BERTREM, "Contamination of concrete in maritime environment", thesis KULeuven, 1993.

8. D. VAN GEMERT, J. HORCKMANS, "Measurement of chloride ion diffusion in PCC", Moskow, 1992.

LONG TERM DURABILITY OF CONCRETE MADE WITH DIFFERENT WATER REDUCING CHEMICAL ADMIXTURES UNDER MARINE ENVIRONMENT

T U Mohammed **T Fukute**

T Yamaji

Port and Airport Research Institute

H Hamada

Ministry of Land, Infrastructure and Transport

Japan

ABSTRACT. A detailed investigation on concrete specimens made with different water-reducing chemical admixtures was carried out. Chemical admixtures include air-entraining admixture (vinsol), water-reducing admixture (lignosulfonate group) and high-range water-reducing and air-entraining admixture (naphthalene, melamine, polycarboxyl and amino-sulfonate group). Cylindrical plain and reinforced concrete specimens were tested after 10-year of exposure in the tidal environment. The test items include compressive strength, Young's modulus, carbonation depths, chloride ingress, pore size distribution of concrete, and electrochemical and physical evaluations of corrosion of steel bars in concrete. Moreover steel-concrete interfaces were examined by Scanning Electron Microscope (SEM). Naphthalene group of high-range water-reducing and air-entraining chemical admixture shows the best performance with respect to the strength development and chloride ingress in concrete. Formation of a good steel-matrix interface prevents the initiation of corrosion even for chloride concentration more than 2% of cement mass.

Keywords: Chemical admixture, Chloride ingress, Corrosion, Durability, Tidal environment.

Mr T U Mohammed, is a Research Engineer at the Materials Division, Port and Airport Research Institute, Independent Administrative Institution, Japan. His research interests include corrosion of steel bars in concrete, and durability of reinforced concrete structures in the marine environment.

Mr H Hamada, is the Chief Research Engineer at the Materials Division, Port and Airport Research Institute, Independent Administrative Institution, Japan. His research interests include durability of concrete materials and corrosion of steel bars in civil structures.

Mr T Yamaji, is a Research Engineer at the Materials Division, Port and Airport Research Institute, Independent Administrative Institution, Japan. His research interests include repair and maintenance of marine concrete structures.

Mr T Fukute, is the Director of Administrative Co-ordination Department, National Institute for Land and Infrastructure Management, Ministry of Land, Infrastructure and Transport, Japan. His research interest includes durability of concrete structures.

INTRODUCTION

Water-reducing chemical admixtures are used to produce concrete of higher strength, obtain a specified strength at lower W/C, or increase the slump of a given mix without an increase in water content. Numerous numbers of study on the properties of fresh concrete mixed with chemical admixtures or concrete properties mixed with chemical admixtures at the early age of exposure were carried out [1]. There were also several international conferences held on the chemical admixtures in the last couple of decades. The detail studies on the long-term performance of concrete mixed with different chemical admixtures are very scarce in the literature [2]. Therefore, studies on the long-term performance of these admixtures will be very useful against the challenges of making long-term durable concrete in the beginning of the 21st century. With this background, a comparative study on the long-term performance of concrete made with commonly used chemical admixtures was carried out under tidal environment. The results are summarized here and will be very useful to the concrete professionals. Moreover, from this study, the importance of improving the steel-concrete interface to make long-term durable concrete structures in the marine environment can be realized.

EXPERIMENTAL METHODS: MATERIALS, MIXTURE PROPORTIONS AND ITEMS OF INVESTIGATION

Materials

Portland cement (PC, ASTM Type I) and blended cements by replacing a portion of the cement with slag were used. Two kinds of slag (Slag 1 (Blaine fineness 8000 cm^2/g) and Slag 2 (Blaine fineness 4000 cm^2/g)) were used. The physical properties and chemical analysis of the cement and slags are shown in Table 1.

Table 1 Physical and chemical compositions of cement and slags

	PC	SLAG 1	SLAG 2
Specific Gravity	3.16	2.90	2.90
Blaine Fineness, cm^2/g	3190	7900	4080
Ignition Loss, %	0.7	-	-
SiO_2, %	21.3	32.7	33.2
Al_2O_3, %	5.3	13.8	14.1
CaO, %	64.4	42.4	42.3
MgO, %	2.2	5.9	5.9
SO_3, %	1.9	2.0	2.0
Na_2O, %	0.28	-	-
K_2O, %	0.6	-	-
TiO_2, %	0.37	-	-
MnO, %	0.1	-	-
Fe_2O_3, %	2.6	0.2	0.2

- Indicate not measured items

Chemical admixtures used in this study include air-entraining (AEA) (vinsol), water-reducing (WRA) (lignosulfonate group) and high-range water-reducing and air-entraining (HRWRAEA) (naphthalene, melamine, polycarboxyl and amino-sulfonate group) admixtures. Crushed river gravel and sand were used as coarse and fine aggregates, respectively. Japanese Industrial Standard steel bars (JIS SR 24) were used. The mill-scale over the steel bar was removed by chemical method before embedded in concrete.

Table 2 Mixture proportions of concrete

CASE	CEMENT TYPE	SLAG CON. (%)	TYPES OF CH. AD.	W/C %	s/a %	UNIT CONTENT (kg/m^3)				WRA or HRWRAEA	AEA % of C
						C	W	S	G		
1	PC	-	Vinsol	51.5	46	330	170	831	977	-	0.025
2			LS Gr.	50.0			165	836	985	250ml /100 kg C	0.002
3			N Gr.	47.0			155	847	1001	1.5% of C	0.0015
4	Slag 1	55	Vinsol	55.5	44.8	330	183	786	972	-	0.06
5			LS Gr.	52.7	44.8		174	797	985	250ml /100 kg C	0.006
6			N Gr.	47.0	45.3		155	828	1001	1.5% of C	0.006
7	Slag 2	55	Vinsol	52.7	45.6	330	174	810	972	-	0.04
8			LS Gr.	50.0	45.5		165	821	985	250ml /100 kg C	0.003
9			N Gr.	47.0	45.5		155	831	1001	1.5% of C	0.005
10	Slag 1	40	N Gr.	47.0	45.5	330	155	834	1001	1.5% of C	0.005
11		70	N Gr.	47.0	45.4			828			0.0095
12	Slag 1	55	N Gr.	40.0	44.0	388	155	784	1001	1.5% of C	0.008
13			N Gr.	50.0	46.0	310		849			0.006
14	Slag 1	55	PC Gr.	47	45.5	330	155	831	1001	1.1% of C	0.006
15			M Gr.							1.3% of C	0.015
16			AS Gr.							1.5% of C	0.003

W-Water, C-Cement, S-Sand, G-Gravel, s/a - Sand-Aggregate Ratio.
AEA – Air-Entraining Admixture, WRA-Water-Reducing Admixture
HRWRAEA- High-Range Water-Reducing and Air-Entraining Admixture
LS – Lignosulfonate, N – Naphthalene, PC-Polycarboxyl, M-Melamine and AS-Amino-sulfonate
For all mixtures, Slump = 12±1 cm, Air Content = 4±1%.

Mixture Proportions

Mixture proportions of concrete are summarized in Table 2. A total of sixteen cases were investigated. Cements and chemical admixtures used in this study were explained in the "Materials" sub-section before. Comparison of the chemical admixtures (lignosulfonate, naphthalene, melamine and polycarboxyl) can be obtained from Case 6 and Case 14~16.

In addition, comparison of the cement types (PC, Slag 1, Slag 2) can be obtained from Case 1~9, fineness of the slag (Blaine fineness 8000 and 4000 cm^2/g) from Case 4~9, replacement amount of cement by slag (55, 40 and 70%) from Case 6, 10 and 11, and comparison of the water to cement ratio (0.47, 0.4 and 0.5) from Case 6, 12 and 13. Standard dosages of the chemical admixtures were used. The slump of the fresh concrete was fixed at 12±1 cm and air content was at 4±1 %. These were kept same for all mixtures to maintain the same workability.

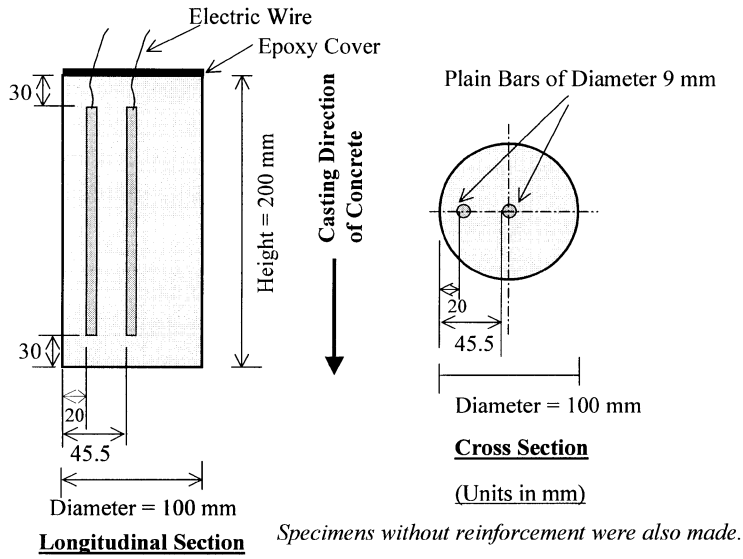

Figure 1 Detail of the specimen

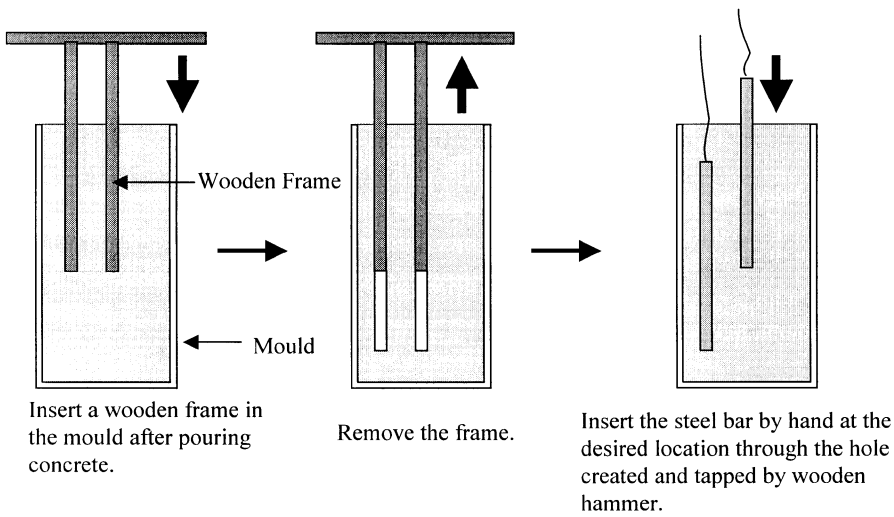

Figure 2 Method of casting concrete

Specimens

Plain and reinforced cylinder specimens of diameter 100 mm and length 200 mm were investigated as shown in Figure 1. Two round steel bars of diameter 9 mm and length 140 mm were embedded at cover depths of 20 and 45.5 mm. The method of casting concrete specimens with steel bars is shown in Figure 2. First a wooden frame was inserted after pouring concrete in the mould. Then it was removed after sometime (about an hour) and the steel bars were inserted manually through the hole. Concrete was compacted with repeated wooden hammer blows on the mould. This special casting technique was adopted to neglect the influence of spacers provided at the bottom of the mould. After 28 days of standard curing, three plain concrete specimens were tested for compressive strength and Young's modulus of concrete. Remaining specimens were exposed in a tidal pool located beside the sea at latitude of about 35° N and longitude of about 138° E. Natural seawater was automatically pumped into and drained out at six-hour interval. Based on the location of the specimens in the tidal pool, the specimens were subjected to a 4-hour wetting and 8-hour air-drying cycle. The specimens were free from freezing and thawing effect.

Items of Investigation

After 10-year of continuous exposure, the specimens were transferred from the exposure site to the laboratory and cleaned. Plain concrete specimens were tested for compressive strength and Young's modulus as per JIS A1108.

Carbonation depth of the specimens was evaluated after spraying 1% phenolphthalein solution on freshly broken or cut surfaces. To measure chloride concentration, a 50 mm disc was cut from the mid-height of the plain concrete specimens. It was cut again in order to take samples at the depths of 0-5, 5-15, 15-25, 25-40 and 40-50 mm. The samples were powdered and water soluble chloride concentrations were measured as per JCI SC4.

The polarization resistance of the steel bars and concrete resistance were measured by AC impedence method. For this, the low frequency was set at 10 mHz and high frequency at 20 Hz. The measurements were carried out keeping the specimen submerged in natural seawater. Utilizing polarization resistance data, micro-cell current density of the steel bars was evaluated from the Stern-Geary Equation given below [3]:

$$I_{mic} = \frac{B}{R_p} \times 10^6$$

$$B = \frac{\beta_a \beta_c}{2.3(\beta_a + \beta_c)}$$

Where, I_{mic} is the micro-cell current density in $\mu A / cm^2$, the value of the B depends on the slopes of the anodic (β_a) and cathodic (β_c) polarization curves. Assuming, β_a and β_c as 120 mV/decade as the average of all corrosion system, the value of B can be estimated at 0.026 V [3]. R_p is the polarization resistance in $\Omega.cm^2$.

Porosity of the mortar samples was measured at a depth of 15-25 mm. For this, mortar pieces (approximate sizes 5 mm) were collected from the required depth and dried. Then pore size distribution of the samples was evaluated by mercury intrusion porosimeter.

The specimens were split opened and the fractured surface normal to the steel bars was checked with SEM. After spilt opened scattered visible voids were found surrounding the steel bars. Also, at the void region deposit of the hydration product over the steel bars was found. The deposit was also checked with SEM. In addition, void surface was also checked with SEM. All samples were carbon coated before SEM observations. In addition to these, XRD analysis of the mortar samples was also carried but detail data are not presented here.

Table 3 Compressive strength and Young's modulus of concrete

CASE	COMPRESSIVE STRENGTH (MPa)		STRENGTH RATIO (10-Year/28-Day)	YOUNG'S MODULUS (MPa)		MODULUS RATIO (10-year /28-day)
	28-Day	10-Year		28-Day	10-Year	
1	43.4	44.7	1.03	3.28×10^4	3.8×10^4	1.16
2	45.5	50.0	1.10	3.39×10^4	4.1×10^4	1.21
3	56.1	55.2	0.98	3.49×10^4	4.4×10^4	1.26
4	41.1	44.8	1.09	3.13×10^4	4.0×10^4	1.28
5	49.1	47.5	0.97	3.25×10^4	4.2×10^4	1.29
6	52.5	59.0	1.12	3.45×10^4	4.6×10^4	1.33
7	33.4	56.4	1.69	2.85×10^4	4.1×10^4	1.44
8	39.1	53.7	1.37	2.92×10^4	4.4×10^4	1.51
9	37.4	50.4	1.35	3.07×10^4	4.5×10^4	1.47
10	50.5	48.7	0.97	3.57×10^4	4.1×10^4	1.15
11	45.2	54.5	1.21	3.24×10^4	4.3×10^4	1.33
12	58.7	55.2	0.94	3.44×10^4	4.5×10^4	1.31
13	48.5	43.8	0.90	3.34×10^4	4.4×10^4	1.32
14	51.7	42.3	0.82	3.39×10^4	4.3×10^4	1.27
15	50.0	53.9	1.08	3.53×10^4	4.3×10^4	1.22
16	51.5	54.2	1.05	3.37×10^4	4.2×10^4	1.25

EXPERIMENTAL RESULTS AND DISCUSSION

The results of this study are explained in three different sub-section entitled as "Compressive Strength and Young's Modulus", "Carbonation Depth and Chloride Profile", and "Micro-cell Corrosion and Physical Evaluation of Steel Bar's Corrosion".

Compressive Strength and Young's Modulus

Compressive strengths of concrete at 28-day and after 10-year of exposure in the tidal environment are listed in Table 3. Compressive strength of concrete is increased in most of the cases. The increment is more in the case of course slag cement (Cases 7~9). At the early

age (28 days), the strength development for the naphthalene group of chemical admixture was the highest (Case 6). This tendency is also the same after 10 years of exposure. However, after 10 years of exposure, polycarboxyl group (Case 14) of admixture shows a 20% reduction in strength from its 28-day strength. The Young's modulus of concrete increased irrespective of the cases investigated here. The observation is clearer for the cases made with water reducing admixture, such as naphthalene group of admixture (Case 3 and 6). The Young's modulus as well as the compressive strength of concrete is the highest for concrete mixed with naphthalene group of chemical admixture (Case 6) after 10-year of exposure compared to the others (Cases 14, 15 and 16). It is clear that naphthalene group of chemical admixture shows the best results with respect to early and long-term strength development.

Carbonation Depth and Chloride Profile

The carbonation depth of the specimens was negligible irrespective of the cases investigated here. Chloride concentrations at the average sampling depths of 2.5, 10, 20, 32.5 and 45 mm from the surface of the specimens are shown in Figure 3 for all of the cases. The use of water- reducing admixture (WRA or HRWRAEA) causes to reduce the chloride ingress in concrete (Case 1~3 for OPC, Case 4~9 for blended cements). The influence of slag contents (Cases 6, 10 and 11) is clearer than the fineness of the slag after 10 years of exposure. Higher water to cement ratio also causes more ingress of chloride into concrete (Case 11 and 12). Comparing the different type of HRWRAEA, such as naphthalene (Case 6), polycarboxyl (Case 14), melamine (Case 15), and amino-sulfonate (Case 16) types of chemical admixture, it is found that the use of polycarboxyl group results in relatively more amount of chloride ingress in concrete after 10 years of exposure in the tidal environment. Contrary naphthalene group of chemical admixture shows the least amount of chloride ingress in concrete.

More chlorides are infiltrated at the inner region of the specimens for the cases made with Portland cement (Case 1~3) compared to the blended cements (Cases 4~9). This is expected due to the significant reduction in capillary pore space with the use of blended cements as shown in Figure 4 (Case 1 and 4). For the case with naphthalene group of admixture the capillary pore volume is relatively higher compared to the case with polycarboxyl type of chemical admixture (Case 6 and 14 of Figure 4). The XRD data showed that more ettringite is formed at the same depth for the case with polycarboxyl group of chemical admixture. Also, more chloride is infiltrated in the case of polycarboxyl type of chemical admixture as explained before. Therefore, less pore space for polycarboxyl group of admixture is expected due to the formation of more chloro-compound and ettringite. More investigation on pore size distribution will be carried out in the near future in order to confirm this observation.

Micro-cell Corrosion and Physical Evaluation of Steel Bar's Corrosion

The micro-cell current density of the steel bars embedded at different cover depths are shown in Figure 5. Generally, a current density of less than 0.2 $\mu A/cm^2$ is defined as negligible corrosion current density or the current density at passive condition [4]. Irrespective of the cases investigated here, the current density is less than 0.2 $\mu A/cm^2$. It indicates that the steel bars are in passive condition in concrete even after 10 years of exposure in the tidal environment.

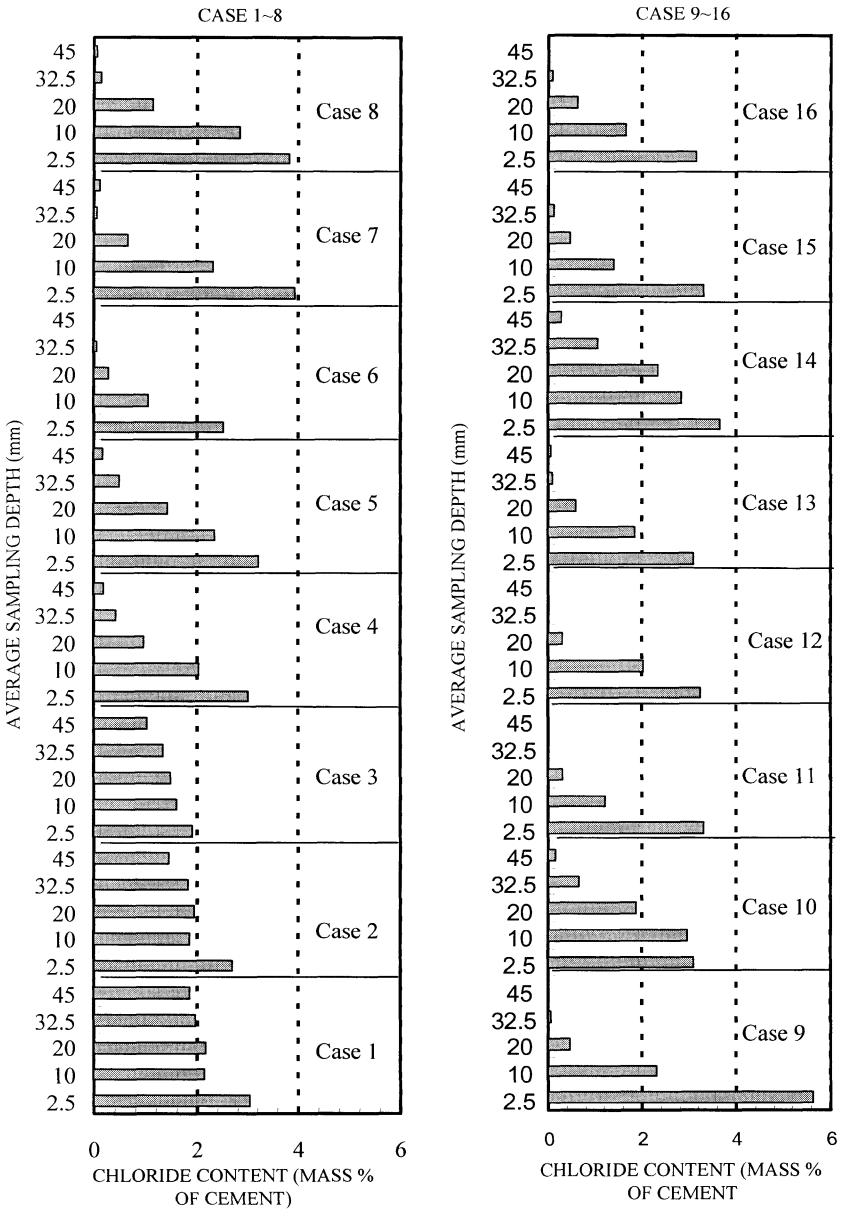

Figure 3 Water soluble chloride contents at different depths

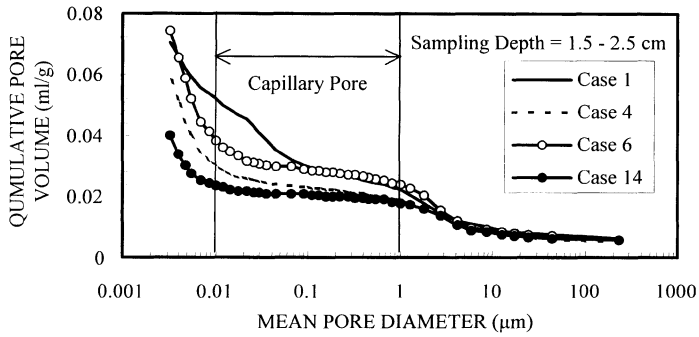

Figure 4 Cumulative pore volume and mean pore diameter

Generally, the chloride threshold level is defined as 0.4 % of cement mass [5]. If it exceeds 2% of cement mass, an active corrosion is defined. The chloride concentrations in concrete were explained before (Figure 3). It was found that the chloride level exceeds the threshold level at 20 mm of cover depth in most of the cases investigated here and for some of the cases even at 45 cm of cover depth. In some cases, it also exceeds 2% of cement mass at cover depth of 20 mm. However, a very low level of corrosion current density is observed irrespective of the cases investigated here. The results indicate the significant improvement of chloride threshold limit. Further discussion on this matter is provided in the next paragraph.

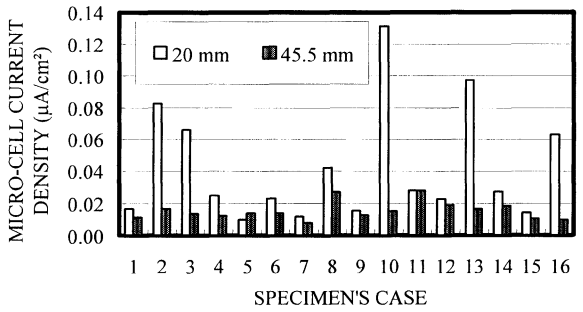

Figure 5 Micro-cell current density

After electrochemical investigation, the specimens were split opened and the steel bars were collected. No corrosion over the steel bars was found. The steel bars were as clear as in the casting time except some deposit of hydration product associated with the voids at the steel-concrete interface. In order to find out the reason of no corrosion over the steel bars for a high chloride content, steel-concrete interfaces, the deposit over the steel bars associated with the voids at the steel-concrete interface and the surface of the voids were checked by SEM. The results are shown in Figure 6. Dense steel-concrete interface is observed (Figure 6a). Deposition of C-S-H is observed over the steel bars associated with the voids at the steel-concrete interface (Figure 6b).

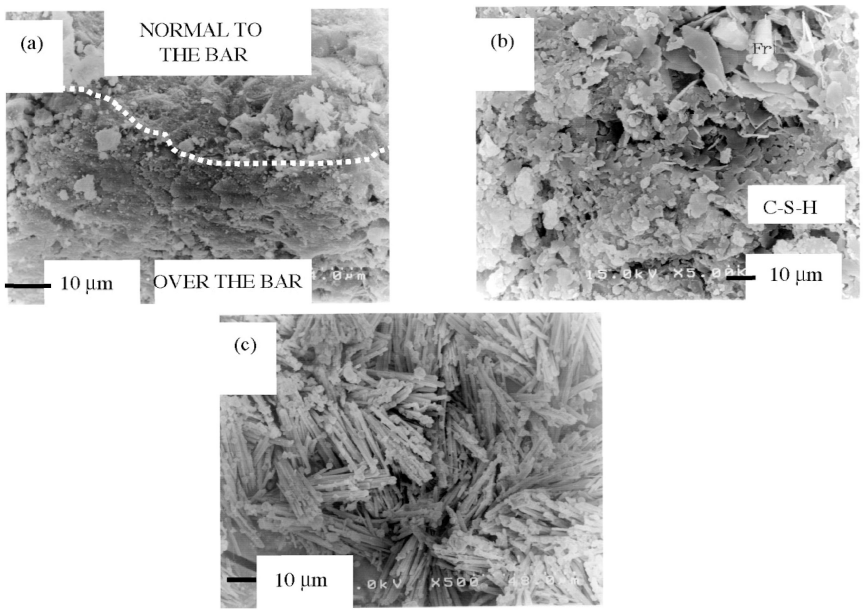

Figure 6 SEM Micrographs (Case 4)
(a) Fractured surface
(b) Deposit over the steel bars associated with the voids at the steel concrete interface
(c) Deposit over the surface of the voids at the steel-concrete interface

The void surface with concrete is densely covered with the ettringite (Figure 6c). The special method of casting concrete (Figure 2) results in the improvement of steel-concrete interface. It causes the improvement of chloride threshold level significantly. The results strongly suggest that the improvement of steel-concrete interface is essential against the challenges of making long-term durable concrete in the marine environment.

CONCLUSIONS

Based on the results of this long-term experimental investigation under tidal environment, the following two main conclusions are drawn:

- Naphthalene group of high-range water-reducing and air-entraining chemical admixture shows the best performance with respect to the strength development and chloride ingress in concrete.

- Formation of a good steel-concrete interface prevents the initiation of corrosion even for chloride concentration more than 2% of cement mass. Steel-concrete interface should be improved to meet the challenges toward making long-term durable concrete structures in the marine environment.

REFERENCES

1. NAGATAKI, S., State of the art report on air-entraining high range water-reducing admixture, Concrete Journal of JCI, Vol 28, No 6, 1990, p5-15.

2. HATTORI, K., Experiences with mighty superplasticizer in Japan, ACI SP 62, 1979, p 37-66.

3. FONTANA, M. G., GREENE, N. D., Corrosion engineering, Second Edition, McGraw-Hill, 1983.

4. ANDRADE, C., ALONSO, C., On-site measurement of corrosion rate of reinforcements, Fifth CANMET/ACI International Conference on Durability of Concrete, Barcelona, Spain 2000, Proceedings of a Special Technical Session on "Near-Surface Testing for Strength and Durability of Concrete", Ed. Basheer, P.A.M., 2000, p 171-183.

5. BROWN, R. D., Mechanism of corrosion of steel in concrete in relation to design, Inspection and Repair of Offshore and Coastal Structures, Performance of Concrete in Marine Environment, ACI SP 65, 1980, p 169-204.

RC CONSTRUCTIONS IN MARINE ENVIRONMENTS

F Kavčič
IGMAT
K Poljanšek
Water Management Institute
Slovenia

ABSTRACT. RC constructions exposed to marine environment exhibit very severe deterioration processes. Besides macroclimate conditions the aggression varies also with microclimate referring to the different position of individual structural element. The established condition of the coastal structures, typical damages of coastal structures and the analysis of chloride profiles on concrete samples taken from different parts of the quay wall structure will be presented. Obtained results were used also to verify and to calibrate mathematical model of diffusion i.e. the 2nd Fick's law of diffusion. The damaged structures are exposed to even faster decay, especially when they are situated in an aggressive marine environment. In this sense, the approach to the execution of repair works with the description of individual phases and the selection of adequate repair materials will be presented. Also, some new coastal structures, which are made in the last five years, will be presented in the paper. Designing of new coastal structures were based on our experience gained from analysis of old coastal structures.

Keywords: High-strength concrete, High-performance concrete, Silica fume, Wharves, Corrosion, Chloride diffusion, Concrete, Cement-polymer mortar

Franci Kavčič, M. Sc., is head concrete technologist at IGMAT (Building Materials Institute in Slovenia). His main research activity is the hydration of cement in concrete. He also works in the field of other concrete properties, like fresh concrete, hardened concrete and repair works on concrete.

Karmen Poljanšek, B. Sc., working as consultant assistant in Maritime Engineering Department of Water Management Institute, Ljubljana, Slovenia.

INTRODUCTION

The investigations were executed on the coastal structures in Port of Koper, only harbor in Slovenia that present the most important infrastructure element in the sea - land connection. The quay wall structures were mostly designed as grid reinforced concrete plates. Most of them are connected with the mainland over two bridges; the other wall structures are part of the land. They are founded on steel piles, which are cathode protected and by concrete pile caps in the tidal and splash zone. By designing of the new coastal structure the similar concept is followed.

Due to a high alkaline environment in the concrete, a passivity film forms on the surface of the steel, which provides good protection against further corrosion. When chloride concentration at the steel level reaches the chloride threshold value this passive layer is destroyed. At this state, the presence of moisture and oxygen around the steel fulfils all the conditions required for the beginning of the active corrosion process (*Figure 1*) and the associated reduction in steel cross section. Tidal and splash zones provide the most ideal circumstances for the corrosion process. This proves to be true also in the analysed construction. When voluminous corrosion products cause cracking, spall and delimitation of the concrete cover the process becomes self-accelerating. The main reason for premature deterioration is inadequate thickness of the construction concrete cover. When the structure was erected, the concrete cover was only 10 to 20 mm thick instead of the designed 40 mm.

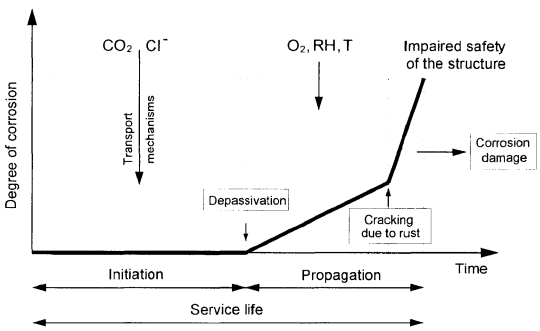

Figure 1 Corrosion model for steel in concrete [1]

The most appropriate method of renovation was determined with regard to the depth of chloride threshold value. This was the main reason to perform this kind of research by drilling a large number of concrete cores.

The results of the research on the 18-year-old quay wall structure provided the opportunity to define the thickness of the concrete cover, which would prevent the beginning of the active corrosion after 18 years. Further on the mathematical model of chloride diffusion, i.e. 2nd Fick's law was verified and calibrated. The model could be used for predicting the service life of the structure if the chloride induced corrosion is the prevailing deterioration mechanism. Such durability design we try to incorporate by construction of the new coastal structures.

MODEL OF CHLORIDE DIFFUSION

The corrosion process of steel is commonly divided into two stages (*Figure 1*):

- **Initial stage**, which includes the transport of aggressive agents to the reinforcement. Its end is defined by depassivity of the reinforcement.
- **Propagation stage,** which includes the active corrosion process where the corrosion products emerge and the safety of the structure is decreased.

Model of the 2nd Fick's law of diffusion in equation (1) enables the prediction of the duration of the initial stage of the corrosion process. The model result is a chloride profile presented as curve of changing chloride concentration C (x,t) with the distance from the surface at a determined duration of environmental aggression.

$$C(x,t) = (C_0 - C_i) \cdot erfc\left(\frac{x}{2\sqrt{D \cdot t}}\right) + C_i \qquad (1)$$

where:

C_0	is the chloride concentration at the concrete surface,
C_i	is the initial chloride concentration in concrete,
t	is the duration of aggressive influences (s),
x	is the distance from the surface (m),
D	is the chloride diffusion coefficient (m^2/s).

The time of the beginning of the corrosion process is the function of environmental aggression (chloride concentration at the concrete surface C_0), concrete quality (chloride diffusion coefficient D) and thickness of the concrete cover. When the concentrations of chlorides in different depths are known, the chloride concentration at the concrete surface and the chloride diffusion coefficient can be calculated. In this way also the quality of the concrete used at the analysed quay wall structure is obtained, and the model can be calibrated to aggressive conditions, which prevail in the Slovenian littoral.

It is assumed that the diffusion is the only form of transport mechanism of chlorides to the reinforcement. The model does not include the other two forms of transport mechanism of chlorides, i.e. capillary absorption and flow under pressure. However, we are aware that they are present only in the surface part of the concrete cover, whereas the diffusion can cause the chlorides to penetrate also further into the level of the reinforcement.

In order to define the end of the initial stage it is necessary to know the chloride threshold value. Numerous codes give the value 0,4% by the weight of cement content in concrete, which is a fairly safe side. The actual value, however, depends on the type of cement, w/c ratio, mineral admixture based on pozzolan, the moisture content in the concrete, etc. Researcher's from Sweden measured the chloride threshold value for different types of concrete's in different exposure zones and they tried to include all these parameters for define the end of the initial stage [2].

RESEARCHES AND RESULTS

The researches were performed at an 18-year-old quay wall structure. The built-in concrete had 350 kg/m^3 OPC with w/c ratio 0,53 and designed concrete strength 30 MPa.

Sixteen cylinder specimens with the diameter of 5 cm were drilled at three different elevations according to the level of seawater (*Figure 2*). In the laboratory the cylinders were cut to a centimeter slices and then in each slice the average total concentrations of chlorides were measured by a photometer. The chloride concentrations are expressed in percentage by the weight of cement content in concrete.

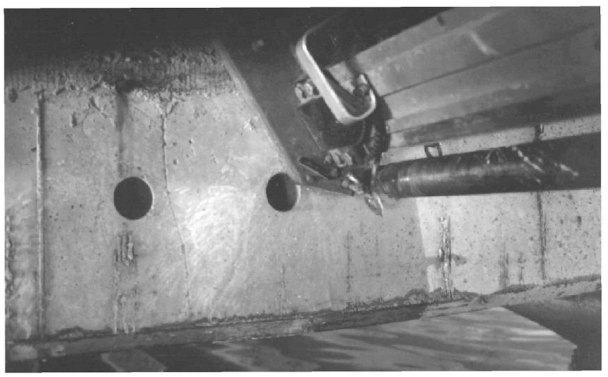

Figure 2 Drilling of cylinder specimens

The intensity of corrosion processes of the reinforcement depends on relative distance of the structural element from the sea surface, the climatic characteristics and composition of the seawater. The Slovenian littoral belongs to temperate climate, for which it is typical to have average summer and winter temperature around 10°C and 20°C, respectively. There is no danger of frost and there is an average of 934 mm rain annually. The sea in the Bay of Koper has the average salinity 36 g/l, 18 to 20 g/l of it are chloride ions and 3 g/l of it are sulphate ions.

The results of measuring the concentrations of chlorides in individual slices of cylinders are presented as chloride profiles. The profiles can be classified into individual exposure zones (*Figure 3*):

- upper tidal zone,
- splash zone,
- marine atmospheric zone.

Figure 3 shows the results together with the best-fit curve of the 2nd Fick's law of diffusion. In the chloride profile from upper tidal zone the Fick's curve and the measurements do not match only in surface part of the concrete cover. Here the capillary absorption and flow under pressure prevail above the diffusion, as this part of the concrete surface is frequently submerged in the time of high water. The maximum concentration of chlorides is found in the depth of 15 mm from the concrete surface and reaches the value of 8,5% by the weight of the cement content. Since the concrete cover was too thin, the reinforcement is in the area of the highest concentrations. The consequence is untimely corrosion of the reinforcement, despite the fact that the concrete is normally saturated in the tidal zone and the diffusion of oxygen is limited.

It is typical for the chloride profile from the splash zone that the influence of capillary absorption and evaporation is even more explicit, since the maximum concentration of chlorides appears even deeper, i.e. at a depth of 25 mm from the concrete surface.

Chloride profile from the atmospheric zone shows that it is a matter of pure diffusion, since the curve of the 2nd Fick's law matches with the measured values along the whole analysed profile.

The exposure zone is very important, since there appear enormous differences in chloride concentrations, even though the specimens are taken within the 0.5 m altitude belt. The diagrams show that the chloride concentrations decrease very quickly by the distance from the concrete surface. At the prescribed depth of the reinforcement 40 or 50 mm (different demands), the values given in Table 1 are measured. As a comparison we can use chloride threshold value as given by the Swedish researchers [2]. It can be established that in the splash and atmospheric zone a 40 mm concrete cover (nominal cover) suffices to prevent the depassivity of the reinforcement in 18 years. In the tidal zone the chloride threshold value is approached by a 50 mm concrete protection cover, however the corrosion risk is lower due to more difficult diffusion of oxygen.

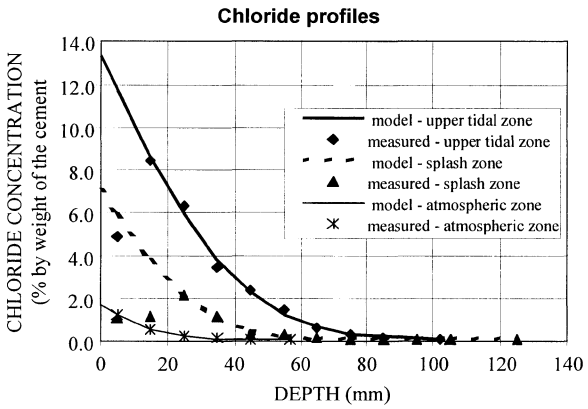

Figure 3 Comparison between chloride profiles from different exposure zones

There appeared also individual micro variations within each exposure zone. *Figure 4* shows two groups of cylinders taken from the same altitudes, but different environmental conditions that the concrete surface is exposed to. At a location sheltered from rain, sun and wind the total chloride ingress was by three times higher as compared to the location that was exposed to rain washout, sun and wind.

The chloride concentration at the concrete surface, which presents the environmental load, is higher:

- if the concrete surface is closer to the water surface (lower altitude),
- if the concrete surface is protected from rain, since there is no washout.

Table 1 Comparison of chloride concentrations with the chloride threshold value [2]

	CHLORIDE CONCENTRATION AT THE DEPTH		CHLORIDE THRESHOLD VALUE (w/c=0,5)
	40 mm	50 mm	
Upper tidal zone	2.97%	1.72%	1.50%
Splash zone	0.12%	0.10%	0.60%
Atmospheric zone	0.11%	0.10%	0.60%

Higher environmental load does not necessarily mean also higher corrosion risk. In the tidal zone where the chloride concentrations are very high, the saturated pores of the concrete prevent the oxygen diffusion to the reinforcement and thus slow down the cathode reaction in the progression stage of the corrosion process.

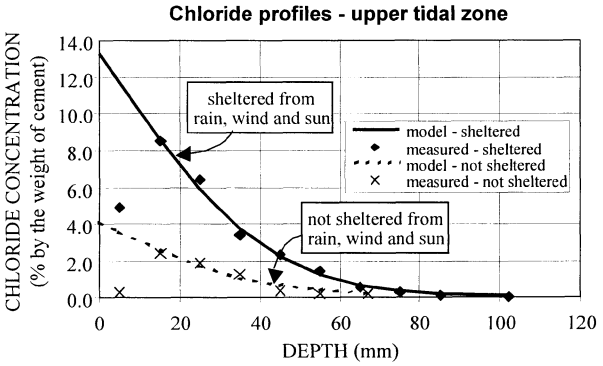

Figure 4 The influence of different external conditions on the chloride profiles of cylinders taken from the same height

REPAIR SYSTEM AND RENOVATION

The repair system consists of one-component polymer-modified Portland cement mortars (PCM), made by TKK Srpenica, Slovenia. The reasons for the choice are:

- Cement base assures better compatibility with damaged concrete surface compared to pure polymer mortars as well as high alkaline reinforcement protection.
- Redispersible polymer and other special admixtures assure good workability properties of fresh mortars and all properties required for the concrete repair mortars, that means to meet strength and durability requirements in the hardened state.
- Mortars are normally one component and they require only mixing with water on site, permanent quality is assured.
- Repair mortar can be applied manually or with the help of machines.
- Economy, mortars have a lower price compared to the pure polymer mortars.

Two mortars are used:

- MCI Antikor, a flexible cementitious polymer modified coating, with MCI (CPP-MCI), was used to protect steel reinforcement against corrosion. It can be also used as a bonding agent between concrete surface and repair mortar.
- Silica MSM is a high quality thixotropic polymer-modified cementitious mortar, which contains polymer and special admixtures for workability and application, synthetic polypropylene fibres, which reduce plastic cracking and shrinkage, and micro silica for reducing permeability and increasing resistance against abrasion and chemical aggression.

High quality cement and carefully selected and graded aggregates are very important, but the main component of the polymer cement system is redispersible polymer powder, which is added in an optimal quantity. This assures that the mortar corresponds to the requirements for concrete repair systems regarding adhesion, bending and compressive strengths, linear deformation, modulus of elasticity, resistance to saponification, carbonation, vapour permeability and freezing and thawing resistance without and in the presence of de-icing salts.

A new generation of corrosion inhibitors are also included, MCI – Migrating Corrosion Inhibitors. MCI molecules allegedly migrate through even the smallest pores and cavities of hardened concrete, condensing on the metal surface either positively charged or negatively charged, creating a protective monomolecular film on the metal. This layer self-adjusts and is self-supplied by condensing other molecules.

According to the established condition of the structure and the possibility of fast expansion of further deterioration of concrete and thus the whole structure (*Figure 1*), the repair was performed, where we could compare the previously shown results with the actual condition in the structure.

The execution of repair was in accordance with the following procedure and depends on the level of damage in an individual element:

1. Removal of the contaminated concrete under the reinforcement up to a depth of 2 to 5 cm.
2. Dry sandblasting of the corroded concrete steel, up to shine PSa $2^1/_2$, and the concrete surface, with additional removal of non-connected particles.
3. Immediate application of anticorrosion protection of the steel MCI Antikor.
4. Additional concreting of individual parts of the structure according to the procedure:
   - ablution under pressure and thus also moistening of the surface,
   - placing of connective layer, MCI Antikor,
   - placing of rough renovation mortar with polypropylene fibres and micro silica (MSM) in one or several layers, machine work - jetting, with smoothing.
5. Execution of protection of concrete surfaces with the help of elastic color coating.

Table 2 Results of laboratory research on the repair materials

TYPE OF MATERIAL	WEIGHT kg/l	VOLUME WEIGHT kg/dm^3	WATER ADDITION l/100 kg	FLOW TEST no shake cm	AIR AVOID %	MORTAR - STRENGTH 28 days		
						Compress MPa	Flexural MPa	Adhere MPa
CPP-MCI	1,10	1,85	35,0	19,5	3,8	37,0	12,0	2,0
MSM	1,46	2,16	12,0	15,5	5,2	62,5	11,9	2,3

Quality control included the following tasks and types of research:

1. Inspection of adequacy of the prepared concrete surface and cleaned concrete steel.
2. Visual inspection of the anticorrosion coating quality.
3. Sampling of individual types of mortar and tests of mechanical properties in the laboratory.
4. Inspection of the quality of repair mortars and the subsequent elastic colour coating.
5. Test of the repaired areas.

The final results of the pull-off tests in-site were as follows:

1. Pull-off of the repair mortar (MSM) averaged 1.7 MPa, with a minimum of the 1.4 MPa. ZTV-SIB 90 specified an average of 1.5 MPa with a minimum of 1.3 MPa.
2. Pull-off of the elastic color coating averaged 1.7 MPa, with a minimum of 1.2 MPa. ZTV-SIB 90 specified an average of 1.3 MPa, with a minimum of 0.8 MPa.

The results show the adequacy of the selected procedures and renovation technology, which should prolong the service life of the concrete structure that was formerly showing significant deterioration.

CONCRETE DESIGN

By analyzing the chloride profiles the conclusion can be drawn that the concrete used in investigated quay wall structure hardly satisfy the durability demands for eighteen years of service. What is more, it would fail in 50 years of service life. If we wish to avoid thicker concrete cover more attention have to be paid to the quality of concrete.

In order to bring the durability design of marine RC structures towards the standards of the bearing capacity design of RC structures the fusion of the experiences gained from the analysis of old structures and the analytical model of 2nd Fick's law of diffusion to predict theoretical chloride profile was applied in the latest project.

The upper tidal zone was taken into consideration as the most aggressive zone regarding chloride induced corrosion of the reinforcement. The estimation was made whether the concrete quality prescribed for XS3 exposure zone in codes [4] meets the requirements for the 50 years service life. Besides, 5% of silica fume was added in the mix to increase the workability of the concrete and decrease the permeability to water.

Calculations using 2nd Fick's law of diffusion, equation (1), have been made based on:

1. $D_0 = 1.4 \times 10^{-12} m^2/s$ [1], a diffusion coefficient, that is being a realistic value for a good portland cement concrete with low w/c ratio. In addition to the measured performance at time t_0, a substantial difference in the time-dependant development of the resistance of the materials was considered. The time-dependency of the achieved chloride diffusion coefficient obeys power function (Maage, Mangat, Takawake, Bjergovič) [6]:

$$D(t) = D_0 \times \left(\frac{t_0}{t}\right)^{\alpha} \tag{2}$$

where α depends on w/c ratio. Poulsen proposed for the ordinary concrete (0.25<w/c<0.6) the following expression [6]:

$$\alpha = \exp\left(-\frac{(w/c)^2}{0.19}\right) + 0.1 \times \exp\left[-\left(\frac{0.1}{w/c}\right)^{2.5}\right] \tag{3}$$

2. *Ccr=1.0% by the weight of the cement content* [2], chloride threshold value is lower, due to negative effect of the silica fume,

3. C_0*=12 % by the weight of the cement content,* chloride concentration at the concrete surface taken from the results of the analysis for the upper tidal zone.

Theoretically chloride threshold value is approached by 30 mm of concrete cover (*Figure 5*). Improper construction practices may result in large variation in the depth of cover actually obtained. Considering altogether the calculated concrete cover has to be increased by 10 mm and finally the 40 mm concrete cover is gained to be adequate for the 50 years service life.

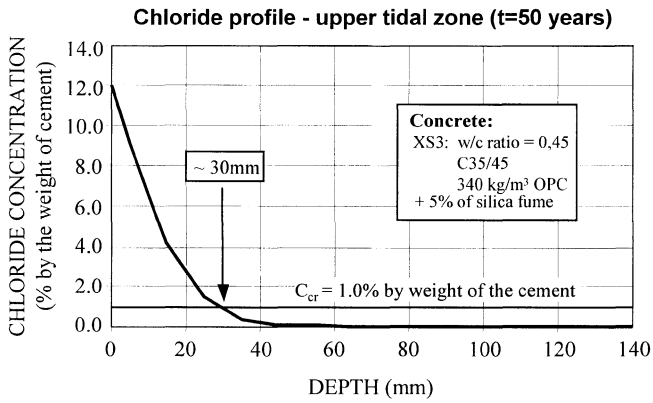

Figure 5 Predicted chloride profile for the upper tidal zone for designed concrete

CONCLUSIONS

Concrete wharves generally experience the deterioration due to chloride-induced corrosion of the reinforcement. This is often the consequence of inadequate cover of concrete over the steel. This occurred in prefabricated concrete elements because of poor inspection. During the analysis of the results of tests carried-out at the coastal structure, we noticed different behaviour in individual parts of the structure. This confirms that the structure shows different levels of aggression due to microclimate referring to the different elevation of individual structural element from the sea level, wind and rain exposure.

The described repair procedure of the concrete wharves on its lower side and the repair system, which consists of polymer-cement mortars with the addition of MCI and micro silica, shows good compatibility with the prepared base. Thus, we managed to increase the alkalinity of the reinforcement's surrounding. The protective layer of the cement-polymer mortar is slightly thicker, but still too thin considering the demands of concrete. However, this layer of cement polymer mortar increased impermeability and is additionally protected with an elastic protective coating.

The results of the research confirmed the application of the 2^{nd} Fick's law of diffusion to concrete structures in marine environment. The basic aim of implication of these findings is to use them in durability design of the new coastal structure. Choosing the concrete recipe in compliance with specification with included micro silica theoretically results in the concrete with the chloride diffusion coefficient low enough to meet the criteria of the service life of 50 years for the concrete with the 40 mm cover.

REFERENCES

1. BENTUR, A., DIAMOND, S., BERKE, N.S., Steel corrosion in concrete: fundamentals and civil engineering practice, E & FN Spon: London, 1997.

2. TUUTTI, K., Repair Philosophy for Concrete Structures, Proceedings of the International Seminar at the University of Dundee, Concrete Durability and Repair Technology, eds. R. K. Dhir, M. J. McCarthy, Thomas Telford, London, p.p. 159-169, 1999.

3. SLATER D., SHARP B.N., Specification for maritime Structures – mythology or methodology? Proceedings of the International Seminar at the University of Dundee, Controlling Concrete Degradation, eds. R. K. Dhir, M. D. Newlands, Thomas Telford, London, pp 45-59, 1999.

4. European pre-standard ENV 206, Concrete – performance, production, conformity, April 1997.

5. CEB Design Guide: Durable concrete structures, Comite Euro-International du Beton, Thomas Telford, UK, 1992.

6. HETEK, Chloride penetration into concrete, State of the Art; Transport processes, corrosion initiation, test methods and prediction models, Report No. 53, 1996

RESISTANCE OF LIGHTWEIGHT AGGREGATE CONCRETE AGAINST CHLORIDE PENETRATION UNDER SIMULATED MARINE EXPOSURE CONDITIONS

K Van Breugel

Delft University of Technology

Netherlands

ABSTRACT. In order to demonstrate the excellent durability characteristic of lightweight aggregate concrete (LWAC), chloride penetration test have been performed on LWAC and normal weight concrete (NWC). Two types of lightweight aggregate were considered, i.e. Lytag and Liapor. The water/cement ratio was the same for all concretes, viz. 0.45. Silica fume was used in order to realise a dense concrete. The concrete was exposed to thermal and hygral cycles, simulating a harsh marine environment. The paper contains a description of the test set-up, mixture composition, curing conditions ("good" curing and "poor" curing) and a presentation of chloride penetration data after 1 and 6 months. Special attention is given to the way in which restrained and unrestrained strain conditions are realised. The penetration depths of the three concretes are compared. Conclusions are drawn as regards the chloride profiles in the different concretes and with respect to the effect of restraint of thermal and hygral strains on the chloride penetration depth. The experiments clearly show that chloride penetration in lightweight aggregate concrete is not more than in normal weight concrete made with the same water/ cement ratio.

Keywords: Chloride penetration, Lightweight aggregate concrete, Marine environment, Thermal cycles, Hygral cycles, Effect of restraint.

K Van Breugel, is employed at Delft University of Technology, Faculty of Civil Engineering and Geosciences, The Netherlands, since 1980. In 1999 he became full Professor at the Department of Concrete Structures. His main topics are numerical simulation of the behaviour of concrete at early ages, durability and the design of concrete structures for environmental protection. He is member of a number of working groups of the fib, RILEM and CEN.

INTRODUCTION

Durability studies on LWAC performed in the past have revealed that these concretes perform quite successfully [1]. However, in spite of many good experiences there is still reluctance as regards the durability of LWAC structures. The reason for this is the (assumed) higher permeability of LWAC and its (assumed) lower resistance against ingress of chloride ions. With the aim to prove the good resistance of LWAC against chloride penetration a special test procedure was developed, whereby the concrete was exposed to a simulated marine environment with thermal and hygral cycles [2,3]. In this test set-up the penetration of chloride ions into the concrete takes place while the concrete is either under restrained of unrestrained condition. The test specimens were large concrete beams, which on top are exposed to thermal and hygral cycles. By applying the thermal and hygral cycles at the top surface of the beams, eigenstresses are generated in the top layer of the beams. These eigenstresses, if tensile stresses, may exceed the tensile strength of the concrete and microcracking may occur. These cracks may grow because of the alternating character of the loading and may promote the penetration of chloride into the concrete.

The main objective of this investigation was to see whether NWC and LWAC behave differently under the aforementioned exposure conditions. The hypothesis was that, due to a better deformational compatibility of the matrix and the LWA, the LWAC would suffer less from temperature-induced microcracking when exposed to thermal loads.

DESCRIPTION OF TEST SET UP

Testing Procedure for Generating Restraint Conditions

For generating small strains and stresses in concrete specimens in a laboratory set-up, with strains and stresses similar to those that might occur in a real structure when exposed to climatic conditions, is very complicated. The required degree of restraint can also be realised by using large beams, which on top are exposed to prescribed thermal and hygral cycles. In Figure 1 the cross section of a beam is shown, with on top a climate chamber. In this chamber alternating temperature cycles and dry-wet cycles are generated. The thermal loading ΔT can be split into the average temperature ΔT_{av}, the temperature difference between top and bottom, ΔT_{fl}, and self-equilibrating temperatures ΔT_{eig}. Predominant in view of stress-generating strains are the self-equilibrating temperatures. These temperatures cause eigenstresses, which are the major reason for surface cracks in massive concrete structures.

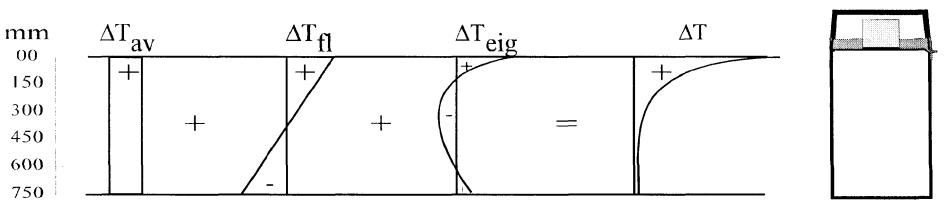

Figure 1 Imposed temperature distribution in the beam (upper part) and its components ΔT_{av}, ΔT_{fl} and ΔT_{eig}. Stresses in the top layer of the beam are hardly affected by the end restraint conditions of the beam

Description of the Experimental Test Set-up and Curing Conditions

Three large reinforced concrete beams, 6.0 m long, 0.4 m wide and 0.75 m deep, were made for this experiment. Each beam consisted of three sections, each two meters long and made with different concrete types. Two sections of each beam were made with lightweight aggregate, i.e. Liapor and Lytag, while the third section was made with normal weight aggregate. After the curing period (see next parapraph), the top surfaces of all the three beams were subjected to wetting-drying cycles. Wetting is done with salt water (5% NaCl by weight). Furthermore, the first and the second beam are also exposed to temperature variations at the surface. The third beam, acting as the reference, is exposed to the laboratory temperature of about 20°C. Climate rooms were used at the top surface of two beams to control the temperature at the surface and prevent loss of heat to the environment. A general plan (top view) of the set-up is shown in Figure 2.

Figure 2 Overview of experimental set-up for large-scale chloride penetration test

All three beams were covered with plastic sheets after casting for one day to prevent plastic shrinkage. The second day after casting the beams 1 and 3 were subjected to a "standard" curing condition, so called "good curing". Beam 2 was subjected to elevated temperature curing, denoted as "poor curing". The elevated temperature curing regime consisted of a temperature of 38°C and a relative humidity of 50%. This curing condition was selected to simulate climatically harsh regions, like in the Gulf Area. Both curing regimes were applied to the beams for two weeks. All three beams were left in open air after the curing period of another two weeks.

EXPOSURE CONDITION

The exposure regime consists of a drying period of 42 hours, consisting of 3.5 temperature cycle, and a short wet period of 6 hours with a constant temperature. The total wetting and drying plus heating and cooling period is 48 hours, and is called an exposure cycle (see Figure 3). The temperature varied between 10 and 60°C.

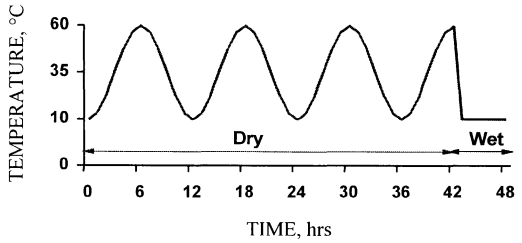

Figure 3 One complete exposure cycle applied to the specimens in the test

This exposure condition was so designed that the tensile stresses after supply of the water would exceed the tensile strength, causing cracking at the concrete surface. In total 87 exposure cycles were applied during the six months of the test.

Chloride Profiles in Restrained and Unrestrained Specimen

The chloride profiles in the concrete were determined on concrete cylinders, diameter 50 mm, drilled from the top surface of the beam. The chloride content was determined on 6 mm thick slices, sawn from the cylinders (see Figure 4). In order to investigate the effect of restraint on the rate of chloride penetration, a number of cylinders were pre-drilled. The drilling of the cylinders was performed before the beams were exposed to the exposure conditions and remained in their positions during the test

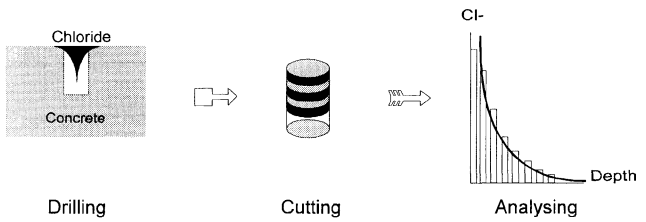

Figure 4 Procedure for determination of chloride profiles

. The annular space between the cylinders and the surrounding concrete was filled with an elastic synthetic material, preventing chloride-containing water to penetrate into this space. These pre-drilled cores are indicated as "unrestrained" specimens. They were cured and tested under exactly the same conditions as the beams. In this way it was possible to compare the rate of chloride ingress in "restrained" beam sections and "unrestrained" cylinders.

Temperature and Temperature-induced Deformations of the Beams

The temperature profiles in the beams and temperature-induced deformations were measured during the whole period of the test. Both length changes and bending of the beams due to imposed temperature differentials over the height of the beam were measured. The temperatures and the measured deformations were used to evaluate the effective degree of restraint experienced by the concrete.

MATERIALS

All concrete beams were made using Portland cement, type CEM I 32.5 R, cement content of 361 kg/m^3 and water-binder ratio 0.45. In all mixtures 17 kg/m^3 of micro silica (5% of cement weight) was used. Two types of lightweight aggregate were used, i.e. Liapor F8 and Lytag, both in 4 - 8 mm. In the NWC crushed aggregate, 4-16 mm, was used. Liapor is an expanded clay, spherical particles with water absorption of 6% (m/m) in 30 minutes. Lytag is a sintered fly ash product, spherical particles with water absorption of 15% (m/m) in 30 minutes. In all mixtures sand, 0-4 mm, was used. The cube compressive strength and the modulus of elasticity of the concrete were measured on 150 mm cubes and prisms, respectively. The mechanical properties at 28 days are presented in Table 1. In spite of the little lower strength of the aggregates the 28-days strength of the three mixtures is about the same. Some suction of mixing water by the LWA might have resulted in a lower effective w/b of the LWAC mixtures, resulting in a stronger paste which might have compensated, at least in part, for the lower strength of the aggregate.

Table 1 Mechanical properties of concrete mixtures at 28 days

	NWC	LIAPOR	LYTAG
Compressive strength of 150 mm cubes [MPa]	62.51	59.78	61.16
Tensile strength of 150 mm cubes [MPa]	3.91	3.69	4.29
Modules of elasticity of 100x100x400 mm^3 prisms [MPa]	34500	25687	26803

TEST RESULTS

Temperature Profiles and Nominal Stresses in the Beams

A maximum temperature of the concrete at a depth of 50 mm was measured of 33°C. Knowing that the maximum imposed temperature at the top was 60°C, steep temperature gradients must have been present in the concrete cover. Linear elastic stress analyses resulted in calculated stresses in the top layer of the beams between 9 and 10.5 MPa in compression and between 3.5 and 4.5 MPa in tension. These tensile stresses would have been high enough to cause fine cracks in the concrete cover.

Effect of Type of Aggregate on Chloride Penetration

The hypothesis at the start of the project was that LWAC might be less susceptible to temperature-induced microcracking because of the lower stiffness of the aggregate and a smaller difference in stiffness between matrix and aggregate. Observations after 6 months exposure are summarised in Figure 5 to 8. The chloride profiles after 6 months measured in beam 1 (standard curing) are presented in Figure 5 and 6 for the restrained and unrestrained specimens, respectively. The figures show that there is hardly any difference in the chloride profiles of the NWC and the two LWAC's. It further appears that the three concretes digest the restrained conditions in the same way.

Figure 7 and 8 show that the chloride profiles measured in the reference beam (beam 3), i.e. the beam not subjected to thermal cycles, have the same shape for all three concretes. All concretes appear to suffer from the drying and wetting cycles in the same way. Due to the imposed hygral cycles the chloride penetration is promoted. The LWAC's do not behave better than the NWC, but certainly not worse.

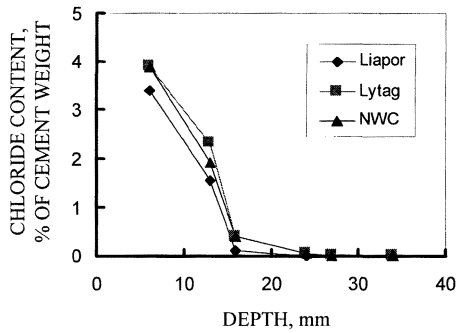

Figure 5 Chloride profile in three types of concretes – Restrained condition thermal and hygral cycles during 6 months, standard curing

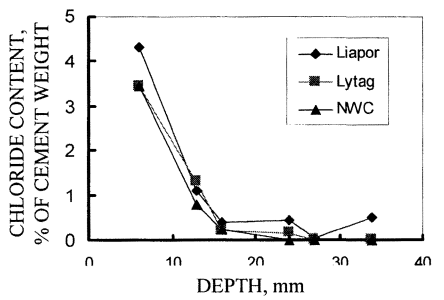

Figure 6 Chloride profile in three types of concretes – Unrestrained condition thermal and hygral cycles during 6 months, standard curing

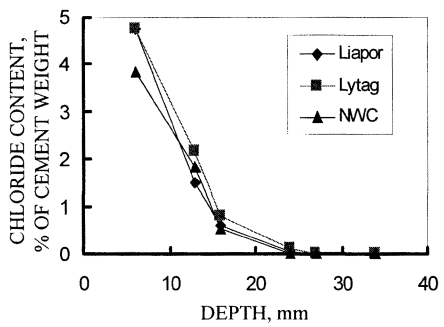

Figure 7 Chloride profile in three types of concretes – Restrained conditions hygral cycles during 6 months, standard curing

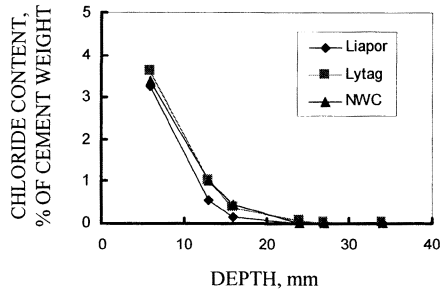

Figure 8 Chloride profile in three types of concretes – Unrestrained condition hygral cycles during 6 months, standard curing

Chloride Profiles – Effect of Degree of Restraint

The second important research parameter was the degree of restraint. The effect of the degree of restraint could be seen already in Figure 5 to 8. In Figure 9 and 10 the effect of restraint is shown for Lytag concrete for poor curing (beam 2) and standard curing (beam 3).

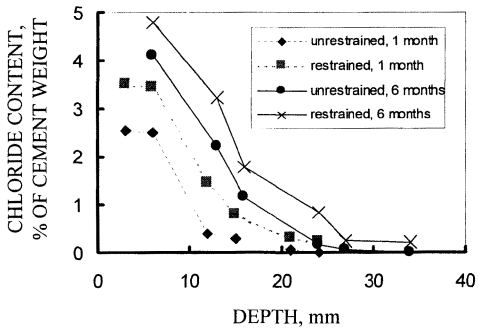

Figure 9 Effect of restraint on chloride penetration. Lytag beams, poor curing

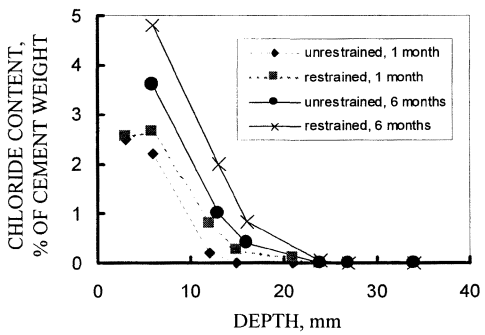

Figure 10 Effect of restraint on chloride penetration. LWAC-Lytag. Only drying-wetting cycles. Standard curing

The figures show the chloride profiles in the Lytag concrete after 1 and 6 month exposure. For all other mixtures a similar effect of restraint on the chloride profiles was found as shown in Figure 9 and 10 for the Lytag concrete, beit less pronounced. In the reference beam 3, i.e. the beam only subjected to drying-wetting cycles, the effect of restraint was very clear for all concrete mixtures. For the Lytag mixture this is shown in Figure 10. It appears that the drying-wetting cycle alone is obviously capable to promote the penetration of chlorides into the concrete. Although the effect of restraint on the shape of the chloride profile is very clear, the depth of penetration appears to be less affected.

CONCLUSIONS

The main hypothesis in this research was that if LWAC and NWC were exposed to thermal and hygral loading, the LWAC would perform as good as, or even better than NWC as far as chloride penetration is concerned. This because of a better compatibility between aggregate and matrix. After 6 months testing the results show that LWAC's and NWC perform largely identical. For three concretes, made with Lytag, Liapor and crushed aggregate, almost the same penetration depths of the chloride profiles were observed after 6 month exposure to severe thermal and hygral cycles. A postulated better performance of LWAC under the prevailing exposure conditions could not be confirmed. However, there was also no indication that the LWAC's performed worse. Further conclusions that could be drawn are:

- After one month exposure the surface concentration of chloride ions in the restrained specimens was higher than that in the unrestrained specimens. After 6 months exposure this was still the case. This is an indication for the possibility of microcracks.
- For the good cured specimens the penetration depth after 6 month in the LWAC's and the NWC was about the same. Only for the poorly cured specimens it was found that the penetration depth in the Lytag concrete was a little bigger than in the other concretes.
- The rate of chloride penetration, deduced from experiments on unrestrained specimens, underestimates the rate of chloride penetration in practical situations where restrained conditions do exist.

ACKNOWLEDGEMENTS

The co-operation with E. Kwint of VASIM during this research project was highly appreciated. The financial support of the EC through the EuroLightcon project was indispensable for performing the research and is gratefully acknowledged.

REFERENCES

1. BREUGEL, K. VAN., VEEN, M. VAN DER., (2000) "Large-Scale chloride penetration test on LWAC-beams exposed to thermal and hygral cycles". EuroLightcon, Document BE96-3942/R13. 37 p.
2. TAHERI, A., (1998) "Durability of Reinforced Concrete Structures in Aggressive Marine Environment" PhD Thesis, TU Delft, 194 pp.
3. TAHERI, A., BREUGEL, K. VAN., Chloride ingress in Marine Concrete Exposed to Thermal Cycles, Proc. Int. Conf. Concrete Durability and Repair Technology, Ed. Dhir et al., 1999, pp. 289-298.

A CONDITION ASSESSMENT OF PILE JACKETS UPON FLORIDA COASTAL BRIDGE SUBSTRUCTURES

W H Hartt
Florida Atlantic University

M Rapa
Ocean Technologies Incorporated

R G Powers
Florida Department of Transportation
United States of America

ABSTRACT. Corrosion and mechanically damaged bridge pilings in Florida coastal waters have, since the 1940's, been repaired and rehabilitated by jacketing; that is, by 1) removing loose concrete, 2) placing a formwork about the damaged zone (usually from mean low water to a height of several meters), and 3) filling the annulus with mortar or concrete. However, removal of jackets from pilings of two bridges that were being rehabilitated revealed that reinforcement corrosion was often severe and structural integrity reduced. Consequently, a condition assessment of jacketed pilings on 19 representative bridges was performed. This involved a visual condition assessment followed by removal of a portion of the jacket and characterization of the underlying condition. The pre- and post-inspection conditions were quantified using a Numerical Condition Rating (NCR) with the difference between the two values (ΔNCR) being taken as a measure of the extent to which piling damage was obscured by the jacket. Influences of jacket age, jacket type, pile reinforcement type (prestressed versus conventional), and piling pre-jacketed condition were evaluated. A mechanism for the deterioration is proposed, and a recommendation was made that jacketing be discontinued as a stand-alone piling repair/rehabilitation strategy.

Keywords: Reinforced concrete pilings, Marine environment, Corrosion, Pile jacketing.

W H Hartt, is Professor of Ocean Engineering and Director of the Center for Marine Materials. His research focuses mainly on corrosion control of offshore structures and of concrete bridge structures in coastal environments.

M Rapa, is a former graduate student. He is presently an engineer with Ocean Technologies, Incorporated in San Diego, CA.

R G Powers, the Assistant Corrosion Engineer with the Florida Department of Transportation Corrosion Laboratory. He is responsible for conducting a corrosion research program, evaluating materials for corrosion control, and advising Department bridge engineers regarding corrosion matters.

INTRODUCTION

General

Concrete normally provides a benign environment for embedded reinforcement because of the alkaline nature of the cement paste (pH~13.5) which promotes formation of a protective passive film upon the steel. However, such protection is often compromised for bridge pilings and related concrete components exposed to marine and coastal waters that contain significant levels of chlorides. Jacketing, which involves encapsulation of either a portion or the entire piling length, is a methodology that has been employed in Florida since the 1940's in an attempt to protect, repair, rehabilitate, and extend the service life of corrosion damaged bridge pilings.

In 1993, the Bryant Patten Bridges between Saint Georges Island and the mainland near Panama City, Florida, were scheduled for repairs and rehabilitation because of concerns regarding deterioration of the pilings, many of which were jacketed. However, upon removing the jackets and loose concrete, it was disclosed that in numerous cases all prestressing tendon had corroded away and concrete cracking and spalling had occurred to such a degree that the piling cross section had been critically reduced. Figure 1 shows example photographs of some of these pilings. Because of this finding, an evaluation commenced to determine the integrity of jacketed pilings on other bridges in the State. Specific objectives were to 1) develop a method for nondestructively characterizing the extent of this deterioration, 2) perform a condition assessment of a representative sampling of jacketed pilings upon State bridges, and 3) develop a deterioration model for jacketed pilings. Results from the first of these objectives have been reported previously [1], while the purpose of this paper is to present results from the second and third.

Figure 1 Four piling bent of the Bryant Patten Bridges. A jacket was removed from the second pile from the left revealing major cross section loss

Repair and Rehabilitation of Florida Pilings by Jacketing

Historically, jacketing was the sole method of piling repair and rehabilitation in Florida, although cathodic protection, either by itself or in combination with conventional concrete repair has been employed increasingly during the past decade [2-5].

Jacketing is accomplished in most cases by mounting a fiber glass form about the pile and filling the interior space with epoxy, mortar, or concrete. In cases where the load bearing capacity has been significantly reduced, a structural jacket is specified for which the fill material is reinforced concrete. The theory behind pile jacketing considers that this approach encapsulates the piling and thereby reduces chloride and oxygen access to the embedded steel and, by so doing, shuts down or moderates corrosion cells. Figure 2 provides a photograph of a typical jacketed piling. Other examples of encapsulation include membranes and overlays as are often employed upon bridge decks in North America where exposure to deicing salts is of concern.

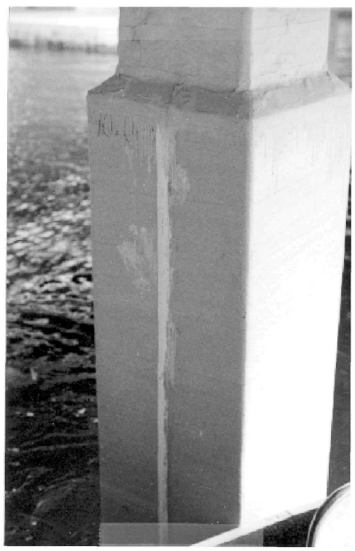

Figure 2 Photograph of a typical jacketed piling

The Florida Department of Transportation (FDOT) Bridge Inventory Database (BID) was employed to provide jacketed piling information. Figure 3 shows the time history of jacket installations and indicates that peaks occurred in the early 1970's and late 1980's. In addition, it was revealed that through 1994 a total of 8,464 jackets totaling 33,250 linear meters had been installed on 279 bridges.

An important consideration in this evaluation was quantification of jacketed piling condition, and for this purpose the Numerical Condition Rating (NCR) was employed. This rating approach is consistent with the Federal Highway Administration document, "Recording and Coding Guide for the Structure Inventory and Appraisal of the Nation's Bridges," and the FDOT document, "Bridge Inventory Database User's Handbook."

A description of the NCRs, as so defined, is provided in Table 1. In development of the jacketed piling database [6], individual FDOT Districts listed the NCR from past bridge inspection reports.

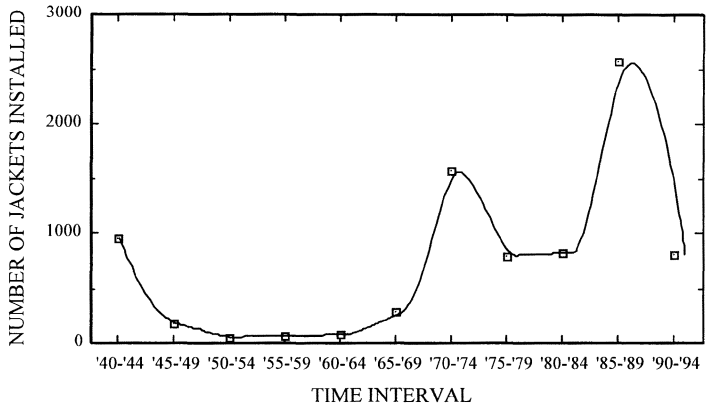

Figure 3 Number of piling jackets installed upon bridges in Florida as a function of time during the period 1940 to 1994

Table 1 Listing and definition of the various NCR categories

NCR	DESCRIPTION
9	Excellent Condition.
8	Very Good Condition - no problems noted.
7	Good Condition - some minor problems.
6	Satisfactory Condition - structural elements show some minor deterioration.
5	Fair Condition - all primary structural elements are sound (i.e., no loss of strength) but may have minor section loss, cracking, spalling, or scour.
4	Poor Condition - advanced section loss, deterioration, spalling, or scour.
3	Serious Condition - loss of section, deterioration, spalling, or scour have seriously affected structural components. Local failures are possible.
2	Critical Condition - advanced deterioration of primary structural elements. Unless closely monitored, it may be necessary to close the bridge until corrective action is taken.
1	"Imminent" Failure Condition - major deterioration or secdtion loss present in critical structural components or obvious vertical or horizontal movement affecting structural stability. Bridge is closed to traffic but corrective action may put back in light service.
0	Failed Condition - out of service - beyond corrective action.

In the present analysis, the NCR for jacketed pilings only was used in cases where such data existed. Otherwise, the NCR for all pilings or, as a final fallback, the substructure was employed. Figure 4 shows the results of this graphically as a plot of the number of bridges with a given NCR. Correspondingly, Figure 5 shows these same data along with the substructure NCR distribution for all State maintained bridges [6]. The two distributions are judged to be essentially the same with the exception that the peak NCR is displaced slightly higher in the case of the overall substructure ratings.

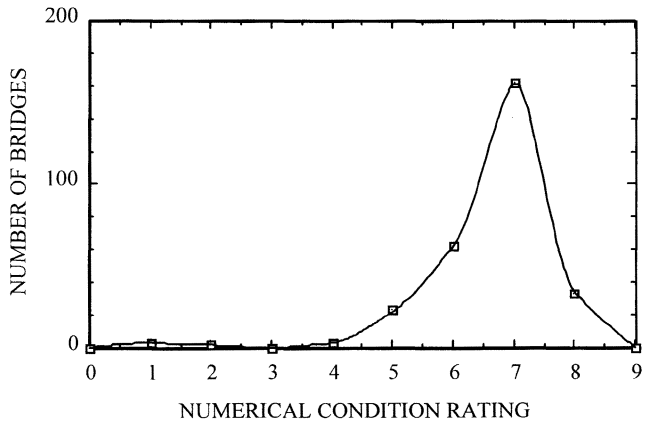

Figure 4 Distribution of NCRs for pilings and substructures of Florida bridges with jacketed pilings

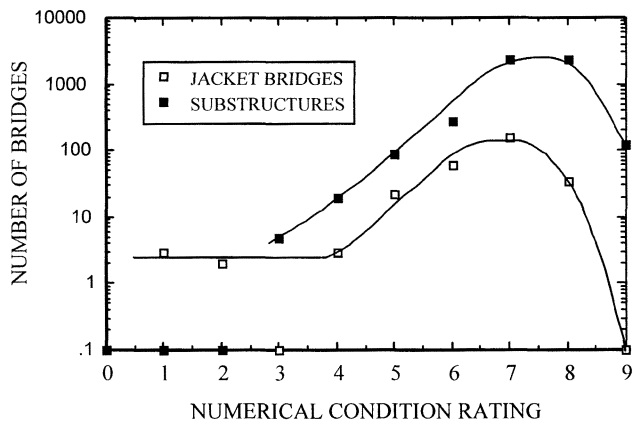

Figure 5 Distribution of NCRs for substructures of the full Florida bridges inventory

This is not unexpected since this database should include new bridges without distress, whereas bridges with jacketed pilings are expected to exhibit some level of deterioration. Note that the slope of the two curves leading to the most common NCR (7 for bridges with jacketed piles and 7-8 for all bridges) is the same in the two cases, suggesting that the distress distribution in this range (NCR 4-7) is similar irrespective of whether or not piles on a particular bridge are jacketed. Amrhein [6] raised the concern, however, that it has been assumed that the condition of the jacket reflects the condition of the piling itself. A focus of the present inspection program was to determine the extent to which this is the case.

FIELD SURVEY AND CONDITION ASSESSMENT

Selection of Bridges and Inspection Protocol

As a part of this project, jacketed pilings upon 19 State inventory bridges were inspected. Table 2 provides a listing of these along with relevant information about each. Although some of these bridges were selected because of simplified logistics, at the same time they are thought to be generally representative of the inventory. Possible exceptions to this are bridges 890060, 890061, 730069, 930005, 930075, and 930117, for which a piling rehabilitation/jacket replacement project was underway at the time of this study. Thus, it can be argued that the jacketed pilings upon these bridges may have been exceptional, worst case examples. At the same time, the fact that most, if not all, jackets were removed from the pilings of these bridges provided the opportunity for a more thorough inspection than would otherwise have been possible. Inspection of jacketed pilings on other bridges was necessarily more limited. The protocol consisted of the following steps:

1. Photographic documentation of the pilings to be autopsied and assignment of a NCR to each based upon visual appearance. It was intended that this NCR be indicative of the visible portion of the piling per se rather than the jacket.

2. Removal of a portion of the jacket form (fiberglass in all cases) from the pile in question. This normally commenced at a corner location since underlying damage was typically most advanced here. If a piling corner spall was present prior to the jacket having been applied, the location of this was determined by visual inspection, if possible, or by non-destructive testing, the instrumentation and procedure for which were described previously [1]. On this basis, the worst location on each piling was examined and characterized.

3. Removal of the jacket fill material. This also began at a jacket corner.

4. Inspection of the underlying piling for cracks and spalls. In cases where cracks or spalls were disclosed, it was determined, where possible, if these preexisted at the time of jacket installation or if they occurred subsequently.

5. Removal of any loose concrete from the piling so that the extent of cracking and spalling could be documented.

6. Measurement of the remaining cross section on any exposed tendon or bar as a function of elevation.

7. Photographic documentation of the piling condition and assignment of a NCR.

8. Replacement of the portion of the jacket that was removed.

Table 2 Listing of general information for inspected bridges

BRIDGE NO.	DATE CONSTR.	PILE TYPE*	JACKET DATE	NO. of JACKETS	PRE-JACKET NCR	Last NCR
150048	1961	PSC	1985	14	5	5
170012	1964	PSC	1986	16	5	5
490034	1990	PSC	1990	5	7	7
700001	1957	PSC	19--,87	110	4	7
730069	1966	PSC	1994	38	5	6
890060	1957	PSC	70,78,85,93	84	3	4
930005	1958	PSC	1978	30	2	7
900016/45	1972	PSC	1987	165	6	8
170021	1958	RC	1986	123	4	6
890061	1958	PSC	1985,87	24	5	6
860161	1965	RC	1986	10	4	6
720011	1958	PSC	1985	38	6	6
30209	1971	PSC	1987	6	8	7
130050	1954	RC	1987	11	5	5
130057	1957	PSC/RC	1978	12	6	7
930075	1956	PSC	1992,94	5	3	4
930117	1956	PSC	1988	6	7	6
100068	1956	RC	19--,87,90	574	5	5
790052	-	RC	1994	-	-	-

* PSC – Prestressed concrete; RC – Conventionally reinforced concrete

The approach involved assigning a NCR value to the pilings based, first, on the initial condition and, second, after jacket removal. The former value (pre-inspection) represented the "apparent" piling condition, irrespective of condition of the jacket. It was considered that this NCR should be comparable to the last FDOT NCR as determined by a bridge inspector. The latter value (post-inspection), on the other hand, should be indicative of the actual piling condition. The difference between these two NCRs (termed ΔNCR) served as a measure of the degree to which any piling deterioration had been concealed by the jacket.

Inspection Results

Bridges with jacketed pilings that showed no corrosion induced deterioration.

Two of the 19 bridges (Bridge Numbers 490034 and 720011) exhibited indications that jackets may have provided some degree of protection. In the former case (Bridge Number 490034) the jackets had been applied at the time of initial construction, apparently because of concerns regarding either pile splices near the waterline or driving damage or both. No corrosion induced deterioration was disclosed, either at the pile splices or at minor longitudinal cracks in the middle of some piling faces beneath the jackets that were excavated. For the latter (Bridge Number 720011), no corrosion induced damage of the inspected jacketed pilings was noted. Apparently, these jackets had been installed on pilings with no deterioration. It was concluded that the jackets upon these two bridges may have provided protection or, at least, had not accelerated deterioration.

Bridges with jacketed pilings that showed corrosion induced deterioration.

General

For bridges other than the two addressed above (17 of 19, Table 2), various degrees of corrosion damage to the jacketed piles were encountered. In an attempt to simplify the characterization and representation of this damage, the bridges were subdivided into two groups: those for which the pilings were prestressed and those that were conventionally reinforced. Primary focus in this project was upon the former (prestressed pilings), because of the Bryant Patten Bridges experience as discussed above. However, four conventionally reinforced piling bridges (Bridge Numbers 170021, 860161, 130050, and 100068) were included. Bridge Number 100068 was intentionally focused upon because of the range of jacket types that were present and because these were available for destructive evaluation since the bridge was being taken out of service. The other three were thought to be prestressed, but this turned out not to be the case. Bridge Number 860161 was not evaluated upon determining that the piles were conventionally reinforced.

Bridges with jacketed conventionally reinforced concrete pilings.

Figure 6 presents a cumulative distribution plot of the pre- and post-inspection NCR values (designated "initial" and "final," respectively) for the four conventionally reinforced piling bridges. From this, it was determined that the median pre-inspection NCR was 7.2 and the post-inspection NCR 5.6 for a difference of 1.6 NCR units. Thus, on average the actual piling condition was 1.6 NCR units lower than appeared to be the case based on visual appearance while jackets were still in place. A total of 29 pilings were represented in this analysis. Figure 7 presents a plot of the average post-inspection piling NCR as a function of

jacket age for these conventionally reinforced examples. The number beside each data point indicates the number of pilings that were examined in arriving at the different averages, and the arrow extending from the one datum indicates that multiple jacket vintages of 6, 11 and greater but unknown years were involved. The lower NCR limit encountered for conventionally reinforced piling bridges was four, and no instances of severe corrosion induced deterioration or concealed deterioration which rendered a condition of potential eminent catastrophic failure were disclosed.

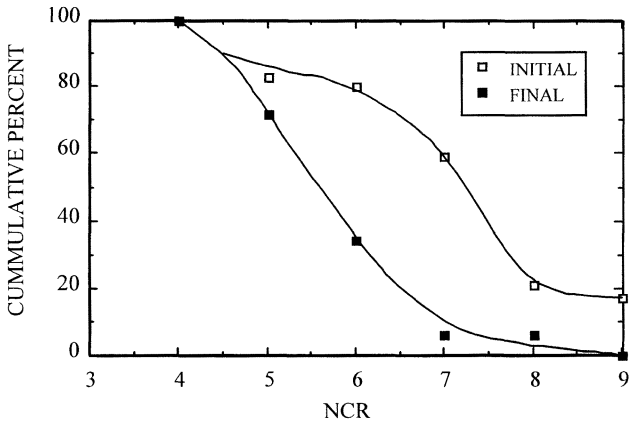

Figure 6 Cumulative distribution plot of pre- and post-inspection NCR values for the four conventionally reinforced jacketed piling bridges

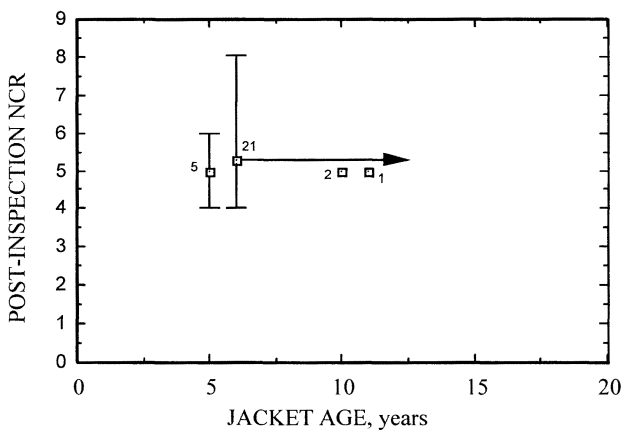

Figure 7 Plot of average post-inspection NCR as a function of jacket age for bridges with conventionally reinforced pilings

Bridges with Prestressed Concrete Pilings and Non-Structural Jackets

Figure 8 presents a pre- and post-inspection cumulative NCR distribution plot for the prestressed pilings with non-structural jackets. Data from Bridge Numbers 490034 and 720011, for which no corrosion or corrosion related deterioration was apparent, were excluded because these were considered exceptional, as discussed above. The data indicate that the median pre-inspection NCR was 7.2, which is identical to the value for the conventionally reinforced pilings, as discussed above. The corresponding post-inspection value, on the other hand, was 4.6 for a decrease of 2.6 NCR units. Also, these two cumulative distribution curves tend to diverge with decreasing NCR, indicating that the difference between the pre- and post-inspection values was greater the poorer the piling condition. For example, the pre-inspection NCR for the 80th cumulative percentile of jacketed pilings (80 percent of the pilings had a pre-inspection NCR which equaled or exceeded this value) was 6.8, whereas the corresponding post-inspection NCR was 3.5 for a difference of 3.3 units. These latter numbers are particularly significant since it is more appropriate in assessing structural integrity to focus upon the worst case than the median.

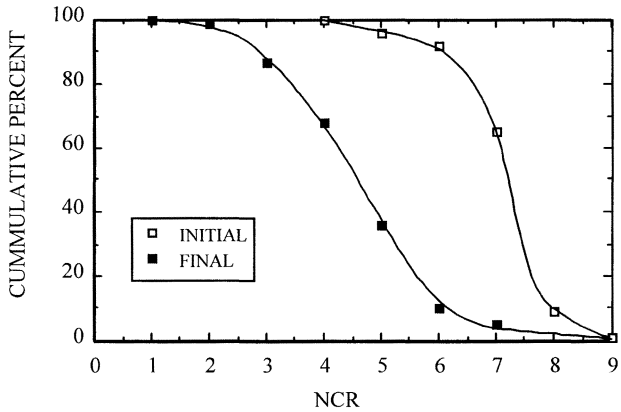

Figure 8 Cumulative distribution plot of pre- and post-inspection NCRs for jacketed prestressed pilings

The above evaluation indicates a more severe situation for jacketed prestress pilings than for conventionally reinforced ones, first, because of the greater difference between the pre- and post-inspection NCR values (median 2.6 compared to 1.6) and, second, because the pre- and post-inspection cumulative distributions diverge with decreasing NCR in the former case (prestressed) and converge in the latter.

The data in Figure 8 represent 91 jacketed piles from 11 bridges. Of these, a post-inspection NCR of four or below resulted for at least one piling on ten of these bridges; and only three pilings were inspected on the one bridge that did not have a NCR this low. Pilings on seven of the bridges had at least one instance of a NCR of 3 or less.

Figure 9 shows a plot of average ΔNCR for each individual bridge in Figure 8 as a function of jacket age. No discernible influence of age upon deterioration is apparent (jacket ages 3-19 years). In should be recognized, however, that the ΔNCR parameter does not indicate the jacket or piling condition per se but the extent to which piling deterioration has been concealed. For example, the two bridges with the highest ΔNCR values (Bridge Numbers 890061 and 930005) both had jackets that were in relatively good condition and which concealed advanced corrosion induced damage to the underlying pilings. On the other hand, pilings of Bridge Number 890060 were in the worst condition and exhibited the lowest post-inspection NCR; but yet the ΔNCR was 2.7 which is only slightly above the average value of 2.5. This resulted because the jackets themselves had deteriorated to an extent that the poor condition of the underlying pilings was visibly apparent. On this basis, it is concluded that the cumulative percent representation of jacketed piling deterioration (Figure 8) is a more revealing approach to damage characterization than is bridge age with the importance of Figure 9 being primarily to demonstrate that significant deterioration to jacketed prestressed pilings apparently transpired in the initial three years.

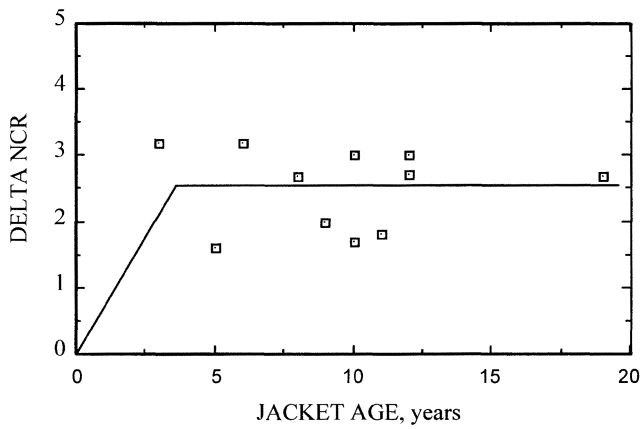

Figure 9 Plot of average ΔNCR for prestressed pilings as a function of jacket age

Bridges with Prestressed Concrete Pilings and Structural Jackets

As noted above, pilings with structural jackets were not the primary focus of this study since it was considered that these are capable of maintaining the load bearing capacity even with major wastage of the prestressing tendons. Also, splitting of the fiberglass and cracking and spalling of the jacket mortar or concrete fill should be visually apparent once corrosion of the jacket reinforcement becomes advanced. Information pertaining to such pilings was acquired from Bridge Number 900016/45 (Table 2). This bridge was initially inspected in February, 1997, at which time no fiberglass splitting or other indications of deterioration was apparent. This inspection included removing the fiberglass from one face of four randomly selected jackets (all structural), which revealed the concrete fill to be sound (no cracks or spalls). Excavation of the jacket fill concrete revealed that, while the epoxy-coating on the reinforcement was disbonded, corrosion was minimal with no significant metal wastage being

apparent. However, inspection of this same bridge approximately one year later (February, 1998) indicated that 41 of the 112 fiberglass jacket forms (37 percent) were split. A section of fiberglass encompassing the split was removed from five of these jackets, and cracking of the underlying fill concrete was apparent for four of these. Such cracking may also have existed in the fifth case; but if it did, it was beyond the area of fiberglass removal. Excavation of the fill concrete for two of these jackets revealed that in one case cracking was a consequence of corrosion of the epoxy-coated jacket reinforcement and in the other corrosion of the piling tendon. These findings indicate that structural jackets installed upon ten year old prestressed pilings in sea water can be expected to exhibit corrosion damage as fiberglass splitting and cracking and spalling of the fill and piling concrete after approximately ten additional years.

DETERIORATION MODEL FOR JACKETED PILINGS

The predominant jacket type encountered in this study was mortar filled fiberglass placed upon a previously spalled pile, as illustrated schematically in Figure 10. As a consequence, the spall exposed steel contacts both the original chloride contaminated concrete and the chloride free jacket mortar. For such a situation, the portion of the tendon that remains in contact with the original, chloride contaminated concrete should be anodic to that in the initially Cl^--free jacket fill mortar and should corrode at an accelerated rate. Continued chloride, moisture, and oxygen availability result from tidal action whereby the water level

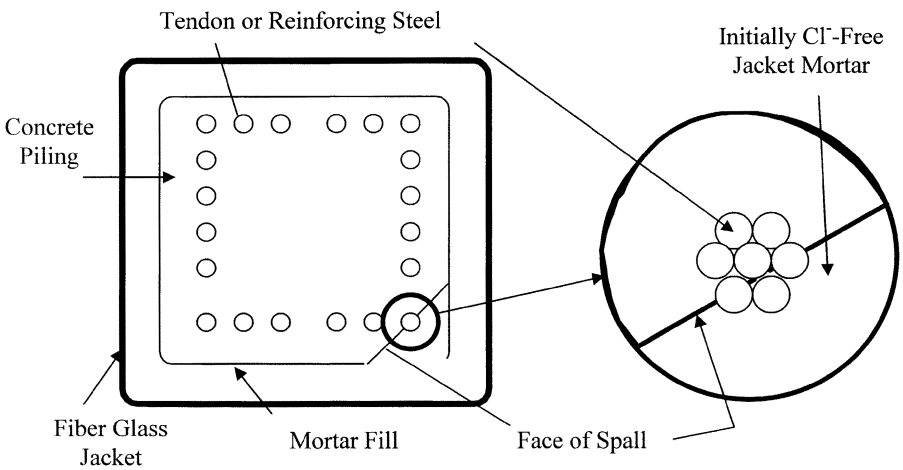

Figure 10 Schematic illustration of the cross section of a spalled piling with mortar filled jacket

cyclically rises and falls. Action of such a cell explains the trend in Figure 9 where significant corrosion induced damage to pilings transpired within three years of jacket

installation. Presence of this type of cell is also consistent with the damage accumulation rate moderating with time, as chlorides accumulate in the mortar. On this basis, application of second and third generation jackets only serves to periodically revitalize the corrosion cell. The inspections indicated that corrosion and corrosion induced concrete damage were more severe for prestressed than conventionally reinforced piles.

Several factors are thought to have contributed to this. First, tendons are typically of smaller diameter than conventional reinforcement (9.5 mm for the former compared to 19 mm or larger for the latter). Consequently, a given amount of corrosion results in a higher percentage of section loss for tendon. Second, because tendons are comprised of six exterior wires spiraled about a central one, the surface-to-volume ratio is greater than for a straight, solid bar.

As a consequence of the findings of this study, the FDOT in 1998 discontinued the use of jacketing as a piling repair method unless the jacket incorporates cathodic protection [5].

CONCLUSIONS

The following conclusions were reached with regard to the utility of fiberglass jacketing for corrosion control of pilings in coastal Florida waters:

1. Jackets installed upon sound, uncracked concrete pilings do not contribute to enhanced deterioration and may provide a modest degree of protection. They do, however, shield the deterioration that eventually occurs from visual detection such that the level of deterioration is likely to be underestimated.

2. Installation of jackets upon prestressed concrete pilings with one or more preexisting spall establishes a corrosion cell that can cause delamination of a piling face and complete section loss of exposed tendons within three years. All four piling faces can become delaminated in less than ten years.

3. Corrosion induced deterioration was more severe for jacketed prestressed pilings than for conventionally reinforced ones. In the former case (prestressed pilings), the median Numerical Condition Rating (NCR) was derated by 2.6 units upon jacket removal and evaluation of concealed deterioration of the underlying piling compared to visual inspection with the jacket in place. The magnitude of this derating was greater the lower the pre-inspection NCR (the more deteriorated the piling). In the case of conventionally reinforced pilings, the median derating was by 1.6 NCR units and was even less for the most deteriorated pilings.

4. Jacketing of concrete pilings should not be employed as a stand-alone approach for corrosion control of marine bridge substructures.

ACKNOWLEDGEMENTS

The authors are indebted to the Florida Department of Transportation for financial support of and technical assistance provide to this project. The assistance of Mr. George Jones in the bridge inspections and data acquisitions is appreciated.

REFERENCES

1. M. RAPA, W.H. HARTT, "Non-Destructive Evaluation of Jacketed Pre-Stressed Concrete Piles for Corrosion Damage," paper no. 566 presented at CORROSION/99, April 25-30, San Antonio.

2. R.J. KESSLER, R.G. POWERS, I.R. LASA, "Update on Sacrificial Anode Cathodic Protection on Steel Reinforced Concrete Structures in Seawater," paper no. 516 presented at CORROSION/95, March 26-31, 1995, Orlando.

3. I. SITTON, R.G. POWERS, J.E. COSTA, "Galvanic Metallized Zinc Cathodic Protection System for a Carbonated Concrete Structure," paper no. 645 presented at CORROSION/98, March 22-27, 1998, San Diego.

4. R.J. KESSLER, R.G. POWERS, I.R. LASA, "Intermittent Cathodic Protection Using Solar Power," paper no. 651 presented at CORROSION/98, March 22-27, 1998, San Diego.

5. D.L. LENG, R.G. POWERS, "Zinc Mesh Cathodic Protection Systems, paper no. 795 presented at CORROSION/00, March 26-31, 2000, Orlando.

6. W. J. AMRHEIN, "Bridge Inventory Presentation," presented at the FDOT Structures Design Conference, Orlando, Aug. 13, 1996.

MAINTENANCE STRATEGY OF REINFORCED CONCRETE STRUCTURES IN MARINE ENVIRONMENT IN HONG KONG

W C Leung

W T K Lai

Government of Hong Kong Special Administrative Region

China

ABSTRACT. The Technical Services Division (TSD) of the Civil Engineering Department is the maintenance authority for most of the Government and public marine facilities in Hong Kong. This paper provides an overview of the strategy of TSD towards the maintenance of the large stock of marine structures. It presents the development process of a specification for marine concrete and an assessment of its in-situ performance as compared to conventional concrete. It describes the condition audit system for marine structures; the preventive maintenance measures instigated for new marine facilities and the maintenance strategy towards the existing stock of marine structures.

Keywords: Concrete specification, Durability, Concrete coating, Condition audit system, Maintenance strategy, Marine structures.

P W C Leung, is a Senior Engineer of Civil Engineering Department, the Government of Hong Kong Special Administrative Region, China. He is a graduate of Civil Engineering from University of Dundee and obtained his MSc and D.I.C. from Imperial College, University of London.

W T K Lai, is an Engineer of Civil Engineering Department, the Government of Hong Kong Special Administrative Region, China. He is a graduate of Civil Engineering at Hong Kong University.

INTRODUCTION

The Technical Services Division (TSD) of the Civil Engineering Department is the maintenance authority for most of the government and public marine structures in Hong Kong. It is responsible for the maintenance of over 300 ferry piers and landing facilities. Most of the piers are located on the outlying islands and on either side of the Victoria Harbour, one of the busiest harbour in the world. The piers may be broadly divided into two categories according to their structural types: solid piers and reinforced suspended deck piers. The design life of the marine facilities in Hong Kong is 50 years generally.

The major task faced by TSD is how to maintain a large stock of marine facilities efficiently. In response, the TSD developed a new maintenance strategy for marine structures. At the start, TSD instigated a consultancy to carry out a comprehensive condition audit of all the ferry piers.

A new marine concrete specification for new construction was then proposed. TSD has also commenced the installation of corrosion monitoring devices in all new marine structures to forewarn the onset of reinforcement corrosion. Coating of all new structures has concurrently been implemented to delay the ingress of chloride. New condition audit procedures for marine structures are also developed. The maintenance strategy of marine structures is presented in this paper.

ENHANCEMENT MEASURES FOR NEW MARINE STRUCTURES

New Marine Concrete Specification

A review of the maintenance record of the marine structures revealed that the durability of concrete produced in accordance with the conventional specification was unsatisfactory in the hot and humid environment of Hong Kong and needs improvement. Corrosion of reinforcement and delamination of concrete are common features found in structures older than 10 years. Structural repairs would certainly have been carried out by the time the structure reaches 15 years of age.

In order to enhance the durability of marine concrete, CED instigated a consultancy to audit the ferry piers and assess the durability of locally produced concrete. A series of trial mixes were produced to assess their performance in respect of chloride diffusion, thermal and sorptivity characteristics under laboratory environment. Details of the concrete mixes and the results of the concrete trials are summarized in Table 1. As the laboratory trials were of short exposure duration, another round of site exposure tests was carried out. Concrete specimens were fixed at splash and tidal zones of selected piers.

The chloride diffusion coefficients were determined by taking cores from the concrete specimens. The cores were taken to laboratory for profile grinding at an increment of 1 mm. The concrete powder at each increment was tested for chloride contents in accordance with CS1 : 1990 : Section 21[1]. The chloride diffusion coefficients were then determined using Fick's Second Law of Diffusion.

The field chloride diffusion results of the mixes after 3 and 6 month's exposure are presented in Table 1.

Fick's Second Law of Diffusion is as follows:

$$C_x = C_s \left[1 - Erf \frac{(x)}{2\sqrt{tD_c}} \right]$$

C_x - Chloride level at depth x and time t
C_s - Surface chloride level
Erf - Error function
D_c - Chloride diffusion coefficient

Table 1 Details of Concrete Trial Mixes

MIX	1	2	3	4	5	6	7	8	9	10	11	12
Cement (kg/m^3)	428	322	314	328	279	292	126	126	377	292	261	126
GGBS (kg/m^3)	-	-	-	-	-	-	294	292	-	-	-	272
PFA (kg/m^3)	-	108	105	109	139	146	-	-	-	104	136	-
CSF (kg/m^3)		-	-	-	-	-	-	-	42	21	21	21
Coarse aggregate (kg/m^3)	1,050	1,055	1,077	1,079	1,064	1,066	1,088	1,057	1,086	1,069	1,060	1,081
Fine aggregate (kg/m^3)	564	567	579	580	573	573	586	569	584	576	570	582
Water/ Cementitious ratio	0.422	0.403	0.381	0.348	0.381	0.353	0.379	0.352	0.382	0.390	0.391	0.381
Superplasticizer (ml/m^3)	2,464	4,445	6,278	6,553	6,276	6,572	6,274	6,281	6,282	6,262	6,252	6,273
Laboratory Test Results												
Final slump (mm)	115	125	60	20	35	10	70	15	15	80	30	45
Compressive strength (MPa)	73	61	64	69	55	63	65	71	83	60	54	67
Water sorptivity (mm/min$^{0.5}$)	0.175	0.150	0.125	0.105	0.110	0.115	0.085	0.095	0.110	0.120	0.130	0.105
Chloride diffusion coefficient* (10^{-12} m^2/sec)	3.25	5.10	5.15	3.60	3.35	6.20	2.10	1.75	2.75	4.50	4.50	1.40
Field Test Results (Chloride diffusion coefficient at tidal zone after exposure for)												
3 months (10^{-12} m^2/sec)	4.2	6.1	4.4	3.9	5.8	4.7	2.7	2.8	2.7	4.6	4.3	2.0
6 months (10^{-12} m^2/sec)	3.2	3.1	3.1	1.9	2.4	2.5	1.6	1.4	2.5	3.0	2.6	1.8

*Immersion of samples in saline water at 23 ± 2°C for 28 days under laboratory conditions

In view of the results of the trial mixes, TSD introduces a marine concrete specification, which differs from the conventional specifications as follows:

(i) Allow the inclusion of ground granulated blast furnace slags (GGBS) to improve the durability of the concrete mix against chloride ingress;
(ii) Introduce the compulsory use of microsilica at a dosage of 5 to 10% of the total cementitious content;
(iii) Lower the maximum water/cementitious content ratio of the concrete mix from 0.42 to 0.38;
(iv) Limit the cementitious content to between 380 and 450 kg/m^3;
(iv) Increase the concrete cover to 75 mm to delay the onset of reinforcement corrosion;
(v) Introduce a tighter specification for aggregates.

Details of the marine concrete specification as well as the conventional concrete specifications are presented in Table 2.

Table 2 Concrete Specification for Marine Structures

COUNTRY	HONG KONG			UK
Specification/Standard	Marine Specification[2] 1998	Interim Specification[3] 1994	Port Works Manual[4] 1992	BS8110[5], BS6349[6]
Design life	Not stated	50 years	50 years	Not stated
Minimum compressive strength	45 MPa	45 MPa	45 MPa	40 MPa
Maximum free water/cementitious ratio	0.38	0.4	0.42	BS6349 states 0.45
Minimum concrete cover for fully immersed, tidal, and splash zones	75 mm	60mm nominal cover	60mm nominal cover	BS6349 states 50mm but preferred 75mm
Minimum concrete cover for aerated zone	75 mm	60 mm nominal cover	50 mm nominal cover	
Cement type	CSF (5-10%); GGBS (60-75% for normal application and up to 90% for low heat application); PFA (25-40%), not to be used with GGBS	OPC; PFA (25-40%) replacement mandatory	OPC	SRPC not permitted. No codes specify PFA, GGBS, CSF
Range of cementitious content	380-450 kg/m^3	360-430 kg/m^3	375-550 kg/m^3	350-400 kg/m^3
Minimum slump	75 mm	75 mm	75 mm	-
Miscellaneous	Equivalent sodium oxide per m^3 of concrete < 3kg Flakiness Index < 30% Elongation Index < 35% Los Angeles Value<30% Sodium sulphate soundness weighted average loss < 6%	-	-	-

Durability Performance of New Marine Concrete Specification

The marine concrete specification was introduced in mid 1998 and has been adopted in all new marine structures. In order to assess the chloride diffusion characteristic of the marine concrete, a pier built in 1999 using the marine specification was selected for testing. Cores were extracted from the structure at splash and tidal zones after one year's exposure to seawater and the chloride profiles obtained by profile grinding technique. It should be noted that the concrete mix was designed by a ready mix supplier based on the requirements of the marine concrete specification. For comparison, similar tests were also carried out on cores obtained at similar zones from a 3-year old pier that adopted the conventional concrete specification. The mix details of both structures are presented in Table 3 and their chloride profiles are presented in Figures 1 and 2 respectively.

Table 3 Mix Details

MIX	GRADE	SLUMP (mm)	CONCRETE COMPOSITION (kg/m^3)					ADMIXTURE (ml/m^3)
			Cement	PFA	CSF	Coarse aggregate	Fine aggregate	
Marine concrete	45D/20	175	310	115	25	1,000	720	4,500
Ordinary concrete	45D/20	75	445	-	-	930	760	890

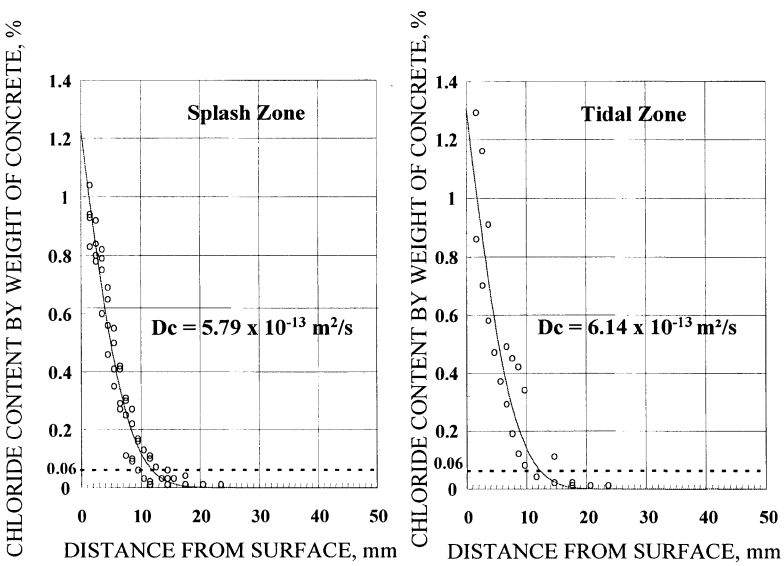

Figure 1 Chloride profiles of marine concrete at splash zone & tidal zone after 1 year of exposure

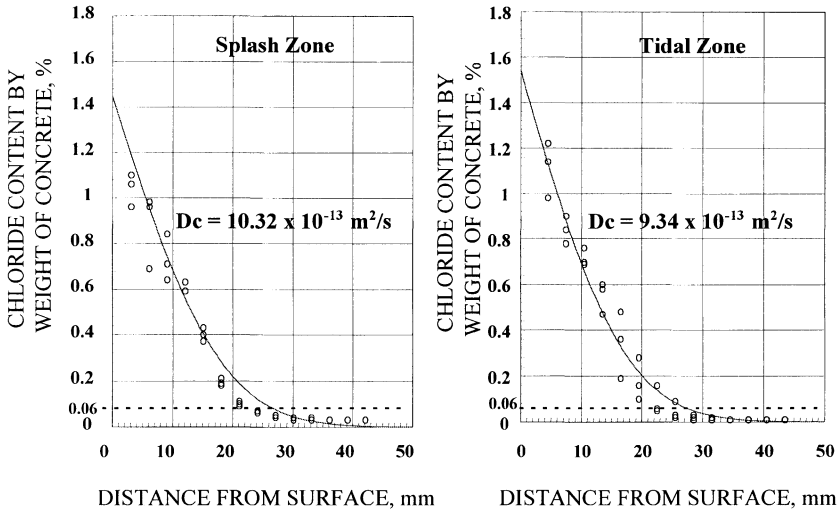

Figure 2 Chloride profiles of conventional concrete at splash zone & tidal zone after 3 years of exposure

It was noticed that the chloride diffusion coefficient of the new structure was substantially lower. An attempt to predict the future ingress of chloride based on the law of diffusion and using the diffusion coefficients extrapolated from the chloride profile results was presented in Figure 3.

The result projects that for structures built using the conventional concrete specification, the chloride content at the reinforcement level would reach the corrosion threshold value (ie 0.06% by weight of concrete) at about 13 years. This ties in well with our maintenance records of existing marine stocks which indicates a major concrete repair would be needed within 12 to 15 years after construction.

For new structures built using the marine concrete specification, it is projected that the chloride ingress would be very slow. With the concrete cover being increased to 75 mm, the pier structure should last for at least 35 years without major concrete repair. This will lead to a substantial saving in the resources needed for maintenance works. However, it should be noted that the structure would still require one or two concrete repair cycles within its 50 years design life if no additional measure was implemented.

To investigate the effectiveness of the coating system, cores were taken from the splash zone of a 3-year old pier, which was constructed using the conventional concrete specification, and coated with silane.

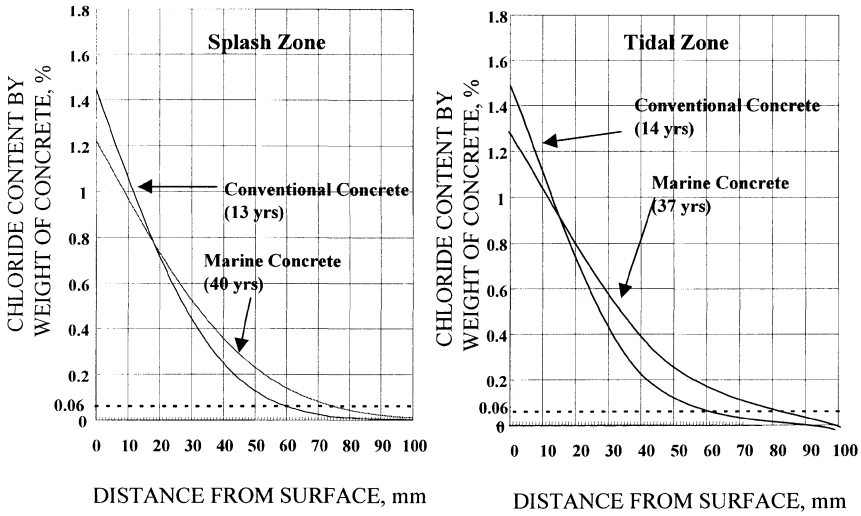

Figure 3 Projected chloride profiles of marine concrete and conventional concrete at splash zone and tidal zone when chloride content at reinforcement level reaches the corrosion threshold value of 0.06% of weight of concrete

The chloride profiles of the cores indicated that the coating has successfully delayed the ingress of chloride after an exposure of more than three years in seawater. A diffusion coefficient as low as 1.7 x 10^{-13} sq. m/s was achieved. This indicates that the structure would not need structural maintenance within its 50 years service life provided that the coating remains effective. In order to monitor the rate of ingress of chloride and detect if the coating remains effective, corrosion monitoring devices such as reference electrodes and chloride ladders are installed in all new pier structures as a general practice.

MAINTENANCE STRATEGY FOR EXISTING PIERS

The piers under TSD's maintenance responsibility may be broadly divided into two structural categories according to their structural types: solid piers and reinforced concrete suspended deck piers. Solid piers are constructed mainly of precast mass concrete blocks and require minimum maintenance. Reinforced concrete suspended structures are mainly used in ferry terminals and the majority of these piers are between 200 to 1,000 m^2 in size. The mean age of the suspended deck piers is 23 years and a quarter of all the reinforced concrete piers is less than 10 years of age.

A maintenance strategy was developed based on TSD's experience in previous repair, trends of deterioration of reinforced concrete piers, diffusion coefficients obtained from both the laboratory specimens and in-situ structures and the protection performance of concrete coatings.

Condition Audit of Piers

To cope with the maintenance responsibility of a stock of aging marine structures, TSD relies on the development of an effective structural audit system to prioritize the maintenance works. The structural audit system comprises visual inspection, detailed inspection and a database assessment system.

The aim of the visual inspection is to identify and record the extent and severity of the visible deterioration. It would normally be conducted at low tide and both photographic and video records would be taken. Each defect type is codified for ease of recording and assessment. The defect codes for the common type of defects are presented in Table 4. The defects are classified into two categories. The category 1 defects are those that adversely affect the serviceability or integrity of structures. The category 2 defects are those that indicate symptoms of deterioration, which need to be recorded and monitored. The observed defects recorded from a visual inspection form a computerised database for assessment.

Table 4 Defect Codes and Category of Defects

DEFECT CODE	CATEGORY 1 DEFECTS	DEFECT CODE	CATEGORY 2 DEFECTS
C3	Concrete cracks 1 - 3mm	C1	Hairline cracks < 0.3mm
C4	Concrete crack 3 - 6mm	C2	Concrete cracks < 1mm
C5	Concrete crack > 6mm	HCB	Honeycombing
S2	Spalling to reinforcement	DP	Damp patch
S3	Spalling behind reinforcement	D	Dripping
RS(N)	Rust stain (Numerous)	PR	Previous repair
B	Broken off	PD	Ponding
		CB	Coating blister
		MC	Map cracking
		S1	Spalling (reinforcement not exposed)
		DLM	Delamination
		EFF	Efflorescence
		CL	Cement loss
		RS(F)	Rust stain (Few)

To supplement the visual inspection, detailed inspection using non-destructive technique (NDT) is also carried out. The NDT commonly used are half-cell mapping technique, concrete resistivity tests, carbonation tests, chloride profiling tests and break out inspection windows. The aim of the detailed inspection is to verify and supplement the results of the visual inspection.

A deterioration index based on the extent of delamination, spalling and the frequency of Category 1 and 2 defects found per unit area will be calculated. Weighted factors are assigned to each type of defect such that defects that will likely cause structural distress (eg spalling and serious cracking) are given a high weighting. The deterioration indices are used to determine the priority of repair for the piers. Unit rates were set in the program to estimate the likely repair cost. The choice of repair options will depend on the remaining service life of the structure.

The Maintenance Options

There are two maintenance strategies for existing stock of piers: the long-term maintenance strategy and the short-term maintenance strategy. The choice will depend on the required remaining service life of the structure.

For structures less than 5 years old, the chloride ingress into the concrete should be minimal. The preferred option will be to treat the structure with a suitable concrete coating to prohibit further chloride ingress. For structures between 5 and 10 years old, the extent of chloride ingress will be assessed first. The coating of the structure will be the preferred option if the chloride ingress is of small quantity and has not reached the reinforcement level. Silane and epoxy coatings are considered suitable for marine application.

For structures over 15 years old, the chloride would have reached the reinforcement level and concrete coating is not considered effective to delay the onset of reinforcement corrosion. Cathodic protection system, which offers long-term protection against reinforcement corrosion, will be considered. This will most likely be installed concurrently with the structural repair works.

For structures with less than 15 years remaining service life, a short-term maintenance strategy will be adopted and conventional concrete repair will be carried out. The option of reconstruction of the pier should be reviewed and planned accordingly.

CONCLUSIONS

1. The chloride ingress rate in marine structure is substantially reduced by the adoption of the marine concrete specification.

2. Although the durability of marine structures is enhanced by the implementation of the marine concrete specification, additional measures such as concrete coating system and corrosion monitoring system would be implemented to minimise the need of structural repair.

3. An effective maintenance strategy based on structural condition audit system and rational prioritization of repair can achieve saving in the maintenance resource.

4. TSD's policy on the maintenance of marine structures will achieve cost saving in the long run. This is achieved by adopting the marine concrete specification, applying concrete coating and installing corrosion monitoring devices to forewarn the occurrence of corrosion, implementing a structured condition audit system to monitor the rate and extent of deterioration and adopting a database system to prioritize the repair works.

ACKNOWLEDGEMENTS

This development work is part of the enhancement programme undertaken by the Civil Engineering Department, the Government of Hong Kong Special Administration Region, China. The authors wish to express their gratitude to the Director of Civil Engineering for his permission to publish this paper.

REFERENCES

1. HONG KONG GOVERNMENT. CS1: Testing Concrete. Volume 1, Section 21, Chemical analysis of hardened concrete, 1990, 33 pp.

2. TECHNICAL SERVICES DIVISION, Recommended Specification for Reinforced Concrete in Marine Environment, Civil Engineering Department, Government of Hong Kong SAR, March 1998, 6 pp.

3. STANDING COMMITTEE ON CONCRETE TECHNOLOGY, Interim Concrete Specification for Reinforced Concrete Structures in Marine Environment, Works Bureau, Government of Hong Kong SAR, November 1994, 2 pp.

4. PORT WORKS DIVISION, Port Works Manual - Design, Construction and Maintenance, Civil Engineering Department, Government of Hong Kong SAR, 1992, 210 pp.

5. BRITISH STANDARDS INSTITUTION. BS 8110: Structural Use of Concrete. Part 1. Code of practice for design and construction, BSI 1997.

6. BRITISH STANDARDS INSTITUTION. BS 6349: Maritime Structures. Part 1. General criteria, BSI 1984.

IMPROVING THE PERFORMANCE OF CONCRETE IN COASTAL AREAS OF BANGLADESH

M S Z Bosunia

J R Choudhury

Bangladesh University of Engineering and Technology

Bangladesh

ABSTRACT. Performance of concrete elements in the coastal areas of Bangladesh is reportedly to be unsatisfactory as the concrete in these areas are found to be deteriorating. The commonest problems are random cracking, corrosion of embedded reinforcements and large scale spalling of concrete. Such deterioration can be caused by a number of physical, chemical and environmental factors, acting alone or in combination. Besides limited availability of suitable materials, absence of relevant specifications and codes of practice together with proper technical know how have adverse effect on durability of concrete and initiate premature deterioration of concrete structures in those areas. This paper briefly describes the results of some studies on the performance of concrete and the related construction practices in the coastal areas of Bangladesh. Based on these studies a number of recommendations have been put forward for improving the performance of concrete structures in the coastal areas of Bangladesh.

Keywords: Concrete, Coastal area, Deterioration, Durability, Construction practices, Quality control.

Professor Shamim Bosunia is a Professor of Civil Engineering Department at Bangladesh University of Engineering and Technology (BUET), Dhaka. He received his BSc(Eng) and MSc(Eng) from BUET in 1965 and 1972 respectively and obtained PhD degree from University of Strathclyde, Glasgow in 1979. His research interests include cement and concrete technology, repair and rehabilitation of concrete structures and low cost construction.

Professor Jamil Choudhury is a Professor of Civil Engineering Department at Bangladesh University of Engineering and Technology (BUET), Dhaka. Presently he is the Vice-Chancellor of BRAC University at Dhaka, Bangladesh. He received his BSc(Eng) from BUET in 1963 and obtained MSc(Eng) and PhD degrees from University of Southampton, UK in 1965 and 1968 respectively. His research interests include high-rise structures, earthquake engineering, disaster management and information technology.

INTRODUCTION

Concrete structures in coastal areas – submerged, partially or completely exposed are inundated by surge water accompanied by the cyclonic storms which quite frequently affect the coastal areas of Bangladesh. The design and construction practices for concrete works in coastal environments assume great importance for proper durability. Performance requirements and structural criteria for such construction in these areas need to be considered separately from those constructions in urban areas.

Premature deterioration of concrete structures in these areas is a common feature. Structures show alarming degree of deterioration by way of cracking in concrete, spalling of concrete and corrosion of reinforcements within years after construction. Achieving long term durability of structures and their adequate performance is considerably more difficult in coastal areas in Bangladesh than in other parts of the country. Lack of durability can be caused by external agents arising from the environments or by internal agents within the concrete. Physical causes arise from the action of alternate wetting and drying and from differences between the thermal properties of aggregates and of the cement paste. Chemical attack takes place within the concrete mass, if the permeability of concrete is favourable for such attack. Environmental factors together with physical and chemical causes have adverse effect both on behaviour of fresh concrete as well as on its performance after hardening. Other constraints such as shortage of suitable materials, construction equipment, skilled labour, proper technical know-how etc. also affect the construction activities in those areas.

Any such construction in the coastal areas, which disregard the environmental and other issues, will affect the quality, performance and durability of concrete structures. Like all other materials, concrete in coastal areas requires the employment of proper design and construction techniques if the proper durability of this material is to be realized in service.

The durability of concrete construction in coastal areas needs to be considered separately from those construction in inland urban areas for various reasons. Firstly the construction shall be made taking mitigatory measures against some causes of disorder/deterioration which may be peculiar to a region. Secondly, a method for the durable construction shall have to be developed by taking into account the local materials and techniques.

The structures in the coastal areas are subjected to extreme wind during cyclones. The cyclonic wind speed for a return period of 50 years is 260 km/hr, whereas the annual maximum wind speed for a return period of 50 years varies for 150 to 190 km/hr along the coastline. The annual maximum temperature (return period of 50 years) is around 40°C and the minimum is around 8°C. The design surge height for a return period of 50 years varies from 4.5 m in the south-east to 7.9 m in the central coastal region.

This paper briefly describes the field studies carried out in the coastal areas of Bangladesh on performance of concrete and construction practices. It also describes how it is hoped to achieve greater durability of the concrete construction in the coastal areas using the experience gained from the field studies and by adoption, where appropriate, of the recommendations contained in recent research reports. Keeping in view the results of the studies and the available information, measures have been suggested in the paper for producing durable concrete in the coastal areas of Bangladesh.

DETERIORATION OF CONCRETE STRUCTURES IN COASTAL AREAS

A field survey was initiated to visit and examine the cyclone shelters along the coastal belt of Bangladesh existing in 1992 (BUET-BIDS, 1992). A total of 227 shelters were visited. These cyclone shelters constructed during 1974-1979 developed serious distresses and large scale deterioration over the years. These are three storied reinforced concrete frame buildings, located at various places of coastal areas, constructed by Public Works Department (PWD) of People's Republic of Bangladesh and funded by International Development Association (IDA). Some typical conditions are shown in Figure 1 (i to iv). These figures clearly demonstrate the distress in major structural elements (viz. columns, slabs and beams) resulting from deficiencies in construction practices. Some of these have been discussed in the following sections.

Due to the serious deterioration of the different structural elements of these concrete buildings, the design criteria, use of construction materials and the construction specifications of the shelters have been reviewed. Some of the construction specifications of these shelters are as follows:

Mix ratio of concrete used by volume - 1 : 2 : 4
Crushing (28 day cylinder) strength of concrete, f'_c = 14 to 16 N/mm^2
High tensile deformed bars with allowable stress in tension, f_s = 158 N/mm^2
Coarse aggregates - Brick chips
Clear cover for reinforcements - Specified as for normal concrete works such as
for slab - 19 mm
for beams and columns - 38 mm

The review of the construction specifications shows that there are deficiencies in those for appropriate concrete construction in coastal areas. Low strength concrete is not durable and use of such low strength for concrete is not normally compatible with the high strength reinforcements used in the structures. The clear covers for the reinforcements in different structural elements are also not suitable for concrete construction in coastal environments and those are inadequate according to codes of practice (e.g. BNBC, ACI or BS). Besides, brick chips as coarse aggregates in concrete construction in coastal environments also invite problems for the durability of the structures. Use of brick chips and the low strength concrete are likely to produce highly porous concrete.

The study of the deterioration process and the analysis of the construction specifications of these cyclone shelters reveal that the distresses in concrete elements are due to deficiencies in design and construction specifications and lack of understanding of properties of indigenous material used. Moreover, lack of repair and timely maintenance works has accelerated the deterioration process over the years.

CONCRETE CONSTRUCTION PRACTICES AND DEFICIENCIES

Concrete construction in the coastal areas of Bangladesh is generally carried out by using indigenous materials, labour-intensive methods and site-mixed concrete. Cast-in-place concrete construction is hardly ever carried out under ideal conditions; as a result the concrete structure may develop defects for different reasons.

(i) Crack in column

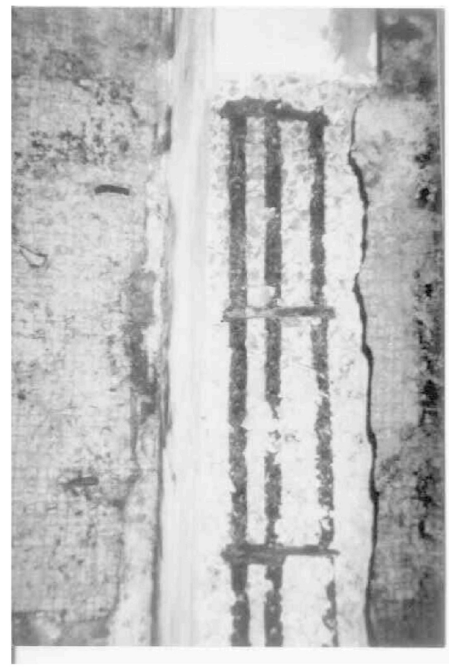

(ii) Spalling in column

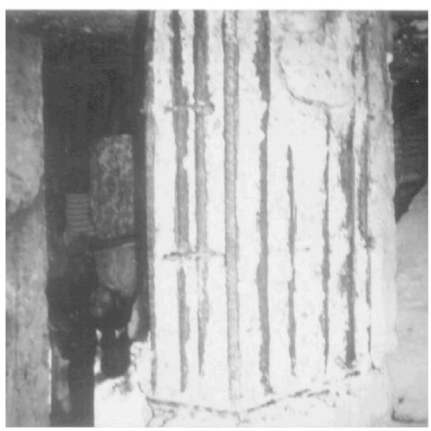

(iii) Spalling in column

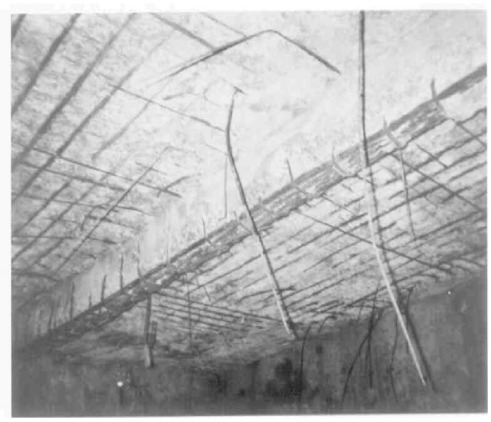

(iv) Spalling in slab and beam

Figure 1 Typical conditions of deteriorated concrete members

Allen and Edwards (1987) listed cracks in horizontal surfaces due to plastic shrinkage, cracks over reinforcing bars due to plastic settlement, surface texture defects and lack of cover to reinforcement as the common type of defects which may occur during in-situ concrete construction. In case of such construction in the coastal areas, other defects such as chemical attack will only accelerate the deterioration process. Experience has shown that in many cases where the design has been properly carried out by using the provisions of the available codes of practice, the constructed structures developed numerous defects because of unforeseen inadequacies in construction. Some of the sources of these inadequacies in terms of materials, site practices, effect of hot weather etc. are identified and discussed below.

Materials

There is an acute shortage of good-quality indigenous building materials in the coastal areas. Locally manufactured bricks are frequently broken to produce the coarse aggregates to be used in concrete construction. These bricks often fail to meet the requirement of standards and occasionally contain salts in them. As these bricks are highly porous, use of such brick aggregates produces porous concrete. The ingress of chemicals, chlorides or sulphates in such pores of concrete allows the crystallization of salts when the environment is dry and favourable. This process in turn exerts a very high pressure inside the pores of the aggregates resulting in volume changes, pattern cracking, spalling and other unpredictable defects within a very short period after the construction.

The rivers in the alluvial plains of the coastal areas deposit a large amount of fine sand after the monsoon period every year. This sand does not fall within the specified grading limits and its use drastically affects the workability and strength of the concrete. The use of these sands increases the water requirement in the concrete mix with consequent decrease in strength and increase in drying shrinkage (Zafar et al. 1989). Besides, these sands contain salts which adversely affect the strength and durability of concrete. Zafar *et al.* (1989) report corrosion of reinforcing steel, salt weathering and environmental cracking due to a number of factors including the use of low quality aggregates contaminated with sulphate and chloride salts.

The quality of available water is also not suitable for concrete making in the coastal areas. In most places the water is saline which is believed to increase the risk of corrosion of the embedded reinforcement.

All concrete works in the coastal areas are produced near the construction sites. Data on site mixed concrete from different sites show that, large variations occur in workability and strength of these concretes due to poor quality control procedures and supervision.

Site practices

Volume batching of concrete mixes, with very little control of water-cement ratio is usually carried out at the construction sites in the coastal areas. In such cases, the quality control requirements are not implemented at the sites because of inadequate testing facilities and lack of understanding of the quality control procedures. This results in poor quality and low strength concrete.

Site practices such as, delay in placing concrete in its final position and addition of water after the concrete mix is discharged from the mixer machine are often observed. These practices produce porous, non-homogeneous and low strength concrete.

Inadequate compaction often produces honeycombed concrete and patch work with plastering on such surfaces is done to hide the honeycombing. This is a very poor substitute for properly compacted concrete. Such concrete does not allow necessary bond to be developed between concrete and embedded reinforcement, and over a period of time the moisture penetrates to corrode the steel causing cracking and subsequent spalling of concrete.

Hot weather

The entire coastal areas have hot climate (with temperature very often reaching 40°C) for the major parts of the year. Concrete construction in hot weather without appropriate measures impairs the properties of fresh as well as hardened concrete. A higher temperature of fresh concrete results in a more rapid hydration and leads, therefore, to accelerated setting and to a lower strength of hardened concrete. Furthermore, rapid evaporation causes plastic shrinkage and crazing and subsequent cooling of hardened concrete introduces tensile stresses resulting cracks in concrete.

Curing practices

Curing practices are sometimes inadequate and defective for the concrete works in coastal areas. Curing is discontinued sometimes too early and the members such as columns, beams, walls etc. are inadequately cured. Bunds often formed with locally available clay to impound water on the surface of horizontal casting allow penetration of chemicals present in clay into the larger pores of very young concrete. This results in early deterioration of concrete.

Summary of problems

The construction practices and the deficiencies identified as above have serious effects on the durability of the concrete structures. Chloride contaminated water enters the highly porous concrete structures very easily and reacts with the embedded reinforcements accelerating the corrosion mechanism of the bars. The inadequate covers of such reinforcements further aggravate the situation, resulting in the formation of cracks. These cracks continue to widen and finally cause the spalling of the total cover exposing the rebars. The rapid corrosion ultimately endangers the safety of the structures and makes the structures unusable only a few years after their construction.

IMPROVED CONSTRUCTION PRACTICES

In order to ensure adequate performance of concrete structures, built under various environmental constraints and difficult climatic conditions of the coastal areas of Bangladesh, appropriate measures of concrete protection can be developed by considering improvements in construction practices. These measures range from selection of suitable constituent materials to moist curing for a definite period and some logical practices in concrete making for safe, economical and durable structures in the coastal areas. To produce the appropriate concrete to be used in structures in coastal areas the essential characteristics of materials and the improved construction practices are listed below.

Aggregates

Aggregates have a definite influence on the behaviour and performance of hardened concrete. The strength and the porosity of the aggregates not only affect the strength of the concrete but their properties also greatly affect durability.

Natural stone aggregates conforming to ASTM C33 shall be used in the concrete construction for the coastal areas. Under no circumstances should brick chips be used in making concrete. The highly porous brick aggregates react with the salts available in the coastal environments causing an expansion of the concrete that initiates the early deterioration of the structure. Crushed, angular pieces of aggregates, well graded, produce a dense and durable concrete with less porosity.

Properly graded good quality sand shall be used in concrete making. If such sand is locally available it must be sufficiently washed before use in concrete making.

It is recommended that all the aggregates shall be washed before use in concrete making. Experimental results reported by Zafar et al. (1989) show that by using washed aggregate in concrete the initiation of corrosion of reinforcement under aggressive environments, is delayed when compared with concrete having same mix proportions, water-cement ratio and unwashed aggregates.

Water

The quality of available water is also not suitable for construction in many parts of the coastal areas. Water from the deep tube wells shall preferably be used. If otherwise water must be free of excessive chlorides (not more than 600 ppm) and sulphates (not more than 1000 ppm). Prior coating of reinforcement with a cement slurry made with fresh water shall be used. These steps help in prolonging the life of reinforced concrete exposed to the action of coastal environments. Sea water should definitely be the last resort for concrete making in the coastal areas.

Concrete mix proportion and strength

Measuring the quantity of materials is an important factor for making good quality concrete. Generally a volumetric measurement is used. The minimum mix proportion of 1:1½:3 (cement: sand : stones) by volume shall be used for the concrete construction. This ratio will require a quantity of cement equal to 390 Kg/m^3 of concrete. If saline water is to be used in concrete making due to non-availability of fresh water the quantity of cement shall be increased to 440 kg/m^3 of concrete. The corresponding mix ratio by volume shall be 1:1¼ :2½. To produce the dense impermeable concrete a low water-cement ratio not more than 0.45 shall be used. Low water-cement ratios diminish the bleed water that may be trapped at the paste/aggregate interface and thus initiate microcracking. The minimum compressive strength of concrete at 28 days shall be 21 N/mm^2 tested on standard cylinders.

The ingredients of concrete shall be thoroughly mixed so as to produce a uniform mixture. The mixing shall be done in a mixing machine. On completion of mixing, the mix shall be discharged carefully. The green concrete should fall vertically into the centre of the receptacle to prevent segregation.

Conveying, placing and compaction of concrete

When the mix is ready, the concrete shall be quickly carried and placed in final position before setting starts. Concrete that has been mixed and left standing for more than 30 minutes shall not be used. No water shall be added to concrete after it has been mixed. Placing of concrete from the pans shall be from a close distance i.e. 18 in. (500 mm) preferably. The rate

of placement of concrete should not be so rapid as to impair proper compaction. Hand compaction shall preferably be avoided. Hand-held mechanical vibrators shall be used for proper compaction. The vibrator shall be inserted at fairly close intervals. It should be withdrawn slowly at each location and should be operated continuously while being withdrawn. Over-vibration must be avoided as it causes bleeding and segregation.

Construction joints are a potential source of weakness and should be located and formed with care and their number shall be kept to a minimum. When fresh concrete is required to be placed on a previously placed and hardened concrete, precaution must be taken to clear the surface of all foreign matter and remove the laitance or scum before the fresh concrete is placed. For securing a good bond and watertight joint, the receiving surface shall be made rough and a rich cement slurry or grouting placed on it just before the placement of fresh concrete.

The initial temperature of concrete is an important consideration in hot weather concreting. The temperature of aggregates can be kept low during hot weather by shading the stockpiles. Shading can also provide an effective, cheap and easily manageable method to protect freshly placed concrete surfaces during the day time. Hasanain et al. (1989) report the results of a field study which shows that shading can reduce the rate of evaporation by 50 percent or more when compared with the rate of evaporation from freshly placed concrete surfaces without any protective measures for hot weather concreting. Before placing concrete the formwork shall be sufficiently wetted.

Curing

Proper curing practice is one of the important steps in making good quality and durable concrete. Moist curing plays an important role in the development of concrete strength particularly in hot weather. A study by Taryal et al. (1986) reports that for hot and dry weather, curing for 14 days by sprinkling water twice a day and keeping the concrete covered by plastic sheets is a very effective method from the view point of strength gain. Based on the experimental results on corrosion of reinforcement Zafar et al. (1989) report that the curing period has a distinct effect on the durability of concrete. The increase in the curing period also improved the resistance against sulphate attack. The normal curing time for concrete construction in the coastal areas shall be 14 days minimum. Besides the method and duration of curing for a particular area shall be decided by considering the weather conditions, type of concrete elements and water supplies at the site. For the slabs, bunds with only cement sand mortar shall be made to allow the curing through ponding. For the beams, columns, walls etc. curing shall be made by sprinkling water at least two to three times a day depending on the weather conditions. Constant vigilant supervision must be employed so that there is no discontinuity in proper curing.

Cover to reinforcement

In order to protect the reinforcing steel from corrosion by exposure to air, moisture and other harmful agents particularly in coastal environments and severe exposure conditions, and to develop necessary bond resistance between the steel and concrete, a minimum cover between the outside faces of steel and concrete shall be provided. For corrosion protection the minimum clear cover to reinforcing bars for any reinforced concrete construction in the coastal areas shall be as follows according to clause R7.7.5 of ACI Code (ACI 318-99). The recommendation in BNBC clause 8.1.8 may also be adapted.

Slabs	-	50 mm
Beams	-	63 mm
Columns	-	63 mm
Concrete cast against and permanently exposed to earth	-	75 mm

All reinforcing bars shall be held in place before and during casting of concrete so that the specified clear covers are strictly maintained. It is frequently noticed that due to labour-intensive concreting operation the clear covers cannot be maintained which ultimately affects for the corrosion of the bars, cracking and spalling of concrete. Sufficient number of mortar blocks shall be used to hold the reinforcing bars from contact with the forms and to ensure correct cover. These blocks shall be made using 1:4 proportion of cement and sand. When used to hold the vertical bars the blocks shall be cast with double wire embedded in them, so that they can be tied with the bars. Blocks must be properly cured earlier and must be wetted before the concreting operation.

QUALITY CONTROL PROGRAMME

In order to ensure that the concrete produced under various environmental constraints and difficult climatic conditions of the coastal areas of Bangladesh meets the prescribed quality norms, quality control at every stage of concreting operations is very important. Quality control is to ensure uniformly good concrete in respect of strength, workability, density etc. Important items of quality control are listed below:

1. Testing of cement received in each consignment.
2. Periodical sieve analysis of aggregates to ensure uniformity in grading and shape.
3. Controlling stock piling of aggregates to avoid segregation during handling.
4. Washing of all aggregates
5. Proper adjustment of proportions of various sizes of aggregates and other constituents such as cement and water in concrete mix.
6. Sampling and testing of concrete for workability, density and strength.
7. Controlling production, transportation and placement of concrete and ensuring proper compaction.
8. Controlling construction joints.
9. Ensuring good formwork with no leakage.
10. Ensuring adequate and proper cover to reinforcement for extreme environment.
11. Ensuring effective curing for adequate period.
12. Effectively controlling temperature of concrete and evaporation of the mix water.

Recent experience

During the period 1992 to 2002, around 1000 new cyclone shelters have been constructed in the coastal areas of Bangladesh. The recommendations related to improved practices stated in this paper have been incorporated during the construction of most of these new shelters. Field observations during the last few years have shown that the performance of these shelters has been relatively much better in comparison with those constructed earlier during 1974-1979. Monitoring of these shelters, particularly the condition of concrete structures elements, is continuing.

CONCLUSIONS

Improving the performance of concrete meeting stringent quality requirements in the coastal areas of Bangladesh is a challenging task. Such concrete construction may be influenced by environmental and climatic condition and also by technical know-how. Adequate measures have to be taken to ensure long-term durability of structural concrete in the coastal areas of Bangladesh and for that there is a need to develop guidelines for proper construction practices, standards and specifications for these areas. For durable concrete structures in the coastal areas of Bangladesh practices and specifications have been suggested taking into account the environmental and climatic conditions in that region, the technical know-how, construction materials and the existing construction practices.

REFERENCES

1. ACI 318-99, "Building Code Requirements for Structural Concrete (318-99) and Commentry (318R-99)
2. ALLEN, R.T.L. and EDWARDS, S.C. "The Repair of Concrete Structures" Blakie & Son Limited, Glasgow, 1987.
3. BNBC, 1993, "Bangladesh National Building Code", HBRI-BSTI, Dhaka.
4. BUET and BIDS, "Repair and Rehabilitation of Existing Shelters and Killas", Final Report Vol. VI, Multipurpose Cyclone Shelter Programme, UNDP/WORLD BANK/GOB Project BGD/91/025, Dhaka, July 1992.
5. HASANAIN, G.S., KHADLAF, T.A. and MAHMOOD, K., "Water Evaporation from Freshly Placed Concrete Surfaces in Hot Weather" Cement and concrete Research, Vol. 19, No. 3, 1989, pp 465-475
6. RASHEDUZZAFAR, AL-GAHTANI, A.S. and AL-SAADOUN, S.S., "Influence of Construction Practices on Concrete Durability" ACI Materials Journal, Nov.-Dec. 1989, pp. 566-575.
7. TARYAL, M.S., CHOWDHURY, M.K., and MALALA, S. "The effect of Practical Methods Used in Saudi Arabia on Compressive Strength of Plain Concrete." Cement and Concrete Research, Vol. 16, No. 5, 1986 pp. 633-645.

SOME PROPERTIES OF UNDERWATER CAST CONCRETE

I A Rostovsky
Bulgarian Academy of Sciences
B D Darakchiev
University of Architecture, Civil Engineering and Geodesy – Sofia
Bulgaria

Abstract. The paper presents the results of lab tests on the washout degree of concrete mixes prepared for underwater concreting by the Contractor method. The effect of various factors on the washout degree is shown such as concrete composition, presence of different admixtures (including antiwashout ones), type of water environment (fresh or sea water), etc. Some properties of underwater cast concrete, obtained from concrete mixes, which have shown the lowest susceptibility to washout, have also been studied. Original lab methods were used for this purpose. The effect of underwater casting on different concrete properties has been examined. The following tests have been carried out:

- washout tests on concrete mixes and specifying some factors influencing on the process;
- comparative strength tests on underwater cast concrete (fresh or sea water) and concrete cast in air;
- the change in the hardness and strength, respectively, of the underwater cast concrete in the surface layer and in depth is examined;
- the porous structure of the underwater cast concrete in the surface layer and its change in depth is studied;
- the change in the pH value of the underwater cast concrete in the surface layer and its change in depth is determined, with the view to identifying corrosion processes in the concrete and protection of the available reinforcement from corrosive attack;

Keywords: Underwater concrete, Washout resistance, Porous structure.

I A Rostovsky, is an Assistant Professor in Central Laboratory of Physico-Chemical Mechanics at Bulgarian Academy of Sciences. His current researches are focused on concrete repair materials, blended binders and high performance concrete.

B D Darakchiev, is a Professor in University of Architecture, Civil Engineering and Geodesy – Sofia

INTRODUCTION

Concrete cast and operating underwater is used in a number of structures and structural elements: pillar foundations, bridge piers and abutments, port and bank consolidation structures, foundations of buildings and structures, concrete piles cast-in-place under high-level groundwater conditions, etc. The underwater concrete works accelerate and cheapen the construction process at the expense of the continuous water pumping which is not always possible.

In such cases there are good reasons to question the properties of underwater-cast concrete.

In some cases, due to the remoteness of fresh water sources, it is necessary to use seawater for preparing the concrete mix, which will later inevitably affect the hardened concrete properties.

In the course of time, several independent methods of underwater concreting have occurred and developed.

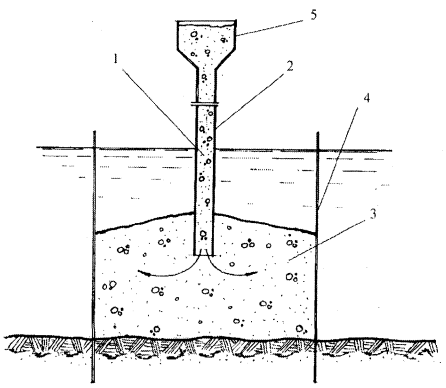

Figure 1 Scheme of underwater concreting by "Contractor" method
1 – tremie; 2 – concrete mixture; 3 – casted concrete; 4 – shape ; 5 – delivery funnel;

The most common method of underwater concreting in the international practice has become the method using vertically displaceable tremies which is also known as "Contractor method". It consists in a continuous discharge of high slump concrete mixture (s=(16-20) cm, in some cases up to 25 cm), through pipes (tremies) positioned at certain intervals, into a space surrounded by framework along the contour. This technology is required in order to obtain qualitative casting and self-compaction of the concrete mixture. When the upper surface level of the cast concrete mixture rises, the tremie also rises but its mouth always remains immersed at a definite depth in the mixture. The schematic diagram illustrating the main idea of the method is shown in Figure 1.

The suitable concrete mixes should be highly compact.

It is known that the underwater-cast concrete mix changes its original composition. Due to the partial washout in the surface layer, the cement quantity decreases as the water-cement ratio increases thus causing a decrease in the strength properties and durability of the concrete. Besides, due to diffusion processes, the water environment penetrates deeply into the forming porous structure of the cement stone, which is accompanied by extraction of part of the easily soluble components. The problem becomes even more complicated when concreting takes place in an aggressive environment (sea or soft water).

LABORATORY STUDIES ON THE PROPERTIES OF CONCRETE MIXES AND CONCRETE IN UNDERWATER CONCRETING

We have adopted the following method of determining the washout degree of concrete mixtures (Figure 2):

1. Thirty minutes after preparing the mixture, it is placed in two polymer net baskets with 2 mm cells;
2. The baskets are immersed three times in a water container having a capacity of 50l;
3. The concrete mixture stays in the water for thirty minutes;

Thus the time for delivering and placing the concrete mixture is taken into account. Besides, it becomes possible to extract partially the highly soluble products from the cement hydration.

The full baskets are weighed to determine their masses m_0 and m_1 before and after performing the experiment, i.e. before and after the washout, respectively. As a criterion for assessment of washout resistance of concrete mixes is the relative loss of mass Δm, calculated by the formula:

$$\Delta m = \frac{m_0 - m_1}{m_0} .100,\%$$

Unfortunately there is no possibility to evaluate what part of the loss of mass is due to washout action of water environment and what – due to bleeding.

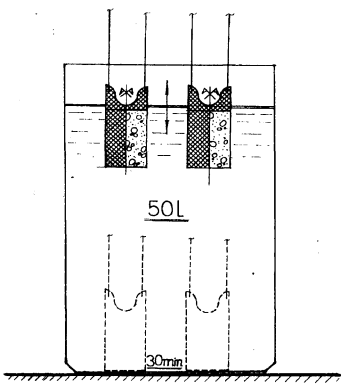

Figure 2 Washout test

This method is considered to reflect more fully the real conditions for the underwater-cast concrete mixtures during concreting.Using the method described above the washout degree of concrete mixes and some factors influencing on the process – temperature of water environment, type of mixing water, use of admixtures etc. , can be examined.

On the basis of the method described above, the washout degree of 15 concrete mixes was determined with the aim to obtain optimal composition in respect of strength and susceptibility to washout.

In order to reach the required consistency - s = (16-20) cm, a superplasticizer based on acetone-formaldehyde resin in a quantity of 2% cement mass was used. Sodium carboxymethyl cellulose (Na-CMC), hydroxyethyl cellulose (HEC), silica fume (SF), bentonite, etc. were applied as antiwashout admixtures for decreasing the concrete mix surface washout.

The water temperature in the containers was 7°C. The concrete mix composition varied within certain limits in view of obtaining the necessary mobility. The mix test results obtained were compared with those from the check concrete mix not containing admixtures. Data on the concrete mixes and the results obtained are presented in Table 1.

Table 1 Concrete mixtures composition and washout test results

MIX No	CEM kg/m^3	SF kg/m^3	AWA type-kg/m^3	HWRA kg/m^3	SAND kg/m^3	CR ST kg/m^3	WATER l/ m^3	W/C	SLUMP cm	Δm %
1	400	-	-	-	650	1000	240	0.60	19.5	3.24
2	418	-	-	+	680	1046	202	0.48	20.0	3.58
3	404	-	Na – CMC -4.04	+	656	1010	230	0.57	18.0	2.83
4	385	33	-	+	680	1046	202	0.48	17.0	0.79
5	372	32	Na – CMC -2.02	+	656	1010	230	0.57	16.0	0.52
6	366	32	Na – CMC -4.04	+	647	996	240	0.60	16.0	1.35
7	369	32	Na – CMC -2.01	+	652	1003	235	0.59	19.0	1.08
8	362	32	Bentonite-41	+	655	1008	231	0.57	20.0	2.01
9	385	32	AD 1*-20.2	+	680	1040	202	0.48	17.5	0.98
10	367	32	GA*-3.6	+	706	1082	175	0.44	21.0	3.9
11	367	31	PEO*-24	+	648	990	227	0.63	16.0	1.2
12	385	33	AD 2*-20.2	+	680	1040	190	0.48	18.0	1.03
13	385	32	P.Alc.*-15	+	680	1040	190	0.51	18.0	1.3
14	354	32	Polym.*-23	+	625	956	255	0.66	18	1.5
15	407	35	HEC-0.23	+	719	1006	194	0.44	18	0.47

AD*1 - acrylate dispersion SIKA 1 - 30% dry content; GA* - gumma arabika; PEO* - polyethylene oxide; AD*2 - acrylate dispersion (vinylacetate, vinylsulphonate, acrilyc acid) - 30% dry content;Polym.* - triple copolymer (acrylamide-methylmetacrylate-vinylsulphonate).

CONCLUSIONS

1) The use of various types of antiwashout admixtures decreases considerably the washout degree of concrete mixes in their surface layer (up to six times higher than that of the check mix) but increases the amount of mixing water for reaching the required consistency, which, in turn, leads either to an increase in the W/C ratio or to overconsumption of cement. The effect is enhanced when a combination of antiwashout admixtures is added (especially for mixes 5 and 15).

2) The mixes with higher susceptibility to water loss, Nos. 1 and 2, have high mass loss thus making them unsuitable for underwater concreting.

3) The most efficient measure for decreasing the washout degree and loss of mass is to decrease the W/C ratio, at the same time increasing the fine particles content in the cement paste thereby enhancing its compactness. This can be achieved by the use of superplasticizers and fine mineral admixtures of the silica fume type.

4) The superplasticizing and plasticizing admixtures do not decrease the washout by themselves, they even increase it since it is well known that they contribute to the dispersion of the cement particles. Besides, they should be carefully used because of the risk of losing quickly the concrete mix mobility, which was unfortunately observed in mix 15.

Tests were performed according to the adopted method at water temperatures of 7°C and 20°C, which are quite real for the weather conditions in Bulgaria, in order to assess the effect of the water environment temperature.

The tendency in all tested mixes was the same. The results obtained are presented in Table 2.

Table 2 Effect of the water environment temperature on the concrete mix washout degree

No.	MASS LOSS IN % At a water environment temperature of:		DIFFERENCE, %
	7^0 C	20^0 C	
1.	3.24	5.48	+69.1
2.	3.58	8.59	+139.9
4.	0.79	0.89	+12.7
8.	2.01	5.0	+148.75
9.	0.98	1.67	+70.4
10	3.9	4.97	+27.4

Note: The concrete mix numbers correspond to Table 1.

The results obtained show definitely that as the water temperature increases, the susceptibility to concrete mix surface washout can increase by over (140 - 150)%.

Two basic reasons could be specified for the loss of mass – washout action of water environment and partially dissolution of easy soluble components of cement stone (mainly calcium hydroxide). It is well known that the permeability and wash ability of water increases as the temperature rises, the solubility of calcium hydroxide decreases in the same time. It is obvious that the first process has much more influence in this case than the second one. Therefore, we can conclude that spring and autumn seem to be more appropriate seasons for underwater concreting.

In underwater concreting using sea water there are two possibilities with regard to the concrete mixing water:

- the mixing water can be fresh water provided that there is a suitable water supply source available;
- the mixing water can be sea water provided that there is no fresh water source and that the construction permits it, i.e. there is no risk of corrosion of the reinforcement in the reinforced concrete;

From what has just been said it follows that there are practically two possibilities with respect to the mixing water and the water environment: fresh mixing water and sea environment or sea mixing water and sea environment.

In the wide range of specialised literature which we consulted, we could not find information on the effect of the type of mixing water and environment on the washout degree of concrete mixtures. The lab tests performed at the University of Architecture, Civil Engineering and Geodesy proved that concrete mixtures prepared with drinking water and natural sea water have actually the same washout.

The results of the tests showed that concrete mixes prepared with drinking and natural seawater from the Varna Port water area practically have the same washout for other conditions being equal. The case was different with the effect of the water environment. It turned out that the same concrete mixes exhibit about 15% higher relative mass loss in sea environment in comparison with fresh water environment both at lower temperatures (7°C) and higher ones (20°C) (see Table 3).

Table 3 Effect of the water environment type on the concrete mix washout degree

COMPO-SITION	MASS LOSS IN % At 7°C water environment temperature:		DIFFERENCE, %	MASS LOSS IN % At 20°C water environment temperature:		DIFFERENCE, %
	fresh	sea		fresh	sea	
1.	3.24	3.76	+16.05	5.48	6.27	+14.42
2.	3.58	4.17	+16.48	8.59	10.0	+16.41
4.	0.79	0.91	+15.19	0.89	1.01	+13.48
8.	2.01	2.35	+16.92	5.0	5.93	+18.6
9.	0.98	1.11	+13.27	1.67	1.91	+14.37
10	3.9	4.64	+18.97	4.97	5.76	+15.9

Note: The concrete mix numbers correspond to Table 1.

Two main conclusion can be drawn from the data above:

1) The type of mixing water - fresh or sea (from the Black Sea) practically does not influence the washout degree of the concrete mixtures.
2) The type of water environment influences the washout degree in the surface layer of the concrete mixtures, it being approx. 15% higher than that in sea water.

The salt content in the Black sea water is the following: NaCl – 11.96 g/l, $MgCl_2$ – 1.436 g/l, $MgSO_4$-1.017g/l, $CaSO_4$-0.509 g/l. The solubility of calcium hydroxide is greater due to presence of chloride, sulphate and other opposite charge ions (see Table 4).

Table 4 Ion composition of the Black sea water

IONS	ION CONTENT OF SALTS:	
	g/dm^3	%
Na^+	4.20 - 4.70	28.74 - 26.02
K^+	0.10 - 0.14	0.68 - 0.78
Ca^{2+}	0.17 - 0.28	1.16 - 1.55
Mg^{2+}	0.52 - 0.68	3.57 - 3.76
Cl^-	8.28 - 10.74	56.67 - 59.47
Br^-	0.01	0.07 - 0.06
SO_4^{2-}	1.16 - 1.34	7.95 - 7.42
CO_3^{2-}	0.17	1.16 - 0.94
Total	14.61	100%

It is experimentally evaluated that the solubility of calcium hydroxide is more than two times greater in the Black sea water than in the drink water.

The method adopted for studying the properties of underwater-cast concrete is based on [1], with certain changes made in order to approximate maximally the real technological conditions. The method allows to obtain samples by which it is easy to determine the physico-mechanical characteristics of the underwater cast concrete By using that method it is possible to model underwater casting under conditions of common and aggressive water environment (Figure 3). A densely perforated 650 mm high PVC pipe (2) is placed in a 700 mm high container (1), pre-filled with water up to level (550-600) mm. A polymer net (2b) and a glass veil (2c) are placed inside the pipe. These two materials form a drain layer which provides all-sided access of water to the cast concrete mixture and prevent the holes of the perforated pipe (2) from blocking.

The concrete mixture is delivered through the PVC tremie (3), which is fitted with a delivery funnel (4) at its upper end.At the lower end of the pipe (3) a rubber valve (5), was provided which prevents water inrush into the tremie before the concreting starts. The rubber valve is very similar to the "go devil" device used in practice, which performs the same function. The valve is kept tight to the tremie mouth by means of a polymer cord (6).

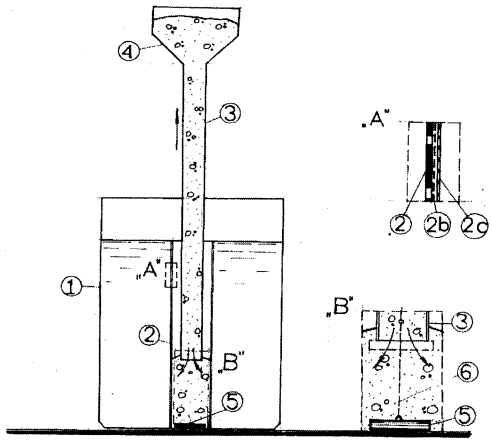

Figure 3 Modelling underwater concreting under lab conditions.
1 - water container; 2 - perforated pipe; 2b - polymer mesh; 2c - glass veil; 3 - tremie; 4 - delivery funnel; 5 - rubber valve; 6 - metal cord.

A layer of sand, gravel or some other material can be placed on the container's bottom so as to model the foundation base.

The casting is carried out continuously, the pipe (2) being filled with the tested concrete mix. The tremie (3) rises smoothly and its lower end should be continuously immersed in the concrete mix.

After concreting is done, a 650 mm high cylinder, about 100-105 mm in diameter, is formed. The stripping of the moulding is carried out after 48 h when the concrete has reached the required strength thus avoiding possible damages. After ageing for at least 7 days, the cylinder is cut into pieces (Figure 4) in order to form samples, which are used to determine the mechanical properties of the concrete obtained.

In order to eliminate the effect of the end sections of the cylindrical moulding, the uppermost and lowermost parts (approx. 5 cm) are cut off.

Similar concrete cylinders are formed simultaneously with the underwater-cast concrete, which are made of a concrete mixture of the same composition but cast in air. After 1 day the "cast in air" concrete is stripped and then stored underwater while being tested. By cutting into pieces, as in the case mentioned above, similar cylindrical samples are obtained (100/100 mm) which are used for check tests.

Several days before testing the compressive sides of the cylinders are smoothed with fine-grained cement-sand mortar.

The method allows to study the effect of a number of factors on the physico-mechanical properties and structural characteristics of underwater-cast concrete.

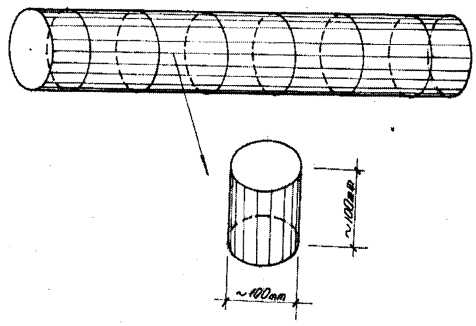

Figure 4 Producing of samples

Two series of samples - cast "in air" and underwater - were prepared from each concrete mixture according to the methods described. On the 28th day the samples were tested to determine their compressive strength. The results obtained are presented in Table 4. The results given in brackets refer to concrete obtained with sea mixing water and cast in sea environment.

Table 5 Strengths of concrete cast underwater and "in air"

COMPOSITION No.	COMPRESSIVE STRENGTH, MPa		DIFFERENCE, %
	under water	in air	
1	20.09 (26.30)	25.02 (29.30)	-19.70 (-10.2)
4	35.04 (50.05)	41.0 (51.90)	-14.59 (-3.55)
5	29.05 (32.08)	30.25 (34.91)	-3.97 (-6.0)
15	35.46 (40.76)	30.25 (38.4)	+17.22 (+7.19)

*Note: 1) The mix numbers correspond to Table 1

GENERAL

1) The method proposed gives a very clear idea of the change in the concrete strength in underwater casting and is suitable for establishing optimal compositions of the concrete mixture when using the respective admixtures (chemical and mineral) under laboratory conditions.

2) The decrease in strength of underwater cast concrete compared with those cast in air varies within 4 - 20%. It is reduced with increasing the concrete mixtures resistance to washout. This is achieved by enhancing the compactness of the cement paste by adding mineral and chemical (antiwashout) admixtures.

3) The use of silica fume and superplasticizer ensures the highest strength in underwater concreting despite the strength decrease by approx. 14.5% as compared with concrete cast in air.

4) The sodium carboxymethyl cellulose decreases the washout degree of the underwater cast concrete by increasing the viscosity of the mixing water. It can be seen that in mixture 3 the difference in the "in air" and underwater cast strengths is minimum, bearing also in mind the fact that the influence of the method of casting here will be considerably higher as compared with the real conditions due to the considerably lower volume of the casts.

5) The concrete with sea water exhibit higher strength than those with drinking water, the difference being between 10 and 40 %. This fact was confirmed by additional tests and allows to use mixing sea water for building concrete structures.

As was mentioned above, the structure of the underwater-cast concrete is formed in continuous contact with the water environment. The concrete changes its original composition in the surface layer (the W/C ratio increases and the cement paste relative content decreases) and hence we should expect a substantial change in the strength properties. Unfortunately, it is impossible to obtain the necessary samples for determining the compressive strength in the surface layer of the underwater-cast concrete.

It is well known that there is a correlation relationship between the surface hardness of the concrete or rather, its mortar component, and its compressive strength. This relationship underlies some non-destructive methods for determining the probable compressive strength of concrete. In this particular case, the relationship was used to get some idea of the change in the hardness and the strength, respectively, of the underwater-cast concrete in its surface layer. For the purpose, cylindrical samples were used, 150 mm in diameter and height. The samples were pressed between the plates of compressive press. The force applied was greater than 30 KN. The plastic imprints were inflicted on the concrete surface by a HPS apparatus. There is a standard correlation between area of imprints and hardness of concrete, and compressive strength respectively. After determining the concrete hardness by the total surface of the samples (actually 0.2-0.3 mm inside), a 1 cm thick layer was cut out of them in tangential direction according to Figure 5. The surfaces of the cut sections were smooth enough and additional grinding was almost unnecessary. New imprints were laid on the cut surfaces and then again a 1 cm layer was cut out, etc.

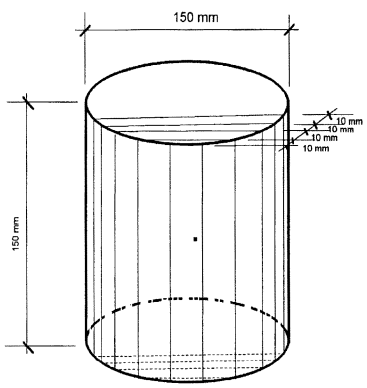

Figure 5 Cut out of 1 cm-layers

Simultaneously, non-destructive testing of concrete of the same composition but cast in air, was being carried out. The testing in depth of concrete continued until the diameters of the imprints obtained on the surface of the underwater-cast concrete and those on the surface of the common concrete became equal, i.e. until their strengths became equal. The results obtained from the determination of the surface hardness of concrete are presented in Figure 6.

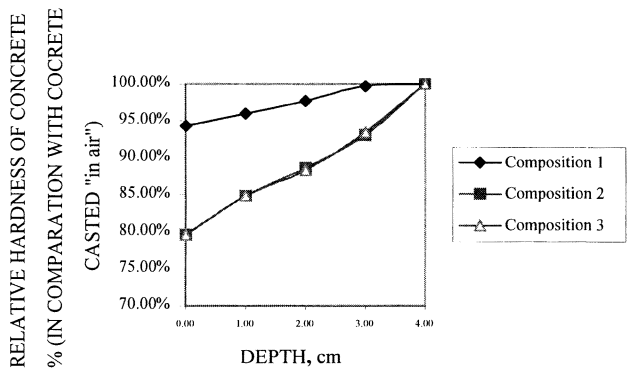

Figure 6 Change in the hardness of the underwater concrete
*Note: 1) The mix numbers correspond to Table 1

It is obvious that at a depth of about 4-5 cm from the concrete surface the hardness, and the probable compressive strength, respectively, of the underwater-cast and the common concrete becomes equal. The change in hardness is more clearly expressed in compositions 2 and 3 which have considerably lower W/C ratio, which definitely accelerates the water diffusion in depth of concrete, whereas in composition 1 the balance between the concrete mix water content and the environment is achieved faster. Taking into account the standard relationship (BSS 3816-84) between the surface hardness and the probable compressive strength, the change of the latter in the underwater-cast surface layer would have the following character (Figure 7):

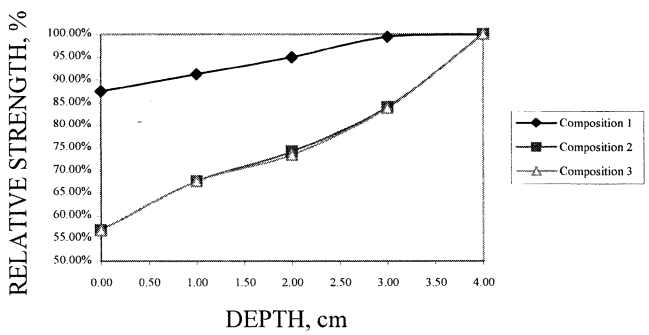

Figure 7 Change in the compressive strength of the underwater concrete
*Note: 1) The mix numbers correspond to Table 1

We can expect that the change in the composition of the underwater-cast concrete will have a considerable effect on its porous structure and its change in depth. From what we have just said it follows that one way of determining the effect of the water environment on the forming concrete structure is by studying its pore space and the changes occurring in that space.

Two series of samples from each concrete mix were prepared - cast "in air" and underwater-cast. At a certain age the samples were tested for determining the concrete compressive strength by the standard destructive method and then samples of the cement mortar component were taken from different depths according to the scheme (Figure 8).The results obtained definitely illustrate the common tendency toward a change in the character of the pore space of the hardened concrete. Figure 9 presents the integral curve of distribution of the pores by sizes for concrete 1 (without admixtures).

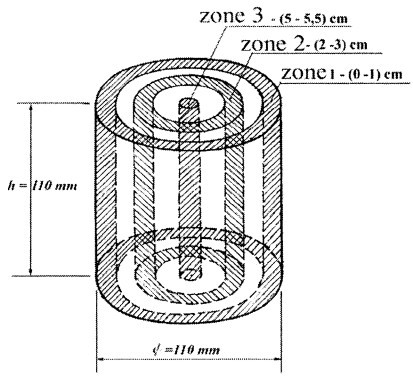

Figure 8 Taking of cement mortar samples

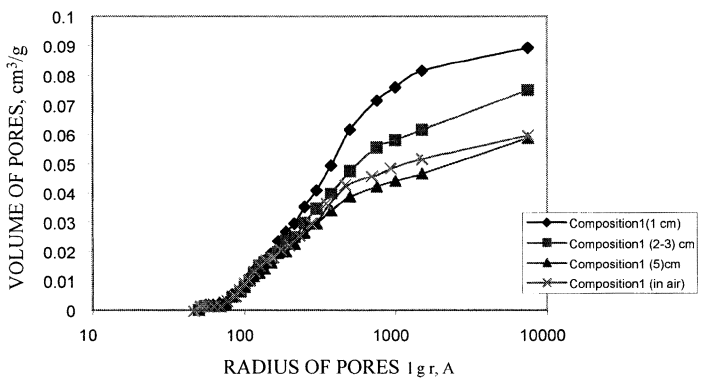

Figure 9 Integral curves of pore-size distribution

There is some displacement of the integral curves in height, i.e. in relation to the pore volume, the increase of the latter concerning the whole investigated range, which is obvious from the differential curves of pore distribution by size - Figure 10.

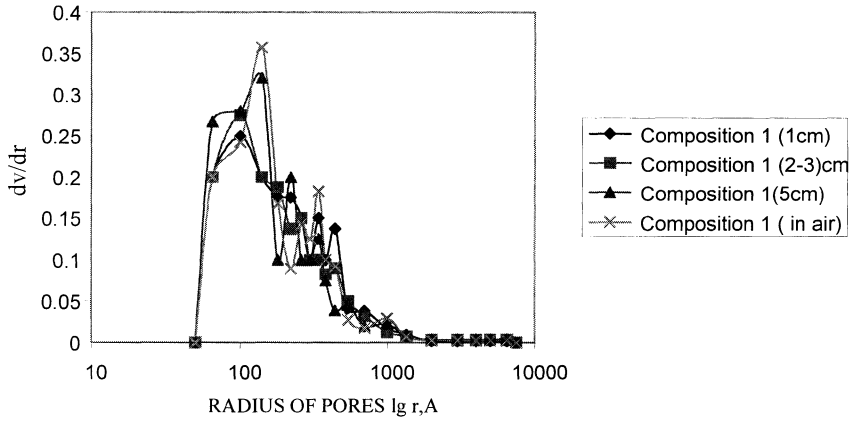

Figure 10 Differential curve of pore-size distribution

On the basis of the results obtained we can draw the following basic conclusions:

1). Due to the water diffusion in the concrete structure, the cement stone in the surface layer forms at a higher W/C ratio thus causing an increase in the cement pore volume. At a depth of 4-5 cm the pore volume is practically identical with that of common concrete cast in air and having the same composition.

2). The increase in the pore volume in the surface layer of the underwater-cast concrete occurs at the expense of the pores from the whole investigated range and not only at the expense of part of them.

The change in pH in depth of underwater-cast concrete was tested by the following method. Cylindrical samples were tested by the standard destructive method for determining the concrete compressive strength. Then, according to Figure 8, sample was taken from soluble concrete component. The single samples were mixed to obtain an average sample.

The compositions of the tested concrete were selected by the method shown in Table 6 in order to take into account the type of mixing water and water environment on the change in pH in the surface layer of the underwater-cast concrete. The concrete age was 1 year.

Concerning the data presented, it is interesting to note that the concrete prepared with fresh water but cast in seawater environment are found in the most unfavourable situation. In this respect, the situation is particularly serious with the check concrete whose structure is more pervious. We should also note the fact that until now a considerable decline in the performance index level for concrete prepared with sea mixing water and cast in sea environment has not been recorded. Certainly, 1 year of age is quite a short period to make

basic conclusions on the development of corrosion in the concrete. The results obtained give good grounds to recommend an increase in the thickness of the protective concrete coating of the reinforcement to over 50 mm in view of its reliable protection against corrosion for a longer service life.

Table 6 Concrete composition, type of water environment and change in pH value in depth of concrete

No.	CONCRETE COMPOSITION	TYPE OF MIXING WATER	TYPE OF WATER ENVIRONMENT	PH VALUE IN DEPTH:		
				0 - 1 cm	2 - 3 cm	5 cm
1	Cem.=400;Sand=650; Cr.St.=1000;W=240.	Fresh	Fresh	11.84	12.17	12.53
2	Cem.=385;SF=33;Sand=680;Cr.St.=1046;W=202; HWRA – 2% from Cem.	Fresh	Fresh	11.84	12.13	12.45
3	As concrete No.1	Fresh	Sea	11.64	12.62	12.77
4	As concrete No.2	Fresh	Sea	12.05	12.44	12.55
5	As concrete No.1	Sea	Sea	12.57	12.8	12.8
6	As concrete No.2	Sea	Sea	12.43	12.73	12.73

It can be expected that, when concreting in sea environment, pH will decrease considerably in the course of time due to the presence of ions in its composition, which favour the dissolution of calcium hydroxide.

REFERENCES

1. DARAKCHIEV, B.D., "Research method for underwater-cast concrete" (Pat. No.47462 от 29.12.1993г.)

2. SAUCIER,-K.L.; NEELEY,-B.D.,"Antiwashout admixtures in underwater concrete, Concrete-international-Design-and-Construction, v.9,no.5, p.42-47, 1987.

3. KHAYAT, K.H., "Effects of antiwashout admixtures on fresh concrete properties", ACI-Materials-Journal, vol.92, No.2, p.164-171, 1995.

4. ROSTOVSKY I. AL., DARAKCHIEV B.D., Factors influencing the washout degree of concrete mixtures for underwater concreting, Proceedings of 9-th International conference on Mechanics and technology of composite materials, September 11-14,Sofia, Bulgaria.

5. DARAKCHIEV B.D., ROSTOVSKY I. A.L., Underwater concreting – modeling and lab strength tests, (as 5).

6. ROSTOVSKY I. A., Porous structure of underwater cast concrete by the "Contractor" method, Proceedings of scientific session 2001", 29.05-01.06.2001, Sofia.

DIVER TRAINING FOR PROFESSIONAL ENGINEERS

T J Collins
Collins Engineers, Inc
United States of America

ABSTRACT. The structural condition of underwater portions of facilities is often crucial to the safety of the general public. Often the responsibility for assessing that condition is left to divers trained as construction workers, rather than structural engineers trained as divers. Training engineers to be divers and using them appropriately poses problems for public and private organizations because of legal constraints such as labor laws and safety concerns. Australia, Canada, the United Kingdom and the United States have such laws, of varying severity and control. Additionally, standards of non-government organizations for training and operations developed for, or adopted or accepted by governmental organizations place further restrictions on the use of engineers as divers. Under some regulations, limited application of those regulations may make it easier to train and employ engineers for limited, specific tasks related to inspection such as engineering inspections but, in general, engineers performing relatively simple underwater observation tasks in shallow benign waters must adhere to the same regulations as divers working at greater depths and performing hazardous tasks such as underwater cutting and salvage. In the U.S., a number of private consulting engineering firms have trained and organized to conduct underwater inspection work in accordance with applicable labor and safety laws. In 2001, the American Society of Civil Engineers developed and published a standard practice manual for underwater investigations which recognizes the importance of engineer-divers and provides guidelines for employing them.

Keywords: Diving, Diver, Engineer-diver, Safety, Training, Underwater.

Thomas J Collins, S.E., P.E., is the President of Collins Engineers, Inc. Chicago, IL, USA, a consulting engineering firm with offices in the U.S. and Ireland, specializing in transportation facilities, especially underwater inspection, and design of repairs and design of new bridge and waterfront structures. Mr. Collins was Principal Instructor of the U.S. Department of Transportation's demonstration projects for Underwater Inspection and Underwater Evaluation and Repair, programs which were presented to governmental agencies throughout the U.S.

INTRODUCTION

Diving operations have been conducted in conjunction with construction and salvage activities since at least the 1830's when Augustus Siebe developed the first practical diving helmet. Historically, divers have been jacks-of-all-trades and might perform any number of underwater construction tasks as needed. The diver, ideally, became more a more proficient diver and underwater tradesman through on-the-job experience. The forces acting on the diver were not fully understood in the early days of diving, and a diver had to be a tough and healthy individual -and lucky [1].

The Siebe diving helmet served with little change or improvement, until the 1940's when Jacques Cousteau and Emil Gagnan developed a practical open circuit scuba (self-contained underwater breathing apparatus), and later led to the current diving helmet. The forces acting on the diver also became better understood during the twentieth century. These developments opened underwater work and recreation to the general public and especially to scientists with less diving training, but better technical skills and a better understanding of the underwater environment.

In the 1960's, engineers began to engage in diving operations to conduct inspections and observe underwater construction activities. By the 1980's, a number of consulting engineering firms and governmental agencies in the United States had trained engineers as divers, recognizing the advantage of using engineers trained as divers to make engineering evaluations and judgments compared with having those evaluations and judgments made by a construction diver who, though he might be an excellent diver and builder, lacked the engineering training and experience to recognize the structural significance of the conditions he encountered.

In fact, it has been the experience of some owners that although a non-engineer may not recognize the importance of subtle damage, such as the uniform erosion of cross sections of a timber pile, it is more likely that the non-engineer diver will raise undue alarm over a minor defect which may appear to the untrained diver to be important, such as an isolated void in a massive concrete unit.

Over the years, as more diving operations were conducted by engineers and as more formalized safety regulations were promulgated for diving, it became clear that recreational dive training, through which many people were introduced to diving, would not suffice for more severe environments in which commercial divers, i.e., both construction divers and engineer-divers, may have to function.

In the United States, although there is competition from firms employing construction divers, and continuing pressure from trade groups dominated by construction divers, to promote their members for the work, most underwater engineering evaluations are conducted by engineer-divers.

Engineer-divers, through the professional activities of the Coasts, Oceans, Ports and Rivers Institute (COPRI) of the American Society of Civil Engineers (ASCE), over about five years, developed an *Underwater Investigations, Standard Practice Manual* which was published in 2001 [2]. The manual provides guidelines and methods for conducting underwater engineering assessments of most types of waterfront facilities, only specifically excepting offshore structures and nuclear facilities. It deals only with the technical qualifications of the

inspectors, and technical inspection and assessment methods, recognizing that diving competence is a necessary component of underwater assessments, but not within the scope of that engineering manual.

LEGAL CONSTRAINTS

There are minimum health and safety requirements and related to diving operations in developed countries. Some countries also mandate periodic underwater inspections of structures such as bridges.

Health and Safety Requirements

United States

In the United States, the federal Occupational Safety and Health Administration (OSHA) establishes the minimum safety regulations for all work places, and specific requirements for diving operations are contained in the Commercial Diving Standards, Subpart N [3]. It proscribes minimum training requirements, minimum operational procedures and equipment requirements, and record keeping requirements. The employer is responsible for ensuring that the employee diver complies with all regulations. The individual states may also operate under their own "mini-OSHA" standards, provided that they are at least as strict as the federal standards, and many states have adopted diving standards very similar to the U.S. federal requirements.

In the U.S., although minimum operational and training requirements are described in general terms, the specificity of the training standards are generally less restrictive than in other parts of the world. The OSHA standards require that the diver be trained for the type of work he will be doing, but leaves it to the employer to determine what that training should be, allows on-the-job training, and does not mandate specific competency testing. All members of the dive team must hold a current certification in first aid.

In the U.S., although a diver may have to demonstrate proficiency and experience to a potential employer in order to be hired, there is no requirement that a diver maintain a log of his diving experience or maintain a record of health examinations. The federal standards do not require a physical examination by a doctor, but most states that have specific dive safety standards require the employer to furnish the medical examination at no cost to the diver.

There is also no requirement for the employer to notify the federal or state OSHA agency when it is performing diving operations and is only required to retain documentation of diving activities in the event of a diving accident.

Canada

In Canada, "Part XVIII - Diving Operations, Canada Occupational Safety and Health Regulations" sets the minimum requirements for diving operations (except for offshore diving). Individual provinces, such as Ontario and British Columbia, have also developed more restrictive diving regulations. The provincial regulations incorporate by reference the Canadian Standards Association Standard (CSA) Z275.2-97, "Competency Standard for Diving Operations [4]."

The Canadian regulations require that prior notice of any diving operation be provided to the ministry so that occupational safety inspectors can be present at the diving operation site. Each diver must keep a personal log in which he records each dive he performs, and this log must be available at the dive site for inspection. The regulations also generally require a minimum of a three-person diving team. Each diver must also have undergone a medical examination.

United Kingdom

In the United Kingdom, health and safety at work, including specific provisions for diving, is regulated by the Health and Safety Executive. Most of the specific regulations governing diving are contained in the Diving at Work Regulations 1997 (DWR) [5]. DWR covers all types of diving and divers at work.

The regulations apply not only to the diver and employer, but also impose a responsibility for health and safety on everyone involved, including the client who has a responsibility to ensure the diving contractor is competent, the work site is safe to use, informing the diving contractor of known hazards, and providing support in the event of an emergency.

Under the DWR, a diving contractor, who plans and conducts a diving project, must be appointed by the person for whom the work is being performed. The diving contractor must appoint a supervisor who is responsible for each diving operation which is part of a diving project.

The diving contractor has the primary responsibility to ensure a safe diving project. He must assess the risks, and ensure that the project is properly planned, that the divers are properly equipped, trained and competent and that all relevant regulations are complied with. The diving supervisor, who must be appointed in writing by the diving contractor, is responsible for the on-site safety and direct control of the diving operation.

The divers must hold an approved qualification for diving and a certificate of medical fitness issued annually by an HSE approved medical examiner. In order to obtain a diving qualification, a diver's competence must be assessed by an organization recognised by HSE. HSE recognises three standards of commercial diving competence: Scuba Diving, Surface Supplied Diving and Closed Bell Diving. Divers must obtain a first aid at work qualification in order to complete their initial diving assessment, and the diving contractor has the responsibility to provide sufficient personnel trained in first aid at the dive site.

The DWR do not specify in detail how the diving work must be carried out, but the Health and Safety Commission (HSC) has published a set of five Approved Codes of Practice (ACOP), one each for Commercial Inland Inshore, Media, Commercial Offshore, Recreational, and Scientific and Archeological diving [6]. The appropriate ACOP, provides practical advice on how to comply with DWR.

Australia

All commercial diving operations in Australia are governed by Australian Standard AS2299, Occupational Diving Operations, a joint standard with New Zealand [7]. Its requirements are similar to the requirements of United Kingdom in many areas. It also requires that divers be trained in accordance with Australian Standard AS 2815 - Training and Certification of

Occupational Divers [8]. Many of the Australian states also have dive safety regulation patterned on the Commonwealth standard.

The Australian Diver Accreditation Scheme (ADAS) is a program designed to meet the training requirements of the standard. It is administered by the Australian Department of Industry, Science and Resources. ADAS provides accreditation to divers who have been assessed by an ADAS accredited diver training establishment as meeting the competency requirements of the relevant standard.

The AS2815 standard provides for four levels of accreditation: Part 1 - Scuba Diving to 30 meters; Part 2 - Air Diving to 30 meters; Part 3 - Air Diving to 50 meters; and Part 4 - Bell Diving [9, 10]. Restricted accreditation is also available for persons whose diving does not require training in all of the underwater tasks in the standard. Generally, certification in accordance with Part 3 is considered the standard for general inshore commercial diving operations. There are other endorsements available that cover supervisory positions and special skills.

ADVISORY AGENCIES AND PRACTICES

American Society of Civil Engineers

In 2001, the American Society of Civil Engineers (ASCE) published *Underwater Investigations Standard Practice Manual* to provide guidelines and methods for conducting underwater engineering assessments of underwater components of existing waterfront structures of all types of facilities except offshore and nuclear structures. The manual is limited to the engineering requirements for conducting underwater facility assessments, and while the manual recognizes the significance of diving and related safety issues, those issues are not within the scope of the manual.

The manual provides an overview of the general requirements for conducting underwater inspections including descriptions of common types of inspections, guidelines for inspection frequency, recommendations for inspector-divers, assessment rating guidelines, guidelines for reports and documentation, descriptions of special testing procedure, and descriptions of approaches to specific types of structures and problem areas associated with those structures.

The manual, which was developed by a task committee of ASCE members and non-members, and peer reviewed, is quite specific recognizing the importance of engineering training and experience, and stating that the underwater inspection team is to be led by and under the direct on-site supervision of a team leader who is a registered, licensed professional civil or structural engineer and a qualified diver who will personally conduct a minimum of 25 percent of the diving inspection work.

The guidelines also require that any inspection team member, involved in underwater inspection, note-taking or documentation, be a trained diver, be a graduate of a four-year engineering curriculum and have been certified as an Engineer-in-Training by one of the United States (or comparable evidence of minimum competence in other countries). The guidelines also permit the inspection work to be performed by technician divers who have successfully completed an 80-hour course of study in structural inspections.

Association of Diving Contractors International

The Association of Diving Contractors International (ADC) has developed Consensus Standards for Commercial Diving Operations which members of ADC pledge to comply with. The Consensus Standards contain recommendations for minimum training, staffing, and diving practices. While ADC has no regulatory authority, many of the provisions of its standards are accepted by most organizations conducting engineering inspection diving operations.

ADC's minimum qualifications for Diver/Tender and Diver are comprehensive, but include many requirements for manual skills training that are not necessary for engineering inspectors. For example, the minimum recommended on-the-job training for a diver includes more than 250 hours of training in cutting, welding and the use of underwater tools.

ADCE was also instrumental in developing an American National Standards Institute, Minimum Standard for Commercial Diver Training, with the Association of Commercial Diving Educators which is similar to the ADC recommendations [11]. In the summary for the standard, however, the Association of Diving Contractors, while endorsing the standard, specifically exempts divers who had achieved equivalent training through field experience or formal instruction.

ADC also provides specific recommendations for staffing diving operations. For surface-supplied air-diving 0-80 feet of sea water (fsw); a 3-man dive team is required; for 80-130 fsw, a 4-person team is required; and for 130-220fsw a 5-man team is required. Additional team members may also be required for some more severe diving operations.

U.S. Navy

The U.S. Navy publishes a comprehensive diving manual which governs its diving operations. The manual is quite comprehensive and covers many types of diving operations. For engineering inspections and evaluations of its waterfront facilities, however, the Navy, despite having the largest number of divers of any organization, retains outside engineering consultants to perform underwater facility inspections.

The standards for its worldwide underwater facility assessments, which began in 1980, require the use of engineer-divers and further require that at least half of all underwater inspections be conducted by engineer-divers who are licensed professional engineers. In evaluating and selecting consultants to conduct their inspections, a qualification-based system is used which places emphasis on engineering competence, while requiring that all diving operations be conducted in accordance with the federal OSHA regulations. Since this is one of the largest and oldest programs in the U.S., its procedures have been adopted by many other organizations.

U.S. Department of Transportation

In the U.S., the National Bridge Inspection Standards (NBIS) require that every bridge be inspected underwater at maximum intervals of five years [12]. The U.S. Department of Transportation's Federal Highway Administration (FHWA) has required that every state establish procedures for conducting the necessary underwater inspections.

FHWA also has established, in very general terms, requirements for the qualifications of underwater inspectors [13]. For complex bridges, the diver should be a qualified team leader, which is a licensed professional engineer or someone with five years bridge inspection experience and who has completed an 80-hour course in bridge inspection. A survey conducted by the Underwater Strictures Inspection and Maintenance Subcommittee of the Transportation Research Board indicated that about two thirds of the individual states that retain outside contractors for underwater inspections consider the services as a professional services contract [14]. Anecdotal evidence indicates that the trend toward the use of engineers as divers by most organizations is to improve the quality of the inspection without significantly increasing the cost.

CONSIDERATIONS FOR TRAINING ENGINEERS AS DIVERS

From a review of the legally mandated safety, training, and certification requirements described above for various jurisdictions, it is apparent that it is much easier for an engineer to conduct underwater inspections in the United States than in other countries. While health and safety requirements of the four countries are generally comparable, the training certification requirements, and the requirements for providing notice of proposed diving operations are more severe in Australia, Canada, and the UK than in the U.S.

In the U.S., there are no specific diver training and certification requirements. The OSHA regulations require that the diver be trained for the task that he will perform, but allow that training to be obtained through the military training and experience, through formal commercial dive school training, or through on-the-job training. There are no federal requirements to obtain any specific certification, although diving schools and the Association of Diving Contractors do provide certification cards. Because of these less stringent regulations, it is easier for an engineer in the U.S., many of whom may have previous recreational diving experience, to obtain sufficient training in the diving skills necessary to conduct underwater inspections.

Because of the engineer's educational background, including physics, chemistry and various structural analysis courses, he has greater in-depth knowledge of the gas laws, pressure relations ships and environmental forces acting on a diver, and understands much of the basic relationships which occupy a large portion of a typical commercial diving school. Similarly, a diver conducting underwater investigations does not need to be trained in underwater welding and burning, and use of underwater power tools, which again occupy a significant portion of a typical commercial dive school curriculum.

CONSULTANT ENGINEER DIVER PRACTICES

In the U.S., there are about ten consulting engineering firms that conduct most of the underwater inspections. These firms generally use diving teams that consist of licensed professional engineer-divers, less experienced graduate engineers-divers, and technician-divers. While some of these engineers were initially trained as divers in the military or in commercial diving schools, most were introduced to diving through recreational diver training, received further practical training on the job. A number of these engineering diving firms have sent their divers to short commercial diver training, or have arranged for special courses in commercial diving that are specifically targeted toward the diving skills that engineers require to safely carry out the diving aspects of their work, and build on the general scientific background of the engineer.

The engineering training related to underwater investigations is similar to the training that would be required for above water inspections, and although most civil engineers have a general background in the assessment of structures, they may not have specific knowledge related to marine damage and deterioration. In the U.S., the most commonly accepted training is an 80-hour bridge inspectors training course developed for FHWA.

CONCLUSION

In the U.S., the practice of training and employing engineers as divers is well established. In Australia, Canada and the United Kingdom, because of more restrictive training laws, it would be more difficult to qualify engineers as divers. However, there are no barriers to using engineers as divers that could not be overcome with sufficient training and obtaining the necessary certifications in these other countries.

REFERENCES

1. U.S. Navy Diving Manual Volume 1 (Air Diving), Revision 3, 15 February 1993

2. AMERICAN SOCIETY OF CIVIL ENGINEERS, Underwater Investigations Standard Practice Manual, Reston, Virginia, 2001, 140pp.

3. OCCUPATIONAL SAFETY AND HEALTH ADMINISTRATION, U.S.A., Subpart N - Commercial Diving Standards.

4. CANADIAN STANDARDS ASSOCIATION, Z275.2-97, Competency Standard for Diving Operations.

5. HEALTH AND SAFETY COMMISSION, UK, The Diving at Work Regulations 1997, London, 1998

6. HEALTH AND SAFETY COMMISSION, U.K., Approved Code of Practice - Commercial diving projects inland/ inshore, Norwich.

7. STANDARDS AUSTRALIA, AS2299.1:1999, Occupational diving operations.

8. STANDARDS AUSTRALIA, AS 2815.1-1992, Training and certification of occupational divers - SCUBA diving.

9. STANDARDS AUSTRALIA, AS 2815.2-1992, Training and certification of occupational divers - Air diving to 30 meters.

10. STANDARDS AUSTRALIA, AS 2815.3-1992, Training and certification of occupational divers - Air Diving to 50 meters.

11. AMERICAN NATIONAL STANDARDS INSTITUTE, ACDE -01-1993, Minimum Standard for Commercial Diver Training, May 1993

12. U.S. DEPARTMENT OF TRANSPORTATION, National Bridge Inspection Standards (NBIS), Title 21, Code of Federal Regulations, Part 650, Subpart C, Revised August 26, 1988

13. U.S. DEPARTMENT OF TRANSPORTATION, Federal Highway Administration, Technical Advisory TA 5140.21 -Revisions to the National Bridge Inspection Standards (NBIS), September 16, 1988

14. TRANSPORTATION RESEARCH BOARD, Unpublished survey conducted by Subcommittee A3CO6(1) Underwater Structures Inspection and Maintenance, 1998

THEME THREE:

TEMPERATURE AND HUMIDITY EFFECTS ON CONCRETE

Keynote Paper

A QUALITY CONTROL SYSTEM FOR READY MIXED CONCRETE IN SAUDI ARABIA

H M Zein-Al-Abideen
Ministry of Public Works and Housing
Saudi Arabia

ABSTRACT: The volume of ready mixed concrete (RMC) construction in The Kingdom of Saudi Arabia (KSA) and other Arab countries has been increasing. There is a misconception that the quality of ready-mixed concrete is always better than concrete mixed on site. The investigation of a large number of cases indicated that the quality of ready-mixed concrete is not up-to-standard and that it fluctuates between good and poor even in one building. It is known that methods of casting, compacting and curing has a big effect on concrete quality; however, things become more critical when the RMC is not conforming to specifications which adds one more factor that may leed to a poor quality concrete. Making sure that plants produced good quality concrete gives the construction industry about half what it takes to obtain good quality buildings and structures. It is very difficult to obtain good quality RMC without having a quality control (QC) system. Quality control systems existing in ready-mixed concrete plants in Saudi Arabia were examined. It was found that in 33% of the cases the systems were not competent. In the remaining 67% of the cases no actual system existed as such. In research, sponsored by King Abdul-Aziz City for Science and Technology (KACST) [1], an effective system is proposed to control quality. The system is developed from one used in most European countries and adapted to suit the conditions of KSA and other Arab Countries. It is based on self quality control (in-house) applied by the plant and complimented by inspection and observation conducted by independent agencies officially authorized to do such work. This paper describes the outlines of a proposed system and how it was adapted from its European counterpart. It is believed that this system will help to substantially improve the quality of concrete. Consequently this reduces building defects and deterioration that result from poor quality concretes.

Keywords: Ready mixed concrete, Quality control, Quality control systems, Concrete standards, Concrete sampling.

Professor H M Zein-Al-Abideen, is the Deputy Minister of Public Works & Housing in Riyadh, Saudi Arabia. He represents the ministry in several national and international organisations. He obtained his Bachelor's Master's and PhD degrees from Hanover and Aachen Universities in Germany. He is a member on ACI Committees 305, Hot Weather Concreting, 364, Rehabilitation; and 437, Strength Evaluation, a member of the Building Research Institute of Germany, and RILEM Committee TC-94. The author of many papers and several books on concrete design and materials, he is the first president of ACI's Saudi Arabia Chapter. Dr Zein-Al-Abideen is a member of the High Commission for the development of Mecca region which undertakes the responsibility of pilgrimage facilities.

INTRODUCTION

Quality control is not a badge to be worn by the engineer or a poster to hang on the wall of his office. Neither it rains from the sky without hard work and persistence. During the construction boom in KSA in the seventies and early eighties there was no clear picture about concrete quality. Information was not available regarding any accurate self monitoring system in RMC plants. There was certainly no follow up or external monitoring over these plants except those performed by some consulting offices or more rarely some governmental agencies. This external supervision was not carried out in a systematic and regular fashion. The task was not assigned to a particular agency to implement. In addition, there is no Saudi standards for RMC that can be referred to for guidance on monitoring QC in plants.

STRENGTH & DURABILITY OF CONCRETE

In the early years of modern urban development of Saudi Arabia (1970s), construction was hasty due to the fast growing needs for building and structures. This has produced much defective concrete and problems started to surface. Some were related to strength and much more due to durability aspects. There is no doubt that the environment in Saudi Arabia may be classified as severe.

The vast area of the Kingdom which occupies the major part of the Arabian Peninsula has undoubtedly a variety of environments. The climate is mostly very hot and varies from arid dry in the middle of the Arabian peninsula to arid humid along the coast of the red sea and more severe along the Arabian Gulf. The geological and geomorphological aspects also affect the concrete industry a great deal vis-a-vis exposure of concrete and reinforced concrete foundations to salts. The contamination of indigenous aggregates with chlorides and /or sulphates is an example of the factors that affect quality of the constituents of RMC which in turn affect the performance of concrete structures from both the strength and more profoundly the durability points of view.

Concrete structures usually have reserved strength and second lines of defence in resisting applied and accidental loads. However, when it comes to durability the defences must be thought about very carefully. The first line of defence in this category is the quality of concrete. Therefore, this paper emphasizes the need for good quality RMC for both strength and durability.

RMC QUALITY INVESTIGATION

In order to find out about the real picture of the quality of RMC in KSA the following procedures were undertaken:

1. Prepared a comprehensive form which was used as a questionnaire.
2. Visited concrete plants and discussed with workers and employees all aspects related to production, storage, maintenance, quality control etc.
3. Attempted to obtain QC figures for both fresh and hardened concrete and constituents of concrete.
4. Depended primarily on figures obtained from the plants over extended periods for several months and sometimes years (where possible).
5. Obtained samples of concrete constituents used in production for independent testing.

The investigation included 33 plants in the major regions of KSA; namely, middle, western and eastern regions which represented 40% of all registered plants. The total production capacity of the plants investigated was 300 000 m^3 per month at the time.

The Rosy Picture Drawn By Plants [2]

When we first received the QC reports that we requested from RMC plants we found that they include magnificent data presented to consultants and owners of public projects. These may be summarized as follows:

- Very low standard deviation for compressive strength 0.5-2.8 MPa.
- Coeffcient of variation indicates that approximately two thirds of the plants provided good or very good quality concrete. The last third produces acceptable quality.
- All factories were achieving the characteristic strength with 5% fractile which is consistent with the low standard deviation values.

This rosy picture did not reflect the real situation indicated by the strength and durability problems in investigations performed on many public and private structures [3], [4] in the seventies and eighties and continuing to surface till these two years of the new Millennium.

Low Standard Deviation (SD)

This section discusses the relationship of standard deviation values and the strength of concrete. It was important to make sure of the correctness of SD reported by RMC plants in KSA compared to those given in countries such as USA & Britain (UK). In 1960 Entroy [5] studied 1600 values of concrete compressive strength and found that average SD = 5.5MPa. Ten years later Metacalf [6] studied 4800 test results of compressive strength after a quality control system was introduced in Britain. The average value of SD obtained was 5.0MPa. In Germany as late as 1989 the reported values of SD [7] range 4-4.5MPa. These values are much larger than the values reported by RMC plants in KSA which is 0.5-2.8MPa. It was hard to believe these figures produced by Saudi plants, especially with the absence of a comprehensive QC system.

Searching for the Truth

From the values of standard deviation discussed above and the impressions the investigation team had visiting plants it was concluded that we can not rely on data provided by plants. Inspite of this suspicion, the information obtained were very important vis-à-vis clarifying the ambiguities and deficiencies in the self-quality control practiced by the plants. The investigation process was three-fold:

- Evaluation of concrete samples taken from the trucks during casting without the prior knowledge of the supplier.
- Evaluation of original records of the plants during a second visit and this was extremely difficult to achieve because of the resistance of the management of the plants.
- Evaluation of concrete constituents used by plants.

The results may be summarized as follows:

a. Actual standard deviation was very high and had very high range 2.7- 9 MPa.
b. Coefficient of variation in 63% of the plants investigated indicates poor to very poor concrete and the rest produce concrete that is merely acceptable.
c. Characteristic strength (with 5% fractile) were not achieved in 60% of the plants under investigation.
d. Cement specifications passed the tests but aggregates and mixing water did not meet the specifications in 50% and 38% of the plants respectively.

PROPOSED QC SYSTEM FOR RMC

A comprehensive system was developed to evaluate the plant production of RMC as well as QC monitoring. The system is comprised of the following main items:

First impression, site, office, administration, aggregates, equipment, storage, fresh concrete, quality control, hot weather concreting precautions transporting concrete etc.

Strategy

1. Classify RMC plants into two categories first and second classes where the first produces only concrete with strength up to 30 MPa whereas the second class produces higher strength concrete and/or special concretes.
2. Develop a new internal QC system which meets the requirements and conditions of KSA connected with an external QC system having a strong enforcement mechanisms capable of motivating good quality and penalizing negligence.
3. Issue standard specifications for RMC.
4. Embark on an awareness campaign for workers, engineers, technicians to educate them for about 6 months. This should be followed by programs to educate the public.
5. Document in organized archives in the plants all information required for external audit by governmental agencies.
6. Pay attention to the quality of aggregates since it comprises the majority of concrete volume and affects most the strength and more profoundly the durability of concrete. Special attention must be given to mixing water since the availability of potent water suitable for concrete is scarce in the Peninsula.
7. In KSA hot weather concerting is a major issue that must be adequately addressed in selecting and storing materials, mixing, transporting, casting and curing.

The Framework of The System

Two main parts of the system:

- Internal monitoring of QC.
- External monitoring of QC.

Two categories of RMC plants:

- Plants that produce concrete of 30 MPa strength, referred to as class RMC1concrete.
- Plants that produce concrete of strength higher than 30 MPa, referred to as class RMC2.

Items included in internal monitoring: (Tables 1and 2):

- Responsibilities (manager, engineers, technicians, laboratories, conformance).
- Requirements (specifications, frequency of testing, procedures if tests fail, statistical evaluation, obtaining samples, reports, hot weather precautions, filing documents. Maintenance).
- QC testing for plants of first category (Table 1).
- QC testing for plants of second category (Table 2).

Only 2 pages of each of Tables 1 and 2 are shown at the end of this paper.

Items included in external monitoring:

- Responsibilities:
- External monitoring has to be performed by an independent agency preferably governmental. However it may be carried out by private agencies under the supervision of the governmental agency which have the fursdiction.

- General requirements:
- The contract, engineers and their experiences training prior to production, data required from the plant, fresh concrete tests, extracting samples, additional testing, times of inspection, unannounced visiting, measures in cases of test failures, joint report prepared by supervising agency, record keeping.

- Inspection:
- Ten unannounced inspection visits every year including four in mid-summer.

- QC Tests:

The tests required to be performed by the independent agency are shown in (Table 3).

Only 2 pages of Table 3 are shown at the end of this paper.

Developing the European (EU) System

The author does not claim that the proposed system has started from scratch; the new system started from the European system and was adapted to be suitable for the conditions in developing countries such as KSA. To this effect the latest versions of the European Codes [10], [11]. The development was carried out under the following main strategies:

1. The general framework of the European systems was utilized [8], [9], [10], [11]. However, a number of modifications were introduced to make it suitable for the industry conditions in the Kingdom as found out from the investigation, and the experiences.
2. The new system is more comprehensive which is very important in the beginning stages to make it easier to apply by including adequate details for the requirements. One of the examples is specifying ten unannounced visits in the new system versus two only in the European. Also, the independent agency for the external monitoring in the EU system may be governmental or from private sector, whereas in the KSA system the supervising agency must be governmental.

3. The two categories of concrete produced in the two systems are the same as explained above. However, in the new system the inclusion of hot weather precautions was included in concrete class 1 (30 MPa and lower) since it is a must in hot countries such as KSA.
4. Standards referred to in the new system had to be a variety of standards from several countries due to the lack of standards in KSA. However, the following new documents were prepared along with the system:
   Specifications for RMC in KSA.
   Equipment and storage guidelines.
   Maintenance guide.
   Indication to local standards/ specifications already prepared in KSA by SASO (Saudi Arabia Standards Organization) such as cement specs.
   aking reference to foreign standards such as ASTM, European, ISO, etc where needed.
5. The new system included more details such as:
   Differentiating between class 1 and 2 concrete from the testing point of view.
   Times of testing are vaguely mentioned in the European system whereas these times are specified distinctly in the new system.
6. Specific tests related to the regions of the country are specified because of the differences in available raw materials.
7. More samples are specified in the new systems to overcome and monitor the effect of larger dispersions in the concrete industry in KSA.
8. The new system indicates specific qualification for the governmental agency which performs the external monitoring.
9. Other factors were included to adapt the system to be suitable for KSA such as:
   Measures to be taken when concrete quality is doubtful.
   Hot weather concreting precautions.
   tandard deviation limits and range in KSA as well as statistical data.
   Educating workers, engineers, administrators and technicians.
10. One of the most important aspects that are included in the system is educating, training, qualifying and certifying all personnel involved in the process.

EFFECTS OF USING THE SYSTEM

The municipality of Riyadh City in collaboration with Professors from King Saud University in Riyadh, have adapted the proposed system and used it since 1995.

A recent investigation was conducted on the performance of RMC plants in the city and it was found that there are noticeable improvements in the quality of RMC produced by the city plants. Samples were taken from plants and tests were carried out on total of 200 samples to obtain characteristics strength (5% fractile i.e. 95% confidence). The samples were taken in groups of twenty. The characteristic compressive strength ranged from 30 – 45 MPa with standard deviation 2.0 – 5.7 MPa compared with a 2.7 – 9.0 MPa previously. These numbers show improvement compared to values obtained prior to the application of the QC monitoring system. The qualitative classification of concrete production showed improvement from poor to acceptable of 20% and from acceptable to good of 22%. Nothing has reached very good or excellent. It is anticipated that the situation will improve further once all aspects of the system are applied and enforced.

COMPUTERIZATION

Program Description

Multimedia Tool Book 3.0 is decided to create a Ready-Mix-Concrete Quality Control computer based system under Microsoft Windows (3.1, 95, 98, ME).

The program is an object-orientated authoring system under Microsoft Windows, which is suitable for design applications as EDUCATION, INFORMATION, INTRODUCTION of PRODUCTS, ORGENIZED DATA BASE, ONLINE PRODUCT DEMONSTRATION programs etc. Toolbook applications consist of DOS FILES called BOOKS, like a printed book with PAGES.

Books in RMC-Q.C. as sample:

1.) Standards
2.) External Q.C.
3.) Internal Q.C.
4.) Site Q.C.
5.) Plant Documentation.
6.) Site Documentation.
7.) Forms.
8.) Researches and Advises.
9.) Advantage of RMC.

The pages are the application's screens, called VIEWERS in "WINDOWS" and contain the information or links to the place of information as well as to other application (word, excel, paint etc.)

- OBJECTS are building the pages and they designed as fields, buttons and graphics. Their function is to act for a special command or to deliver information. They could be accessible from one page only or for the whole book from the background.
- FIELDS are areas in which text, hot words as actor or object-function are placed
- BUTTONS are objects, they act to its behavior by pushing, holding or clicking.
- GRAPHICS are objects direct designed or imported with function or none.

The program allows creating programmed object behavior with many functions as:

MOVE through the book or to other books, QUESTIONING-ANSWERING, HYPERLINK to other application, SOUND and MOVIE-playing, ANIMATION etc.

It is possible to write the ENGLISH and/or ARABIC Language in the so-called book, on page and object. The Programmer Language is called OPENSCRIPT (a kind of BASIC-language) and special designed for this program. The CPU-System must full fill several requirements to run Toolbook. The MICROSOFT products MS-DOS 3.1 or higher, WINDOWS 3.1 or higher must be installed as a basic. The computer should have a CPU with a 20MHz 80386 SX PROCESSOR.A "WINDOWS" compatible MOUSE or POINTING DEVICE should be connected. CD-ROM DRIVE must be present. To store the data on the computer there must be a HARD DISK with 120-MB FREE DISK SPACE and the RANDOM-ACCESS MEMORY of 8MB.A GRAPHIC ADAPTER CARD (Windows-compatible card) is needed to display the graphic with the min resolution of 800 X 600.

EDUCATION

Computer Programs to be Developed in Conjunction with the Research

This section explains proposal regarding computer programs to be developed for education and training purposes and to enable users (RMC Plant personnel, personnel of the External Supervising Agency, and the site engineers of the purchaser) to prepare, run and document all procedures and activities required to perform a comprehensive quality system as specified in the research. It is proposed to develop for each of these purposes separate facilities, namely:

System 1: Programs Supporting Training and Education

The user will be guided through the original research text. By paging through this text he will find highlighted or otherwise marked text. By clicking this highlighted text, he will be able to see explanations to help him to understand the content of the research; e.g. when coming to the place in the research where the 'characteristic strength' is highlighted, the user will be guided to the content of Ref. 4 book explaining the relationship between normal distribution, standard deviation and characteristic strength.

As another example, when the highlighted text is referring to a certain standard or test procedure, by clicking this highlighted text the user will be able to see the content of this standard, may be supplemented by our comments when necessary.

Pictures and sketches may be implemented when explaining the function of a mixer or other mixing equipment or when explaining correct storage of aggregate and appropriate measures providing sun protection. In any way, all subjects we feel are necessary to explain should be highlighted in the text of the research by the research team well in advance as specified in the research.

System 2: Programs Supporting and Controlling Activities and Procedures in a RMC Plant to Establish and Run a Quality Control System

The user of this program facility might be personnel of a RMC plant or a person who has passed already a training course to subsequently work in a RMC plant in the field of quality control.

The user will be guided through topics established and based on the titles and headings of the updated research paper. The overall goal of this program facility will be t to enable the user to establish and run a quality control system as specified in the research paper.

The tool by guiding the user through all activities and procedures of quality control will be on the basis of a 'Quality Control Manual' which has to be established by RMC plants being certified and assessed by an external surveillance agency.

System 3: Programs Supporting and Controlling Activities and Procedures of the External Surveillance Agency

The user of the system will be guided through topics established and based on tiles and headings of the updated research paper.

System 4: Programs Supporting and Controlling Activities and Procedures of the Site (Purchaser)

The user of the system will be guided through topics established and based on Tables 4 and 5 of the research paper

Since the task to develop the computer programs as described is very huge, the programs shall be prepared in 4 phases, starting with the development of the education and training system.

CONCLUSIONS

A comprehensive system has been developed for the quality control (QC) for ready-mixed concrete (RMC) in the Kingdom of Saudi Arabia (KSA). Two major classes of plants are established: one for plants which produce concretes with characteristic compressive strength up to 250 Kg/cm2 (25 MPa). The other class of plants produce concretes with strength greater than 25 MPa and special concretes. The system is supplemented with required specification as well as guides to all its aspects. Internal and external monitoring details were give. Qualifications of governmental agencies assigned to conduct the external monitoring are explained. The system is computer based which facilitates its application and upgrading. The QC system is also linked to an education mechanism to teach plant technicians, engineers, administrators and management as well as employees of the governmental agency(s) responsible for the external monitoring.

An early version of the system was applied in the city of Riyadh where considerable improvement was noticed in the quality of concrete produced by randomly chosen two of the city plants. It is hoped that when the developed system is applied fully will have a very positive impact on the quality of concrete and construction industry in KSA.

REFERENCES

1. ZEIN-AL-ABIDEEN, H M, The quality of ready-mixed concrete in the Kingdom of Saudi Arabia, Progress and Final Reports of a Research Project sponsored by King Abdul-Aziz City for Science and Technology, Riyadh, KSA, 1991.

2. First Progress Report of above Reference.

3. MINISTRY OF BUPLIC WORKS AND HOUSING, Reports on the assessment of existing concrete buildings and structures, authored by several engineers, experts and consultants. MPWH, Riyadh,KSA, 1975-2002.

4. ZEIN-AL-ABIDEEN, H M, Safety assessment of concrete buildings and structures, 2nd edition, Obekan Publishing Co, Riyadh, 1992.

5. ENTROY, H C, The variation of test cubes, Cement and Concrete Association, Research Report 10, 1960.

6. METCALF, J B, The specification of concrete strength, part II, Report LR 300, Research Laboratories, Crowthorn Road.

7. FEDERAL INSTITUTION for Testing Building Materials, Information given by researchers in Munic and Stuttgart, Germany and Graz, Austria, 1989.

8. DIN 1045, Beton and Stahlbeton: Bemesung und Ausfuhrung.

9. DIN 1084/3, Uberwachung (guteeuberwachung) im beton und stahlbetonbau: Teil 3 transportbeton.

10. EN 206-1: 2000, Concrete- Part 1: Specification, performance, production and conformity.

11. EUROCODE 2, Common unified rules for concrete, reinforced concrete and prestressed concrete construction, Chapter 6.4, Quality Control.

Table 1: RMC Manufacturer's Internal Production Control					Plant Type RMC1
CONCRETE CONSTITUENTS		Required Inspections and Tests		Requirements	Frequency
			INITIAL AND PERIODICAL INSPECTIONS		
		1	Check suppliers test certificate	To ascertain compliance with requirements e.g. that tests have been performed and specified properties are confirmed	Prior to first delivery and each shipment that comes from another source than the previous accepted one, but at least every 3 months
		2	Check suppliers delivery ticket and bag/silo labels	To confirm compliance with supply order and delivery to be from the correct source	Each delivery prior to discharge
		3	Check correct storage	To prevent cement from deteriorating	Once per week
			INITIAL TESTS		
1	**CEMENT**		No tests required! Perform initial inspections as mentioned above		
			PERIODICAL TESTS		
			No tests required! Perform periodical inspections as mentioned above		

Table 1: RMC Manufacturer's Internal Production Control						Plant Type RMC1
CONCRETE CONSTITUENTS		**Required Inspections and Tests**			**Requirements**	**Frequency**
		INITIAL AND PERIODICAL INSPECTIONS				
		1	Check supplier's test certificate		To ascertain compliance with requirements e.g. that tests have been performed and specified properties are confirmed	Prior to first delivery and each shipment that comes from another source than the previous accepted one, but at least every 3 months
		2	Check suppliers delivery ticket		To ascertain compliance with supply order and delivery to be from the correct source	Each delivery prior to discharge
		3	Check type of aggregate		For comparison with normal appearance	
		4	Check shape of aggregate			
		5	Check for harmful impurities			
		6	Check correct storage			Once per week
		INITIAL TESTS				
2	**AGGREGATE**	1	Sieve analysis (grading)	SASO 249-1	To assess compliance with RMC specification	Prior to first delivery and each shipment that comes from another source than the previous accepted one
		2	Organic impurities	SASO 250-2	To asses the presence and quantity of impurities	
		3	Water absorption	EN 1097-6	To assess the effective water content	
		4	Impact strength	SASO 251-3	To assess compliance with requirements	
		5	Clay, silt and fines content	SASO 278-4	To ascertain compliance with approved limit values in RMC specifications	
		6	Water soluble chloride	EN 1744-1 SASO 806??	To ascertain compliance with approved limit values	
		7	Acid soluble sulphate	EN 1744-1 SASO 806??	To ascertain compliance with approved limit values	
		8	Alkali reactivity (optional)	ASTM C 586 ASTM C 289 or others	To indicate the general level of reactivity and whether further tests should be made with this type of aggregate	In case of doubts

Table 2: RMC Manufacturer's Internal Production Control					Plant Type RMC 2
CONCRETE CONSTITUENTS		Required Inspections and Tests		Requirements	Frequency
		INITIAL AND PERIODICAL INSPECTIONS			
		1	Check suppliers test certificate	To ascertain compliance with requirements e.g. that tests have been performed and specified properties are confirmed	Prior to first delivery and each shipment that comes from another source than the previous accepted one, but at least every 3 months
		2	Check suppliers delivery ticket and bag/silo labels	To confirm compliance with supply order and delivery to be from the correct source	Each delivery prior to discharge
		3	Check correct storage	To prevent cement from deteriorating	Once per week
		INITIAL TESTS			
1	CEMENT	1	Perform tests of any cement type other than Portland cement (SASO 142) or Sulphate-resistant Portland cement (SASO 570) Tests shall comply with EN 196 or equivalent approved by the Surveillance Agency	To ascertain compliance with requirements of approved standards	Prior to first delivery
		PERIODICAL TESTS			
		1	Perform tests of any cement type other than Portland cement (SASO 142) or Sulphate-resistant Portland cement (SASO 570) Tests shall comply with EN 196 or equivalent approved by the Surveillance Agency	To ascertain compliance with requirements of approved standards	Each delivery that comes from another source than that delivery used for initial testing of fresh and hardened concrete but at least once per year

Table 2: RMC Manufacturer's Internal Production Control

CONCRETE CONSTITUENTS		Required Inspections and Tests			Requirements	Frequency
		INITIAL AND PERIODICAL INSPECTIONS				
2	AGGREGATE	1	Check supplier's test certificate		To ascertain compliance with requirements e.g. that tests have been performed and specified properties are confirmed	Prior to first delivery and each shipment that comes from another source than the previous accepted one, but at least every 3 months
		2	Check suppliers delivery ticket		To ascertain compliance with supply order and delivery to be from the correct source	Each delivery prior to discharge
		3	Check type of aggregate		For comparison with normal appearance	
		4	Check shape of aggregate			
		5	Check for harmful impurities			
		6	Check correct storage		*See comments of Ministry of Health!*	Once per week
		INITIAL TESTS				
		1	Sieve analysis (grading)	SASO 249-1	To assess compliance with RMC specification	Prior to first delivery and each shipment that comes from another source than the previous accepted one
		2	Organic impurities	SASO 250-2	To asses the presence and quantity of impurities	
		3	Water absorption	EN 1097-6	To assess the effective water content	
		4	Impact strength	SASO 251-3	To assess compliance with requirements	
		5	Clay, silt and fines content	SASO 278-4	To ascertain compliance with approved limit values in RMC specifications	
		6	Water soluble chloride	EN 1744-1 SASO 806	To ascertain compliance with approved limit values	
		7	Acid soluble sulphate	EN 1744-1 SASO 806	To ascertain compliance with approved limit values	
		8	Alkali reactivity (optional)	ASTM C 586 ASTM C 289 or others	To indicate the general level of reactivity and whether further tests should be made with this type of aggregate	In case of doubts

Table 3: Monitoring and Certification of Ready-mixed Concrete (RMC) Manufacturers				RMC 1 RMC 2
SUBJECT		**Required Inspections and Tests**	**Requirements**	**Frequency**
		INITIAL ASSESSMENT		
1	**ASSESSMENT OF RMC MANUFACTURER'S INTERNAL PRODUCTION CONTROL**	1 Check RMC manufacturer's production control manual	To assess RMC manufacturer's capability to perform the required production control procedures	Each time before a new RMC plant under a surveillance contract comes into operation or when an already commercially registered RMC manufacturer has asked for assessment, surveillance and certification of his running production
		2 Check the availability of relevant documents being available to the relevant persons		
		3 Check RMC plant manager's qualification		
		4 Check the knowledge, training and experience of RMC manufacturer's staff for production and internal production control		
		5 Check RMC manufacturer's laboratory equipment		
		6 Check the capability of the laboratory when contracted and named by the RMC manufacturer to perform testing as part of his internal production control		
2	**ASSESSMENT OF RMC MANUFACTURER'S PLANT EQUIPMENT**	1 Check stockpiles, bins, store rooms, etc	To ascertain compliance with requirements stipulated in the documents 'Quality Control of Ready-mixed Concrete' and 'Specification of Ready-mixed Concrete'	
		2 Check weighing equipment		
		3 Check admixture dispenser		
		4 Check water meter		
		5 Check equipment for measurement of moisture content of aggregates		
		6 Check the batching system		
		7 Check mixers (including truck mixers and/or agitating trucks)		
		8 Check RMC manufacturer's calibration reports and records		

Table 3: Monitoring and Certification of Ready-mixed Concrete (RMC) Manufacturers				RMC 1 RMC 2
SUBJECT		**Required Inspections and Tests**	**Requirements**	**Frequency**
			INITIAL ASSESSMENT	
3	**ASSESSMENT OF RMC MANUFACTURER'S PRODUCTION AND DELIVERY**	1 Check concrete type catalog	To ascertain compliance with requirements stipulated in the documents 'Quality Control of Ready-mixed Concrete' and 'Specification of Ready-mixed Concrete'	Each time before a new RMC plant under a surveillance contract comes into operation or when an already commercially registered RMC manufacturer has asked for assessment, surveillance and certification of his running production
		2 Check plant diary		
		3 Check batching and mixing instructions		
		4 Check delivery tickets		
		5 Check delivery instructions		
		6 Check other available relevant production reports and records		
4	**ASSESSMENT OF RMC MANUFACTURER'S HOT WEATHER PRECAUTIONS**	1 Check sun protection of aggregate		
		2 Check sun protection of water tanks		
		3 Check sun protection of mixers, truck mixers and/or agitating trucks		
		4 Check aggregate water spraying		
		5 Check water chillers and/or facility for addition of ice		
5	**CERTIFICATION OF RMC MANUFACTURER**	1 Assess RMC manufacturer's internal production control, staff and equipment if he appears capable to run an orderly concrete production	Issue a certificate if requirements are fulfilled and classify the RMC manufacturer as RMC1 or RMC2 as appropriate	

THE PECULIARITIES OF CONCRETE MIXTURE PROPERTIES IN DRY AND HOT CLIMATES

K Abdrakhmanova
Kazakh State Academy of Civil Engineering
Kazakhstan

ABSTRACT. In the present study, the properties of concrete mixture on low water consumption binder basis in dry and hot climate are investigated. It was established the forming of concrete mixture on low water consumption binder basis in high temperature condition is depends from composition, structure, rheological and technological parameters. It was developed the method and the device for complex estimation of forming of concrete mixture on low water consumption binder basis in different temperatures by value of structural viscosity and tixotropy parameters. It was developed the method and the device for definition of lamination of concrete mixture on low water consumption binder by value of solution separation by vibration. Taking into account an influence of the high temperature the kinetics of the change of the technological properties of concrete mixture of different composition on low water consumption binder has been studied. It has been determined that the concrete on low water consumption binder are achieve of required strength in 2-3 days at natural hardening. It will allow producing the concrete materials without thermal-moisture treatment.

Keywords: Low water consumption binder (LWCB), Fine- milled concrete (FMC), Period of outflow, Thixotropy factor, Dry and hot climate.

Dr K Abdrakhmanova, is a Lecturer of the Department of Construction Materials, Products and Construction Technology, Kazakh State Academy of Civil Engineering, Almaty, Kazakhstan. She specialises in the field of resource-saving technologies development of binders systems on the basis of technogenic wastes utilization. Her research interests also include the investigation and use additives in concrete.

INTRODUCTION

The improvement of quality and effectiveness of any concrete and reinforced-concrete products in conditions of dry and hot climate is primarily related to decreasing of defectiveness of the structure subject to environmental influence.

Over the last years, as a result of the elaboration of effective additives including superplasticizers (SP) as well as the methods of production of multi-component binders for mechanical-chemical activation including re-crushing of cement with fine-milled mineral additives and superplasticizers, there are more possibilities to solve problems in improving technology of concrete and reinforced-concrete products in conditions of dry and hot climate at a new level [1].

Properties of any concrete mixture are determined by character and value of effective forces between particles of solid phase and liquid. In concrete mixtures on low water-consumption binder (LWCB) and fine-milled cements (FMC), as a result of higher specific surface of cement particles and the introduction of significant amount of SP, balance of effective forces changes considerably. Internal cohesion increases, but its value is impacted by changes in water-content and vibrating effects.

However, any possible changes in temperature will be at lesser degree manifested in changes in properties of concrete mixture because sufficient saturation of superplasticizers will to some degree neutralize the influence of new cement formations. Since improvement in fineness of cement grind and increasing in the amount of SP is most considerably manifested in concrete mixture but not in hardened concrete, then in changing in cement properties and in saving of cement with the use of LWCB and FMC, great effectiveness (up to 70-80 %) is determined by changing of rheological and technological properties of concrete mixture [2]. Therefore, the determination of these properties subject to any influence of different factors is of great scientific and practical significance.

EXPERIMENTAL DETAILS

Materials

In the works for investigating concrete mixtures and concrete the following materials have been used: Portland cement M-400, as multi-component binder LWCB -50 with slag fillers, FMC-50 with slag and ash fillers, as superplasticizing agent S-3. Big filler –granite rubble with fraction of 5-20 mm, small filler – river quartz sand with gradation factor of 2.03.

Test Method and Equipment

Since concrete mixtures on basis of LWCB and FMC have some features that are difficult to determine through standard methods, the original tools and methods have been worked out: tool for determining rheological features of concrete mixtures that are quickly heated by electric current, tool for determining unmixness of concrete mixtures at different temperatures.

The tool for determining rheological characteristics consists of a plastic cylinder with height of 450 mm and diameter of 132 mm in the bottom of which there is a 100 x 100 mm hole for mixture outflow. The tool is supplied with a controlling device that indicates the concrete mixture level. Power for heating the mixture to the required temperature is supplied through a running disk. Voltage value is regulated by a latr. The base of the tool is isolated. The tool is safely mounted on a platform vibrator with the help of a magnetic device.

The tool for determining pulling force consists of a bunker for fraction, a magnet-controlled damper and potentiometer for registering readings of movements of a rod with a ball in concrete mixture at various temperature. The tool for determining unmixness of concrete mixtures at various temperature is characterized by the fact that a net with 3-5-mm cells is installed through a calibrated hole in the tool for determining concrete mixture outflow.

With the help of these original tools now it is possible to determine period of concrete mixture outflow at various temperatures; factor of concrete mixture thixotropy, viability and water-loss of concrete mixture, unmixness of concrete mixtures of different composition at temperature of 25…45^{0}C, that is typical for dry and hot climate.

To define the temperature influence on placeability of concrete mixture, it was placed in container, in which temperature was maintained at 25°, 35^0, 45°C at relative air moisture of 45-60%. Placeability of concrete mixture during the first 3 hours was determined every 15 minutes and then every 30 minutes.

Based on the investigation of the temperature influence on mouldability of LWCB-based concrete mixtures subject to influence of consumption of binder, water-binder ratio and proportion of sand in filler mixtures, the index of changing in water content in equally workable concrete mixtures at increasing in temperature (K_1) is justified. In number terms it represents increasing in water volume at given temperature to water content required for producing the concrete mixture of given placeability at temperature of 25^{0}C.

To evaluate properties of LWCB-based concrete mixtures that have high thixotropy, it was proposed to use conditional factor of thixotropy, which represents ratio of force of pulling the ball rod from the concrete mixture in the state of rest to force of pulling the ball rod at vibration $K_{thix} = P_1/P_2$ Thixotropy factor approximately characterizes the concrete mixture behavior at vibration. The higher the factor the higher effectiveness of vibration effects.

Optimization of Technology Parameters

The investigation of changing of mobility and period of outflowing of equally workable LWCB-based concrete mixtures and portland cement including those with S-3 additives has shown that the character of their change is different. For portland- cement-based concrete mixtures losses of mobility at increasing in temperature are accompanied by significant increasing in period of outflowing. The application of S-3 reduces mixture viscosity but the character of dependence remains, although mobility loss decreases. In LWCB-based concrete mixture, as temperature increases mixture mobility to be determined by slump decreases while outflowing time that characterizes mixture behavior at vibration changes insignificantly (Figures 1, 2).

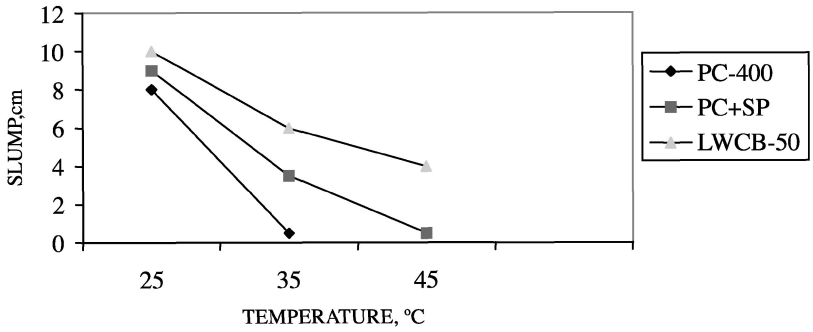

Figure 1 Influence of binder type and concrete mix temperature on mobility of concrete mixture

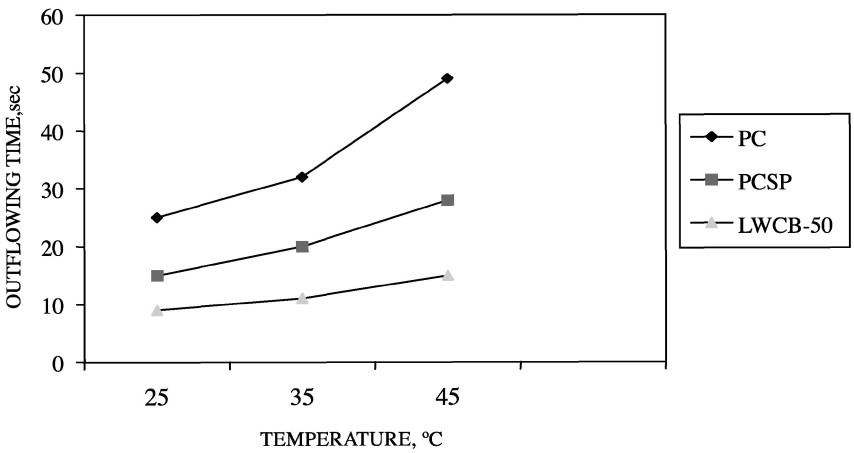

Figure 2 Influence of binder type and concrete temperature on period of concrete mixure outflow

This way, the investigation shows that the binder has a substantial influence on the concrete mixture behavior when temperature increases.

At investigation, binder consumption, water-cement ratio, sand proportion in filler mixtures, SP consumption and concrete mixture temperature have been assumed to be basic factors. Variability interval was set depending on limits of rational oscillations of factors. In accordance with the requirements of mathematic planning of the experiment it was reasonable to aply Box-Benkin plan that, in our opinion, has optimum properties from the viewpoint of the volume of experimental works and to-be-obtained information [3].

Levels and intervals of variability of properties of portland-cement-based concrete mixture with plasticizing additives S-3 are presented in Table 1. Sand proportion in filler mixture was assumed to be 0,42.

Table 1 Factors and levels of variability

FACTOR	LEVELS OF VARIABILITY			INTERVAL OF VARIABILITY
	-1	0	+1	δXi
Consumption of cement , C, kg, (X_1)	250	350	450	100
Water-cement ratio, W/C, (X_2)	0.4	0.5	0.6	0.1
Content of additive , A, %, (X_3)	0	0.6	1.2	0.6
Temperature of mix, T, ^{0}C ,(X_4)	25	35	45	10

Levels and intervals of variability of properties of LWCB-based concrete mix are presented in Table 2.

Table 2 Factors and levels of variability

FACTOR	LEVELS OF VARIABILITY			INTERVAL OF VARIABILITY
	-1	0	+1	δXi
Consumption of low water consumption binder, LWCB, kg ,(X_1)	250	350	450	100
Water-binder ratio, W/B, (X_2)	0.3	0.35	0.4	0.05
Proportion of sand P, (X_3)	0.32	0.42	0.52	0.1
Temperature of mix, T, ^{0}C ,(X_4)	25	35	45	10

Since for LWCB-based concrete mixture the sand proportion influence on mixture properties is not completely studied, the sand proportion is taken into account as one of the factors of the experiment.

As a result of processing of experiment data, polynomial mathematical models of concrete mixture properties have been obtained. After exclusion of insignificant regression factors and check-up of conformity there have been obtained the following equations that describe dependence of concrete mixtures and concrete on to-be-investigated factors:

-concrete mix on PC-based

$$\tau=1417,7 - 716C - 1642W/C - 182A + 0,3T + 127,5C^2 + 592,6W/C^2 + 8,7A^2 + 0,04T^2 + +294,1C*W/C + 65,8C*A - 1,4C*T + 79,1W/C*A - 1,1W/C*T - 0,07A*T$$

-concrete mix on LWCB-50-based

$$\tau = 2441,4 - 2,2LWCB - 9892,5W/B - 1441,4P + 2,8T + 0,001LWCB^2 + 11354,4W/B^2 + +737,1P^2 + 2,2LWCB*W/B + 1,3LWCB*P + 2221,5LWCB*T - 3,6W/B*T$$

-strength of concrete on PC-based at 28-days

$$R = 458,1 + 1,45C + 1055,7W/C + 80,2A - 2,24T - 0,4C^2 - 627,3W/C^2 - 0,2A^2 - 1,3C*W/C - -0,2C*A - 0,4C*T - 56,8W/C*A + 0,04W/C*T - 0,3A*T$$

-strength of concrete on LWCB-50 at 28-days

$$R = 673,4 + 1,35LWCB + 2149,89W/B + 212\ ,39P + 2,45T - 0,3LWCB^2 - 2651,15W/B^2 -$$
$$-165,5P^2 - 0,038T^2 - 0,62LWCB*W/B + 0,099LWCB*P - 0,4LWCB*T - 266,8W/B*P +$$
$$+1,3W/B*T - 0,83P*T$$

Analysis of surface of response of four factor models has shown that as binder consumption increases, viscosity of Portland-cement-based and LWCB-based concrete mixtures increases with increasing in temperature. And vice versa when water-binder ratio increases. Increasing in content of S-3 smoothes out temperature influence on concrete mixture viscosity. Increasing in sand proportion in filler mixture from 0.32 to 0.52 results in decreasing in viscosity at increase of temperature.

When forecasting the water-consumption of concrete mixtures of given mobility or hardness there were investigations for determining the dependence of these properties on the basic factors: normal density of binder, water-demand of sand and rubble and factor that allows for changing of mixture viscosity due to temperature (K_t). Levels of variability of factors are presented in Tables 3 and 4. Sand proportion in filler mixture was assumed to be 0,42.

Table 3 Factors and levels of variability (by slump)

FACTOR	LEVELS OF VARIABILITY			INTERVAL OF VARIABILITY
	+1	0	-1	δXi
Slump, S, cm,(X_1)	13	7	1	6
Water demand of sand W_s, %, (X_2)	9	6	3	3
Water demand of rubble W_r, %,(X_3)	4	3	2	1
Normal density, ND, %,(X_4)	18	17	16	1
Index K_t, (X_5)	1.12	1.06	1	0.06

Table 4 Factors and levels of variability (by hardness on technical viscosimeter)

FACTOR	LEVELS OF VARIABILITY			INTERVAL OF VARIABILITY
	+1	0	-1	δXi
Hardness, H, sec, (X_1)	100	60	20	40
Water demand of sand W_s,%, (X_2)	9	6	3	3
Water demand of rubble W_r, %,(X_3)	4	3	2	1
Normal density, ND, %,(X_4)	18	17	16	1
Index K_t, (X_5)	1.12	1.06	1	0.06

When planning experiments,5-factor plan of Box-Benkin has been used.

As a result of the investigation, mathematical models of the water-consumption of concrete mixture of given placeability have been obtained from to-be-studied factors:

- mobile concrete mixture on LWCB-based

$$W = -1054,6 + 5,4S + 9,26W_s + 14,95W_r + 46,58ND + 1170,82K_t - 0,06S^2 - 0,08W_s^2 + 1,75W_r^2 - 0,89ND^2 - 415,74K_t - 0,03S*W_s - 0,16S*W_r - 0,1S*ND + 1,54SK_t - 0,23W_s*W_r - -0,24W_s*ND + 1,67W_s*K_t - 0,72W_r*ND + 4,9W_r*Kt - 11,7ND*K_t$$

- hard concrete mixture on LWCB-based

$$W = -1204,3 - 0,61H + 2,17W_s + 10,02W_r + 57,36ND + 1373K_t - 0,3H^2 - 0,17W_s^2 - 1,52W_r^2 - - 1,69ND^2 - 632,1K_t^2 - 0,6H*W_s - 0,6H*W_r - 0,3H*ND - 0,21H*K_t + 0,04W_s*W_r - - 0,3W_s*ND + 4,8W_s*K_t - 0,33W_r*ND + 14,42W_r*K_t + 0,13ND*K_t$$

Figure 3 shows isolines of mobility and hardness of concrete mixture of given placeability depending on water-consumption, temperature and for different values of slump and hardness.

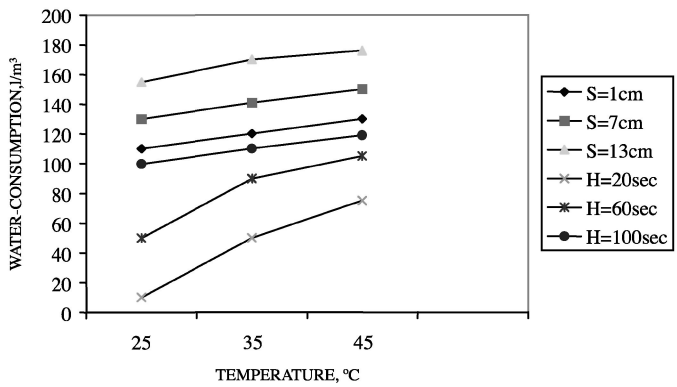

Figure 3 Isolines of mobility and hardness of given placeability depending on water-consumption and temperature

With the help of these dependence it is possible to carry out the task of rational selection parameters to produce concrete mixture and concrete with given properties to apple then in construction in conditions of dry and hot climate.

DISCUSSION

Results of experiments on the evaluation the influence of binder type and concrete mixture temperature on thixotropy factor, which are presented in Table 5, indicate that LWCB-and FMC-based concrete mixtures are characterized by increased internal cohesion in initial state at unbroken structure. Subject to vibration, these mixtures quickly lose their internal cohesion indicating increased thixotropy. As a result, these mixtures subject to vibration are well placed and packed.

Table 5 Influence of binder type and temperature on concrete mix thixotropy factor

TYPE OF BINDER	W/B	ADDITIVE S-3,%	SLUMP cm	FORCE OF PULLING*, kg/cm^2, BY TEMPERATURE,^{0}C			THIXOTROPY FACTOR, BY TEMPERATURE,^{0}C		
				25	35	45	25	35	45
PC-400	0,61	-	11	12.4 / 0.77	23.8 / 0.87	36.1 / 0.95	16.1	27.3	38.0
PC-400	0,52	0,6	10	21.1 / 0.75	36.8 / 0.85	43.3 / 0.98	28.1	43.3	44.2
LWCB-50	0,39	-	12	26.7 / 0.35	44.1 / 0.41	47.4 / 0.45	62.1	107.5	108.3
FMC-50	0,53	-	10	13.2 / 0.55	17.5 / 0.59	32.6 / 0.61	24.0	29.6	53.0
FMC-50	0,43	1	12	21.5 / 0.47	31.1 / 0.49	36.2 / 0.51	45.7	63.5	71.0

* over the line – force of pulling without vibration
under the line – force of pulling by vibration

Temperature at lesser degree impacts on the internal cohesion of LWCB-and FMC-based concrete mixture as compared with PC-based concrete mixtures. These properties of LWCB and FMC-based concrete mixtures confirm their high effectiveness when applied in conditions of dry and hot climate.

One of the important characteristics of concrete mixtures, which condition on possibility of their application in conditions of dry and hot climate is kinetics of their placeability by time.

It has been determined that LWCB-50-based concrete mixtures with binder consumption of 350 kg/m^3 at initial slump of 10 cm, in 1,5-2 hours of exposure at 35^{0}C had the slump of 6-7 cm, while PC-based concrete mixtures had the same slump only in 45 min. The rates of decreasing in mobility of concrete mixtures on the basis of LWCB and those on portland - cement with S-3 additive are almost the same.

Decreasing in placeability at high temperature depends on concrete mixture water-loss rates. Based on experimental data, it may be assumed that quantity of water to be evaporated from LWCB-based concrete mixture at high temperature is considerably higher then from portland-cement-based concrete mixture for the same period. It is related to properties of the LWCB-based concrete mixture structure, in which quantity of free water is considerably lower.

When applying mushy LWCB-based concrete mixtures, one of the important task is to secure their resistance to unmixness. The rates of unmixness of concrete mixtures on the basis of PC, LWCB-50 and FMC-50 at consumption rate of 350 kg/m^3 were determined by quantity of separated cement slurry at 3 min vibration.

Results of testing are presented in Table 6.

Table 6 Consumption of materials and results of the investigation of separated cement slurry

CONSUMPTION OF MATERIALS, kg/m^3				W/B	ADDITIVE S-3, %	SLUMP cm	DENSITY OF CONCRETE MIX kg/m^3	QUANTITY OF SEPARATED CEMENT SLURRY, %, BY TEMPERATURE, ^{0}C		
Binder	Water	Sand	Rubble					25	35	45
PC-400										
350	175	778	1074	0.5	-	1	2350	5.21	4.89	3.72
350	222,5	725	1000	0.64	-	12	2260	9.7	9.29	8.43
350	235	713	984	0.67	-	20	2255	16.35	15.52	14.08
350	175	778	1084	0.5	0.6	2	2310	7.25	6.49	5.48
350	180	770	1064	0.52	0.6	10	2245	8.13	8.0	7.79
350	210	740	1021	0.6	0.6	20	2235	19.18	17.6	14.9
LWCB-50										
350	135	824	1140	0.38	-	1	2375	4.36	4.0	3.8
350	140	816	1127	0.4	-	10	2395	6.26	6.0	5.38
350	175	778	1074	0.5	-	20	2285	15.7	14.5	13.6
FMC-50										
350	126	812	1126	0.42	1	1.5	2205	8.5	7.9	7.59
350	160	805	1111	0.47	1	10	2295	9.47	8.7	8.3
350	180	778	1074	0.52	1	20	2270	14.76	14.04	13.05
350	144	824	1140	0.39	2	1.5	2296	5.17	4.4	3.9
350	146	816	1127	0.42	2	10	2380	5.98	5.2	5.5
350	175	778	1074	0.5	2	20	2320	14.5	14.0	13.89

As slump of to-be-investigated concrete mixtures increases, quantity of separated cement slurry increases. Increasing in temperature from 25 ^{0}C to 45 ^{0}C insignificantly impacts on value of cement slurry separation. Therefore, the application of mushy LWCB-based concrete mixtures in conditions of dry and hot climate is effective because these mixtures contain lesser quantity of water and they are insignificantly influenced by temperature. LWCB-based concrete mixtures are set for longer periods. However, further they are set more quickly as compared with portland-cement-based concrete. Kinetics of setting of some concretes with different binder is presented in Table 7. From these data it is apparent that LWCB-based concrete in conditions of dry and hot climate achieves temper hardness (70%) for 2-3 days of natural setting.

Table 7 Kinetics of setting of some concretes with different binder

CONSUMPTION OF BINDERS, kg/m^3	W/B	ADDITIVE, S-3, %	SLUMP, cm	DENSITY OF CONCRETE MIX, kg/m^3	STRENGTH OF CONCRETE AT THE AGE, DAYS, %, BY TEMPERATURE, ^{0}C								
					25^{0}C			35^{0}C			45^{0}C		
					1	7	28	1	7	28	1	7	28
PC-400													
350	0.5	0.6	1	2376	26.4	77.5	100	26.7	86.5	100	30.2	84.9	100
350	0.55	0.6	10	2360	27.9	83.5	100	30.5	85.7	100	32.1	75.5	100
350	0.6	0.6	20	2357	28.4	80.0	100	31.5	81.5	100	32.5	77.5	100
LWCB-50													
350	0.3	-	1	2380	32.3	88.8	100	35	89.5	100	40.4	91.2	100
350	0.35	-	10	2420	34.8	91.0	100	35	92.7	100	35.7	92.0	100
350	0.4	-	20	2380	28.8	89.5	100	34	87.0	100	33.5	86.0	100
FMC-50													
350	0.35	1	1	2360	34.1	90.4	100	36.2	90.1	100	40.6	91.9	100
350	0.4	1	12	2365	35.0	89.0	100	37.9	89.4	100	36.5	90.5	100
350	0.65	1	20	2361	30.4	84.0	100	36.7	86.7	100	25.2	88.7	100

CONCLUSIONS

- As a result of the investigation, the relation of LWCB- and FMC-based concrete mixture mouldability to their composition and structure and rheological and technological characteristics in conditions of high temperature is substantiated.
- There has been proposed a conditional thixotropy factor that allows evaluating features of behavior of concrete mixtures with high content of SP in conditions of high temperature.
- The determining influence of binder type and temperature on concrete mixture sensitivity to vibration effect is shown.
- Kinetics of changing of technological properties of concrete mixtures of different composition based on LWCB and FMC subject to temperature is determined.
- Based on the investigation of LWCB- and FMC-based concrete mixture properties in conditions of dry and hot climate it is concluded that it is possible to organize manufacturing of products without thermal - moisture processing.

REFERENCES

1. BATRAKOV, V, Modified concrete, Moscow, 1990, p 400.
2. BAZHENOV, Y, Increase of effectiveness of concrete technology, Concrete and reinforced concrete, No 9, 1988, p 19-23.
3. Use of mathematical planning of the experiment in concrete technology, Moscow, NIIGB, 1982, p103.

MECHANICAL BEHAVIOUR OF REINFORCED CONCRETE BEAM-TO-COLUMN JOINTS SUBJECT TO CORROSION OF REBARS

F Sato

Technical Research Institute at Maeda Corporation

M Iwanami **H Yokota**

Port and Airport Research Institute

Japan

ABSTRACT. Corrosion of rebars embedded in concrete is one of the important issues when considering structural performance and durability in marine environment. At present, it has not been well investigated quantitatively how the corrosion affects those performances. In this study, the influence of corrosion in longitudinal rebars on mechanical behaviours of T-shaped reinforced concrete beam-to-column joint was investigated by loading tests with four specimens suffered from artificially accelerated corrosion. In order to evaluate the failure process inside concrete, acoustic emission signals were detected during loading. As a result, it was found that the load bearing capacity was declined as corrosion of rebars progressed. Furthermore, by analysing acoustic emission signals, the difference in fracture mechanism was made clear between specimens with corroded rebars and sound ones.

Keywords: Reinforced concrete beam-to-column joint, Rebar corrosion, Load bearing capacity, Local deflection, Acoustic emission

F Sato, is a Civil Engineer of the Technical Research Institute at Maeda Corporation, Japan. His research interests are related to durability of reinforced concrete and high performance concrete.

M Iwanami, is a Researcher of Structural Mechanics Division of the Port and Airport Research Institute, Independent Administrative Institution, Japan. He received his Doctor of Engineering Degree from Tokyo Institute of Technology in 1999. His research focuses on maintenance techniques for harbour structures and non-destructive testing of concrete structure.

H Yokota, is a Head of Structural Mechanics Division of the Port and Airport Research Institute, Independent Administrative Institution, Japan. He specialises on structural behaviours and design of RC, PC, and steel-concrete composites. His recent research interests include the effect of the deterioration of materials to overall performance of concrete structures.

INTRODUCTION

Port and harbour concrete structures suffer from the attack of chloride ion that may cause degradation of materials. As a result, expansion of rebars due to corrosion may induce cracks in concrete and consequent fall of cover concrete. Therefore, it is essential to keep those concrete structures in serviceable conditions during their service lives by means of periodic maintenance and repair or strengthening when required. For this purpose, it is necessary to evaluate the remaining structural performances such as load-carrying capacity and ductility [1]. The timing and methods of measures against chloride-induced deterioration should be well examined with the extent of damages. However, the timing and methods have been vaguely judged by visual inspection in practice. From these points of view, the present study has been undertaken experimentally on the relationship between the degree of rebar corrosion and the basic mechanical behaviours of deteriorated concrete members. As a part of the study, this paper presents the experimental results and discussion on the mechanical behaviours of T-shaped reinforced concrete beam-to-column joints subjected to rebar corrosion.

EXPERIMENTAL PROCEDURE

Specimens

The specimens used for the test are T-shaped reinforced concrete beam-to-column joints. Four specimens were prepared, of which cross sectional dimensions and longitudinal rebars arrangement were identical. Eight deformed rebars with nominal diameter of 19mm (D19) were used as longitudinal reinforcement. Figure 1 shows the dimensions of specimens. The cross section and rebar arrangement are shown in Figure 2. The nominal compressive strength of concrete used for the specimen was 30N/mm^2. The maximum size of coarse aggregate was 20mm. Mechanical characteristics of concrete and rabars used are summarised in Tables 1 and 2 respectively. Rebars in the joint part suffered from artificially accelerated corrosion by means of the electrolytic technique as shown in Figure 1. Stainless steel plates as the cathode were attatched on the both sides of the joint part in the specimen, whose dimensions were 400mm by 400mm. Tap water was sprinkled to corrode certainly only at the joint part.

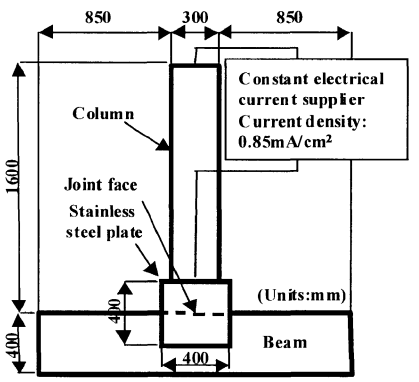

Figure 1 Dimensions of specimen and galvanostatic corrosion system

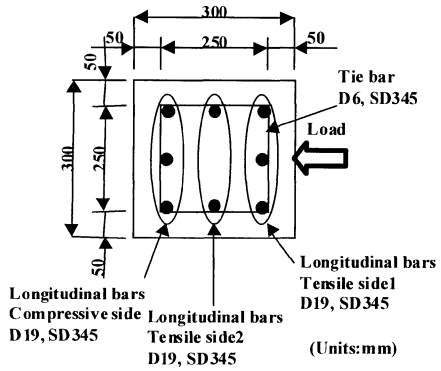

Figure 2 Rebars arrangement and cross section of column

Table 1 Mechanical properties of rebar

REBAR	DIAMETER	YIELD POINT (N/mm^2)	BREAKING POINT (N/mm^2)
Longitudinal rebar	D19	413	574
Tie	D6	391	585

Table 2 Mechanical properties of concrete

COMPRESSIVE STRENGTH (N/mm^2)	YOUNG'S MODULUS (N/mm^2)
31.2	2.65×10^4

The degree of corrosion was controlled by changing the duration of electric current applied. The state of deterioration in the joint part was characterised based on visual inspection as follows: Level 1: Rebars were not corroded (sound specimen), Level 2: Longitudinal cracks were observed on the concrete surface, Level 3: Longitudinal cracks considerably increased from the state of Level 2 and rust stain was found partially on the concrete surface, Level 4: Many longitudinal cracks developed and rust stain spread widely.

Loading Tests

The test setup is shown in Figure 3. The specimen was fixed to the floor through the beam by PC steel bars. Repeated horizontal force was applied 1400mm high above the joint face. The loading program in the tests is schematically shown in Figure 4. Three repetitions were carried out on the following each load level: 1) Flexural cracking load, 2) Allowable load, 30kN, 3) Intermediate load between 1) and 2); 20kN, 4) First yield load. The yield load was determined

by rapidly increasing in displacement at the loading point. The applied load, horizontal displacements of the column, pullout of longitudinal rebars from the beam, crack widths, and compressive strains of the concrete surface were measured. After the loading test, longitudinal rebars were taken out from the specimen to estimate the corrosion loss. The corrosion loss was measured by JCI method [2], where the effect of the dissolution of mill scale into the diammonium hydrogen citrate solution was taken into account.

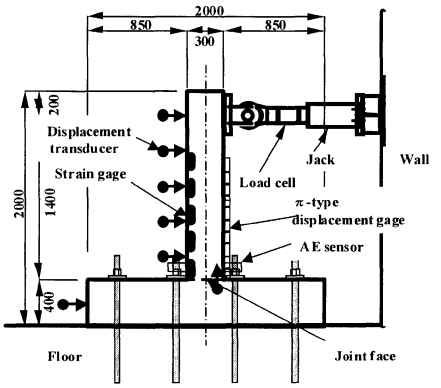

Figure 3 Loading method

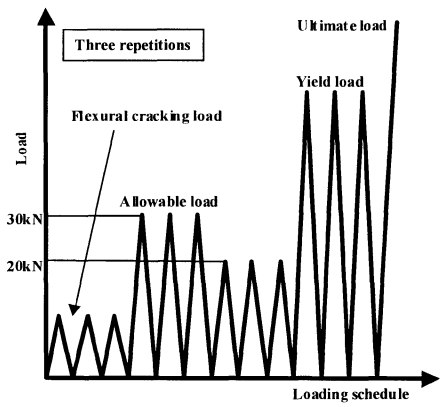

Figure 4 Loading procedure

Acoustic Emission Measurement

In order to examine the applicability of the AE technique to quantitative estimation of the deterioration degree of an actual concrete structure, acoustic emission signals were measured during the loading test. Acoustic emission (AE) is known as the generation of elastic waves related directly to fracture [3]. Arrangements of AE sensors are shown in Figure 4.

A two-channel AE system was used for the measurement of AE parameters. AE signals detected by the two sensors with resonant frequency of 60kHz were amplified by 40dB in preamplifiers. Furthermore, the signals were amplified by 40dB in main amplifiers. The signals exceeding 50dB were recorded for analysis.

RESULTS AND DISCUSSION

Condition of Rebars Corrosion in The Joint Part

The distributions of corrosion loss along the height of the column are shown in Figure 5. Regarding to stress condition during the loading test, longitudinal rebars are classified into three groups in terms of their positions (Tensile side 1, Tensile side 2, and Compressive side). The corrosion loss shown in the figure is defined as an average value of the area reduction of rebars. The maximum value of corrosion loss existed within the region up to 200mm above the joint. The maximum value of corrosion loss in Tensile sides 1 and 2 became large as the degree of deterioration progressed to severer levels.

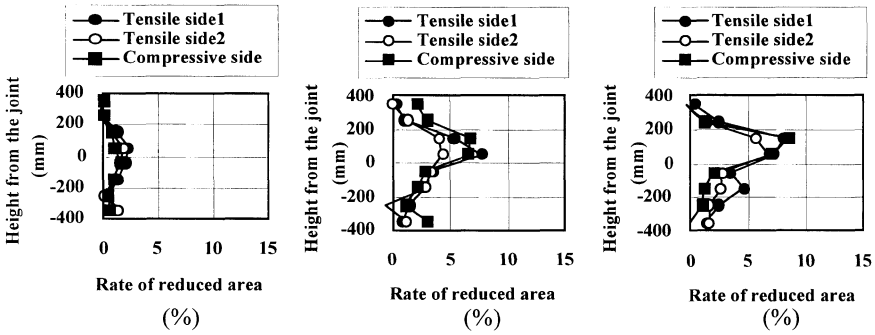

Figure 5 Distribution of corrosion loss

Influence of Corrosion on Load Bearing Capacity

Table 3 shows the influence of corrosion loss on the loads of yield and ultimate. The values in Table 3 are defined as the remaining rate of yield and ultimate loads that was normalised on the load of the sound specimen (Level 1). Yield and ultimate loads decreased more as amount of corrosion loss increased more. Furthermore, the rate of decrease on ultimate load was larger than that on yield load, and corrosion loss clearly affected the load carrying capacity at the high stress conditions. In order to evaluate the influence of rebars corrosion on load bearing capacity quantitatively, ultimate moment at each cross section was calculated by taking into account the corrosion loss of the longitudinal rebars. The effects of concentration of stress induced by pits and area reduction of longitudinal rabars were considered on calculation. The effects of pits on concentration of stress can be expressed as follows [4]:

$$f_{ycorr} = (1.00\text{-}1.32 \cdot d_w) \cdot f_y \quad (1)$$

where, $f_{y\,corr}$ is yield stress of corroded rebar, d_w is ratio of corrosion area, and f_y is yield stress of sound rebar.

Table 3 Influence of corrosion loss on yield and ultimate loads

ISSUES		DEGREE OF DETERIORATION			
		Level 1	Level 2	Level 3	Level 4
Maximum area reduction (%)	Tensile side1	0.00	2.31	7.65	8.05
	Tensile side 2	0.00	1.80	4.25	6.77
	Compressive side	0.00	1.70	6.65	8.45
Remaining rate on yield load (%)		100	97.1	96.5	95.5
Remaining rate on ultimate load (%)		100	94.6	92.2	87.1

Figure 6 shows the calculated ultimate moment at each cross section of the column. The ultimate loads are also plotted, which was converted from the ultimate moment. From this figure, the ultimate moments were significantly different at each cross section according as difference of corrosion loss along the longitudinal rebars. Therefore, load-carrying capacity was not determined by the ultimate moment at the joint face, because the ultimate moments varied along the height of the column. Figure 7 shows the relationship between calculated and experimental rates of reduction. The calculated rates of reduction on ultimate load corresponded to experimental rate of reduction. On the other hand, experimental rates of reduction did not decrease so much as calculated rates of reduction on the yield state. However, the calculating method used in this study is very easy and practical to evaluate the influence of corrosion, and gives the safety value.

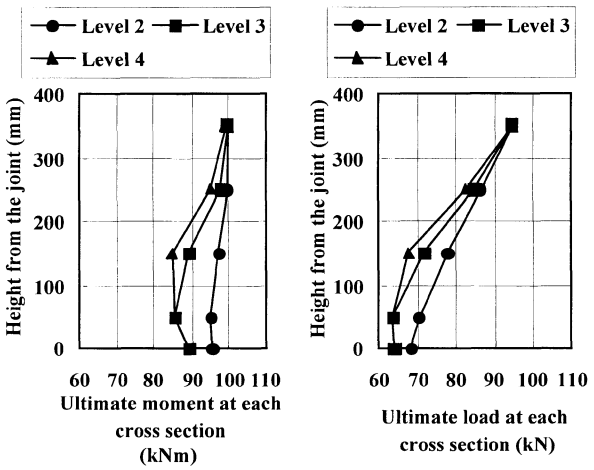

Figure 6 Influence of corrosion on flexural moment and ultimate load

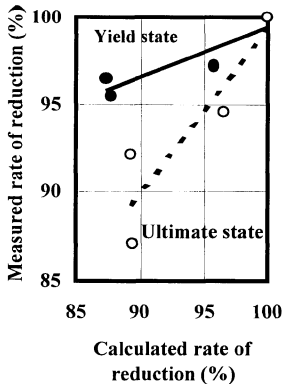

Figure 7 Measured and calculated rates of corrosion

Influence of Corrosion on Deformation

Figure 8 shows an example of the relationship between load and displacement at the loading point. The displacement at the loading point consists of two components: 1) flexural deformation, 2) rotation resulting from pullout of longitudinal rebars from the joint. Therefore, it is required to separate the flexural deformation from the total displacement of loading point in order to evaluate the stiffness of column. The rotation was calculated by considering the measured value of pullout of longitudinal rebars from the joint, effective depth, and neutral axis. Furthermore, flexural displacement was calculated by subtracting the displacement resulting from pullout of longitudinal rebars from the total displacement at the loading point. From Figure 8, the flexural stiffness was considerably lager than that of the sound specimen due to the progress of deterioration. This implies that the bond-performance between rebars and concrete was considerably deteriorated due to rebers corrosion. As a result, distributive performance of cracks became worse and the deformation of column concentrated in the joint part.

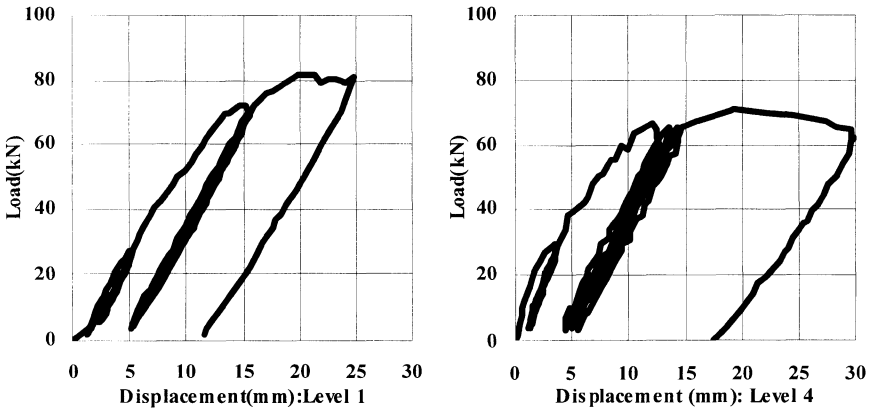

Figure 8 Example of the relationship between load and displacement at the loading point

Figure 9 shows the example on the distribution of crack widths measured at tensile side by π -type gages. The crack widths of the sound specimen (Level 1) gradually decreased from the joint part to the loading point, the shape of distribution corresponded to the gradient of actual moment. On the other hand, an only crack in the joint part opened extremely wider than the other cracks when the longitudinal cracks due to corrosion rebars have been induced in the column. This tendency was conspicuous and the number of flexural cracks became less, as corrosion of rebars progressed. Therefore, in the case where rabars in concrete corroded, it was made clear that the local fracture was induced due to deterioration of bond between rebars and concrete.

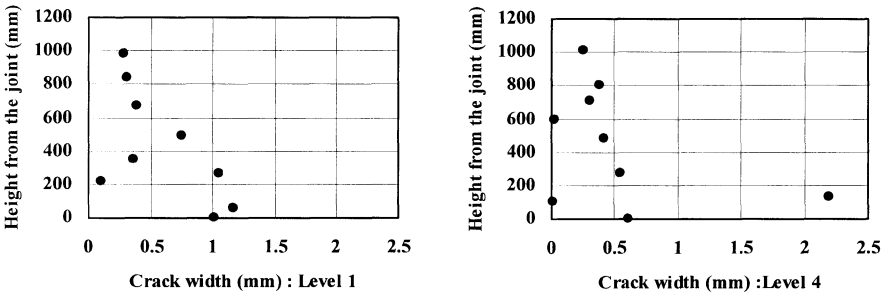

Figure 9 Example of distribution of crack width

Influence of Corrosion on Acoustic Emission Characteristics

It is necessary to accurately evaluate the degree of deterioration under working stress level in order to apply the AE technique to actual concrete structures on site. For that reason, the recorded AE signals were evaluated at the allowable stress level. Figure 10 shows AE hits of all the specimens, which were generated at the allowable stress level. The largest number of AE hits was obtained in the specimen whose deterioration degree was Level 2, because potential AE sources increased due to inducement of bond-crack between rebars and concrete and tensile stress of concrete around the corroded rebars. AE hits decreased according to the following order; Level 1, Level 3, and Level 4. On the other hand, in case where the deterioration degree became greater than Level 2, AE hits, namely, potential AE sources decreased according to progress of the deterioration degree. This result was caused by decreasing in AE source on the boundary surface between rebars and concrete and decreasing in number of flexural cracks due to deterioration of bond.

CONCLUSIONS

The influence of corrosion was investigated on mechanical behaviours of T-shaped reinforced concrete beam-to-column joints subject to accelerated galvanostatic corrosion through the loading tests. Furthermore, acoustic emission signals were detected to evaluate the fracture process inside concrete during the loading tests. The results obtained in this study are summarised as follows:

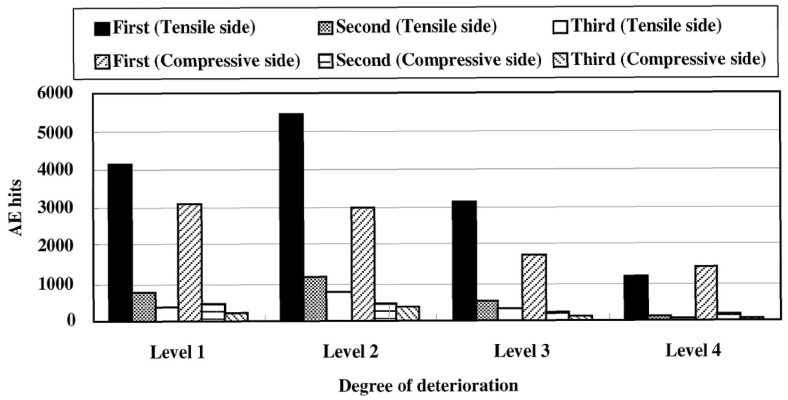

Figure 10 AE hits at the allowable stress level

(1) The load bearing capacities on yield and ultimate states were reduced according to increase of corrosion loss. It was confirmed that there was a good relationship between corrosion loss and load bearing capacity. Furthermore, the influence of rebar corrosion on the load bearing capacity could be evaluated considering both reduced area of longitudinal rebars and stress concentration due to the pits.

(2) The corrosion of rebars caused the degradation of performance on bond between rebars and concrete. As a result, the number of flexural cracks decreased, because the stress of rabars could not be transmitted effectively to concrete. From this reason, the deformation concentrated at the joint part and the column showed the local fracture at the ultimate limit state.

(3) The influence of corrosion on AE activity depended on the interactive relationship between increase in potential AE source due to rebar corrosion and decrease in potential AE source due to degradation of performance on distribution of cracks.

REFERENCES

1. OKADA, K, KOBAYASHI, K and MIYAGAWA, T, "Influence of Longitudinal Cracking due to Reinforcement Corrosion on Characteristics of Reinforced Concrete Members", ACI Structural Journal , Mar. , 1988 , pp.134-140

2. JCI TECHNICAL COMMITTEE ON STEEL CORROSION AND CORROSION PROTECTION, "Test Methods and Standards about Steel Corrosion and Corrosion Protection in Concrete Structures (Draft)", 1987 (in Japanese)

3. JCI TECHNICAL COMMITTEE ON REHABILITATION OF CONCRETE STRUCTURES, "Committee Report on Rehabilitation of Concrete Structures", Oct., 1998 ,pp.43-46 (in Japanese)

4. OHTSU, M, "The History and Development of Acoustic Emission in Concrete Engineering", Journal of Materials, Concrete Structures and Pavemant, No.496/V-24, Aug., 1994, pp.9-19 (in Japanese)

DURABILITY OF HIGH PERFORMANCE CONCRETE WITH FLY ASH

A Camões

R M Ferreira

J B Aguiar

S Jalali

University of Minho

Portugal

ABSTRACT. High-performance concrete (HPC) is usually produced using high quality materials. These high quality constituents drastically increase the initial cost of HPC, hence hindering its more widespread use. Therefore, the main goal of this research project was to produce a low cost enhanced performance concrete or even a low cost HPC, using low quality fly ash and locally available crushed aggregates. In this way, a significant reduction in the use of Portland cement, as well as that of scarce natural resources, would be obtained. The effect of high percentages of fly ash and crushed aggregates on concrete performance was studied by comparing the mechanical and durability performances of such concretes with nominally similar types of concrete with no fly ash incorporated. The results obtained indicate that it is possible to produce concrete in the low range of HPC with up to 65 MPa at 56 days by replacing up to 40% of cement with as received fly ash using crushed granite aggregates. Furthermore, it was observed that workability and durability both increased significantly when fly ash partially replaced Portland cement.

Keywords: High performance concrete, High volume fly ash concrete, Durability, Sustainability, Chloride diffusion, Electrical resistivity, Capillary absorption.

Dr A Camões, is Research Assistant in the Department of Civil Engineering at the University of Minho, Guimarães, Portugal, presently researching high performance concrete material properties.

Dr R M Ferreira, is Research Assistant at the University of Minho, Guimarães, Portugal, presently researching durability design and quality assurance in concrete construction.

Professor J B Aguiar, is Associate Professor, teaching construction materials at the University of Minho and is principal research area is focused in adhesion between polymers and concrete.

Professor S Jalali, is Associate Professor, teaching construction materials at the University of Minho, is coordinator of EU and of nationally funded research projects on Eco-efficient and innovative construction materials.

INTRODUCTION

The world's eco-system is faced with the growing problem of global warming which is associated with the emission of CO_2 into the atmosphere. It is a well known fact that for every ton of Portland cement produced, approximately one ton of CO_2 is released. To reduce the CO_2 emissions related to cement production, the use of Portland cement needs to be reduced without compromising the performance of the concrete structures.

The emission of CO_2 is only one of the many problems presently facing the construction industry. The increase in the volume of construction in the last few decades has resulted in a rampage of our natural resources. The natural resources employed in concrete are finite, and so the sustainability of construction needs to be taken into consideration.

High-performance concrete (HPC) is a viable alternative to the conventional concrete for special structures. It is usually produced using high quality materials. These constituents drastically increase the initial cost of HPC, hence hindering its more widespread use.

The main goal of this research project was to produce a HPC in which a significant percentage of Portland cement was replaced by fly ash, and in which the aggregates used were obtained from locally available crushed granite, thus eliminating the use of river sand or natural coarse aggregates. In Portugal, the massive utilisation of natural aggregates during the last decades is causing environmental problems associated with alterations in river morphology, which in turn affect the safety of infrastructures.

In order to achieve the aims of this research, an experimental program was performed which included the evaluation of the mechanical properties, workability and durability of the proposed concretes. The research work studied performance of concretes with 0, 20%, 40% and 60% Portland cement replacement by fly ash, while the total binders employed were 400 kg/m^3, 500 kg/m^3 and 600 kg/m^3.

The effect of a high volume of fly ash was studied by evaluating the mechanical and durability performances of the designed concretes. The durability of the concretes produced was evaluated through a capillary water absorption test, an electrical resistivity test and an apparent coefficient of diffusion using non-steady state chloride migration tests (CTH rapid method).

EXPERIMENTAL PROGRAM

Materials

Aggregates

All the aggregates used in this research work were obtained from crushed granite. Two sands with maximum aggregate sizes (D_{MAX}) of 2.38 mm and 4.76 mm, and a coarse aggregate with a D_{MAX} of 9.53 mm were used as received, with no previous treatment.

Cement and fly ash

The cement used was an ordinary Portland cement type CEM I 42.5 R. The fly ash came from the Pego Power Plant in Portugal, with a loss on ignition (LOI) which varied between 6% and 9%. The LOI exceeded the maximum values established by European standards [1]. However, studies have shown that, at least for this fly ash, a high LOI does not have a deleterious effect on the cement pastes and mortars [2]. Table 1 shows the oxide content of the cement and the fly ash used. Table 2 presents the estimated compound composition of the cement using Bogue's expressions [3]. Table 3 shows some physical characteristics of the cement and the fly ash.

Table 1 Oxide composition of the cement and fly ash

CHEMICAL COMPOSITION	CEMENT (%)	FLY ASH (%)
SiO_2	19.71	42.16 – 58.46
Al_2O_3	5.41	21.04 – 32.65
Fe_2O_3	3.34	3.51 – 9.13
CaO	61.49	1.67 – 9.18
MgO	2.58	0.65 – 2.59
SO_3	3.22	0.22 – 1.04
Cl^-	0.01	0.00 – 0.06
Free Lime	0.81	0 – 0.12
Loss on ignition	2.52	5.60 – 9.28
Insoluble residue	1.94	–

Table 2 Estimated compound composition of the cement

COMPOUND COMPOSITION	(%)
C_3S	61.61
C_2S	4.55
C_3A	8.69
C_4AF	10.15
CSH	5.47

Table 3 Physical characteristics of the cement and the fly ash

PHYSICAL CHARACTERISTICS	CEMENT	FLY ASH
Specific Weight (kg/m^3)	3150	2360
Blaine Specific Surface (m^2/kg)	358.4	387.9
Fineness - μm (%)	(>90) 1.7	(>45) 14.1 – 31.6
Water demand (%)	28.0	29.7

Superplasticizer

The superplasticizer used had a chemical composition based on naphthalene sulphonate formaldehyde condensates. The amount of SP used was estimated measuring the fluidity of mortars and pastes. Results indicated the saturation point (optimum quantity of SP) to be between 0.5% and 1.0% weight of binder [4,5]. For economic reasons, the value of 0.5% was adopted in this research.

Mix Design

Twelve different mixes corresponding to 3 binder contents and 4 levels of cement replacement were used. The binder contents, B, were fixed at 400 kg/m^3, 500 kg/m^3 and 600 kg/m^3 whilst the water/binder ratios, W/B, were respectively 0.40, 0.30 and 0.25. The aggregate composition was determined using the Faury method. The mix designs workability obtained using the Slump and the Flow Table tests used are presented in Table 4.

Table 4 Concrete mix proportions and workability

MIX	W/B	C (kg/m^3)	FA (kg/m^3)	SAND 1 (kg/m^3)	SAND 2 (kg/m^3)	COURSE AGGREGATE (kg/m^3)	SLUMP (cm)	FLOW TABLE (cm)
B400FA0	0.40	400	0	613.56	233.55	857.45	10.5	45.0
B400FA20	0.40	320	80	591.96	262.38	878.58	21.0	48.5
B400FA40	0.40	240	160	552.99	284.75	875.65	18.0	55.0
B400FA60	0.40	160	240	503.44	300.96	855.01	20.5	53.5
B500FA0	0.30	500	0	502.92	308.43	865.61	2.5	31.5
B500FA20	0.30	400	100	461.85	334.01	869.82	10.5	39.5
B500FA40	0.30	300	200	406.91	349.01	847.11	20.5	47.4
B500FA60	0.30	200	300	364.24	373.70	848.70	23.0	55.0
B600FA0	0.25	600	0	377.30	367.85	850.73	3.5	35.0
B600FA20	0.25	480	120	326.57	399.51	856.01	12.5	36.5
B600FA40	0.25	360	240	271.28	407.93	832.76	20.0	51.0
B600FA60	0.25	240	360	223.26	421.23	824.23	23.0	53.0

The specimen moulded from the concrete mixes was stored in a chamber with a temperature of 21°C and a constant relative humidity of 80%. At 24 hours, the specimens were removed from the moulds and stored in water (21°C), until the date of testing.

EXPERIMENT RESULT AND DISCUSSION

Compressive Strength

The effect of fly ash on the mechanical properties of the concrete was evaluated by compressive strength tests performed on a 100x100x100 mm^3 cube specimen in a displacement-controlled universal testing machine. In Figures 1-3, the compressive strength test results versus curing times are presented for the B400, the B500 and the B600 concretes. The Equation proposed by Jalali [6,7] for the prediction of strength gain with time was used to evaluate the overall strength gain behaviour of the mixes studied. The best fits of data are presented in Figures 1-3.

The results obtained indicate that during the initial curing period the strength gain is slower as the amount of fly ash increases. For B500 and B600, a 20% replacement of cement by fly ash positively influences the compressive strength for curing times of 150 to 200 days. For B600 concrete, even a substitution of up to 40% enhances the compressive strength. This can be explained by the large amounts of calcium hydroxide produced, due to the large amount of cement which fly ash could react with. Results from the B400 mix indicate a reduction in compressive strength, even for 20% replacement, for up to 200 days curing. This result was not expected, as it is widely accepted that the compressive strength for 20% replacement is usually equal to that of concrete with no fly ash. The low quality of the fly ash used is probably responsible for the results obtained. Figure 2 clearly indicates two levels of strength: B500 with no fly ash and 20% fly ash exhibit similar compressive strengths, while 40% and 60% replacements present a clearly lower level of strength. This distinction is not apparent in the case of B400 concrete. For B600 concrete, two distinct levels of strength, one for 60% replacement and one for the rest of the mixes, can be seen. It is interesting to note that the percentage of cement replacement, while strength is maintained, increases as binder content is increased.

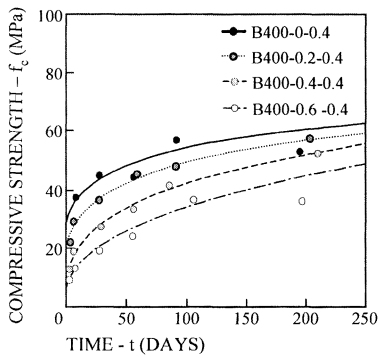

Figure 1 Compressive strength with time for concrete B400

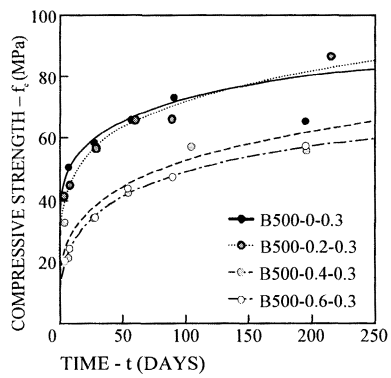

Figure 2 Compressive strength with time for concrete B500

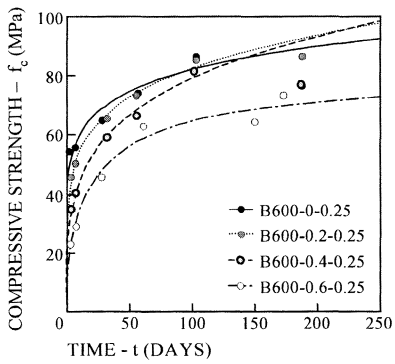

Figure 3 Compressive strength with time for concrete B600

Considering the effect of binder content on strength, it can be seen that higher compressive strengths are achieved with higher binder contents. B400, B500 and B600 mixes achieved 60, 80 and 90 MPa at 200 days, while at 250 days they achieved 62, 85 and 100 MPa. When comparing these strength gains it can be seen that 5 kg and 6.7 kg of binder rendered a 1 MPa increase of strength for B500 and B600 at 200 days, while at 250 days only 4.4 and 5.3 kg were needed. It can be stated that the efficiency of the binder in terms of compressive strength increases as the curing time increases.

Chloride Migration Test

The durability of mixes used was evaluated by estimating the chloride diffusion coefficient using the CTH Rapid Method procedure, developed by Luping [8]. In this method the diffusion coefficient is determined for a non-steady state when a potential of 40 V across a 50 mm thick specimen for a recommended duration, based on the initial current, is applied. The depth of penetration of the chloride front is determined by a colorimetric method using silver nitrate. The average penetration, measured with a precision of 0.5 mm, was considered to be the depth of penetration. The diffusion coefficient is obtained using the Equation:

$$D = \frac{R \cdot T \cdot L}{z \cdot F \cdot U} \cdot \frac{x_d - \alpha \cdot \sqrt{x_d}}{t} \tag{1}$$

with:

$$\alpha = 2 \cdot \sqrt{\frac{R \cdot T \cdot L}{z \cdot F \cdot U}} \cdot erf^{-1}\left(1 - \frac{2 \cdot c_d}{c_0}\right) \tag{2}$$

where:

D: diffusion coefficient, m^2/s;
z: absolute value for ion valence, for chlorides, $z = 1$;
F: Faraday constant, $F = 9.648 \times 10^4$ J/(V.mol);
U: absolute value of potential difference, V;
R: gas constant, $R = 8.314$ J/(K.mol);
T: solution temperature, K;
L: specimen thickness, m;
x_d: penetration depth, m;
t: test duration, seconds, $t = t_{CTH} \times 3600$;
erf^{-1}: inverse of error function;
c_d: chloride concentration at which the colour changes, $c_d \approx 0.07$ N;
c_0: chloride concentration in the upstream cell, N;

Each coefficient of chloride diffusion obtained is the average of six tests done on 6 nominally identical specimens.

Figure 4 presents the results of the diffusion coefficients for one year old specimen. The effect of fly ash content on the diffusion coefficient is clearly visible. A 20 % replacement of cement by fly ash indicates a significant reduction in the diffusion coefficient for the concrete with a binder content of 400 kg/m^3 and to a lesser degree for the remaining concretes.

Further increase of fly ash content seems to have a marginal effect on the diffusion coefficient. With respect to durability and the diffusion coefficient, there seem no be no gains in increasing the overall content of binder from 500 kg/m^3 to 600 kg/m^3. It is interesting to note that even for the lowest binder content, B400, with 60% fly ash, the diffusion coefficient (D) obtained is lower than that of the mixtures with the higher cement content, B600FA0 with no fly ash.

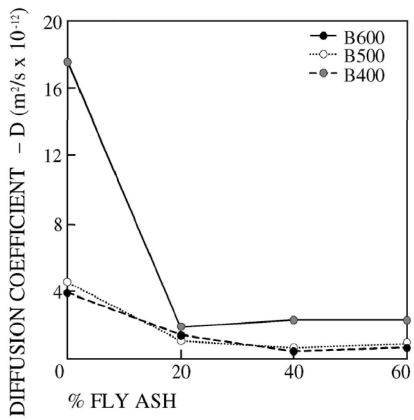

Figure 4 Evolution of the diffusion coefficient with fly ash and binder contents

Based on the classification presented by Gjørv [9] in which the diffusion coefficient values are divided into five categories (i.e.: from low to extremely high) based on the concrete's resistance against chloride diffusion (see Table 5), the substitution of up to 20% of cement by fly ash in the case of the B400 concrete results in the qualitative improvement of the concrete's chlorides diffusion resistance, moving it from a classification of low to very high. For the other concretes, B500 and B600, the qualitative improvement is less pronounced and moves them from the very good classification to extremely good.

Table 5 Relationship between accelerated chloride diffusivity based on non-steady state migration testing and resistance against chloride diffusion [9]

CHLORIDE DIFFUSIVITY ($m^2/s \times 10^{-12}$)	RESISTANCE
> 15	Low
10 – 15	Moderate
5 – 10	High
2.5 – 5	Very high
< 2.5	Extremely high

Electrical Resistivity

The electrical resistivity was determined using the initial current intensity values of the CTH Rapid Method test. Ohm's Law was used to estimate the resistivity values.

Each value of electrical resistivity represents an average of six tests done on individual specimens.

Figure 5 indicates that the replacement of cement by fly ash increases the resistivity of all the mixes studied and is more significant for high binder content concretes. For B500 and B600 there is a significant increase for up to 40% cement replacement and a rapid decrease for higher fly ash content. Results indicate the highest resistivity values for 40% fly ash content, irrespective of binder content. This does not match the compressive strength tests, but is in general agreement with the apparent coefficient of diffusion estimated.

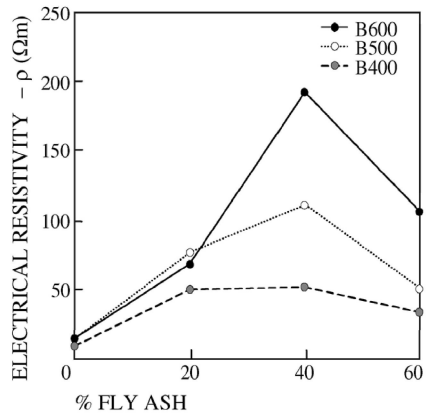

Figure 5 Variation of the electrical resistivity with fly ash and binder contents

It is interesting to note that this test can not distinguish between plain concretes with different cement content, while the CTH Rapid test clearly distinguished B400 from the other concretes. For the concretes with fly ash, however, the electrical resistivity test seemed more sensitive and clearly distinguished the different concretes. It remains to be determined what part of this effect is due to the presence of fly ash and what portion is due to a more compact structure, resulting from the finer hydration products from fly ash lime reaction.

Capillary Absorption

The capillary water absorption test was performed to obtain more data regarding the durability behaviour of the mixes studied. The test followed the LNEC specification E393 [10], which is based on the RILEM CPC11.2 draft recommendation [11]. The coefficient of capillarity absorption, S, is the slope of the curves representing water absorbed per unit area versus square root of time during the initial four hours of testing for all the mixes studied. Each coefficient of capillary absorption is the average of four tests performed on four nominally identical specimens.

The results presented in Figure 6 indicate that the addition of fly ash decreases the coefficient of capillary water absorption (S). The increasing of the quantity of binder, associated with a lower W/B ratio, also decreases this coefficient (S). This effect is, however, only pronounced up to 500 kg/m^3 binder content. Higher binder contents do not seem to affect S significantly.

CONCLUSIONS

In order to evaluate the possibility of producing high performance-low cost concrete, laboratory tests were performed on specimen of concrete with increasing binder contents and cement replacements by fly ash. The compressive strength tests indicate that concrete with 65 MPa strength at 56 days can be produced using B500 with up to 20% cement replacement and B600 with up to 40% cement replacement. This strength was obtained with the specimens cured in water until 56 days. If these curing conditions were not maintained during this time, surely the strength would decrease. The other mixes studied did not achieve this level of strength at this age. It is noted that the efficiency of the binder, i.e. the amount needed for each 1 MPa increase in strength compared to B400, increases with increasing curing time. Furthermore, it was noted that the optimum amount of cement replacement increases with curing time and binder content.

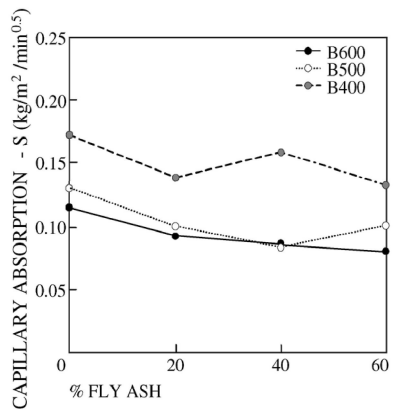

Figure 6 Variation of the capillary absorption with fly ash and binder contents

The addition of FA = 60% allows the obtaining of concrete with considerably lower mechanical characteristics, in comparison of the others. However, concerning the low quantities of cement existing in the mix, those may be considered as concrete with a good economic performance.

The durability of the mixes was evaluated using three different tests. They were selected between those commonly considered to characterise durability. All the tests indicate a better performance for concretes with fly ash. However, the optimum percentage of replacement varies between the performed tests. While the resistivity test indicates higher values for 40% substitution, the other two tests showed a tendency towards amelioration of durability without indicating a specific optimum point. Further research is needed to determine the effect of fly ash on the resistivity of concrete by itself and after changing the microstructure of concrete when reacted with lime.

The CTH Rapid test is sensitive to the quality of concrete with no fly ash content, but is only marginally sensitive to the level of cement replacement or even to the binder content when fly ash has been added. On the contrary, the electrical resistivity test is not sensitive when fly ash is not used, but is clearly sensitive to the amount of binder content and level of cement replacement, when fly ash is used.

The resistivity tests performed indicate that the optimum fly ash content, for studied mixes, is 40 %. This may be due to the fact that for higher amounts of substitution enough lime is not formed for complete pozolanic reaction.

The capillary water absorption test is capable of distinguishing concretes with different binder contents and is somehow sensitive to the amount of fly ash present in the mix.

REFERENCES

1. EN450 1994, Fly Ash for Concrete, Definitions, Requirements and Quality Control, CEN, European Committee for Standardization, September 1994.

2. ROCHA, P., High Performance Concrete Using Common Materials and Procedures, Master Thesis, University of Minho, October 1999. (In Portuguese).

3. BOGUE, R. H., Chemistry of Portland Cement, Reinhold, New York, 1955.

4. CAMÕES, A., et al, Mechanical Characterization of High Performance Concrete Using Fly Ash, JPEE98, Portuguese Seminar in Structural Engineering, Lisbon, 25/28 November 1998, pp 517-525. (In Portuguese).

5. CAMÕES, A., et al, Low cost high performance concrete using low quality fly ash, ERMCO98, 12th European Ready Mixed Concrete Congress, Lisbon, June 1998, p 478-486.

6. JALALI, S., ABYANEH, M. Y., Prediction of Final Concrete Strength in Hot Climates, Magazine of Concrete Research, Vol 47, No 173, December 1995.

7. JALALI, S., SANTOS, L. M. V., The Effect of Curing Temperature on the Strength Gain of Concrete, Safe and Early Formwork Removal and Quality Control, ENCO Engineering Concrete, No 724,-September 1997, pp 676-684.

8. LUPING, T., Chloride transport in concrete, measurement and prediction, Doctoral Thesis, Chalmers University of Technology, Gotemborg, Sweden, 1996.

9. GJØRV, O. E., Controlled service life of concrete structures and environmental consciousness, Concrete Technology for a Sustainable Development in the 21st Century, Lofoten, Norway, 2000.

10. E393-1993, Concrete. Determination of the Absorption of Water Through Capillarity, LNEC, 1993. (In Portuguese).

11. RILEM CPC11.2, Absorption of water by concrete by capillarity, 1982, 2nd edition, RILEM Recommendations for the Testing and use of Construction Materials, E&FN SPON, Great Britain, 1994, pp 34-35.

WHEN READYMIX CONCRETE TURNS T(r)OPICAL

K Nath

P Jha

RMC Readymix (India) Pvt Limited

India

ABSTRACT. Ready mixed concrete is a new Industry in India. It was only towards the end of 1994 that serious attempts were made to introduce ready mixed concrete. The initiators of the business had to face a variety of challenges, one such being the ability to develop concrete mixes with good slump retention. The concrete properties had to compensate for the hot weather, increased travel time due to traffic delays and accommodate elementary placing methods of a construction industry plagued by lack of mechanization. The paper examines the various challenges faced in the production and transportation of ready mixed concrete in India. The paper details the progress made in overcoming these difficulties. It also looks at the successful case study of temperature-controlled concrete (concrete placing temperature less then 23°C), supplied at ambient temperature of 36°C, developing special concrete for mass pours and triple blend mixes for high performance concrete. Finally the paper concludes by suggesting various means of controlling the peak core temperature while producing concrete in hot and tropical climates.

Keywords: Ready mixed concrete, Cement, Admixture, Aggregates, Ggbs, Pfa, Batching plants, Truck mixers, Slump retention, Peak core temperature, Concrete placing temperature, Temperature controlled concrete, High performance concrete.

Kshemendra Nath, General Manager (Technical and Marketing), RMC Readymix (India) Pvt Limited. He has qualified as a BTech (Civil Engineering) and also passed "Concrete Technology and Construction" examination conducted by City & Guilds London Institute. He has 15 years experience in the cement, construction and building material industry, the last six being with RMC Readymix (India) Limited.

Prashant Gopal Jha, Technical Manager, RMC Readymix (India) Pvt Limited. He has qualified as a BE (Civil Engineering) and also passed "Concrete Technology and Construction" examination conducted by City & Guilds London Institute. He has 11 years experience in the construction and building material industry, the last four being with RMC Readymix (India) Limited.

INTRODUCTION

Ready mixed concrete is a new industry in India. It was only from 1994, that serious attempts were made to introduce ready mixed concrete to the Indian market. Today the ready mixed concrete Industry has an annual turnover of 2.1 million m^3 of concrete. In a country producing 100 million MT of cement annually, the industry has only touched the proverbial tip of the iceberg. Even this modest progress was achieved with considerable effort. One major challenge was to produce workable concrete in the hot tropical climate. The problem was compounded by the lack of consistent raw materials and heavy dependence on manual placing methods. This paper describes the first hand experience of the authors who have been associated with the ready mixed concrete industry in India since 1994, specifically dealing in detail how mixes were evolved to combat the tropical conditions and overcome problems related to slump loss with time. It details the successful development of special concrete for mass foundation with a view to restrict the peak temperature below 70°C. The paper also briefly describes two case studies involving supply of temperature-controlled concrete and high-performance concrete with triple blend (Cement, Micro-silica and PFA) in Mumbai (formerly Bombay). It concludes by suggesting various methods for controlling the placing temperature of concrete with a view to restrict the peak core temperature in mass concrete.

TYPICAL PROBLEMS FACED BY RMC PRODUCERS IN INDIA

As mentioned earlier, ready-mixed concrete is a new concept in India. Therefore for the concept to take shape in the country the initiators of the business had to face a lot of problems. From a technical viewpoint, the tropical climate and the unique Socio-Economic conditions threw considerable challenge to the RMC producers in India in the formative years. A brief description of the some of these are listed below:

Ambient Temperature

India is a tropical country where the ambient temperature in summer can be as high as 46°C. Generally in most of the cities the temperatures are in excess of 30°C throughout the year. Table 1 shows the average day temperature in select cities in different months. *

Table1 Average day temperatures in select cities in India

	JAN	FEB	MAR	APR	MAY	JUNE	JULY	AUG	SEPT	OCT	NOV	DEC
Delhi	21	23	29	36	39	38	34	33	34	33	28	23
Mumbai	29	29	31	33	36	33	30	29	30	34	33	31
Chennai	28	31	33	36	38	37	35	34	33	32	29	28
Hyderabad	28	32	35	38	39	34	31	30	31	31	28	28
Bangalore	27	80	32	34	32	29	28	27	28	28	27	26

Road Condition

Although the road network of India is the third largest in the world, majority of them is unpaved. Vehicular population has grown from 0.3 million in 1951 to 40 million in 1997, while the road network has only grown from 0.4 million kms to 3 million kilometers during the same period. The road networks in the cities are also ill equipped to cope with the increasing vehicular traffic. Mumbai, for example, has only 10% of its area covered by roads as against a world norm of 25-30%. The average speed of trucks and buses in the central business district of Mumbai during the peak hours is as low as 6 km/hour. To a ready mixed concrete producer, these traffic conditions are potentially detrimental because it adversely affects the slump retention.

Raw Materials

Quality of cement available in India is comparable to international standards, but the quality of aggregates continues to be a major cause of concern. The aggregate production in India is more of a cottage Industry and is highly fragmented. The variability in size and shape makes it extremely difficult to estimate the water demand. There is also tremendous seasonal variation in both quality and quantity of natural sand, which is manually dredged. During the initial phase of the business, none of the admixtures available in India provided for slump retention because concrete never used to be transported to long distances. Therefore, retaining the slump in hot climate proved to be extremely difficult. To overcome this problem, transporting concrete to longer distances was attempted only during night to take advantage of the improved traffic conditions and reduced ambient temperatures.

But as the demand for ready mixed concrete increased, this hardly looked to be a sustainable solution. Trial mixes were conducted to arrive at the best possible combination of the available admixtures to produce concrete capable of retaining a slump of 100 mm after one hour of mixing. Eventually, success came in the form of split dosage. The retarding plastisizers were dosed at the plant while super-plastisers were added to the truck on its arrival at site.

This method worked reasonably well for some time but it had it's own drawback. A trained technical supervisor was required at the site to eliminate the risk of overdosing of admixture. Through consistent endeviour and effective communications with the admixture producers, suitable admixtures were developed that could be totally added at the batching plant and achieve the desired slump retention. Development activity is still continuing to optimize the dosage rates for the required performance.

Construction Practices

Prior to the introduction of ready mixed concrete, concrete used to be made at the site by small portable mixers at an average rate of 5 cum per hour. The placing and laying techniques adopted were suited to handle only small volumes of concrete. The placing methods, which were highly labour-intensive, proved inadequate to place 6 cum of concrete from a truck mixer within reasonable time. Pumping the concrete was a logical solution but had its limitations for members like columns. Due to this reason, placing ready mixed concrete in members such as columns and walls, till date defies an effective solution.

Re-dosing the admixture midway through the discharge of concrete is risk prone. Although, today, it is possible to supply pump mixes to distances more than three hours from the plant, ready-mixed concrete is generally not preferred for columns.

CONCRETE FOR MASS FOUNDATIONS

ACI 116 R defines mass concrete as "any volume of concrete with dimensions large enough to require that measures be taken to cope with generation of heat from hydration of the cement and attendant volume change to minimize cracking".

For slabs and thin sections, risk of thermal cracks arising out of internal restraint is not critical. However, in mass concrete, if the difference in temperature between the core and the surface exceeds 20°C, it can lead to thermal cracking from internal restraint. For this reason, the peak temperature of concrete is normally restricted to a maximum of 70°C. One of the ways to control this would be to reduce the placing temperature of concrete. Many International standards restrict the maximum placing temperature of concrete to 30°C. But the code for practices in India allows placing temperatures for concrete as high as 40°C, which the authors feel needs immediate revision.

Apart from the risk of thermal cracking, high peak temperature in the core of the concrete, can lead to other durability issues. Of late, considerable interest is being generated on the damage mechanism initiated by Delayed Ettringite Formation (DEF) in concrete subjected to temperatures greater than 70°C. DEF can cause internal cracking of concrete, which may occur years later. Higher concrete temperatures leads to coarser pore structure of the cement paste and results in reduced ultimate strength of concrete. A high peak temperature can also restrict the hydration process due to self-desiccation.

In India, some specifiers stipulate that the placing temperature of concrete in mass foundations should be limited to a maximum of 23°C. RMC India ventured to validate this figure through confirmatory trials and develop special concrete designed to restrict the peak temperature to less than 70°C.

As a starting point, experiments were conducted on a number of cement types to compare the rate of heat generation and the time of the peak temperature. This was done using the **quick binder test** apparatus, developed by RMC Group Company, Readymix Kies-Union AG of Austria. This equipment consists of temperature probes, a data logger and a PC. Neat cement pastes of the cements or cement blends to be tested are filled in a polystyrene container. The temperature probes are then inserted into the container. The temperature probe transmits data via a multi-point transmitter to the PC. The data is stored and saved for further process. These data results in a different characteristic curve for each cement type. Figure 1 illustrate the temperature record for various locally available cements and the cement blends.

As observed from the graph, different cements not only develop different peak temperatures but they also peak at different times. Even different 53 grade OPC had different characteristic curves. It was not surprising that cement blends with PFA and GGBS exhibited lower peak temperatures and took longer time to reach their peak temperature.

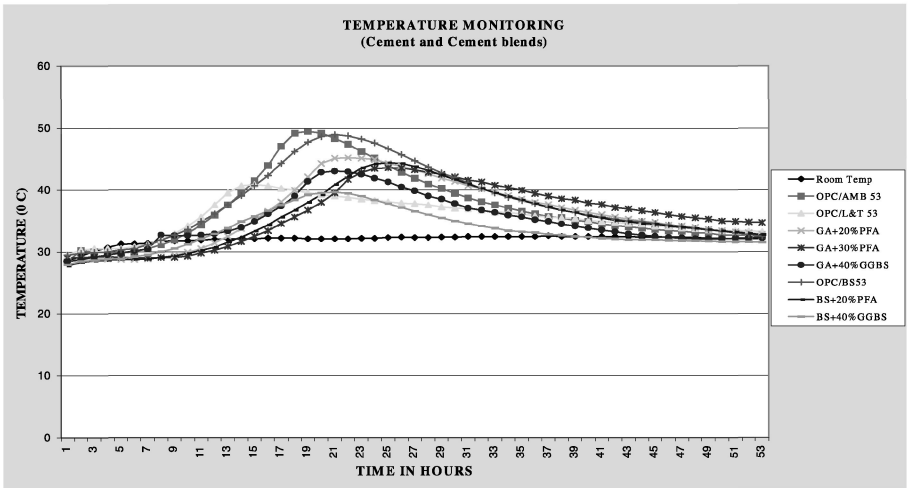

Figure 1 Graph depicting the temperature development of different types of cement and cement blends

The quick binder tests were only a starting point as mentioned earlier. The placing and the subsequent peak concrete temperatures would depend on a lot of other factors like the ambient temperature, the type of aggregates, thickness of the section etc. Therefore, the next logical step was to simulate the site conditions as close to reality as possible. Concrete of grade M40 (40 N/mm^2), produced from RMC's Mumbai plant with the normal aggregates and the cement that gave the least peak temperature was placed in a wooden box measuring 1 m* 1 m* 1 m 100 mm thick polystyrene strips fixed on all sides including the bottom provided thermal insulation. Thermocouples were inserted in the core of the concrete to measure the temperature rise with time. The temperature was monitored at 2 hours interval on the data logger. The trial block reached a peak core temperature of 90°C in 48 hours, significantly higher then the desired peak core temperature of 70°C. The experiment was repeated with different replacement levels of GGBS (40% and 70%) and unclassified PFA @ 25% sourced from a nearby thermal power station. This time there was a reduction in the peak temperature as they recorded 84°C, 68°C and 81°C respectively. Figure 2 shows the temperature recorded during the trials on the $1m^3$ insulated trial block.

Although it was established successfully that the peak temperature could be controlled by the use of blends like GGBS and PFA, their availability was a major problem. While GGBS was not readily available in and around Mumbai, the consistency of the quality of the available GGBS was yet to be established. At high replacement levels of 70%, the confidence of consistency was absolutely necessary to minimize risks. Similar was the case with the unprocessed PFA. Therefore, a second series of trials had to be undertaken to develop the concrete with the desired properties.

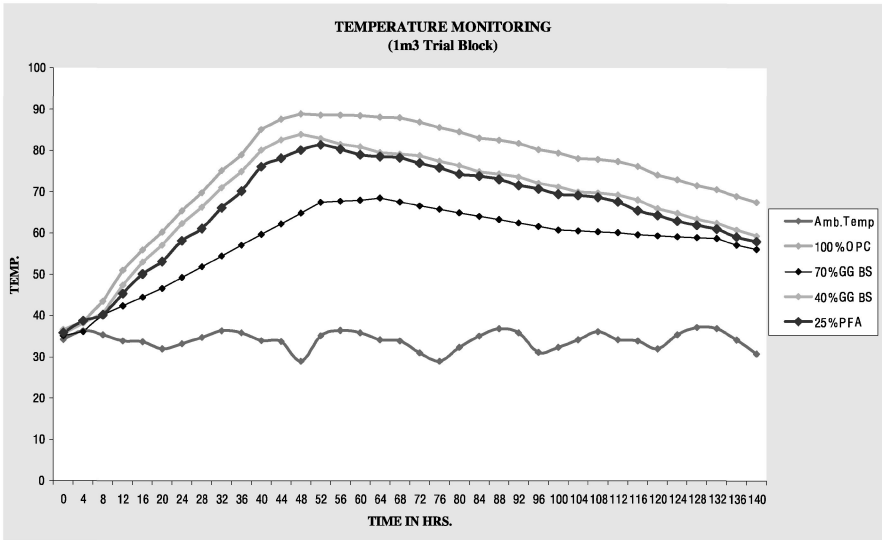

Figure 2 Graph depicting the temperature development of concrete with different types of cement and cement blends in simulated trial block

Since the options were limited on the use of blends, this time the focus was to reduce the placing temperature of concrete as low as possible. Numbers of experiments were conducted at the lab by reducing the temperatures of the various ingredients. The target was to produce concrete at a temperature less than 23°C in laboratory conditions before resorting to 1 cubic meter trial blocks. Since water had the highest specific heat, it had the maximum influence on the resultant temperature of the concrete. Therefore attempts were made to reduce the water temperature to the minimum. Under laboratory conditions, the minimum concrete temperature that could be achieved was 27°C. Ultimately, the desired reduction in concrete temperatures was achieved when ice flakes replaced the mixing water. The resultant temperature of concrete was 16°C. The phenomenon was due to the fact that the latent heat of ice on melting absorbed the heat of concrete thereby cooling it substantially. Subsequently trials were conducted on the 1 cubic meter trial blocks with mixing water at normal temperature (30°C), chilled water (10°C) and by using 100% flaked ice. This time the block reached a peak temperature of 90°C, 75°C and 66°C respectively. Figure 3 shows the temperatures recorded in the $1m^3$ insulated trial block with chilled water and ice –flakes.

CASE STUDY OF TWO SPECIAL CONCRETES

A) Temperature Controlled Concrete:
Project: - Mahindra Heights: 27 Storey Residential Building
Consultant: - Mahimtura And Associates
Contractors: - Mahindra Construction Company Limited

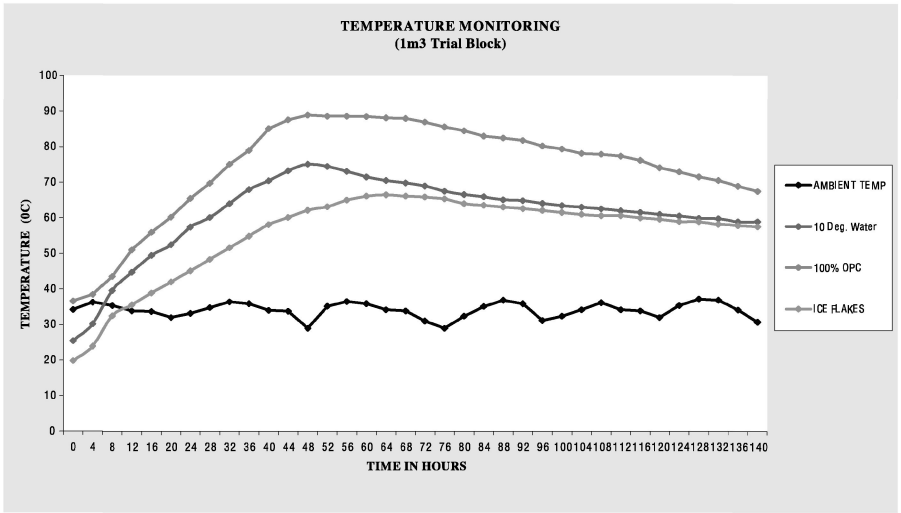

Figure 3 Graph depicting the effect of chilled water and ice flakes on temperature development of concrete in simulated trial block

In Mumbai, where land costs are prohibitive, vertical expansion is the most viable alternative. Therefore multi storied building are very common. Generally the foundation depths vary from 1.5 meter to 2 meters. 2000 m^3 of M-40 grade concrete was to be supplied for the raft foundation for this prestigious residential complex in south Mumbai. The raft was 2 meter thick and the specified maximum placing temperature of concrete was 25°C.

Owing to the variability in aggregate size and shape and the traveling time involved, cement content for producing grade M-40 concrete worked out to be 450 kgs/m^3. At ambient temperatures of 35-36°C, the placing temperature of the concrete would be around 38°C. Hence it was necessary to reduce the concrete temperature by at least 13°C.

Buoyed by the success of the trials conducted, efforts were made to produce the concrete from RMC's closest ready mixed concrete plant, which was about 60 minutes away from the site. Apart from using ice in flaked form, the aggregates piles were pre-cooled by proper shading and sprinkling them with chilled water to reduce their effect on the temperature of concrete.

Since the batching plant did not have the provision to weigh ice, the first issue to address was to weigh the ice exactly so as to maintain the w/c ratio. The total volume of concrete was to be placed in three pours, the largest one being 1200 m^3. Lack of proper means of weighing the flaked ice would seriously affect the quality and the rate of pour. After considering a series of options, the most effective and practical solution was to weigh the ice through the weighbridge in the plant. Empty truck was driven on to the weighbridge, the ice flakes as required was accurately weighed and loaded into the truck mixer and the concrete was then batched dry into the truck mixer.

With experience it was observed that after approximately 25 minutes, ice melted completely to form plastic concrete. Knowing this, the admixture addition time was determined. Since the travel time to the site during peak hours could be as high as 90 minutes, it became necessary to add admixture to the truck, 30 minutes after it was batched. Thus by a pragmatic approach based on the established norms of hot weather concreting, concrete with temperature less than 23°C was placed at an ambient temperature of 35°C.

Due to other technical considerations, primarily to achieve a monolithic structure, the concrete was placed in full depth of 2 meters. Therefore it might be possible that the peak core temperature could have exceeded 70°C. Today, with the confidence of the practical experience of producing more than 100,000 cubic meters of concrete with blends like GGBS and PFA, it is very well possible to restrict the peak temperature to less than 70°C. The success of this project also clearly established the savings in admixture costs that could be accrued by reducing the temperature of concrete. Therefore, when RMC Readymix established their next plant at chennai, where the climate is hotter than Mumbai, a water-chiller plant formed an integral part of the plant setup.

B) High Performance Concrete for Bandra-Worli Sea Link Project, Mumbai

Consultants: - M/s Sverdrup Civil Inc (USA)

Contractors: - M/s Hindustan Construction Company, Mumbai

The Bandra-Worli Sea-link is a 5.6 km bridge joining Mumbai with its western suburbs and is being built at an estimated cost of £ 60 Million. M/s Sverdrup civil Inc (USA), is the lead consultant for this project which is being developed as an "Intelligent Bridge" with facilities for electronic tolls, close-circuit television, traffic counting, remote weather information system etc. This 8-lane bridge also has a single tower supported 500 meter long cable-stayed portion. Once complete, the Bandra-Worli sea-link will provide a fast moving road link, which will relieve traffic congestion at peak times and result in £15 million of annual savings in vehicle operating costs as well as saving travel time and reducing pollution.

Owing to the extreme exposure conditions, high performance concrete incorporating micro-silica in a slurry form was specified for the project. For the piling mix to be cast in the sea, the requirement was to retain a slump of 175 mm after 4 hours of mixing. This time frame was to facilitate transport from batching plant to the nearest landmass, transferring the concrete from the truck mixer to a mixer unit mounted on a barge, which will then transport the concrete through the sea before finally pouring into the pile. RMC's expertise was called upon to design and execute the mix to the consultant's stringent specifications. This also helped the concreting process to begin months before the contractor could set up his batching plant.

The thixotropic nature of silica fume concrete and the increased rate of slump loss at high ambient temperatures posed grave challenges in the initial stages of the trials. The mix design, especially the grading of the aggregates needed fine-tuning to take into account the addition of silica fumes. Also for the concrete to retain a slump of 175 mm for 4 hours, a totally different type of high range water reducing admixture, at very high dosages was required. Numerous admixtures were tried to arrive at the mix.

Finally, a new generation admixture, based on Poly-carboxylic ether (PCE) and specially formulated to suit the locally available cement and the fine aggregates gave the desired performance. Once the trial mixes was established and approved by the client, a trial pour of 20 m^3 was conducted for a test pile to verify the field performance. Minor adjustments were necessary at the batching plant to dispense the micro-silica in the slurry form.

For the pile caps, a triple blend of OPC, Silica-fume and PFA was specified. This concrete of grade M60 had a restriction that the peak core temperature should not exceed 70°C and the temperature difference between the core and surface should not be greater than 20°C. Therefore, the specified placing temperature of concrete was not to exceed 30°C.

The experience gained in producing temperature-controlled concrete in the past stood the company in good ground to achieve the desired specifications without great difficulty. Although the specified maximum temperature was 30°C, it was obvious that the concrete placing temperatures need to be targeted close to 20°C, to restrict the maximum peak temperature below 70°C.

CONCLUSIONS

To ensure durability of concrete in a tropical country like India, it is necessary to limit the peak temperature of concrete. There are many ways in which this can be achieved. Reducing the cement contents is a good option. But in higher grades of concrete, it may not be always practical. Using replacements like GGBS/PFA should be encouraged as an effective method to reduce the peak temperature and also for the other important benefits it provides for the durability of concrete. Using chilled water helps to reduce the placing temperatures of concrete. But in mass concrete, to minimize the risk of thermal cracking due to internal restraint, use of GGBS/PFA and partial or full replacement of mixing water with ice may be required. Shading the aggregate stockpiles and sprinkling cold water will help to reduce the concrete temperatures. Other factors to be considered are to paint the truck mixer drums, the cement silos and the batting plants in white, as it would reflect the heat and thereby influence the concrete temperatures. The maximum placing temperature of concrete should not exceed 30°C for general concreting works.

REFERENCES

1. ACI COMMITTEE 207, Mass Concrete (ACI207.1R-96).
2. ACI COMMITTEE 116, Cement and Concrete Terminology (ACI 116R-00).
3. BAMFORTH, PROF PHIL B., BSc, PhD, C:Engg, MICE, Taywood Engineering. Concreting Large Volume (Mass) Pours.
4. CONCRETE SOCIETY, The use of ggbs and pfa in concrete, Concrete Society Technical Report-40, 1991.
5. IS: 7861, (Part I) – 1975, Indian Standard Code of Practice for Extreme weather Concreting, part I, Recommended Practice for hot weather concreting.
6. GORDON, D., KSHEMENDRA NATH, P., - Setting-up of Ready mixed concrete industry in India: Challenges and the Opportunities. "Creating with concrete" – International Congress: Dundee, Sept: 1999.

CONCRETE STRUCTURE DESIGN AND CONSTRUCTION AT 4,000 METERS ABOVE SEA LEVEL

R Uribe-Afif

L Garcia-Chowell

M Flores-Morales

Cementos Mexicanos

Mexico

ABSTRACT. In the state of Puebla is located a hill called "La Negra" and it is the place chosen to construct a Millimeter Radio-Telescope, the biggest one in the world. The hill corresponds to a volcano system 4,000 meters above sea level and it takes part of the "Faja Volcánica Trans-Mexicana" that goes through the central part of the country from east to west. This place was chosen because it attends to the equipment operation needs, which are defined according to the location and atmospheric conditions of the installation. The final selection was decided after analyzing more than one hundred different places around the world. The millimeter radio telescope has a concrete base that houses an operations building and a dish aerial with a maximum diameter of 50 meters. The equipment base was built over a reinforced concrete structure that is placed "in situ" with an altitude of 4000 meters above sea level. The atmospheric conditions have different temperatures from –5 to 25 °C, cycles of humidity and drying with relative humidity over 60%, wind velocity between 5 and 10 m/s, maximum 14 m/s. The mix was designed reviewing the specific mechanical requirements and the conditions of the place where the mix was to be produced, with a controlled temperature no lower than 10 °C to accomplish the specified properties. To satisfy the concrete rules it was necessary to modify the production plant of concrete to guarantee total control over the mix temperature when fresh and obtain the required hardened properties.

Keywords: Radio-telescope, Placing, Production, Extreme conditions, f'c, Control mix, Temperature.

R Uribe, is currently undertaking research in to the development of performance specifications for durability. His research focuses mainly on concrete durability, pathology and aggregates.

L García, is a Chartered Civil Engineer and his mainly function is a technical manager for several years in the concrete production.

M Flores, is a Civil Engineer and his main function is the supervision of reinforced concrete structures.

INTRODUCTION

In the state of Puebla, México, is located the highest hill of the country with a maximum altitude of 4600 meters over the sea level and also placed in the central part of the Mexican territory belonged to the "Faja Volcánica Trans-Mexicana" fisiographic province, it contains the biggest Millimeter Radio-Telescope (MRT) in the world with a receiver frequency plate with 50 meters diameter. The selection of the place included to analyze and review of 160 different places in all over the Mexican country, also this place was chose among hundred different places, from these different places was very important to find good conditions to have more hours of viewing without any interference of the waves that sometimes appear in this kind of equipment; the important conditions to take decisions are: environmental humidity, wind velocity, Clear days, variety of temperature, etc. This place does not have any infrastructure, so it is necessary to develop all processes to manufacture concrete in an industrial way.

The MRT corresponds to an international project with the participation of different countries like: The United States Of America, Germany and Mexico, it develops new technologies in the manufacturing of this kind of operative systems; as a prove, it is necessary to mention a building industry with the finality to manufacture different pieces and after being assembled the telescope is ready; for this structure was necessary to assure that the specifications were done with exactitude rules and dimensions were established for each piece that take part of the plate, even though does not exist any commercial instrument with the measurement required to accomplish with the exactitude the assemble.

The installation considers as an important task of the project, the construction of a concrete base, also the base for the telescope and other accessories to make the equipment work. All these structures will be built over an altitude upper 4000 meters over the sea level where the placing conditions are qualified less common, in other cases adverse for the concrete manufacture.

OBJECTIVE

To develop concrete specifications and technical propose to design and manufacture a concrete structure under extreme conditions; all these have to satisfy the structural and durability requirements that allow to assure the good performance of the material under different conditions, all this established by the place of the MRT.

SPECIFICATIONS

The concrete advertises for the project include the following requirements:

Template f´c 15 N/mm², 5 cm thick, maximum aggregate size 19 mm, Volumetric Weight 2200 kg/m^3 Cement Type IP (ASTM C 595) or type II cement with low alkali 8ASTM C 150;in bulk with a quality certificate of the producer; in another cases it is possible manage cement bags.

Aggregates: brittle particles <3% elongated and flat <15% as crushed dust, the percentage that goes by the mesh 200 has to be less than 2%, lose by washed sand <3% and grave <1%.

Note: there is a confusion in regard to the crushed material, the specific gravity <2.5, modulus of refinement from 2.5 to 2.9.

Water; there is a consume higher than 0.19 m^3 in each m^3 of concrete, it is very important to use water reducer and initial set retarded admixtures in the set (type D o G according to ASTM C 494).

As we can see, these advertises include the selection of components and also the grade of the same ones, it assumes that it is very important to elect and review the raw material and wait if the final combination gives as a result a mix with the correct characteristics. It is important to mention that these can accept the mix after evaluating fresh concrete, for its consistence and when the compressed resistance becomes hard, according to ASTM.

This task will specify the analysis of the structural concrete uses, although the other type mentioned is also considered basic with the specific criterion that at the same time are defined according with the used row material in the material production.

Technical Suggestion

With the finality to attend to all the requirements to this project, it was done a technical suggestion that are added to the specifications, all this represented a general guide to define the necessary activities to accomplish, the concrete manufacture process. In this suggestion [1], there were concepts no included in the original advertises as the selection of the special aggregates that allow to accomplish with specified elastic modulus and it was not considered as a part of the original property of the product. The use and management of the alternative cement, the inclusion of system pores in the concrete who will help to prevent the repetitive action of the freeze cycles, the definition of the minimum temperatures in the fresh mix (13 and 16 °C) for each element based in particular characteristics [3], the established requirements for the minimum conditions [4] (minimum temperature 4 °C and the appearance of rain and fog) to stop the production and to place the concrete finally the schedule for the set, established according to atmospheric conditions that are being review at the moment.

EXPOSURE AND SERVICE CONDITION

The faceable atmospheric conditions [5] for the structures set:

- Temperatures between –5 °C and 25 °C, it means that there is an unfavorable risk during the concrete manufacture resulting from the low temperatures.
- Relative humidity upper than 60%.
- Wind velocity between 5 and 10 m/s, with a maximum of 1m/s in certain moments.
- Exposure and service conditions during the operation.
- Minimal temperatures from –5 °C.
- Freezing and defrosting cycles.
- Exposure to a moist environment.
- There are no presence or abrasive actions.

- There is no risk of any chemical attack with the direct contact between the material and the aggressive.
- There is no possibility to get any chemical reaction between the cement alkali and the employment in the concrete manufacture, also this elements have been evaluated, also have been proved their inoffensive behavior.

According with the exposure and service conditions defined by MRT structures, the main big risks of the problem are the following:

When the concrete is fresh or in process of becoming stiff it is necessary to pay special attention on the concrete temperature to assure the cement hydration.

In another way, when the concrete is stiff it is important to take care of the internal structure capable to support the degrading action resulted from exposure to the current action from freezing and defrosting cycles; also, concrete has to be manufactured with a permeability level that closes the possibility of any corrosive process over the steel reinforcement, since the natural environment is very wet and the rainy periods are common.

MANUFACTURING AND CONSTRUCTION PROCEDURES RECOMMENDED

Taking in consideration the placement of the project there is no any infrastructure for the materials transportation and processes done for the project construction are not the best quality, even, some traces have a pendant in around 10%.

To put in practice MRT, it was necessary to implement a plant (Figure 1) in the place to avoid any problem when the concrete was provided. To perform this task it was necessary to divide the concrete production plant in different parts and after that it was replaced along 1 km from the chosen place for the construction, as a plant support was included a truck mixer as a base and in different periods, if would be more demand there is an extra equipment to accomplish a correct delivery of concrete.

Material delivery: for a deficient infrastructure during a construction, the delivery where the cement and aggregates are, it is necessary to transport them in 2 stages: first of all, take the cement and aggregates to the nearest town and place them in a warehouse and second, to take them through the production plan; in the case of the cement only 15 tons can be transport and the aggregates only charges of 4 m^3; the delivery time between the warehouse and the plant is around 4 hours.

Concrete production: to make a production it is necessary to modify the plant and include:

A water heater system that has the blank to search a minimum temperature of 70°C, to accomplish this task was necessary to install at water tank and withaheater like, also used in petroleum asphalt plants.

To get the specified temperatures in the project the production system existent, the tube circuit, the cement silo, the additive tank and water were recovered totally with polyurethane being apart from the low environmental temperatures; in another way the aggregates warehouses are covered with canvas to maintain the temperature apart of outdoor conditions; in all the equipment's the oil was substituted by oil that do not get freeze.

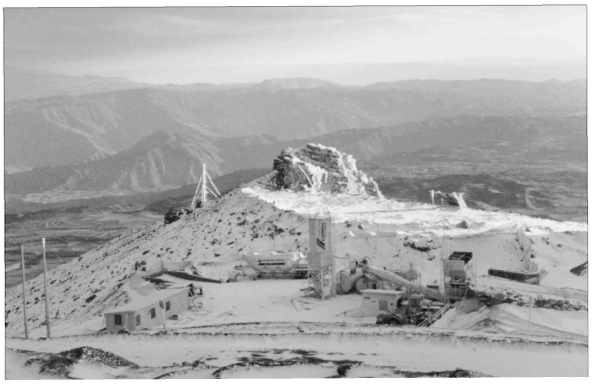

Figure 1 Concrete production plant

Before starting the current delivery, there were manufacture concrete proves with the finality of verifying the specific characteristics and authorize the project mixes; when the set is starting, are prepared 2 mixes with low volume (3 m^3) to make valid results, when it is proved starts the total delivery made in trucks of 7 m^3 and at the same time they delivery volumes no more than 6m^3; the material delivery schedule were always favorable for the concrete to get a high environmental temperature in the set, 90% of the sets were done after 13 hours.

The sets are programmed at least 24 hours and the total volume has to be assured.

Concrete set: the concrete set area, at the beginning of the set is covered with canvas, the same is injected with steam to avoid contrast temperatures, this task is done after 2 or 4 hours after the set is finished and at the end is recovered with canvas in the case of a frustum of a cone that is the main support of the observation plate there were specific steeps, for example the placement of a thermal cover in the (forms) at the same time it is cured with water steam.

RESULTS

Fresh and Hydrating Concrete

In the following are presented the results after the concrete [6] is placed in a 95% that correspond to a MRT base structure and support.

The results of the fresh mix are presented on Table 1 and it shows the good management of the concrete temperature before the setting, the same one was placed in all cases under specification.

The Figure 2 shows the environmental temperature conditions and the main characteristics of the elements, all cases presented the minimum temperature for the concrete mix, where the task under analysis establishes 2 ranks.

Table 1 Results of the fresh mixes

CONCEPT	SAMPLE NUMBER	X	S	C.V. (%)	MINIMUM VALUE	MAXIMUM VALUE
Slump (cm)	44	20.00	2	8	15	22.00
Concrete Temperature (°C)	44	21.00	3	13	16	26.00
Environmental Temperature (°C)	44	9.00	3	30	3	16.00
Air Content (%)	44	4.62	2	22	22	6.98
Fresh Volumetric Weight (kg/m^3)	44	2242.00	45	45	2187	2292.00

In the Figure 3 is demonstrated what: independently of the environmental temperature conditions and the particular characteristics of the elements, the minimum temperature specified is fulfilled in every case, were in the analysis case is established two acceptation ranges.

Note: In the figures, the temperature does not show all the measured results but we can consider as a representative samples the obtained results from the MRT construction.

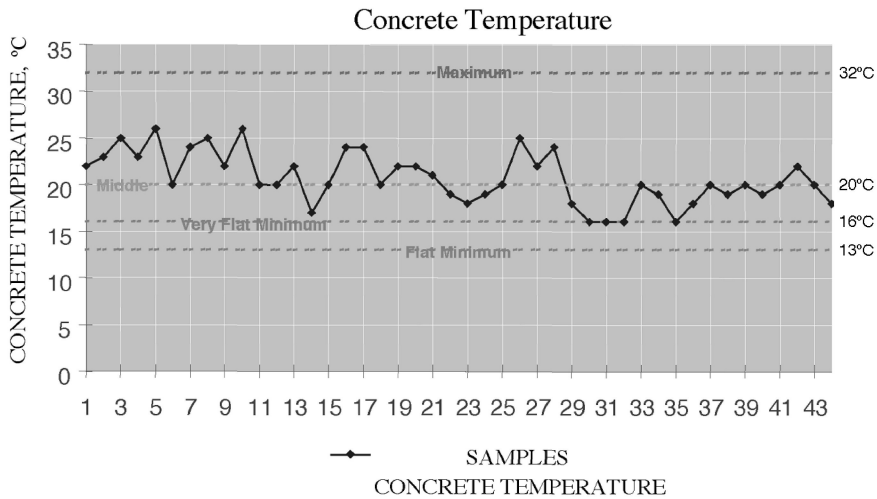

Figure 2 Fresh concrete temperature during the placement in centigrade degrees

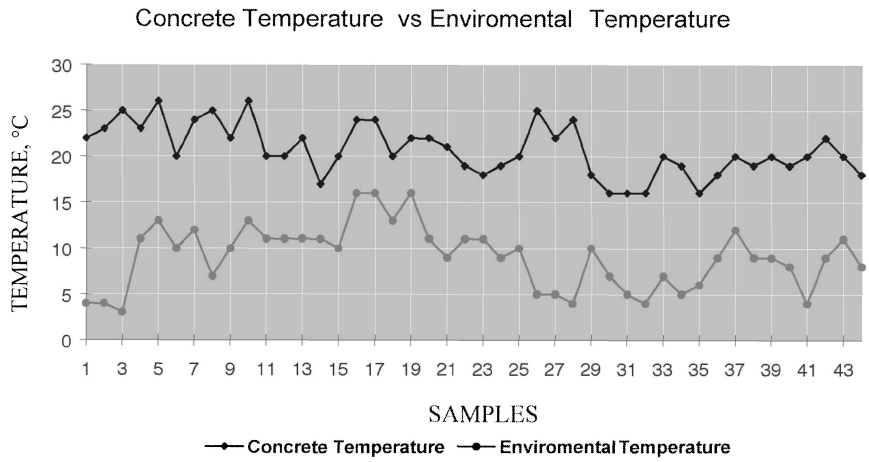

Figure 3 Comparision between the fresh concrete temperature and the enviremental temperature in centigrade degrees

Hardened concrete

The compression strength results are shown in the Table 2, these show what the admixture have a light excess performance in relation to the original acceptance approach what suggest a f'c of 35 N/mm², in the basis of that it's possible to comment the following points.

Table 2 Compressive strength results of the concrete

f'c (N/mm²)	AGE (days)	SLUMP (cm)	SAMPLE NUMBER	S (N/mm²)	X (N/mm²)	C.V.	MINIMUM VALUE	MAXIMUM VALUE	% f'c	CEMENT CONTENT (kg/m³)
35	3	18	29	4.4	25.3	18	149	329	101	350
35	7	18	34	4.1	35.8	11	287	441	143	350
35	28	18	37	2.2	43.8	5	388	471	175	350

According with the project owner was necessary to define the minimum cement amount for each m3 of concrete (350 kg/m³) to satisfy the durability conditions for the same structure. To obtain efficiency during the use of the forms in the project, the owner asked to deliver the concrete accomplishes the 80% of performance in 3 days.

The group of these variants with a low a/c relationship (0.45) establishes an increase in the natural develop of the compression performance of the product. It is important to mention that the 2 specified compression performances, only one maintains itself (35 N/mm²) according with the owner project interests.

The static modulus of elasticity results can be checked in the Table 3, we can see that the aggregate inclusion with calcareous composition has an excellent quality, the obtain values over the minimum specified by design, where the minimum was 221 35.9 N/mm², this value mentioned before was not accepted at all.

Table 3 Static modulus of elasticity results of the concrete

AGE (days)	SLUMP (cm)	SAMPLE NUMBER	S (N/mm²)	X (N/mm²)	C.V.	MINIMUM VALUE	MAXIMUM VALUE	% Ec
7	18	6	2537.6	30022.2	9	270806	348117	136
28	18	15	3589.9	33259.5	11	284082	397455	175

CONCLUSIONS

Related with the original project specifications it is considered the structural needs of the product that are less important to the exposure and service conditions of the elements.

The final opinions are consider for the concrete production and set, for example to unify owners interest, designers, masonries, supervisors, and project producers, in this way, everybody stay with the same position to get the collective goal.

The good obtain results of the fresh concrete properties in fresh state, becoming stiff prove the measurements effectiveness taking in programming, production and concrete placement. In particular, the temperature control was effective to assure the material production in regard to a minimum value defined by a temperature placement.

REFERENCES

1. DIRAC. "Especificaciones de Concreto del Radio Telescopio Milimétrico". Instituto Nacional de Astrofísica Óptica y Eléctrica, Universidad Nacional Autónoma de México, Puebla, México,1999.
2. URIBE, A.R. "Análisis y Recomendaciones Relativas a la Construcción de la Cimentación del Gran Telescopio Milimétrico". Informe Técnico, Centro de Tecnología Cemento y Concreto, Dirección Técnica, Unidad Concreto, Cementos Mexicanos, México,1999.
3. MENA, F., *et al.* "Guía para la Durabilidad del Concreto, Suplemento Mexicano del Informe del Comité ACI 201". Ed. American Concrete Institute Sección México-Capital. México,1989.
4. ACI 201. " Guide To Durable Concrete". ACI Manual of Practice, Detroit, Michigan, USA1999.
5. INAOE,. "Reporte de las Condiciones Atmosféricas y Climatológicas en el Cerro de la Negra, Puebla, México". Instituto Nacional de Astrofísica, Óptica y Eléctrica, Universidad Nacional Autónoma de México, Puebla, México,1999.
6. FLORES, M.M.,. "Informe de Control de Calidad del Concreto para el Proyecto del Gran Telescopio Milimétrico". Informe Interno, CEMEX Concretos, Unidad, 2000.

HOW TEMPERATURE AFFECTS EARLY AGE CONCRETE BEHAVIOR UNDER LOCAL CONDITIONS

B Toumi

Z Guemmadi

H Houari

University Constantine

Algeria

ABSTRACT. The present paper aims to present the evolution of compressive concrete strength at early age under local conditions. In this fact, a large scale test has been investigated using concrete with type II cement for assessing the mechanical strength development in function of curing mode and temperature of treatment that simulate Algeria climate. The different curing mode were saturated, without evaporation and ambient. The curing temperature were 20, 30 and 50°C successively. Measurements were taken at the ages of 0.42, 1, 2, 3, 7 and 28 days. Three others concrete mixes were used at water-cement ratio of 0.45, 0.55 and 0.65 to determine the temperature evolution in core of massive concrete elements that have volume-exposed surface ratio of 0.05, 0.10 and 0.15. The temperature evolution was continuously followed from 24 hours and up to three days of concrete age. Obtained results attest that, at early age, the compressive strength rate is affected by temperature, type of moulds and curing conditions. Tensile strength was affected as like as the compressive strength. The temperature in the core of test-specimens varies with the type of moulds (plastic, steel, cardboard), curing conditions and with the concrete massivity.

Keywords: Concrete, Early age, Temperature, Curing, Mould, Massivity, Strength.

Toumi Belkacem, is a PhD candidate at Constantine university and is researcher in the LMDC laboratory. His research interests include mathematical modeling and high-strength concrete behavior under high temperatures.

Guemmadi Z'hor, is civil engineer at the LTPEst laboratory and PhD student researcher at LMDC laboratory. Currently she is a teacher in the university of Constantine, her research interests include alkali aggregate reactions and durability of concrete.

Houari Hacene, is postdoctoral follow and director of LMDC laboratory. He received his PhD degree from INSA at France. His research interests are in durability of concrete, high-strength concrete and new materials behavior.

INTRODUCTION

Early age concrete behavior is a major industrial problem and is of greet interest to modern concrete technologies. Currently, we are facing an acceleration in the rate of construction that result from the great technical developments, economic considerations and environmental constraints. These constraints, stimulate concrete firms to look how they can quickly get a compressive strength that permit them to manipulate manufactured concrete elements without damaging there long-term properties. This objective need not only a proper understood of concrete hardening process at early age, but also a computing method that permit assess the concrete properties at any time.

Hhydraulic concretes, always need a waiting time to acquire their final strength by a natural hardening. This constitutes one of the major inconveniences of these materials. This waiting time is more and more mismatched with the productivity of concretes firms. In concrete industry, it exist several ways for accelerating the process of concrete hardening. If the thermal treatment remained the most efficient means to get the critical strength, it may be intensified by climatic conditions particularly in hot climate as the case of Algeria in witch mean of temperature in summer is about 45°C that may involve a large thermal gradient between the inside and concrete element surface. This thermal considerations affect both concrete durability and its mechanical properties. Consequently, mathematical models for concrete strength assessment must not neglect the temperature effect on thermo mechanical concrete properties.

The object of this article is to present the concrete behaviour at early age, and to put in evidence how concretes performances are influenced by moulds nature, curing mode, curing temperature, W/C and the Volume to Surface ratio. So, a vast experimental program was realized in odder to follow the development of the mechanical strength and within test-tubes temperature evolution at early age.

The obtained results have permitted us to collect several knowledge on the early age concrete behavior, and demonstrate to us that the curing mode and temperature affect compressive strength increase as well as the tensile strength. The temperature within test-tube is affected by the type of mould, by curing mode, by W/C and also by the V/S ratio.

EXPERIMENTAL PROGRAM

The concrete submitted to tests is an ordinary concrete. It results of mixing gravel, sand, cement and water. These constituent are of local produces. All tests have been realized in according to Algerians standard.

The selected parameters were:

- mould nature (steel, cardboard, plastic)
- curing mode (ambient, saturated, without evaporation).
- curing temperature (20°C, 30°C, 50°C).
- water to cement ratio
- volume to surface ratio

Tests were organized into two groups of measures:

The first group of measures corresponds to the assessments of the influence of the moulds type, the curing mode and the curing temperatures on the compressive and tensile strength at the ages of 0.42, 1, 2, 3, 7 and 28 days.

The second group of measures corresponds to the measures of the within test-tube temperature evolution (continuously followed from 24 hours and up to three days of concrete age).

MATERIAL USED AND CONCRETE CONFECTION

Granulates

Granulates that form the skeleton of the concrete come from the career of Ain Smara. The granular classes used are 0/3, 3/8, 8/15 and 15/25.

Cement

The cement type is CPJ 45. It comes from the ERCE factory and is conform to the Algerian's norms (NA 442).

Concrete confection

The formulation of the concrete mix has been made according to the method of Dreux and Gorisse. Three concrete mixes M1, M2 and M3 that defer only by the W/C ratio (W/C = 0.45; 0.55; 0.65 respectively) have been prepared. The dosages of the final constituent are ported on Table 1. The mixture M1 is destined to follow the resistances and the temperature evolution within test-tubes under the influence of the moulds type and the mode of conservation. For the following of the influence of the W/C and the Volume/Surface on the temperature evolution, the three mixes M1, M2 and M3 has been use.

Table 1 Dosages of concrete constituents

CONSTITUENTS	DOSAGE, Kg/m^3		
	M1	M2	M3
Sable 0/3	435.9	418.7	449.2
Sable 3/8	133.2	127.9	137.2
Gravel 8/15	400.5	384.7	412.7
Gravel 15/25	805.3	773.5	829.8
Cement	350.0	426.7	295.4
Water	192.0	192.0	192.0
W/C	0.55	0.45	0.65
Slump	11 cm	9 cm	13 cm

RESULTS AND DISCUSSION

The concrete presents an evolutionary behaviour in the time. its complex mechanical behaviour, results in the differed deformation, of the mechanical effects often no linear and irreversible. This behaviour is not manifested at the level of granulates that are considered like being inert by their nature, but it is at the level the paste cement that it take place. without a doubt, when cement and water are mixed, three major effect begins to develop at the level of the past, mechanical strength , heat generation and volume reduction. These three effect are generally coupled and influenced by conditions to the limit

Influence of the mould type

The nature of the mould influence on the compressive strength. Plastic moulds (Figure1), give a compressive strength better then that obtained with steel moulds (Figure.2) and cardboard moulds (Figure 3) and this for all curing mode. This gain in strength, can be explained by the insulating nature (thermal insulation) of plastic moulds. A certain quantity of the heat generated by the hydration of the cement is kept by the mould, it confers to the concrete a certain auto maturation that accelerate the process of the hardening.

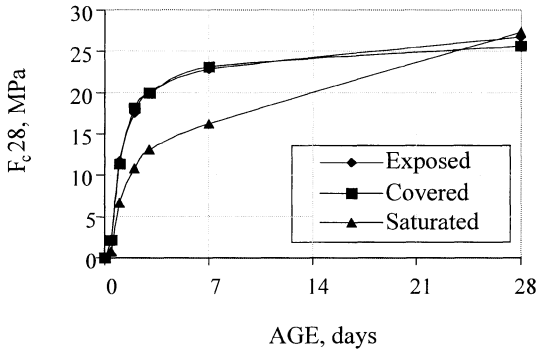

Figure 1 Compressive strength versus age – steel moulds

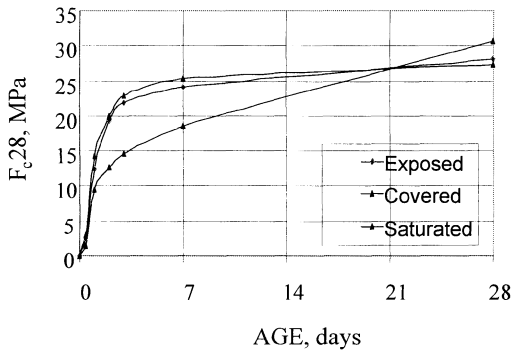

Figure 2 Compressive strength versus age – plastic moulds

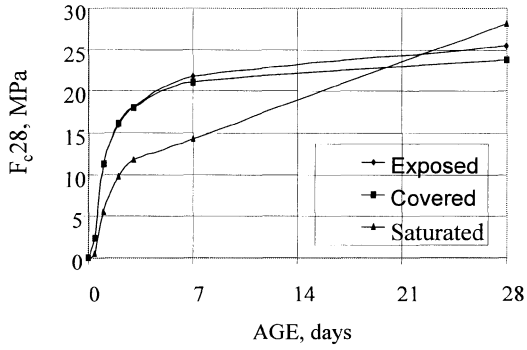

Figure 3 Compressive strength versus age – Cardbord n moulds

This auto maturity explain by following of temperatures in the centre of test-tubes that proves that the more raised temperatures are given by plastic moulds. Moulds made of steel give the less important compared to that in plastic this for the three curing modes. This can be explained by the strong thermal conductivity of metal. Moulds in cardboard, although they are more insulating than moulds made of steel, give the weaker strengths that those gotten by the two others type of moulds. This reduction can be owed to their rigidity (requires the against moulds) and to the impact that appears in the microstructure of the concrete (inflation éttraingite, thermal expansion...). The nature of mould influences considerably on the underground of the concrete.

Influence of the fashion of conservation

At early age, the given strengths in curing mode "saturated" are less important then those procured in curing mode "without evaporation and ambient". Because the water consumed by the cement hydration is continually replace by outside contribution and the pore are not empty by auto desiccation of the concrete. This saturation of water is noted at the time of the bruising of test-tubes at the age of 10 hours and 1 days. To these ages test-tubes break themselves as the humid soil.

At long term test-tubes conserved in water, present a resistances superior to the two another's one. this may be explains by the more advanced hydration state because there is sufficiently water quantity so that the process of hydration contained contrary to the two other that present a lack of water by evaporation and by auto desiccation.

The gotten strength, by the ambient conservation and without evaporation modes are approximately identical for the same type of mould. concretes Strength are affected by the mode of conservation.

Influence of the treatment temperature

The gotten results (Figures 4, 5 and 6) show that the strengths, at early age, increases with the elevation of the temperature. at long term, the strongest temperature of treatment at the young age of the concrete, give the weakest strengths. This results is reinforced by the bibliographic analysis that shows that several researcher have raise this point. The influence of the temperature is appreciable, for the main thing, on the kinetics of the hydration what laws obey to Arhenius law.

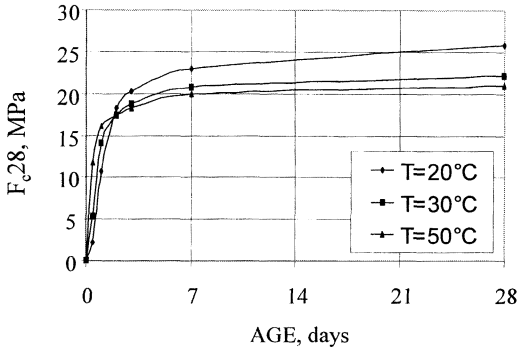

Figure 4 Compressive strength versus age – steel moulds

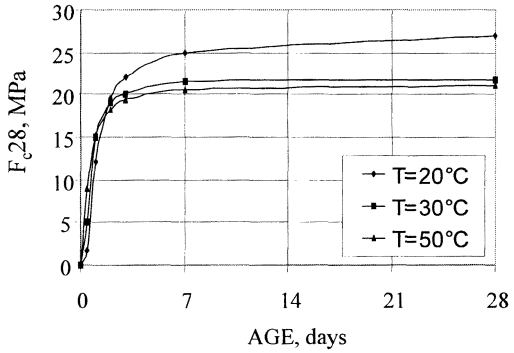

Figure 5 Compressive strength versus age – Plastique moulds

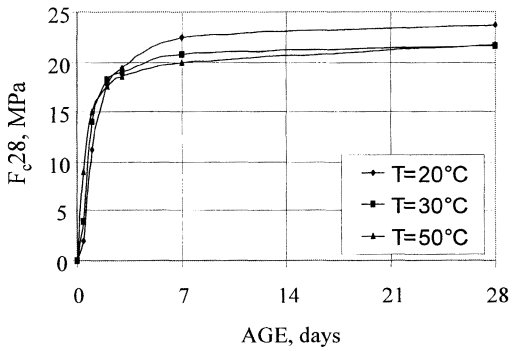

Figure 6 Compressive strength versus age – cardboard moulds

The experimental results [1,2,3] analysis by the least square method, has permits us to calculate the different constants of the three models (Tables 2 to 7).

Table 2 Parameters of Models, T = 20°C

MODEL	$R = a + b \log(t_e)$			$R = t_e/(a\,t_e + b)$			$R = a \exp(-b/t_e)$		
Parameters	a	b	VAR	a	b	VAR	a	b	VAR
	10,4628	7,6601	93.88%	0,0353	0,0538	93.53%	26,8654	0,9009	99.15%

Table 3 Observed values, esteemed values and models curves (P = 95%)

Model	Age	Value Observed	Value Esteemed	MODEL TENDENCY CURVE	OBSERVED VALUES VERSUS PREDICTED VALUES (P = 95%)
$R = a + b \log(t_e)$	0,42	2,1	6,19	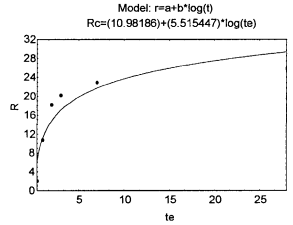	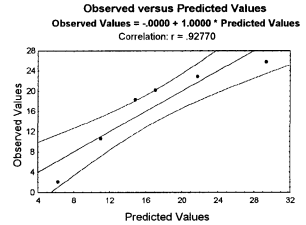
	1	10,7	10,98		
	2	18,3	14,80		
	3	20,3	17,04		
	7	22,9	21,71		
	28	25,8	29,36		
$R = t_e/(a\,t_e + b)$	0,42	2,1	6,10	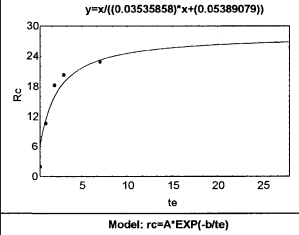	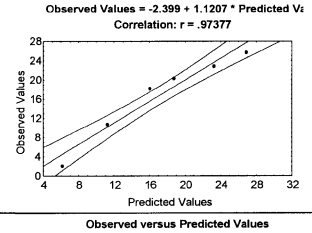
	1	10,7	11,20		
	2	18,3	16,05		
	3	20,3	18,75		
	7	22,9	23,22		
	28	25,8	26,82		
$R = a \exp(-b/t_e)$	0,42	2,1	3,14	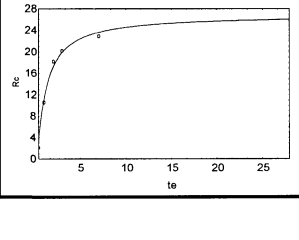	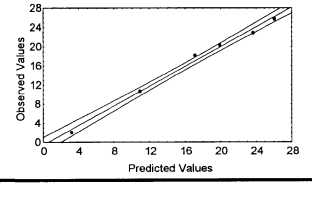
	1	10,7	10,91		
	2	18,3	17,12		
	3	20,3	19,89		
	7	22,9	23,62		
	28	25,8	26,01		

Table 4 Parameters of Models, T = 30°C

MODEL	$R = a + b \log(t_e)$			$R = t_e/(a\,t_e + b)$			$R = a \exp(-b/t_e)$		
Parameters	a	b	VAR	a	b	VAR	a	b	VAR
	12,6107	3,6817	80.12%	0,0426	0,0357	95.06%	22,6653	0,5447	99.17%

Table 5 Observed values, Esteemed values and models curves P = 95%

Model	Age	Value Observed	Value Esteemed	MODEL TENDENCY CURVE	OBSERVED VALUES VERSUS PREDICTED VALUES (P = 95%)
$R = a + b \log(t_e)$	0,42	5,4	9,41	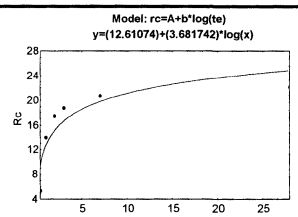	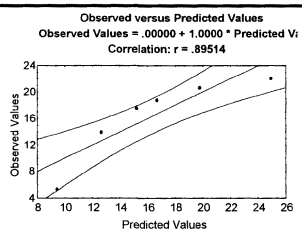
	1	14	12,61		
	2	17,5	15,16		
	3	18,8	16,65		
	7	20,7	19,77		
	28	22,1	24,87		
$R = t_e /(a\ t_e + b)$	0,42	5,4	7,83	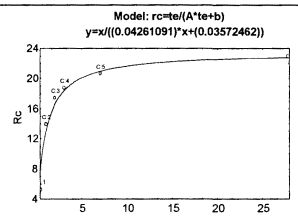	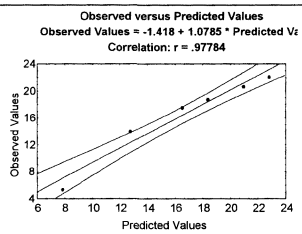
	1	14	12,76		
	2	17,5	16,53		
	3	18,8	18,34		
	7	20,7	20,95		
	28	22,1	22,78		
$R = a \exp(-b/t_e)$	0,42	5,4	6,195	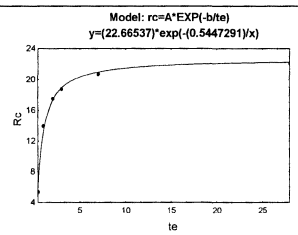	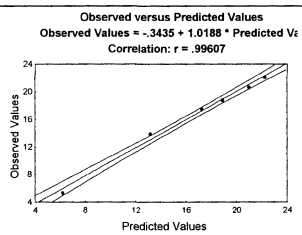
	1	14	13,14		
	2	17,5	17,26		
	3	18,8	18,90		
	7	20,7	20,96		
	28	22,1	22,22		

Table 6 Parameters of Models, T = 50°C

MODEL	$R = a + b \log(t_e)$			$R = t_e /(a\ t_e + b)$			$R = a \exp(-b/t_e)$		
Parameters	a	b	VAR	a	b	VAR	a	b	VAR
	15,2339	2,0954	87.90%	0,04803	0,01587	97.09%	20,4433	0,24450	98.30%

Observing these results, we can note that for the three temperatures, the exponential model (model 3) deal a better interrelationship that the logarithmic model (model 1) and model hyperbolic (model 2).

The logarithmic model under esteem strengths at early age and on esteem ulterior strengths, at later ages for all temperature, then final strength of a treated concrete is less important than that of not treated concrete.

Table 7 Observed values, Esteemed values and models curves P = 95%

Model	Age	Value Observed	Value Esteemed	MODEL TENDENCY CURVE	OBSERVED VALUES VERSUS PREDICTED VALUES (P = 95%)
$R = a + b \log(t_e)$	0,42	11,7	13,41	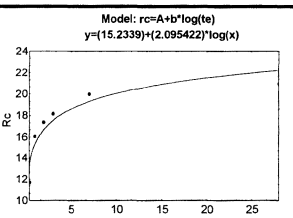	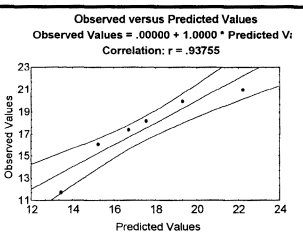
	1	16,1	15,23		
	2	17,4	16,68		
	3	18,2	17,53		
	7	20,0	19,31		
	28	21,0	22,21		
$R = t_e/(a\,t_e + b)$	0,42	11,7	11,65	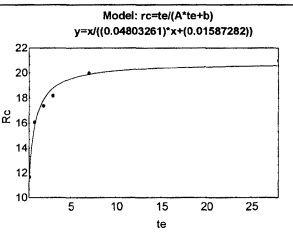	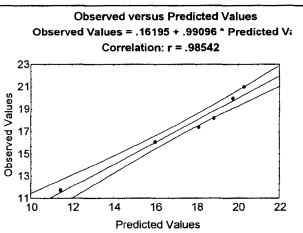
	1	16,1	15,64		
	2	17,4	17,86		
	3	18,2	18,75		
	7	20,0	19,88		
	28	21,0	20,57		
$R = a\exp(-b/t_e)$	0,42	11,7	11,42	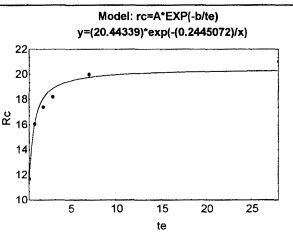	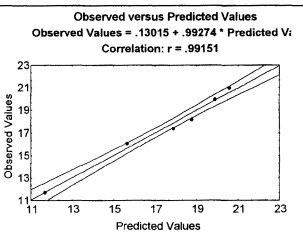
	1	16,1	16,00		
	2	17,4	18,09		
	3	18,2	18,84		
	7	20,0	19,74		
	28	21,0	20,26		

At relatively elevated temperatures, hyperbolic and exponential models, foresee final strength less important then those gotten experimentally. At early age, the exponential model converges very well with the experimental results. This model will be therefore preferential for software development to assess the mechanical strength at early age of the concrete.

Influence of the W/C ratio on the evolution of the temperature within concrete elements

The elevation of the temperature in a massif concrete element is inversely proportional to the W/C ratio, it comes back to say that the elevation of the temperature within concrete is directly linked to the cement content. This observation is verified in this study for the three W/C ratios (Figures 7, 8 and 9).

Influence of the V/S ratio on the temperature evolution within concrete elements

The V/S ratio constitutes a balance between the generation of heat and its dispersion. The concrete is a material having a weak thermal conductivity, so the diffusion of the heat from

the centre toward the outside is very weak what explains that more the V/S ratio is large more the value of the temperature in the centre is large. The V/S report can constitute a measure to predict the elevation of the temperature in the massive elements (ratio of Heat Generation laws to the heat dispersion).

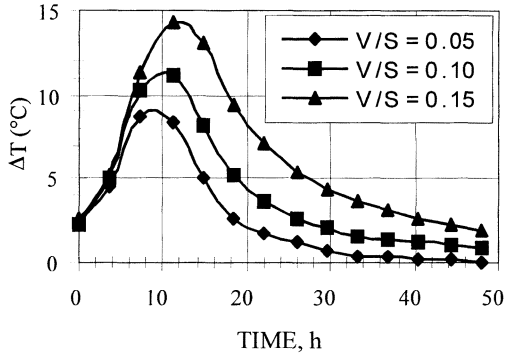

Figure 7 Evolution of temperature in function of rapport W/C (W/C=0.45)

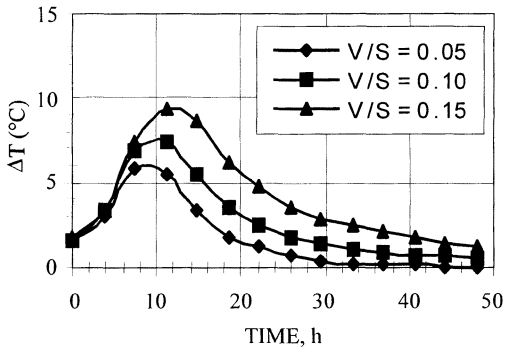

Figure 8 Evolution of temperature in function of rapport W/C (W/C=0.55)

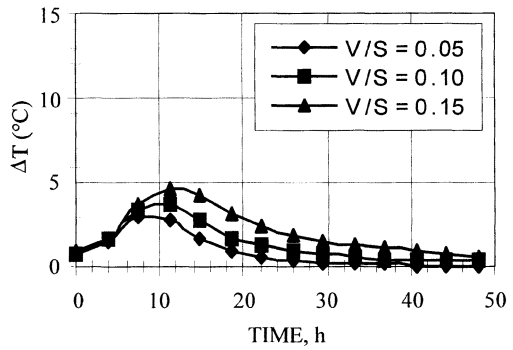

Figure 9 Evolution of temperature in function of rapport W/C (W/C=0.65)

The influence of the V/S ratio is also sees by the instant of the pick apparition of the heat and in the phase of cooling. The three V/S, show that the more this ratio increases the higher the temperature becomes.

Perhaps, from this Bournazel reports that cracks owed to the thermal withdrawal appear in dams during the winter that follows their construction.

CONCLUSIONS

Moulds influence the concrete resistances by their nature, their rigidities and their shape. For current curing mode, plastic moulds give the best strength in compression. The saturated curing mode, give the weakest strength at early age and the strongest at long-term. The tensile strength is affected by both conservation and temperature.

The strong temperature of treatment gives the raised strength at early age and the weak strength at long-term.

The equivalent age concept constitutes a convenient method permitting to predict concrete mechanical strength required in the establishment of concrete project scheduling for an optimal exploitation.

Since mechanical property evolution is strongly affected by temperature, and the advancement of hydration reactions obeys to the Arhenius law, maturity functions based on this last law, give a realist predictions of those gotten in tests.

The cement content is directly linked to concrete pieces temperature elevations. The concrete is a bad driver of the heat, the necessary time to the cooling can be considerable for the massif pieces.

BIBLIOGRAPHIES

TOUMI B. *Contribution à l'étude du comportement du béton au jeune âge sous conditions locales.* Thèse de magister, Université Constantine 1999.

TOUMI B., GUEMMADI Z., HOUARI H., Effet de la température sur la résistance du béton au jeune âge. Séminaire national du Génie Civil, SNGC Sidi bel Abbes 15/16 mai 2001.

TOUMI B., GUEMMADI Z., HOUARI H., *Etude du caractère thermo-mécanique du béton au jeune âge Models de prévision de la résistance mécanique.* Séminaire internationale sur la modélisation numérique en structure et géomatériaux SMNSG 2001, Batna, 22-24 Octobre 2001

GUO CHENGJU Maturity *of concrete : Method for Predicting Early Stage Strength. ACI Materials Journal Vol. 86 N°4 July-August 1989 P. 341-353*

BYFORS J. *Plain concrete at early ages*, Stockholm : Swedish Cement and concrete Research institute, 1980, 345 P, Rapport N° Fo 3/80.

BOURNAZEL J. P., REGOURD M. M. *Matthematical Modeling of concrete Durability : The use of Thermodynamics Processes* Concrete durability Sp 144-12 PP 233-249

BRESON J. *Prediction of Strength of Concrete Products*, RILEM International Conferance on concrete at Early ages, Paris: Ecole National des Ponts et Chaussés 1982, vol. P111-115

PLOWMAN *Maturity and Stength of concrete* Magazine of Concrete Research 1958 Vol. 8 No. 22 PP 13-22

CARINO N. J., TANK R. C. *Maturity functions for concrete made with various cements and admixtures* ACI Materials Journal Vol. 92 N°2 March - April 1992 P. 188-196

CHANVILLARD, G. D'ALOÏA, L. *Concrete Strength Estimation at Early Age : Modification of the method of Equivalent Age*. ACI Materials Journal Vol. 94 N

ALLOWANCE FOR NON-LINEAR PROPERTIES OF REINFORCED CONCRETE STRUCTURES IN FINITE ELEMENT ANALYSIS

A Ermakova
Southern Ural State University
Russia

ABSTRACT. The method of additional loads is used for non-linear finite element analysis of reinforced concrete structures. The main difficulty of realization of this method in programs is the definition of theoretical functions for formation of additional loads and correcting stresses. For example, the algorithm for formation of additional loads was carried out for taking into account of progressive cracking on the basis of developed triangular finite element with conditional crack. This algorithm was realized in program "Element-1", which gave the good results for analysis of some structures under plane stress-strain state. Besides this algorithm has opened the possibilities for formation of additional loads for any structure and non-linear property. It was proved by finite element analysis of Chelyabinsk shopping center long-span shell.

Keywords: Finite element method, Additional loads, Non-linear property, Reinforced concrete.

A Ermakova, is Cand. Tech. Sc, Assistant Prof. ("dotsent") of Department of Building Structures of Southern Ural State University, Chelyabinsk, Russia.

INTRODUCTION

The finite element method considers any structure as an assembly of elements of simple form and finite size. In the end it permits to lead a design to the solving of algebraic system of linear equations

$$KV=P \tag{1}$$

where V = column matrix of unknown displacements of points;
P = column matrix of external loads;
K = stiffness matrix of the calculated structures.

The solution of linear problem ends at this stage, but the result does not lead to real data of stress-strain state of the structure if it has strongly pronounced non-linear properties.

At present two methods are used for accounting of nonlinear properties of material. The first method is the variation of coefficients of matrix K at each step of load and each iteration.

The second method is the transformation of column of constant terms by means of additional loads. In this case the system of linear equations (1) takes the next form:

$$KV = P + F \tag{2}$$

where F = vector of additional loads taking into account the non-linear properties of analysed system.

The essence of method is that the application of vectors F and P deforms the displacements of the structure with linear properties to the state of displacements of the same structure with non-linear properties under the action of external loads P.

This paper considers some problems of this method for non-linear finite element analysis of reinforced concrete structures.

COMPUTER PROBLEMS

At present the method of additional loads is used in a few programs for analysis of structures by means of the finite element method because it requires the essential modification of solution of algebraic system of linear equations.

Programs

The application of additional loads for non-linear finite element analysis requires the programs with next steps:

1. Composition of design diagram.
2. Calculation of stiffness matrix of finite elements.
3. Formation of stiffness matrix of the system K.
4. Allowance for non-linear properties with the help of vector of additional loads F.

5. Solution of algebraic system of linear equations by Gauss elimination.
6. Calculation of strains, stresses and nodal reactions.
7. Analysis of stress-strain state of the structure.

Thus, the using of this method leads to the reorganization of the solution of a system of algebraic equations as the main part of such programs.

Gauss Elimination

The application packages realizing the finite element method use Gauss elimination of unknowns for solution of algebraic system of linear equations. According to this method the definition of unknowns is realised at first by direct motion and then by inverse motion. The use of the method of additional loads allow to eliminate the most labour consuming operation of obtaining of inverse stiffness matrix K^{-1} in solution of system of equations (2) at every step of load and at each iteration of the step except the first iteration of the first step, Figure1. Only operations connected with calculation of constant terms remain among the operations of direct running of solution of algebraic system of linear equations and then the operations of inverse running take place. Such flowchart saves three forth of time for solution of system of linear equations at all iterations except the first iteration of the first step.

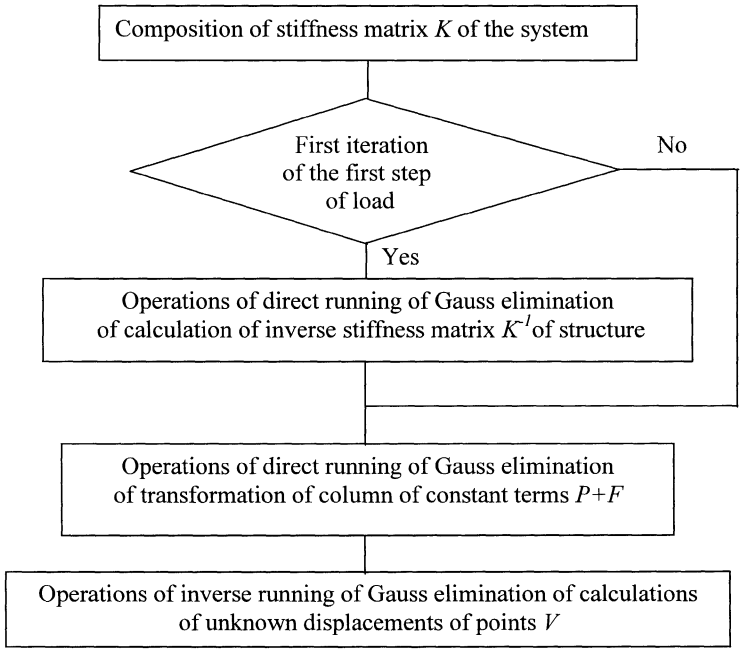

Figure 1 Flowchart of solution of algebraic system of linear equations $KV=P+F$

VECTOR FOR ADDITIONAL LOADS FOR NON-LINEAR PROPERTIES

It is well known that the analysis of reinforced concrete structures by means of the finite element method is connected with some serious difficulties because of brightly expressed specific non-linear properties. The obtaining of the theoretical dependencies for formation of the vectors of additional loads and correcting stresses in the finite elements is the actual problem.

Vector of Additional Load and Correcting Vector of Stress

The main non-linear properties of concrete are plasticity, progressive cracking, bond, presstressing, repeated loading, temperature action. Therefore at every stage of design the vector of additional loads determines by the formulae:

$$F = \sum_{i=1}^{n} F_i \tag{3}$$

where F_i = vector of additional load taking into account the character of manifestation of non-linear property;

n – number of non-linear properties taking into account at the present stage of analysis.

The essence of the given process may be graphically represented by axial tension (compression), Figure 2.

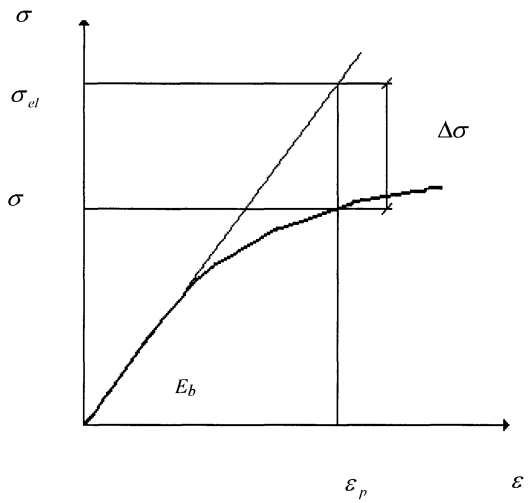

Figure 2 Diagram for taking into account of non-linear properties by means of vector of additional load for axial tension (compression).

E_b = initial modulus of elasticity of material;

ε_p = strain taking into account of non-linear properties;

σ_{el} = elastic stress corresponding to non-linear strains ε_p,

i.e. simultaneous application of external load P and additional load F;

σ = stress taking into account of non-linear properties;

$\Delta\sigma$= correcting vector of stress which takes into account the change of elastic stress due to appearance of non-linear properties.

Table 1 shows the example of formation of vector F for reinforced concrete structures taking into account most typical non-linear properties.

Table 1 Formation of vector of additional load and correcting vector of stress of allowance for non-linear properties of reinforced concrete

Number of Non-Linear Property	Non-Linear Property	Considered of Non-Linear Properties	VECTOR OF ADDITIONAL LOAD		CORRECTING VECTOR OF STRESS	
			Notation	$F=\sum_{i=1}^{6}F_i$	Notation	$\Delta\sigma=\sum_{i=1}^{6}\Delta\sigma_i$
1	Plastic properties of concrete	1	F_{pl}	F_{pl}	$\Delta\sigma_{pl}$	$\Delta\sigma_{pl}$
2	Bond of concrete and reinforcement	1,2	F_{bond}	$F_{pl}+F_{bond}$	$\Delta\sigma_{bond}$	$\Delta\sigma_{pl}+\Delta\sigma_{bond}$
3	Cracking	1,2,3	F_{crc}	$F_{pl}+F_{bond}+F_{crc}$	$\Delta\sigma_{crc}$	$\Delta\sigma_{pl}+\Delta\sigma_{bond}+\Delta\sigma_{crc}$
4	Prestressing	1,2,3,4	F_{pr}	$F_{pl}+F_{bond}+F_{crc}+F_{pr}$	$\Delta\sigma_{pr}$	$\Delta\sigma_{pl}+\Delta\sigma_{bond}+\Delta\sigma_{crc}+\Delta\sigma_{pr}$
5	Repeated load and discharge	1,2,3,4,5	F_{rep}	$F_{pl}+F_{bond}+F_{crc}+F_{pr}+F_{rep}$	$\Delta\sigma_{rep}$	$\Delta\sigma_{pl}+\Delta\sigma_{bond}+\Delta\sigma_{crc}+\Delta\sigma_{pr}+\Delta\sigma_{rep}$
6	Temperature action	1,2,3,4,5	F_t	$F_{pl}+F_{bond}+F_{crc}+F_{pr}+F_{rep}+F_t$	$\Delta\sigma_t$	$\Delta\sigma_{pl}+\Delta\sigma_{bond}+\Delta\sigma_{crc}+\Delta\sigma_{pr}+\Delta\sigma_{rep}+\Delta\sigma_t$

By analogy with formula (3) the correcting vector of stress $\Delta\sigma$ is determined by all types of non-linear properties considered at the given stage of analysis of structure:

$$\Delta\sigma = \sum_{i=1}^{n} \Delta\sigma_i \tag{4}$$

where $\Delta\sigma_i$ is the correcting vector of stress which takes into account the change of value of elastic stress due to appearance of definite type of non-linear property.

The correcting vector of stress $\Delta\sigma$ is formed by the separate vectors of stress $\Delta\sigma_i$. Each of these vectors takes into account the change of elastic stress due to appearance of corresponding non-linear property.

The Table 1 shows the formation of correcting vector of stress, which takes into account non-linear properties of reinforced concrete.

Previous Research

A number of works dealing with analysis of non-linear reinforced concrete structures by the finite element method was done under the leadership of Prof. Oatul A.A. at Chelyabinsk Polytechnic Institute (then Chelyabinsk State Technical University, at present Southern Ural State University).

Thus thesis for a candidate degree written by Karyakin A.A. (assistant professor ("dotsent") of department of building constructions) and was concerning with the development of algorithm allowing for plastic properties of concrete by means of additional load vector F_{pl} on the theory of plasticity by Geniev G.A. [1].

The logical continuation of this work was concerned with the development of algorithm for formation of additional load vector with allowance for bond F_{bond} and cracking F_{crc}. So, vector F_{crc} is formed on the basis of properties of special developed triangular finite element with conditional crack [2]. This method has been carried out for analysis of structures under plane stress-strain state (deep beams). It gives the opportunity with allowance for any non-linear property of any reinforced concrete structures under any type of stress-strain state [8].

Program "ELEMENT-1"

Efficiency of additional loads was proved by program "ELEMENT-1". This program saves computer resources essentially and decreases the time of problem solution from 1.2 to 3.5 times depending on the stage of analysis [3]. The use of this program for analysis of structures under plane stress-strain state gives the possibility to obtain the detailed information about behaviour of structures. In a number of cases the analysis of this state leads to more rational design, economic effect and saving of material resources.

Fibrous Concrete Beams

Design of prestressed fibrous concrete beams was done with the view to evaluate the efficiency of steel fibrous concrete use in such members. In this connection the efficiency of the used program "ELEMENT-1"evaluated too. The values of experimental and theoretical cracking loads for five considered types of beams differed from 2.16 to 13.32% [7].

Wall Basement Panels

The necessity of analysis of the interior wall basement panels of large panel residential buildings was based on the following problems: a) the increase of static loads on the panel due to transition from 9-floor to 10-floor structure of the residential building; b) the support of basement panels on the pile heads without grid foundations as it was in initial variant; c) the change of concrete grade of basement panels from B20 to B15. The panels differ from each other in dimensions, outlines, values of uniformly distributed loads per linear metre and numbers of supporting piles and openings. Four types were considered. The use of program "ELEMENT-1"[3] in design of these panels led to positive decisions of these problems.

Long Span Shell

The efficiency of this method for space structures and another program was proved by analysis of Chelyabinsk Shopping centre long span shell (102x102 m) for daily temperature difference. Allowance for non-linear property caused by the action of daily temperature difference was carried out by formation of vector of additional load F_t [4,5,6]. The realised analysis allowed to find out the maximum daily temperature difference for this shell and to prove the necessity of allowance for such temperature difference in design of the same long span shells.

Requirements of the Formation of Additional Loads

Some requirements on the formation of additional loads were postulated on the base of using this method for non-linear finite element analysis of reinforced concrete structures.

This algorithm must:

1) follow logic of the finite element analysis;
2) be universal and similar for all of non-linear properties;
3) consider the peculiarity of each type of non-linear property;
4) indicate the change of deformed state of analysed structure under the action of the considered type of non-linear property;
5) provide the change of stress state of analysed structure under the action of the considered type of non-linear property;
6) be easy to program;
7) give the opportunity for carrying out of auxiliary programs for transformation of linear programs into non-linear ones.

It should be marked that these requirements are not equal. For example the first one is the basic requirement, the second, third, forth and fifth ones are auxiliary requirements, the sixth and the seventh are the results of computation.

CONCLUSIONS

Since the method of additional loads for non-linear finite element analysis is effective from the point of view the speed and quality of obtained results it is necessary to carry out:

- the way of formation of additional loads for allowance of various non-linear properties responding to mentioned above requirements;
- the auxiliary algorithm for transformation of the program realizing linear analysis into program for non-linear analysis of reinforced concrete structures by the finite element method.

ACKNOWLEDGMENTS

All researches were made at Southern Ural State University at its Civil Engineer Faculty. At present these researches are continued.

REFERENCES

1. Computer-aided design of reinforced concrete structural elements. Collected lectures. Part 4, edited by Prof. OATUL, A.A. Chelyabinsk, Polytechnic Institute. Chelyabinsk, 1980, p 67.
2. KARYAKIN A.A., ERMAKOVA A.V., Procedure of allowance for cracking in analysis by means of the finite element method. Research in structural mechanics and structural elements., Chelyabinsk Polytechnic Institute. Chelyabinsk, 1985, p 131-133.
3. ERMAKOVA A.V., Computation of reinforced concrete structures operating under condition of plane stress-stain state by means of program "Element-1". Researches into concrete and reinforced concrete. Chelyabinsk Polytechnic Institute. Chelyabinsk, 1989, p 15-18.
4. ERMAKOVA A.V., MAXIMOV Yu.V., OATUL A.A., Analysis of operation of Chelyabinsk shopping centre shell with allowance for thermal loads. Research into structural mechanics and structural elements. Chelyabinsk Polytechnic Institute. Chelyabinsk, 1996, p 81-85.
5. MAXIMOV Yu.V., ERMAKOBA A.V., Analysis of Chelyabinsk shopping centre shell under thermal, static and dynamic loads. Proceedings. International congress ICSS-98. June 22-26, 1998, Moscow, Russia, v.1, p. 368-373.
6. MAXIMOV I., ERMAKOBA A., Necessity of allowance for daily temperature difference in design and operation of long-span shells. Proceedings of the Third international conference on concrete under severe conditions, CONSEC'01. Vancouver, BC, Canada 18-20 June 2001, v.1, p 1017-1024.
7. ERMAKOVA A.V., MAXIMOV Yu.V., Allowance for prestressing in analysis of reinforced concrete structures by the finite element method. Proceedings of the First Russia conference on concrete and reinforced concrete problems. September 9-14, 2001, Moskow, Russia, v.2, p 968-973.
8. ERMAKOVA A.V., Allowance for nonlinear properties of reinforced concrete by means of additional loads in finite element analysis. Proceedings of the First Russia conference on concrete and reinforced concrete problems. September 9-14, 2001, Moskow, Russia v.2, 974-979.

APPLICATION AND RESEARCH OF THE HOUSING BASE CONCRETE TO THE CURING USING HEATING SHEET

M Sugiyama
Hokkai-Gakuen University
Japan

ABSTRACT. This study evaluated the viability of electric heating sheets for the curing of concrete housing foundations in severe, low-temperature environment. The heating sheets tested use PTC (positive temperature coefficient resistor) ceramic elements. The heating temperature is automatically adjusted by these elements in response to adjacent air temperature. The experiment was carried out in two series. The first series was carried out at -10° C in a thermostatic chamber. The second series involved on-site testing. Under severe, low-temperature conditions, of up to -11° C outside air temperature, it was found that curing was possible at about +15° C through the use of heating sheets. Compressive strength was found to be sufficient. The heating sheet is considered to be extremely useful for curing concrete in cold regions.

Keywords: Compressive strength, Heating sheet, Low-temperature, Curing, On-site testing.

Dr Sugiyama Masashi is a professor of the Hokkai-Gakuen University engineering department in Sapporo City, Japan. He received his doctorate in engineering from Hokkaido Univ. in 1981. His doctoral dissertation was "The effect of concrete in structure of the drying on physical property". His specialty is research into technologies which improve the durability of concrete. He received a prize for research into super-high durable concrete from Japan Concrete Institute in 1988. His interests are chemical admixtures and compressive strength and elastic modulus and freezing and thawing resistances and neutralization, etc.

INTRODUCTION

This study evaluated the viability of electric heating sheets for the curing of concrete housing foundations in severe, low-temperature environments. The heating sheets tested use PTC (positive temperature coefficient resistor) ceramic elements. The experiment was carried out in two series. The first series, which used small test specimens, evaluated the compressive strength of concrete that had been cured using the heating sheet. The second series involved on-site testing.

BASIC EXPERIMENT USING SMALL SPECIMENS

An Outline of the PTC Electric Heating Sheet

In the past, heating sheets that used nichrome wire displayed erratic temperature changes with the attendant risk of fire and damage to the sheet. Likewise in the case of oil-stove heating, toxic gases were produced and fire was a potential hazard. The PTC (Positive Temperature Coefficient Resistor) element has many advantages over previous technologies used in heating sheets. The PTC element is extremely durable, safe and flexible and is thus resistant to damage. The PTC element is able to maintain temperature stability by automatically detecting ambient temperature and adjusting if necessary. Heating sheets that utilize PTC elements run on domestic electricity at 100 (V), which makes the power source convenient and efficient.

Plan and Method

The first series evaluated the compressive strength of concrete that had been cured using the heating sheet. This series was carried out using small test specimens. The experiments were carried out in a thermostatic chamber at -10° C and outdoor in Sapporo in November. First, a box that simulated the footing foundations of the concrete was produced. Next, specimens of the fresh concrete were inserted into this box, and the heating sheet was placed on the upper surface. Compressive strength was tested after the 3rd, 7th and 28th day of curing. The dimensions of the specimen were 10φ × 20 cm. The box was made of 10 mm thick wood, and the dimensions were L400 × W120 × H200. Three pieces of the concrete specimen (100φ × 200) were positioned in this box. The box was filled with foam beads, 3~5 mm in diameter. Steel plates L400 × H200 × @4.2 mm) acted as inner walls in three of the test boxes. Because steel reacts more sensitively to outside temperature, we were able to reproduce severe curing conditions. Table 1 shows the design of the experiments. Table 2 shows curing conditions. Table 3 shows the concrete mix proportions.

Table 1 Plan of experiment

CURING CONDITION	IN CHAMBER	OUTDOOR
Temperature	-10°C	Open Air
Curing Period	4 weeks	
Strength	After 3 days, 7 days, 28 days	

Table 2 Curing conditions

SYMBOL	HEATING SHEET	CONDITIONS
A	With	In wood box
B	With	In steel plates box
C	Without	Out Air
D	20 °C water	

Table 3 Concrete mix proportions

W/C %	SLUMP cm	AIR %	WATER kg/m^3	CEMENT kg/m^3	SAND kg/m^3	GRAVEL kg/m^3
50	18	4	165	330	762	1122

cement (density 3.16), river sand (density 2.69), river gravel (density 2.75)

The Results

The temperature results for concrete specimens cured at -10° C are shown in Figure 1. The concrete was mixed at a temperature of 24° C. Specimens A and B (cured under the heating sheet) cooled slowly. However, specimen C (cured without the heating sheet) cooled rapidly and froze at a temperature of -10° C. Mean temperatures after 3 days of curing were as follows; Specimen A (wooden frame) cured under the heating sheet was 5.1° C. Specimen B (steel plate) cured under the heating sheet was 5.5° C. Specimen C cured in outside air was -8.9° C. The air under the heating sheet was 3.4° C. The difference in mean temperature between specimen A (with the heating sheet) and specimen C (without the heating sheet) was 14° C.

Compressive strength is shown in Figure 2. Compressive strength after 3 days of curing was as follows; Specimen A (wooden frame) cured under the heating sheet was 7.24 N/mm^2. Specimen B (steel plate) cured under the heating sheet was 6.85 N/mm^2. Both specimens reached the target strength of 5 N/mm^2 for mould removal. The strength of specimen C could not be assessed due to freezing damage in the initial stages.

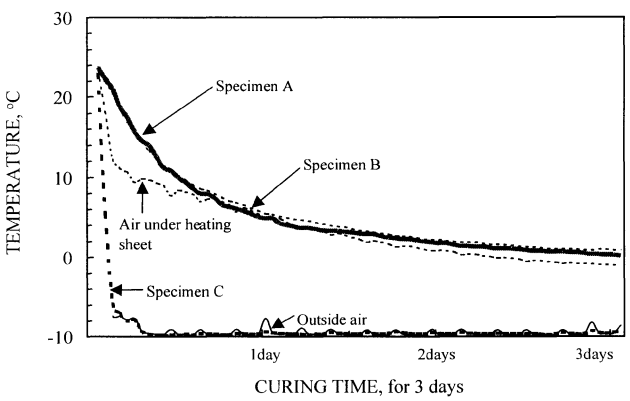

Figure 1 Temperature of concrete specimens (-10° C)

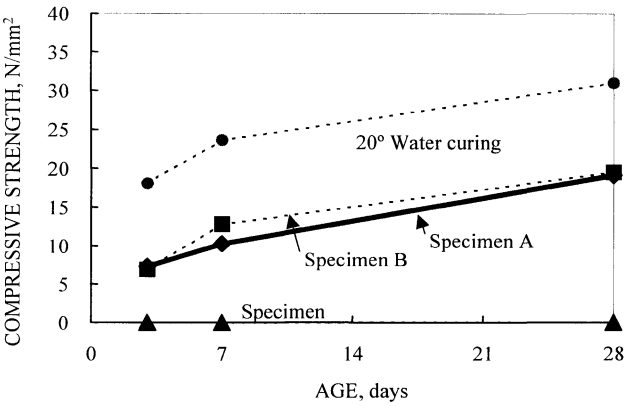

Figure 2 Compressive strength (-10° C)

The temperature results for concrete specimens cured outside in November in Sapporo are shown in Figure 3. Specimen A and B (cured under the heating sheet) once again, cooled slowly. However, specimen C (cured without the heating sheet) cooled rapidly. Mean temperatures after 3 days of curing were as follows; Specimen A (wooden frame) cured under the heating sheet was 12.4° C. Specimen B (steel plate) cured under the heating sheet was 12.3° C. Specimen C cured in outside air was 0.4° C. The air under the heating sheet was 7.7° C. The mean temperature of outside air was 1.0° C. The difference in mean temperature between specimen A (with the heating sheet) and specimen C (without the heating sheet) was about 12° C.

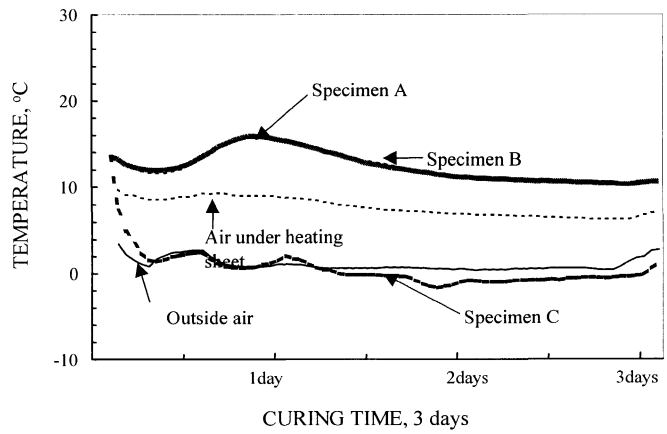

Figure 3 Temperature of concrete specimens (outdoors in November, Sapporo, Japan)

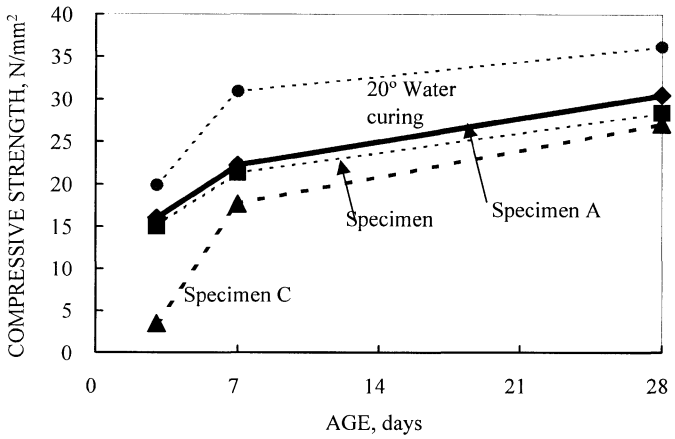

Figure 4 Compressive strength (outdoors in November, Japan)

Compressive strength is shown in Figure 4. Compressive strength after 3 days of curing was as follows; Specimen A (wooden frame) cured under the heating sheet was 16.0 N/mm^2. Specimen B (steel plate) cured under the heating sheet was 15.1 N/mm^2. Specimen C cured in outside air was 3.44 N/mm^2. Specimen A and B reached the target strength of 5 N/mm^2 for mould removal. Specimen C, cured without the heating sheet, could not reach the required strength target.

The results show that curing, using the heating sheet, produces concrete of sufficient strength, even in severe low temperature conditions.

THE FIELD EXPERIMENT

Outlines

The second series involved on-site testing. The tests were carried out in Sapporo City, Hokkaido prefecture, the northern-most region of Japan. Under severe, low-temperature conditions, of up to -11° C outside air temperature, it was found that curing was possible at about +15° C through the use of heating sheets.

Plan and Method

The foundation plan is shown in Figure 5. The experiment was carried out using an actual foundation with metal mould. Foundation dimensions were 6 × 6 m square, wall thickness was 16 cm and the height varied – in sections 1.1 m and in others 1.4 m. The foundation was covered with the heating sheets about 1 hour after the concrete had been poured. The foundation cross section is shown in Figure 6. The heating sheet was activated 4 days after the initial pouring.

The plan of the experiment is shown in Table 4. An outline of the test-pieces used is shown in Table 5. A core test-piece was used to examine the foundation strength. The concrete mix proportions are shown in Table 6. The water/cement ratio was 50%, the slump was 15 cm and the temperature was 13° C.

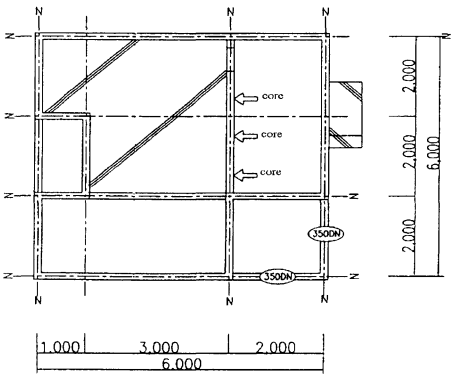

Figure 5 Foundation

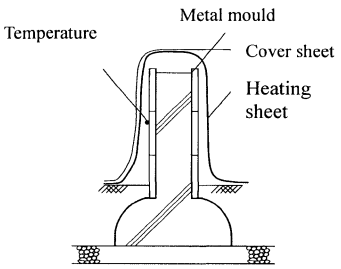

Figure 6 Section of foundation

Table 4 Plan of experiment

PLACE	SAPPORO CITY, JAPAN
Period	Feb 4th-Mar 3th, 2000
Curing Period	4 days
Compressive Strength	After 4 days, 7 days, 28 days

Table 5 Curing conditions

SYMBOL	HEATING SHEET	POSITION	COMPRESSIVE STRENGTH SPECIMEN
A	With	Upper foundation	10φ Core
B	With	Lower foundation	10φ Core
C	Without	Center foundation	10φ Core
D	With	-	10φ20 cm Cylinder
O	Outdoor	-	10φ20 cm Cylinder
S	20°C Water	-	10φ20 cm Cylinder

Table 6 Concrete mix proportions

W/C %	SLUMP cm	AIR %	TEMP °C	WATER kg/m^3	CEMENT kg/m^3	SAND	kg/m^3	GRAVEL kg/m^3
50	15	4.4	13	155	310	□539	□236	1075

cement (density 3.16), sand (density □2.69, □2.68), gravel (density 2.64)

The Results

Temperature

The temperature results are shown in Figure 7. The temperature of the foundation concrete lowered slowly. Mean temperatures after 4 days of curing are as follows; □Center of the foundation concrete (cured under the heating sheet) was 16.5° C. □T division of the foundation concrete (cured under the heating sheet) was 17.6° C. □Foundation concrete without heating sheet was 3.4° C. □Temperature of outdoor air was -4.4° C(-11° C lowest temperature). □Air temperature in the tent was -0.7° C. □Air temperature under the heating sheet was 12.3° C. □Air temperature between the heating sheet and vinyl sheet was 8.6° C.

In an environment where the lowest outside air temperature reached -11° C, curing at about +16° C was possible for concrete cured under the heating sheet. The temperature of the concrete cured under the heating sheet (□and □) was between 13° C to 14° C higher than in concrete cured without the heating sheet (□). The temperature of the concrete cured under the heating sheet (□and□) remained stable when compared to the change in outside air temperature.

Compressive Strength

Compressive strength is shown in Figure 8. After the 4th day of curing, the compressive strength of the core drilled from the upper part of the concrete (cured with the heating sheet) (A) was 14 N/mm^2, while the core drilled from the lower part of the concrete (B) was 12 N/mm^2. Both A and B exceeded the minimum strength of 5 N/mm^2 required to prevent freezing damage in the initial state. Core strength C (cured without the heating sheet) was 4 N/mm^2 after the 4th day. The effectiveness of the heating sheet is clear.

In the case of specimen D, the temperature lowered significantly before the heating sheet was put in place (due to the small size of the specimen) and therefore compressive strength was extremely low.

The Merits of the PTC Heating Sheet for Curing

The advantages of the PTC heating sheet are shown in Table 7.

In regards to the PTC electric heating sheet, there are no temperature irregularities, no risk of fire, and no adverse effects on the environment whereas, in the case of the nichrome wire sheets, a temperature regulator is necessary, there is a substantial risk of fire and damage to the sheet and carbon dioxide is generated in the case of fire.

In the case of the stove heating method (charcoal or oil heater use), there is substantial variation between air temperature close to the heating source and in the corners. A temperature regulator is necessary when using this method and there is a great risk of fire and burn damage to the sheet. A large amount of carbon dioxide gas is produced which has a negative effect on the environment.

The PTC electric heating sheet therefore, has substantial advantages over traditional heating methods.

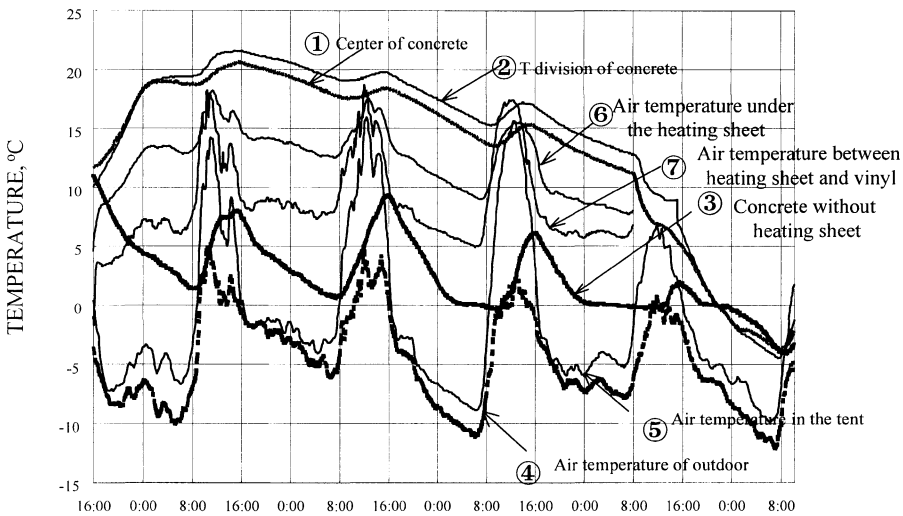

Figure 7 Temperature survey result of field concrete

CONCLUSIONS

This study evaluated the viability of electric heating sheets for the curing of concrete housing foundations in severe, low-temperature environment. The heating sheets tested use PTC (positive temperature coefficient resistor) ceramic elements. The heating temperature is automatically adjusted by these elements in response to adjacent air temperature. The experiment was carried out in two series. The first series was carried out at -10° C in a thermostatic chamber.

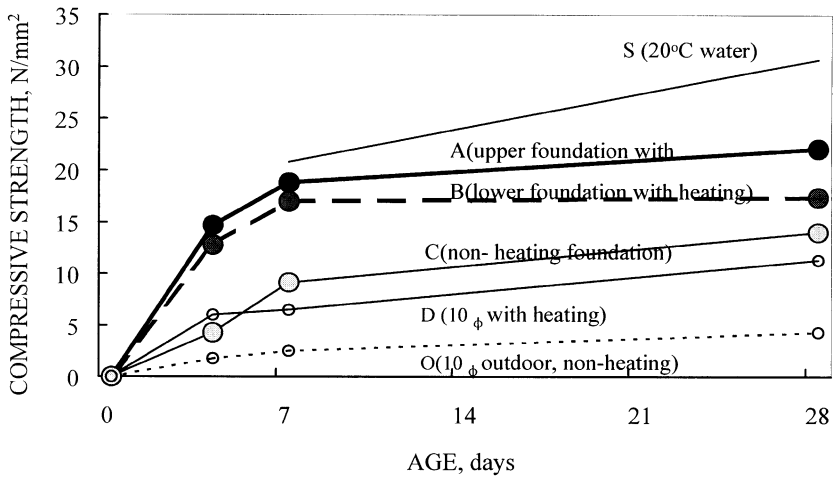

Figure 8 Compressive strength in field concrete

Table 7 The advantages of the PTC heating sheet

THE HEATING CURING METHOD	THE PTC ELECTRIC HEATING SHEET	THE NICHROME WIRE HEATING SHEET	THE STOVE HEATING (CHARCOAL OR OIL HEATER)
Temperature irregularity	Nothing	There is a little variation in temperature	There is temperature variation
Temperature regulator	Nothing. The PTC semiconductor is controlled automatically.	Necessary	Necessary
Safety	Little risk of fire or damage. 100V domestic electric power source.	There is risk of fire and damage to the sheet.	There is great risk of fire and damage to the sheet.
Effect on global environment	Nothing	In the case of a short fire is generated and carbon dioxide is produced.	Large amounts of carbon dioxide produced. Air is contaminated.
Total evaluation	O	×	×

The second series involved on-site testing. Under severe, low-temperature conditions, of up to -11° C outside air temperature, it was found that curing was possible at about +15° C through the use of heating sheets. Compressive strength was found to be sufficient. The PTC heating sheet is extremely durable, safe and flexible and is thus resistant to damage. It has significant benefits when compared to traditional heating methods. This heating sheet is considered to be extremely useful for curing concrete in cold regions.

REFERENCES

1. SUGIYAMA MASASHI, FUKAI AKIRA, Curing experiment of housing foundation concrete using the new heating curing sheet, Annual Meeting of Architectural Inst of Japan, pp 425-428, 2000.

2. SUGIYAMA MASASHI, FUKAI AKIRA, Curing experiment of housing foundation concrete using the new heating curing sheet, Annual Meeting of Architectural Inst of Japan, pp 319-322, 2001.

3. SUGIYAMA MASASHI, SASAKI R., A curing experiment of the concrete using the new thermal curing sheet, Architectural Inst. of Japan, Hokkaido branch research report No 73, pp 431-434, 2000.

4. SUGIYAMA MASASHI, SASAKI R., Curing experiment of housing foundation concrete using the new the heating curing sheet, Bulletin of the Faculty of Engineering HOKKAAI-GAKUEN University, pp 121-129, No 28, 2001.

5. A.I.J., Japanese Architectural Standard Specification, JASS5 Reinforced Concrete Work, 1997.

6. A.I.J., Recommendation for Practice of Cold Weather Concreting, 1998.

7. SEKISUI House Ltd., Technical Report, Japan.

EFFECTS OF DIFFERENT CURING TEMPERATURES AND DURATIONS ON SOME MECHANICAL PROPERTIES OF STEAM-CURED CONCRETE

L Turanli

Middle East Technical University

B Baran

STFA Enercom Industrial Manufacturing and Trade Co

Turkey

ABSTRACT. In this study, effects of steam curing on some mechanical properties of concrete; compressive and split tension strength, and modulus of elasticity of hardened concrete were investigated. For these purposes, three different concrete mixes were prepared. Three different curing temperatures as 40 ^{o}C, 60 ^{o}C, and 75 ^{o}C, and also two different curing durations as 4h and 8h were applied in the program. The interpretation of the results of tests revealed that the rate of development in early strength values of steam-cured specimens were relatively higher with respect to their controls as the steam curing temperatures were increased. However, the gain in early strength values became smaller according to the control specimens for higher strength classes of concretes. Moreover, the rate of improvement in early strength values of steam-cured specimens was also greater according to the controls when the steam curing durations were increased. Finally, slight reductions in late strength values of all steam- cured specimens were observed when they were compared with the control specimens.

Keywords: Steam-curing, Accelerated curing, Early strength, Late strength, Compressive strength, Split tension, Modulus of elasticity.

Dr L Turanli, is an Instructor at the Department of Civil Engineering, Middle East Technical University, Ankara, Turkey. His current research interests are primarily in the areas of the use of supplementary cementing materials and durability of concrete. He has published several papers on concrete technology.

Mr B Baran, is a Senior Engineer STFA Enercom Industrial Manufacturing and Trade Co. and he obtained his M.S. degree in the Department of Civil Engineering, Middle East Technical University, Ankara, Turkey.

INTRODUCTION

The process of steam curing is probably the most widely used method of accelerated curing which is used extensively in the production of precast concrete structural members, pipe, masonry units, and prestressed products. It provides a significant improvement in the early strength of concrete and gives possibility to the removal of the forms in a quick manner. However, the most serious drawback is the reduction in the late strength values with respect to normal cured concretes [1]. This reduction is attributed to the change in hydration characteristics of cement paste when encountered to early maturation due to high temperature. At normal temperatures, cement hydrates slowly and hydration products diffuse to interstitial pores leading to a fine and dense structure. However, mature pastes cured at high temperatures, i.e. <50 ^{o}C, exhibit a coarser morphology and pore structure than those characteristics of pastes cured under ambient conditions. At elevated temperatures, cement hydrates so rapidly that hydration shells develop around grains. Hydration shells act as diffusion barriers reducing the ultimate degree of hydration consequently leading to increased porosity and accompanied strength reduction at later ages [2, 3].

A number of considerations govern the choices of steam curing cycle, namely the precuring period, the rate of increase and decrease of temperature, and the level in time of constant temperature [4].

In most cases, steam curing is employed only for achieving 50 to 70 percent of specified strength in a short period instead of full treatment for 2 to 3 days required to obtain specified strength. This would result in the economy of reuse of molds and equipment by achieving stripping strength, which is normally about 50 percent of the specified strength. The stripping strength will be sufficient to take care of any impacts, which may be produced during their demoulding and transportation to the stockyard [5].

Over the past several decades, numerous failures of concrete structures during construction and economic pressures to accelerate construction schedules have emphasized the need to predict the early-stage strength gain of concrete. Many of the failures have been attributed to the removal of formwork or to the application of construction loads before concrete has reached adequate strength [6].

The combined influence of time and curing temperature on the strength development of concrete has been under investigation during the past several decades. Saul [7] proposed a "law" of strength gain with maturity as "Concrete of the same mix at the same maturity has approximately the same strength whatever combination of temperature and time go to make that maturity [8]. So, by using the curing temperature and duration in an introduced maturity function, one can predict the early strength development of a steam-cured concrete and/or also decide to an appropriate steam curing duration and temperature for a required early strength of concrete easily.

The object of this study was to determine the effects of steam curing on some mechanical properties; especially on compressive strength, split tension strength, and modulus of elasticity, of hardened concrete. In addition to this, the most important objective was to examine the increase in early strength values, and to set up an approach for compressive strength influenced by time and temperature history of concrete. By this purpose, a maturity function was introduced to predict the early strength according to the curing condition applied and to be able to prove the reliability and the accuracy of the strength tests performed throughout this study.

For these purposes, six different steam-curing conditions were applied to three different strength classes of concretes by the consideration of curing temperature and duration as the changing parameters. The effects of steam curing on some mechanical properties of hardened concrete were examined by using three different curing temperatures as 40 °C, 60 °C, and 75 °C, and also 4h and 8h of curing duration.

EXPERIMENTAL STUDY

Experimental Program

In order to observe the effects of initial curing on some mechanical properties of concrete; three different concrete mixes were subjected to steam curing under different temperature and for different duration conditions. Each of the mixes was applied to six different curing regimes. Slump value was not considered as a parameter, and fixed to a constant value as 7 cm for all three mixes, on concrete properties in this research. The applied accelerated steam curing temperatures and curing durations for each mix are shown in Table 1.

Table 1 Concrete mixes produced for the experimental study

TYPE OF CONCRETE MIX	DESIGNATION*	CURING TEMPERATURE (°C)	CURING DURATION (h)
I	C30	20	-
II	C30	40	4
III	C30	40	8
IV	C30	60	4
V	C30	60	8
VI	C30	75	4
VII	C30	75	8
VIII	C40	20	-
IX	C40	40	4
X	C40	40	8
XI	C40	60	4
XII	C40	60	8
XIII	C40	75	4
XIV	C40	75	8
XV	C50	20	-
XVI	C50	40	4
XVII	C50	40	8
XVIII	C50	60	4
XIX	C50	60	8
XX	C50	75	4
XXI	C50	75	8

* "C" stands for "Concrete Mix". The number indicates 28-day strength of concrete.

Firstly, tests were performed on cement, cement paste, mortar and also on aggregates to be able to determine physical and chemical properties; thereafter, the concrete mix proportioning method given by ACI 211 [1] was followed to obtain the designs of the mixtures mentioned above.

The three different mixes were designed as C30, C40 and C50 having 400, 500, and 650 kg/m^3 cement contents respectively. All of the three mixes were prepared to have 6-8 cm slump value. Three different temperatures of curing as 40 °C, 60 °C, 75 °C by using and, two different steam curing time, as 4 h and 8 h, for each temperature condition, were applied to these batches.

By applying one of the specified temperature condition the required numbers of specimens (30) were put into the curing tank, thereafter while half of the specimens have being taken out from the curing tank after 4 hours, remaining ones were left for an additional 4 hours in tank to complete the 8 h steam curing duration. After having been taken out from steam curing, all specimens were cured under 100% relative humidity and 20 °C temperature till testing date. After casting, specimens were rested at room temperature for approximately 1 hour before steam curing was applied. After placement in curing tank, temperature rise was controlled in order to not exceed 25 °C / hour. For curing temperature of 40, 60 and 75 °C temperature rise periods were 1, 1 ¾ and 2 hours respectively. Curing history of various conditions are shown in Figure 1.

Besides the steam-cured specimens, control concrete specimens were also cast for each mix (C30, C40 and C50) in order to make comparisons with the cured ones. Control concretes were stored in 20 °C and 100% relative humidity curing condition. For these purposes, 105 standard cylindrical specimens were taken to perform compressive strength, modulus of elasticity, and split tension tests on hardened concrete at different test ages for each mix. Each test set was consisted of three samples for each condition at each testing date, which were 1, 7, 28 and 90-days for compressive strength and 28-days for split tension tests. A commercial superplasticizer was also used for the production of concretes to be able to reduce the w/c ratios as possible and so to obtain high strength concrete mixes.

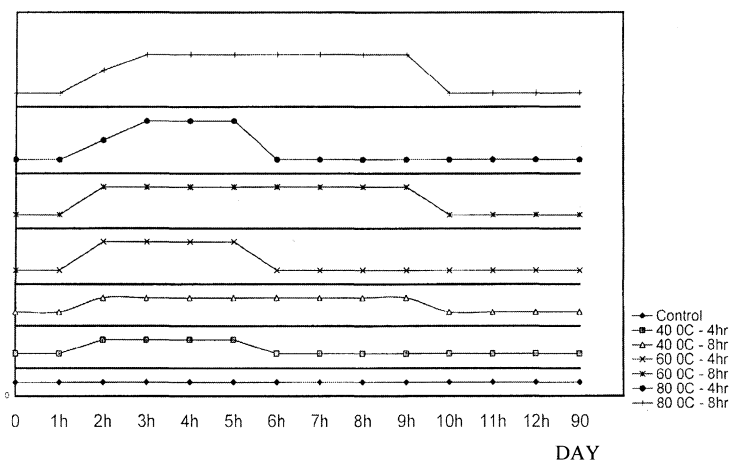

Figure 1 History of the curing conditions

Materials Used

Portland Cement

An Ordinary Turkish Portland Cement, PÇ 42.5 that corresponds to ASTM Type I cement was used for the preparation of paste, mortar and concrete specimens.

The chemical and physical properties of this cement are shown in Tables 2 and 3, respectively.

Table 2 Chemical composition of portland cement

OXIDES	(%)	ASTM C150 LIMITS
CaO	61.88	-
SiO_2	19.83	-
Al_2O_3	5.32	-
Fe_2O_3	3.47	-
MgO	1.78	max. 6.0%
SO_3	2.84	max. 3.5%
K_2O	0.82	-
Na_2O	0.20	-
LoI	3.06	max. 3.0%

Table 3 Physical properties of portland cement

PROPERTY		ASTM C150 LIMITS
Density (g/cm^3)	3.08	-
Specific Surface (cm^2/g)	3250	min. 2800
Time of Setting (minutes)		
Initial	70	min. 45
Final	230	max. 375
Compressive Strength (MPa)		
3 days	23.2	min. 12.4
7 days	32.6	min. 19.3
28 days	45.3	-

Aggregates

A natural river sand having a particle size interval between 0 and 7 mm and a crushed stone having particle sizes from 0 to 3 mm were used as fine aggregate. The size groups (3-9 mm and 10-25 mm) of crushed stone were used as coarse aggregates. 32% of river sand (0-7 mm), 27% of 0-3 mm size crushed stone, 7% of 3-9 mm, and 34% of 10-25 mm size crushed stone groups were combined to form the suitable gradation for coarse aggregates.

Table 4 gives the results of the specific gravity and absorption tests conducted on aggregates.

Table 4 Specific gravity, and absorption of aggregates

SPECIFIC GRAVITY	
Coarse Aggregate (3-9 mm) (Dry)	2.72
Coarse Aggregate (3-9 mm) (SSD)	2.73
Coarse Aggregate (10-25 mm) (Dry)	2.69
Coarse Aggregate (10-25 mm) (SSD)	2.70
Fine Aggregate (0-3) (Dry)	2.71
Fine Aggregate (0-3) (SSD)	2.72
Fine Aggregate (0-7) (Dry)	2.44
Fine Aggregate (0-7) (SSD)	2.54
ABSORPTION (%)	
Coarse Aggregate (3-9 mm)	0.32
Coarse Aggregate (10-25 mm)	0.09
Fine Aggregate (0-7) (Dry)	0.40
Fine Aggregate (0-7) (SSD)	3.84

Mixing Water, Superplasticizer and Admixture

Normal, drinkable tap water, which was assumed to be free from oil, organic matter and alkalies, was used as mixing water.

A commercial superplasticizer agent, which was in a liquid form, and having a dark color and a density of approximately 1.00 g/cm^3, was used for the purpose of using as possible as low w/c ratios and obtaining high strength concretes. Superplasticizer agent was introduced into the concrete as a part of the mixing water.

Concrete Mixes

Cement dosages of 400, 500 and 650 kg/m^3 by using PÇ 42.5 cement were used for mixes C30, C40, and C50 respectively.

Concrete mix proportions of all batches were designed for saturated surface dry (SSD) conditions of aggregates and moisture corrections were made when necessary. The concrete mix proportioning method given by ACI 211 [1] was followed to design the concrete mixtures. Concrete mix proportions in this study are given in Table 5.

The amount of superplasticizer that should be introduced into concrete mixtures, was determined experimentally for three different water/cement ratios as 0.44, 0.46, and 0.48 for a constant slump value of 7 cm as described in Table 6.

Table 5 Concrete mix proportions

	C30	C40	C50
Cement (kg/m^3)	400	500	650
Water (kg/m^3)	193	231	286
FA (0-3 mm)	501	447	366
FA (0-7 mm)	538	477	391
CA (3-9 mm)	136	117	99
CA (10-25 mm)	627	564	464
Total Weight (kg)	2395	2336	2256
Admixture content (%)	1.25	1.20	1.23
Admixture amount (kg)	5	6	8

TEST RESULTS AND DISCUSSION

Tests on Fresh Concrete

Slump, unit weight, and air content tests were the types of tests performed on all concrete mixes and the results were given in Table 6.

Table 6 Characteristics of fresh concrete used in the investigation (cement content = 400 kg/m^3)

CONCRETE MIX	W/C	SLUMP (cm)	AIR CONTENT (%)	UNIT WEIGHT (kg/m^3)
C30	0.48	7	1.90	2395
C40	0.46	7	1.75	2336
C50	0.44	7	1.70	2256

Tests on Hardened Concrete

Compressive strength, modulus of elasticity, and split tension tests were conducted on hardened concrete specimens for all concrete mixes which were exposed to 6 different accelerated steam curing conditions by using three different accelerated steam curing temperatures as 40 °C, 60 °C, and 75 °C and also two different curing durations as 4h and 8 h at the same time.

To be able to perform the tests mentioned above, cylindrical steel molds having standard nominal dimensions of 15 cm in diameter and 30 cm height were used. The specimens were cast and put into the steam-curing tank of which the temperature had been adjusted to the specified value before and then they were kept in the tank until the end of the required curing durations. After having been removed from the tank, the specimens were stored in the moisture room to complete 24 h. Thereafter they were demoulded and stored in the curing room again until the time of testing age. By the way, control specimens were stored at 20 °C and 100% relative humidity in the moist room until the test ages.

Compressive Strength Test

Compressive strength tests of all concrete specimens were performed according to ASTM C39. The results are tabulated in Table 7. Compressive strength tests were performed on the specimens at the ages of 1, 7, 28, and 90 days.

Table 7 Compressive strength development of C30, C40 and C50 concrete cured at different durations and temperatures

	CONTROL	CURING TEMPERATURE 40 °C		CURING TEMPERATURE 60 °C		CURING TEMPERATURE 75 °C	
Curing Duration (h)	-	4	8	4	8	4	8
			C30 (MPa)				
1-day	17	20	21	22	24	23	26
7-day	30	26	28	27	28	28	30
28-day	37	33	33	33	33	35	35
90-day	40	36	38	36	39	37	39
			C40 (MPa)				
1-day	26	28	29	29	31	30	32
7-day	38	31	33	31	35	32	36
28-day	43	37	36	38	39	38	39
90-day	46	40	41	41	42	41	42
			C50 (MPa)				
1-day	33	34	34	34	35	35	36
7-day	45	42	39	40	39	37	37
28-day	51	45	43	42	41	39	39
90-day	53	47	46	45	45	43	43

It is obvious from Table 7 that both temperature and duration of steam curing were directly proportional to early strength. An increase either in curing temperature or in duration provided an increase in 1-day compressive strengths of all steam-cured specimens. Steam curing duration of 8h at any temperature was more beneficial than that of 4h conditions from

the early strength point of view, and 75 °C curing temperature at any duration provided higher rates of increase in 1-day compressive strengths when compared with 40 °C and 60 °C for all strength classes of concrete.

However, the rates of gain in early strengths of steam-cured specimens were decreased as the strength classes of concretes were increased. While 1-day compressive strengths of C30 and C40 concretes were improved considerably by steam curing, C50 could not demonstrate the same level of development from this point of view.

The rates of reductions in late strengths of steam-cured specimens were increased as the strength classes of concretes increased when compared with the controls.

For concretes C30 and C40, 8h steam curing duration has given better late strength results than 4h duration at any temperature conditions. On the contrary, it was observed a reverse effect for C50 class of concrete; in other words, 8h steam curing duration has shown lower late strength results than 4h duration at any temperature conditions. Moreover, it can easily be concluded that, steam-cured specimens have higher late strength results as temperature has been increased from 40 °C to 75 °C for C30 and C40 concretes. In spite of this, it was seen a reverse effect for C50 class of concrete; in other words, C50 has shown lower late strength results as steam curing temperatures have been increased from 40 °C to 75 °C at any curing duration conditions.

Split tension Test

The split-cylinder test was used in this study in accordance with the specifications of ASTM C 496. The split tension test is accomplished by loading the standard test cylinder along two diametrically opposite lines. The load is distributed over a width of about one-twelfth the diameter of the cylinder by a strip of plywood. The cylinder fails suddenly by splitting along a vertical plane. Split-cylinder tests were performed at 28 days. The results are tabulated in Table 8.

Table 8 28-day split tensile strengths of concretes cured at different temperatures and durations

	CONTROL	CURING TEMPERATURE 40 °C		CURING TEMPERATURE 60 °C		CURING TEMPERATURE 75 °C	
Curing Duration (h)	-	4	8	4	8	4	8
C30 (MPa)	3.1	3.0	3.1	2.8	3.1	3.2	3.2
C40 (MPa)	3.6	3.0	3.1	3.1	3.6	3.0	3.4
C50 (MPa)	3.8	3.6	3.7	3.3	3.8	3.1	3.6

As it was seen from Table 8, Split Tensile strength tests were demonstrated for the concrete C30, C40 and C50 at an age of 28 day. Whatever the curing temperature, the split tensile strength of the batches, which were subjected to 8 h curing, indicated higher values than that hour curing condition. The rates of reductions in split tensile strengths with respect to controls were less than that in compressive strengths at the age of 28-days. Even for some

cases, split tension strengths were slightly greater when compared with the controls. It can also be concluded that, extension of the steam curing duration from 4h to 8h have indicated a small amount of improvement in split tensile strength values.

Modulus of Elasticity Test

Modulus of elasticity tests of all concrete specimens were performed according to ASTM C 469. The results are tabulated in Table 9. Modulus of elasticity tests were performed at 7, 28, and 90 days.

Table 9 Modulus of elasticity improvement of C30, C40 and C50 concrete cured at different durations and temperatures

	CONTROL	CURING TEMPERATURE 40 °C		CURING TEMPERATURE 60 °C		CURING TEMPERATURE 75 °C	
Curing Duration (h)	-	4	8	4	8	4	8
			C30 (MPa)				
7-day	28	24	23	24	24	26	24
28-day	35	27	28	29	29	31	30
90-day	39	33	36	33	34	34	35
			C40 (MPa)				
7-day	28	22	23	23	23	25	24
28-day	35	30	28	30	30	31	30
90-day	39	37	35	38	35	38	36
			C50 (MPa)				
7-day	37	34	31	32	30	31	30
28-day	43	36	36	36	36	34	34
90-day	47	39	41	41	41	35	38

It was a known fact that, the property of modulus of elasticity is directly related with compressive strength. Test results for all curing conditions pointed out that, the trends of modulus of elasticity values were exactly the same with the compressive strengths at all test ages, and for all strength classes of concretes.

CONCLUSIONS

In order to investigate the effects of steam curing on some mechanical properties of different concrete classes, three mix designs were made to get C30, C40, and C50 concretes. Thereafter, these concretes were subjected to six different curing conditions by considering three different steam curing temperatures and two different curing durations.

In addition to them, control specimens from each class of concrete were stored in the moist room and tested together with the steam-cured specimens.

1. Application of steam curing by any of the six conditions increased the 1-day compressive strength values of all cured C30, C40, and C50 concretes with respect to controls.

2. As it was expected, reductions in compressive strengths with respect to controls for the ages of later than 7-days were unavoidable when steam curing was applied.

3. Both C30 and C40 classes of concretes, the most appropriate curing condition was found to be at 75 ^{o}C and for duration of 8 hours. Under subjection of this steam curing an increase of 55% at 1-day and a reduction of 5% at 28-day compressive strengths were provided for C30 and an increase of 25% at 1-day and 8% reduction at 28-day compressive strengths were observed for C40.

4. For C50 class of concrete none of the curing conditions could provide neither a high rate of early strength improvement nor an acceptable rate of late strength reduction. That is why steam curing is not advised for C50 by considering the results of this study.

5. Data analysis performed to set up a relation between early strength and combined time and temperature effect of curing concluded that, C30 was much more sensitive while C40 was moderate and C50 was least sensitive to any curing variations from the early strength improvement point of view.

6. The results of the tests showed that, the rates of reductions in split tensile strengths with respect to controls were less than that in compressive strengths at the age of 28-days. Even for some cases, split tension strengths were slightly greater when compared with the controls. It can also be concluded that, extension of the steam curing duration from 4h to 8h have indicated a small amount of improvement in split tensile strength values.

7. It was a known fact that, the property of modulus of elasticity is directly related with compressive strength. Test results for all curing conditions pointed out that, the trends of modulus of elasticity values were exactly the same with the compressive strengths at all test ages, and for all strength classes of concretes.

REFERENCES

1. AMERICAN CONCRETE INSTITUTE, Masonry Precast Concrete Special Processes, ACI Manual of Concrete Practice, Part I, 1997.

2. PATEL, H H, BLAND, C H, POOLE, A B, The microstructure of concrete cured at elevated temperatures, Cement and Concrete Research, Vol 25, No 3, 1995.

3. KJELLSEN, K O, DETWILER, R J, GJORV, O E, Development of microstructures in plain cement pastes hydrated at different temperatures, Cement and Concrete Research, Vol 21, 1991.

4. WADDELL, J J, DOBROWOLSKI, J A, Concrete Construction Handbook, McGraw-Hill, 1993.

5. HANSON, J A, Optimum Steam Curing Procedure in Precasting Plants, ACI Journal, 1983.

6. KIM, J K, MOON, Y H, EO, S H, Compressive strength development of concrete with different curing time and temperature, Cement and Concrete Research, 1998.

7. SAUL, A G A, Principles underlying the steam curing of concrete at atmospheric pressure, Magazine of Concrete Research, Vol 2, 1951.

8. TAN, K, GJORV, O E, Performance of concrete under different curing conditions, Cement and Concrete Research, 1996.

9. HIGGINSON, E C, Effect of steam curing on the important properties of concrete, ACI Journal Proceedings, Vol 58, No 3, 1961.

10. TANK, R J, CARINO, N J, Rate constant functions for strength development of concrete, ACI Material Journal, 1991.

11. OLUOUKUN, F A, BURDETE, E G, DEATHERAGE, J H, Elastic moduls, poisson's ratio, and compressive strength relationships at early ages, ACI Materials Journal, 1991.

12. AL-KHATAT, H, HAQUE, M N, Effect of initial curing on early strength and physical properties of a lightweight concrete, Cement and Concrete Research, 1998.

QUANTATIVE EVALUATION OF INFLUENCE OF REBAR CORROSION ON STRUCTURAL PERFORMANCE OF DETERIORATED RC BEAMS

M Iwanami **H Yokota**
Port and Airport Research Institute
F Sato
Maeda Corporation
Japan

ABSTRACT. This paper describes the relationship between corrosion of rebars and structural performance of reinforced concrete (RC) beams subject to corrosion damage. By quantifying the degree of corrosion using an index of cross-sectional loss of rebars, decrease in load carrying capacity of deteriorated RC beams was well explained. It also coincided with the result from the long-term exposure test under actual marine environment. Moreover, the applicability of electrochemical measurement was examined to a nondestructive estimation method of corrosion of rebars in concrete. As a result, polarization resistance was a more useful index than half-cell potential in heavily deteriorated RC beams. Integrating the inverse of polarization resistance along exposed time enabled to evaluate corrosion of rebars in concrete accurately and quantitatively.

Keywords: Marine concrete structure, Chloride attack, Corrosion, Load carrying capacity, Nondestructive testing, Half-cell potential, Polarization resistance.

Dr M Iwanami, is a Researcher of Structural Mechanics Division of the Port and Airport Research Institute, Independent Administrative Institution, Japan. He received his Doctor of Engineering Degree from Tokyo Institute of Technology in 1999. His research field is maintenance of port and harbour facilities and nondestructive testing of concrete structures.

Mr F Sato, is a Civil Engineer of the Technical Research Institute at Maeda Corporation, Japan. His research covers durability of reinforced concrete and high performance concrete.

Dr H Yokota, is a Head of Structural Mechanics Division of the Port and Airport Research Institute, Independent Administrative Institution, Japan. He received his Doctor of Engineering Degree from Tokyo Institute of Technology in 1993. He specialises in structural behaviours and design of RC, PC, and steel-concrete composites. His recent research interests include the effect of deterioration of materials to overall performance of concrete structures.

INTRODUCTION

Ports and harbours in Japan play important roles in both domestic and international sea transportation because its land is surrounded by ocean. Therefore, port and harbour facilities are essential to stability of our economical activities. Almost all port and harbour facilities are made of reinforced concrete (RC), for example, quay walls, piers, breakwaters, etc. However, marine environment is extremely severe to RC structures; that is, chloride ions in sea water induce corrosion of reinforcing bars in concrete and humid condition in marine areas supplies water enough to progress corrosion reaction. Hence, structural performance and durability of marine RC structures gradually decrease due to corrosion of rebars in concrete during in-service. In order to keep various performance of those structures at the required level, rational maintenance and repair work should be planned and conducted systematically. At present, the relationship between corrosion of rebars and structural performance remains unclear so that appropriate schemes for maintenance and repair work to those structures have not been determined to date.

In structural performance assessment of existing deteriorated RC structures, quantitative information about corrosion of rebars in concrete is required. However, corrosion reaction occurs inside concrete so that it is generally impossible to evaluate the state and the degree of corrosion by visual observation from the outer surface. Therefore, nondestructive evaluation methods of corrosion of rebars are expected to be established soon.

In this study, influence of rebar corrosion was investigated on load carrying capacity of RC beams subject to electrolytic corrosion in order to obtain basic data about the relationship between rebar corrosion and structural performance of RC structures in marine environment. The results obtained were compared with those from the 23-year exposure test under actual marine environment [1]. Furthermore, electrochemical measurement was applied to deteriorated RC beams to nondestructively evaluate corrosion of rebars in concrete. On the basis of the experimental results, the applicability of electrochemical measurement was examined to a nondestructive estimation method of rebar corrosion.

EXPERIMENTAL PROCEDURES

Test Beams

The specimens used in this study were RC beams as shown in Figure 1. The shape, size, rebar arrangement, and mechanical properties of the ingredients for the beams were the same as those for the previous long-term exposure test [1] to compare between the two results.

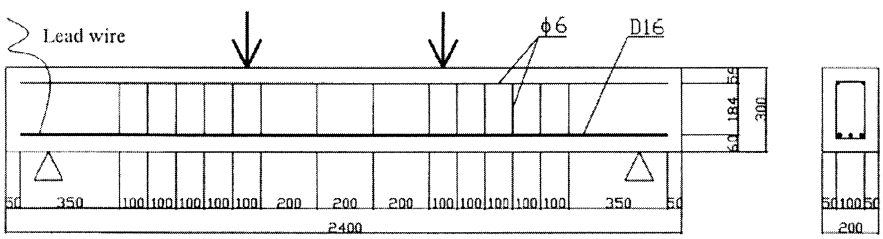

Figure 1 RC beam specimen

Table 1 Mixture proportion of concrete

UNIT WEIGHT (kg/m^3)				
W	C	S	G	Ad
180	265	1015	860	3.33

The dimensions of the beams were 200mm wide, 300mm high, and 2400mm long. The arrangement of rebars is also shown in Figure 1. Three deformed bars of 16mm in diameter were used as main rebars, and 12 stirrups were embedded with an interval of 100mm. Yield and tensile strengths were 382 and 560 N/mm^2 for the main rebar, and 306 and 444 N/mm^2 for the stirrup. At either end of the main rebar, a lead wire was attached for electrolytic test and electrochemical measurement. Concrete cover of rebars is considered to greatly affect durability of concrete structures in marine areas. In this study, the thickness of cover was set to be 42mm, which was almost the same as actual structures.

Mixture proportion of the concrete is presented in Table 1. The maximum size of coarse aggregate was 20mm, and target slump and air content of the concrete were 12cm and 4%, respectively. Air entraining agent was added in mixing as chemical admixtures. The compressive strength and Young's modulus of the concrete at the bending test were $26.6N/mm^2$ and $24.0kN/mm^2$, respectively. As mentioned above, the beams used in this study were reproduction of the beams for the long-term exposure test [1], which were manufactured more than 25 years ago. Therefore, mechanical properties of the concrete were low compared with the recent ordinary one.

Preliminary Loading

For investigating influence of cracks on structural performance of RC beams subject to corrosion damage, some beams were preliminarily bend-loaded before electrolytic test until the maximum crack width reached the allowable value of 0.15mm determined from the viewpoint of durability [2]. The applied load was approximately 40kN, and set-up of loading was identical to that of the bending test mentioned later. The beams with and without initial cracks induced by the preliminary loading were designated as C-series and U-series, respectively.

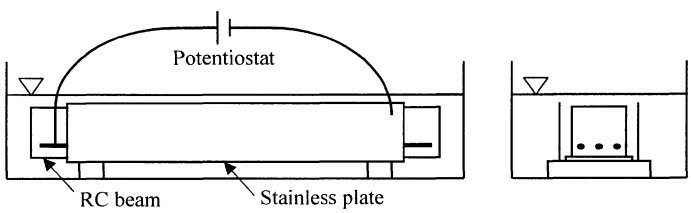

Figure 2 Electrolytic test

Electrolytic Test

An electrolytic test was conducted as an acceleration test of rebar corrosion. In this test, rebars in concrete were corroded artificially by applying direct current to the rebars. The test set-up is shown in Figure 2. An RC beam in a sea water tank was surrounded by a stainless plate of 0.3mm thick and approximately 2000mm long. After connecting lead wires from 3 main rebars and the stainless plate to a potentiostat, direct current of 2.95A was applied to this electrical circuit. The current density, defined as current per unit surface area of main rebars, was 0.85mA/cm^2, which was determined based on the previous test conducted by Hamada et al [3].

In the experiment of this study, an axial crack started to form in U-series after applying the direct current for 32 hours. The axial crack was initiated due to expansion of corroded rebars in concrete. In this study, this electrolytic duration of 32 hours was determined as a fundamental period of electrolytic test, which is represented by Q. The direct current was applied to C-series and U-series for the duration of $1Q$, $2Q$, $4Q$, and $8Q$. In U-series, a test case of $0.5Q$ was added to examine the mechanical behaviours before an axial crack occurred. For comparison, a sound beam was prepared without the application of direct current.

Loading Test

For investigating structural performance of RC beams subject to corrosion of rebars, the bending test was performed on the beams. The positions of loading and supporting points are illustrated in Figure 1. During loading, applied load, midspan deflection, strain at the compressive fibre, and widths of both existing and newly-formed cracks were measured.

Corrosion Evaluation

For quantifying the degree of corrosion of rebars in RC beams subject to electrolytic test, a cross-sectional loss of main rebars was measured. After the loading test, main rebars in concrete were taken out from the beam, and corrosion product was removed by both sand-blasting and chemical reaction with citric acid. Then, by measuring the length and the weight of rebars, unit weight per length of corroded rebars was calculated. Finally, a cross-sectional loss of rebars, which was equal to a weight loss of rebars, was obtained by comparing with unit weight per length of a sound one. This value could not evaluate a kind of concentrated corrosion, but averaged degree of corrosion. In this procedure, only the part of a main rebar in pure bending span was focused in consideration with its influence on flexural behaviours of deteriorated RC beams.

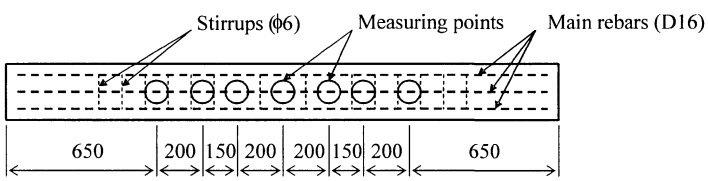

Figure 3 Points of electrochemical measurement (view from the bottom)

Electrochemical Measurement for Nondestructive Corrosion Estimation

A nondestructive testing method to accurately evaluate rebar corrosion in concrete is keenly required to develop because corrosion reaction occurs inside concrete and is not visible from the outer surface. Corrosion reaction of iron can be understood on the basis of electrochemistry. Therefore, some electrochemical parameters are thought to be effective for estimating the state and the degree of corrosion of rebars in concrete. In this study, half-cell potential and polarization resistance were picked, and the applicability of these parameters was investigated to corrosion estimation for rebars in concrete. A half-cell potential is related to the state of rebars so that it is effective to find if corrosion occurs at the surface of rebars. By using half-cell potential, however, it is impossible to obtain quantitative information about the degree or the rate of corrosion. On the other hand, it is known that polarization resistance has a distinct correlation with the rate of corrosion. In the field of electrochemistry, the inverse of polarization resistance is proportional to the rate of corrosion; that is, corrosion current is expressed by the following Equation [4].

$$I_{corr.} = \frac{K}{R_p} \tag{1}$$

where $I_{corr.}$: corrosion current
K : constant
R_p : polarization resistance

The constant K in the Equation was influenced by many factors, such as concrete properties, chloride concentration, temperature, humid condition, etc. Therefore, the exact value of K was not determined to date so that polarization resistance was used as an evaluation index in this study, instead of corrosion current. In electrochemical measurement of this study, an Ag/AgCl electrode was attached to the bottom surface of deteriorated RC beams, and half-cell potential of the central main rebar of the three was measured at the points illustrated in Figure 3. The measuring procedure proposed by ASTM [5] was followed in this study. Polarization resistance was measured by the alternative current impedance method [6] at the same points as those of half-cell potential. The frequencies of alternative current used in this measurement were both 10Hz and 20mHz, and the applied voltage was 10mV. In order to accurately localize the polarized area on the surface of rebars, a special sensor with a guard counter electrode [6] was used. Since the moisture content of concrete will greatly affect the result of measurement, it was kept almost constant. The influence of temperature changes on the results was neglected because these measurements were conducted under almost the same temperature conditions.

RESULTS AND DISCUSSION

Visual Observation

Table 2 summarizes the results of visual observation to surface appearance of RC beams subject to corrosion damage. Deterioration levels in this Table were judged according to the Manual for Maintenance and Repair to RC Structures of Japanese Ports [7]. In this judgement, deterioration levels are determined by the results of visual observation only, which are categorized to six levels from O to V. Level O has no damage or deterioration observed in the outer surface, and the level changes toward V as the deterioration progresses. The deterioration levels of the beams in this experiment varied from O to III. From this Table, it was found that existence of initial cracks had no major influence on the deterioration level.

Quantification of Corrosion of Rebars

Figure 4 shows the relationship between cross-sectional loss of rebars and electrolytic duration. The cross-sectional loss of rebars increased in proportion to electrolytic duration. In the beam subject to electrolytic damage for $8Q$, more than 10% loss in cross-section of rebars was observed.

In the case of $1Q$ beam of U-series, the cross-sectional loss of rebars was 1.3%. This value is thought to be critical to initiate an axial crack due to corrosion of rebars, which agreed well with that proposed in the previous study [8].

Table 2 Results of visual observation

C-SERIES (WITH INITIAL CRACKS)					
Electrolytic duration	$0.5Q$	$1Q$	$2Q$	$4Q$	$8Q$
Axial crack	—	yes	yes	yes	yes
Axial crack width (mm)	—	0-0.04	0.04-0.1	0.15-0.35	0.3-0.9
Rust stain	—	no	little	much	too much
Delamination	—	no	no	no	no
Deterioration level	—	I	II	III	III
U-series (without initial cracks)					
Electrolytic duration	$0.5Q$	$1Q$	$2Q$	$4Q$	$8Q$
Axial crack	no	no	yes	yes	yes
Axial crack width (mm)	—	—	0.04-0.1	0.1-0.2	0.3-0.7
Rust stain	no	no	little	much	too much
Delamination	no	no	no	no	no
Deterioration level	O	I	II	III	III

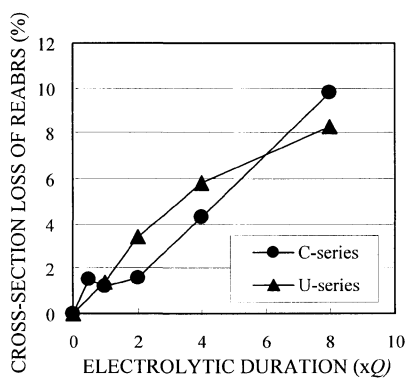

Figure 4 Change in cross-sectional loss of rebars with electrolytic duration

Structural Performance

Figure 5 shows the change in load carrying capacity of deteriorated beams against electrolytic duration. From this Figure, yield and ultimate loads slightly decreased with increase in electrolytic duration, indicating that influence of corrosion on load carrying capacity was not so significant. Moreover, it was found that existence of initial cracks did not affect the test results. Therefore, the test results of U-series and C-series were not distinguished in the following discussion.

For making clear the relationship between load carrying capacity and rebar corrosion, the results described above were rearranged by using cross-sectional loss of rebars, as shown in Figure 6. The yield and ultimate loads were normalized by those measured in the sound specimen. The influence of corrosion was greater on the yield load than on the ultimate load. It was because slippage between concrete and rebars occurred after rebars yielded, and corrosion of rebars brought about more slippage due to deterioration of bond between concrete and rebars.

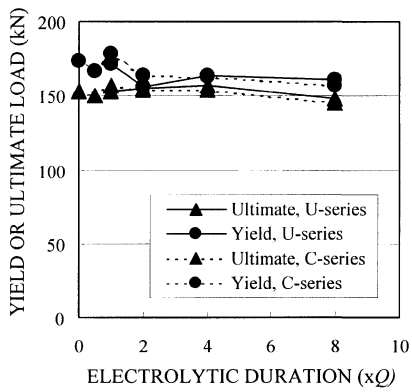

Figure 5 Change in load carrying capacity with electrolytic duration

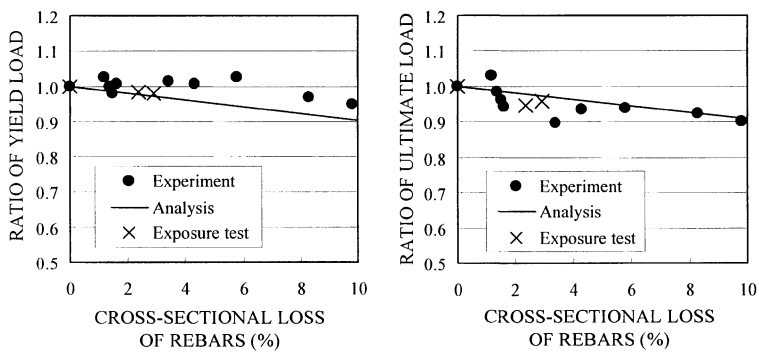

Figure 6 Relationship between cross-sectional loss and load carrying capacity

The analytical solution was also illustrated in Figure 6. In this analysis, rebar corrosion was reflected not only to decrease in cross-section, but also to decrease in yield strength and Young's modulus, as expressed in the following Equations [9].

$$\frac{f_y}{f_{y0}} = 1 - 0.0132\,w \tag{2}$$

$$\frac{E}{E_0} = \frac{1 - 0.0113\,w}{1 - \frac{w}{100}} \tag{3}$$

where f_{y0} , f_y : yield strength of rebar without and with corrosion
E_0 , E : Young's modulus of rebar without and with corrosion
w : cross-sectional loss of rebars (%)

Comparing between the experimental results and the analytical results, the measured yield loads were slightly larger than the calculated ones. As to the ultimate loads, the analytical results coincided approximately with the experimental ones. Therefore, it was found that this analysis was a useful tool for evaluation of load carrying capacity of deteriorated RC beams subject to corrosion damage in the safe side.

The results from the long-term exposure test were also plotted in Figure 6. The trend was similar to that obtained in this study. It was said that the electrolytic test condition in this study was equivalent to natural marine environment from the viewpoint of rebar corrosion. On the basis of the discussion above, it was concluded that the load carrying capacity of deteriorated RC beams could be quantitatively estimated by using the cross-sectional loss of rebars in concrete.

Nondestructive Estimation of Corrosion in Concrete

A cross-sectional loss of rebars was found to be an effective parameter to assess the structural performance of deteriorated RC beams. Nondestructive evaluation methods should be adopted to estimate the cross-sectional loss of rebars in existing RC structures. In this study, corrosion of rebars was tried to quantitatively estimate with electrochemical parameters.

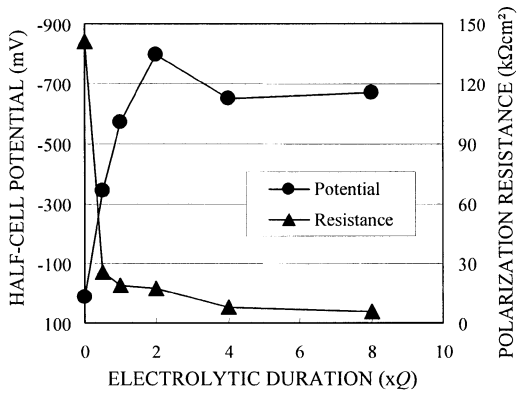

Figure 7 Change in electrochemical parameters with electrolytic duration

Figure 7 shows the change in half-cell potential and polarization resistance against electrolytic duration. The values of half-cell potential in this Figure are against $Cu/CuSo_4$ electrode, by converting from the values against Ag/AgCl electrode. When the electrolytic duration was shorter than $2Q$: equivalent to light or moderate corrosion, half-cell potential decreased monotonically with corrosion progressing. In such cases, therefore, the degree of rebar corrosion in concrete could be estimated by measuring the half-cell potential of rebars.

On the other hand, when the electrolytic duration was longer than $2Q$, half-cell potential kept almost constant. This was because half-cell potential indicated the state of corrosion, not the rate of corrosion. In such a heavy corrosion, it was considered that corrosion occurred all over the surface of rebars and its reaction progressed even inside rebars. Even if almost the same states of corrosion on the surface of rebars were observed, the rate or depth of corrosion might be different. Therefore, estimation of rebar corrosion was difficult only by the half-cell potential on heavily deteriorated RC beams.

Overcoming this difficulty, polarization resistance was introduced to evaluate the rate of corrosion. The result of measurement for polarization resistance is also provided in Figure 7. It was found that polarization resistance decreased with increase in electrolytic duration even in the cases of longer than $2Q$. It was suggested that the measured values of polarization resistance less than $10k\Omega \cdot cm^2$ indicated heavy corrosion with significant loss in cross-section of rebars. By measuring not only half-cell potential but also polarization resistance, it was possible to estimate the degree of heavy corrosion of rebars.

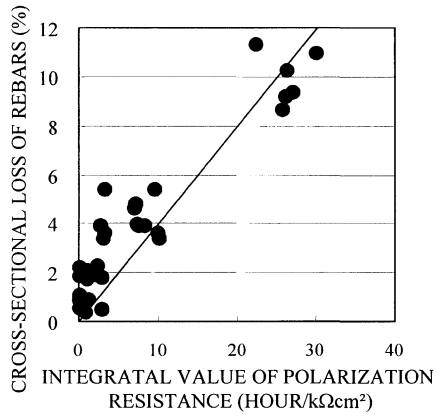

Figure 8 Relationship between cross-sectional loss and integral value of inverse of polarization resistance

Therefore, integrating the inverse of polarization resistance along exposed time is considered to allow quantitative estimation of the cross-sectional loss of rebars. The result of integral calculation is shown in Figure 8. It was found that there existed an obvious correlation between the cross-sectional loss of rebars and the integral value. Its correlation coefficient was 0.88. From this fact, the possibility was confirmed to quantitatively estimate the cross-sectional loss of rebars by measuring and analyzing polarization resistance, which was essential to evaluation of structural performance of RC structures subject to corrosion damage.

CONCLUSIONS

The following conclusions were drawn from the tests on deteriorated RC beams subject to corrosion damage:

1) The load carrying capacity decreased slightly with increase in the cross-sectional loss of rebars due to corrosion. This tendency was identical to that for the long-term exposure test under actual marine environment. The analysis, in which corrosion was appropriately reflected, enabled to evaluate the load carrying capacity of deteriorated RC beams in the safe side.

2) In the case of lightly corroded rebars, it was possible to evaluate the degree of corrosion by measuring half-cell potential of rebars. On the other hand, for evaluating rebar corrosion in heavily deteriorated RC beams, it was effective to measure both half-cell potential and polarization resistance at the same time. Quantitative estimation of the cross-sectional loss of rebars due to corrosion will be achieved by calculating integration of the inverse of polarization resistance along exposed time.

REFERENCES

1. YOKOTA, H, FUKUTE, T, HAMADA, H, AKIYAMA, T, Structural assessment of deteriorated RC and PC beams exposed to marine environment for more than 20 years, Proceedings of the 2nd International RILEM/CSIRO/ACRA Conference, Melbourne, Australia, 1998, p 209-219.

2. JAPAN SOCIETY OF CIVIL ENGINEERS, Standard specification for design and construction of concrete structures [design], 1996, p 86-90.

3. HAMADA, H, FUKUTE, T, ABE, M, DOZONO, A, Application of AE (acoustic emission) technique as a non-destructive test method to deteriorated port and harbor concrete structures, Technical Report of Port and Harbour Research Institute, No 872, 1997, p 10-12.

4. STERN, M, GEARY, A L, Electrochemical polarization I. A theoretical analysis of shape of polarization curves, Journal of the Electrochemical Society, Vol 104, No 1, 1957, p 56.

5. AMERICAN SOCIETY OF TESTING AND MATERIALS, Standard test method for half-cell potentials of uncoated reinforcing steel in concrete, ASTM C876-91, 1991.

6. MIYUKI, H, OHNO, T, YOKOTA, M, YOSHIDA, M, Corrosion monitoring of steel rebars in concrete structures by AC impedance method, Proceedings of the International Symposium on Plant Ageing and Life Prediction of Corrodible Structures, Sapporo, Japan, 1995, p 447-451.

7. PORT AND HARBOUR RESEARCH INSTITUTE ed, Manual on maintenance and rehabilitation of port and harbour structures, Coastal Development Institute of Technology, 1999, p 91-103.

8. TAKEWAKA, K, MATSUMOTO, S, Behaviours of reinforced concrete members deteriorated by corrosion of reinforcement, Proceedings of the 6th Japan Concrete Institute Conference, 1984, p 177-180.

9. JAPAN CONCRETE INSTITUTE, Committee report on rehabilitation of concrete structures, 1998, p 36-52.

FREEZE-THAW RESISTANCE OF CONCRETE SUBJECTED TO DRYING AT EARLY AGES

N Yuasa Y Kasai I Matsui
Nihon University
E Kamada
Hokkaido University
Japan

ABSTRACT. Freeze-thaw expansion of concretes is mainly controlled by air. However with a 4.5 % of air content, considerable may occur when subjected to dying at early ages depending on the types of cement and water-cement ratios. The use of blended cement with a high water-cement ratio should be accompanied by sufficient moist curing at early ages. Difference in pore volume at the radius ranging from 180 to 1,000 nm was found between damaged and undamaged. Freeze-thaw scaling also increased when drying initiation age became earlier. Amount of scaling was highly correlated to a pore of surface layer concrete, especially to a pore volume of larger than 56 nm in the radius. These pore regions increased are likely to increase when subjected to drying at early ages.

Keywords: Structural concrete, Freeze-thaw resistance, Scaling, Curing, Porosity.

Dr N Yuasa, is a Lecturer of College of Industrial Technology, Nihon University. His main research interest lies in the area of durability of concrete structures from the viewpoint of pore structure and moisture.

Dr Y Kasai, is an Emeritus Professor of Nihon University. His 50 years' research on concrete technology extends over a wide range including the early-age properties, NDT of concrete structures, demolition and reuse of concrete and high-fluidity concrete.

Dr I Matsui, is a Professor of College of Industrial Technology, Nihon University. His research focuses mainly on evaluation method of tactile impression for building finishing material.

Dr E Kamada, was a Professor of Hokkaido University. His main research interest was in the area of frost resistance of concrete. He passed away three years ago.

INTRODUCTION

The moisture content of surface layer concrete decreases with drying. In the case where the start of drying is halfway through the hydration of cement, it could hinder the hydrating cement of the surface layer concrete and thus causes the surface layer concrete to be porous just as it is before the drying [1], [2]. In the case where the concrete receives freezing and thawing reaction after these phenomena, it is conceivable that these phenomena promote the frost damage to the surface layer concrete through scaling and expansion deterioration. In Japan, Tabata showed that the expansion of hardened cement paste with freezing and thawing was larger as the underwater curing term before drying is shorter [3]. The committee on concrete in Japan Cement Association pointed out that the scaling of earlier dried concrete is larger with the increasing number of cycle for freezing and thawing [4]. However, these studies concentrated only on the relationship between the condition of curing and the results of the free-thaw resistance and did not deal with the deterioration mechanism from the viewpoint of inhomogeneous porosity subjected to drying. Saeki tried to evaluate the scaling resistance from the surface layer strength by the pull-out method (Draw method) [5]. This example explains the resistance of freezing and thawing from concrete qualities. However, this study did not discuss about the freeze-thaw resistance of early dried concrete through the effected concrete qualities by the drying. This paper discusses about the changes to the dynamic modulus of elasticity, expansion and scaling content of freeze-thaw resistance test from concrete porosity and compressive strength before freezing and thawing. Finally, from these discussions, the control method for curing of concrete subjected to freezing and thawing is presented.

EXPERIMENTAL DETAILS

Producing Method of Specimens

Ordinary Portland cement (OPC), high-early-strength Portland cement (HPC), moderate heat Portland cement (MPC), type B Portland blast furnace slag cement (SCB) and type B Portland fly ash (FCB) as shown in Table 1 were used. Every cement, river sand (surface-dry density of 2.62 d/cm^3 and F.M. of 2.83), river gravel (surface-dry density of 2.66 d/cm^3 and F.M. of 6.96) and chemical admixture were mixed at different water-cement ratio according to the mixture proportions given in Table 2. Specimens were cast in standard metal forms of 10x10x40 cm with two pin gauges embedded for measuring expansion. Compressive strengths of these concretes, sealed cured at 20°C, are also shown in Table 2.

Table 1 Properties of used cement

TYPE OF CEMENT	DENSITY	SPECIFIC SURFACE AREA (cm^2/g)	SETTING			COMPRESSIVE STRENGTH (MPa)*		
			WATER (%)	INITIAL SETTING (h-m)	FINAL SETTING (h-m)	3 DAYS	7 DAYS	28 DAYS
OPC	3.16	3260	28.1	2-18	3-47	14.9	25.1	42.1
HPC	3.14	4310	29.7	2-19	3-42	26.8	39.5	49.9
MPC	3.21	3150	28.5	5-02	6-45	11.6	17.0	37.9
SCB	3.04	4090	29.8	2-55	4-30	12.5	20.2	41.2
FCB	2.97	3200	28.0	3-07	5-02	13.1	20.0	35.6

(Based on JIS R 5201)

After casting, specimens were set in an air-conditioned room at a temperature of 20 C. and relative humidity of 60 %. All surfaces of specimens were exposed for drying at the age of 1, 3 and 7 days. At the age of 28 days, these and the non-dried specimens were immersed in 20 °C water for 24 hours. This is done to remove the dynamic modulus of elasticity and length with drying due to the outward changes to the weight. After immersing in the water for 24 hours, all specimens would recover their original weight at the removal of forms.

Test Method for Resistance of Concrete to Rapid Freezing and Thawing

The freezing and thawing test was carried out in conformity to method A of ASTM C666 "Standard Test Method for Resistance of Concrete to Rapid Freezing and Thawing" at the age of 29 days.

Measuring Method

In order to obtain a sample for the determination of the pore structure before freezing and thawing, 1 cm thick parts were cut from the concrete prism at a depth of 0-1, 1-2, 2-3, 4.5-5.5 cm from the side of the drying surface. These parts were crushed to a particle size of between 2.5 to 5.0 mm, soaked in acetone and then dry ice dried. These samples were subjected to mercury porosimetry to determine the porosity that ranged from 3 nm to 3.2×10^5 nm in radius.

On the other hand, rates of aggregate in samples were measured. The porosity samples were heated at 600 C for 1 hour, mixed with 10 % hydrochloric acid and then stirred for 2 hours to dissolve the cement components. Subsequently, the wet insoluble residue was heated at 600 C for 1 hour, cooled in a desiccator and weighed as an insoluble residue Wns (g). The soluble component content (cement paste content in g/g) WRs can be calculated by Equation (1). W_0 (g) is the mass of the porosity sample before heating,

$$WRs = (W_0 - Wns) / W_0 \quad (1)$$

Table 2 Mixture proportions and properties of concrete

TYPE OF CEMENT	W/C	REQUIRED AIR CONT. (%)	WATER CONT. (kg/m³)	WEIGHT (kg/m³)			ADMIXTURE (cc/m³)			TEMP AS MIXED (°C)	SLUMP (cm)	MEASURED AIR CONTENT (%)	COMPRESSIVE STRENGTH 28 DAYS (MPa)
				Cement	Fine Agg.	Coarse Agg.	No 70	SP-8N	No 303A				
	0.4	1.0	185	463	671	1008	-	1600	1080	20.30	19.50	4.5	41.2
		1.0	185	308	747	957	-	-	-	20.00	17.50	1.3	27.5
OPC	0.6	3.0	185	308	799	957	770	-	700	22.00	21.50	3.3	31.3
		4.5	185	308	838	957	770	-	1900	21.00	22.00	4.5	25.2
	0.8	4.5	185	231	865	1008	578	-	1560	19.80	21.00	4.6	14.9
HPC	0.6	1.0	185	308	781	987	-	-	-	20.00	19.50	1.8	29.2
		4.5	185	308	873	987	770	-	2450	22.00	22.00	4.5	31.0
MPC	0.6	1.0	186	311	781	987	-	-	-	19.80	21.00	0.6	22.3
		4.5	186	311	873	987	770	-	2410	20.80	22.00	4.7	24.5
SCB	0.6	1.0	183	304	781	987	-	-	-	21.00	16.00	1.1	29.5
		4.5	183	304	873	987	770	-	2730	21.00	21.50	4.5	25.5
FCB	0.6	1.0	181	303	781	987	-	-	-	22.50	18.00	0.9	21.3
		4.5	181	303	873	987	770	-	4230	20.80	20.50	4.7	23.4

The total effective pore volume Vep (cc/g), that is the pore volume present in the cement paste, in the sample can be calculated from the measured pore volume Vmp (cc/g) by Equation (2).

$$Vep = Vmp / WRs \quad (2)$$

The dynamic modulus of elasticity, expansion content and scaling content were measured during test for freezing and thawing.

The dynamic modulus of elasticity of specimen was measured in conformity with JIS A 1127. The length of specimen was measured in conformity with JSTM C7301T-1992. Every measured value was calculated into the relative value for the one before the test of freezing and thawing.

The scaling content Vsn (cm^3/cm^2) at "n" cycle was calculated from the surface-dry specimen weight Wsn (g) at "n" cycle, weight Wwn (g) in water at "n" cycle, the water density ρw, the specimen surface area A (cm^2) before testing, the surface-dry specimen weight Wso (g) before testing and weight Wwo (g) in water before testing by Equation (3).

$$Vsn =((Wso - Wwo) \times \rho w) - (Wsn - Wwn) \times \rho w)) / A \quad (3)$$

RESULTS AND DISCUSSION

Deterioration with Expansion

Changes to the relative dynamic modulus of elasticity are shown in Figure 1. This clearly shows that the air volume in concrete is the most important factor for freeze-thaw resistance. In the case of 3 % air concrete, the relative dynamic modulus of elasticity decreases earlier when the start of drying is earlier. Though concrete involved 4.5 % air, the decrease of relative dynamic modulus of elasticity of the specimen using type B Portland blast furnace slag cement and type B Portland fly-ash can be seen at the drying age of 1 and 3 days.

These results can also be recognized from changes of the specimen length [7], [8]. The changes of length show deterioration clearly in comparison with the changes of relative dynamic modulus of elasticity.

From these results, in order to avoid deterioration with expansion, it is important firstly to keep the 4.5 % air volume and secondly to reduce the water cement ratio.

However, by merely maintaining the air volume or reducing the water cement ratio is not sufficient, early moist curing plays an important role for the resistance to freezing and thawing. So, it is important to ensure enough curing term at early ages when using moderate heat Portland cement, Portland blast furnace slag cement, or Portland fly ash that hydrates slower.

The distributions of moisture content [9] in concrete shown at 28 days was almost even. This is due to the small specimen dried from all surfaces [1]. Therefore pore structures also showed homogeneity in specimens except for the case where the water cement ratio is 0.4.

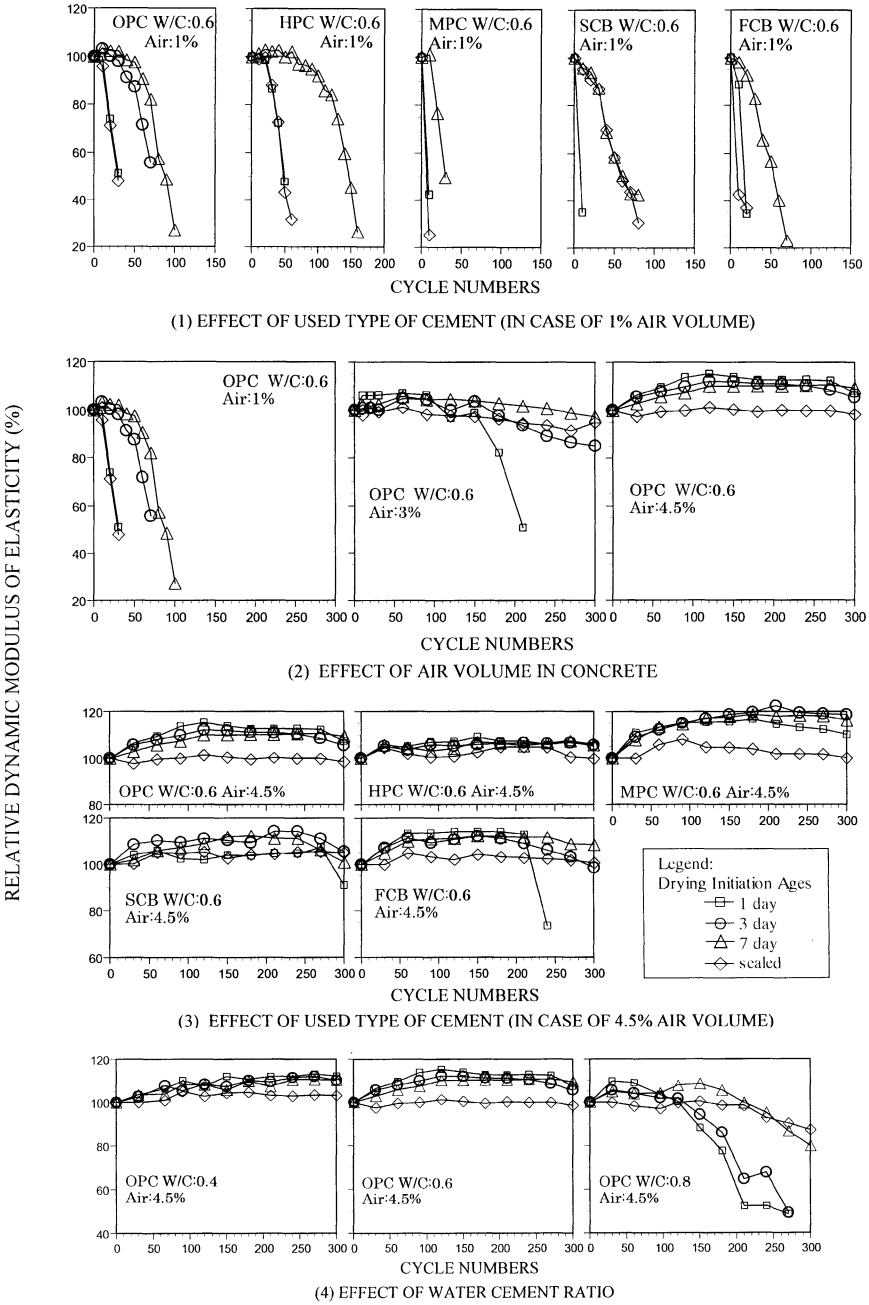

Figure 1 Changes of relative dynamic modulus of elasticity

In concretes that involve 4.5 % of air, the pore size distributions of seven concretes that show reducing dynamic modulus of elasticity and increasing expansion for test of freezing and thawing at the age of 28 days are shown in Figure 2 (1) and the pore size distributions of twenty-one concretes that did not show these changes for test are shown in Figure 2 (2). In Figure 2, only surface layer (0-1 cm) distributions are shown because of the above reasons.

Most concretes that show reducing dynamic modulus of elasticity and increasing expansion have more pores in the range of 180 nm to 1,000 nm in radius than concretes that don't. The respective two concretes shown by broken lines in Figure 2 (1) and (2) are exceptions from this tendency. Kamada one of authors noted that the pores in the range of 75 nm to 7,500 nm in radius has relationship with the frost damage [10]. For this pore, Trinker has pointed out from the range of 100 nm to 1,000 nm in radius [11], Kokufu from 24 nm to 7,500 nm in radius [12] and Sumiyoshi from 42 nm to 7,500 nm in radius [13]. The results from our experiment roughly agree with those from other studies.

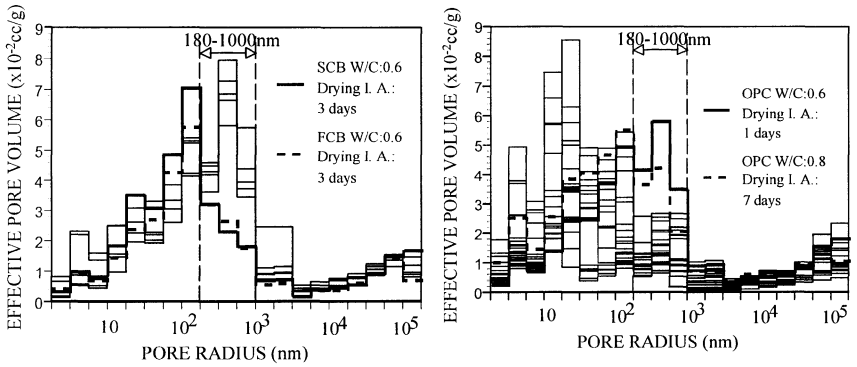

(1) EXPANDED SPECIMENS (2) NON-EXPANDED SPECIMENS

Figure 2 Effect of pore size distribution on expansion deterioration

Furthermore, Kamada explained this relationship from the theory of the falling of melting pot and developed it into the theory on the mechanism of frost damage [14], [15]. Yuasa, one of the authors, noted that pores of larger than 18 nm in radius, especially from 100 nm to 1,000 nm, has a tendency to increase when concrete is dried from early ages [1]. So, in order to avoid expansion due to the action of freezing and thawing, drying of concrete at early ages needs to be carried out careful.

Scaling

The Scaling contents of concrete are shown in Figure 3. The Scaling contents increase accordingly as concrete is dried earlier. Though reducing water cement ratio is effective in avoiding scaling as pointed out by JASS 5, keeping moist curing is more important at early ages. In other words, after controlling the air volume and water cement ratio to avoid expansion, keeping moist curing at early ages is more effective in avoiding scaling than reducing water cement ratio immoderately.

In the case of using Portland blast furnace slag cement, the dried concretes have a remarkably higher amount of scaling than non-dried concrete. For non-dried concrete, concretes using type B Portland fly ash have a higher amount of scaling. In reality, for the case of using type B Portland blast furnace slag cement and type B Portland fly ash, reducing water cement ratio sharply may be needed to resist scaling. As air volume increases, the amount of scaling reduces. But the difference between 3% and 4.5% of air volume is small and may be improved by narrowly lowering the water cement ratio or lengthening the moist curing term. Though keeping air volume in concrete is important to avoid expansion, it is not very effective to resist scaling. It is easier for water in larger pores to freeze than for water in smaller pores to freeze [14], [15]. So the correlations between the surface layer (0-1 cm) effective pore volume in the range of larger than certain pore sizes and the scaling content per cycle were calculated as shown in Figure 4. In this discussion, the scaling content per cycle was calculated from the scaling content after 240 cycles of freezing and thawing because one of concretes using type B Portland fly ash broke after completing 240 cycles. As a result, the effective pore volume of more than 56 nm in radius is best related to the scaling as shown in Figure 5. This 56 nm as the lower limit radius can be considered as reasonable by the analogy from background studies [15], [16]. As mentioned above, the pore of larger than 56 nm in radius is mostly found in concrete dried at early ages [1]. Accordingly, moist curing at early ages is extremely important to prevent scaling by the freezing and thawing reaction.

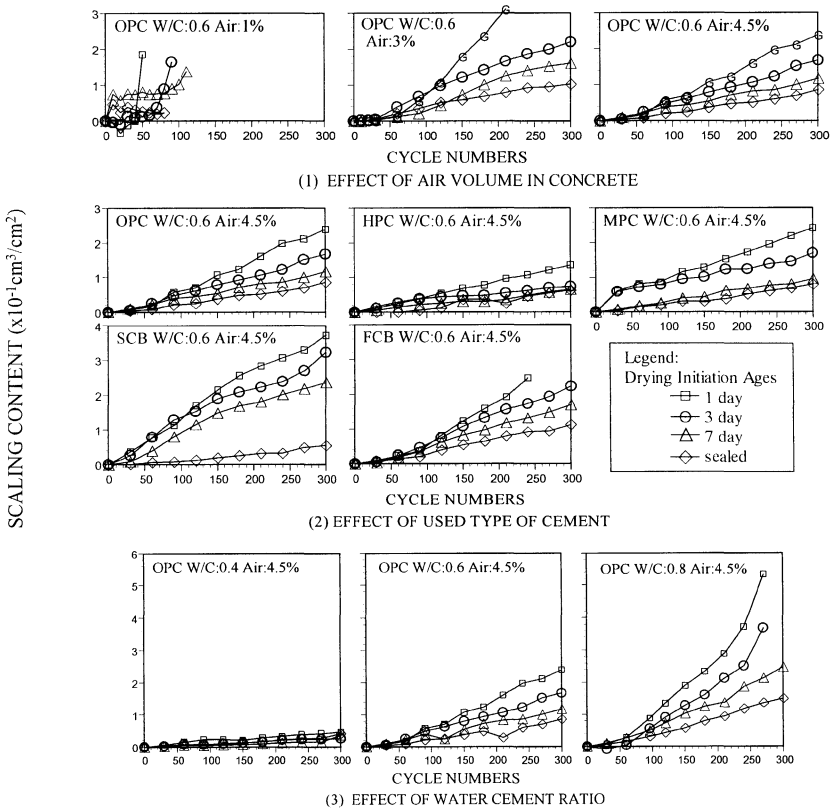

Figure 3 Change of scaling content

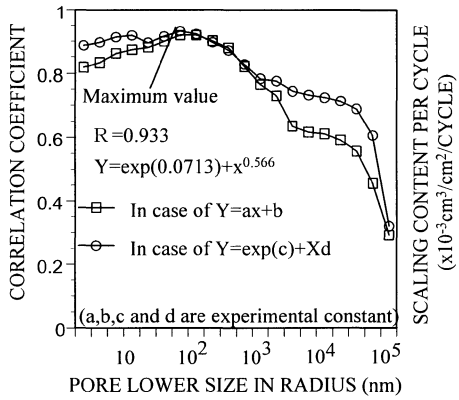

Figure 4 Effect of pore smaller size on scaling

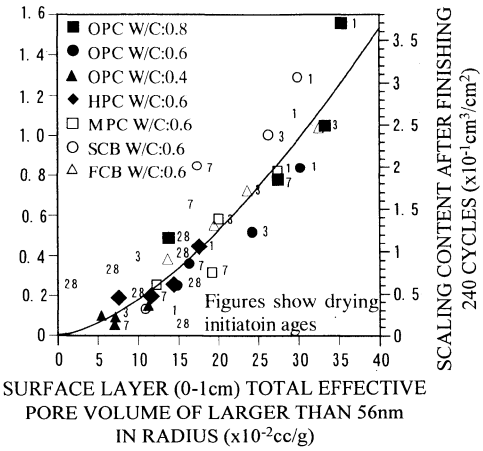

Figure 5 Relationship between surface layer total effective pore volume of larger than 56 nm in radius and scaling content

CONCLUSIONS

The freeze-thaw resistance of concretes subjected to drying at early ages has been discussed, and major findings of the work carried out, are as follows.

1. Freeze-thaw expansion of concretes is mainly controlled by air content rather than the types of cement or drying initiation ages. However with a 4.5 % of air content, considerable expansion at 300 freeze-thaw cycles, leading to a fracture, may occur when subjected to drying at early ages and depending on the types of cement and water-cement ratios. Use of blended cement with a high water-cement ratio should be accompanied by sufficient moist curing at early ages.

2. Difference in pore volume at the radius ranging from 180 to 1,000 nm was found between damaged and undamaged concretes during freeze-thaw test. These pore regions increased considerably with drying at early ages.
3. Freeze-thaw scaling increased when a drying initiation age became earlier. Scaling resistance can be increased by a moist curing immediately after concrete placement, but a decrease in water-cement ratio was still necessary when blended cement was used.
4. Amount of scaling was highly correlated to a pore size distribution within 1 cm from the surface, especially to a pore volume of larger than 56 nm in the radius. Pore volume in this region is likely to increase when subjected to drying at early ages.

REFERENCES

1. YUASA, N., KASAI, Y , MATSUI, I., Inhomogeneous distribution of moisture content and porosity in concrete, Creating with concrete, Concrete durability and repair technology, 1999, p 93-101.

2. YUASA, N., KASAI, Y., MATSUI, I., Inhomogeneous distribution of compressive strength from the surface layer to internal parts of concrete in structures, CANMET/ACI/JCI, Fifth International Conference on Durability of Concrete, 2000, p 269-281.

3. TABATA, M., A study on the influence of environmental conditions on frost damage of concrete, Doctor paper of Hokkaido University, 1986, p 45-54.

4. COMMITTEE ON CONCRETE, Properties of concrete affected by drying condition in early age, CAJ, Cement & Concrete, No 466, 1985, p 20-30.

5. SAEKI, N., HORIGUCHI, T, SUGAWARA, T., Concrete strength of surface layer, Concrete Journal, Vol 33, No 10, 1995, p 5-12.

6. HIRAI, K., NARITA, T., MIHASHI, H., Influence of curing method and pore structure on the frost damage of concrete, JCI, Symposium on National Environment and Concrete Performance, 1993, p 67-72.

7. KAMADA, E., KOH, E., Length change as a measure of frost resistance of concrete, The Cement Association of Japan, Review of the 25th General Meeting - Technical Session, No 25, 1971, p 182-183.

8. KOH, E., HASEGAWA, T., On the test method for resistance of concrete to freezing and thawing, Vol 16, No 9, 1981, p 16-22.

9. YUASA, N., KASAI, Y., MATSUI, I., Measuring method for moisture content in hardened concrete using electric properties of a ceramic sensor, Journal of Structure and Construction Engineering, Architectural Institute of Japan, No 498, 1997, p 13-20.

10. KAMADA, E., KOH, E., TAKAHASHI, A., Freeze-thaw resistance and porosity of hardened cement paste used every types of cement, Proceeding of the 35th meeting of Hokkaido Branch of Architectural Institute of Japan, 1971, p 7-10.

11. TRINKER, B. D., et al, Methods of structure resistance in estimating the life of heavy concretes, Primary Report of RILEM Symposium, Durability of Concrete III, 1969.

12. KOKUBU, K., Fundamental studies on freeze-thaw durability of expansive concrete, Japan Society of Civil Engineers, Proceedings of the Japan Society of Civil Engineers No 334, 1983, p 145-154.

13. SUMIYOSHI, H., KUBOYAMA, K., IMAHASHI, T., SHIOYA, M., Effect of steam curing on micro structure and other properties of concrete, The Cement Association of Japan, Review of the 25th General Meeting -Technical Session, No 35, 1981, p 151-153.

14. KAMADA, E., SENBU, O., TABATA, M., TANAKA, H., Statistical investigation concerning the effects of pore structure on the frost resistance of concrete, Journal of Structure and Construction Engineering, Architectural Institute of Japan, No 487, 1996, p 1-8.

15. OKAMOTO, S., UOMOTO, T., Frost damage of concrete and pore structure of hardened cement paste, Proceedings of the Japan Concrete Institute Vol 10, No 1, 1988, p 51-60.

AN ASSESSMENT OF THE RAPID CHLORIDE ION PENETRABILITY TEST

M Hale **B W Russell**
University of Oklahoma
T D Bush
Frankfurt Short Burza Associates
United States of America

ABSTRACT. Many researchers have begun to question the validity of the Rapid Chloride Ion Penetrability Test (ASTM C 1202) as a means to assess the permeability of concrete. Many researchers believe the Rapid Chloride Ion Penetrability Test (RCIP) measures the concrete's conductivity not necessarily the permeability [1]. The researchers believe the addition of mineral admixtures such as blast furnace slag (BFS), fly ash (FA), and silica fume (SF) may alter the pore fluid chemistry of the concrete, which would produce RCIP results that were either too high or too low. This paper examines the RCIP results of over 30 different concrete mixtures. The results of the research further support the view that the RCIP test may not be an adequate test for measuring the permeability of concrete.

Keywords: Rapid chloride ion penetrability (ASTM C 1202), Concrete permeability, Pozzolans.

Mr W M Hale, is a Research Assistant at The University of Oklahoma. He has been involved in concrete materials research and its applications to prestressed concrete bridge girders.

Dr B W Russell, is an Associate Professor at Oklahoma State University. His research interests include prestressed concrete and concrete materials.

Dr T D Bush, is a structural engineer with Frankfurt Short Bruza Associates.

INTRODUCTION

There are several different standardized tests that measure the permeability of concrete. Many of the tests require a significant amount of time to measure the concrete's permeability. In 1991 a test was adopted by American Society for Testing and Materials (ASTM) that measured the concrete's permeability in six hours. This test is known as the Rapid Chloride Ion Penetrability Test (RCIP). Theoretically, the test measures the number of chloride ions that pass through a sample of concrete in a six-hour period of time. In general, the lower the permeability of the concrete the lower the amount of coulombs passed. Therefore, concrete with a high permeability will pass more coulombs.

Some researchers believe that the Rapid Chloride Ion Penetrability Test (ASTM C 1202) measures the concrete's conductivity but not necessarily the concrete's permeability [1]. The addition of mineral admixtures such as fly ash, blast furnace slag, and silica fume may alter the concrete's conductivity by altering the pH of the pore solution, which could either increase or decrease the RCIP value. The pore fluid of hardened concrete consists mainly of Na, K, and OH ions. Shi et al (1998) reported that the addition of mineral admixtures might increase or decrease the concentrations of these ions. They reported that BFS decreases the concentration of the OH and K ions, but increases the Na concentration [1]. Shi et al (1998) also reported that the replacement of cement with 5 percent silica fume "can lead to order of magnitude reductions in Na, K, and OH ion concentrations." They also reported that the addition of fly ash might either increase or decrease the Na and K concentrations [1].

It is theorized that these changes in concentrations of the pore fluid result in changes in the concretes' specific conductivity. When compared to the control mixture (100 percent portland cement), the addition of 50 percent BFS reduced the concrete's specific conductivity by 3.25 percent at 28 days and up to 24 percent by 730 days. A specific conductivity of a concrete mixture containing 5 percent silica saw a reduction of 70.6 percent at 28 days. Shi et al (1998) concluded that "it was not correct" to use the RCIP test to evaluate the rapid chloride penetrability of concrete containing mineral admixtures [1].

Zhao et al (1999) also examined the pore chemicals in concretes with mineral admixtures. They measured the concretes' resistivity and its RCIP [2]. They also found that the concretes' resistivity increased with the addition of mineral admixtures and as the concretes' resistivity increased its RCIP values decreased. These findings are similar to the results of a study conducted by Wee et al (2000) [3].

Pfiefer et al (1994) examined the correlation of the RCIP test to the 90-day salt ponding test (AASHTO T259). They, like Shi et al, also state that the addition of silica fume can substantially reduce the number of coulombs passed. Pfiefer et al states that typical concrete "may have a 5- to 10-fold decrease in coulombs passed when 7 silica fume is added, while the actual chloride ingress after 90-day ponding tests may decrease only one to two times." For selecting materials for low permeability concretes, Pfiefer et al recommended that the selection should based on the 90-day salt ponding tests (AASHTO T259) not the RCIP test (ASTM C 1202) [4]. Scanlon et al (1996) also examined the correlation between the 90-day ponding test (AASHTO T259) and the RCIP test (ASTM C 1202) for concretes containing fly ash and/or silica fume. They too concluded that there were inconsistencies between the permeability determined by the RCIP test and the permeability measured by the 90-day ponding test.

Scanlon et al stated that the correlation between coulomb values and chloride ingress given in AASHTO T277 or ASTM C 1202 "appears invalid for use with concretes containing silica fume, fly ash or a HRWRA [5]."

EXPERIMENTAL PROGRAM

Scope

This paper presents and examines the RCIP test results of over 30 different concrete mixtures. The mixtures investigated were developed from two separate research programs. The variables of the mixtures were the water to cementitious material ratio (w/cm), the total air content, and the amount and type of mineral admixture. The w/cm ranged from 0.26 to 0.50. The total air contents ranged from approximately one percent to seven percent. The types of mineral admixtures used were fly ash, blast furnace slag, and silica fume. The replacement rates ranged from zero percent to 50 percent. The RCIP test was performed at two different ages. All mixtures were tested at 28 days of age and also at either 56 or 90 days of age

Materials

Type I or Type III Cement was used in the mixtures. The coarse aggregate was 9.5 mm., crushed limestone. For the fine aggregate, natural river sand with a fineness modulus of 2.50 was used in all mixtures. The mineral admixtures used in the research included Class C FA, Grade 120 BFS, and silica fume. The Class C FA was obtained in bulk from two different sources. The BFS and SF were obtained in bulk from the same source. The chemical admixtures that were used included an air entraining agent and a normal and high range water reducer. All chemical admixtures are commercially available.

Mixture Designations

As previously stated the mixtures tested were part of two separate research programs. Mixtures AP through ABB in Table 1 and 2 were part of a study that examined the influence of blast furnace slag on the fresh and hardened properties of concrete. The first letter in the designation represents the cement brand. Cements A, B, and C were the three different brands of Type I Cements examined in the study. The second group of letters represents the type of pozzolan added to the mixture. A mixture whose second letter is P contains only portland cement. Mixtures whose second group of letters is FA or BFS contain fly ash or blast furnace slag, respectively. FB designates mixtures that contain both fly ash and blast furnace slag, and BB designates mixtures in which 50 percent of the cement was replaced with blast furnace slag. For example, Mixture CFA contains Cement C and fly ash.

The second set of mixtures was part of a research program that investigated the freeze-thaw durability of high performance concrete. These mixtures are listed in Tables 2 through 5. The mixtures are designated by their w/cm and measured total air content. The first number is the w/cm, and the second number is the total air content. Any additional letter at the end of the designation represents fly ash (F), silica fume (S) or the use of Type I Cements (T1).

For example, Mixture 42-2.4S has a w/cm of 0.42, a total air content of 2.4, and contains silica fume.

Tests

The concrete mixtures were subjected to several fresh and hardened property tests. For most mixtures, the slump (ASTM C 143), total air content (ASTM C 231), and unit weight (ASTM C 136) were the fresh properties measured. The hardened properties examined were compressive strength (ASTM C 39) and Rapid Chloride Ion Penetrability (ASTM C 1202) at 28 days of age and at either 56 or 90 days of age.

RESULTS & DISCUSSION

The results from the compressive strength tests and RCIP tests are shown Tables 1 through 5. The compressive strength reported is the average of three cylinders (101.6 mm x 203.2 mm). For most mixtures, the RCIP value reported is the average of four tests. The results from the 28-day RCIP tests are shown in Figure 1. The 56 and 90-day test results are shown in Figure 2. Also shown in the Figures are the ASTM C 1202 permeability classifications.

PC Mixtures

PC mixtures are mixtures that do not contain any pozzolanic material. From examination of Figures 1 and 2, it is apparent that increases in w/cm resulted in increases in the number of coulombs passed for mixtures containing only portland cement. This increase in the number of coulombs passed was expected. The effect of the w/cm on the permeability of concrete has been well documented [6,7]. A decrease in the w/cm reduces the porosity of the concrete, which results in a more impermeable concrete.

At 28 days of age, the total charge passed ranged from 671 coulombs for mixture 0.26-3.8 to 9450 coulombs for mixture 0.50-0.9. At later ages (56 days or 90 days), the RCIP value decreased for most mixtures. At 56 and 90 days of age, mixtures with a w/cm equal to or less than 0.39 had moderate permeability based on ASTM C 1202 classifications. The only mixtures to achieve low permeability (according to ASTM C 1202) were mixtures with a w/cm equal to or less than 0.34.

FA Mixtures

FA mixtures are mixtures that contain some amount of fly ash. The mixtures examined in this paper contained fly ash at replacement rates of either 15 percent (mixtures 42-2.2F and 50-1.5F) or 19.5 percent (mixtures AFA, BFA, and CFA). Class C fly ash was used in the mixtures. Two separate power plants provided the fly ash. The fly ash used for mixtures 42-2.2F and 50-1.5F came from one source, while the fly ash used for mixtures AFA, BFA, and CFA came from another source.

Table 1 Mixture proportions and properties

Materials	MIXTURE DESIGNATIONS							
	AP	BP	CP	AFA	BFA	CFA	ABFS	BBFS
Cement (kg/m^3)	392	392	392	333	333	333	293	293
Fly Ash (kg/m^3)	0	0	0	80	80	80	0	0
BFS (kg/m^3)	0	0	0	0	0	0	98	98
SF (kg/m^3)	0	0	0	0	0	0	0	0
Water (kg/m^3)	151	151	151	151	151	151	151	151
Coarse Agg. (kg/m^3)	1125	1125	1125	1125	1125	1125	1125	1125
Fine Agg. (kg/m^3)	677	677	677	677	677	677	677	677
WR (L/m^3)	0	0	0	0	0	0	0	0
HRWR (L/m^3)	0	0	0	0	0	0	0	0
AEA (L/m^3)	3.6	3.6	3.6	3.6	3.6	3.6	3.6	3.6
w/cm	0.39	0.39	0.39	0.37	0.37	0.37	0.39	0.39
Air Content (%)	6.9	5.9	5.3	6.9	6.6	6.3	5.2	5.2
Slump (mm.)	76	57	45	57	83	64	32	25
Unit Weight (kg/m^3)	2265	2307	2320	2275	2251	2313	2315	2358
28 D Comp. (MPa)	31.1	29.5	33.2	25.9	35.1	31.1	40.2	37.7
28 D RCIP (coulombs)	4130	4580	4010	6350	6860	8860	1820	2380
56 D RCIP (coulombs)	-	-	-	-	-	-	-	-
90 D RCIP (coulombs)	3500	2670	3560	3670	4230	4225	1285	1930

Table 2 Mixture proportions and properties

Materials	MIXTURE DESIGNATIONS							
	CBFS	AFB	BFB	CFB	ABB	26-2.4	26-2.1T1	26-3.8
Cement (kg/m^3)	293	235	235	235	196	534	534	534
Fly Ash (kg/m^3)	0	80	80	80	0	0	0	0
BFS (kg/m^3)	98	98	98	98	196	0	0	0
SF (kg/m^3)	0	0	0	0	0	0	0	0
Water (kg/m^3)	151	151	151	151	151	139	139	139
Coarse Agg. (kg/m^3)	1125	1125	1125	1125	1125	1062	1062	1062
Fine Agg. (kg/m^3)	677	677	677	677	677	722	722	669
WR (L/m^3)	0	0	0	0	0	1.0	1.0	1.0
HRWR (L/m^3)	0	0	0	0	0	5.2	5.2	5.2
AEA (L/m^3)	3.6	3.6	3.6	3.6	3.6	0	0	3.5
w/cm	0.39	0.37	0.37	0.37	0.39	0.26	0.26	0.26
Air Content (%)	5.1	5.4	5.3	5.1	3.4	2.4	2.1	3.8
Slump (mm.)	38	38	45	38	13	165	165	203
Unit Weight (kg/m^3)	2345	2326	2308	2315	2406	2439	2431	2392
28 D Comp. (MPa)	37.6	35.1	36.0	35.9	44.1	84.1	81.4	77.7
28 D RCIP (coulombs)	2310	3900	3300	4260	1053	710	1210	671
56 D RCIP (coulombs)	-	-	-	-	-	520	877	660
90 D RCIP (coulombs)	1660	2770	2280	3025	1054	-	-	-

Table 3 Mixture proportions and properties

	MIXTURE DESIGNATIONS							
Materials	26-5.6	30-2T1	30-1.1	30-4.5	30-5.7	32-4.1	34-2.0	36-2.4T1
Cement (kg/m^3)	534	534	534	534	534	534	534	534
Fly Ash (kg/m^3)	0	0	0	0	0	0	0	0
BFS (kg/m^3)	0	0	0	0	0	0	0	0
SF (kg/m^3)	0	0	0	0	0	0	0	0
Water (kg/m^3)	139	160	160	160	160	171	182	192
Coarse Agg. (kg/m^3)	1062	1062	1062	1062	1062	1062	1062	1062
Fine Agg. (kg/m^3)	617	665	665	614	561	585	610	582
WR (L/m^3)	1.0	1.0	1.0	1.0	1.0	1.0	1.0	1.0
HRWR (L/m^3)	5.2	3.5	3.5	3.5	3.5	2.8	2.8	0.9
AEA (L/m^3)	5.2	0	0	0.2	0.3	0.1	0	0
w/cm	0.26	0.30	0.30	0.30	0.30	0.32	0.34	0.36
Air Content (%)	5.6	3.5	1.1	4.5	5.7	4.1	2.0	2.4
Slump (mm.)	108	-	254	38	273	165	292	69
Unit Weight (kg/m^3)	2358	-	2417	2363	2342	2358	2412	2377
28 D Comp. (MPa)	72.8	-	84.1	68.7	70.8	66.6	70.7	50.8
28 D RCIP (coulombs)	956	1226	1270	1789	1222	1534	2471	2675
56 D RCIP (coulombs)	799	454	849	1281	756	811	1739	2560
90 D RCIP (coulombs)	-	-	-	-	-	-	-	-

Table 4 Mixture proportions and properties

	MIXTURE DESIGNATIONS							
Materials	36-2.6	36-3.8	36-6.2	42-1.8	42-2.2F	42-2.4S	42-4.4	42-5.9
Cement (kg/m^3)	534	534	534	534	454	507	534	534
Fly Ash (kg/m^3)	0	0	0	0	80	0	0	0
BFS (kg/m^3)	0	0	0	0	0	0	0	0
SF (kg/m^3)	0	0	0	0	0	27	0	0
Water (kg/m^3)	192	192	192	224	224	224	224	224
Coarse Agg. (kg/m^3)	1062	1062	1062	1062	1062	1062	1062	1062
Fine Agg. (kg/m^3)	582	529	477	498	498	498	445	393
WR (L/m^3)	1.0	1.0	1.0	0	0	0	0	0
HRWR (L/m^3)	0.9	0.9	0.9	0	0	0	0	0
AEA (L/m^3)	0	0.3	0.4	0	0	0	0.3	0.4
w/cm	0.36	0.36	0.36	0.42	0.42	0.42	0.42	0.42
Air Content (%)	2.6	3.8	6.2	1.8	2.2	2.4	4.4	5.9
Slump (mm.)	64	89	51	83	51	25	95	102
Unit Weight (kg/m^3)	2368	2352	2236	2335	2337	2304	2286	2228
28 D Comp. (MPa)	63.3	57.5	53.1	59.9	59.9	53.6	44.6	42.1
28 D RCIP (coulombs)	2453	3416	3500	4546	4639	1343	5905	5430
56 D RCIP (coulombs)	2319	2949	2166	4551	3514	1134	5110	4216
90 D RCIP (coulombs)	-	-	-	-	-	-	-	-

Table 5 Mixture proportions and properties

Materials	MIXTURE DESIGNATIONS					
	45-4.1	50-0.9	50-1.5F	50-2.2S	50-3.6	50-6.6
Cement (kg/m^3)	534	534	454	507	534	534
Fly Ash (kg/m^3)	0	0	80	0	0	0
BFS (kg/m^3)	0	0	0	0	0	0
SF (kg/m^3)	0	0	0	27	0	0
Water (kg/m^3)	240	267	267	267	267	267
Coarse Agg. (kg/m^3)	1062	1062	1062	1062	1062	1062
Fine Agg. (kg/m^3)	403	386	386	386	333	281
WR (L/m^3)	0	0	0	0	0	0
HRWR (L/m^3)	0	0	0	0	0	0
AEA (L/m^3)	0.3	0	0	0	0.2	0.3
w/cm	0.45	0.50	0.50	0.50	0.50	0.50
Air Content (%)	4.1	0.9	1.5	2.2	3.6	6.6
Slump (mm.)	140	159	203	83	241	254
Unit Weight (kg/m^3)	2247	2297	2279	2247	2164	2137
28 D Comp. (MPa)	42.1	42.9	50.8	42.1	43.7	38.3
28 D RCIP (coulombs)	5969	9450	8624	1868	8057	8623
56 D RCIP (coulombs)	5413	7410	5491	1484	7549	8467
90 D RCIP (coulombs)	--	-	-	-	-	-

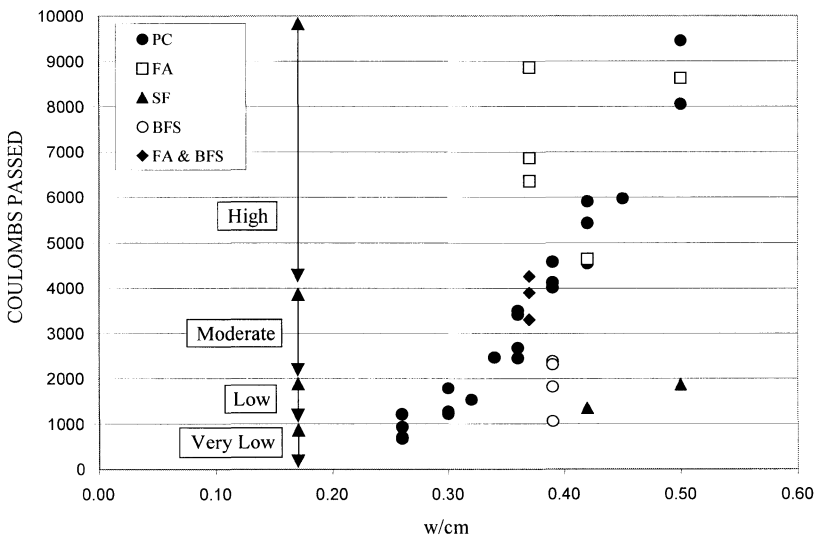

Figure 1 28-Day RCIP Results and ASTM C 1202 Permeability Classifications

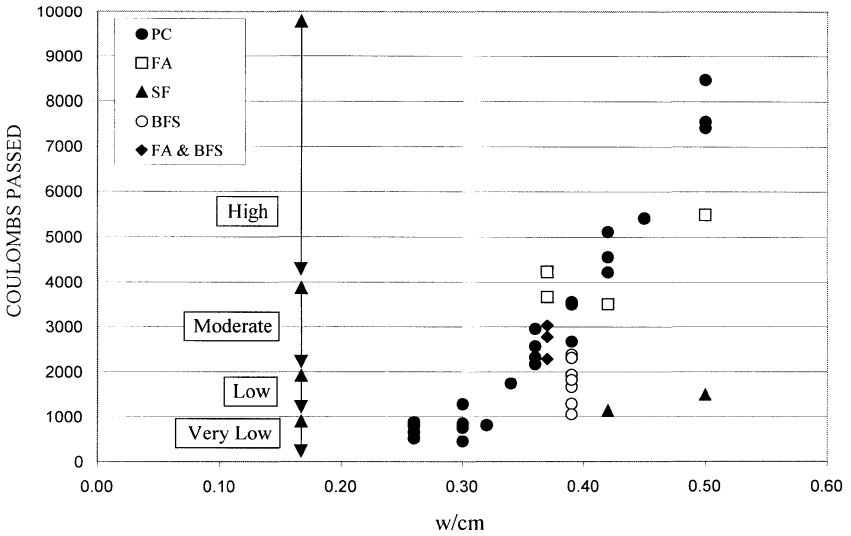

Figure 2 56 and 90-Day RCIP Results and ASTM C 1202 Permeability Classifications.

From examination of Figure 1, the addition of fly ash increased the charge passed for mixtures AFA, BFA, and CFA when compared to identical mixtures without fly ash (AP, BP, and CP). At 28 days of age, the total coulombs passed for mixtures AFA, BFA, and CFA ranged from approximately 50 percent to 100 percent greater than that of similar mixtures (AP, BP, and CP) without fly ash. By 90 days of age, the RCIP value for the fly ash mixtures had decreased by as much 50 percent but was still greater than the RCIP values for mixtures without fly ash.

Mixtures 42-2.2F and 50-1.5F contained fly ash at a replacement rate of 15 percent. As previously stated the fly ash for these mixtures was obtained from a different source than that of mixtures AFA, BFA, and CFA. When compared to similar mixtures (42-1.8 and 50-0.9), the addition of fly ash did not appear to affect the total charge passed at 28 days. By 56 days of age, the total charge passed for mixtures 42-2.2F and 50-1.5F was approximately 20 and 25 percent less than that of similar mixtures (42-1.8 and 50-0.9) without fly ash.

The fact that the two different fly ashes came from different sources appeared to have a significant effect on the mixtures' RCIP value. The fly ash used in mixtures AFA, BFA, and CFA increased the total coulombs passed at both 28 and 90 days of age, whereas the fly ash used in mixtures 42-2.2F and 50-1.5F decreased the coulombs passed at both 28 and 56 days of age. These findings are consistent with the report of Shi et al who stated that fly ash could either increase or decrease the Na and K concentrations of the pore fluid.

BFS Mixtures

BFS mixtures are those mixtures that contain some amount of blast furnace slag. The mixtures examined in this paper contained BFS at replacement rates of either 25 percent (ABFS, BBFS, and CBFS) or 50 percent (ABB). At 28 and 90 days of age, the total coulombs passed for the BFS mixtures were approximately 50 percent less than that of

similar mixtures (AP, BP, and CP) without BFS. The total charge passed for the mixture containing 50 percent BFS (ABB) was approximately 75 percent less than that of similar mixtures (AP, BP, and CP) without BFS at 28 days of age. According to ASTM C 1202, at 90 days of age all mixtures containing BFS would be classified as having low chloride permeability.

FA and BFS Mixtures

FA and BFS mixtures are those mixtures that contained both fly ash and blast furnace slag. The mixtures examined in this paper (AFB, BFB, and CFB) contained FA at a replacement rate of 19.5 percent and BFS at a replacement rate of 25 percent. For these mixtures, the combination of FA and BFS accounted for 44.5 percent of the total cementitious material. As shown in Figure 1, the addition of both FA and BFS had little effect on the chloride ion penetrability when compared to similar control mixtures at 28 days of age. At 90 days of age the RCIP values (Figure 2) for these mixtures were approximately 15 to 20 percent less than that of similar mixtures (AP, BP, and CP).

The FA used in these mixtures was the same fly ash that was used in mixtures AFA, BFA, and CFA. The addition of the FA significantly increased the total coulombs passed for those mixtures. However, mixtures AFB, BFB, and CFB did not see such increases in the number of coulombs passed due to the addition of BFS. The addition of BFS counteracted the negative effects of the FA. At 90 days of age, mixtures AFB, BFB, and CFB would be classified as having moderate permeability.

Silica Fume Mixtures

Mixtures 42-2.4S and 50-2.2S contained silica fume at a replacement rate of 5 percent. Figures 1 and 2 show the dramatic effect that the addition of silica fume has on the rapid chloride ion penetrability of the concrete. At 28 and 56 days of age, the total coulombs passed for the silica fume mixtures was more than 75 percent less than for identical mixtures (42-1.8 and 50-0.9) without silica fume. These results are consistent with Shi et al who reported that the replacement of cement with 5 percent silica fume "can lead to order of magnitude reductions in Na, K, and OH ion concentrations."

CONCLUSIONS

The purpose of the paper was to provide additional data on the effectiveness of the RCIP Test (ASTM C 1202) as a means to measure concrete penetrability. Although this test is a measure of the concrete's resistance to the migration of chloride ions under a forced current, the concrete's permeability should be directly related to its penetrability. Increases in permeability should result in increases in penetrability. The mixtures containing no mineral admixtures (FA, BFS, or SF) substantiated this trend, in that as the w/cm increased, the RCIP increased which was expected since increases in w/cm results in increases in permeability. For mixtures not containing any mineral admixtures, the test appears to be effective in measuring concrete's chloride ion penetrability. As shown in Figure 1 and 2, the concrete's penetrability increases as the w/cm increase, which is expected. All mixtures containing portland cement only follow this trend.

However, once mineral admixtures are introduced, this trend is no longer valid. The introduction of one Class C FA increased the concrete's RCIP while the introduction of another Class C FA had little effect at 28 days of age and decreased the concrete's RCIP at 90 days of age. For all mixtures, the addition of BFS and silica fume decreased the chloride ion penetrability at all ages. When compared to similar control mixtures, silica fume reduced the chloride ion penetrability by more than 75 percent.

In conclusion, the Rapid Chloride Ion Penetrability Test (ASTM C 1202) can be used as a method to assess concrete's permeability, but one must take caution when testing concrete with mineral admixtures. For concrete containing no mineral admixtures, the use of the RCIP test to provide an indirect indication of permeability produced results that followed expectations, and appeared to have validity. Since the RCIP test does not directly measure permeability, other factors can influence the parameter the test actually does measure, which is concrete resistivity. Therefore, other factors (such as pore fluid chemistry) may influence the parameter actually measured, leading to a basic need for users to understand what the test actually measures so that results can be put into proper perspective. When testing concrete containing mineral admixtures, one should compare the results to an identical mixture without mineral admixtures. This comparison with mixtures containing only portland cement may provide a better idea as to the true permeability of the concrete.

ACKNOWLEDGEMENTS

The authors would like to acknowledge the Oklahoma Department of Transportation for providing the funding and support for the project. The authors would also like to acknowledge Dolese Bros. Co., Ash Grove Cement, and W.R.Grace for providing the materials used in the research.

REFERENCES

1. SHI, C., STEGEMANN, J. A., CALDWELL, R. J., Effect of Supplementary Cementing Materials on the Specific Conductivity of Pore Solution and its Implications on the Rapid Chloride Permeability Test (AASHTO T277 and ASTM C1202), ACI Materials Journal, 1998, Vol 95, No 4, July-August, p 389-394.
2. WEE, T. H., SURYAVANSHI, A. K., TIN, S S, Evaluation of Rapid Chloride Permeability Test (RCPT) Results for Concrete Containing Mineral Admixtures, ACI Materials Journal, 2000, Vol 97, No 2, March-April, p 221-232.
3. ZHAO, T. J., ZHU, J. Q., CHI, P. Y., Modification of Pore Chemicals in Evaluation of High-Performance Concrete Permeability, ACI Materials Journal, 1999, Vol 96, No 1, January-February, p 84-89.
4. PFIEFER, D. W., MCDONALD, D. B., KRAUSS, P. D., The Rapid Chloride Permeability Test and Its Correlation to the 90-Day Chloride Ponding Test, PCI Journal, 1994, January-February, 1994, p 38-47.
5. SCANLON, J. M., SHERMAN, M. R., Fly Ash Concrete: An Evaluation of Chloride Penetration Testing Methods, Concrete International, 1996, June, p 57-62.
6. NEVILLE, A. M., Properties of Concrete, John Wiley and Sons, Inc., New York. New York, 1997, p 844.
7. MINDESS, S., YOUNG, J. F., Concrete, Prentice-Hall, Englewood Cliffs, New Jersey, 1981, p 671.

INFLUENCE OF POROSITY ON THE FREEZE-THAW SALT RESISTANCE OF HIGH PERFORMANCE MORTAR

A Šajna
Engineering Company of Public Roads
Slovenia

ABSTRACT. The goal of the research work was to experimentally evaluate the influence of porosity on the freeze–thaw-salt resistance of the high strength concrete and mortar. Seven different high strength mortar admixtures were prepared to clear up the structure – durability relations. To gain mortars of different porosity, the content of microsilica, the content of polypropylene fibres and the water/binder factor were changed. In the extensive experimental program the fresh and hard mortar properties including He-porosity, mercury porosimetry and the freeze–thaw–salt resistance were evaluated. The influence of different admixture proportions on the total pore volume and pore distribution was observed, but no influence on the freeze–thaw–salt durability was detected.

Keywords: High strength mortar, Durability, Freeze–thaw-salt resistance, Porosity.

A Šajna is a Senior Advisor for concrete and concrete structures in the Sector for Quality, Research and Technology of the Engineering Company of Public Roads, Ljubljana, Slovenia.

INTRODUCTION

Nowadays road pavements are mostly made of bituminous materials. Due to higher chemical resistance to oil products (petrol stations), lower plasticity at high temperatures (building of ruts in the cross-road zones and bus-stops), brighter colour (tunnels) and higher strength (industry) asphalt is replaced by (cement) concrete. During wintertime de-icing solutions are applied on road surfaces. In spite of extensive research work, the freeze-thaw-salt resistance of cementitious materials is still a serious problem. The freeze-thaw-salt resistance is usually improved by adding air-entraining agents to concrete mixtures. These agents form small, well-distributed air voids in the cement paste and increase the frost resistance of the concrete.

Because the freeze-thaw-salt destruction occurs mostly in the binder or in the transition zone between binder and aggregate, the resistance of cementitious materials can also be increased by making a high quality, condense cement paste.

A higher quality of the cement binder and better binder-aggregate contact can be reached by using selected materials, by the admixture optimization and by adding spatial additives. In so-called high performance concretes and mortars (HPC, HPM) lower water to cement (or binder) factors (< 0,3) in combination with (super)plasticizers, aggregates of higher strength, pozzolanic additives such as microsilica (MS) and polypropylene or steel fibres are used.

The effects of MS and small water content on the microstructure and the composition of the mortar results in a reduction of total porosity, a decrease of pore volume of both capillary and gel pores, a shift of the maximum of pore size distribution to smaller pore radii, a reduction of specific surface area and a decrease of Ca $(OH)_2$-content.

Hence, the advantages of a HPC are obvious: Because of its homogeneous and dense pore structure, the permeability of concrete is reduced and thus the penetration of moisture and external ions (alkali, sulphate) is limited. The uniform and dense pore system and the smaller content of water provide a good resistance to frost attacks. But there are also disadvantages which have to be considered: During the hydration process micro-cracks can arise due to self-desiccation (low w/c factor), the reactivity of MS can lead to an undesirable formation of gel in hardened concrete and finally, unhydrated clinker minerals can be reactivated for hydration by moisture ingress, which leads to micro-cracking and destruction of the material.

The goal of the program was to investigate the influence of the pore structure of the cement paste on the freeze-thaw-salt resistance of high performance mortar.

EXPERIMENTAL PROGRAM

Admixture Proportions

For the preparation of high strength mortars the following materials were used: Portland cement CEM I 52,5 R, microsilica, sand of 4 mm maximum aggregate size, 6 mm polypropylene fibres and a melamine-formaldehyde based superplasticizer (powder).

To gain proper characteristics and compositions of the cement and MS, the chemical composition and the characteristics were determined (Table 1).

Table 1 Characteristic and compositions of the cement and MS

MATERIAL	SPEC. WEIGHT [g/cm³]	SPEC. SURFACE [m²/g]	LOSS ON IGNITION [%]	CHEMICAL COMPOSITION [M-%]							
				SiO_2	Al_2O_3	CaO	MgO	Fe_2O_3	SO_3	Na_2O_3	K_2O
Cement	3.16	1.69	1.56	20.42	6.03	64.45	0.21	2.36	3.22	0.43	1.21
MS	2.28	18.40	2.42	92.49	-	0.47	-	0.62	0.27	-	-

Seven different mortar mixtures were prepared and tested in the study. Different cement matrix porosity was achieved by changing the amount of microsilica, the water to binder (microsilica + cement) ratio and the amount of polypropylene fibres.

The water to binder ratio was changed between 0.28 and 0.4. The amount of MS was changed from 0 to 8 % and the amount of polypropylene fibres from 0 to 2 % (in both cases in mass relation to cement). For mortars with higher water to binder ratio different aggregate distribution was used. Similar workability was reach by adding different amount of superplasticizer (see Table 2 and Figure 1).

For all mortars the consistence, the air content and the volume mass were evaluated according to DIN 18555-2. The values were compared with the theoretically calculated ones.

Table 2 Admixture proportions

ADMIXTURE	CEMENT	MS	SUPERPLASTI-CIZER	PP FIBRES	W/C-FACTOR	AGGREGATE (B)	AGGREGATE (C)
	[kg/m³]	[kg/m³]	[kg/m³]	[kg/m³]	[-]	[kg/m³]	[kg/m³]
M0W28F0	900	0	18.0	0	0.28	1173	-
M0W28F2	900	0	18.0	2	0.28	1169	-
M4W28F0	900	36	18.72	0	0.28	1089	-
M8W28F0	900	72	19.44	0	0.28	1001	-
M8W28F2	900	72	19.44	2	0.28	996	-
M8W35F0	575	46	9.32	0	0.35	-	1481
M8W40F0	500	40	7.5	0	0.40	-	1558

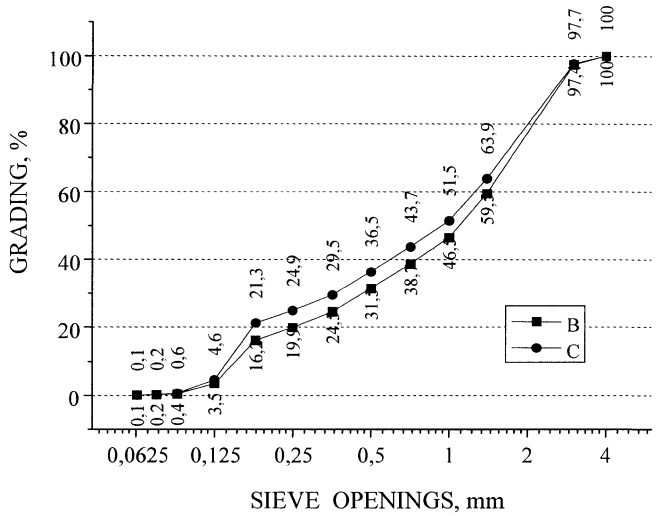

Figure 1 Sieving curves of used aggregates

Preparation of Test Samples

The complete amount of mortar necessary for the preparation off all test samples was prepared at once, in a 50 l concrete mixer. As a superplasticizer in powder was added, a special mixing procedure was used: dry mixing of aggregate (in mixer, 0.5 min), dry mixing of cement and microslica (by hand, 0.5 min), dry mixing of aggregate, cement and MS (mixer, 0.5 min), addition of water, mixing by mixer for 3 min, addition of superplasticizer, mixing by mixer for 2.5 to 3.5 min.

Fresh mortar was poured into standard iron moulds and compacted by a vibration table.

After 24 hours, the specimens were demoulded and for 27 days stored under water (20 °C). Until the test, specimens were stored under standard laboratory conditions (except for the time of transportation).

Test Methods

At 28 and 90 days the compressive and the bending strength (DIN 18555-3) as well as the modulus of elasticity (DIN 18555-4) were determined for all mortars. At an age greater than 90 days the capillary suction of all mortars was measured according to DIN 52617. Six 40 × 40 mm specimens instead three specimens of 50 cm^2 test area for each admixture were used. At an age of minimum 90 days the pore structure of the materials was characterized. Two methods were used: the He- porosity and the mercury porosimetry. The freeze-thaw-salt resistance was studied by the CDF test (capillary suction of de-icing solution and freeze-thaw test).

All the specimens were prepared at the Institute for Research in Materials and Applications IRMA, Ljubljana, Slovenia where the mechanical material parameters including the capillary suction were determined as well. The pore structure measurements by mercury porosimetry and by helium pycnometry as well as the tests of freeze-thaw resistance (CDF-test) were carried out in the Laboratory VII.11 "Physical and Chemical Characteristics of Building Materials" of the Federal Institute for Materials Research and Testing (BAM) in Berlin, Germany.

TEST RESULTS

In the investigation standard fresh and hard mortar parameters were determined, pore structure was investigated and freeze-thaw resistance was tested.

Standard Fresh and Hard Mortar Parameters

Standard fresh and hard mortar parameters were determined as described in the previous section. In the following tables standard fresh (Table 3) and hard (Table 4) mortar characteristics are listed.

Since in the preliminary tests similar consistence for all mortars was reach by changing the amount of superplatiziser, the differences in the consistence of the main investigation are higher than expected. The reason could be found in different mixer used in the main instigation. The measured values of the bulk density compare well to the theoretical predictions.

From the test results presented in the Table 4 it can be concluded, that all mortars produced can be classified as high strength mortars (compr. str. > 80 MPa).

Table 3 Standard fresh mortar characteristics

ADMIXTURE	CONSISTENCE	AIR CONTENT	BULK DENSITY
	[mm]	[%]	[kg/m^3]
M0W28F0	-	2.6	2308
M0W28F2	171	3.3	2312
M4W28F0	210	3.7	2281
M8W28F0	218	3.8	2275
M8W28F2	223	4.1	2263
M8W35F0	250	2.4	2333
M8W40F0	233	2.0	2330

Table 4 Standard hard mortar characteristics

ADMIXTURE	28 DAYS			90 DAYS		
	Compr. Strength	Bending Strength	E-Modulus	Compr. Strength	Bending Strength	E-Modulus
	[MPa]	[MPa]	[GPa]	[MPa]	[MPa]	[GPa]
M0W28F0	83.27	9.83	36.35	105.23	9.16	42.73
M0W28F2	93.77	8.96	36.42	110.93	8.70	39.55
M4W28F0	86.77	6.62	30.23	104.53	8.77	29.93
M8W28F0	83.73	7.15	27.21	103.70	9.66	27.24
M8W28F2	98.07	6.56	28.21	120.90	7.82	31.06
M8W35F0	104.67	7.29	40.37	115.20	8.53	42.09
M8W40F0	89.70	8.27	40.25	104.03	10.51	38.16

Pore Structure Investigation

Two different methods were used in the pore structure investigation: the helium pycnometry and the mercury porosimetry. As a measure of the pore structure and the freeze-thaw-salt resistance the capillary suction of the material was investigated, too. The results are presented in the Table 5.

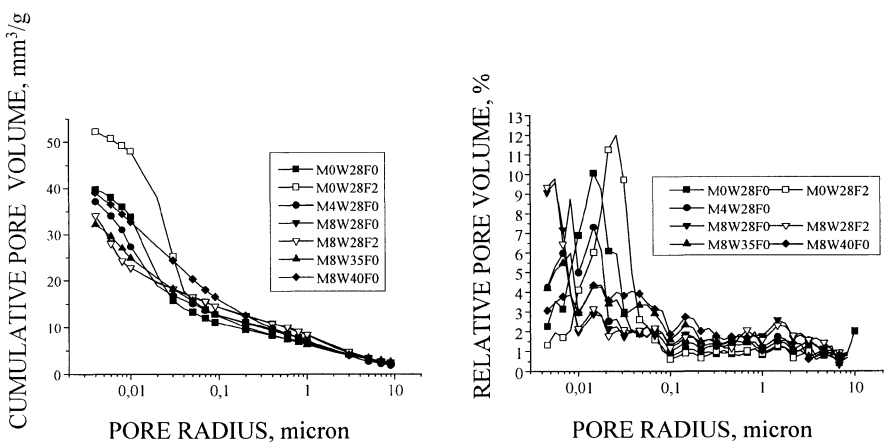

Figure 2 Pore distribution resulting from the mercury porosimetry (cumulative and relative)

Table 5 Results of the pore structure investigation

ADMIXTURE	MERCURY POROSIMETRY					HELIUM-PYCNOMETRY	DIN
	Total Pore Volume	Mean Pore Radius	Porosity	Specific Weight	Corrected Specific Weight	Specific Weight	Capillary Suction
	[mm³/g]	[nm]	[%]	[g/cm³]	[g/cm³]	[g/cm³]	$[\frac{g}{m^2 \cdot \sqrt{h}}]$
M0W28F0	39.2	17	8.9	2.27	2.50	2.57	0.21
M0W28F2	45.6	23	10.3	2.26	2.52	2.56	0.20
M4W28F0	37.8	10	8.5	2.24	2.45	2.54	0.30
M8W28F0	35.9	7	7.9	2.21	2.40	2.50	0.30
M8W28F2	35.7	6	7.9	2.21	2.40	2.50	0.34
M8W35F0	32.6	9	7.4	2.26	2.44	2.52	0.23
M8W40F0	40.1	9	9.0	2.25	2.47	2.52	0.56

As pore size distribution has a greater influence on the freeze-thaw-salt resistance than the total amount of pores, the pore size distribution has been determined by the mercury porosimetry, too. The pore size distribution diagrams resulting from the investigation are presented in Figure 2. Basic information about the pore distribution can be reached from the mean pore radii listed in Table 5.

Freeze-Thaw-Salt Resistance Tests

The freeze-thaw resistance of the mortars was tested according to the CDF procedure. Within the test, the 7 day capillary suction and the loss of mass were measured. The results are presented in the Table 6.

Table 6 CDF test results

ADMIXTURE	CAPILLARY	LOSS OF MASS AFTER				
	Suction	14 Cycles	28 Cycles	34 Cycles	50 Cycles	56 Cycles
	[g/m²]	[g/m²]	[g/m²]	[g/m²]	[g/m²]	[g/m²]
M0W28F0	551	20.7	83.5	100.89	-	-
M0W28F2	522	30.5	91.6	130.3	-	-
M4W28F0	508	11.56	36.0	-	-	131.6
M8W28F0	782	21.9	55.9	-	-	125.5
M8W28F2	515	24.7	58.9	-	157.7	-
M8W35F0	485	23.8	56.4	-	188.9	-
M8W40F0	783	148.3	371.3	-	951.0	-

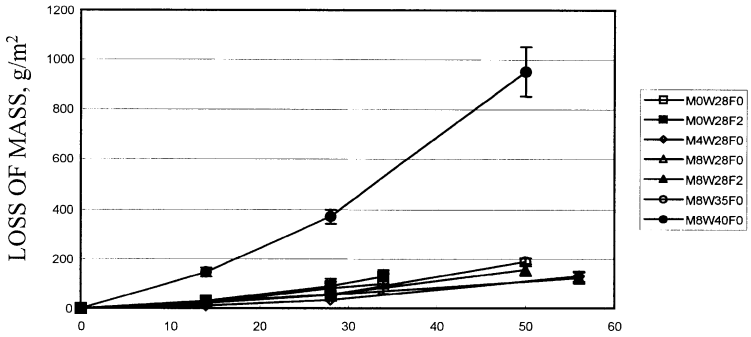

NUMBER OF CYCLES

Figure 3 CDF test results

As the loss of mass is smaller then 1500 g/m^2 (at 28 cycles), all the tested mortars can be considered as freeze–thaw-salt resistant.

DISCUSSION AND CONCLUSIONS

From the test results presented in the previous section following conclusions can be made:

- All produced and tested mortars have a compressive strength higher than 80 MPa and can be therefore considered as high strength materials.

- The capillary suction of the tested mortars is three to four times smaller than that of a normal mortar. Slightly higher suction can be observed for the mortar with higher water/binder factor (w/(c + MS) = 0.4). In mortars (concretes) with w/c factors higher than 0.3, the hydration processes are fully completed and the capillary pore system is formed.

- All tested materials can be considered as freeze–thaw-salt resistant. Slightly higher loss of mass (but still freeze-thaw resistant) can be observed for the mortar with higher water/binder factor (w/(c + MS) = 0.4). The observed lower resistance is a result of higher capillary suction of the material.

- By this pore structure investigation the well known influences of the w/c factor, microsilica and PP fibres has been (with some exemptions) confirmed:
  - an increase in w/c factor results in an increase in the pore volume and in an increase of pore radii, which lead to a better freeze–thaw-salt resistance,
  - the use of polypropylene fibres results in the increase of pore volume and in an increase of pore radii, which lead to a better freeze–thaw-salt resistance,
  - the use of microsilica results in the decease of pore volume and in the decrease of pore radii, which lead to a better freeze–thaw-salt resistance,
  - the use of microsilica reduces the effects of higher w/c factor and the use of PP fibres on the pore structure.

ACKNOWLEDGEMENT

The author would like to acknowledge the support provided for the project by the Ministry of Education, Science and Sport of the Republic of Slovenia, the Federal Ministery of Education and Research of the Federal Republic of Germany and the Federal Institute for Materials Research and Testing (BAM) in Berlin, Germany.

REFERENCES

1. SCHRAGE, I., Schriftenreihe des Deutschen Ausschuß für Stahlbeton, Heft 438, Beuth Verlag GmbH, Berlin (1994).

2. FIP-CEB Working Group on High Strength Concrete, FIP SR 90/1/, CEB Bulletin d'Information, No 197, Chameleon Press, London (1990).

3. MALHOTRA, V.M., RAMACHANDRAN, V.S., FELDMAN, R.F., AITCIN, P.-C., Condensed Silica Fume in Concrete, CRC Press, Boca Raton (1987).

4. M. REGOURD, Mat. Res. Soc. Symp. Proceedings, Pennsylvania, 42, 3 (1985).

5. ABENTUR, Proceedings of Darmstädter Massivbau-Seminar, Darmstadt, Vol 6, Paper IV (1991).

6. MÜLLER, H.S., RÜBNER, K., Proceedings of the International RILEM Workshop on Durability of High Performance Concrete, Wien, RILEM Secrétariat Général, Cachan Cedex, 23 (1995).

7. HILSDORF, H.K., Proceedings of Darmstädter Massivbau-Seminar, Darmstadt, Vol 6, Paper VII (1991).

8. GJØRV, O.E., "Vom Werkstoff zur Konstruktion", Festschrift H. K. Hilsdorf, Ernst und Sohn, Berlin 423, (1990).

9. HÄRDTL, R., Schriftenreihe des Deutschen Ausschuß für Stahlbeton, Heft 448, Beuth Verlag GmbH, Berlin 199.

10. KUKKO, H., Proceedings of the International RILEM Workshop on Durability of High Performance Concrete, Wien, RILEM Secrétariat Général, Cachan Cedex, 100 (1995)

11. SETZER, M.J., FAGERLUND, G., JANSSEN, D.J., RILEM Recommendation, Beton + Fertigteil Technik 4, 101 (1997).

12. ASTM-Designation C 227-71, Annual Book of ASTM-Standards, Part 14, 142 (1974).

13. KOCH, A., STEINEGGER, H., Zement-Kalk-Gips 7, 317 (1960).

14. DIN 18555-2, Publication date: 1982-09 Testing of mortars containing mineral binders; freshly mixed mortars containing aggregates of dense structure (heavy aggregates); determination of consistence, bulk density and air content.

15. DIN 18555-3, Publication date: 1982-09 Testing of mortars containing mineral binders; hardened mortars; determination of flexural strength, compressive strength and bulk density.

16. DIN 18555-4, Publication date:1986-03 Testing of mortars containing mineral binders; hardened mortars; determination of linear and transverse strain and of deformation characteristics of masonry mortars by the static pressure test.

17. DIN 52617, Publication date:1987-05 Determination of the water absorption coefficient of construction materials.

MONITORING OF MULTISPAN CONSTRUCTION DURABILITY

I A Koudriavtsev
Belarussian University of Transport
Belarus

ABSTRACT. The conduct of span structure elements under long exploitation term was investigated. The influence of pH factor and accelerations on strength change was revealed. An equation for physical wear of waterproofing and construction in general was suggested. Quantitative estimation of clorine ions influence on durability taking into account defects revealed was made and method of strengthening for span structure beams was given.

Keywords: Waterproofing, Durability, Vibration, pH-factor, Corrosion, Destruction.

I A Koudriavtsev, is Doctor of science, Professor, Head of the chair "Building constructions, bases and foundations" and is engaged in the field of transport communication lifetime forecasting, including underground.

INTRODUCTION

Problems of durability of multi-span structures have come under scrutiny recently. Yet, it is impossible to predict their durability accurately because of a large scatter of the data. In addition to the workmanship and types of materials the weather factors play an essential role accounting for over 90% of causes of premature loss of durability by multi-span structures. Still, there are practically no methods allowing to assess quantitative factors, such as temperature and humidity conditions which govern the durability, traffic intensity, maintenance schedule, etc.

PROBLEM CONDITION

Year-long observations in the European part of the NIS over the condition of prestressed reinforced concrete girders up to 33 m long used in some multi-span automobile overbridges have revealed the effect of certain factors on the term of their life. An example can be a 4-span overbridge, each span has the dimensions 2×33 m and 2×18 m. Automotive and electric vehicles (trolleybuses) move over its upper level crossing the railway. The mean load over the traffic area of the overbridge by automotive vehicles is 52 kN, and 200 kN by electric vehicles, the level of acceleration transmitted by automotive vehicles is 0.20 m/s^2; 0.23 m/s^2 by electric vehicles and 0.50 m/s^2 by railway trains, Figure 1 shows the cross section of one span 33 m long.

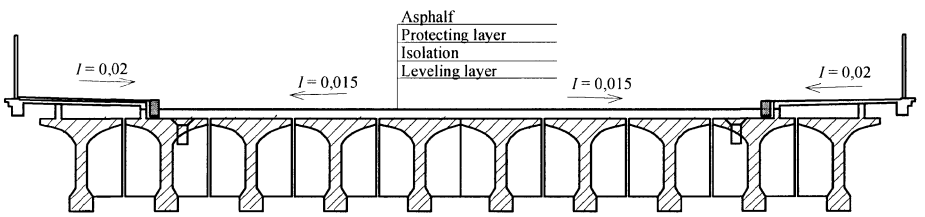

Figure 1 Cross section of span structure

Prestressed reinforced girders are made from cast concrete class B25. The term of operation is 30 years. The leveling blanket is 50 mm thick; it underlies a waterproofing material coated with a protective layer 40 mm thick, the latter is then covered with asphalt.

The analysis of the condition allows to conclude that the protective layer ceases to fulfill its functions already after 5–8 years both in respect to the coefficient of water permeability and the strength of reinforced concrete. The pH value of the protective layer reduces in addition to the loss of strength and the rise of the water saturation factor. The single-layer waterproofer begins to disintegrate already after 10 years, in case it is a double-layered waterproofer its disintegration begins after 13–15 лет [1].

The wear of the single-layer waterproofer (Y, in %) is sufficiently well correlated by the equation of the type:

$$Y = 6{,}12X_1 + 0{,}94X_1X_2 + 0{,}16X_1X_3$$

that of the double-layered waterproofer:

$$Y = 4{,}57X_1 + 0{,}83X_1X_2 + 0{,}14X_1X_3$$

Where X_1 – the term of operation, years;
X_2 – the level of acceleration transmitted to the span, m/s^2;
X_3 – the loading acting on the axis, kN.

The physical wear of span structures under normal conditions of operation is correlated sufficiently well by the expression:

$$Y = 1{,}54X_1 + 0{,}27X_1X_2 + 0{,}23X_3 + 10{,}8X_1X_4$$

Where X_1 – the term of operation, years
X_2 – the level of acceleration transmitted to the span, m/s^2
X_3 – wear of the waterproofer, %
X_4 – the indicator of the presence of chlorides.

Examination of a variety of structures after different terms of operation in the atmospheric conditions (outdoors and indoors) has revealed a clear relationship between R (strength) and pH of water extracts from the cement rock.

Reinforced concrete structures with pH between 11.5–12.8 are the strongest. When pH is below 11.5 the strength of the reinforced concrete in any structure shows reduction. The pH value 11.5 is the limit of the steady state of reinforced concretes. The relationship R–pH does not allow to judge how the factor of operation time affects pH and how much this value depends on the carbonate component (CC). The main cause of pH drop in the atmosphere is that reinforced concrete reacts with CO_2 and moisture. In fact, this relationship does occur (Figure 2).

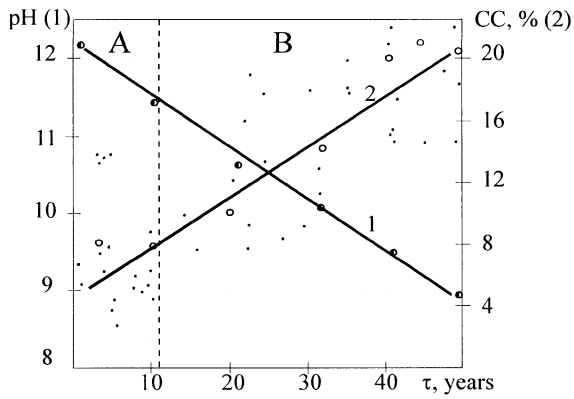

Figure 2 Effect of time of operation (τ) of reinforced concrete structures on CC and pH:
• – experimental data, ○ – mean values of CC, ◐ – mean values of pH

After some years the CC increases, meanwhile pH reduces to very low values (pH < 10,5) at which reinforced concrete manifests accelerated degradation. The latter is accompanied by the loss of adhesion between the cement rock and the filler, protective characteristics in respect to the reinforcement vanish completely. The experimental data show that in all the cases the scatter of the indicators is large. The dispersion of readings of CC reaches 25 % of the mean values that of pH reaches 15 %. High dispersion is due to the use of different brands of concrete in reinforced concrete structures, therefore many factors govern their behavior [2]. If the obtained data are approached from the probability statistical viewpoint, a steady relationship can be assumed to exist between the time of life of the existing layer, *R*, pH and CC. Only mean values are shown for pH in Figure 2 omitting the experimental data for clarity.

In any case the surface *R* of reinforced concrete should not be identified as *R* through the body of a structure. Hence it is worthwhile to trace how pH changes through the depth in order to judge about *R*. The results in Figure 3 are obtained for the lower fillets of the overbridge after 40 years of life, the structure has been in service for 7 years.

The outer side of the first girder (facing south) was exposed to seasonal rains, sunlight, temperature drops, it is free of the soot film, the cement rock is carbonized to the maximum depth (Figure 3, curve 2). The Δ pH equal to approximately 3 has the maximum deviation from the steady state limit of the reinforced concrete (pH ≈ 11.5). The reinforced concrete loses its protective properties in respect to the reinforcement below this value and its degradation begins (Figure 3, curve1). *R* = 14 MPa on the surface at pH = 8.5; pH = 11.5 at a depth 50 mm where *R* = 35 – 50 MPa.

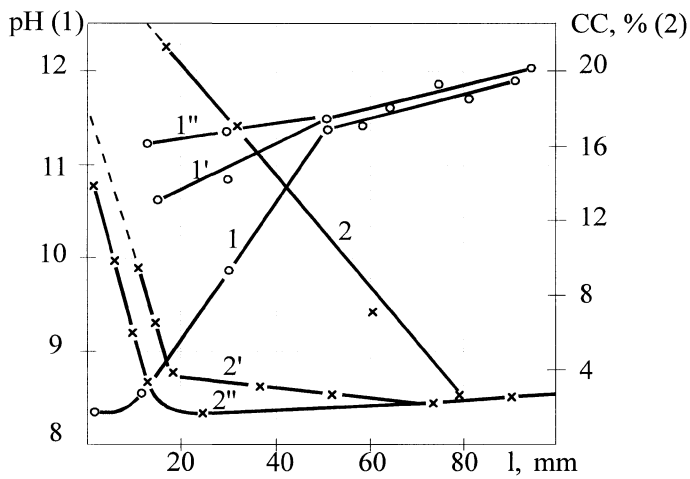

Figure 3 Dependence of pH (1), CC (2) on depth of structure in cast concrete and conditions of operation: 1, 2 – outer girder; 1', 2' – soot coating; 1'', 2'' – after 7 years of life

Inner girders coated with soot from the exhaust of railway diesel engines have the carbonized layer which is 4 times thinner and Δ pH = 0.9, i.e. the process of carbonization shows significant sluggishness, the surface *R* approaches to the *R* in the reinforced concrete body (Figure 3, curves 1', 2'). This data proves that the soot produces a protective effect because it contains carbon black, unburnt heavy fractions of fuel and oils. This blend possesses good hydrophobic and insulating characteristics.

Inspection of 160 structures has allowed us to determine approximate quantitative criteria for assessment of their condition (Table 1). The data relate to the analyses of cement and sand samples from which crushed stone was separate during blend preparation.

Brines serving to melt ice on the bridge ways in the wintertime filter through in case of unsatisfactory maintenance of movement joints. As a result the protective layer in the upper and lower fillets of the girder destroys, the reinforcement rod bundles corrode in the lower fillet of the girder. The girder walls show destruction of the protective layer also (Figure 4).

Table 1 Criteria of chemophysical indicator of reinforced concrete structure condition

NOS.	pH	CC, %	R, MPa	CONDITION OF REINFORCED CONCRETE AND REINFORCEMENT
1	11,5-12,8	2-8	30-50	Cast concrete strong, reinforcement in a passive state.
2	10,5-11,5	8-14	25-30	Strength characteristics of the cement rock begin to change. The reinforcement begins to corrode in the humid environment. Corrosion is strongly inhibited in dry conditions due to the ohmic resistance of cast concrete.
3	9,5-10,5	14-20	15-22	Degradation of cast concrete and corrosion of the reinforcement evolve with acceleration, causes should be eliminated, the structure should repaired (or replaced).
4	<9,5	>20	<12	The protective layer peels off of the reinforcement, adhesion of the cement rock to the filler becomes loose (full degradation). An emergency situation.
5	<9,5	2-8	<12	Faulty cement slurry composition (lack of cement, excess of fillers).

Note. When carbonate rock is used the tolerable CC concentration is up to 16 %.

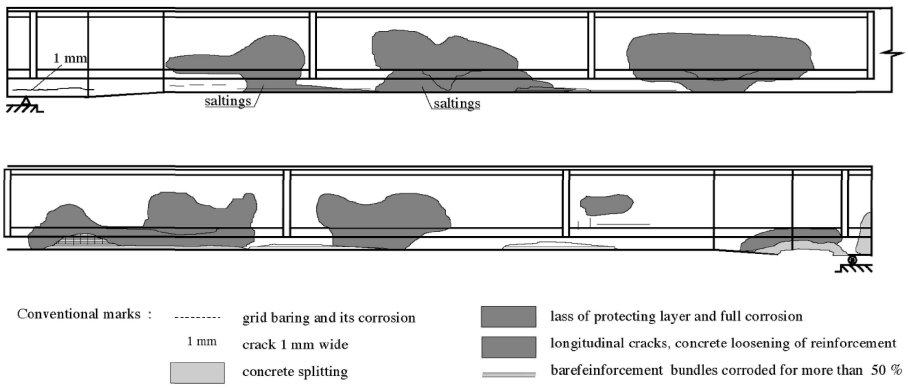

Figure 4 Diagram of girder with indication of detected defects

To eliminate the detected defects the destroyed concrete, corroded reinforcement should be cleaned, the lower fillet of the girder should be encased, and stresses in the reinforcement should be boosted.

The obtained results have served to elaborate methods of reinforcing the structure after a long time in use, these methods allow to extend durability 1.5 times, actions are also proposed to improve maintenance of similar structures.

CONCLUSIONS

On the basis of long term monitoring of wide span structures there were determined quantitative indices of factors which influence their durability. It has made an attempt to estimate concrete strength properties by means of pH factor, on its basis there were suggested criteria of physical chemical condition of ferroconcrete structures and strengthening methods for structures subjected to corrosion.

REFERENCES

1. KUDRYAVTSEV I.A., Hydroinsulating Systems (in Russian), 2000, 443 pp.
2. KUDRYAVTSEV I.A., BOGDANOV V.P., Study of Carbonization of Reinforced Concrete Structure After Protracted Life, Materials, Technologies, Tools (in Russian), Vol. 5, No. 3 2000, pp. 13-16

INNOVATIVE COMPOSITE STRUCTURAL ELEMENTS FOR BUILDINGS IN THE MIDDLE EASTERN ENVIRONMENT

W H Mirza

A A Alhamrani

Alhamrani Industrial Group

Saudi Arabia

ABSTRACT. Structures built in the Middle East during the previous two to three decades, using conventional reinforced concrete, showed premature damage owing to the exposure to aggressive ambient environment. A considerable effort has therefore been put in the region to come up with materials, design practices and construction processes for building more durable structures. This paper describes the results of an extensive research and development activity carried out by local industry to manufacture composite structural elements more suited to the Middle Eastern environment. These elements consist of burned clay-prestressed concrete panels and loadbearing brick walls. The ceiling and wall panels form a structural system, which is pre-manufactured under factory controlled conditions, ready for delivery and installation at site. This innovative structural system is not only time-saving and cost effective but also has a number of advantages over conventional reinforced concrete construction, notably, improved serviceability, reduced dependence on in situ concreting, higher thermal insulation, greater fire protection and increased sound attenuation. This system can be easily incorporated in development projects like schools, shopping arcades, residential compounds, private villas and apartment buildings.

Keywords: Prestressed concrete, Burned clay brick, Composite structural element, Ceiling Panel, Loadbearing wall, Aggressive environment, Durable construction, Serviceability.

Sheikh A A Alhamrani, is a member of the Executive Board of Al Hamrani Industrial Group. He administers a number of industrial units and is constantly involved in the development and setting up of processes to improve both quality and characteristics of a range of building products.

Dr W H Mirza, a former Professor of Civil Engineering, currently heads a technical department in Alhamrani Industrial Group. He supervises the development and production of composite structural elements. His research interests include formulations for high performance construction materials and durability aspects of cementitious products.

INTRODUCTION

Concrete structures built during the final quarter of the last century in the Arabian peninsula showed signs of premature damage. The service life of such structures was severely curtailed when exposed to the Middle Eastern environment. Concerns were expressed by a number of authors about the ability of conventional reinforced concrete to provide a long, maintenance free service under severe ground/water salinity and the widely fluctuating hot weather condition [1,2]. Concrete structures, which would normally remain serviceable for fifty years or more, deteriorated at an accelerated rate and required maintenance soon after occupancy [3].

A concerted and coordinated effort has been in place to improve the durability of structures in the Middle East. Regular conferences and symposia are held in the region, not only to highlight the factors contributing towards rapid deterioration of concrete structures but also to suggest ways and means to improve their behaviour under sustained aggressive environment [4,5]. Since this issue is directly related to the construction industry, a number of dynamic industrial groups in the region have been collaborating with the educational institutions, research establishments and other experts, both at the local and international level, to find solutions to the problem.

OBJECTIVES OF PRESENT WORK

This paper describes a study, carried out jointly by Alhamrani Industrial Group and Bautechnische Institut, Austria, which led to the development and industrial production of composite structural elements. This collaborative effort focused its attention towards realizing the following objectives:

1. Utilization of locally- available materials and other natural resources.
2. Reduce the amount of concrete in the construction by incorporating other materials which show greater durability under local conditions.
3. Minimize direct exposure of concrete to the climatic variations and other aggressive agents.
4. Develop durable composite structural elements, geared towards prefabricated production on an industrial scale.

DEVELOPMENT OF THE STRUCTURAL SYSTEM

The criteria for selecting materials for producing structural elements were based on the performance of different building components. A recourse was made to study the possibility of using burned clay bricks. In the recent past, majority of structures in the Middle East have been built by relying on the conventional reinforced concrete frame concept. The hollow red clay bricks were used in partition walls or as hordy blocks in slabs. In both cases, the brick contribution was to act as a non-loadbearing filler material. However, it is common knowledge, that a kiln-fired clay brick exhibits greater resistance to aggressive agents, both from the climatic conditions and the chemical attack from its surroundings when compared with common cementitious building products. It was therefore considered prudent that this important characteristic of a burned clay brick be gainfully employed in modifying the structural system in two ways.

Firstly, the beam-column arrangement can be replaced completely by a loadbearing wall system. Secondly, reinforced concrete ribs can be encased in specially designed ceiling bricks to form a composite slab unit with high load-carrying capacity.

Having agreed on the proposed structural system, the joint research and development study then undertook a number of technical activities like design and theoretical analyses, selection and testing of individual materials and components, forming composite sections, evaluating the final products and finally, the development of a plant technology to mass produce the structural elements. Some aspects of this extensive work are explained in the following 3 sections.

COMPOSITE STRUCTURAL SYSTEM

In its basic form the composite structural system consists of two main components; prefabricated ceiling panels and loadbearing masonry walls on which the ceiling panels are supported.

Ceiling Panels

The ceiling panels are large formatted slabs, produced by adopting an industrial technology in which clay bricks and prestressed concrete are utilized.

Specially designed red clay bricks with pre-determined perforated profile, occupy nearly 80% of the panel cross-section. These bricks are produced by first extruding, under pressure, a moist but stiff mixture of red clay and other ingredients through a shape-forming die. After cutting to size, the moulded bricks are kiln-fried at high temperature. Standard bricks of a width 240 mm yield a compressive strength in excess of 30kN/mm^2.

Very high strength steel tendons are used in pre-stressing the concrete. For a given height of the panel, its design load capacity is dependent on the number of pre-stressing tendons provided at the top and bottom of each concrete rib in the panel cross-section. The steel tendons are a very low relaxation type, 7 mm in diameter, having an ultimate tensile strength of 1670N/mm^2 and a modulus of elasticity of 200,000N/mm^2.

To complement the high quality of both the clay bricks and the prestressing tendons, a high performance, high early strength concrete mixture has been developed for casting the panel ribs. This self-compacting dense concrete is batched by incorporating special mineral and chemical admixtures into the mix. In order to maintain a strict production schedule, the hardened concrete achieves a 16-hour compressive strength of 35 N/mm^2 and its 28 day compressive strength exceeds 75 N/mm^2.

Each ceiling panel is manufactured with a standard width of 1200 mm, achieved by placing on the casting table, 4 full brick units (each 240 mm wide), flanked by two half bricks, one at each end, forming a panel cross-section of 5 concrete ribs, as shown in Figure 1. For special requirements, panel widths of 480, 720 and 960 mm can also be produced. Based on the brick height, panels have thicknesses of 160, 200, 250 and 290 mm (designated as Z1, Z2, Z3 and Z4 respectively). Whenever necessitated by design/finishing considerations, 40 mm concrete screed can be provided on the top surface of the panel at site.

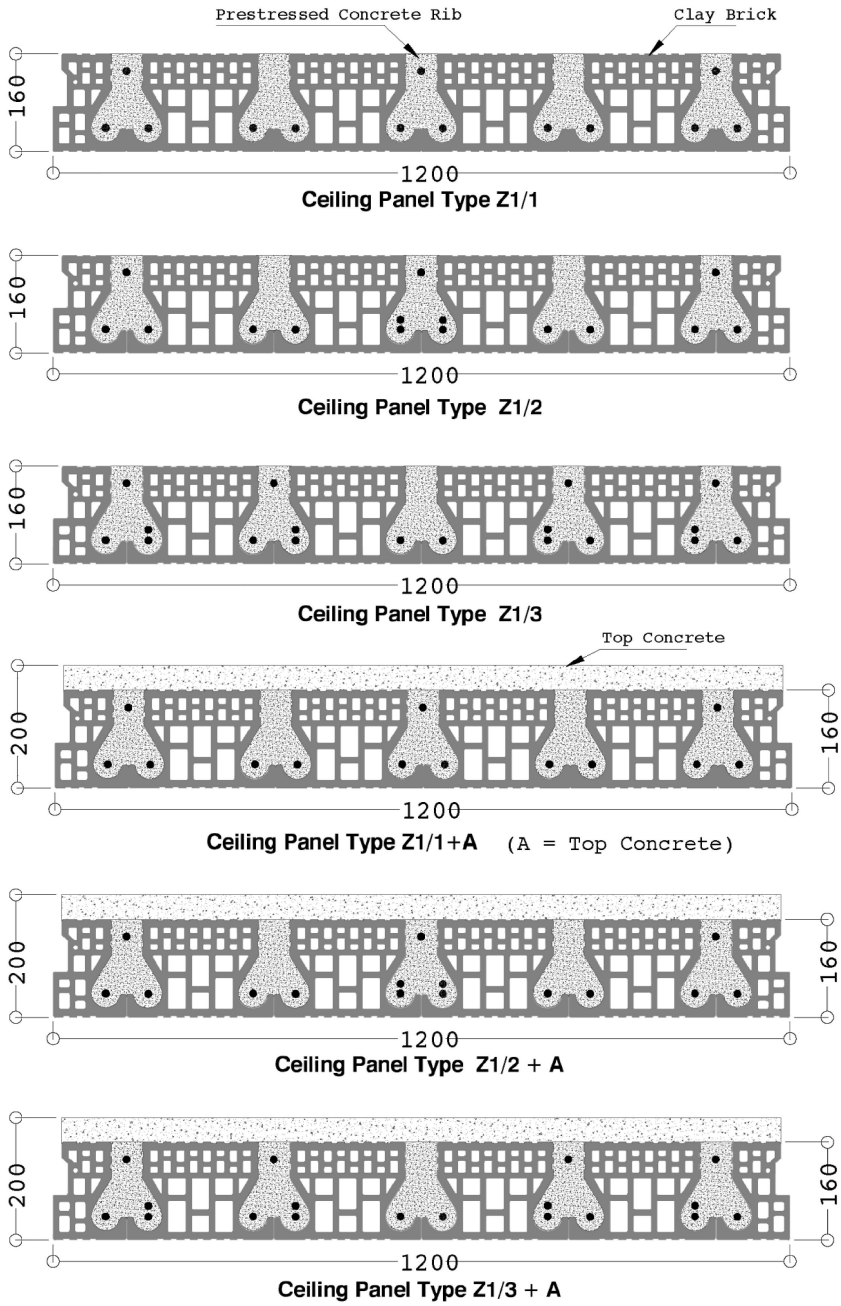

Figure 1 Typical Cross-Section of the Clay Brick Pre stressed Concrete Ceiling Panel Z1
(All Dimensions are in Millimeters)

The ceiling panels are cast under factory controlled conditions on a row of casting beds, each about 100 m long. Prestressing of steel tendons and subsequent concreting operations like transporation, pouring and compaction are all fully automated. Concrete is mixed in a batching plant from where it is transported by a motorised trolley and poured into the panel ribs.

While the concrete is filling the ribs, prepositioned vibrating flaps on the trolley impart the compactive effort to ensure an adequate bond, both with the prestressing tendons and the brick sides. Once the concrete has achieved its compressive strength of 35N/mm² in 16 hours, the panels can be cut to the required lengths by an electrically-operated diamond saw.

Ceiling Panel Characteristics

The panel height, coupled with the number of prestressing steel tendons per cross section determine the design load capacity of each panel. Tables 1 to 4 list the design loads along with other physical properties of Z1, Z2, Z3 and Z4 panels.

A high brick content (80% of a more) in the ceiling panels results in a thermal conductivity value of 0.60 W/mk., far lower than that of conventional reinforced concrete. Also an attenuation of 53dB to 59dB is achieved for airborne sound. A 40 mm concrete topping further decreases the sound transmission by 3dB to 5dB.

The burned clay – prestressed concrete composition in ceiling panels provides a high degree of fire resistance, chiefly because the clay bricks pass through temperatures in excess of 900 degrees centigrade during their production. This helps them to impart an excellent shielding property to the concrete ribs and hence the ceiling panels easily can exceed three hour fire rating.

Load-Deflection Test

To a structural engineer, the deflection of a slab under an applied load is of major interest. A typical ceiling panel (Z1/1) was, therefore, tested to ascertain its load-deflection behaviour. The panel was simply-supported with a clear span of 5000 mm and the load was applied at an increment of 1kN/m². This was achieved by placing appropriate number of lintels, of known weight, uniformly distributed over entire panel span. At each applied load, the midspan deflection was noted.

When the panel was loaded up to a maximum of 9.0kN/m² (1.7 times its design load capacity of 5.3kN/m²), it gave an average midspan deflection of 8.29mm. The net deflection is therefore 2.29 mm after taking into consideration the initial camber of 6.0 mm. This maximum load was sustained on the panel for 24 hours, and the net deflection showed a marginal increase of only 0.39mm.

The applied load was removed by successive decrements of 1 kN/m² and the midspan deflection recovery was recorded. When the entire applied load was removed, the panel showed a small residual gross deflection of 1.49mm indicating thereby excellent elastic behaviour of the composite ceiling panel. The deflection behaviour of the ceiling panel was closely monitored at each application/removal of load, specially to observe the development of any signs of crack, either in the brick or in the concrete.

Table 1 Design Load Values for Ceiling Panel Type Z1 (Panel Width = 1200 mm)

PANEL TYPE	Z1/1	Z1/2	Z1/3	Z1/1+A	Z1/2+A	Z1/3+A
Depth of the Ceiling Construction, mm	160	160	160	200	200	200
Self-weight, KN/m²	2.6	2.6	2.6	3.6	3.6	3.6
No. of Top Tendons	3	3	4	3	3	4
No. of Bottom Tendons	10	12	14	10	12	14
Maximum Clear Span, m	Design Load, kN/m² (without self-weight)					
6.50			3.6			4.2
6.25		3.3	4.1			5
6.00	2.9	3.8	4.6		4.5	5.9
5.75	3.4	4.3	5.3	3.9	5.5	6.9
5.50	4.0	5.0	6.0	4.8	6.5	8.1
5.25	4.6	5.7	6.8	5.8	7.7	9.4
5.00	5.3	6.6	7.8	7.0	9.1	11.0
4.75	6.2	7.6	8.9	8.4	10.6	12.5
4.50	7.2	8.7	10.2	9.9	12.2	14.3
4.25	8.4	10.1	11.8	11.6	14.1	15.3
4.00	9.8	11.7	13.6	13.5	16.4	16.6

Table 2 Design Load Values for Ceiling Panel Type Z2 (Panel Width = 1200mm)

PANEL TYPE	Z2/1	Z2/2	Z2/3	Z2/1+A	Z2/2+A	Z2/3+A
Depth of the Ceiling Construction, mm	200	200	200	240	240	240
Self-weight, KN/m²	3.1	3.1	3.1	4.2	4.2	4.2
No. of Top Tendons	3	4	5	3	4	5
No. of Bottom Tendons	12	16	19	12	16	19
Maximum Clear Span, m	Design Load, kN/m² (without self-weight)					
8.00		3.2	4.1		3.6	5.0
7.75		4.6	4.1		3.9	5.4
7.50		4.0	5.1		4.6	6.2
7.25	3.0	4.6	5.7	3.0	5.3	7.0
7.00	3.4	5.1	6.4	3.6	6.1	8.0
6.75	4.3	5.7	7.1	4.3	7.0	9.0
6.50	4.9	6.4	7.9	5.2	8.1	10.2
6.25	5.1	7.2	8.8	6.1	9.2	11.5
6.00	5.8	8.1	9.8	7.1	10.5	12.3
5.75	6.6	9.1	10.9	8.3	11.9	13.1
5.50	7.5	10.2	12.0	9.4	13.4	13.9
5.00	9.5	12.9	13.6	12.5	15.7	15.7
4.75	11.0	14.5	14.5	14.2	16.8	16.8
4.50	12.7	15.5	15.5	16.3	18.0	18.0
4.25	14.6	16.6	16.6	18.8	19.4	19.4
4.00	16.9	17.9	17.9	20.9	20.9	20.9

Table 3 Design Load Values for Ceiling Panel Type Z3 (Panel Width = 1200 mm)

PANEL TYPE	Z3/1	Z3/2	Z3/3	Z3/1+A	Z3/2+A	Z3/3+A
Depth of the Ceiling Construction, mm	250	250	250	290	290	290
Self-weight, KN/m²	3.8	3.8	3.8	4.8	4.8	4.8
No. of Bottom Tendons	16	18	20	16	18	20
Maximum Clear Span, m	Design Load, kN/m² (without self-weight)					
8.75	3.3	4.1	4.9		4.3	5.4
8.50	3.8	4.6	5.4	3.9	5.0	6.1
8.00	4.7	5.6	6.5	5.2	6.5	7.7
7.75	5.3	6.3	7.2	6.0	7.3	8.6
7.50	5.9	6.9	8.0	6.8	8.2	9.7
7.25	6.6	7.7	8.8	7.8	9.3	10.8
7.00	7.3	8.5	9.7	8.8	10.4	12.1
6.75	8.2	9.5	10.7	10.0	11.7	13.3
6.50	9.1	10.5	11.9	11.13	13.1	14.0
6.25	10.2	11.7	12.9	12.7	14.7	14.8
6.00	11.4	13.0	13.6	14.3	15.7	15.7
5.75	12.7	14.5	14.4	1.0	16.6	16.6
5.50	14.2	15.2	15.2	17.6	17.6	17.6
5.25	16.2	16.2	16.2	18.7	18.7	18.7
5.00	17.2	17.2	17.2	19.9	19.9	19.9
4.75	18.4	18.4	18.4	21.3	21.3	21.3
4.50	20.0	20.0	20.0	22.8	22.8	22.8

Table 4 Design Load Values for Ceiling Panel Type Z4 (Panel Width = 1200 mm)

PANEL TYPE	Z4/1	Z4/2	Z4/3	Z4/1+A	Z4/2+A	Z4/3+A
Depth of the Ceiling Construction, mm	290	290	290	330	330	330
Self-weight, KN/m²	4.3	4.3	4.3	5.3	5.3	5.3
No. of Top Tendons	5	5	5	5	5	5
No. of Bottom Tendons	17	20	22	17	20	22
Maximum Clear Span, m	Design Load, kN/m² (without self-weight)					
9.75	3.1	4.2	4.8		4.3	5.1
9.50	3.5	4.6	5.3		4.9	5.8
9.25	3.9	5.1	5.8	3.9	5.5	6.5
9.00	4.3	5.6	6.4	4.5	6.2	7.2
8.75	4.8	6.2	7.0	5.2	7.0	8.1
8.50	5.4	6.8	7.7	5.9	7.8	9.0
8.25	6.0	7.5	8.4	6.7	8.7	9.9
8.00	6.6	8.3	9.2	7.6	9.7	11.0
7.75	7.4	9.1	10.1	8.5	10.8	12.2
7.50	8.2	10.0	11.1	9.6	12.0	13.5
7.25	9.0	11.0	12.0	10.7	13.4	14.2
7.00	10.0	11.8	12.6	12.0	14.2	14.9
6.75	11.1	12.4	13.3	13.5	14.9	15.7
6.50	12.3	13.1	14.0	15.0	15.8	16.5
6.25	13.8	13.8	14.8	16.6	16.6	17.4
6.00	14.6	14.6	15.6	17.6	17.6	18.4
5.75	15.4	15.4	16.5	18.6	18.6	19.5
5.50	16.4	16.4	17.5	19.8	19.8	20.7
5.25	17.4	17.4	18.6	21.0	21.0	21.9
5.00	18.8	18.8	20.0	22.4	22.4	23.4

No cracks or separations at brick-concrete interface were observed during either the loading or the unloading stages of the test. Results of the load-deflection test are plotted in Figure 2.

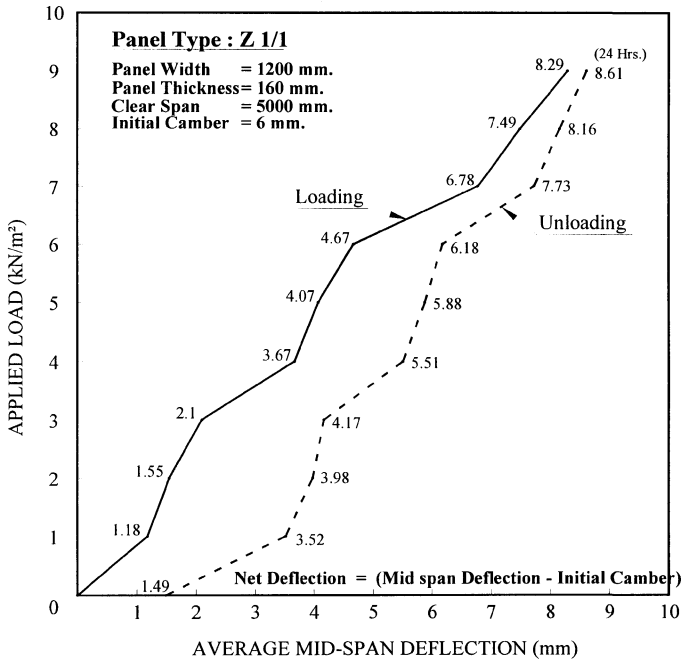

Figure 2 Load-Deflection Test Data of Composite Ceiling Panel

Loadbearing Masonry Walls

The second major component of the structural system is loadbearing masonry walls. These 200 mm thick walls are built, layer by layer, in a pre-programmed assembly setup wherein each, brick of size 500x250x200 mm is embedded in a strong, cementitious mortar. Standard walls are of 3 m high and the length can vary, up to a maximum of 7m. Six horizontal steel bars, each 5 mm in diameter, are provided at wall heights of 0.25m, 1.25m and 2.25m. These bars span the entire length of the wall. Vertical anchors, shaped like twisted bars with hooked ends, are inserted in the wall, their specific location and spacing having been pre-determined automatically by computer aided design. These anchors are grouted into the wall perforation and help later in lifting and placing of the wall panels. Wherever openings for doors, windows, air-conditioning, etc. occur in the walls, lintels are provided. In order to achieve compatibility between the masonry wall and the lintels and to avoid the risk of subsequent plaster separation at the interface, the lintels are factory-produced with special red clay bricks and prestressed concrete. Due to the high flexural strength of such lintels, openings up to 3m wide can be accommodated in the loadbearing walls.

INSTALLATION OF THE COMPOSITE STRUCTURAL SYSTEM

Pre-manufactured ceiling panels and walls can both be transported to the construction site on flat-bed trailers. A mobile, telescopic crane can lift these units for placement at the exact location in the structure. The walls are placed vertically on a 15 mm thick mortar bed on an existing ground beam/foundation. A typical wall foundation anchoring arrangement is shown in Figure 3. Once the walls are properly anchored to the ground, ceiling panels are placed on them with an edge support of 5 cm to 8 cm.

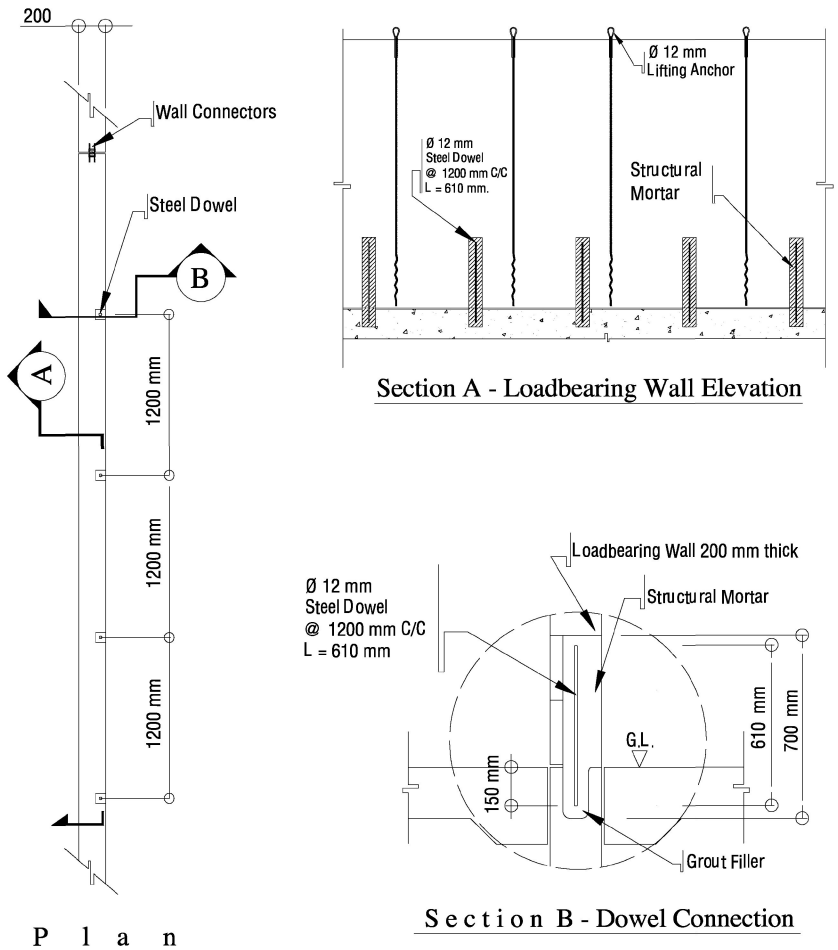

Figure 3 Wall–Foundation Anchors

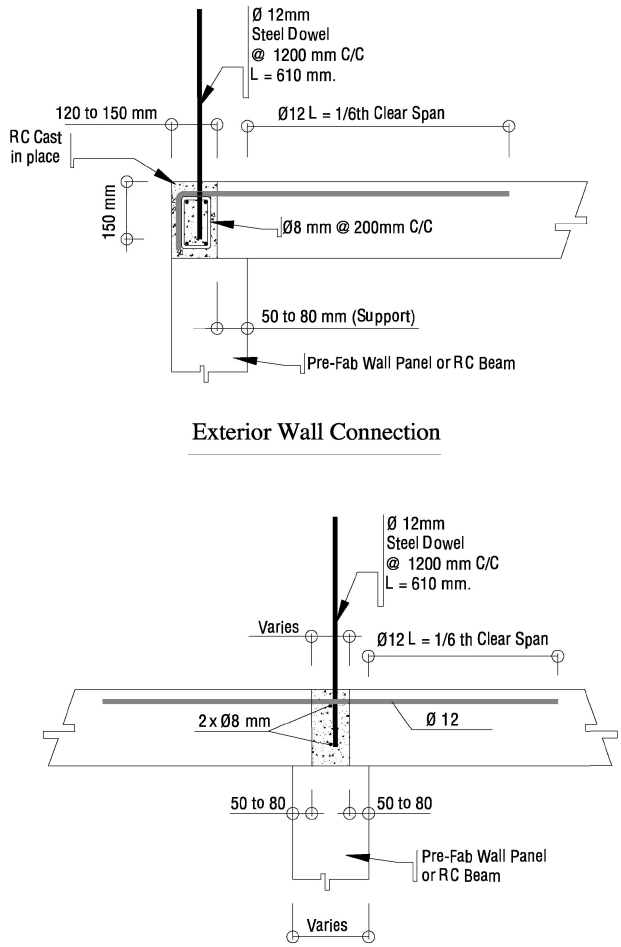

Figure 4 Wall–Ceiling Panel Connections

Since the wall is 200 mm thick, the remaining space is utilized in casting a ring beam all around the exposed ceiling panel sections. Wall-ceiling panel connections, both interior and exterior reinforced concrete, have been properly designed as shown in Figure 4. As soon as the ceiling panels are supported onto the loadbearing walls, these are ready to be walked upon and work on the next stage of the superstructure can begin immediately. The composite ceiling-wall system has been designed on the principle of a rigid box structure. All walls, which carry ceiling panels as floors or roof slabs, act as shear walls. The system is fully capable of resisting lateral forces due to wind or seismic loading as per the limiting specifications of the Uniform Building Code [6].

CONCLUDING REMARKS

The structural system, based on burned clay loadbearing walls and clay brick-prestressed concrete ceiling panels, is an innovative, cost effective and versatile construction method. In this system, need for reinforced concrete columns and beams is largely eliminated because the floor and roof loads are transmitted to the foundations via the strong loadbearing masonry walls. The composite nature of the ceiling panels ensures that high strength, high performance prestressed concrete ribs are fully encased in specially designed clay bricks, thereby minimising the direct exposure of concrete to external elements. Starting from the selection of the raw materials to the final production of each component of the structural system, all operations are carried out under a complete quality assurance production process. Being both simple and efficient, the composite structural system described in this paper is easily adaptable to a variety of infrastructure developmental activities like schools, housing projects and shopping arcades. Once in use, the system offers durable service life with low maintenance costs in addition to better thermal insulation, low sound transmission and an excellent fire rating, all features directly beneficial in the Middle Eastern environment.

REFERENCES

1. RESHEEDUZZAFAR, DAKHIL, F., AL-GAHTANI, A. S., The deterioration of concrete structures in the environment of environment of the Middle East, Journal, American Concrete Institute, No 1, January-February 1984, p 13-20.

2. MIRZA, W. H., AL-NOURY, S. I., Performance of construction materials in hot weather, Journal of Precast Concrete Technology, Munich, Germany, January, 1988, p 5-11.

3. AL-TAYYIB, A. J., MIRZA, W. H., Durability of building materials in Saudi Arabia, Proceedings, Third International Conference on the Durability of Building Materials and Components, CIB/RILEM/ASTM, Espoo, Finland, August 12-15, 1985, Vol II, p 284-297.

4. KFUPM, SYMPOSIUM PROCEEDINGS, Performance of concrete structures in Arabian Gulf Environment, Dhahran, Saudi Arabia, November 15-17, 1998.

5. CIVIL ENGINEERING SOCIETY, Bahrain, Sixth International Conference on Deterioration and Repair of Reinforced Concrete in the Arabian Gulf, Bahrain, November 20-22, 2000.

6. UNIFORM BUILDING CODE (UBC), International Conference of Building Officials, USA, 1997.

USE OF CRUMB RUBBER TO ACHIEVE FREEZE/THAW RESISTING CONCRETE

K A Paine

R K Dhir

R Moroney

K Kopasakis

University of Dundee

United Kingdom

ABSTRACT. The initial results of a laboratory study to investigate the use of crumb rubber, a product of shredding used tyres, as an alternative to air-entrainment for providing freeze/thaw resisting concrete are reported. Three sizes of crumb rubber, obtained from mechanical shredding of lorry tyres, were investigated: 0.5-1.5 mm, 2-8 mm and 5-25 mm. Concrete mixes were designed for both a compressive cube strength of 37 N/mm^2, complying with the minimum strength allowed by BS 8500 where air-entrainment is used, and 50 N/mm^2, the minimum strength without air-entrainment, and crumb rubber contents up to 6% by volume were investigated. Tests were carried out using the CEN slab test, which measures freeze/thaw damage by means of scaling from a concrete surface, and the ASTM prism test, where damage results from disintegration of the concrete mass. The results showed that there is potential for using crumb rubber as a freeze/thaw resisting agent in concrete. The crumb rubber concrete performed significantly better under freeze/thaw conditions than plain concrete, and the performance of crumb rubber concrete in terms of scaling was similar to that of air-entrained concrete.

Keywords: Freeze/thaw, Crumb rubber, Scaling, Air-entrainment, Used tyres, Waste materials, Relative dynamic modulus

Dr Kevin A Paine is a Research/Teaching Fellow in the Concrete Technology Unit, University of Dundee. His research interests are concerned with the use of waste and recycled materials as binder and aggregate components in concrete.

Professor Ravindra K Dhir is Director of the Concrete Technology Unit, University of Dundee. He specialises in binder technology, permeation, durability and protection of concrete. His interests also include the use of construction and industrial wastes in concrete to meet the challenges of sustainable construction.

Mr Robert Moroney is a Research Student at the University of Dundee. He is currently carrying out a PhD into the potential use of crumb rubber in cementitious materials.

Mr Kyriakos Kopasakis is a Research Student at the University of Dundee. His research has centred on the use of crumb rubber in pavement quality concrete.

INTRODUCTION

Concrete surfaces in the UK and other temperate zones are susceptible to freeze/thaw damage due to hydraulic pressures created within the microstructure during sub-zero temperatures, and horizontal pavement surfaces are particularly prone to damage because of the practice of using de-icing salts with the intention of delaying or preventing ice formation in winter. This creates a thermal shock magnifying the damaging mechanism should freezing occur.

Although, the UK environment is particularly severe for this type of exposure, there is a relatively low incidence of serious damage reported. This is largely as a result of the recognised practice of entraining-air in concrete where exposure to a freeze/thaw environment is suspected. Generally roads in the UK have been designed for a very severe exposure [1,2] requiring a minimum strength of 35 N/mm^2 and a mean air content (3.5-5.5%) appropriate to the aggregate size. Whilst traditional methods of specifying for freeze/thaw resistance have been largely successful, it does not follow that they are necessarily economical. Furthermore, there are a number of concerns with the use of air-entrainment as a method for providing freeze/thaw resistance. These include [3]: losses in air-content during transportation, erratic air-entrainment when using pulverised-fuel ash (pfa), reduced air-entrainment with low alkali/sulfate resisting cements, difficulties with air-entraining low workability concretes, and the formation of blowholes on the surface following vibration.

An alternative solution is to add solid, compressible, inert particles into the concrete mix that can be accurately batched and give the necessary compressibility under stresses imposed by the freezing water. One possible material is crumb rubber, a product of shredding used tyres.

This paper reports initial results of a laboratory study investigating the use of crumb rubber as an alternative to air-entrainment for providing freeze/thaw resisting concrete. The work described is part of a much broader research programme being undertaken by the Concrete Technology Unit at the University of Dundee to examine the feasibility of recycling rubber tyres for use in concrete.

CRUMB RUBBER

The disposal of used tyres is a major waste disposal problem in the UK, and it is estimated that 37 million car and truck tyres are being discarded annually [4] with this number set to increase, in line with growth in road traffic, by a further 39% by 2011 and 63% by 2021 [5]. At present, over 11 million tyres are disposed of in landfill (shredded tyres) or are stockpiled (whole tyres). However, these routes will be not be available with the implementation of European legislation banning the disposal of whole and shredded tyres by 2003 and 2006, respectively [6].

There is, therefore, an urgent need to identify alternative outlets for these tyres, with the emphasis on recycling in line with the UK Governments waste management hierarchy [4]. One possible outlet is to produce crumb rubber (CR) components for use in concrete. Indeed, CR is uniquely different to other waste materials, because its production method is now well developed and commercial shredding and processing machinery are available economically. Hence, the successful use of this material in concrete could provide one of the most environmentally responsible and economically viable ways of converting this waste into a valuable resource.

MATERIALS

The CR used in this study was obtained from mechanical shredding of lorry tyres, and was supplied in three sizes 0.5-1.5 mm, 2-8 mm and 5-25 mm, referred to, respectively as SCR 1, SCR 8, and SCR 20 throughout this paper. The particle size distribution (psd) of the CR is shown in Figure 1, and compared with the natural aggregate (river sand and gravel) used in the study.

It can be seen that the grading of the two coarsest crumb rubbers (SCR 8 and SCR 20) had similar particle size distributions to 5-10 mm and 10-20 mm natural aggregates, respectively. Furthermore, they both fell within the current limits for single sized aggregate specified in BS 882. For this reason, SCR 8 was treated as 10mm aggregate and SCR 20 as 20mm aggregate. The finest crumb rubber (SCR 1) did not meet the requirements for sand specified in BS 882, falling on the coarse side.

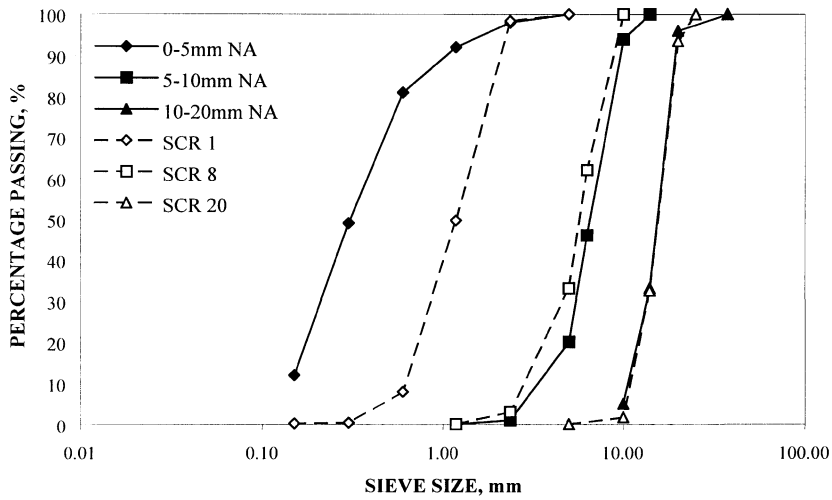

Figure 1 Particle size distribution of crumb rubber and natural aggregates

The main physical aggregate properties of crumb rubber and natural aggregate are given in Table 1. As these properties are defined for natural aggregate, they were not necessarily applicable to the crumb rubber. For example, shape, defined by a visual interpretation, is so irregular with crumb rubber that it did not meet one single criterion. It was therefore described as angular/flaky/elongated.

Similarly, tests to assess the resistance of aggregate to crushing (Aggregate crushing value) and impact (aggregate impact value) failed to cause any damage to crumb rubber. Values of 0% were therefore recorded.

Table 1 Physical properties of crumb rubber and natural aggregate calculated in accordance with British and European standards

PROPERTY	CRUMB RUBBER			NATURAL AGGREGATE		
	SCR 1	SCR 8	SCR 20	Sand	5-10 mm	10-20 mm
Shape, Visual	--	Angular/Flaky/Elongated		--	Rounded	
Elongation Index, %	--	44		--	14	
Aggregate Impact Value‡, %	--	--	0	--	--	24
Aggregate Crushing Value‡, %	--	--	0	--	--	20
Water Absorption, %	0.6	1.0	0.9	0.5	1.3	1.2
Particle Density (dry), kg/m^3	1020	1110	1120	--	--	--
Particle Density (SSD), kg/m^3	1020	1130	1130	2630	2590	2590
Apparent Particle Density, kg/m^3	1020	1130	1140	--	--	--
Bulk Density (SSD)						
Loose, kg/m^3	--	460	470	1580	1590	1550
Compacted, kg/m^3	--	520	530	1680	1660	1650

-- Not applicable ‡ *10 to 14 mm sample*

Water absorption values were found to be very similar to those of natural aggregate. However, this test and the associated density tests were somewhat difficult to carry out because of the nature of crumb rubber, i.e. despite carrying out the tests in non-aerated water, a substantial amount of air bubbles still attach themselves to the crumb rubber. Subsequently, the values recorded will be on the low side. Furthermore, the results show that crumb rubber has a mean particle density of between 1020 and 1140 kg/m^3, although in all three-size fractions approximately 5% by mass of the crumb rubber was found to float. Loose bulk density values were between 460 and 470 kg/m^3. These clearly indicate that crumb rubber can be classified as a lightweight aggregate as they fall below the limit of 1200kg/m^3, specified in BS [7].

The results of tests to determine the physical properties of crumb rubber defined in ASTM D5603 [8] are shown in Table 2. The ash content is defined as that remaining after one hours ignition at 550°C. It can be seen that all three-size fractions were under the maximum of 8% permitted by ASTM D5603. However, the crumb rubber used contained large amounts of fibrous material. For the two coarsest size fractions this was generally attached to the rubber particles, and the free fibre content was below the specified limit of 0.5%. However for the finer fraction, the additional shredding had led to separation, of the fibres and subsequently this did not meet the ASTM limits. For the two finest crumb rubbers, the magnetic removal of iron during processing meant that no iron was found, although some iron threads were attached to SCR 20. However, these limits are specific to use of CR in the USA for rubber compounding and, therefore, do not necessarily preclude it from use in concrete, particularly in Europe where no such standards apply. They should, therefore, be treated only as a guide to the quality of the material.

The cement used was strength class 42.5N Portland cement conforming with BS 12 [9].

Table 2 Rubber characteristics of crumb rubber calculated in accordance with ASTM D5603

	CRUMB RUBBER			ASTM D5603 LIMITS
	0.5–1.5 mm	2-8 mm	8-25 mm	
Ash content, %	6.8	5.1	7.3	8.0
Fiber content, %	1.1	2.4	2.0	--
Free fiber content, %	1.1	0.5	0.4	0.5
Iron content	0.0	0.0	0.5	0.1

MIX PROPORTIONS

Mixes were designed to give a compressive cube strength of 37 N/mm^2, conforming with the minimum strength allowed by BS 8500 [10] where air-entrainment is used. Three additional mixes were designed for 50 N/mm^2, the minimum strength without air-entrainment. A mix design procedure devised for normal strength concretes [11] was used to design the control concrete mixes.

For mixes including SCR 8 and SCR 20, the CR was included as direct replacement volume for volume for the 10 mm and 20 mm aggregate, respectively, since the CR and natural aggregate were of nominally identical size (Figure 1). SCR 1 was also used as direct replacement volume for volume, with the sand. In this case it was considered that it may be necessary to reduce the natural coarse aggregate proportions and increase the fine proportions as the CR content increased. However, since the intention was to investigate the use of SCR 1 as a freeze/thaw resisting agent, it was decided to treat this size fraction in the same manner as air in air entrained mixes. Therefore, only the sand was reduced as the CR content increased.

Mix proportions are given in Table 3. These show that a reduction in water/cement ratio (w/c) was made as the CR content increased. The reduction was based on the earlier work carried out by the CTU, which showed that the loss in strength when using CR was similar in magnitude to that for an equivalent amount of air.

TEST PROCEDURES AND RESULTS

Cube Strength

Cube tests were carried out in accordance with BS 1881: Part 116 [12], on 100mm specimens at 3, 7 and 28 days.

The results are given in Table 4, and shown graphically in Figure 2 for the 37 N/mm^2 design strength mixes. It can be seen from Figure 2 that the cube strength reduces as the CR content increases, despite the lower w/c ratio used in the mix proportions. Furthermore, the cube strength of the 6% CR concretes is lower than that of 6% air-entrained concrete at the equal

w/c ratio. This may be due to additional air that becomes entrapped within the concrete as a result of being attached to the CR. This has been discussed previously [13], and is the subject of on-going work at the CTU.

Flexural Strength

Flexural Strength tests were performed in accordance with BS 1881: Part 118 [14]. Tests were carried out on 100 x 100 x 500mm prisms.

The results are shown in Table 4 and Figure 3. Unlike in some earlier studies [15,16] there appears to be little benefit of CR on flexural strength. Indeed flexural strengths recorded at 6% addition are lower than those of equivalent air-entrained concrete.

Table 3 Mix proportions

MIX	AIR, %	CR, %	MIX CONSTITUENTS, kg/m^3						w/c
			PC	water	CR	Aggregates			
						sand	10mm	20mm	
Design Strength = 37 N/mm^2									
Plain	0	0	330	180	-	660	410	815	0.55
	6[a]	0	400	160	-	505	395	790	0.40
CCR	0	2	360	180	20	640	420	840	0.50
SCR1	0	2	360	180	20	640	420	840	0.50
	0	4	400	180	40	515	400	795	0.45
	0	6	450	180	60	485	375	750	0.40
SCR8	0	2	360	180	25	555	380	865	0.50
	0	4	400	180	45	545	320	845	0.45
	0	6	450	180	70	530	255	825	0.40
SCR20	0	2	360	180	25	555	435	810	0.50
	0	4	400	180	45	545	425	740	0.45
	0	6	450	180	70	530	410	670	0.40
Design Strength = 50 N/mm^2									
Plain	0	0	400	180	-	635	395	785	0.45
SCR1	0	4	515	180	40	480	370	745	0.35
SCR8	0	4	515	180	45	510	290	795	0.35

[a] Actual measured air content = 6.4%

Table 4 Results of engineering and durability tests

MIX	AIR, %	CR, %	CUBE STRENGTH, N/mm^2	FLEXURAL STRENGTH, N/mm^2	SCALING, kg/m^2	RELATIVE DYNAMIC MODULUS
			28 Days	*28 days*	*56 Cycles*	*294 Cycles*
Plain	0	0	40.0	3.50	0.94	47.1
	6	0	31.0	3.10	0.06	85.3
SCR1	0	2	38.0	3.60	0.73	71.9
	0	4	31.0	2.80	0.14	71.4
	0	6	28.0	2.70	0.08	60.0
SCR8	0	2	36.0	3.40	0.82	76.5
	0	4	28.0	2.70	0.18	65.0
	0	6	26.0	2.50	0.10	61.4
SCR20	0	2	35.5	3.10	1.12	74.1
	0	4	27.0	2.50	0.62	61.0
	0	6	25.0	2.40	0.26	53.7
Plain	0	0	51.0	4.00	0.34	49.4
SCR1	0	4	47.5	3.90	0.06	72.4
SCR8	0	4	45.0	3.70	0.08	65.3

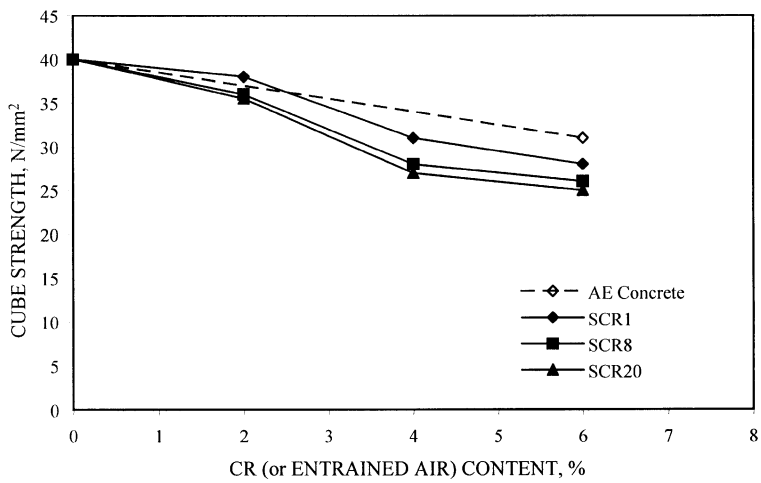

Figure 2 Effect of CR on cube strength

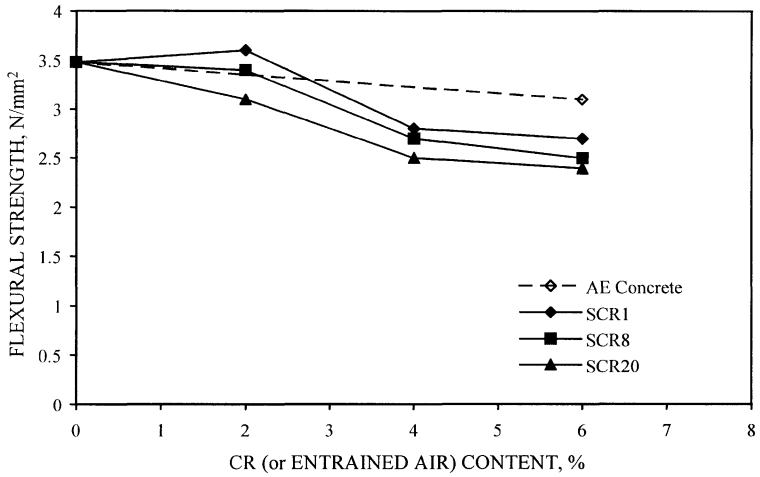

Figure 3 Effect of CR on flexural strength

Freeze/Thaw Test Methods

Freeze/thaw testing was carried out using two methods: the CEN slab test, described by CEN/TC 51 [17], which measures freeze/thaw damage by means of scaling from a concrete surface, and the ASTM prism test, ASTM C666, Procedure A [18], where damage results from disintegration of the concrete mass. The two test methods are described below.

Scaling Test

For this test, 150mm cubes sawn to the required dimensions of 150 mm x 150 mm x 50 mm (at 21 days) were used. At 28 days, a pond was created on the sawn surface by gluing rubber sheeting to all sides of the test specimen, except the test surface. This pond was filled with a 3mm layer of tap water and left for 3 days, to allow re-saturation before testing.

At 31 days, the tap water was replaced with 67 ml of 3% sodium chloride solution and each specimen covered in thermal insulation, except for the test surface, which was covered with a polyethylene sheet to prevent evaporation from the surface (see Figure 4). The specimens were then subjected to repeated freezing and thawing cycles. Each cycle lasted 24 hours, with the temperature at the surface of the specimen ranging from 20 ± 4°C to -18 ± 2°C.

After 7, 14, 28, 42 and 56 cycles, the test solution was drained and material that had scaled from the surface collected and weighed. The freezing medium was then replaced with a fresh 67 ml sample of 3% sodium chloride solution.

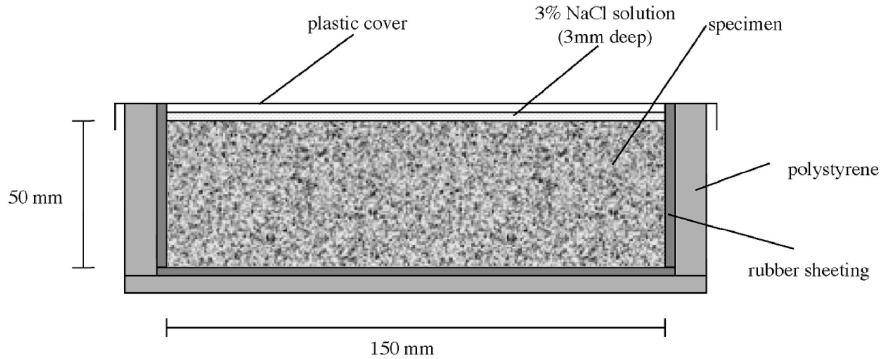

Figure 4 Test specimen used in slab test

The effect of CR content on the resistance of concrete to freeze/thaw scaling is shown in Figure 5, for all three CR sizes. It is clear that as the CR content increases the resistance of concrete to freeze/thaw scaling also increases, and improves from acceptable at 0% CR to very good resistance at 6% CR. Resistance to freeze/thaw also increases as the SCR size diminishes, SCR 20 concretes having clearly less resistance to scaling than SCR 1 and SCR 8.

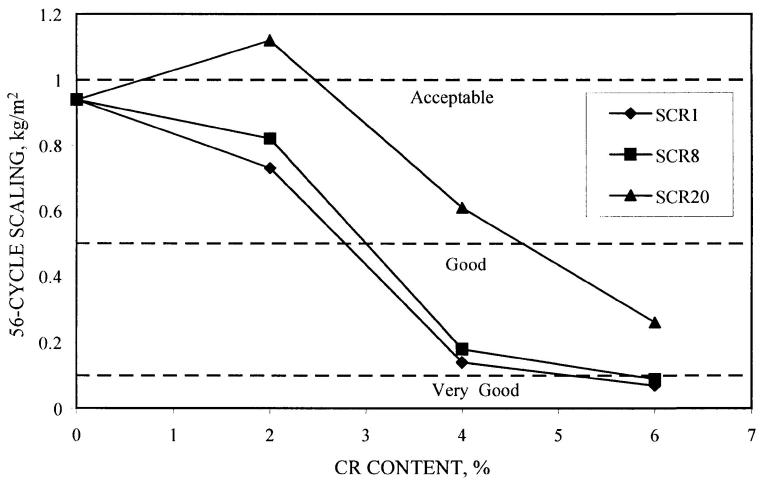

Figure 5 Effect of CR content on scaling resistance

A comparison of the resistance to freeze/thaw scaling for 6% CR and 6% air entrained concrete are shown in Figure 6. The results show that 6% air–entrained concrete gives only marginally better resistance than SCR1 and SCR8 concretes. All three of these concretes having scaling less than 0.1 kg/m^2 after 56 cycles, corresponding to very good resistance in the Swedish criteria (Table 5) [19]. For SCR 20, the amount of scaling after 56 cycles was 0.25 kg/m^2, corresponding to good resistance (< 0.5 kg/m^2).

The scaling from non-air entrained concretes, designed for a strength of 50 N/mm^2, after 56 cycles was 0.3 kg/m^2 – much lower than that of concrete designed for the lower strength (Figure 7). With respect to this performance, it can be seen that it is necessary to use a CR content greater than 4% to achieve improved freeze/thaw resistance when using the lower cube strength. Clearly, the use of CR in concretes designed for 50 N/mm^2 improves resistance further. The total scaling of all specimens after 56 cycles is given in Table 4.

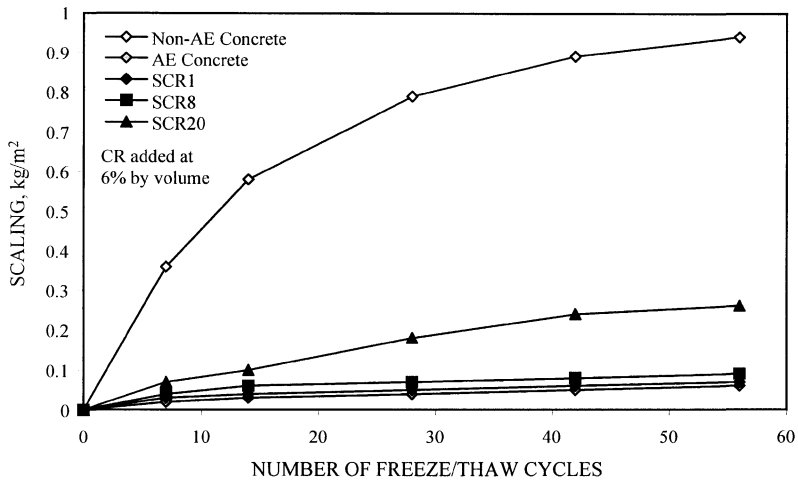

Figure 6 Comparison of cumulative scaling of non-air entrained, air entrained and CR concretes

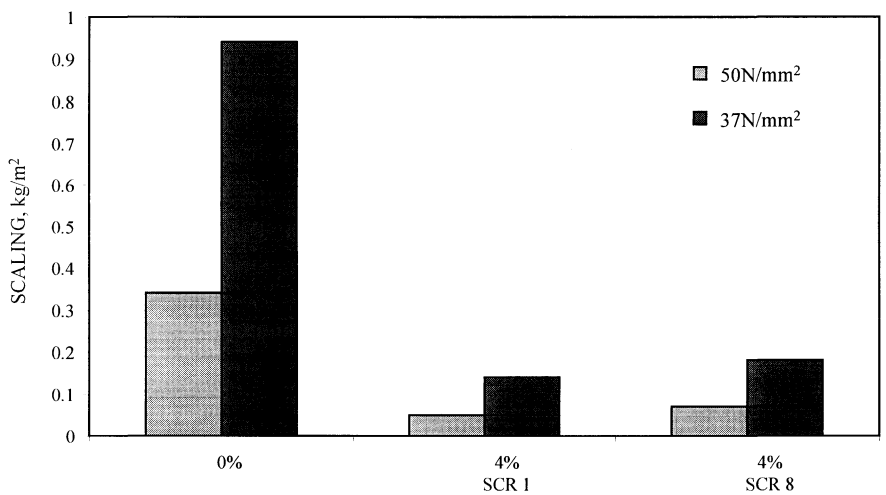

Figure 7 Effect of cube strength and CR size on 56 day scaling

Table 5 Swedish criteria for comparative scaling resistance given in SS 13 72 44 [19]

SCALING RESISTANCE	REQUIREMENT
Very Good	No specimen has more than 0.1 kg/m^2 scaled after 56 cycles
Good	The mean value for the material scaled after 56 cycles (m_{56}) is less than 0.5 kg/m^2, and m_{56}/m_{28} is less than 2
Acceptable	The mean value for the material scaled after 56 cycles (m_{56}) is less than 1.0 kg/m^2, and m_{56}/m_{28} is less than 2
Unacceptable	The net requirements for acceptable scaling resistance are not met

Relative Dynamic Modulus

In this method, 75 x 75 x 300mm prisms were used with reference studs cast in at both ends. At 28 days the specimens were stored in individual metallic containers, which were filled with water and located in a refrigeration unit. The freezing/thawing system followed an eight-hour cycle, with four hours freezing (-17 ± 1.7°C) and four hours thawing (4.4 ± 1.7°C). Specimens were therefore exposed to three freeze/thaw cycles per day. Tests were continued to 294 cycles.

Specimens were periodically tested for deterioration using linear expansion and dynamic modulus of elasticity.

The effect of CR content on relative dynamic modulus after 294 freeze/thaw cycles is shown in Figure 8. Clearly, the loss of dynamic modulus as a result of freeze/thaw is less than that of non-air entrained suggesting that CR does provide some resistance to spalling. However, although resistance to deterioration is better for CR concrete than non-air entrained concrete, the best resistance was found at a CR content of 2%, with relative dynamic moduli approximately 15% lower at CR contents of 6%. Again, greatest resistance was found using smaller CR sizes.

However, as shown in Figure 9, the resistance of CR concretes to deterioration is significantly less than that of air-entrained concrete. The relative dynamic modulus of 6% air-entrained concrete being greater than 90% after 296 cycles, compared with 60% for the equivalent amount of CR. This may be due to a gradual loss in the bond between the rubber and cement paste during the test. This is clearly not detrimental to the performance of the concrete since the CR is not intended to give any strength or stiffness. This needs further investigation.

The relative dynamic modulus of non-air entrained concrete, designed for a strength of 50 N/mm^2, after 296 cycles was found to be 50% - similar to that of the lower strength (37 N/mm^2) concretes (Figure 10). Therefore, it is clear that all CR concretes give better resistance to internal freeze/thaw disintegration than non-air entrained concretes. However, performance is not as good as that obtained using air-entrained concrete.

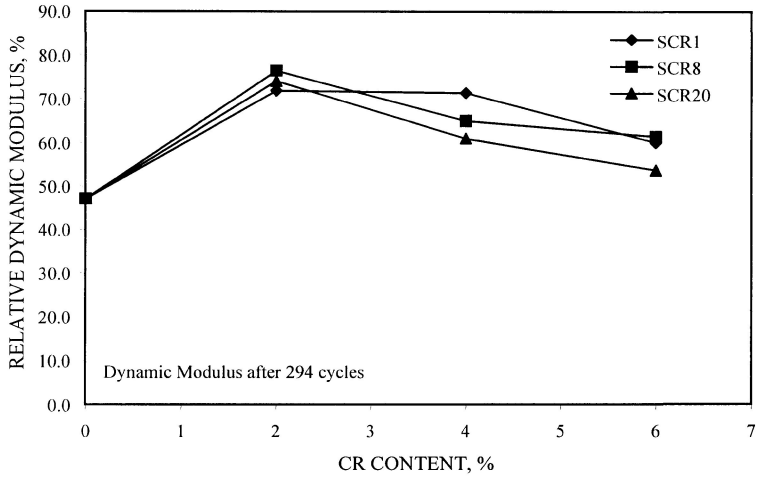

Figure 8 Effect of CR content on relative dynamic modulus

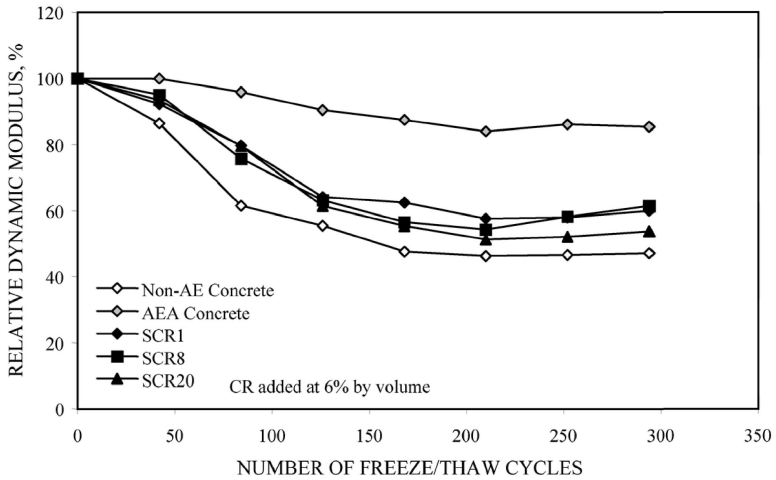

Figure 9 Change in relative dynamic modulus during freeze/thaw cycles

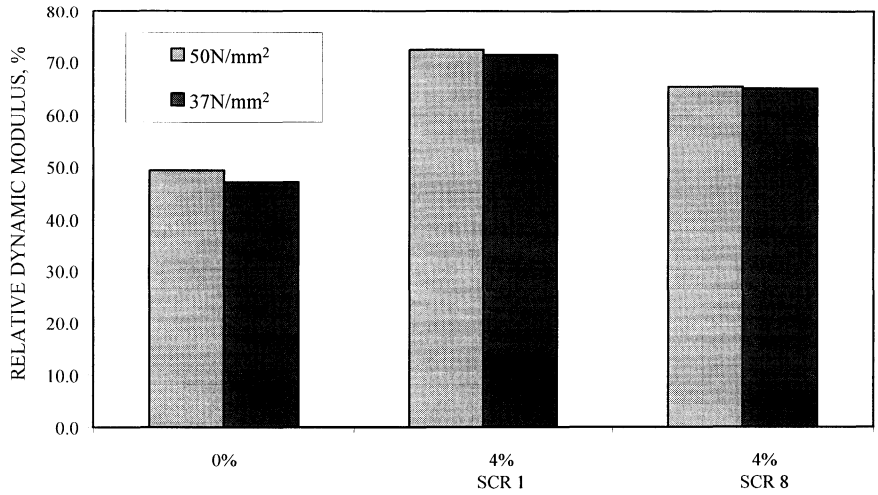

Figure 10 Effect of cube strength and CR size on relative dynamic modulus

SUMMARY AND CONCLUSIONS

This study has shown that there is potential for using CR as a freeze/thaw resisting agent in concrete. CR concrete performs significantly better under freeze/thaw conditions than plain concrete, both in terms of scaling performance measured using the CEN test and relative dynamic modulus using the ASTM test method.

Furthermore, the performance of CR concrete in terms of scaling is similar to that of air-entrained concrete, and when compared with the Swedish Criteria for freeze/thaw resistance gives very good resistance for a CR content of 6%. The performance of CR concrete in the ASTM test appears less impressive than air-entrained concrete, but may be due to a loss in bond between the CR and cement paste which is not detrimental. This requires further investigation.

The use of CR in concrete leads to lower cube strengths than that of equivalent air-entrained concrete. At the low contents used, there is also no effect on flexural strength. Reasons for the lower strength may include the entrapment of additional air that was attached to the CR particles.

ACKNOWLEDGEMENTS

This work was carried out as part of a Partners in Innovation collaborative research project. The authors are grateful to the Department of Trade and Industry, and all the industrial partners for funding the project. The Charles Lawrence Group kindly supplied the crumb rubber used.

REFERENCES

1. BRITISH STANDARDS INSTITUTION. BS 8110: Part 1. Structural use of concrete. Code of practice for design and construction. 1997
2. BRITISH STANDARDS INSTITUTION. BS 5328: Part 1. Guide to Specifying Concrete. 1997
3. HARRISON, T A, DEWAR, J D, BROWN, B V. Freeze-thaw resisting concrete: its achievement in the UK. CIRIA Report C559, London, 2001, 79pp
4. SCRAP TYRE WORKING GROUP. Second annual report to ministers. STWG, 1997.
5. ENVIRONMENT AGENCY. Annual report on tyres in the environment, London, 1998
6. ENVIRONMENT AGENCY. Environment action: Let's act now to beat tyre glut. The Environment Agency's bi-monthly newspaper. Issue 18, Feb. / March 1999
7. BRITISH STANDARDS INSTITUTION. BS 3797. Specification for lightweight aggregates for masonry units and structural concrete.
8. AMERICAN SOCIETY OF TESTING AND MATERIALS. ASTM D5603 Standard classification for rubber compounding materials – recycled vulcanizate particulate rubber.
9. BRITISH STANDARDS INSTITUTION. BS 12. Specification for Portland cement.
10. BRITISH STANDARDS INSTITUTION. BS 8500. Concrete. Complementary British Standard to BS EN 206-1. Specification for constituent materials and concrete
11. TEYCHENNE, D C, FRANKLIN, R E, ERNTROY, H C, MARSH, B K. Design of Normal Concrete mixes; Second Edition, Building Research Establishment, 1997
12. BRITISH STANDARDS INSTITUTION. BS 1881: Part 116. Testing concrete. Method for determination of compressive strength of concrete cubes
13. ALI, N A, AMOS, A D, ROBERTS, M. Use of ground rubber tyres in Portland cement concrete. Concrete 2000 - Economic and Durable Construction Through Excellence., International Conference, Dundee, 7-9 September 1993, pp 379-390
14. BRITISH STANDARDS INSTITUTION. BS 1881: Part 118. ddd Testing concrete. Method for determination of flexural strength
15. LEE, H S, LEE, H, MOON, J S, JUNG, H W. Development of tire-added latex concrete. ACI Materials Journal, Vol. 95, No. 4, 1998, pp 356-364
16. LI, Z, LI, F, LI, J S L. Properties of concrete incorporating rubber tyre particles. Magazine of Concrete Research, Vol. 50 No. 4, 1998, pp 297-304
17. COMITÉ EUROPÉEN DE NORMALISATION. Test methods for the freeze-thaw resistance of concrete - Tests with water or sodium chloride solution. Part 1: Scaling. CEN/TC51/WG12/TG4. 1994
18. AMERICAN SOCIETY OF TESTING AND MATERIALS. ASTM C666. Test for resistance of concrete to rapid freezing and thawing. 1992
19. SWEDISH STANDARDS. SS 13 72 44. Betonproving – Hrdnad betong – Avflagning vid frysning

EFFECTIVE SULFATE CONTENT IN CONCRETE INGREDIENTS

R S Al-Rawi

R A W Al-Salihi

M H M Ali

University of Baghdad

Iraq

ABSTRACT. The problem of internal sulfate attack in concrete is widespread in Iraq and neighboring countries. This is because of the high gypsum content usually present in sand and gravel used in concrete. Specifications usually put upper limits of SO_3 content in cement, aggregate and concrete. The upper limit of SO_3 content is calculated assuming that sulfates from all concrete ingredients have the same effect. Based on the results of an extensive experimental program, it is suggested to adopt the effective sulfate concept. It is shown that sulfate in cement are more effective than sulfates in sand and the latter is more effective than sulfate in coarse aggregate i.e. with increased size of gypsum particles the sulfate effectiveness decreases. A new formula is presented to define sulfate effectiveness. Adopting this concept may facilitate the use of aggregate reserves that are not used at present.

Keywords: Concrete compressive strength, Expansion in water, Effective sulfate, Sand, Coarse aggregate, Fineness modulus.

Professor R S Al-Rawi, is a Professor of Civil Engineering, University of Baghdad. His research focuses on durability of concrete including internal and external sulfate attack, shrinkage, creep and cracking of concrete under hot weather conditions.

Mr R A W Al-Salihi, is a former Research Student at the Civil Engineering Department, University of Baghdad.

Mr N H M Ali, is a former Research Student at the Civil Engineering Department, University of Baghdad.

INTRODUCTION

In the current Iraqi specification [1] and because of the scarcity of sand and coarse aggregates with low sulfate content, the upper limits of SO_3 was lowered to 2.8% in OPC. This is considerably lower than the limits in other specifications, e.g. in B.S.12 specification [2] the SO_3 content in OPC is limited to not more than 3.5% and in ASTM specification [3], the limit SO_3 content is 3.0 - 3.5% (type I) cement.

Lowering SO_3 content in cement made it possible to increase the upper limit of SO_3 in sand to between 0.5-1.0 % and in coarse aggregates to 0.1%. However, such sands and coarse aggregates are scarce and usually quite far from main cities. This raises the need for a new more precise method for calculating the effective SO_3 content in concrete, instead of the current method, which gives equal effectiveness to sulfates from all concrete ingredients. Such a new method may, in some cases, make it possible to use sands and coarse aggregates with higher SO_3 content.

LITERATURE REVIEW

Most of the research results concerning the upper limit of SO_3 in concrete ingredients are contradictory e.g. German Specifications [4] allow 1% SO_3 in both sand and coarse aggregate. While British Specifications [5] allow 0.4% SO_3 in both sand and coarse aggregate. At the same time British specifications allow 4% SO_3 in concrete measured as a percentage of the weight of cement. Local literature also shows considerable contradictions regarding the allowable SO_3 content in aggregates and in concrete as a whole. One possible reason for these contradictions is the variation of chemical composition and the fineness of cement of the same type [6].

The main source of sulfate in cement, sand and coarse aggregate is gypsum, which has a very low solubility in water of 0.2%. Naturally gypsum in cement is ground to a very high fineness. This means fast solubility in water and quick combination with C_3A and water and to a lesser extent with C_4AF and water. In a previous work [7], medium gypsum content in cement depleted within eight weeks of curing in water. But medium gypsum content in sand did not deplete after twenty-six weeks of curing in water [8]. This may be because of the relatively coarse particles of gypsum in sand compared with those in cement. This indicates that the present method of calculation of SO_3 in concrete needs to be revised to take into consideration the effectiveness of gypsum from various concrete constituents.

EXPERIMENTAL WORK

The experimental work was carried out in two stages. In the first stage, the relative effects of SO_3 in cement and sand were studied [9]. In the second stage, the relative effects of SO_3 in sand and coarse aggregates were studied [10]. In both stages, concrete mixes were made and cast in 100 mm cubes and in 75 x 75 x 285 mm prisms. In the first stage some 450 cubes and 50 prisms were cast. In the second stage some 525 cubes and 70 prisms were cast.

The mix proportion in the first stage were 170 kg / m^3 water, 315 kg / m^3 cement, 630 kg / m^3 sand and 1260 kg / m^3 coarse aggregate. The SO_3 contents of the cement were 1.0%, 1.5%, 2.0%, 2.5% and 2.8%. These SO_3 contents were obtained by grinding a cement clinker brought from a cement factory with the appropriate gypsum content in a ball mill to a surface

area of around 3000 cm^3 / gm (Blaine). The resulting cement conformed to Iraqi and British specifications. Details of the clinker composition are given in Table 1. The SO_3 contents of the sand were 0.2%, 0.5%, 1.0%, 1.5% and 2.0%. These SO_3 contents were obtained by mixing sand with SO_3 content of 0.2% with the appropriate amount of gypsum collected from a sand quarry. The SO_3 content of the coarse aggregate was kept virtually zero by thorough washing in water. The cubes were tested for compressive strength after curing in water for 7, 28, 56, 90 and 250 days. The prisms were tested for expansion after curing in water for 3, 7, 28, 56, 90, 150, 180 and 250 days. The curing water temperature was $23^o \pm 5^oC$.

In the second stage, the mix proportions were: 200 kg / m^3 water, 315 kg / m^3 cement, 700 kg / m^3 sand and 1145 kg / m^3 coarse aggregate. The SO_3 contents of the sand were: 0.08%, 0.50%, 1.00%, 1.50% and 2.00%. The SO_3 contents of the coarse aggregate were 0.10%, 0.25, 0.50%, 0.75%, 1.00%, 1.25% and 1.50%. The SO_3 contents of the coarse aggregates were obtained by mixing coarse aggregate with low SO_3 content with the appropriate amount of coarse aggregate with high SO_3 content. Chemical composition of the cement is given in Table 1. Again concrete cubes and prisms were cast, cured and tested as in the first stage

Table 1 Oxide and calculated compound compositions of the clinker and ordinary Portland cement used

OXIDE	CEMENT CLINKER FIRST STAGE	CEMENT CHEMICAL ANALYSIS SECOND STAGE	LIMITS OF IRAQI SPECIFICATIONS [1]
CaO	64.30	60.02	-
SiO_2	22.96	21.62	-
Al_2O_3	5.10	5.26	-
Fe_2O_3	2.30	3.00	-
SO_3	0.75	2.06	≤2.80
MgO	3.40	4.11	≤5.00
Na_2O	0.94	0.60	-
K_2O	-	0.31	-
L.O.I.	0.20	1.62	≤4.00
I.R.	-	1.36	≤1.50
Chloride	-	0.04	-
C_3S	41.00	35.00	-
C_2S	34.00	36.00	-
C_3A	9.00	9.00	-
C_4AF	9.00	9.00	-

RESULTS AND DISCUSSION

Relative Effect of SO_3 in Cement and Sand

Figure 1 shows that a compressive strength of 38 N/mm^2 at the age of 90 days can be obtained with SO_3=1.5% in cement and SO_3 =2.0% in sand i.e. a total of 5.5% SO_3 by weight of cement. Figure 2 shows that about the same compressive strength at the same age is obtained with SO3 =2.5% in cement and SO_3 =1.0% in sand i.e. a total of SO_3 =4.5%. This

shows that an increase of 1% SO_3 in cement is equivalent to a decrease in SO_3 in sand =2.0%. Noting that the sand content in this case is twice the cement content. The results of all the other compressive strength tests also show that SO_3 in cement is about twice more effective than SO_3 in sand.

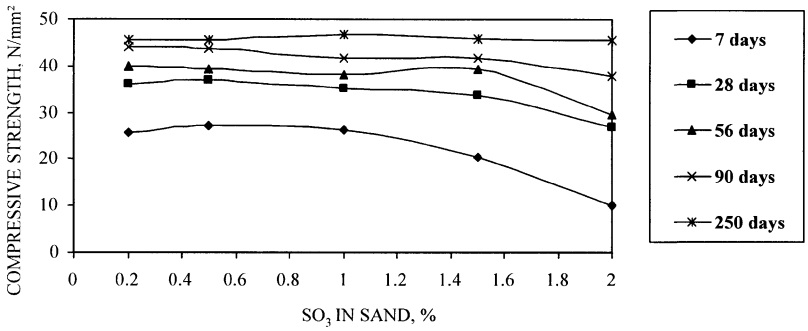

Figure 1 Effect of sulphate in sand on concrete compressive strength with 1.5% SO_3 in cement – first stage

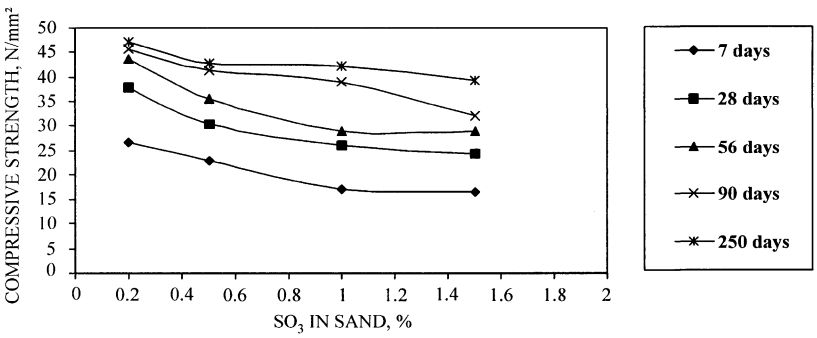

Figure 2 Effect of sulphate in sand on concrete compressive strength with 2.5% SO_3 in cement – first stage

Total (SO_3) Content in Concrete

Table 2 shows that for the same total SO_3 in concrete, there is a large variation in concrete compressive strength, especially at later ages when significant deterioration of strength may or may not take place. Both the Iraqi specification and the British specification give an upper limit of SO_3 content in concrete. In both specifications, the SO_3 contents are calculated by direct addition of SO_3 from various concrete ingredients. These specifications need to be revised to take in to consideration the relative effect of SO_3 from concrete ingredients on compressive strength.

Expansion of Concrete in Water Related to SO_3 Content

Due to the relatively slow rate of reaction of sulfates from sand compared with that from cement, there may be some doubt about the long-term effect of sulfates in sand on concrete. The results of expansion of concrete in water are given in Table 3. These results shows that, for the same total SO_3 content in concrete, the mixes having more sulfates in sand and less sulfates in cement expand less at early ages and more at later ages compared with mixes having less sulfates in sand and more sulfates in cement. But Table 2 shows that the first mixes, despite their high expansion at later ages show more gain in strength between the ages of 90 days and 250 days compared with the latter mixes. This shows that the occurrence of relatively slow expansion in concrete at later ages may not lead to concrete deterioration i.e. in the present case deterioration could not be detected by expansion. Also no visual damage was detected. The stress induced by this expansion is partially relieved by creep of concrete, which takes place over a relatively long period of time. Therefore, it is better to base specification of SO_3 content on strength results rather than on expansion results.

Table 2 Concrete compressive strength – first stage

TOTAL SO_3 BY WEIGHT OF CEMENT, %	C:SO_3 IN CEMENT, %	CONCRETE COMPRESSIVE STRENGTH, N/mm^2				
	S:SO_3 in sand by weight of cement, %	Age, days				
		7	28	56	90	250
4.5	C=1.5 , S=3.0	20.5	33.8	39.3	41.7	46.0
	C=2.5 , S=2.0	17.0	26.0	29.0	39.0	42.3
4.8-5.0	C=1.0 , S=4.0	19.0	27.4	32.9	42.9	45.4
	C=2.0 , S=3.0	17.2	25.4	31.5	35.4	45.9
	C=2.8 , S=2.0	16.6	23.1	26.6	34.9	37.9
5.5	C=1.5 , S=4.0	18.2	26.9	29.7	37.9	45.7
	C=2.5 , S=3.0	16.4	24.3	29.0	32.2	39.2
5.8-6.0	C=2.0 , S=4.0	18.4	23.2	24.6	29.7	35.7
	C=2.8 , S=3.0	15.9	22.4	26.0	27.6	28.9

Table 3 Expansion of concrete – first stage

TOTAL SO_3 BY WEIGHT OF CEMENT, %	C:SO_3 IN CEMENT, %	CONCRETE EXPANSION * 10^{-5}				
	S:SO_3 in sand by weight of cement, %	Age, days				
		7	28	56	90	250
4.5	C=1.5 , S=3.0	11.0	19.0	24.5	30.0	32.0
	C=2.5 , S=2.0	12.0	20.0	25.5	29.0	31.0
4.8-5.0	C=1.0 , S=4.0	12.0	24.0	30.5	36.0	38.5
	C=2.0 , S=3.0	13.0	23.0	29.5	34.0	36.5
	C=2.8 , S=2.0	13.0	23.5	27.5	32.0	35.0
5.5	C=1.5 , S=4.0	14.0	25.0	31.5	38.0	43.0
	C=2.5 , S=3.0	14.5	26.0	31.5	38.0	40.0
5.8-6.0	C=2.0 , S=4.0	15.0	26.0	32.5	40.0	47.0
	C=2.8 , S=3.0	15.0	27.0	32.5	38.0	41.5

Relative Effect of SO_3 in Sand and in Coarse Aggregate

The results of the second stage of the work show that the decrease in compressive strength of concrete due to increased SO_3 content in coarse aggregate is considerably less than that due to increased SO_3 content in sand. Figure 3 shows that with increase in sulfate content of coarse aggregate from 0.1% to 1.37% and to get the same compressive strength of concrete at the age of 7 days, the SO_3 content in sand must be decreased from 2.0% to 1.5%. Calculations show that the effectiveness of SO_3 in sand in this case is more than twice the effectiveness of SO_3 in coarse aggregate. Other curves in Figure 3 show the same trend. Figure 4 also shows the same trend, i.e. for the same 180-day's compressive strength, the increase in SO_3 in coarse aggregate is more than twice the decrease in SO_3 of sand. The expansion in water tests results show that for concrete with sand having low SO_3 content 0.08%, expansion is very low for SO_3 content in coarse aggregate ranging from 0.25% to 1.5% as can be seen from Figure 5. This is despite the fact that the total SO_3 content in concrete in the second case reaches 7.161%, which is quite high. Figure 5 also shows that expansion of curve 1 is much higher than expansion of curve 2 even through they both having about the same total SO_3 content. This is because for curve 1, the SO_3 in sand is relatively high. It may be concluded that the upper limit of SO_3 is 0.1% in coarse aggregate given in current Iraqi specifications is too low and may be increased.

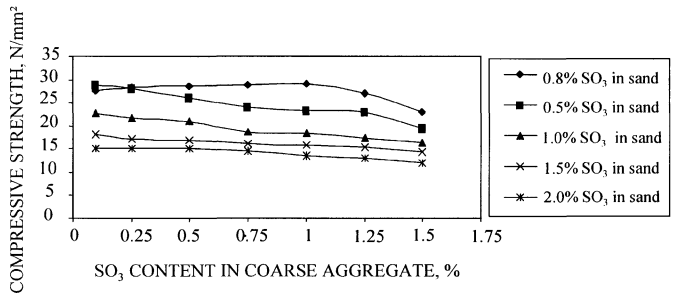

Figure 3 Compressive strength with different percentage of SO_3 in sand and coarse aggregate at age of 7 days – second stage

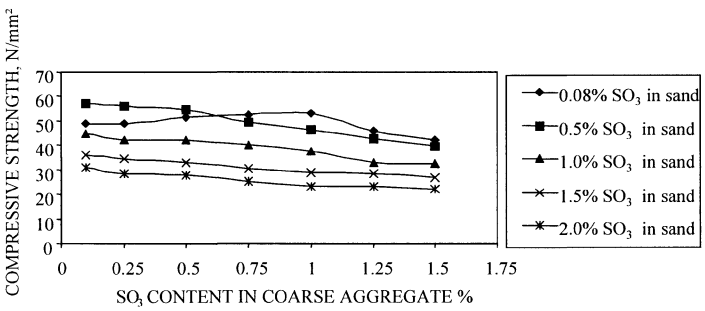

Figure 4 Compressive strength with different percentage of SO_3 in sand and coarse aggregate at age of 180 days – second stage

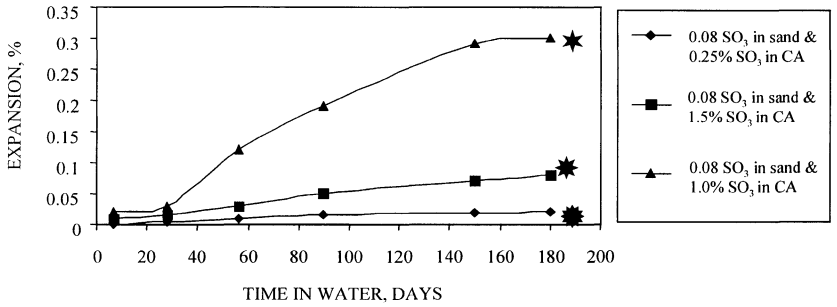

Figure 5 Expansion in concrete with varying SO_3 content in sand and in coarse aggregate – second stage

Relative Effect of SO_3 in Sand with Different Fineness Modulus

Increased fineness modulus of sand means increased particle size of gypsum in that sand, which means lower activity and consequently lower effectiveness of SO_3. To test this hypothesis, sands with fineness modulus of 1.05, 2.49 and 3.45 were used in concrete mixes designed according to ACI method. The results showed that, as expected, with increased fineness modulus of sand the effectiveness of sulfates in sand decreases. These results confirm the above hypothesis. Therefore, the fineness modulus of sand should be taken in consideration when determining the effectiveness of SO_3 in sand and the same may be applicable to coarse aggregate i.e. decreased effectiveness with increased fineness modulus.

Effective SO_3 in Concrete

Reduction in the upper limit of SO_3 content in cement may allow increasing the allowable SO_3 in sand and coarse aggregate significantly. It seems clear that adopting the concept of total effective SO_3% in concrete will facilitate the use of huge sand and coarse aggregate reserves which are not allowed in concrete under the current specifications and the current method of calculation of total SO_3% content.

CALCULATION OF EFFECTIVE SO_3 IN SAND AND COARSE AGGREGATES

Based on the results of the present work, the following formula was developed for the effective SO_3 content in sand and coarse aggregates used in concrete.

$$SO_{3\,(effective)} = SO_3 \text{ content } (0.9 - 0.25\ (F.M.)^{1/2})$$

Where F. M. is the fineness modulus of sand or coarse aggregates. The factor adopted for effective SO_3 content in cement and water is unity. The effective total SO_3 content in concrete as a percentage by the weight of cement is then calculated as follows:

SO_3 content in cement + SO_3 content in water multiplied by w/c ratio + $SO_{3\,(effective)}$ in sand multiplied by sand/cement ratio + $SO_{3\,(effective)}$ in coarse aggregate multiplied by coarse aggregate/ cement ratio.

CONCLUSIONS

Under the present test conditions, the following conclusions could be drawn:

1. The effect of SO_3 on concrete compressive strength depends on its source. SO_3 from sand has less effect than SO_3 from cement. With increased fineness modulus of sand, the effectiveness of SO_3 decreases.
2. SO_3 from coarse aggregates has less effect on concrete compressive strength and expansion in water than SO_3 from sand. Because of the very low activity of SO_3 from coarse aggregate, the current Iraqi specification for upper limit of SO_3 content in coarse aggregate 0.1% does not seem to be justifiable.
3. Concrete with the same total SO_3 content could show significant variation in compressive strength and expansion in water, if the percentages of SO_3 in various ingredients are varied. Specifications of upper limit of SO_3 content in concrete need to be revised to take into consideration the relative effects of SO_3 from various concrete ingredients.
4. Concrete showing continuous slow expansion in water could at the same time show relatively high strength development. Therefore, it is better to base specifications of SO_3 content on compressive strength results than on expansion in water results.
5. A new formula is presented for calculation of effective SO_3 content in sand and coarse aggregates. Adopting this formula and specifying lower SO_3 content in cement, may facilitate the use of huge sand and coarse aggregates reserves, not used at present.

REFERENCES

1. IRAQI STANDARDS No.5, Iraqi standard specification for Portland cements, ICOSQC, Baghdad, Iraq, 1984.
2. BRITISH SPECIFICATION, 12-1991, British standard specification for Portland cements, British Standards Institution, UK.
3. ASTM, C150, Standard specification for Portland cement, Annual Book of ASTM Standards, Vol.04.08, 1995.
4. DIN, 4226-1983, Regulation of the German committee for concrete aggregate from natural sources, Deutsche Norman, Berlin, Germany.
5. BRITISH SPECIFICATION, 882-1992, British standards specification for aggregate from natural sources for concrete, British Standards Institution, UK.
6. ABDUL-LATIF, A M, Compatibility of sulfates content in concrete ingredients M.Sc. Thesis, Baghdad University, May, 1997.
7. Al-RAWI, R S, Gypsum content of cement used in concrete cured by accelerated methods, ASTM, Journal of Testing and Evaluation, Vol 5, No 3, 1977, p 231-327.
8. YOUSIF, S H, Effect of sulfates on lean and medium richness concrete, M.Sc. Thesis, Baghdad University, 1980.
9. ALI, N H M, Effect of sulfates on concrete with different gypsum content cements, M.Sc. Thesis, Baghdad University, 1980.
10. AL-SALIHI, R A, Proposed revision of Iraqi specifications for concrete ingredients to cope with post war era, M.Sc. Thesis, Baghdad University, January, 1994.

THE EFFECT OF COMPRESSION PRE-LOADING ON THE STRENGTH OF CONCRETE

T Kukai

P Lenkei

Pécs University

Hungary

ABSTRACT. This paper describes a study carried out to determine the effect of compression pre-loading on the strength of concrete. In the first part of the study the concrete strength variations of cubes and beams (made from C13 and C18 concrete classes) during loading tests are reported. The strength variations of non pre-loaded and pre-loaded tests specimens are compared. The maximum strength increase of the specimens due to pre-loading were of the order of 2-10%. In the second part of the study tests with core samples taken from prestressed concrete structure are described. The concrete strength increases of the samples due to prestressing were of the order of 2-3% and 5-6% depending on the angle included between the direction of the prestressing and the direction of the sample axis.

Keywords: Concrete strength, Compression pre-loading, Beam tests, Cube tests, Core sample tests, Ultrasonic measurements.

Dr T Kukai is currently Associate Dean of Engineering, Pécs University, Hungary. His professional activities focuses mainly on the concrete construction technologies and quality assessment methods.

Dr P Lenkei is currently Széchenyi Professor of Structural Engineering, Pécs University, Hungary. His main research fields are ageing management of concrete structures, non-linear design of concrete structures and structural standardization.

INTRODUCTION

Several modern concrete technologies are using the compressing pre-loading (pressing) at early phases of concrete setting to obtain better concrete performance. There is a wide range of investigations dealing with the effect of compressive pre-loading at later ages of concrete setting and early hardening. The study reported herein is aimed to contribute to this general problem. The specific goal was to determine both the variation of the strength increases in relation to the acting compressive stress (from the payload) and the influence of the direction of this pre-loading.

TESTS ON PRE-LOADED SPECIMENS

The tests reported in this chapter [1] were carried out in the laboratories of the Engineering College, Pecs University.

The test specimens

Two types of test specimens were used. The beam specimens were of 150*300 mm rectangular cross section and 3150 mm long. The beam span was 3000 mm (Figure 1a).

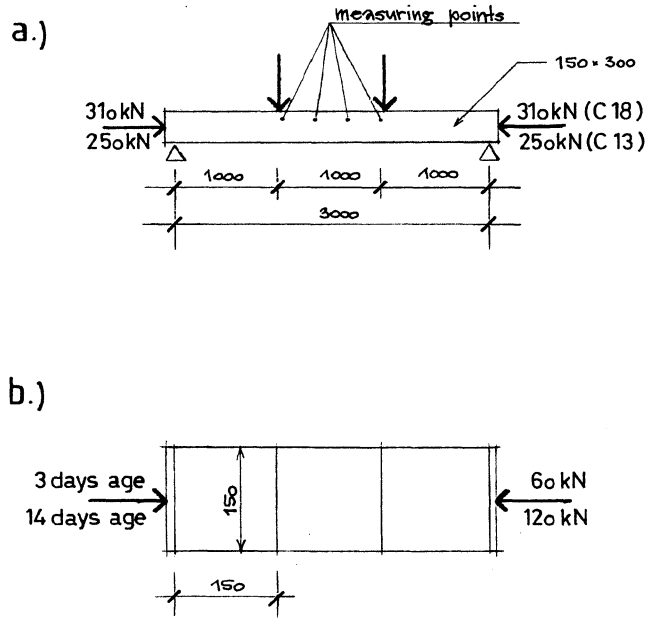

Figure 1 The test beams (a) and the test cubes (b)

The longitudinal compressive pre-loading was applied in the center of the cross section by means of small steel frames. The vertical load was applied at the thirds of the span. The 150*150*150 mm cube specimens (Figure 1b) were pre-loaded in another frame.

Three cubes were in one frame. The design concrete strength classes were equivalent to C13 and C18 strength classes. From each concrete class 3 beams and 10 cubes were produced. The beam types are shown in Table 1. The beams were over reinforced to induce concrete crushing failure.

Table 1 The test beam types

TEST BEAMS	CONCRETE CLASS	NON PRE-LOADED NATURAL CURING	PRE-LOADED NATURAL CURING	PRE-LOADED THERMAL CURING
C 18/1	C18		X	
C 18/2	C18	X		
C 18/3	C18			X
C 13/4	C13			X
C 13/5	C13		X	
C 13/6	C13	X		

TEST PROCEDURE AND THE RESULTS

The applied compressive pre-loading at the age of 5 days was about 60% of the final value and it was increased at ages of 14 and 28 days. The values are shown in Table 2, where

P – the pre-loading force,
σ_{cp} – the concrete stress from pre-loading,
f_{cm} – the average concrete compressive strength.

Table 2 The compressive pre-loading of the test beams

TEST BEAMS	**P** [kN]	σ_{cp} [N/mm^2]	f_{cm} [N/mm^2]	σ_{cp}/f_{cm}
		5 days age		
C 18/1	218	4.84	26.4	0.183
C 18/3	189	4.20	29.2	0.143
C 13/4	164	3.64	20.7	0.176
C 13/5	171	3.80	21.7	0.175
		14 days age		
C 18/1	288	6.40	28.3	0.226
C 18/3	276	6.13	33.0	0.186
C 13/4	235	5.22	22.5	0.232
C 13/5	220	4.88	22.8	0.214
		28 days age		
C 18/1	310	6.88	33.6	0.205
C 18/3	310	6.88	36.0	0.191
C 13/4	256	4.78	29.1	0.165
C 13/5	243	5.40	29.8	0.181

The vertical loads were applied stepwise and the tests were continued until the failure of the beams. The stresses in the beams were measured by ultrasonic equipment. The measuring points are shown on Figure 1a.

The ultrasonic test results are shown in Table 3, where lower index i is the beam number and

v_{io} - the ultrasonic velocity without bending in m/s
v_{imax} - the velocity at maximum bending in m/s,
$\Delta v_i = v_{imax} - v_{io}$ the difference in ultrasonic velocities in m/s,
$\Delta v_{max} = v_{imax} - v_{2o}$ or v_{6o} respectively, the difference in ultrasonic velocities in pre-loaded and non pre-loaded beams [m/s].

The average ultrasonic velocity values were calculated on the bases of 3-3 measurements taken in 4 points on the compressed concrete zone of the constant bending moment fraction, all together 12 measurements for each value.

Table 3 The ultrasonic test results

TEST BEAMS	PRE-LOAD	v_{io} [m/s]	v_{imax} [m/s]	$\Delta v_i = v_{imax} - v_{io}$	$\Delta v_{max} = v_{imax} - v_{2o}$	$\Delta v_{max} = v_{imax} - v_{6o}$	v_{io}/v_{2o}	v_{io}/v_{6o}	v_{imax}/v_{io}	v_{imax}/v_{2max}	v_{imax}/v_{6max}
C 18/1	+	4196	4272	76	170	n/a	1.023	n/a	1.018	1.010	n/a
C 18/3	+	4254	4303	49	201	n/a	1.037	n/a	1.012	1.017	n/a
C 18/2	n/a	4102	4229	127	127	n/a	1.000	n/a	1.031	1.000	n/a
C 13/4	+	3830	3905	75	n/a	203	n/a	1.035	1.020	n/a	1.017
C 13/5	+	3809	3922	113	n/a	220	n/a	1.029	1.030	n/a	1.021
C 13/6	n/a	3702	3840	138	n/a	138	n/a	1.000	1.037	n/a	1.000

The resulting diagrams of the ultrasonic velocities for beams are shown in Figure 2 and for cubes in Figure 3.

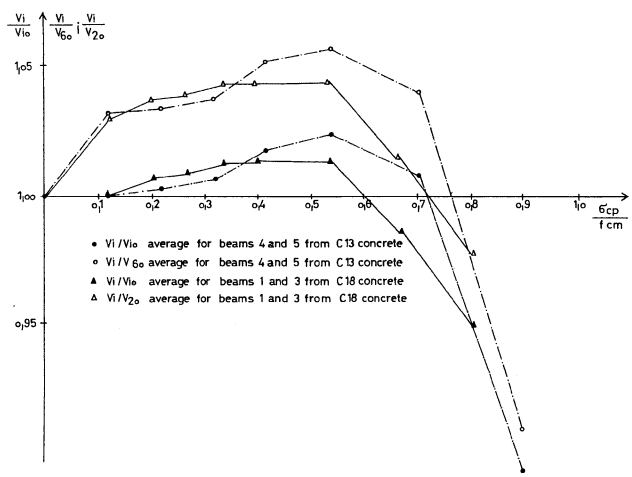

Figure 2 Ultrasonic velocities for test beam measurements

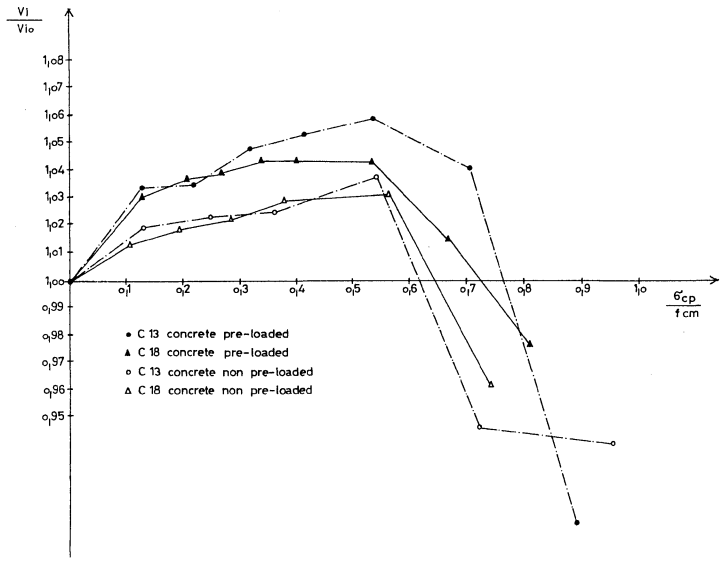

Figure 3 Ultrasonic velocities for test cube measurements

Table 4 The concrete strength variations in N/mm^2

TEST BEAMS	PRE-LOAD	σ_{io} [N/mm^2]	σ_{io}/σ_{2o}	σ_{io}/σ_{6o}	σ_{imax} [N/mm^2]	$\sigma_{imax}/\sigma_{io}$	$\sigma_{imax}/\sigma_{2max}$	$\sigma_{imax}/\sigma_{6max}$
C 18/1	+	34.8	1.18	n/a	39.6	1.14	1.17	n/a
C 18/3	+	38.3	1.29	n/a	41.8	1.09	1.24	n/a
C 18/2	n/a	29.6	1.00	n/a	33.7	1.14	1.00	n/a
C 13/4	+	18.7	n/a	1.23	21.2	1.13	n/a	1.12
C 13/5	+	18.2	n/a	1.20	21.9	1.20	n/a	1.15
C 13/6	n/a	15.1	n/a	1.00	19.0	1.26	n/a	1.00

The concrete strengths were calculated on the bases of the average ultrasonic velocities. The ultrasonic velocities were calibrated using the f_{cm} test values.

Discussion of the results

The pre-loaded beam and cube specimens showed 2-5% higher ultrasonic velocity than the non pre-loaded ones. This was due to higher density and consequently higher strength at each loading step. The relative strength increases were of the same range for both concrete classes (C13 and C18). The relative values of the ultrasonic velocity increases were the highest in the range of 0.5-0.6 of the ultimate strength. After these values the density of the concrete decreases a little due to the loosening of the microstructure and, consequently, the measured ultrasonic velocity, which is mainly based on concrete density, decreases too.

This is a very important remark for the load tests of existing structures. Such tests usually are carried out under a so-called "service load level", which very often constitute only 50-60% of the ultimate load. In this way one can get from the tests a 5-10% higher estimate for the ultimate concrete strength. This could lead to wrong conclusions and consequences.

Having this result, one could formulate a question whether or not these strength increases are only in the intermediate loading phases. To answer this question more tests would be of good use. But as far as at almost all the loading steps this range of relative increases were observed due to pre-loading (only the non pre-loaded elements had a smaller velocity range) the answer is no, the highest increases over initial strength values were taken at intermediate loading steps, but the relative strength increases were constant.

MATERIAL TESTS OF PRESTRESSED STRUCTURAL ELEMENTS

It was decided to demolish some large span prestressed concrete trusses after 40 years of service in a chemical factory. This gave a rare opportunity to make destructive tests [2], [3]. Core samples were taken from the prestressed and non prestressed parts of the structure. Altogether 14 core samples were tested. Most of the core samples were taken from the prestressed chord. Some of these samples were taken from the direction of prestressing and some at right angle to this direction.

The core samples were tested and two interesting remarks could be formulated. The first was in agreement with the results reported in the previous section. The core samples taken from the direction of prestressing showed 5-6% higher strength than the core samples taken from the right angle to this direction. This is resulting from the fact, that the compaction (density increase) is the highest in the direction of pre-loading or prestressing. If there are no lateral boundaries the pre-loading due to prestressing in the right angle to the prestressing direction will create no or much less compaction.

The second remark is also relative to the previous section. From the first remark one could estimate a further strength increase in the direction of the pre-loading if it would be possible to have made measurements along the longitudinal direction.

CONCLUSIONS

- The moderate pre-loading or prestressing of concrete structural elements at early ages leads to the compaction of concrete microstructure resulting in higher density and strength. This is the main reason of the concrete strength increase observed in the tests reported. The degree of this strength increase was in the range of 2-10%.

- The relative increase is the highest at the stress level of 50-60% of the concrete crushing strength., but will be observed throughout the whole loading process up to failure.

- Strength increase is observed first of all in the direction of pre-loading or prestressing.

ACKNOWLEDGEMENTS

The authors would like to acknowledge the support provided for the reported study by the Mecsek Ore Co., the Department of Bridges and Structures as well as the Department of Building Materials and Geology of the Budapest University of Technology and Economy, the Plc. for Quality Control and Innovation in Building (ÉMI, Budapest) and the Department of Strength of Materials and Structures of the Pécs University (Hungary).

REFERENCES

1. KUKAI T., Effect of pre-loading and stress level on the non destructive test results and on the compressive strength of concrete (in Hungarian), Doctoral Thesis, Budapest University of Technology, 1986 p. 1-105

2. LENKEI P., KOVÁCS K., Programme for comparison of NDT and DT methods of structural concrete evaluation, Proceedings of the RILEM-IMEKO International Conference *Non Destructive Testing and Experimental Stress Analysis,* Kosice 1998 p 125-132

3. LENKEI P., Report on the material testing results connected with the demolition of the chemical factory of the Mecsek Ore Co. (in Hungarian) 2001 p 1-

EFFECT OF LONGITUDINAL STEEL OR RCC MEMBERS UNDER TORSION

M P Aryal

N N Maharjan

Tribhuvan University

Nepal

ABSTRACT. This paper describes an experimental study carried out to determine the effect of longitudinal reinforcement on torsional parameters of reinforced concrete torsion dominant element with torque to flexural moment ratio (T/M) as 1. The study has been carried out in rectangular reinforced concrete beams with cross section 180 mm x 125 mm and length 1300 mm. Three groups of beam-specimens were prepared for the investigation with varying percentage of longitudinal reinforcement in tension as well as in compression. The percentage of shear reinforcements were the same in all types of beams. Nine types of reinforcement arrangements were adopted for study. Experimental studies show that under combined loading (T/M = 1), ultimate torque increases with the increase in the percentage of tensile steel, however with the increase of the compression steel, no significant change has been observed in the torque value. Experimental studies also show that under the combined loading, torsional toughness increases significantly with the increment of tensile reinforcement when the compression steel and stirrups are kept constant, whereas the same parameters does not increase with the increment of compression steel when the tensile steel and stirrups are kept constant. Study has also shown that the nature of torque - twist curve of a RCC beam in pre-cracking stage can be represented by a linear relationship up to half cracking torque and after that it can be represented by the second degree parabola up to the value of cracking torque. In the post-cracking stage, torque-twist relationship can be best represented by cubic parabola.

Keywords: Torsion, Torsional toughness, Torsional rigidity, Torque-twist curve, Cracking, Best-fit curve, Trend line.

M P Aryal is an associate Professor of Civil Engineering in the Institute of Engineering, Tribhuvan University, Kathmandu, Nepal. His research area focuses on concrete technology, durability of concrete and design of reinforced concrete structures.

N N Maharjan is a structural engineer in a consulting firm. He is currently involved in the design and construction activities in Nepal.

INTRODUCTION

Reinforced cement concrete (RCC) elements, widely used in construction works, undergo different types of loading in various combinations such as bending, shear, axial force and torsion. Domination of one or the other type of loading depends upon the type of the structural element. In most of the designs, in the past, torsion had been considered as secondary in importance due to the less complexities of structures. But the modern structures with their complex configurations require the consideration of torsional behaviour. Studies have shown that the capacity of a structure significantly decreases due to the effect of torsion in combination with transverse loading. Researches are underway in recent years to study the behaviour of RCC structures under torsion.

The problem of torsion in an elastic circular member was first studied at the end of the seventeenth and at the start of eighteenth centuries. The first theory for reinforced concrete elements subjected to torsion was proposed by Rausch in 1929 and it was later extended by Cowan, Lessig, Lampert and other researchers [1, 2].

Recent studies have established the interaction among torsion, flexure, shear and axial forces. But, in the behaviour of torsion in RCC structures many other parameters are also involved, which still require to be studied to consider all the aspects of complex behaviour. This paper presents some of the results of the experimental studies about the effect of longitudinal reinforcements on the behaviour of RCC beam under combined action of bending and torsion.

TORSIONAL CHARACTERISTICS OF CONCRETE BEAM

Behaviour of reinforced concrete elements under transverse loading and torque vary not only with respect to the level of loading but also with the type and percentage of reinforcement. Three theories are generally available to predict the torsional strength of plain concrete beams. They are elastic, plastic and skew-bending theories [1, 2]. The ultimate torsional strength of reinforced concrete beam is made up of two parts, namely, the contribution of concrete and that of the reinforcement. As mentioned by various authors, the behaviour of a reinforced concrete beam subjected to pure torsion is very different in pre-cracking and post-cracking stages. Knowledge of the complete behaviour of the structural element up to the failure in torsion domain structure is also an essential part in limit state design conception to forecast the vulnerability of the structure in case of major earthquakes or other similar catastrophic events.

There may be various parameters to consider the behaviour of RCC element under different levels of loading under torsion. Study on the torsional toughness of RCC beam with respect to equal volume of longitudinal steel and stirrups were carried out by the author [3]. In this paper, effect of tensile and compressive reinforcement on three torsional parameters of RCC beam i. e, torque, torsional toughness and torsional rigidity have been considered.

Torsion in concrete structures is generally accompanied by bending and shear. In order to consider this aspect as well as to limit the complications of experiments under torsion, the above mentioned torsional parameters have been studied with torque to bending moment ratio as 1 (T/M =1).

BASIS OF STUDIES AND INTERPRETATION

Experimental studies are the basis for the present investigation. Tests were conducted in cantilever beams with different percentages of tensile and compressive longitudinal reinforcements. Similarly, the three different parameters, adopted to reflect the behaviour of the beam, have been studied at various stages of loading. The torque-twist relationships at different levels of loading up to failure, has been interpreted from the experimental tests diagrams. (Refer figures 1, 2 and 3).

The slope of the torque - twist curve has been adopted as torsinal rigidity of the beam. The torque-twist diagram has been divided into pre-cracking and post-cracking parts with the distinction of linear and non-linear stages in the pre-cracking range. In order to observe the torsional rigidity at different stages, three points such as A, B and C have been selected in the torque-twist curve. Point A denotes the stage at half of the cracking torque, point B - cracking torque and point C - ultimate torque. The inclination of the lines joining the origin of the diagram with the points A, B and C are designated as torsional rigidity at half-cracking, cracking and ultimate loads. Similarly, the area under the torque-twist curve has been considered as torsional toughness of the beam and this has also been categorized at half cracking, cracking and ultimate loads. In calculating the torsional toughness and torsional rigidity, the respective angle of twist has been considered in radians.

The above mentioned parameters have been calculated for beams with various longitudinal reinforcements. The experimental results are presented in the forms of figures, equations and tables.

LIMITATION

The study has been conducted on rectangular beams. Only three groups of beam-specimens have been studied. These groups differ from each other in terms of the percentage of tensile and compressive reinforcements. The shear reinforcements are kept constant for all types of beams. Similarly, the results are limited to the torque to bending moment ratio as 1 and no effect of shear force has been considered.

EXPERIMENTAL INVESTIGATION

Preparation of Specimens

Nine different types of reinforced beam-specimens were prepared for investigation. The cross-sectional area of the specimen was 180 x 150 mm and the overall length was 1300 mm. Three groups of specimens were prepared for the investigation. In each of the sets 3 to 4 beams were prepared and altogether 34 beams were casted. The characteristic cube strength of concrete used was 25 MPa. In the first group, the compression steel was 0.5 percent of the cross sectional area of the section and the stirrups were 4.75 mm diameter placed at 55 mm center to center, the percentage of tensile steel (p_t) were 0.50, 1.04 and 1.52. In the second group, the compression steel used was 0.79 percent and the spacing of the stirrups were kept constant but the percentage of tensile reinforcements were 1.13, 1.52, 2.02 and 2.40. And in the third group, the percentage of tensile reinforcements and the spacing of the stirrups were kept constant (p_t = 1.52 percent and stirrups - 4.75 mm diameter placed at 55 mm center to

center) but the percentage of the compressive reinforcements were 0.50, 1.04 and 1.40. The steel grade was Fe 415 for longitudinal bars and Fe 500 for stirrups. The details of the specimens are shown in Table 1.

Table 1 Reinforced concrete beam-specimen details

SN	BEAM IDENTIFICATION	p_t, %	p_c, %	s_v*, mm
Group - I				
1	$RBAL_1S$	0.50	0.50	55
2	$RBAL_2S$	1.04	0.50	55
3	$RBAL_9S$	1.52	0.50	55
Group - II				
4	$RBAL_6S$	1.13	0.79	55
5	$RBAL_7S$	1.52	0.79	55
6	$RBAL_8S$	2.02	0.79	55
7	$RBAL_{8a}S$	2.40	0.79	55
Group - III				
8	$RBAL_9S$	1.52	0.50	55
9	$RBAL_{10}S$	1.52	1.04	55
10	$RBAL_{11}S$	1.52	1.40	55

s_v* - spacing of 2 legged stirrups.

Note: Yield stress of longitudinal reinforcing bar (f_y) = 415 MPa;
Yield stress of stirrups (f_{yv}) = 500 MPa.

Testing

Testing was carried out in the universal testing machine with its loading capacity of 22 KN. The specimens were tested as cantilever beams. In order to provide fixed support condition at one end and loading at another, special steel frame arrangements with the loading system were prepared. Under such arrangements the torque to bending moment ratio (T/M) can be varied from 4.0 to 1.0. However, in this study the value was limited to 1.0. The RCC beam was fixed at one end in the supporting frame; at the other end, loading frame was attached. The loading frame itself to the next end was loaded by the machine at its loading axis. Both of the effective lengths of the beam as well as loading frame to create bending moment and torque were 1.0 m.

The load - deflection curve along the loading axis of the machine was continuously observed in computer screen. The bending moment in the beam-specimen was calculated directly multiplying the machine load and half of the loading frame weight with the effective span of the beam, whereas, the torque (T) and twist angle (θ) were calculated as follows:

$$T = P \cdot L_f + P_f \cdot \frac{L_f}{2} \qquad (1)$$

$$\theta = \tan^{-1} \frac{\left(\frac{a}{b}\right)}{c} \qquad (2)$$

Where P = machine load; L_f = effective span of loading frame;
P_f = weight of loading frame; θ = twist angle in degree/unit length;
a = deflection along machine load axis due to torque only;
b = effective span of the loading frame; c = effective span of the beam.

Torque-twist (T - θ) relationships, torsional toughness and torsional rigidity were obtained for each type of the specimens. In order to calculate the torsional toughness and torsional rigidity, twist angles in each testing were converted to radians.

The torque-twist diagrams (Figures 1, 2 and 3) reflect the behaviour of the beams at different levels of loading. The first cracking load was observed in the diagram on the monitor and this was simultaneously verified by observing the cracks developed in the beams during the process of testing.

Result Analysis and Discussion

Based on the results of the torque - twist diagrams presented in figures 1, 2 and 3 as well as torsional toughness and torsional rigidity presented in Table 2, the behaviour of each of the beam specimens has been analyzed in pre and post cracking stages.

Table 2 Torque, torsional toughness and torsional rigidity of reinforced concrete beams.

BEAM SPECIMENS	ULTIMATE TORQUE (T_u)	TORSIONAL TOUGHNESS, N-mm^2 x 10^{12}			TORSIONAL RIGIDITY (T/θ), N-mm^2 x10^{10}		
	KN-m	Upto $T_{cr}/2$	Upto T_{cr}	Upto T_u	Upto $T_{cr}/2$	Upto T_{cr}	Upto T_u
1	2	3	4	5	6	7	8
Group I							
$RBAL_1S$	3.35	2.36	13.52	237.15	18.40	14.60	3.70
$RBAL_2S$	3.57	4.33	19.73	226.70	18.70	17.20	4.40
$RBAL_9S$	4.25	3.68	40.04	268.56	35.80	17.70	5.40
Group II							
$RBAL_6S$	4.16	5.77	39.95	211.99	22.50	15.50	6.20
$RBAL_7S$	4.47	5.52	61.25	304.72	25.10	12.20	5.00
$RBAL_8S$	4.90	4.77	64.77	337.99	32.60	13.50	5.50
$RBAL_{8a}S$	5.26	7.16	76.23	403.85	30.90	15.70	5.60
Group III							
$RBAL_9S$	4.25	3.68	40.04	268.56	35.80	17.70	5.40
$RBAL_{10}S$	4.22	5.52	35.67	262.78	17.10	12.30	4.90
$RBAL_{11}S$	4.00	3.79	28.77	287.99	18.20	11.20	4.10

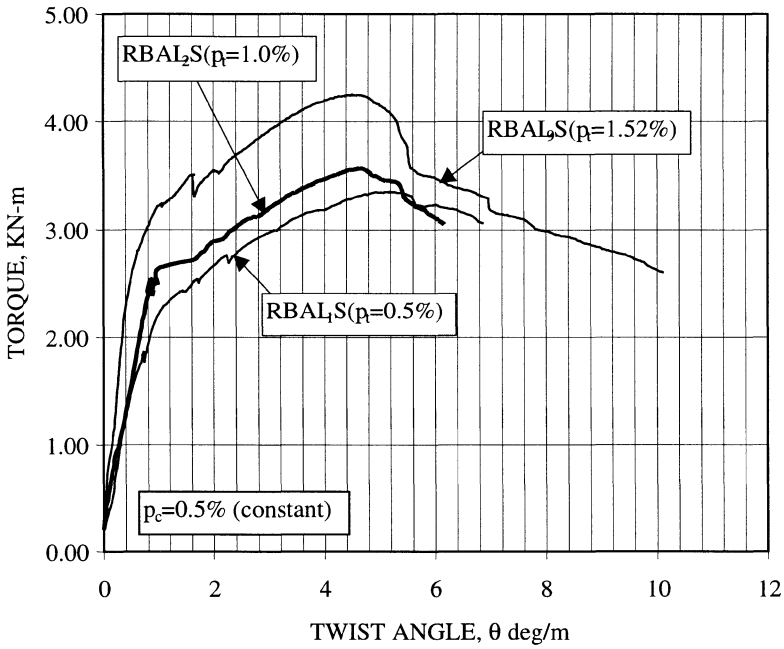

Figure 1 Torque-twist curve of beams $RBAL_1S$, $RBAL_2S$ & $RBAL_9S$

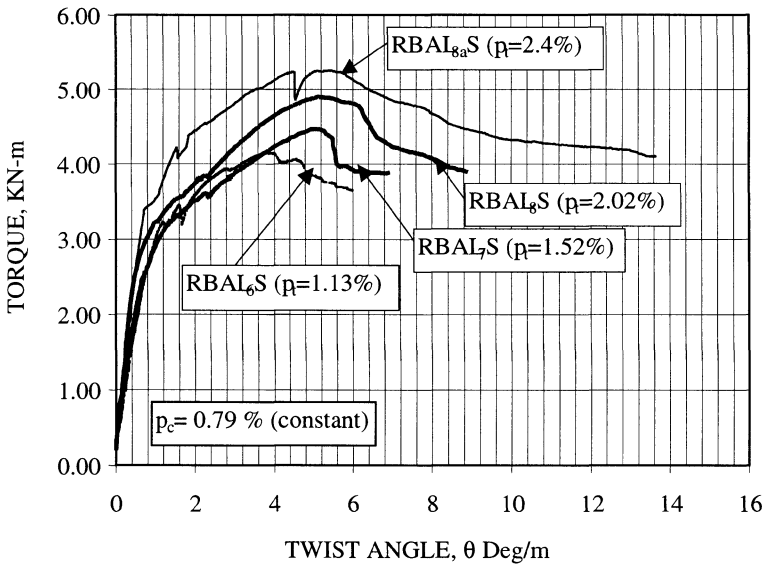

Figure 2 Torque-twist curve of Beams $RBAL_6S$, $RBAL_7S$, $RBAL_8S$ & $RBAL_{8a}S$

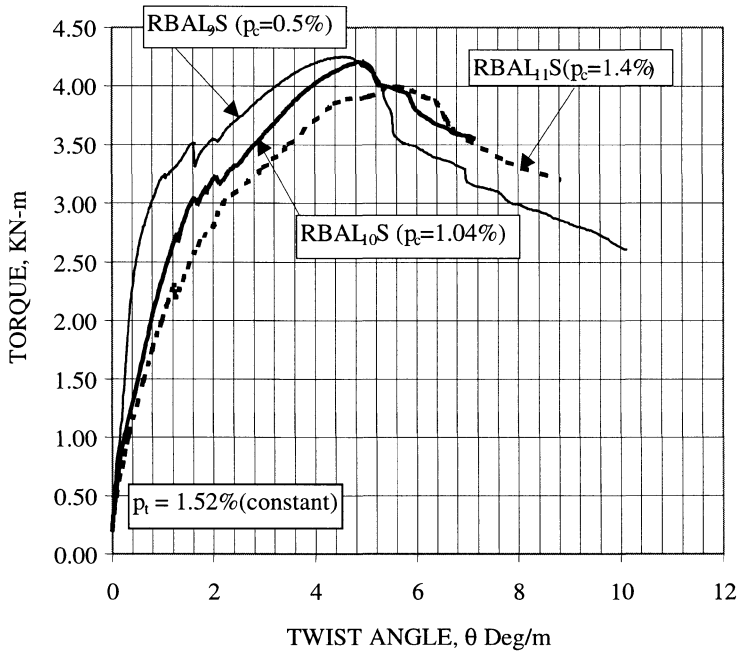

Figure 3 Torque-twist curve of beams $RBAL_9S$, $RBAL_{10}S$ & $RBAL_{11}S$

Pre-cracking stage of the torque - twist diagram has been divided into two parts - linear and non-linear. The torque-twist relationship up to half cracking torque ($T_{cr}/2$) is taken as linear and beyond it up to cracking - nonlinear. The non-linearity continues up to ultimate torque. The best-fit curves of the torque-twist diagrams were developed for each of the linear and non-linear parts for all of the nine specimens. The best-fit curve for the non-linear pre-cracking range is found in the form of second degree parabola, whereas in the range of post-cracking stage the torque-twist relationship can be best represented by cubic parabola.

Data of the torque-twist curve from the first group of the specimen show that the ultimate torque increases with the increase of tensile reinforcement. The increment of ultimate torque is about 26 percent with the increment of tensile reinforcement from 0.50 to 1.52 percent. In the second group of the specimen as well, with the higher percentage of the compression steel compared to the specimens in first group, the behaviour remains almost the same. In this group the ultimate torque is increased by about 26 percent with the increase of tensile reinforcement from 1.13 to 2.40 percent. However, in the third group of the specimen, the ultimate torque decreases by about 6 percent with the increment of compression reinforcement from 0.50 to 1.40 percent.

Experimental investigation also shows that the tensile reinforcement has insignificant effect on torsional toughness at half cracking load. But at the cracking and ultimate loads the effect is relatively significant. From the results of the first and second groups of specimens it has

been observed that the average increase of torsional toughness at the half cracking load is about 40 percent; at the cracking and ultimate loads the parameter increase by about 150 and 50 percents respectively. But from the results of the third group of specimens it can be observed that the parameter does not change at half cracking and ultimate loads. But at the cracking load its value has been decreased by about 28 percent.

Similarly, data on the torsional rigidities show that at half cracking load, this parameter, with the specimens from the first and second groups, is increased by an average value of about 65 percent with the increment of tensile reinforcement. However, at cracking and ultimate loads the increment is very insignificant. But in the case of third group of the specimens the respective values have been found decreased by about 45, 35 and 25 percents.

Trend lines have been proposed for all of the three torsional characteristics with respect to the change in longitudinal reinforcements. This has been done in order to minimize the effect of the scatter of the test data. The equations of the trend lines for ultimate torque as well as for torsional toughness and torsional rigidity at three different levels of loading are presented in Table 3.

Table 3 Equations of trend lines

PARAMETERS	LOADING LEVEL	SPECIMEN GROUP I	SPECIMEN GROUP II	SPECIMEN GROUP III
Torque, KN-m	Ultimate	$y = 0.873x + 2.833$	$y = 0.863x + 0.172$	$y = 0.476x - 0.930$
Torsional Toughness,	Half cracking	$y = 1.343x + 2.087$	$y = -0.133x + 6.310$	$y = 1.855x + 0.992$
N-mm^2 x10^{12}	Cracking	$y = 25.699x - 1.783$	$y = 25.704x + 5.119$	$y = -7.045x + 0.401$
	Ultimate	$y = 29.754x + 213.79$	$y = 139.8x + 67.547$	$y = 65.829x + 23.84$
Torsional Rigidity,	Half cracking	$y = 16.717x + 7.249$	$y = 8.9372x + 12.479$	$y = -21.257x + 4.365$
N-mm^2 x 10^{10}	Cracking	$y = 3.076x + 13.362$	$y = -1.420x + 20.635$	$y = -5.9064x + 0.022$
	Ultimate	$y = 1.659x + 2.808$	$y = -0.278x + 6.067$	$y = -0.5848x + .6398$

Note:

y - respective values of torque / torsional rigidity / torsional toughness.

x - percentage of respective longitudinal reinforcement for different specimen groups as mentioned in Table 1.

CONCLUSION

The following conclusion are drawn from the investigation:

1. Under the combined action of torsion and transverse loading (T/M = 1), ultimate torque increases with the increase in the percentage of tensile steel. However, with the increase of the compression steel, there is no increment of the ultimate torque.

2. There is no effect of tensile reinforcement on torsional toughness at half cracking load, however, the parameter is increased at the cracking and ultimate loads. The increment has been observed more at pre-cracking load compared to the ultimate one.

3. Torsional rigidity of RCC beams at half cracking load moderately increases with the increment of compression reinforcement. However, at cracking and ultimate loads this parameter decreases with the increment of compressive reinforcement.

REFERENCES

1. THOMAS, T.C. HSU, Torsion of Reinforced Concrete, Van Nostrand Reinhold Company, 1984, 516 pp.

2. PANDIT, G.S., GUPTA, S.P., Torsion in Concrete Structures, CBS Publishers and Distributors, New Delhi, 1983, 512 pp.

3. ARYAL, M.P., SHRESTHA, J.M., Torsional Toughness of Reinforced Concrete Beam. South-Asian Countries Conference on Challenges to Architects and Civil Engineers during Twenty-First Century. Nepal Engineering College in Association with Nepal Engineer's Association, Vol. 2, April 7–9, 1999, pp 962-969.

THEME FOUR:

DESIGN FOR ACCIDENTAL DAMAGE

Keynote Paper

PERFORMANCE OF REINFORCED CONCRETE PILES EXPOSED TO MARINE ENVIRONMENT

P Paramasivam

C T E Lim

K C G Ong

National University of Singapore

Singapore

ABSTRACT. Six marine piles were extracted from the Port of Singapore after 32 years in service. The wharf was repaired 22 years after installation due to excessive corrosion of its under deck structures. Remedial work using the jacketing method with prepacked aggregates and grouting techniques was used to reinstate the deteriorated concrete. The wharf was eventually demolished to make way for modern container facilities. The piles were extracted in the process to examine their residual properties. This present paper compares numerical predictions, using Fick's second law of diffusion, against concentration profile of water-soluble chloride obtained from the atmospheric, tidal and submerged zones of the piles. Concentrations of water-soluble chloride at the level of steel reinforcement were compared with the loss in mass of the reinforcing bars. The results show that the numerical estimates were in good agreement with the actual values of water-soluble chloride concentrations obtained under Singapore conditions. From regression analysis, diffusion parameters and threshold concentrations of water-soluble chloride for steel corrosion were calculated and these provided useful means in design of estimating the service life of concrete in the local marine environment.

Keywords: Concrete marine environment, Fick's second law of diffusion, Service life, Water-soluble chloride.

P Paramasivam is Professor in the Department of Civil Engineering, National University of Singapore. He has been actively involved in R&D application of ferrocement and fibre reinforced cement composites.

C T E Lim is Senior Professional Officer in the Department of Civil Engineering, National University of Singapore. His fields of interest are in fracture of concrete, and repair and strengthening of reinforced concrete structures.

K C G Ong is an Associate Professor in the Department of Civil Engineering, National University of Singapore. His research interest includes ferrocement, composite materials, and repair and appraisal of reinforced concrete structures.

INTRODUCTION

Research over the years has shown that permeability of concrete is an important factor affecting the durability of concrete structures. Permeability, rather than cement composition, has been identified as one of the more important parameters affecting the chemical resistance of concrete structures when exposed to seawater [1]. The alkaline nature of concrete made from normal Portland cements serves to provide a natural protection against corrosion of steel bars embedded as reinforcement. However, the presence of chloride in small quantities, depending on the Cl /OH ratio, tends to destroy this passivity of steel reinforcement even at a pH considerably above 11.5 [2]. Chloride may enter into concrete as a result of exposure to high chloride environment. Using various mathematical models, the rate of chloride ingress into concrete due to long-term exposure to marine environments may be estimated and the service life and maintenance programme for such structures planned in advance [3]. In the present study, the ingress of water-soluble chloride into concrete piles extracted after 32years of service and exposure to the local marine environment was investigated. Lengths of the extracted piles covered the atmospheric, tidal and submerged zones. Concentration of water-soluble chloride in the concrete was compared with numerical predictions using Fick's second law of diffusion [4 and 5]. Presence of water-soluble chloride at the level of steel reinforcement was compared with the loss in mass of the reinforcing bars. The results demonstrate the usefulness of this mathematical model in predicting the service life of reinforced concrete structures exposed to the local marine environment.

BACKGROUND

Located on the eastern section of Keppel Harbour at the south of Singapore island, the wharf was designed to handle shipments of general cargo with provision for storage facilities (godowns). Built during the period March 1960 to 1962, the wharf was constructed as a piled structure with decks supported on bents of cast in-situ reinforced concrete beams spanning between 406mm (16in.) or 457mm (18in.) square piles as shown in Figure 1. The spacing between beams was about 4.57m (15ft). Spacing of supporting piles along the beams varied from 3.05m (10ft) under the storage section (godowns) to 4.95m (16ft 3in.) at the apron.

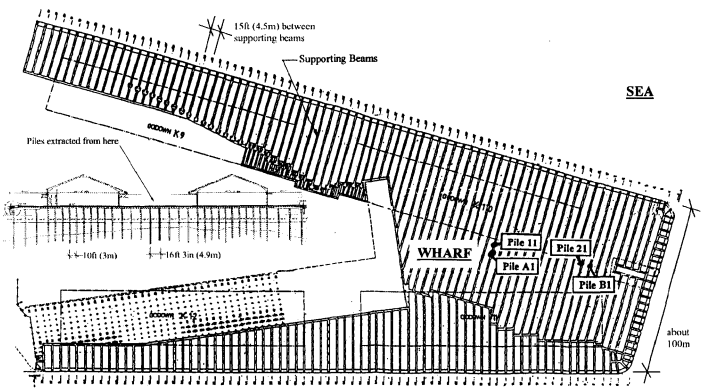

Figure 1 Plan of wharf and locations of extracted piles

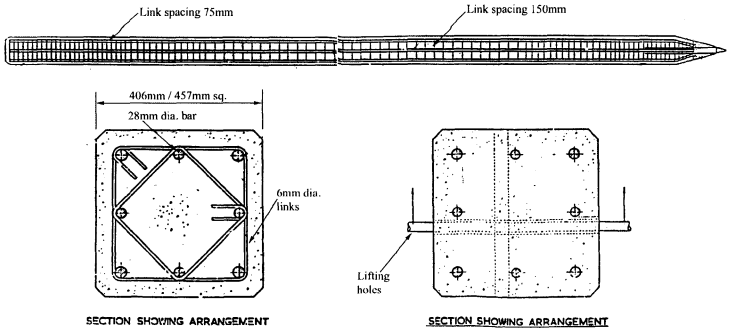

Figure 2 Reinforcement details of piles

The piles were of plain reinforced concrete, without any surface coating, fitted with rock shoes and driven to a minimum penetration depth of 1.52m (5ft) into underlying shale to ensure fixity. The depth to the shale varied between 4.57m (15ft) to 18.29m (60ft) below the soffits of the crossbeams. The piles extracted were reinforced with 28mm ($1^1/_8$in.) diameter longitudinal bars and 6mm ($^1/_4$in.) diameter links at 75mm and 150mm spacing with 50mm notional concrete cover. Reinforcement details of the piles are shown in Figure. 2. A concrete mixture of 414kg Portland cement, 621kg fine aggregate, 1242kg coarse aggregate per m^3 of concrete with water/cement ratio (W/C) of 0.4 was used. Minimum cube strengths of 28MPa at 7days and 38MPa at 28days were obtained from work tests during construction.

After about 22years in service, maintenance inspection revealed that the underdeck reinforced concrete beams, slabs and top 1m section of the piles, within the atmospheric and upper tidal zones, were badly spalled and the reinforcements severely corroded. Remedial work using the jacketing method with prepacked aggregates and grouting techniques to reinstate the deteriorated concrete was carried out in February 1985 and completed in September 1986.

ANALYTICAL CONSIDERATION

Theoretical Concentration Profile

The ingress of water-soluble chloride into concrete is commonly assumed to be a pure diffusion process through pore waters held in the concrete microstructures, [4-7]. The mode of transport of the water-soluble chloride may be described by Fick's second law of diffusion, effects of hydrostatic pressure on diffusion are neglected in this analysis [5]. The one-dimensional diffusion equation takes the form of:

$$\frac{\partial C_{x,t}}{\partial t} = D_c \frac{\partial^2 C_{x,t}}{\partial x^2} \tag{1}$$

where $C_{x,t}$ is the chloride concentration at depth, x, at time, t,
D_c is the chloride diffusion coefficient of the concrete,
x is the depth from the exposed surface of the piles,
and t is the exposure duration.

In a semi-infinite medium and where the surface concentration, $C_{x,t}$ at x =0 is unchanging, the solution of Equation (1) yields;

$$C_{x,t} = C_o[1 - erf(\frac{x}{2\sqrt{D_c t}})] \tag{2}$$

where C_o is the apparent concentration at the surface, assumed to be constant,
and $erf(z)$ is the error function which was proposed by Crank [5] as:

$$erf(z) = 1 - (1 + a_1 z + a_2 z^2 + a_3 z^3 + a_4 z^4)^{-4} \tag{3}$$

with constants $a_1 = 0.278393$,
$a_2 = 0.230389$,
$a_3 = 0.000972$, and
$a_4 = 0.078108$.

When concrete is always in seawater, it may be assumed that the chloride content of the exposed surface, C_o, is in equilibrium with the concentration of the salt in seawater, and is constant. Equation (2) is therefore appropriate to describe the case of concrete in the submerged zones.

Takewaka and Mastumoto [6] modified the solution of Equation (1) to take into account the repeated wetting and drying which occurs in the splash or tidal zones. They assumed a constant rate of deposition per unit time, W_o, on the exposed surface and that eventually all the deposited chloride penetrates into the concrete. The accumulation of each individual diffusion profile is found by integrating Equation (1) over the exposure period. The following diffusion profile for chloride ion intrusion in the splash or tidal zones was thus obtained as:

$$C_{x,t} = 2W_o\{\sqrt{\frac{t}{\pi D_c}} \times e^{-x^2/4D_c t} - \frac{x}{2D_c}[1 - erf(\frac{x}{2\sqrt{D_c t}})]\} \tag{4}$$

The value of W_o is expected to vary considerably depending on geographical conditions, wind direction, etc.

Given a specific external environment, categorised by the values of C_o and W_o, the diffusion coefficient, D_c, determines the rate of ingress of chloride ions into the concrete and is solely a function of its permeability. It is expected that D_c is affected by W/C and type of cement used, and that it would decrease with longer exposure duration. The diffusion coefficient, D_c, was empirically determined by Takewaka and Mastumoto [6] for temperate conditions;

$$\log(D_{w/c}) = -6.274 - 0.076(w/c) + 0.00113(w/c)^2 \tag{5}$$

and $$D_c = D_{w/c} \times D_1 \times T^{-0.1} \tag{6}$$

where $D_{w/c}$ is the diffusion coefficient affected by W/C of the concrete,
w/c is the W/C of the concrete expressed in percent
T is the exposure period in years,

and D_1 is a constant depending on cement type, which is:
= 1.00 for ordinary Portland cement,
= 1.20 for high early strength Portland cement,
= 0.30 for blast furnace Portland cement,
= 0.08 for high alumina cement.

By fitting the above equations to water-soluble chloride concentration profiles experimentally obtained from specimens exposed, for up to 30years, under various marine environments in Japan, both simulated and actual, Takewaka and Mastumoto [6] found that the environmental parameters typically varied between the following ranges;

C_o ≅ 0.7% to 1.0% by mass of concrete
W_o ≅ 0.01% to 0.1% by mass of concrete . mm per month in the splash and tidal zones,
≅ 0.001% to 0.01% by mass of concrete . mm per month in the atmospheric zone, and
D_c ≅ 10^{-6} to 10×10^{-6}mm^2/s depending on W/C used.

Values reported by Browne [7] for data obtained from offshore and coastal structures in the Baltic Sea and Atlantic Ocean also showed that:

D_c ≅ 5×10^{-6}mm^2/s for grade 30 concrete
≅ 0.1×10^{-6}mm^2/s for grade 50 concrete.

Threshold Concentration of Water-Soluble Chloride to Initiate Corrosion

Takewaka and Mastumoto [6] observed that under temperate conditions the critical concentration of water-soluble chloride to cause steel corrosion ranged between 0.03 to 0.10% by mass of concrete. The former occurred mainly in the atmospheric and splash/tidal zones while the latter in the submerged zones. The disparity was attributed to the difference in the availability of oxygen needed for corrosion to take place in the various zones. Investigations by Browne [7] revealed that under temperate conditions the concentration of water-soluble chloride to initiate corrosion was between 0.2 to 0.4% by mass of cement. Thus, assuming for the present study, a mixture proportion as given above and density of 2442kg/m^3 as documented in available construction records, these threshold concentrations to initiate corrosion of reinforcement steel would therefore be between 0.034 to 0.068% by mass of concrete. Similarly, Mindess and Young [8] noted that the critical water-soluble chloride concentration to initiate corrosion was 0.6 to 1.2kg Cl /m^3 of concrete (or approximately 0.025 to 0.050% by mass of concrete). Mehta and Monteiro [9] reported that for typical concrete mixtures, normally used in practice, the threshold water-soluble chloride content to initiate corrosion is in the range 0.6 to 0.9 kg of Cl /m^3 of concrete (or approximately, 0.025 to 0.037% by mass of concrete). Hussain et al [2] found that, from specimens tested in the Arabian Gulf region, the threshold of free (water-soluble) chloride content was 0.22 to 0.29% by mass of cement (approximately 0.037 to 0.050% by mass of concrete) and was independent of the tricalcium aluminate content of the cement. The wide range in threshold values reported maybe due to differences in the Cl /OH ratio of the concretes used, availability of oxygen needed for steel corrosion and electric resistivity of the concrete tested.

In summary therefore, the threshold concentration of water-soluble chloride to initiate steel reinforcement corrosion in concrete may be about 0.025% by mass of concrete for the atmospheric zone and about 0.037 to 0.1% by mass of concrete for the tidal/submerged zones.

EXPERIMENTAL INVESTIGATION

In this study the concentration profile of water-soluble chloride and the corresponding degree of corrosion of reinforcing steel in piles extracted from a wharf structure in Singapore were examined. Samples were taken from the atmospheric, tidal, and submerged zones. The piles were extracted from the interior of the wharf, midway between the seaward and landward side, as shown in Figure 1. Locations of piles E11 and E21 were not documented but it is likely that they came from the same area as the rest of the piles because they were extracted at about the same time as the wharf was being demolished. Figure 3 shows a typical pile being examined.

Visual Observation

Generally, the top portions of the extracted piles were thickly coated with fuel oil, while barnacles were found in abundance on sections of the piles in the submerge zones. In Pile B1, the concrete cover over a length of about 1m within the upper tidal zone was spalled, exposing badly corroded main reinforcement bars and missing links. Cracks running along the longitudinal reinforcement bars were discovered at the tidal zones of Piles 11, 21, A1, B1, and E11. Rust stains and yellowish-orange leachate could be seen exuding from some of the cracks indicating that corrosion was still active in the extracted piles. The submerged zones of all the piles were generally in good condition with no visible signs of cracks or rust stains when the barnacles were removed.

Determination of Water-Soluble Chloride

The ingress of chloride into the concrete was determined from the concentration of water-soluble chloride in concrete fines extracted using the drill and suction method, shown in Figure 3. Samples were taken from boreholes at depth intervals of 20mm to a depth of 200mm. Two adjacent boreholes spaced 200mm apart were made at approximately 1m intervals along the entire length of the piles, thus giving samples from the atmospheric, tidal and submerged zones. The concrete fines were sieved through a screen of 150μm aperture. The finer material was then weighed and dissolved in 100ml of deionised water after stirring for an hour. The solution was filtered to remove any remaining suspension and the filtrate analysed for water-soluble chloride in an ion-chromatograph. The concentration of water-soluble chloride obtained was expressed as percentage by mass of the concrete fines. In total 1020 samples were obtained and analysed.

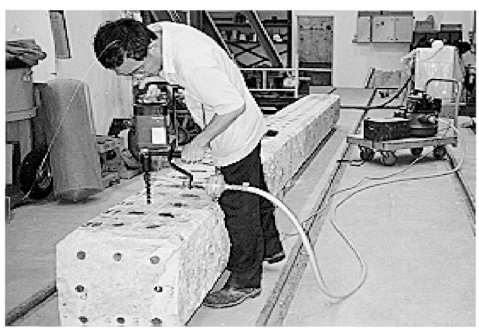

Figure 3 Typical pile being sampled for water-soluble chloride

Determination of Reinforcement Corrosion

The degree of corrosion was determined by measuring the gravimetric weight loss of the reinforcement bars extracted from 100mm diameter cores taken at about 2m intervals along the entire length of the piles at sections in the atmospheric, tidal and submerged zones. A solution of concentrated hydrochloric acid with antimony trioxide and stannous chloride, commonly known as Clarke's solution, was used to dissolve the oxidation products present on the steel reinforcement. After chemical etching, gross diameters of the less corroded bars extracted were measured physically using a vernier calliper of accuracy 0.005mm, and found on average to be about 28.08mm with a standard deviation of 0.37mm for the main longitudinal bars and about 6.13mm with a standard deviation of 0.19mm for the links. These agree with the specified diameters of 28.57mm ($1^1/_8$ in.) and 6.35mm ($^1/_4$ in.) from the original design drawings, as shown in Figure 2. Since the actual initial diameters of the reinforcement bars embedded in the piles some 32years ago were not documented, the difference between the effective diameter after treatment and that of the least corroded reinforcement bar was used as an indication of the degree of corrosion. The effective diameter after treatment was obtained from the ratio of volume of the treated bar, measured using buoyancy method, divided by its length. The bars were then weighed and their densities calculated. The change in diameters was then expressed as the loss in weight due to corrosion. In total 96 bar samples extracted from the atmospheric, tidal, and submerged zones of the piles were examined.

RESULTS AND DISCUSSION

Figure 4 shows the result of the various tests performed on the extracted piles. As the piles were extracted without clear demarcation of the actual exposure conditions, locations of atmospheric, tidal and submerged zones were distinguished by visual inspection. The upper limit of the barnacle growth was taken to be the level of the lowest low tide, L.W.O.S.T. (Lowest Water of Spring Tide), as was done by Gourley and Bieniak [4], to differentiate the submerged zones from the tidal zones. This level was found to range between 3.8m and 4.4m below the top of the piles. From the PSA report on underdeck repairs [10], the tidal range was taken as 3m from L.W.O.S.T. at 0.00ft Singapore Harbour Board (S.H.B.) Datum to H.W.O.S.T. (Highest Water of Spring Tide) at 9.00ft (approximately 3m) S.H.B. Datum.

Concentration of Water-Soluble Chloride

Chemical analysis of the concrete fines showed the concentration of water-soluble chloride decreasing with depth into the interior of the piles. Typically, the presence of water-soluble chloride was more concentrated in sections in the tidal zones and least concentrated in sections in the atmospheric zones of the piles. The apparent surface concentrations were about 0.7% by mass of concrete at sections of about 1.5m above the L.W.O.S.T., in the tidal zones. Further down the length of the piles, however, the apparent surface concentration reduced to about 0.4% by mass of concrete at sections about 2m below the L.W.O.S.T., in the submerged zones. In comparison, the apparent surface concentrations within the atmospheric zones were only about 0.2% by mass of concrete. The periodic wetting and drying due to wave and tidal action therefore contributed to the greater accumulation and penetration of water-soluble chloride into the concrete in the tidal zones. This is consistent with observations made by Gourley and Bieniak [4] and Takewaka and Mastumoto [6].

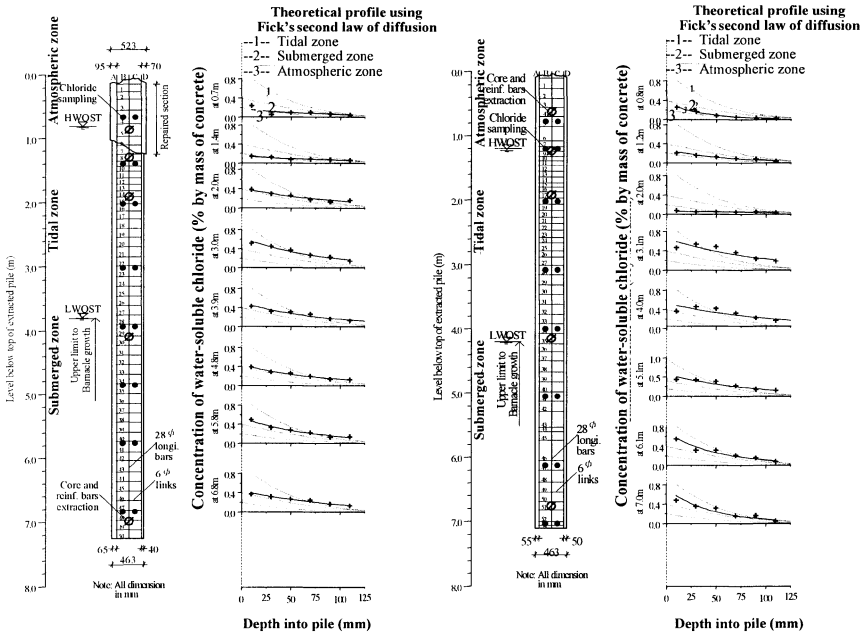

Pile 11, top 1.5m was repaired in 1985 Pile A1, did not require repair in 1985

Figure 4 Typical results of repaired and original piles, respectively

The concentration of water-soluble chloride along the piles may be divided into three distinct concentration profiles corresponding to the atmospheric, tidal and submerged zones as approximated by theoretical concentration profiles calculated using Fick's second law of diffusion, Equations (2) and (4). These are plotted as dashed line in Figure 4. In general, the concentration profiles obtained for the atmospheric, tidal and submerged zones are in agreement with the theoretical distributions calculated using Fick's second law.

Figure 5 show the concentration profile plotted according to the assumed atmospheric, tidal and submerged zones. By curve fitting, the theoretical profile onto the experimental data the following environmental parameters were obtained:

$$C_o = 0.391\% \text{ by mass of concrete}$$
$$W_o = 0.21\% \text{ by mass of concrete . mm per month for tidal zone}$$
$$= 0.04\% \text{ by mass of concrete . mm per month in atmospheric zone}$$
$$D_{w/c} = 3.12\times10^{-6}\text{mm}^2/\text{s}$$
$$D_c = D_{w/c}\times1\times(32)^{-0.1} = 2.21\times10^{-6}\text{mm}^2/\text{s}$$

The results showed a lower C_o but higher W_o than reported by Takewaka and Mastumoto [6] which was obtained for temperate conditions. The value of D_c was within the range discovered by Takewaka and Mastumoto [6] of 10^{-6}mm^2/s to 10×10^{-6}mm^2/s and Browne [7] of 5×10^{-6}mm^2/s for grade 30 concrete.

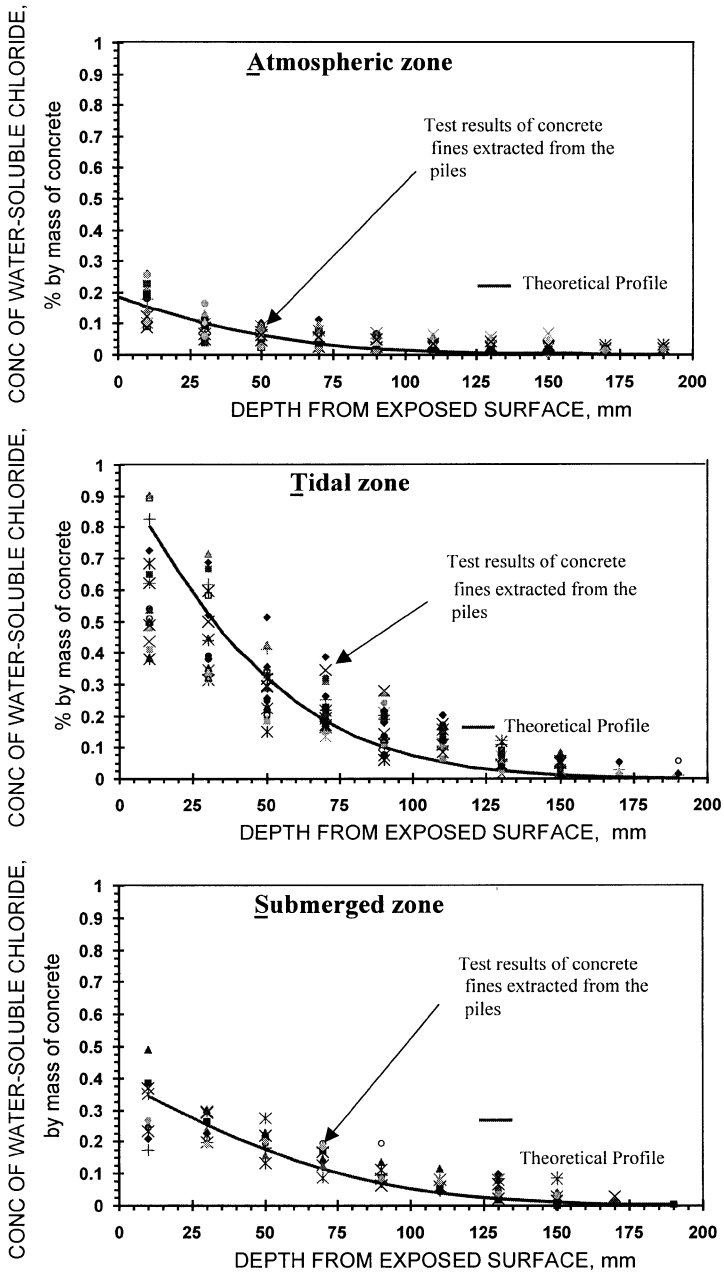

Figure 5 Concentration profile of water-soluble chloride in the various zones

Threshold Concentration

A plot of water-soluble chloride concentrations at the depth of the steel reinforcements and the corresponding loss in mass of the extracted reinforcement bar samples is shown in Figure 6. There is, however, no obvious relationship between these parameters. This is expected as the water-soluble chloride may have migrated to the level of the reinforcement bars through the concrete or through cracks resulting from the expansive formation of steel corrosion products.

In the atmospheric zone, significant loss in reinforcement mass was found even where water-soluble chloride concentrations was as low as 0.025% by mass of concrete. However, in the tidal and submerged zones, loss in reinforcement mass was only found where water-soluble chloride concentration exceeded 0.05% by mass of concrete. Therefore, the threshold concentration of water-soluble chloride to initiate steel reinforcement corrosion in Singapore's marine environment maybe appropriately taken as about 0.025% and 0.05% by mass of concrete, corresponding to the atmospheric and tidal/submerged zones, respectively.

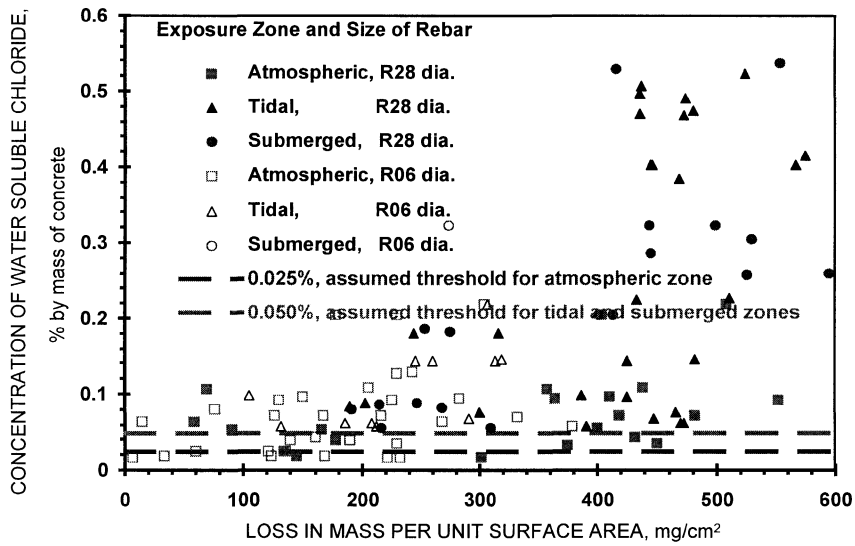

Figure 6 Concentration of water-soluble chloride present at the depth of reinforcement and their corresponding apparent loss in mass of reinforcement bars due to corrosion

Comparison of Numerical Model with Actual Observation

The results therefore show that for a concrete cover of 50mm, as was found in the original piles, the concentration of water-soluble chloride exceeded the threshold to initiate corrosion within a period of about 20, 7 and 10years in the atmospheric, tidal, and submerged zones, respectively.

These are estimated assuming a threshold concentration of 0.025% and 0.05% by mass of concrete for the atmospheric and tidal/submerged zones, respectively. The results therefore agree with observations made during maintenance inspections [11] carried out on the piles after 22years in service which revealed that severe reinforcement corrosion had occurred in the underdeck structure and supporting piles (in the atmospheric zone) of the wharf. This agrees with the prediction of service life described by Vesikari [12]. Equation (2) and (4) may thus be used, with the environmental parameters obtained above, to estimates of the service life of the structure under tropical conditions. Procedure for the prediction of service life is described in detail by Vesikari [12]. It is expected that the above graphs may not be readily applicable to new structures constructed in recent years as they do not take into account the significant mineralogical changes in the composition of ordinary Portland cement, new mix design and concrete manufacturing methods, and widespread use of admixtures such as ground granulated blast-furnace slag and fly ash.

CONCLUSIONS

In summary, therefore, the findings from the above experimental investigation into the condition of 32 year-old reinforced concrete marine piles may be summarised as follows:

1. The concentration profiles of water-soluble chloride into the piles in the submerged zones were in close agreement with theoretical distributions based on Fick's second law of diffusion.

2. Diffusion profile proposed, by Takewaka and Mastumoto [6], for chloride ion intrusion in the splash or tidal zones, Equation (4), may be used to estimate the concentration profile of water-soluble chloride in concrete in the atmospheric and tidal zones.

3. From the concrete samples extracted, the associated environmental parameters for humid tropical conditions were found to be:

$$
\begin{aligned}
C_o &= 0.391\% \text{ by mass of concrete} \\
W_o &= 0.21\% \text{ by mass of concrete . mm per month for tidal zone} \\
&= 0.04\% \text{ by mass of concrete . mm per month in atmospheric zone} \\
D_{w/c} &= 3.12\times10^{-6}\text{mm}^2/\text{s} \\
D_c &= D_{w/c}\times1\times(32)^{-0.1} = 2.21\times10^{-6}\text{mm}^2/\text{s}
\end{aligned}
$$

4. The estimated reductions in mass of reinforcement bars were most severe where high concentrations of water-soluble chloride were present in the concrete at the depth of the reinforcing steel. Threshold concentrations of water-soluble chloride of 0.025% and 0.05% by mass of concrete (or approximately 0.15% to 0.30% by mass of cement), corresponding to the atmospheric and tidal/submerged zones, respectively, may be considered appropriate for Singapore.

ACKNOWLEDGEMENTS

This project has been carried out in collaboration with the Port of Singapore Authority (PSA) under grant GR6266 and research project R264000043112. The authors wish to thank: Mr. K.H. Law, Mr. Tan Gak Peng and Mr. Ng Chee Yong for their collaboration and assistance in arranging for the extraction and transportation of the test piles.

REFERENCES

1. MEHTA, P.K., Concrete in the Marine Environment, Elsevier Science Publisher, London, UK, 1991, pp.59-71.

2. HUSSAIN, S.E., AL-GAHTANI, A.S., RASHEEDUZZAFAR, Chloride Threshold for Corrosion of Reinforcement in Concrete, ACI Materials Journal, V.93, No.6, Nov-Dec 1996, pp. 534-538.

3. MAAGE, M., HELLAND, S., POULSEN, E., VENNESLAND, Ø., CARLSEN, J.E., Service Life Prediction of Existing Concrete Structures Exposed to Marine Environment, ACI Materials Journal, V.93, No.6, Nov-Dec 1996, pp. 602-607.

4. GOURLEY, J.T., BIENIAK, D.T., Diffusion of Chloride into Reinforced Concrete Piles, Material for Tomorrow's Demand, Sym. on Concrete 1983, Perth, Oct. 1983, pp.44-45.

5. CRANK, J., Mathematics of Diffusion, 2nd edition, Oxford University Press, UK, 1975

6. TAKEWAKA, K., MASTUMOTO, S., Quality and Cover Thickness of Concrete Based on the Estimation of Chloride Penetration in Marine Environments, Proc. Second Int. Conf. on Concrete in Marine Environment, American Concrete Institute Special Publication, (ACI SP-109), 1988, pp.381-400.

7. BROWNE, R.D., Mechanisms of Corrosion of Steel in Concrete in Relation to Design, Inspection and Repair of Offshore and Coastal Structures, Proc. Conf. on Performance of Concrete in Marine Environment, American Concrete Institute Special Publication, (ACI SP-65), 1980, pp.169-204.

8. MINDESS, S., YOUNG, J.F., Concrete, Prentice-Hall, NJ, 1981, 671pp.

9. MEHTA, P.K., MONTEIRO, P.J.M., Concrete: Microstructure, Properties, and Materials, Indian Edition, Indian Concrete Institute, India, 1997, 548pp.

10. PORT OF SINGAPORE AUTHORITY, Underdeck Repairs to East Wharf (K9-K12), 1986, 77pp.

11. PORT OF SINGAPORE AUTHORITY, Report on Defective Marine Structures at East Wharf, Berths 44, 45, 46, and 47, 1983, 37pp.

12. VESIKARI, E, Service Life of Concrete Structures with regard to Corrosion of Reinforcements, Research Report 553, Technical Research Centre of Finland, 1988, 53pp.

DEVELOPMENT OF GENERALISED STRENGTH MODELS INVOLVING NON-DIMENSIONAL PARAMETERS FOR SILICA FUME CONCRETE

S Bhanja
Bengal Engineering College
B Sengupta
Jadavpur University
India

ABSTRACT. The present paper deals with mathematical models developed using statistical methods to predict the 28-day compressive strength of silica fume concrete. Extensive experimentation was carried out to determine the isolated effect of silica fume on concrete and analyzing the strength results of 32 concrete mixes performed over a wide range of water-binder ratios and silica fume replacement percentages, simplified relationships have been proposed. In the present investigation, silica fume-binder ratios ranged from 0.0 to 0.3 and water binder ratios from 0.26 to 0.42. The ratios of compressive strengths between silica fume and control concrete have been related to silica fume replacement percentage. The expressions, being derived with strength ratios and not with absolute values of strength, are independent of the specimen parameters and are applicable to all types of specimens. These simplified models might serve as useful guides for proportioning concrete mixes incorporating silica fume.

Keywords: Concrete, Silica fume, Compressive strength, Regression analysis, Models, Non-dimensional parameters.

Dr S Bhanja, Lecturer, Department of Civil Engineering, Bengal Engineering College (D.U.), Howrah - 711103, West Bengal, India.

Dr B Sengupta, Professor in Civil Engineering, Jadavpur University, India.

INTRODUCTION

The concept of concrete making has undergone radical changes since the last fifty years. The most challenging problem faced by the environmental engineers nowadays is the disposal of millions of tonnes of industrial byproducts produced throughout the globe every year. Widespread research has proved that concrete is the safest home for these byproducts. Gradually concrete technologists realized that not only from ecological aspects but these materials have tremendous potentials in modifying many specific properties of concrete. The present day new generation concretes almost invariably incorporate mineral admixtures and silica fume is foremost amongst them due to its finely divided form and very high percentage of amorphous silica. The existing literature is rich in reporting on silica fume concrete but relationships to evaluate the compressive strength of silica fume concrete or to optimize the effect of silica fume on concrete are very limited. Slanicka [1] developed models for SF concrete by modifications of the Abrams and Bolomey expressions. Guttierrez and Canovas [2] developed a model of the compressive strength of silica fume concrete based on the results on 15 × 30 cm cylinders. Duval and Kadri [3] proposed a model to determine the compressive strength of SF concrete based on the 28-day compressive strength of standardized mortar. All these models deal with absolute strength values and thus are valid for a particular type of specimen. The aim of the present investigation is to overcome this inherent weakness and develop a regression model involving non-dimensional parameters so that the effect of specimen shape and size can be eliminated. The absolute values of the compressive strength of concrete depend on a host of parameters like quality of ingredients, mix proportions including the dosage of SP, mixing procedures, curing conditions and testing procedures. It is impossible to define a model that can cater to all these variables simultaneously and can make accurate predictions under all conditions [4]. But if the strengths of SF concrete are defined with respect to the control concrete and expressed in the form of ratios, then the uncertainties involved in the predictions are considerably reduced. Moreover, for a particular set of concretes, the changes in the prevailing conditions for the SF and control concretes are generally not very significant.

EXPERIMENTAL PROGRAM

Materials

The constituent materials used in the program were tested to comply with the relevant Indian Standards. To assure uniformity of supply, the materials were subjected to periodical control tests. Cement used was Ordinary Portland Cement, having a 28-day compressive strength of 54 MPa. Silica fume, containing 90.9% SiO_2 and having a BET specific surface area of 18000 m^2/ kg, from Elkem Materials A/S, Norway was used. Natural river sand having Fineness Modulus of 2.5 was used. The specific gravity and water absorption values were obtained as 2.65 and 0.8% respectively. Crushed, angular, graded coarse aggregates of nominal maximum size 12.5 mm were used in the investigation. The specific gravity and the water absorption of the aggregates were 2.85 and 0.9% respectively. Potable water and a high dosage of high range water reducing admixtures were employed for the mixing.

Experimental Procedure

The experimental research program was carefully designated to determine the isolated effect of silica fume on the properties of concrete over a wide range of water-binder ratios by eliminating the effect of other mix design factors [5]. Therefore while performing the investigations only cement was replaced by silica fume, keeping other mix design variables

constant. To minimize variations in workability the compaction energy had to be varied to achieve proper compaction. The strength of silica fume concrete depends on the water-binder ratio and silica fume content of the mix. The experimental program included five sets of concrete mixes, at w/cm ratios of 0.26, 0.30, 0.34, 0.38 and 0.42, prepared by partial replacement of cement by equal weight of silica fume. Each set had mixes at six different percentages of cement replacement. The dosages of silica fume were 0% (control mix), 5%, 10%, 15%, 20% and 25% of the total cementitious materials. For w/cm ratios of 0.38 and 0.42 even 30% silica fume dosage was adopted. The mix proportion was adopted as C: FA: CA = 1: 1.28: 2.2 for all the mixes. The total binder content was fixed at about 500 kg/m^3 varying from 520 kg/m^3 at w/cm ratio of 0.26 to 480 kg/m^3 at w/cm ratio of 0.42. According to Neville [6] superplasticizers can affect the concrete strength even at constant water cement ratio. Hence the dosage of superplasticizer was also kept constant for all the mixes and thus the change in concrete properties at any constant water-binder ratio occurred primarily due to silica fume incorporation. 100 × 100 × 100 mm cubes and 100 × 200 mm cylinder specimens were used for compressive strength determination. All the specimens were moist cured under water at room temperature till testing. Each strength value was the average of the strength of three specimens.

ANALYSIS OF RESULTS AND STATISTICAL MODELING

The compressive strengths of concrete as obtained on the different specimens and the strength ratios of silica fume and control (reference concrete with 0 % silica fume) concrete are presented in Table 1. If absolutely identical methods of preparation and testing conditions can be ensured, then the ratio of the strengths of two concrete measured on different specimens should be identical and independent of the specimen parameters. Hence for the same SF and same control concretes, the ratios of strengths measured on different specimens should be similar. But absolutely identical conditions of sample preparation and testing are virtually impossible to achieve in practice. Hence the ratios of strengths for the same concretes are observed to be somewhat different for different specimens. These ratios can be utilized for the development of generalized expressions which, being free from the influence of specimen parameters, can be used for the strength prediction of any type of specimen. Such a model, being independent of the specimen parameters, will have an immense potential of strength prediction and will depict the effect of cement replacement by silica fume on the concrete strength. The primary factor that governs the compressive strength of concrete is the water to cementitious material ratio. Again at a particular w/cm ratio, the percentage of cement replaced by silica fume also affects the compressive strength. As per the classical formulation of Abrams' law, there exists an inverse relationship between the compressive strength and water to cement ratio of concrete. But the relationship of compressive strength with silica fume replacement percentage is yet to be well established. In situations where there is no prior relationship known between variables, a scatter diagram is prepared and the information portrayed in the diagram is used in the search for an appropriate mathematical model. The scatter diagrams for both the specimens exhibited a non-linear relationship. From the scatter diagrams it was observed that a third degree polynomial might be appropriate for the test results. Regression analysis was performed to formulate the model and using the method of least squares the unknown regression parameters were determined. The validity of the expressions has been investigated by examining the relevant statistical co-efficients [7].

Table 1 Compressive strengths (28-day) of silica fume and control concrete on 100 mm cubes and 100 × 200 mm cylinders

w/cm RATIOS	SILICA FUME REPLACEMENT %	CUBES		CYLINDERS	
		f	f_{sf}/f_c	f	f_{sf}/f_c
0.26	0	87.67	1.0	63.88	1.0
	5	96.33	1.0988	69.61	1.0897
	10	102.00	1.1635	70.88	1.1096
	15	109.67	1.2509	74.27	1.1626
	20	104.67	1.1939	73.00	1.1428
	25	94.33	1.0760	65.15	1.0199
0.3	0	74.67	1.0	58.15	1.0
	5	80.00	1.0714	63.88	1.0985
	10	88.33	1.1829	64.30	1.1058
	15	99.00	1.3258	67.70	1.1642
	20	99.67	1.3348	72.15	1.2408
	25	97.67	1.3080	70.88	1.2189
0.34	0	69.00	1.0	49.67	1.0
	5	73.67	1.0677	58.79	1.1836
	10	79.67	1.1546	61.12	1.2305
	15	88.33	1.2801	65.36	1.3159
	20	90.00	1.3043	66.63	1.3415
	25	85.00	1.2319	64.09	1.2903
0.38	0	58.00	1.0	40.11	1.0
	5	66.00	1.1379	46.69	1.164
	10	69.67	1.2012	50.93	1.2698
	15	70.33	1.2126	56.02	1.3967
	20	72.67	1.2529	59.42	1.4814
	25	79.00	1.321	63.24	1.5767
	30	75.67	1.3047	53.26	1.3278
0.42	0	55.00	1.0	36.5	1.0
	5	58.33	1.0605	39.69	1.0874
	10	59.33	1.0787	43.51	1.1921
	15	65.67	1.1940	50.08	1.3721
	20	66.33	1.2060	52.84	1.4477
	25	68.00	1.2364	55.39	1.5175
	30	60.33	1.0969	40.32	1.1047

f represents the strength of concrete, f_c refers to the strength of control concrete and f_{sf} refers to the strength of silica fume concrete

For the present investigation, the total binder content was fixed at about 500 kg/m^3 and hence the water contents of the mixes varied with the water-cementitious material ratios. The results indicate that the effect of silica fume on the strength of concrete is a function of the water-cementitious material ratios i.e. water content of the mix. Similar observations were

obtained by Oluokun [8]. Hence while developing the strength models for silica fume concrete based on the present test results the effect of water-cementitious material ratios have been taken into consideration. Examining the values of errors and correlation coefficients, two types of models have been proposed – one for water-cementitious material ratios less than 0.3 and the other for 0.3 and above.

The relationship between the 28-day strength ratios of SF and control concrete and silica fume replacement percentage for w/cm ratios less than 0.3 has been obtained as

$$\frac{f_{SF}}{f_C} = 1.0034 + 0.014(SF\%) + 0.0006(SF\%)^2 - 0.00004(SF\%)^3 \quad (1)$$

where SF% refers to the silica fume replacement percentage and f_{SF} and f_C denote the strengths of silica fume and control concrete respectively. The values of the standard error of estimate and correlation coefficient have been obtained as 0.035 and 0.926 respectively.

The relationship between the 28-day strength ratios of SF and control concrete and silica fume replacement percentage for w/cm ratios equal to or greater than 0.3 has been obtained as

$$\frac{f_{SF}}{f_C} = 1.0071 + 0.0127(SF\%) + 0.0009(SF\%)^2 - 0.00004(SF\%)^3 \quad (2)$$

where the notations have the same meaning as in Equation 1. The values of the standard error of estimate and correlation coefficient have been obtained as 0.085 and 0.823 respectively.

CONCLUSIONS

Extensive experimentation was performed to determine the isolated effect of silica fume on the properties of concrete over a wide range of water to cementitious material ratios varying from 0.26 to 0.42 and silica fume replacement percentages ranging from 5 to 30. By performing regression analysis on a large number of experimental results, statistical models have been developed which can serve as useful tools for optimizing and predicting the strengths of silica fume concretes. For the determination of compressive strengths, different types of specimens are used in different countries. The existing strength models generally deal with the absolute strength values and hence are applicable for that specific specimen type. The present models, involving non-dimensional variables, are independent of the specimen parameters and might find widespread application in the strength prediction of any type of specimens.

REFERENCES

1. SLANICK, A. S., The Influence of Condensed Silica Fume on the Concrete Strength, Cement and Concrete Research, 1991, Vol 21, No 4, p 462 - 470.

2. GUTIERREZ, P. A., CANOVAS, M. F., High Performance Concrete: Requirements for Constituent Materials and Mix Proportioning, ACI Materials Journal, Vol 93, No 3, 1996, p 233 - 241.

3. DUVAL, R., KADRI, E. H., Influence of Silica Fume on the Workability and the Compressive Strength of High Performance Concretes, Cement and Concrete Research, Vol 28, No 4, 1998, p 533 - 548.

4. BHANJA, S., SENGUPTA, B., Investigations on the compressive strength of silica fume concrete using statistical methods, Cement and Concrete Research, Accepted for publication.

5. BHANJA, S., PhD Dissertation submitted to Jadavpur University, Kolkata, India, 2001.

6. NEVILLE, A. M., Properties of Concrete, Fourth Edition ELBS with Addison Wesley Longman Limited, England, 1996.

7. BHATTACHARYA, G. K., JOHNSON, R. A, Statistical Concepts and Methods, John Wiley and Sons, New York, 1977.

8. OLUOKUN, F. A., Fly Ash Concrete Mix Design and the Water-Cement Ratio Law, ACI Materials Journal, Vol 91, No 4, 1994, p 362 - 371.

APPLICATION OF IMMUNE ALGORITHM TO IMPACT RESISTANCE DESIGN FOR REINFORCED CONCRETE SLABS

H Nakamura **A Miyamoto**

Yamaguchi University

Japan

K Brandes

Federal Institute for Material Research and Testing (BAM)

Germany

ABSTRACT. Design of concrete structures subjected to impact loads is usually based on design impact loads, which are characteristic data obtained empirically. However, concrete structures under impact loads, unlike those under static loads, exhibit highly complicated failure modes that change with time by the influence of stress waves. A 3-D layered nonlinear dynamic finite element method (FEM) was applied to evaluate the ultimate behavior and failure modes of reinforced concrete (RC) slabs subjected to soft impact loads. Immune algorithm is combined with a 3-D layered nonlinear dynamic FEM analysis for the purpose of proposing the design of RC slabs subject to soft impact loads. The results give evidence that it presents complicated failure modes, and that Immune algorithms can be applied to the design of RC slabs effectively.

Keywords: Soft impact load, Reinforced concrete slab, Impact resistance design, Immune algorithm, Design support system.

Professor H Nakamura, is an Associate Professor in the Department of Computer Science and Systems Engineering at Yamaguchi University, Yamaguchi, Japan. His research interests include thermal stress in mass concrete structure, integrated management system for existing bridges.

Professor A Miyamoto, is a Professor in the Department of Computer Science and Systems Engineering at Yamaguchi University, Yamaguchi, Japan. His recent research activities are in the areas of nonlinear dynamic (impact) analysis of reinforced and prestressed concrete slabs and serviceability rating on concrete bridges.

Dr K Brandes, is a Head of Laboratory "Steel Structures" in the Federal Institute for Material Research and Testing (BAM), Berlin, Germany. His research interests include impact analysis of structures.

INTRODUCTION

Conventionally, nonlinear discrete programming, which is an extended branch-and-bound technique, and the gradient method, which is applied according to calculated sensitivity values, have been used to solve various design problems. These techniques, however, often require long computation times and are hard to apply to design problems that have many constrains. Genetic algorithms (GAs), which can more or less cope with these difficulties, were proposed recently, and many applied studies, including design support systems based on GAs, have been carried out [1]. However, designers have to present multiple design plans with different features to investigate a wide range of design possibilities in consideration of construction, installation, and environmental conditions. The use of GAs appears insufficient because they provide only one quasi-optimum solution even when there are multiple optimum solutions. We tried in this study to develop a useful design support system for RC slabs by combining a layered nonlinear FEM developed newly in our laboratory for impact failure behavior and an immune algorithm (IA) with which multiple quasi-optimum solutions can be obtained.

DEVELOPMENT OF DESIGN SUPPORT SYSTEMS

RC slabs under impact loads exhibit very complicated time-dependent failure behavior under the influence of stress waves and inertial forces. Because it appears difficult to withstand impact loads by simply taking into account static design loads at the time of failure, construction of a design support system based on the FEM analysis of impact failure behavior is attempted in this study. Because such factors as construction, installation, and environmental conditions, which are difficult to quantify, are involved in design, it is desirable to present multiple design plans in consideration of the designer's intention. We have therefore introduced a modified immune algorithm, which is considered suitable for deducing multiple optimum solutions.

Immune Algorithm [2]

Immune System [2]

In immune responses, a living organism's own tissue is distinguished from foreign substances (antigens) by immunocytes to protect the organism from antigens, and such foreign substances as viruses and malign part of own tissue are eliminated. The immune system in a living organism produces antibodies to combat invading antigens by rearranging genes, and expels the antigens by proliferating the produced antibodies

Outline of the Modified Immune Algorithm

Immune algorithms (IAs) are based on engineered models of antibody production and self-control mechanisms of immune systems. A conventional IA [2] was modified in this study to maintain diversity and obtain multiple quasi-optimum solutions more reliably. The IA used in this study is outlined in Figure 1.

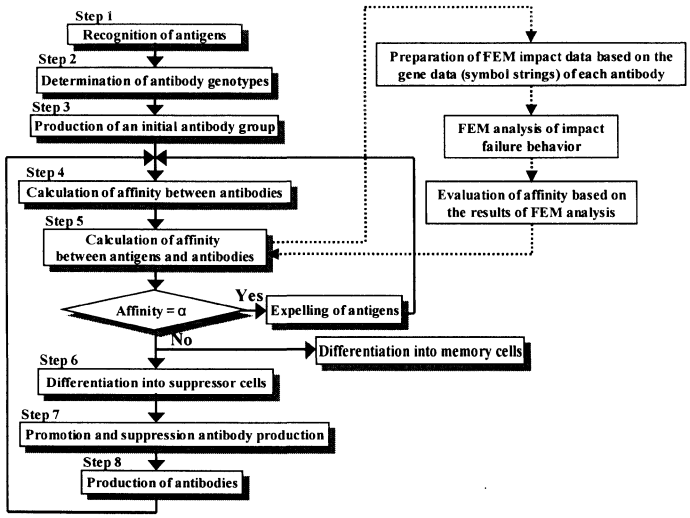

Figure 1 Outline of the modified immune algorithm

Step 1: Recognition of Antigens

The system recognizes the presence of antigens. In optimization problems, antigens correspond to objective functions and constraints. Thus, antigens can be recognized by incorporating objective functions and constraints into the system and providing any input parameters to control them.

Step 2: Determination of Antibody Genotypes

An IA can be applied to a problem by expressing the gene elements of antibodies (events of the problem) with symbol strings. To apply the IA, therefore, input data of the problem need to be converted to symbol strings (antibodies).

Step 3: Production of an Initial Antibody Group

A number of strings are generated based on the model prepared in step 2. An initial antibody group is formed by determining each antibody gene randomly to generate antibodies of different genes.

Step 4: Calculation of Affinity Between Antibodies

Each antibody's affinity (similarity) with all the other antibodies is calculated.

Step 5: Calculation of Affinity Between Antigens and Antibodies

The affinity of each antibody with an antigen (evaluation of solution) is calculated.

Step 6: Differentiation into Memory and Suppressor Cells

Memory and suppressor cells are produced from antibodies that have been found to be effective. The memory cells produced are the candidates of optimum solutions.

Step 7: Promotion and Suppression of Antibody Production

1. $N/2$ antibodies having the lowest affinity with the antigen are extinguished.
2. Each of the remained antibodies is extinguished if its affinity with a suppressor cell exceeds a threshold. This is for averting duplicative production of memory cells.

Step 8: Production of Antibodies

1. Antibodies are produced in place of the ones extinguished in 2) of step 7.
2. Among the antibodies remained after step 7 and the newly produced antibodies, $N/4$ pairs are selected while allowing duplication. Antibodies with higher expectation are more likely to be selected. Genes are crossed over for each antibody pair, and $N/2$ antibodies are newly generated.

Steps 4 through **8** are performed until a predetermined final generation is reached.

Coding of RC Slab Characteristics

The RC slabs analyzed in this study are double-reinforcement concrete slabs with a length of 132 cm, a width of 132 cm, and arbitrary thickness (Figure 2). Each slab is supported by two-side simple supports with a span of 120 cm.

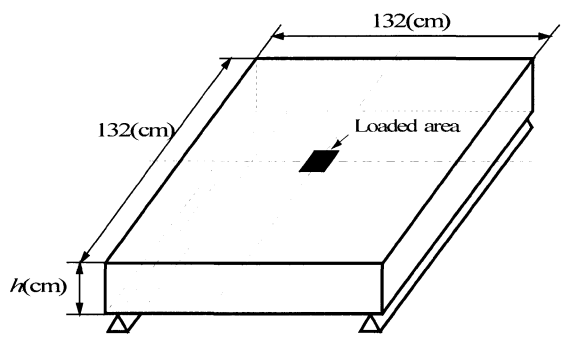

Figure 2 Outline of RC slab used for analysis

To combine the IA with the FEM analysis of impact failure behavior, the input data of RC slab characteristics needs to be coded as symbol strings (binary numbers in general). In the present study, RC slab characteristics are coded as binary data of antibodies and individuals.

The RC slab characteristics addressed in this study are: (1) the width of the concrete slab, (2) the type of concrete, (3) the shape of reinforcements, (4) the number of reinforcement bars, and (5) the type of reinforcement material. These characteristics, coded as binary data, are listed in Tables 1 to 5. If a code that does not exist (lethal gene) is obtained (for example, "11" for the type of concrete), random selection from the other codes is repeated.

Table 1 Coding for concrete material

CONCRETE TYPE	CODE
Ordinary concrete	00
Steel fibre mixed concrete	01
High-strength concrete	10

Table 2 Coding of reinforcement material

REINFORCEMENT TYPE	CODE
Ordinary bars	00
High-strength bars	01
Type A FRP bars	10
Type B FRP bars	11

Table 3 Coding of slab thickness

SLAB THICKNESS	CODE
17/20	00
18/20	01
19/20	10
20/20	11

Table 4 Coding of reinforcement shape

REINFORCEMENT SHAPE	CODE
D6	000
D10	001
D13	010
D16	011
D19	100
D22	101
D25	110
D29	111

Table 5 Coding of the number of rebars (quarter portion)

NUMBER OF REBARS	CODE
3	000
4	001
5	010
6	011
7	100
8	101
9	110
10	111

Layered Nonlinear FEM Analysis [4]

The layered nonlinear FEM model of the RC slab consists of six concrete layers and reinforcement layers consisting of the elements of main reinforcement and distributing bars. Then, different types of concrete or reinforcement can therefore be used in different layers. To take into consideration the tensile stress in the lower part of the slab and the compressive stress in the upper part of the slab, concrete types were selected separately for the upper three and lower three layers. For the convenience of construction, the same type and shape of main reinforcement and distributing bars were used in each reinforcement layer. However, different numbers of bars were used for different layers. The heights of reinforcement layers, which can be set arbitrarily, were determined according to the predetermined thickness of cover concrete and the diameter of reinforcing bars. Directions of bars in each reinforcement layer are usually in the order of upper main reinforcement, upper distribution bars, lower distribution bars, and lower main reinforcement from the upper side of the slab. An example of the coding of RC slab characteristics is presented in Figure 3.

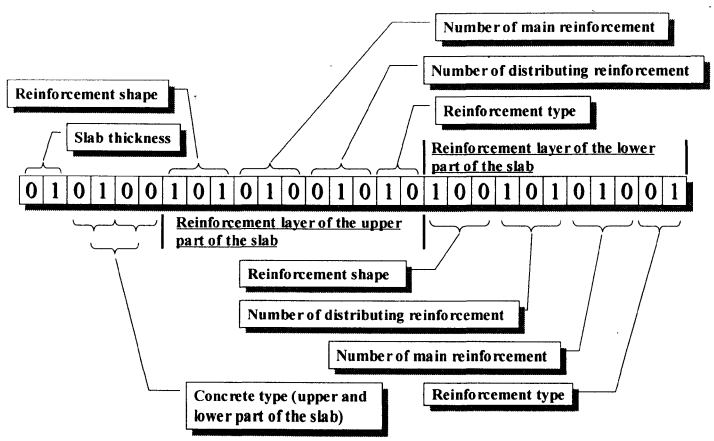

Figure 3 Example of the coding of RC slab characteristics (layered FEM)

Verification of the Precision of the Design Support System

A certain level of precision is generally required in design. In particular, inappropriate designing of concrete structures can cause casualties. To verify the precision of the design support system based on the IA, analyses were carried out for all the combinations of the characteristics of the RC slab model, and the analytical results were compared with the results obtained by the design support system. Comparison was also made with the results obtained by using a GA [3]. In a simulation test for the verification of precision, the design problem presented below was addressed with a loading rate of 50 tf/msec (490 kN/msec), 200 generations, 30 antibodies or individuals, a crossing-over probability of 1.00, and a mutation rate of 1%. In the GA, selection was first made by the elite preservation method and then the roulette method. The thresholds of the IA were set to $T_{ac1} = 0.50$, $T_{ac2} = 0.50$, $T_{ac3} = 0.50$, and $T_c = 0.45$, and suppress power was set to 1.5.

Design Problem

- Objective function: design of a RC slab that fails at a local deformation index [13] of 0.0020.
- Constraint: maximum weight of the RC slab is 540 kgf (5.30 kN).

Here, the local deformation index [5] is the curvature at the time of failure divided by the displacement at the loading point. The index, closely correlated with failure mode, decreases with decreasing local displacement.

Because a long time is required to analyze all the combinations of RC slab characteristics, the number of types coded were reduced by the following criteria to shorten the time required for analysis and design simulation:

- The concrete material used for the upper and lower part of the slab was unified.
- D6 (000) and D10 (001) for the shape of reinforcements were treated as lethal genes.
- The number of distributing bars were half the number of main reinforcements.
- The number of main reinforcements to be arranged in the quarter portion of RC slab was either 4 (00), 6 (01), 8 (10), or 10 (11).

An example of the coding of RC slab characteristics based on the above criteria is presented in Figure 4. The total number of combinations of RC slab characteristics is 110,592 ($4\times3\times6\times4\times4\times6\times4\times4$) cases.

The ten most preferable RC slab models are presented in Table 6, based on the results obtained by the layered nonlinear FEM analysis of all the combinations for the design problem. The shaded models are the design plans obtained by using the IA. As shown in Table 6, the best two models, design plans 1 and 2, as well as the 4th and 8th best models were obtained by using the IA. Although not shown in the Table, the 11th best model, having a sufficient precision with a slab thickness of 12.35 cm and a local deformation index of 0.0019996, was also obtained by using the IA. Accordingly, design plans with high precisions were obtained by using the IA for slab thicknesses of 11.05, 11.70, and 12.35 cm. This demonstrates the ability of the IA in presenting multiple, diverse solutions with high precisions.

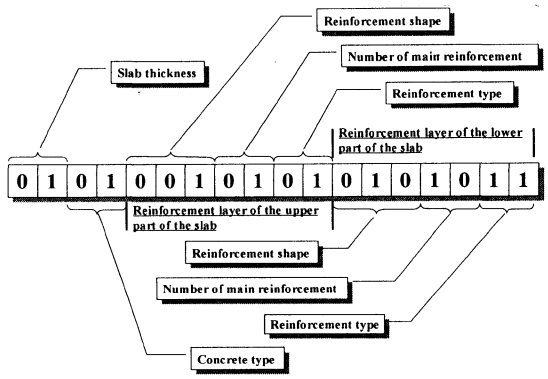

Figure 4 Example of the coding of RC slab characteristics for verification

Table 6 Design plans obtained by using the immune algorithm for design problem 1

DESIGN PLAN	SLAB THICKNESS (cm)	CONCRETE TYPE	REINFORCEMENT IN THE UPPER PART			REINFORCEMENT IN THE LOWER PART			LOCAL DEFORMATION INDEX (10^{-2}/cm^2)
			Shape	Number of rebar	Type	Shape	Number of rebar	Type	
1	11.70	Steel fiber mixed	D22	8	Type B FRP	D16	12	Type B FRP	0.2000025
2	11.05	High-strength	D13	8	Type B FRP	D13	8	Type B FRP	0.2000104
3	12.35	Steel fiber mixed	D22	8	Type B FRP	D16	8	Type B FRP	0.1999868
4	11.70	Steel fiber mixed	D16	12	Type B FRP	D16	12	Type A FRP	0.1999843
5	11.05	High-strength	D13	8	Type A FRP	D13	8	Type B FRP	0.1999835
6	12.35	Steel fiber mixed	D19	12	Type B FRP	D16	8	Type A FRP	0.2000199
7	11.70	Steel fiber mixed	D13	20	Type A FRP	D16	12	Type B FRP	0.1999782
8	12.35	Steel fiber mixed	D19	8	Type B FRP	D19	8	Type B FRP	0.1999776
9	11.05	High-strength	D16	16	Type B FRP	D13	8	Ordinary	0.1999738
10	12.35	Steel fiber mixed	D16	20	Type B FRP	D13	12	Type B FRP	0.2000333

Note: The shaded design plans were obtained by design simulation

Table 7 Design plans obtained by using the genetic algorithm for a design problem with a mutation rate of 1 %

GENERATION	SLAB THICKNESS (cm)	CONCRETE TYPE	REINFORCEMENT IN THE UPPER PART			REINFORCEMENT IN THE LOWER PART			LOCAL DEFORMATION INDEX (10^{-2}/cm^2)
			Shape	Number of rebar	Type	Shape	Number of rebar	Type	
10	11.05	High-strength	D16	16	Type B FRP	D13	8	Ordinary	0.1999738
	11.05	High-strength	D13	20	Type B FRP	D13	8	Ordinary	0.2015199
20	11.05	High-strength	D13	16	Ordinary	D13	8	Ordinary	0.2018071
	11.05	High-strength	D16	16	Type B FRP	D13	8	Ordinary	0.1999738
30	11.06	High-strength	D16	16	Type B FRP	D13	8	Ordinary	0.1999738

Table 8 Design plans obtained by using the genetic algorithm for a design problem with a mutation rate of 5 %

GENERATION	SLAB THICKNESS (cm)	CONCRETE TYPE	REINFORCEMENT IN THE UPPER PART			REINFORCEMENT IN THE LOWER PART			LOCAL DEFORMATION INDEX (10^{-2}/cm^2)
			Shape	Number of rebar	Type	Shape	Number of rebar	Type	
10	11.70	Steel fiber mixed	D13	12	Type B FRP	D13	16	Type B FRP	0.1999266
	11.70	Steel fiber mixed	D13	16	Type A FRP	D16	12	Type B FRP	0.2000815
20	11.70	Steel fiber mixed	D13	20	Type A FRP	D16	12	Type B FRP	0.1999782
30	11.70	Steel fiber mixed	D13	20	Type A FRP	D16	12	Type B FRP	0.1999782

Note 1: The listed design plans are the models having evaluated values equal to or higher than the evaluated value of the converged model of each generation.
Note 2: The shaded design plans are the models converged in the relevant generations.

On the contrary, design plans obtained by using the GA resulted in the 9th best model in the 10th generation, and all RC slab models converged to this model in the 20th generation as shown in Table 7. No additional model was presented thereafter. This is probably due to an early convergence to a local solution, which is the behavior characteristic of GAs. When the mutation rate was increased from 1% to 5% (Table 8), convergence was weakened because diversity was more or less preserved but a better design plan was obtained in the 20th generation. Although the results obtained by using the IA are more precise than the results obtained by using the GA, the GA requires only about 20 generations to obtain a precise solution whereas the IA requires at least 100 generations to obtain multiple solutions with sufficient precisions.

As discussed above, the IA-based design support system provides better precision than the GA-based design support system. This is probably because of the early convergence that is characteristic of GAs; in a problem with a complicated objective function, early convergence to an event with a high evaluation level tends to occur, and wide-range searches thereafter are mostly dependent on mutation. In the IA, however, a new search is initiated after an event with a high evaluation level is memorized as a candidate solution in a memory cell. Wide-range searches are ensured in this case because candidate solutions other than those already detected are searched for by the function of suppressor cells. As a result, the IA can provide multiple, diverse design plans with higher precisions.

Design Simulation

Generally, RC slabs subjected to impact loads must be designed to avoid failure or to fail in bending failure mode in which energy absorption is great. As an effective way to avoid failure, RC slabs may be designed so that they do not fail while their design loads are not exceeded. However, it is difficult to determine design loads according to the purpose of use because there is no established method to convert impact loads into static loads. Thus, the design problem presented in the previous section is not a practical one. To construct a more practical design support system, a design problem was set as follows for an RC slab with a maximum impact resistance and a constraint on the amount of reinforcement, which is the largest cost factor:

Design Problem

- Objective function: design of a RC slab with high impact resistance; impact resistance is evaluated by dividing the impact load at the time of failure by the local deformation index [5], in consideration of loading capacity and the mode of deformation.
- Constraints: maximum weight of the RC slab is 1.0 tf (9.8 kN); the maximum volume of reinforcement in the slab is either 2.5×10^3 cm^3, 1.0×10^4 cm^3, or 3.0×10^4 cm^3.

Because cost was not taken into account in the above problem, high-strength concrete was not adopted as a concrete type. The problem was addressed with 150 generations, 30 antibodies, a crossing-over probability of 1.00, and a mutation rate of 1%.

The slab was designed by using the IA, with loading rates of 25 tf/msec (245 kN/msec), 50 tf/msec (490 kN/msec), and 75 tf/msec (735 kN/msec). Among multiple design plans obtained for different constraints, representative plans with high impact resistance are presented in Figure 5. In all the design plans obtained, a higher amount of reinforcement was inserted in the lower part than the upper part of the slab. In a concrete structure loaded from one side, great tensile stress generally occurs on the other side of the structure. In such an application as a rock shed, therefore, a higher amount of reinforcement is preferably inserted in the lower part rather than the upper part of the RC slab. Thus, the obtained design plans appear to reflect the evaluation of impact resistance required in the objective function. Various plans were obtained for different conditions, and the arrangement of reinforcement was significantly changed by changing the material type of reinforcement. Conclusively, multiple design plans were effectively obtained by using the IA.

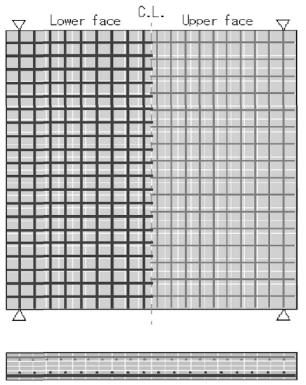

[Concrete]
Upper part: steel fiber mixed concrete
Lower part: steel fiber mixed concrete
Slab thickness: 130mm

[Reinforcement]
Main reinforcement in the upper part
Type A FRP bars
Shape: D10; 16 bars
Distributing reinforcement in the upper part
Type A FRP bars
Shape: D10; 20 bars
Main reinforcement in the lower part
Ordinary bars
Shape: D13; 20 bars
Distributing reinforcement in the lower part
Ordinary bars
Shape: D13; 18 bars

(1) Design plan 1

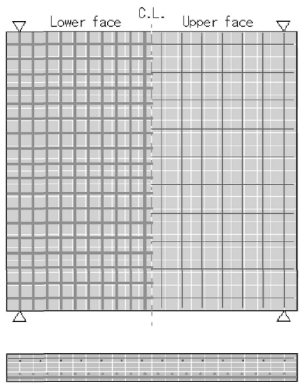

[Concrete]
Upper part: steel fiber mixed concrete
Lower part: steel fiber mixed concrete
Slab thickness: 130mm

[Reinforcement]
Main reinforcement in the upper part
High-strength bars
Shape: D6; 10 bars
Distributing reinforcement in the upper part
High-strength bars
Shape: D6; 14 bars
Main reinforcement in the lower part
Type B FRP bars
Shape: D13; 18 bars
Distributing reinforcement in the lower part
Type B FRP bars
Shape: D13; 20 bars

(2) Design plan 2

Figure 5 Examples of design plan
(maximum reinforcement volume less than 1.0x104cm3; loading rate=735kN/ms)

CONCLUSIONS

The impact resistant design of RC slabs that exhibit complicated failure behavior in response to impact loads was investigated based on the FEM analysis of impact failure behavior. An IA was introduced to solve design problems, and its effectiveness was studied in comparison with the results obtained by a GA. Design simulation was then conducted based on the layered FEM analysis, and the adequacy of the design plans obtained were evaluated together with the search performance of the immune and genetic algorithms. The results obtained in the present study are summarized as follows:

1) The IA, which maintains versatility with the help of suppressor cells and extends the range of search, provides more precise solutions than the GA.

2) Multiple design plans for impact resistant RC slabs can be obtained precisely with the IA. However, the method of making a selection from the obtained design plans still need to be established.

3) In the GA-based design support system, design plans with fair precisions were obtained in a very short period of time because of the early convergence that is characteristic of GAs. GAs therefore are useful when design plans need to be obtained quickly or when only impact resistance need to be taken into consideration.

4) When an impact load is applied on the top of the RC slab at a relatively low loading rate and a large volume of reinforcement is arranged in the lower part of the slab, tensile stress is suppressed and compressive stress becomes dominant in the lower part. Thus, impact resistance is improved by adopting concrete material resistant to compression in the lower part.

REFERENCES

1. CHIJIIWA, H., MIHARA, T., OHTA, T., An optimal location design method of steel pile foundation using genetic algorithm, Proceedings of Japan Society of Civil Engineers, No 549/I-37, October 1996, p 97-105.

2. MORI, K., TSUKIYAMA, M., FUKUDA, T., Application of an immune algorithm to multi-optimization problems, Journal of Electrical Engineering, C117, No 5, 1997, p 593-597.

3. ADELI, H., HUNG, S. L., Machine learning, Neural networks, Genetic algorithms, and Fuzzy systems, John Wiley & Sons, 1997.

4. MIYAMOTO, A., KING, W. M., FUJII, M., Nonlinear dynamic analysis of reinforced concrete slabs under impulsive loads, ACI Structural Journal, Vol 88, No 4, 1991, p 411-419.

5. MIYAMOTO, A., ISHIBASHI, T., MITO, M., Evaluation of impact resistance for reinforced concrete slab structures, JSCE Journal of Structural Engineering, Vol 40A, March 1994, p 1605-1618.

6. MIYAMOTO, A., KITAYAMA, A., GOTOU, M., 3-D nonlinear dynamic analysis and its verification of failure modes for reinforced concrete slab under soft impact loads, JSCE Journal of Structural Engineering, Vol 42A, March 1996, p 1325-1336.

RELIABILITY OF CONCRETE COLUMN EXPOSED TO ACCIDENTAL ACTION DUE TO IMPACT

M Holický

J Marková

Czech Technical University

Czech Republic

ABSTRACT. Reliability analysis of a reinforced concrete bridge column exposed to persistent and accidental design situations is based on the application of probabilistic methods. Principles and rules of the Eurocodes and recommendations given in UIC 777-2 R are taken into account. Accidental design situation due to impact caused by the rail traffic under the bridge is considered. Results of the analysis show, that the reliability of the designed bridge column is sufficient at the persistent design situation (the reliability index β is approximately 4,7 for one year). The probability of the column failure given accidental impact of rail traffic determined using probabilistic methods seems to be relatively high, around 0,3. The total probability of failure for the bridge column, taking into account both the persistent and accidental designed situation, may exceed the target value $1{,}3\times10^{-6}$ ($\beta = 4{,}7$) recommended in EN 1990. Further research of bridge columns and other structures near railway under impact loading should be focused on probabilistic models of accidental impact forces and on probabilistic risk assessment using appropriate data for possible consequences of structural failure.

Keywords: Structures near railway, Train impact, Impact model, Risk assessment, Probability of failure, Reliability of bridge column.

Dr M Holický, is a Research Fellow at the Klokner Institute of the Czech Technical University in Prague, Head of the Department of Structural Reliability, Deputy Director of the Klokner Institute and Associated Professor at the Faculty of Civil Engineering of the Czech Technical University in Prague, Czech Republic.

Dr J Marková, is a Researcher at Klokner Institute of the Czech Technical University in Prague, Czech Republic.

INTRODUCTION

It is well known that accidental actions may significantly endanger human lives and affect reliability of construction works near railway. As the requirements for the rail traffic and the train speed are gradually increasing, the subcommittee for bridges of the International Union of Railways (UIC) has recently carried out investigations related to the impacts on structures near railway lines. These investigations have been used to develop a new document UIC Code 777-2 R [1], which recommends several measures to reduce the effects of an accidental impact from a derailed trains.

Previous documents of UIC have been used during the development of the prenormative document ENV 1991-2-7 [2], "Accidental actions due to impact and explosions" that is currently at the stage of transformation to normative standard EN 1991-1-7. This document should be soon used in most European countries. Each Member state of CEN will have to prepare its National annex and to compare accidental impact forces given in national standards with those, provided in new European standards. This may be a difficult task as some values recommended for impact forces on supporting substructures of bridges significantly exceed the values specified in national standards.

The following analysis of a bridge column under persistent and accidental design situation due to impact is based on the recommendations of UIC Code 777-2 R [1] and ENV 1991-2-7 [2]. General theoretical principles are illustrated by an example of a motorway bridge located in the north-western part of the Czech Republic. The bridge is a continuous beam of two equal spans of 21 m. The cross section of the bridge superstructure (a concrete slab on two concrete beams) supported by two columns of height L is shown in Figure 1. A railway track, perpendicular to the motorway bridge, passes under this bridge. Accidental design situation may arise due to the impact of derailed train to the columns of the motorway bridge represented in Figure 1 by the impact force A_d at the height r above top of the track level.

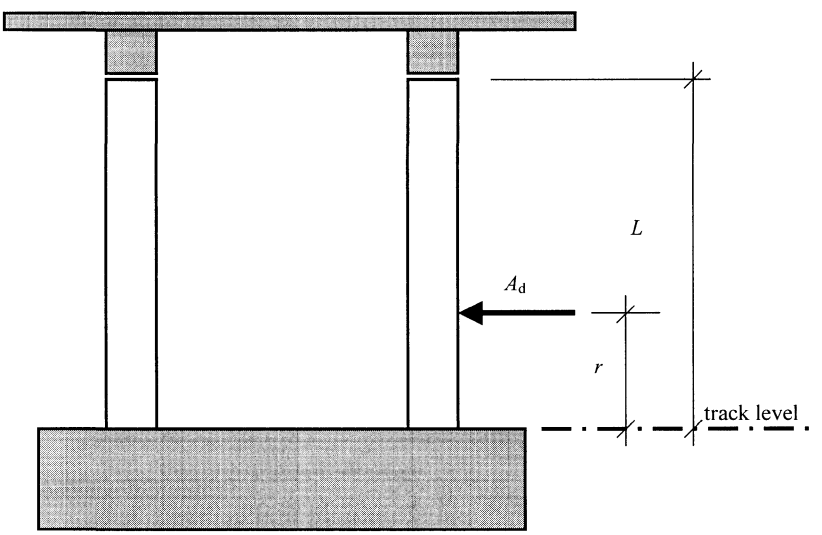

Figure 1 Cross section of the bridge

PROBABILITY ASSESSMENT OF THE COLUMN FAILURE

Two different design situations are considered in the following assessment of failure probability for the bridge column located in the vicinity of the track:

- persistent (normal) design situation N, which is assumed to occur with the probability P_N;
- accidental design situation A (for simplicity considering only accidental impact due to the rail traffic), which is assumed to occur with the probability P_A.

Obviously, for mutually exclusive events N and A it holds that $P_N + P_A = 1$. Using the total probability theorem, the failure probability P_f may be expressed as

$$P_f = P_{fN}\, P_N + P_{fA}\, P_A \cong P_{fN} + P_{fA}\, P_A \tag{1}$$

Note, that the approximation indicated in Equation (1) may be justified, as the probability of the accidental design situation P_A is usually very small and the complementary probability is approximately unity, $P_N = 1 - P_A \approx 1$. If the total probability P_f is limited by the target value P_t (e.g. $1{,}3\times10^{-6}$ per year), then it follows from (1) that the probability of failure P_{fA} should satisfy the following condition

$$P_{fA} \le (P_t - P_{fN})/P_A \tag{2}$$

The conditional probability P_{fA} of the column failure given accidental design situation, and the conditional probability P_{fN} of the column failure given persistent design situation are assessed in the following sections using probabilistic methods of structural reliability. However, according to the Draft 7 of UIC [1], the conditional probability P_{fA} may be assessed using the empirical formula

$$P_{fA} = \{1 - 2/3\ [t\,(2v^{0,55} - 2a - t)/(v^{0,55} - a)^2]\}\,\alpha \tag{3}$$

In this Equation, v denotes the train speed, a is the axial distance of the track to the bridge column, t is the lateral deviation over which the remaining speed of the train felt down below 60 km/h, $t = 45\ a\ (v^2/80 - 45)^{-1}$ and assuming the reduction factor $\alpha = 0{,}95$ for the robustness of column [1].

The probability P_A of the accidental design situation A can be determined as

$$P_A = P_D\, P_{Im} \tag{4}$$

where P_D is the probability of the train derailment and P_{Im} is the probability of the train impact to the column.

In accordance to the Draft 7 of UIC 777-2 R [1], the probability of the train derailment P_D and the probability of the train impact P_{Im} may be assessed using formulas

$$P_D = 365\ e_r\, d\, Z_d \tag{5}$$

$$P_{Im} = 0{,}5\ [(v^{0,55} - a)/\ v^{0,55}]^3 \tag{6}$$

In these Equations e_r is the derailment rate and d is the longest derailment path, $d = v^2/80$, Z_d is the number of trains per day.

As an example, it is considered single track line without switches (Z_d =100 trains/per day for a single track, $e_r = 2{,}5\times10^{-9}$ [1]), a passenger train of the speed 120 km/h (the maximum line speed considered in ENV 1991-2-7 [2] for impact models), and the distance of column from the axis of track a = 3 m. The probability of the column failure under the accidental design situation P_{fA} may be assessed using Equation (3)

$$P_{fA} = \{1\text{-}2/3\ [1\times(2\times120^{0,55} - 2\times3 - 1)\times(120^{0,55} - 3)^2]\} \times 0{,}95 = 0{,}84$$

The probability of the accidental design situation P_A follows from Equations (4), (5) and (6)

$P_D = 365\times2{,}5\times10^{-9}\times120^2/80\times100/100^3 = 1{,}64\times10^{-5}$ and $P_{Im} = 0{,}5\ [(120^{0,55} - 3)/120^{0,55}]^3 = 0{,}241$

$$P_A = P_{Im}\, P_{fD} = 0{,}241 \times 1{,}64 \times10^{-5} = 3{,}95 \times 10^{-6}$$

Note, that the probability of failure P_{fA} should satisfy the condition given by Equation (2)

$$P_{fA} \le (1{,}3\times10^{-6} - P_{fN})/\ 3{,}95 \times 10^{-6} < 0{,}33$$

where the target probability $P_t = 1{,}3\times10^{-6}$ (β_t = 4,7) per one year is considered according to the recommendations of EN 1990 [3] and the probability of failure P_{fN} is assumed to be significantly less than P_t. Thus, the probability of failure P_{fA} = 0,84 estimated using Equation (3) given in Draft 7 of UIC 777-2 R [1] is greater than the required value of 0,33. Obviously, the total probability P_f given by Equation (1) shall exceed the target value $P_t = 1{,}3\times10^{-6}$ for any failure probability P_{fN} at the persistent design situation.

LOAD COMBINATIONS

The column is designed for the persistent design situation, considering the combination of actions according to EN 1990 [3], Annex A.2 and prEN 1991-2 [4] given as

$$\sum_{j\ge1} \gamma_{G,j} G_{k,j} "+" \gamma_{Q,1} Q_{k,1} "+" \sum_{i>1} \gamma_{Q,i} \psi_{0,i} Q_{k,i} \tag{7}$$

Considering the accidental design situation the column is designed assuming the impact of the rail traffic using the load combination given in [3]

$$\sum_{j\ge1} G_{k,j} "+" A_d "+" \psi_{1,1}\ Q_{k,1} "+" \sum_{i>1} \psi_{2,i} Q_{k,i} \tag{8}$$

The partial factors γ_G, γ_Q and reduction factors ψ_0, ψ_1, ψ_2, recommended in EN 1990 [3] are used in the design.

Permanent actions, traffic load models and impact load considered in the design of the bridge column are listed in Table 1.

Table 1 Actions considered in the design of the column.

TYPE OF LOADING	ACTION
Self-weight of superstructure	147,5 kN/m
Surfacing layers	23,96 kN/m
Pavements and corbels	26 kN/m
Self-weight of column $b \times h$	$bh\,L\,\gamma_{con}$
Load model LM1[(1)] (TS)	448 kN ($Q_{k,1}$ = 300 kN, $Q_{k,2}$ = 200 kN)
(ULS)	35,86 kN/m ($q_{k,1}$ = 9 kNm^{-2}, $q_{k,2}$ = 2,5 kNm^{-2})
Load on footways	7,5 kN/m [(2)]
Braking forces	345 kN
Accidental force A_d	4000 (10000) kN

[(1)] Adjustment factors $\alpha_{Q1} = \alpha_{Q2} = 0{,}8$ and $\alpha_{qi} = 1$ are considered.
[(2)] Combination value.

The design value of bending moment M_d of the column is given as

$$M_d = N_d (e_0 + e_a + e_2) \tag{9}$$

where e_0 denotes the first order eccentricity, e_a is the additional eccentricity taking into account geometric imperfections and e_2 is the second order eccentricity due to the deformations of the column. The eccentricities e_a and e_2 are determined in accordance with Section 4 of ENV 1992-1-1 [5]. The additional eccentricity e_a is given as

$$e_a = v_a L_0/2 \tag{10}$$

where L_0 is the effective length of the bridge column considered as $L_0 = 2L$ and the inclination v from the vertical $v = 1/200$, thus $e_a = 1/200\ L$. The second order eccentricity e_2 is

$$e_2 = 0{,}1\ K_1 L_0^2\ (1/r) \tag{11}$$

where the coefficient K_1 depends on the slenderness ratio $\lambda = L_0/i$ (i is radius of gyration). For the slenderness ratio $\lambda \geq 35$ the recommended value $K_1 = 1$, and for $15 \leq \lambda \leq 35$ K_1 is

$$K_1 = \frac{\lambda}{20} - 0{,}75 \tag{12}$$

The curvature $1/r$ is determined as

$$\frac{1}{r} = \frac{2 K_2\, \varepsilon_{yd}}{0{,}9(h - d_1)}, \text{ where } K_2 = \frac{N_{ud} - N_d}{N_{ud} - N_{bal,d}} \leq 1 \tag{13}$$

N_{ud} is the design ultimate capacity of the cross-section $N_{ud} = \alpha f_{cd} A_c + f_{yd} A_s$, N_d is the design axial force and $N_{bal,d}$ is the axial force which, when applied to a section, maximises ultimate moment capacity of the cross-section. The force $N_{bal,d} = 0{,}5 \alpha f_{cd} A_c$ is considered for symmetrical reinforcement. The coefficient α takes account of the long-term effects on the compressive strength, $\alpha = 0{,}85$ according to ENV 1992-2, Concrete bridges [6].

Material Characteristics of the Column

The following material characteristics for concrete and reinforcing steel are considered

– concrete class C 25/30 having the characteristics

$$f_{ck} = 25 \text{ MPa}, \gamma_c = 1{,}5, f_{cd} = 16{,}7 \text{ MPa} \tag{14}$$

– reinforcement S 500 having the strength values

$$f_{yk} = 500 \text{ MPa}, \gamma_s = 1{,}15, f_{yd} = 435 \text{ MPa} \tag{15}$$

The modulus of elasticity E_s = 200 GPa, the design yield strain ε_{yd} = 2,17 % corresponds to the design value of yield strength f_{yd} given above.

Design of the Cross-section

The column has height of L = 6,3 m and a rectangular cross-section $b \times h$ is considered in the design. The reinforcement of the column is symmetrical ($A_{s1} = A_{s2} = A_s/2$), the axial distance of the reinforcement from the edge d_1 = 0,05 m. The column cross-section is designed considering the design axial force N_d and the design bending moment M_d using a simplified interaction diagram described by the following formulas:

for $N_d < 0{,}5 \alpha\, b\, h\, f_{cd}$:

$$[A_s f_{yd} (h - 2\, d_1) + h\, N_d (1 - N_d/(\alpha\, b\, h\, f_{cd})]/2 - M_d > 0 \tag{16}$$

for $N_d > 0{,}5 \alpha\, b\, h\, f_{cd}$:

$$K_2 [A_s f_{yd} (h - 2\, d_1)/2 + \alpha\, b\, h^2 f_{cd}/8] - M_d > 0 \tag{17}$$

These relationships approximate well appropriate rules of ENV 1992-1-1 [5].

The designed reinforcement area A_s should satisfy the conditions for the minimum and the maximum area of reinforcement specified in Clause 5.4 of ENV 1992-1-1 [5]

$$0{,}15\, |N_d| / f_{yd} < A_s, \;\; 0{,}003\, b\, h \; < A_s < 0{,}08\, b\, h \tag{18}$$

Using relationships (16) and (17), material properties in Equations (14) and (15), the resulting cross-sectional dimensions $b \times h$, reinforcement area A_s, cross-sectional capacity moment M_R and moment M_E due to action effects are shown in Tables 2a and 2b. Groups of traffic load gr1a and gr2 according to prEN 1991-2 [4] are considered in the first two study cases of the design of column at persistent design situation.

The horizontal equivalent design force A_d, caused by rail traffic, is applied at a height r (see Figure 1) above the track level in accordance to the recommendations of UIC 777-2 R [1] and ENV 1991-2-7 [2]. The height r is reduced by 20 % taking into account interaction of the column with superstructure.

Table 2a Design of the bridge column $b \times h$ (8 study cases)

CASE	N_d [MN]	M_0 [MNm]	e_0 [m]	e_a [m]	$A_s\ 10^4$ [m^2]	b [m]	h [m]	N_{bal} [MN]
1.	4,35	0,09	0,02	0,032	9,5	0,8	0,8	4,53
2.	3,67	0,48	0,13	0,032	28	0,8	0,8	4,53
3.	2,89	5,76	1,99	0,032	65	1,15	2,2	17,92
4.	2,35	5,76	2,45	0,032	76	1,15	2,2	17,92
5.	2,76	3,33	1,20	0,032	60	1,15	1,45	11,81
6.	2,22	3,33	1,50	0,032	70	1,15	1,45	11,81
7.	3,04	8,32	2,74	0,032	64	1,15	3,05	24,85
8.	2,49	8,31	3,34	0,032	75	1,15	3,05	24,85

Table 2b Design of the bridge column $b \times h$ (8 study cases)

CASE	N_u [MN]	λ	K_1	K_2	e_2 [m]	M_E [MNm]	M_R [MNm]	$M_R - M_E$ [MNm]
1.	9,48	54,56	1	1	0,10	0,67	1,05	0,38
2.	10,28	54,56	1	1	0,10	0,97	1,30	0,34
3.	38,67	19,84	0,24	1	0,01	5,88	5,90	0,01
4.	39,12	19,84	0,24	1	0,01	5,85	5,87	0,03
5.	26,23	30,1	0,76	1	0,04	3,53	3,54	0,05
6.	26,67	30,1	0,76	1	0,04	3,49	3,52	0,03
7.	52,47	14,31	0	1	0	8,42	8,46	0,01
8.	52,95	14,31	0	1	0	8,40	8,43	0,00

In the study cases 3 to 6, the axial distance 3 m $\leq a \leq$ 5 m and following accidental load combinations are considered:

Case 3: A_d = 4 MN acting at height r = 1,8 m above the track level, combined with frequent combination of traffic loads;
Case 4: A_d = 4 MN (r = 1,8 m) combined with permanent actions;
Case 5: as in the case 3, however the height r is reduced to r = 1,8 – 0,76 = 1,04 m as allowed by additional measures of UIC 777-2R [1];
Case 6: as in case 4, however with the reduced height r = 1,04 m;

In the study cases 7 to 8, the axial distance a < 3 m and following accidental load combinations are considered:

Case 7: A_d = 10 MN acting at height r = 1,04 m, combined with frequent values of traffic loads;
Case 8: as in case 7, however without traffic loads.

In the study cases 5 to 8, it is assumed that the columns are protected by elevated foundations height by 0,76 m above the track level (the minimum value recommended in UIC 777-2 R [1]).

RELIABILITY ANALYSIS

The limit state function g is expressed as the difference of resistance bending moment and the actual bending moment due to the effect of external forces

$$g = \xi_R M_R - \xi_E M_E \tag{19}$$

where coefficients of model uncertainties ξ_R and ξ_E are considered as random variables to cover imprecision and incompleteness of the relevant theoretical models. Taking into account Equations (16 and 17), the limit state functions are given

for $N < 0{,}5\alpha\, b\, h f_c$:

$$\xi_R [A_s f_y (h - 2\, d_1) + h\, N(1\text{-}N/(\alpha\, b\, h f_c)]/2 - \xi_E M_E > 0 \tag{20}$$

for $N > 0{,}5\alpha\, b\, h f_c$:

$$\xi_R [A_s f_y (h - 2\, d_1)/2 + \alpha\, b\, h^2 f_c/8] - \xi_E M > 0 \tag{21}$$

Basic variables applied in the reliability analysis are listed in Table 3.

Table 3 Statistical properties of basic variables for bridge column

BASIC VARIABLES	NAME OF BASIC VARIABLES	SYMBOL	DISTR. TYPE	DIMEN-SION	MEAN	STANDARD DEVIATION
Material properties	Compression concrete strength	f_c	LN	MPa	35	5
	Yield strength	f_y	LN	MPa	560	30
	Modulus of elasticity of steel	E_s	DET	GPa	200	0
	Reduction factor	α	REC (1)	-		
Geometric data	Width of cross-section	b	DET	m	nom.	0,01
	Height of cross-section	h	DET	m	nom.	0,01
	Distance of bars from edge	d_1	GAM	m	nom.	0,01
	Reinforcement area	A_s	DET	m^2	nom.	0
Model uncertainty	Uncertainty of resistance	ξ_R	N	-	1,1	0,11
	Uncertainty of load effect	ξ_E	N	-	1,0	0,10
Actions	Weight density of concrete	γ_{con}	N	MN/m^3	0,025	0,0025
	Traffic load – TS	Q_{TS}	GUM	MN	nom	0,3 nom
	Traffic load – UDL	q_{UDL}	GAM	MN/m^2	nom.	0,1 nom
	Load on footways	q_f	GAM	MN/m^2	nom.	0,1 nom
	Braking forces	Q_b	GUM	MN	nom.	0,1 nom
	Accidental action	A	GUM	MN	nom.	0,75 nom

(1) lower bound 0,8 and upper bound 0,9

Some of the basic variables are assumed to be deterministic values - denoted "DET" (A_s, L, E_s), while the others are considered as random variables having the rectangular distribution "REC", normal distribution - "N", lognormal distribution - "LN", Gamma distribution - "GAM" and Gumbel distribution - "GUM".

Statistical properties of the random variables are further described by the moment characteristics, the mean and standard deviation, partly taken from the previous studies in the Klokner Institute and following recommendations of the JCSS Probabilistic Model Code [7].

Accidental impact force depends on the train speed, its mass and deformation behaviour, the way of the train derailment, the distance from the point of derailment to the point of impact, friction coefficients (roughness of terrain) and on direction of impact. In the case of road vehicle impacts, various theoretical and experimental studies are available. However, in the case of train impacts only very few investigations were made (e.g. Train Derailment and Its Impact on Structures [8]). Appropriate information enabling to develop more advanced impact models does not exist. The numerical evaluation of engine or carriage impacts needs further research, in particular experimental investigation. The probabilistic model used in this contribution is mostly based on subjective judgement.

Reliability analysis of the bridge column designed for the persistent design situation shows, that the resulting reliability index β_N is higher than the recommended value of 4,7 (see cases 1 and 2 in Table 4).

Reliability of the bridge column designed also for the accidental impact due to rail traffic is high only if the ultimate limit states (STR) are verified (reliability index β_N is around 8). Reliability of the column is low in the case of accidental impact (β_A is from 0,4 to 0,5, which corresponds to P_{fA} approximately 0,3).

Table 4 Reliability indexes β (in brackets probabilities of failure P_f) for 8 study cases (cases 1–2 considering only persistent design situation N in the design of column, cases 3–8 for accidental design situation A)

CASE	β (P_f)	CASE	β (P_f)
1 (N)	5,46 ($1{,}9\times10^{-8}$)	5 (A)	0,52 (0,30)
2 (N)	4,73 ($1{,}1\times10^{-6}$)	6 (A)	0,43 (0,33)
3 (A)	0,51 (0,31)	7 (A)	0,50 (0,31)
4 (A)	0,42 (0,34)	8 (A)	0,41 (0,34)

The reliability analysis of the actually built bridge column shows, that for the persistent design situation the reliability index β_N = 7,3 is rather high. However, the reliability of the column is completely insufficient if accidental impact force A_d = 4 MN recommended in ENV 1991-2-7 [2] is considered (according to the Czech provisions the impact force A_d = 1 MN may be used only).

CONCLUSIONS

The reliability of the bridge column at the persistent design situation is sufficient; the reliability index β is greater than the value of 4,7 recommended in EN 1990 Basis of Structural Design for a reference period of one year.

The probability of the column failure P_{fA} under accidental train impact assessed in accordance with the empirical formula recommended in the Draft 7 of UIC 777-2 R is 0,84. Probabilistic reliability analysis, based on static equivalent impact models recommended in previous documents of UIC and ENV 1991-2-7, indicates that the probability P_{fA} is around 0,3 (less than the empirical value of 0,84).

The total probability of failure P_f of the bridge column considering both the persistent and accidental design situation may exceed (for $P_{fA} > 0{,}33$) the target value of $1{,}3\times10^{-6}$ ($\beta = 4{,}7$).

Advanced impact models based on new theoretical and experimental investigation, which should encompass new requirements for railway traffic are still missing. Probabilistic impact model accepted in this contribution for the reliability assessment of a bridge column should be updated using newly obtained data.

Further research of impact resistance of concrete elements should be focused on probabilistic models of accidental impact forces, and on probabilistic risk assessment based on appropriate data for possible consequences of structural failure.

ACKNOWLEDGEMENTS

This research has been conducted at the Klokner Institute of the Czech Technical University in Prague, Czech Republic as a part of the research project CEZ J04/98/210000029 „Risk Engineering and Reliability of Technical Systems“ supported by the Ministry of Education and as a part of the project No. 803120110 “Thermal and Accidental Action Models for Bridge Structures according to the Eurocodes” supported by the Ministry of Transport and Communications of the Czech Republic.

REFERENCES

1. UIC Code 777-2 R, Structures Built over Railway Lines, Recommendations for Structures in the Track Zone, 1997 and Draft 7, UIC Paris, 03/2001, pp 51.
2. ENV 1991-2-7 Eurocode 1, Basis of Design and Actions on Structures, Part 2-7, Actions on Structures, Accidental Actions due to Impact and Explosions, CEN, 1998, pp 38.
3. EN 1990 Eurocode, Basis of Structural Design, 07/2001, pp 89, and Annex A.2, CEN, 08/2001, pp 30.
4. prEN 1991-2, Actions on Structures, Part 2, General Actions, Traffic Loads on Bridges, CEN, 06/2001.
5. ENV 1992-1-1 Design of Concrete Structures, Part 1, General Rules and Rules for Buildings, CEN, 1991, pp 311.
6. ENV 1992-2, Design of Concrete Structures, Part 2, Concrete Bridges, CEN, 1996, pp 50.
7. JCSS, Probabilistic Model Code, Part 2, Load Models, 02/2001.
8. GROB, J., HAJDIN, N., Train Derailment and Its Impact on Structures, Structural Engineering International, 2, 1993, pp 88-94.

COST FOR AIRCRAFT IMPACT DESIGN OF CONCRETE PROTECTIVE STRUCTURES

K van Breugel
Delft University of Technology
Netherlands

ABSTRACT. Structures for storage of hazardous materials and, more general, buildings and structures that accommodate risk-bearing activities, like nuclear power plants and storage of LNG and LPG, should be able to resist the impact caused by and aircraft crash. In this contribution of the probability of aircraft crashes is discussed. For different type of aeroplanes, ranging from small jetfighters to large passenger planes, the force-time diagrams are shown. For four types of jetfighters the required thickness of a concrete protective structure to withstand the impact of these planes was investigated. The extra costs of an aircraft impact design are determined. These extra costs are compared with the cost of catastrophic accidents. By comparing additional building costs and potential costs in case of a catastrophic impact load it is made plausible that concrete protective structures are cost effective components of advanced protective systems.

Keywords: Protective structures, Concrete, Aircraft crashes, Statistics, Aircraft impact, Impact resistance, Costs.

K van Breugel is employed at Delft University of Technology, Faculty of Civil Engineering and Geosciences, The Netherlands, since 1980. In 1999 he became full professor in the Department of Concrete Structures. He main topics are numerical simulation of the behaviour of concrete at early ages and the design of concrete structures for environmental protection. He is member of a number of working groups of the fib, RILEM and CEN.

INTRODUCTION

The growth of industrial activities goes along with a large increase in energy consumption and an intensive use of raw materials. Energy carriers and raw materials are often stored in large quantities in large tank farms. Depending on the type of product stored, the bulk storage of these materials constitutes a potential hazard for people and environment. Moreover, the size and complexity of modern storage facilities make them more and more non-transparent and difficult to survey. In many cases they are vulnerable to extreme accidental loads. Escalation of an accident and the occurrence of domino effects once an accident has started is a point of major concern of all plant owners. Where domino effects have occurred, the losses are generally extremely high. In the thirty years period from 1950 to 1980 the number of large-scale accidents at industrial facilities with direct losses exceeding US$ 10,000,000 exhibits a linear correlation with the overall energy consumption per capita [1]. Bearing in mind that the consumption of energy is prognosticated to increase drastically in the coming decades, the safety levels of risk bearing activities, including large-scale storage facilities for hazardous materials, should be improved on penalty of facing a huge increase in the number of large accidents.

One possible cause of a major accident is an impact load by a crashing aircraft. The cost for an aircraft resistant design of a structure can be very high. Whether these costs are justified will depend on the potential losses in the case an aircraft impact occurs. For judging this kind of issues information is needed about the extra costs for an impact resistant design on the one hand and estimates of the losses in case an accident might happen on the other hand. This paper concentrates on the additional costs of an aircraft impact resistant design of a concrete storage tank for liquefied petroleum gas. First the question will be addressed how realistic an extreme impact load caused by a crashing plane is.

PROBABILITY OF AIRCRAFT CRASHES ON BUILDINGS

From the civil engineering point of view aircraft crash statistics are of utmost importance for specifying extreme load cases for structures with a high risk potential. In this respect nuclear power plants have to be mentioned and tanks for storage of liquefied natural gas (LNG) [2] and liquefied petroleum gas (LPG). The probability of an aircraft crash follows from the number of crashes in the past. In the period from 1954 to 1983 about 5,000 airliners crashed. This means a frequency of 166 crashes per year. In this figure crashes in the former USSR and China are not included. From the number of crashes per year a probability of an aircraft impact of about 10^{-6}/10,000 m^2 per year can be calculated. Assuming that 1% of the land is covered with buildings, the probability that a crashing aircraft hits a building is about 10^{-8} per year. Although this is a small probability, it is known by experience that crashing planes do destroy buildings regularly. In 1992 a Boeing 747 destroyed a multi-story apartment building near Amsterdam. In the same week a crashing plane destroyed a private house in the United States. Table 1 gives an overview of aircraft crashes in the period from 1986 to 2000 in which buildings were damaged or destroyed. Still assuming a number of 166 crashes per year, the total number of crashes in this fifteen-year period would be 2490. Table 1 shows that in that period 16 accidents happened in which buildings were damaged or destroyed. These 16 accidents make out about 0.64 per cent of the estimated total number of accidents in that period. This figure matches quite well with the assumed 1 per cent of the land that consists of built-up area.

Even though the previously mentioned probability of an aircraft impact on a building is as low as 10^{-8} per year, accidents statistics show that even these small probabilities do represent real events that may occur in space in time. The events summarised in Table 1 confirm this. The consequences of these accidents in terms of deaths and injured people and loss of property was sometimes very high, but always limited to a rather small area. The consequences can be much more severe if the buildings that are destroyed accommodate risk-bearing activities.

Although the number of that kind of buildings is only a small portion of the total number of buildings, the probability of a aircraft impact on such structures is not beyond our experience horizon. In this respect it is opportune to mention that in 1988 an F-16 crashed at 15 kilometres from a nuclear power plant in Germany. In the same year a Mirage F-1 crashed 1.5 kilometres from the nuclear power station in Landshut, also in Germany. These events, as well as the impacts on buildings listed in Table 1, are to be considered as precursor events [3]. They point to future events with a very low probability of occurrence but with consequences far exceeding those of the crashes on buildings we have seen so far.

Table 1 Aircraft crashes on buildings in period 1986 to 2000 (after [3], extended)

Year	Country	Description	Death	Injured
1987	Germany	Private aeroplane hit restaurant near Munich	6	--
1987	USA	A-7 Corsair crashed on hotel in Indianapolis	14	--
1987	Germany	Harrier jet-fighter crashed on farm near Detmold	1	--
1988	Germany/ Remscheid	A10 Thunderbolt II crashed and hit twelve buildings. Six apartment blocks caught fire	6	40
1988	Scotland	Boeing 747 crashed in Scotland and hit fuel station and three houses at Lockerbie	280	--
1989	Brazil	Boeing 707 on shanty houses near Sao Paulo	17	200
1990	Italy	Military aeroplane crashed on a school	12	19
1992	USA	Hercules carrier crashed on restaurant and motel in Evansville	16	11
1992	Netherlands	Boeing 747 crashed on 10 story apartment building	43	--
1992	USA	C 130 carrier crashed on house in West Verginia	6	--
1996	Brazil	Fokker-100 crashed in Sao Palo. Many houses in fire	98	--
1996	Paraguay	DC-8 on houses in Asuncion	15	--
1996	Ecuador	Boeing 707 hit tower of church and crashed	>30	80
2000	Greece	Military plane crashed on house	4	--
2000	India	Boeing 737-200 crashed near Patna. Houses burnt down	57	--
2000	France	Concorde crashed on motel near Paris	113	--

AIRCRAFT IMPACT LOADS

Like all impact loads, aircraft impact loads are determined by the velocity of the plane, its mass and distribution of the mass over the length of the plane and the shape and size of the impact area. For design purposes force-time diagrams have been proposed. Examples of such diagrams are shown in Figure 1 for five different aircraft types. From the figure it is clear that there is a big difference between the impact loads caused by different planes. Meanwhile the load-time diagrams of the individual impacts loads have turned out to be plausible. For one aircraft impact, i.e. a F4 Phantom II, the load-time diagram has been verified experimentally in a full-scale test. The result of this test is shown in Figure 2. From the relatively good agreement between design diagram and experiment is has been inferred that also the other design diagrams are appropriate.

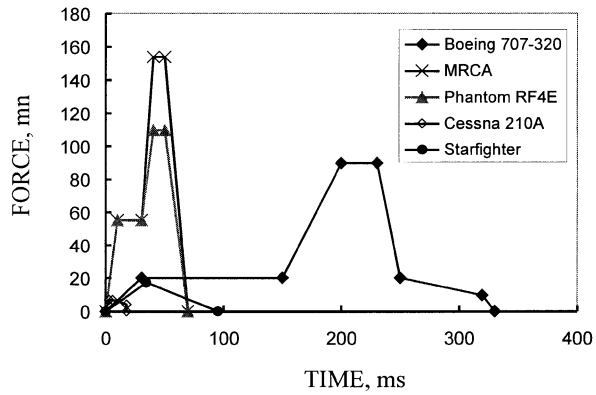

Figure 1 Force-time diagrams for aircraft impact

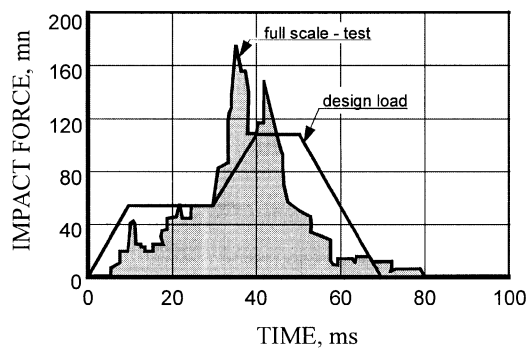

Figure 2 Load-time diagram for aircraft impact: full scale test and design diagram (after [5])

STRUCTURAL RESPONSE UNDER AIRCRAFT IMPACT

Description Of The Protective Structure

The aim of this study is to analyse the additional costs for an aircraft resistant design of a concrete protective structure. For the protective structure a cylindrical concrete structure was adopted, provide with a concrete roof. This structure was designed for storage of Liquefied Petroleum Gas (LPG, atmospheric storage at – 50°C). The diameter of the structure was 50 m, height of the wall 30 m. The thickness of wall and roof and the amount of reinforcing and prestressing steel were designed for carrying the dead load, hydrostatic load and thermal loads, including the thermal shock in case of the failure of an inner tank (Note: an LPG tank generally consists of an insulated steel inner tank and a concrete outer tank). The wall was monolithically connected with the floor slab and with the spherical concrete roof. The initial thickness of the wall and the roof for carrying the "standard loads" was 800 mm and 200 mm, respectively. The relative large wall thickness was required of carrying the high shear forces in the monolithic wall-to-base connection. For the sake of simplicity and while the aircraft impact will finally determine the thickness of the wall, the wall thickness was taken constant over the full height of the tank.

Response Under Aircraft Impact Loads

In literature different methods have been proposed for determining the response of concrete structures under aircraft impact. For this study the relatively simple method proposed by Herzog and the TUV-formula have been used for determining the required concrete thickness for resisting and aircraft impact. Since the main aim of this study was to quantify the extra costs for an aircraft resistant design of a protective structure, the details of the individual calculation procedures will not be dealt with here.

The Herzog-method [5,6] concentrates on the punching resistance of concrete shells. The concrete compressive strength and shear strength of the concrete, dynamic effects, the curvature of the concrete shell and the amount of reinforcement are considered explicitly in the calculated punching shear resistance. The calculated shell thickness includes a prescribed safety factor, for which a value of 1.2 to 1.5 is often used. A value of 1.54 is considered to result in a safe estimate of the punching shear resistance.

For the resistance against scabbing, i.e. the loss of material at the rear side of the shell, NUCON [5,7] uses the TUV-formula (concrete shell loaded by fuselage or engine):

$$S = 1.13\ X + 5.69\ Y$$

where:
S = scabbing thickness [cm]
$X = 0.326 \cdot A \cdot D^{-1,785}$
$Y = 0.446 \cdot A^{0.359} \cdot \exp(-2.1\ D\ A^{-0.359})$
$A = W \cdot V^{1.5} \cdot \sqrt{10.f_c}$
D = diameter of the aircraft fuselage [cm]
W = weight of the aircraft [kg]
V = impact velocity [m/s]
f_c = 28 day concrete cube compressive strength [MPa]

Required Concrete Thickness

For four aircraft impact loads, representative for a starfighter, F16, F4 Phantom II and a MRCA tornado, the shell thickness of a cylindrical concrete structure is calculated. The shell

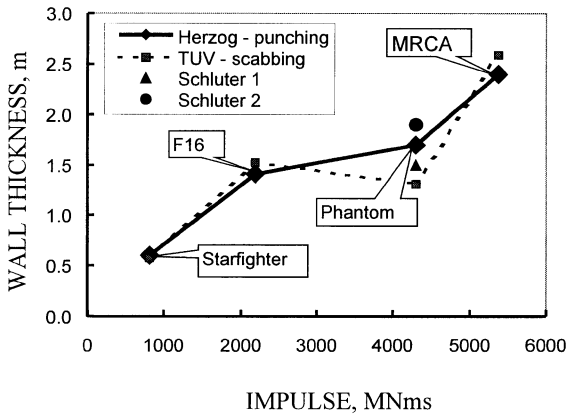

Figure 3 Required shell thickness for aircraft impact design (after [10])

thickness for punching and scabbing were calculated with the Herzog concept and the TUV formula. The required shell thickness for resisting the impact loads is presented in figure 3 as a function of the impulse, i.e. the area under the force-time diagram of the individual impact loads. For the Phantom also the results of Schlüter [9] are presented. Schlüter determined the required shell thickness using a multiple-mass-spring model. In his calculation procedure the typical shape of the load-time diagram was taken into account explicitly.

Figure 3 shows that, except for the F4 Phantom II, the punching resistance according to Herzog and the scabbing thickness found with the TUV-formula were almost the same. The shell thickness found by Schlüter for the Phantom II, obtained using a quite different approach, was in good agreement with the values yielded with the punching shear calculation according to Herzog. From Figure 3 it can be inferred that the calculated shell thickness, obtained using different procedures, is sufficiently reliable to use them as a basis for the analysis of the extra cost for an aircraft impact resistant design.

COST ANALYSIS OF IMPACT RESISTANT DESIGN

The extra costs for increasing the thickness of the concrete roof and the cylindrical shell in order to resist heavy impact loads consist of the costs for material, labour and design costs. Additionally, an increasing shell thickness will result in higher costs for installations, local penetrations of the concrete shell, etc.

The result of the cost analyses are shown in Figure 4. The 100% level refers to the original, non-impact resistant design with a roof thickness of 0.2 m and a wall thickness of 0.8 m. For increasing the roof thickness up to 1.0 m the cost materials and labour costs increased by 40%. For higher impact loads the thickness of both the roof and the cylindrical wall had to be increased. In Figure 4 the extra costs are presented in two ways, i.e. as a percentage of the initial materials and labour costs for the 50,000 m^3 concrete tank and as a percentage of the total project costs. The total project costs are estimated on the basis of integral cost of \$150 per m^3 LPG stored. Already from these two curves it is clear that it makes out all the difference how the extra costs for an impact resistant design are presented. For a comprehensive judgement of the extra costs and whether it is warranted to spend this extra money for extreme loads with a very low probability of occurrence, all the anticipated losses in case of an aircraft impact should be considered.

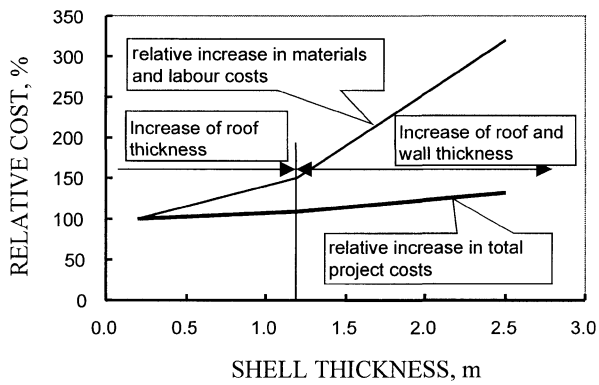

Figure 4 Relative additional cost for an aircraft impact resistant design of a 50,000 m^3 LPG storage tank (after [10])

JUSTIFICATION OF COSTS FOR AIRCRAFT IMPACT RESISTANT DESIGN

Whether the extra costs for an aircraft impact resistant design are justified depends on the potential consequences of a major accident caused by a crashing plane. These consequences will depend on the type of building and the activities that take place inside the building. For a comprehensive judgement of the consequences the complete set of consequence aspects has to be considered. Such a complete set includes not only direct financial losses, but also the long-term financial losses. Besides these short- and long-term losses also social, cultural, psycholo-gical and environmental consequences have to be considered. In many cases the long-term losses and indirect losses of catastrophic accidents exceed the direct losses several times. As an illustration of this, Figure 5 shows the short- and long-term losses of the Chernobyl disaster. The estimates were made shortly after the accident and four years later. In this figure the loss of life and costs for heath care are not included. Meanwhile 30,000 people have been reported to have died as a result of radiation. For new projects Schneider [4] suggests that for each human life saved in case of an industrial accident an additional investment at time zero of about US\$ 250,000 is justified, either for additional active of

passive safety measures. Knowing the number of 30,000 fatalities caused by uncontrolled release of radiating material, additional safety measured would have been warranted of US$ 7.5 billion. This amount is additional to the amount to be taken from Figure 5. The Chernobyl case clearly reveals that the capitalised consequences soon exceed the extra costs for an case clearly reveals that the capitalised consequences soon exceed the extra costs for an aircraft resistant protective structure (Note: extra costs for a 50,000 m^3 impact resistant storage tank, wall thickness 2,5 m, were, in absolute terms, about US$ 3 million).

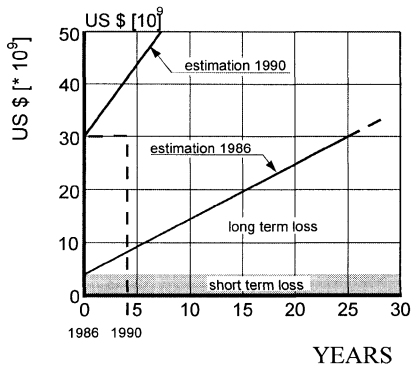

Figure 5 Estimation of short and long-term losses of the Chernobyl disaster [1]

CONCLUSIONS

Consistent scenario thinking and completeness of hazard scenarios are the corner stones of sound safety considerations. A special load case comes from aircraft crashes. Whether impact loads caused by aeroplanes should be considered depends on the consequences in case such an accident occurs. In this paper a number of aspects that affect the decision concerning the need to adopt an aircraft impact as a design load have been envisaged. The following conclusions can be drawn.

- Aircraft impact on buildings is a realistic load case. Its probability can be determined sufficiently accurate on the basis of accident statistics.
- Punching shear resistance of a concrete shell, calculated with the formula proposed by Herzog, and the scabbing thickness calculated with the TUV-formula, give about the same thickness for the concrete shell.
- For impacts caused by different types of jetfighters the required shell thickness to resist these impacts exhibit a good correlation with the impulse.
- For a 50,000 m^3 concrete storage structure for LPG the additional cost for an impact resistant design were up to 40% of the total project costs. This 40% increase of the project costs was due to the increase of the thickness of wall and roof up to 2.2 and 2.5 m, respectively, thick enough to withstand the highest design impact load of an MRCA.
- Justification of the extra costs of an aircraft impact resistant design should be based on a multidisciplinary evaluation of all short and long-term consequences of an aircraft impact.

REFERENCES

1. BOMHARD, H., BREUGEL, K. VAN (ed.), Protective systems against hazards – Nature a nd Extent of the Problem, fib-bulletin 5, 1999, 58 p.

2. BUREAU VERITAS, Liquefied gas storage installations under atmospheric pressure. Guidance Note NI 002 CMI OCT. 84, 1984, 56 p.

3. BREUGEL, K. VAN, About the role of precursor events in the judgement of Low Probability – High Consequence risks. Proc. 8th Int. Conf. on Safety and Reliability, 2001, California, ICOSSAR'01 (in print).

4. SCHNEIDER, J., Safety – A matter of Risk, Cost and Consensus. Structural Engineering International, 2000, 4, pp. 266-169.

5. RAMLER, J.P.G., BREUGEL, K. VAN, Impact – Loads and response (In Dutch). Delft University of Technology, Report 25.5-89-06/A1, 1989, 220 p.

6. HERZOG, M., Durchtanzen der Abschirmkuppel eines Reaktorgebaudes bei Flugzeugauf-prall. Der Bauingenieur, 1978, 53, pp. 109-111.

7. NUCON-Report, Dynamic calculation methods for the design of buildings, structures, systems and components. NUCON Engineering and Contracting, 1986, Project no. N3513-02.

8. BREUGEL, K. VAN, Beyond the Risk Concept. Proc. 7th Int. Conference on Structural Safety and Reliability, Kyoto, Vol. I, 1997 pp. 255-262.

9. SCHLUTER, F.H., 1990. Dynamische Beanspruchung von Platten. Colloquium Deutscher Ausschuss fur Stahlbeton, 1990, Karlsruhe.

10. MEYDAM, L., WIJK, M.H. VAN, Concrete protective structures under aircraft impact (in Dutch). Msc-Thesis, TU Delft, 1990, 198 p.

FIRE RESISTANCE REQUIREMENTS FOR BUILDINGS

S Kumar
Harcourt Butler Technological Institute
India

ABSTRACT. One aspect of building regulation, which is directly concerned with the design of structures, is the fire resistance of the structure. This review outlined some of the major developments that have occurred in structural fire engineering design during recent years. The general principles are discussed together with the various approaches that can be adopted by an architect or engineer to design a structure capable of withstanding the attack of fire without collapsing using scientific concepts as a basis for determining the fire resistance and protection requirements. The fire resistance of various structural members can be determined by testing or, in many cases by calculation, which is far expensive and time consuming. The development of realistic methods for calculating fire resistance in an actual fire enables the building designer to adopt a rational approach to fire safety in building design. The most notable factors considered in this study are fire load intensity and size and shape of the openings. This paper summarizes some of the fire loads data conducted in office and residential buildings in Kanpur, India. The structural interaction and response in an elevated temperature environment are explained.

Keywords: Accidental damage, Buildings, Durability, Fire damage, Fire proofing, Fire resistance, Fire resistant structures, Fire safety, Fire-temperature curve, Structural fire engineering.

Dr Sunil Kumar, is Assistant Professor in Civil Engineering at Harcourt Butler Technological Institute, Kanpur, India. He received his B.Sc. Engineering in Civil Engineering from Aligarh Muslim University, Aligarh, M. Tech. From Kurukshetra University, Kurukshetra and Ph. D. from Kanpur University, Kanpur. His main research interests include the durability of concrete structures in aggressive environments, structural fire engineering, probabilistic design loads in buildings and waste management. Dr. Kumar has published research papers widely in National and International Journals and Seminars. He has several years of experience in designing a number of concrete structures including tall buildings, water retaining structures, and water and sewage treatment plants in India.

INTRODUCTION

Providing structural elements of an appropriate fire resistance, specified in building regulations, so that in the event of a fire they continue to perform their design function, ensures the safety of a structure against fire. The fire resistance of an element is measured by its endurance in terms of time in a standard furnace test. While this test may be useful for establishing comparative fire rating for different structural components, it may not provide a good indication of how they might behave during an actual fire. Standard fire test is generally a conservative representation of a natural fire because it implies that there is an inexhaustible supply of fuel.

With increasing sophistication in methods of predicting fire resistance, the need increases for more refinement in determine how much fire resistance has to be provided. During the last three decades, rapid progress has been made in the development of realistic methods for fire engineering design of structural members. Advances have been made both in understanding the behavior of real fires in buildings and their correlation with experimental and standard fire tests. Therefore, it is now possible to design and more precisely calculate the fire resistance requirements of a building and where necessary, specify the type and thickness of fire protection required by structural members using an alternative fire engineering approach.

Numerous compartment fire tests have indicated that while the fire curves depend on many factors, the two significant parameters are the fire loads and an opening factor. With fire loads and opening factor defined, realistic fire curves for design can be generated.

First is the determination of fire load, i.e., the combustible contents, on which the fire resistance design of the building should be based. At the present time, there are limitations in our knowledge base, which have to be considered when adopting a probability based design guide for structural fire safety.

This paper provide a summary of practical information intended for use by architects, engineers, and building officials who must design concrete structures for particular levels of fire resistance or evaluate structures as designed. Therefore the purpose of this paper is to introduce the general principles of an alternative, more rational fire engineering approach which can be used in assessing the fire resistance requirements of a structure and the ability to withstand the natural fire.

FIRE RESISTANCE

The building must be capable of maintaining its structural integrity during a fire over a period of time, determined by actual fire conditions and the required safety level, meanwhile protecting its occupants and providing them with a safe means of escape. This period of time over which structure will resist the effects of a fire is termed as fire resistance. Provision of appropriate fire resistance is one of the requirements in buildings. The fire resistance of various structural members can be determined by standard fire resistance test or by using alternative methods based on real fire conditions.

The standard fire resistance test is based on standard fire exposure curve, which is defined by a temperature-versus-time relationship and increases monotonically during the rating period and is the same for all building occupancies. Although not long ago fire resistance of

members could only be determined by costly and time consuming tests, calculation methods are more and more replacing them. Many fire resistance design formulas derived from results of computer simulations and validated by furnace tests have been developed in recent years. They can be used for the purpose of satisfying building code requirement.

Fire Resistance by Testing

In laboratory tests, time temperature curve of an international standard taking the same form [1] in ISO, ASTM, BS 476 Part 20 and other national codes of different countries is used. There is a substantial evidence [2-8] to show that the laboratory fire test may be inappropriate indicator of how a structural element behaves during an actual fire. The use of one unique increasing fire fails to recognize that the amount and composition of materials in the compartment, as well as ventilation effects, will cause variations in the rate of heat generated and the peak temperature reached. The decrease in temperature following the exhaustion of the finite amount of fuel is characteristic of realistic fire curves [3,9] but currently is not taken into account in standard fire tests, since performance is considered during the rising temperature portion.

It may be advantageous to allow the use of one of several natural fire exposures, depending on building occupancy, in fire resistant structural design and in component quantification testing for various occupancies. The temperature obtained in a fire and the duration for which they are maintained depends on fire loading, ventilation rate and the thermal properties of the enclosed construction materials.

Conceptually, different fire curves can be generated for any combination of fire load and opening factor, including the effect of different bounding surface composition [6]. Consequently, to investigate the requirements for fire resistance, in buildings with different type of occupancies, in general would necessitate fire load density and ventilation being collected in a number of buildings.

There are only limited data available to describe fire loads. Assuming that the fire load is known, the fire temperature curves of a building compartment can be obtained by using energy - balance equation. These natural fire curves are to be used in classifying the structural members with respect to fire by performing experiments in the standard furnace as an alternative to the internationally prevalent method of classification based on results of standard fire resistance test.

Fire Resistance by Calculation

A study of the available information was carried out by Law [10]. The study showed that the fire resistance required in any building could be calculated by using the relation:

$$t_f = \frac{k.L}{(A_w.A_t)^{1/2}} \qquad (1)$$

Where t_f is the required fire resistance time, k is a constant, which, depending on circumstance, takes a value between 1.0 and 1.3 min. $m^2 kg^{-1}$, L is the total fire load in kg, A_w is the area of ventilation in m^2, and A_t is the area of walls and ceilings of the compartment in m^2, excluding the ventilation openings.

Equation 1 has been well tested for both kinds of fire behavior, that is, the air controlled regime and fuel-controlled regimes. Further large scale experiments in bricks and concrete compartments and different fire loads gave a value for k approximating to unity. Hence, equation 1 may be written as

$$t_f = \frac{L}{A_f} x \frac{A_f}{(A_w . A_t)^{1/2}} \tag{2}$$

Where A_f is the floor area in m^2. It can be seen that the first term in the above equation is the conventional fire load and the second term is a geometric one determined by building designer. Hence if fire load intensity is correctly known, the building designer can control the geometry and ventilation of the building compartment to increase its fire resistance. Malhotra [11] gave two further equations based on work by Pettersson [12] for determining the equivalent fire resistance necessary for construction components located in fire compartments.

FIRE LOAD INTENSITY

The fire load determines the duration of the fire, whereas the openings influence both intensity and duration. From this it is possible to determine the fire temperature course for a given building.

The fire load is a measure of the amount of material available to burn, whether it forms part of the structure (static) or its contents (mobile). At present only limited data exist concerning the values of fire loads in buildings [13-21]. Moreover these data are in terms of fire load per unit area rather than bounding surface area.

The size and shape of a compartment can have a significant effect upon the burning rate and consequently the atmospheric temperature attained during a fire. To some extent this is taken into account by defining fire load density in terms of MJ/m^2 of bounding surfaces. This implies that for the same floor coverage, a tall room will have a greater volume of air as well as an increased wall area over which heat can be lost.

Surveys have shown that fire load is dependent on occupancy; for example, residences, offices, libraries, hotels etc. have different values of fire load. Since the nature of building components change, there is a continuing need to update fire load survey data to reflect current conditions. Most of the previous surveys were conducted mostly in office buildings. Moreover most of the surveys were done about 20 years back in developed countries. Hence, there is a need to update load surveys data to reflect current condition.

Fire load density q is derived from

$$q = \frac{1}{A} \sum m_v H_v (m_i) \tag{3}$$

Where A is the bounding surface area in m^2, m_v is the total mass of the vth combustible material in kg, H_v is the calorific value for the vth combustible material in MJ/kg and m_i is the combustible factor. The actual value of m_i is a function of the type of fuel, and the position of fuel in fire compartment, among other things.

The masses of the different items are obtained by using the combustible factor and are multiplied by their respective calorific values, and then added to get the total amount of combustible items. The total quantity of combustibles present in a room is divided by the total interior area of the surface bounding that room, including all openings, to get the fire load corresponding to that room. A detailed description of the survey data collection and the data processing procedure is given in the previous paper of Kumar and Rao [20]. Since, failure depends on extreme vale of the fire load, the assessment of fire load, which was previously based on professional judgment, just on the mean and standard deviation, can now be carried out more accurately by probabilistic model prediction.

Ideally in full structural engineering design calculations the fire load density should be determined for each compartment within the building. However, this is usually impractical. Therefore, for specific occupancies statistical data can be referred to which have been derived from analyses of a large number of rooms. The author has conducted an extensive survey of offices and residential buildings in Kanpur, India and the results of this survey are reported elsewhere [20, 21]. Typical results are given in Tables 1-3.

Table 1 Influence of category of housing on fire load (residential buildings)

CATEGORY OF HOUSING	FIRE LOAD (MJ/m^2)		
	Maximum	Mean	Standard Deviation
One room housing	790.9	502.4	128.7
Two room housing	735.7	432.2	118.7
Three room housing	601.9	401.3	105.3
Four room housing	649.2	382.1	102.8
Greater than four room housing	570.6	361.2	86.1

OPENING FACTOR

Apart from the characteristics of the fire load, the temperature attained inside a compartment may also be controlled by the size and shape of the openings. When the window opening is small the amount of air reaching a fire will be limited, as the window opening is increased the rate of burning of fire will increase because of the greater supply of air. This kind of fire behavior is called a ventilation-controlled fire.

Table 2 Influence of room use on fire load

ROOM USE	FIRE LOAD (MJ/m^2)			
	Residential Buildings		Office Buildings	
	Mean	Standard deviation	Mean	Standard deviation
Drawing room	427.6	86.9	--	--
Dining room	428.9	146.7	--	--
Bed room	495.7	170.1	--	--
Corridor	278.8	112.0	153.0	139.6
Kitchen	673.0	206.9	--	--
Store room	852.3	621.6	601.1	371.6
Reception	--	--	536.7	349.4
Technical	--	--	433.9	301.8
General	--	--	300.1	191.4
Clerical	--	--	431.8	199.8
Auditorium	--	--	188.5	39.3
Bathroom/Lavatory	382.5	124.1	146.3	143.0
All rooms	487.0	255.0	348.2	261.7

Table 3 Influence of floor level on fire load

FLOOR LEVEL	FIRE LOAD (MJ/m^2)			
	Residential Buildings		Office Buildings	
	Mean	Standard deviation	Mean	Standard deviation
Ground floor	389.6	95.3	369.9	173.1
First floor	408.8	101.6	306.4	78.6
Second floor	391.2	112.4	346.5	106.2
Third floor	377.5	79.8	303.5	26.8

As the window opening is increased still further, the stage is reached where the combustibles have a sufficient supply of air and any further increase will not cause a greater rate of burning. When this stage is reached the fire is said to be fuel controlled. That is, the rate of burning is now determined by the nature and disposition of the combustible material.

Magnuson and Thelandersson [22] have suggested that the problem of ventilation control v/s fuel control is by no means only of academic interest. To make it possible for the practicing engineer to use this differentiated approach, all the design curves in the manuals published are based on the assumption that fire development is ventilation controlled for all ratio of fire load to ventilation openings

The basic parameter for describing the ventilation condition of the room or fire compartment is the opening factor. The opening factor represents the influence of the ventilation of the room or fire compartment and is defined as, $A_w\sqrt{h}/A$ ($m^{1/2}$), where A_w is the total area of door and window openings in m^2, h is the average height of the openings weighted with respect to each individual opening area in m, and A is the total interior surface of the room including openings in m^2 [6,7].

With regard to window and door openings considered in the assessment, it has to be ensured that any covers of openings are either automatically released or is destroyed early in the fire process. A wide squint window is better than a tall narrow window of the same area, with the former the rate of burning of the combustibles will be less than with the latter. One much publicized aim of the fire prevention education has been to persuade people to shut doors and windows in houses at night in order to delay the growth of a fire by restricting the air supply.

TEMPERATURE EFFECT ON CONSTRUCTION MATERIALS

Reinforced concrete is perhaps one of the best fire resistant materials in common structural use. The need to understand its behavior in fire and other industrial disaster conditions has resulted in considerable research into the effect of elevated temperatures on the properties of reinforced concrete [23].

Concrete is subjected to a form of damage due to excessive heat, which is known as spalling. When fire causes spalling of the concrete, the reinforcing steel may be exposed, and the heated steel will lose its strength. Spalling can occur when moisture within the concrete expands and causes cracks or chunks of the concrete to break off. Spalling can also occur due to thermal expansion of the outer surface in contact under compression as in columns, walls, or prestressed structural members.

The effect of increase in temperature on the strength of concrete is small and somewhat irregular below 250^0C [24], but above 300^0C a definite loss of strength takes place. Concrete heated by a building fire loses compressive strength and continues to lose it on cooling. Where the temperature has not exceeded 300^0C most of the strength will eventually be recovered. Harda [25] has shown that concrete, which has been heated at a temperature below 500^0C, will rehydrate when cooled down and gradually regain most of its strength. After about one year, the recovery in strength is about 90%.

If the temperature is of short duration, a slow recovery of strength may take place. The loss in strength at higher temperatures is greater in saturated than in dry concrete, and it is the

moisture content of the concrete that is the most important factor determining its structural behavior at higher temperatures [26]. Leaner mixes appear to suffer a relatively lower loss of strength than richer ones. The temperature of 400^0C is an upper limit for O.P.C. concretes, since any concrete heated to a significant duration will deteriorate on subsequent post cooling exposure in air. However, this limit can be virtually eliminated by using pozzolanic Portland cement replacement agents, which reduce the free lime in hydrated paste [23].

It is readily appreciated that any exposed steel will begin to show a reduction in its strength from 300^0C [27]. Unless the hot rolled reinforcement has been exposed for any length of time to temperatures exceeding 600^0C due to early spalling of its concrete cover, the possibility of permanent reduction in strength is remote [27]. Cold worked reinforcement heated above 400^0C will; however lose a measurable proportion of the strength obtained due to cold working. The steel in prestressed concrete will lose approximately 20% of the strength at 600^0F and it does not regain their strength when it is cooled [28].

In calculating the atmosphere heating rate inside a compartment consideration is given to the type of materials used in its construction. Building which is poorly insulated will lose a substantially larger portion of the heat through its surfaces than a building, which is constructed from materials that have good insulation properties.

Methods exist for calculating the temperatures in fire exposed structural members. In these, the dependence of material properties on temperature can be taken into account and a high accuracy obtained if the material properties are known.

When temperature rises in fire - exposed members, their strength is reduced. If the fire load is sufficient and the duration of the fire long enough a stage will be reached at which the strength of the member will no longer be adequate to support the structural load. The fire load that is just sufficient to reduce strength to this critical point is defined as the critical load. The aim of fire resistant buildings is to make the critical fire load for a member sufficiently high to allow it to withstand burn out of the design fire load. In general, this can be achieved by selecting appropriate protecting materials of adequate thickness and appropriate dimensions of the members.

CONCLUSIONS

This paper has introduced the main concepts involved in structural fire engineering design, important developments that have taken place in recent years and how they have been applied in actual situations. The alternative of continuing to base acceptance of one universal standard test appears to impose an economical penalty. The use of one unique increasing fire fails to recognize that the amount and composition of material in the compartment, as well as ventilation effects, will cause variations in the rate of heat generated and the peak temperature reached.

It may be advantageous to allow the use of one of several natural fire exposures, depending on building occupancy, in fire resistant structural design and in component quantification testing for various occupancies. The main advantage of structural fire engineering design calculations is the availability of an alternative design approach leading to economical and safe solutions, which can be introduced at an early stage in a project by architects and engineer.

However, additional research is required to develop an ensemble of fire exposure curves that could be used for this purpose. More and more data collection and use of probabilistic modeling techniques is required to predict design fire loads which will provide a more rational approach to design and quantification of fire safety.

REFERENCES

1. CONNOR, D.J.O., Structural engineering design for fire safety in building. The Structural Engineer. 1995, 73 (4), pp 53-58.

2. MAGNUSSON, S.E., THELANDERSSON, S., Temperature-time curves for the complete process of fire development. Acta Polytechnica Scandinavica. Civil Engineering and Building Construction Series No. 65. Stockholm, Sweden, 1970.

3. LIE, T.T., Characteristic temperature curves for various fire severities. Fire Technology. 1974, 10 (4), pp 315-326.

4. HARMATHY, T.Z., Fire resistance versus flame spread resistance. Fire Technology. 1976, 12 (4), pp 290-302.

5. PETTERSSON, O., Theoretical design of fire exposed structures. Division of Structural Mechanics and Concrete Construction Bulletin 51. Lund Institute of Technology, Lund, Sweden, 1976.

6. ELLINGWOOD, B., SHAVER, J.R., Effects of fire on reinforced concrete members. Journal of Structural Division. ASCE 1980, 106 (11), pp 2151-2166.

7. ELLINGWOOD, B., Impact of fire exposure on heat transmission in concrete slabs. Journal of Structural Division. ASCE 1991, 117 (6), pp 1870-1875.

8. HOSSER, D., DORN, T., RICHTER, E., Evaluation of simplified calculation methods for structural fire design. Fire Safety Journal. 1994, 22, pp 249-304.

9. LIE, T.T., Calculating resistance to fire. Division of Building Research. Canadian Building Digest. May 1979, CBD 204-204-4.

10. LAW, M., Prediction of fire resistance requirements for buildings: a new approach. J.F.R.O. Symposium No. 5, Her Majesty's Stationery Office, London, 1971.

11. MALHOTRA, H.L., Design of fire resisting structures. Surrey University Press, London, 1982.

12. PETTERSSON, O., Fire engineering design of tall buildings. ASCE-IABSE Int. Conf. Reprints, Lehigh University, Pennsylvania, 1972.

13. Fire Resistance Classification of Building Construction. Building Mat. Struct. Report BMS 92, Nat. Bureau of Standards, Washington, D.C., 1942.

14. KAWAGOE, K., SEKINE, T., Estimation of fire temperature-time curve in rooms. Building Research Occasional Report No. 17, Building Research Institute, Ministry of Construction, Tokyo, 1964.

15. BRYSON, J.O., GROSS, D., Techniques for the survey and evaluation of live floor loads and fire loads in modern office buildings. Building Sc. Ser. No. 16, Nat. Bureau of Standards, Washington, D.C., 1967.

16. BALDWIN, R., ET AL., Survey of fire loads in modern office buildings – some preliminary results. JFRO Fire Res. Note No. 808, Her Majesty's Stationery Office, London, 1970.

17. CULVER, C.G., Survey results for fire loads and live loads in office buildings. Build. Sc. Ser. No. 85, Nat. Bureau of Standards, Washington, D.C., 1975.

18. A conceptual approach towards a probability based design guide on fire safety. 1983. CIB W 14, Fire safety Journal, 6, pp 1-59.

19. CHOI, E.C.C., Data structure and data processing procedures for live loads and fire loads in office buildings. Tech. Rec. 524, Nat. Build. Tech. Centre, Sydney, 1988.

20. KUMAR, S., RAO, C.V.S.K., Fire loads in office buildings. Journal of Structural Engineering. ASCE 1997, 123 (3), pp 365-368.

21. KUMAR, S., RAO, C.V.S.K., Fire load in residential building. Building and Environment 1995, 30 (2), pp 299-305.

22. MAGNUSSON, S.E., THELANDERSSON, S. A., Discussion of compartment fires. Fire Technology 1974, 10, pp 228-245.

23. DIAS, W.P.S., Some properties of hardened cement paste and reinforcing bars upon cooling from elevated temperatures. Fire and Materials. 1992, 16, pp 29-35.

24. SAEMANN, J.C., WASSHA, G.W., Variation of mortar and concrete with temperature. ACI Material Journal 1957, 54, pp 385-395.

25. HARDA, T., ET AL., Strength, elasticity and thermal properties of concrete subjected to elevated temperatures. Int. Sem. on Concrete for Nuclear Reactors. ACI Sp. Publn. No. 34, 1972, pp 1: 377-406.

26. LANKARD, D.R., ET AL., Effects of moisture content on the structural properties of Portland cement concrete exposed to temperatures up to 500^0 F. Temperature and Concrete. ACI Sp. Publn. No. 25, 1971, pp 59-102.

27. VIRDI, K.S., Fire resistant design of the structures, Int. Sem. on Civil Engg. Practices in the Twenty First Century, Roorkee, India, 1996, pp 1736-1755.

28. PRAKASH, A., Fire damage assessment, design check and strengthening of a R.C. frame building. Int. Sem. on Civil Engg. Practices in the Twenty First Century, Roorkee, India, 1996, pp 1719-1735.

BEHAVIOUR OF HIGH STRENGTH REINFORCED CONCRETE BEAMS EXPOSED TO DIRECT FIRE

H H Ghith

Building Research Center

M Awad

Dar El-Handsa Consulting

Egypt

ABSTRACT. The performance of high strength reinforced concrete beams at elevated temperatures is critical especially in case of the evaluation of building behavior in fire conditions. Many researches reported and explained the fire effect on the mechanical properties of the normal concrete and reinforcement. As the need of high strength concrete arises with increasing demands for an unproved efficiency and reduced concrete construction cost, the effect of fire on high strength concrete beams were studied in this research. In this research twelve high strength concrete beams were casted to study the factors affecting this behavior. The factors taking into consideration in this research were the thickness of concrete cover and time exposure to fire. The cover thicknesses taking in this research were 1.5 cm, 3.0 cm and 4.5 cm. Time exposures to fire taken into account in this research were 0, 30 minutes, 60 minutes and 120 minutes. The temperature inside the oven used was 650°C. The tested beams were exposed to direct flame for the test time, beams were left to cool gradually. The temperature inside the oven was raised till 650°C in 3 minutes. The results of testing were illustrated in charts for load - deflection relationship, load maximum - tensile strains, load - maximum compressive strains. Deformation shapes and the modes of failures were presented. Conclusions according to the test results were drawn.

Keywords: High strength concrete, Fire, Deformations, Concrete cover, Heating, Time of exposure to fire.

H H Ghith is a Associated Professor of reinforced concrete structures, in the Building Research Center, Cairo, Egypt.

M Awad is a an engineer at Dar El-Handsa Consulting Firm at Cairo Branch, Egypt.

INTRODUCTION

Since the use of high strength concrete is a recent development, there is a little information on the effects of high temperature on its properties. The ability of concrete to withstand high temperature can be hampered considered by spalling. Most of the previous researches covered agree that moisture content, in combination with one or more unfavorable working factors, is the cause of spalling. Theoritically speaking, high strength should have a higher tendancy to spall because of its low permeability, which leads to intrap of the internal moisture and causes extra tensile stresses which causes the sudden noisy failure. Researchers [1] studied the effect of high temperature on high strength concrete obtained by using type (F) super-plasticizer, they found that an initial loss in the strength at 100 °C was 10 to 20% of the room temperature strength, after 200 °C a recovery strength reached a peak value that was 8 to 13% above the room temperature strength. In temperature ranges of 400 to 800 °C, the strength in each case dropped sharply, reaching a low of about 30% of room temperature strength.

It was pointed [2] that the risk of explosion of concrete increases with increased moisture content, increased heating rate, decreased permeability and decreased tensile strength of concrete. His tests confirmed the following results: the free water which the spalling is unlikely to occur is less than 3 to 4 % by weight for concrete defined by silica fume. The results indicated that for dry specimens the chemically bound water is an essential part of the moisture causing the explosions, for concretes containing various proportions of silica fume, it was found that these concretes may explode at a heating rate of only 1 °C per minute, whereas heating rates of 10 °C per minute and greater are required for other concretes to explode (a heating rate of 10 to 20 °C per minute is normal to fire exposed structures) i.e. these tests indicate that concrete densified by using silica fume are more likely to explode.

Tests [3] were conducted a fire test on two full size T-beams, one of high strength concrete and the other of normal strength concrete with 28 day compressive strength of 920 and 250 kg/cm^2 respectively. Sever explosive spalling of high strength concrete specimens started at temperature of 715 °C, while no spalling was observed in the normal concrete specimens. The spalling of high strength concrete specimen occurred in the flange of T – beam where the cover of the steel was very large and equal to 7.5 cm. There was no spalling in the flange with 2.5 cm cover. It apears that in common construction types, where the cover to steel is not as large as 7.5 cm, high strength concrete may be safe from spalling, although high strength concrete might be more prone to spalling in a fire than normal strength concrete.

Experiments[4] Carried out no significant difference in behavior between high strength concrete and normal strength concrete. They have conducted a fire test on model sized reinforced slab speciemens (90x90x10cm) with normal compressive strength of 345 and 945 kg/cm^2. The specimens were subjected to a 4 hours fire exposure following the time versus temperature relationship specified in the ASTM 119-83. Results of the testd specimens exhibited spalling of the exposed surface nor was any explosive behavior observed.

EXPERIMENTAL PROGRAM

The previous introduction makes it possible to introduce the objectives of this research. The experimental program was performed to investigate the behavioral characteristics of reinforced concrete beams exposed to direct fire for different time intervals and then cooled

gradually in air. After that they were tested under monotonically increasing vertical loads until failure. Load – deflection relationships were recorded at each load increments. The main parameters studied through this test program were as follows:

Concrete cover:

Three concrete covers were taken into account in this research. These concrete covers are 1.5, 3.0 and 4.5 cm.

Time exposure to fire:

Four time intervals of exposure to direct flame were taken into consideration in this research. These time intervals are 0, 30, 60 and 120 minutes. The first interval with zero time is taken as a reference to compare the effect of fired beams with the normal beams.

Specimens

Twelve reinforced concrete beams were constructed with the following dimensions:

- Rectangular cross section b x d = 12.0 x 23.0 cms
- Length = 2.60 m.
- Clear span between supports = 2.40 m.
- Reinforcement ratio = 0.833 %
- Compressive characteristic strength = 967.7 kg/cm^2
- Main steel = 2 ϕ 12
- Type of main steel = 36 / 52 (high tensile steel)
- Type of stirrups steel = 24 / 36 (mild steel)
- Stirrups = 5 ϕ 8 mm/m
- Cement = Super Fine Portland Cement
- Cement Content = 400 kg/ m^3
- Admixtures = Silica fume content 8% of cement weight.

Six standard concrete cubes (15.0 x 15.0 x 15.0 cms) were also casted with each beam to determine the compressive strength.

Material properties

Locally produced available materials were used as follows:

- Super Fine Portland cement confirming to the Egyptian standard specifications was used.
- Natural siliceous sand and dolomite stones with maximum nominal size 20mms were used as fine and coarse aggregate respectively. Quality control tests took place on sand and stone specimens to assure their appliance for Egyptian standard specifications.
- Steel reinforcement used was as follows, mild steel reinforcement defined as (24/35) for stirrups and, while high-grade steel reinforcement defined as (36/52) for longitudinal bars.
- Water used in all test specimens was tap drinking clean and free from impurities.

Casting

Mix proportions by weight was 1: 1.75: 3.5 (C: S: G) and the water to cement ratio was 0.40 by weight The target standard cube compressive strength was 933.0 Kg/cm^2 after 28days. The concrete was mixed in revolving drum type electrical mixer of capacity 0.1m^3 and vibrated carefully after being placed in the molds with dimensions listed. All specimens were removed from the molds after 24 hr. They were cured under wet burlap for two weeks, after which they were left to dry in the air for another two weeks in lab temperature.

Test Procedure:

One week before testing, all the beams were painted with diluted white lime solution to facilitate observation of cracks during testing. Beams and cubes had exposed to fire for the required intervals. Figure 1 shows the experimental work group. . Figure 2 shows the details of tested beams and also the details of reinforcement. Figure 3 shows the corresponding time temperature curve for the oven used to burn the tested beams. The beams were exposed to direct fire flame. Temperature inside the oven was measured each 5 minutes to be sure that the applied temperature is as shown in Figure 3. After the removal of the tested beams out of the oven they were left in air to cool gradually. No water was added to cool the beams.

After cooling the beams cubes were tested to determine the strength of concrete used after burn. Figure 4 shows the shape of loading these beams. Deflections under applied load and also under the mid-span of the beams were measured using dial gauges with accuracy of 0.001 mm. The strains along the mid-span height were also measured using demic points. Cracks were marked each load increment.

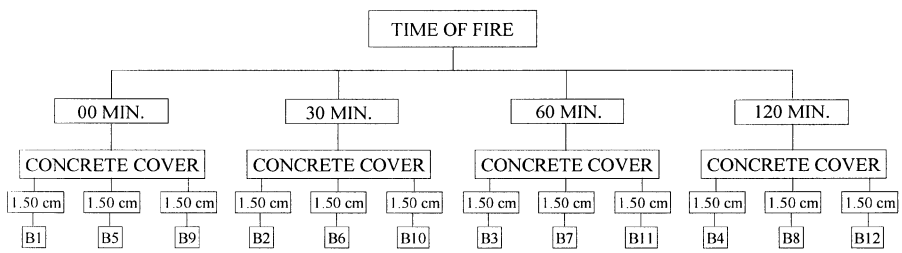

Figure 1 Experimental work program

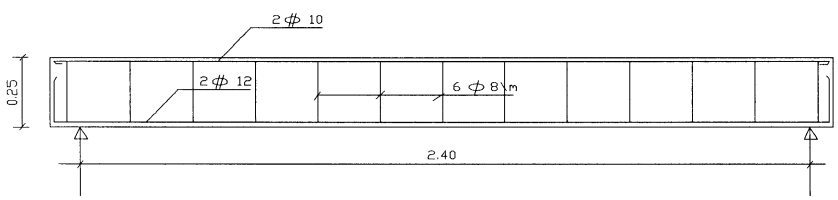

Figure 2 Details of tested beams reinforcement and dimensions

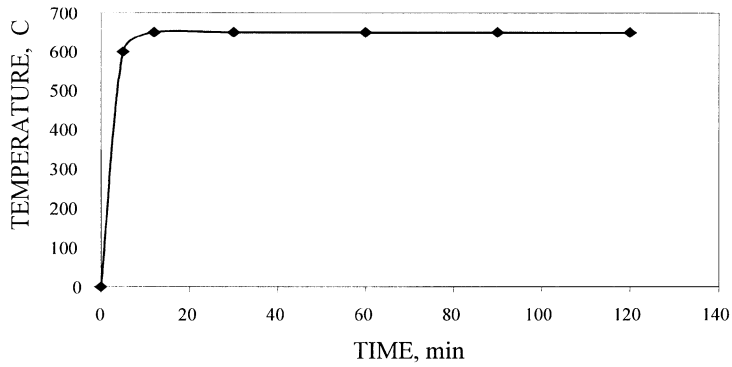

Figure 3 Time temperature applied for the tested beams

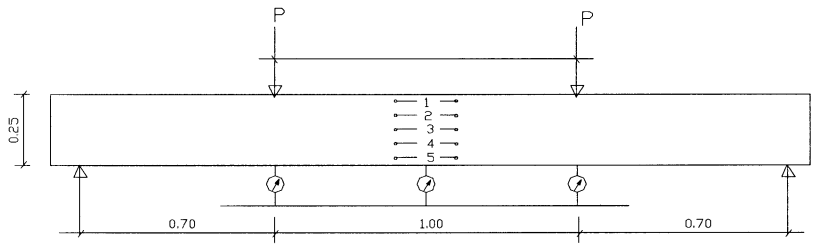

Figure 4 Details of beams loading and measurements

ANALYSIS AND TEST RESULTS

Ultimate load

Table (1) shows the ultimate load of the tested beams. It is seen that the ultimate load decreases with the increase of time exposure to fire. The ultimate load decreases by about 6% when exposed to fire 30 minutes, decreases by about 11% when exposed to fire 60 minutes and decreases by about 15% when exposed to fire 120 minutes. These values are nearly the same for all cases of the beams. It is also seen from the figure the decreases of the ultimate decreases with the increase in cover thickness.

Deflections - Effect of time exposure to fire

Measured deflections were recorded for all the investigated beams. The test results are arranged presented in figures giving the maximum measured deformations for each beam and the corresponding loads up to the failure loads.

Figure 6 shows the relation between the applied load and the deflection at mid span of the beams B1, B2, B3 and B4 which have the same properties (with concrete cover equal 1.5 cm) but have differ time of exposure to fire. It is seen the measured deflections exceed with the increase of time exposure to fire. The deflections of the beams burned for 2 hours (B4) have deflection about 152.3% of the deflection of the original beam (B1). It is also noticed that there was a sharp increase on the deflection after about 35% of the ultimate load.

Figure 7 shows the load deflection curve for the beams B5, B6, B7 and B8. These beams have concrete cover equals 3.0 cm. It is noticed that the maximum deflection of the burned beams is bigger than that of the original beam B9. The increase in that deflections of the beams B6, B7and B8 are 14.3, 32.4 and 61% bigger than the deflection of beam B9.

Table 1 Ultimate loads for the tested beams

BEAM	ULTIMATE LOAD (ton)	% OF ULT. LOAD/ REF. BEAM LOAD	MAX. MEASURED DEFLECTION (cm)	% OF ULT. DEFL./ REF. BEAM DEFL.
B1	8.30	100	0.88	100
B2	7.80	93.98	1.13	128.4
B3	7.65	92.17	1.21	137.5
B4	7.15	86.14	1.34	152.3
B5	8.40	100	0.77	100
B6	8.20	97.62	0.88	114.3
B7	8.00	95.24	1.02	132.4
B8	7.50	89.29	1.24	161.0
B9	8.45	100	0.71	100
B10	8.38	99.17	0.79	111.3
B11	8.20	97.04	0.88	114.3
B12	7.80	92.31	1.13	159.2

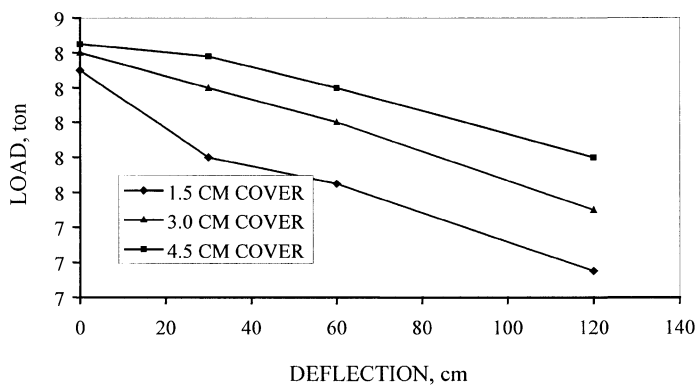

Figure 5 Load time exposure curve

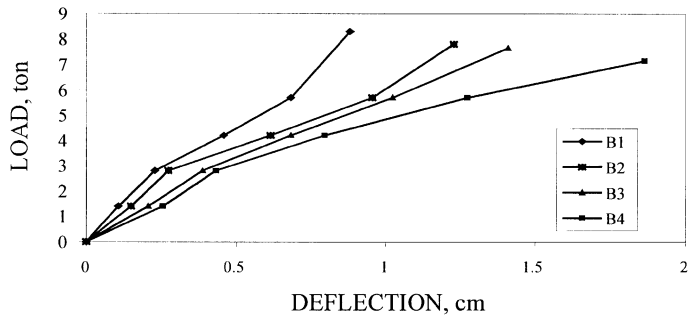

Figure 6 Load deflection curves for beams have 1.5 cm cover

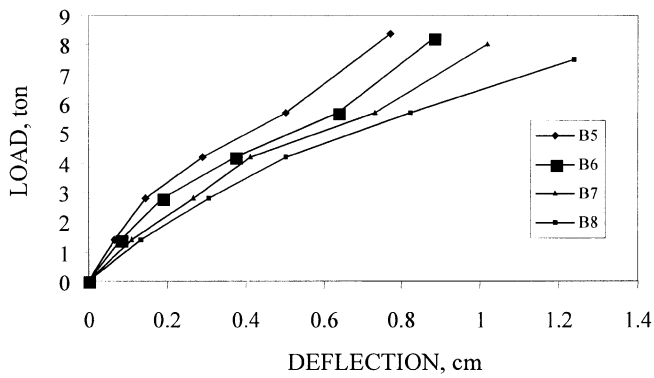

Figure 7 Load deflection curves for the beams have 3.0 cm cover

Figure 8 shows the load deflection curve for the beams B9, B10, B11 and B12. These beams have concrete cover equals 4.5 cm. It is noticed that the maximum deflection of the burned beams is bigger than that of the original beam B12. The increase in those deflections of the beams B10, B11 and B12 are 11.3, 14.3 and 59.2% bigger than the deflection of beam B9. It is also noticed that the deflections of this group are less than the deflections of the previous groups for the same time of exposure.

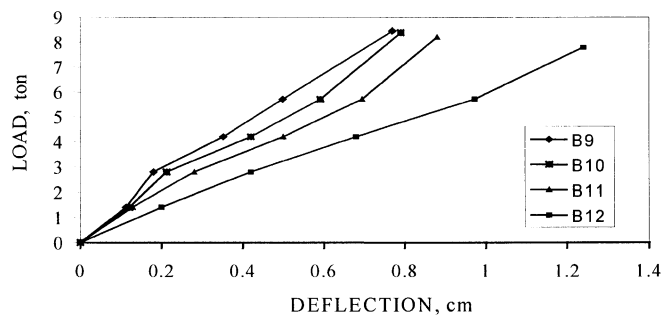

Figure 8 Load deflection curves for the beams have 4.5 cm cover

Longitudinal strains

For concrete cover equals 1.5 cm for beams B1, B2, B3 and B4, the compression and tension strains increased by increasing the duration of fire at different stages of loading. The maximum compressive strains of beams B2, B3 and B4 increased by 10%, 20% and 30% respectively than that for reference beam B1. The maximum tensile strains of beams B2, B3 and B4 increased by 25%, 32% and 50% respectively than that for reference beam B1. Figure 9 shows the loads maximum tensile strains for the beams of this group.

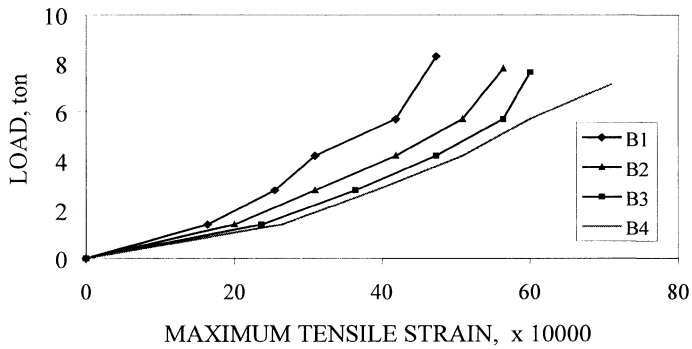

Figure 9 Load maximum tensile strain curves for the beams have 1.5 cm

For concrete cover equals 3.0 cm for beams B5, B6, B7 and B8, the compression and tension strains increased by increasing the duration of fire at different stages of loading. The maximum compressive strains of beams B6, B7 and B8 increased by 8%, 10% and 30% respectively than that for reference beam B5. The maximum tensile strains of beams B6, B7 and B8 increased by 10%, 25% and 35% respectively than that for reference beam B5. . Figure 10 shows the loads maximum tensile strains for the beams of this group.

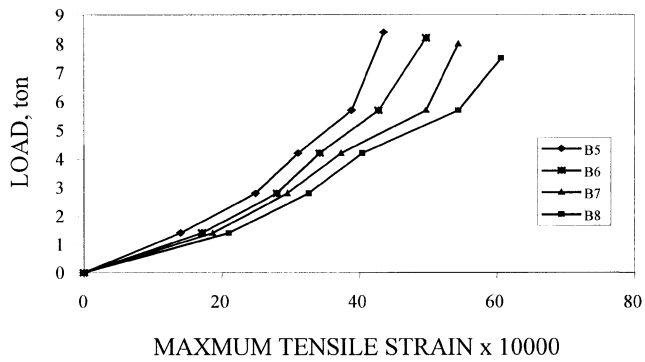

Figure 10 Load maximum tensile strain curves for the beams have 3.0 cm

For concrete cover equals 4.5 cm for beams B9, B10, B11 and B12, the compression and tension strains increased by increasing the duration of fire at different stages of loading. The maximum compressive strains of beams B10, B11 and B12 increased by 10%, 20% and 30% respectively than that for reference beam B19. The maximum tensile strains of beams B10, B11 and B12 increased by 10%, 20% and 50% respectively than that for reference beam B9. From the test results also it is seen that using high strength steel as a main reinforcement reduces the values of compressive and tensile strains for the same exposure time and same concrete cover. It is also noticed that for the same exposure time to fire the compressive and tensile strain increases with the decrease in concrete cover. Figure 9 shows the loads maximum tensile strains for the beams of this group.

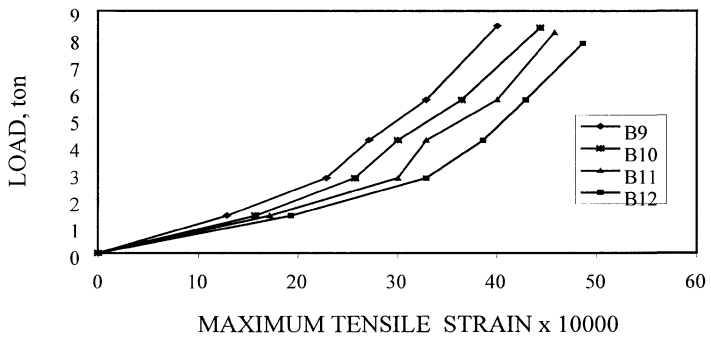

Figure 11 Load maximum tensile strain curves for the beams have 4.5 cm

Modes of failure

As the load was applied to the beams, vertical cracks initiated in the extreme tension fiber in the maximum moment region and other flexural cracks were formed in the shear span. However, inclined cracks then begins due to the presence of shear stresses as the load is increased resulting in a flexural – shear crack. The failure occurs due to the propagation of these cracks towards the vicinity of the point load at compressive face of the beam.

Toughness

The areas of load deflection (p- δ) curve of each beam are given in table (1). Beams B1, B2, B3 and B4 which have concrete cover equals 1.5 cm, the percentage of the area under curve relative to reference beam B1 were 103%, 106% and 113% for beams B2, B3 and B4 respectively.

Beams B5, B6, B7 and B8 which have concrete cover equals 3.0 cm and have longitudinal mild steel, the percentage of the area under curve relative to reference beam B1 were 101%, 102% and 107% for beams B6, B7 and B8 respectively.

Beams B9, B10, B11 and B12 which have concrete cover equals 4.5 cm the percentage of the area under curve relative to reference beam B9 were 101%, 102% and 106% for beams B10, B11 and B12 respectively.

From the above results the area under load deflection curve was increased by the increase of exposure time to fire which means that there is an increase in the toughness for the tested beams by increasing the time exposure to fire. The gain occurred in the toughness was reduced by increasing the concrete cover of the longitudinal steel.

CONCLUSIONS

Based on the above results and analysis of these results, the following conclusions can be drawn:

- Increasing the time exposure to fire increases the total number of cracks, decreases the spaces between cracks and also increases the crack width for at the same load till failure for the same concrete cover thickness.
- Increasing the time exposure to fire decreases the flexural capacity for the same concrete cover.
- Reducing the concrete cover of the longitudinal steel reduces the ultimate capacity of the beams for a certain exposure time to fire.
- Tensile and compressive strains increase with the increase of time exposure to fire. The increase in these strains dependent on the exposure time and it is nearly 50 % more that the reference beam in case of exposure time equals 2.0 hr.
- Increasing the time exposure to fire increase the measured deflection, the increase in this deflection decrease with the increase of the concrete cover.
- Toughness (The area under load deflection curve) increases with the increase of time exposure to fire. And also decreased with the increase in concrete cover.
- Using high tensile steel in beams reduces deflections, tensile strains and compressive strains for the same time exposure and concrete cover.

REFERENCES

1. CASTILLO, C., DURRANI, A. J., Effect of transient high temperature on high strength concrete. ACI Materials Journal, V. 89, No. 4, July – August 1992, pp. 345- 347.
2. HERTZ, K. D. Danish investigations on silica fume concrete at elevated temperature. ACI Materials Journal, V. 89, No. 4, July – August 1992, pp. 345- 347.
3. SANJAYAN G., STOCKS , L.J. Spalling of high strength silica fume concrete in fire. ACI Materials Journal , V. 90, No. 2 , March – April 1993, pp. 170-173.
4. SHIRLEY, S. T. , BURG, R.G. and Fiorato, A. E., Fire Endurance of high strength concrete slabs. ACI Materials Journal, V. 85, No. 2 , March – April 1988, pp. 102-108.
5. AWAD, M. Effect of fire on the behavior of high strength reinforced concrete beams. M. Sc. Thesis 1998, Cairo Univ. .
6. KAMAL, M. M. and others, (1999), The Effect of High Temperature on Mechanical Properties of Concrete. Civil Eng. Research Magazine, Faculty of Eng. Al-AZHAR University , Cairo.
7. FAROUK EL-Sayed and others, (2000), Effect of Fire On The Compressive Strength of High Strength Concrete Using Different Tests. Proceedings of the Eighth Arab Structural Engineering Conference, V.4, pp. 1437.

ASSESSMENT OF FIRE DAMAGE OF CONCRETE BY USING INFRARED THERMAL IMAGING METHOD

X Zhang Tongji University

H X Du Taiyuan University

China

B Zhang University of Glasgow

D V Phillips United Kingdom

ABSTRACT. According to the principle of infrared radiation, the infrared thermal imaging technique was applied to study the fire damage of concrete. The average temperature rise of infrared thermal images on the surfaces of concrete specimens heated up to 900°C was continuously monitored for five minutes. There existed linear relationships of the average temperature rise with the fire temperature and the relative residual concrete strength above 200°C. When the temperature was below 200°C, the damage of concrete was insignificant. The fire damage of concrete structures in situ was also assessed using this technique.

Keywords: Concrete, Fire damage, Infrared thermal image.

X Zhang, is Professor and Deputy Director in State Key Laboratory of Concrete Materials Research at Tongji University, Shanghai, China. His research interests include environmentally friendly building materials, and the test and evaluation of damaged constructions.

H X Du, is an Associate Professor in the Department of Civil Engineering at Taiyuan University of Technology, Shanxi, China. Her research interests include the physical, chemical and mechanical properties of concrete materials, the fundamental behaviour of concrete structures at high temperature and the NDT techniques on existing concrete structures.

B Zhang, is a Research Fellow in the Department of Civil Engineering at University of Glasgow, UK. His research interests include the physical, chemical and mechanical properties of concrete materials and fundamental behaviour of reinforced concrete under varied loading and environmental conditions.

D V Phillips, is a Senior Lecturer in the Department of Civil Engineering at University of Glasgow, UK. His research interests include finite element methods, experimental investigations of reinforced and prestressed concrete properties and design methods for reinforced concrete.

INTRODUCTION

Research on the fire damage of concrete structures began in the 1950's. With the economical development and the increase in population, cities have been inundated with industrial and domestic buildings. The probability of fire damage of these buildings increases rapidly and this causes heavy losses in property and human life. It is of significant importance to quickly but accurately test and evaluate the damage degree of buildings that sustain fire because this not only directly affects the reliability and economy of repair programs, but also greatly helps to reduce the losses and reuse the fire-ruined buildings.

Traditional methods to assess the fire damage of concrete structures mainly include *resilience*, *hammer-tapping*, *ultrasonic wave*, *core strength test*, etc. However, there still exist many imperfections. The resilience method is not very reliable because the surface strength of fire-damaged concrete is different from the strength inside. The hammer-tapping method is relatively slow and unreliable. The ultrasonic wave method is very sensitive to the fire-damaged concrete because the test surface is required to be highly smooth. The core strength test is more direct and accurate for testing the residual strength of the fire-damaged concrete, but sometimes it is difficult to obtain a good specimen because the structural components are either too small or seriously damaged or even fully destroyed, especially when the residual concrete strength is below 10 MPa. These imperfections significantly affect the assessment of fire-damaged concrete structures. The infrared thermal imaging as an NDT method [1] offers a new technology to assess the fire damage of concrete structures [2].

So far, traditional destructive or non-destructive methods have limitations for assessing the fire damage of concrete materials and structures and more feasible and accurate non-destructive methods need to be adopted. By using the infrared thermal imaging technique, the maximum fire temperature, the residual concrete strength, the damage depth of concrete cover, the damage of reinforcing bars and the damage of the bond between the bars and the surrounding concrete could be assessed for fire-damaged concrete structures.

PRINCIPLE OF MEASURING TEMPERATURE BY INFRARED RAYS

Infrared radiation, also called infrared ray, is a kind of electromagnetic wave or radiation with the wavelength between 0.75 to 1000 μm. Naturally, any object above the absolute zero degree (0°K or -273°C) continuously radiates infrared energy and its amount is closely related to the temperature the object is exposed to. In other words, the amount of the radiated infrared energy varies with the sustained temperature. Infrared thermal imaging is a special technique for measuring this radiation and displaying it as a visual thermal image. Heated objects are better sources of infrared radiation.

Testing Principle of Infrared Thermal Imaging

The infrared thermal imaging method is based on the heat radiation law and the differential equation of heat conduction. The heat radiation law for an object is expressed as:

$$P = \varepsilon \sigma T^4 \tag{1}$$

Where P = the power of infrared radiation, W/cm^2
σ = Stefan-Boltzmann constant, equal to 5.673×10^{-12} W/cm^2 °K^4
T = the thermodynamic temperature on the surface of the object, °K
ε = emissivity ($0 < \varepsilon < 1$).

Any heated object has its own infrared radiation that depends on the heating temperature and the emissivity. The differential equation of heat conduction for an object can be expressed as:

$$\frac{\partial T}{\partial t} = \frac{\lambda}{\rho\, c}\left(\frac{\partial^2 t}{\partial x^2} + \frac{\partial^2 t}{\partial y^2} + \frac{\partial^2 t}{\partial z^2}\right) \tag{2}$$

Where t = the time, hour or sec
λ = the coefficient of heat conduction, W/cm °K
ρ = the density, kg/m^3
c = the coefficient of thermal capacity, J/kg °K
x, y and z = co-ordinates, mm.

Different values of λ, ρ and c lead objects to have different surface temperatures and emissivities so the amounts of infrared radiation are accordingly different and a variety of infrared thermal images are formed.

For a fire-damaged concrete, its surface state and composition vary with different temperatures it is exposed to. Under certain ambient conditions, the damaged concrete radiates different amounts of infrared radiation. Using suitable thermographs, the surface of a building or a concrete structure can be rapidly scanned and the defective areas will show different transmittances of infrared radiation. Obtained information can be read and analysed immediately and various damage degrees can be predicted.

Working System for Forming Thermal Images

When the detector is used to optically scan the surface of an object, the infrared energy radiated from surface is collected and converted into electrical signals that are proportional to the incident energy. These signals are amplified and processed using an electronic system, and then converted into video signals. Thus, a two-dimensional colour temperature image map can be displayed on the colour monitor [3].

EXPERIMENTAL INVESTIGATIONS

In this study, 100 mm cubes of normal strength concrete (Grade C30) were used for the infrared thermal imaging tests. The concrete was made of ordinary Portland cement (42.5 N), natural river sand and 20 mm graded crushed calcareous aggregates. The slump of the concrete was controlled between 30 and 50 mm. Specimens were cured in the curing room (20 ± 2°C and RH over 90%) for 28 days, and then moved out of the curing room and stored in air at room temperature for at least two days before testing.

The concrete specimens were heated in a furnace with the designed heating temperature T_m varying between 100°C and 900°C at an interval of 100°C. Soon after the designated T levels were reached, the cubes were placed in the furnace and continuously heated for 90 minutes. Thereafter, they were naturally cooled in air for at least 24 hour prior to the infrared thermal imaging tests. For each heating temperature, three specimens were tested, with three unheated cubes for comparison. Thus, a total of 30 specimens were used.

Infrared Thermal Imaging Testing

The infrared thermal imaging tests were conducted using TH1101 Thermo Tracer, a non-contact highly sensible infrared thermometer. The thermal tracer could process a variety of images using a built-in CPU. It had multi-functions including sharp colour liquid crystal display, image data recording and storing to floppy disks, automatic setting of focus, temperature and sensitivity, continuous measurement for a short period of time and powerful image processing ability, etc.

Ambient temperature was calibrated using CAL key before testing. The emissivity of concrete was adopted as 0.92. Focus, temperature level and sensitivity were also set automatically. Infrared ray lamps were used as the external heating source with a fixed distance between the lamps and the concrete samples as 1 m. The heating time was 5 min.

INFRARED THERMAL IMAGES OF FIRE-DAMAGED CONCRETE

Figure 1 shows the infrared thermal images of concrete specimens exposed to various temperatures. Different damage degrees of concrete specimens could be found for varied heating temperatures so that different infrared thermal images could be formed from the same external heating source due to the difference in the physical parameters of heat conduction. The right column in Figure 1 shows the infrared thermal images of concrete specimens exposed to very high temperatures (600°C and 800°C). The damages were more serious and the temperature rises in the infrared thermal images were higher than those measured on the cubes unheated and at relatively high temperature (500°C), see the left column in Figure 1. When the concrete specimens were exposed to higher temperatures, the surfaces became loose and some microcracks were induced. The higher the heating temperature, the looser the concrete surfaces became and the more microcracks formed.

When the external heating source shone on the surface of the concrete specimens, the heat would be conducted through the concrete mass. The loose surfaces or microcracks, however, would be heated up faster because the fracture surface of loose layer acted as a small insulator, trapping the heat near the surface. The accumulated heat would make these surfaces a few degrees warmer than those of the unheated concrete. These temperature changes were detectable and also visible by using the infrared thermal imaging technique. In other words, the more heat piled up, the higher the temperature of infrared thermal images. The average temperature rise, T_i, of infrared thermal image on the surfaces (100 × 100 mm) of the fire-damaged concrete specimens was calculated using a built-in microprocessor. The test results are listed in Table 1, including the heating temperature T_m, the average temperature rise of the infrared thermal images T_i, the compressive strength of concrete f_{cu}, the relative residual concrete strength $f_{cu}/f_{cu,20°C}$ (the ratio of the strength of the fire-damaged concrete to the strength of un-heated concrete) and the apparent examinations.

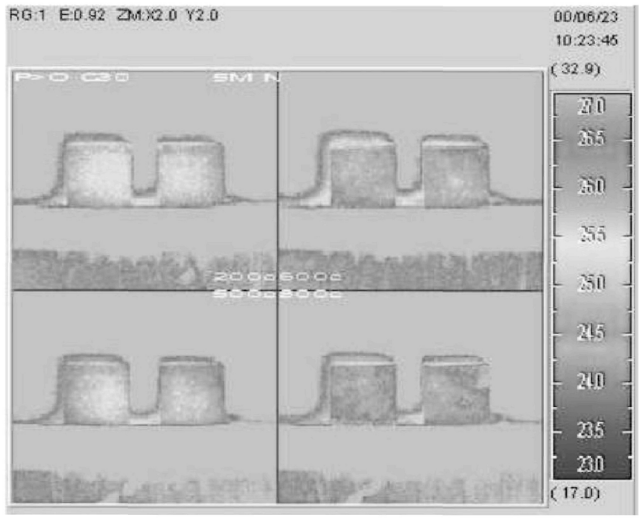

Figure 1 Infrared thermal images of concrete at different heating temperatures

Table 1 Infrared thermal imaging results and material properties

T_m (°C)	T_i (°C)	f_{cu} (MPa)	$f_{cu}/f_{cu,20°C}$ (%)	APPARENT EXAMINATIONS
20	1.65	39.50	100.0	No significant changes in the exterior of the concrete
100	1.65	38.00	96.0	
200	1.50	38.75	98.2	
300	1.65	35.05	88.7	Slightly yellow and no cracks
400	1.70	32.65	82.7	
500	1.85	25.00	63.3	Slightly yellow and a few fine cracks
600	2.00	19.75	50.0	Grey-blue at 600°C, white at 700°C and a few big cracks with some fine cracks
700	2.15	14.50	36.7	
800	2.15	13.00	33.0	Grey-white and a few big penetrating cracks and some small cracks
900	2.30	3.50	8.9	Grey-pink-white and many penetrating cracks and some broken parts

Average Temperature Rise of Infrared Thermal Images During Heating and Cooling

Figure 2 shows the average temperature rise of the infrared thermal images, T_i, on the fire-damaged concrete during heating and cooling periods (both 5 minutes) for different heating temperatures up to 900°C. In general, T_i monotonically increased with the increasing heating time t_h. Below 300°C, there was no significant difference in T_i at any heating stage. Above 300°C, however, the average temperature rise T_i increased with the increasing heating temperature T_m for any heating time, i.e. the higher the heating temperature T_m, the larger the average temperature rise T_i. During the cooling period, the average temperature rise T_i

monotonically decreased with the increasing cooling time t_C. In the first three minutes, T_i decreased very rapidly with t_h and then the decrease rate became smaller. At t_C = 5 min, T_i dropped down to 1.2°C for $T_m \geq$ 500°C and to between 0.9 and 1.0°C for $T_m \leq$ 400°C.

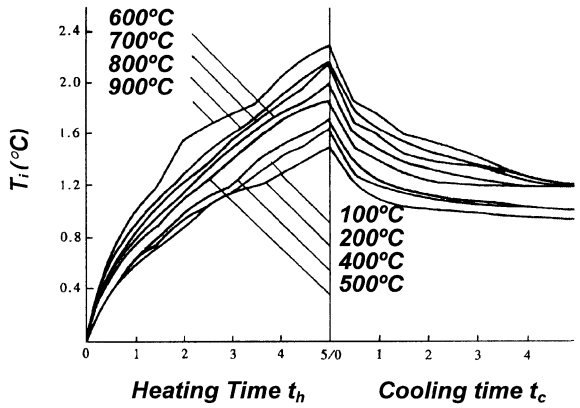

Figure 2 Average temperature rise of infrared thermal images on fire-damaged concrete during heating and cooling

Relationship Between T_m and T_i

The above observations show that for higher heating temperatures (above 200°C), the average temperature rise of the infrared thermal images, T_i, could be used to predict the maximum heating temperature a concrete specimen was exposed to. Here, a heating time t_h = 5 min was adopted for such prediction. Table 1 shows the development of the heating temperature, T_m, with the average temperature rise of the infrared thermal images, T_i, for the heating time t_h = 5 min. Below 200°C, T_m changed very little with T_i. Above 200°C, T_m monotonically increased with T_i. A linear expression can be used to represent this relationship for $T_m \geq$ 200°C as

$$T_m = 859.06\, T_i - 1092.95 \ (°C) \tag{3}$$

with a linear correlation coefficient r = 0.991. As soon as the temperature rise T_i for any fire-damaged concrete structure is detected using the infrared thermal imaging technique, the maximum heating temperature T_m the concrete has been exposed to (above 200°C) can be accurately predicted using Equation (3). Below 200°C, the change in the heating temperature T_m did not cause T_i to change significantly. In other words, T_i was not sensitive to the change of the heating temperature below 200°C. Actually, the structural damage of concrete heated below 200°C should be very small.

Relationship Between $f_{cu}/f_{cu,20°C}$ and T_i

Table 1 also shows the development of the relative residual compressive strength on concrete cubes, $f_{cu}/f_{cu,20°C}$, with the average temperature rise of the infrared thermal images, T_i, for

the heating time t_h = 5 min. Below 200°C, f_{cu} changed very little with T_i and only dropped by 1.8% at 200°C. Above 200°C, f_{cu} monotonically decreased with T_i and dropped by 17.3% at 400°C, 46.7% at 500°C, 50% at 600°C, 63.3% at 700°C and 91.1% at 900°C. A linear expression can be used to represent this trend for $T_m \geq 200$°C as

$$f_{cu}/f_{cu,20°C} = -109.07\ T_i + 266.29\ (\%) \tag{4}$$

with r = 0.992. As soon as the average temperature rise T_i for any concrete structure that is exposed to the temperature over 200°C is measured using the infrared thermal imaging technique, the residual concrete strength can be accurately predicted using Equation (4). Below 200°C, both f_{cu} and T_i did not change significantly.

DISCUSSION

When T_m was below 200°C, lower heating temperature helped the further hydration, accompanied with the evaporation of capillary water, which made cement particles cohere closely. During this physical process, concrete strengths would not sustain a significant reduction with T_m, and the temperature rise of infrared thermal images did not change very much. For T_m > 200°C, the concrete strengths decreased and the temperature rise of the thermal images increased with T_m. This is mainly associated with the evaporation of gel water and chemically combined water and decomposition. Some phases changed and a large number of interfacial cracks formed. High temperatures over 500°C also caused chemical and micro-structural changes and increased dehydration, interfacial thermal incompatibility and chemical decomposition of hardened cement paste and aggregates. All these changes caused large internal stresses and led to a large number of microcracks and visible macrocracks. Finally, the strength of concrete decreased and the irreversible deformation increased. For the heating temperature of 900°C with an exposure of 1.5 hours, the aggregates totally separated from the cement paste.

The above test results and analyses have shown that the concrete strength did not lose very much when the heating temperatures was below 200°C, whereas the loss of the concrete strength became very significant when T_m varied between 400°C and 900°C. Similar trends of the concrete strength with the heating temperature have also been observed before [4,5].

EVALUATION OF FIRE-DAMAGED CONCRETE STRUCTURES

If the average temperature rise of infrared thermal images on the concrete surfaces is measured, the maximum fire temperature the concrete structure has sustained and the residual concrete strength can be predicted by using Equations (3) and (4). The expose time to fire can be calculated by using the ISO standard curve of temperature rising. The internal temperature distribution of concrete structural components can be conjectured using Equation (2). For concrete,

$$\lambda(T) = 1.16 \times (1.4 - 1.5 \times 10^{-3} T + 6 \times 10^{-7} T^2), W/m\,°C \tag{5}$$

$$\rho(T) = 2400 - 0.56\,T, kg/m^3 \tag{6}$$

$$c(T) = 92.0, J/kg\,°C \tag{7}$$

Here, if we let $\alpha(T) = \lambda(T)/[\rho(T)\, c(T)]$, then we have

$$\alpha(T) = \frac{1.4 - 1.5\times10^{-3}\, T + 6\times10^{-7}\, T^2}{3600\,(528 - 0.1232\, T)},\ m^2/s \tag{8}$$

Hence, the thermal conduction equation (2), can be simplified for concrete as

$$\frac{\partial T}{\partial t} = \alpha\left(\frac{\partial^2 t}{\partial x^2} + \frac{\partial^2 t}{\partial y^2} + \frac{\partial^2 t}{\partial z^2}\right) \tag{9}$$

Thus, the damage depth and extent of concrete structural components caused by fire can be determined based on Equation (9). The strength loss of concrete can be conjectured based on the measurements of the temperature rise of infrared thermal images in corporation with Equation (4). Meanwhile, the maximum fire temperature the reinforcing bars have sustained can be inferred by considering some conclusions by $CIBW_{14}$ (the 14th Section of the Committee of International Building Science and Technology and Works), and the residual mechanical properties of the reinforcing bars and their cohesive strength with the concrete can be deduced. Thus, the damage degrees of concrete structural components can be evaluated synthetically and comprehensively. In this section, an example shows how the infrared thermal imaging technique could be used to predict the fire damage of a concrete structure.

The building investigated was located at 776/778 Huayuan Road of Kunshan City in Jiangsu Province, China. The first and second floors were made of C30 concrete, with the heights of 3.6 and 3.0 metres respectively, and strengthened by using reinforced concrete frames. Further higher levels were made of C25 concrete and bricks. The build-up area of each floor was 95 m^2. The concrete floors were reinforced by using D-LL550 steel bars. Fire was caused due to leaking liquid fuel. Figure 3 shows the thermal infrared imaging on the concrete roof of this fire damaged building and Table 2 lists the details of the measured and predicted results on the first and second floors of this building.

From Table 2, it can be seen that the column sustained the least damage from fire. The calculated maximum fire temperature was only 196°C with negligible heating time. No damage happened on concrete, reinforcing bars and the bond between the concrete and reinforcement. The damage of beams was medium but severer than that of the column. On the first floor, the calculated maximum fire temperature sustained by the beams varied from 797°C to 883°C with the heating time between 22 and 36 minutes. The concrete strength loss was calculated as high as 74% to 85%, with a reinforcement damage of 5% and a bond damage of 15%. On the second floor, the calculated maximum fire temperature for the only studied beam was 539°C with an exposure time of 11 minutes. The concrete strength lost by 41%, with a reinforcement damage of 5% and the bond damage of 10%. The beams on the first floor seemed to sustained severer damage than the beam on the second floor. Also, the concrete had severer damage than the reinforcement and the bond. Finally, the slabs sustained the severest damage. The calculated maximum fire temperature varied from 625°C to 797°C with the heating time between 11 and 22 minutes.

The concrete strength loss was calculated between 52% and 74%, with the reinforcement damage from 5% up to 30% and serious bond damage as high as 80% to 97%. Meanwhile, Figure 3 also shows higher temperature rises on the reinforced concrete slabs than those on the beams, which means that the slabs indeed sustained severer damage than the beams.

Table 2 Thermal infrared imaging test results of a fire-damaged concrete building

COMP	NO	T_i	T_{cal}	$t_{h,cal}$	DAMAGE DEPTH (mm)		DAMAGE DEGREES (%)			OVERALL DAMAGE
		(°C)	(°C)	(min)	Btm	Side	Concrete	Bar	Bond	
Column	1	1.5	196	/	/	/	0	0	0	No
Beam	1	2.3	883	36	20	18	85	5	15	Medium
	2	2.3	883	36	22	18	85	5	15	Medium
	2	2.2	797	22	20	16	74	5	15	Medium
	4	1.9	539	11	/	12	41	5	10	Medium
Slab	1	2.2	797	22	25	/	74	30	95	Severe
	2	2.1	711	13	18	/	63	20	80	Severe
	3	2.1	711	18	25	/	63	30	95	Severe
	4	2.0	625	11	20	/	52	5	97	Severe

Figure 3 Infrared thermal images of a fire-damaged concrete building

CONCLUSIONS

The characteristics of the infrared thermal images on concrete surface significantly varied with heating temperatures, so it is feasible to assess the fire damage of concrete using the infrared thermal imaging technique. The average temperature rise on concrete surface could be used as a useful parameter for such study.

The average temperature rise on concrete surface linearly increased with the increasing heating temperature when the temperature was above 200°C. This relationship would allow predicting the fire temperature concrete structures could have sustained. Below 200°C, the average temperature rise changed little with the heating temperature.

The average temperature rise on concrete surface linearly increased with the decreasing residual concrete strength due to the increasing heating temperature when the temperature was above 200°C. This relationship would allow assessing the residual concrete strength of fire damaged concrete structures. Below 200°C, the average temperature rise changed little with the concrete strength.

Using the infrared thermal imaging technique, the damaged degrees of concrete structures and components for a fire damaged building have been evaluated, including the maximum fire temperature each component sustained, the loss of concrete strength, the damage depth of concrete, the damage in the reinforcing bars and the damage of the bond strength of the reinforcing bars with the surrounding concrete. This study could provide a scientific basis for repairing, reinforcing and demolishing the fire damaged concrete structures.

REFERENCES

1. BAR-COHEN, Y., Emerging NDT technologies and challenges at the beginning of the third millennium, Part 1, Material Evaluation, Jan. 2000, pp 17-30.

2. DU, H.-X., ZHANG, X., HAN, J.-H., Test and evaluation on the fire harm and damages of concrete structures, Journal of Building Materials, 1(2), 1998, pp 175-181 (in Chinese).

3. DU, H.-X., ZHANG, X., HAN, J.-H., LI, X.-F., Test and analysis of fire damage of concrete using infrared thermal imaging technique, Journal of Building Materials, 1(3), 1998, pp 223-226 (in Chinese).

4. ZHANG, B., BICANIC, N., PEARCE, C.J., BALABANIC, G., Residual fracture properties of normal and high strength concrete subjected to elevated temperatures, Magazine of Concrete Research, 52(2), April 2000, pp 123-136.

5. ZHANG, B., BICANIC, N., PEARCE, C.J., BALABANIC, G., Assessment of toughness of concrete subjected to elevated temperatures from complete load-displacement curve — Part I: General introduction; Part II: Experimental investigations, ACI Materials Journal, 97(5), Sept.-Otc. 2000, pp 550-566.

EARTHQUAKE IN BHUJ (INDIA) – WAS IT A MAN-MADE CALAMITY?

C M Dordi
Gujarat Ambuja Cements Ltd
A Goyal **R Sinha**
Indian Institute of Technology
India

ABSTRACT. In this paper, structural failures due to the recent earthquake in Bhuj, India, on 26 January 2001, are presented and discussed. The various causes of failures due to inadequate splicing of longitudinal reinforcement, inadequacy of transverse reinforcement, weak columns and vulnerable RCC framing are illustrated and reviewed. The amplification effect due to inadequate foundations and weak founding strata had caused failures several kms away from the epicenter. The deficiencies due to which failures occurred in several areas are listed out based on the study made after the earthquake. The additions and alterations done by occupants or owners of structures also contributed to the various failures besides reasons due to poor structural design and construction practices. The failures are broadly summarized and concluded.

Keywords: Mechanical splices, Transverse reinforcement, Weak columns, Structural System, Foundations, Founding strata.

Mr C M Dordi, is the Vice President (Technical Services) of Gujarat Ambuja Cements Ltd., India. He looks after consumer training and technical services in India in Mumbai, Pune, Nasik in Maharashtra State, entire Kerala State, Mangalore in Karnataka State and abroad in Sri Lanka. His main interests are concrete, good construction practices, training and knowledge sharing.

Dr A Goyal, is Professor of Civil Engineering in Indian Institute of Technology, Bombay, India. His main interests are structural and earthquake engineering, bridge design and structural assessment and rehabilitation work.

Dr R Sinha, is an Associate Professor of Civil Engineering in Indian Institute of Technology Bombay India. His main interests are structural and earthquake engineering, structural condition assessment and disaster management.

THEME FIVE:

EXTREME LOADING CONDITIONS

INTRODUCTION

As the nation was about to commence celebrating its 52nd Republic Day on 26 January 2001 a severe earthquake struck Bhuj in the State of Gujarat. It was 08:46:54.82 Indian Standard time when this severe earthquake shook most parts of our Nation including cities of Mumbai, Delhi and Chennai. The shocks were felt in neighbouring countries Pakistan, Afghanistan, Nepal, Bhutan and Bangladesh. The epicenter was in Western India at latitude 23.45 Deg.N and Longitude 70.34 Deg. E. The earlier earthquakes which have occurred in the near about locations were on 16 June 1819 and on 21 July 1959 at 23.6 Deg. N, 68.6 Deg E and 23.3 Deg. N., 70.0 Deg. E respectively. Within a matter of about 90 seconds several structures were flattened causing insurmountable losses to human lives and properties. Cities of Bhuj, Anjar, Bachau, Sukhpur were converted into heaps of rubble. Cities like Gandhidham, Kandla, Adipur and few others had many structures which had either completely collapsed or were badly damaged. The city of Ahmedabad, which was located 350 km from the epicentre was also badly affected. 69 multistoreyed buildings mainly constructed using RCC frame work and unreinforced masonry infill collapsed either partially or completely causing 746 human casualties. These buildings were between ground + four storeys to ground + ten storeys high.

Besides damages in urban areas, it is reported that nearly 1700 villages perished and the total death toll of around 30,000 people was reported. The total loss after accounting for partially or totally damaged structures along with personal properties of the occupants is estimated to be nearly Rs. 300,000 million. This earthquake besides causing heavy destruction and loss of lives has caused unimaginable mental agony, stress and suffering to those who survived with or without injuries. It has instantaneously changed the lives of millions of people.

If a simple question, "Is earthquake a natural or a man made calamity?" is asked, the answer is definitely that, while the cause is due to nature, the calamity is greatly man made. Is it possible to face such calamities in future with the present technology and developments? The answer is, to a great extent, YES. Loss of life and valuable property can certainly be greatly reduced but some damage or injuries to human beings cannot be totally ruled out.

Most of the high rise structures, which collapsed during this earthquake, were developed by Builders. Such builders generally appoint Architects to draw out the plans and details of the structure to suit their requirements, ensuring maximum possible built up area and financial benefit. The Architects get the structural designs worked out by Structural Consultants generally with total disregard to earthquake forces. The statutory authorities inspect mainly the architectural layout and certify the plans, at times with total disregard to building byelaws and statutory requirements, due to corrupt practices. After the building is completed, ignorant buyers will purchase the apartment / flat in the same. The main considerations for purchase being the cost, location of the building, external beauty of the building, additional amenities etc. We can therefore, conclude that ignorance, greed, carelessness and negligence are essentially the underlying causes of failures which one witnessed in the recent earthquake.

SHEAR AND LATERAL FORCES DUE TO SEISMIC SHOCK

The Indian sub continent is divided in five zones for the purpose of determining the seismic forces. The shear force, due to earthquake, on the structure will be maximum at the base of the structure and will depend on many factors. The shear force gradually reduces at higher elevations. Maximum shear force occurs at ground level hence most of the shear failures of columns occur at lower elevations.

Figure 1 Building collapsed due to construction of swimming pool on the terrace besides other reasons

Figure 2 Dislodging of weakly connected overhead water tank

Figure 3 Dislodging of weakly connected lift machine room

However, lateral forces are higher at higher elevations with the maximum force occurring at the roof level. Heavy loads on the upper floors (see Figure 1) due to roof gardens, swimming pools, overhead water storage tanks can cause failures during earthquakes. There are also chances of dislodging weakly connected overhead storage tanks (see Figure 2) or lift machine rooms (see Figure 3).

MECHANICAL SPLICES ON LONGITUDINAL REINFORCEMENT

During an earthquake, structures undergo inelastic deformations resulting in tensile stresses in reinforcement approaching the tensile strength of the steel. It is therefore most essential to avoid splices in regions of potential yield in members resisting earthquake effects. Column failures seen were as a result of splicing of longitudinal reinforcement provided in regions of potential yield and also due to inadequate transverse steel, both in terms of size and spacing provided along the lapped (spliced) longitudinal steel.

Lap (mechanical) splices must be provided only in the central half of the member length and not more than 50% of the bars shall be spliced at one section. This is because at mid height, stress reversal is likely to be of a smaller stress range than locations near the joints. On some occasions, discontinuity of the longitudinal reinforcement without proper confinement can lead to joint failure and subsequent collapse of the structure located above the joints.

TRANSVERSE REINFORCEMENT

The transverse reinforcement is required for confining the concrete and providing lateral support to the longitudinal reinforcement. When earthquake forces act on columns and beams concrete shell cracks up and spalls due to inadequate transverse (shear) reinforcement. The longitudinal bars in columns buckle and concrete in the core portion gets crushed (see Figure 4). This separation of portions of the concrete from the core caused by local spalling creates a falling hazard and can ultimately lead to structural collapse.

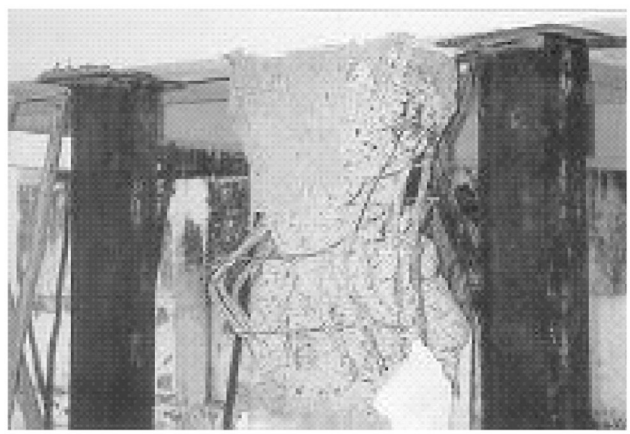

Figure 4 Buckling failure of longitudinal bars of a column

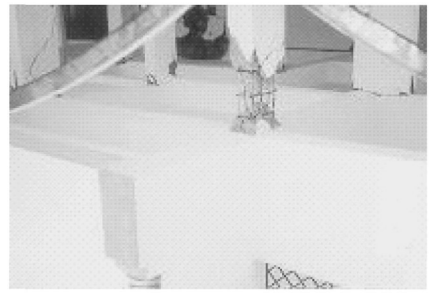

Figure 5 Column failure due to formation of strong beam - weak column connection

Added conservatism on shear is therefore necessary in locations where potential flexural hinging may occur as a result of non-linear displacements caused by earthquake. The most vulnerable locations are beam column junctions at plinth level or a first floor slab level where shear forces are maximum as compared to shear forces at higher elevations.

Special precautions are required to be taken for designing and detailing structural members such as beams and columns as elaborated in IS 13920-1993 for ductile detailing of reinforced concrete structures subjected to seismic forces. Most of the failures observed were due to non-compliance with this code of practice.

Important stipulations in codes of practices are summarised below:

- The spacing of transverse reinforcement should not exceed one-quarter (as per ACI) or one half (as per BIS) of the minimum member dimension. This helps concrete confinement.
- Spacing of transverse reinforcement should not exceed six times longitudinal bar diameter. This helps to restrain longitudinal reinforcement from buckling. Inadequate lateral restraint causes buckling of longitudinal bars.
- 135 degree hooks are more effective than 90 degree hooks in transverse reinforcement. The hooks should have, 10 times the diameter or minimum of 75mm, length extension.
- Cross ties are required to be provided if length of any side of the columns exceeds 300 mm.
- Special confining transverse reinforcement is also required to be placed at beam- column junctions, at column-footing junctions and for columns under discontinued walls. These provisions are clearly detailed in IS 13920-1993.

WEAK COLUMNS

If column dimensions are smaller in size they result in flexible and weak vertical elements relative to the adjoining horizontal members at beam-column junctions. This results in strong beam - weak column and places heavy burden on columns especially at first storey level, increasing storey drifts and forcing hinging to occur in the columns. Figure 5 shows column damage as a result of formation of strong beam - weak column connection. This often results in column failure at both ends in a given storey resulting in a complete column failure mechanism of all columns leading to a total collapse of the entire storey (see Figure 6).

Some precautions for prevention of these failures are stated below:

Figure 6 Weak column connections resulting in total collapse of the entire storey

Figure 7 Shear failure of a column causing a soft storey collapse

- The minimum dimension of the column should not be less than 200 mm. However, the minimum dimension necessary to be provided is 300 mm when centre to centre unsupported beam span exceeds 5 m or the unsupported length of the columns is more than 4m.
- The ratio of the shorter cross sectional dimension to the longer perpendicular dimensions shall not be less than 0.40.
- Sum of moments at the faces of the joint corresponding to the nominal flexural strength of the columns framing into the joint should be 1.2 times or greater than sum of moment at the faces of the joint corresponding to the nominal flexural strengths of the beams framing into the joint.
- The longitudinal reinforcement bars in beams and columns must be continued through the joints as per requirements of IS 13920-1993.

STRUCTURAL SYSTEM

During the earthquake the horizontal load is transferred from the soil strata on to the foundations which in turn transfers this load to columns. This horizontal load creates shear and therefore it is important to design the column to take the desired shear force without failure. This horizontal shear force is resisted by the columns and transferred to beams above and below via the beam column joint or junction. It is therefore extremely important to design the joints and columns between the two floors adequately so that hinging due to inelastic deformation does not occur causing flexural yielding.

Soft Storey

To a certain extent even unreinforced infill walls between the columns restrain the flexural yielding. This flexural yielding is more severe at lower elevations of a high rise building (see Figure 7) than at higher elevations as shear reduces from bottom to top of a high rise structure. Building on stilts, to facilitate car parking at ground floor level, are generally without infill wall panels and are therefore most vulnerable to collapse specially when columns at ground level are not tied together by plinth beams in both directions and/or the foundations are not resting on hard strata. This storey at ground level, without infill walls, is therefore termed as "Soft Storey" due to its vulnerability to collapse while other storeys remain intact. Several buildings during the recent earthquake failed due to this reason.

Vulnerable RCC Framing with Cantilever Beams

Typical construction in the city of Ahmedabad and various other cities could also be held responsible for structural failures and damages. The Municipal Corporations restrict the built up area depending on the area of the plot. This restriction is based on floor space index (FSI). This index is the ratio of the plot area divided by the constructable built up area. Balconies and open stilted areas are not counted in the built up area. In order to get maximum advantage for construction of larger areas at the ground floor, no walls are provided.

Besides this, at first floor level, balconies are generally constructed on large cantilever beams projecting outside the columns on the ground floor (see Figure 8). The FSI calculations are based on the smaller area of the ground floor into the number of storeys. The excess areas on all floors on cantilever beams benefit the builder.

Most of the buildings had only two columns in a frame on the ground floor and then a beam over them cantilevered on both sides. These columns are generally terminated at first floor level and three or more floating columns emerge above the cantilever beams from first floor onwards. This is a very unstable and vulnerable structural system from the earthquake resistance point of view. This forms a soft storey, at ground floor level. Shear failure of a single column would lead to a collapse of the ground floor.

Staircases

The general tendency of the human being during an earthquake is to escape out of the structure. It is obvious that the escape route is through the staircase. There have been cases reported of staircase failures (see Figure 1) causing death of human beings as they were trying to escape. It is recommended that staircases should be designed as per provisions given in codes of practice and also considering higher importance factor which gives higher factor of safety during an earthquake. Cantilevered staircases should not be built in seismic zones as such staircases act like diagonal bracing between the connected floors and get damaged.

All precautions required to be taken are well illustrated in IS 4326-1993 and need to be followed religiously.

Figure 8 Large cantilever beams projecting outside the columns on the ground floor

Parapets and Cantilevered Members

Cantilever parapet walls, cantilever beams, sunshades/canopies (chajjas) have a peculiar character of being affected by earthquake as they form terminal extremities in a building. They should be firmly anchored to the slabs, or RCC frame work to prevent collapse. In strong earthquake zones brick/block masonry parapet walls should be avoided as chances of their collapse are much higher than RCC parapets.

Overhead Water Tanks and Swimming Pools

The overhead water tanks located on the terrace are subjected to higher acceleration force and high vibrations. In some structures the overhead were supported on short RCC columns. Presence of heavy mass of water and stone masonry infill in the overhead water caused collapse as supporting columns sheared off due to high acceleration. The water in the tanks create secondary vibrations causing additional shear force and if the tank's supporting columns are not adequately detailed the tank topples from the roof top (see Figure 2). One ground + ten storey structure had a swimming pool and additional water tanks constructed at a later date creating additional loads without strengthening the columns. This probably acted as a last straw to break the camel's back as the building already had shallow foundations and poor design of soft storey. The collapse of two out of the four blocks in this building caused 46 deaths (see Figure 1).

FOUNDATIONS AND FOUNDING STRATA

In the recent earthquake it was observed that damage due to the earthquake was intense even in regions 350 km away from the epicenter. This was mainly due to presence of soft soils and construction of shallow foundations in them. It is therefore important to recognize the amplifying role of soft soil on structural performance.

Local geotechnical conditions and site amplification partially influenced the damage patterns in buildings situated on sites underlain by thick alluvial deposits along the Sabarmati River. Most of the buildings that collapsed or were badly damaged rested on shallow open footings. For a ground + four storey building foundation depths were usually 1.5 m and for a ground + 10 storey foundation depths were 2.0 to 2.7 m.

The soil was alluvial (N value 10 to 25) at the founding level and at many locations ponds had been filled up to construct high rise buildings. This resulted in amplification of earthquake induced vibrations and caused collapses or damage to structures. Local soil conditions influence the magnitude as well as the form of earthquake loading as stated below:

- Loose granular soils may get compacted by ground vibrations induced by earthquake resulting in large settlements and differential settlements.
- The type of soil immediately below and adjacent to the foundation of any structure will contribute to overall dynamic response of the structure because of soil structure interaction effects.
- The distances from epicenter of earthquake may be similar, the intensities of damage in the areas differ with soil conditions at the said locations i.e. the magnitude and the form of earthquake loading is significantly influenced.
- Frequency characteristics of the ground motion and its duration also plays a prominent role in damage potential.

Foundations

Additional precautions are necessary for designing and constructing foundations in earthquake zones. They are listed below:

- The subgrade below the entire area of the building shall be of the same type of soil. If it is not possible, a suitable separation or crumple section shall be provided.
- Loose fine sand, soft silt and expensive clays should be avoided. If unavoidable the building shall rest either on a rigid raft foundation or on piles taken to a firm stratum. Sand piling and/or stabilization measures may be taken to improve soil in case of light construction.
- All individual footings and pile caps shall be connected by RCC ties in two directions at right angles to each other.
- For structures without basement all columns must be connected to each other in both directions at or below plinth level. For structures with basement all columns must be connected to each other at the level of the basement floor.

BUILDING SYSTEMS

Before discussing basic design requirements and preventive measures it is important to briefly review the building systems which existed in the affected areas. The structures can be broadly categorised in two parts as given below:

- The older non-engineered structures made with load bearing masonry walls supporting tiled roof on wooden trusses or RCC slab. The masonry generally consisted of large sized random rubble (25 x 40 x 60 cm) bounded together either by mud mortar or low strength cement sand mortar. Other materials used for masonry were small to large cut stones, clay bricks or concrete blocks.
- The newer engineered RCC framed multistoried structures with unreinforced masonry infills. The infills of varied nature were used such as concrete hollow or solid blocks or large or small blocks of rubble or clay bricks. The masonry generally used cement sand mortar as a bonding material.

The non-engineered structures failed because of inadequate bond between rubble or bricks as they were not tied together by RCC bands. The walls failed and disintegrated specially at corners, failure of wooden trusses supporting the heavy tiled roof and inadequate tie between roof and masonry were other notable deficiencies of such structures. The engineered structures had the following deficiencies:

- Existence of soft storey on the ground floor.
- Absence of masonry infill between columns.
- There was no reinforcement provided for the infill walls specially necessary for their strength and stiffness.
- Inadequate longitudinal and transverse steel reinforcement in columns and beams.
- Incorrect framing of beams and columns.
- Inadequate foundation or founding strata.
- Excessive use of cantilever in RCC framing above first floor level with floating columns over them.
- Absence of counter balancing beam on the backside of cantilever.
- Omission of plinth/tie beams at ground/plinth level.
- Inadequate ties provided for overhead water tanks and lift machine rooms.
- Staircases supported by cantilever beams.
- Poor maintenance of the structure.
- Poor quality of steel bars (rerolled scrap steel) used.
- Poor construction practices.
- False economy deployed in design and construction practices to match the low rates of real estate.

Figure 9 High rise RCC structure close to the epicenter but not damaged

Figure 10 Three structures at same location - one totally collapsed, one badly damaged and one slightly damaged

PREVENTIVE MEASURES IN CONSTRUCTION PRACTICES

Number of failures have occurred due to bad construction practices. It was reported that while constructing several structures virtually no technical supervision at site was available. Most of the construction was done using 1:2:4 mixes. The concrete specified for superstructure for high rise structures was generally of M15 grade. With non-availability of standard aggregates of proper grading and fineness, poor control of water addition and poor curing, the quality of low grade concrete was far from satisfactory as some concrete failures virtually showed piles of powdered concrete.

There is a great need for specifying much higher grades of concrete and designing the mixes in a scientific manner.

Besides the above, following preventive measures are necessary:

- Strict supervision by qualified and competent Engineers.
- Compliance with drawings and specifications.
- Selection of good quality materials such as steel, cement, aggregates, blocks and bricks.
- Proper proportioning of materials in concrete mix with tight control of water to cement ratio and batching of all ingredients.
- Production of high strength and highly workable concrete mixes.
- Careful supervision of reinforcement steel work in beam-column junction and along the entire length of all columns.
- Careful placing and compaction of concrete without segregation at densely reinforced beam-column junctions and in the full length of the column.
- Production of dense concrete free from honeycombs, entrapped air, cracks and cold joints.
- Proper curing.

MODIFICATIONS BY OCCUPANTS / OWNER

The most important factor which is responsible for structural stability is the way the occupants maintain and at times tamper with the structure. The common man often feels that as the structure or a portion of the structure belongs to him, he can make any number of additions or alterations. Either due to ignorance or negligence or carelessness, he gets alterations done in his premises often endangering the entire structure. At times additional loads are introduced or structural load bearing members are tampered with, without consulting a Structural Engineer. Many buildings in our cities have collapsed without an earthquake due to these dangerous or rather murderous acts. The common man must be aware that the structure is systematically designed and therefore will not and cannot tolerate abuse of any sort. It is a must to consult a Structural Engineer and not an Architect if he desires to do any additions or alterations.

SUMMARY

To summarise, the failures in this earthquake were essentially due to the combination of the following causes.

- Structural Design
- Construction Practices
- Additions & Alterations

Eight combinations of these causes and their resultant status are summarised in Table 1.

The responsibilities have to be fixed on different agencies such as the purchaser, statutory authorities, owner or builder, architect, structural consultant and contractor. However, if one has to seriously think of the consequences of this earthquake which destroyed over 3,39,000 structures and damaged over 7,83,000 structures within 90 to 120 seconds, then perhaps nothing could be more appropriate than each agency involved in the business of construction realising their responsibility and acting accordingly in future.

Table 1 Combination of causes for failures during earthquakes

SR. NO.	STRUCTURAL DESIGN	CONSTRUCTION PRACTICE	ADDITIONS & ALTERATION	STATUS	FIG. NO.
1	Good	Good	Not Done	Intact	9
2	Good	Good	Done	Intact/Damaged	-
3	Good	Bad	Not Done	Damaged	3
4	Good	Bad	Done	Damaged/ Badly Damaged/ Collapsed	8, 10
5	Bad	Good	Not Done	Damaged	5, 10
6	Bad	Good	Done	Damaged / Badly Damaged / Collapsed	4
7	Bad	Bad	Not Done	Badly Damaged / Collapsed	2,6,10
8	Bad	Bad	Done	Collapsed	1, 7

The present earthquake took place in relatively less populated areas of the country. What would have been the extent of loss of life and damage to property if a similar earthquake were to occur closer to the mega metros of our country?

Predictions suggest that by 2025, more than 5.5 billion people worldwide will live in cities, and a large population of them close to regions with high seismic zones. In the next century, it is statistically inevitable that powerful earthquakes will assault several large urban areas. The fatalities from quakes are certainly going to rise in the next two decades and more so if nothing is done. It is said that "Disasters don't kill the people Buildings do". In our country, the number of unsafe buildings is increasing each day. It is therefore high time that following actions should be taken immediately.

- Stop unsafe building design and construction practices.
- Stop tampering with the structures by damaging the structural elements.
- Stop overloading the structures to create short term facilities.
- Massive programme for retrofitting of the buildings have to start in mega metros and other towns close to high seismic zones.

CONCLUSIONS

Earthquake - Is it a man made calamity? All natural disasters - floods, storms, earthquakes are entirely outside human control. As lethal as the earthquake of 26th January 2001 was, its destructiveness was highly magnified by human failings. Most fatalities were the consequence of poorly constructed and designed buildings crushing its occupants. The quake struck in a region known to seismic activities but the effects were also felt in regions not known for seismic activities in the past. The fact remains that there was wide spread disregard for the building codes and out dated construction practices were continued. Many people must share this blame for such shortcomings. Pleas of ignorance about the dangers are not to be trusted now. From the common man, politicians, bureaucrats to owners, builders, architects and structural engineers everyone needs an awakening. We have to learn our lessons from failures now and not wait for more lethal attacks of earthquakes on our densely populated cities and other areas.

This massive load test due to act of God must cause a serious awakening not only of the professionals but also of the common man. It is high time that we learn our lessons from this earthquake. The answer to the above question is therefore left to each individual to answer.

REFERENCES

1. AMBUJA TECHNICAL LITERATURE SERIES - 63, Earthquake - Is it a man made calamity? April 2001.

2. ENGINEERS (INDIA) -MAHARASHTRA STATE CENTRE, Earthquake you and your abode - do's and dont's, 2001.

3. BUREAU OF INDIAN STANDARDS - Codes of practice, Earthquake resistant design of structures, IS 1893, 1984.

4. BUREAU OF INDIAN STANDARDS - Codes of practice, Earthquake resistant design and construction of buildings, IS 4326, 1993.

5. BUREAU OF INDIAN STANDARDS - Codes of practice, Ductile detailing of reinforced concrete structures subject to seismic forces, IS 13920, 1993.

6. INDIAN SOCIETY OF STRUTURAL ENGINEERS, Post earthquake reflections, Quarterly Journal, Vol 3, No 1, April 2001.

7. AMERICAN CONCRETE INSTITUTE, Code of Practice, ACI 318, 1999.

PERFORMANCE OF BEAM-COLUMN CONNECTIONS STRENGTHENED WITH GFRP UNDER SEISMIC LOADS

H S Hadad **H H Shaheen**
Housing and Building Research Center
M El Kafrawy
Cairo University
Egypt

ABSTRACT. Thousands of Egyptian buildings are lightly - reinforced concrete structures in which, the gravity loads have dominated the design only. Moreover, most of the structural details used in these structures are improper as a seismic detailing. Therefore, these structures have a shortage in the lateral load resistance. According to the observations of many consultants after the October 12th earthquake, hundreds of buildings were totally collapsed or severely cracked. Most of the failure cases were initiated at the beam - column joints. This paper is intended to focus on upgrading an ordinary (non - seismic) exterior beam- column joint to withstand the lateral load expected in moderate earthquake zone using traditional (Concrete and steel plates) and nontraditional methods (GFRP).

Keywords: Behavior, Strengthening, Glass fiber reinforced plastic (GFRP), Stiffness, Energy dissipation, Ductility.

Hadad Said Hadad is an assistant Professor in the Concrete Structures Department of the Housing and Building Research Center. His researches focus on strengthening and repair of the structures.

Hamdy H Shaheen is a Professor in the Concrete Structures Department of the Housing and Building Research Center, Giza, Egypt.

Mostafa El Kafrawy is a Professor in the Concrete Structures Department, faculty of engineering of Cairo University, Giza, Egypt.

INTRODUCTION

During the past few decades, it was a common practice in Egypt to design and detail low to medium rise buildings to resist gravity loads only, with no consideration to any lateral loads caused by earthquakes or wind. In fact, the majority of residential and public buildings were designed according to this concept. However, the amount of damage observed in reinforced concrete structures during the October 12th 1992 earthquake pointed out the urgent need to consider these forces in designing and detailing. This was reflected in the Egyptian Code of Practice ECP - 89[3], and the subsequent edition ECP-95[5],where regulations for lateral loads caused by earthquakes are included. Lateral loads are now explicitly specified in a special code for loads and forces ECP- 93[4]. The important issue of detailing the structure to fulfill these design requirements is still not fully addressed.

According to the observations of many consultants after the October 12th earthquake, hundreds of buildings were totally collapsed or severely cracked due to poor reinforcement details. In many of these cases the initial failure started at the beam - column joints.

The lack of adequate design or appropriate detailing of the beam - column connection leads to a less ductility and more brittle failure of the structure. To mitigate the risk posed by lateral loads, building officials and owners find that strengthening of existing structures is a feasible way to provide the safety to the building occupants and to protect their investments.

The main objective of this paper is to focus on upgrading an ordinary (non - seismic) exterior beam- column joint to withstand the lateral load expected in moderate earthquake zone using traditional materials such as steel plates and R. C. haunch and nontraditional materials such as GFRP.

METHODOLGY

In this paper, five exterior beam-column joints simulating connections in a multi-storey residential building were tested, a control specimen J1 and other four strengthened specimensJ2, J3, J4 and J5. The boundary conditions were set to simulate the point of contra-flexure in the beams and columns. Beam mid-span and column mid-height represent the points of contra-flexure under lateral loads with an acceptable accuracy. The overall dimensions of the test specimen are shown in Figure 1. The specimens were designed and detailed according to the practical case in Egypt to carry gravity loads only without any precautions for horizontal loads. The testing frame used for all specimens is shown in Figure 2. For all specimens, the loading was controlled by the displacement of the beam at the intended loading point. The controlled loading history used is shown in Figure 3.

STRENGTHENING SCHEMES

The joint region and the critical parts from the column and the beam adjacent to the joint were strengthened. Three types of strengthening schemes (R. C. haunch, Steel plates and GFRP) were adopted and applied to four specimens (J2, J3, J4 and J5). The details of the strengthening schemes for the four specimens are shown in Figure 4.

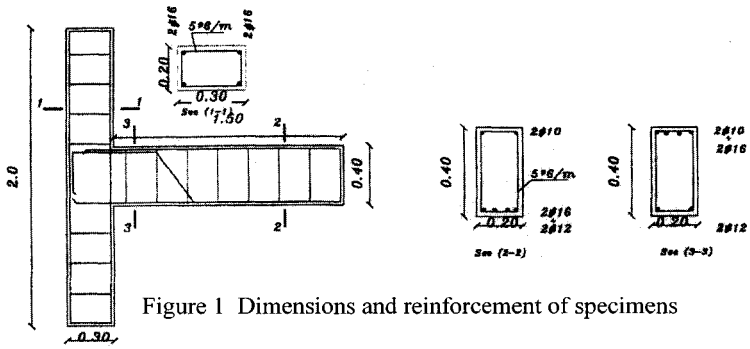

Figure 1 Dimensions and reinforcement of specimens

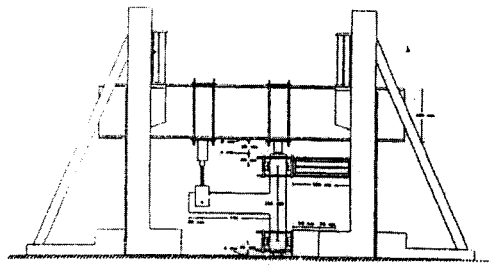

Figure 2 Testing frame

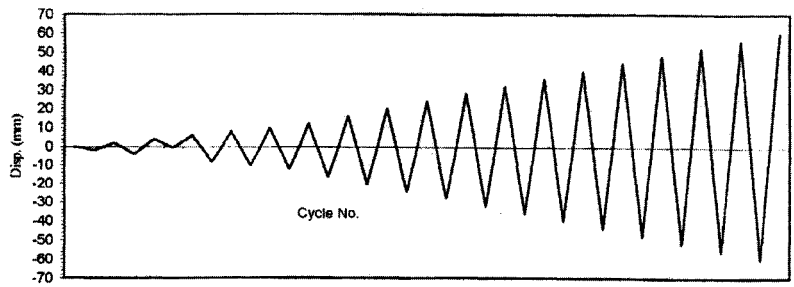

Figure 3 Loading history

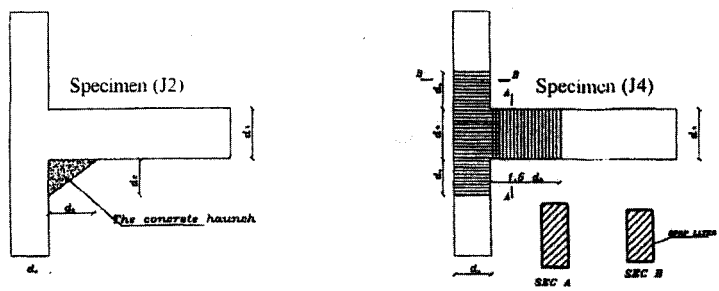

Figure 4 Details of strengthened specimens

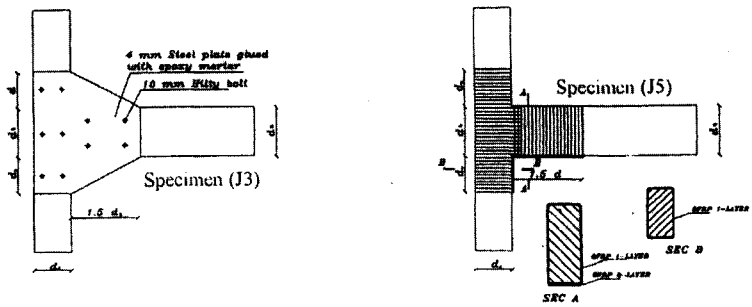

Figure 4 Details of the strengthened specimens (continued)

TEST PROCEDURE

The specimens were tested with the column portions placed vertically in the testing frame. The specimens were tied down by applying an axial load to the column and that kept constant throughout the test. Reversed cyclic displacements were applied to the free end of the beam simulating an earthquake-type loading. The data acquisition controls the loading process of the test specimen. All data gathered from load sensors, displacement transducers, and strain gauges were recorded continuously during the test. Cracks were obvserved and traced for each load level.

EXPERIMENTAL RESULTS AND DISCUSSION

Modes of failure and crack patterns

The crack patterns and mode of failure for the different specimens are shown in Figure 5. The figure shows that the traditional Egyptian exterior joint does not fail down due to one reason. The mode of failure of J1 was a combination between brittle shear filure in the joint region and slippage of the stirrups hanger, which initiated and increased the diagonal crack in the beam parallel to the bent bar. Using concrete haunch as a strenthening technique did not improve the behaviour of the specimen J2 since partial separation of the concrete haunch took place and then the specimen began to behave as J1, and the mode of failure of J2 was approximately the same as J1. For specimen J3, the steel plates improved the behaviour of the specimen where the failure mode was a flexural failure at the far edge of steel plates. However, a sudden drop in the load capacity was noticed due to a pull out of the corner bolt which suffered from a concentration of forces.

For specimens J4 and J5, which were strenghened with GFRP sheets, peeling of the FRP at the joint region began to occur at the fifth cycle (11.5 mm displacement approximately). At successive loading levels peeling area increased, with vertical and horizontal cracks in the FRP sheet. After removing the FRP layer from the two specimens (Figure 5) there were no shear cracks in the joint or in the critical part from the beam. The mode of failure was flexure in the beam at the inner beam edge. For specimen J5, which was strengthened by an additional longitudinal lower layer to overcome the shortage of the lower beam reinforcement, the specimen behaved approximately as a frame joint.

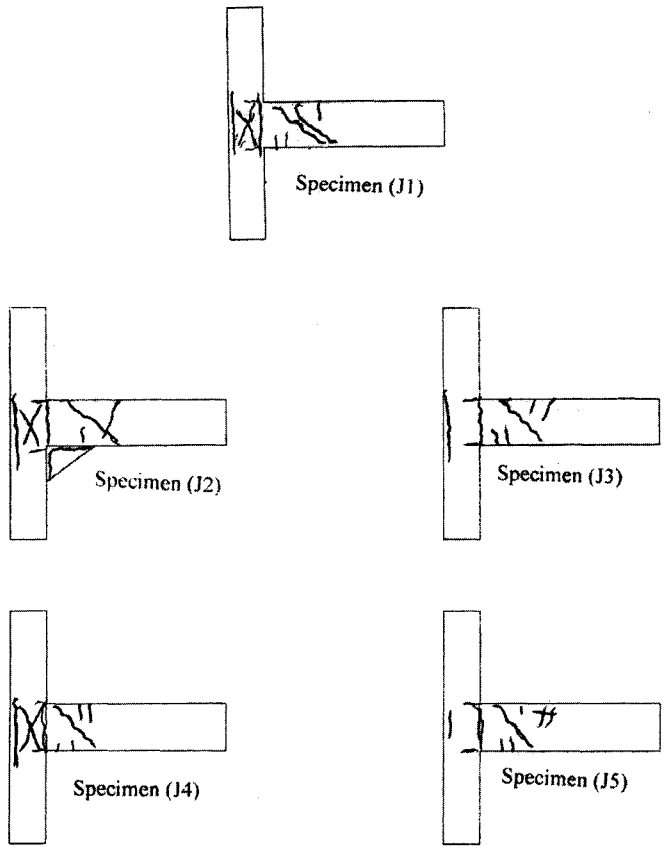

Figure 5 Crack pattern and mode of failure of the test specimens

Strength evaluation

The strength capacity of the test specimens were evaluated and compared using the hysteresis loop envelope, which relates the peak load in each cycle and the corresponding displacement. The hysteresis envelopes of the different specimens are presented in Figure 6. Table 1 shows a comparison between the strength evaluation of the specimens, as a factor of the control specimen J1 and the cycle at failure with the definition that failure load corresponds to 75% of the ultimate load on the descending branch. The results show that all the strengthening techniques increased the lateral strength of the original specimen that (J1) by 127, 208, 232 ad 283% for J2, J3, J4 and J5 respectively.

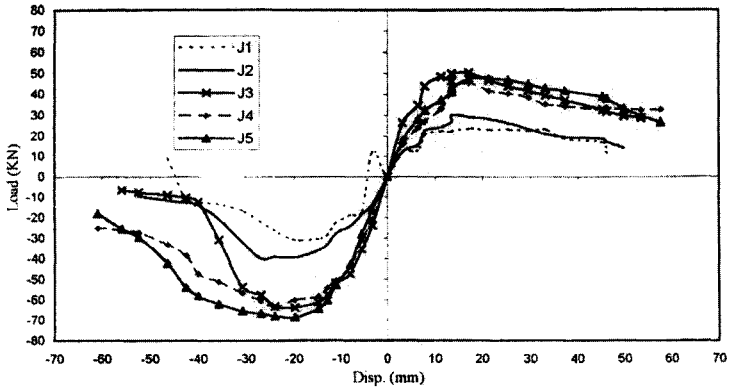

Figure 6 Hysteresis loop envelope of test specimens

Stiffness analysis

The cracked stiffness of each test specimen was calculated for each loading cycle. The cracked cyclic stiffness K_i was computed as follows:

$$K_i = (P_{ci} + P_{ti}) / (\Delta_{ci} + \Delta_{ti}) \quad (1)$$

Where:

P_{ci} is the maximum compression load at cycle i
P_{ti} is the maximum tension load at cycle i
Δ_{ci} is the maximum compression displacement at cycle i
Δ_{ti} is the maximum tension displacement at cycle i

The cracked cyclic stiffness was presented versus the number of cycles to represent the stiffness degradation due to cyclic loading, as in Figure 7. In addition, Table 1 shows a comparison between the cracked stiffness of the specimens after the first cycle, as a factor of the control specimen (J1). It can be seen from the table that all strengthening techniques, generally, improved the behaviour of the specimens to different degrees. However, strengthening with double layer of GFRP showed excellent response since the specimen J5 sustained a large number of cycles until failure compared with other specimens. It is worth mention that the cracked stiffness for specimen J3, strengthened by steel plates, was the best compared with the others.

Table 1 Comparison between the failure load, failure cycle, strength evaluation and cracked stiffness of the test specimens

SPECIMEN	FAILURE CYCLE	FAILURE LOAD (kN)	STRENGTH EVALUATION (ratio of J1)	CRACKED STIFFNESS (ratio of J1)
J1	9	20.4	1	1
J2	10	26.0	1.27	1.76
J3	10	42.4	2.08	2.24
J4	12	47.4	2.32	1.7
J5	14	57.7	2.83	1.95

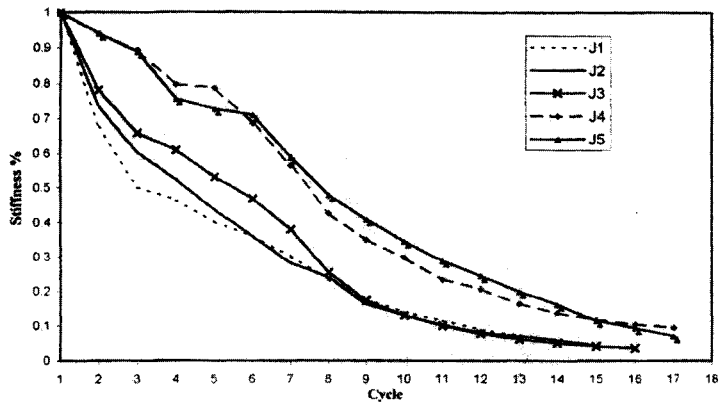

Figure 7 Stiffness degradation curves of test specimens

Energy dissipation

The dissipated energy was computed for each cycle as the area enclosed by the lateral load-displacement hysteresis loop for the cycle. Energy dissipated per cycle, E_i is calculated as follows [6]:

$$E_i + \Sigma [(P_{i+1} + P_i) * (\Delta_{i+1} - \Delta_i)/2] \quad (2)$$

The accumulated dissipated energy is plotted versus the number of cycles for the test specimens in Figure 8.

The non-dimensional energy index [6] is used to evaluate the energy dissipated by different test specimens. This energy index is expressed as follows:

$$I_{EN} = (\Sigma E_i (K_i/K_y) * (\Delta_i / \Delta_y)^2) / (P_y * \Delta_y) \quad (3)$$

Where:

I_{EN} is normalized energy index
E_i is the dissipated energy at cycle number i
K_i, K_y are the stiffness at cycle number i and the stiffness at yield, respectively
Δ_i is the average of maximum compression and tension displacements at cycle no i
Δ_y, P_y are the yield displacement and yield load, respectively.

The specimen having a normalized energy dissipation index of 60 or higher posseses sufficient ductility to satisfy the intent of ACI Committee 352 recommendation [1]. The energy indexes of the test specimens are shown in Table 2.

The index appears to be a reliable indicator of the performance of subassemblies. A major advantage of this index is the incorporation of the effect of different loading histories by including the actual displacement and stiffness of each cycle. Moreover, the non-dimensional form of the index facilitates the comparison of specimens of different sizes and scales.

Figure 8 and Table 2 shown small amount energy dissipation for the specimen J1 and a high value for J5 compared with the other specimens. The energy dissipation for the specimens J5 is higher than that for J2 and J3 by 240% and 36.5% respectively. Comparing the energy index of the different specimens through Table 2 shows that the practical Egyptian joint does not cover the ACI requirements, even when it was strengthened by concrete haunch. Using steel plate in specimen J3 barely covers the ACI requirements, using the GFRP increased the energy index of the specimen to be higher than the ACI requirement by 24–44% approximately as shown for the results of J4 and J5 respectively.

Table 2 Accumlated energy and energy index of the test specimens

SPECIMEN	TOTAL ACCUMULATED ENERGY (kN mm)	ENERGY INDEX
J1	4950	20.1
J2	5757	33
J3	14263	58
J4	17818	74.3
J5	19611	87.45

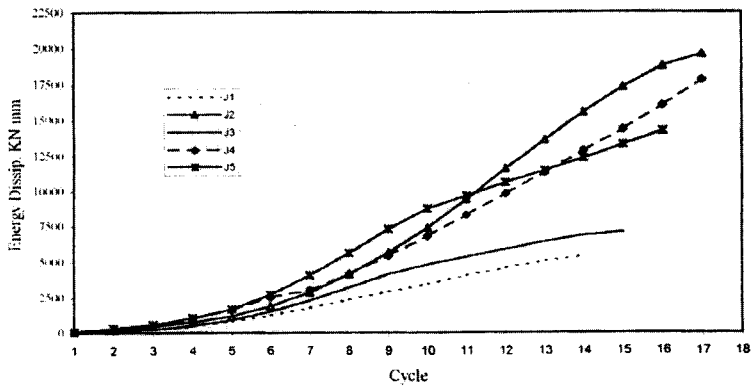

Figure 8 Accumulated energy dissipation of teest specimens

Displacement ductility factor and accumulated displacement ductility

The failure load was taken equal to 75% of the ultimate load on the descending branch. The corresponding displacement (at the failure load) was computed from the strength envelope. The displacement ductility is defined as the ratio between the maximum displacement at cycle number i, Δ_i, and the yield displacement Δ_y. The displacement ductility factor is defined as the ratio between the displacement at failure load, Δ_f, and the yield displacement, Δ_y.

Displacement Ductility = Δ_i / Δ_y.
Displacement Ductility factor = Δ_f / Δ_y,
The accumulate displacement ductility is defined as the sum of the displacement ductility accumulated up to the defined failure load as shown by Equation 4.
Accumulated displacement ductility = ? (Δ_i / Δ_y)
Where Δ_i is the maximum displacement at cycle number i.

Table 3 shows the displacement ductility factors and the accumulated displacement ductility for the test specimens. In addition, Table 3 shows also the ductility of the specimens as a percentage of that for specimen s detailed according to ACI for gravity loads and that for moderate seismic zone, experimentally tested b by Fahad A. Aljahaliedt et al [7]. Strengthening by GFRP increased the ductility of the traditional joint to be more than the requirements of ACI for moderate seismic zone by 5-20% for J4 and J5 respectively.

Table 3 Displacement ductility of the test specimen

SPECIMEN	DUCTILITY FACTOR	ACCUMULATED DUCTILITY	% OF ACI-MODERATE SEISMIC ZONE (FAHAD ET AL) [7]	% OF ACI-GRAVITY LOAD FAHAD ET AL) [7]
J1	1.98	31.6	66	74.5
J2	2.56	37.81	75	85
J3	3.2	39.9	106.6	120
J4	2.86	35.1	105	118.8
J5	3.65	41.7	121.6	137

CONCLUSIONS

1- Failure mode of the traditional Egyptian exterior joint is a combination of cracks due to the slippage of the stirrups hanger and shear in the joint region. The absence of lateral level horizontal reinforcement in the joint decreases the seismic performance.

2- The ductility factor of the Egyptian traditional exterior joint is about 1.9 and the maximum drift ratio is about 1.5%. This conclusion had been drawn from the specimen (J1). This ductility factor is approximately 75% of that detailed for gravity load according to ACI. Moreover, it is 65% of the ductility factor of the joint detailed according to ACI for moderate seismic zone.

3- Using a concrete haunch is considered the cheapest method to strengthen the exterior joint. However, this method is suitable to resist low cyclic loading (low earthquake) as it may separate from the concrete surface at small displacement level. The concrete haunch increases the ductility factor of the original specimen by about 29%. The joint becomes as ductile as the joint detailed according to ACI for gravity loads only , but its ductility is still less than the requirements of ACI for the moderate seismic zone .

4- Using steel plates to increase the seismic performance of the exterior joint is considered as the easiest method for field applications. However, the failure or pullout of one (or more) bolts of the connection may cause a sudden failure. Therefore it is recommended that the corner bolts in the connection must be away as possible from beam edges. Using steel plates to improve the seismic performance of the exterior joints increase its lateral strength, ductility factor, and drift ratio by 71%, 39%, and 60% respectively. The ductility factor for such joint becomes higher than that of the joint detailed according to ACI for moderate seismic zone. This method may be more suitable for displacement of medium level

6. Using GFRP for strengthening the joints led to a higher ductility than that of the joints detailed according to the ACI for gravity loads by 20 - 50% and those detailed for moderate seismic zones up to 30%.

7. Adding a longitudinal layer of GFRP to cover the shortage of the beam bottom reinforcement at the joint led to an increase of the lateral strength and the ductility factor of the joint by 115%, 85% and 153% respectively. Moreover, it changed the behaviour of the joint, as it acts as a frame joint that can resist more lateral loads.

REFERENCES

1. ACI- ASCE Joint Committee 352, Recommendations for Design of Beam- Column Joints in Monolithic Reinforced Concrete Structures, ACI Journal, July 1976, pp 375-393.

2. CHRIS P. PANTELID et al, Rehabilitation Of Beam-Column Joints With Carbon Fiber Jacket Proceeding Of The Third International Symposium (FRPR C3-3) Sapporo - Japan- October-1997.

3. ECP-1989, Egyptian Code of Practice for Reinforced Concrete Structure, Housing and Building Research Center, Egypt 1989.

4. ECP-1993, Egyptian Code of Practice for Loads and Forces in Buildings, Housing and Building Research Center, Egypt 1993.

5. ECP-1995, Egyptian Code of Practice for Reinforced Concrete Structure, Housing and Building Research Center, Egypt 1995.

6. EHSANI M. R., and WIGHT J. K., Confinement Steel Requirements for Connections in Ductile Frames, Journal of Structural Engineering, ASCE, Vol 116, No 3, March, 1990.

7. FAHAD A. ALJAHDALI et al " Seismic Performance of Strengthened Exterior Beam - Columns Joints, PhD Research, Ain Shams Univ., 1998.

8. GENG et al, "Retrofit of Reinforced Concrete Column -to-Beam Connections," Composites Science and Technology, 1998.

9. HADAD SAID HADAD et al, Strengthening of the Beam - Columns Connections with GFRP (to resist cyclic loading), PhD Research, Cairo Univ, 2000.

APPLICATION OF HIGH-PERFORMANCE CONCRETE ON CONTRACT C708 OF SINGAPORE'S NORTH-EAST MRT LINE

C K Nmai
Master Builders Inc
United States of America

P Broome
Nishimatsu Construction Co Ltd
Singapore

P C Robery
FaberMaunsell
United Kingdom

ABSTRACT: In early 1996, the Singapore Government announced its decision to expand the country's mass rapid transit (MRT) system by building the North-East Line from the World Trade Centre in the south of the island to the new towns of Hougang, Sengkang and Punggol in the north-eastern part of Singapore. The £2.55bn North-East Line is approximately 20 km long and is built primarily underground using precast tunnel-lining segments. Contract C708 of this project included a stretch of bored tunnel passing through bacterially active marine clays and underneath the Singapore River, possibly the worst soil and groundwater conditions to be found in Singapore. The specification requirements for the project referred to a 100-year design life and included the use of high-performance concrete with a maximum water-cementitious material ratio of 0.45 and a minimum 28-day compressive strength of 60 MPa for the concrete used in the precast tunnel segments. In addition, the specification included the use of high yield bars with a fused epoxy coating to mitigate corrosion of the reinforcing steel due to chlorides in the groundwater. At the request of the contractor, the specifying agency accepted the use of a dense silica-fume concrete and integral waterproofing corrosion inhibitor as an alternative to the epoxy-coated bar. Over 8,000 precast, high-performance concrete tunnel-lining segments were produced for the construction of the underground tunnels, which were completed in December 2000. This paper summarises the development of the high-performance concrete mixes for the tunnel lining segments, production issues and QA/QC measures that were implemented to ensure compliance with the specification.

Keywords: High performance concrete, Water-proofing, Silica fume, Corrosion inhibitor, Tunnels.

Mr C K Nmai, is currently employed with Master Builders Inc., United States of America.

Mr P Broome, is currently employed by Nishimatsu Construction Co Ltd, Singapore.

Professor P C Robery, is Business Stream Leader with FaberMaunsell, United Kingdom.

INTRODUCTION

In September 1995, the Singapore Government established the Land Transport Authority (LTA) to integrate the development of land transport with an overall mission to provide Singaporeans with a world-class transport system. Shortly thereafter, in January 1996, the Singapore Government announced its decision to expand the existing 83 km long Phase I of the mass rapid transit (MRT) system, by building the North-East Line from the World Trade Centre in the south of the island to the new towns of Hougang, Sengkang and Punggol in the north-eastern part of Singapore. The £2.5bn North-East Line is approximately 20 km long and was built primarily underground using precast tunnel-lining segments, with an internal tunnel diameter of 5.8 m and subjected to between 18 m and 65 m of overburden pressure. A fully assembled ring for C 708 consists of five 68° segments and one key bolt. The segments have a width of 1.2 m and are 250 mm thick. Contracts for the civil engineering work were awarded beginning in April 1997 and tunnelling and station structure work was started in late 1997 with the civil engineering and structure work completed by December 2000.

Design and Build Contract C 708 for the Clarke Quay Project was awarded to the Japan-Singapore-France joint venture group of Nishimatsu Construction Co Ltd., Lum Chang Building Contractors Pte Ltd., and Bachy-Soletanche Singapore Pte Ltd, with Maunsell Consultants (Singapore) Pte Ltd as the main designer. Contract C 708 is in a particularly severe part of the line with respect to concrete durability. The line of the bored tunnel passes through the highly variable and bacterially active estuarine and marine clay soils, which had caused much concern during the Phase I construction due the potential risk of sulphuric acid formation when exposed to oxygen. Also, the tunnel passed underneath the Singapore River, resulting in very high chloride ion contents in the groundwater.

This paper presents information on the development of the high-performance concrete (HPC) mixes for the tunnel-lining segments, covering the production issues and the quality control measures that have been implemented to ensure compliance with the specification, which required a 100-year design life.

DESIGN CONSIDERATIONS & SPECIFICATION REQUIREMENTS

The existing two lines that constitute Phase I of the Singapore MRT system were constructed between 1984 and 1986 using bored tunnels with a specified internal diameter of 5.2 m and precast concrete segmental linings. The presence of chlorides, sulfates and acids in the soil and groundwater and issues regarding accessibility for maintenance were important design considerations[1]. The tunnel linings form a critical element in the smooth operation of the transit system but are not readily accessible for routine maintenance. The Mass Rapid Transit Corporation (now the LTA) adopted a design philosophy that resulted in the production and use of tunnel linings that were rugged, durable and required low maintenance. The Phase I tunnel linings were cast with a Grade 45 reinforced concrete mix and had a minimum concrete cover requirement of 25 mm to the inner face and 30 mm to the external face[1]. For additional protection from groundwater, a coal tar epoxy coating was used on the extrados, that is, the exterior curved surfaces. This coating provided both protection against chloride ion ingress into the concrete and resistance to acid-forming bacterial attack.

For Phase II, with a specified design service life of 100 years, the LTA placed greater emphasis on the long-term durability of the tunnel segments compared with Phase I. In particular, the LTA improved the specification of the concrete used in the precast segments, requiring a higher compressive strength, resulting in a lower concrete permeability, an

increased concrete cover and the use of fusion bonded epoxy powder coated reinforcement. In addition, the LTA required the contractors to produce a Durability Strategy Report for their specific section of the line, commenting on the LTA specification and proposing alternative strategies to achieve the 100-year design life.

The LTA specification requirements for the concrete mix used in the precast tunnel segments of contract C 708 is summarised in Table 1. The minimum characteristic concrete strength was 60 MPa, an increase of 33% compared with the concrete used in the manufacture of the tunnel linings in Phase I. In the specification, the type of cement was left to the contractor, and included the use of blended cements containing pulverized fuel ash (fly ash) and ground granulated blast-furnace slag, with the choice to be based on the actual results from the soil and groundwater analysis, in accordance with the LTA's Design Criteria.

Table 1 Specification requirements for concrete mixes for the C708 bored tunnels

CONCRETE GRADE	60 MPa
Minimum 28-day Characteristic Strength	60 MPa
Minimum Cement Content	370 kg/m^3
Maximum Cement Content	400 kg/m^3
Maximum Water-Cement Ratio	0.45
Maximum Aggregate Size	20 mm
Maximum Placing Temperature	32°C

Consistent with the objective of using low permeability concrete as the primarily means of meeting the durability requirements of the tunnel segments, the LTA would have accepted the use of silica fume. However, because of concern regarding explosive spalling of saturated very low permeability concrete during a fire, the amount of silica fume that could be used in the concrete mix for the C 708 tunnel linings was limited to 7% by mass of cementitious material. The specification permitted the use of an approved high-range water-reducing admixture to achieve the minimum possible water-cementitious ratio consistent with the contractor's workability requirements, provided the specification also permitted the contractor to propose the use of admixtures provided the dosage remained within stated boundaries. The minimum concrete cover over the reinforcement was specified at 40 mm. The specification required the use of deformed high-yield steel reinforcing bars meeting the requirements of BS 4449:1988, with a fusion-bonded epoxy coating meeting ASTM A 775 requirements. For tunnel lining segments containing steel reinforcement the specification also required the application of a coal tar epoxy coating to the exterior curved surface, the sides and the inside of all bolt and grout holes.

DESIGN MODIFICATIONS TO ENHANCE DURABILITY

The contractor was permitted to propose the use of other admixtures that would provide benefits consistent with the intent of the specification. Working closely with Maunsell, alternative design proposals were developed that gave greater surety that the concrete would meet the LTA's required design life of 100 years.

The contract required the contractor to produce a Durability Strategy Report, so scheme designers Maunsell used their UK Infrastructure Maintenance team in Birmingham to carry out this task. The team already had knowledge of the particularly aggressive Singapore ground conditions from previous projects and it was soon established that Contract C708 was in one of the most aggressive areas of soil and groundwater towards concrete, running directly underneath the saline Singapore River [1].

The first durability design recommendation to the LTA proposed a fundamental change in strategy, namely not to use epoxy-coated reinforcement. The reasons were as follows:

- Damage to the epoxy coating during handling, fabrication of the reinforcement cages and casting of the tunnel linings could not be eliminated. With very severe exposure conditions, arising from high chloride ion concentrations in the groundwater, pinhole defects in the coating could lead to significant corrosion problems that would be difficult to detect and rectify.
- Even though consideration was given to the use of a fluidised bed technique for applying the epoxy powder to pre-bent bar fixed in tack-welded cages, no such plant existed local to the construction works. Hence, the time, expense and quality control required to coat, protect and then transport the assembled reinforcement cages using this process could have jeopardised the construction programme.
- If pre-bent coated bar was used and then assembled, the lack of rigidity of the reinforcement cage would cause a handling problem, as spot welding of the epoxy-coated bar would not be permitted.

Without the epoxy-coated bar, the main protection for the embedded reinforcement had to be provided primarily by the concrete used in the manufacture of the tunnel linings and the key property was the permeability of the concrete. The tar epoxy coating applied to the extrados of the segments provided a complete barrier to water and water borne salts such as chloride and sulfate ions, provided it remained intact during installation. However, the main area of concern was seepage of groundwater through the segment joints and down the face of the segments.

Reportedly, under controlled curing conditions, a water permeability of $5x10^{-13}$ m/s could be achieved in a Grade 60 concrete with a carefully selected mix proportion [1]. Simple modelling of chloride ion diffusion through Grade 60 concrete under normal exposure conditions indicated that unprotected concrete was unlikely to provide the necessary protection to the reinforcement over the specified 100-year life. The situation in the tunnels of the MRT system would be more severe, as it would be a very warm environment, with fast air movements, with the potential to concentrate even low levels of chloride ion present in the groundwater to a crystalline state on the surface of the segment. If chlorides were therefore going to absorb and diffuse through the cover zone, then measures would be needed to control corrosion of the reinforcement in the medium to long term.

The LTA would have permitted calcium nitrite corrosion-inhibiting admixture be added to the concrete mix. This additive was known to suppress pitting corrosion of reinforcement in chloride-contaminated concrete. However, published evidence had indicated that while calcium nitrite was a highly effective corrosion inhibitor, if the dosage of calcium nitrite was too low for the chloride exposure conditions, then pitting corrosion could occur.

The economical inhibitor dosage considered for C 708 was 15 L/m^3 for groundwater chloride contents of up to 4500 ppm. Clearly, the conditions on the inside of the segments would be much higher than this, due to the likely build-up of salt on the concrete surface, and therefore the dosage would have to be increased significantly.

Rather than increase the calcium nitrite dosage, Maunsell examined alternative approaches, such as waterproofing the concrete to reduce the absorption rate and using combination waterproofing and corrosion inhibiting admixtures that would not result in a risk of pitting corrosion at high chloride ion concentrations. Following considerable research and review of published papers, the most cost effective solution was identified as an organic corrosion-inhibiting and waterproofing admixture consisting of amines and esters [2], [3], and this was subsequently approved by the LTA for use in the manufacture of the tunnel linings in lieu of the epoxy-coated reinforcement. However, as a secondary durability strategy, regular inspection and maintenance of the structure was recommended to identify and treat any areas of leakage that developed over the coming years, with options for installing monitoring probes and even impressed current cathodic protection to the segments should significant chloride ion penetration occur.

Amine/Ester Organic Corrosion Inhibitor

Developed and used extensively in the U.S. since 1990, the amine/ester organic inhibitor protects embedded steel reinforcement by reducing the permeability of concrete and by forming a protective coating at the surface of the steel [2], [3]. The effectiveness of the amine/ester organic corrosion inhibitor (OCI) in delaying the time to corrosion initiation is demonstrated by the macro cell corrosion current data shown in Figure 1 from an ongoing comparative, long-term, accelerated corrosion investigation.

The graph shows virtually no corrosion activity in the OCI test specimens through about 1550 days of ponding with a 15% solution of sodium chloride. The OCI was used at its recommended dosage of 5 L/m^3. By contrast, the control untreated specimens exhibited signs of corrosion activity after about 200 days and specimens containing a 20 L/m^3 dosage of a calcium nitrite inhibitor started corroding between 800 and 900 days. All the concretes had a low water-cement ratio of 0.40 and the ponding cycle being utilized in this accelerated corrosion test consists of 4 days of ponding with the 15 percent sodium chloride solution at between 16°C and 27°C, followed by 3 days of drying at 38°C. This test cycle is similar to that used in earlier studies [5], [6] and it creates a macro cell within the specimen with the top layer of reinforcing steel becoming anodic and the bottom layer of steel cathodic, with the relative humidity maintained at between 60% and 80%. Additional test details, such as specimen preparation prior to testing, are given in the references [5], [6].

DEVELOPMENT OF HIGH PERFORMANCE CONCRETE MIXES

As would be expected in a project of this magnitude, particularly in light of the specification requirements to meet the design service life of 100 years, laboratory and field trials had to be performed to develop the correct concrete mix.

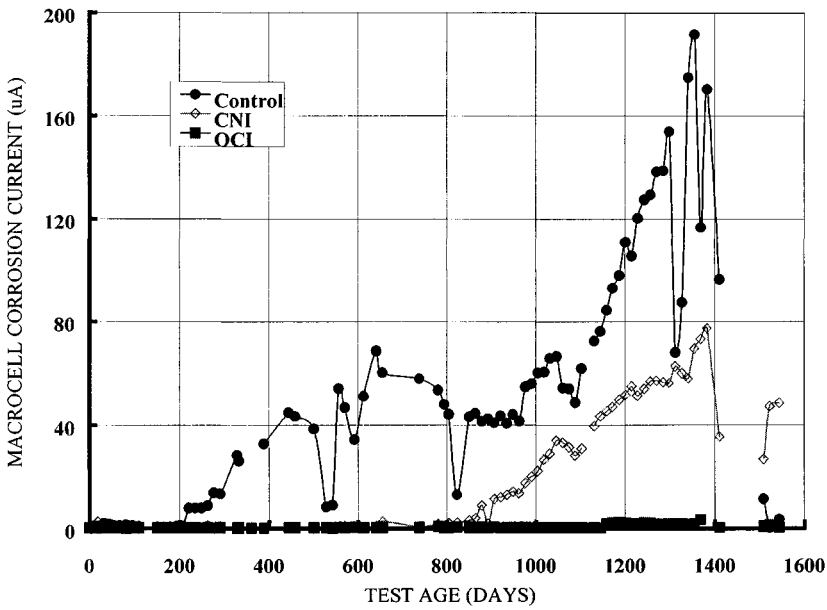

Figure 1 Macro cell corrosion current data from comparative long-term accelerated corrosion investigation

In most instances, durability and not strength is the controlling factor when a concrete mix has to be designed to meet specific durability requirements. This is because the low water-cementitious ratios needed from a durability perspective, invariably produce compressive strengths that significantly exceed the requirements from a structural design perspective.

Rapid durability proof tests would therefore be required to demonstrate the durability resistance of the concrete used in the precast segments. Tests such as the water permeability test alone would only give an indication of the pore structure of the concrete and not indicate the resistance to either absorption of chloride ions or subsequent diffusion through the cementitious paste matrix. However, steady-state chloride ion diffusion tests, such as the "Bulk diffusion test" favoured in Europe, would be impractical as a quality control test, taking over 90-days for a pass/fail test result. Therefore, in addition to compressive strength, both the water permeability and resistance to chloride ion penetration by the electrically-driven "Rapid Chloride Permeability" (RCP) method of ASTM 1202 were chosen for this purpose.

The primary target in the development of the concrete mix for the tunnel linings was a 28-day RCP value of less than 1000 coulombs, which was accepted by the LTA as a minimum practical value for the segment concrete. Changes in this value would serve as a check on concrete quality, in terms of ionic conductivity, which can be affected by increased chloride/sulfate content of the mix water and aggregate, as well as obvious changes in the water/cementitious ratio.

In March 1998, two concrete mixes, one containing pulverized fly ash cement (PFAC) and silica fume and the other a ternary blend of ordinary Portland cement (OPC), PFAC and silica fume, were evaluated. The fly ash content of PFAC was 20 percent and the mix proportions are as shown in Table 2. Two 100-mm diameter by 50-mm thick core slices were obtained from cast slab specimens and air-freighted in a moist condition to the U.S. for rapid chloride permeability (RCP) testing at Construction Technology Laboratories Inc. (CTL) in Skokie, Illinois. The core slices were tested in accordance with ASTM C 1202, "Standard Test Method for Electrical Indication of Concrete's Ability to Resist Chloride Ion Penetration" [4]. As indicated in Table 2, the RCP charge passed at 28 days averaged 806 coulombs for the PFAC-silica fume mix and 872 coulombs for the OPC-PFAC-silica fume mix. Thus, it was established that the requirement of <1000 coulombs at 28 days was achievable with the selected mix proportions.

Table 2 Concrete data for C 708 trial mixes

MIX ID	TM 5	TM 14
Concrete Grade	60 MPa	60 MPa
Target Slump	25 – 35 mm	25 – 35 mm
Ordinary Portland Cement	--	200 kg/m^3
Pulverized Fly Ash Cement	400 kg/m^3	200 kg/m^3
Fly ash content (%)	20%	10%
Silica Fume	15 kg/m^3	20 kg/m^3
Water	155 kg/m^3	155 kg/m^3
Fine Aggregate	808 kg/m^3	807 kg/m^3
Coarse Aggregate	1017 kg/m^3	1015 kg/m^3
High-Range Water-Reducing Admixture	1.3 L/100 kg	1.3 L/100 kg
	28-day RCP (coulombs)	
Specimen #1	830	964
Specimen #2	782	781
Average	806	872

In June 1998 a local testing laboratory in Singapore carried out additional RCP testing on specimens cast from two trial mixes, designated T1 and T2. On average, RCP values of 595 and 628 coulombs were obtained for Mix T1 at 60 and 90 days, respectively. For Mix T2, the 60-day and 90-day RCP values averaged 536 and 778 coulombs, respectively. Though the 90-day RCP values were slightly higher than the values obtained at 60 days, the data again demonstrated that the specification requirement of 1000 coulombs was achievable. Also, prior to the MRT Phase II project there had been only minimal specification and use of the RCP test in Singapore and the trials provided Maunsell with the assurance that the test could be performed locally. Following the trials, the mix proportions shown in Table 3 were submitted by the contractor and approved by the LTA for use in the manufacture of the tunnel-lining segments for C 708.

Table 3 Concrete Mix Proportions for C 708 Tunnel-Lining Segments

DESIGN STRENGTH	60 MPa @ 28 DAYS
Cement	400 kg/m^3
Silica Fume	20 kg/m^3
Water	138 kg/m^3
Fine Aggregate	762 kg/m^3
Coarse Aggregate	1109 kg/m^3
High-Range Water-Reducing Admixture	1.2 L/100 kg
Amine/Ester Organic Corrosion Inhibitor	5.0 L/m^3
Target Slump	40 mm

The final specification for the concrete segments was therefore a hybrid of the original LTA specification with additional requirements added by Maunsell:

- The reinforcement should be conventional uncoated bar at 40mm cover, tack-welded to provide electrical continuity.
- The concrete should be 25mm slump, with Silica Fume and superplasticising admixture.
- Water/cementitious ratio of 0.38 and at least C60 cube strength at 28-days.
- Average water permeability of 5x10-13 m/s at 28-days.
- Average chloride ion permeability to ASTM C1202 of <1,000 coulombs.
- Use of a combination waterproofing and corrosion-resisting admixture.

In addition, with uncoated bar and tack-welded cages, the segments would be suitable for corrosion monitoring or impressed current cathodic protection should the reinforcing bar ever begin to corrode.

PRODUCTION OF TUNNEL LININGS / QUALITY CONTROL OF HPC

For production, the Durability Strategy Report contained proposals for quality control checks on samples taken from concrete segments cured under the standard conditions for the specified period. These tests included the following:

- Compressive strength: - 1 sample per 50 m^3, testing for 7 and 28-day strengths.
- Chloride resistance: - ASTM C1202, three cores/month or every 1000 m^3.
- Water permeability: - SISIR method I-118568/2/TT, three cores/month or every 1000 m^3.

Production of the precast, HPC tunnel-lining segments for C 708 started at the beginning of 1999 in Malaysia. Over eight thousand units were produced for construction of the underground tunnels for this contract of the MRT Phase II project.

Statistical analysis of data obtained from about 350 pours for C 708 over a four-month period spanning late May through early October 1999 showed that the average slump was approximately 35 mm with a standard deviation of 7 mm. The target slump was 40 mm. The measured ambient temperatures were between 24°C and 31°C, with an average of 29°C and a standard deviation of 1.6°C. The non-accelerating effect of the amine/ester organic corrosion inhibitor proved to be an added benefit under these hot temperature conditions.

The concrete mix had adequate workability to facilitate placement and consolidation in the curved forms but, as can be expected with relatively low-slump silica fume mixes, it was sticky and initially made finishing a difficult task. To reduce stickiness, the use of an ASTM C 494 Type A, water reducing, admixture[4] in combination with the high-range water-reducing admixture or the partial replacement of a portion of the cement with fly ash, or both, was recommended. The forms could be typically stripped 8 to 10 hours after casting, after the concrete had achieved a compressive strength of 15 MPa.

Figure 2 Handling of the precast segments following demoulding

Cube Compressive Strength Data

Four-point moving averages of the 1-day, 7-day and 28-day cube compressive strengths obtained over the four-month period spanning late May through early October 1999 are presented in Figure 3. The smooth curves also shown in the Figure through each data set are the corresponding fourth-order polynomial trend lines. It should be noted that some of the 1-day strength tests were performed between 25 hours and 48 hours after casting, but are included in the Figure and data analysis to show the early-age strength development of the concrete mix. The results of a statistical analysis on the actual data within this period are presented in Table 4.

The data show an average 1-day cube compressive strength of approximately 38.4 MPa with a standard deviation of 6.2 MPa. The corresponding values at 7 days are 62.8 MPa and 4.8 MPa, respectively, and as shown in Table 4, the cube strength averaged 76.8 MPa at 28 days with a standard deviation of 6.8 MPa. The high early-age strengths facilitated early demoulding and reuse of the forms without the need for steam curing that had been used on Phase 1 of the MRT system[1]. The data also show that on average the specified design compressive strength of 60 MPa was achieved at around 7 days.

From Figure 2 it can be seen that the compressive strengths decreased in the period to 15 July 1999, but were maintained thereafter. Therefore, as indicated by the statistical data in Table 4, analysis of the cube compressive strength data obtained between July 15, 1999 and early October 1999 was also performed.

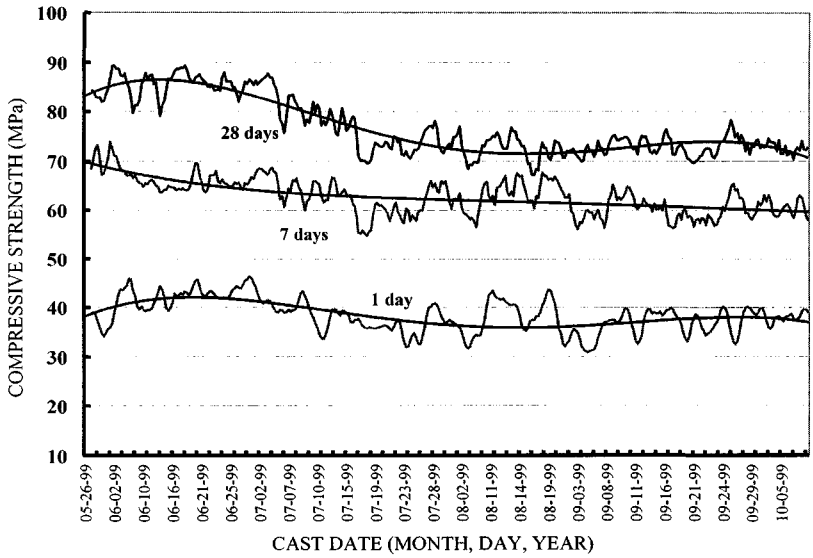

Figure 2 Four-point moving average of cube compressive strength data for C 708

Table 4 Summary of statistical analysis of cube compressive strength data for C 708

	CUBE COMPRESSIVE STRENGTH, MPa		
	1 Day**	7 Days	28 Days
	All data		
Range	22.5 – 58.5	50.5 – 76.8	64.4 – 92.3
Average	38.4	62.8	76.8
Standard Deviation	6.2	4.8	6.8
Coefficient of Variation	16.1	7.7	8.8
Degree of Control (ACI 363.2R[8])	--	Very Good	Very Good
	From 15 July 1999 to early October 1999		
Range	22.5 – 52.6	50.5 – 70.8	64.4 – 88.7
Average	37.0	61.0	72.9
Standard Deviation	5.8	4.5	3.8
Coefficient of Variation	15.5	7.4	5.3
Degree of Control (ACI 363.2R[8])	--	Very Good	Excellent

** Includes results performed between 25 hours and 48 hours of casting

Traditionally, the standard deviation of compressive strength data has been used as a measure of the degree of control. However, as discussed in ACI 363.2R, the coefficient of variation provides a better measure of the dispersion of compressive strengths, especially for high-strength concrete, and in Table 5.1.1 of the report suggested standards of quality control are given [8]. Based on the ACI 363.2R quality control standards, the calculated coefficient of variation for the 28-day cube compressive strength indicates very good control for the entire data set (late May to early October 1999) and excellent control for the data from mid-July to early October 1999.

RCP Durability Testing

RCP testing, using core samples from companion slabs cast during concrete placement in the tunnel lining forms, was performed routinely to ensure that the production units met the quality measures detailed in the modified specification. The frequency of testing was greater at the start of production and subsequently for segments representing the production for the 20th tunnel lining ring, where testing was performed on core samples representing the extrados, middle and intrados of the slab. Further tests were carried out on samples from the extrados and intrados representative of the 40th, 60th, 80th, 100th, and 120th rings. Thereafter, testing was performed only on the extrados core samples.

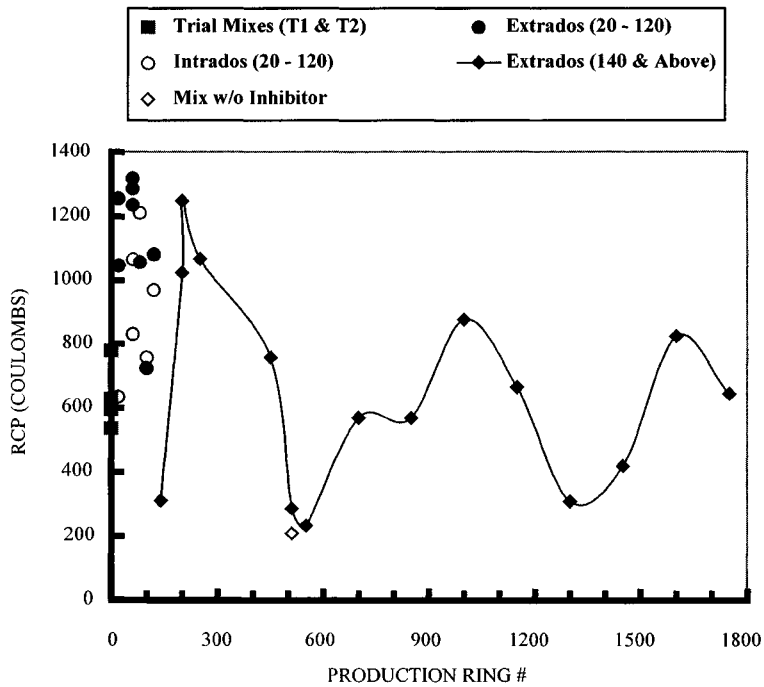

Figure 4 RCP Data for C 708 Tunnel Linings

As shown in Figure 4, RCP data from the first series of tests performed, representing the production of the 20th, 60th and 80th rings, produced results greater than the specification limit of 1000 coulombs. This led to a critical review of the various factors that could affect RCP test results such as batching sequence, mixing time, actual water content, specimen preparation, curing and testing, and the potential effect of the various admixtures used in the concrete mix. For example, RCP testing of concrete with and without the amine/ester organic corrosion inhibitor was performed and confirmed that the inhibitor had no effect on total charge passed in the RCP test (see data points representing testing for production ring # 510 in Figure 3). For reference purposes, the average values obtained from the RCP testing of Trial Mixes T1 and T2 are also shown in Figure 4.

Figure 5 Precast segments following application of coal-tar epoxy resin coating

The review indicated that, inadvertently, a slight modification in the computer program for the batch plant had affected the time of addition of the high-range water-reducing admixture, changing it from a delayed addition to an up-front addition at the very beginning of batching with the fine and coarse aggregates. The batching sequence for the high-range water-reducing admixture was changed to a delayed addition and, simultaneously, the mixing time was increased from 110 to 150 seconds. These modifications and other minor quality control measures that were implemented resulted in RCP values less than the required value of 1000 coulombs as shown in Figure 4.

Figure 6 View down the part-completed tunnel

As indicated in Figure 4, very low RCP values ranging from about 200 to 300 were obtained immediately after the review effort. It can also be inferred from Figure 4 that the quality control measures were revisited and reinforced whenever the RCP test results crept towards the 800 to 1000 coulomb range. Though the actual causes of the higher than expected RCP values obtained initially were not pinpointed, it is believed that day-to-day and batch-to-batch variability in the concrete mixes and, quite possibly, testing variances were all contributing factors. The review effort, which involved the contractor, precast manufacturer, admixture supplier and other parties, was instrumental in establishing the quality control factors critical to the production of the C 708 precast, HPC tunnel-lining segments. Subsequently, the frequency of testing was changed to every 150 rings.

CONCLUSIONS

The 100-year design service life for Singapore's MRT expansion project ranks it as a major application of HPC based on corrosion inhibitor in recent years, of the same magnitude as the recently completed Confederation Bridge that links Prince Edward Island with the Canadian mainland [7]. The information presented in this paper represents a significant milestone in concreting technology in Singapore and Malaysia and the developments in the specification have been built upon in subsequent LTA projects [9].

The data presented show that both the specified compressive strength of 60 MPa and the RCP durability requirement of <1000 coulombs were met during production of the precast concrete tunnel-lining segments. The specified compressive strength was achieved in 7 days. Based on the criteria published in ACI 363.2R, the coefficients of variation obtained from statistical analyses of the 28-day cube compressive strengths indicate very good to excellent control of the production and testing of the concrete mixes.

The high early-age strength development of the HPC mixes provided several benefits in the production of the tunnel-lining segments including early demoulding and increased mould turnover, the elimination of steam curing, and less damage to the units during handling, lifting and stacking at early ages. The overall benefit was a higher production rate to meet tunnel construction needs, and cost savings from not having to establish and maintain steam-curing facilities or perform extensive repairs to damaged segments.

Macrocell corrosion current data from an ongoing, independent, comparative accelerated corrosion evaluation show the significant benefit that the amine/ester organic corrosion inhibitor will provide in protecting the steel reinforcement in the tunnel-lining segments.

ACKNOWLEDGEMENT

The authors would like to express their thanks to the LTA for giving their permission for this paper to be published. As is the case in nearly all HPC applications of this magnitude, team effort among all parties was essential to guarantee achievement of the durability parameters required by the specification. The design team, contractor group and their consultants, the precast concrete manufacturer (ACP Industries Berhad, Malaysia) and the admixture supplier all contributed in various ways towards the success of the concreting operations of the project.

REFERENCES

1. ROBERY, P.C., DORAN, S.R, ONG, H. AND ROBINSON, S.A. Corrosion Protection to Buried Structures, Proc. Singapore Mass Rapid Transit Conference '87, 6-9 Apr. 1987.

2. NMAI, C.K., FARRINGTON, S.A., AND BOBROWSKI, G.S., Organic-Based Corrosion-Inhibiting Admixture for Reinforced Concrete, Concrete International, American Concrete Institute, Vol. 14, No. 4, April 1992, pp. 45-51.

3. NMAI, C.K., AND MCDONALD, D., Long-Term Effectiveness of Corrosion-Inhibiting Admixtures and Implications on the Design of Durable Reinforced Concrete Structures: A Laboratory Investigation, Supplementary Proceedings, RILEM TC-158 AHC International Symposium on The Role of Admixtures in High Performance Concrete, Monterrey, Mexico, March 1999.

4. ANNUAL BOOK OF ASTM STANDARDS, SECTION 4 – Construction, Volume 04.02 – Concrete and Aggregates, American Society for Testing and Materials, West Conshohocken, PA.

5. PFEIFER, D.W., LANDGREN, J.R., AND ZOOB, A.B., Protective Systems for New Prestressed and Substructure Concrete, *Report No. FHWA/RD-86/193*, U.S. Department of Transportation, Federal Highway Administration, April 1987, 126 pp.

6. MCDONALD, D.B., PFEIFER, D.W., AND BLAKE, G.T., The Corrosion Performance of Inorganic-, Ceramic- and Metallic-Clad Reinforcing Bars and Solid Metallic Reinforcing Bars in Accelerated Screening Tests, *Report No. FHWA-RD-96-085*, Federal Highway Administration, Office of Engineering and Highway Operations R&D, McLean, VA, October 1996, 112 pp.

7. LANGLEY, W., Concrete Mix Proportioning to Meet Durability Concerns for Confederation Bridge, SP-186, High-Performance Concrete – Performance and Quality of Concrete Structures, Proceedings, Second CANMET/ACI International Conference, Gramado, RS, Brazil, Malhotra V.M., Helene P, Prudencio, Jr. L.R., Dal Molin, D.C.C., eds., ACI International, 1999, pp. 129 – 148.

8. ACI COMMITTEE 363, Guide to Quality Control and Testing of High-Strength Concrete, ACI 363.2R-98, ACI International, Farmington Hills, MI, Dec. 1998, 18 pp.

9. NMAI, C.K., SEOW K.H, KHOR E.L. & ROBERY,P.C., Application of High-Performance Concrete in Singapore's North-East and Changi MRT Lines, Fifth CANMET/ACI International Conference on Recent Advances in Concrete Technology, Singapore, August 2001.

CONCRETE PLASTICITY DIAGRAM

A Voytsekhovsky N Kucherenko
Vinnytsya State University
A Barashikov
Kyiv National University of Civil Engineering and Architecture
Ukraine

ABSTRACT. In determining real bearing power of reinforced concrete structures it is necessary to know the amount of deformation limits of both reinforcement steel and concrete. Deformation limits of these materials are known to depend on many factors: stress distribution, loading history, and for concrete - on its age as well. While defining bearing power of reinforced concrete structures working under real loads, estimation of deformation limits for reinforcement steel and concrete become much more important task. If the question is approached more generally, in the process of designing any material or structure we predetermine its serviceability, ie the energy to be applied, for its destruction. Depending upon the presumable working conditions of the structure or material its wearing can be determined and probable further service life can be forecast. Thus, while assessing technical state of any material or structure we must know its strain characteristics as well as such an important material's parameter as deformation limits.

Keywords: Concrete, Plasticity, Load capacity, Deformation.

A Barashikov, Doctor of Engineering Sciences, Head of Chair of Reinforced Concrete Structures, Kyiv National University of Civil Engineering and Architecture.

A Voytsekhovsky, Candidate of Engineering Sciences, Head of Building Structures Laboratory, Vinnytsya State Technical University.

N Kucherenko, Post-graduate student of Vinnytsya State Technical University.

INTRODUCTION

Plasticity Diagram Plotting Technique

According to well-known theories of material plasticity, deformation limits for each material have functional dependence on relative hydrostatic pressure, common for different stressed states and deformation histories. For finding values of material deformation limits, plasticity diagram is used. Material plasticity diagram is the mechanical characteristic, which enlarges engineer's comprehension of material plasticity when the deformation sign is changed and characterizes plasticity dependence upon the kind of stress under simple deforming and fixed temperature-velocity conditions. This diagram establishes interrelation between material deformation limits intensity e_p and change of stressed state index η_k.

Since stressed state is characterized by three invariants, its kind can be described with two indices of η_k (k=1,2), which are constant under stress changes under simple loading. According to plastic state equation, simple stress appears with simple deformation, if average normal stress (σ) to stress intensity ratio (σ_u) is a constant figure. For the majority of reinforced concrete structures under ordinary working conditions only the first stress index of η_1 (k=1) is applicable and calculated as follows:

$$\eta_1 = \eta = \frac{3\sigma}{\sigma_u} = \frac{\sigma_1 + \sigma_2 + \sigma_3}{\sigma_u}, \qquad (1)$$

where $\sigma_1, \sigma_2, \sigma_3$ - are the main stresses in a three-dimensional space.

To plot a plasticity diagram in "e_p-η" coordinates the material is tested in different stressed states under simple loading, when the stress varies in proportion to one parameter as well as deformation, namely uniaxial tension (η=1), torsion (η=0), uniaxial compression (η= –1) and biaxial compression (-2<η<-1). Ultimate stresses $\sigma_1, \sigma_2, \sigma_3$ are assumed to correspond to the moment of material destruction.

In (1) stresses intensity σ_u is calculated by the formula

$$\sigma_u = \frac{1}{\sqrt{2}}\sqrt{(\sigma_1 - \sigma_2)^2 + (\sigma_2 - \sigma_3)^2 + (\sigma_1 - \sigma_3)^2}. \qquad (2)$$

Deformation limits intensity e_p that occurs with ultimate stresses should be found by the next equation

$$e_p = e_u = \frac{\sqrt{2}}{3}\sqrt{(e_1 - e_2)^2 + (e_2 - e_3)^2 + (e_3 - e_1)^2}, \qquad (3)$$

where e_1, e_2, e_3- are logarithmic deformations

$$e_i = \ln(1 + \varepsilon_i), \text{ where } i = 1 - 3. \qquad (4)$$

In accordance with this technique, investigations and tests have been carried out and plasticity diagram for grade A400C reinforcement steel has been suggested - Figure 1.

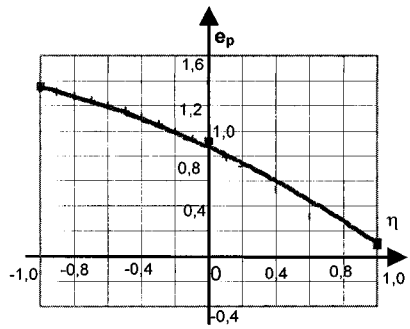

Figure 1 Experimental plasticity diagram for grade

Analytical dependence of this diagram can be represented as [1]

$$e_p(\eta_i)=e_p(\eta=0)\left\{(1-\eta)^2+\frac{1}{2}\eta\left[(1+\eta)e^{-\lambda_1}-(1-\eta)e^{\lambda_2}\right]\right\}, \tag{5}$$

where coefficients that characterize plasticity sensitivity to strain change

$$\lambda_1=\ln\frac{e_p(\eta=0)}{e_p(\eta=1)},\ \lambda_2=\ln\frac{e_p(\eta=-1)}{e_p(\eta=0)}. \tag{6}$$

Because of the fact that load-bearing strain values e_i in concrete are in the range from 0 to 1500 x 10^{-5} (0.015), ie are negligible, the equation for finding the amount of logarithmic deformations can be as follows:

$$e_i = \varepsilon_i. \tag{7}$$

Then deformation limits intensity will be

$$e_p=e_u=\frac{\sqrt{2}}{3}\sqrt{(\varepsilon_1-\varepsilon_2)^2+(\varepsilon_2-\varepsilon_3)^2+(\varepsilon_3-\varepsilon_1)^2}. \tag{8}$$

As far as concrete is concerned, there is a great number of experimental studies aimed at finding relationship between acting stresses and strains in concrete under different loading patterns that enable to define their ultimate values. Thus, to plot concrete plasticity diagram one can use investigations [2, 3, 4], each of them giving the way to find stresses and deformations in concrete under plane stressed state.

Concrete Deformation Under Uniaxial Tension, Torsion Tension, Compressive Torsion And Uniaxial Compression

To define the nature of concrete plasticity diagram in the interval of $-1<\eta<1$ we use investigation [2], which puts forward analytic functions necessary for finding basic concrete deformation characteristics under uniaxial tension ($\eta=1$), torsion tension ($1<\eta<0$), torsion ($\eta=0$), combined torsion and compressive action ($0<\eta<-1$) and uniaxial compression ($\eta=1$).

Depending on the relationship between principal stresses, strength condition is supposed to be as follows:

$$\sigma_1 = R_{bt}(1 + \sigma_2/R_b) = R_{bt} \cdot k_{p.c}, \tag{9}$$

Stress values in equation (9) are taken with their signs, ie tensional stresses are supposed to be positive while compressive ones - negative.

Ultimate compressive stress in accordance with $\beta=\sigma_1/\sigma_2$ is defined by the equation

$$R^*_{rp} = \frac{R_b R_{bt}}{\beta R_b - R_{bt}}. \tag{10}$$

Under the conditions of "tension - compression" plane stress, concrete is considered to be orthotropic material, all orthotropies of which run along the directions of principal stress areas (σ_1) and (σ_2).

The investigations also showed that concrete deformations in the directions of main axes are definitely non-linear. The non-linearity can be seen even with low levels of stresses, so interrelations between stresses and deformations are suggested to be performed with the help of physical equations for orthotropic body, but with its non-linearity taken into account, as well as effects of principal stresses β for the given element

$$\begin{aligned} \varepsilon_1 &= \frac{\sigma_1}{E'_{b1}} - \mu_{21} \frac{(1 + |\beta|)\sigma_2}{E'_{b1}|\beta| + E'_{b2}}; \\ \varepsilon_2 &= -\mu_{12} \frac{(1 + |\beta|)\sigma_1}{E'_{b1}|\beta| + E'_{b2}} + \frac{\sigma_2}{E'_{b2}}. \end{aligned} \tag{11}$$

Lateral strain coefficient of concrete μ_{ij} is not a constant value and depends upon stress variations.

Hence, under uniaxial load this figure can change from 0.15 to 0,4 depending on the stress level.

In [2] coefficients μ_{ij} for concretes under " tension-compression" plane stress conditions were assessed. For specimens with $\beta= -1$ the magnitude of μ_{ij} was approximately 0.15 , for specimens with $\beta= -1$ to$\beta= -1/6$ the value of μ_{ij} ranged from 0.15 to 0.20 and with $\beta= -1/12$ to $\beta= -0$ the coefficient μ_{ij} was observed to increase from 0.2 to 0.4.

Thus, as the result of the mentioned above, the following relation between transverse deformation coefficient change μ_{ij} can be suggested

$$\mu_{ij}=f(\beta)=0{,}25\cdot\beta^2+0{,}5\cdot\beta+0{,}4. \tag{12}$$

In equations (11) variable values for module of concrete deformations $E'_{б1}$, $E'_{б2}$ in the directions of principal tensile and compressive stresses action is used. In their turn $E'_{б1}$ and

$E'_{б2}$ depend upon β coefficient and design grade of concrete. Because of different properties manifested by concrete under tension and compression, values of concrete deformation module $E'_{б1}$ and $E'_{б2}$ are not the same. In [2] the next formulae for finding deformation module of concrete are recommended:

- in the direction of main tension stresses
-

$$E'_{b1} = E_b \text{ with } \sigma_1 \le 0{,}5 \cdot R_{bt} \cdot k_{p.c};$$

$$E'_{b1} = 0{,}5 \cdot E_b R_{bt} k_{p.c} \Big/ \sigma_1 \text{ with } \sigma_1 > 0{,}5 \cdot R_{bt} \cdot k_{p.c}; \qquad (13)$$

- in the direction of principal compressive stresses
-

$$E'_{b2} = E_b \upsilon_2 = E_{b6}\left[\tilde{\upsilon}_2 + (1 - \tilde{\upsilon}_2)\sqrt{1 - S}\right];$$

where

$$\tilde{\upsilon}_2 = \frac{Rb}{E_b \varepsilon_{rp}} \Big/ \left(1 - 0{,}25\sqrt{1 - \chi^2}\right), \qquad (14)$$

S-level of principal compressive forces, $S = \sigma_2 / R^*_{rp} \le 1$, $E_б$– concrete modulus of elasticity, ε_{rp}-ultimate strain for concrete under axial compression $\varepsilon_{rp} = \varepsilon_{br}$, χ- ratio of extreme principal compressive force to prism strength of concrete $(\chi = \sigma_2 / R_b)$.

While plotting plasticity diagram let us use the above equations (9)-(14) and the following explanations. In case of unidirectional tension $(\eta = 1)$ and taking into account negligible (in absolute meaning) value of concrete tensional strength R_{bt}, we assume $\sigma_2 = \sigma_3 = 0$.

Then $$\eta = \frac{\sigma_1 + \sigma_2 + \sigma_3}{\sigma_u} = \frac{\sigma_1 + \sigma_2 + \sigma_3}{\frac{1}{\sqrt{2}}\sqrt{(\sigma_1 - \sigma_2)^2 + (\sigma_2 - \sigma_3)^2 + (\sigma_1 - \sigma_3)^2}} = \frac{R_{bt}}{\frac{1}{\sqrt{2}}\sqrt{2R_{bt}^2}} = 1$$

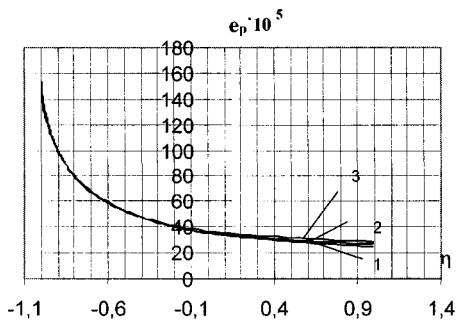

Figure 2 Concrete plasticity diagram by [2]:1 – for concrete With R_b = 20 Mpa; 2 – R_b = 30 Mpa; 3 – R_b = 40 MPa

and deformation intensity in this case

$$e_p = \frac{\sqrt{2}}{3}\sqrt{(e_1 - e_2)^2 + (e_2 - e_3)^2 + (e_3 - e_1)^2} = \frac{2}{3}e_1,$$

when $e_1 = \varepsilon_{btu} = 2\frac{R_{bt}}{E_b}$; $R_{bt} = 0{,}65\sqrt[3]{R_b^2}$.

The above-mentioned enables us to plot concrete plasticity diagram for section. $-1 < \eta < 1$ (see Fig.2), where it can be approximated

$$e_p(\eta, Rb) = \frac{(0{,}0127 \cdot Rb^2 - 0{,}9155 \cdot Rb + 41{,}18)}{\eta + (1 \cdot 10^{-4} \cdot Rb^2 - 0{,}0073 \cdot Rb + 1{,}32)} + \\ + (-0{,}007 \cdot Rb^2 + 0{,}5925 \cdot Rb + 3{,}87) \qquad (15)$$

Concrete Deformations Under Uniaxial And Biaxial Compression

Work of concrete under uniaxial (η= -1), as well as biaxial (η= -2), compression was examined in research papers [3,4]. These studies deal with plane stress-strain state, ie the case when σ_3=0. Then, equations (1) and (2) look as follows:

$$\eta = \frac{\sigma_1 + \sigma_2}{\sigma_u}$$

where $$\sigma_u = \frac{1}{\sqrt{2}}\sqrt{(\sigma_1 - \sigma_2)^2 + \sigma_2^2 + \sigma_1^2} = \sqrt{\sigma_1^2 + \sigma_2^2 - \sigma_1\sigma_2}\,.$$

In [3] the next equation for finding σ_1 with known σ_2 is suggested:

$$\sigma_{b1} = \hat{\sigma}_{b1} \cdot \sum_{i=1}^{5} a_i \cdot \bar{\varepsilon}_{b1}^{i} \qquad (16)$$

where $\bar{\varepsilon}_{b1} = \frac{\varepsilon_{b1}}{\hat{\varepsilon}_{b1}}$; $\hat{\sigma}_{b1}$, $\hat{\varepsilon}_{b1}$ - are ultimate stresses and corresponding deformations. (Further $\sigma_1=\sigma_{b1}$; $\sigma_2=\sigma_{b2}$; $\varepsilon_1=\varepsilon_{b1}$; $\varepsilon_2=\varepsilon_{b2}$).

Average experimental magnitudes for a_i coefficients of "σ–ε" concrete diagram are taken in accordance with its compressive strength (Rb) as suggested in [5]. For intermediate values of Rb, diagram parameters can be defined with the help of linear interpolation.

Finding ultimate deformations $\hat{\varepsilon}_{b1}$ and stresses $\hat{\sigma}_{b1}$ are proposed as follows:

$$\hat{\varepsilon}_{b1} = \left[1 + 2{,}15\frac{\sigma_{b2}}{R_b} - 1{,}95\left(\frac{\sigma_{b2}}{R_b}\right)^2\right] \cdot \varepsilon_{bR}, \qquad (17)$$

$$\tilde{\sigma}_{b1} = \left[1+1{,}38\frac{\sigma_{b2}}{R_b} - 1{,}15\left(\frac{\sigma_{b2}}{R_b}\right)^2\right]\cdot R_b,$$

where ε_{bR} - strains of concrete compression, which correspond to stresses $\sigma_b=R_b$. Then, polynomial (17) will look so:

$$w_{\sigma_{b1}} = R_b\cdot\left[1+1{,}38\frac{\sigma_{b2}}{R_b} - 1{,}15\left(\frac{\sigma_{b2}}{R_b}\right)^2\right]\cdot\sum_{i=1}^{5} a_i\left\{\frac{\varepsilon_{b1}}{\left[1+2{,}15\frac{\sigma_{b2}}{R_b} - 1{,}95\left(\frac{\sigma_{b2}}{R_b}\right)^2\right]\cdot\varepsilon_{bR}}\right\}^i. \qquad (18)$$

Application of (16) - (18) equations allow us to obtain concrete plasticity diagram for $-2<\eta<-1$ section (see Figures 3 and 4).

Paper [4] contains a somewhat different approach to the problem and suggests that relative deformation changes are to be dealt by introduction of lateral strain coefficients μ_{ij}. Then, magnitudes of actual strains ε'_{b1} and ε'_{b2} are found by the equations:

$$\varepsilon'_{b1} = \varepsilon_1 - \mu_{21}\cdot\varepsilon_2; \quad \varepsilon'_{b2} = \varepsilon_2 - \mu_{12}\cdot\varepsilon_1. \qquad (19)$$

Lateral strain coefficients

$$\mu_{12} = \sqrt{\mu_1\mu_2\cdot\frac{E_{b1}}{E_{b2}}}; \quad \mu_{21} = \sqrt{\mu_2\mu_1\cdot\frac{E_{b2}}{E_{b1}}}, \qquad (20)$$

where μ_1,μ_2 - lateral strain coefficients in the direction of main axes that are calculated, as for uniaxial compression, by the equation:

$$\mu_i = 0{,}16 + \left(\frac{\sigma_i}{k_c R_b} - 0{,}164\right)^6, \qquad (21)$$

where *i* - orthography axis direction coinciding with principal stress direction; k_c - coefficient characterizing increase in concrete strength under biaxial compression and depending upon μ_σ - Lode-Nadai coefficient; φ_R -coefficient of concrete strength increase under biaxial compression relative to uniaxial; e_1 - maximum state index k_c ($0<e_1<1$).

Application of equations (19)-(21) enables us to obtain concrete plasticity diagram for- $-2<\eta<-1$ section (see Figures 3 and 4).

From the above Figures the plasticity diagram is seen to be identical in both cases. Although, the approach suggested in [4] takes into consideration a wider range of factors that affect concrete deformation under biaxial compression. While approximating plasticity diagrams, thus, we use curves 1-3 from Figure 4. Plasticity diagram for this section can be approximated by the function:

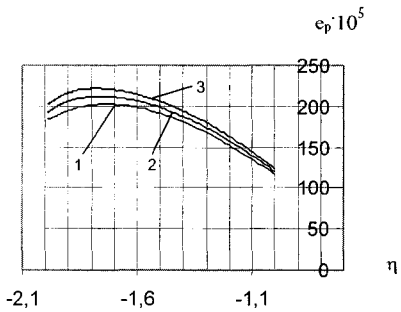

Figure 3 Concrete plasticity diagram by [3]
1 – for concrete with R_b = 20 MPa;
2 – R_b = 30 MPa; 3 – R_b = 40 MPa

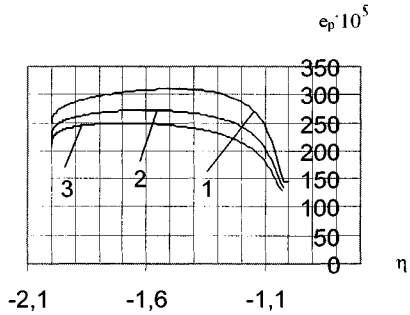

Figure 4 Concrete plasticity diagram by [4]
1 – for concrete with R_b = 20 MPa;
2 – R_b = 30 MPa; 3 – R_b = 40 MPa

$$e_p(\eta, Rb) = \eta^4(-0{,}0815 \cdot Rb^2 + 33{,}615 \cdot Rb - 2342{,}6) + \eta^3(-0{,}693 \cdot Rb^2 + 227{,}1 \cdot Rb - 15105) +$$
$$+ \eta^2(-2{,}085 \cdot Rb^2 + 571{,}75 \cdot Rb - 36416) + \eta \cdot (-2{,}605 \cdot Rb^2 + 628{,}85 \cdot Rb - 38765) +$$
$$+ (-1{,}076 \cdot Rb^2 + 245{,}91 \cdot Rb - 14905) \qquad (22)$$

Diagram For Concrete Plasticity Under Uniaxial And Biaxial Compression With Considering Of Down Going Section Of Deformation

In papers [3,4] relationships given by equations (16)-(21) permit to define dependence of deformations upon stresses from 0 to ε_{br}, that is, for up going section of deformation. For reinforced concrete structures bearing capacity of which is determined by the moment of gaining maximum stress within concrete (R_b), such an approach is quite adequate and plasticity diagram presented by (15) and (22) is applicable.

In the case of proportioning statically indeterminate and some other reinforced concrete structures their bearing capacity is determined by moment of reaching ultimate (maximum) deformations ε_{bu}. Down going sections of concrete deformation curves are crucial for such structures.

To plot a diagram of concrete plasticity with provision for down going section, equations (9-14) and (16-21) are assumed to be true within the whole deformation period, as it can be seen from analysis of test results given in [3]. Then, the equations (14) according to [2] will look as follows:

$$\tilde{\upsilon}_2 = \frac{Rb}{E_b \varepsilon_{bu}} \Big/ \left(1 - 0{,}25\sqrt{1-\chi^2}\right);$$

and equation (17) from [3]: $\hat{\varepsilon}_{b1} = \left[1 + 2{,}15\,\frac{\sigma_{b2}}{R_b} - 1{,}95\left(\frac{\sigma_{b2}}{R_b}\right)^2\right] \cdot \varepsilon_{bu}$.

With these changes taken into account, concrete plasticity diagram looks as shown in Figure 5 and 6.

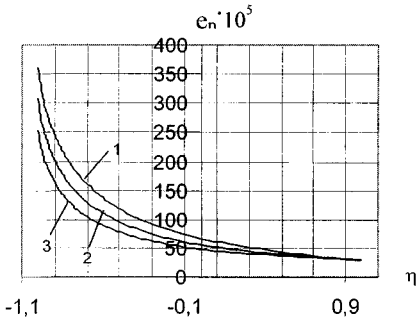

Figure 5 Concrete plasticity diagram by [2] taking into account drop-down branch of curve of concrete derformation: 1 – for concrete with R_b = 20 MPa; 2 – R_b = 30 MPa; 3 – R_b = 40 MPa

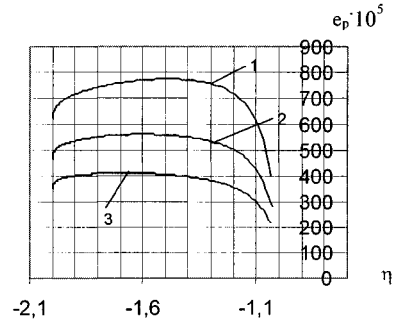

Figure 6 Concrete plasticity diagram by [4] taking into account drop-down branch of curve of concrete deformation: 1 – for concrete with R_b = 20 MPa; 2 – R_b = 30 Ma; 3 – R_b = 40 MPa

Approximation for this diagrams may be suggested as the equations:

- for section $-2 < \eta < -1$:

$$e_p(\eta, Rb) = \eta^4\left(-1{,}6755 \cdot Rb^2 + 222{,}38 \cdot Rb - 8070{,}5\right) + \eta^3\left(-11{,}11 \cdot Rb^2 + 1446{,}3 \cdot Rb - 51{,}801\right) + \\ + \eta^2\left(-27{,}42 \cdot Rb^2 + 3508{,}4 \cdot Rb - 124228\right) + \eta \cdot \left(-29{,}63 \cdot Rb^2 + 3743{,}3 \cdot Rb - 131567\right) + \\ + \left(-11{,}465 \cdot Rb^2 + 1440{,}1 \cdot Rb - 50430\right) \tag{23}$$

- for section $-1 < \eta < 1$:

$$e_p(\eta, Rb) = \frac{\left(0{,}0576 \cdot Rb^2 - 5{,}91 \cdot Rb + 191{,}06\right)}{\eta + \left(1 \cdot 10^{-4} \cdot Rb^2 - 0{,}0103 \cdot Rb + 1{,}422\right)} + \left(-0{,}0215 \cdot Rb^2 + 2{,}275 \cdot Rb - 47{,}9\right) \tag{24}$$

CONCLUSIONS

The conducted investigations permit to suggest the following concrete plasticity diagrams.

1. In cases when moment of gaining maximal stresses, ($\sigma_b = R_b$.) serves as the criterion of concrete destruction, plasticity diagram looks as the curve 1 in Figure7, its analytic description being equations (15) and (22).
2. In cases when moment of gaining maximal deformations, ($\varepsilon_b = \varepsilon_{bu}$) is taken for the criterion of concrete destruction, the plasticity diagram looks like curve 2 in Figure 7, its analytic description being equations (23) and (24).

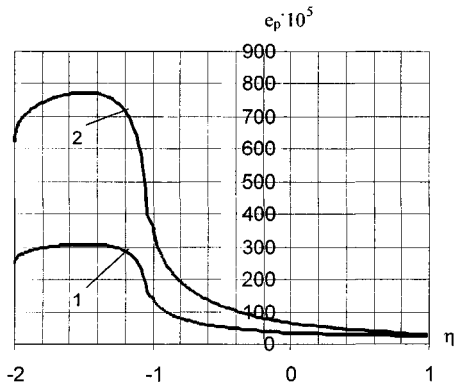

Figure 7 The concrete plasticity diagrams when R_b = 20 MPa:
1 – peak voltages serve as a criterion;
2 – peak deformations serve as a criterion

REFERENCES

1. VOYTSEKHOVSKY O.V. AND KUCHERENKO N.Y., Technological Maker's Data Sheet as Main Document Characterizing Serviceability of Material, Resource-saving materials, buildings and structures, Journal of Rivne State Technical University, Vol 3, Rivne: RSTU, 1999. –310 p.

2. SHUBERT I.M., Investigation of Stress-strain State of Centrifugal Circular Piers under Torsion Compression//Dissertation for Candidate of Engineering Degree, Minsk, 1983. – 227 p.

3. DAVYDENKO A.I., Complex Strain Influence on Concrete Compression Diagram Parameters in Proportioning Reinforced Concrete Beams on Deformed Base //Dissertation for Candidate of Engineering Degree, Kyiv, RIBS, 1988. –150 p.

4. ZHURAVSKY A.D., Stress-Strain State of Reinforced Concrete Slabs with Biaxial Recompression//Dissertation for Candidate of Engineering Degree, Kyiv, KICE, 1988. – 158 p.

5. Methodological Recommendations for Precise Proportioning of Reinforced Concrete Parts with account for Diagram of Full Concrete Compression, Kyiv, RIBS, 1987. – 23 p.

EXPERIMENTS ON CONCRETE UNDER SHOCK LOADING

N Herrmann

J Eibl

L Stempniewski

University of Karlsruhe

Germany

ABSTRACT. In the case of loading a concrete structure by detonation or hypervelocity impact shockwaves are generated. These shockwaves cause a steep increase in pressure within the wavefront which propagates with high velocity. For a numerical simulation of such actions a constitutive material law $F = \dot{f}(\varepsilon, \dot{\varepsilon}, T)$ is needed to describe concrete under these conditions adequately.

We report our approach to measure stress, strain and temperature during tests on concrete slabs under loading with contact charges in the pressure range up to 20 000 MPa. The known measuring methods with carbon-resistors, strain gauges and manganin gauges with a specially developed encapsulation were used. First experiences in using a new temperature-sensor called the atomic-layer thermopile are gained. The measurement results are shown and remaining problems are discussed.

Keywords: Shockwaves, Measuring technique, Extreme conditions, High pressure, Material characterization.

N Herrmann, is a Physicist and Manager of the Institute of Reinforced-Concrete Structures and Building Materials at the University of Karlsruhe and the main person in charge of the reported tests.

J Eibl, is the former Head of the Institute of Reinforced-Concrete Structures and Building Materials at the University of Karlsruhe.

L Stempniewski, is the Head of the Institute of Reinforced-Concrete Structures and Building Materials at the University of Karlsruhe.

INTRODUCTION

In order to develop material models as many as possible data should be gained by performing tests. The measuring of data within concrete under shock loading during tests with contact charges is a challenge for the measuring technique because of the fast rise time of the signals. In the literature only a small number of publications can be found containing data for standard concrete under these condition.

Tests for measuring the volumetric pressure were made earlier at our institute and a material law by disregarding deviatoric stress and analytically discribing the adiabatic temperature rise within the concrete was developed. To describe the stress-state including the deviatoric part, it is necessary to measure the stresses in different directions, or minimally by measuring the hydrostatic pressure and the stress in one direction. To check the assumptions for the adiabatic heat a new attempt to measure the temperature rise was made.

THEORY

Shockwaves in concrete are formed because of the nonlinearity of the volumetric stress-strain-relation (Figure 1). The propagation velocity c of the wave depends on the slope of the non-linear stress-strain-relation:

$$c = \sqrt{\frac{H}{\rho}} \quad \text{with} \quad H = \frac{d\sigma}{d\varepsilon}$$

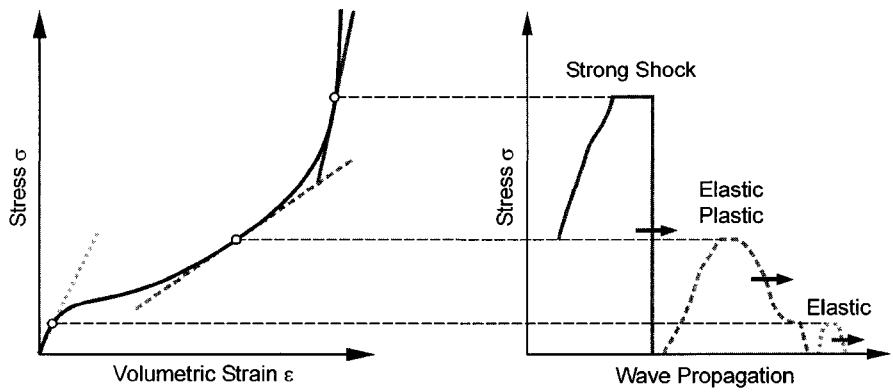

Figure1 Shockwave formation due to the nonlinearity of the volumetric stress-strain-relation for concrete

In the elastic range all parts of the wave propagate with the same velocity, so the original shape is only disturbed by the inhomogenity of the material. If the amplitude of the wave is higher, so that the plastic range of the stress-strain-relation is achieved, the pores are destroyed and the velocity for the plastic part of the wave is lower, the wave smoothes out.

In the high pressure range, the material is highly volumetric compacted and the propagation velocity for the higher amplitudes increases, so that the wave profile steeps up to a sharp discontinuity in pressure named shockwave [1].

The description of a shock wave transition through a material is given by the Hugoniot-Equation. The Conservation-Equations for mass, momentum and energy for the material before and after the wave transition can be combined to the Hugoniot-Equation describing all possible states of the material loaded by a shockwave:

$$\rho_1 \cdot (u_S - u_p) = \rho_0 \cdot u_S \qquad \text{conservation of mass}$$

$$\rho_0 \cdot u_S - u_p = p_1 - p_0 \qquad \text{conservation of momentum}$$

$$\rho_0 \cdot u_S \left(E_1 - E_0\right) + \frac{1}{2} \cdot (\rho_0 \cdot u_S \cdot u_p)^2 = p_1 \cdot u_p \qquad \text{conservation of energy}$$

$$E_1 - E_0 = \frac{1}{2}(p_1 + p_0) \cdot (V_0 - V_1) \qquad \text{Hugoniot-Equation}$$

The transition between the initial state and the final state is given by the Raleigh-Line, since the states in between are not run through:

$$\frac{p_1 - p_0}{V_0 - V_1} = \left(\frac{u_S}{V_0}\right)^2 \qquad \text{Raleigh-Line}$$

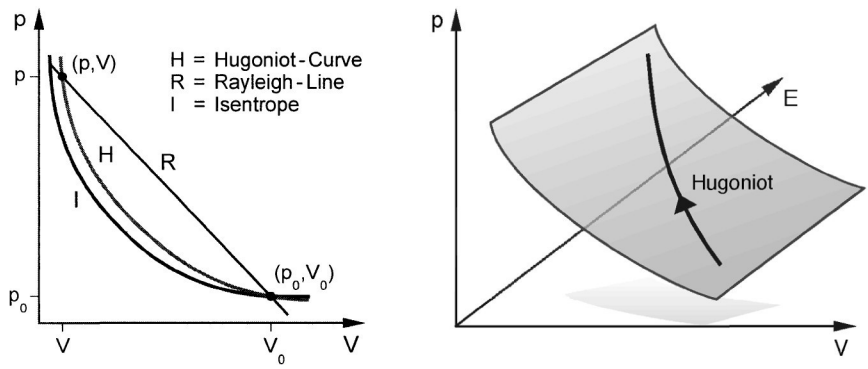

Figure 2 Hugoniot-Curve in p-V-plane and as part of the EOS in p-V-E-space

The Hugoniot-Curve is generally a line lying in a plane representing the Equation of State (EOS) in the pressure-volume-energy-space (Figure 2). Many assumptions for the EOS were made. To gain more information on the best fitting EOS it is necessary to know the adiabatic part for the Hugoniot [9].

In Figure 3 the failure surface for concrete is shown. The pressure region up to 1000 MPa is known from static tests, but in the high pressure region only a few points on the hydrostatic axis have been measured. The development of the deviatoric part is not known. There are three possibilities for the shape of this part. The first possibility is that the deviatoric part of the failure state increases with the hydrostatic part because of the increasing of the friction between the destroyed material parts, the second possibility is that the deviatoric part comes to a constant value or thirdly it decreases due to the decrease of friction between the remaining particles of the material. To get some information on the shape of the deviatoric it is necessary to measure stress in different directions.

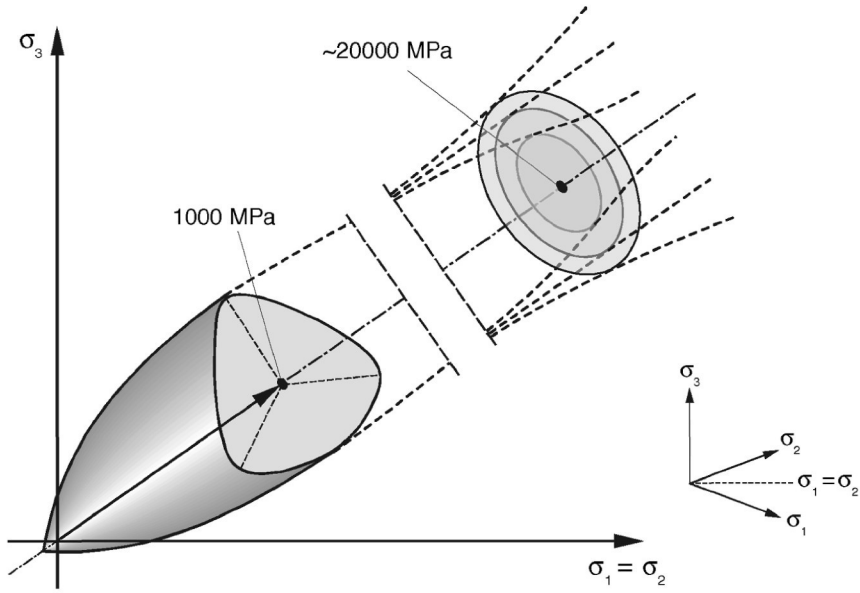

Figure 3 The known failure surface for concrete and the possibilities for the failure surface in the region above

EXPERIMENTS

A series of 3 tests were performed on concrete slabs loaded with contact charges. The concrete strength was chosen to 35 MPa. In 2 cases the load was 2 kg TNT and in another case the load had a weight of 0.7 kg TNT. As charge a so-called plane-wave-generator was used and slabs with a = 0.5 m were used (Figure 4).

The outer part of this conical charge consists of Composition B, an explosive with a detonation velocity of 7900 m/s, the inner cone is made of TNT with a detonation velocity of 6800 m/s, so the detonation wave of the faster explosive holds the inner detonation wave within the cone. The base angle of the geometry of the charge depends on the detonation velocities and is responsible for the formation of a plane wave that loads the slab on the upper surface.

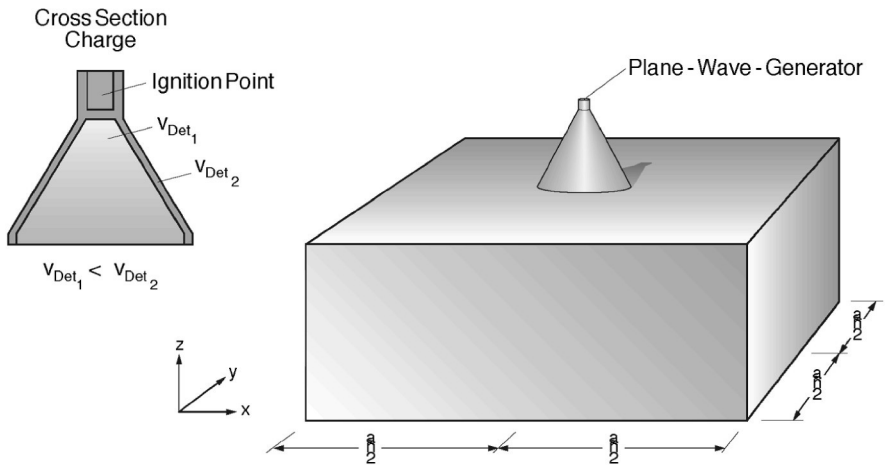

Figure 4 Test set up with plane-wave-generator

MEASURING TECHNIQUE

To collect the desired data a new measurement system was used and partially developed. For measuring the volumetric pressure p within the concrete carbon-resistors were used. At our institute a dimensionless calibration curve based on the results of many authors has been established [9]. The resistors are encapsulated by an epoxid-bonding-agent which is injected in a small casting form in which the resistors are positioned and connected by a coaxial cable. It is important that the connection wires pass the sensor on the opposite side to the load direction in order to avoid destruction of the sensor before it is hit by the pressure wave (Figure 5).

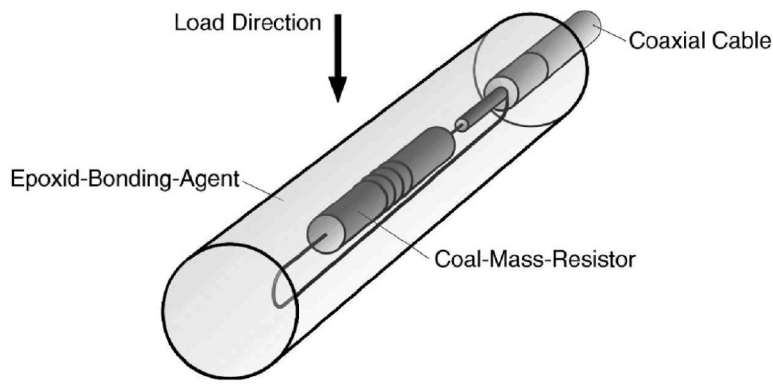

Figure 5 Encapsulation for carbon-resistor

In earlier tests at our institute only the method of the carbon-resistors was used to measure the volumetric pressure within the concrete and the deviatoric stress was neglected. In order to check the assumption that in the case of a slab loaded by a contact charge the stress state in the region directly under the charge is hydrostatic not only the volumetric pressure p should be measured. The pressure p is given by the following equation:

$$p = \frac{1}{3}(\sigma_{11} + \sigma_{22} + \sigma_{33})$$

One of the objectives of this study was to determine the deviatoric part of the stress state. Therefore it is necessary to record the stress in two different directions or minimally to measure the volumetric pressure and stress in one direction. With the assumption $\sigma_{22} = \sigma_{33}$ one can calculate the deviatoric stress τ_0 which is given by [3]:

$$\tau_0 = \sqrt{2/9}\,(\sigma_{11} - \sigma_{22}) \qquad \text{with:} \quad \sigma_{11} \neq 0\,;\, \sigma_{22} = \sigma_{33} \neq 0$$

The tests were performed with manganin sensors which are thin foil-sensors measuring the stress perpendicular to the foil-plane. The sensors have a thickness of 13 µm and an area of (44.45 x 6.35) mm. As the foil itself and especially the connection wires are very sensitive they have been embedded in a sandwiched encapsulation made of aluminium (Figure 6). Aluminium was chosen because of the similar modulus of elasticity in comparison to the concrete. The wires were led to the opposite site of the load, to avoid a pre-event destruction [2].

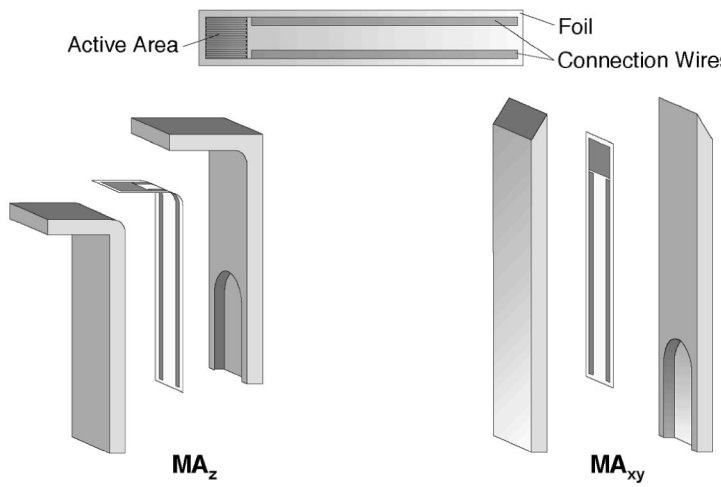

Figure 6 Encapsulation for manganin gauges

For the strain measurement high performance strain gauges of a type that can measure strains up to 15% were used (Figure 7).

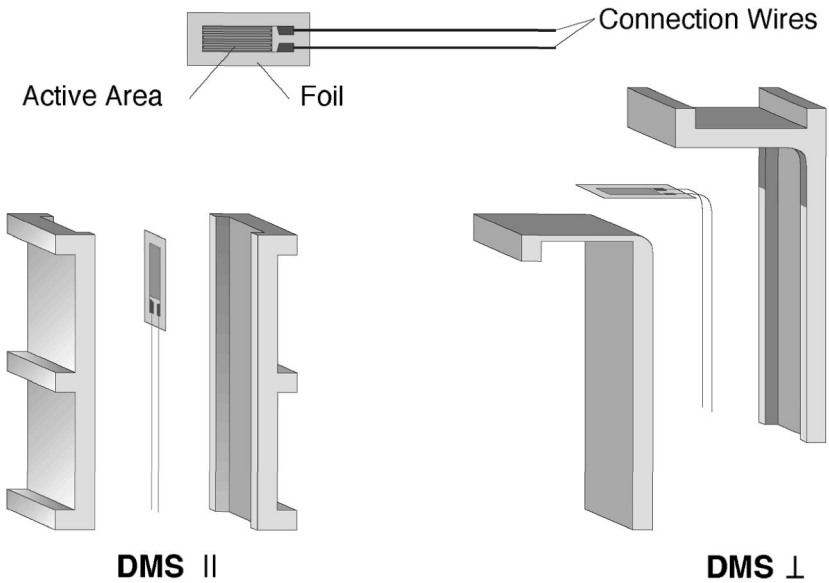

Figure 7 Encapsulation for strain gauges

Very similar to the manganin gauges they were bonded in an sandwiched aluminium encapsulation. In addition to the manganin-type encapsulation they have been ribbed in order to assure the bonding between the sensor and the concrete.

An innovative measurement system was developed to measure the temperature rise during the adiabatic compression. A sensor was used that is able to register a temperature rise in the time of some nanoseconds when used in open form. This sensor called the atomic-layer thermopile was originally developed for power measurement of high energy lasers. The principle of this measurement is the Seebeck-Effect. This effect is well known as it is the physical principle of thermocouples [6].

Bringing two different metals in contact causes a contact voltage that is originated by the two different Fermi levels of the metals. From the metal with the higher occupied electron states to that with the lower occupation occurs a diffusion in order to equalize the potentials. The difference of the potentials depends on the temperature. When considering a ring of the two metals in which one contact is kept at a constant temperature, the temperature at the other contact will cause a voltage proportional to the temperature difference that can be measured between the two contacts (Figure 8).

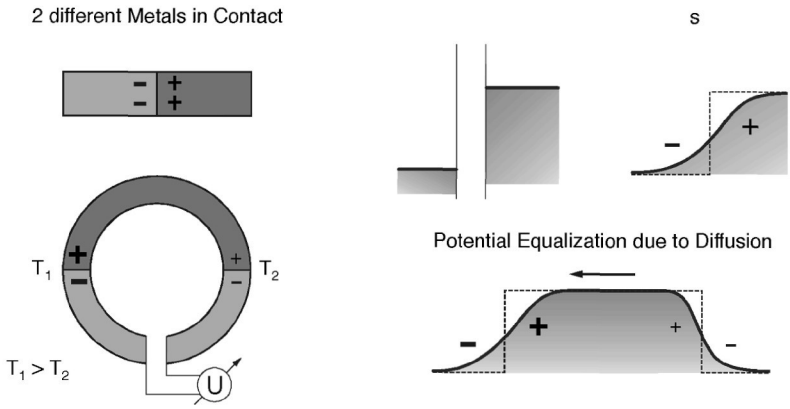

Figure 8 Physical principle of thermocouples – Seebeck-Effect

Considering many layers of two different metals on a substrate that is kept at constant temperature a voltage is caused by heating the surface of the multilayer (Figure 9a, 10a). This voltage is the sum of all the contact voltages at the layer boundaries. As it is difficult to pick up the voltage between the surface and the substrate the angle of the layers can be tilted so that the electric field caused by the temperature gradient can be divided in a parallel and a transversal part (Figure 9b). The voltage caused by this transversal field can be picked up at the sides of the sensor which is called an atomiclayer thermopile. The multilayer is given by the anisotropy of the high temperature superconductor $YBa_2Cu_3O_7$ whose crystal structure is shown in Figure 9c. Layers of good conducting copper-oxide are alternating with the Ytterbium and Barium layers that are rather bad conductive [8].

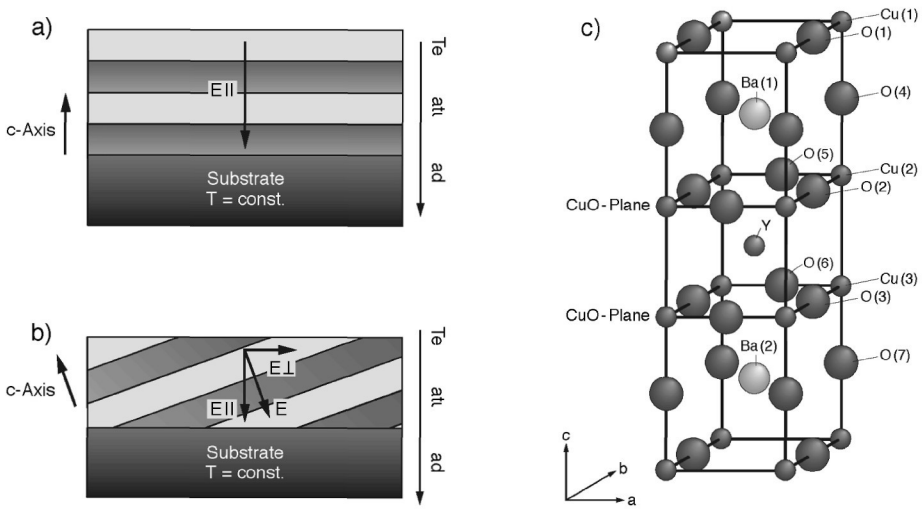

Figure 9 Transversal Seebeck-Effect and Crystal Structure of $YBa_2Cu_3O_7$

This type of sensor has rise times of a few nanoseconds when used in unencapsulated form as it is in power measurement of lasers for which the sensor was developed [7]. For application in concrete the very sensitive sensor should be encapsulated. This is done by casting it within the same epoxid-bonding-agent as used for the carbon resistors. For the calibration of the signal many assumptions for the heat transfer to the sensor must be taken into account. These assumptions lead to a sensitivity of 0.01 V/K.

As for the other sensors also in the case of the thermopile it is important to take into account the connection points and wires. Normally the sensors are connected in a way that the gold-contacts lie above the active surface (Figure 10c).

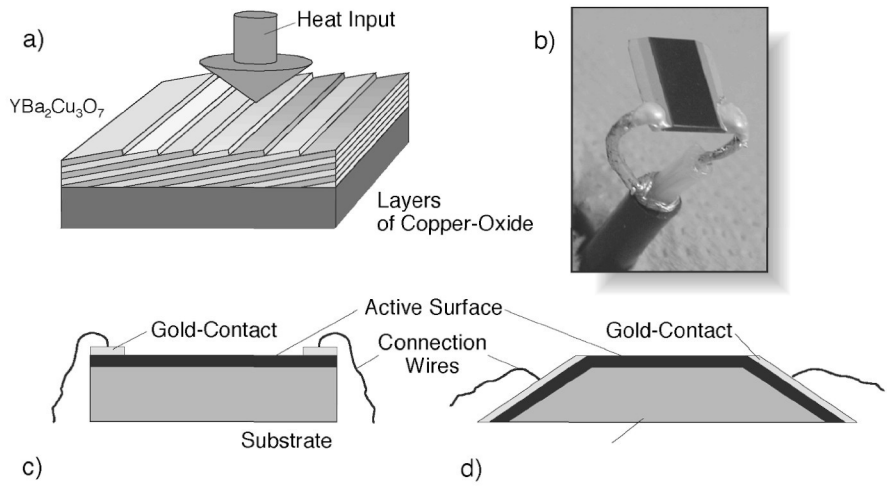

Figure 10 Thermopile in principle and after contacting, principle of contacting

Together with the manufacturer we developed a sensor setup with sloped contact-planes on both sides of the sensor so first the active surface is striked by the incoming pressure wave, before destruction of the contacts can occur (Figure 10d). The contacting was made by a conducting silver bond (Figure 10b).

EXPERIMENTAL RESULTS

The test data was recorded with a transient recorder with a sample rate of 25 MHz and transmitted and evaluated with a personal computer. Out of the series of tests some results will be shown in the following.

A typical pressure profile measured by carbon-resistors in the high pressure region is presented in Figure 11. As expected the peak pressure is reducing very fast. The pressure of 18000 MPa in a depth of 2 cm decreases to a value of 2000 MPa in a depth of 7 cm.

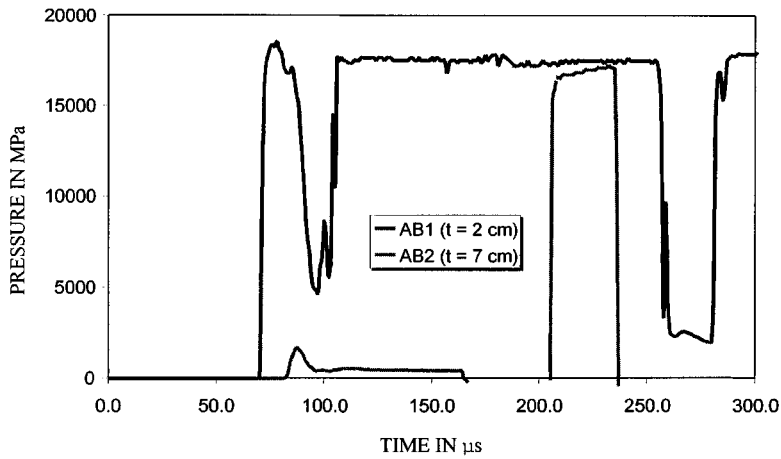

Figure 11 Pressure profiles in the upper region of slab III

In the lower region of the slab the signals are overlaid by noise but amplitudes down to 5 MPa can still be resolved. In Figure 12 some curves with lower peak pressures evaluated from the data of slab III are presented.

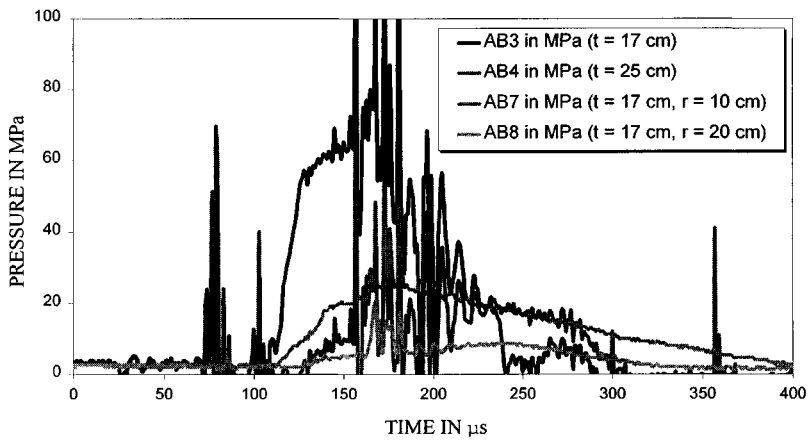

Figure 12 Pressure profiles in the lower region of slab III

The sensors AB7 and AB8 were positioned in the same horizontal plane as sensor AB3 but with the radius r = 10 cm resp. r = 20 cm apart from the vertical middle axis of the slab, so that the decrease also in horizontal direction can be seen.

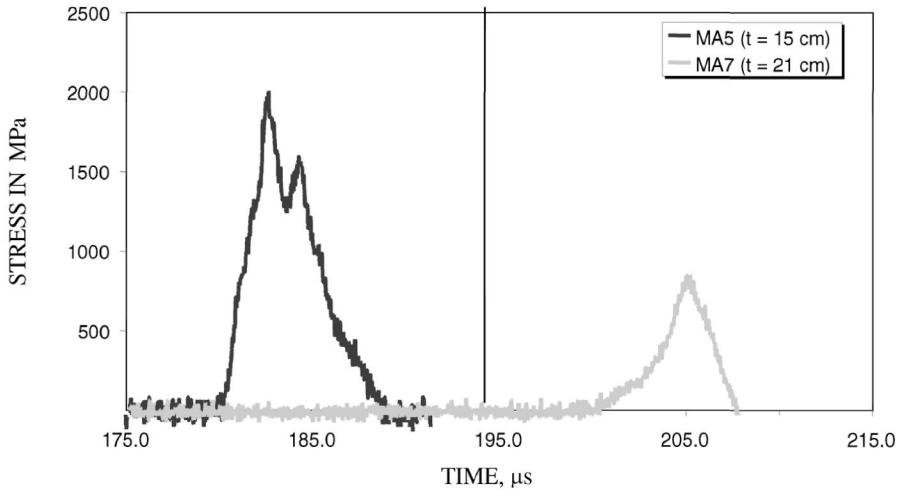

Figure 13 Stress measurement with manganin gauges in slab II

The stress measurement is rather difficult due to the higher sensitivity of the sensors. The sensors perpendicular to the load direction are very easily destroyed so that the best results can be gathered in the load direction. In Figure 13 two stress curves from slab II are shown. The rise time for the stress-signals is very short and the peaks are sharper than the pressure peaks. As the measured pressure is a result of the superpositioning of the stress parts, the pressure peaks are much more broadened.

The strain measurement leads to results as presented in Figure 14.

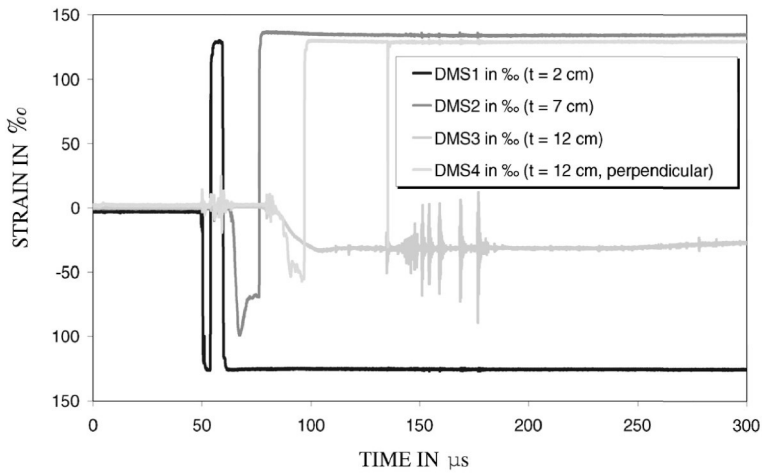

Figure 14 Strain measurement in slab III

The highest strain of 12% (DMS1) is measured in the upper part of the slab, which decreases to 3% in a depth of 12 cm (DMS3). In this level a gauge was also embedded perpendicular to the load direction (DMS4). This gauge also registered a negative strain of about 5% what leads to the assumption that in this region the incoming wave is more and more spreading in the horizontal direction and is no longer propagating as a plane wave in this part of the slab. In addition to the temperature curve the pressure registered in a position that lies symmetric to the position of the thermopile in slab III is also shown in Figure 15. The coincidence of the signals can be seen and a temperature rise of 17K for a pressure of 25 MPa has been measured. To extend the Hugoniot-Curve it is necessary to know the arrival times of the wave at the pressure sensors. This leads to a propagation-time-history for each slab (Figure 16)

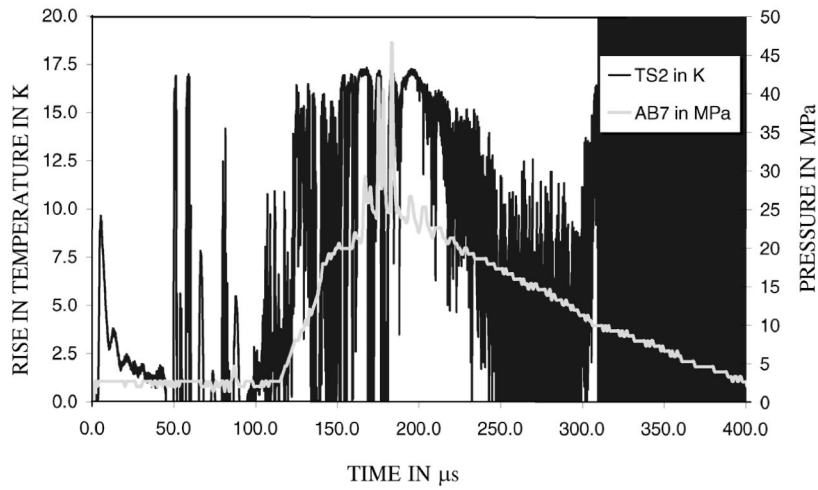

Figure 15 Temperature with pressure curve of a symmetric position in slab III

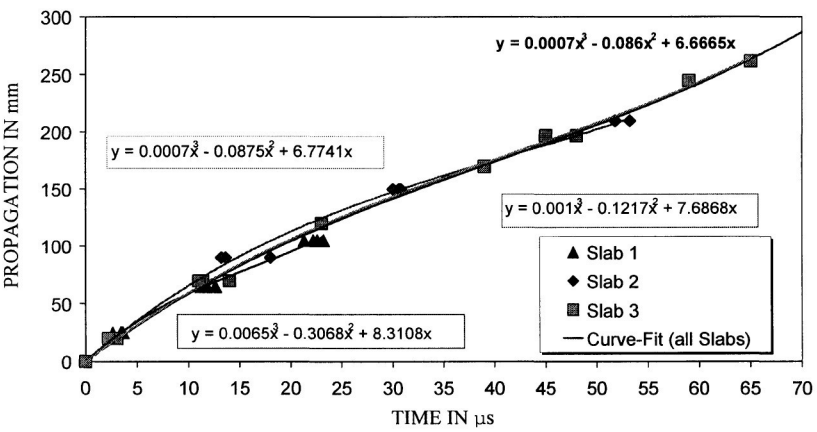

Figure 16 Propagation-Time-History for single slabs and for all slabs

For the same explosive used for the charge the wave-velocity can be determined by derivation of a polynomial-fit of third degree of the time-history for all the tests. The result is a function for the wave-velocity in dependence of the depth of wave-propagation. Using the resulting wave velocities points of the Hugoniot can be gained by calculating for each point with a known pressure the relation V/V_0 with the following equation [9]:

$$\frac{V}{V_0} = \frac{p}{\rho \cdot u_s^2}$$

The new Hugoniot points gained in this series are presented together with known points in Figure 17.

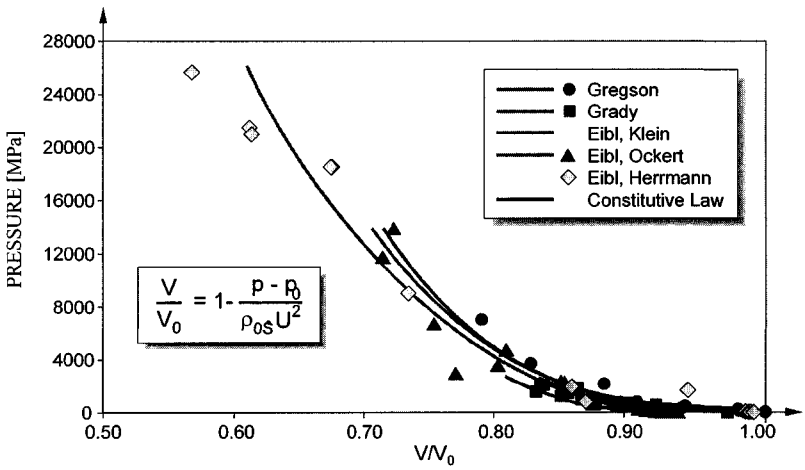

Figure 17 Hugoniot-Curve with new points from recent test series [4], [5], [9]

CONCLUSIONS

In order to get more material data for standard concrete of a compressive strength of 35 MPa new points of the Hugoniot-Curve were gained by the presented test series of concrete slabs under shock loading caused by contact charges.

The technique using carbon-resistors has been improved. Successful stress and strain measurement in the load direction has been performed and shown. For these measurements special encapsulations have been developed.

A new attempt for measuring the rise in temperature during an adiabatic compression was made and a first curve was presented. This technique seems to be worth to be developed further in order to get a fast temperature sensor for the application of temperature measurement in opaque materials where optical methods cannot be used.

REFERENCES

1. ASAY, J. R.; SHAHINPOOR, M., editors; High-Pressure Shock Compression of Solids; Springer-Verlag, 1993.

2. CHARTAGNAC, P. F., Determination of Mean and Deviatoric Stresses in Shock Loaded Solids; J. Appl. Phys. 53(2), February 1982, pp 948-953.

3. CHEN, W.; SALEEB, A. F.; Constitutive Equations for Engineering Materials, Volume 1: Elasticity and Modeling; John Wiley & Sons; 1982.

4. GRADY, E. D.; Impact Compression of Concrete; Sixth International Symposium on Interaction of Nonnuclear Munitions with Structures; Panama City Beach; Florida;1993.

5. GREGSON, V. R.: A Shock Wave Study of Fondu-Fyre WA-1 and Concrete; General Motors Materials and Structures Laboratory; Report MSL-70-30;1971.

6. IBACH, H.; LÜTH, H.; Festkörperphysik, Springer-Verlag, 1990.

7. KAUF, M. et. al.; Atomlagen-Thermosäule; Laser Magazin, 5/1994, pp 12-16.

8. LENGFELLNER, H., et. al.; Thermoelectric Effect in Normal State $YBa_2Cu_3O_{7-\square}$ Films; Europhys. Lett. 25 (5), 1994, pp. 375-378.

9. OCKERT, J.; Ein Stoffgesetz für die Schockwellenausbreitung in Beton; Schriftenreihe des Instituts für Massivbau und Baustofftechnolologie; Dissertation; Universität Karlsruhe; 1997.

STRESS CONCENTRATIONS AND CRACKED MODE OF CONCRETE

F Belhamel
CNERIB
Algeria

ABSTRACT. The knowledge of failure parameters of ordinary concretes such as failure energy and equivalent length of cracked zone is very important to be inquired about the evolution state of the damaged zone. For this purpose , and considering the complexity of the local phenomenon of cracking related to the non-linearity in the tip of the cracking , we must have recourse to bending tests "three points on notched specimens" in order to determine these parameters.

These tests are unstable when carried out with a controlled force. Their stability is assured by very rigid presses (5000 to 9000 N/m) working in a displacement mode controlled at speeds of 0.05 mm/mn at least. Badly equipped laboratories are hence not able to carry out these tests.

That is why empirical formula of estimations are very useful to calculate these parameters in order to know previously their magnitude order.

Keywords: Non-linearity, Instability, Imposed displacement, Brittle, Quasi-brittle, Fracture mode.

M F Belhamel is a researcher in the Department of Structure and Building Technologies at the CNERIB, Algeria.

INTRODUCTION

The study and the characterization of ordinary concretes in their cracked state requires the knowledge of the fracture parameters as fracture energy G_F and the equivalent length a_{eq} of the damaged zone. These parameters are generally used to develop the propagation criteria of the crack. They depend on the intrinsic properties of the material and must be the subject matter of tests on notched specimens. Among these tests, the one concerning the three points test bending will be presented. It gives rise to the fracture mode I of the crack opening.

THREE POINTS BENDING TESTS

The three points bending test [1,2,3] is easy to carry out with regard to the direct tensile test which could give rise to accidental eccentricities that could largely affect the results. The test must be stable [4,5,6] that means that the curve (σ-CMOD) must be completely followed until the end of the test. The obtained results depend on the specimens' dimensions because of the size effect [7,8,9].

Fracture Energy

The fracture energy G_F is defined on the basis of the curve (σ - w) according to the following formula:

$$G_F = \int_0^{w_c} \sigma(w)\, dw \qquad (1)$$

Where W_c = the maximal opening of the crack when $\sigma = 0$.

This integral simply represents the area delimited by the curve (σ - w) and the straight lines of the equations $w = 0$ and $w = w_c$ (Figure 1).

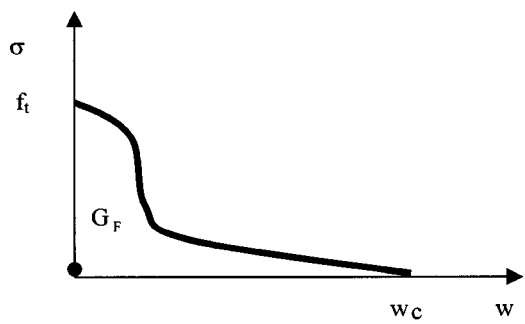

Figure 1 Experimental shape curve (σ - w) of a three points bending test.

For numerical calculus needs, some models, as Hillerborg mode, simplifies the curve (σ - w) representing it by a straight line providing the following basic condition G_F = Cste (Figure 2).

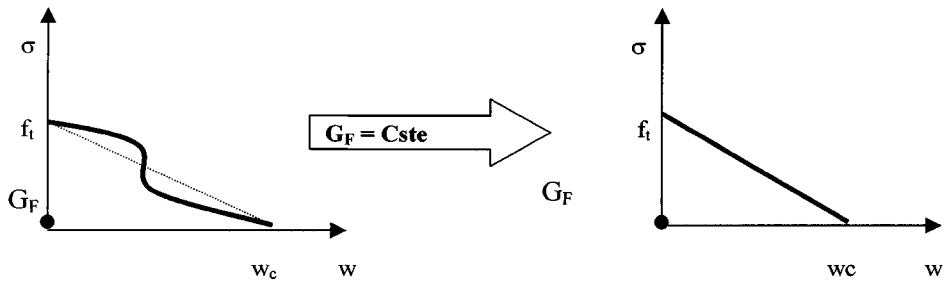

Figure 2 The curve approximation (σ - w) by a straight line

This fracture energy is obtained from the three points bending test according to the RILEM recommendations [10]. Knowing that this test, allows also, the obtaining of the curve (P - δ), the following formula of fracture energy is obtained:

$$G_F = \frac{\int_0^{\delta_0} P(\delta)d\delta + mg\delta_0}{B(H-a_0)} \quad (2)$$

Where δ_0 = the maximal deflection when P is cancelled.
m = the specimen mass.
g = the gravity acceleration.
B = the specimen width.
H = the specimen height.
a_0 = the initial length of the notch.

The weight of the specimen is in the order of 2 to 5% of bending moment due to loading.

Figure 3 illustrates this three points bending test on a notched specimen.

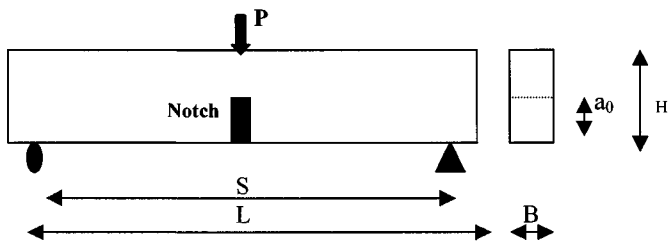

Figure 3 Static diagram of a three points bending test

For lack of appropriated tests equipments, we can avoid these tests by using the following empirical formula checked by acceptable results given as a first approximation [11].

$$G_F = \frac{58 \ .4 \ .f_t.d_{\max}}{E_C} \quad (3)$$

Where f_t = the tensile strength of the concrete (N/mm² or Mpa).
d_{max} = the maximal diameter of aggregates (mm).
E_C = the elastic modulus of the concrete (N/mm²or Mpa).
G_F in N/mm.

If the experimental value of E_c is once more not obtained, we can use the following empirical formula:

$$E_c = 4733. \sqrt{f_c} \quad (4)$$

Where f_e is the compressive strength of the concrete (N/mm² or Mpa).

Example:

Given an ordinary concrete having the following properties:

F_c = 25 Mpa f_t = 2 Mpa
$E_c = 4733 \sqrt{25} = 23665$ Mpa
d_{max} = 15 mm

$G_F \approx 74$ N/m

The Equivalent Length of the Crack

It is very difficult to estimate exactly the propagation of a crack and its length because the zone in proximity of the crack tip is singular and disrupted by the developing of micro cracks. This propagation depends on the concrete matrix, the notch, specimens' dimensions and loading mode. The destructive and non-destructive results present, sometimes, significant gaps. Figure 4 shows the definition of this equivalent crack length.

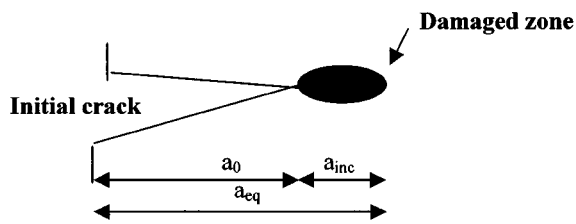

Figure 4 Definition of equivalent crack length in mode I

In this case, we can also obtain an approximate prediction of this parameter. The following empirical formula gives acceptable results

$$a_{inc}=[0.8+0.258(H-a_0)]d_{max}^{0.5} \quad (5)$$

Where H, a_0 and d_{max}, previously defined, having as a unity the centimeter (cm).

Example:

Given dimensions of a notched specimen according to RILEM recommendations:

$H = 100\ mm = 10\ cm$
$a_0 = 50\ mm = 5\ cm$
$d_{max} = 15\ mm = 1.5\ cm$
$a_{inc} = [0.8+0.258(10-5)].\sqrt{1.5} \approx 2.5cm$
$a_{eq} = a_0 + q_{inc} = 5 + 2.5$

$$\mathbf{a_{eq} = 7.5\ cm}$$

CONCLUSIONS

For lack of tests, forecasting formulas given in this paper allow the obtaining of acceptable results. Among the most significant conclusions, we mention:

- The fracture energy is largely influenced by granular inclusion and the weak aggregate-mortar interface.
- The size effect has also an influence on the fracture parameters.
- The fracture energy of ordinary concretes is in the order of 80 N/m.

REFERENCES

1. GUINEA, G. V., PLANAS, J., ELICE, M., "Measurement of the fracture energy using three point bend tests: 1- influence of experimental procedures ". Ibid .25 (148) (1992) 212-218.
2. BROBERG, K. B., "On stable crack growth". Journal of the mechanics and physics of solids, vol.23, 1975 pp.215-237.
3. GUO, Z. H., ZHANG, X.Q., (1987) "investigation of complete stress – deformation curves for concrete in tension". ACI Mat., J ., 84 (4), 278 – 285.
4. JANSON, J., (1978) "damage model for crack growth and instability". Eng., Fracture mechanics, vol.10, pp. 795-806.

5. MARZOUK, H., Chen, Z. W., (1995) "fracture energy and tension properties of high-strength concrete". Journal of Mechanics in Civil Engineering N° 108.

6. HILLERBORG, A., PETERSSON, P. E., (1981) "Fracture mechanical calculations, test methods and results for concrete and similar materials" advances in fracture research. 5th international conference on fracture, Cannes 29 March – 2 April – 1981 pp. 1515-1522 Ed. D. Français, Pergamon Press.

7. BAZANT, Z. P., Kim, J. K., 1984, PLEIFFER, P. A., 1986 "determination of fracture properties from size effect tests". J. of Struct. Eng., ASCE, V. 112 N° 2 pp. 289 –307.

8. BAZANT, Z. P., 1989a "identification of strain softening constitutive equations from specimens of different sizes". Cem. And Concrete Res. V.19 pp. 937 – 979.

9. BAZANT, Z. P., Pleiffer, P. A., 1987 "determination of fracture energy proprieties from size effect and brittleness number". ACI Mater. J. V. 84 N° 6 pp . 463-480.

10. RILEM TC-50 FMC (Draft Recommandation), "determination of fracture energy of mortar and concrete by means of three point bend tests on notched beams". Mater. Struct. 18 (106) (1985) 285-290.

11. BYUNG HWAN, O.H., "fracture energy of concrete and equivalent crack length". Kwanak-ku-Seoul – Korea (1989).

DETERMINATION OF THE BOND CREEP COEFFICIENT FOR LIGHTWEIGHT AGGREGATE CONCRETE (LWAC) UNDER CYCLIC LOADING

G König

University of Leipzig

F Dehn

MFPA Leipzig GmbH

K Holschemacher **D Weiße**

Leipzig University of Applied Sciences

Germany

ABSRTACT. The bond behaviour between reinforcement and concrete influences considerably the structural behaviour of reinforced concrete members. Whereas the bond properties of Normal Weight Concrete (NWC) are mostly known even for non-static loading, for Structural Lightweight Aggregate Concrete (LWAC) only a few investigations for repeated loading are known. Due to an enormous increase of the attraction of this concrete in Germany and in other countries, a wider application of LWAC e.g. in bridge construction is expected. This paper outlines the experimental programme and its results on the bond behaviour of conventional rebars in Lightweight Aggregate Concrete under cyclic loading. The aim of the research work was to evaluate the long-term behaviour of LWAC under cyclic loading in order to determine the corresponding bond creep coefficient.

Keywords: Lightweight aggregate concrete, Bond behaviour, Monotonic loading, Cyclic loading, Bond creep coefficient.

Professor G König, is Partner in the design and construction office "König, Heunisch + Partner" and Professor of Civil Engineering at the Institute for Structural Concrete and Building Materials, University of Leipzig.

Professor K Holschemacher, is Professor of Civil Engineering at the Leipzig University of Applied Sciences (HTWK Leipzig).

Mr F Dehn, is Manager of the MFPA Leipzig GmbH and a former Research Engineer at the Institute for Structural Concrete and Building Materials, University of Leipzig.

Mr D Weiße, is currently undertaking research into the bond behaviour of SCC and LWAC in the Unit of Reinforced and Prestressed Concrete at the Leipzig University of Applied Sciences (HTWK Leipzig).

INTRODUCTION

Nowadays, Structural Lightweight Aggregate Concrete (LWAC) plays more and more a significant role in the design and construction of innovative and economic concrete structures in Germany after years of stagnation. In this context the Karl-Heine pedestrian bridge in Leipzig [1] and the facade structure of the Kai-Center in Düsseldorf [2] are mentionable. These and other structures all over the world [3] demonstrate the economic and technical advantages of LWAC and point the way to the future. Through the existing advantage of the lower self-weight in opposite to Normal Weight Concrete (NWC), the application of LWAC can increase the effective span, leads to slender structures and can lower the amount of reinforcement in concrete members and therefore has economic advantages. The lower self-weight has also a positive effect on the formwork and falsework, the columns and the foundations. In precast members the advantage is a lower montage and transportation weight and therefore leads to lower montage costs. Possible reductions of costs extend not only to lower maintenance, improved durability and material savings, but also to the expenditure of columns, foundations and to the required reinforcing and prestressing steel.

Crucial to a wide spread application is besides the development of efficient mixtures mainly the provision of new design concepts, that considers the speciality of LWAC or High Strength LWAC. On one hand the new German standard DIN 1045-1 [4] and the Eurocode 2 [5] correspond to this new situation, Normal Weight Concrete and Lightweight Aggregate Concrete are included in the same standard and will be treated in the same manner. On the other hand it should be kept in mind that LWAC differs from NWC with respect to fresh and hardened concrete properties like strength and deformation values because of its contents. These differences have to be considered when designing with LWAC. One of these aspects is the bond behaviour between reinforcement and LWAC. The load bearing capacity of a reinforced concrete structure is considerably influenced by the bond behaviour between the rebars and the concrete. In this context, the anchorage of the reinforcing bars, crack width control, lapped reinforcing bars and the rotation capacity of the concrete structures are mentionable. Because of the lack of knowledge on bond tests with LWAC under cyclic loading a systematic research work on the bond behaviour was started within the scope of a common research project of the University of Leipzig, Institute for Structural Concrete and Building Materials, and the Leipzig University of Applied Sciences (HTWK Leipzig). This paper reports on first experimental tests on the bond behaviour of LWAC under cyclic loading.

BOND IN CONCRETE

The bond properties of rebars in concrete are normally described in bond stress-slip relationships, whereby a fictive bond stress is plotted against the measured displacement of the rebar. In the literature this relationship is called "bond law", but in reality it is not a material law, because the bond stress is not distributed continuously over the bond length, the force transfer is concentrated at the ribs of the rebars.

Whereas in the CEB-FIP Model Code 90 [6] a bond law is included, in other design codes like Eurocode 2 [5] the design rules based on the bond are hidden in design tables. So it is difficult to reproduce the design parameter. The following bond law for NWC is integrated in the CEB-FIP Model Code 90 [6] (Figure 1, Equation 1). The parameters depending on the bond conditions in this bond law are shown in Table 1.

$$\tau = \begin{cases} \tau_{max} \cdot (s/s_1)^{\alpha} & \text{for } 0 \le s \le s_1 \\ \tau_{max} & \text{for } s_1 \le s \le s_2 \\ \tau_{max} + \dfrac{\tau_f - \tau_{max}}{s_3 - s_2} \cdot (s - s_2) & \text{for } s_2 \le s \le s_3 \\ \tau_f & \text{for } s > s_3 \end{cases} \quad (1)$$

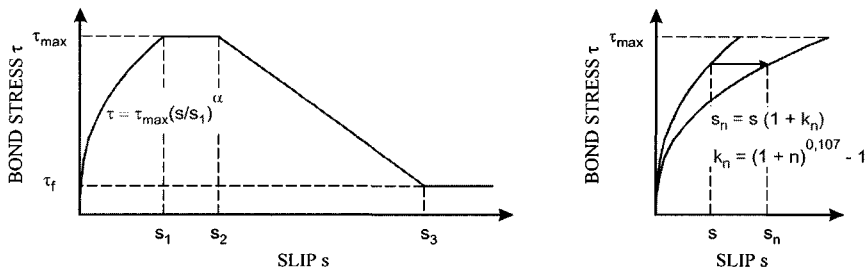

Figure 1 Bond law according to Model Code MC 90 [6]

Table 1 Bond model parameters for NWC according to Model Code MC 90 [6]

	s_1 [mm]	s_2 [mm]	s_3 [mm]	α	τ_{max} [N/mm²]	τ_f [N/mm²]
Good Bond	0.6	0.6	1.0	0.4	$2.0 \cdot \sqrt{f_{ck}}$	$0.30 \cdot \sqrt{f_{ck}}$
Other Bond	0.6	0.6	2.5	0.4	$1.0 \cdot \sqrt{f_{ck}}$	$0.15 \cdot \sqrt{f_{ck}}$

Out of numerous investigations on pull-out specimens made of NWC it is well known that cyclic loading with an increasing number of load cycles leads to a decrease in the bond strength accompanied with an increasing displacement ([7] to [12]). This influence can be recognised in the area of the increasing branch, while the displacement after first loading is multiplied by the bond creep coefficient. Therefore it is possible to generate a bond law affine to static loading for cyclic loading (Equation (2) and (3) according to Model Code MC 90 [6]):

$$s_n = s_0 \cdot (1 + k_n) \quad (2)$$

$$k_n = (1 + n)^{0.107} - 1 \quad (3)$$

n – number of load cycles
k_n – bond creep coefficient

A reduction of the bond strength depending on the number of load cycles is not included in the Model Code MC 90. It seems reasonable, because for design rules in the service limit states, like crack width control, the height of the loading action is relative low.

Whereas numerous researchers investigated the bond behaviour of reinforcement in NWC both under short-term and long-term, static and non-static loading, bond in LWAC and especially in High Strength LWAC was of less interest. A summary of the reached knowledge is among other in [13] enclosed. In [14] a recommendation of the extension to the bond law according to Model Code MC 90 is included, which suggests an adaptation of the bond parameters (Table 2).

Considerably not cleared is nowadays, whether this extension of the bond law is applicable also for LWAC. Because of an increase and a wider application of LWAC in e.g. bridge design, with the described test series concerning the bond behaviour under cyclic loading it will be possible to determine the bond creep of reinforcement.

Table 2 Bond model parameters for LWAC according to [14]

	s_1 [mm]	s_2 [mm]	s_3 [mm]	α	τ_{max} [N/mm^2]	τ_f [N/mm^2]
Good Bond	1.0	2.0	clear rib spacing	0.35	$0.6 \cdot f_{ck}^{0.82}$	$0.09 \cdot f_{ck}^{0.82}$
Other Bond	1.0	2.0	clear rib spacing	0.35	$0.3 \cdot f_{ck}^{0.82}$	$0.045 \cdot f_{ck}^{0.82}$

TEST PROGRAMME

Mix Design

For the test series two different aggregate types were used: Liapor (test series 1) and Ulopor (test series 2). Liapor is made of expanded clay and Ulopor is an expanded shale. The mix designs are summarised in Table 3.

Table 3 Mix design for test series 1 and 2

CONTENTS	TEST SERIES 1 [kg/m^3]		TEST SERIES 2 [kg/m^3]	
Cement	395.0	(42.5 R)	350.0	(52.5 R)
Water	160.0		122.0	
Superplasticizer	7.9	(2 m.-% of C.)	7.0	(2 m.-% of C.)
Retarder	1.6	(0.4 m.-% of C.)	-	
Microsilica	55.3	(14 m.-% of C.)	42.0	
Light-weight Sand 0/4	410.9		-	
Liapor 4/8	490.2		-	
Ulopor 0/2	-		400.1	
Ulopor 2/4	-		109.8	
Ulopor 4/8	-		346.7	
Ulopor 8/16	-		166.7	

Pull-out Specimens

All pull-out tests were performed on modified RILEM-specimens (Figure 2). Different from the conventional RILEM-specimen [15] a cylindrical geometry with a concentrically placed reinforcement bar was chosen, which has been used successfully in previous test series [16]. During the concreting, the rebars were placed vertically. The advantage of this modification is the constant concrete cover around the rebar. To avoid an unplanned force transfer between the reinforcement and the concrete in the unbonded length of 5 d_s, the rebars were encased with a plastic tube and sealed with a highly elastic silicone material. The bond length was also 5 d_s, whereby d_s is the diameter of the rebar.

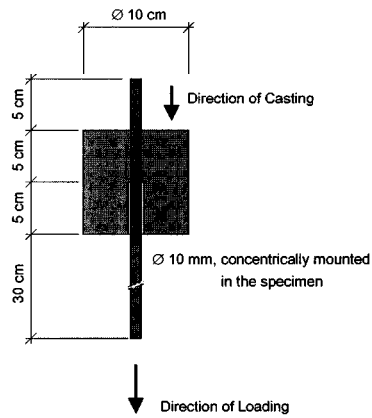

Figure 2 Pull-out specimen

As reinforcement it was used deformed reinforcing steel BSt 500 S according to the German Standard DIN 488 [17] measuring 10 mm in diameter. The application of other diameters was not necessary because from numerous publications it is known, that the influence of the different rebar diameters with constant relative rib area to the bond behaviour is of secondary importance. The relative rib area f_R of the used rebars was determined individually for each specimen and measured between 0.085 and 0.091. The relative rib area of the used rebars has to be at minimum 0.052 according to the standard DIN 488.

The slip between rebar and concrete was measured both at the loaded and unloaded rebar end of the specimen with three rotation symmetrically around the rebar fixed Linear Variable Differential Transformers (LVDT's) with a measuring accuracy of 1/1000 mm. The pull-out specimens were loaded in concrete placing direction (Figure 2).

Pull-out Tests

In preparation of a cyclic test, three pull-out tests under monotonic (static) were performed. These pull-out specimens were loaded path-controlled with a loading rate of 0.001 mm/s. Out of the measured bond stress-slip relationships the average of maximum bond stresses was determined to set the lower and upper level of the bond stress for the cyclic loading.

The amplitude $\Delta \tau_b$ was 25 % and the upper level τ_b^u was 50 % of the maximum bond stress τ_{bu} (Table 4).

Table 4 Summary of the test programme

TEST SERIES	LIGHTWEIGHT AGGREGATE	BOND LENGTH l_b	BAR DIAMETER d_s	RELATIVE AMPLITUDE $\Delta \tau_b / \tau_{bu}$	RELATIVE UPPER LEVEL τ_b^u / τ_{bu}
1	Liapor	$5 \cdot d_s$	10 mm	0.25	0.50
2	Ulopor	$5 \cdot d_s$	10 mm	0.25	0.50

The pull-out specimens were loaded with 10^6 load cycles at a frequency of 5 Hz. One pull-out test lasted therefore about 55 hours. By means of a servo-hydraulic testing machine a cyclic tension loading was applied. The first step of the cyclic tests was loading up to the upper level and measuring the initial displacement s_0. After the load was reduced to the mean, the force-controlled sinusoidal oscillation was started. The relevant data were measured at regular intervals of 3 to 15 minutes. After the cyclic loading the specimens were tested monotonic regarding there residual bond strength.

TEST RESULTS

Fresh and Hardened Concrete Properties

Tables 5 and 6 show the fresh and hardened concrete properties of the used LWAC-mixtures. Because of the spherical shape of Liapor, the flow of test series 1 was better and therefore the placing is more economic. All specimens were water cured until the test after 28 days. The cylinder compressive strength and the modulus of elasticity were tested on cylinders measuring Ø150/300 mm³, the cube compressive strength and splitting tensile strength on cubes 150x150x150 mm³. It was found out, that the compressive strength of LWAC is less related to the slenderness of the specimens. This means, that the typical difference between cylinder and cube compressive strength, known from normal weight concrete, is smeared (Table 6). The same effect was monitored on SCC [16].

Table 5 Properties of the fresh concrete (test series 1 and 2)

TEST SERIES	LIGHTWEIGHT AGGREGATE	FLOW [mm]	PLASTIC DENSITY [kg/dm³]
1	Liapor	510	1.55
2	Ulopor	440	1.74

Table 6 Properties of the hardened concrete (test series 1 and 2)

TEST SERIES	LIGHTWEIGHT AGGREGATE	COMPRESSIVE STRENGTH $f_{lc,\,cyl}$ [N/mm²]	COMPRESSIVE STRENGTH $f_{lc,\,cube}$ [N/mm²]	SPLITTING TENSILE STRENGTH $f_{lct,\,sp}$ [N/mm²]	MODULUS OF ELASTICITY E_{lc} [N/mm²]	MODULUS OF ELASTICITY [kg/dm³]
1	Liapor	48.0	44.1	2.9	14,600	1.35
2	Ulopor	51.6	54.8	3.8	19,300	1.65

Pull-out Tests – Monotonic Short-term Loading

All of the specimens failed by splitting of the concrete cover. Therefore it was only partly possible to determine the bond behaviour after reaching the maximum bond stress τ_{bu}, namely the descending branch of the bond stress-slip relationship. The basis for the evaluation and presentation are the test results of the unloaded rebar end. In Figure 3 the bond stress relative to the concrete compressive strength is displayed, every curve is an average of 3 measurements. Out of Figure 3 it is evident that LWAC under utilisation of Ulopor reaches higher bond stresses at lower displacements at the same time (see also in Table 7). The main reason could be the higher strength and density of the Lightweight Aggregate Ulopor and referring to this the higher compressive and splitting tensile strength.

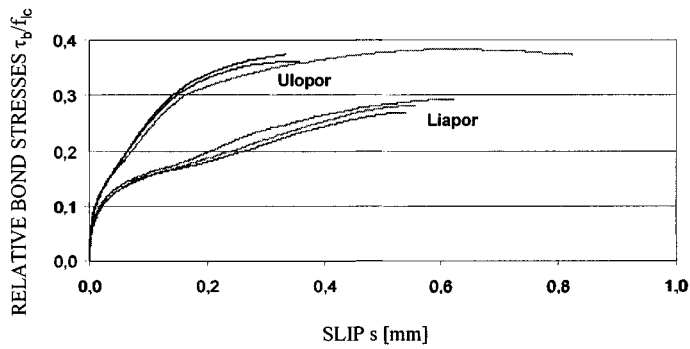

Figure 3 Relative bond stress of monotonic short-term loading

Table 7 Relative bond stress at 28 days

LIGHTWEIGHT AGGREGATE	LIAPOR	ULOPOR
Relative Bond Stress $\tau_{b;0.1}$ [1] / f_{lc}	0.16	0.25
Relative Bond Stress τ_{bu} / f_{lc}	0.28	0.36
Relative Slip s_u at τ_{bu}	0.51mm	0.34mm

[1] Bond Stress at 0.1 mm Slip

Pull-out Tests – Cyclic Long-term Loading

These tests can be presented in so called Wöhler-diagrams indicating the relationship between the slip s versus the number of load cycles n. Figure 4 shows this relationship for the performed tests (Indication: used Lightweight Aggregate and Specimen No.). The results confirm the observation from the monotonic short-term loading that LWAC with Liapor has a greater initial slip. Nevertheless the type of aggregate has no influence on the slip increase during the cyclic loading.

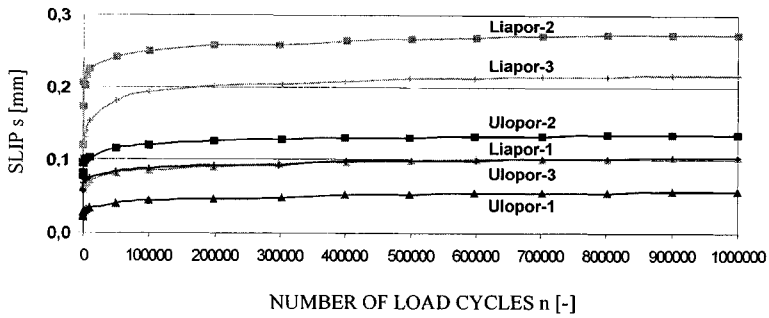

Figure 4 Increase of slip during cyclic loading as a function of load reversals

Residual Bond Strength after 10^6 Load Cycles

The specimens, that did not fail during cyclic loading, were finally tested monotonic. Tests on NWC performed by Rehm / Eligehausen [8] could be verified for LWAC that previous cyclic loading does not negatively influence the bond stress versus slip behaviour near ultimate load compared with the monotonic loading behaviour. The maximum bond stress τ_{bu} was about 10 % higher than with specimens without cyclic loading. Furthermore a steeper increase of the bond stress was observed due to the anticipation of the initial slip.

BOND CREEP COEFFICIENT UNDER REPEATED LOADING

The measured relationships between the slip and the number of load cycles are shown in a double-logarithmic scale (Figure 5). It is evident from this image, that there is a nearly linear connection between lg s and lg n. Through the application of regression analysis the bond creep coefficient k_n could be determined. For a bond length of 5 d_s and loading below the fatigue strength of the bond, the bond creep coefficient is:

$$k_n = (1+n)^{0.063} - 1 \qquad (4)$$

In comparison to the bond creep coefficient in Model Code MC 90 for NWC based on the experimental programme of Rehm / Eligehausen [8] (Equation 3) leads the found bond creep coefficient (Equation 4) for the investigated LWAC to lower slip increase.

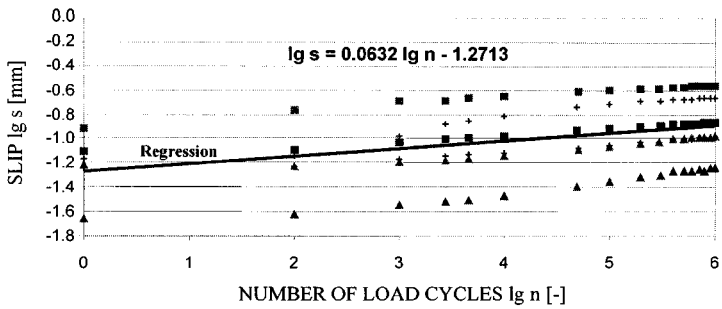

Figure 5 Slip-number of loading-relationship in a double-logarithmic scale

EFFECTS OF BOND CREEP

The most important results of the bond creep under repeated loading can qualitatively summarised as follows:

- Peak values of the bond stress will be relieved due the bond becomes softer, i.e. the distribution of the bond stress along the rebar becomes more fully;
- Transfer length and crack width will increase;
- Anchorage length of the reinforcement will be longer.

It is possible to calculate effects of the bond creep with bond orientated crack theories ([18] to [20]). When the in this test series investigated bond properties and the bond creep coefficient will be taken as a basis, then the transfer length and the initial crack width increase of about 25 to 30 % during $2 \cdot 10^6$ load cycles opposite to the values measured under monotonic short-term loading. About 40 - 50% of the slip increase will be reached only after about 10,000 load cycles.

CONCLUSIONS AND OUTLOOK

It could be shown with the performed test series, that the bond creep due to cyclic loading is less distinctive compared with results of NWC out of the literature [8]. Therefore, concrete structures made of LWAC show a better behaviour under cyclic loading in the ultimate limit states as well as in the serviceability limit states. From the bond properties point of view LWAC is suitable for concrete members and structures with repeated loading so that new applications for LWAC are possible, e.g. in bridge construction.

Nevertheless it has be taken account of the fact that the tested LWAC-mixes do not represent the whole spectrum of LWAC. Furthermore, the reached data are restricted to one specimen geometry and one loading level. On the other hand the complex investigation of the bond behaviour under repeated loading is very time and cost intensive, so it is not possible to expect short-dated results, whereby all possibilities of varying parameters concerning the concrete and bond aspects had been considered. At present it can be recommended both for NWC and for LWAC within the design to use the same bond creep coefficient (Equation 3) after Model Code MC 90 and so close the gap in the design rules.

REFERENCES

1. KÖNIG, G; NOVÁK, B, FISCHER, M; BARTHEL, K, Der Karl-Heine-Bogen in Leipzig. Bautechnik 77, No 8, 2000, pp 523-535.
2. HELD, M, Hochfester Konstruktions-Leichtbeton - Unkonventionelle Fassade für Bürogebäude in Düsseldorf. Beton 46, No 7, 1996, pp 411-415.
3. Lightweight Aggregate Concrete, Guidance Documents Structural, Part 3: Case studies, fib-Bulletin No 8, May 2000.
4. DIN 1045-1, Tragwerke aus Beton, Stahlbeton und Spannbeton. Teil 1: Bemessung und Konstruktion, (Concrete, reinforced and prestressed concrete structures-Part 1: Design), July 2001.
5. Eurocode 2, Design of concrete structures, 1992.
6. Structural Concrete. Textbook on Behaviour, Design and Performance, Vol 1, Introduction - Design process – Materials, fib-Bulletin No 1.
7. PERRY, E S, JUNDI, N, Pullout bond stress distribution under static and dynamic repeated loadings, ACI-Journal, May 1969.
8. REHM, G, ELIGEHAUSEN, R, Einfluß einer nicht ruhenden Belastung auf das Verbundverhalten von Rippenstählen, Betonwerk+Fertigteil-Technik 1977, H 6, pp 295-299.
9. GÜNTHER, G, MEHLHORN, G, Untersuchungen zur Mitwirkung des Betons zwischen den Rissen für monoton steigende und schwellende Belastungen, Universität Gesamthochschule Kassel, Forschungsbericht, 1987.
10. ROHLING, A, Zum Einfluß des Verbundkriechens auf die Rissbreitenentwicklung sowie die Mitwirkung des Betons auf Zug zwischen den Rissen. Dissertation, TU Braunschweig, 1987.
11. KOCH, R, BALÁZS, G, Verbund unter nicht ruhender Beanspruchung, Beton- und Stahlbetonbau 93, H 7, 1988, pp 220-223.
12. LUNDGREN, K, Pull-out tests of steel-encased specimens subjected to reversed cyclic loading, Materials and Structures 33, 2000, pp 450-456.
13. WALRAVEN, J; DEN UIJL, J, STROBAND, J, AL-ZUBI, N, GIJSBERS, J, NAAKTGEBOREN, M, Structural lightweight concrete: recent research, Heron 40, No 1, 1985, pp 5-30.
14. Lightweight Aggregate Concrete. Guidance Documents Structural, Part 1: Recommended extensions to Model Code 90, fib-Bulletin No 8, May 2000.
15. RILEM/CEB/FIP, Bond test for reinforcing steel. I. Beam-Test, II. Pull-Out Test. RILEM 3, No 15, 1970.
16. KÖNIG, G, HOLSCHEMACHER, K, DEHN, F, WEIßE, D, SCC - Time Development of Material Properties and Bond Behaviour. Second International Symposium on Self-Compacting Concrete in Tokyo/ Japan, October 2001.

17. DIN 488, Teil 2: Betonstahl; Betonstabstahl; Maße und Gewichte, (Reinforcing steel; reinforcing bars; dimensions and masses), 1984.

18. NOAKOWSKI, P, Nachweisverfahren für Verankerung, Verformung, Zwangbeanspruchung und Rissbreite. Deutscher Ausschuß für Stahlbeton, Heft 394, Berlin 1988.

19. KRIPS, M, Rissbreitenbeschränkung im Stahlbeton und Spannbeton. Dissertation, TH Darmstadt 1984.

20. HOLSCHEMACHER, K, Zur Berechnung von Rissbreiten und Zwangschnittgrößen in Stahlbeton und Spannbetonbauteilen. Dissertation, TH Leipzig 1992.

MODAL DAMPING ASSESSMENT IN CRACKED REINFORCED CONCRETE BEAMS

J-M Ndambi

J Vantomme

Royal Military Academy of Belgium

Belgium

ABSTRACT. In the present work a fundamental study of modal damping in cracked reinforced concrete beams based on finite element modelling is performed. The objective is to improve the understanding of the damping evolution in the case of a cracked reinforced concrete beam. The study is performed on a reinforced concrete beam and is based on the energy balance approach. In the model, two degradation processes in the concrete matrix are considered: the decrease of rigidity in the cracked section and the friction effects due to relative motion of the crack edges. The total damping of the beam is evaluated using the two-phase model which is already used for polymeric composite materials and is derived on the one hand from the damping coefficients of the steel reinforcement and of the concrete matrix and on the other hand from the strain energy distribution between the two components of the reinforced concrete beam. The model shows that the decrease of rigidity in the concrete matrix apparently leads to a decrease of the total damping of the reinforced concrete beam while the later is apparently increased by the friction effect. This study shows that damping in reinforced concrete structures is a complex phenomenon, depending on the actual status of the structure, and it is affected by two mechanisms that lead to opposite damping evolutions.

Keywords: Damping, Reinforced concrete beam, Energy balance approach, Non-destructive dynamic testing, Finite element modelling.

J-M Ndambi, is a Doctoral Researcher at the Royal Military Academy of Belgium. He specialises in the use of the dynamic system identification for the characterisation of reinforced concrete structures and the influence of damage on the dynamic properties.

Dr J Vantomme, is a Professor at the Civil Engineering department of the Royal Military Academy of Belgium. His main research interests include the parametric study of damping in composite and concrete materials, the influence of damage on the dynamic properties and the effects of explosions on structures.

INTRODUCTION

The monitoring of changes of dynamic system characteristics in the evaluation of the damage in structures is a method that has been widely used in the last years. Modal testing methods are frequently used as non-destructive tools in many engineering applications to detect and evaluate damage, including civil engineering applications. The basic idea of damage evaluation techniques based on vibration is that the dynamic system characteristics (DSC's) are function of the physical properties of the structure and therefore, any change in these properties caused by damage result in the change of DSC's [1]. In concrete structures, it is already proven that damage either local or global is associated with structural modifications, which can be observed through changes in modal parameters: eigenfrequencies, modal damping ratios, modes shapes and derivatives [2, 3].

In general, crack damage in reinforced concrete (RC) structures leads to an overall decrease of resonant frequencies and to an increase of modal displacements in the damaged sections. These observations are the consequence of a decrease of the bending stiffness in the structure due to crack damage and allows to have a global idea on the state of health of the RC structure. Although, the evolution of resonant frequencies and mode shapes can be easily explained, the case of damping remains quite different, it either increases or decreases during the progressive cracking process in RC beams [4, 5]

The present work focuses on damping study and is based on the idea of expressing the damping of RC elements in function of stored strain energies in RC components (steel reinforcement and concrete matrix) and basic damping factors of each RC component. This idea has been exploited in [6] for the case of composite materials. The goal is to understand in a better way the energy transfer mechanism occurring in RC beams during the cracking process and to determine the dissipated energy by friction in crack edges during vibrating motions. A finite element model (FE) model of a RC beam is considered, where one cylindrical steel bar is embedded in the concrete matrix. The adherence condition between steel and concrete matrix is considered to be perfect. Interface elements are inserted in the cracked model to reproduce the decrease of rigidity in cracked sections and to maintain the stress transfer mechanism between the crack edges. The strain and dissipated energies allow to calculate the damping of the RC beam.

DAMPING IN RC ELEMENTS: THEORETICAL ASPECTS

All engineering materials show deviations from ideal elastic behaviour, even at very small strain values. Under cyclic deformation, these deviations result in irreversible energy losses in the material, and the causes of such losses are many, include damping. The damping mechanisms occurring in structures depend on material properties, composition and on the way the structure is loaded. Materials or elements with internal interfaces can also dissipate mechanical energy through the relative motions of the interface by mechanisms such as friction [7]. The damping measured on such materials corresponds thus to a combination of different types of damping (material and structural). Although it is difficult to analyse all individual damping mechanisms for a material or a structure, some mechanical considerations may allow to predict the damping of RC elements.

The damping of an element or a structure is often expressed as the loss factor η. Knowing the relation between the loss factor and the damping ratio ξ, the calculated and measured damping factors may be easily compared [6, 8], The loss factor η is defined as:

$$\eta = \frac{1}{2\pi}\frac{\Delta W}{W} = 2\xi \tag{1}$$

where, ΔW and W are the dissipated and the stored energies during a loading cycle, respectively.

In the case of a RC element, two materials with different mechanical and vibration characteristics work together (steel and concrete). To take into account the contribution of each material in the global loss factor, it appears to be necessary to divide the expression written for a homogeneous and continuous elements (equation 1) in different terms which correspond to each type of material. In addition to this, the energy dissipated at interfaces can also be considered, the complete expression of the loss factor for RC elements can then be written as follows:

$$\eta = \frac{1}{2\pi}\frac{\Delta W_c + \Delta W_s + \Delta W_i}{W} \tag{2}$$

where *c* refers to the concrete matrix, *s* to the steel reinforcement and *i* to the interface.

Yet, according to the theory established for composite material, the dissipated strain energy due to bending loading in a beam can be divided into different terms corresponding to each stress type [9, 10]. Working in two-dimensional configuration (plane x, y), the stress types σ_x, σ_y and τ_{xy} can be considered and result in equation (3) for the dissipated energy:

$$(\Delta W)_j=(\Delta W_x+\Delta W_y+\Delta W_{xy})_j \tag{3}$$

where j=c, s, i, and ΔW_x, ΔW_y, ΔW_{xy} are the dissipated strain energies related to σ_x, σ_y and τ_{xy}.

It should be noted that the dissipated energy ΔW is not only due to material behaviour, related to stress content, but also due to structural phenomena; this leads to the additional interface term in (4):

$$\eta = \left|\frac{\Delta W_x}{2\pi W_x}\frac{W_x}{W} + \frac{\Delta W_y}{2\pi W_y}\frac{W_y}{W} + \frac{\Delta W_{xy}}{2\pi W_{xy}}\frac{W_{xy}}{W}\right|_j + \frac{\Delta W_i}{2\pi W} = \left|\eta_{\sigma_x}\frac{W_x}{W} + \eta_{\sigma_y}\frac{W_y}{W} + \eta_{\tau_{xy}}\frac{W_{xy}}{W}\right|_j + \frac{\Delta W_i}{2\pi W} \tag{4}$$

where W_x, W_y, W_{xy} are the stored strain energies related to σ_x, σ_y and τ_{xy}; $\eta_{\sigma x}$, $\eta_{\sigma y}$ and $\eta_{\tau xy}$ are the basic loss factors corresponding to the axial, transverse and shear loading of the element.

Equation (4) allows to calculate the damping of a RC element from the basic loss factors of each material, the stored strain energy in each component and the dissipated energy at interfaces. In the case of a vibration solicitation, equation (4) can be written for each vibration mode. Due the small value of the loss factor for steel (η_s), η_s is often considered to be independent of stress type, which highly simplifies equation (4). For the interfaces, due to the lack of data for friction loss factors, the related term in equation (4) is kept the same, which leads to equation (5).

$$\eta = \left|\eta_{\sigma_x}\frac{W_x}{W}\right|_c + \left|\eta_{\sigma_y}\frac{W_y}{W}\right|_c + \left|\eta_{\tau_{xy}}\frac{W_{xy}}{W}\right|_c + \eta_s\frac{W_s}{W} + \frac{\Delta W_i}{2\pi W} \tag{5}$$

Friction effect

The cracking process in the concrete matrix of a RC element leads not only to a strain energy redistribution, but also to friction in the crack edges. Indeed, the transfer of stresses over a crack in concrete is possible because of friction forces acting between the grains and matrix. If a cracked concrete element is subjected to cyclic loading, crack edges rub against each other and cause energy dissipation which may only be calculated if the stress-crack opening law is known. Some models are mentioned in [11] and include the *continuous function model*. The *continuous function model* consists basically of three continuous functions as shown in figure 1: envelope, unloading and loading curves.

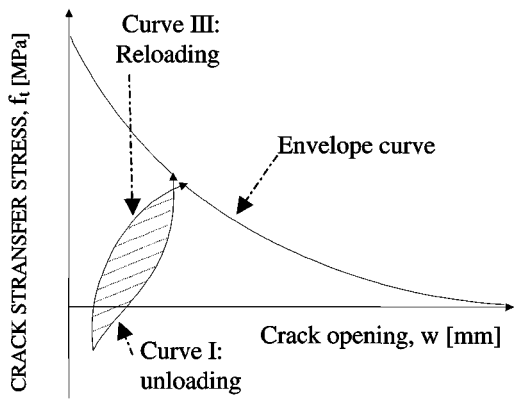

Figure 1 Continuous function model; (w_c : the ultimate crack opening; f_t: concrete ultimate tensile stress)

Details on the analytical expressions of envelope (softening), loading and unloading curves can be found in [12]. The energy dissipated by friction can be estimated by energy contained in the loading and unloading loop and corresponds to the shaded area in figure 1. The dissipated energy by friction is calculated using the following expression:

$$\Delta W_i = \int_s \left(\int_{reloading} \sigma dw \right) ds - \int_s \left(\int_{unloading} \sigma dw \right) ds \tag{7}$$

where, σ is the normal stress through the crack, w the crack opening and s the friction surface.

FINITE ELEMENT MODELLING

The idea to establish a correlation between crack damage and damping evolution in RC structures has been attracted some researchers. Experiments made on RC beams subjected to crack damage show that the relative changes in damping factors with damage are large (up to 100 %), while for the same damage level the change in eigenfrequencies reaches 20 % [4], [5]. Yet, the variation of eigenfrequencies is easy to explain, the damping evolution remains difficult to explain, it can either increase or decrease with damage and does not correspond with the increase which is generally reported in the literature [2, 3].

De Visscher et al. [5] emphasise in their research work the fact that the use of damping to evaluate structural damage depends on the understanding of all the damping mechanisms occurring in damaged structures. However, the damping mechanisms are strongly influenced by a number of non-controllable factors such as composition and material properties, state of stress, duration of load application and the degree of structural damage [13, 14].

In the present study, two processes of degradation in a RC beam are considered: the decrease of the rigidity in the section where the crack occurs which leads to redistribution of strain energies and the friction effect in the crack edges of the cracked concrete matrix. The model consists of a RC beam of 500 mm length with a rectangular cross section (40x60mm). The reinforcement is one cylindrical steel bar placed in the vertical symmetric plane of the cross section and at the mid-height of the beam.

FE models

For the numerical calculations and because of the vertical symmetry, the beam is reduced to a plane object assuming the concrete matrix and the steel reinforcement to be thin plates in two-dimensional configuration. The FE code ANSYS (INFINITE) is used for the numerical analysis. The mesh is made using linear rectangular elements with two degrees of freedom (DOF's) at each node, where the elements near the crack are arranged to be more closely spaced to improve the accuracy of the model. In the damaged state, cracks are simulated in the concrete matrix, perpendicularly to the reinforcement direction, as geometrical discontinuities by means of separated finite elements. This way of modelling the damage only changes the geometry but does not introduce nonlinearities in the behaviour of the model [15]. The non-linear behaviour appears after introducing interface elements between the crack edges in the cracked section. The models are loaded by defining the DOF's arising from the numerically calculated mode shapes (see section Interface elements).

The physical properties used in the model are as follows: E_c= 30000 MPa; E_s= 21000 MPa; ν_c =0.2; ν_s=0.3; ρ_c=2500 kg/m³, ρ_s=7800 kg/m³, where E_c, E_s are the concrete and steel Young's modulus; ν_c, ν_s are the concrete and steel Poisson's ratios; ρ_c, ρ_s are the concrete and steel densities.

Interface elements

The strain energy redistribution plays an important role for the damping evolution in cracked RC element. In order to take into account the decrease of rigidity in the cracked section, separate finite elements are not sufficient, because of lack of interaction between the two crack edges; interface elements have thus to be introduced. Therefore, in the considered models, the *ANSYS* non-linear interface element *combin-39* is used. The element *combin-39* connects two nodes of the model and is characterised by only one parameter K, which expresses the rigidity. Figure 2 presents the FE model of the cracked RC beam and gives the description of the element *combin-39.*

When a cracked RC element is subjected to bending vibration, the cracks open and close periodically. The value of the parameter K should reproduce the real behaviour of a crack in a RC element, that means to reproduce the stiffness degradation and restoration due to the opening and closing of the crack. The value of K can be drawn from the secant interlock stiffness versus crack opening w as mentioned in [16] by the following relation:

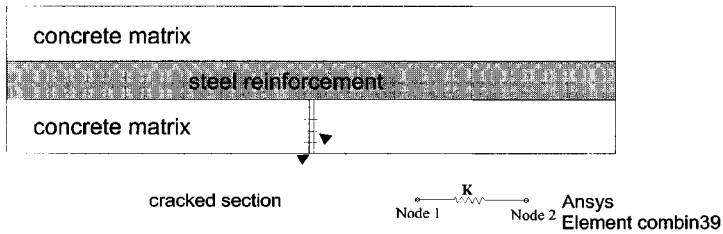

Figure 2 FE model of the cracked RC beam, description and location of the element *combin39*

$$K = \frac{k}{w} \tag{8}$$

Where k is a dimensional constant depending on the concrete type and equals to 1.2 N/mm² for normal gravel concrete. The left graph of figure 3 shows the evolution of the crack stiffness in function of the crack opening while the right graph shows the crack transfer force in the concrete cracked section.

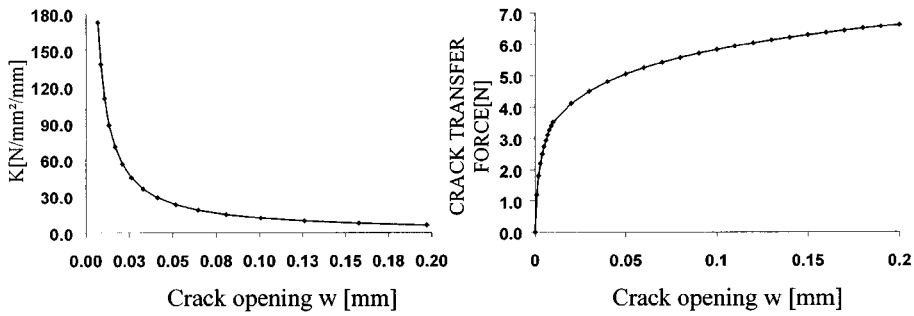

Figure 3 Crack parameters: left graph: interlock stiffness versus crack opening w; right graph: crack transfer force versus crack opening w

Static equivalent models

The strain energy distribution in the RC element is calculated for a well-defined loading configuration. Two loading cases are possible: the first using directly the mode shape displacements from numerical modal analysis and the second considers the static equivalent models (SEM's). The SEM's are the static reproductions of mode shapes. The second solution is preferred in FE modelling in order to take into account the nonlinearities arising from the interface elements, which are completely ignored in classical modal analysis. In this paper, the first three bending modes are investigated and the number of cracks considered is 1, 3, 5 or 7.

RESULTS AND DISCUSSION

Two cases are considered in the loss factor evaluation for the case of a cracked reinforced concrete beam: the first case where only the phenomenon of energy redistribution due to crack appearance is considered, and the second case where the two phenomena are combined: the friction effect in the crack edges and the energy redistribution due to crack damage.

Strain energy redistribution

The SEM's allow to calculate the stress redistribution in the RC models taking into account the nonlinearities introduced by interface elements. It is noted that the stress state changes with the accumulation of cracks, decreasing in the concrete matrix and increasing in the steel reinforcement. The stored strain energies in steel and concrete are calculated from the stress distributions, figure 4 shows the evolution of strain energies in function of the number of cracks for the three investigated bending modes.

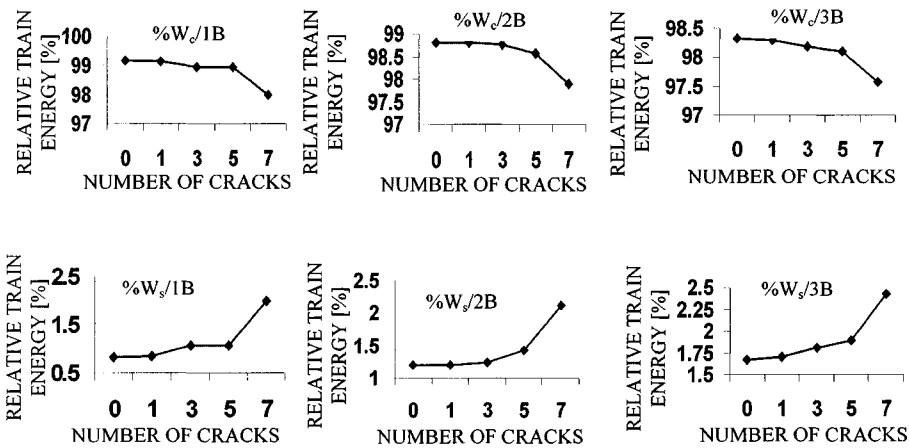

Figure 4 Strain energy distribution as function of the number of cracks; $\%W_c$, $\%W_s$ refer to the strain energy fraction in the steel and concrete matrix respectively in %; iB refers to the i^{th} bending mode

From figure 4, one can see that a redistribution of strain energy from cracked concrete matrix to the steel reinforcement is observed. Indeed, crack accumulation leads to an increase of stresses in steel reinforcement and a decrease of stresses in the concrete matrix, the strain energies being related to stress distribution should vary in the same way.

Loss factor (Damping)

Figure 8 shows the calculated loss factors as function of the number of cracks. The values of 1.18 % and 1.07 % are used for the basic loss factors of the concrete matrix for the normal and shear stresses respectively and the value of 0.1 % is used for the basic steel loss factors for all stress types. One can see that the damping decreases for the three bending modes investigated, because the new energy distribution increases the contribution of the steel

damping in the RC while on the same time, the contribution of the concrete matrix is reduced. Due to the small value of the steel damping, the total damping of the RC beam decreases as shown in figure 5.

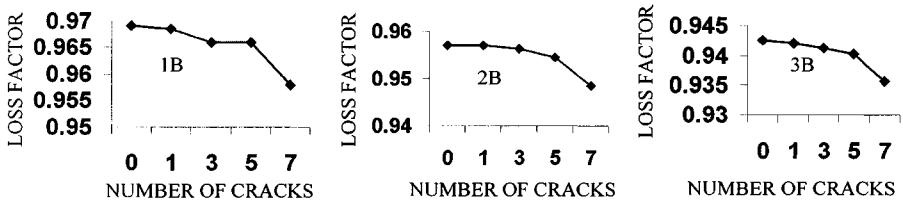

Figure 5 Loss factor as function of the number of cracks; iB refers to the i^{th} bending mode

Friction Effect

Using equation 7 (*continuous function model)*, the friction dissipated energy ΔW can be estimated for each mode shape. Tables 1, 2 and 3 present the stored and dissipated energies for the first three bending modes, where W_c and W_s are the stored energies; ΔW_i is the friction dissipated energy in the crack edges and %W is the energy fraction expressed in %.

Table 1 Fraction of stored and friction dissipated energies, mode 1B.

Number of cracks	0	1	3	5	7
$\%W_c$	99.18	97.67	92.04	82.85	80.72
$\%W_s$	0.82	0.84	0.99	0.89	1.65
$\%\Delta Wi$	0	1.49	6.97	16.25	17.63

Table 2 Fraction of stored and friction dissipated energies, mode 2B.

Number of cracks	0	1	3	5	7
$\%W_c$	99.81	98.81	97.37	89.16	81.01
$\%W_s$	1.19	1.19	1.22	1.29	1.74
$\%\Delta Wi$	0	0	1.40	9.54	17.24

Table 3 Fraction of stored and friction dissipated energies, mode 3B.

Number of cracks	0	1	3	5	7
$\%W_c$	98.33	97.53	94.75	93.04	85.57
$\%W_s$	1.67	1.69	1.75	1.79	2.12
$\%\Delta Wi$	0	0.771	3.50	5.17	12.30

Figure 6 presents the global loss factors as function of the number of cracks when taking into account the energy dissipated by friction for the first three bending modes. In contrast to figure 5, the loss factors increase with the increasing number of cracks. This is due the extra energy dissipated by friction in the crack edges.

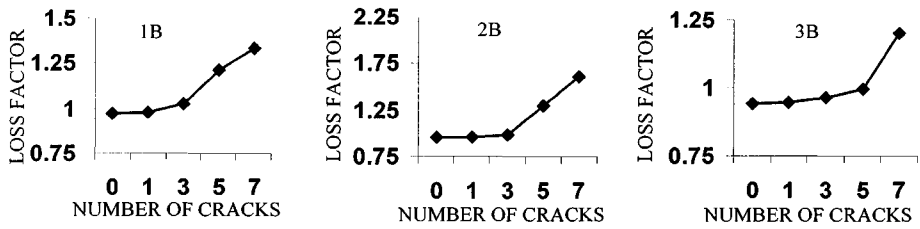

Figure 6 RC loss factor as function of the number of cracks for the first three bending modes

CONCLUSIONS

In the present work, an approach of damping study based on FE modelling is proposed. FE models of a RC beam are implemented in order to understand the experimental damping evolution due to crack damage. In the FE models, the *Ansys* interface elements *combin39* are introduced to simulate the real crack behaviour in RC elements. The SEM's are derived from the mode shape displacement fields and allow to calculate the fractions of stored strain energy taking into account the nonlinearities due to interface elements. The friction dissipated energy is calculated using the continuous function model. The total damping loss factors of the RC beam are calculated from the energy fractions and the friction dissipated energy.

It appears that the crack damage accumulation in RC beams leads to a new strain energy redistribution from concrete to steel, which results in a decrease of the damping factor. Indeed, the crack damage increases the contribution of steel damping while on the same time it decreases those of the concrete matrix and results in the monotonical decrease of the global damping factor. Taking into account the friction dissipated energy, the damping factor has as tendency to increase, and this observation may thus explain the experimental non-monotonical evolution in the global loss factor of RC beams subjected to crack damage, that increases at lower levels of crack damage and decrease at higher levels.

ACKNOWLEDGEMENTS

This work is a part of a research project G-0243.96 sponsored by the Flanders Fund for Scientific Research of Belgium. Its financial support is gratefully acknowledged.

REFERENCES

1. DOEBLING, S.W., FARRAR, C.R., PRIME, M.B., SHEVITZ D.W. "Damage Identification and Health Monitoring of Structural and Mechanical Systems from changes in their Vibration Characteristics". 'A literature Review', Los Alamos National Laboratory; New Mexico,1996.

2. PANDEY, A.K., BISWAS, M., SAMMAN, M.M., "Damage Detection from Changes in Curvature Mode Shapes", in 'Journal of Sound and Vibration', 145(2), pages 321-332, 1991.

3. ZAKIC, B.D., "Vibrations in Diagnosis of Damages in Concrete Bridges", in 'Proc. of the 2nd RILEM Int. Conf. on Diagnosis of Concrete Structures'; Strbské pleso, Slovakia, pages 320-323, 1996.

4. NDAMBI, J.M., PEETERS, B., MAECK, J., De VISSCHER, J., WAHAB, M.A., De ROECK, G., De WILDE, W.P., 'Material Property Assessment in Cracked Reinforced Concrete by Dynamic System Identification ', in ' Proc. of the Euromech Colloquium'; Kerkrade, The Netherlands, pages 223-232, 1997.

5. De VISSCHER, J., NDAMBI, J.M., PEETERS, B., 'An Experimental Study of Damping in Reinforced Concrete', in 'Proc of the Int Conf on Concrete Durability and repair technology'; Dundee, Scotland, UK, pages 629-636, 1999.

6. VANTOMME, J., 'A Parametric Study of Material Damping in Glass Fibre Reinforced Thermosetting plastics', Doctoral Thesis, VUB, Department of Mechanics of Material and Constructions, 1992.

7. JONG H, Y., GILLESPIE, J.W., Jr, 'Damping Characterization of 0° and 90° AS4/3501-06 unidirectional laminates including the transverse shear effect', in Composite structures, 50 (2000), pages 217-225, 2000.

8. De VISSCHER, J., BOSSELAERS, R., 'Experimentel Bepaling van de Demping van Compositematerialen', Afstudeerwerk van Bugerlijk Werktuigkundig-Electrotechnisch Ingenieur, VUB, 1988.

9. NI, R.G., ADAMS, R.D., 'The Damping and Dynamic Moduli of Symmetric Laminated Composite Beams-Theoretical and Experimental Results', in Journal of Composites Materials, Vol 8, 1984.

10. GOUMARIS, G.D., ANIFANTIS, N.K., 'Structural Damping Determination by finite element approach', in 'Computers & Structures', 73(1999) pages, 445-452, 1999.

11. TELFORD, T., 'RC Elements under Cyclic Loading: State of The art Report', 'Comité Euro International du béton', 1996.

12. HORDIJK, D.A., 'Local approach to fatigue of concrete', Ph.D. thesis, technisch Universiteit Delft,1991.

13. CIESIELSKI, R., KUZNIAR, K., MACIAG, E., TATARA, T., 'Damping of Vibration in Precast Buildings with bearing concrete walls', in 'Archives of civil engineering', XLI,3, 1995.

14. ELLIS, B.R., 'Damping and Non-Linear Behaviour in buildings', in 'Structural Engineering World Wide', Ed. Srivastava N.K., Paper T193-5,1998.

15. JAUREGUI, D.V., Farrar, C.R., 'Damage Identification Algorithms Applied to numerical Modal Data From Bridges', in 'Proc. of the IMAC XVII Int Conf'; Honolulu, Hawaii, 1994.

16. Magazine of concrete research: vol. 32, N°111: June 1980.

USING HIGH PERFORMANCE CONCRETE TO BUILD THE 100 YEAR HIGHWAY

P J Tikalsky

S Goel

S Camisa

Pennsylvania State University

United States of America

ABSTRACT. The wide ranging environmental conditions and raw materials of the northeastern United States have created conditions that accelerate the deterioration of highway bridges and structures. The saturated freeze-thaw cycling, alkali-silica reaction susceptible aggregates, annual thermal cycles, and heavy use of deicing salts have reduced the life of the average bridge superstructure to 28 years. The use of high performance concrete specifications is being used to increase the life of new bridges and highway structures and decrease the life-cycle costs of the bridge inventory in the northeastern United States. The specifications require an evaluation of the structures loadings and environments, classification of the exposure and risk level, performance based concrete mixtures and new quality control measures to place and cure long-life structural elements.

Keywords: High performance concrete, Durability, Environmental loadings, Specifications, Concrete, Life-cycle

Dr P J Tikalsky, is a registered professional Engineer, Fellow of the American Concrete Institute and Associate Professor of Civil Engineering at The Pennsylvania State University. His research is focused on the durability of cementitious systems and the infrastructure.

Drs S Goel and S J Camisa, are graduate Research Assistants at the Pennsylvania Transportation Institute at The Pennsylvania State University. Their work is on performance based specifications for highway bridges.

INTRODUCTION

The bridges in the Northeastern United State undergo some of the most damaging loadings in the word. The combination of loadings is so severe that bridges rarely last more than 30 years. Statistics from the National Bridge Inventory show the traffic on the interstate highways in the region is nearly 65 percent trucks with single or double trailers weighing 36,000 kg and permit trucks weighing up to 180,000 kg. While the bridges can be designed to sustain these heavy cyclic loadings, the more damaging factors are environmental in nature. The Northeastern United States goes through up to 40 hard freeze-thaw cycles per winter, safety concerns require up to 6 tons of deicing salt per lane mile annually, annual temperatures cycle from –18°C in the winter to 35°C in the summer, and the region has alkali reactive aggregates throughout [1].

The combinations of physical and environmental loadings have created a situation where a typical northeastern state, such as Pennsylvania, has 24 percent of its bridges labeled structurally deficient and another 18 percent functionally obsolete. Substantial changes in these statistics have not occurred in the past decade, as shown in Table 1. The funding for infrastructure allows for the replacement or repair of between 1 and 1.5 percent of the bridges annually. With a current bridge performance life of 25-30 years, this leave about 2500 bridges in the region to be posted for reduced capacity or removed from service, annually. The solution to the bridge life problem is a longer lasting infrastructure. The boom in highway construction in the 1950s never envisioned the mass of deicing salt used on the roads, the volume of trucks or the size of permit vehicles driving the interstate highway system in the northeastern corridor. The new paradigm is a 100-year highway. This starts with bridges and extends to pavements, parapets and tunnels. To design and construct the 100-year highway, the highway agencies are turning to more durable materials, design methods that include durability requirements, performance based specifications and payment tied to performance. The initial change is often referred to as "high performance" concrete, where engineers and maintenance managers define the desired level of performance and the exposure of bridge components, and concrete materials engineers and contractors design concrete to meet the new performance standards [2].

Table 1 U.S. National Bridge Inventory data for Pennsylvania

PENNSYLVANIA HIGHWAY BRIDGES							
Year	Total # of Bridges	Structurally Deficient		Functionally Obsolete		Total of Both	
		#	%	#	%	#	%
1992	23,804	6,006	25.23	4,519	18.98	10,525	44.22
1994	23,535	5,907	25.10	4,411	18.74	10,318	43.84
1996	23,411	5,924	25.30	4,257	18.18	10,181	43.49
1998	22,742	5,745	25.26	3,842	16.89	9,587	42.16
2000	22,052	5,405	24.51	4,096	18.57	9,501	43.08

DEFINING HIGH PERFORMANCE

Defining high performance for most bridges is synonymous with defining high durability concrete. High durability is needed to increase the life and performance of concrete bridges, pavements and structures. Any concrete, which satisfies criteria to overcome the limitations of conventional concretes, may be referred to as high performance concrete (HPC). It may include concrete that benefits the construction process (e.g. reduces construction time to permit rapid opening of roads or bridges without compromising service life performance), provides substantially improved resistance to environmental influences (e.g. reduced permeability to resist the ingress of chemical species), or improved mechanical properties for structural applications (e.g. high strength to reduce section size or span length). Therefore, it is not possible to provide a unique definition of HPC without considering the performance requirements of the intended use of the concrete [3,4]. The definition of HPC is that which uniquely defines the structural elements intended use in construction and service, as well as, its resilience to deterioration and environmental extremes.

It is widely understood that species such as alkali, sulfate, and chloride have a detrimental effect on concrete service life of bridges. Until now, the engineer has not been able to translate this knowledge into specifications. This knowledge gap requires guidelines that define the required level of performance of the concrete mixture designs and hardened concrete for a known use or environment. By using information on structural loading, environmental conditions, aggregate sources, exposure to moisture or salts, lifetime expectancy, and soil conditions and composition, guidelines can assist engineers or highway agencies in optimizing the life and cost of their structures.

The increased durability of concrete impacts the life expectancy, life-cycle, capital cost and maintenance of the transportation infrastructure. For the purposes of the transportation infrastructure uses of concrete, high performance can be further defined into specific performance characteristics. Table 2 defines twelve specific characteristics and performance grades for concrete used in the transportation infrastructure [1]. Each characteristic has three grades of performance that can be specified, depending on the anticipated exposure and desired design life. The levels of performance were determined by experience and correlation with standards of other agencies [1,3]. Grade 1 represents good quality concrete for general transportation applications. The higher grades represent higher performance levels to increase the life of the highway infrastructure, reduce maintenance, improve constructability or optimize structural systems. The high performance concrete requires contractors and engineers to use advanced knowledge of concrete materials, proportioning technology and quality control. Each of these performance characteristics must consider the technical, economic and practical ability of a contractor to attain the desired hpc properties. because many characteristics of high performance concrete are interrelated, a change in one property usually results in changes in one or more of the other characteristics. Consequently, if several performance characteristics have to be taken into account in producing concrete for the intended application, each of these characteristics must be clearly specified in the contract documents and can not be contrary to the other properties, e.g. high strength and low modulus. Each of the characteristics in table 2 benefits certain components of the highway infrastructure. However, the specification of a performance grade requires that engineers and contractors understand the exposure conditions and the potential deleterious effects of the effects. It is not necessary to specify the performance grade of all characteristics of concrete or all types of potential deterioration.

Table 2 Grades of performance for high performance concrete

PERFORMANCE CHARACTERISTICS	STANDARD TEST METHOD	PROPOSED HPC PERFORMANCE GRADE		
		1	2	3
FT Freeze-Thaw durability (DF)	AASHTO T161-A	60%≤X≤80%	80%≤ X≤90%	90%≤ X
SR Scaling resistance (50 cycles)	ASTM C 672	X=2,3	X=1	X=0
AB Abrasion Resistance (wear depth, mm)	ASTM C994	2.0>X≥1.0	1.0>X≥0.5	0.5>X
AS Alkali Silica Reaction	ASTM C1293 C1290	X<0.10% At 14 Days C1290	X<0.04% At 1 Year C1293	X<0.04% At 2 Years C1293
	ASTM C441		X<0.10% At 56 Days	X<0.05% At 56 days
CP Chloride Permeability, Coulombs	AASHTO T 277	4000≥X>2500	2500≥X>1500	1500≥X
CS Compressive Strength, MPa	AASHTO T 22	24≤X<32	32≤X<55	55≤X<82
SD Strength Ratio (28day f_c)/(7day f_c)	AASHTO T 22	1.15	1.33	1.45
ME Elasticity, GPa	ASTM C 469	20≤X<30	30≤X<45	45≤X
SH Shrinkage, με	ASTM C 157	800>X≥500	500≥X200	200≥X
SU Sulfate resistance, % Expansion	ASTM C1012	X<0.10% At 6 months	X<0.10% At 12 months	X<0.10% At 18 months
TS Tensile Strength, MPa	ASTM C78	4 >X≥5	5 >X≥6	X > 6
WK Workability, mm	ASTM C143	50>X≥125	125>X≥200	200<X

100-YEAR HIGH PERFORMANCE FACTORS

Design Engineers must define the environment the bridge with service before completing a design. Both the structural design and the environmental exposure must be translated into specifications before the bridge can be bid and subsequently constructed. Using the defined environment factors, the engineer can select a grade of performance to optimize the life of the bridge structure. Table 3 is an environmental guideline that should be included in every design.

The design team should use this guide to define the exposure conditions and the subsequent performance grades needed to optimize the life of the structure. The designer must define the freeze-thaw conditions, average number of cycles per year, and the moisture condition of the structural element and whether it will be saturated during freezing. The exposure to deicing salts or seawater is needed, as well as, the nature of the exposure, i.e. direct or indirect, or wet dry of the tidal zone. The sulfate and chloride exposure should be determined, along with the concentrations. Elements that must be watertight or directly exposed to surface loadings should be defined, e.g. tire, rails, pipes. Finally, the necessity of early opening to construction or service loadings should be defined. Using the responses to these questions, the engineer should use the guidelines in Figure 1 to define the durability requirements for the performance specification in Table 2. The resulting performance specification is used in parallel with the structural design to design a long-life structural element. Used on all elements, the specification can be used to enhance the life of the system.

Table 3 Engineering guide for durability requirements

CONDITIONS			*IF CONDITION IS PRESENT,		
Freeze-Thaw Cycles	Yes*	No	Number of Cycles/year		
Periodically Saturated	Yes*	No	Saturated while freezing	Yes	No
Deicing Salts	Yes*	No	Application	Direct	Indirect
Reactive Aggregates	Yes*	No	Level of Reactivity	Moderate	Severe
Tire or surface wear	Yes*	No	Studs, Chains or Scour	Yes	No
Sulfate Exposure	Yes*	No	Concentration, % or ppm		
Seawater Exposure	Yes*	No	Wet-dry cycling	Yes	No
Watertight Design	Yes*	No	Lining	Yes	No
Early Age Use	Yes*	No	Service Loads in 7-days	Yes	No

FIELD IMPLEMENTATION

The Pennsylvania Department of Transportation is currently implementing many elements of the presented high performance concrete program. Two long span bridges were cast using the program in 2001, and six more will be cast in 2002. The monitoring of these bridges will continue throughout their life. In addition, fifteen interstate highway bridges will be fully instrumented in an ongoing implementation program. The in-situ performance will be monitored and compared to the lab performance test and standards. The program is expected to evolve into improved specifications for the entire United States.

SUMMARY

The performance guide in Table 2 is based on 75-100 year service life, if the desired service life is considerably less, the grade of performance can be reduced by one or more grades. While it is difficult to correlate the guide and specifications to 75-100 years field data, the concept is developed to mitigate or prevent known distress mechanisms. Many of these distress mechanisms are interrelated; therefore, the design must mitigate all the contributing factors to be effective. The basis for the durability requirements is to prevent freeze-thaw related distress, mitigate alkali silica reaction and sulfate attack, and delay the onset of

scaling and corrosion by reducing the permeability and cracking of concrete. The state of practice in concrete technology and construction is such that all of the desired performance characteristics can be met simultaneously through the use of good quality control, the proper use of pozzolans and chemical admixtures and careful attention to curing practices.

Figure 1 Performance specifications for durability

FT Freeze Thaw Durability	Is the concrete exposed to freezing and thawing environments?	Yes	Is the member exposed to deicing salts?	Yes	Will the member be saturated during freezing?	Yes. Use FT-Grade 3
						No. Use FT-Grade 2
					No. Use FT- Grade 1	
		No. FT grade should not be specified.				
SR Scaling Durability	Is the concrete exposed to deicing salts?	Yes	Is the exposure a direct application of salt?	Yes	Will the member be subjected to surface loadings?	Yes. Use SR-Grade 3
						No. Use SR-Grade 2
					No. Use SR - Grade 1	
		No. SR grade should not be specified				
AB Abrasion Durability	Is the concrete exposed to surface abrasion?	Yes	Is the member subjected to other than tire wear?	Yes	Will the member be exposed to tire studs or chains?	Yes. Use AB-Grade 3
						No. Use AB-Grade 2
					No. Use AB- Grade 1	
		No. AB grade should not be specified.				
AS Alkali Silica Reaction Durability	Does the concrete contain reactive aggregates?	Yes	Is the concrete exposed to moisture?	Yes	Will the member be saturated during freezing?	Yes. Use AS - Grade 3
						No. Use AS - Grade 2
					No. Use AS - Grade 1	
		No. AS grade should not be specified.				
CP Chloride Permeabili ty Durability	Is the concrete exposed to chloride salts or soluble sulfates environments?	Yes	Is the membe exposed in a potentially moist environment?	Yes	Will the member be saturated during freezing?	Yes. Use CP-Grade 3
						No. Use CP-Grade 2
					No. Use CP- Grade 1	
		No. CP grade should not be specified.				
SD Strength Ratio	Will the concrete go into service after a minimum of 7 days after being cast?	Yes	Will the member benefit from long-term strength gain?	Yes	Is thermal cracking a potential in the member?	Yes. Use SD-Grade 3
						No. Use SD-Grade 2
					No. Use SD- Grade 1	
		No. SD grade should not be specified				

Figure 1 Performance Specifications for Durability (continued)

SH Shrinkage	Is the concrete exposed to moisture, chloride salts or soluble sulfates environments?	Yes	Is the member constructed without joints?	Yes	Is the member designed to be watertight or crack free?	Yes. Use SH-Grade 3
						No. Use SH-Grade 2
				No. Use SH- Grade 1		
		No. SH grade should not be specified.				
SU Sulfate Resistance	Is the concrete exposed to more than 0.10 percent soluble sulfates?	Yes	Is the member exposed to more than 0.20 percent soluble sulfates?	Yes	Is the member exposed to wet-dry cycles?	Yes. Specify a compressive strength within SU - Grade 3
						No. Specify a compressive strength within SU - Grade 2
				No. Use SU - Grade 1		
		No. SU grade should not be specified.				

ACKNOWLEDGMENTS

The authors would like to acknowledge the support provided for the project by the Pennsylvania Department of Transportation, as well as the cooperation of the Federal Highway Administration.

REFERENCES

1. TIKALSKY, P J, SCANLON, A, Defining the High Performance Concrete Requirements for Highway Structures, PCI/FHWA/FIB International Symposium on High Performance Concrete, September 25-27, 2000, pp 1-10.

2. ZIA, P, AHMAD, S, LEMING, M, High-Performance Concretes A State-of-Art Report (1989-1994), Federal Highway Administration, Report FHWA-RD-97-030, Washington, DC, 1997, www.tfhrc.gov/structur/hpc/hpc2/ack.htm.

3. GOODSPEED, C, VANIKAR, S, COOK, R, High-Performance Concrete (HPC) Defined for Highway Structures, Concrete International, American Concrete Institute, Vol 18, No 2, February 1996.

4. FORSTER, S W, High-Performance Concrete-Stretching the Paradigm, Concrete International, Vol 16, No 10, October 1994.

A CASE STUDY OF A CONCRETE DAMAGING OF WATER-COOLING TOWER IN ROMANIA

M Muntean
University Politehnica Bucharest
A Viorel C Virban
JT International Manufacturing
B Florin
Conel
Romania

ABSTRACT. This study is a working part of a national program for concrete structure diagnosis-investigation for water cooling towers, gas evacuating towers from thermoelectric plants, dams, channels lining and underground adduction galleries. The data from this paper represent the results assessed on the basis of the initial documentation, site evidences of the water characteristics, environmental measurements, non-destructive site examination, structural expertise and analyses realised by several laboratories. The initial expert supposition was that the structure is affected mainly by alkali-aggregate reaction, but based on team work, knowledge deployment inside the group, standardised analytical methodology and reporting, it was found that the concrete it is affected not only by AAR. The concrete is damaged by steel corrosion, sulphate attack, carbonation, and alkali-silica reaction, in correlation with a poor initial concrete quality. This paper relates only the AAR results assessments.

Keywords: Concrete structure diagnosis-investigation, Analytical algorithm, Carbonation, Alkali-silica reaction.

Professor M Muntean, is Professor at "Politehnica" University of Bucharest, Oxide Materials Science, with contributions in the field of cement, building materials, ceramics, mortars and concrete investigations, co-ordinating and participating in different European Research Programs.

Dr A Viorel, is an Engineer in physics and PhD in Alkali-Aggregate Reactions, with contributions in monuments and concretes laboratory diagnosis, and analytical developments for Cement Industry.

Mrs C Virban, is a Chemical Engineer and PhD student in the field of early age cement hardening by electrical conductivity, contributions in research and old monuments investigation.

Mr B Florin, is a Civil Engineer, National Company for Electricity, Concrete Laboratory, expert.

INTRODUCTION

The general stages of the concrete diagnosis are: site inspection and testing, sampling, laboratory investigations, assessment of site and laboratory findings, evaluation of the risk. The aspects detailed below are in respect only with the physico-chemical investigation of the concrete samples, as part of standard final report issue by laboratory.

History of the Structure

This step must consider whether conditions are such that internal and external chemical attack could occur: the source of the aggregate, the location of the structure, its use and exposure conditions, which part of the structure have suffered damage, preliminaries tests and reports.

Results of the Visual Examination-Inspection

Results of the visual examination-inspection of the concrete surface are necessary to describe the patterns of cracking, seepage, discoloration, staining, softening, erosion, or other damages as described by RILEM, 1994, "Draft Recommendation for Damage Classification of concrete structure" [1].

Actual Stage in the Damaging Factor Classification

The classification and definitions o the damaging factors must be clear despite controverts of the data from the literature. For the laboratory it is necessary to separate the chemical deterioration from the physical and mechanical factors. The synthesis of the actual stage in damaging factor classification was realised from related literature.

Actual Stage in the Analytical Field of Concrete Diagnosis

The diagnosis is mainly in respect with the quality of the hardened concrete, the question being raised to the composition, with primary interest for the cement content and water/cement ratio. Unfortunately there exist no direct method of determining the content of cement, even Portland cement alone, in a sample of concrete, ASTM 1084-92, BS 1881:part 124:1989, BS 1881:Part 124:1989, for chemical methods, ASTM 856-83, (1988), ASTM C 457-90, for microscopically methods. Other aspects are in correlation with the nature of the reaction products, which can be regarded as an investigation activity that need the use of non standardised analytical techniques, e.g. X-ray diffraction, differential analysis, infrared spectroscopy, scanning-transmission electron microscopy, electron microanalysis, etc. Generally it must be known that there are to kinds of investigation, e.g. so-called analytical and visual examination that must finally be assessed to have a good probability of the final result.

Sampling Information

Sample history from site to the laboratory, e.g. extracting mode, place into the structure, association with damaged areas, transportation, keeping, notices from site concerning there characteristics, etc., are the main information used by the laboratory in respect with samples that must be analysed.

The Minimal Analytical Procedure

For mortars and concrete diagnosis, it was developed a special analytical algorithm, as a compromise between expert requirements (number of samples, cost, time, precision) and laboratory interests (price, luck of information, assessment risk of the results, synthetically results).

The algorithm it is based on:

Analytical techniques:

- Chemical analysis, (mean sample, soluble fraction plus ignited fraction);
- X-ray diffraction (mean sample, enriched hardened cement paste samples);
- Optical microscopy by transmission.

Quantitative results assessment:

- Special software for correction and calculation;
- Standard final report.

DESCRIPTION OF THE TOWER

Execution:	1982-1984.
Location:	Giurgiu, south of Romania, near Danube.
Environmental conditions:	In the vicinity of the chemical plant "Verachim", situated at aprox.1000 m from his gas-evacuating tower.
External aspects:	Individual cracks, longitudinal and horizontal on the concrete surface; Map cracking in limited area of the concrete surface, near the superior collecting basin; Insufficient covering layer; Steel corrosion; Carbonation; Black colour of the map cracking.

The vertical and horizontal structural elements have fissures with white efflorescence belong the fissures, identified as calcite.

PRELIMINARY RESULTS

The concrete was investigated in several laboratories before to diagnose the nature of the chemical deterioration. In Table 1 it is indicated the synthesis of the results obtained by the expert in another laboratory, in respect with minimal requirements for a rapid diagnosis and archive documentation.

Table 1 Preliminaries results for the concrete investigations

COMPRESSIVE STRENGTH	334...554 daN/cm^2
Density	2.28...2.33 t/m^3
Porosity	9.7...11.5 %
PH	7.5...12
Soluble chloride	96...994 mg/Kg
Soluble sulphate	205...4049 mg/Kg
Total sulphate	6450...20140 mg/Kg
$Na_2O_{equivalent}$	1.22...1.72 %
Aggregate origin [1]	From Danube
Estimated cement type [2]	OPC

[1]In the absence of the original testing certificate, this supposion was made on he proximity carrier and colateral reports for other concrete structure from this zone.
[2]From the original testing certificate.

The cross-functional team collected all data analysed the water compositions by the chemical laboratory of the electrical plant, from the last 5 years. The results there were assessed as a graphs, analysed and introduced in the final report, as shown for example in Figure 1 for SO_4^{2-} and Cl^-. In the vicinity of the electrical plant there is a chemical plant. Based on archive investigation and on site discussions it was found that before 1989 the chemical plant has a contribution of air and water pollution in that region. Two assumptions had to be checked during on site inspection of the cross-functional team:

- ✓ Air pollution, due to uncontrolled emissions of chloride and sulphate gases.
- ✓ Water pollution with chemical residues, mainly as sulphate type, of the feeding channel, down to the electrical plant.

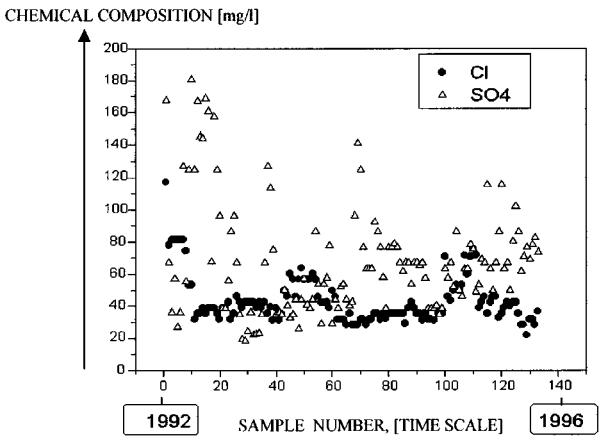

Figure 1 SO_4^{2-} and Cl^- content in the water used for the condenser cooling (Note: this water is coming from Danube, through a 5-km long channel, passing through the chemical plant from the vicinity.)

Despite complex investigation, the influence of the chemical plant was not so obvious as direct results. The biggest values for chloride and sulphate and the lowest values for pH and compressive strength are for the external concrete surface.

On site inspection shown the following major characteristics:

- ✓ High concrete porosity.
- ✓ Small covering concrete surface.
- ✓ Metallic insertion corrosion.
- ✓ Horizontal and vertical pillars crack.
- ✓ Map cracking fissure on the external concrete surface, the border crack being black coloured and with humid aspect, see Figure 2, Section B-B.

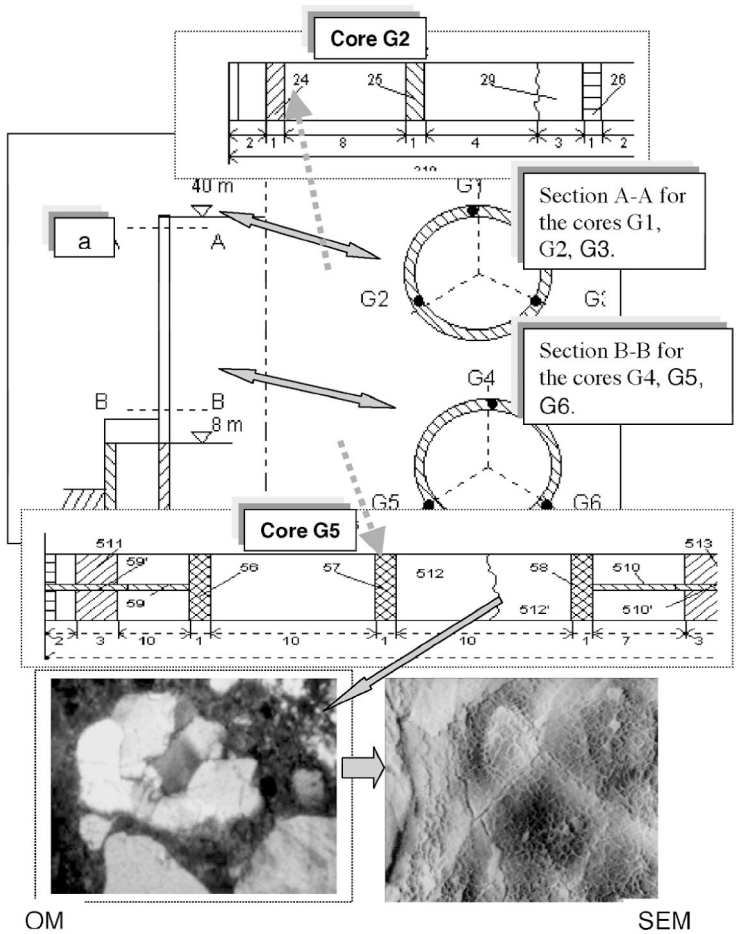

Figure 2 Investigated samples, cores position in the structure and AAR localisation in the core sample and concrete structure
(OM-Optical Microscopy, SEM-Scanning Electron Microscopy)

The marked different parts of the cores, as shown in Figure 2, for cores with codes G2 and G5, there investigated by physico-chemical methods as separate samples, based on special algorithm. Some results are systematised in Table 2 and Table 3.

RESULTS OF THE CHEMICAL AND PHYSICO-CHEMICAL INVESTIGATION

The chemical damaging and the extent of the observed in the concrete masse was investigated with the special analytical procedure. The analysed samples are those indicated in Figure 2, being from two different heights of the cooling tower, samples G1, G2, G3 from the top of the tower, and from 10 m height from soil, G4, G5, G6.

Table 2 Chemical compositions

	CONCRETE [%]		AGGREGATE [%]		HARDENED CEMENT PASTE [%]	
	Mean value	1σ	Mean value	1σ	Mean value	1σ
SiO_2	71.16	3.10	75.65	1.78	20.58	0.64
Al_2O_3	9.31	0.93	13.00	1.84	6.93	0.55
Fe_2O_3	6.19	0.96	2.21	0.20	3.96	0.27
CaO	1.67	0.21	2.08	0.90	57.82	2.06
MgO	1.11	0.38	0.74	0.26	4.29	1.82
SO_3	1.03	0.09	0.24	0.14	2.75	0.22
Na_2O	1.22	0.16	3.17	0.26	0.77	0.08
K_2O	1.26	0.34	2.38	0.20	1.03	0.23
TiO_2	0.74	0.08	0.53	0.35	1.82	0.14
$Na_2O_{quivalent}$	2.05	0.37	4.71	0.34	1.44	0.22
Insoluble	76.82	2.03	-	-	-	-
LOI 580°C	5.21	0.50	-	-	-	-
LOI 1050°C	6.60	0.69	-	-	-	-

Note: Mean value- mean value of all investigated samples, 1σ-Standard deviation of the mean values, as dispersion indicator.

Table 3 Mineralogical compositions

COMPOUND	X-RAY DIFFRACTION	TRANSMISSION OPTICAL MICROSCOPY
Quartz	50-60%	30%Quartz 40% quartzite micro crystalline 30% quartzite shiest
Feldspar	15-20%	-
Calcite	<5%	-
Illite-micas	10-15%	-
Chlorite	<<5%	-
Vaterite	<<5%	-
$Ca(OH)_2$	~5%	-
Gypsum	~2	-

CONCLUSIONS

The corrosion of the metallic insertion was identified to be the main damaging factors, as it was identified during on site expertise, by visual and ultrasound tests. Mainly the insufficient covering layer and pour concrete quality caused the corrosion of the metallic insertion.

The presence of the gypsum at the level of hardened cement paste, after 10 years of tower using, can be associated with the sulphate attack. The sulphate attack was found mainly in the superficial concrete layer, and it seems to be produced by the air and water rich in sulphate from a neighboured chemical plant, as external factors, in correlation with pour concrete quality, (density, high C_3A content).

The carbonation of the concrete mass was correlated with the initial high porosity, and leaching phenomena too, due to condensed water. Portlandite and carbonate are present in concrete composition, as found by mineralogical analysis, X-ray diffraction and optical microscopy. The carbonate is in crystallized form as Vaterite, this being very probable an indicator of high amount of alkali content.

The first expert as main deterioration factor initially assumed The Alkali Aggregate Reaction. His arguments were based on the map cracks presence on the concrete surface, and assumptions related to aggregate origin and cement quality used initially. For samples coming from B-B section, Figure 2, the equivalent alkali content exceeds the normal values, ~2%Na_2O_{equiv}, indicating the potential risk for AAR. The aggregate contains ~70% quartzite (40% micro crystalline and 30% shiest). The alkali aggregate reaction was very often associated by optical microscopy with quartzite from the concrete mass, only in the region of the concrete mass situated at +8 and + 10 m. AAR was confirmed mainly by visual methods, (on site map cracking, optical microscopy and scanning electron microscopy). For the rest of hardened cement paste, the alkali content it is greater than the normal, this situation being most probably correlated with the high C_3A content, different from cement specification. For these samples, alkali aggregate reaction was not evidenced by optical microscopy.

Based on laboratory assessment and structural final results, the structure management was informed that the structure couldn't be in use longer than 5 years, being more economically to build another cooling tower instead to repair and maintain the existing one.

REFERENCES

1. MUNTEAN, M, Investigation of old concrete of 100-110th years durability, Politechnica University Bucharest, 1986.

2. ANDREI, V, CRIAUD A, COLOMBET, P, Secondary reactions associated with alkali-aggregate reactions at 150°C investigated by SEM-EDAX", Proc. 4th NCB International Seminar on Cement and Building Materials, New Delhi, India, December 12-15, 1994.

3. ANDREI, V, CRIAUD, A, Alkali-aggregate reaction products identified in concrete after high temperature cure in alkaline solution at 150°C, Proc. 10th International Conference on Alkali Aggregate Reaction in Concrete, Ed Shayan, A, Melbourne, Australia, August 18-23, 1996, p 957.

4. ANDREI, V, MUNTEAN, M, OLTEAN, A, Investigation of alkali aggregate reactions by physico-chemical analysis in the case of different constructions from Romania, Proc. 10th International Conference on Alkali Aggregate Reaction in Concrete, Ed Shayan, A, Melbourne, Australia, 18-23 August, 1996, p.227.

5. ANDREI V, MUNTEAN, M., OLTEAN, A, Three case studies for alkali aggregate reactions investigated with a complex physico-chemical procedure, Proc. 5th NCB International Seminar on Cement and Building Materials, New Delhi, India. November 25-29, 1996, Vol 3, p XV 97-XV 107.

6. ANDREI, V, MUNTEN, M, BOIAN, F, OLTEAN, A, Investigation by instrumental laboratory physico-chemical analysis in different real concrete structure from Romania, International Conference "Cement and Concrete Science", 8-8 September,1998, University of Leeds, U.K.

7. ANDREI, V, VIRBAN, C, MUNTEAN, M, IONESCU, A, OLTEAN, A, BOIAN, F, Case study of long term concrete durability investigation for the Dragan-Iad hydrotechnique site in Romania, Proc .International Conference on Infrastructure, Regeneration and Rehabilitation, Improving the Quality of Life Through Better Construction, A Vision for the Next Generation., University of Shefield, UK, 1999.

8. ANDREI, V, Alkali-Aggregate Reaction, PhD Thesis, "Politehnica" University, 2001.

RESIDUAL DEFORMATIONS OF A REINFORCING ROD IN THE CRACK OF A DEEP REINFORCED CONCRETE BEAM

O G Kumpyak

D G Kopanitsa

Tomsk State University of Architecture and Building

Russia

ABSTRACT. The paper presents the results of the experimental and theoretical investigations of a steel reinforcing rod under tension and shear. Stresses and deformations of the rods fractured in test machines as well as of those removed from the destructed deep reinforced concrete beam are considered. In the process of the experiment there have been determined changes in the structure of steel in the zone of plastic deformations and destruction. Electron microscopy and X-ray examination have been used to determine the structure of steel and values of residual stresses. Residual deformations have been measured along both the rod depth and length. The results are given in the diagrams of residual deformations for rods removed from the destructed reinforced concrete beam. Values of deformations and pattern of their distribution for rods subjected to tension of various intensity have been compared. The experiments have shown no influence of squeezing concrete medium on the character of residual plastic deformation distribution in the fracture zone of the rod.

Keywords: Reinforced concrete structure, Reinforcing rod, Tension, Shear, Residual (plastic) deformations, Microstresses, Longitudinal deformations, Lateral deformations, Translucent electron microscopy, X-ray (diffraction) analysis.

Professor O G Kumpyak, is PhD, Professor, honorary worker of Higher and Vocational Education of the Russian Federation, head of the department "Reinforced concrete and stone buildings and structures", Tomsk State University of Architecture and Building; conducts research on calculation of reinforced concrete structures subjected to intensive dynamic loading, as well as on reinforced concrete structure restoration.

Professor D G Kopanitsa, is Candidate of Tech. Sc., Associate Professor, Tomsk State University of Architecture and Building; conducts theoretical and experimental research on reinforced concrete structures subjected to considerable deformations and destruction under intensive dynamic loading.

INTRODUCTION

The problem of reinforced concrete structure calculation is critical with the regard for crack formation in concrete and development of considerable plastic deformations in reinforcement. It is connected with a number of problems, in particular, with a reinforcing rod resistance to longitudinal, lateral forces, and bending in the crack of a reinforced concrete structure. The experiments show that in the destruction process deformations in the reinforcement reach considerable values and can be determined only indirectly as the direct measurements are impossible. Quantitative evaluation of the stressed state in the zone of plastic deformations or reinforcement destruction can be given on the basis of the data on residual deformations obtained by direct measurements. It is known that in a crack, reinforcement resistance to shear force, according to various data, is within the limit of 10 to 40 % of the value of the lateral force in the section. Investigations showed the dependence of tangent stresses in a reinforcing rod on reinforcement percentage, aggregate size grading, concrete quality and other factors, including load value, time of operation and recurrence [1, 2]. Besides normal stresses, in the crack of a reinforcing rod there arise tangent stresses developing longitudinally on a limited section. Shear of the crack edges results in curvature of the longitudinal axis of the rod and the appearance of bending moments.

MATERIALS AND METHODS OF RESEARCH

The object of investigation was a steel rod widely used as a reinforcement in reinforced concrete structures. The experiments were conducted in three stages. At first, 10 mm diam. rods were tested on a rupture machine at a speed of $4 \cdot 10^{-4} c^{-1}$. The diagram σ - ε built in the process of testing is shown in Figure 1.

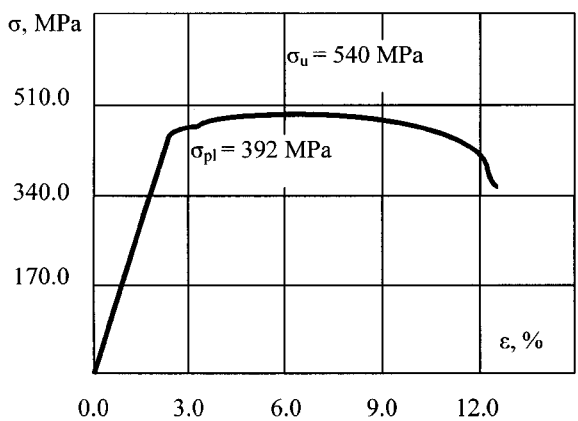

Figure 1 Diagram $\sigma - \varepsilon$ for the tested rod

At the second stage the reinforcing rods were tested for the action of external shear forces. A 12-mm diam. reinforcing rod was used as a specimen. Its rupture strength was 540 MPa. The experiments were conducted on a hydraulic press with the use of a special device in the form of a thick –walled hollow cylinder with the inner diameter equal to the reinforcement diameter and the external one equal to 60 mm. The cylinder was cut into three parts along its

length. The two edge parts of it were fastened to the press support. The middle part was mobile and was intended for transmission of the press shear force to the rod inserted into the device hole. At fracture the surfaces of the shearing parts of the thick-walled cylinder were very close to each other. To smooth out stress concentrations, the cutting edges of shearing surfaces were rounded off. The third stage included the tests on a deep reinforced concrete beam. Its structure caused the appearance of cracks dividing the beam into three parts. The static load was applied to an upper side from top to bottom. Figure 2 shows the scheme of the test on reinforced concrete beams strengthened with 16-mm diam. rods.

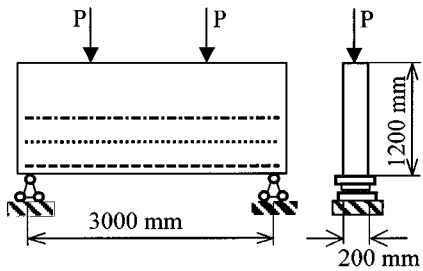

Figure 2 Scheme of a deep reinforced concrete beam testing
The rods are shown by dotted lines

The rods were distributed through the depth of the beam body due to which forces of various values arose in them under the applied load. At the last stage of the experiment the lower rod was fractured and in the above - lying rods there appeared local plastic deformations of various intensity. After the beam destruction the rods were removed from the concrete.

Methods of physics of metals were used to study the material structure and determine residual deformations in the investigated rods. The latter were cut into plates (foils) by electrospark method in a kerosene medium. The distance between the sections was taken as a multiple of the rod diameter, as it's shown in Figure 3. The steel structure was studied by the methods of translucent electronic microscopy and X –ray diffraction analysis. Thin foils were prepared in the following way. Metal plates (thin foils) 0.25 mm thick were thinned electrolytically in the oversaturated solution of chromium anhydride and orthophosphorus acid up to ~ 0,17 mkm. They were examined through electronic microscope at the accelerating voltage of 125 kV with 4000 through 40000 magnification. The final magnification was obtained by photo printing. The diffraction analysis with the use of dark field technique was applied to identify material phases [1]. Electron - microscopic images of the investigated material were used to a) classify the structure according to morphological features; b) determine dimensions, volume, fraction and secondary phases localization; c) determine scalar $<\rho>$and redundant $\rho_{\pm}$ of dislocation density and curvature -torsion amplitude χ of the material crystal lattice.

X-ray diffraction analysis was carried out on diffractometer in the filtrated $Cu_{k\alpha}$-radiation.

It consisted in measuring the sizes of coherent scattering regions (D_{HKL}) and microstresses of the second type (σ_{II}). The latter were determined according to the formula [2]:

$$\sigma_{II} = E\frac{\Delta d}{d}$$

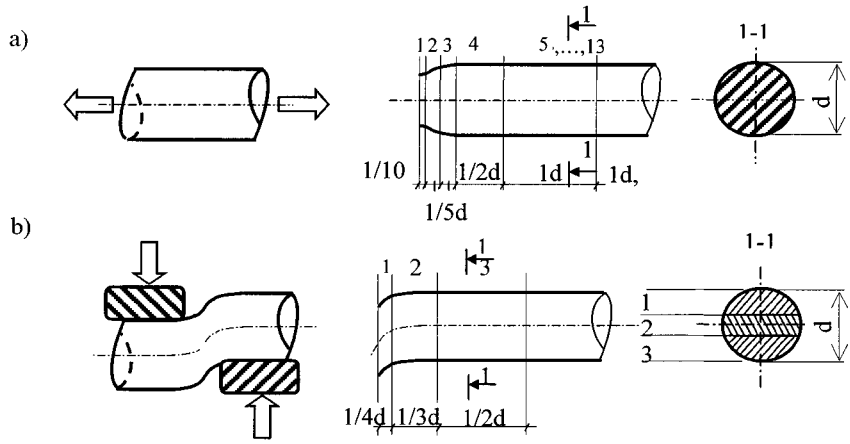

Figure 3 Cutting schemes of rods: a) destructed by tension; b) destructed by shear

Two types of residual stresses are usually distinguished in metal alloys. These types differ in volumes in which they are counterbalanced. Stresses of the first type (σ_I), that are sometimes called zonal or macrostresses, are counterbalanced in macroscopic volumes or in the volume of the whole specimen. Microstresses of the second type (σ_{II}) are counterbalanced in the volumes of separate crystals or mosaic blocks.

RESULTS OF THE TENSION TESTS

The electron microscopic analysis showed that the structure of steel in a non - deformed state was a mixture of ferrite and perlite grains oblong in shape. Their average lateral and longitudinal sizes are equal to 3.2 mkm and 5 mkm respectively. The dislocation structure of ferrite grains and ferrite layers in perlite colonies is characterised by a random disposition of dislocations. Curvature contours indicative of the presence of elastic fields of stresses in specimens were observed inside perlite and ferrite grains. Increase in the deformation degree (approximation to the specimen destruction zone) results in the following:

1) The dislocation scalar density increases;

2) The value of elastic fields of stress increases and their distribution in the material changes.

This conclusion can be made from the change in the form and lateral sizes of the curvature contours. In the initial state they are diffusive (indistinct) and extend through the whole grain from boundary to boundary. With the increase in deformation degree the contour outlines become sharper and the form gets more complicated. In the fracture zone there can be observed contours located inside the grains and closed on themselves. Measurement results are summed up in Table 1, where foil numbers correspond to section numbers in Figure 3.

X-ray diffraction examination showed that microstresses (σ_{II}) were changing nonuniformly on the specimen length reaching their maximum value in the rupture point.

Table 1

FOIL NUMBERS	$<\rho>\cdot 10^{10}cm^{-2}$		$\rho_{\pm}\cdot 10^{10}cm^{-2}$		σ_{el}, N/mm^2		σ_{pl}, N/mm^2	
	ferrite	perlite	ferrite	perlite	ferrite	perlite	ferrite	perlite
2	7.2	9.1	8.0	9.3	6.0	7.0	2.8	3.1
3	5.2	9.8	7.5	10.0	4.0	7.6	2.7	3.2
5	5.5	8.8	7.4	8.2	3.2	6.8	2.7	2.9
7	2.6	3.9	6.2	7.0	1.8	2.5	2.5	2.6
9	2.5	2.6	5.0	5.2	2.2	2.4	2.2	2.2
13	2.0	2.0	4.0	4.0	2.0	1.8	2.0	2.0

The diagrams were plotted according to measurement results, where the basic changes of microstresses (σ_{II}) occur on the part equal to one diameter of the rod, Figure 4.

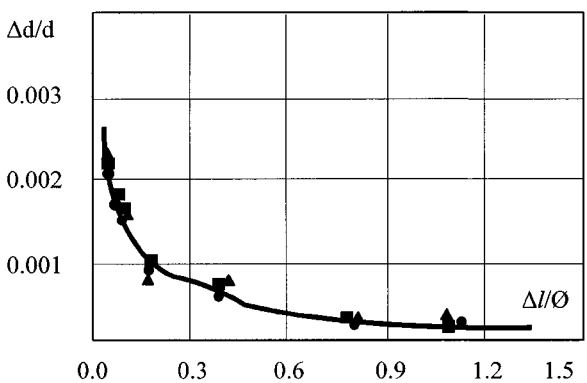

Figure 4 Diagram of axial residual deformations for a 10-mm diam. rod

It should be noted that the level of residual stresses at a distance of 1/10d from the rupture point was four times as high as the level of residual stresses at a distance of one diameter. The stresses (σ_{II}) became stable at a distance of 3 to 7 diameters from the rupture point. The analysis of long-range fields of stresses showed that their value in perlite grains was somewhat higher than in ferrite ones. The pattern of distribution of long-range fields of stresses along the length coincided with the distribution of microstresses(σ_{II}).

RESULTS OF THE SHEAR TESTS

Methods of metallography and electronic diffraction microscopy of thin foils enabled to find out that the steel in its initial state was morphologically a two-phased material and consisted of the mixture of ferrite, Figure 5a and perlite, Figure 5b grains. In ferrite grains a net dislocation substructure was observed in which the dislocation scalar density was $\approx 1.5 \cdot 10^{10}$ cm^{-2}. In ferrite layers of perlite grains the dislocation substructure in chaotic form had the dislocation density equal to $\approx 10^{9}$ cm^{-2}. In cementite plates practically no dislocations were observed.

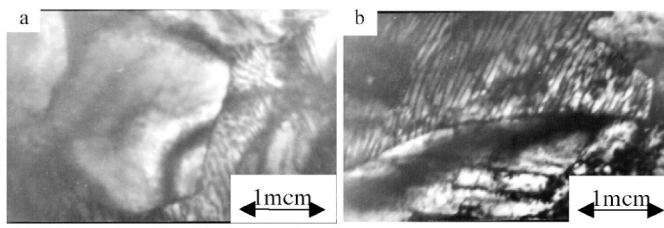

Figure 5 Structure of steel in its initial state

Mechanical testing of the material resulted first of all, in a change in the dislocation substructure in ferrite component of the steel. Close to the destruction zone (3-mm) a fragmented dislocation substructure was formed in ferrite grains, Figure 6a. In perlite grains the type of dislocation substructure did not change. However, the dislocation scalar density increased up to $\approx 2.5 \cdot 10^{10}$ cm^{-2}, Figure 6b.

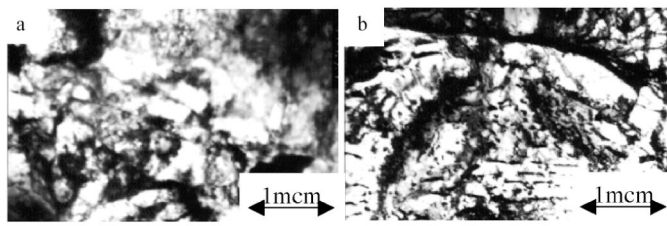

Figure 6 Structure of steel at a distance of 3-mm (1/4 of the rod diam) from the fracture point

The increase in dislocation scalar density was accompanied by cementite plates destruction. The plates were cut and cracked by moving dislocations. Dislocations entangled the edges of plates. Cementite plate destruction was accompanied by plate dissolution basically because of carbon atoms moving from carbide crystal lattice into dislocation nucleus [3].

At a distance of ~ 6 mm from the destruction zone, a change in the dislocation substructure of the ferrite component of the material was observed only in quantitative respect. As well as in the initial state, a net substructure was observed. However the dislocation density $\approx 5 \cdot 10^{10}$ cm^{-2} was much higher, than that in the initial state.

In ferrite layers of a perlite structure the dislocation substructure did not change either (as compared to the initial one), but the dislocation density increased up to $8 \cdot 10^9 \, cm^{-2}$. Such increase in dislocation density didn't have a noticeable influence on the state of cementite plates. Specific electronic – microscopic shapes of the steel structure on the given distance from the area of fracture point shown for ferrite, Figure 7a and perlite, Figure 7b grains.

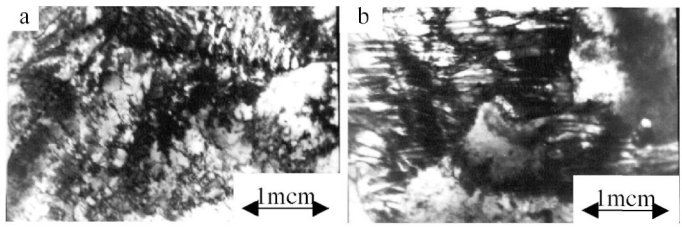

Figure 7 Structure of steel at a distance of 6mm (1/2 of the rod diam) from the fracture point

For the plotted sections (Figure 3b) measurements oriented along the rod axis of the steel residual deformations, i.e. longitudinal (ε_x) and lateral (ε_y) were made. Figure 8a shows the diagrams of residual deformations ε_y, where normal section 1 is made in the zone of rod destruction at a distance of 3 mm from the shear plane. Section 3 is made at a distance of 12 mm, i.e. at of one diameter. As it is shown, the pattern of lateral deformation distribution changes with greater distance from the fracture point. The highest values of lateral deformations arose on external fibers of the rod. Transformation of the diagram of lateral deformations in section 3 testifies to decrease in the value of shear force and of damping of bearing deformations at a distance of one diameter from the shear plane.

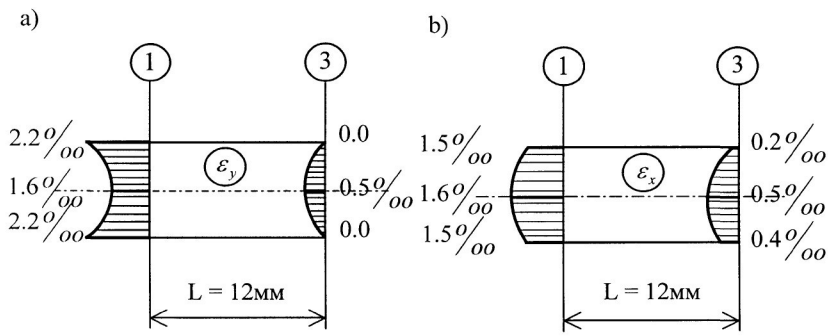

Figure 8 Diagrams of residual deformations: a) lateral ones ε_y; b) longitudinal ones ε_x

Figure 8, b shows diagrams of longitudinal residual deformations (ε_x). Section 1 is made in the destruction zone and coincides with the shear plane. Normal section 3 was made at distances 12 mm from the destruction plane. Longitudinal deformations were measured in three points on the height of the rod section. The highest values of longitudinal deformations were found in close proximity with the shear plane. With greater distance from the fracture point, the deformation values decreased and the moment component increased.

RESIDUAL TENSILE DEFORMATION OF THE RODS REMOVED FROM CONCRETE

The diagrams of microdeformation ($\varepsilon_{//}$) for the rods removed from a deep beam are shown in Figure 9. The upper curve is built for the fractured rod; the other two correspond to distribution of residual deformations in the rods located above the fractured one.

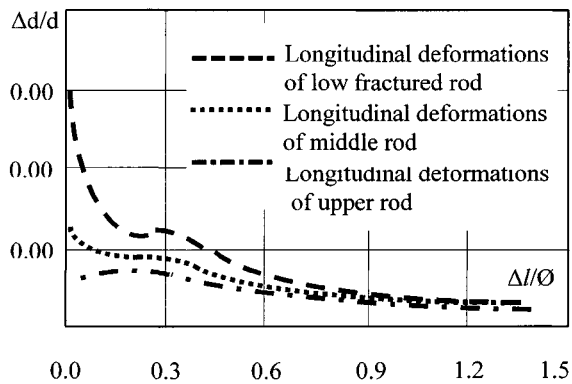

Figure 9 Diagram of longitudinal residual deformations for reinforcing rods Removed from the destructed beam

Transformations of residual deformation diagrams depend on tension intensity. They can be represented in the form of analytical expressions showing limiting state of a reinforcing rod in the crack. For example, under loads causing local plastic deformations, formed on the limited length of the rod, distribution of deformations can be represented by a quadratic curve. Distribution of considerable plastic deformations resulting in the appearance of a neck or in destruction has a more complicated definition.

Analysis of the test results revealed the importance of the problem concerning the influence of squeezing concrete medium on the pattern of deformation distribution and the value of deformations in the reinforcement. Comparison of the results obtained for the rods tested on a rupture machine and for those removed from the beam concrete showed the absence of concrete influence on relative values of deformations, as well as on character of their distribution in the zone of plastic deformations or destruction.

REFERENCES

1. UTEVSKY, L., Diffraction electron microscopy in physical metallurgy, M, Metallurgy, 1973, p 584.

2. TAILOR, A., X-ray metallography, M, Metallurgy, 1965, p 664.

3. GROMOV, V., KOZLOV, E., BAZAIKIN, V., et al, Physics and mechanics of drawing and die forging, M, Nedra, 1997, p 293.

RPC IN CROATIA

D Bjegovic

M Skazlic

V Candrlic

University of Zagreb

Croatia

ABSTRACT. Over the past twenty years high strength concrete and reactive powder concrete (RPC) have been investigated by many researchers. At present, preliminary experiments to produce RPC are in progress in Croatia. The preliminary investigation described in this paper involved testing of concrete mixtures having different concrete components. Sand and superplasticizer samples used in the tests were varied as for their respective origins, while steel fibers, cement and silica fume were obtained from the same sources. The compressive and flexural strengths were measured after 7 and 28 days. The selection of the right sand was done based on the strength results obtained. The results of testing will serve as guidelines for further investigations.

Key words: Concrete, Strength, Durability, Reactive powder concrete.

Professor D Bjegovic, is Vice Dean and Professor of Materials Science and Prefabrication Technology in the Materials Department at Faculty of Civil Engineering Zagreb, Croatia. Her research focuses mainly on prefabrication, concrete durability and repair and maintenance.

Mr M Skazlic, is young Researcher in the Materials Department at Faculty of Civil Engineering Zagreb, Croatia. He is currently undertaking research into the development of high performance fibre reinforced concrete.

Professor V Candrlic, is retired Professor of Bridge Construction in the Construction Department at Faculty of Civil Engineering Zagreb, Croatia. He is author or coauthor of many projects and publications in the field above indicated.

INTRODUCTION

Building of modern structures of various architectural shapes, and reconstruction of the existing ones impose strict requirements with regard to the quality of materials used for their construction. For this reason, continuing researches aimed at the development of concrete - the most often used building material - has been carried out. As a result, maximum strength of concrete that can be obtained at the present stage of development is several times greater than that achievable a few years ago.

This information gains in importance considering that strength of concrete was until recently considered to be the main factor in deciding on its suitability, while all other properties were found to be related to its strength. However, the number of newly developed concrete materials has been increasing, and the properties achieved do not necessary depend on strength of concrete. It has been realized that required, predetermined properties of concrete can be achieved by adjusting the composition of a concrete mixture. In addition, the selection of components of the mixture should be given careful consideration, i.e. the components should be of satisfactory quality in terms of required properties. Also, the technology to prepare high-performance concrete materials is itself of crucial importance.

Researches done worldwide over the past few years on the basis of the above mentioned principles resulted in concrete of superior characteristics known as Reactive Powder Concrete (RPC). RPC is based on a principle that a material with a minimum of defects such as micro cracks and voids will be able to realize a greater percentage of potential strength defined by its components [1, 2, 3, 4, 18].

In our country, certain preliminary researches in terms of analyses of components to be used in RPC-a have been conducted, and the results obtained will be useful guidelines for further investigations. The purpose of the above researches was the possible construction of a concrete arch bridge over the Bakar Straits, Croatia, with a span of 432 meters. A preliminary design of the bridge has been made and, according to the design, the whole bridge is planned to be built by using prefabricated segments made of RPC concrete. This bridge would be a continuation of Croatian achievements in bridge construction on the global scale [14, 15].

RESEARCH WORK

RPC materials exhibit very high compressive and tensile strengths and possess outstanding properties such as high durability and energy absorption, superior ductility, very low shrinkage and creep. Therefore, these materials are suitable for a number of structural applications.

In addition to standard components such as cement, fine aggregate and water, RPC materials consist of high strength cements crushed quartz, superplasticizers, silica fume, and micro fibers. Such concrete contains particles of less than 0.1 μm up to about 600 μm in order to achieve a more homogenous mixture with minimum portion of micro pores. It is for its composition, i.e. such fine particles, that this concrete material is called Reactive Powder Concrete [6, 11].

The development of RPC was aimed at meeting some basic requirements as follows [8]:

- A more homogenous material by eliminating course aggregate;
- Increase in density of the placed concrete by optimizing grain size distribution and application of pressure prior to and during the placing of concrete;
- Improved microstructure by thermal treatment of the concrete placed (i.e. heating of concrete after it has set);
- Improved ductility by adding fine steel fibers; and
- Possible production in the existing plants.

The components of RPC must satisfy demanding criteria and strict requirements concerning quality. For this reason, at the Faculty of Civil Engineering in Zagreb, preliminary tests of RPC were carried out [16, 17]. The components of RPC mixtures used in these tests were varied in order to test them for their respective qualities; those which exhibited required qualities were used in further tests. Testing was aimed at obtaining RPC 200, i.e. concrete with compressive strength of 200 MPa.

Aggregate and superplasticizers used for testing purposes were of different types, while steel fibers, cement and silica fume were not changed, i.e. from the same sources. Since aggregate is required to achieve high strength, small grain types of quartz sand were used. The three types of aggregate materials (max grain size 2 mm) originated from different parts of Croatia (the towns of Lipik, Lepoglava, and Đurđevac), and the sand for testing cement was standard three-fraction sand.

Water cement ratio in RPC is very low and, therefore, workability of such concrete is improved by adding significant quantities of superplasticizers. The superplasticizers used in the tests were of SMF type, manufactured by different producers.

Since silica fume has very fine particles of 0.1 up to 0.5 μm, its function is to fill in the space between the cement particles and to bond free lime (a component of cement having the poorest qualities), which would result in significant increase in density of hardened concrete. For the purposes of the subject experiment, a product containing a certain percentage of silica fume, available on the Croatian market, was used.

By adding steel fibers, tensile strength is increased and so is the desired degree of ductility, i.e. ultra-high capacity of energy absorption. is achieved. The steel fibers added to RPC act as reinforcing steel compared to a small size of the biggest grain of aggregate. On the basis of this fact, RPC can be considered as fibre reinforced concrete. In this case, the fibers should have a aspect ratio that corresponds to fibre reinforced concrete. In our experiments, amorphous steel fibers of 13 mm length, 0.2 mm diameter and 1500 MPa strength were used. The cement was Portland cement of Class 45 produced by a Croatian producer.

A fresh concrete mixture was cast into steel moulds by using a standard procedure and compacted on a vibrating plate. The concrete samples were being cured in a moisture chamber at 95 % relative humidity until the date set for testing.

The tests on the samples of mixtures consisting of the above mentioned components were carried out to determine consistency of fresh concrete by using the method of settlement, and compressive and flexural strengths after 7 and 28 days. The compositions of mixtures and the results of testing are given in Tables 1 and 2.

DISCUSSION ABOUT RESULTS

The test results given in the Tables show that expected compressive strengths of 200 MPa were not achieved; however, through this work guidelines for further experiments have been provided. The maximum compressive strength of 113 MPa, and maximum flexural strength of a little less than 35 MPa were obtained.

The analysis of results showed that the compressive and flexural strengths characteristic of RPC were not achieved as expected, which is caused by a number of various factors; for example, during testing some basic procedures necessary to produce RPC were not used.

Table 1 Results of testing concrete mixtures

COMPOSITIONS OF MIXTURES (kg/m^3)								
Sand	Lipik				Lepoglava			
	995,80	995,80	855,90	855,90	782,00	782,00	719,50	719,50
Cement	677,90	677,90	588,60	571,30	571,30	571,30	533,30	533,30
Silica fume	203,40	203,40	176,50	176,50	171,40	171,40	159,90	159,90
Water	322,00	322,00	389,70	389,70	428,50	428,50	450,00	450,00
Superplasticizer 1	20,30	20,30	17,60	17,60	17,10	17,10	15,90	15,90
Superplasticizer 2	-	-	-	-	-	-	-	-
Steel fibers	-	-	146,80	146,80	-	-	133,30	133,30
Water/cement	0,36	0,36	0,51	0,51	0,57	0,57	0,64	0,64
Properties of fresh concrete								
Consistency(mm)	160,00	160,00	160,00	160,00	160,00	160,00	160,00	160,00
Strengths of samples (after 7 days)								
Flexural (N/mm^2)	10,50	13,80	28,42	30,45	7,43	7,48	20,94	21,58
Compressive (N/mm^2)	53,95	57,17	41,61	39,02	28,28	33,62	26,31	24,03
Strengths of samples (after 28 days)								
Flexural (N/mm^2)	14,78	16,04	32,41	32,37	11,71	14,52	27,97	33,12
Compressive (N/mm^2)	74,31	69,69	54,27	55,68	42,31	47,12	36,10	39,71

This refers in particular to the technology used in preparing concrete mixtures because it did not involve either thermal treatment of the concrete placed or the application of pressure before and during the placement of concrete samples. In addition, the process of compacting concrete samples should be optimized. As for the components used to prepare RPC, it was found out that the material containing silica fume was not of the required quality. Also, aggregate of grain sizes having less than 1 mm should be used. According to the test results it can be concluded that the best results are achieved with aggregate originating from the depot of Đurđevac, and with superplasticizers marked with number 2.

The results obtained provide useful guidelines for the continuation of research work aimed at producing RPC suitable for structural applications.

Table 2 Results of testing concrete mixtures

COMPOSITIONS OF MIXTURES (kg/m³)										
Sand	Đurđevac								Standard sand	
	1009	1009,4	832,30	832,30	1026,6	842,70	955,20	908,50	914,20	851,70
Cement	745,50	745,50	624,90	624,90	722,30	613,40	644,50	638,80	660,60	623,30
Silica fume	223,60	223,60	187,50	187,50	224,30	190,50	389,40	378,30	205,10	193,50
Water	252,50	252,50	351,50	351,50	261,70	357,00	269,80	280,50	330,80	349,20
1	22,30	22,30	18,70	18,70	-	-	-	-	20.50	19,30
2	-	-	-	-	15,00	12,70	16,60	16,40	-	-
Steel fibers	-	-	156,20	156,20	-	158,7	-	90,10	-	161,20
Water/ cement	0,26	0,26	0,43	0,43	0,27	0,44	0,26	0,27	0,38	0,43
Properties of fresh concrete										
Consistency (mm)	160,000	160,000	160,000	160,000	160,000	160,000	160,000	160,000	160,000	160,000
Strengths of samples (after 7 days)										
Flexural (N/mm²)	17,33	16,67	36,12	27,87	19,28	31,60	16,36	28,46	17,62	28,68
Compressive (N/mm²)	68,17	67,65	47,46	44,49	71,31	49,99	75,18	78,71	67,89	51,49
Strengths of samples (after 28 days)										
Flexural (N/m²)	22,57	24,85	34,98	27,26	20,82	33,15	23,65	31,24	19,25	31,46
Compressive (N/mm²)	8257	80,43	62,60	71,71	90,77	89,70	89,62	113,55	86,40	92,20

PRELIMINARY DESIGN OF AN ARCH BRIDGE-THE FIRST APPLICATION OF RPC IN CROATIA

The main purpose of the research work described in this paper is the development of RPC, the quality and properties of which would primarily meet requirements set for the possible building of the first structure in Croatia to be made of RPC. Naturally, when designing and building such a complex structure, one should draw on practical experience gained by experts worldwide. It refers particularly to the application of RPC in the construction of the first structure made of this material, namely the pedestrian and bikeway bridge in Sherbrooke, Canada, completed in 1997 [10, 12, 13].

Improved mechanical properties and durability of RPC in relation to regular concrete provide the following advantages [5, 7, 9]:

- Very high strength allows reduction in sizes of structural members;
- High ductility and energy absorption provide greater structure reliability either under overload conditions or earthquakes;
- The elimination of conventional reinforcement allows freedom to introduce new structural member shapes;

- Enhanced abrasion resistance provides extended service life for bridge decks and industrial floors;
- Very low porosity enhances corrosion resistance providing longer service life of the structure in unfavourable and aggresive environments; and
- The fine structure of the material allows high-quality surface finish.

Wishing to carry on the Croatian tradition of contributing to the world achievements in construction of bridges, and taking into consideration both the above benefits of RPC and the fact that Croatia has its own natural resources to produce this material, a group of experts headed by Professor Vinko Candrlic has prepared a preliminary design of an arched bridge which is to be made of RPC. This will be the first application of this product in Croatia. The bridge which will have the span of 432 meters and the total length of 820 meters (Figure 1) will carry the Rijeka-Senj motorway across the Bakar Strait. In this way the Adriatic Highway running around the Bakar Bay would be shortened by about 7 kilometers. In addition, it should be noted that a roadway will be fully protected against gusts of bora, one of the most adverse conditions influencing the usability of the Adriatic bridges in bad weather [14, 15].

Except bridge and arch foundations of MB-40 (MB is an abbreviation for concrete segments) and the highest columns of MB-50 at arch springers, which are the only concrete components placed in the field, the whole bridge would be constructed by using precast members made of RPC with compressive strength of 200 MPa. The bridge members would be fabricated in the plant by using the method of concreting tongue-and-groove segments; during their erection on the bridge the segments would be joined together by using epoxide resins and then prestressed with external cables. The use of RPC allows significant reduction in sizes of cross sections and in member weight, and, owing to this, the upper flange of box girder cross section could have the thickness of only 12 cm.

Thus, this new, original technology for the 21st century could be applied by our own experts to construct the Bakar bridge in a very short time, by using industrial products. The existing concrete mixing plants could be engaged in the production of precast elements made of RPC that would be used for the construction of the bridge. In this way a solid basis for the Croatian construction industry would be provided.

It is also important to notice that bridge construction industry can be proud of the structures completed so far; thanks to these structures, our builders have gained worldwide reputation. This especially refers to one of the first stressed bridges in the world that was constructed over the river Sava in Zagreb in 1939, and has been used ever since. Another impressive achievement of the Croatian bridge building industry is the bridge that connects the mainland and the island of Krk, constructed in 1980. Until recently, this bridge, made of reinforced concrete, was placed first among arch bridges owing to its span of 390 meters.

CONCLUSIONS

The beginning of the 21st century is characterized by the use of concrete materials exhibiting very high strengths and high-performance properties, a typical example of which is Reactive Powder Concrete. Owing to the present stage of its development, concrete has satisfied increasingly strict requirements for a building material.

Figure 1 Preliminary design of the arch bridge over the Bakar Strait in Croatia

In Croatia, preliminary researches to achieve RPC were done, and the results obtained provide useful guidelines for the continuation of investigations. The final aim of the research is to produce RPC to be used in the possible construction of the first structure made of RPC in Croatia, i.e. the arch bridge over the Bakar Strait with the span of 432 meters, whose preliminary design has already been made.

The development of new concrete technologies allows wider applications in the fields in which concrete has been under-represented so far. However, the application of concrete materials calls for new approaches in designing, constructing and maintaining structures, which provides not only Croatian, but also foreign experts and scientists with sufficient research matter to deal with.

REFERENCES

1. BJEGOVIC, D., SKAZLIC, M., BALIC, M., Development of Concrete Through Centuries, Convention of Croatian Civil Engineers 2000, Civil Engineers' Contribution to the Development of Croatia, p 319-326.

2. UKRAINCZYK, V., Concrete - Structure, Properties, Technology, Alcor, Zagreb, 1994.

3. WALRAVEN, J., The Evolution of Concrete, Structural Concrete, Vol P1,1, 1999, p3-11.

4. UKRAINCZYK, V., BJEGOVIC, D., Material Testing within the System of Providing Durability of Concrete Structures, Civil Engineering Yearbook 1995, Croatian Society of Civil Engineers, Zagreb, 1995, p 209-285.

5. ROUX, N., ANDRADE, C., SANJUAN, M. A., Experimental Study of Durability of Reactive Powder Concretes, Journal of Materials in Civil Engineering, February 1996, p 1-6.

6. DOWD, W. M., Construction Materials for the Next Millenium Reactive Powder Concrete, http://www.sr.ex.state.ut.us/1996conf/dowd.htm

7. MORANVILLE-REGOURD, M., Portland Cement-Based Binders – Cements for the Next Millennium, in Modern Concrete Materials: Binders, Additions and Admixtures, Proceedings of the International Conference Creating with Concrete, Dundee, Scotland, 8-10 September 1999, Thomas Telford, 1999, p 87-100.

8. CHEYREZY, M., Structural Applications of RPC, FIP International Conference New Technologies in Structural Engineering, on CD, Lisbon, Portugal, July 2-5, 1997.

9. DAURIAC, C., Special Concrete May Give Steel Stiff Competition, http://www.djc.com/special/concrete97/10024304.htm

10. AITCIN, P. C., LACHEMI, M., ADELINE, R., RICHARD, P., The Sherbrooke Reactive Powder Concrete Footbridge, Structural Engineering International, 2/1998, p 140-144.

11. EMERGING CONSTRUCTION TECHNOLOGIES-REACTIVE POWDER CONCRETE, http://www.new-technologies.org/ECT/Civil/reactive.htm

12. ADELINE, R., GANZ, H R, DOWD, B, The First RPC Structure, Concrete Engineering International, April 1998, p 23-26.

13. BEHLOUL, M., CHEYREZY, M., LACHEMI, M., The Sherbrooke Footbridge, Structural Concrete-The Bridge Between People, FIB Symposium 1999, Prague, Czech Republic, p 711-715.

14. CANDRLIC, V., et al, Concrete Arch Bridge over the Bakar Strait, Convention of Croatian Civil Engineers 2000, Civil Engineers' Contribution to the Development of Croatia, p 357-364.

15. CANDRLIC, V., MRAKOVCIC, S., HRELJA, G., Concrete Bridges with Arch Members of Precast Concrete Segments, Građevinar, V 51, 3/1999, p 205-214.

16. BOBIC, I., RPC – Ultra High-Performance Concretes, Diploma Thesis at the Faculty of Civil Engineering in Zagreb, 1999.

17. DEVIC, M., RPC - Ultra High-Performance Concretes, Diploma Thesis at the Faculty of Civil Engineering in Zagreb, 1999.

18. NAWY, E., Fundamentals of High-Performance Concrete, John Wiley & Sons Inc, New York, 2001.

ENHANCING THE PROPERTIES OF REINFORCED CONCRETE BEAMS BY USING HELICAL REINFORCEMENT

M N S Hadi

L C Schmidt

University of Woolanging

Australia

ABSTRACT. This paper considers the strength gain and ductility of high strength reinforced concrete beams incorporating high strength tensile and helical reinforcement. The effect on ductility through the application of helical reinforcement located in the compressive region of the beam is highlighted. Beams of span 1.2 meters were subjected to flexural loading, with an emphasis placed on the mid span deflection. The results indicate that helical reinforcement is an effective way of increasing ductility in high strength reinforced concrete beams. If the correct pitch is utilised for effective confinement, helical reinforcement will provide an economical solution in enhancing the strength and ductility of flexural members made from high strength concrete.

Keywords: Beams, High strength concrete, Ductility, Helical reinforcement

M N S Hadi is Director of Studies and Senior Lecturer in Civil Engineering. He obtained his BSc in 1977 and his MSc in 1980 from the University of Baghdad, Iraq. His PhD was from the University of Leeds, UK in 1989. His research interests are in the field of concrete analysis and design where he has published over one hundred and ten research papers in international journals and conferences. He has organised two international conferences and has presented his research findings in twelve countries.

L C Schmidt is Emeritus Professor of Civil Engineering. He has significant experience in structural engineering. He has the Pioneers' award for the development of research in Space Structures, 1993, awarded annually by the Space Structures Research Centre, University of Surrey, to one person worldwide. He was Commonwealth Fellow at St Johns College, Cambridge, 1976, and had been awarded a Royal Society Award, London, 1976. He is reviewer for seven international journals related to structural engineering. Since 1992, he has received $570,000 from various sources for research.

INTRODUCTION

Current developments of the construction industry have led to the continuous improvement of construction materials. However, continuous improvements in a material's strength capacity are often burdened by a decrease in ductility. To increase the ductility will allow new materials to be used, as well as harness the full potential flexural strength of reinforced concrete beams. Improved ductility through the incorporation of helical reinforcement located in the compression region is investigated herein. Helical reinforcement has been successfully used to improve the ductility of high strength concrete columns, but is yet to be implemented into beams. The helix must successfully confine the inner core in order for substantial ductility improvements to occur. In this study, different helical configurations are investigated, in order to determine the full implications of their use.

HIGH STRENGTH CONCRETE CHARACTERISTICS

High strength concrete has become increasingly popular in recent years. The Australian Standard (AS 3600) [1] recognises the use of concrete up to 50 MPa, although a modification allowing the use of 60 MPa is expected in the near future. Recently, concretes of 70, 80 and 90 MPa have been used on a small number of projects throughout Australia, whilst in other countries compressive strengths up to 130 MPa have been used [2]. As a result of its highly brittle nature, its immediate use throughout the industry is restricted by limitations placed by the Australian Standard. A full understanding into its behaviour is required before it can be successfully incorporated into present and future structures.

The high compressive strength of high strength concrete can be obtained from a low water to cement ratio and the use of potential high strength cements, such as silica fume (Cement and Concrete Association of Australia and National Ready Mixed Concrete Association of Australasia) [3].

Silica fume is a by-product from the production of silicon and ferrosilicon alloys in an arc furnace. The resulting powder is extremely fine (surface area of approximately 20,000 m^2/kg) and highly reactive (Cement and Concrete Association of Australia and National Ready Mixed Concrete Association of Australasia) [3]. The fine cementitous material will completely react, filling any small voids and providing a highly dense material. Incorporation of a low water-cement ratio ($\approx$ 0.25) and an increase in water demand from the silica fume, results in a highly unworkable mix. To improve the workability a superplasticiser may be incorporated. The superplasticiser increases the slump of the mix, but does not affect the composition or characteristics of the concrete. However, the period of high workability is limited to around an hour.

DUCTILITY INVESTIGATIONS – HELICAL REINFORCEMENT

Lateral reinforcement will provide confinement to the concrete, and hence increase the compressive strength of the member. It achieves this confinement by resisting the lateral expansion due to the Poisson's effect upon loading, and thus acts on the concrete with a lateral compressive force. This allows the core of the member to be subjected to a beneficial triaxial compression. In this state, both the deformation capacity and strength of the concrete are enhanced [4]. A helical configuration will provide a reasonably even distribution of lateral forces to the enclosed core of concrete.

Experiments preformed by Pessiki and Pieroni [4] looked at the axial loading of large-scale helically reinforced concrete columns. During the experimentation, it was observed that large cracks occurred along the length of the concrete, and nearing the ultimate loading capacity the concrete cover split and buckled, and fell away. The closely spaced reinforcement physically separated the concrete cover from the core, causing the early failure of the cover. It was then suggested that a decrease in spiral pitch was required for the high strength column to achieve the same ductility as that of normal strength columns.

Helix (spiral) reinforcement has been used mainly in columns, however it may be incorporated into other applications to improve ductility or compressive strength. To be effective, the helical reinforcement must be placed in the compression zone and the pitch must be small enough to confine the concrete core. Herein, the exploration of helical reinforcement in the compressive region of the reinforced concrete beams is considered, so as to determine whether the helix will increase the strength and ductility of the beams. Single and double helices were used.

The helical pitch size is a major influence on the effectiveness of the confinement. If the concrete is sufficiently confined, only the cover will be shed near the ultimate loading capacity. However, if the pitch is increased the concrete core may not be effectively confined, causing some of the core to spall with the concrete cover. The reduction in cross sectional area will then affect the ultimate load capacity.

Pessiki and Pieroni [4] developed equations for the effective compressive strength of confined concrete:

$$f_{cc} = 0.85f_c^{'} + 4.0f_2(1-\frac{s}{d_c}) \tag{1}$$

and

$$f_2 = \frac{2A_{sp}f_{sp}}{d_c s} \tag{2}$$

where f_{cc} is the compressive strength of the confined core of the column, f_c' is the compressive strength of concrete cylinders, f_2 is lateral pressure, A_{sp} is the area of a helical reinforcement bar, f_{sp} is the stress in the helical reinforcement, s is the pitch of the spiral reinforcement and d_c is the diameter of core of helically reinforced measured to outside diameter of helix.

EXPERIMENTAL PROGRAM

Beam Composition

Twelve beams were subjected to four point flexural loading. Six different beams were tested, and each beam was duplicated in order to observe the typical behaviour. Table 1 shows a summary of the beams' composition.

Table 1 Summary of beam composition

SPECIMEN	CONCRETE STRENGTH (MPa)	TENSILE STEEL	HELICAL REINFORCEMENT					
			Steel		Type	Dia. D (mm)	Pitch P (mm)	P/D
			Bar Size	Dia., d (mm)				
UR – PL	70	2Y12[1]	R6[2]	6	-	-	-	-
OR – PL	70	2Y16	R6	6	-	-	-	-
OR – SH – P1	70	2Y16	R6	6	Single	50	15	0.3
OR – SH – P2	70	2Y16	R6	6	Single	50	45	0.9
OR – DH – P1	70	2Y16	R6	6	Dual	25	15	0.6
OR – DH – P2	70	2Y16	R6	6	Dual	25	45	1.8

[1] Y indicates 400 MPa yield strength
[2] R indicates 250 MPa yield strength

Throughout this research a plain beam (PL) is classified as a reinforced concrete beam that does not contain any helical reinforcement in the pure moment region, while SH and DH indicate a single helix and double helices, respectively. Although the beams are all under-reinforced, the notation of UR (Under reinforced) and OR (Over reinforced) is used to indicate respective design specifications. The pitches of the helices are alternated between 15 mm (P1) and 45 mm (P2).

Modifications to a design mix obtained from Van and Montgomery [5] were used with a targeted characteristic strength of 90 MPa, but the compressive strength obtained was approximately 25% lower than the intended design strength.

The beams' dimensions and reinforcement placement are shown in Figure 1(a) through (c). Cover for all reinforcement was 20 mm, which a significant percentage of the beam depth (13%).

Beam Fabrication

The reinforcing cages were constructed through the use of wire ties. Deformed steel bars located in the compression region of the beam were not considered in resisting flexural loads, but were used to support the shear stirrups and helical reinforcement. The helical reinforcement was coiled through cold working straight R6 steel around a hollow tube. To obtain the desired pitch, the helices were pulled longitudinally and cut to the desired length.

Superplasticiser was added to all the mixes to obtain a normal structural slump. The maximum aggregate size used in this study was 10 mm. The beams were then quickly poured and compacted through the use of an internal vibrator. All beams were left in their moulds until adequate strength was obtained, and were cured by covering with wet hessian bags. To obtain a comparative concrete strength, the test cylinders were cured in the same manner.

Test Details

All beams were tested in an INSTRON 8500 (500 kN capacity) in the Wollongong University Laboratory. Strain gauges were used to monitor strains in the midspan longitudinal steel and

helical reinforcement. The INSTRON has an internal deflection monitor, however a deflection gauge was still situated at midspan to measure vertical deflection. Demec gauges were approximately placed at the location of the longitudinal steel and 25 mm from the top of the cross section at midspan.

The rate of loading was 0.01 mm/s, with readings taken in 5 kN increments. A plotter was used to graph the load versus the deflection of the beam during loading. Loading of the beam was ceased upon failure, or due to the inability to continue effective loading

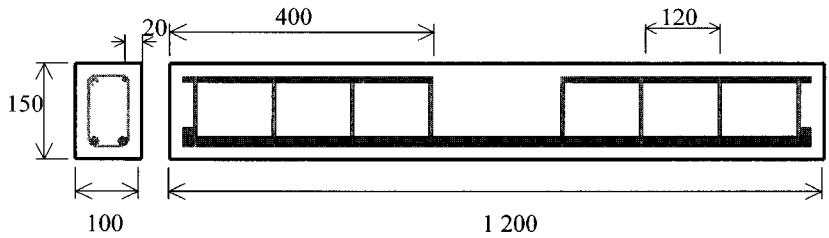

(a) Universal beam dimensions

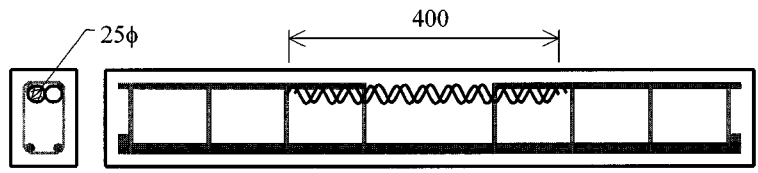

(b) Dual Helices

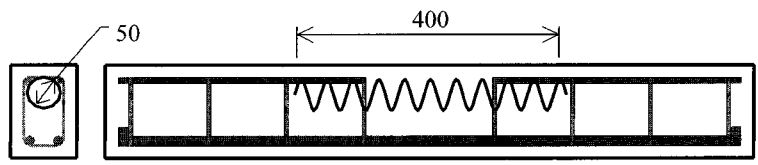

(c) Single Helix

Figure1 Beam dimensions (mm)

EXPERIMENTAL RESULTS

Flexural Behaviour

The majority of failures were compressive, while some beams failed in shear. Figure 2 shows the resulting photos for the relevant beams. The dual and single helical beams are each represented once as there was no different behaviour observed between any two identical beams.

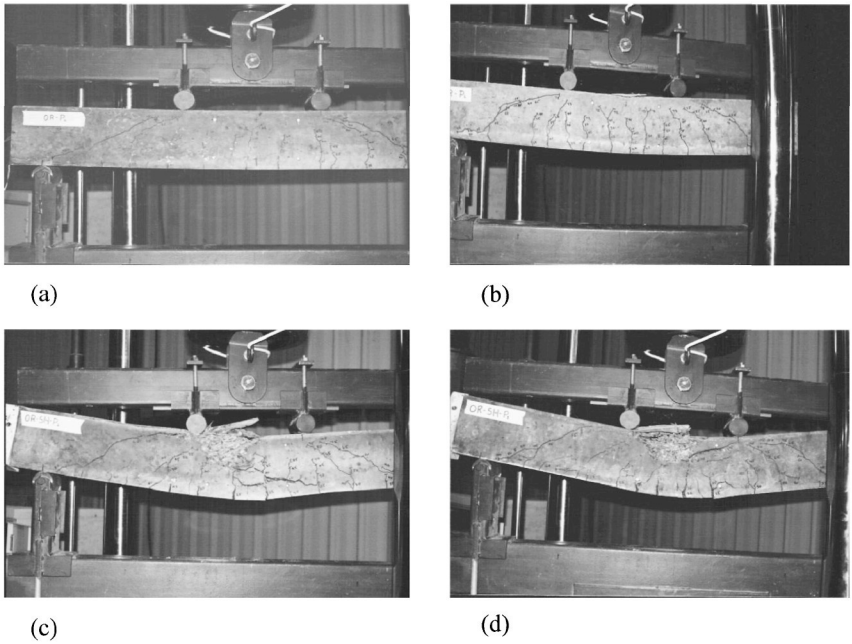

(a) (b)

(c) (d)

Figure2 Photos prior to failure for (a) UR Plain, (b) OR Plain, (c) 15 mm pitch Helix and (d) 45 mm pitch Helix.

The loading of the beams incorporating a 15 mm pitch had to be stopped as the corner of the loading beam came in contact with the test beam.

The helical beams experienced an initial failure of the compression region. The concrete cover failed and crumbled, yet loading was still maintained. Inspection of the beams after loading showed that the concrete was effectively confined in the 15 mm pitch, while the 45 mm pitch furnished a less effective confinement. Figure 3 presents the load deflection curves for the beams tested.

Figure 4 shows moment versus curvature relationships for the tested beams. It is clear that beams with helical reinforcement which 15 mm pitch and helix diameter of 50 mm have the highest ductility and strength.

The following tables provide a summary of the experimental results. Table 2 compares the strength and consequential reduction in ductility due to increasing the tensile reinforcement. Comparisons of strength (Table 3) and deflection (Table 4) are made between plain beams and similar beams incorporating helical reinforcement.

Assuming that the concrete in the confined area of the helix will reach the ultimate strength and the lever arm is the distance between the reinforcing steel and the centre of the helix and using the equation proposed by Pessiki and Pieroni [4] to calculate the ultimate strength of the beams, Table 5 presents a summary of the beams' capacity. It is to be noted here that the unconfined concrete is ignored and the confined concrete in the helix is assumed to have a constant strain.

Table 2 Comparison of Y12 and Y16 tensile reinforcement (Plain Beams)

Beam Type	Yield Strength[1] (kN)	Yield Strength Ratio[2]	Max. Strength (kN)	Max. Strength Ratio[2]	Yield Defl. (mm)	Max. Defl. (mm)	Ductility[3] (mm)	Ductility Ratio[4]
UR – PL	71.8	1	81.8	1	6.0	18.6	12.7	1
OR – PL	114.1	1.6	120.2	1.5	8.3	14.5	6.2	0.49

1 – The yield point is defined as the point where linear deflection changes to non-linear
2 – Yield strength ratio is defined as yield strength of beam relative to that of the UR-PL
3 – Ductility is defined as the distance measured from the yield point to failure
4 – Ductility ratio is defined as measured deflection of beam relative to that of the UR-PL

Table 3 Strength comparison of helical beams

Beam Type	Tensile Reinf.	Helix			Yield Strength (kN)	Yield Ratio	Max. Strength (kN)	Max. Ratio
		Number	Dia. (mm)	Pitch (mm)				
OR – PL	2Y16	-	-	-	114	1	120	1
OR – SH – P1	2Y16	1	50	15	123	1.08	119	0.99
OR – SH – P2	2Y16	1	50	45	111	0.98	115	0.95
OR – DH – P1	2Y16	2	25	15	107	0.94	112	0.93
OR – DH – P2	2Y16	2	25	45	108	0.95	113	0.94

Table 4 Deflection comparisons of helical beams

Beam Type	Tensile Reinf.	No.	Helix Dia. (mm)	Helix Pitch (mm)	Yield Strain Defl. (mm)	Yield Ratio[1]	Max. Defl. (mm)	Defl. Ratio	Ductility (mm)	Ductility Ratio[2]
OR - PL	2Y16	-	-	-	8.3	1	14.3	1	6	1
OR – SH - P1	2Y16	1	50	15	7.9	0.95	56.1	3.9	48.2	8.0
OR – SH - P2	2Y16	1	50	45	8.3	1	38.6	2.7	30.3	5.1
OR – DH - P1	2Y16	2	25	15	8.2	0.99	60.1	4.2	51.9	8.7
OR – DH - P2	2Y16	2	25	45	8.5	1.02	38.1	2.7	29.6	4.9

1 – OR-PL used as reference value
2 – OR-PL used as reference value

It obvious that the beams with helical reinforcement with pitch greater than the helix diameter will yield in reduction in the beam's capacity. Using the same compressive strength of the concrete for such a beams rather than the confined strength will yield values of maximum loads as shown in parentheses in Table 5.

Table 5 Calculated ultimate moments of tested beams

PARAMETER	BEAM			
	OR-SH-P1	OR-SH-P2	OR-DH-P1	OR-DH-P2
Helix bar diameter, mm	6	6	6	6
Helix tensile strength, MPa	250	250	250	250
Helix Diameter, mm	50	50	25	25
Pitch, mm	15	45	15	45
Comp. strength of concrete, f_c', MPa	70	70	70	70
f_2, MPa	18.85	6.28	37.70	12.57
f_{cc}, MPa	112.28	62.01 (70)	119.81	19.29 (70)
Ultimate Moment, kN-m	16.09	8.89 (10) [(1)]	10.06	1.62 (5.9) [(1)]
Maximum Load, kN	80.5	44.4 (50.2)[(1)]	50.3	8.1 (29.4)[(1)]

[(1)] Values in parentheses are when assuming $f_{cc} = f_c' = 70$ MPa.

EXPERIMENTAL ANALYSIS

Ductility of Increased Tensile Reinforced Beams

As shown in Table 2 an increase in tensile reinforcement increases by about 50% the load resistance of the beam. The large increase in strength was accomplished by a simple increase in tensile steel to the next available deformed bar. However, the increase in strength produced a 50% reduction in structural ductility, which is defined in this paper as the measured deflection between the yield point and final failure regardless of load capacity.

If the amount of tensile steel is further increased, the member will surpass the suggested k_u (the ratio of the depth to the neutral axis from the extreme compressive fibre to the distance to the resultant tensile force in the reinforcing steel) limit of 0.4 [1]. The strength of the member will become enhanced, however the ductility will be significantly reduced. To achieve a suitable value of ductility, most design standards limit the amount of tensile steel.

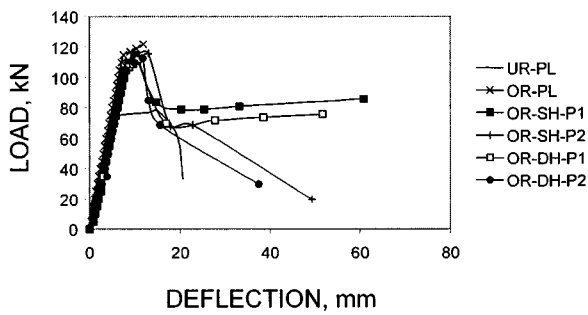

Figure3 Load deflection curves of the test beams

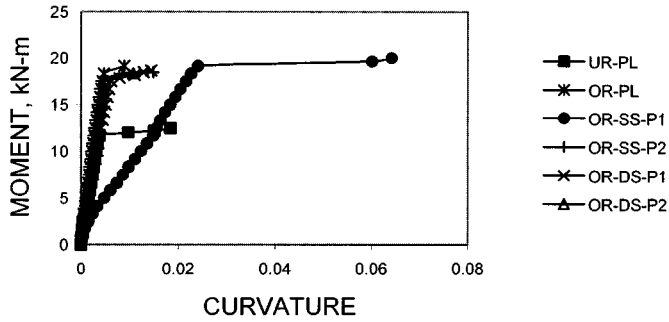

Figure 4 Moment-curvature relationship for tested beams

Ductility of Helical Beams

The application of helical reinforcement made a substantial difference in the flexural behaviour, by significantly increasing the beams' ductility. The flexural strengths of the helical beams were slightly decreased as observed in Table 3. Except for the single helix with 15 mm pitch, all helical beams experienced a 5% reduction in strength when compared with the over-reinforced beams. This was due to early failure of the concrete cover, lowering the compressive resistant area of concrete.

On the other hand, the ductility was significantly increased through the use of helical reinforcement. In the case of the 15 mm pitch, the ductility was increased by a factor of 800% (Figure 2 (c) and Figure 3). The actual increase in ductility is not known, as the final failure of the beams was not observed due to testing equipment limitations. The helical beams with 45 mm pitch experienced a 500% (Figure 2 (d) and Figure 3) increase in ductility; however, high flexural resistance was not sustained.

Comparisons of the single helix and dual helices yielded similar results. In the experiments performed no significant difference in strength or ductility was observed between the two sets of results. As the amount of steel required for the single helix was less than that of the dual helices, the single helix would present the most economical solution.

Both the plain (with no helical reinforcement) and helical beams, behaved in an identical manner prior to the ultimate load. Where the plain beams deflected and then ultimately failed, the helical beams shed their cover and continued to deflect at a substantial load. However, the maximum loading plateau achieved was less for the helical beams. This was due to the concrete cover being separated by the presence of the helical reinforcement.

Once the concrete cover was spalled off, the flexural capacity of the beam decreased. As the beams were quite small, compared with that used in current structures, the concrete cover of 20 mm was a significant portion of the total area as stated above. This left a small amount of concrete to resist all compressive forces. The reduction of flexural loading would not be as predominant in larger sized beams.

CONCLUSIONS

Based on this study, the following observations can be made on the basis of the specimens considered:

- Due to the size of the beams cross sections, a significant cross-sectional area of concrete cover existed and subsequently a significant fall in load capacity occurred due to spalling when the ultimate load was reached.
- The reduced ductility, due to the increase in tensile steel and the use of high strength concrete was overcome through the use of helical reinforcement in the compression region of the beam.
- The use of helical reinforcement was effective due to the lateral confinement of the concrete.

The results from this research are encouraging in improving the strength and ductility of reinforced concrete beams. To improve further the effects of helical reinforcement on beam ductility, additional investigations into helical configuration and structural behaviour is required.

REFERENCES

1. AS3600, Concrete Structures. Standards Australia, 1994, 156 pp.

2. WEBB, J., High-Strength Concrete: Economics, Design and Ductility, Concrete International: Design and Construction, ACI, Vol 15, No 1, Jan. 1993, pp 27-32.

3. CCAA, High-Strength Concrete, Cement and Concrete Association of Australia and National Ready Mixed Concrete Association of Australasia, 1992.

4. PESSIKI, S. and PIERONI, A., Axial Behaviour of Large-Scale Spirally-Reinforced High-Strength Concrete Columns, ACI Structural Journal, Vol 94, No3, May-June 1997, pp 304-314.

5. VAN, B. and MONTGOMERY, D., High-Performance Concrete Containing Limestone Modified Cements. International Conference on HPHSC, Perth, Australia, 1998, pp 701-713.

BEHAVIOUR OF SHALLOW STRIP FOUNDATIONS WITH STRUCTURAL SKIRTS RESTING ON DENSE SAND

M Y Al-Aghbari

Sultan Qaboos University

Oman

A J Khan

BUET University

Bangladesh

ABSTRACT. Skirts of sufficient stiffness may be used for improving the bearing capacity of an existing shallow concrete foundation or for obtaining enhanced bearing capacity of a new shallow foundation. The degree of improvement of bearing capacity for skirt foundations is likely to depend on several factors namely foundation base friction factor, skirt depth factor, skirt side roughness factor and soil compressibility factor. A series of small tank testing was carried out to study the effect of these factors on the bearing capacity of foundations with skirts. On the basis of these test results a modified bearing capacity equation for the centrally loaded foundation with skirts has been suggested. The results obtained from this proposed equation show that the use of structural skirts can produce enhanced bearing capacity ratios in the range of 1.4 to 3.5, depending on particular geometric and loading condition.

Keywords: Skirt foundation, Skirt factor, Extreme loading condition, Bearing capacity, Improvement ratio.

M Y S Al-Aghbari is an Assistant Professor in the Department of Civil Engineering, Sultan Qaboos University, His research focuses mainly on behaviour of shallow foundations with structural skirts.

A J Khan is an Assistant Professor in the Department of Civil Engineering, BUET University, Dhaka-1000, Bangladesh.

INTRODUCTION

Foundation resting on sand has been widely employed and the relevant theory for the calculation of ultimate bearing capacity is available since the proposal of Terzaghi in 1943. It is evident from the general shear failure mechanism involved in the development of bearing capacity theory, everything else remaining the same, the bearing capacity of a foundation resting on a homogeneous layer of sand increases with the increase in width of the foundation. In effect, an increase in width of the footing increases the total length of the failure surface which mobilises higher shear resistance than that for a footing with smaller width. It is therefore plausible to envisage that structural skirts may be fixed to the edges of shallow foundations to increase the length of failure surface that would develop under extreme central vertical loading condition and therefore improve the bearing capacity of the foundations resting on sand.

Structural skirts fixed to the edges of shallow foundations have been used for a considerable time in marine and other situations where water scour may be a problem. Bransby et al (1998) have provided a valuable detailed consideration of their use in such applications. However, the use of such structural skirts in conjunction with conventional shallow structural foundations has not been widely employed, nor have the improvements in bearing capacity occurring from their use been investigated in detail. On this basis an experimental study has been undertaken to establish the degree of improvement in ultimate bearing capacity to be gained from increasing the effective depth of shallow strip foundations on dense sand by fixing structural skirts to their edges. The various factors influencing the bearing capacity improvements to be derived from the use of these skirts are identified and combined into a Skirt Factor. It is suggested that this Skirt Factor can be introduced into the general ultimate bearing capacity equation for shallow strip foundations resting on dense sand.

BEARING CAPACITY EQUATIONS FOR SHALLOW STRIP FOUNDATIONS WITH STRUCTURAL SKIRTS RESTING ON DENSE SAND

Terzaghi (1943) first proposed a formula for the ultimate bearing capacity of shallow strip foundations on dense sand subjected to central vertical loading, Figure 1. This has the following form:

$$q_{ult} = \gamma D_f N_q + \tfrac{1}{2} B \gamma N_\gamma \qquad (1)$$

where q_{ult} = ultimate bearing capacity
γ = unit weight of the soil
D_f = foundation depth
B = foundation width
N_q and N_γ are bearing capacity factors

Values for N_q and N_γ were given by Terzaghi (1943) and related to the peak angle of friction (ϕ'). Following this many other researchers have proposed alternative values for the bearing capacity factors, based on different assumptions, e.g. Meyerhof (1963), Hansen (1970) and Vesic (1973).

For shallow strip foundations with structural skirts resting on dense sand and subjected to central vertical load, Figure 2, modifications to the general ultimate bearing capacity equation are required.

These are as follows:

i) For all situations, the soil above the lower edges of the skirts should be treated as a surcharge, in a similar manner to that proposed for shallow strip foundations by Terzaghi (1943).

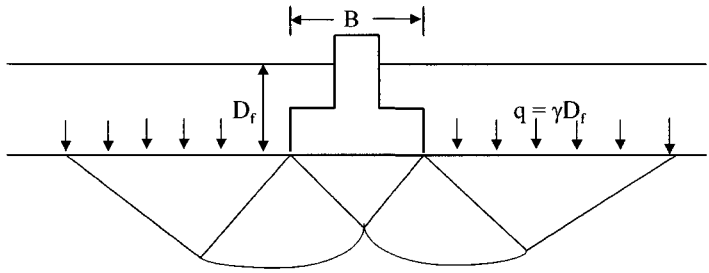

Figure 1 Bearing capacity failure mechanism in soil under a rough rigid continuous foundation subjected to vertical central load

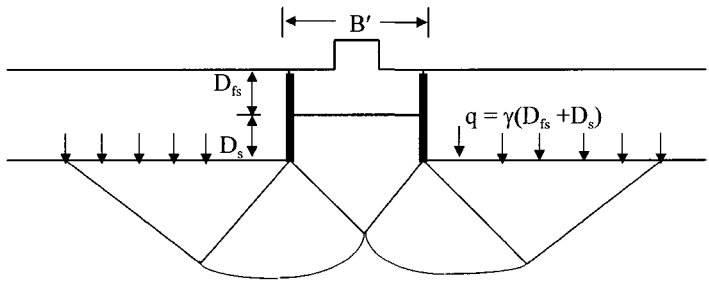

Figure 2 Bearing capacity failure mechanism in soil under continuous foundation with structural skirt subjected to vertical central load

ii) To determine the ultimate bearing capacity of a shallow strip foundation with structural skirts, a Skirt Factor (F_γ) should be introduced into the second part of the general equation, to take account of all the characteristics of the structural skirts, the soil, the foundation and the loading, which influence the ultimate bearing capacity of the foundation. Thus the modified ultimate bearing capacity equation may be written as:

$$q_{ult} = \gamma\,(D_{fs} + D_s)\,N_q + \tfrac{1}{2}\,B'\,\gamma\,N_\gamma\,F_\gamma \qquad (2)$$

where D_{fs} = depth to the foundation base below ground level
D_s = depth to the lower edge of the skirt below the foundation base
B' = total foundation width with skirts ($B + 2B_s$)
B_s = skirt thickness

The Skirt Factor (F_γ) is likely to be influenced by:

Angle of friction of the base of the foundation , (δ_f).
Angle of friction of the side of the skirt, (δ_s).
Compressibility of the soil between the skirts.

The Skirt Factor (F_γ) may now be written in the following form:

$$F_\gamma = F_{\gamma f} \cdot F_{\gamma r} \cdot F_{\gamma c} \quad (3)$$

where $F_{\gamma f}$ = Foundation base friction factor.
$F_{\gamma r}$ = Skirt side roughness factor.
$F_{\gamma c}$ = Soil compressibility factor.

Employing Equations 1, 2 and 3, the improvements in bearing capacity to be derived from the use of structural skirts can be determined for central vertical loading condition.

TEST APPARATUS, PROCEDURES AND MATERIALS

Testing on small scale foundation was performed in a test tank formed by a rigid steel frame and glass side. The inner dimensions of the tank were 600mm long, 300mm deep and 150mm wide, (Figure 3). The foundation was placed centrally across the width of the tank. It was constructed from smooth steel plate and was 50mm wide and 150mm long. The skirts are manufactured from smooth steel sheets. Central vertical loads were applied using a triaxial test frame. A load cell measured the applied load and a LVDT measured the displacement of the foundation. At the beginning of any test, the glass side plates were cleaned with acetone and lubricated with silicon grease. Detailed lubrication method is given by Al-Aghbari (1999).

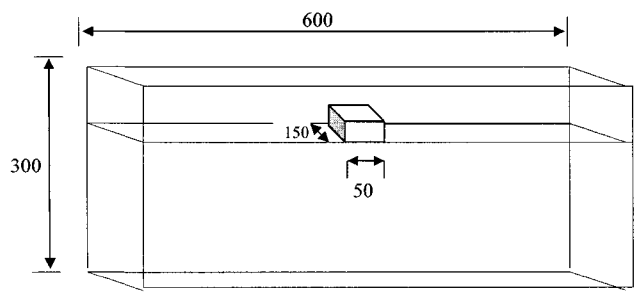

All dimensions in mm

Figure 3 The dimensions of the tank

The sand filling the tank was Leighton Buzzard Sand with a particle size range from 0.3 to 2.0mm and mean particle diameter of 0.82mm. The sand was placed in the tank by a sand raining technique and an uniform dense state achieved, (a relative density of 86 per cent). Detailed description of the sand placement and foundation and skirts installation are given by Al-Aghbari (1999). The peak angle of friction for the dense sand was determined over the confining stress range 40 to 200 kN/m^2 using the shear box, triaxial and plane strain apparatus and found to be 45°, 46° and 49°, respectively.

The angle of friction between the dense sand and smooth steel skirt was determined in the shear box over the same stress range and found to be 27°. The skirts were also treated to make them smoother or rougher. The angles of friction between the dense sand and the treated steel skirt were found to vary from 15° up to a maximum value of 37° depending upon the surface treatment employed for the skirts.

RESULTS FROM TESTS USING SHALLOW STRIP FOUNDATIONS WITHOUT STRUCTURAL SKIRTS

The data from the bearing capacity tests using strip foundations without skirts were compared with the theoretical ultimate bearing capacity. For the comparisons between the experimental and theoretical computations, a representative value of the peak angle of friction for the soil (ϕ') is required. A value of $\phi' = 47.5°$ is selected which is mid-way between the triaxial and plane strain test values. Figure 4 shows that the data obtained from the test falls well within the spread of the valus obtained using the equations proposed by Terzaghi (1943) Meyerhof (1963), Hansen (1970) and Vesic (1973).

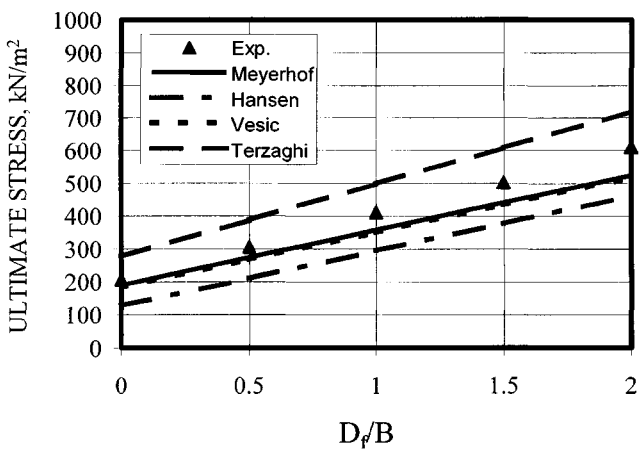

Figure 4 Theoretical and experimental ultimate bearing capacities at different depths using the operational value of $\phi' = 47.5°$

RESULTS FROM TESTS USING STRIP FOUNDATIONS WITH STRUCTURAL SKIRTS

The test programme investigated separately each influence factor within the Skirt Factor (F_γ). The results are given in Table 1. The tests undertaken are analyzed in the following sections:

Table 1 Vertical Testing Programme, Foundation with Skirts

TEST No.	D_S/B'	FOUNDATION BASE FRICTION δ_f	SKIRT SIDE FRICTION δ_s	RELATIVE DENSITY OF SOIL BETWEEN THE SKIRTS D_r	q_u kN/m^2	FACTORS TO BE STUDIED
1	0.04	27°	27°	89	353.4	
2	0.04	35°	27°	89	352.0	$F_{\gamma f}$
3	0.04	37°	27°	89	355.3	
4	0.8	27°	15°	89	521.3	
5	0.4	27°	27°	89	459.8	
6	0.8	27°	27°	89	573.2	
7	1.2	27°	27°	89	672.9	
8	1.6	27°	27°	89	722.9	
9	0.4	27°	35°	89	490.8	$F_{\gamma r}$
10	0.8	27°	35°	89	619.2	
11	1.2	27°	35°	89	741.9	
12	0.4	27°	37°	89	494.8	
13	0.8	27°	37°	89	653.8	
14	1.2	27°	37°	89	794.7	
15	1.21	27°	27°	86	680.4	
16	1.21	27°	27°	54.8	705.8	$F_{\gamma c}$
17	1.21	27°	27°	37.8	718.6	
18	1.21	27°	27°	12	747.1	

Foundation Base Friction Factors ($F_{\gamma f}$)

Tests were conducted on surface foundations with a range of base friction values. Three surface foundations without skirts and with different Foundation Base Frictions (δ_f) were carried out. The same tests of surface foundation were repeated with skirts using a very short skirt with a Skirt Depth Ratio (D_s/B) of only 0.04. The Foundation Base Friction (δ_f) and the peak angle of friction (ϕ') of the soil, were related using the Base Friction Ratio ($\tan\phi'/\tan\delta_f$).

The test results were plotted in the form of Foundation Base Friction Factor ($F_{\gamma f}$) against the Base Friction Ratio ($\tan\phi'/\tan\delta_f$), as shown in Figure 5, and indicate that the following relationship can be assumed:

$$F_{\gamma f} = 0.5\,[1+(\tan\phi'/\tan\delta_f)] \quad (4)$$

where ϕ' : Operational Value for the Peak Angle of Friction of the soil
δ_f : Foundation Base Friction obtained by direct shear testing.

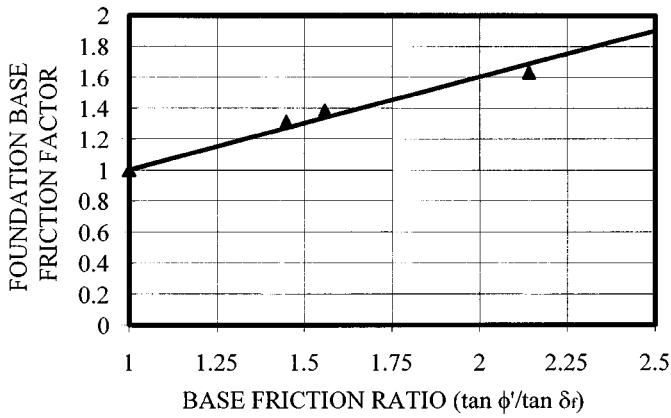

Figure 5 The relationship between foundation base friction factor, $F_{\gamma f}$, and base friction ratio ($\tan\phi'/\tan\delta_f$)

Skirt Side Roughness Factors ($F_{\gamma r}$)

The test series referred to above were extended to include different Skirt Side Friction values of 15, 27, 35 and 37° for different values of Ds/B′. The data plotted is in the form of Skirt Side Roughness Factor ($F_{\gamma r}$) against Skirt Depth Ratios (Ds/B′) for different Side Friction Ratio ($\tan\delta_s/\tan\delta_f$), as shown in Fig. 6, and the following relationship is obtained:

$$F_{\gamma r} = 0.35\,[\,(\tan\delta_s/\tan\delta_f) - 1]\,D_s/B' + 1 \quad (5)$$

Where δ_f and δ_s are obtained by direct shear testing.

Soil Compressibility Factors ($F_{\gamma c}$)

Tests were conducted on surface strip foundations with Skirt Depth Ratios (D_s/B') of 1.21. The Relative Density of the soil between the skirts was varied from 12 to 89 %. Comparisons were made between these test data and data from a strip foundation without structural skirts but with the same overall depth. The Soil Compressibility Factor ($F_{\gamma c}$) so calculated were then plotted against the Relative Density (D_r) of the soil between the skirts, as shown in Figure 7, and the following relationships is obtained:

$$F_{\gamma c} = 1.20 - 0.002\,D_r \quad (6)$$

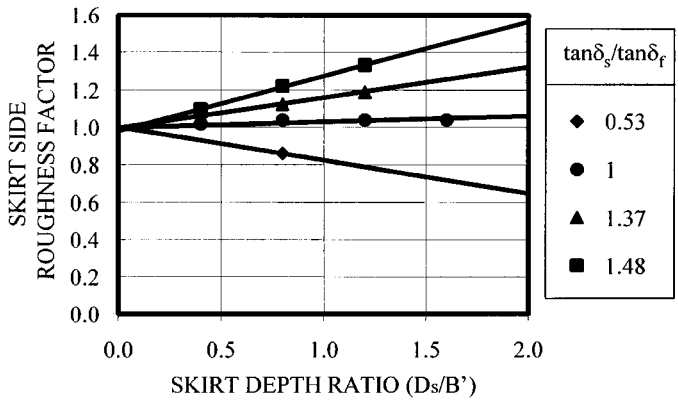

Figure 6 The relationship between skirt side roughness factor, $F_{\gamma r}$, and skirt depth ratio (Ds/B') for different skirt side friction values ratio ($\tan\delta_s/\tan\delta_f$)

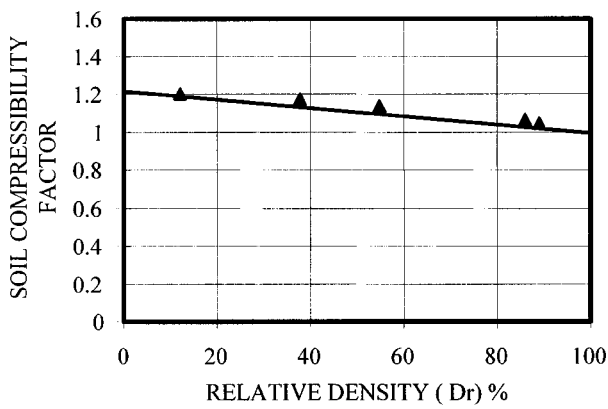

Figure 7 The relationship between soil compressibility factor, $F_{\gamma c}$, and relative density (D_r) of the soil between the skirts

Equation for Skirt Factor

On the basis of the test programme with the model foundation and the analysis described above, it was shown that some of the assumed influence factors were not significant. Therefore, the Skirt Factor (F_γ) may be taken to be as follows:

$$F_\gamma = \{0.5\,[1+(\tan\phi'/\tan\delta_f)\}\,.\{\,0.35\,[\,(\tan\delta_s/\tan\delta_f)-1]\,D_s/B'+1\}.\{1.2-0.002D_r\} \quad (7)$$

The above Skirt Factor (F_γ) can be used to estimate the improvements that can be derived from the use of structural skirts fixed to the edges of shallow strip foundation resting on dense sands.

PREDICTED IMPROVEMENTS DERIVED FROM THE USE OF STRUCTURAL SKIRTS

Equations 1, 2 and 7 can be used to predict the bearing capacity of strip footing with structural skirts resting on sand. To identify the likely magnitudes of these improvements, typical values were assigned to the various design parameters as follows:

Peak Angle of Friction of the Soil (ϕ') = 30 to 50°

Angle of Side and Base Friction of the Foundation (δ_f) = ($^2/_3$)ϕ'

Angle of Side Friction of the Structural Skirts (δ_s) = 0.4ϕ'

Relative Density of the Soil between the skirts (D_r) = 90%

Skirt Depths (D_s) = 0.5 and 1.0B

Skirt Thickness B_s = 0.05B

Eccentricity of the loads at the base of the skirts (e) = < B′/6

Using these values the Skirt Factor is in the range:

F_γ = 1.20 to 1.36

Calculations to determine the improvements to be gained from the use of structural skirts, were undertaken using the bearing capacity factors suggested by Terzaghi (1943), Meyerhof (1963), Hansen (1970) and Vesic (1973), and the skirts factor. The results obtained from these calculations are given in Table 2. They are presented in terms of Improvement Ratio, that is the ratio of the ultimate bearing capacity for strip foundations with structural skirts over the bearing capacity for strip foundation without structural skirts.

Table 2 Improvement ratios for ultimate bearing capacity for central vertical loading

$D_f = D_{fs}$	D_s	IMPROVEMENT RATIOS FOR PEAK ANGLES OF FRICTION (ϕ') = 30 to 50°			
		Terzaghi (1943)	Meyerhof (1963)	Hansen (1970)	Vesic (1975)
0	0.5	2.5-1.8	2.5-1.8	2.5-2.0	2.3-1.9
	1.0	3.4-2.0	3.4-2.0	3.5-2.4	2.9-2.1
0.5	0.5	1.7-1.6	1.7-1.6	1.7-1.6	1.7-1.6
	1.0	2.1-1.8	2.1-1.8	2.1-1.9	2.0-1.8
1.0	0.5	1.4-1.5	1.4-1.5	1.4-1.5	1.5-1.5
	1.0	1.7-1.6	1.7-1.6	1.7-1.7	1.7-1.6

Overall, the calculated values of Improvement Ratio suggest that the benefits to be gained from the use of structural skirts are very significant and that this method of bearing capacity improvement in sand is of practical value.

DISCUSSION AND CONCLUSIONS

An equation has been proposed for the estimation of the bearing capacity of shallow strip foundations with structural skirts resting on sand. This equation is a modified version of the presently widely adopted general ultimate bearing capacity equation. The characteristics of the foundation, skirts, soil and loading which influence the bearing capacity of foundations with structural skirts were individually quantified and combined to determine the values of the Skirt Factor used in the modified bearing capacity equation.

On the basis of this experimental study and the comparisons made using various bearing capacity theories it is concluded that the use of structural skirts to improve the bearing capacity of new or existing shallow strip foundations resting on sand is a technically viable methodology. These comparisons show that the use of structural skirts can produce enhanced bearing capacity ratio in the range 1.4 to 3.5, depending on the particular geometric and loading conditions.

REFERENCES

1. Al-AGHBARI, M.Y. S., Bearing capacity of shallow strip foundation with structural skirts resting on dense sand, Ph.D.Thesis, University of Strathclyde, Glasgow, UK, 1999.

2. BRANSBY, M.F AND RANDOLPH, M.F, Combined loading of skirted foundation, Geotechnique 48, No 5, 1998, pp. 637-655

3. HANSEN, J.B., A revised and extended formula for bearing capacity, Bulletin No.28, Danish Geotechnical Institute, Copenhagen, 1970, pp. 5-11.

4. MEYERHOF, G.G., Some recent research on the bearing capacity of foundations, Can. Geotech. J., Vol. 1, 1963, pp. 16-26.

5. TERZAGHI, K., Theoretical Soil Mechanic, John Wiley & Sons, New York. 1943.

6. VESIC, A.S., Analysis of ultimate loads of shallow foundations, Proc. ASCE, J. of SMFED, Vol. 99, SM1, 1973, pp. 45-73.

THEME SIX:

CONCRETE FOR SPECIALIST SITUATIONS

Keynote Paper

NUCLEAR POWER PLANT CONCRETE STRUCTURES – AGING CONSIDERATIONS

D J Naus
Oak Ridge National Laboratory

B R Ellingwood
Georgia Institute of Technology

J I Braverman
Brookhaven National Laboratory

H L Graves, III
U.S. Nuclear Regulatory Commission

United States of America

ABSTRACT. Concrete structures in nuclear power plants provide foundation, structural support, biological shielding, containment, and protection against internal and external hazards. Aging of these structures occurs and has the potential, if not controlled, to increase the risk to public health and safety. Research providing guidance on aging management of reinforced concrete structures is summarized. Topics include a materials property database, an aging assessment methodology to identify critical structures and degradation factors, guidelines and evaluation criteria for use in condition assessments, and a reliability-based methodology for current condition assessments and estimations of future performance. Fragility analysis is used to compare the response of a degraded and undegraded propped cantilever beam. Several international activities addressing aging of nuclear power plant concrete structures are also summarized.

Keywords: Aging management, Condition assessment, Durability and aging, Fragility analysis, In-service inspection, Material properties database, Nuclear power, Probability theory, Reliability, Repair, Structural engineering

D J Naus, is a senior development staff member in the metals and ceramics division at the Oak Ridge national laboratory. His research interests are related to aging management of nuclear power plant civil engineering structures and he is a member of several ACI, ASME, and RILEM technical committees.

B R Ellingwood, is college of engineering distinguished professor and chair of the school of civil and environmental engineering at the Georgia Institute of Technology. His research focuses on applications of methods of probability and statistics to structural engineering.

J I Braverman, is a research engineer staff member in the nuclear energy and infrastructure systems division at Brookhaven national laboratory. His research currently deals with age-related degradation issues of structures and passive components at nuclear power plants.

H L Graves, III, is a senior structural engineer at the U.S. Nuclear Regulatory Commission. His research interests are related to structural aging, soil-structure interaction, and anchorage to concrete. He is a member of ACI Committees 349, Concrete nuclear structures, and 355, Anchorage to concrete, and a member of ASME Section XI Working group on containment.

INTRODUCTION

All commercial nuclear power plants (NPPs) contain concrete structures whose performance and function are necessary for protection of the safety of plant operating personnel, the general public, and the environment. Structural loads incurred by these structures during normal plant operation are generally not significant enough to cause appreciable degradation. Nuclear power plants, however, involve complex engineering structures and components operating in demanding environments that potentially can challenge the high level of safety (i.e., safety margins) required throughout the operating life of the plant. Aging can occur with the passage of time and has the potential, if its effects are not controlled, to affect the engineering properties, structural resistance/capacity, failure mode, and location of failure initiation.

SAFETY-RELATED CONCRETE STRUCTURES

The reinforced concrete structures in NPPs are designed according to consensus codes and standards to withstand loads from a number of low-probability external and internal events, such as earthquakes, tornadoes, and loss-of-coolant accidents (LOCAs). Although these structures are essentially passive under normal operating conditions, they play a key role in mitigating the impact of extreme environmental events such as earthquakes, high winds, and tornadoes. Moreover, the importance of these structures in accident mitigation is amplified by the so-called "common cause" effect, in which failure of a structure may lead to failure or loss of function of appurtenant mechanical or electrical components and systems.

Each pressurized-water reactor (PWR) or boiling-water reactor (BWR) unit is housed within a much larger metal or concrete containment. The primary purpose of the containment is to prevent the release of fission products to the environment in the event of a LOCA in the primary system and to provide a shield against radiation under normal operation. In addition to being designed to withstand internal pressures and temperatures resulting from design basis events, containments are designed to provide protection against severe external events. Concrete containments for PWRs are fabricated from reinforced concrete, that in some cases may be post-tensioned, and enclose the entire primary circuit (i.e., pressure vessel, steam generators, and piping). Although the majority of BWR plants utilize a steel containment vessel, a number of units utilize either prestressed- or reinforced-concrete vessels. Typical material systems used to fabricate concrete containments include: moderate heat of hydration and sulfate-resistant portland cement, fine and coarse aggregate and water obtained primarily from local sources, carbon steel deformed bar reinforcement having a minimum yield strength of 415 MPa, and wire or strand post-tensioning systems having capacities to 10.7 MN. Leak-tightness of the U.S. concrete containments is provided by a thin steel liner (e.g., 6 mm in thickness) that is anchored to the concrete. Depending on the functional design, U.S. concrete containments can be on the order of 40 to 50-m diameter and 60 to 70-m high, with dome and wall thicknesses from 0.9 to 1.4 m, and base slabs from 2.7 to 4.1 m. Descriptions of other concrete-based structures are provided elsewhere [1].

DEGRADATION CONCERNS

Degradation of concrete can be caused by adverse performance of either its cement-paste matrix or aggregate materials under chemical or physical attack. Chemical attack may occur

in several forms: efflorescence or leaching, sulfate attack, delayed ettringite formation, attack by acids and bases, salt crystallization, and alkali-aggregate reactions. Physical attack mechanisms for concrete include freeze-thaw cycling, thermal exposure/thermal cycling, settlement, abrasion/erosion/cavitation, and fatigue or vibration. Degradation of steel reinforcing materials can occur as a result of corrosion, irradiation, elevated temperature, or fatigue effects. Prestressing steels are susceptible to the same degradation mechanisms as the steel reinforcement, plus loss of prestressing force, primarily due to steel relaxation and concrete creep and shrinkage. Examples of some of the degradation occurrences that have been observed in NPP structures include basemat cracking, prestressing tendon wire failure, steel reinforcement corrosion in water-intake structures, tendon gallery concrete leaching, and containment dome concrete freeze/thaw damage [1]. Current aging concerns are related to inaccessibility of reinforced concrete basemats for inspection, availability of proven nondestructive evaluation techniques for inspection of thick heavily-reinforced concrete sections, and corrosion of embedded portions of the steel pressure boundary (liner). Even though concrete structural components generally have substantial structural margins when properly designed and constructed, available margins for aged or degraded structures are not known.

STRUCTURAL AGING PROGRAM

The Structural Aging (SAG) Program had the overall objectives of providing background data and information for identification and evaluation of the potential structural degradation processes; identifying issues to be addressed during continued service reviews of NPP concrete structures, as well as criteria, and their bases, for resolution of these issues; assessing relevant in-service inspection, structural assessment or remedial measures programs; and formulating methodologies to perform current assessments and reliability-based life predictions of reinforced concrete structures. Activities were conducted under three task areas: (1) materials property database/service life, (2) structural component assessment/repair technologies, and (3) quantitative methodology for continued service determinations.

Material Properties Database/Service Life

Development of a reference source that contains data and information on the time variation of material properties under the influence of pertinent environmental stressors and aging factors provides a means to assist in the prediction of potential long-term deterioration of critical concrete structural components and to establish limits on hostile environmental exposure for these structures. The Structural Materials Information Center consists of the *Structural Materials Handbook* and the *Structural Materials Electronic Database* [1]. The *Structural Materials Handbook* is an expandable, hard-copy reference document containing complete sets of data and information for each material (e.g., material composition, constituent material properties, and performance and analysis information useful for structural assessments and safety margins determinations). The *Structural Materials Electronic Database* is an electronically accessible version of the *Structural Materials Handbook* providing an efficient means for searching the various database files to locate materials with similar characteristics or properties. Reference sources and testing of concrete samples obtained from NPP facilities have been used to develop over 140 material property databases for SMIC [2].

A review and evaluation was conducted of accelerated aging techniques and tests that can either provide data for service life models or that by themselves can be used to predict the service life or performance of reinforced concrete [3]. Mathematical models were identified and evaluated for each of the degradation processes that can potentially impact the performance of concrete structures. A major conclusion of this study was that theoretical models need to be developed, rather than relying solely on empirical models, because predictions from theoretical models are more reliable, far less data are needed, and the theoretical models would have wider applications.

Structural Component Assessment/Repair Technologies

New structures can be designed for improved durability based on operating experience (e.g., use of high performance concrete materials). Existing structures, however, have already been designed and constructed, so apart from possibly the addition of barrier materials and sealants to accessible surfaces to prevent ingress of hostile environments, the most prudent approach to maintaining adequate structural performance is through an aging management program that involves application of in-service inspection and maintenance strategies. Primary activities under this task have addressed structural component prioritization, in-service inspection and condition assessment, and repair practices.

Structural Component Prioritization

For practical reasons, structural condition assessments must focus on a few critical structural components that are dominant contributors to plant risk. A methodology has been developed that provides a logical basis for identifying the critical concrete structural elements and the degradation factors that can potentially impact their performance [4]. This approach has been applied to NPP concrete structures through the use of plant logic models to identify structural components of most importance. Selection of structural components for evaluation can also be based on an evaluation of the impact on plant risk due to structural aging [5].

In-Service Inspection and Condition Assessment

The stability and durability of a concrete structure can only be guaranteed when it has an appropriate safety margin against expected loads and environmental influences during its intended lifetime. To assess deterioration in a concrete structure, an inspection is needed. In-service inspection programs for safety-related NPP reinforced concrete structures have the primary goal of ensuring that these structures have sufficient structural margins to continue to perform in a reliable and safe manner. A secondary goal of these programs is to provide a means to identify any environmental stressor or aging factor effects before they reach sufficient intensity to potentially degrade structural margins.

The condition survey usually begins with a review of the "as-built" drawings and other information pertaining to the original design and construction so that information, such as accessibility and the position and orientation of embedded steel reinforcing and plates in the concrete, is known prior to the site visit. Next is a detailed visual examination of the structure to document easily obtained information on instances that can result from or lead to structural distress. Locations and widths of cracks are drawn on copies of project plans and degraded areas of significance noted and measured. The condition of the surrounding

structures is examined to detect occurrence of differential settlement or note aggressiveness of the local operating environment. Distress associated with cracks such as efflorescence, rust stains, or spalling is noted. After the visual survey has been completed, the need for additional surveys such as delamination plane, corrosion, or pachometer is determined. Results of the visual and delamination surveys are used to select portions of the structure that will be studied in greater detail. To locate areas of corrosion activity within reinforced concrete, copper-copper sulfate half-cell studies can be performed. Where significant chloride penetration is suspected, concrete powder samples or cores should be removed from several depths extending to and beyond the embedded outer layer of reinforcing steel. Where there is evidence of severe corrosion, the steel bar should be uncovered to allow visual inspection and measurement of cross-sectional area loss. Any elements that appear to be structurally marginal, due either to unconservative design or deterioration effects, are identified and appropriate calculation checks made. After all the data and information have been collated and studied, a report is prepared.

Two approaches have been developed for assistance in the classification and treatment of results that might emanate from condition assessments of NPP reinforced concrete structures – visual-based and degradation-based. These approaches primarily are based on the results of visual inspections since these inspections provide the cornerstone of any condition assessment program for concrete structures.

The visual-based approach uses a "three-tiered" hierarchy: acceptance without further evaluation, acceptance after review, and additional evaluation required [6]. If conditions found do not conform to criteria for acceptance without further evaluation, a review is required that involves determining the likely source of degradation, its activity level, and its net effect on the component. Possible approaches resulting from the review include acceptance as-is, further evaluation using enhanced visual inspection (e.g., magnification), scheduling follow-up inspections at a later date, or use of nondestructive or destructive testing techniques. If conditions fail to conform to criteria for acceptance after review, an evaluation is performed to determine the appropriate course of action. This will generally involve extensive application of both nondestructive and destructive testing methods. Detailed analytical evaluations frequently will be required to better characterize the current condition of the structure and provide the basis for formulation of a repair strategy (if needed).

The degradation-based approach is founded on the concept that degradation of a component in service is manifested in physical evidence or signs (e.g., measurable values), and that these signs can be categorized or classified into distinct stages or conditions in accordance with their potential impact on performance (e.g., structural margins). Cracks are a frequent manifestation of reinforced concrete degradation and are significant in that they may indicate major structural problems (e.g., active cracks), provide an avenue for ingress of hostile environments (e.g., chloride ions), and inhibit a structure from meeting its performance requirements (e.g., water retention). Crack width, location, and environmental exposure are important. Several studies have attempted to relate crack widths to environmental factors through specified limits to reduce the potential for ingress of contaminants [7]. Information is available on classification of environmental exposure conditions in terms of aggressiveness, chemical attack of concrete by soils and water containing aggressive agents, and influence of moisture condition on several durability processes (e.g. carbonation,

corrosion, frost attack, and chemical attack) [8]. This information has been used to prepare example damage-state charts to assist in the resolution of results obtained from in-service inspections or testing [9].

Remedial/Preventative Measures Considerations

Reinforced concrete structures almost from the time of construction may start to deteriorate due to environmental exposure. Deterioration rate is dependent on the component's structural design, materials selection, quality of construction, curing, and aggressiveness of environmental exposure. Termination of a component's service life occurs when it can no longer meet its functional and structural requirements. Results provided through periodic application of in-service inspection techniques as part of a condition assessment program can be used to develop and implement a remedial action prior to the structure achieving an unacceptable level of performance.

Damage repair practices commonly used for reinforced concrete structures in Europe and North America have been reviewed. In Europe, repair solutions have concentrated on repair of damage resulting from corrosion of steel reinforcement [10] and include: (1) realkalization; (2) limiting the corrosion rate by changing the environment (e.g., drying) to reduce the electrolytic conductivity; (3) steel reinforcement coating (e.g., epoxy); (4) chloride extraction; and (5) cathodic protection. In North America, activities have primarily addressed repair of infrastructure-related facilities (e.g., highways and bridges). A report has been prepared that summarizes techniques and materials available for mitigation and repair of concrete experiencing cracking, spalling, delaminations, water seepage, honeycomb and voids, alkali-aggregate attack, external sulfate attack, and corrosion damage [7].

Quantitative Methodology for Continued Service

Evaluation of structures for continued service should provide quantitative evidence that their capacity is sufficient to withstand future demands within the proposed service period with a level of reliability sufficient for public safety. Structural aging causes the integrity of structures to evolve over time. Uncertainties that complicate the evaluation of aging effects arise from a number of sources: inherent randomness in structural loads, initial strength, and degradation mechanisms; inadequacies in nondestructive evaluation; and shortcomings in existing methods to account for repair. Any evaluation of the reliability of a reinforced concrete structure during its service life must take into account these effects, plus any previous challenges to the integrity that may have occurred.

Time-Dependent Reliability Approach

Time-dependent reliability analysis methods provide a framework for performing condition assessments of existing structures and for determining whether in-service inspection and maintenance are required to maintain reliability and performance at the desired level. The duration of structural loads that arise from rare operating or environmental events, such as accidental impact, earthquakes, and tornadoes, is short and such events occupy a negligible fraction of a structure's service life. Such loads can be modeled as a sequence of short-duration load pulses occurring randomly in time.

The occurrence in time of such loads is described by a Poisson process, with the mean (stationary) rate of occurrence, λ, random intensity, S_j, and duration, τ. The number of events, N(t), to occur during service life, t, is described by the probability mass function,

$$P[N(t) = n] = \frac{(\lambda t)^n \cdot \exp(-\lambda t)}{n!}; n = 0, 1, 2, \ldots \quad (1)$$

The intensity of each load is a random variable, described by cumulative distribution function (CDF) $F_i(x)$. This process can be generalized to one in which the load process is intermittent and the duration of each load pulse has an exponential distribution,

$$F_{T_d} = 1 - \exp[-t/\tau]; t \geq 0 \quad (2)$$

in which τ = average duration of the load pulse. The probability that the load process is nonzero at any arbitrary time is $p = \lambda\tau$. Loads due to normal facility operation or climatic variations may be modeled by continuous load processes. A Poisson process with rate λ may be used to model changes in load intensity if the loads are relatively constant for extended periods of time. The duration of each load is exponential, with average duration $\tau = 1/\lambda$.

The strength, R, of a reinforced concrete component is described by

$$R = B \bullet R_m(X_1, X_2, \ldots, X_m) \quad (3)$$

in which X_1, X_2, ... are basic random variables that describe yield strength of reinforcement, compressive or tensile strength of concrete, and structural component dimensions or section properties. The function $R_m(\ldots)$ describes the strength based on principles of structural mechanics. Modeling assumptions invariably must be made in deriving $R_m(\ldots)$ and the factor B describes errors introduced by modeling and scaling effects. The probability distribution of B describes bias and uncertainty that are not explained by the model $R_m(\ldots)$ when values of all variables X_i are known. The probability distribution of B can be assumed to be normal. A more accurate behavioral model leads to a decrease in the mean and variability in B and thus in R. Probability models for R usually must be determined from the statistics of the basic variables, X_i, since it seldom is feasible to test a sufficient sample of structural components to determine the cumulative distribution function (CDF) of R directly.

The failure probability of a structural component can be evaluated as a function of (or an interval of) time if the stochastic processes defining the residual strength and the probabilistic characteristics of the loads at any time are known. The strength, R(t), of the structure and applied loads, S(t), are both random functions of time. Assuming that degradation is independent of load history, at any time t the margin of safety, M(t), is

$$M(t) = R(t) - S(t). \quad (4)$$

Making the customary assumption that R and S are statistically independent random variables, the (instantaneous) probability of failure is,

$$P_f(t) = P[M(t) < 0] = \int_0^\infty F_R(x)\, f_S(x)\, dx \quad (5)$$

in which $F_R(x)$ and $f_S(x)$ are the cumulative distribution function of R and probability density function (PDF) of S. Equation (5) provides an instantaneous quantitative measure of structural reliability, provided that $P_f(t)$ can be estimated and/or validated [11]. It does not convey information on how future performance can be inferred from past performance.

For service life prediction and reliability assessment, one is more interested in the probability of satisfactory performance over some period of time, say (0,t), than in the snapshot of the reliability of the structure at a particular time provided by Eqn. (5). Indeed, it is difficult to use reliability analysis for engineering decision analysis without having some time period (e.g., an in-service maintenance interval) in mind. The probability that a structure survives during interval of time (0,t) is defined by a reliability function, L(0,t). If, for example, n discrete loads S_1, S_2, ..., S_n occur at times t_1, t_2, ..., t_n during (0,t), the reliability function becomes,

$$L(t) = P[R(t_1) > S_1, \ldots, R(t_n) > S_n] \tag{6}$$

in which $R(t_i)$ = strength at time of loading S_i.

Taking into account the randomness in the number of loads and the times at which they occur as well as initial strength, the reliability function becomes [12]

$$L(t) = \int_0^\infty \exp\left(-\lambda t\left[1 - t^{-1}\int_0^t F_s(g_i r)dt\right]\right) f_{R_0}(r)\, dt \tag{7}$$

in which f_{R_0} = PDF of the initial strength R_0 and g_i = fraction of initial strength remaining at time of load S_i. The probability of failure during (0,t) is

$$F(t) = 1 - L(t). \tag{8}$$

The conditional probability of failure within time interval (t, t+□t), given that the component has survived up to t, is defined by the hazard function which can be expressed as

$$h(t) = -d \ln L(t)/dt. \tag{9}$$

The reliability and hazard functions are integrally related

$$L(t) = P[R(t_1) > S_1, \ldots, R(t_n) > S_n] \tag{10}$$

The hazard function is especially useful in analyzing structural failures due to aging or deterioration. For example, if the structure has survived during the interval (0, t_1), it may be of interest in scheduling in-service inspections to determine the probability that it will fail before t_2. Such an assessment can be performed if h(t) is known. If the time-to-failure is T_f, this probability can be expressed as

$$P[T_f < t_2 | T_f > t_1] = 1 - \exp\left(-\int_{t_1}^{t_2} h(x)dx\right) \tag{11}$$

In turn, the structural reliability for a succession of inspection periods is

$$L(0,t) = \prod_i L(t_{i-1}, t_i) \exp\left\{\int_{t_{i-1}} h(x)dx\right\} \tag{12}$$

in which $t_{i-1} = 0$ when $i = 1$.

Intervals of inspection and maintenance that may be required as a condition for continued operation can be determined from the time-dependent reliability analysis. Forecasts of reliability enable the analyst to determine the time period beyond which the desired reliability of the structure cannot be assured. At such a time, the structure should be inspected. The density function of strength, based on prior knowledge of the materials in the structure, construction, and standard methods of analysis, is indicated by $f_R(r)$. The information gained during scheduled inspection, maintenance and repair causes the characteristics of strength to change; this is denoted by the (conditional) density $f_R(r|B)$, in which B is an event dependent on in-service inspection. Information gained from the inspection usually involves several structural variables including dimensions, defects, and perhaps an indirect measure of strength or stiffness. If these variables can be related through event B, then the updated density of R following in-service inspection is,

$$f_R(r|B) = P[r < R \le r + dr, B] / P[B] = c\, K(r)\, f_R(r)$$

in which $f_R(r)$ is termed the prior density of strength, K(r) is denoted the likelihood function, and c is a normalizing constant. The time-dependent reliability analysis then is re-initialized following in-service inspection/repair using the updated $f_R(r|B)$ in place of $f_R(r)$. The updating causes the hazard function to be discontinuous.

Optimal intervals of inspection and repair for maintaining a desired level of reliability can be determined based on minimum life cycle expected cost considerations. Preliminary investigations of such policies have found that they are sensitive to relative costs of inspection, maintenance, and failure [13]. If the cost of failure is an order (or more) of magnitude larger than inspection and maintenance costs, the optimal policy is to inspect at nearly uniform intervals of time. However, additional research is required before such policies can be finalized as part of an aging management plan.

Time-dependent reliability concepts are illustrated with a simple conceptual example of a reinforced concrete slab designed using the requirements for flexure strength found in ACI Standard 318 [14]

$$0.9\, R_n = 1.4\, D_n + 1.7\, L_n, \tag{14}$$

in which R_n is the nominal or code resistance, and D_n and L_n are the code-specified dead and live loads, respectively. Three scenarios are considered: (1) the strength of the slab changes with time, initially increasing as the concrete matures and then decreasing due to (unspecified) environmental attack, (2) the strength degrades linearly to 90% of its initial strength at 40 years, and (3) the strength remains constant with time (Figure 1).

In general, the behavior of resistance over time must be obtained from mathematical models describing the degradation mechanism(s) present. The statistics used in this example are provided elsewhere [1].

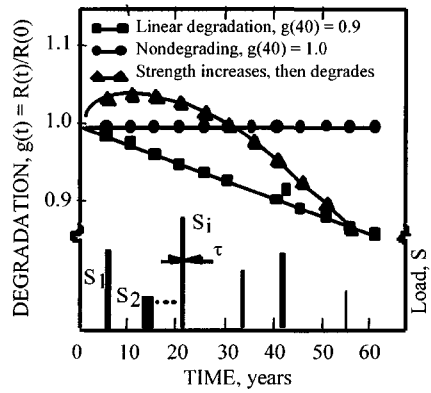

Figure 1 Mean degradation function of one-way slab

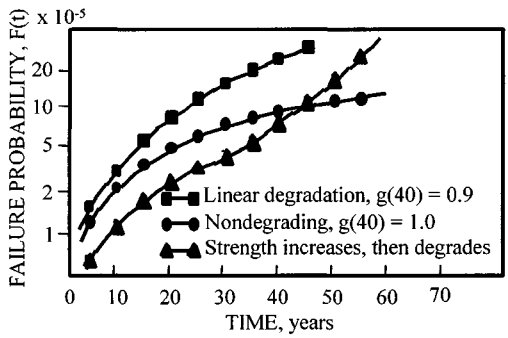

Figure 2 Failure probability of one-way slab

Figure 2 compares the limit state probabilities [F(t) = 1 - L(t) in Eqn. (7)] obtained for the three degradation models considered in Figure 1 for service lives (0,t) ranging up to 60 years. When R(t) = R(0) and no degradation of strength occurs, a result is obtained analogous to what has been done in probability-based code work to date [11]. Neglecting strength degradation entirely in a time-dependent reliability assessment can be unconservative, depending on the time-dependent characteristics of strength.

If we now consider the following conditions involving a single inspection/repair:

a. Every part of the structure is fully inspected and all detected damages are repaired completely.
b. The initiation of damages is described by a stationary Poisson process with a parameter υ = 5/yr that is dependent on the surface area or volume of the structure.

c. Damage grows linearly with time as described below with $\alpha = 1$ (i.e., linear)

$$X_j(t) = \begin{cases} 0 & ; 0 \le t < T_{I_j} \\ C_j\left(t - T_{I_j}\right)^{\alpha} & ; t \ge T_{I_j} \end{cases}$$

in which $X_j(t)$ j = 1, 2, ... is the intensity of damage at time t; T_{Ij}, j = 1, 2, ... are the random initiation times of damage; Cj's are damage growth rates that are identically distributed and statistically independent random variables described by a CDF $F_C(c)$; and α is a deterministic parameter. The assumption of independent Cj's provides a conservative estimate of failure probability. Parameters C and α depend on the degradation mechanism.

d. The degradation rate, C, is lognormally distributed with mean value, $\mu_C = 0.00125$, that corresponds to $E[X(40)|T_I = 0] = 0.05$, and with a coefficient of variation, $V_C = 0.5$.

The effect on the mean degradation function of inspection/repair described by several detectability functions, d(x), is illustrated in Figure 3. The first detectability function considered is a step function in which $x_{th} = 0.03$; in the second, d(x) is linear between x_{min} and x_{max}, where $d(x_{min}) = 0$ and $d(x_{max}) = 1$; in the third and fourth, d(x) has the shape of a lognormal distribution, with mean, $\mu_{x_{th}}$, equal to 0.03, and coefficient of variation, $V_{x_{th}}$, equal to 0.3 or 0.5. It is assumed that inspection/repair is carried out at $t_{R_{in}} = 20$ years. The mean degradation function decreases as $V_{x_{th}}$ increases (that would result in lower reliability); however, the effect of the general shape of d(x) is not significant and decreases with time elapsed since inspection. This insensitivity of the mean degradation to the choice of detectability function suggests that a general detectability function might be approximated for practical purposes by a step function with $x_{th} = \mu_{x_{th}}$. This would be advantageous for NDE technologies currently used for reinforced concrete structures because information on $\mu_{x_{th}}$ may be more readily available than information on d(x).

The effect of multiple inspection/repair and the mean degradation function is illustrated in Figure 4, assuming a step detectability function and the same assumptions as used in the previous example. Inspection/repairs are carried out at 20, 30, 40, and 50 years with $x_{th} = 0.05$ when $E[X(40)|T_I = 0] = 0.05$. For comparison, the mean degradation function for a component without repair and for a component with one repair at 30 years with $x_{th} = 0.01$ is also presented in the figure. With multiple inspections/repairs, the mean degradation function can be kept within a narrow range during the service life of the structure.

RESPONSE OF DEGRADED CONCRETE STRUCTURES

Degradation effects can be quantified with fragility curves developed for both undegraded and degraded components. A fragility analysis assesses, in probabilistic terms, the capability of an engineered system to withstand a specified event. It requires a focus on the behavior of the system as a whole, with an emphasis on what can go wrong. The fragility modeling process leads to a median-centered (or most likely) estimate of system performance, coupled

with an estimate of the variability or uncertainty in performance. Considered below is a reinforced concrete flexural member typical of what could be found in NPPs whose loss of integrity could impact the plant safety envelope. Results are also available for a short reinforced concrete shear wall [15].

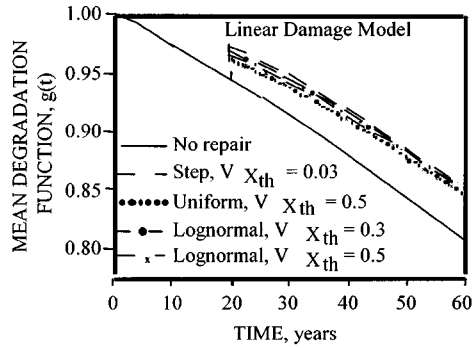

Figure 3 Effect of several detectability functions on mean degradation function of inspection/repair

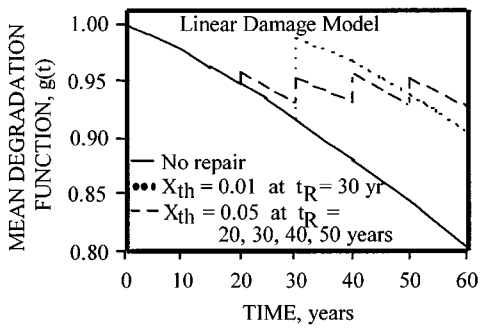

Figure 4 Effect of multiple inspection/repairs on mean degradation function

The structural fragility is modeled by a lognormal cumulative distribution function (CDF),

$$F_R(x) = \Phi[\ln(x/m_R)/\beta_R] \tag{16}$$

in which Φ [ ] = standard normal probability integral, m_R = median capacity, and β_R = logarithmic standard deviation, approximately equal to the coefficient of variation, V_R, when $V_R < 0.3$. Sources of uncertainty impacting structural performance, including both aleatory, β_R (e.g., inherent variability in concrete and steel reinforcement strength, and dimensions) and epistemic, β_U (e.g., simplifying assumptions regarding structural mechanics and data limitations), must be included in the logarithmic standard deviation. In the present analysis, aleatory and epistemic uncertainties are combined through

$$\beta_c = \sqrt{(\beta_R^2 + \beta_U^2)}$$

and β_R is replaced with β_C in Eqn. (16).

Statistical data to describe the strength of reinforced concrete flexural members (beams and slabs) are provided in Table 1 [16]. Epistemic uncertainty arising from idealizations of behavior in the analytical model of the structure is accounted for by the factor β_f, where $\beta_f = 1.04$ with $V_R = 0.07$. Uncertainties are propagated through the analyses using Latin Hypercube Sampling with 19 samples used for each analysis to facilitate probability plotting within the center 90% range of the fragility curve.

Table 1 Structural Response Statistics

PROPERTY	MEAN	V_R	CDF
Concrete (27.6 MPa)			
Comp. str.	24.5 MPa	0.16	N
Splitting strength	2.47 MPa	0.18	N
Init. tangent mod.	26.2 GPa	0.18	
Max. comp. strain	0.004	0.20	N
Grade 60 Reinf.			
Yield strength	455 MPa	0.10	LN
Elastic modulus	200 GPa	NA	

The specific example addressed is a propped cantilever beam (Figure 5) designed using procedures in ACI 318 to accommodate a dead load of 14.6 kN/m and a live load of 43.8 kN/m. Reinforcement ratios in the negative and positive moment regions are 0.0145 and 0.0087, respectively. Evaluating the beam load-deflection behavior according to ACI 318, the loading to produce cracking is 14.4 kN/m, with the first and second plastic hinges occurring at loadings of 105 kN/m (support) and 114 kN/m (3.81 m from fixed support), respectively. Beam deflections at the location of the second plastic hinge when first and second plastic hinges form were 1.17 cm and 1.37 cm, respectively. Finite-element analyses were used to verify these results.

Using information in Table 1, fragility curves were generated for the undegraded and degraded beams. Beam strength for each of the samples was evaluated through

$$w_u = 2\left[M_u^- + M_u^+ L / (L - x)\right] / Lx \qquad (18)$$

in which M_u^- and M_u^+ are, respectively, the negative and positive moment capacities and x is the location of the second plastic hinge. The resulting mean strength was found to be 126 kN/m with $V_R = 0.11$.

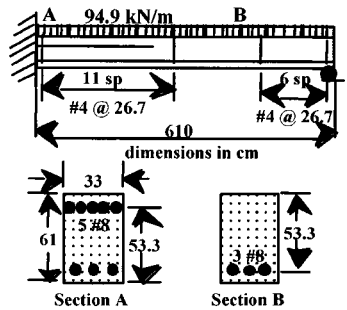

Figure 5 Cantilever beam details

Age-related degradation effects included in the study were loss of steel area and reduction in concrete area. Steel area losses of 20% and 10%, with coefficients of variations of 0.11 and 0.07, respectively, were considered and treated as random variables. Spalling of cover concrete was considered and had a coefficient of variation of 0.36. In addition to individual effects, cover spalling in combination with loss of steel section was also included. The mean and standard deviation for the degraded cases are summarized in Table 2. For the worst case considered, 20% loss of steel area plus bottom spall, the strength of the beam is reduced by less than 18%. This condition is associated with severe concrete section cracking which could be readily observed during an inspection. Current in-service inspections would identify such potential problems before serious degradation could occur.

Table 2 Fragility Curve Statistics

CASE	MEAN CAPACITY kN/m	VR
Undegraded	126.4	0.11
Bottom spall	120.1	0.12
Top spall	117.6	0.12
Top and bottom spall	115.1	0.13
10% loss top and bottom steel	114.0	0.12
20% loss top and bottom steel	106.4	0.13
20% loss steel + spall, at bottom	103.8	0.12
20% loss steel + spall, at top	108.8	0.12

INTERNATIONAL ACTIVITIES

Internationally, about 25% of NPPs have been operating for over 20 years, with some having been in operation for over 30 years. Although the individual national programs (e.g., United Kingdom, France, and Switzerland) focus on the plants within each country, there are common generic aging effects. Issues presented by aging NPPs are therefore of international

interest and experience and information has been exchanged with a view of determining best practice. The principal organizations that have involved in these activities include Réunion Internationale des Laboratoires d'Essais et de Recherches sur les Matériaux (RILEM), Organization for Economic Co-operation and Development - Nuclear Energy Agency (OECD-NEA), and International Atomic Energy Agency (IAEA).

RILEM Committee TC-160 MLN, "Methodology for Life Prediction of Concrete Structures in Nuclear Power Plants," was established in 1994 to review existing guidelines and procedures used to monitor and evaluate concrete structures in NPPs as well as their performance history. In order to provide the basis for development of a life prediction methodology, a series of state-of-the-art papers related to current practices for aging management of concrete structures in NPPs has been prepared (e.g., service life, instrumentation systems, creep methodologies, and probabilistic methods) [17]. The committee also organized an international conference [18] and a workshop [19] on life prediction and aging management of concrete structures.

The Committee on the Safety of Nuclear Installations (CSNI) of the OECD-NEA has established a task group to study aging of NPP concrete structures. The basic mandate of the task group is to review current international (and, where appropriate, national) activities in the area of aging (both structural and functional), and to formulate recommendations for a medium-to-long term program of work. Recommendations of this group [20] are being implemented through a series of workshops addressing specific issues associated with aging: prestress losses in NPP containments, development priorities for non-destructive examination of concrete structures, response of degraded structures (including finite-element analysis techniques), and instrumentation and monitoring of concrete structures. Planned activities include a workshop on repair and condition assessment, and state-of-the-art reports addressing finite-element analysis of concrete structures and electrochemical techniques to detect corrosion.

To assist Member States in understanding aging of structures, systems, and components important to safety, the Safety Division of IAEA in 1989 initiated pilot studies related to evaluation and management of the safety aspects of NPP aging. Concrete containment buildings were included in these studies. Under Phase I [21], paper assessments of the current knowledge on age-related degradation, and its detection and mitigation, were conducted, and recommendations developed for Phase II studies. Phase II activities (comprehensive aging studies) were implemented through IAEA Co-ordinated Research Programs (CRPs) that took place over a three- to five-year period. Under the CRP involving NPP concrete containment buildings two primary activities took place. Under the first activity a questionnaire was developed and sent to approximately 200 plant owners/operators to obtain information regarding aging and its management (i.e., general plant information; inspection, investigation, and preventative maintenance; and age-related degradation experience). Responses representing over 150 nuclear power units were provided from 15 countries. General conclusions resulting from responses were that over half the plants responding had some form of aging management program in place but only about 10% addressed the concrete structures; visual examinations, leakage-rate testing, and testing of prestressing systems were the commonly used methods of inspection; utilities whose containments were instrumented generally used longer inspection intervals; and concrete cracking was the most common form of degradation. Under the second activity results of the

questionnaire and experience of the CRP participants were used to identify current practices for detecting and mitigating the effects of aging, and to provide the technical basis for developing and implementing a systematic aging management program for concrete containment buildings. Drawing on international experience and best practice, a framework for an aging management program for concrete containment buildings was developed that is based on an understanding of the issues involved [22].

ACKNOWLEDGEMENTS

Research sponsored by the Office of Nuclear Regulatory Research, U.S. Nuclear Regulatory Commission, under Interagency Agreement 1886-N604-3J with the U.S. Department of Energy under Contract No. DE-AC05-00OR22725. The U.S. Government retains a nonexclusive, royalty-free license to publish or reproduce the published form of this contribution, or allow others to do so, for U.S. Government purposes. The findings and opinions stated in the paper are those of the authors and not necessarily the views of the employing organizations.

REFERENCES

1. NAUS, D.J., OLAND, C.B., and ELLINGWOOD, B.R., Report on Aging of Nuclear Power Plant Concrete Structures, NUREG/CR-6424, U.S. Nuclear Regulatory Commission, Washington, DC, March 1996.

2. OLAND, C.B., and NAUS, D.J., Summary of Materials Contained in the Structural Materials Information Center, ORNL/NRC/LTR-94/22, Martin Marietta Energy Systems, Inc., Oak Ridge National Laboratory, Oak Ridge, Tennessee, 1994.

3. CLIFTON, J.R., Predicting the Remaining Service Life of Concrete, NISTIR 4712, U.S. Department of Commerce, National Institute of Standards and Technology, Gaithersburg, Maryland, 1991.

4. HOOKHAM, C.J., Structural Aging Assessment Methodology for Concrete Structures in Nuclear Power Plants, ORNL/NRC/LTR-90/17, Martin Marietta Energy Systems, Inc., Oak Ridge National Laboratory, Oak Ridge, Tennessee, March 1991.

5. ELLINGWOOD, B.R., Issues Related to Structural Aging in Probabilistic Risk Analysis of Nuclear Power Plants, J. Rel. Engrg. & System Safety 62(3):171-183, 1998.

6. HOOKHAM, C.J., In-Service Inspection Guidelines for Concrete Structures in Nuclear Power Plants, ORNL/NRC/LTR-95/14, Lockheed Marietta Energy Systems, Inc., Oak Ridge National Laboratory, Oak Ridge, Tennessee, August 1995.

7. KRAUSS, P.D., Repair Materials and Techniques for Concrete Structures in Nuclear Power Plants, ORNL/NRC/LTR-93/28, Martin Marietta Energy Systems, Inc., Oak Ridge National Laboratory, Oak Ridge, Tennessee, March 1994.

8. COMITE EURO-INTERNATIONAL DU BETON, Durable Concrete Structures — Design Guide, Thomas Telford Services Publisher, London, England,1992.

9. NAUS, D.J., BRAVERMAN, J.I., MILLER, C.A., ELLINGWOOD, B.R., and HOFMAYER, C.A., Factors Related to Degradation of Nuclear Power Plant Concrete Structures, Proc. of International RILEM Workshop on Life Prediction and Aging Management of Concrete Structures, Proceedings PRO 16, International Union of Testing and Research Laboratories for Materials and Structures, Cachan Cedex, France, 2000.

10. PRICE, W.F., BAMFORTH, P.B., and GLASS, G.K., Review of European Repair Practice for Corrosion Damaged Reinforced Concrete, Report No. 1303/91/5823, Taywood Engineering Ltd., R & D Division, London, England 1993.

11. ELLINGWOOD, B.R., Probabilistic Risk Assessment, Engineering Safety, pp. 89–116, McGraw-Hill Book Co., Ltd., London, England, 1992.

12. ELLINGWOOD, B.R. and MORI, Y., Probabilistic Methods for Condition Assessment and Life Prediction of Concrete Structures in Nuclear Power Plants, Nuclear Engineering and Design 142, pp. 155-166, Elsevier Science S.A., North-Holland, Amsterdam. The Netherlands, 1993.

13. MORI, Y. and ELLINGWOOD, B.R., Maintaining Reliability of Concrete Structures II: Optimum Inspection/Repair, Journal of Structural Engineering 120(3), pp. 846-862, American Society of Civil Engineers, New York, New York, March 1994.

14. AMERICAN CONCRETE INSTITUTE, Building Code Requirements for Reinforced Concrete, ACI Standard 318-99, Farmington Hills, Michigan, November 1999.

15. BRAVERMAN, J.I., MILLER, C.A., ELLINGWOOD, B.R., NAUS, D.J., HOFMAYER, C.H., SHTEYNGART, S., and BEZLER, P., Probability-Based Evaluation of Degraded Reinforced Concrete Components in Nuclear Power Plants, NUREG/CR-6715, U.S. Nuclear Regulatory Commission, Washington, DC, April 2001.

16. ELLINGWOOD, B.R. and HWANG, H, Probabilistic Descriptions of Resistance of Safety-Related Structures in Nuclear Plants, Nuclear Engineering and Design 88(2), pp. 169–178, Elsevier Science S.A., North-Holland, Amsterdam, The Netherlands, 1985.

17. NAUS, D.J. (Editor), *State-Of-The-Art:* Considerations for Use In Managing the Aging of Nuclear Power Plant Concrete Structures, Report No. 19, International Union of Testing and Research Laboratories for Materials and Structures, Cachan Cedex, France, 1999.

18. JAVOR, T. (Editor), Proceedings of International Conference on Life Prediction and Aging Management of Concrete Structures, EXPERTDCENTRUM, Bratislava, Slovakia, July 6-8, 1999.

19. NAUS, D.J. (Editor), Proceedings of International RILEM Workshop on Aging Management and Life Prediction of Concrete Structures, Proceedings PRO 16, International Union of Testing and Research Laboratories for Materials and Structures, Cachan Cedex, France, 2000.

20. ORGANIZATION FOR ECONOMIC COOPERATION AND DEVELOPMENT, Report of the Task Group reviewing National and International Activities in the Area of Aging of NPP Concrete Structures, NEA/CSNI/R(95)19, Nuclear Energy Agency, Issy-les-Moulineaux, France, 1995.

21. INTERNATIONAL ATOMIC ENERGY AGENCY, Pilot Studies on Management of Ageing of Nuclear Power Plant Components – Results of Phase I, IAEA-TECDOC-670, Vienna, Austria, 1992.

22. INTERNATIONAL ATOMIC ENERGY AGENCY, Assessment and Management of Ageing of Major Nuclear Power Plant Components Important to Safety: Concrete Containment Buildings, IAEA-TECDOC-1025, Vienna, Austria, 1998.

HYGRIC AND THERMAL PROPERTIES OF HPC FOR CONCRETE CONTAINMENTS OF NUCLEAR POWER PLANTS

J Drchalová J Toman

R Černý

Czech Technical University

P Rovnaníková

Technical University of Brno

Czech Republic

ABSTRACT. Thermal conductivity, specific heat and linear thermal expansion coefficient are measured in the temperature range from 100^0C to 800^0C and in the moisture range from dry material to saturation water content. Linear hygric expansion coefficient is measured in the whole moisture range from dry material to full water saturation. Moisture diffusivity is measured as a function of temperature up to 80^0C, and the effects of high-temperature exposure up to 800^0C and freeze/thaw cycles on its value are studied. In order to analyze the observed changes in moisture diffusivity and thermal parameters, thermal analysis and visual analysis are performed. As the main reason for these changes, the crack formation is identified. Particularly, the magnitude of variations of moisture diffusivity is found to be affected by the quality of aggregates rather than by the quality of cement. High quality quartzitic aggregates with very low porosity and very good mechanical properties perform much better than other, more porous siliceous aggregates such as opal, and than the calcareous aggregates such as chalk.

Keywords: Moisture diffusivity, Thermal conductivity, Specific heat, Linear thermal expansion coefficient, HPC, Containment.

Dr J Drchalová, is an Assistant Professor at the Department of Physics, FCE CTU Prague. She specializes in measuring hygric properties of building materials.

Professor J Toman, is Professor of Physics at the Department of Physics, FCE CTU Prague. His main research interest is in measuring thermal properties of building materials under nonstandard conditions.

Professor R Černý, is a Professor at the Department of Structural Mechanics, FCE CTU Prague. He works in the field of mathematical modeling and experimental monitoring of heat, moisture and salt transport processes in building materials.

Associate Professor P Rovnaníková, is an Associate Professor of Chemistry, Head of the Institute of Chemistry, Faculty of Civil Engineering, Technical University of Brno. Her main research interests are in the field of concrete chemistry, hydration processes and thermal analysis.

INTRODUCTION

High performance concretes used in nuclear power plants for the nuclear safety related structures have to satisfy special requirements, for instance they should resist well to higher temperatures, frost cycles, etc., in addition to the common high strength necessity. In this paper, the properties of two high performance concretes used in concrete containment buildings of nuclear power plants are tested from the point of view of hygrothermal properties, and their performance is evaluated.

METHODS FOR MEASURING HYGRIC AND THERMAL PROPERTIES

Moisture Diffusivity

For determination of moisture diffusivity κ we employed a simple method based on the assumption that κ can be considered as piecewise constant with respect to the moisture content (PCK method in what follows). Contrary to the most frequently used methods for κ determination, the PCK method is very fast even for materials with low κ, and in addition it exhibits a reasonable precision [1]. Therefore, its application for concrete is very suitable.

The experimental setup of the PCK method is identical with that of a common water sorption experiment (see e.g. [2]). As a result of the experiment, the amount of water in the specimen as a function of time is determined. Assuming κ to be constant in certain (not very wide) range of moisture content, we can employ analytical solution of the moisture transport equation to the identification of κ which is the only unknown parameter.

In practical measurements we perform the experiment with a set of specimens with various values of the initial partial moisture content u, and determine the corresponding set of values of the moisture diffusivity $\kappa(u_i)$. In this way we obtain a pointwise given $\kappa(u)$ function, i.e., the dependence of the moisture diffusivity on the moisture content.

In this paper, we measured just one characteristic value of moisture diffusivity for every group of specimens because our primary aim was only basic comparison of the various effects on the moisture transport. The initial state of specimens was dry material, so that the measured values of κ correspond to approximately one half of the water saturation value.

Specific Heat

A nonadiabatic method was used for determining the temperature dependent specific heat (see [3], for details). The nonadiabatic calorimeter that we used has a mixing vessel with a volume of 2,5 litres. The volume of the measuring fluid (water in this case) is about 1 litre. The maximum volume of the measured samples is 1 litre. The amount of heat loss of the nonadiabatic system is determined using a calibration.

The measuring method itself is based on well-known principles. The sample is heated to a predetermined temperature T_s in a furnace and then put into the calorimeter with water. Then, the relation of water temperature to time $T_w(t)$ is measured, the water being slowly stirred all

the time, until the temperatures of the measured sample and the calorimeter are equal. Finally, the change of specific enthalpy h corresponding to the change of sample temperature from room temperature to the temperature T_s is determined using the classical calorimetric equation. Performing a set of measurements for various sample temperatures T_i, we obtain a set of points $[T_i, h(T_i)]$. A regression analysis of this pointwise given function results in a functional relationship for $h=h(T)$ and, using the definition relation for specific heat, also in the function $c = c(T)$ as the first derivative of h with respect to T.

Thermal Conductivity

For room temperature measurements, we employed a commercial device ISOMET 104 (Applied Precision, Ltd.), which is based on an impulse technique. For high temperature measurements, we used a double integration method based on the analysis of the temperature field (see [4] for details, [5] for a short view). The basic principle of this method consists in measuring temperature field in the sample at one-sided heating and the subsequent solution of the inverse heat conduction problem. Using this method, we have to know the specific heat and the density of the material as functions of temperature.

The procedure for $\lambda(T)$ function determination consists in the following. One-side heating of a specimen (for concrete typically 71x71x71 mm) with thermally insulated lateral faces is realized using a furnace, where a constant temperature is maintained. Along the longitudinal axis of the sample, a set of temperature sensors is positioned, which makes it possible to record the temperature field through a measuring unit by a PC. From the measured $T(x,t_i)$ curves, a set of 8-10 curves is chosen, and these curves are used in the computational treatment. First, the measured $T(x,t_i)$ curves are subject of a regression analysis. Then, we choose a temperature τ_i, determine the integration area for this value and calculate the corresponding value of thermal conductivity $\lambda(\tau_i)$. This procedure is repeated for a sufficient number of τ_i values, so that we finally obtain a pointwise given function $[\tau_i, \lambda(\tau_i)]$.

Linear Thermal and Hygric Expansion Coefficients

In measuring the high-temperature linear thermal expansion coefficient, we employed an experimental device developed in our laboratory (see [6]). The device consists of a cylindrical, vertically placed electric furnace with two bar samples located in the furnace. The first sample is the measured material, the second sample is a reference material with the known dependence of the thermal expansion coefficient on temperature. The length changes of the samples are measured mechanically outside the furnace by thin ceramic rods which pass through the furnace cover and are fixed on the top side of the measured sample. These ceramic rods pass by an indefinite temperature field, so that their elongation cannot be determined mathematically and a comparative method is used.

In measuring the linear hygric expansion coefficient, we measured the length changes by the Carl Zeiss optical contact comparator with ±1 μm accuracy, and the mass changes were determined by the Sartorius electronic balance with ± 1 mg accuracy. he basic set of points $l_i(m_i,T_i)$ necessary for determining the $\alpha(u)$ function was obtained in this way. he experiments were performed under isothermal conditions, with $T=(25.0\pm0.5)^0C$.

MATERIAL SAMPLES

The experimental work was done with two types of high performance concrete used in nuclear power plants: Penly concrete and Temelin concrete.

Penly concrete was used for a concrete containment building in a nuclear power plant in France (samples were obtained from M. Dugat, Bouygues Company, France). t had a dry density of 2290 kg/m^3, the maximum water saturation 4 %kg/kg, and consisted of the following components: Cement CPA HP Le Havre (290 kg/m^3), sand 0/5 size fraction (831 kg/m^3), gravel sand 5/12.5 size fraction (287 kg/m^3), gravel sand 12.5/25 size fraction (752 kg/m^3), calcareous filler PIKETTY (105 kg/m^3), silica fume (30 kg/m^3), water (131 kg/m^3), retarder CHRYTARD 1.7, super-plasticizer Resine GT 10.62. he compressive strength after 28 days was 64 MPa [7].

The Temelin concrete used for the concrete containment building of the Temelin nuclear power plant in the Czech Republic had a dry density of 2200 kg/m^3 and maximum water saturation 7 %kg/kg. he composition was as follows: Cement 42.5 R Mokrá (499 kg/m^3), sand 0/4 size fraction (705 kg/m^3), gravel sand 8/16 size fraction (460 kg/m^3), gravel sand 16/22 size fraction (527 kg/m^3), water (215 kg/m^3), plasticizer 4.5 l/m^3. The compressive strength after 28 days was 52 MPa [7].

The specimens for determination of moisture diffusivity had prismatic shape, 100x100x50 mm and before the measurements of moisture diffusivity they were exposed to various external conditions. The first group of the specimens (supposed to be applied for the measurements of κ dependence on temperature up to 80^{0}C) was left in laboratory conditions and the moisture diffusivity measurements were done 6 months after the production of specimens. The second group was exposed to thermal load. The chosen temperatures were 200^{0}C, 400^{0}C, 600^{0}C, and 800^{0}C. Measurements of moisture diffusivity were done 6 months after specimens production. The third group of the specimens was exposed to several hundreds of frost cycles according to the Czech standard ČSN 731322 just after the 28 days curing period. One frost cycle consisted in freezing to -20^{0}C for 4 hours and subsequent thawing at +20^{0}C for 2 hours. Measurements of moisture diffusivity were done again 6 months after the end of the frost cycling procedure. The final, fourth group of the specimens was employed as a reference for the frost exposed materials. They were kept at room temperature in water for the whole time of the cycling procedure (about 10 months), then they were left for additional 6 months on the air in laboratory conditions before measurements of moisture diffusivity. Always three specimens exposed to the same conditions were employed for every particular measurement of moisture diffusivity.

The specimens for measuring the specific heat were cubic in shape, 71x71x71 mm for both materials. Twenty measurements were made for each material.

For high temperature measurements of thermal conductivity, we used cubic specimens 71x71x71 mm, and for room temperature measurements prismatic specimens 40x40x160 mm.

The measurements of both linear thermal expansion and linear hygric expansion were performed on 12 samples each. The dimensions of the samples were 40x40x120 mm, and the centers of the 40x40 mm faces were provided with contact seats for use with the contact comparator.

EXPERIMENTAL RESULTS

The results of measurements of moisture diffusivity are shown in Figures 1 to 3. Figure 1 presents the dependence of moisture diffusivity on temperature in the temperature range of 5^0C to 80^0C. Apparently, the moisture diffusivity of both materials increases with temperature in a significant way, and the values of κ for Temelin concrete are approximately two times higher compared to Penly concrete. Figure 2 shows the effect of high temperature exposure prior to the measurement on moisture diffusivity. We can see that moisture diffusivity of both materials increases with the heating temperature very fast. An interesting feature can be observed. While in the temperature range up to 400^0C, the moisture diffusivity of Penly concrete remains approximately two times lower than of Temelin concrete similarly as at room temperature, for temperatures 600^0C and higher the situation is changed dramatically, and Penly concrete has more than one order of magnitude higher moisture diffusivity than Temelin concrete. Figure 3 shows the effect of frost cycles on moisture diffusivity. We can observe that for specimens not exposed to frost cycles, Penly concrete has again about 2 times lower moisture diffusivity than Temelin concrete. However, while the moisture diffusivity of Temelin concrete increases only slowly with the number of frost cycles, approximately one half order of magnitude after 400 cycles, the moisture diffusivity of Penly concrete increases much faster, after 50 cycles it is already higher than moisture diffusivity of Temelin concrete, and after 200 cycles it is about one order of magnitude higher compared to the reference specimens. As it is quite apparent, that the mentioned changes in moisture diffusivity were due to the crack formation after high temperature exposure, in Figure 4 there is presented a digital photograph of Penly concrete after being exposed consecutively to 200, 400, 600 and 800^0C, in order to show the extent of damage on the

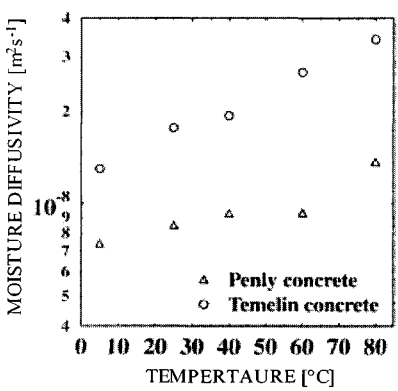

Figure 1 Dependence of moisture diffusivity of Penly concrete and Temelin concrete on temperature

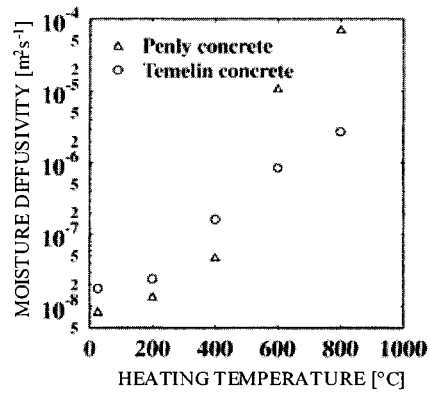

Figure 2 Dependence of moisture diffusivity of Penly concrete and Temelin concrete concrete on heating temperature

Figure 5 shows the dependence of specific heat on temperature. In the temperature range to 400^0C, both materials behaved in a similar way, and we observed a characteristic increase of specific heat with temperature. The measured data were very close to those determined earlier for similar concrete mixes.

For temperatures above 400^{0}C, the specific heat of Temelin concrete slowed down its increase with temperature, and for temperatures higher than 600^{0}C the specific heat began to decrease. The dependence of specific heat on moisture content is presented in Figure 6.

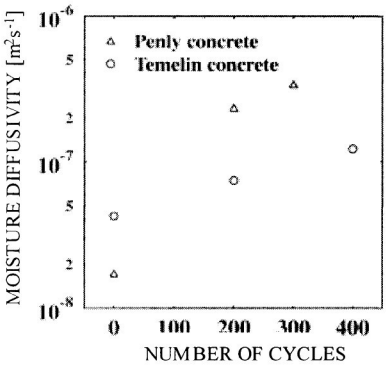

Figure 3 Dependence of moisture diffusivity of Penly concrete and Temelin concrete on the number of frost cycles

Figure 4 Digital photograph of the Penly concrete specimens exposed to 1 hour at 200, 400, 600 and 800^{0}C

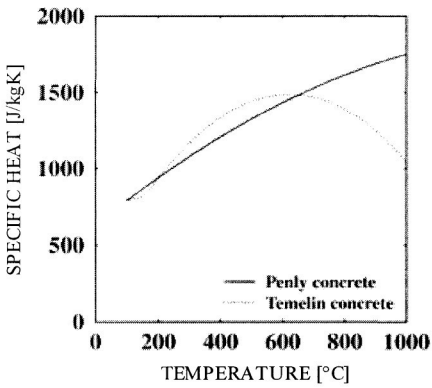

Figure 5 Dependence of the specific heat of Penly concrete and Temelin concrete on temperature

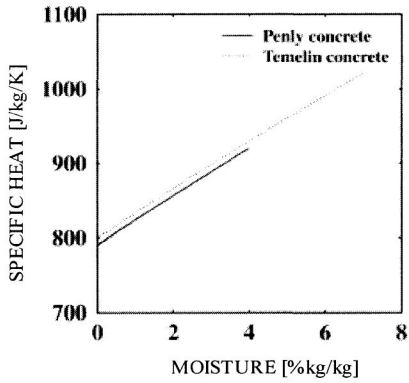

Figure 6 Dependence of the specific heat of Penly concrete and Temelin concrete on moisture

Figure 7 shows the dependence of thermal conductivity on the moisture content. The measured results exhibit significant changes in thermal conductivity due to the moisture variations.

The data for high values of moisture, close to the saturation moisture content, are split, which might be a consequence of structural damage caused by the water saturation process. Figure 8 presents the high temperature data of thermal conductivity. The two materials exhibited very similar behavior. In the temperature range to 400^{0}C, we observed a characteristic decrease of thermal conductivity which is well known for instance for monocrystalline metals or semiconductors. For temperatures above 400^{0}C, the thermal conductivity began to increase, which is an unexpected behavior.

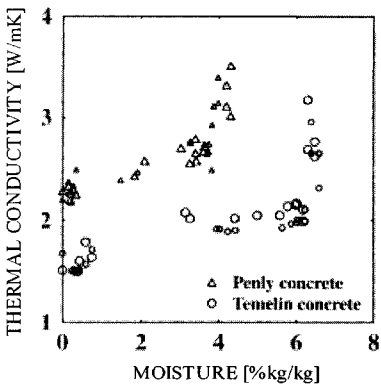

Figure 7 Dependence of the thermal conductivity of Penly concrete and Temelin concrete on moisture

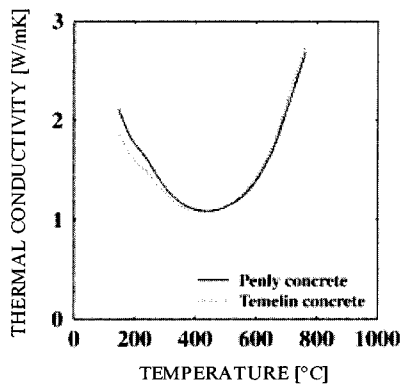

Figure 8 Dependence of the thermal conductivity of Penly concrete and Temelin concrete on temperature

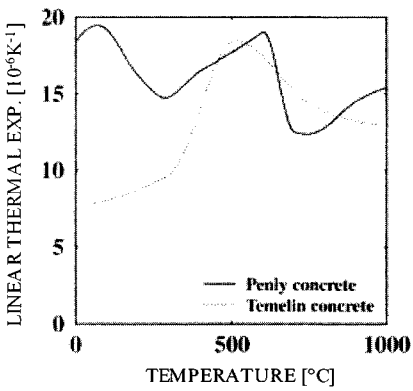

Figure 9 Dependence of the linear thermal expansion coefficient of Penly concrete and Temelin concrete on temperature

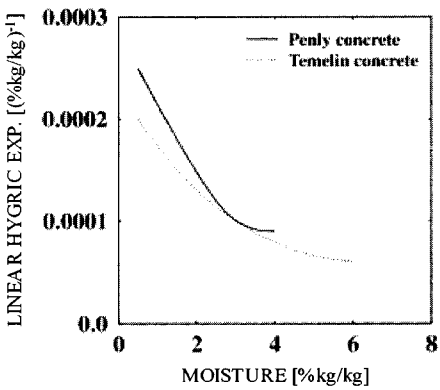

Figure 10 Dependence of the linear hygric expansion coefficient of Penly concrete and Temelin concrete on moisture

Figure 9 shows the measured linear thermal expansion coefficient of both types of high performance concrete in the temperature range from 20^{0}C to 1000^{0}C. The experimental results for Temelin concrete show an abrupt change in the character of the $\alpha(T)$ function at approximately 500^{0}C. The course of the $\alpha(T)$ function for Penly concrete is even more

dramatic, with several maxima and minima. Figure 10 presents the dependence of linear hygric expansion coefficient on the moisture content. Both types of high performance concrete exhibited a very similar behavior, and their linear hygric expansion coefficient decreased with the moisture content.

DISCUSSION

The very fast increase of moisture diffusivity of both materials with the heating temperature corresponds to the theoretical predictions of the effects of high temperatures on concrete in general. From the point of view of structural changes, for the temperature range up to 1000^0C two processes are the most important, namely the decomposition of $Ca(OH)_2$ at about 460^0C and decomposition of calcium silicate hydrates at about 700^0C. During these processes, gaseous substances are released, water vapor in the first case, and carbon dioxide in the second. Therefore, the amount of bigger pores increases which makes the liquid water transport easier and faster. In addition, due to the fast generation of a substantial amount of the mentioned gaseous substances, the local overpressure in some parts of the porous system may lead to crack appearance, and consequently to the opening of preferential paths for the pore water flow.

The increase in moisture diffusivity of Penly concrete between 400^0C and 800^0C (Figure 2) was much faster than for Temelin concrete. This is most probably a consequence of opening of wider preferential paths after the high temperature exposure because in normal conditions Penly concrete possesses lower moisture diffusivity than Temelin concrete.

First supporting arguments to this hypothesis can be found in a dramatic increase in the saturation moisture content (i.e. in the content of open pores) of Penly concrete between 400^0C and 600^0C (more than 30 %) while for Temelin concrete we found only an about 20 % increase. As Penly concrete contains a significantly lower amount of cement than Temelin concrete, the $Ca(OH)_2$ production after heating to more than 460^0C should be lower. Therefore, a logical conclusion is that the significant increase of porosity at about 500^0C was caused mostly by crack appearance in the aggregates and on the grain boundaries due to the local overpressure.

In order to prove this statement, we have done visual observations, at first. We realized that on the specimens of Penly concrete, the most of the pebbles appeared cracked or split after being exposed to the temperatures higher than $400\text{-}500^0$C, and well visible cracks $\approx 500\mu$m wide were also observed on the grain boundaries. The appearance of thermal cracks at elevated temperatures is documented in Figure 4. Apparently, the main reason for crack formation is the low quality of aggregates in Penly concrete which consists of submicrocrystalline silicon dioxide, like chalcedony and opal, and limestone, mainly chalks with 90-99 % of $CaCO_3$ and microfossiliferrous covering.

Siliceous and calcareous aggregates were further analyzed by differential thermal analysis (DTA) and thermogravimetry. We observed that the chalk starts to decompose at 782^0C, the weight loss is 43.83 %, which means that the chalk is an almost pure calcium carbonate. The siliceous compounds are decomposed during an exposure to a temperature of at least 580^0C. The weight loss of 3.20 % is attributed to leakage of water vapor from the microporous system of opal. Further reason for the crack formation is the thermal decomposition of very small limestone grains in cement stone at 755^0C. These grains are apparently identical with the calcareous filler in the mixture.

For the sake of comparison of the effect of high temperatures on both types of concrete investigated throughout this paper, the cracks in Temelin concrete appeared in the cement binder only, no visible cracks were observed in the aggregates. The quality of aggregates was therefore apparently much better than in Penly concrete.

The lower-quality aggregates in the Penly concrete were probably also responsible for the differences in moisture diffusivity of both materials induced by the frost cycles (Figure 3). The moisture content at saturation of Penly concrete increased by 10 % after only 200 cycles and by additional about 10 % after another 100 cycles. The dry density decreased by about 2 % after 300 cycles which is again an illustration of substantial deterioration processes taking place in the material. On the other hand, the dry density of Temelin concrete remained unchanged even after 400 cycles, and the saturation moisture content increase began not until 200 cycles.

Comparing the results of κ measurements in Figures 1 and 3, we can observe that the values of moisture diffusivity of both Temelin and Penly concrete measured on the 6 months old specimens (i.e. just after their delivery) were about two times lower than those which were measured on the specimens left for additional 10 months in water (reference specimens for the frost cycling procedure). The main reason of this fact is probably the "natural" aging of both materials. As the observed changes were for both materials about the same, we believe that the aggregates did not play any significant role in this case.

CONCLUSIONS

On the basis of results obtained in this paper, we can conclude that the quality of aggregates plays more important role for the concrete durability in both high temperature conditions and in the conditions of cyclic freezing and thawing than the quality of cement.

The calcareous aggregates should be avoided in concrete with presumed high temperature exposure, as well as any calcareous fillers, because of their thermal decomposition accompanied by release of substantial amount of carbon dioxide, which can damage the internal microstructure of the matrix due to the increase of internal pressure. Also, the presence of opal in aggregates is not suitable because its microporous system contains water, which can evaporate and damage the porous matrix. Fully quartzitic aggregates perform much better in high temperature conditions.

High quality siliceous aggregates with very low porosity and very good mechanical properties are also the most proper solution for concrete supposedly exposed to freeze/thaw cycles. The siliceous aggregates with higher porosity such as opal are more sensitive to water freezing in the porous system because they contain a higher amount of water in natural conditions, and the stress increase after freezing is higher than in low porosity aggregates. The calcareous aggregates have significantly worse mechanical properties than quartzitic aggregates, and therefore also their resistance to water freezing resulting in significant internal stress increase in the porous system is worse.

For the particular application of concrete in this paper, namely concrete containment buildings of nuclear power plants, the above conclusions may be considered as a warning into the future. Several hundreds of freeze/thaw cycles can be achieved during 10-20 years in the European climate, and this is a critical limit for concretes with calcareous aggregates. Concrete containment buildings were not yet designed for high-temperature exposure above 200^0C. Such temperature could not be achieved in the containment even during a nuclear

accident in the plant, so that the poor performance of concretes with calcareous aggregates in the high-temperature range should not result in performance problems. However, it should be noted that regarding what happened September 11, 2001, high temperature exposure of a concrete containment building from outside should not be excluded any more in the design of future nuclear power plants. Therefore, a logical conclusion is that calcareous aggregates should be avoided in future concrete mix design for containments buildings.

ACKNOWLEDGEMENTS

This research has been supported partially by the Ministry of Education of the Czech Republic, under contract No. MSM: 210000004, and partially by the Grant Agency of the Czech Republic, under grant No. 103/97/K003.

REFERENCES

1. DRCHALOVÁ, J., ČERNÝ, R., HAVRDA, J., The effect of anisotropy of building materials on the moisture transfer, Acta Polytechnica, Vol 40, 2000, p 32-35.

2. SABIR, B. B., WILD, S., O'FARRELL, M., A water sorptivity test for mortar and concrete, Materials and Structures, Vol 31, 1998, p 568-574.

3. TOMAN, J., ČERNÝ, R., High-temperature measurement of the specific heat of building Materials, High Temp-High Press, Vol 25, 1993, p 643-647.

4. ČERNÝ, R., TOMAN, J., Determination of temperature- and moisture-dependent thermal conductivity by solving the inverse problem of heat conduction, Proc. of International Symposium on Moisture Problems in Building Walls, V P de Freitas, V Abrantes (Eds), p 299-308, University of Porto, Porto, 1995.

5. ČERNÝ, R., MADĚRA, J., PODĚBRADSKÁ, J., TOMAN, J., DRCHALOVÁ, J., KLEČKA, T., JUREK, K., ROVNANÍKOVÁ, P., The effect of compressive stress on thermal and hygric properties of Portland cement mortar in wide temperature and moisture ranges, Cement and Concrete Research, Vol 30, 2000, p 1267-1276.

6. TOMAN, J., KOUDELOVÁ, P., ČERNÝ, R., A measuring method for the determination of linear thermal expansion of porous materials at high temperatures, High Temp-High Press, Vol 31, 1999, p 595-600.

7. VODÁK, F., et al, Tables of Physical Properties of Concretes for Nuclear-Safety Structures, CTU Reports Vol 4, No 5, 2000, p 5-66.

CRACKING IN CONCRETE NUCLEAR WASTE CONTAINERS

I Tovena

CEA – Commissariat a'lEnergie Atomique

France

ABSTRACT. The main cracking mechanisms of concrete nuclear waste containers have been identified in storage. They include physical mechanisms (plastic shrinkage, thermal expansion, thermal shrinkage, thermal cycling, freezing-thawing, irradiation), chemical attack (leaching, sulfate or alkali-aggregate reaction and embedded metal corrosion) and microbial action. To the extent that knowledge permits, these mechanisms are generically evaluated and classified into non significant and potentially significant. The most potentially significant mechanisms are chemical ones such as sulfate attack or metal corrosion.

Keywords: Cracking, Durability, Chemical attack, Physical attack, Nuclear container.

Dr I Tovena, is a Doctor in Material Science. After a thesis on glass durability, she worked as a project manager on the durability issue of different materials such as zircaloy and plastics. Today, she focusses on concrete durability in unsaturated conditions at CEA-Saclay –Laboratory of Study of Concrete and Clay.

INTRODUCTION

The main functions of the nuclear waste containers in storage are confinment, limited dispersion and mechanic resistance. Each of these functions should be maintained as long as there is no critical cracks in the containers. The difficulty is to precise this critical value. For, cracking occurs in virtually all concrete structures and, because of concrete's inherently low tensile strength and lack of ductility, cracking can never be totally eliminated. In this paper, a global approach is first discussed to assess the cracking sources, then the more likely cracking mechanisms are evaluated. The identified potentially significant cracking mechanisms include:

- physical attack (shrinkage aggregates, drying shrinkage,crazing, freeze-thaw cycles, wet-dry cycles and irradiation),
- chemical attack (calcium hydroxide leaching, sulfate attack, alkali-aggregate reaction and embedded metal corrosion),
- microbial action (effects of sulfur oxidising and nitrifying bacteria).

In the following sections, some among the more common types of cracking are considered.

CONCRETE CONTAINER SYSTEMS

The durability of concrete containers can be limited as a result of adverse performance of its cement-paste matrix or aggregate constituents or embedded metallic parts under either chemical or physical or bio attack. In practice, these processes may occur concurrently to reinforce each other. In nearly all durability issue of concrete structures, dominant factors involved include transport mechanisms within the pores and cracks and the presence of water. In the following, cracking is considered as a consequence of the degradation process and its influence on the degradation process is not considered.

Water is present in the concrete structure itself (free water in the porosity or physisorbed water or engaged in the hydrates constitutive of the cement paste). Free water is the only one to consider as a degradation intrinsic factor. But, water could be present in the environment ; its form (liquid or gaseous) depends on the environmental relative humidity and temperature. The ratio of gaseous to liquid water has direct consequence on the kinetics of the degradation mechanisms and cracking effects.

PHYSICAL ATTACK

Physical attack involves the degradation of concrete due to external influences mostly temperature and relative humidity. Concrete attack due to overload conditions is not considered as an aging mechanism.

Thermal expansion

This kind of cracking due to the material's low diffusivity is not frequently observed. In the case of large structures, the heat developped within these structures is dispersed into the environment very slowly. The temperature in the bulk can reach 70°C or more, while the outer portion beeing cooled in the air after striking of the forms, quickly reaches values near ambiant temperature [1]. This temperature distribution causes an expansion of the core that generates tractional forces at the transition between the core and the outside shell.

Drying/Thermal exposure/ Thermal cycling

The cement paste in contact with a relative humidity lower than 95 % tends to progressively lose water. Therefore the hydrated cement particles approach to one another giving rise to hygrometric shrinkage [1].

High temperature exposure and thermal gradients are important to concrete structures in that they affect the concrete's strength and stiffness. Significant deterioration of the concrete strength does not generally occur until the exposure temperature reaches around 400 °C when high dehydration of calcium hydroxide occurs [2]. Thermal cycling, even at relatively low temperatures (<65 °C due to daily temperature) can have some deleterious effects on concrete's mechanical properties (compressive, tensile, bond strengths and modulus of elasticity are reduced) and at the end cause cracking especially when the thermal expansion values are quite different between cement paste and aggregates (see Table 1).

Freezing and thawing

While freezing and thawing are repeated, the material gradually lose its strength and stiffness[3]. It is commonly accepted that when concrete is frozen, water stored in micropores expands 9 % in volume. This expansion induces large tensile stress locally and damages the micropores [4]. Water flows through the fractured micropores when the material is thawed, which accelerates the damage [5]. The process of deterioration is not fully clarified since it depends on various external factors such as the range of cooling and heating temperatures, the repetition of freezing and thawing and the applied stress (see Table 1).

Irradiation[1]

The fast neutron are mainly responsible for the considerable growth, caused by atomic displacements, that has been measured in certain aggregate (e.g.flint). Nuclear heating occurs as a result of energy introduced into the concrete. For, the neutrons or gamma radiation interact with the molecules within the concrete material. The nuclear heating should be negligible for incident energy fluxes less than 10^{10} MeV/cm^2 per s [6].

Gamma rays produce radiolysis of water in cement paste that can affect concrete's creep and shrinkage behavior to a limited extent and also result in evolution of gas [7, 8].

CHEMICAL ATTACK

Chemical attack involves the alteration of concrete through chemical reaction with either the cement paste or coarse aggregate, or embedded metal. Chemical causes of deterioration can be grouped into three categories : hydrolysis of cement paste components by soft water; cation exchange reactions between aggressive fluids and the cement paste and reactions leading to formation of the aggressive products (sulfate attack, alkali aggregate reaction and reinforcement corrosion) [9].

[1] Irradiation is physical but generates both physical (elevated temperature)and chemical effects (radiolysis, H_2 production and O_2 consumption) which are difficult to assess.

Leaching

For calcium hydroxide leaching, water (or other aqueous solutions) must be flowing on the cement not just filling a crack or a void.

The most readily soluble material is calcium hydroxide. When calcium hydroxide has been leached away, other cementitious constituents become exposed to chemical decomposition. This could leave behind silica and alumina gels with little or no strength. Because of the high alkalinity of concrete (pH>12.5), it is degraded by strong acids whenever the concrete is exposed to such solutions because of the waste for example [7, 9, 10, 12].

Leaching over long periods increases the porosity and permeability of concrete making it more susceptible to other forms of aggressive attack and eventually reducing its strength and stiffness [11]. The only outward manifestation of this degradation is the appearance of a pock marked surface which ultimately leads to spalling and cracking.

Sulfate attack

Magnesium and alkali sulfates present in wastes react with calcium hydroxide and alumina bearing phases of portland cement to form gypsum and ettringite.

Conceptual model for the ettringite formation[13, 14]

⊇Gypsum formation after diffusion of sulfate ions to calcium hydroxide :

$$Ca(OH)_2+SO_4^{2-}+2H_2O \rightarrow CaSO_4.2H_2O+2\ OH^-$$

⊄Monosulfoaluminate formation

$$3\ CaO.Al_2O_3.6H_2O + (Ca^{2+}+SO_4^{2-})+6H_2O \rightarrow 3CaO.Al_2O_3.CaSO_4.12\ H_2O$$

⊂Ettringite formation

$$3\ CaO.Al_2O_3.CaSO_4.12H_2O+2\ (Ca^{2+}+SO_4^{2-})+20H_2O \rightarrow 3CaO.Al_2O_3\ .3(CaSO_4).32H_2O$$

These reactions, if enough water is present, result in expansion and irregular cracking of concrete that can lead to progressive loss of strength [15].

But sulfate attack may be external or internal (presence in the waste or agregate or cement). Damage of concrete due to internal sulfate attack (often referred to as delayed ettringite formation (DEF)) has been reported primarily in concrete members submitted to high temperature curing followed by open-air weathering and hence drying-re-wetting cycles[16,17]. But Diamond [18] suggests that the DEF problem is not just confined to steam cured concrete at excessive temperatures: the effectiveness of prior alkali-silica reaction-induced cracking in stimulating the development of DEF has been noted. Anyway, three critical conditions are commonly reported to govern internal sulfate attack [16]: portland cement composition i.e. high contents of $3CaO.Al_2O_3$ and SO_3 (4-5% SO_3), high curing temperatures, exposure to a moist environment.

Concretes undergoing DEF suffer a general loss in dynamic elastic modulus, even if sampled in apparently sound areas between visible cracks (one third the normal modulus of unaffected concrete). In extreme cases, the concrete becomes crumbly and soft and it is evident that the effectiveness of the cement paste binder has been destroyed [18, 19].

Alkali aggregate reactions

Alkali-aggregate reactions comprise different chemical processes between alkali ions of the concrete pore fluid and the aggregate material. Three types of allkali-aggregate reaction are distinguished in the «standard classification« [20,21] :

*Alkali silica reaction (ASR)
ASR can be considered in a simplified manner as an acid base reaction between the alkaline pore solution and an amorphous or reactive silica content of the aggregate [22].

*Alkali silicate reaction (ASSR)
ASSR occurs between interlayer precipitates of phyllosilicates and the alkaline pore solution [23].

*Alkali carbonate reaction (ACR)
ACR is a reaction between the carbonates of the aggregate and the alkaline pore solution of concrete.

Most of the research work has been devoted to the alkali silica reaction, only little work has been done so far to explore the mechanisms and consequences of the alkali carbonate reaction. Thus, this paper will focus on the allkali silica reaction.

The ASR deterioration can be attributed, on the microstructural level, to the formation of a hydrophilic gel from reactive silica in the aggregates, alkalies in the cement klinker (namely K^+ and Na^+) and water in the concrete pore solution [22]. The mechanism of the second stage, leading to the formation of the expansive reaction products is still not well known. It seems that the dissolved ions diffuse due to differential spatial concentrations through the pore solution to microvoids, pores and cracks, forming various reaction productions (gels, precipitates and even crystals). Depending on the amount of water available and on the location, this gel formation generates an increasing internal pressure in the cementitious matrix on the concrete skeleton [23], a pressure that triggers the macroscopic expansion and map cracking (see Table 1).

Corrosion of embedded steel

Concrete is a highly alkaline material (pH>12.5) which provides an ideal environment to protect the embedded reinforcing steel rods or metallic waste from corrosion. However, when the pH of the environment in contact with the steel is reduced, then corrosion of the embedded steel can occur [24].

A reduction in the pH requires an ongoing intrusion of agressive ions (most notably , chlorides in the presence of carbonation or acidic materials from the waste). There is no consensus on the solid corrosion products [25] but when corrosion occurs, the rust products exert tensile stresses in the concrete, causing longitudinal cracking (coincident cracks following the line of the reinforcement). Spalling of the concrete cover may then follow (see Table 1).

MICROBIAL ACTION

Unlike chemical reactions, biological reactions depend on a biocatalyst which must be synthesised by an intact cell. Thus, in order to generate the cellular biomass, key elements must be present in roughly the right proportions. The most crucial elements (after the

hydrogen and oxygen provided by water) are carbon, nitrogen, phosphorus and sulphur, though metal ions are needed in trace amounts, particularly potassium, magnesium and iron. In the container, phosphorous would be limiting. The nature of the limiting substrate is important since it determines which element will be scavenged down to a low equilibrium concentration. Other minor nutrients are needed to maintain a viable microbial population. Small amounts of magnesium, potassium, iron, copper, manganese, zinc and other common metal ions must be present but are generally found at acceptable levels in water in natural environment. However, if their concentration is suppressed, cells may adapt [26].

Biodegration in the container system

Concrete degradation is not a direct biodegradation mechanism but more commonly a consequence of the bacterias growing on the concrete surface. Tache quotes different examples of this kind of concrete degradation [27]:

- dissimilation of H_2S and bacterial oxidation in sulphuric acid (essentially *by Thiobacillus thiooxidans*). This acid may affect the concrete where bacteria grow with the gypsum formation (see previous chapter on sulfate attack), then the DEF cracking.
- dissimilation of nitrates or nitrites by *Nitrosomonas* or *Nitrobacter*. *Nitrosomonas* transform ammonium ion in nitrite and *Nitrobacter,* nitrites in nitrates. Their growing in mineral medium is slow and dependant on the pH (neutral or slightly alkaline).

METHODOLOGY FOR THE ASSESSMENT OF THE MORE LIKELY CRACKING MECHANISMS

In this section, the previous phenomena are classified into non-significant and potentially significant. For each degradation phenomenon, the specific needed parameters that control the physical or chemical or microbial mechanisms are mentioned in Table 2.

The probabibility of the phenomenon to occur P_{Deg} is qualitatively assessed as below:

$$P_{Deg} = P_{int} * P_{ext}$$

P_{Deg} : probability for the degradation phenomenon to occur in the storage concrete container
P_{int} : probability for the degradation controlling factors being in the container
P_{ext} : probability for the degradation controlling associated factors being in the environment of the container

With : $0<P...<1$ 0: less probable
1: more probable

Five levels **A** to **E** are proposed for P. **A** ($\cong 0$) corresponds to the least probable phenomenon and **E** ($\cong$**1**) corresponds to the most probable one.

Based on review and evaluation of the operating history of the storage containers, relevant laboratory test data, and related experience of similar structures in other industries, the probabilities have been qualitatively evaluated. All the probabilities for each degradation mechanism are reported in Table 2.

Table 2 represents for each cracking phenomenon, the main specific degradation factor and the reliant internal or external parameter if present. The cracking probability is then assessed as previously explained.

Table 1 Qualitative description of common cracking phenomena

CRACKING PHENOMENA	TIME[2]	FORM AND ORIENTATION	SIZE (m)	PART OF THE CONTAINER AFFECTED
Thermal expansion	On striking the forms	Parallel to the long side and linear along the bars	Width:up to 1.10^{-3} Depth: several tenths Length: up to a few metres	Very massive structural elements(>one or two metres)
Thermal exposure/ Thermal cycling	Variable	Parallel to the short side	Width: 0.2. 10^{-3} up to 1.10^{-3} Depth: several tenths Length: up to a few metres	Walls and floors
Frost attack	One or several years	Several forms: scaling, spalling and pattern cracking	?	Variable
Leaching	Variable	?	Variable: function of the agressivity of the medium	Exposed surface
Sulfate attack	One of several years	Macroscopic crack pattern controlled by the geometry of the restraint system (parallel to the direction of the prestressing cables)	Gross cracking (network with component crack segments running partly along aggregate peripheries (rim cracks) but generally connecting through segments running through the cement paste (paste cracks)	Anywhere
Alkali-aggregate reaction	Up to 10 years (ASR) Up to 20 years (ASSR) Up to 5 years (ACR)	«map cracking» or oriented cracking in function of the restraint system	Width: 0.1. 10^{-3} up to 1.10^{-3} Depth: several 10^{-2} m Length: mesh from 10^{-2} to 10^{-1} m	Anywhere if sufficient water
Reinforcement corrosion	From one year to 30-50 years	Longitudinal cracking following the line of the reinforcement	Width: 0.1. 10^{-3} up to 1.10^{-3} following the line of the reinforcement	Anywhere in presence of metallic part
Microbial action	One to several years	Variable in function of the bacteria class (*sulphur oxiding bacteria* see sulfate attack ; *nitrifying bacteria* see leaching)	Variable in function of the bacteria class (*sulphur oxiding bacteria* see sulfate attack; *nitrifying bacteria* see leaching)	Exposed surface

This qualitative assessment allows a classification of the differents cracking phenomena from the more probable to the less probable as follows :

Reinforcement corosion > Irradiation > Thermal exposure and cycling ≅ Sulfate attack >Salt crystallization > Alkali Agregate reaction> Thermal expansion > Frost attack> Leaching> Sulfur oxidising bacteria and nitrifyng bacteria.

[2] Depends on the concrete quality (W/C) and agressive factor level. Here in standard natural conditions

CONCLUSIONS

The potentially significant cracking mechanisms for nuclear waste container in storage have been identified. They include physical or chemical or microbial mechanisms. Physical mechanisms generally are controled by the temperature and humidity level in and above all out of the container. That's why these mechanisms could be generally easily avoided by a control of the ambiant atmosphere of the container. It is not the case for chemical degradation such as those induced by sulfate attack or embedded metal corrosion or radiochemical attack because the controling parameters are parts of the containers (irradiation sources, metallic or sulfate waste, pore water or salts.). Anyway, for each of these chemical attack, water level in the container has a direct impact on the degradation kinetics and should be studied to minimize the cracking risk.

Table 2 Qualitative Assessment of the probability for physical , chemical and microbial cracking in the nuclear waste concrete container

CRACKING PHENOMENA	MAIN SPECIFIC DEGRADATION FACTORS	RELIANT INTERNAL PARAMETER	RELIANT EXTERNAL PARAMETER	CRACKING PROBABILITY		
				P_{int}	P_{ext}	P
Physical attack						
Thermal expansion	Temperature	Very massive structural elements>1m, high heat of cement hydration	Temperature	B	C	BC
Thermal exposure	Temperature	Gamma Irradiation	Temperature	E	C	CE
Frost attack	Water, temperature	Internal water	Temperature<0°C, HR	E	<B	<EB
Irradiation	Irradiation source	Irradiation source, water or other solvents for gas generation	Irradiation source gamma essentially	D	D	DD
Chemical attack						
Leaching	Flowing water or acids, $Ca(OH)_2$, CSH	Flowing water or acids, $Ca(OH)_2$, CSH, W/C ratio	Flowing water or acids	B	B	BB
Salt crystallization	Salt concentration, thermal cycling	Salt concentration, W/C ratio	Thermal cycling	D	C	CD
See next Sulfate attack	Sulfate, water, temperature curing	Sulfate, water, temperature curing	Sulfate or temperature,water	E	C	CE
Alkali-aggregate reaction	Silica or carbonate aggregate, water	Silica or carbonate aggregate, water	Water	D	B	BD
Reinforcement corrosion	Reduced alkalinity or Chlorides, water, oxygen	pH<11.5 , Chlorides, water or acids	CO_2 or Chlorides, water, oxygen	E	E	EE
Microbial action						

Sulfur oxidising bacteria	C- H-O-N-P-S Elements, water	C- H-O-N-P-S Elements, water	Water	B	B	BB

ACKNOWLEDGMENTS

The author would like to acknowledge the support provided by the Laboratory of Study of Concrete and Clay, namely C. Richet, P.Bouniol, P. Le Bescop and J.Sercombe.

REFERENCES

1. ROSSETTI, VA, ROSSI, M, Recognizing and preventing cracking in concrete and reinforced concrete, L'industria italiana del cemento, Decembre 1997, pp 962-971.

2. BAZANT, Z P, Normal and refractory concretes for LMFRB Applications, Vol.1: Review of literature on high temperature behavior of Portland Cement and refactory concrete, EPRI NP 2437, Electric Power Research Institute, Palo Alto, California, June 1982.

3. PIGEON, M, La durabilité au gel du béton, Materials and structures, 22, 1989, pp 3-14.

4. HORI, M, MORIHORI, H, Micromechanical analysis on deterioration due to freezing and thawing in porous brittle materials, Int. Engng Sci., Vol.36, No 4, 1998, pp 511-522.

5. VEEN, I C, Properties of concrete at very low temperatures : a survey of the literature. Report of the faculty of civil Engineering, Delft University of Technology, 1987.

6. AMERICAN NUCLEAR SOCIETY, Guidelines on the Nuclear Analysis and Design of Concrete Radiation Shielding for Nuclear Power Plants, American National Standard ANSI/ANS-6.4-1985, La Grange Park, Illinois, 1985.

7. NAUS, J, OLAND, C B, ELLINGWOOD, B R, Report on aging of Nuclear Power Plant Reinforced Concrete structures, BNL NUREG 13148, Mars 1996.

8. BOUNIOL, P, ASPART, A, Disappearance of oxygen in concrete under irradiation : the role of peroxides in radiolysis, Cement and Concrete Research, Vol. 28, 11, 1998.

9. KASSIR, M, BANDYOPADHYAY, K, BUSH S, MATHER B, SHEWMAN P, Aging mechanisms for concrete components of high level waste storage tanks, in Service experience, structural integrity, severe accidents, and corrosion in nuclear and fossil plants, PVP-Vol 303, NY ASME, 425, 1995 pp117-123.

10. ADENOT, F, RICHET, C, FAUCON, P, Long term prediction of concrete durability in radioactive waste management: influence of the pH of the aggressive solution, Int. Conf. Engineering Materials, 8-11 June 1997, Ottawa, Canada, Vol 2, pp 107, 1997.

11. FAUCON, P, ADENOT, F, JACQUINOT, J F, PETIT, J C, CABRILLAC, R, JORDA, M., Long term behaviour of cement pastes used for nuclear waste disposal, review of physico-chemical mechanisms of water degradation, Cement and Concrete Research, Vol 28, No 6, 1998, pp 847-857.

12. Comité Euro- International du béton (CEB), Durable Concrete Structures-design Guide, published by Thomas Telford Services Ltd., London, England, 1989.
13. ATKINSON, A, HEARNE, A, Mechanistic model for the durability of concrete barriers exposed to sulfate bearing groundwaters, Mater. Res. Soc., 784, 1990, pp 149-156.

14. POMMERSHEIM, J M, CLIFTON, J R, Expansion of cementitious materials exposed to sulfate solutions, Mater. Res. Soc., 333, 1994, pp 363-368.

15. PLANEL, D, SERCOMBE, J, LE BESCOP, P, ADENOT, F, SELLIER, F, CAPRA, B, TORRENTI, J M, Experimental and numerical studt on the effect of sulfates on calcium leaching of cement paste, Fracture Mechanics of Concrete structures, de Borst et al. (ed1) Vol 1, 2001, pp 287-292.

16. FU, Y, DING, J, BEAUDOIN, J J, Expansion of Portland cement mortar due to internal sulfate attack, cement and concrete research, Vol 27, No 9, 1997, pp 1299-1306.

17. ODLER, I, GLASSER, M, Mechanism of sulfate expansion in Hydrated Portland cement, J. Am.Ceram. Soc., 71, 11, 1988, pp 1015-1020.

18. DIAMOND, S, Delayed Ettringite Formation-Processes and Problems, Cement and Concrete Composites 18, 1996, pp 205-214.

19. LANE, D S, OZYILDIRIM, H C, Evaluation of the Potential for Internal Sulfate attack through adaptation of ASTM C 342 and the Duggan Test, American Society for testing and materials, 1999, pp 43-58.

20. GRATTAN-BELLEW, P E, Alkali-silica reaction-Canadian experience in: The alkali-silica reaction in concrete, ed.R.N. Swamy, Blackie, Van Nostrand Reinhold, 1992, pp 30-53.

21. TSCHEGG, E K, ROTTER, H., HAMMERSCHLAG, J G, KREUZER, H, Alkali Aggregate Reaction in Mass concrete, 1998,Verbund Band 33 .

22. UHLM, F-J, COUSSY, O, KEFEI, L, LARIVE, C, Thermo-Chemo-Mechanics of ASR expansion in concrete structures, J. Eng. Mechanics, March 2000, pp 233-242.

23. HOBBS, D W, Alkali-silica reaction in concrete, 1988,Thomas Telford, London.

24. ACI 222R-89, Corrosion of metals in concrete, American Concrete Institute, Manual of Concrete Practice, Part I, Detroit, Michigan, 1993.

25. STEWART, M G, ROSOWSKY, D V, Structural safety and serviceability of concrete bridges subjectto corrosion, J. Infra. Systems, December 1998, pp 146-155.

26. GREENFIELD, B F, ROSEVEAR, A, WILLIAMS, S J, Review of the Microbiological, Chemical and Radiolytic degradation of organic Material likely to be present in Intermediate Level and Low level Radioactive Waste, DOE Report 7/9/552, 1990.

27. TACHE, G, Corrosion bactérienne des bétons in Biodétérioration des matériaux, (ed Lemaitre, C, Pébère, N, Festy, D) 1998.

MODULUS OF ELASTICITY OF TWO-STAGE CONCRETE

H S Abdelgader

J A Górski,

Technical University of Gdańsk

Poland

ABSTRACT. Two-stage concrete is made by forcing cement grout into the voids of a compacted mass of stone aggregate. The two-stage concrete differs from ordinary concrete in that it contains a higher proportion of stone aggregate and the aggregate stays in point-to-point contact as placed. Thus, the mechanical characteristics of the two-stage concrete in failure conditions are distinctly different from the ordinary concrete. Moreover, there is no background information for evaluating the two-stage concrete elastic modulus. This paper presents the results of some experimental tests of two types of stone aggregates and three different mix proportions of grout. Stress-strain relations in function of water-cement and cement-sand ratios are elaborated. A relationship between the initial tangent elastic modulus and the compressive strength of two-stage concrete is statistically derived.

Keywords: Two-stage concrete, Aggregate, Modulus of elasticity, Compressive strength, Grouting, Preplaced aggregate concrete, Mass concrete.

Dr H S Abdelgader, is a researcher of Civil Engineering, Secretariat of High Education, Libya. Presently resident at the Technical University of Gdańsk, Poland, where in 1996 he received his PhD from the Faculty of Civil Engineering, Department of Building Materials and Concrete Technology. He specializes in concrete mix design and concrete repair. His research interests include two-stage concrete technology and its practical applications. A member of American Concrete Institute (ACI).

Dr J Górski, is employed at the Faculty of Civil Engineering, Technical University of Gdańsk, Poland. Research fellowship at the TU Wuppertal, Germany (1992 and 1993) and TU Bochum, Germany (1998–1999, 2001–2002). His research area includes: stochastic analysis, description of damage of materials, concrete constitutive relations.

INTRODUCTION

Two-stage concrete is produced in two phases. First, stone aggregate is placed into a prepared formwork. Then, a high flow cement/sand grout is introduced into the bottom of the form, in open air or under water. The two-stage concrete can be applied to concreting mass structures (of at least 0.5 m in size), in places hard to reach (e.g. in zones of great thickness of reinforcement), and where there is enough amount of stone aggregate [1].

High-density concrete may contain high amount of cement, which is characterized by an increase in creep and shrinkage. Moreover, because of the high density of aggregates, there will be noted a tendency to segregation. To avoid theses, two-stage concrete can be adopted [2]. Other names commonly given to two-stage concrete are: preplaced aggregate concrete, prepacked concrete, grouted concrete, and "prepakt concrete" (a trade name) [3].

The published literature describing the two-stage concreting method has been very limited until now. Especially it is difficult to find any details of the influence of the stone aggregate type used and the grout mix proportions on the concrete stress-strain relations and its elastic properties.

The modulus of elasticity is particularly important from the design point of view in plain or reinforced concrete, since it can describe the concrete mechanical behaviour. The elastic modulus and the failure characteristic of the two-stage concrete differ from the ordinary concrete. The difference results mainly from the method of placement and from a higher proportion of stone aggregate. The two-stage concrete may be regarded as skeleton concrete because the stones rest one on another [4]. In this way the point-to-point contact of the aggregate can be observed, whereas in normal concrete the aggregate is rather dispersed.

To avoid the laborious and time-consuming direct determination of the concrete mechanical parameters, it seems to be useful to find a simple relationship between the compressive strength and the modulus of elasticity of the two-stage concrete. Therefore, a set of experiments has been carried out. Some aspects of the test results are presented in this paper.

MATERIALS AND TEST PROCEDURES

In the manufacture process of two-stage concrete the stone aggregate and the grout are the basic constituents. The stone aggregate used in this investigation was rounded aggregate and crushed (basalt) aggregate. The rounded aggregate was brought from Rybaki quarry near Gdańsk, Poland, and was sieved from the unsorted mass in three fractions: 16/32mm (34%), 32/50mm (60%), and 50/63mm (6%). The crushed (basalt) aggregate was brought from the Polish Railway plant in Gdańsk and was also sieved in three fractions: 16/32mm (46%), 32/50mm (49%), and 50/63mm (5%). The physical properties of the stone aggregates are shown in Table 1.

The fine aggregate used for the manufacture of grout was clean sand brought from a quarry at Borowiec near Gdańsk. The largest particles of sand do not exceed the size which passes through sieve No. 2 (2 mm) conforming to Polish standard. The water absorption value equals 1.05% by mass. The particle size distribution of sand is divided into three fractions: 0/0.25 mm (20%), 0.25/1.0 mm (67%), and 1.0/2.0 mm (13%). Ordinary portland cement (Type I) was used throughout the study.

Table 1 Physical properties of stone aggregates

TYPE OF STONE AGGREGATE	BULK DENSITY kg/m^3	TEST NO	COMPRESSIVE CYLINDRICAL STRENGTH (f) MPa		APPARENT SPECIFIC GRAVITY	VOID RATIO %	ABSORPTION %	GRAIN SIZE mm
			f	Average f				
Rounded	1540	1	10.97	11.30	2.607	43.0	0.62	16 - 63
		2	11.37					
		3	11.54					
Crushed	143	1	14.14	14.14	2.687	47.0	0.34	16 - 63
		2	13.58					
		3	14.71					

The mix proportions of the grout were prepared in water/cement ratios of 0.45, 0.50, and 0.55, and cement/sand ratios of 1/1.5, 1/1, and 1/0.8. Superplasticizer was used for all mixes and was added at the rate of 2% by mass of cement [4].

54 specimens of 196 mm in diameter and 392 mm high cylinders with different grout proportions were made. In this way, for each of the two-stage concrete type, three cylinders were subjected to a compressive test after 28 days of curing. During the loading procedure, the vertical deformations were measured on three sides of the specimen with respect to axial force increment. On the basis of these results, stress and appropriate strain values were calculated. Some of the test results are presented in Figure 1.

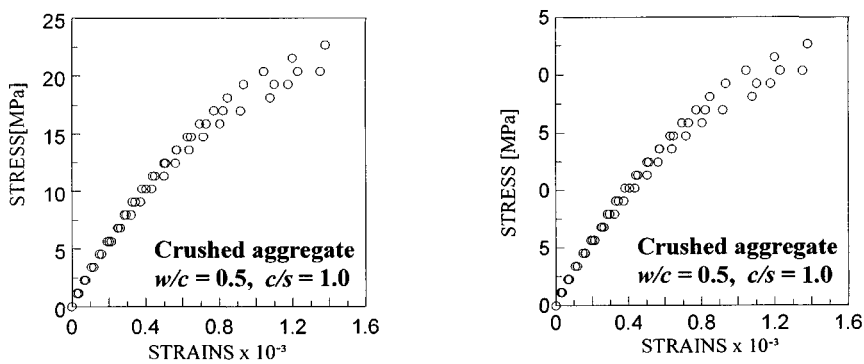

Figure 1 Some results of compressive tests of two-stage concrete cylinder samples

At the same time 108 concrete cube samples (3 *w/c* ratios, 3 *c/s* ratios and 2 types of stone aggregates) of 300×300×300 mm were tested for compressive strength. Six readings of concrete strength were made in all measurement series. The results presented in Table 2 were calculated according to an algorithm, which was proposed earlier for designing of two-stage concrete [5].

Table 2 Cube compressive strength for various two-stage concrete types

WATER-CEMENT RATIO, *w/c*	CEMENT-SAND RATIO, *c/s*	COMPRESSIVE STRENGTH [MPa]	
		Rounded	Crushed
0.45		30.36	30.82
0.50	1/1.5	26.60	27.27
0.55		22.84	23.72
0.45		30.34	30.65
0.50	1/1	26.58	27.10
0.55		22.82	23.55
0.45		30.33	30.78
0.50	1/0.8	26.57	27.23
0.55		22.80	23.68

STATISTICAL ANALYSIS OF TEST RESULTS

The obtained results are statistically analysed to estimate equations for the compressive strain-stress relations of various two-stage concrete types. The statistical analysis is performed by use of the MINITAB program [6]. The code fits an equation to the experimental data by the least square method. The calculation can be divided into the following steps: assumption of the mathematical relation, estimation of the equation coefficients, testing of the assumed equation and choice of the best model.

The statistical analysis of the two-stage concrete test data is performed in two successive phases.

First, the stress-strain relations for each type of stone aggregates and different grout proportions are derived. In this step the data consist of 54 (3×18) stress-strain sets of experimental results obtained from cylinder compressive tests. After various trials the following simple relation for all concrete types is assumed:

$$\hat{\sigma} = a\varepsilon_1^3 + b\varepsilon_1^2 + c\varepsilon_1 \qquad \text{[MPa]} \tag{1}$$

Where $\hat{\sigma}$ = the estimated concrete stresses,
$\varepsilon_1 = \varepsilon \times 10^3$
ε = concrete strain,
a, b, c = regression coefficients.

The coefficients of regression a, b, and c in Equation (1) are statistically obtained for each concrete type separately. In Table 3 some results (6 out of 18 test data sets) for c/s = 1/1.5 and various w/c ratios are presented. Equation (1) gives reliable results in the following range of strains:

$$0 \le \varepsilon \le 0.001 \tag{2}$$

Typical statistically obtained stress-strain curves for two-stage concrete characterized by different grout proportions and two types of the stone aggregates are presented in Figure 2.

Table 3 Constants a, b, c of Equation (1) for two aggregate types and c/s = 1/1.5

AGGREGATE TYPE	*w/c*	*a*	*b*	*c*	CORRELATION COEFFICIENT
rounded	0.45	18.20	-32.5	34.0	0.9941
	0.50	1.00	-9.4	28.5	0.9978
	0.55	5.81	-22.0	32.1	0.9861
crushed	0.45	9.15	-27.0	34.9	0.9846
	0.50	0.08	-17.2	33.3	0.9931
	0.55	5.84	-23.4	36.2	0.9983

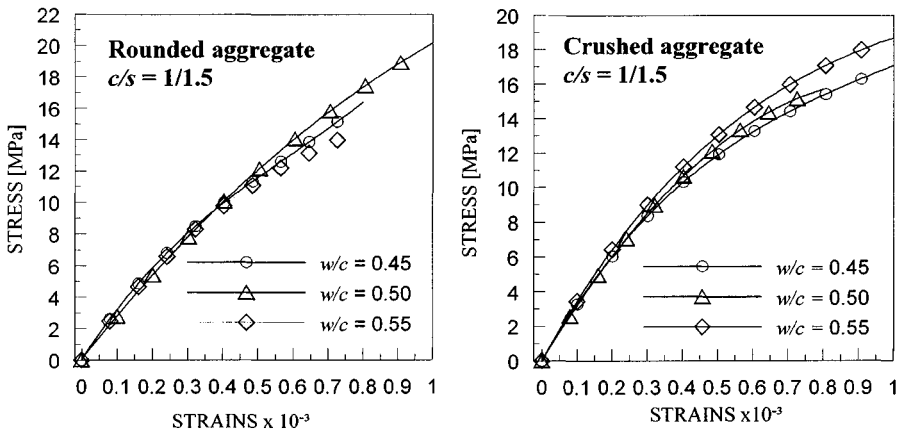

Figure 2 Graphical presentation of the stress-strain relations (Equation 1) for various two-stage concrete types

In the second step the statistical analysis is used to obtain the two-stage concrete stress-strain relations as function of water-cement (ω = w/c) and cement-sand (ς = c/s) ratios. After a complex analysis the functions $a = a(\omega,\varsigma)$, $b = b(\omega,\varsigma)$ and $c = c(\omega,\varsigma)$ in Equation (1) are assumed as follows:

for rounded aggregate:

$$\begin{aligned} a(\omega,\varsigma) &= 38.9 - 51.2\omega - 7.59\varsigma \\ b(\omega,\varsigma) &= -40.8 + 30.1\omega + 5.80\varsigma \\ c(\omega,\varsigma) &= 40.7 - 11.1\omega - 4.46\varsigma \end{aligned} \tag{3}$$

for crushed aggregate:

$$\begin{aligned} a(\omega,\varsigma) &= 14.9 - 17.1\omega + 1.89\varsigma \\ b(\omega,\varsigma) &= -28.7 + 1.0\omega + 9.63\varsigma \\ c(\omega,\varsigma) &= 37.9 + 4.0\omega - 7.82\varsigma \end{aligned} \tag{4}$$

Table 4 Function $a(\omega,\varsigma)$, $b(\omega,\varsigma)$, and $c(\omega,\varsigma)$ calculated according to relation (3) and (4)

AGGREGATE TYPE	*w/c*	$a(\omega,\varsigma)$	$b(\omega,\varsigma)$	$c(\omega,\varsigma)$	CORRELATION COEFFICIENT
Rounded	0.45	10.80	–23.39	32.73	0.8275
	0.50	8.24	–21.88	32.18	0.7976
	0.55	5.68	–20.38	32.62	0.6525
Crushed	0.45	8.47	–21.83	34.49	0.8083
	0.50	7.61	–21.78	34.69	0.8143
	0.55	6.76	–21.73	34.89	0.7357

Some results calculated according to Equations (3) and (4) are presented in Table 4. The values of the correlation coefficient reveal that using the functions $a(\omega,\varsigma)$, $b(\omega,\varsigma)$, and $c(\omega,\varsigma)$ the test results and their estimators are more dispersed (compare Table 3 and 4).

DISCUSSION OF RESULTS

Stress-Strain Relations

The test observations and the statistical analysis have proved that the linear part of the stress-strain curve in two-stage concrete may reach 60% of the ultimate cylinder strength (see Figure 2). The obtained stress-strain curves (Figure 2) and the compressive strength (Table 1) are influenced by the aggregate types. This may result from a very good contact between the aggregate particles. In consequence the applied load seems to be distributed mainly by the stone skeleton.

During the laboratory tests it was observed that the aggregate skeleton of the two-stage concrete carried the load until the whole specimen collapsed. It was the reason why the failure of the two-stage concrete was not sudden and explosive but rather gradual. The failure specimen showed extensive lateral expansion in the form of bulging [7].

The specific stress-strain characteristics of the two-stage concrete can be explained by a dominant influence of the rigid stone skeleton. It should be pointed out that the stress-strain relations of traditional concrete result from transfer of stress through the mortar-aggregate uniform matrix. In the two-stage concrete there are no such uniform relations because the mechanical properties of two-stage concrete are mainly determined by the characteristics of the stone aggregate. Therefore, the subsequent fracture of the two-stage concrete takes place through the stone aggregate particles [4].

In the two-stage concrete the compressive stresses in the aggregate and in the grout cannot be equal. The compressive stress is influenced by the shear stresses occurring not only in the vertical section but also in the horizontal contact surfaces. The produced shear stress caused the tearing off of the aggregate grains from grout.

It was also observed that some microcracking or interfacial cracks were randomly distributed even before the specimens were subjected to the load testing.

It seems that these cracks were caused by bleeding, settlements of grout, or by shrinkage stresses induced by the drying process. The cracks formed within the grout may be considered to be isolated or discontinuous.

Modulus of Elasticity

The experimental data analysis and the statistically obtained stress-strain relations allow for formulating the relationship between the modulus of elasticity and the compressive strength of the two-stage concrete. The compressive strength (Table 2) is calculated according to the algorithm for designing the two-stage concrete proposed by Abdelgader, [5]:

$$\overline{f}_c = \beta_0 + \beta_1 \cdot \overline{f}_g^{\beta_2} \qquad \text{[MPa]} \tag{5}$$

where $\overline{f}_g$ = compressive strength of grout,

β_0, β_1, β_2 = constants assumed for the specific aggregate (see [5], Table 6).

The modulus of elasticity of the two-stage concrete is mainly affected by the physical properties of the stone aggregate, i.e. its cylindrical compressive strength (see Table 1). The influence of the content of grout in the concrete is rather meaningless. It has been observed that the same factors that affect the compressive strength also alter the elastic modulus of the two-stage concrete.

The elastic modulus is obtained from the analysis of the stress-strain curves for each type of stone aggregate and the mix proportions. The initial tangent modulus of elasticity of the two-stage concrete is derived with reference to the tangent line drawn to the stress-strain curve at the starting point (compare some examples presented in Figure 3).

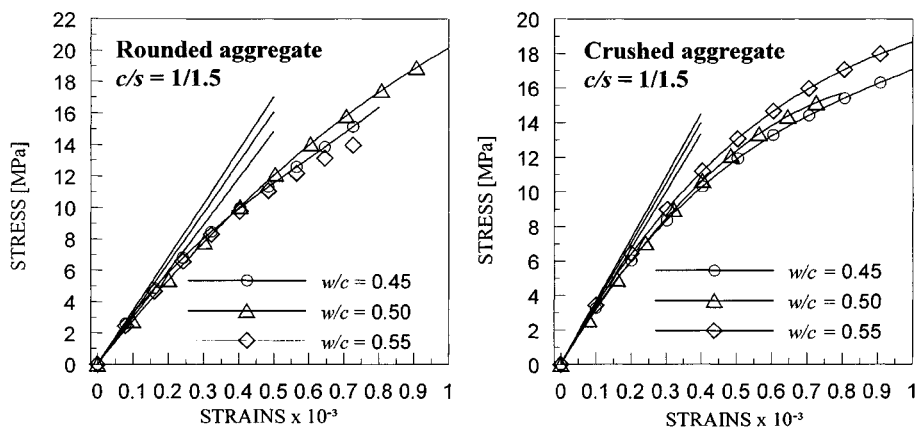

Figure 3 Graphical presentation of estimating the two-stage concrete modulus of elasticity

The modulus of elasticity of two-stage concrete $E_{tsc}(\varepsilon_1)$, determined as a function of strains ε ($\varepsilon_1 = \varepsilon \cdot 10^3$), can be calculated from Equation (1) as follows:

$$E_{tsc}(\varepsilon_1) = \frac{d\hat{\sigma}}{d\varepsilon_1} = 3 \cdot a(\omega,\varsigma) \cdot \varepsilon_1^2 - 2 \cdot b(\omega,\varsigma) \cdot \varepsilon_1 + c(\omega,\varsigma) \qquad \text{[GPa]} \qquad (6)$$

Assuming that $\varepsilon_1 = 0$ the concrete modulus E_{tsc} is estimated as:

$$E_{tsc} = c(\omega,\varsigma) \qquad \text{[GPa]} \qquad (7)$$

Equation (7) indicates that function $c(\omega,\varsigma)$, calculated according to Equations 3 and 4, determines the elastic modulus of the two-stage concrete. It should be mentioned that the values of the elastic modulus obtained for 30% of the cylinder ultimate strength are approximately the same.

It is possible to elaborate an alternative version of the elastic modulus formulae. Making use of the regression analysis of the experimental data, expressions describing the relationship between the elastic modulus of the two-stage concrete and its compressive strength, the following assumption can be made:

rounded aggregate $\quad E_{tsc} = 28.7\text{–}0.080\,\bar{f}_c \quad$ [GPa] (8)

crushed aggregate $\quad E_{tsc} = 33.9\text{-}0.049\,\bar{f}_c \quad$ [GPa] (9)

Where $\bar{f}_c$ = the concrete cube strength (Equation 5 and Table 2).

The limit values of the compressive strengths $\bar{f}_c$ of the two-stage concrete in Equations 8 and 9 are:

$$22 \text{ MPa} \le \bar{f}_c \le 32 \text{ MPa} \qquad (10)$$

The obtained relations indicate that the initial modulus of elasticity for various aggregate types are described by similar relations. The concrete design by use of the rounded aggregate has shown that its mechanical characteristics are of lower quality compared to crushed aggregate concrete types. This may be explained by the area of contact surfaces between various aggregates. In the case of rounded stones the contact area is limited only to points (see [8]).

CONCLUSIONS

1. The stress-strain relationships for different grout mixes (water/cement ratios and cement/sand ratios) do not show a big difference. The initial stress-strain curves can be estimated by linear relations. This may result from the stresses distributed mainly by the particles of stone aggregate (skeleton of stones). The specific way of stress transmission may also contribute to the initiation and propagation of cracks.

2. The modulus of elasticity as a function of compressive strength of the two-stage concrete is elaborated. The modulus values for specific types of aggregate can be described by linear constant functions. The obtained equations can help engineers to design the two-stage concrete according to the algorithm presented in [5].

3. It is proved that the crushed aggregate is better than the rounded aggregate for designing the two-stage concrete. The crushed aggregate makes it possible for a better contact between the grains of the aggregates than the rounded stones.

4. The mechanical behaviour of the two-stage concrete specimens is noticeably determined by random placement of stone aggregate into the forms.

5. This method can be used for shielding constructions to prevent external or internal radiation.

ACKNOWLEDGEMENTS

This work was done to honour the late Professor Kazimierz Braun who supervised the study. The research was carried out at the Civil Engineering Department of the Technical University of Gdańsk, Poland.

REFERENCES

1. ALLEN, R T L, EDWARDS, S C, SHAW, D N, The repair of concrete structures, Second Edition, Chapman & Hall, UK, 1993.

2. DAVIS, H E, High-density concrete for shielding atomic energe plant, Am. Concr. Inst. 1958, Vol. 54, No 11, pp 965-977.

3. ACI Committee 304, (Reapproved 1997), Guide for the use of preplaced aggregate concrete for structural and mass concrete applications, Am. Concr. Inst., (1992).

4. ABDELGADER, H S, Effect of quantity of sand on the compressive strength of two-stage concrete, Magazine of Concrete Research, 1996, Vol. 48, No 177, pp 353-360.

5. ABDELGADER, H S, How to design concrete produced by a two-stage concreting method. Cement and Concrete Research, 1999, Vol 29, No 3, pp 331-337.

6. SCHAEFER, R L, ANDERSON, R B, The students edition of MINITAB statistical software adapted for education, Addison–Weslley Publishing Company Inc., Reading, Massachusetts, USA, 1989.

7. ABDUL AWAL, A S M, Failure mechanism of prepacked concrete, Journal of Structures Engineering, 1988, Vol 114, No 3, pp 727-732.

8. ABDELGADER, H S, GÓRSKI, J, Influence of grout proportions on modulus of elasticity of two-stage concrete, Magazine of Concrete Research, 2002. In print.

CONCRETE IN CONTAMINATED LAND: RESULTS OF 5 YEAR TESTS

S L Garvin

J P Ridal

Building Research Establishment

United Kingdom

ABSTRACT. This report discusses the results of tests on concrete samples that were undertaken over a five-year period. A series of concrete samples was based on different cement types and cement contents. Solutions of contaminants were developed to simulate conditions found on contaminated land sites. The results of tests after five years show that the majority of test samples have been affected to some degree. A number of concrete samples were not considered resistant to high concentrations of contaminants and these generally performed poorly. However, concrete with higher cement content and combinations of resistant cements had better performance. Mechanisms for the chemical attack by contaminants are proposed and a risk based approach to the use of concrete in contaminated land is discussed.

Keywords: Concrete, Contaminated land, Chemical attack, Solutions of contaminants.

Dr S L Garvin, is a Principal Consultant and Head of Construction Technology at BRE Scotland (East Kilbride). His main research topics are concerned with building materials technology and performance, in particular the durability of building materials in aggressive environments. He is a Member of the Concrete Society (MCS) and the Royal Society of Chemistry (CChem. MRSC).

Dr J P Ridal, is a Senior Consultant at BRE Scotland, his research is concerned with the performance of building materials and the impact of construction on the environment. He is a Member of the Royal Society of Chemistry (CChem. MRSC).

INTRODUCTION

Chemical attack on concrete and other materials in aggressive ground conditions has been known about for many years. Sulfate attack from soils and ground water is well known (1–3). Sulfates occur in natural soils, but also in former industrial sites. Guidance on the use of concrete in sulfate bearing soils has been extensively revised by the Building Research Establishment, United Kingdom (2). This guidance now encourages a risk based approach to assessing and managing sulfate bearing ground. The emphasis of the guidance switches to a more detailed assessment of the ground conditions, and at the same time more detailed guidance on concrete specification and form. However, the contaminated soil environment can vary considerably in the nature of the contaminants and the properties of the ground. Other contaminants also attack concrete and although some guidance is provided in the new sulfate guidance there is still uncertainty as to how mixtures of contaminants affect materials in the ground. In particular, the question of whether or not mixtures of contaminants increase the risk to concrete.

The Building Research Establishment (BRE) has therefore been undertaking tests to assess the performance of concrete in contaminated land (4–6). This research aims to produce risk based guidance for contaminated land redevelopment and will lead to a comprehensive revision of BRE Report BR255 on the performance of building materials in contaminated land (1). This work builds on research undertaken for the Environment Agency to develop guidance on risks from contaminated land to construction (3).

The research has involved a four point test programme as follows:

- Immersion of small mortar prisms in aqueous solutions of single and combined contaminants (duration of exposure of 2-4 months);
- Immersion of concrete cubes in aqueous solutions of contaminants (duration of exposure of 5 years);
- Exposure of concrete cylinders in the laboratory to a contaminated slurry (minimum duration of exposure of 10 years);
- A field trial involving the burial of concrete piles in a contaminated site (minimum duration of exposure of 10 years).

The four point programme scales the testing upwards from short term tests with representative material types to realistic field trials of long term duration.

This report describes the testing of samples of concrete that have been exposed to solutions of contaminants and the contaminated slurry for five years, previously samples had been tested at one, two and three years. The results of tests up to the three year period have been reported in previous Congress Papers (5, 6). The field trial commenced at a later stage than the laboratory based tests and therefore five year results are not yet available for this paper.

RISK FACTORS FOR CONTAINMENT ATTACK ON CONCRETE

In aggressive soils the risk factors for contaminant attack on concrete are as follows (2):

- The presence of water as a carrier of aggressive contaminants (except in the case of free-phase liquid organic contamination).

- The availability of the contaminant in terms of sufficient concentration, solubility in water and replenishment rate of the aggressive solution at the concrete surface.
- Contact between the contaminant and the building material.
- The sensitivity of the material to the contaminant, in other words the inherent durability of the material and the properties that cause it to react or not with the contaminant.

Other risk factors also influence whether or not deterioration will take place and the rate of deterioration. Identification and management of these factors are part of the risk management process. Risk factors include the following:

- The use of unsuitable materials, for example the wrong choice of cement or aggregates for the ground conditions.
- Poor production or placing of concrete that leaves the concrete with a more open texture and permeable structure.
- Placing a vulnerable material in an aggressive environment without appropriate protection from ground conditions.
- Lack of maintenance of materials to maximise their life.

The design of the building or its components will also influence the potential for contaminants to attack building materials and therefore cause damage to the structure. Issues such as the thickness of elements and if the material is part of a piled foundation, foundation strip or wall can contribute to the degree of attack experienced. In general the thicker the building material then the less likelihood there is for contaminant attack to cause significant damage to the component or structure. More slender elements are potentially more at risk than thicker elements.

The potential for contaminants to cause damage to the structure also depends on whether or not contaminant ingress into porous materials such as concrete and masonry are likely to be encouraged by both ground conditions and the structure's design. A particular example is where ground floor slabs allow evaporation of water from their upper surface and therefore capillary forces draw contaminated groundwater from soils or fill. This has been known to cause damage where ground floor slabs have been laid on sulfate contaminated fill.

EXPERIMENTAL

Concrete samples were made from several types of cement, including Portland cement (PC), Portland cement/blastfurnace slag (PC/ggbs), Portland cement/pulverised fuel ash (PC/pfa), sulfate resisting Portland cement (SRPC) and high alumina cement/blastfurnace slag (HAC/ggbs – BRECEM). Table 1 details the mixes used, a number of which met criteria for aggressive sulfate soils and their performance was expected to be good. These were based on Portland cement with replacement materials and a SRPC mix. However, other mixes were included that were not thought to be resistant to contaminants.

Solutions of contaminants used for the immersion tests were based on data from site investigation reports of gasworks, chemical works and scrapyards, Table 2. The pH of the solutions were checked on a weekly basis and the solutions replaced at three month intervals. A slurry was made from contaminated soils from various sites plus additional chemicals in order to produce a contaminated soil type environment. The slurry was replaced on an annual basis. After five years immersion concrete cubes were removed from the solutions and their condition assessed.

A number of the cubes were in good condition and could be tested directly for compressive strength. However, in most cases deterioration had progressed to the extent that the cubes had to be capped with a mortar before being tested. Some cubes had deteriorated to the stage where they could not be tested. In addition, cylinders were also tested after they were capped with a mortar.

Table 1 Details of concrete mixes used in test programme

MIX NO.	CEMENT COMPOSITION	CEMENT RATIO	w/c RATIO	CEMENT CONTENT (kg/m^3)	FINE AGG. (kg/m^3)	COARSE AGG. (kg/m^3)	28 Day CS (N/mm^2)
1	PC	100	0.55	220	1200	910	34
2	PC	100	0.55	300	772	1192	59
3	PC	100	0.6	300	772	1192	42
4	PC/ggbs	30:70	0.57	320	769	1075	36.5
5	PC/ggbs	30:70	0.45	380	729	1055	52
6	PC/pfa	70:30	0.58	320	829	1025	38.5
7	PC/pfa	70:30	0.45	380	799	995	30
8	SRPC	100	0.45	360	710	1175	73
9	HAC/ggbs (BRECEM)	50:50	0.55	320	700	1175	21

PC = Portland cement, ggbs = ground granulated blast furnace slag, pfa = pulverised fuel ash, SRPC = sulfate resisting Portland cement, BRECEM = 50:50 mix of High Alumina Cement (HAC) and ggbs, Mix 1 had a superplasticiser addition (no other admixtures used)

Table 2 Solutions of contaminants used in concrete immersion tests

CONTAMINANT	SOLN A	SOLN B	SOLN C	SOLN D	SOLN E	SOLN F
pH	7.8	2.5	8	7.8	7	2.5
Sulphate	4200	4200	4200	4200	4200	4200
Sulphide	34	34	-	-		
Chloride	-	-	218	24		
Arsenic	5	5	65	1		
Cadmium	-	-	-	0.8		
Chromium	23	23	39	41		
Cobalt	-	-	-	11		
Copper	26.5	26.5	180	103		
Lead	91	91	530	130		
Manganese	355	355	-	730		
Mercury	-	-	2	0.1		
Nickel	23.5	23.5	28	43		
Vanadium	-	-	-	47		
Zinc	65	65	351	175		
Phenol	1	1	3.5	-		
Toluene	100	100	100	100		

note - all concentrations in mg/l (except pH), water control solution termed soln G

RESULTS

The results of compressive strength tests after 5 years have been compared with the 28 day water cured strength (Table 3) and control samples that have been stored in water for five years (Table 4).

PC Concrete (Mixes 1 – 3)

The only remaining PC concrete at five years was mix 1 (PC = 220 kg/m^3, w/c = 0.55). Mixes 2 and 3 were badly deteriorated at 3 years and no further samples remained for test. The concrete was in reasonable condition that it could be tested in most of the solutions with the exception of the acidified solutions (B and F).

ggbs Concrete (Mixes 4 and 5)

Mix 4 was tested at 1, 2 and 3 years but no samples remained for test at 5 years. Concrete cubes of Mix 5 could not be tested for compressive strength at 5 years due to deterioration, although, they survived for longer than mix 4.

pfa Concrete (Mixes 6 and 7)

The pfa concrete mixes were still in moderate to good condition in the solutions after five years. Mix 6 (PC/pfa = 320 kg/m^3, w/c = 0.6) was tested for strength from all solutions except the acidified solutions (B and F) and non-acidified solutions (A and D) where considerable deterioration had occurred. Mix 7 (PC/pfa = 380 kg/m^3, w/c = 0.45) was tested for strength from all solutions except the acidified solutions (B and F).

Mix 6 was found to have gained strength in all solutions up to one year. After three years there were also strength gains in all but the acidified solutions. After five years there was generally a loss of strength in comparison with one and three years.

Mix 7 had gained strength in all the solutions up to one year. At three years there were further strength gains in most of the solutions with the exception of the acidified solutions. The most dramatic drop in strength was in solution B that contained the mix of contaminants and acid. After five years the strength of this concrete was still high in all solutions with the exception of the acid solutions. However, greater deterioration was found in solution B and the cubes could not be tested. The residual strength in the other acidified solution (F - sulfate/acid) was only 20% of the 28 day strength. Comparison with the water control samples has shown that strength loss in all but the acidified solution was negligible at five years, Table 4.

SRPC Concrete (Mix 8)

The SRPC concrete (SRPC = 360 kg/m^3, w/c = 0.45) had a high 28 day strength and it does not typically gain strength significantly after this time. In general, the SRPC concrete gained 5 – 10% strength over the first year in most of the solutions (Table 3). Indeed the concrete tended, over this period, to gain more strength in the solutions than in the water control (Table 4). The main impact on the SRPC concrete was that the cubes in the acidified solutions were badly attacked and could not be tested for strength after five years.

Table 3 Compressive strength of concrete as a percentage of 28 day water cured strength

	MIX 1	MIX 2	MIX 3	MIX 4	MIX 5	MIX 6	MIX 7	MIX 8	MIX 9
Sol A									
1 year	88.2	67.8	47.4	148.7	125.7	128.6	160.2	101.6	184.8
2 year	-	24.6	15.8	115.5	-	-	-	-	-
3 year	73.5	NT	NT	80.5	108.1	131.2	146.7	98.9	204.0
5 year	41.8	NP	NP	NP	NT	NT	141.3	65.1	186.7
Sol B									
1 year	72.0	67.8	52.2	110.5	108.1	116.9	114.6	107.8	170.4
2 year	-	27.4	23.3	81.8	-	-	-	-	-
3 year	60.3	22.0	17.8	NT	93.5	61.0	57.3	81.9	146.4
5 year	NT	NP	NP	NP	NT	NT	NT	NT	NT
Sol C									
1 year	91.2	90.7	69.9	120.0	128.6	131.2	156.8	111.2	158.4
2 year	-	51.4	16.2	16.2	-	-	-	-	-
3 year	73.5	NT	NT	NT	128.6	131.2	175.3	107.1	206.4
5 year	52.6	NP	NP	NP	NT	113.5	150.7	83.5	175.2
Sol D									
1 year	98.5	72.0	48.6	143.2	125.7	129.9	161.8	111.9	146.4
2 year	-	40.9	17.8	102.7	-	-	-	-	-
3 year	73.5	NT	NT	103.7	120.8	139.0	168.6	109.8	211.2
5 year	50.9	NP	NP	NP	NT	NT	157.8	57.6	177.1
Sol E									
1 year	98.5	83.1	72.3	141.8	128.6	146.8	145.0	116.0	177.6
2 year	-	41.2	40.7	103.6	-	-	-	-	-
3 year	70.6	22.0	22.5	102.3	124.7	131.2	166.9	102.3	196.8
5 year	45.9	NP	NP	NP	NT	NT	151.7	83.5	182.4
Sol F									
1 year	92.7	86.4	75.9	121.4	111.1	123.4	111.3	106.4	172.8
2 year	-	61.5	41.5	91.4	-	-	-	-	-
3 year	69.1	39.0	36.8	80.5	88.6	83.1	96.1	85.9	148.8
5 year	NT	NP	NP	NP	NT	NT	20.9	NT	NT
Sol G									
1 year	102.9	94.1	96.1	144.6	128.6	129.9	165.2	107.1	153.6
2 year	-	100.0	105.0	154.6	-	-	-	-	-
3 year	116.2	102.5	104.4	160.9	140.3	139.0	170.3	120.1	208.8
5 year	111.2	NP	NP	NP	132.9	134.8	157.8	83.1	193.5

Sol = solution, Sol G = water control: NP – not available for test after five years: NT = Samples too badly deteriorated to be tested

BRECEM Concrete (Mix 9)

This concrete initially had a low compressive strength at 28 days, in the region of 20N/mm^2. However, considerable strength gains were experienced in all solutions after one year (Table 3). Indeed in comparison with the water control samples there were higher strength gains in the solutions than in the water control (Table 4).

At three years there were further strength gains in the solutions, except the acidified solutions. In these acidified solutions strength was reducing. At five years strength losses were found for all solutions, although the strengths remained well above the 28 day value.

Table 4 Compressive strength of concrete cubes as a percentage of water cured samples

	MIX 1	MIX 2	MIX 3	MIX 4	MIX 5	MIX 6	MIX 7	MIX	MIX 9
Sol A									
1 year	85.7	72.1	49.4	102.8	97.7	99.0	96.9	94.9	120.3
2 year	-	21.5	15.0	74.7	-	-	-	-	-
3 year	63.3	NT	NT	50.0	77.1	94.4	86.1	82.4	97.7
5 year	37.6	NP	NP	NP	NT	NT	89.5	77.8	96.5
Sol B									
1 year	70.0	72.1	54.3	76.4	84.1	90.0	69.4	100.6	110.9
2 year	-	27.4	22.2	52.9	-	-	-	-	-
3 year	51.9	21.5	17.0	NT	66.7	66.7	33.7	68.2	70.1
5 year	NT	NP	NP	NP	NT	NT	NT	NT	NT
Sol C									
1 year	88.6	96.4	72.8	83.0	100.0	101.0	94.9	103.8	103.1
2 year	-	51.4	15.4	74.7	-	-	-	-	-
3 year	63.3	NT	NT	86.4	84.0	94.4	103.0	89.2	98.9
5 year	47.4	NP	NP	NP	NT	84.2	95.5	100.5	90.6
Sol D									
1 year	95.7	76.6	50.6	99.1	97.7	100.0	98.0	104.5	95.3
2 year	-	40.9	16.9	66.5	-	-	-	-	-
3 year	63.3	NT	NT	64.4	86.1	100.0	99.0	91.5	101.1
5 year	45.8	NP	NP	NP	NT	NT	100.0	69.3	91.6
Sol E									
1 year	95.7	88.3	75.3	98.1	100.0	113.0	87.8	108.3	115.6
2 year	-	41.2	38.7	67.1	-	-	-	-	-
3 year	60.8	21.5	21.6	63.6	88.9	94.4	98.0	85.2	94.3
5 year	41.3	NP	NP	NP	NT	69.4	96.1	100.5	94.3
Sol F									
1 year	90.0	91.9	79.0	84.0	86.4	95.0	67.4	99.4	112.5
2 year	-	61.9	39.5	59.1	-	-	-	-	-
3 year	59.5	38.0	35.2	50.0	63.2	59.8	56.4	71.6	71.3
5 year	NT	NP	NP	NP	NT	NT	13.2	NT	NT

Sol = solution, NT = Samples too badly deteriorated to be tested: NP – Not available for test after 5 years

Slurry Results

As the physical appearance of the cylinders was good samples were available for compressive strength tests. The results for tests on six cylinder samples of each mix are given in Table 5. The strength results have been supplemented with observations on the failure mode, as follows:

- Mix 1 – Normal cylinder failure mode, fracture through weakest plane of whole cylinder.
- Mix 2 – The outside of the cylinder crumbled, but the inside was rigid.
- Mix 3 – The outside of the cylinder crumbled, but the inside was rigid.
- Mix 4 – The cylinder exploded at the point of failure.
- Mix 5 – The cylinder exploded at the point of failure.
- Mix 6 – The outside of the cylinder crumbled, but the inside was rigid.
- Mix 7 – The outside of the cylinder crumbled, but the inside was rigid.
- Mix 8 – The cylinder exploded at the point of failure.
- Mix 9 – The cylinder exploded at the point of failure.

Table 5 Strength results of cylinders in slurry at 5 years, and as % of 28 day strength

MIX NO.	DENSITY kg/m^3	COMPRESSIVE STRENGTH N/mm^2	STATIC ELASTIC MODULUS GPa	*STRENGTH AS % OF 28 DAYS CS*		
				1 year	*3 years*	*5 years*
1	2386	29.0	19.8	*131*	*153*	*115*
2	2395	38.8	23.2	*94*	*106*	*75*
3	2389	24.6	18.5	*110*	*120*	*70*
4	2384	39.2	23.8	*165*	*169*	*130*
5	2386	47.2	26.1	*130*	*169*	*125*
6	2372	31.8	20.6	*117*	*136*	*95*
7	2336	31.7	20.7	*156*	*171*	*124*
8	2447	50.3	26.3	*112*	*152*	*99*
9	2407	27.5	20.1	*271*	*299*	*235*

DISCUSSION

Concrete Cube in Solution Tests

The range of concrete mixes tested was intended to provide information on the performance of different cement types and different mix proportions. The guidance on concrete in aggressive soils advises (1, 3) on the use of replacement materials such as ground granulated blastfurnace slag (ggbs) and pulverised fuel ash (pfa), although, sulfate resisting Portland cement (SRPC) is also used. The action of replacement with materials such as pfa and ggbs is as follows:

- Dilution of the C_3A content of the cement, i.e. the main phase that reacts with sulfate ions to form ettringite and cause expansion. SRPC has a low C_3A content (approximately 3%) and is therefore less susceptible to attack from sulfates than Portland cement (typically 8 – 12%).
- Removal of the free calcium hydroxide from Portland cement hydration by reaction with silica from the replacement materials. This decreases the permeability of the concrete as well as reducing the calcium hydroxide phase that is vulnerable to sulfate attack.
- A reduction in the stability of hydrated calcium aluminate. Ettringite is stable in lime solution, but if the calcium hydroxide is removed from the pore space then it is less likely to form.

Deterioration of the PC concrete (mixes 2 and 3) and one PC/ggbs concrete (mix 4) was typified by expansion, cracking, edge loss and corner loss. This form of attack is associated with sulfate attack on the concrete. Sulfate ions permeate into the surface layers of the concrete and react with the calcium hydroxide and calcium aluminates. The expansive reactions are the result of the formation of gypsum and ettringite.

In the acidified solutions there was less visible deterioration of the concrete samples. However, there was advanced strength loss of the samples in these solutions. There are two possible reasons for this occurrence, as follows:

- The acid leaches calcium hydroxide from the pore structure of the cement paste and a more open and porous structure results. There is therefore little formation of gypsum as a result. The subsequent formation of ettringite is also less disruptive as it has room to grow within the pore structure. The expansion of the cubes is therefore much reduced.
- The formation of ettringite is reduced in the acid conditions that are created in the concrete pores. The result is that expansion does not occur.

The overall impact of the solutions of contaminants is to enhance the amount of chemical attack in comparison with sulfate, or sulfate and acid solutions. In all the solutions tested sulfate was present to a high concentration, approximating to class IV sulfate conditions by the previous sulfate guidance. However, there were also metal and organic concentrations in the solutions and these appear to have had an impact. The cause of the enhanced attack is not fully understood, and if any of the individual contaminants is responsible for the enhanced attack. Further tests are, at the time of writing, underway to try to assess the effect of some of these contaminants on the chemical attack. It is possible that the metal ions provide a stabilisation of the ettringite formation in the concrete and therefore the expansion is greater and more destructive. This would not necessarily be the case in acid conditions where the ettringite would be less stable, however, the acid would be more aggressive than neutral sulfate conditions.

Concrete Cylinders in Slurry Tests

After one year the strength of the concrete cylinders had generally gained over the 28 day water cured value, Table 5. This trend was repeated at three years where further gains were found. However, after five years the situation had altered and there were strength reductions experienced by a number of the concrete mixes. These strength reductions, in comparison with three year values, could indicate that some form of chemical attack is taking place.

The observations of the failure modes of the cylinders indicated that although the cylinders remained in good condition and with high strength there is evidence of chemical attack on the outer surface. The crumbling of the external surface in the strength test particularly indicates that some attack affect may have taken place. Further tests are planned for 10 years and these tests should determine whether or not deterioration has taken place to the same extent as 1, 2, 3 or 5 years immersion in solutions.

Risk Assessment

The results of the long term experiments have indicated that there a need for risk assessment for concrete in contaminated land. The main points that should be considered are as follows:

- Mixtures of contaminants have been shown to enhance the attack on concrete compared with sulfate alone.
- Acid conditions caused enhanced deterioration of all the concrete that was tested; this was worse when the test solution contained a mixture of contaminants.
- In general, the concrete mixes that were specified in accordance with current guidance (1) performed well. Less deterioration was found for these concrete types, although, the mixtures of contaminants were still more aggressive than sulfate alone.

Guidance being developed by BRE is in the form of procedures for risk assessment and management. The process of risk assessment should include site investigation to determine the type, nature and concentration of contaminants. The risks from the ground contaminants should then be estimated and evaluated based on available knowledge of materials-contaminant interaction. The tests described in this paper will help to provide the information for risk evaluation.

Risk management for contaminated land covers a number of options. These are based on risk avoidance, risk minimisation and risk reduction. In most cases durable good quality concrete can be developed for most ground conditions and this tends to dictate that appropriate materials selection is the key to managing risks. However, the range of contaminants being considered on most contaminated land sites also brings into question the risks to other receptors, for example humans. In some cases it may not be appropriate to leave contamination in place if short or long term risks to other receptors exist. However, the risk assessment should also include a risk model involving the source of contamination, pathways to the receptors and the vulnerability of the receptor (3). The guidance from BRE is developing in this direction and risk based guidance for concrete in contaminated sites will be produced in 2002.

CONCLUSIONS

These experiments have shown that concrete is vulnerable to contaminant attack if it is specified incorrectly or the wrong mix is used. However, good quality concrete with suitable chemical resistance should perform well. The slurry tests show a much reduced degree of chemical attack than the solution tests. This finding supports the risk factors that affect the degree of chemical attack experienced, although effects were beginning to be seen after five years. The contaminants are more static in the slurry than the solutions and therefore the

replenishment rate at the surface is low. The contaminants are also more likely to be bound up in the slurry matrix. These tests require a longer testing period, but they do indicate that even in static conditions that some chemical attack is likely.

ACKNOWLEDGEMENTS

The authors would like to thank the Department of the Environment, Transport and the Regions of the UK for funding this work with industry through the Partners in Innovation programme.

REFERENCES

1. BUILDING RESEARCH ESTABLISHMENT, Performance of Building Materials in Contaminated Land, BRE Report BR255, Construction Research Communications Ltd, Watford, 1994.

2. BUILDING RESEARCH ESTABLISHMENT, Concrete in Aggressive Ground, Parts 1 to 4, BRE Special Digest 1, Construction Research Communications Ltd, Watford, 2001.

3. GARVIN, S L, HARTLESS, R, MANCHESTER, S, TEDD, P, SMITH, MA, Risks of contaminated land to buildings, building materials and services, A literature review, Environment Agency R&D Technical Report, 2000, p 331.

4. GARVIN, S. L., LEWRY, A. J., RIDAL, J. P., Building materials performance in contaminated land: experimental and field work, pp 835-837 in the Proceedings of the Third International Symposium and Exhibition on Environmental Contamination in Central and Eastern Europe, September 1996, Warsaw, Poland.

5. GARVIN, S. L., LEWRY, A. J., The performance of concrete in contaminated land, Proceedings of the Conference on Concrete in the Service of Mankind, Concrete for Environment Enhancement and Protection, Editors R K Dhir and T D Dyer, pp457–469, Dundee 1996.

6. GARVIN, S. L., RIDAL, J. P., HALLIWELL, M, Performance of concrete in contaminated land, pages 201-210 in Extending performance of concrete structures, Ravindra K Dhir and Paul A J Tittle (Editors), Thomas Telford Publishing, Part of the Proceedings of Creating with Concrete International Congress, University of Dundee, Scotland, United Kingdom, 6-10 September, 1999.

ENHANCED CHROMIUM CONFINEMENT BY BLENDING PFA WITH CEMENT

L J Csetenyi
University of Dundee
United Kingdom
A Herendi
University of Veszprém
Hungary

ABSTRACT. A typical constituent of galvanic sludge is chromium, whose immobilization potential in hydrating Portland cement has been assessed using matrices with various replacement levels of pulverized fly ash (PFA). PC:PFA ratios of 10:0, 9:1, 8:2, 7:3, 6:4, 5:5, 4:6 and 3:7 were applied. The rate of Cr retention was measured by two different extraction techniques — either by immersing the granular sample in water (static method) or by seeping water through the granules at a very low flow rate (quasi-dynamic method). The matrix material was found to retain chromium most efficiently if cement is replaced by 20-30% PFA in the blend. Comparison of the results shows that the relatively short period of quasi-dynamic leaching can be used to predict a much longer-term static leaching at a reasonable accuracy.

Keywords: Chromium, Immobilization, Cement, Fly ash, Leaching, Static, Quasi-dynamic.

Dr L J Csetenyi, is Research Fellow in the Concrete Technology Unit, University of Dundee. His main areas of interest include cement and concrete science and binder technology with emphasis on waste stabilisation/solidification and value added uses of wastes in construction.

Mr A Herendi, is a final year Materials Engineering Student at the University of Veszprém, Hungary. He has undertaken research into stabilisation/solidification of chromium containing electroplating wastes using cementitious materials. He expects to obtain his MSc degree in 2002.

INTRODUCTION

Immobilization of chromium in cement is achieved by precipitation of this heavy metal in the form of sparingly soluble $Cr(OH)_3$ if the high pH environment of hydrated cement paste is also accompanied by reducing character. Otherwise the readily soluble six-valent form of chromium prevails. Portland cement exhibits a slightly positive (about +200 mV) electrode potential and therefore it is unsuitable for immobilization of Cr unless admixed with significant quantities of blast furnace slag or pulverized fuel ash resulting in a matrix with electrode potentials of about minus 200-300 mV (Figure 1) [1].

Optimum proportions of matrix constituents were investigated earlier on a series of samples leached for 48 hours using the quasi-dynamic leaching technique [2]. That assessment included the following matrices: PC:BFS blends at 1:1, 1:3 and 1:9 ratios and PC:PFA blends at 10:0, 9:1, 8:2, 7:3, 6:4, 5:5, 4:6, 3:7 ratios.

The highest retention rates were found for the 1:9 PC:BFS blend and for the 7:3 PC:PFA blend. Present work focuses on the PC:PFA compositions, but at an extended time scale and attempts to correlate results of the two different leaching methods used (static and quasi-dynamic leaching) in view of faster assessment of leachability.

EXPERIMENTAL

Chromium was introduced as $K_2Cr_2O_7$ dissolved in the mixing water to obtain a 0.2M Cr solution; and the water/cement ratio was kept constant at 0.5. Samples were cured for 24 months, crushed and sifted to obtain grains of 1-1.6 diameter for static and for quasi-dynamic leaching with distilled water as leachant for both tests. For the former the leachate was renewed at 1, 3, 7, 14 and 21 days. The latter arrangement comprised a peristaltic pump, a sample holder tube, a collector vessel and a reservoir for the leachant (Figure 2).

The sample holder tube accommodated about 7 g of the granular sample over a glass sieve. Leachates were passed at 32 ml/h leach rate and collected at 2 hours, 6 hours, 24 hours and then daily for 7 days. Cr concentration of leachates were determined by spectrophotometry using 3 ml H_2SO_4 and 2 ml diphenyl-carbazole for a 100 ml volumetric flask and measuring at 541 nm wavelength.

RESULTS AND OBSERVATIONS

The experimental results are given in Tables 1 and 2 as well as depicted in Figure 3. It is observed that neither extremes of the composition range give acceptable retention for chromium. However, the optimal proportion seems to be slightly different depending on the leaching technique used. For the static leaching method the 9:1 and 8:2 PC:PFA ratios release the least Cr, whereas the quasi-dynamic method identifies the 7:3 ratio blend as the most advantageous one.

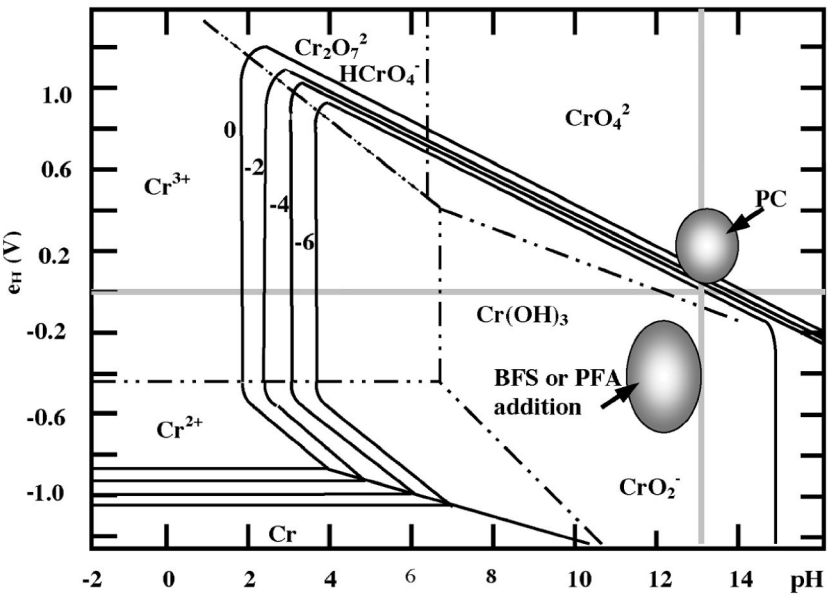

Figure 1 Pourbaix diagram of chromium at 10^x M concentrations (x = 0, -2, -4, -6) at 25°C [3]

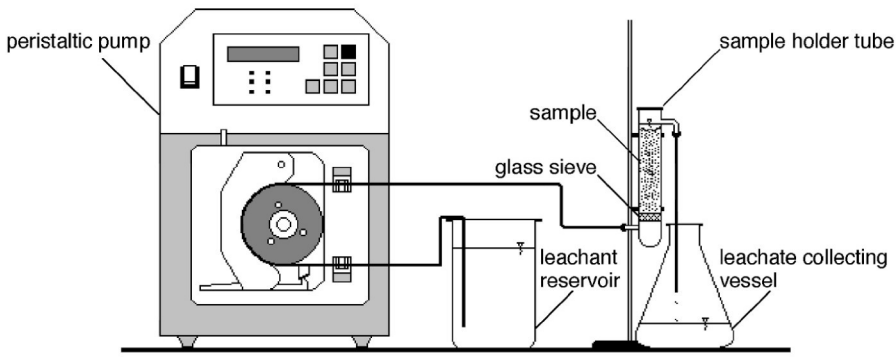

Figure 2 Quasi-dynamic leaching apparatus

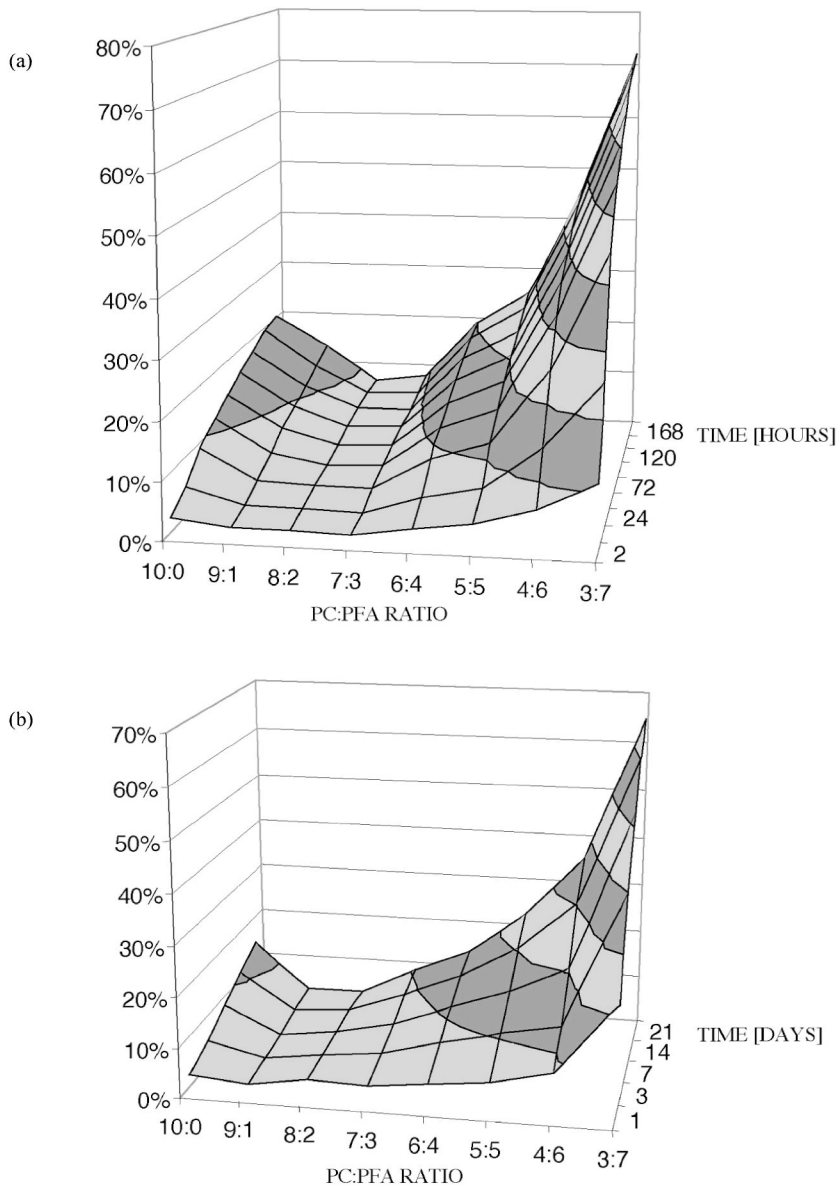

Figure 3 Cumulative leaching rates from X:Y PC:PFA blends relative to the admixed Cr
(a) Quasi-dynamic leaching, time scale 168 hours
(b) Static leaching, time scale 21 days

Table 1 Cumulative release rates for Cr from X:Y PC/PFA blends relative to admixed chromium, quasi-dynamic method

LEACHING PERIOD, HOURS	PC/PFA RATIO OF BLEND							
	10:0	9:1	8:2	7:3	6:4	5:5	4:6	3:7
0-2	0.0198	0.0131	0.0141	0.0104	0.0255	0.0366	0.0659	0.1128
0-6	0.0421	0.0200	0.0206	0.0177	0.0493	0.0685	0.1419	0.2538
0-24	0.1244	0.0377	0.0320	0.0315	0.0888	0.1199	0.2484	0.4500
0-48	0.2113	0.0592	0.0413	0.0440	0.1159	0.1539	0.3195	0.5492
0-72	0.2862	0.0776	0.0520	0.0541	0.1357	0.1799	0.3606	0.6040
0-96	0.3527	0.0932	0.0612	0.0649	0.1546	0.2041	0.3913	0.6447
0-120	0.4198	0.1095	0.0699	0.0730	0.1730	0.2278	0.4222	0.6784
0-144	0.4888	0.1265	0.0783	0.0821	0.1912	0.2500	0.4510	0.7079
0-168	0.5546	0.1443	0.0793	0.0915	0.2007	0.2617	0.4655	0.7235

Table 2 Cumulative release rates for Cr from X:Y PC/PFA blends relative to admixed chromium, static method, w/s=10

LEACHING PERIOD, DAYS	PC/PFA RATIO OF BLEND							
	10:0	9:1	8:2	7:3	6:4	5:5	4:6	3:7
0-1	0.0229	0.0138	0.0299	0.0287	0.0401	0.0523	0.0793	0.2204
0-3	0.0483	0.0208	0.0380	0.0485	0.0796	0.1055	0.1271	0.3976
0-7	0.0805	0.0275	0.0413	0.0680	0.1099	0.1512	0.2064	0.5221
0-14	0.1132	0.0383	0.0453	0.0892	0.1353	0.2049	0.3019	0.6057
0-21	0.1433	0.0467	0.0488	0.1040	0.1514	0.2412	0.3672	0.6587

Comparison between the static and the quasi-dynamic leach techniques concludes that the quasi-dynamic leaching is more intensive and removes more Cr from the sample. A less obvious observation, however, that the difference between cumulative release rates measured by the two leaching techniques for each PC:PFA ratios can be closely approximated by a linear relationship ($y \sim 0.06t + C$, where t is time in days, C is constant). Moreover, the fit is better ($R^2>0.99$) for matrices with higher Cr-retention. Based on these, one can predict longer-term static leaching values by measuring the leaching rates for as short as 3 days by both techniques and then comparing the cumulative release rates (*i.e.* total released Cr by a given day over total Cr content of the sample). The extrapolation to several weeks seems to be of reasonable accuracy. Confirmation of this hypothesis is currently under way by leaching tests extending to several months and will be reported later.

CONCLUSIONS

Certain cementitious supplementary materials (BFS, PFA) significantly improve the immobilisation potential of chromium due to their S^{2-} content and hence reducing character. Their lower porosity and permeability also contribute to this effect. Compositions containing 15-30% PFA seem to be optimal against leaching.

The reported quasi-dynamic leaching method produces comparable results to those obtained using prolonged static leaching tests and can be applied both at the design stage and to assess performance of hazardous waste repositories.

REFERENCES

1. KINDNESS, A., MACIAS, A., GLASSER, F. P., Immobilisation of chromium in cement matrices, Waste Management, Vol 14, No 1, 1994, p 3-11.

2. CSETENYI, L. J., TRITTHART, J., Stabilisation of chromium-containing electroplating sludge by cementation, World Cement, Vol 28, No 4, 1997, p 114-116.

3. MACPHEE, D. E., GLASSER, F. P., Immobilization science of cement systems, MRS Bulletin, Vol 18, No 3, 1993, p 66-71.

NO ALTERNATIVE TO VERTICAL EXPANSION

J Goyal
Indian Institute of Technology - Bombay
India

ABSTRACT. Time is ripe to develop a high-rise science in India. Population explosion, rapid urbanization, a revolution in information technology and area of land available remaining fixed, there is no alternative left except to expand vertically and to fulfill the housing and commercial accommodation needs of the country. While the country looks skywards, there is an urgent need to lay specific guidelines for earthquake resistance, fire safety, efficient vertical transportation, usage of modern construction equipment and safety during construction of high-rise buildings. This paper examines these aspects and puts forth the steps that have accumulated at the back of author's mind on his study of foreign experiences over the years.

Keywords: Jagvir Goyal, Safety, Vertical expansion, Sky-scrapers, Earthquake, High rise, Fire safety, Vertical transport.

Er J Goyal, was born on 9th October, 1958, did his Bachelor of Engineering (Civil) in 1978 with Honours from Thapar Institute of Engineering and Technology, Patiala, Punjab State, India and secured the second top position in the University. His first technical book 'RCC structure construction with slip-forms' on high-rise construction technology was published in 1992. His second voluminous and detailed technical book, 'Expeditious construction of tall RCC chimneys' was published in 1994. His third book, a literary one, about the life of a civil engineer 'The Forlorn Phoenix' (477 pages) was published in 1995. He was honoured by the Punjab State Electricity Board in 1995 with a cash award and an appreciation letter. To date, he has written more than 50 papers and articles in the technical magazines and newspapers of repute. He has presented papers at National and International Conferences. Presently, he is serving as a Senior Executive Engineer (Civil) with Punjab Government and has 23 years of experience in construction work to his credit. He has been in charge of construction of tall RCC chimneys and natural draught cooling towers for thermal power projects.

INTRODUCTION

A 'High-rise movement' is in the offing in India too. Population explosion coupled with the hard fact that area of land available with us is fixed has changed the direction of 'development arrow' from horizontal to vertical. Urbanization is approaching its peak. There is a revolution in Information Technology front with more and more citizens becoming 'netizens'. Such a situation tends to break all restrictions and force its way to expansion. With the available 'Earth-space' shrinking day by day, the only alternative left is to look towards the 'sky' and give birth to sky-scrappers.

New York's famous night-view makes one believe as if the high-rise towers are not scrapping the sky but intruding into it. The 102 storeyed Empire State Building, inaugurated way back on August 30, 1929, still fascinates the onlookers. At that time, it could have been a case of giving shape to one's dreams but today, high-rise structures have become a necessity. Land becoming dearer, its cost can be divided among dwelling units only if multi-storeyed buildings are erected. Cost of external services can also be cut down and parking facilities can be increased if horizontal development gives way to vertical expansion. Keeping India's economic conditions in view, vertical expansion becomes all the more necessary.

Housing Shortage

In India, the VEB (Vertical Expansion Bug) has bitten the metros only [1]. The population has crossed one billion! Yet people are having four-canal houses, single-storeyed buildings, horizontal commercial centers and Government offices opened in the old, dilapidated buildings. There is an urgent need to demolish all unsafe and old structures, to free the precious land, to utilize it in a judicious manner and to erect multi-storeyed, tall buildings wherever possible. The housing shortage has been estimated to be around 41 million [2]. Though shelter was enshrined as a Fundamental Right in the Constitution of India, housing could not get the attention it deserved as there were multiple problems to be tackled at other fronts. Of the houses available in the country, only 40% can be reckoned as properly built while the rest come under temporary category. In order to fulfill the shortage and to make available such a large number of dwelling units, the only solution is to build tall, multi-storeyed buildings having different sizes of accommodation for lower, middle and upper income categories. If there is no action now, soon we will be forced to do so. There is no alternative! Time is ripe to develop a high-rise science. So far as tall industrial structures are concerned, well defined written word is available. However multi-storeyed commercial, residential and office towers are demanding ready availability of detailed guidelines that need to be followed as and when the VEB bites more and more cities [1].

As the country gears itself to expand vertically, many new factors that need to be given special attention, raise their heads. Devastation caused by the Bhuj earthquake sent the country reeling and sheer necessity of having earthquake resistant buildings was felt by the country. Occasional sight of towering infernos draws attention towards fire safety measures. Provision of fast and quick vertical transport systems in high rise buildings is mandatory to keep the buildings efficient and this is an additional factor to be watched. Maximum usage of modern construction equipment to ensure faster and better construction is a must and equipment manufacturers all over the world are to be encouraged to market their equipment in India. Above all, safety measures an aspect often neglected by the builders in India, is to be given due consideration. An overview of these aspects is important.

EARTHQUAKE RESISTANT BUILDINGS

The Bhuj Experience

The earthquake that shook Bhuj and surrounding areas of Gujarat, India on 26th January, 2001 left the state gasping for breath. There was death and devastation all around. Cities and towns on the whole were destroyed. Major cause of an alarming death toll was construction of tall buildings without making them earthquake resistant. These buildings were unable to withstand an earthquake of just 6.8 magnitude on Richter's scale. No earthquake safety measures were taken by the builders though the area fell under severe seismic zone.

Avoiding Collapse Of Buildings

It is not the earthquake but the collapse of buildings that causes destruction and loss of human lives. Earthquakes will do least harm if the collapse of buildings is avoided. The buildings may sway, deform, crack or distort but must not collapse. Seismic forces assume greater significance with the increase in height of buildings and affect the structural design of the building in a big way. 'Total deflection' at the top of the building increases with the increase in its slenderness ratio and this has to be taken care of. The Architect however will not compromise over the services to be given to end-users of the building and will ask for wall free or column free floors where necessary. The ceilings too may be required to be flat and unhindered to accommodate AC-ducts and electrical fixtures above false-ceilings. Under such circumstances, the following guidelines may prove very useful.

(i) A tube-structure may be found highly effective in resisting seismic loads. Such a structure was first suggested by Owings and Merill, Chicago. In this structure, the core of the building is kept stiff while columns are provided along its periphery and are connected by spandrel beams. A 'Flat-slab' design is preferred for ceilings as it does away with the beams [3].

(ii) The structural frame-work should be kept as highly redundant or indeterminate during design. Such a structure will provide better resistance to lateral earthquake forces [3].

(iii) The mass of the buildings should be kept as least possible. Light weight materials should be brought under use. Lesser is the self-weight of the building, lesser will be the earthquake force affecting it [3].

(iv) The seismic zone of the area having the building must be kept in view during design along with the wind velocity in that area.

(v) Deflection-diagram of the building should be studied and joints should be so designed that a cumulative effect of deflection does not occur in any member.

(vi) Sub-soil investigations must be carried out in the field to ascertain the bearing capacity of the soil and other factors. The investigating agency must carry a high rating. Investigation results must be realistic and authenticated [4].

(vii) For buildings taller than 30 meters, model analysis should be carried out to study the behavior of the building under random motion of ground.

(viii) For buildings taller than 75 meters, dynamic behavior of the structure must be studied.

(ix) A large damage occurs due to break-out of fires on occurrence of an earthquake. No time may be available to operate fire fighting equipment. The buildings should therefore be provided with escape routes for instant use by the occupants [4].

(x) The vibrations due to earthquakes rise in buildings from foundation upwards. The buildings should therefore be provided with bearings that are able to absorb shock waves [5].

FIRE SAFETY

From time to time, reports of high rise buildings getting destroyed by major fires and loss of several lives have been hitting the newspaper headlines. A few such instances can be listed here:

- October, 1992: Krishi Bhavan, New Delhi holding many important offices in it completely gutted.
- April, 1990: Prestigious Vigyan Bhavan, New Delhi, a host to many national and international events completely ravaged by the intense blaze.
- January, 1986: Siddhartha Continental Hotel, New Delhi destroyed in fire claiming 37 lives.
- June, 1983: Gopala Towers, New Delhi got engulfed in fire, trapping 400 people in it.
- January, 1972: 21-storeyed SBI Building, Mumbai destroyed in fire claiming 9 lives.

Each mishap sends a grim reminder to the builders in the country to adopt minimum required safety measures and evacuation facilities for high rise buildings. In addition to earthquake resistance, fire safety is the second most important factor to be kept in mind. The country has not to give birth to 'Towering Infernos'. The guidelines in this regard should include the following :

(i) In case of fire, the main stairs of the high-rise buildings should get isolated from the rest of building by automatic closing of fire-doors and should further be pressurized with whiffs of fresh air.

(ii) An automatic system should close the air-conditioning system of the building thus stopping re-circulation of air and smoke and at the same time should activate ventilation fans to suck in fresh air to all those floors that are not affected by fire.

(iii) Provision of a computer-system loaded with software to analyze the fire situation and make announcements over public address system should be mandatory [1].

(iv) The electrical equipment and installations provided in the buildings must be of high standard. The building should be designed to carry an emergency power supply in addition to the main supply. The main supply should automatically switch off in case of fire. The emergency supply should turn on to run ventilation fans.

(v) Safe exit routes and escape stairs should be planned in the design of the building.

(vi) Sufficient area around each high rise building should be kept open and unoccupied for free movement of fire-tenders.

(vii) Provision of exhaust machinery and water tanks of sufficient capacity in the basement of buildings should be ensured as the basements are susceptible to fire.

(viii) Shafts for electric cables should be separate and not common with those for water supply and telephone lines. These should be provided with fire resistance seals.

(ix) Provision of smoke detectors, automatic fire sensing systems, breathing apparatuses and sprinkler systems should be made on each floor of the high rise buildings.

(x) Existence of combustible materials in the buildings proves to be of major disadvantage in controlling a fire. Wherever such materials are used, these should be painted with intumescent coatings to avoid spread of fire [1].

VERTICAL TRANSPORT SYSTEM

Having a fast and efficient Vertical Transport System is another factor that must be counted while planning to raise a high-rise building. The following points should be given due consideration in this regard:

(i) A 'Traffic study' involving accurate assessment of building users must be made. Traffic flow measurements should tell the number of persons that ride the elevators in a five minute period. Peak demand hours should be identified.

(ii) Elevators should be located in the central core of the building for the quickest and efficient carriage of vertical traffic.

(iii) All elevators should operate under 'Group control' system rather than independent control to avoid disproportionate loading. Under the 'Group control' system, several cars respond to a call. Thus a centralized and group-controlled system responds maximum.

(iv) All cars(elevators) should be fitted with overload devices. Such a device keeps the car-doors open, sounds a buzzer and switches on a warning light whenever the car-load exceeds 10% of rated capacity.

(v) All cars should be provided with Automatic Rescue Devices (ARD). These devices send the cars to nearest floors in case of power failures and even open the doors.

Sears Tower in USA is a 110-story building and is reckoned as the tallest office building in the world. It carries a 106-cab elevator system including 16 double decker elevators. The top deck known as Skydeck rises 1353 feet above ground and two express elevators soar to this altitude in just over a minute - so efficient is the 'vertical transport system'!

MODERN CONSTRUCTION EQUIPMENT

Maximum usage of Modern Construction Equipment should be made while raising tall buildings and sky-scrappers if good quality work and faster construction is to be ensured. The equipment manufacturers all around the world have developed amazingly fast, accurate and durable construction equipment. They must be encouraged to market their equipment in India. The following specifications should be compulsorily adopted:

(i) RMC plants should be installed at the site of high-rise building and all concrete used be Ready Mixed Concrete only [6].

(ii) Use of super-plasticizers that are fully compatible with the cement under use should be made to maximum possible extent.

(iii) Maximum concrete pouring should be done by use of concrete-pumps. Super-plasticizers will help in free flow of concrete through placer booms without increasing water-cement ratio.

(iv) Sophisticated form-work systems such as slip-forms, hydraulic jump-forms, should be put to use wherever possible. This factor should be kept in mind at the time of building-design itself.

SAFETY MEASURES

Importance

Safety in construction is one area often relegated to the bottom rung of priorities by the builders and the engineers. Irreparable loss of money, manpower and progress may occur whenever a scaffolding fails, a roof collapses or a fatal accident takes place at site of work. It has been a common experience that once a worker loses his life in an accident at site, the morale of the working force sinks to a new low. The spirit of working and the progress of work never remain the same as have been earlier. Despite this realization, safety aspect is often ignored. The Indians are habitual of getting shock treatment. Only then when some untoward incident occurs, they begin to take safeguards. This tendency needs to be curbed.

Situation In India

Findings of International Labor Organization reveal that the accident rate among industrial workers is highest in India, touching 4 per 1000 and a major share of it goes to the construction sector [7]. Indian construction industry is highly labor-intensive. Though mechanization in construction projects is inevitable but machines are being adopted in a very slow manner. The labor is cheap, unorganized, unaware of its rights and mostly struggling to make both ends meet. The builders, therefore, find it convenient and profitable to use manpower than machines.

Builders dread occurrence of an accident at their work-sites. They know that one fatal accident may result in closure of work for a few days and rise of fear among workers who may refuse to work at higher elevations. Not only this, the credibility of the builder may be at stake. He may have to pay a large amount on account of compensation if the workers are not covered under group insurance. Besides, he has to wriggle out of legal complications arising upon occurrence of the accident. Now certain organizations have begun to ask for 'certified accident record' of the builders before allotting works to them [7]. A high incidence may result in disqualification of a builder. So much trouble an may cause yet the only 'safety measure' the builders take is to keep praying to the god to keep their site free of accidents. No other measures are taken.

Construction Safety Manual

It is time that a 'Construction Safety Manual' is evolved, made a part of standard tender document in every organization and strictly enforced by the supervising agency. Some teething troubles may arise in doing so but gradually the safety aspect will become a part and parcel of every site and the builders will not hesitate in making expenditure on this account [7].

Looking for a concise guideline on safety in construction, some of the requirements may be summed up and classified in a few categories as under:

Safety Measures While Handling Tools, Equipment and Machinery

1. All electric tools must be properly insulated.
2. All winches and hoists shall be provided with magnetic brakes for automatic operation on failure of electricity.
3. No metallic ladders shall be used when high voltage electric wires are passing overhead.
4. Only skilled persons shall be allowed to handle equipment or machinery.
5. All compressed gas cylinders shall be stored in upright position only, with their valve caps in position.
6. All equipment shall be properly earthed.
7. No electric tools shall be used while standing in water and without taking proper precautions.
8. All wire ropes shall be thoroughly checked against any broken strands.
9. Flash back arrestors shall be provided on gas cylinders.
10. All machine guards shall be kept in position while the machines are running.
11. No discarded tools, equipment or machinery shall be allowed to use.
12. The scaffoldings and the wooden planks used shall be strong and durable.

Accessories To Be Provided To The Workers

1. All workers shall be provided with safety helmets when work at higher elevations is in progress.
2. All workers deployed at higher elevations shall wear safety belts.
3. Protective gloves, shoes and aprons shall be provided to all workers handling electric equipment and chemicals.
4. Ear plugs shall be provided to workers deployed in high noise level locations.

5. Face masks or nose filters shall be worn by workers in areas where obnoxious gases are released by chimneys or chemical plants. Respiratory equipment shall be available for use when required.
6. Safety goggles and shields shall be used by workers engaged in welding work.
7. Gum-boots and torches shall be provided to workers working inside tunnels.
8. Breathing air hoods shall be provided to workers doing sand blasting or spray painting work.
9. Other accessories as suggested by 'Safety organization' with respect to the nature of work shall be provided.

Safety Arrangements To Be Made At Site Of Work

1. 'Men working overhead' sign boards shall be placed around structures on which work is in progress at higher elevations.
2. All floor openings in intermediate floors of a building shall be kept covered with gratings. Otherwise temporary protective railings shall be provided.
3. Warning lights (during night) and red flags (during daytime) shall be provided around dangerous areas of working, near ground-level water tanks and near trenches and excavations.
4. Proper railing shall be provided around all working platforms at higher levels.
5. Nylon safety-mesh shall enwrap working platforms of high-rise structures.
6. Sufficient illumination of all working levels and access arrangements shall be ensured.
7. Any spill-over of oil or grease on ladders, stairs or landings shall be cleaned at once.
8. The height of ladders shall be restricted. Too long ladders shall not be allowed. Intermediate platforms shall be provided to give relief to workers going up.
9. All access arrangements shall be inspected by the engineer to be safe and well supported before allowing their use by the workers.
10. Proper bearing shall be provided to the planks and battens used in temporary platforms. No overhangs shall be permitted.
11. All scaffoldings and shuttering shall be well braced and supported. It must be examined and passed by the engineer before allowing pouring of concrete.
12. In 'enclosed' working areas such as tunnels, proper ventilation arrangements shall be made.
13. Full arrangements for storage and handling of explosives, radio-active elements and chemicals shall be made.
14. Fire fighting equipment shall always be kept ready. Fire extinguishers shall not be allowed to expire.
15. All working platforms shall be kept clear of projecting nails in wooden planks.

Safety Measures When Work Is In Progress

1. Vertical cuts in excavation, if any, shall be fully braced or shored.
2. All excavated earth shall be stacked away from the cutting edge to avoid its falling over workers and burying them.
3. Site-offices and stores shall be located at a safe distance from the working area. This shall be specially ensured while constructing a high-rise structure.
4. All vehicles shall be parked away from work-site and the excavated area.
5. Periodic checks of wire-ropes, wooden planks, scaffoldings, shuttering, electric wires and cables, and access arrangements shall be carried out.

Safety Organization

On major projects, a Safety Organization should be established that should lay concerted efforts to ensure safety. On minor projects or construction sites, safety engineers should be appointed. They should ensure implementation of above points. In addition, they should see that i) medical facilities and first aid is available at site; ii) an ambulance or a vehicle is always available to carry an accident victim to hospital; iii) one or two persons are trained in giving artificial respiration; iv) accidents are reported at once to the project heads. Safety organization should celebrate 'Safety weeks' to create awareness among workers. Safety awards should be instituted. Accident investigations, lodging of claims and payment of compensation should be ensured by this organization.

Accidents must be declared intolerable. Safety must be assigned priority. As per a recent survey, Indian construction industry employs 32 million people of whom 24 million are workers. No doubt, it is a big force. Making it undergo safety training programs may not look feasible at this stage, but it can certainly be motivated to follow safety rules by holding safety talks from time to time.

CONCLUSIONS

A look at the world's tallest twin towers in Kuala Lumpur with a height of 1483 feet, the 1454 feet high Sears tower in USA, 75-storeyed Interstate and many other such structures make the necks bend at 90^0 and enthrall one and all. It is heartening to note that hundreds of tall super-structures in USA have been designed and built by Indians. High-tech support including most wonderful software packages are becoming available in India and brilliant academic achievements are galore. If the latest equipment is made to arrive in plenty, there is nothing to hold the country back. Now is the right time to touch the dizzy heights. India must not lose any more time in seizing the opportunity.

REFERENCES

1. GOYAL, J, Vertical expansion, The Tribune, September 1999, p16.
2. S K, Housing, India at 50, Express Publications (Madurai) Ltd, Chennai, 1997, p 688.

3. ALPA, S, High rise offices - A structural engineer's viewpoint, Indian Architect and Builder, September 1992, p 84.

4. INDIAN STANDARD INSTITUTION, Criteria for earthquake resistant design of structures, IS1893, New Delhi, 1983, p 72.

5. GOYAL, J, Coping with the calamity, The Tribune, February 2001, p 16.

6. GOYAL, J, Time to switch over to RMC, The Tribune, May 1999, p 16.

7. GOYAL, J, Criminal neglect of safety, The Tribune, February 1998, p 16.

CLOSING PAPER

CONDITION SURVEY OF SALT DAMAGE TO REINFORCED CONCRETE BUILDINGS IN JAPAN

M Y Masuda
Utsunomiya University
Japan

ABSTRACT. This paper reports on the results of comprehensive survey on the degree of salt damage, chloride content, and the relationship between the chloride content and the rate of corrosion of reinforcement in reinforced concrete buildings in Japan.

The survey consisted of the following:

(1) Condition survey of concrete by appearance observation.
(2) Survey of chloride content of concrete.
(3) Survey of rate of corrosion of reinforcement related to chloride content of concrete.

The progress of deterioration is nearly levels off 10 to 15 years after completion for buildings at a long distance from the sea and those containing no sea sand, whereas buildings near the sea and those containing sea sand tend to continue to deteriorate for a long period. The rate of corrosion is almost inversely proportional to the cover depth and nearly proportional to the chloride content.

Keywords: Condition survey, Salt damage, Reinforced concrete building, Appearance observation, Chloride content, Rate of corrosion, Building near the sea, Buildings containing sea sand, Concrete cover.

Professor M Y Masuda, is the Professor at the Department of Architecture and Civil Engineering, Utsunomiya University. He received Dr. Eng. from Tokyo Institute of technology in 1982. The main themes of studies are deterioration mechanism and repair system for reinforced concrete and performance evaluation of high performance concrete.

INTRODUCTION

Deterioration of reinforced concrete buildings due to salt damage generally includes expansive cracking of concrete due to such salts as magnesium sulfate and magnesium chloride contained in seawater. In this paper, however, it refers to corrosion of reinforcement and other steel embedded in concrete by the action of penetrating chlorides, causing such damage as cracking and delamination.

Chloride content in concrete is one of the most important factors which affect the durability of reinforced concrete. Reinforcing bar in concrete is protected from corrosion by alkalinity of concrete, however, when concrete contains certain amount of chloride, the reinforcing bar would no longer be protected and begin to corrode.

Most chlorides gain access to the inside of concrete through two paths: one is the case where chlorides contained in the materials of concrete, such as sea sand and chemical admixtures, are included during mixing and the other is the case where splashes of seawater and air-borne salt deposit on coastal buildings, gradually penetrating concrete [1][2].

This paper reports on the results of comprehensive survey on the degree of salt damage, chloride content, and the relationship between the chloride content and the rate of corrosion of reinforcement in rein forced concrete buildings in Japan.
The survey consisted of the following:

(1) Condition survey of concrete by appearance observation.
(2) Survey of chloride content of concrete.
(3) Survey of corrosion of reinforcement related to chloride content of concrete.

1) Delamination

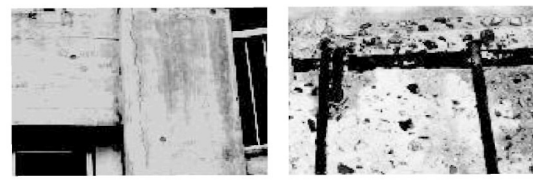

2) Crack

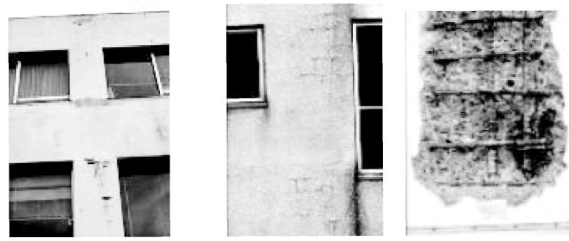

3) Peeling

Figure1 Deterioration of reinforced concrete buildings

CONDITION SURVEY OF CONCRETE BY APPEARANCE OBSERVATION

Method of investigation

In order to grasp the state of the deterioration of reinforced concrete structures as a whole, appearance observation was carried out on 4,363 reinforced concrete buildings, examining deterioration phenomena, such as cracking, reinforcement corrosion, and spalling, and their degrees and portions in the structure. The buildings under study were classified by the distance from the coast, while the presence of sea sand as a component material was examined to analyze its effects on the deterioration.

Buildings were sampled to equalize the numbers in each group classified by the distance from the coast and building age. Random selection was made in regard to the use of the buildings. Table 1 gives the numbers of buildings classified by their use.

Table 1 Surveyed buildings classified by uses

USE	NUMBER	PERCENTAGE
Residence	1,552	34.9
Office	687	15.7
School	851	19.5
Culture	321	7.4
Hospital	653	15.0
Commercial	196	4.5
Industrial	92	2.1
Other	41	0.9
Total	4,363	100

In the survey, sample buildings were examined in portions of columns, beams, walls, areas near the openings, parapets, eaves, and balconies facing the north, south, east, and west. The presence/absence of the following deterioration and their degrees (less than 5 or 5 or more) were investigated:

R: rust exudation.

C: cracking along reinforcement.

Em: delamination of finishing materials, such as mortar.

Ex: reinforcement exposure.

The degree of cover depth and whether the portion contains sea sand were also examined where practicable by visual observation or checking the drawings/documents.

Results

(1) Deterioration

The results of the condition survey are summarized as follows:

1) Out of the 4,363 buildings surveyed, those exhibiting no deterioration amounted to 2,586 buildings (59.3%). Certain deterioration was observed in at least one aspect or portion of the remaining 1,777 buildings (40.7%), such as rust exudation, cracking, and reinforcement exposure.
2) Among those involving deterioration, 691 buildings (15.8%) exhibited relatively severe deterioration, such as reinforcement exposure.
3) Buildings having one or more aspect or portion in which reinforcement is exposed at 5 or more points, indicating more significant deterioration than 2) above, amounted to 255 buildings (5.8%).
4) Out of the buildings counted in 3) above, those having such deterioration in critical portions in regard to structural capacity, such as columns, beams, and walls, were limited to 91 buildings (2.1%). Deterioration was found mostly in parapets and eaves.

(2) Analysis of causes of deterioration

a) Effect of cover depth.
Out of 521 buildings having exposed reinforcement, 469 buildings (90.0%) had insufficient cover, suggesting that it was one of the major causes of deterioration.

b) Effect of deterioration with age.
The buildings having exposed reinforcement were tabulated in Table 2 according to the age after completion. The percentage of deteriorated buildings increases 10 years after completion.

Table 2 Ratio of buildings having exposed reinforcement classified by age

AGE (YEARS)	TOTAL NO. OF BUILDINGS*	NO. OF BUILDINGS HAVING EXPOSED REBAR	PERCENTAGE OF BUILDINGS HAVING EXPOSED REBAR
0-9	1,527 (35.0)	90	5.9
10-19	1,595 (36.6)	333	20.9
20-	1,227 (27.8)	265	21.8
Unknown	24 (0.6)	3	12.5
Total	4,363 (100)	691	Average: 15.8

Note: * Values in parentheses are percentages in the total.

c) Effect of Distance from the Sea.
Buildings having any one point of reinforcement exposure in any one portion are tabulated in Table 3 according to the distance from the sea. Exposed reinforcement was found in 22% of the buildings located within 200 m from the sea, which is 1.5 times the value, 15%, for buildings located farther than 200 m from the sea. This suggests salt damage from outside of the buildings near the sea.

Table 3 Ratio of buildings having exposed reinforcement classified by distance from the sea

DISTANCE FROM THE SEA (KM)	TOTAL NO. OF BUILDINGS	NO. OF BUILDINGS HAVING EXPOSED REBAR	PERCENTAGE OF BUILDINGS HAVING EXPOSED REBAR
0-0.2	1,003 (23.0)	225	22.4
0.2-1.0	1,179 (27.0)	181	15.4
1.0-10	1,138 (26.1)	173	15.2
10-	977 (22.4)	102	10.0
Unknown	66 (1.5)	10	15.2
Total	4,363 (100)	691	Average: 18.8

Note: * Values in parentheses are percentages in the total.

d) Effect of sea sand as a component material.
Table 4 tabulates buildings having exposed reinforcement according to the presence/absence of sea sand as a component material. Exposed reinforcement was found in 18% of buildings containing sea sand as a component material of concrete, which is 1.3 times the value, 14%, for buildings containing no sea sand.

Table 4 Ratio of buildings having exposed reinforcement classified by presence of sea sand

PRESENCE/ABSENCE OF SEA SAND	TOTAL NO. OF BUILDINGS	NO. OF BUILDINGS HAVING EXPOSED REBAR	PERCENTAGE
Buildings containing sea sand	578	104	18.0
Buildings with no sea sand	2,571	362	14.1
Unknown	1,214	225	18.5
Total	4,363	691	15.8

e) Effect of marine salt on deterioration with age.

The deterioration condition of each column, beam, wall, area near openings, balcony, eave, and parapet in the north, south, east, and west aspects was assessed according to the criteria given in Table 5. The total of such points of each building divided by 1.4 was defined as the degree of deterioration of the building.

Figures 2 and 3 show the average degrees of deterioration of buildings classified by the distance from the sea, presence/absence of sea sand, and age after completion.

Table 5 Grade of deterioration and points

DETERIORATION	POINT
Five or more exposed rebars in at least one portion in at least one aspect	5
1 to 4 rebars in at least one portion in at least one aspect	3
Cracking but no exposed rebar	1

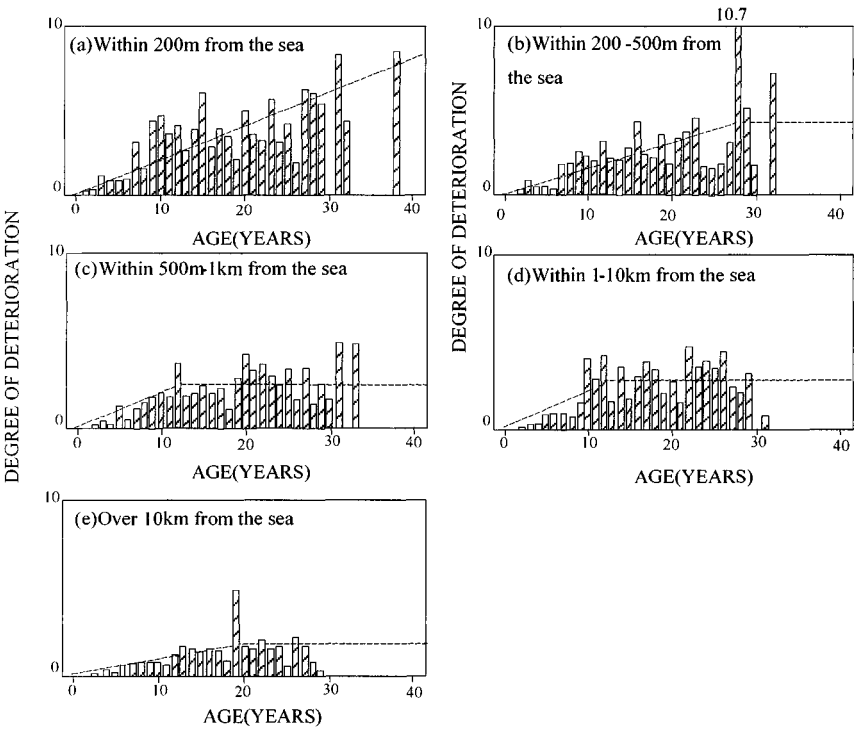

Figure 2 Effect of distance from the sea by appearance survey

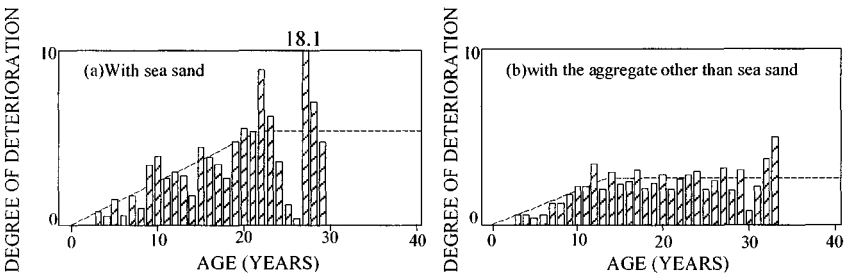

Figure 3 Effect of use of sea sand by appearance survey

These Figures reveal that the progress of deterioration nearly levels off 10 to 15 years after completion for buildings at a long distance from the sea and those containing no sea sand, whereas buildings near the sea and those containing sea sand tend to continue to deteriorate for a long period.

CHLORIDE CONTENT OF CONCRETE IN BUILDINGS

Survey Method

Fifty buildings near the sea and ten buildings containing sea sand were examined to grasp the actual chloride ion content of concrete in buildings. These buildings have been used as flats, offices, public halls, laboratory and so on. The age of the investigated buildings varied in the range of 7 years and 46 years, but most of them were between 10 years and 20 years. Sea sand was applied to 44% and river sand was to 53% of the investigated buildings and the rest was not clear. The type of admixture applied to concrete was unknown. Design strength of concrete were between 15 N/mm^2 and $21N/mm^2$, but most of them were $18N/mm^2$. In the survey, concrete cores 10 cm in diameter were drilled from columns, walls, and other parts on the exterior, cut into disks 1 to 2 cm thick, and ground into powder. The powder samples were then entirely dissolved in nitric acid and subjected to analysis by potentiometric titration and absorptiometry to determine the chloride ion content.

RESULTS

Figure 4 shows the averages of the inward distributions of chloride ion concentrations on the aspect facing the sea and other aspects of each building

This Figure reveals the following:

1) When sea sand is used, the chloride ion content is high at deep sections. The chloride ion concentration in buildings containing sea sand and located at long distances from the sea is highest at a depth of 3 to 4 cm while being low on the surfaces. In buildings containing sea sand and located near the sea, the concentration is very high on the surfaces.
2) On the aspect facing the sea, the chloride penetration in concrete is greater than on the other aspects, and the difference widens as the distance from the sea decreases.
3) The chloride ion penetration in concrete on the ground floor is greater than on upper floors. In buildings within a distance of 50 m from the sea, which are occasionally exposed to splashes of seawater, the chloride ion concentration is very high on the surfaces, as well as into significantly deep sections.
4) In buildings within a distance of 50 m from the sea, which are occasionally exposed to splashes of seawater, the chloride ion concentration is very high on the surfaces, as well as into significantly deep sections.
5) In buildings at 100 m from the sea and beyond, the chloride ion concentrations are high on the surfaces but low in deep sections. On the west coast of the northern part of Honshu Island, buildings 100 m or more away from the sea exhibit extremely high chloride ion concentrations. The chloride ion concentration at the deepest section was then subtracted from the concentration at each depth and the difference was integrated in the direction of the depth

Table 6 Buildings surveyed

NO	LOCATION	AGE (YEAR)	USE	NUMBER OF BUILDINGS	DESIGN STRENGTH (N/mm^2)	DISTANCE FROM SEA (m)	FINE AGGREGATE
1	Hokkaido	25	Flats	1	Unknown	590	River sand
2	Aomori	17	Laboratory	2	21	140	River sand
3	Aomori	12	Office	1	Unknown	20	River sand
4	Akita	7	Flats	1	21	150	River sand
5	Yamagata	11	Flats	1	18	800	River sand
6	Chiba	3 – 24	facility	2	Unknown	20	River sand
7	Chiba	22	Market	2	21	10	River sand
8	Chiba	21	Flats	2	Unknown	50	River sand
9	Chiba	20	hall	1	18	50	River sand
10	Chiba	18	tower	1	Unknown	50	River sand
11	Chiba	15	Flats	1	Unknown	30	River sand
12	Niigata	28	Flats	1	Unknown	1200	River sand
13	Niigata	21	Flats	1	18	120	River sand
14	Toyama	15	Flats	1	18	360	River sand
15	Ishikawa	15	Flats	1	18	700	River sand
16	Fukui	12	Flats	1	21	470	River sand
17	Shizuoka	13-15	Flats	4	Unknown	700	River sand
18	Shizuoka	8	Flats	4	Unknown	230~350	River sand
19	Aichi	12	Flats	1	18	40	River sand
20	Kyoto	7	Flats	1	18	150	River sand
21	Osaka	15	Flats	2	18	10~50	Sea sand
22	Osaka	14	Office	1	18	20	Sea sand
23	Hyogo	16	Flats	1	18	150	Sea sand
24	Hyogo	8	Flats	1	18	100	Sea sand
25	Tottori	14	Flats	1	18	10	River sand
26	Shimane	15-16	Flats	2	18	60~80	River sand
27	Hiroshima	15	Office	1	Unknown	50	Sea sand
28	Yamaguchi	13	Flats	1	18	250	Sea sand
29	Ehime	19	Office	1	18	5	River sand
30	Ehime	10	Flats	1	18	350	Sea sand
31	Fukuoka	27	Flats	1	15	150	River sand
32	Saga	30	Flats	1	18	100	Unknown
33	Kumamoto	10-12	Flats	2	18	300	Sea sand
34	Oita	10-15	Flats	2	18	450-550	Sea sand
35	Miyazaki	9	Flats	1	18	5	River sand
36	Kagoshima	24	Flats	1	15	200	River sand
37	Okayama	15	Flats	1	Unknown	2300	Sea sand
38	Hiroshima	12	Flats	1	Unknown	2400	Sea sand
39	Hiroshima	13-14	Flats	2	Unknown	7000	Sea sand
40	Hiroshima	7-12	Flats	4	Unknown	6000	Sea sand
41	Kagawa	13	Flats	1	Unknown	6000	Sea sand
42	Fukuoka	17	Flats	1	Unknown	3000	Sea sand

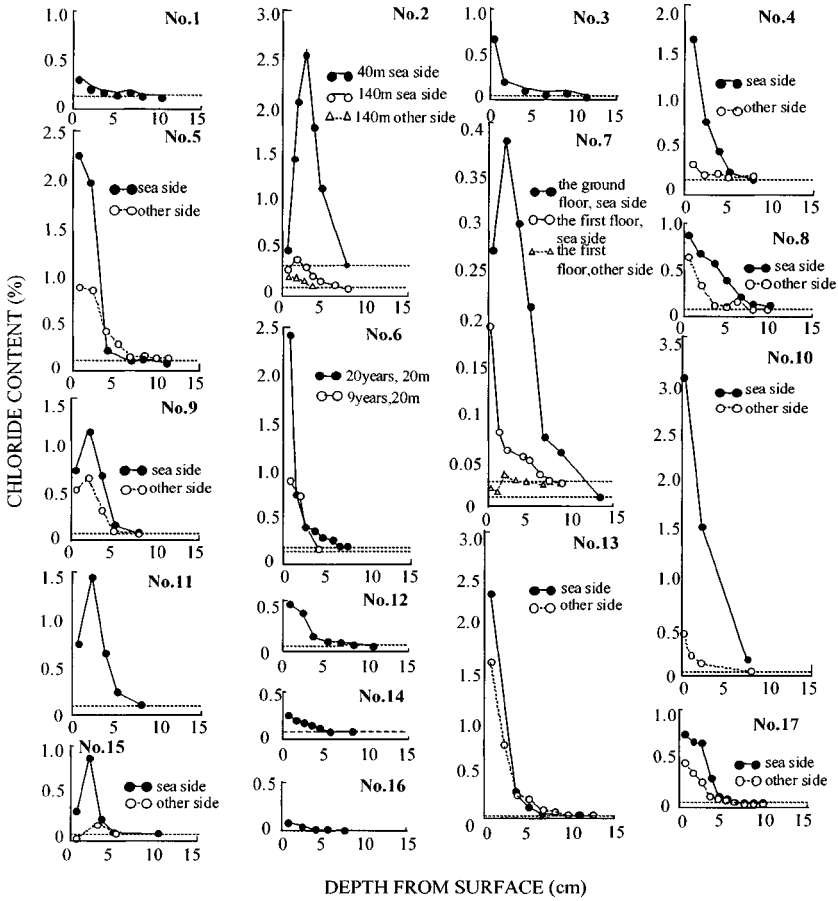

Figure4-1 Inward distribution of chloride content in actual buildings

The result was divided by the number of years after completion to determine the chloride ion penetration per unit time and unit area. Figure 5 shows the results plotted over the distance from the sea, indicating that the chloride ion penetration decreases as the distance from the sea increases, excepting those of the buildings on the west coast of the northern part of Honshu.

CHLORIDE CONTENT AND RATE OF CORROSION OF BUILDINGS

Survey Method

In order to quantitatively grasp the effect of chloride content on the rate of reinforcement corrosion, the chloride content of concrete was surveyed in fifty of the buildings given in Table 6.

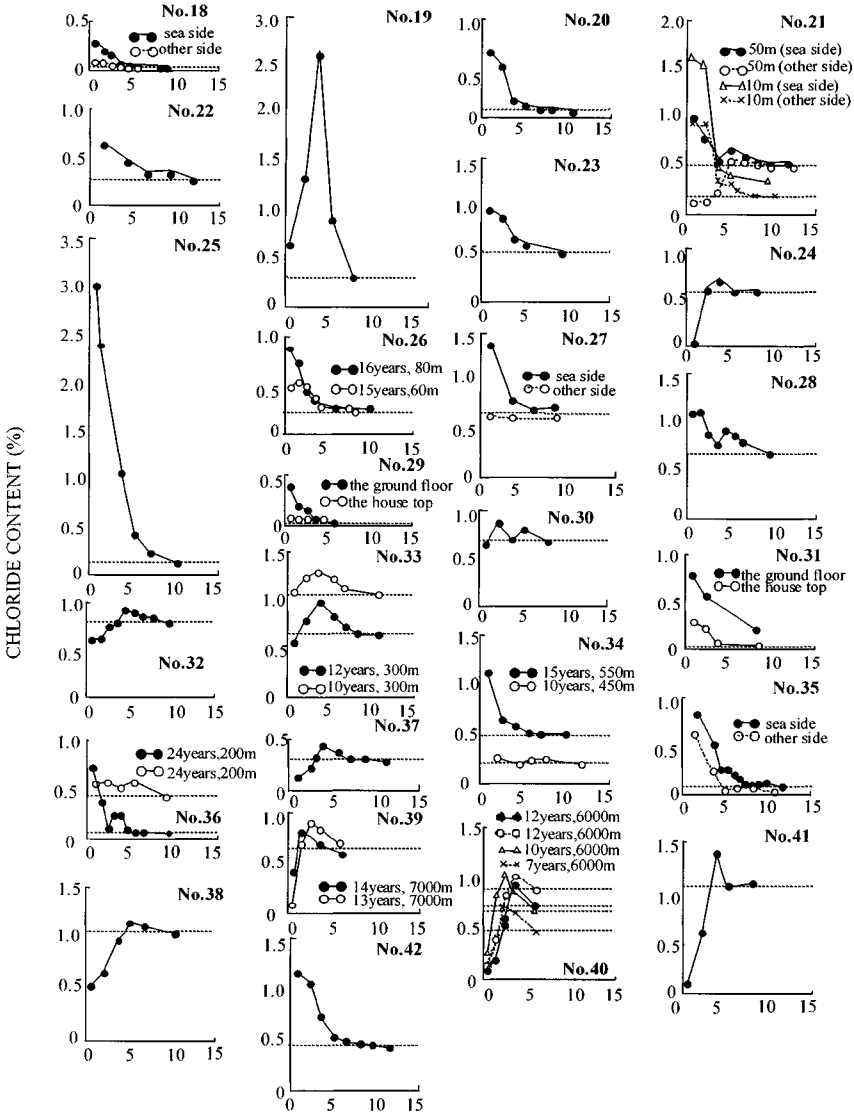

Figure 4-2 Inward distribution of chloride content in actual buildings

The degree of reinforcement corrosion was also investigated by chipping off cover concrete to expose the reinforcement for visual observation based on the scale of five given in Table 7. The mass loss ratios of reinforcement by corrosion determined by Table 7 were divided by the number of years after completion to determine the rate of corrosion [3].

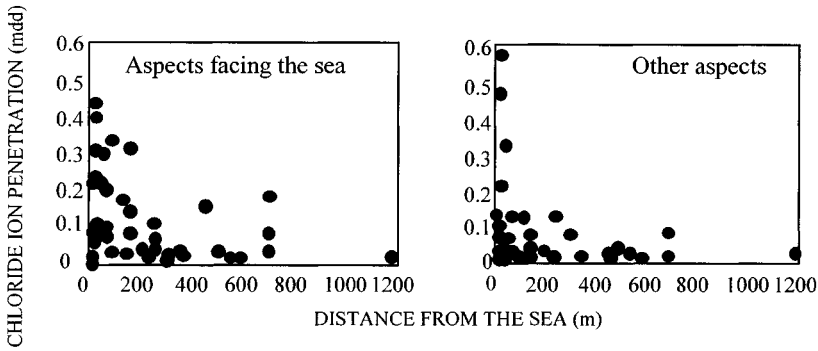

Figure 5 Relationship between distance from the sea and chloride ion penetration

Results

The following results were obtained:

1. The corrosion-inhibiting effect of a thickness of finishing mortar corresponds to that of concrete cover having half the thickness. The equivalent cover depth including 1/2 the thickness of finishing mortar is used hereafter[4].

2. Figure 6 shows the relationship between the chloride ion content at the depth of the cover and the rate of reinforcement corrosion. In this Figure, each point is plotted to represent the age after completion of the building and average mass loss by corrosion at the point. The inclination of each straight line indicates the rate of corrosion (%/year). Figure 7 shows the relationship between the cover depth and the rate of reinforcement corrosion plotted for each chloride concentration. These Figures reveal that the rate of corrosion is almost inversely proportional to the cover depth and nearly proportional to the chloride content.

Table 7 Rating of reinforcement corrosion

DEGREE OF CORROSION	CRITERION	AVERAGE MASS LOSS BY CORROSION (%)
I	Steel retains mill scale with no corrosion.	0
II	Slight pitting appears on steel surface.	1.5
III	Thin rust flakes develop on steel surfaces. Rust stains concrete.	3.25
IV	Relatively thick blistering rust grows, but cross-sectional losses are limited.	6.13
V	Steel is entirely covered with thick blistering rust. Cross-sectional losses are significant.	11.0

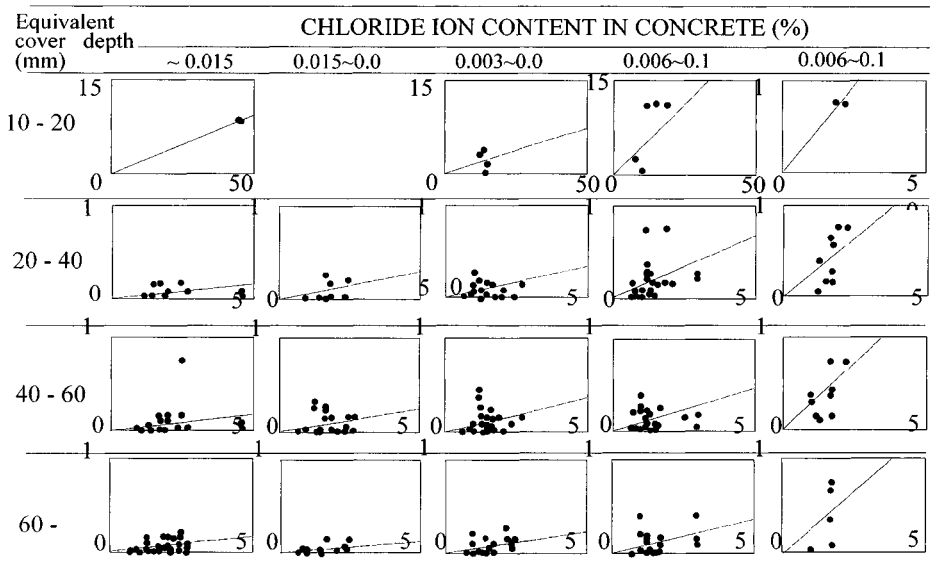

[Note] Abscissa: Age (10years/pitch), Ordinate: Mass loss (%) (5%/pitch)

Figure 6 Chloride content in concrete and mass loss by corrosion classified by cover

In this light, the service life of reinforced concrete is estimated for each chloride ion concentration as follows:

(a) When the chloride ion concentration in concrete is less than 0.015% (equivalent to 0.30 kg/m^3 or less in terms of chloride ion content), the rate of reinforcement corrosion will be as low as between 0.04 and 0.05 (%/year), provided the cover depth is not less than 20 mm. At this rate, the mass loss by corrosion will be 1% or less after 20 years, with the degree of corrosion being I or II, posing no problem for the durability of the structure.

(b) When the chloride ion concentration in concrete is 0.015% or more and less than 0.03% (equivalent to 0.30 kg/m3 or more and less than 0.60 kg/m3), the rate of reinforcement corrosion will be very low at around 0.04 (%/year), provided the cover depth is not less than 60 mm. However, with a cover of less than 60 mm, the rate of reinforcement corrosion will be between 0.07 and 0.1 (%/year), leading to a mass loss between 1.5 and 2% 20 years later, with the degree of corrosion being II or III.

(c) When the chloride ion concentration is 0.03% or more and less than 0.06% (equivalent to 0.60 kg/m3 or more corresponding to the case of using sea sand without washing with fresh water), the rate of reinforcement corrosion will be between 0.09 and 0.13 (%/year), leading to a mass loss of 2 to 3% after 20 years. If this rate of reinforcement corrosion is maintained for 50 years, then the mass loss by corrosion will be between 5 and 8%, with the degree of corrosion being IV. In other words, serious problems may be posed for the durability of the structure 50 years after completion.

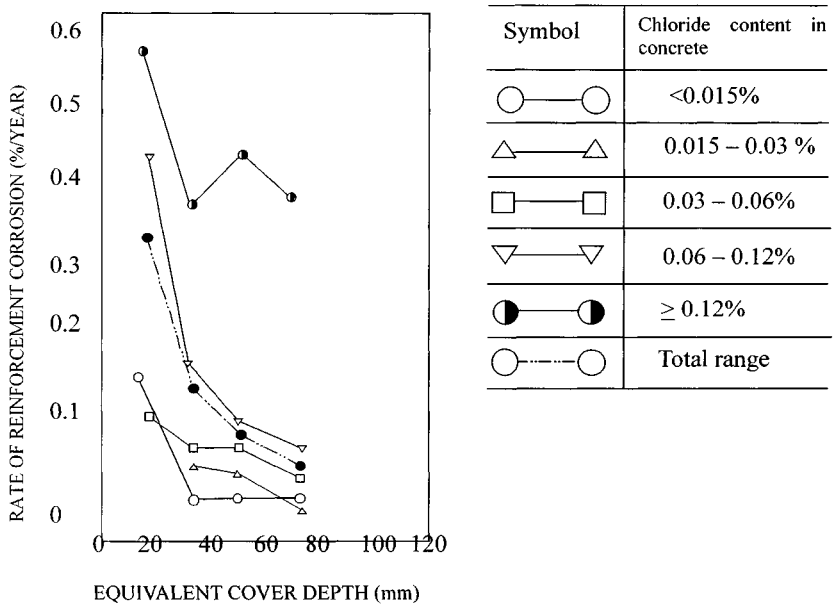

Figure 7 Relationship between equivalent cover depth and rate of reinforcement corrosion

(d) When the chloride ion concentration is 0.06% or more, the rate of reinforcement corrosion will be significantly high even if the cover is sufficient. The rate of reinforcement corrosion will be between 0.16 and 0.25 (%/year) even with a cover depth between 40 and 60 mm, leading to a mass loss between 3 and 5% and between 5 and 8% 20 and 30 years after completion, respectively. The degree of corrosion of reinforcement under a cover depth of 40 to 60 mm will be IV, posing serious problems for the durability of the building.

CONCLUSIONS

In this paper, the results of an extensive survey on the salt damage of reinforced concrete buildings in Japan have been reported. Since chloride ions produce a critical impact on the durability of reinforced concrete buildings, concrete specifications should be adequately established to prevent deleterious amounts of chloride ions from penetrating concrete in areas with a high risk of salt damage. It is also important to promote researches on the methods of repair and corrosion inhibition of buildings in which chlorides have already penetrated.

ACKNOWLEDGEMENTS

This survey was carried out in the Comprehensive Research Project, "Development of Technology for Durability Improvement of Concrete" by Ministry of Construction of Japan. The Author was in change of the subject on salt damage in this project. The author expresses the gratitude to Prof. Tomosawa of Hokkaido University, Prof. Abe of Kogakuin University, Mr. Tanaka of Tobishima Corporation and Mr. Yasuda of Toyo Construction Co. Ltd. for their cooperation.

REFERENCES

1. YAMADA, Y, Study on penetration of chloride ions into concrete under chloride contaminated Environment, A thesis for the degree, Utsunomiya University, Japan, February 2000.

2. KAWAKAMI, H, et al, Chloride permeation into concrete and estimation of saline environment, Journal of structural and construction engineering, Transactions of AIJ, No 453, November 1993, p 9-14.

3. MORINAGA, S, Study on prediction of service lives reinforced concrete buildings based on rate of corrosion of reinforcing steel, A thesis for the degree, The University of Tokyo, Japan, November 1986.

4. TOMOSAWA, F, MASUDA, Y, et al, Influence of chloride content on the rate of corrosion of reinforcing bar in concrete, Report of the Building Research Institute, Published by B.R.I, Ministry of Construction, Japan, No 118, November 1988.

CONGRESS CLOSING PAPER

CONCRETE: VADE MECUM

P C Hewlett
British Board of Agrément
United Kingdom

ABSTRACT. In putting together this Congress review from the many papers submitted, I have been looking for significant trends that can give direction to the way forward. Both the Seminars and Conferences have been taken into account but it has been written in advance. As a consequence the views expressed and conclusions drawn may well change as a result of the Congress itself and the exchanges that will occur during the event. There will be opportunity to cover such developments during the Closing Address Ceremony.

A number of ongoing challenges for concrete have been identified that suggest a way forward. The intent to change is serious but the consequences of not changing are even more so. Quo Vardis?

Keywords: Cement, Environment, Durability, Composite materials, Toughness, Pathology, Sustainability, Aesthetics, Waste, Deconstruction.

P C Hewlett is a chartered chemist and Chief Executive of the British Board of Agrément. He is visiting Industrial Professor in the Department of Civil Engineering at the University of Dundee and an active member of the Concrete Technology Unit. He is Chairman of the Technical Executive Committee of the UK Concrete Society and Chairman of the Editorial Board of the Magazine of Concrete Research.

Particular research interests cover durability, surface and bulk characteristics of concrete modified using chemical additions.

INTRODUCTION

A Congress is defined as a formal meeting of delegates with the purpose of discussing between those present issues such as special studies. In this regard, a Congress about concrete is both timely and needed and since concrete is a global material an International Congress seems very appropriate. This is now the 5th event held in Dundee on a triennial basis, the others being:

'Protection of Concrete' 1990
'Concrete 2000' 1993
'Concrete in the Service of Mankind' 1996
'Creating with Concrete' 1999

For those not involved with concrete it may seem strange after so many years of use, thousands of published papers and many books on the subject, all that could be known about concrete was known. So why does the debate and development continue?

Firstly, concrete is the most widely used construction material globally, it has become established in technically advanced countries and it has been estimated that some 1,200-2,400 kg per head of population are made per year [1]

Secondly, because of its adaptability it can be used for almost all construction situations, both structural and non-structural.

Thirdly, it is capable of being developed further in response to environmental concerns, energy considerations and new functional demands extending the material's performance in answer to engineering needs.

In other words, concrete and concreting are dynamic and will never reach a static position, unless of course our imaginations stagnate and we run out of ideas. For all of these reasons concrete is a material of opportunity and the debate will continue.

The theme of the present Congress is 'Challenges of Concrete Construction' embracing the weather, fire, seismic and marine situations and all that interlinks them. However, concrete faces other challenges from alternative materials such as steel, wood, glass, plastics and natural masonry. Alternatives do not readily have their justification in being straight material's replacements so much as finding their own niche in the design and functional requirements of buildings.

Other challenges covered at this Congress are,

1. Exploitation of the planet – Awakening of conscience in our own self interest
   – Environmental concerns/auditing/marking

2. Adoption of cleaner technologies

3. Sustainability – Design aspects
   – Brownfield development
   – Role of taxing and charging (landfill and aggregate tax)
   – Standardisation of components to assist reuse.

4. Elimination of waste
5. Whole life costing – life and death
6. Design for deconstruction
7. Alternatives to Portland cement
8. Wide/mandated use of cement replacement materials
9. High volume use of by-products
10. Energy conservation
11. Education for such involvements

Notwithstanding such challenges, concrete remains the most widely used construction material globally and that situation is likely to continue.

There is a constant probing for new developments reflecting drivers for change both direct and indirect and some suggested drivers are noted below.

- functional
- decorative
- competitiveness
- opportunity
- serviceability
- environmental issues
- safety
- fashion

These matters are dealt with in the Congress that comprises three Seminars and three Conferences.

CONGRESS REVIEW

Seminar 1 is concerned with 'Composite Materials used Internally and Externally', both organic and in-organic. These new materials offer better durability, lower weight and higher strength, ease of transportation, low thermal conductivity and reduced energy to make. For all of these reasons, adoption of composite materials technology should be welcomed but as with so many innovations in our industry, exploitation is guarded. It is clear that questions are being raised over slowness to adopt new ideas and innovations within concrete construction.

Conceptually fibre reinforced composites are not new and the ground rules for design and selecting them are established [2]. However, reinforced concrete is still conceptually large steel fibres (rebar) as reinforcement in an inorganic matrix rather than organic.

Proven performance based on unequivocal data are key to acceptance by specifiers and users alike to give confidence in the adoption of such new technologies.

Ironically, reinforced concrete itself was originally not backed up by a great deal of pre-use data as are fibre reinforced composites today and yet it was adopted with commitment. Why was this? Perhaps we are both set in our ways as well as worried about litigation. In this respect the composite beam example of Van Elp, Cattel and Heldt [3] is a good one that contradicts the apparent trend. The logical and prospective replacement of the established convention by optimum use of new materials resulting in a hybrid beam that outperforms the traditional reinforced concrete beam. The new types of beam have high load capacity, excellent fatigue resistance, outstanding durability, although detailed reaction to fire and comparable costs need to be addressed.

Are such radical developments welcomed and do we express the functional benefits well enough to persuade clients and specifiers and designers to adopt the new options? When considering new possibilities there is also the issue of appropriate technology. It is sometimes tacitly assumed that technologies rooted in advanced industrialised countries, may be used with equal effect in less developed countries where materials and skills may be different. Since concrete in one form or another is global, it should be possible to evolve appropriate applications for different locations. We talk readily of buildability but in the area of new ideas we should also consider adoptability.

There is merit in simplicity, both in concept, manufacture and use and a shift in Europe to prefabrication, giving better control over the process and a reduction in the need for established site skills.

Composite materials should respond in a ductile manner, eg be tough rather than simply strong. The issue of toughness is repeated throughout the Congress papers. The same trend applies to the development of lightweight structural materials, probably based on waste products, reflecting the emergence of conscience as well as functional and cost requirements. The phrase 'priorities for change' appears in Lowe's keynote paper [4].

It is suggested that value should replace cost in selecting options. This is compatible with the concept of whole life costing, another strand repeated throughout the Congress.

Do regulations and standardisation stimulate or impede innovation? Regulation can stimulate by demanding new and more exacting performance levels. The means of showing compliance with the regulation, eg conforming to a standard or established technical specification may not assist change. Performance based not on prescriptive specifications are an answer but to implement such an approach requires a will to adopt and change.

Mention is made to high temperature and fire effects on organic binders and one paper by Ballaguru [5] introduced an inorganic adhesive for bonding carbon fibre sheets to concrete beams. The water-based adhesive is composed of an alumna-silicate and is stable up to 1000°C. Despite a very complicated application procedure it is indicative of what can be achieved.

One stimulant to development of fibre-reinforced plastics has been seismic performance. Typical fibres are carbon, glass and aramids maintaining cohesion beyond the point of failure.

The pursuit of lightweight and toughness is highly desirable and whilst carbon fibres have a role to play in achieving this objective it needs to be remembered that carbon can act as a noble metal in the galvanic series and whilst it will not corrode it may cause less noble metals relative to it to do so. The carbon itself is conductive and given the right combination of conditions may exacerbate the process.

Seminar 2 is concerned with 'Floors and Slabs' with an emphasis on flooring that seems to represent a typical case of 'we seem to know what to do but do not always do it'. Self imposed inadequacy!

Flooring is undoubtedly a substantial activity in the distribution depot and monolithic construction sectors that use some $1.5m^3$ of concrete a year of concrete in the UK alone.

However, what in principle could be simpler than a slab? What could be simpler than a slab made of concrete? The physical principles of which are known – or are they? When you take regard of the conditions under which concrete for flooring is laid that assumption might be questioned.

There would appear to be too many homespun practices observes Harvey [7] but the problems with floors are global and commonplace. Notwithstanding all of this there would appear to be no substitute for concrete.

There is still much emphasis on Concrete Society Report TR34 [8]

Seidler [9] challenged that notwithstanding progress in concrete generally over the last 150-200 years, concrete flooring has not advanced significantly.

Incipient cheapness whilst a determining factor in this apparent lack of progress at some 27 Euros per square metre (approximately £17.50 per square metre) the equivalent of a medium quality fitted carpet! I cannot image the average fitted carpet functioning like an industrial floor. The requirements of industrial floors are clearly stated, namely,

- non shrink concrete
- monolithic construction
- non dusting
- adequate strength and surface resistance
- complex serviceability requirements

Chemical modifications can help overcome the known problems but the addition of polymers increases the cost substantially.

An industrial floor is a good example of a multi faceted performance requirement from something that is basically very simple. Why has this topic received so little attention? Value, longevity and robust performance rather than cost might be a better approach. In this sector cost seems to dominate.

Fast track construction leading to long strip and large bays are a trend to be acknowledged, together with joint-free slabs with speciality surface finishing and finishes. These are added demands to what superficially is a simple functional element.

Floor quality appears to have reached a plateau in terms of economically obtained quality. Again a plea for whole life costing.

The paper by Watanabe et al [10], suggests a form of flooring categorisation in the range 1-7, linked to the use to which the floor may be put and the development of a so-called U-scale as a measure of anti-static performance.

Seminar 3 deals with 'Repair, Rejuvenation and Enhancement of Concrete'.

Concrete repair and rehabilitation still dominate the concrete scene and yet concrete's failures are a relatively small proportion of concrete's use. Failure is also small, relative to new applications of concrete, eg, self compacting and ultra-high strength concrete and in relation to major projects such as the second Severn Crossing. However, in money and nuisance value terms, the profile of rehabilitation and repair is high and in that sense it attracts attention. It is the longer term inadequacies such as poor appearance, sulphate and chloride attack, sulphation and carbonation, that need to be addressed. Have these problems resulted from pursuing cost containment, lower cement contents, reduced cover rather than long term value?

The entire topic of concrete's pathology and degradation processes is worthy of our attention, how do we extend with confidence, the lifespan of concrete structures?

I refer to the paper of Tuutti [11] that quotes some telling figures relating capital values of buildings and structures to the value of all stocks as they apply to Sweden but may well reflect global trends in industrialised countries. Much of this stock has to be repaired and/or replaced on a 50 year cycle and that represents vast sums of money. If that is so, do we simply use concrete and design buildings, towns and cities as we have always done? Is such an approach sustainable?

Exploitation of new materials options that will have a longer service life and perhaps even be 'smart' will become the norm. Autogenous healing of cracked concrete is an example of a 'smart' material. It is difficult to predict where the initiative for change will come from. Will it be radical design, reflecting efficient function or will it be ad hoc picking up on personal preferences and available options? Will the drive be regulation or market opportunism? Did the development of self-compacting concrete start with an engineering need or more the availability of such a material's option, driven in turn by dispersant technology applied to cementitious suspensions rather than sound market research? In a capitalist economy the ultimate drive is financial well-being and planning and opportunism will live close together resulting in a somewhat volatile cocktail. So will concrete's future development be ad hoc and random or will sustainability, efficiency and environmental concerns dominate? Will such concerns only be responded to by wealthy economies with the less endowed creating their own appropriate technologies?

The existence of historical structures built from concrete is tangible evidence of the material's good latent durability. However, what remains is the best and a great deal has not lasted and for many reasons. Therefore the historical legacy has lessons to teach us and they are worthy of study.

In determining the effect of challenges to concrete, the diagnosis stage is very important. A comparison with forensic science is justified and the diagnostician has many techniques at his disposal. I am of course referring to the paper by Sims [12].

Threats, such as thaumasite sulphate attack (TSA), alkali-silica reaction (ASR), alkali-carbonate reaction (ACR) and delayed ettringite formation (DEF), all challenge concrete but we have to keep the potential problems in context. Notwithstanding this the avoidance of alkali-silica and alkali-carbonate reaction by selecting suitable aggregates remains a global issue.

Physico-chemical techniques have resulted in preventative and remedial measures such as cathodic protection, electro chemical realkalisation and chloride removal. All have a place and the last two may well have moved on from being something of a curiosity to full-scale practical application [13].

The themes developed in the Seminars enlarge and extend into the three Conferences. Conference 1 is concerned with 'Innovations and Developments in Concrete Materials and Construction' and Shah [14] sees the following targets for concrete in the 21st Century,

- more durable
- more constructable
- more predictable
- greener

I would add, more sustainable and more competitive.

By judicious use of investigative and monitoring techniques, all these objectives are attainable. However, since concrete is a global material, a case could be made for such developments to be globally supported with the results available to all. At the present time research cultures are very national and even regional, resulting in considerable duplication of effort on the one hand but also inventive variety on the other. The basic principle of such issues as rheology, hydration, corrosion and loading characteristics could be conducted in one or two locations whereas much effort is dispersed at numerous locations around the world, competing for funds and technical recognition. It is only when we draw people together in a Congress such as this that we identify the common features. It depends upon whether a global material such as concrete requires global development in a global economy with appropriate planning and prioritising or whether the more parochial approach is more beneficial if somewhat wasteful.

For instance, the use of electronic speckle pattern interferometry (ESPI) to study cracking in fibre reinforced concrete [14] compared with the K and F functions to describe fibre distributions resulting in stress intensity factors that govern crack propagation, assists in defining the capability limits of such reinforcements. Do such studies need to be duplicated? Is the study itself not definitive?

Shah et al's work[14] has shown that extrusion can improve fibre distribution and result in a stronger and tougher composite. Prefabricated components might well lend themselves to such techniques.

In the area of self compacting concrete, rheological studies assisted the optimisation of concrete mixes. A balance has to be struck between high flow and no segregation with yield values permitting deformability of the concrete to accommodate awkward shapes. The absolute rheological terms of yield value and viscosity do not relate directly to deformability, placeability and segregation that describe what the material has to do in practice. However, such an approach permits judgements and selection to be made.

Rossi [15] has developed ultra high strength performance fibre reinforced concrete (UHPFRC) to the point that concrete without conventional reinforcement might be a prospect. This concept is represented by the MSCC (multi scale concept concrete) that consists of short fibres (6mm) and long fibres (13mm) mixed together at 7% of the cement content.

Perhaps we have too many options e.g.

- MDF (macro defect free) concrete
- DSP (densified small particle concrete)
- CRC (compact reinforced composites) and its BPR variant (similar to CRC but with longer fibres)
- RPC (reactive powder concrete)
- MSCC (multi-scale cement composite)
- SIFCON (slurry infiltrated fibre concrete)
- ECC (engineered cementitous composite)

to mention but a few.

Having developed new materials, techniques of placing and finishing them have to be considered. These are not concretes as we know them. With approximately 1000 kg/m^3 of cement and cement:aggregate ratios of 4:1 and tensile strengths of 40-50 MPa being attainable!

Costs of these developments, at this stage, are not given but clearly it is cost effectiveness and value that matters – they are not like for like replacements of normal concretes. The importance of such extreme developments as this is that it shows what can be done and, like radical fashions, they set a pattern within which there is general advancement.

It is encouraging to note in a paper by Garshol and Constantiner [16] that at long last the concept of incorporating chemicals to control and modify the plastic and harden states of concretes and mortars has consolidated into normal practice. Indeed without certain admixtures and reactive additives these new concepts would remain only a wish.

Admixtures are now being tailored to the known chemistry of cements and the required physical and chemical characteristics of resulting mortars and concretes. Science is replacing intuitive flair and materials engineering replacing a 'try and see' approach. Integrating disciplines in this way will bring construction in line with other process engineered activities, eg, aircraft construction. Such trends are predicted in the Egan Report – 'Rethinking Construction' [17].

Having made and placed the concrete its maintained appearance does not receive the status it deserves. The visual impact of concrete is not popular with the community at large and Kronlof [18] is concerned with the aesthetics of concrete, as we all should be. The phrase 'concrete is beautiful when it makes the designer and user happy' can hardly be argued with.

Concrete's form and appearance should be predictable – no unpleasant surprises. Natural ageing should be taken into account and neatness should be a prime aim for concrete development but again a low cost outlook does not aid aesthetic development.

General expectations of society and designers may differ from those of the industry and users. Kukko [19] considers that designers and society may be concerned with image and public benefit, but industry is more concerned with economic and technical profits. Is this division true? If it is how can it ever be reconciled?

Production of high quality surfaces, edges and joints is a priority with high quality materials being required, resulting in ready for finishing details, eg, painting and wallpapering.

There are opportunities for higher strengths and toughness – thinner and slender structures, shells, lattices, profiled beams and columns, all are attainable. Kukko identifies some aims, namely,

- environmental friendliness
- improving the quality of life
- competitiveness
- improved employment prospects
- improved working conditions, in particular, safety

Concrete is 'a material for all reasons' and, if its permanency could be assured, we might invest more in some of these value added options.

Conference 2 deals with 'Sustainable Concrete Construction' and Nixon's paper [20] is both forthright, to the point and very relevant. He makes some telling criticisms of man's exploitation of the planet. He contends we should be concerned with,

- adaptable buildings
- minimum waste
- design for deconstruction
- low energy cements
- reduced energy in use by using concrete intelligently

In attaining these aims concrete is the premier construction material.

Firstly, some disturbing facts.

In the UK about 25% of the energy used in industry is accounted for by the manufacture and transportation of building materials.

- It is estimated that 8% of global CO_2 emissions result from concrete production.
- One ton of CO_2 is produced per ton of Portland cement.
- Cement production is growing, particularly in developing countries and what we gain by going in one direction to save the environment may be offset by trends in the opposite direction.
- In summary we need an alternative to Portland cement – such options are coming into play already.

Cements that require reduced energy for production (less by 16%) and in turn produce less carbon dioxide (less by 10%) are seemingly attainable. Cements based upon belite with properties comparable to Portland cements and with some evidence to indicate that durability of resulting concretes might even be improved have been produced on a commercial scale in China. There is also the recent TecEco development based on magnesium oxide.[21] What is the future for these alternatives?

Nixon also makes the point that we should use concrete innovatively, taking regard of its high thermal mass resulting in substantial economies in the running of buildings.

Jensen and Glavind [22] remind us that to make $1m^3$ of office space requires something in the region of 500 MJ whereas for the same office space it requires 15,000 MJ to heat and light. How can concrete assist in the use and running of buildings is an issue that needs to be addressed.

Jensen and Glavind continue a similar theme noting that 2-6% of worldwide CO_2 stems from cement production and cement manufacture is increasing at 5% per year, equivalent to an increase of 10 million tons of CO_2 per year.

Perhaps we will only take the environmental issues seriously when failure to achieve set aims is legislated for. The Eco Management and Audit Scheme (EMAS) coupled with a statutory instrument against which a company can be registered might be a way forward. Various tools are available to engendering an environmental culture but what creates the will to do so? The principles of life cycle assessment (LCA) and life cycle inventory (LCI) can have aims and set targets such as,

- CO_2 reduction by at least 30%
- 20% of all concrete should use residual products as aggregates
- use concrete industry's own residual products
- CO_2 neutral waste derived fuel being used at a rate of at least 10% of all fuel used in cement production

In the USA some 5 billion tons of non hazardous by-product materials are produced annually (NAIK [23]). Major inputs from agriculture (2.1 billion tons) and mineral sources (1.8 billion tons).The UK construction industry produces 20% of all UK waste [24].

The use of fly ash and bottom ash and clean coal ash in cement production with new energy generating technologies yielding different coal derived ashes assists the quest for energy containment. There are many new end uses for waste materials, for instance, sewage sludge for lightweight aggregates and for making clay bricks.

The task of carrying the environmental banner often falls to the lot of the manufacturer but contractors have a role to play as well (Goring [25]). Greater integration and co-operation emphasising quality and safety and less so cost, as has been the habit to date. These principles are set out in Egan's 'Rethinking Construction' [25]. How do these attitudes impinge upon concreting activities? Firstly, starting with design concepts – concrete can play a role by way of its thermal mass in providing better air quality and natural ventilation. To effect radical change we need an integrated approach involving concrete design and function and increasing the overlap between environmental concerns and how we build.

Torring and Lauritzen [26] estimate a potential of 400 million tons of reusable concrete, stone and brick from industrialised countries. We have to consider the means of deconstruction and reclaiming the materials used. – Joined up construction underwritten by a joined up sense of public conscience.

Pocklington and Glass [24] believe that the energy performance of buildings are a key to sustainability in which case there is good reason for using concrete. Phrases such as 'burn and bury', 'dilute and disperse' and 'end of pipe' are no longer acceptable. The term anthropogenic was used – greenhouse gas emissions caused by man. We need some form of fiscal encouragement to create a culture of change. We also need to plan for longer life and adaptability of buildings.

Further telling statistics supplied by Glavind and Munch-Petersen [27]. Some 5 km^3 of concrete are used per year globally and whilst some would contend that CO_2 produced per ton of cement is small in itself, it becomes large due to the amount of concrete produced. The prospect of quantified benchmarking of attainable objectives for CO_2 reduction say by 30% and recycled concrete used as aggregate, making an energy reduction of 20% is tantalising. The authors also consider that waste derived fuels should replace 10% of fossil fuels and their paper results in a specification for 'green' concrete types – some 14 in number. The authors were very conscious of solving one problem but creating a second order unwelcome legacy, eg, kiln dust containing zinc, vanadium, lead and copper as well as phosphorus pentoxide. We have to maintain a sense of proportion and perspective. The various phases of materials production and construction activity cannot be dealt with in isolation, one from the other.

Conference 3 deals with 'Concrete for Extreme Conditions' and the paper by De Vries [28] endeavours to put the problems of durability into perspective. On balance the performance of concrete is not as bad as many would contend. However, there are problems of poor workmanship and with new materials. Codes and specifications are not particular enough and matters of maintenance and repair not covered sufficiently well. De Vries would like to see performance and reliability based service life design and makes reference to the European Brite/Euram research project – 'Duracrete'. A plea is made to involve the client and give contractors a number of options.

Durability design should get as much attention as structural design. The Eastern Schedlt barrier has a service life-span of some 200 years! However, a period of 85 years was settled for the concrete when it was accepted that the cover will have to be replaced. An example of integrating maintenance with design life. We have to quantify the anticipated functional life-span. To do this a knowledge of the durability of materials is required and the effect of workmanship on achieving these properties needs to be addressed.

De Vries is also concerned with the interaction of structure and the environment and uses a probabilistic technique to determine the likelihood of failure and target service life. There are problems of defining the limit state requirements eg the onset of corrosion. Models exist for defining degradation conditions and the design can be modified to offset adverse predictions of service life based on such models – a preemptive approach.

Slater [29] concentrates on marine structures and these represent a severe exposure condition but relates the data so that it is relevant to all types of construction. The emphasis is on buildability and durability. Buildability covering such issues as safety and economy and durability fixed by design and exposure (environment). Reassuring to see a preference for

low w:c ratios and a useful quoted rule of thumb 'a reduction in w:c ratio of .05 is the equivalent of an increase in a cover of 5mm'. Slater concludes with an excellent series of pragmatic recommendations.

Over recent times there has been much discussion on the existence of threshold chloride levels below which passivation is maintained and above which active corrosion commences. The paper by Paramasivam et al [30] is a good example of data obtained on an actual structure, in this case a 32 year old wharf from which 6 marine piles (driven) were recovered and analysed for chloride content and penetration. Comparisons were made of the actual with predicted ingress levels of chloride and the relationship between such levels and loss in mass of reinforcing bars. Reference is made to threshold chloride levels (Reference 2 of [30])again and the establishment of critical chloride levels in the range .03 - .1% weight/weight concrete, covering in the first instance the splash zone and the latter submerged (Reference 6 [30]). Alternatively, Browne (Reference 7 of [3]) again showed such values to be in the range .2 - .49% w/w cement. Therefore values of .034 - .068% w/w concrete were considered appropriate.

These figures are to be doubted where a plentiful supply of oxygen is available. There was broad agreement between predicted and actual values confirming the various models used. As an extension to the problems caused by chloride ingress and contamination, Masuda [31] considered salt damage to reinforced concrete buildings resulting from both seawater and airborne salt. Some 4,363 buildings were investigated, covering everything from domestic to industrial, schools, offices, hospitals, etc resulting in 60% or so being perfectly satisfactory in the age range 7-46 years old. The distance from the coast was a significant factor in determining the residual chloride levels. Insufficient cover was the cause of deterioration in most cases but the examination was primarily visual. The threshold levels in this study were broadly corroborated.

CONCLUSIONS

This Congress has brought together a great deal of data and experience that within itself has trends that indicate the way ahead and help to establish attitudes and create priorities. Some noted trends are given below.

1. Concrete is capable of considerable further performance-based development and should not posture as a low technology stereotype .

2. Sustainability will remain a motivator for regulators, designers and concrete material providers. Is there a sustainable alternative to Portland cement?

3. Adopted technology should be in proportion to prevailing local conditions.

4. Creating a concrete culture at operative level with recognition of skill status will help to exploit new developments and make the aim of best practice a reality.

5. Laboratory-based data must reconcile with what happens in practice — transfer of micro mechanisms to macro fact. Methods of diagnosis should be accurate and unambiguous, performed by those qualified to do so and interpretation should be subject to severe scrutiny.

6. The role of water needs more committed study. It is necessary for cement to transform into masonry but is also responsible for much of concrete's degradation.

7. Development of tough concrete rather than high strength but brittle concretes.

8. The visual appearance of concrete with time is of concern. Concrete should remain pristine and not take on a patina of industrial downgrading.

9. Coating and sealing may not be sufficient. We have to understand how concrete behaves to fluctuations in its surroundings at a micro mechanistic level.

10. Does a true threshold chloride level exist before steel corrosion occurs?

11. Can we consider structures that do not contain normal reinforcement but rely solely on metal fibres and a reconstituted matrix?

12. The use of recycled and waste materials should be encouraged using legislation and tax incentives for those that comply – a stick and carrot approach.

ACKNOWLEDGEMENTS

I am indebted to all the authors of those Congress papers to which I have made reference and indeed those that I have not, I also thank colleagues with whom I have endless discussions about concrete, without which opinions and viewpoints could not be formed and conclusions drawn.

REFERENCES

With the exception of References 1, 8, 17 and 21, all are drawn from papers given at the Dundee Congress 'Challenges of Concrete Construction' 5-11 September 2002. To simplify the listing only the relevant Seminar or Conference is identified.

1. GLASSER F. P., Private Communication

2. All Authors, Composite Materials in Concrete Construction, Seminar 1.

3. VAN ERP G., CATTEL C., HELDT T., Fibre Composites in Civil Engineering: An Opportunity for a Novel Approach to Traditional Reinforced Concrete Concepts. Proceedings of International Congress: Challenges of Concrete Construction, Seminar 1 – Composite Materials in Concrete Construction, Dundee, Scotland, 5-6 September, 2002, pp 1-16

4. LOWE P., Composite Materials in Concrete Construction, Proceedings of International Congress: Challenges of Concrete Construction, Seminar 1 – Composite Materials in Concrete Construction, Dundee, Scotland, 5-6 September, 2002, pp 17-30

5. BALAGURU P.N., Inorganic Polymer Composites in Concrete Construction: Properties, Opportunities and Challenges, Proceedings of International Congress: Challenges of Concrete Construction, Seminar 1 – Composite Materials in Concrete Construction, Dundee, Scotland, 5-6 September, 2002, pp 109-126

6. VAN GEMERT D., BROSENS K., Non-Metallic Reinforcements for Concrete Construction, Proceedings of International Congress: Challenges of Concrete Construction, Seminar 1 – Composite Materials in Concrete Construction, Dundee, Scotland, 5-6 September, 2002, pp 225-236

7. HARVEY D.J.J., Developing a Greater Understanding of the Nature and Usability of Concrete in Industrial Floor Applications, Proceedings of International Congress: Challenges of Concrete Construction, Seminar 2 – Concrete Floors and Slabs, Dundee, Scotland, 5-6 September, 2002, pp 183-194

8. CONCRETE SOCIETY, Concrete Industrial Ground Floors – A Guide to their Design and Construction, Technical Report No 34, 1994, pp 170.

9. SEIDLER P., How Polymers Improve Floors – Possibilities Today and Prospects for the Future, Proceedings of International Congress: Challenges of Concrete Construction, Seminar 2 – Concrete Floors and Slabs, Dundee, Scotland, 5-6 September, 2002, pp 1-14

10. WATANABE H., ONO H., KAIZU H., Performance Evaluation of Floors for Static Charge on Human Body – Proposal of a New Method, Proceedings of International Congress: Challenges of Concrete Construction, Seminar 2 –Concrete Floors and Slabs, Dundee, Scotland, 5-6 September, 2002, pp 233-244

11. TUUTTI K., Repair, Rejuvenation and Enhancement of Concrete – A Fast Growing Market, Proceedings of International Congress: Challenges of Concrete Construction, Seminar 3 – Repair, Rejuvenation and Enhancement of Concrete, Dundee, Scotland, 5-6 September, 2002, pp 1-10

12. SIMS I., Diagnosing and Avoiding the Causes of Concrete Degradation, Proceedings of International Congress: Challenges of Concrete Construction, Seminar 3 – Repair, Rejuvenation and Enhancement of Concrete, Dundee, Scotland, 5-6 September, 2002, pp 11-24

13. VENNESLAND O., Documentation of Electrochemical Maintenance Methods, Proceedings of International Congress: Challenges of Concrete Construction, Seminar 3 – Repair, Rejuvenation and Enhancement of Concrete, Dundee, Scotland, 5-6 September, 2002, pp 191-198

14. SHAH S.P., AKKAYA Y., BUI V.K., Innovations in Microstructure, Processing and Properties, Proceedings of International Congress: Challenges of Concrete Construction, Conference 1 - Innovations and Developments in Concrete Materials and Construction, Dundee, Scotland, 9-11 September, 2002, pp 1-16

15. ROSSI P., Developments of New Cement Composite Materials for Construction, Proceedings of International Congress: Challenges of Concrete Construction, Conference 1 - Innovations and Developments in Concrete Materials and Construction, Dundee, Scotland, 9-11 September, 2002, pp 17-30

16. GARSHOL K.F., CONSTANTINER D., Super-Concrete Examples: Complete Rheology Control and Passive Fire Protection, Proceedings of International Congress: Challenges of Concrete Construction, Conference 1 - Innovations and Developments in Concrete Materials and Construction, Dundee, Scotland, 9-11 September, 2002, pp 411-422

17. EGAN J., Rethinking Construction, July 1998, pp 39.

18. KRONLÖF A., Concrete Aesthetics: Flexible or Stiff – Humble or Arrogant, Proceedings of International Congress: Challenges of Concrete Construction, Conference 1 - Innovations and Developments in Concrete Materials and Construction, Dundee, Scotland, 9-11 September, 2002, pp 751-762

19. KUKKO H., Requirements for Advanced Concrete Materials, Proceedings of International Congress: Challenges of Concrete Construction, Conference 1 - Innovations and Developments in Concrete Materials and Construction, Dundee, Scotland, 9-11 September, 2002, pp 949-956

20. NIXON P.J., More Sustainable Construction: The Role of Concrete, Proceedings of International Congress: Challenges of Concrete Construction, Conference 2 – Sustainable Concrete Construction, Dundee, Scotland, 9-11 September, 2002, pp 1-12

21. GLASSER F.P., TecEco: Cements Based on Magnesium Oxide, A Private Communication, 2001, pp 9.

22. JENSEN B.L., GLAVIND M., Consider the Environment – Why and How, Proceedings of International Congress: Challenges of Concrete Construction, Conference 2 – Sustainable Concrete Construction, Dundee, Scotland, 9-11 September, 2002, pp 13-22

23. NAIK T.R., The Role of Combustion By-Products in Sustainable Construction Materials, Proceedings of International Congress: Challenges of Concrete Construction, Conference 2 – Sustainable Concrete Construction, Dundee, Scotland, 9-11 September, 2002, pp 117-130

24. POCKLINGTON D., GLASS J., Economics, Sustainability and Concrete, Proceedings of International Congress: Challenges of Concrete Construction, Conference 2 – Sustainable Concrete Construction, Dundee, Scotland, 9-11 September, 2002, pp 683-694

25. GORING P.G., Rethinking Sustainable Concrete Construction, Proceedings of International Congress: Challenges of Concrete Construction, Conference 2 – Sustainable Concrete Construction, Dundee, Scotland, 9-11 September, 2002, pp 439-456

26. TORRING M., LAURITZEN E., Total Recycling Opportunities – Tasting the Topics for the Conference Session, Proceedings of International Congress: Challenges of Concrete Construction, Conference 2 – Sustainable Concrete Construction, Dundee, Scotland, 9-11 September, 2002, pp 501-510

27. GLAVIND M., MUNCH-PETERSEN C., Green Concrete – A Life Cycle Approach, Proceedings of International Congress: Challenges of Concrete Construction, Conference 2 – Sustainable Concrete Construction, Dundee, Scotland, 9-11 September, 2002, pp 771-786

28. DE VRIES H., Durability of Concrete : A Major Concern to Owners of Reinforced Concrete Structures, Proceedings of International Congress: Challenges of Concrete Construction, Conference 3 – Concrete for Extreme Conditions, Dundee, Scotland, 9-11 September, 2002, pp 1-16

29. SLATER D., Marine and Underwater Concrete – Buildability and Durability, Proceedings of International Congress: Challenges of Concrete Construction, Conference 3 – Concrete for Extreme Conditions, Dundee, Scotland, 9-11 September, 2002, pp 189-204

30. PARAMASIVAM P., LIM C.T.E., ONG K.C.G., Performance of Reinforced Concrete Piles Exposed to Marine Environment, Proceedings of International Congress: Challenges of Concrete Construction, Conference 3 – Concrete for Extreme Conditions, Dundee, Scotland, 9-11 September, 2002, pp 525-536

31. MASUDA M.Y., Condition Survey of Salt Damage to Reinforced Concrete Buildings in Japan. Proceedings of International Congress: Challenges of Concrete Construction, Conference 3 – Concrete for Extreme Conditions, Dundee, Scotland, 9-11 September, 2002, pp 823-836

INDEX OF AUTHORS

SUBJECT INDEX

This index has been compiled from the keywords assigned to the papers, edited and extended as appropriate. Th page references are to the first page of the relevant paper.